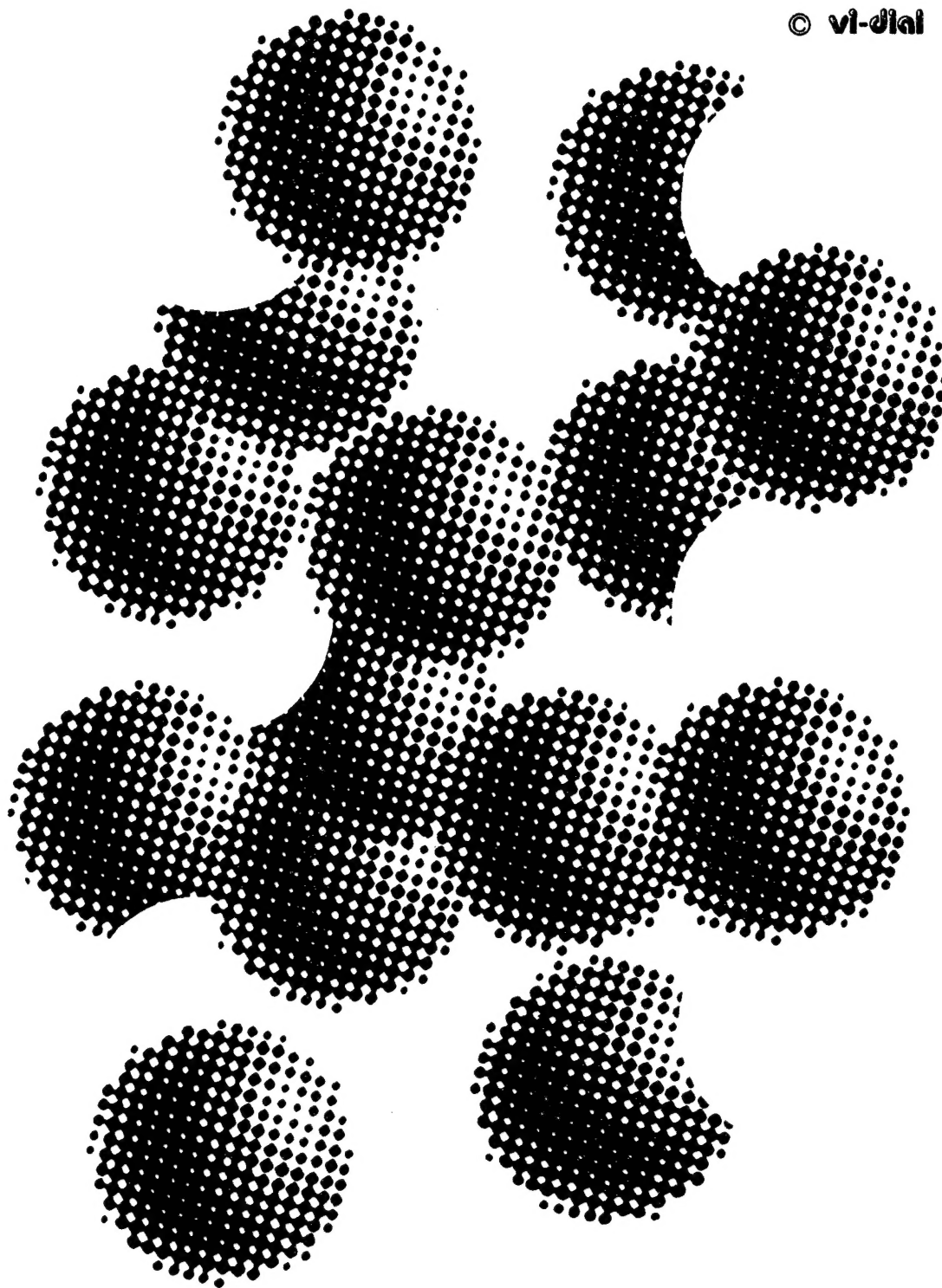


electromagnetic compatibility

part —2

© vi-dial



DISTRIBUTION STATEMENT A
Approved for Public Release
Distribution Unlimited



Fifteenth
International Wrocław
Symposium and Exhibition
on Electromagnetic Compatibility
June 27-30. 2000

FIFTEENTH INTERNATIONAL
WROCŁAW SYMPOSIUM AND EXHIBITION

ELECTROMAGNETIC COMPATIBILITY 2000

PART II

EDITORS:

J.M. JANISZEWSKI

W. MOROŃ

W. SĘGA

Published by the National Institute of Telecommunications

AQ F00-12-3818

All papers are published on responsibility of the authors

©Copyright by Wrocław Symposium on EMC

Applications for reproduction of this book or parts thereof
should be directed to EMC Proceedings Editor

Organizers address:

EMC Symposium, Box 2141
51-625 Wrocław 12, Poland
fax: +4871 3728878
e-mail: emc@il.wroc.pl
www.emc.wroc.pl

ISBN 83-901999-8-X

REPORT DOCUMENTATION PAGE			Form Approved OMB No. 0704-0188	
Public reporting burden for this collection of information is estimated to average 1 hour per response, including the time for reviewing instructions, searching existing data sources, gathering and maintaining the data needed, and completing and reviewing the collection of information. Send comments regarding this burden estimate or any other aspect of this collection of information, including suggestions for reducing this burden to Washington Headquarters Services, Directorate for Information Operations and Reports, 1215 Jefferson Davis Highway, Suite 1204, Arlington, VA 22202-4302, and to the Office of Management and Budget, Paperwork Reduction Project (0704-0188), Washington, DC 20503.				
1. AGENCY USE ONLY (Leave blank)		2. REPORT DATE 24 July 2000		3. REPORT TYPE AND DATES COVERED Conference Proceedings
4. TITLE AND SUBTITLE Emc - 15TH International Wroclaw Symposium And Exhibition On Emc , <i>Part 2</i>			5. FUNDING NUMBERS F61775-00-WF074	
6. AUTHOR(S) M.M. Janiszewski, W. Moron, W. Segal (Editors)				
7. PERFORMING ORGANIZATION NAME(S) AND ADDRESS(ES) Institute of Telecommunications ul. Swojczycka 38 Wroclaw 51-501 Poland			8. PERFORMING ORGANIZATION REPORT NUMBER N/A	
9. SPONSORING/MONITORING AGENCY NAME(S) AND ADDRESS(ES) EOARD PSC 802 BOX 14 FPO 09499-0200			10. SPONSORING/MONITORING AGENCY REPORT NUMBER CSP 00-5074	
11. SUPPLEMENTARY NOTES Two volumes. <i>Part 1</i>				
12a. DISTRIBUTION/AVAILABILITY STATEMENT Approved for public release; distribution is unlimited.			12b. DISTRIBUTION CODE A	
13. ABSTRACT (Maximum 200 words) The Final Proceedings for 15th INTERNATIONAL WROCLAW SYMPOSIUM AND EXHIBITION ON EMC, 27 June 2000 - 30 June 2000 This is an interdisciplinary conference. Subject matter will include all aspects of Electromagnetic Compatibility (EMC) theory and practice as seen in this partial list of topics for planned sessions: EMC on Component and PCB Level; Lightning and ESD; EMC in Communication and Power Systems; Modeling and Simulation Theory and Practice. NATO EMC issues: Military vs Civil EMC Standards - Comparisons and Problems, Standard Procedures for Simulation, Prediction and Modeling Antennas and Propagation, Biological Effects of EM Radiation - Technical Aspects, Spectrum Management and Monitoring, EM Hazards and Terrorism, EMC Matters and Satellite-based Systems I, Computational EM Technique in Mobile Wireless Communications				
14. SUBJECT TERMS EOARD, Modelling & Simulation, Electromagnetics, Electromagnetic Compatibility			15. NUMBER OF PAGES 924 + cover matter (two volumes)	
			16. PRICE CODE N/A	
17. SECURITY CLASSIFICATION OF REPORT UNCLASSIFIED	18. SECURITY CLASSIFICATION OF THIS PAGE UNCLASSIFIED	19. SECURITY CLASSIFICATION OF ABSTRACT UNCLASSIFIED	20. LIMITATION OF ABSTRACT UL	

NSN 7540-01-280-5500

Standard Form 298 (Rev. 2-89)
Prescribed by ANSI Std. Z39-18
298-102

20000913 037

DQC QUALITY INSPECTED 4

Patron:

T. Szyszko
Minister of Posts and Telecommunications of
the Republic of Poland

Under the auspices of:

Polish Academy of Sciences (PAN)
Committee of Electronics and Telecommunication

Organizers:

The Association of Polish Electrical Engineers
The Wroclaw University of Technology
The National Institute of Telecommunications

Cosponsor:

International Union of Radio Science



Cooperating:

International organizations

International Union of Radio Science (URSI); International Telecommunication Union: Radiocommunication Bureau (ITU-R), Telecommunication Standardization Bureau (ITU-T) and Telecommunication Development Bureau (ITU-D); International Electrotechnical Commission (IEC); International Special Committee on Radio Interference (CISPR) and TC 77 Electromagnetic Compatibility (IEC TC77); UNESCO International Centre for Theoretical Physics (ICTP); European Broadcasting Union (EBU); European Telecommunications Standards Institute (ETSI); Pacific Telecommunication Council (PTC); Region 8 (Europe) and Poland Section of the Institute of Electrical and Electronics Engineers (IEEE); International Amateur Radio Union (IARU) – Region 1

Convention of National Societies of Electrical Engineers of Europe – EUREL

Austrian Electrotechnical Association – ÖVE (*Austria*); Association of Electrical Engineers Graduated from the Montefiore Institute – AIM (*Belgium*); Royal Flemish Society of Engineers – TI-KVIV (*Belgium*); Royal Belgium Society of Electrical Engineers (*Belgium*); The Association of Electrical, Electronics and Automation Societies in Finland – FINEL (*Finland*); Association of Electrical and Electronics Engineers – SEE (*France*); Association for Electrical, Electronic & Information Technologies – VDE (*Germany*); Hungarian Electrotechnical Association – MEE (*Hungary*); Institution of Engineers of Ireland – IEI (*Ireland*); Italian Electrotechnic and Electronic Association – AEI (*Italy*); Association of Polish Electrical Engineers – SEP (*Poland*); Portuguese Association of Engineers – OE (*Portugal*); Slovak Electrotechnic Society – SES (*Slovakia*); Swedish Society of Electrical and Computer Engineers – SER (*Sweden*); Swiss Electrotechnical Association – SEV (*Switzerland*); Institution of Electrical Engineers – IEE (*United Kingdom*)

Other Associations

Scientific Technical Society for Radio Technology, Electronics and Electrocommunications – BORES (*Belarus*); Union of Electronics, Electrotechnics and Telecommunications – UEEEC (*Bulgaria*); Association for the Protection against Electromagnetic Interference – EMCAS (*Czech Republic*); Estonian Electronics Society – EES (*Estonia*); Association of Electrical Engineers – AEE (*Finland*); Scientific Society for Telecommunication – HTE (*Hungary*); The Institute of Electronics, Information and Communication Engineers – IECE (*Japan*); Latvian Society of Radioelectronic and Communication Engineers – AERE (*Latvia*); Lithuanian Society of Informatics, Communications and Electronics – LIREB (*Lithuania*); Association of Electronics and Radio Engineers – NERG (*The Netherlands*); Pakistan Institute of Telecom Engineers – PITE (*Pakistan*); A.S. Popov Scientific Technical Society for Radio Technology, Electronics and Electrocommunications – RORES (*Russian Federation*); Chamber of Turkish Electrical Engineers – EMO (*Turkey*); Ukrainian Scientific and Engineering Radio, Electronics and Communication Society – UORES (*Ukraine*); Institute of Electrical and Electronics Engineers, EMC Society – IEEE EMCS (*USA*)

Symposium Council:

Chairman:

Prof. W. Majewski, *Poland*

V-chairmen:

Prof. A. Pilatowicz, *Poland*; Dr M. Rusin, *Poland*

Prof. M. Amanowicz, *Poland*; Prof. G. Balodis (AERE), *Latvia*; V. Bulavas (LIREB), *Lithuania*; Prof. K. Feser (VDE), *Germany*; G. Goldberg (SEV), *Switzerland*; W. Grabowski, *Poland*; S. Grela (PAR), *Poland*; J. Grzybowski (SEP), *Poland*; Prof. S. Hahn (URSI-Nat. Com.), *Poland*; Prof. V. Heinrichsen (EES), *Estonia*; M. Javed (PITE), *Pakistan*; Dr E. Joffe (IEEE-EMCS), *Israel*; R. Jones, *ITU-R*; P.J. Kerry, *IEC-CISPR*; Dr W. Kromolowski, *Poland*; A. Kornatowski (PAR), *Poland*; P. Laven, *EBU*; Prof. P.E. Leuthold (EMC Symp.), *Switzerland*; W. Nietyksza, *IARU-Region 1*; A. Peurala (AEE), *Finland*; Prof. V.V. Pilinsky (UORES), *Ukraine*; Dr A. Radasky, *IEC-ACEC*; Prof. S.M. Radicella, *UNESCO-ICTP*; K.H. Rosenbrock, *ETSI*; P. Rzepka (TP S.A.), *Poland*; Prof. H.R. Schmeer (EMC Congress), *Germany*; Prof. B. Smólski, *Poland*; Dr M. Suchanski, *Poland*; Dr J. Svoboda (EMCAS), *Czech Republic*; Dr B. Szentkuti, *IEC - TC77*; Prof. A. Wierzbicki (IL), *Poland*; B. Wojtynski (POLKOMTEL), *Poland*; Prof. W. Wolinski (PAN), *Poland*; Prof. T. Yoshino (IEICE), *Japan*; H. Zhao *ITU-T*; Prof. M. Zientalski, *Poland*; Dr Yu.B. Zubarev (RORES), *Russian Federation*; Dr E. Zernicki, *Poland*

Scientific Program Committee:

Honorary Chairman:

Prof. F.L. Stumpers, *The Netherlands*

Chairman:

Prof. R.G. Struzak, *Poland*

Prof. J. Bach Andersen, *Denmark*; T. Boe, *Norway*; Prof. J.A. Catrysse, *Belgium*; Prof. P. Degauque, *France*; G. Goldberg, *Switzerland*; Prof. E. Habiger, *Germany*; Prof. M. Hayakawa, *Japan*; G. Hurt, *USA*; Prof. M. Ianoz, *Switzerland*; Prof. A. Karwowski, *Poland*; W. Luther, *USA*; Prof. A. Marvin, *United Kingdom*; Prof. H. Mikolajczyk, *Poland*; Prof. E. Nano, *Italy*; Dr. A. Pavliouk, *Russian Federation*; Dr. A. Schiavoni, *Italy*; Dr. J. Shapira, *Israel*; Prof. G. Varju, *Hungary*; M.C. Vrolijk, *The Netherlands*; Prof. T. Yoshino, *Japan*

Symposium Organization:

Prof. D.J. Bem (*Symposium Chairman*)

J. Rutkowski (*Co-chairman*)

W. Moroń (*Organizing Chairman*)

Dr M.J. Grzybkowski, Dr J.M. Janiszewski, H. Ługowska, Prof. J. Malko, Dr T. Niewodniczański (*Public Relations*), Dr M. Pietranik, Z. Rabiej, Dr W. Sęga (*Program Coordinator*), Prof. T.W. Więckowski, Dr R.J. Zieliński (*Exhibition Coordinator*), Dr R. Żarko

Author's index

A

Aboaba O. 624
Agostinelli M. 825
Aizawa T. 59
Akino T. 566
Allahverdiev A. 397
Alter L. 679
Altman Z. 240
Amemiya F. 346
Aniserowicz K. 144
Aporovitch V. 605
Araz I. 841
Augustyniak L. 159
Aust D. 865
Azaro R. 309, 341
Azoulay M. 79, 441
Azzarone R. 16

B

Baker S. 294
Ball R. 294
Bandinelli M. 807
Batueva E. 626
Baum C. 898
Baumann J. 410
Beletsky A. 637
Bellan D. 260, 265
Bem D. 829
Benamar A. 884
Benedetti A. 807
Bertotto P. 245
Bielli P. 245
Blaunstein N. 479
Blikrud E. 868
Blocher T. 314
Bochkov K. 444, 453
Boscovic D. 884
Bose R. 84
Boudreau D. 703
Brunello F. 250
Budai A. 683

C

Can M. 397
Caorsi S. 309, 341
Cerri G. 168
Cesky T. 721
Chan G. 657

Charalampakis I. 448
Charrere M. 250
Chavka G. 609
Cheparin V. 571
Chernikova L. 587
Chiarandini S. 168
Chiti S. 807
Christodouloupoulos C. 448
Cioni R. 807, 812
Cooray V. 173
Czajkowski J. 687

D

Daguillon O. 280
Darizhapov D. 626
Davydenko S. 483
De Brito G. 872
De Leo R. 168
Despres B. 441
Dhamrait M. 661
Di Laura S. 816
Dikmarova L. 583
Dimitrov D. 791
Dinan U. 502
Disco D. 250
Doebbelin R. 89
Dole C. 208
Donelli M. 309
Dostert K. 98
Drozd A. 314
Dub P. 383
Dufour M. 703
Dymarkowski K. 846

E

Eged B. 64
Egorova N. 319

F

Faizoulaev B. 457
Fei Xikang 137
Feix N. 194
Felic G. 94
Filcev J. 724
Fiori F. 41
Floreani M. 270
Foster K. 413
Fujiwara O. 255

G

Galvan A. 173
 Gambin D. 250
 Garbe H. 289
 Gardner R. 178, 466, 889, 896, 898
 Gattoufi L. 240
 Gavan J. 921
 Gazizov T. 45, 469
 Gelencser I. 64
 Gianola P. 250
 Goldberg G. 31, 103, 410, 418, 427
 Gonschorek K. 216, 336
 Gorisch A. 230
 Gorobets N. 630
 Gouliaev A. 691
 Gragnani G. 309
 Griesse E. 70

H

Habiger E. 304
 Haehner T. 198
 Haga A. 149
 Halme L. 203
 Hamid E. 902
 Hansen D. 107, 361
 Harms H. 284
 Harms R. 850
 Hattori K. 546
 Hayakawa M. 275, 523, 536, 546, 561, 915
 Heidemann M. 289
 Heyder D. 89
 Hiroshima Y. 346

I

Ianoz M. 183, 908
 Ishibashi N. 275
 Itoh T. 546
 Iudin D. 523, 528

J

Jakobus U. 221, 642
 Jecko B. 194, 575
 Jennings P. 294
 Joskiewicz Z. 829

K

Kaluski M. 436
 Kanzaki H. 536
 Karwowski A. 240
 Katulski R. 121
 Katz M. 125

Kawamata K. 149
 Kawasaki Z. 902
 Kazama S. 50
 Kazik J. 854
 Kebel R. 289
 Kharkovsky S. 397
 Kharlap S. 453
 Kho K. 749
 Kikuchi H. 488, 493, 910
 Kincaid J. 208
 Kinsht N. 125
 Kitaytsev A. 571
 Klima J. 728
 Klok H. 794
 Klosok W. 646
 Kogan V. 708
 Kolakowski J. 128
 Kolchigin N. 319
 Koledintseva M. 571
 Kolodziej H. 579
 Korovkin N. 523
 Kosinski A. 121
 Kostenko M. 188
 Kourennyi E. 322, 587
 Kovalev K. 683
 Kowalczyk P. 370
 Kozel V. 683
 Krzysztofik W. 401, 614
 Kuleshova V. 473
 Kurby C. 736
 Kurgan E. 326
 Kurowski T. 591
 Kus A. 770
 Kuwabara N. 346
 Kuznetsova-Tadjibaeva O. 45

L

Lalande-Guionie M. 194
 Larkin V. 551
 Larkina V. 506, 551, 556
 Lascu D. 75
 Lascu M. 75
 Lavell-Smith A. 799
 Laven P. 8
 Lee S. 275
 Leenders H. 420
 Lenivenko V. 596
 Leontiev N. 45
 Lever P. 294
 Lodge J. 703
 Logatchev V. 457
 Loginov N. 708

Loyka S. 132
 Luszcz J. 601
 Luther W. 713
 Lyubimov V. 379

M

Macdonald-Bradley C. 294
 Macher M. 436
 Makita K. 561
 Mamtchenkov P. 691
 Manara G. 820
 Mandzij B. 55
 Mardiana R. 902
 Mareev E. 498
 Mariani Primiani V. 168
 Martinod E. 194
 Masada E. 406, 432
 Maslowski G. 154
 Mazzetti C. 183
 Mecke H. 89
 Medeisis A. 619
 Meidan R. 741
 Michalak M. 366
 Mikhailovsky L. 571
 Mikolajczyk H. 475
 Minegishi S. 149
 Missala T. 299
 Misuri G. 836
 Mizuma T. 406
 Monorchio A. 820
 Moorut P. 884
 Mordachev V. 331, 683
 Mund B. 198

N

Nadeau P. 575
 Nalbandian A. 666
 Nichoga V. 383, 583
 Nickolaenko A. 528, 532
 Nikonov V. 683
 Nitsch J. 225
 Nomicos C. 512
 Nucci C. 183

O

Ohta K. 536, 561
 Ohtsuka M. 517
 Okyere P. 304
 Oraevsky K. 457
 Oraevsky V. 508

P

Paskovich D. 703
 Patenaude F. 703
 Pavelka C. 733
 Pavliouk A. 670, 708
 Pawlowski W. 121, 633
 Pazar S. 841
 Pesta A. 314
 Petropavlovsky Y. 125
 Petrosov V. 322, 587
 Pietranik M. 695
 Pignari S. 260, 265
 Pilinsky V. 591
 Pirjola R. 915
 Pivnenko S. 319, 387
 Podgorski A. 366
 Podgorski E. 366
 Pogrebnyak N. 322
 Preobragenskaya O. 125
 Procacci V. 836
 Pulinets S. 473

R

Rabinowicz L. 532
 Rachidi F. 183
 Radasky W. 3, 893, 896
 Radulescu M. 448
 Raffetto M. 309
 Reineix A. 575
 Repacholi M. 413
 Revermann L. 850
 Richiardi G. 245
 Ristau D. 361
 Rodionova M. 591
 Rozycki S. 436
 Rucinski D. 448
 Russo P. 168
 Ruzhin Y. 506, 508, 512
 Ryazantseva N. 444
 Rybin A. 591

S

Sadowski M. 609
 Sato R. 50, 59, 566
 Schiavoni A. 245
 Schwarz H. 424
 Segal W. 695, 699, 718
 Selivanov M. 691
 Semenikhina D. 637
 Senin B. 556
 Sergeeva N. 556

Shagimuratov I. 508
 Sharpe M. 876
 Shihab S. 94
 Shinohara S. 50, 59, 566
 Shvets A. 541
 Siebert P. 753
 Silin N. 125
 Siwiak K. 744
 Smirnov N. 691
 Sowa A. 159, 370, 579
 Spoelstra T. 758, 775
 Sroka J. 374
 Stecher M. 351
 Steinmetz T. 225
 Stewart F. 804, 859
 Stoudt D. 466, 898
 Struzak R. 21, 890

T

Tarafi R. 280
 Teti F. 812
 Tiedemann R. 336
 Trakhtengerts V. 523
 Trigubovich V. 461
 Trzaska H. 646
 Tyczynski W. 699, 718

U

Ucziwek J. 846
 Ustuner F. 841

V

Vaananen A. 356, 650
 Vallianatos F. 512
 Van Driel W. 779
 Varshney P. 314
 Vasiltssov I. 55
 Vercellotti G. 163
 Verduijn J. 675
 Verholt C. 655
 Vick R. 111
 Villien P. 213
 Vogt A. 579

W

Wang J. 255
 Weiner D. 314
 Wheaton O. 881
 Wiat J. 240
 Wieckowski T. 391, 829
 Wik M. 893, 896
 Wilhelmsen P. 116
 Winkler T. 89
 Winnberg A. 784
 Wolfesperger H. 235
 Wollenberg G. 230
 Wong M. 240
 Wu Yunxi 137

Y

Yamamoto H. 59
 Yang Shiwu 137
 Yazici M. 841
 Yeliseyeva N. 630
 Yoshino T. 502, 517
 Yumoto K. 546

Z

Zagoskin V. 708
 Zajac R. 846
 Zarko R. 695
 Zawadzki P. 280
 Zeddam A. 280
 Zich R. 163, 235, 270
 Zielinski R. 763
 Zivic T. 140
 Zlahtic F. 140
 Zorman M. 140

CONTENTS

PART I

I PLENARY SESSIONS

PLENARY SESSION I

Chairman: PROF. R. STRUZAK, *Co-Chair, URSI WG on SM, Member ITU RRB, Poland*

- W. RADASKY, *Metatech Corporation, Goleta, USA: Electromagnetic Compatibility Strategy for the Future* 3
- P. LAVEN, *European Broadcasting Union, Geneva, Switzerland: The Future of Broadcasting* 8

PLENARY SESSION II

Chairman: PROF. D.J. BEM, *University of Technology, Wroclaw, Poland*

- R. AZZARONE, *General Directorate TELEDIFE, Rome, Italy: Civilian vs Military EMC Standardization - View of NATO Special Working Group 10 on Electromagnetic Environment Effects* 16
- R. STRUZAK, *Co-Chair, URSI WG, ITU RRB, Poland: Noise Interference in Radiocommunication Networks: Shannon's Formula Revisited* 21

PLENARY SESSION III

Chairman: DR W.A. RADASKY, *IEC-ACEC Chairman, Metatech Corporation, Goleta, USA*

- G. GOLDBERG, *Past chairman IEC-ACEC, Zurich, Switzerland: EM Phenomena and Implications for Standardization. EMC - Safety - Human Exposure* 31

II SECTIONAL SESSIONS

EMC ON COMPONENT AND PCB LEVEL - PART I

Chairman: DR E. GRIESE, *Siemens AG IC, Paderborn, Germany*

- F. FIORI, *Technical University, Torino, Italy: ICs Susceptibility: A Critical Assessment of the Test Procedures* 41
- T. GAZIZOV, N.A. LEONTIEV, *State University of Control Systems and Radioelectronics, O.M. KUZNETSOVA-TADJIBAEVA, Research and Design Center "Polus", Tomsk, Russian Federation: Far-End Crosstalk Reduction in Coupled Microstrip Lines with Covering Dielectric Layer* 45
- S. KAZAMA, S. SHINOHARA, R. SATO, *EMC Research Laboratories Co Ltd, Sendai, Japan: Estimation of Current and Voltage Distributions in a Digital IC Package* 50
- I. VASILTSOV, *Academy of National Economy, Ternopil, B.A. MANDZIJ, State University "Lvivska Politechnika", Lviv, Ukraine: New 3D Model of Internal Electromagnetic Noises in VLSI Chip* 55

EMC ON COMPONENT AND PCB LEVEL - PART II

Chairman: PROF. T.R. GAZIZOV, *State University of Control Systems and Radioelectronics, Tomsk, Russian Federation*

- T. AIZAWA, H. YAMAMOTO, S. SHINOHARA, R. SATO, *EMC Research Laboratories Co Ltd, Sendai, Japan: Evaluation of the Radiated and Immunity Characteristics of Optical Transceiver Modules* 59
- B. EGED, I. GELENCSEI, *Technical University, Budapest, Hungary: The Effect of Discontinuities on Ground/Power Planes of High-Speed Printed Circuit Boards* 64
- E. GRIESE, *Siemens AG, Paderborn, Germany: A Hybrid Electrical/Optical Interconnection Technology for Printed Circuit Boards* 70
- M. LASCU, D. LASCU, *Technical University, Timisoara, Romania: Finite Element Method Applied in Modelling Perturbations on Printed Circuit Boards* 75

EMC IN COMMUNICATION AND POWER SYSTEMS

Chairman: DR R. VICK, *EMC Consulting and Management, Dresden, Germany*

- M. AZOULAY, *TDF, Saint Quentin en Yvelines, France: Radio Interference Cases on Broadcasting Sites* 79
- R. BOSE, *Indian Institute of Technology, Delhi, India: Optimally Placing Base Stations in a Microcellular Urban Environment* 84
- R. DOEBBELIN, D. HEYDER, H. MECKE, T. WINKLER, *Otto-von-Guericke University, Magdeburg, Germany: Resistance Welding Machines - a Critical Power Supply Network Load Concerning Power Quality and Electromagnetic Emissions* 89
- S. SHIHAB, G. FELIC, *Royal Melbourne Inst of Technology, Melbourne, Australia: Monitoring of Electromagnetic Interference in High Voltage Substations* 94

POWER-LINE COMMUNICATION - EMC PROBLEMS

Invited session

Organizer/Chairman: DR R. VICK, *EMC Consulting and Management, Dresden, Germany*

- K. DOSTERT, *University of Karlsruhe, Karlsruhe, Germany: EMC Aspects of High Speed Power Line Communications* 98
- G. GOLDBERG, *Past chairman IEC-ACEC, Zurich, Switzerland: Evaluation of Power Line Communication Systems* 103
- D. HANSEN, *EURO EMC SERVICE (EES), Berikon, Switzerland: Megabits per Second on 50 Hz Power Lines?* 107
- R. VICK, *EMC Consulting and Management, Dresden, Germany: Radiated Emission of Domestic Main Wiring Caused by Power-Line Communication Systems* 111
- P. WILHELMSSEN, *Norwegian Post and Telecommunications Authority, Oslo, Norway: A Regulatory Authority's Evaluation of PLC and EMC* 116

EMC IN COMMUNICATION, POWER AND TRANSPORT SYSTEMS

- R. KATULSKI, *Technical University, Gdansk*, A. KOSINSKI, *Naval Academy, Gdynia*, W. PAWLOWSKI, *Technical University, Gdansk, Poland*: **Radiocommunication Aspects of EMC Analysis and Measurements on a Ship**..... 121
- N. KINSHT, M.A. KATZ, N.V. SILIN, O.V. PREOBRAZHENSKAYA, Y.B. PETROPAVLOVSKY, *State Far-Eastern Technical University, Vladivostok, Russian Federation*: **Application of Electromagnetic Radiation of High-Voltage Equipment for Diagnostic of its Technical State** 125
- J. KOLAKOWSKI, *University of Technology, Warsaw, Poland*: **Application of Wavelet Transform for Adjacent Channel Transient Power Measurements** 128
- S. LOYKA, *Belarusian State University of Informatics & Radioelectronics, Minsk, Belarus*: **Numerical Modeling of Nonlinear Interference and Distortions for Wireless Communications** 132
- YANG SHIWU, FEI XIKANG, WU YUNXI, *Northern Jiaotong University, Beijing, China*: **New Approach to Suppress Impulsive Interference on Track Circuit of Electrified Railways** 137
- F. ZLAHTIC, M. ZORMAN, T. ZIVIC, *Elektroinstitut Milan Vidmar, Ljubljana, Slovenia*: **Electromagnetic Compatibility Assurance in Electric Power Substations**..... 140

LIGHTNING AND ESD

Chairman: PROF. R.E. ZICH, *Technical University, Milano, Italy*

- K. ANISEROWICZ, *Technical University, Bialystok, Poland*: **Comparison of the Lumped- and Distributed-Circuit Model of the Lightning Protection System** 144
- K. KAWAMATA, *Hachinohe Institute of Technology, Aomori*, S. MINEGISHI, A. HAGA, *Tohoku Gakuin University, Tohoku, Japan*: **Time Domain Measurement of Very Fast Transition Durations Due to Gap Discharge in Air as a Simulation of the CDM ESD**..... 149
- G. MASLOWSKI, *University of Technology, Rzeszow, Poland*: **Modeling of the Lightning Electric Field for Different Models of the Channel-Base Current with Standard Parameters**..... 154
- A. SOWA, L. AUGUSTYNIAK, *Technical University, Bialystok, Poland*: **Lightning Overvoltages in Structural Cabling Systems** 159
- G. VERCELLOTTI, R.E. ZICH, *Technical University, Milano, Italy*: **LEMP-Like Effects on Railways Systems** 163

LIGHTNING EFFECTS AND COUPLING MODELS

Invited session (sponsored by URSI Commission E)

Organizer/Chairman: PROF. M.V. IANOZ, *Swiss Federal Institute of Technology, Lausanne, Switzerland*

- R. DE LEO, G. CERRI, S. CHIARANDINI, V. MARIANI PRIMIANI, P. RUSSO, *University of Ancona, Ancona, Italy*: **A Hybrid Method for the Analysis of Transients in EMC Problems** 168
- A. GALVAN, V. COORAY, *Uppsala University, Uppsala, Sweden*: **On the Maximum Overvoltages Induced in Low Voltage Power Installation Networks Due to Indirect Lightning Flashes** 173
- R. GARDNER, *Spectral Synthesis Labs, Alexandria, USA*: **Modeling of the Base of a Lightning Return Stroke**..... 178

- M. IANOZ, *Swiss Federal Institute of Technology, Lausanne, Switzerland*, C. MAZZETTI, *University of Rome "La Sapienza", Rome*, C.A. NUCCI, *University of Bologna, Bologna, Italy*, F. RACHIDI, *Swiss Federal Institute of Technology, Lausanne, Switzerland*: **Lightning Indirect Effects Modeling Applied to Protection Design and Evaluation** 183
- M. KOSTENKO, *State Technical University, St Petersburg, Russian Federation*: **Associative Modeling of Incoming and Reflected Waves in Lightning Channel and in Stroked Overhead Line** 188
- E. MARTINOD, N. FEIX, M. LALANDE-GUIONIE, *IRCOM, Brive la Gaillarde*, B. JECKO, *IRCOM, Limoges, France*: **Analysis of Connectors Behaviour in Term of Electromagnetic Compatibility** 194

EMC PERFORMANCE OF SYMMETRICAL AND COAXIAL CABLINGS

Invited session

Organizer/Chairman: DR L. HALME, *University of Technology, Helsinki, Finland*

- T. HAEHNER, *Alcatel Cable France, Paillart, France*, B. MUND, *bedea Berkenhoff & Drebes GmbH, Asslar, Germany*: **Background, Content and Future of the EMC Measurement Standard prEN 50289-1-6 - Open/Shielded Test Methods** 198
- L. HALME, *University of Technology, Hut, Finland*: **Primary and Secondary Electro-Magnetic Screening (Shielding) Parameters** 203
- J. KINCAID, C. DOLE, *Belden Electronics Division, Richmond, USA*: **Shielded Screening Attenuation Test Method Down to 5 MHz** 208
- P. VILLIEN, *3P Third Party Testing, Hoersholm, Denmark*: **Future Development of Standardisation of Coupling Attenuation** 213

EMC MODELLING AND ANALYSIS

Invited session

Organizer: PROF. K. GONSCHOREK, *University of Technology, Dresden, Germany*

Chairman: DR H. HARMS, *Thyssen Nordseewerke GmbH, Emden, Germany*

- K. GONSCHOREK, *University of Technology, Dresden, Germany*: **Introduction to MOM, GTD/UTD and Their Combination** 216
- U. JAKOBUS, *University of Stuttgart, Stuttgart, Germany*: **Latest Developments in the Method of Moments for an Efficient Numerical Solution of Complicated and Large Scale EMC Problems** 221
- T. STEINMETZ, J. NITSCH, *Otto-von-Guericke University, Magdeburg, Germany*: **Analysis of Complex Systems with Cables Using Electromagnetic Topology** 225
- G. WOLLENBERG, A. GORISCH, *Otto-von-Guericke University Magdeburg, Germany*: **Using Hybrid PEEC-MTL Models for the Analysis of Interconnection Structures** 230
- R. ZICH, *Technical University, Milano, Italy*, H.A. WOLFSPERGER, *Karlsruhe University, Karlsruhe, Germany*: **Analysis of the Shielding Performances of Loaded Perforated Shields** 235

COMPUTATIONAL EM TECHNIQUES IN MOBILE WIRELESS COMMUNICATIONS

Invited session

Organizer/Chairman: PROF. A. KARWOWSKI, *Silesian Technical University, Gliwice, Poland*

- Z. ALTMAN, *CNET, Issy les Moulineaux, France*, A. KARWOWSKI, *Silesian Technical University, Gliwice, Poland*, M. WONG, J. WIART, *CNET, Issy les Moulineaux*, L. GATTOUFI, *Bouygues Telecom, Velizy, France*: **Dosimetric Analysis of Base Station Antennas via Simulation and Measurements** 240
- P. BERTOTTO, A. SCHIAVONI, G. RICHIARDI, P. BIELLI, *CSELT, Torino, Italy*: **Directional Antennas for the Reduction of SAR Inside the Human Head** 245
- F. BRUNELLO, M. CHARRERE, D. DISCO, D. GAMBIN, P. GIANOLA, *CSELT, Torino, Italy*: **Electromagnetic Fields in Proximity of GSM Base Stations** 250
- J. WANG, O. FUJIWARA, *Institute of Technology, Nagoya, Japan*: **The Role of Head Tissue Complexity in the Peak SAR Assessment for Mobile Phones** 255

EMC MODELLING - PART I

Chairman: DR E.B. JOFFE, *KTM Project Eng. Ltd, Ramat Hasharon, Israel*

- D. BELLAN, S. PIGNARI, *Technical University, Milano, Italy*: **A Probabilistic Model for Transmission Line Voltages Induced by an External Field** 260
- D. BELLAN, S. PIGNARI, *Technical University, Milano, Italy*: **A Prediction Model for Crosstalk in Large and Densely-Packed Random Wire-Bundles** 265
- M. FLOREANI, R.E. ZICH, *Technical University, Milano, Italy*: **Analysis of the Shielding Effectiveness of a Truncated Chiral Cylinder** 270
- N. ISHIBASHI, S. LEE, M. HAYAKAWA, *University of Electro-Communications, Tokyo, Japan*: **Theory and Experiment on Radiation from a Bent Transmission Line** 275
- P. ZAWADZKI, *Silesian Technical University, Gliwice, Poland*, R. TARAfi, O. DAGUILLON, A. ZEDDAM, *CNET Technopole Anticipa, Lannion Cedex, France*: **An Efficient Method for Calculation of the Radiation from Copper Installations with Wideband Transmission Systems** 280

EMC MODELLING - PART II

Chairman: PROF. D.J. BEM, *University of Technology, Wroclaw, Poland*

- H. HARMS, *Thyssen Nordseewerke GmbH, Emden, Germany*: **EMC Analysis for Frequencies Above 1 GHz in Naval Shipbuilding** 284
- M. HEIDEMANN, H. GARBE, *University of Hannover, Hannover*, R. KEBEL, *Daimler-Chrysler Aerospace AG, Bremen, Germany*: **Calculation of Electromagnetically and Thermally Coupled Fields in Real Soil Decontamination** 289
- C. MACDONALD-BRADLEY, P.A. JENNINGS, R.J. BALL, P.H. LEVER, S. BAKER, *University of Warwick, Coventry, UK*: **A Statistical Approach for Computational Electromagnetics** 294
- T. MISSALA, *Industrial Research Institute for Automation and Measurements, Warsaw, Poland*: **Models for Simulation of Fieldbus Transmission Line EMC Testing** 299

- P. OKYERE, E. HABIGER, *University of Technology, Dresden, Germany*: **Cost-Effective EMC-Conforming Design of Switched-Mode Power Supplies**..... 304

EMC MODELLING - PART III

- R. AZARO, *University of Genoa, Genoa*, S. CAORSI, *University of Pavia, Pavia*, M. DONELLI, G.L. GRAGNANI, M. RAFFETTO, *University of Genoa, Genoa, Italy*: **A Software for the Evaluation of Field Penetration Inside Shielding Box with Apertures**..... 309
- A. DROZD, *ANDRO Consulting Services, Rome, NY*, T.W. BLOCHER, A.J. PESTA, *Air Force Research Laboratory, Rome NY*, D.D. WEINER, P.K. VARSHNEY, *Syracuse University, Syracuse, NY, USA*: **Predicting EMI Rejection Requirements Using Expert System Based Modeling & Simulation Techniques** 314
- N. KOLCHIGIN, N.P. EGOROVA, S.N. PIVNENKO, *State University, Kharkov, Ukraine*: **Modeling the Measurement of the Transient Wave from the Object Located over Earth Surface** 319
- E. KOURENNYI, *State Technical University, Donetsk*, V.A. PETROSOV, *The Priasovsk State Technical University, Mariupol*, N.M. POGREBNYAK, *State Technical University, Donetsk, Ukraine*: **Squaring and Smoothing in EMC Models: A Statistical Solution**..... 322
- E. KURGAN, *University of Mining and Metallurgy, Krakow, Poland*: **Magnetic Analysis of Inhomogeneous Double-Layer Shields at Low Frequencies**..... 326
- V. MORDACHEV, *Belarusian State University of Informatics & Radioelectronics, Minsk, Belarus*: **Radiosignals Dynamic Range in Space-Scattered Mobile Radiocommunication Networks**..... 331
- R. TIEDEMANN, K. GONSCHOREK, *University of Technology, Dresden, Germany*: **Rebuilding the Screen of a Cable by a Double Layer of Parallel Wires**..... 336

EM INTERFERENCE MEASUREMENTS

Chairman: DR D. HANSEN, *EURO EM Service, Berikon 2, Switzerland*

- R. AZARO, *University of Genoa, Genoa*, S. CAORSI, *University of Pavia, Pavia, Italy*: **Determination of the Field Reduction Properties of Shielding Devices by Modulated Scattering Measurements** 341
- N. KUWABARA, Y. HIROSHIMA, F. AMEMIYA, *NTT Corp., Tokyo, Japan*: **An Investigation on Measurement Method of Disturbances at Telecommunication Ports by Using Both Voltage and Current Probe**..... 346
- M. STECHER, *Rohde & Schwarz GmbH & Co KG, Munchen, Germany*: **Weighting of Interference for its Effect on Digital Radiocommunication Services**..... 351
- A. VAANANEN, *Polytechnic University, Vaasa, Finland*: **Screening Effectiveness of CATV Networks - Field Measurements** 356

EMC MEASUREMENT TECHNIQUES

Chairman: DR A.S. PODGORSKI, *ASR Technologies, Ottawa, Canada*

- D. HANSEN, D. RISTAU, *EURO EMC SERVICE (EES), Berikon, Switzerland*: **Antenna Factors of the New EUROTREM Cell for Fully Compliant Emission and Immunity Testing**..... 361

- A. PODGORSKI, E. PODGORSKI, *ASR Technologies, Ottawa, Canada*, M.P. MICHALAK, *National Institute of Telecom, Wroclaw, Poland*: **Semi-Anechoic Chamber BGF Facility for Measurements of Emission and Immunity - Latest Advancements** 366
- A. SOWA, P. KOWALCZYK, *University of Technology, Wroclaw, Poland*: **Test Chamber Characteristics - Important Factor Determining Required RF Power of Amplifier in Radiated Immunity Tests** 370
- J. SROKA, *Schaffner EMV AG, Luterbach, Switzerland*: **On the Proper Use of the Injection Clamps in IEC/EN 61000-4-6 Test** 374

EMC MEASUREMENTS

- V. LYUBIMOV, IZMIRAN, *Troitsk, Russian Federation*: **Instruments for the Natural Magnetic Fields Registration in the City Conditions: The Magnetic Storm Indicators** 379
- V. NICHOGA, P. DUB, *National Academy of Sciences of Ukraine, Lviv, Ukraine*: **Analysis of Noise Parameters of Highly Sensitive Induction Sensors for Measurement of Very Weak Electromagnetic Fields** 383
- S. PIVNENKO, *State University, Kharkov, Ukraine*: **Slotline Sensor for Pulse Measurements** 387
- T. WIECKOWSKI, *University of Technology, Wroclaw, Poland*: **Loop Antenna in the Emission Measurements** 391

BIOLOGICAL EFFECTS OF EM RADIATION - TECHNICAL ASPECTS

- S. KHARKOVSKY, A. ALLAHVERDIEV, M. CAN, *Cukurova University, Balcali, Turkey*: **Calibration of the Microwave Oven for Studies of Microwave Electromagnetic Radiation Effects on Cell Cultures** 397
- W. KRZYSZTOFIK, *University of Technology, Wroclaw, Poland*: **The Near-Field of GSM 900/1800 Handset Terminals with Build-in Antennas** 401
- E. MASADA, *Science University of Tokyo, Noda*, T. MIZUMA, *Traffic Safety and Nuisance Research Institute, Mitaka-city Tokyo, Japan*: **Electromagnetic Environment in Railway Systems** 406

REGULATIONS FOR THE LIMITATION OF HUMAN EXPOSURE TO EM FIELDS - PART I

Invited session

Organizer/Chairman: G. GOLDBERG, *Past Chairman IEC ACEC, Zurich, Switzerland*

- J. BAUMANN, *Swiss Agency for the Environment, Forest and Landscape, Bern*, G. GOLDBERG, *Past chairman IEC-ACEC, Zurich, Switzerland*: **Regulations for the Protection of the General Population in Switzerland** 410
- K. FOSTER, *University of Pennsylvania, Philadelphia, USA*, M. REPACHOLI, *WHO, Geneva, Switzerland*: **Biological Effects of Electromagnetic Fields with Emphasis on Health and Safety** 413
- G. GOLDBERG, *Past chairman IEC-ACEC, Zurich, Switzerland*: **The Different Kinds of EMF Standards** 418

- H. LEENDERS, *Philips Corporate Standardization Dept., Eindhoven, Netherlands*: **European EMF Legislation - Turning the Thread of Trade Barriers into an Opportunity by Means of Standardization** 420
- H. SCHWARZ, *Safety Test Solutions, Enningen, Germany*: **Standardisation and Regulation in Germany** 424

REGULATIONS FOR THE LIMITATION OF HUMAN EXPOSURE TO EM FIELDS - PART II

Invited session

Organizer/Chairman: G. GOLDBERG, *Past Chairman IEC ACEC, Zurich, Switzerland*

- G. GOLDBERG, *Past chairman IEC-ACEC, Zurich, Switzerland*: **Regulations for the Limitation of Human Exposure to EM Fields - An Overview** 427
- E. MASADA, *Science University of Tokyo, Noda, Japan*: **Regulations for the Limitation of Human Exposure to EM Fields in Japan** 432
- S. ROZYCKI, *Institute of Power Engineering, Warsaw*, M. KALUSKI, M. MACHER, *National Institute of Telecom, Wroclaw, Poland*: **Regulations for the Limitation of Human Exposure to EM Fields in Poland** 436

EMC REGULATIONS

Chairman: DR N.V. RYAZANTSEVA, *State University of Transport, Gomel, Belarus*

- M. AZOULAY, *TDF, Saint Quentin en Yvelines*, B. DESPRES, *France Telecom Research and Development, Issy les Moulineaux, France*: **Presentation of CISPR/H Activities** 441
- K. BOCHKOV, N.V. RYAZANTSEVA, *State University of Transport, Gomel, Belarus*: **Determination of Rated EMC Parameters Based on the Probabilistic Approach and Consideration of Actual Conditions** 444
- M. RADULESCU, *INSCC*, D.C. RUCINSCHI, *University "Politehnica", Bucharest, Romania*, C. CHRISTODOULOPOULOS, *INTRACOM S.A., Peania Attika*, I. CHARALAMPAKIS, *INTRACOM S.A., Athens, Greece*: **Technical EMC Specifications for Telecommunications Products** 448

IMMUNITY

- K. BOCHKOV, S.N. KHARLAP, *State University of Transport, Gomel, Belarus*: **Computer Analysis of the Performance of Essential Microelectronic Circuits in Intricate Electromagnetic Environment** 453
- B. FAIZOULAEV, V.V. LOGATCHEV, K.S. ORAEVSKY, *EMC Scientific & Test Center "IMPULS", Moscow, Russian Federation*: **Immunity Investigation of Electronic Equipment Under Simulation of Indirect Electrostatic Discharge** 457
- V. TRIGUBOVICH, *Belarusian State University of Informatics and Radioelectronics, Minsk, Belarus*: **Multi-Signal Method to Receiver's Selectivity Estimation** 461

EM HAZARDS AND TERRORISM

Chairman: R.L. GARDNER, *URSI Com. E Chairman, USA*

- R. GARDNER, *Spectral Synthesis Labs, Alexandria, D.C.* STOUT, *Naval Surface Warfare Center, Dahlgren, USA: Requirements for Mitigation in Intentional Electromagnetic Interference* 466
- T. GAZIZOV, *State University of Control Systems and Radioelectronics, Tomsk, Russian Federation: Design of Electronic Systems Protected from Electromagnetic Terrorism* 469
- V. KULESHOVA, S.A. PULINETS, *IZMIRAN, Troitsk, Russian Federation: The Human Health Dependence on the Geomagnetic Activity* 473
- H. MIKOLAJCZYK, *Prof. emeritus of Occupational Hygiene, Lodz, Poland: ELF EM Radiations and Intrinsic EM Phenomena in Human Organism Need for a Convention* 475

PART II

GRAVITO-ELECTRODYNAMICS, EHD, SELF-ORGANIZATION, AND PRE-EARTHQUAKE EFFECTS IN THE ATMOSPHERE, IONOSPHERE AND MAGNETOSPHERE

Invited session (sponsored by URSI Commission E)

Organizer: PROF. H. KIKUCHI, *Institute for Environmental Electromagnetics, Tokyo, Japan*

Chairman: PROF. S.A. PULINETS, *IZMIRAN, Troitsk, Russian Federation*

- N. BLAUNSTEIN, *Ben-Gurion University of the Negev, Beer Sheva, Israel: Modulation of AGW-Induced Plasma Inhomogeneities in the Disturbed Ionosphere in Period of Earthquake Preparation* 479
- S. DAVYDENKO, *Russian Academy of Science, Nizhny Novgorod, Russian Federation: On the Calculation of the Quasistatic Atmospheric Electric Field and Current* 483
- H. KIKUCHI, *Institute for Environmental Electromagnetics, Tokyo, Japan: Gravito-Electrodynamics of Dust in Electric Cusps and Electric Mirrors with Electric Reconnection and Its Applications to Diffuse Dust Layer in the Troposphere and Pre-Earthquake Atmospheric and Ionospheric Effects* 488
- H. KIKUCHI, *Institute for Environmental Electromagnetics, Tokyo, Japan: A Model of Fireball or Plasmoid Produced by a Supersonic Gas Flow in the Laboratory and by Inter-Cloud and Airplane Discharges in the Atmosphere Based on Concept of Critical Ionization Velocity and Electric Reconnection* 493
- E. MAREEV, *Russian Academy of Science, Nizhny Novgorod, Russian Federation: Dusty Particles Effects on Terrestrial Electromagnetic Environment and their EHD Description* 498

ENERGY TRANSMISSION FROM EARTHQUAKE FOCUS AND EM EMISSION WAVE GENERATED ON THE GROUND SURFACE AND IN THE IONOSPHERE

Invited session (sponsored by URSI Commission E)

Organizer/Chairman: PROF. T. YOSHINO, *University of Technology, Fukui, Japan*

- U. DINAN, *University of Ankara, Ankara, Turkey, T. YOSHINO, Fukui University of Technology, Tokyo, Japan: The Anomaly Unstable Polarization Fading of HF Wave Propagation Appeared at the Earthquake in Turkey of 1999* 502

- V. LARKINA, Y.Y. RUZHIN, *IZMIRAN, Troitsk, Russian Federation: Plasmaspheric Low-Frequency Emission Intensity and Spectrum Variations over Preparation Zones of Quick (Seismogenous) and Slow Geodynamic Processes in the Earth Crust*..... 506
- V. ORAEVSKY, Y.Y. RUZHIN, I.I. SHAGIMURATOV, *IZMIRAN, Troitsk, Russian Federation: Anomalies of Ionospheric TEC Above the Turkey Before Two Strong Earthquake at 1999* 508
- Y. RUZHIN, *IZMIRAN, Troitsk, Russian Federation*, C. NOMICOS, *TEI, Athens*, F. VALLIANATOS, *TEI Chania Branch, Crete, Greece: High Frequency Seismoprecursor Emissions*..... 512
- T. YOSHINO, M. OHTSUKA, *Fukui University of Technology, Tokyo, Japan: The Study of the Energy Correspondence Between Bottom Ionosphere and Earthquake Focus for Seismogenic EM Emission* 517

TERRESTRIAL EM NOISE ENVIRONMENT - PART I

Invited session (sponsored by URSI Commission E)

Organizer/Chairman: PROF. M. HAYAKAWA, *University of Electro-Communications, Tokyo, Japan*

- M. HAYAKAWA, D. IUDIN, N.V. KOROVKIN, *University of Electro-Communications, Tokyo, Japan*, V. TRAKHTENGERTS, *Russian Academy of Science, Nizhny Novgorod, Russian Federation: Cellular Automaton Model of Lightning Discharge Preliminary Stage* 523
- A. NICKOLAENKO, *National Academy of Sciences of Ukraine, Kharkov, Ukraine*, D. IUDIN, *University of Electro-Communications, Tokyo, Japan: Hurst Exponent Derived for Natural ELF Electromagnetic Noise* 528
- A. NICKOLAENKO, L. RABINOWICZ, *National Academy of Sciences of Ukraine, Kharkov, Ukraine: A Compact Solution for Natural ELF Pulse in Time Domain* 532
- K. OHTA, H. KANZAKI, *Chubu University, Kasugai Aichi*, M. HAYAKAWA, *University of Electro-Communications, Tokyo, Japan: Three Dimensional Ray-Tracing for Very Low Latitude Whistlers with Considering the Latitudinal and Longitudinal Gradients of the Ionosphere*..... 536
- A. SHVETS, *National Academy of Sciences of Ukraine, Kharkov, Ukraine: Worldwide Lightning Mapping with ELF Tomography*..... 541

TERRESTRIAL EM NOISE ENVIRONMENT - PART II

Invited session (sponsored by URSI Commission E)

Organizer/Chairman: PROF. M. HAYAKAWA, *University of Electro-Communications, Tokyo, Japan*

- M. HAYAKAWA, T. ITOH, *University of Electro-Communications, Tokyo*, K. HATTORI, *Institute of Physical and Chemical Research, Shizuoka*, K. YUMOTO, *Kyushu University, Fukuoka, Japan: ULF Electromagnetic Precursors for an Earthquake at Biak, Indonesia on February 17, 1996*..... 546
- V. LARKIN, V.I. LARKINA, *IZMIRAN, Troitsk, Russian Federation: Natural Low-Frequency Emissions as a Tool of Research of Processes Occurring in the Plasmasphere* 551
- V. LARKINA, *IZMIRAN, Troitsk*, N.G. SERGEEVA, *Polar Geophysical Institute, Murmansk*, B.V. SENIN, *SoyuzMorGeo, Gelendzhik, Russian Federation: Ionospheric Electromagnetic Effects Above Various Eurasia Arctic Tectonic Areas* 556
- K. OHTA, K. MAKITA, *Chubu University, Kasugai Aichi*, M. HAYAKAWA, *University of Electro-Communications, Tokyo, Japan: On the Association of Anomalies in Subionospheric VLF Propagation at Kasugai with Earthquakes at the Center of Japan*..... 561

EMI REDUCTION TECHNIQUES

Chairman: PROF. B. JECKO, *IRCOM, Limoges Cedex, France*

- T. AKINO, S. SHINOHARA, R. SATO, *EMC Research Laboratories Co Ltd, Sendai, Japan: Estimation of Attenuation Characteristics of Feed-Through Type EMI Filters Using Fe-Si Alloy Flake-Polymer Composite*566
- L. MIKHAILOVSKY, A.A. KITAYTSEV, M.Y. KOLEDINTSEVA, V. CHEPARIN, *Power Engineering Institute, Moscow, Russian Federation: Research and Design of Gyromagnetic Media and Devices on Their Base for EMC and Ecology Problems*571
- P. NADEAU, A. REINEIX, *IRCOM, Limoges Cedex*, B. JECKO, *IRCOM, Limoges, France: Transmission Link Radiation And Common Current Generation by 15 Pin D Connector*575
- A. VOGT, H.A. KOLODZIEJ, *University of Wroclaw*, A.E. SOWA, *University of Technology, Wroclaw, Poland: New Generation of Absorbing Materials*579

EMI SOURCES, COUPLING PATH TO VICTIMS AND REDUCTION TECHNIQUES

- L. DIKMAROVA, V. NICHOGA, *National Academy of Sciences of Ukraine, Lviv, Ukraine: Electromagnetic Radiation of Multipair Balanced Cables with Double Twisted Conductors*583
- E. KOURENNYI, *State Technical University, Donetsk*, V.A. PETROSOV, *The Priasovsk State Technical University, Mariupol*, L.V. CHERNIKOVA, *State Technical University, Donetsk, Ukraine: Linear Filtration of Random Processes in EMC Models: The "Partial Reactions" Method*587
- T. KUROWSKI, *Technical University, Zielona Gora, Poland*, V.V. PILINSKY, M.V. RODIONOVA, A.I. RYBIN, *National Technical University of Ukraine, Kiev, Ukraine: Mains RFI-Filters Design Methodology*591
- V. LENIVENKO, *EM Solutions, Yeerongpilly, Australia: High Frequency Spurious Response of Rectangular Waveguide Components*596
- J. LUSZCZ, *Technical University, Gdansk, Poland: Conducted Electromagnetic Interference Propagation through the Power Transformer*601

ANTENNAS AND PROPAGATION

Chairman: A. MEDEISIS, *State Radiofrequency Service, Vilnius, Lithuania*

- V. APOROVITCH, *Research Institute of Automation Facilities, Minsk, Belarus: Multiple-Knife-Edge Diffraction Loss Estimation by the Logarithmic-Cell- Simulation Method*605
- G. CHAVKA, M. SADOWSKI, *Technical University, Bialystok, Poland: Frequency-Domain and Pulse Radiation of Broadband Matched Antenna Array*609
- W. KRZYSZTOFIK, *University of Technology, Wroclaw, Poland: Reception Conditions of Communication Satellites in Poland*614
- A. MEDEISIS, *State Radiofrequency Service, Vilnius, Lithuania: Fine Tuning of the Okumura-Hata Propagation Prediction Model Using the Minimum Squares Method and Fuzzy Logic Approach*619

ANTENNAS AND PROPAGATION

- O. ABOABA, *Obafemi Awolowo University, Ile-Ife, Nigeria*: **Interference Due to Superrefraction and Ducting in the VHF Band in a Tropical Location in Nigeria** 624
- E. BATUEVA, D.D. DARIZHAPOV, *Siberian Branch of RAS, Ulan-Ude, Russian Federation*: **Fluctuations of VHF/UHF Signal Level in Distant Tropospheric Propagation over the Far-Eastern Region of Russia** 626
- N. GOROBETS, N.P. YELISEYEVA, *State University, Kharkov, Ukraine*: **Reducing Level of Side Radiation of Vibrator and Microstrip Antennas in Definite Direction** 630
- W. PAWLOWSKI, *Technical University, Gdansk, Poland*: **Statistical Studies of VHF and UHF Radio Waves Propagation in the South Baltic Area** 633
- D. SEMENIKHINA, A.A. BELETSKY, *State Radio Engineering University, Taganrog, Russian Federation*: **Excitation of the Infinite Perfect Conducting Nonlinear Loaded Circular Cylinder Coated with the Dielectric** 637

EMC IN AMATEUR RADIO SERVICE

Invited session (sponsored by IARU Region 1 WG EMC)

Organizer: PROF. H. TRZASKA, *University of Technology, Wroclaw, Poland*

Chairman: C.M. VERHOLT, *IARU Region 1 EMC WG, Copenhagen, Denmark*

- U. JAKOBUS, *University of Stuttgart, Stuttgart, Germany*: **Numerical Computation of the Near-Field of Typical Amateur Radio Antennas and Comparison with Approximate Result of Far-Field Formulas Applied in the Near-Field Region** 642
- W. KLOSOK, *Polish Amateur Radio Union, Leszno*, H. TRZASKA, *University of Technology, Wroclaw, Poland*: **EM Radiation Hazard in Residential Areas** 646
- A. VAANANEN, *Polytechnic University, Vaasa, Finland*: **Very High Power Scientific Radio Emissions as EMI Sources to Radio Amateur Service** 650
- C. VERHOLT, *Danish Standards Association, Charlottenlund, Denmark*: **EMC Work in IARU** 655

RADIO SPECTRUM ISSUES IN 2000

Invited session

Organizer/Chairman: R.J. MAYHER, *SMILE Associates, Edgewater, USA*

- G. CHAN, *Industry Canada, Ottawa, Canada*: **The Determination of the Coordination Area Around Earth Stations** 657
- M. DHAMRAIT, *Radiocommunication Agency, London, UK*: **Work of the ITU-R Task Group 1/5: Unwanted Emissions** 661
- A. NALBANDIAN, *ITU BR, Geneva, Switzerland*: **ITU Spectrum Management Process and Results of WRC 2000** 666
- A. PAVLIOUK, *Radio Research and Development Institute - NIIR, Moscow, Russian Federation*: **Spectrum Sharing and Spectrum Fees in 2000** 670
- J. VERDIJN, *Radiocommunications Agency, Nederhorst den Berg, Netherlands*: **The Changing Role of Monitoring in the Spectrum Management Process** 675

SPECTRUM ENGINEERING

- L. ALTER, *LONIIR, St Petersburg, Russian Federation: Probability of Intermodulation Interference of Land Mobile Cellular Radio Systems*..... 679
- A. BUDAI, *Belarus Ministry of Post and Telecommunications, K. KOVALEV, V. KOZEL, V.I. MORDACHEV, Belarusian State University of Informatics & Radioelectronics, V. NIKONOV, Belarus State Supervisory Dept for Telecommunications, Minsk, Belarus: Generalized EMC Analysis of Air Navigation and GSM Networks in Belarus*..... 683
- J. CZAJKOWSKI, *Merchant Marine Academy, Gdynia, Poland: The Problem of Generating False Alert Signals with Help of Digital Selective Calling - DSC in the GMDSS System*..... 687
- A. GOULIAEV, P.N. MAMTCHENKOV, M. SELIVANOV, N. SMIRNOV, *NIIR, Moscow, Russian Federation: Problems of UMTS Networks EMC with Radio Relay Systems of the Fixed Service in Russia*..... 691
- M. PIETRANIK, W. SEGA, *National Institute of Telecom, R. ZARKO, University of Technology, Wroclaw, Poland: Compatibility Between Mobile Services and TV Broadcasting in VHF Band. Practical Experiences*..... 695
- W. SEGA, W. TYCZYNSKI, *National Institute of Telecom, Wroclaw, Poland: Assessment of the International Coordination Necessity of Microwave Radio Relay Links*..... 699

SPECTRUM MANAGEMENT AND MONITORING

Chairman: W.A. LUTHER, *Federal Communications Commission, Washington, USA*

- D. BOUDREAU, M. DUFOUR, J. LODGE, *Communications Research Centre, D.H. PASKOVICH, Directorate of Automated Spectrum Monitoring, F. PATENAUD, Communications Research Centre, Ottawa, Canada: Monitoring of the Radio-Frequency Spectrum with a Digital Analysis System*..... 703
- V. KOGAN, *NIIRDAR, N. LOGINOV, GOSSVIAZNADZOR of the RF, A.P. PAVLIOUK, Radio Research and Development Institute - NIIR, V. ZAGOSKIN, GOSSVIAZNADZOR of the RF, Moscow, Russian Federation: Accuracy Analysis of the HF Transmitter Location Procedure by the Single Station Location (SSL) Method*..... 708
- W. LUTHER, *Federal Communications Commission, Washington, USA: Interferometric System Direction Finding Improvements on Circularly-Disposed Wide-Aperture Direction Finding System Accuracy*..... 713
- W. SEGA, W. TYCZYNSKI, *National Institute of Telecom, Wroclaw, Poland: Compatibility Criteria of Microwave Links Used in International Coordination*..... 718

COMPUTER SUPPORT OF INTERNATIONAL FREQUENCY MANAGEMENT ACTIVITIES

Invited session

Organizer/Chairman: T. CESKY, *SES Astra, Luxemburg, Luxemburg*

- T. CESKY, *SES Astra, Chateau de Betzdorf, Luxemburg: Support of Introduction of Digital Broadcasting in Europe*..... 721
- J. FILCEV, *CRC Data, Prague, Czech Republic: Implementation of Component-based Frequency Spectrum Management Software*..... 724

- J. KLIMA, *University of Mathias Bel & PTT Research Institute, Banska Bystrica, Slovak Republic: Vienna Agreement '99 - Harmonized Calculation Method Activities* 728
- C. PAVELKA, *TESTCOM, Praha, Czech Republic: Exchange of Data for Frequency Spectrum Management* 733

EMC MATTERS AND SATELLITE-BASED SYSTEMS - PART I

Invited session

Organizer/Chairman: DR R. MEIDAN, *MOTOROLA, Tel-Aviv, Israel*

- C. KURBY, *Motorola Inc, Libertyville, USA: Emissions Control Techniques for MSS Handset Transmitters* 736
- R. MEIDAN, *Motorola, Tel-Aviv, Israel: Out-of-Band Emission Limits for Mobile Satellite Earth Terminals* 741
- K. SIWIAK, *Motorola Inc, Boynton Beach, USA: Polarization Cross-Coupling in LEO and MEO Satellite Links* 744

EMC MATTERS AND SATELLITE-BASED SYSTEMS - PART II

Invited session

Organizer/Chairman: DR R. MEIDAN, *Motorola, Tel-Aviv, Israel*

- K. KHO, *NATO HQ C3 Staff, Brussels, Belgium: Sharing Properties of Mobile Satellite Service (MSS) Below 1 GHz and NATO Military Terrestrial Communications Systems* 749
- P. SIEBERT, *Societe Europeenne des Satellites, Chateau de Betzdorf, Luxemburg: Standardization of Ka-band Satellite Terminals* 753
- T. SPOELSTRA, *ESF Committee on Radio Astronomy Frequencies, Dwingeloo, Netherlands: Oh Satellite, Oh Satellite!* 758
- R. ZIELINSKI, *University of Technology, Wroclaw, Poland: Risk of Interference to Aircraft from VSAT, SNG and SIT Terminals* 763

SCIENTIFIC USE OF RADIO - REGULATIONS AND FACTS

Invited session (sponsored by ESF-CRAF)

Organizer/Chairman: DR T.A. SPOELSTRA, *Committee on Radio Astronomy Frequencies, Dwingeloo, Netherlands*

- A. KUS, *Nicholas Copernicus University, Torun, Poland: Radio Astronomy in Poland* 770
- T. SPOELSTRA, *ESF Committee on Radio Astronomy Frequencies, Dwingeloo, Netherlands: Regulations and Scientific Use of Radio Frequencies* 775
- W. VAN DRIEL, *Unite Scientifique Nancay, Observatoire de Paris, Section de Meudon, Meudon, France: The Need for Radio Astronomical Line Observations: From Hydrogen to Alcohol* 779
- A. WINNBERG, *Space Observatory, Onsala, Sweden: Scientific Use of Radio - Challenges from Space* 784

NATO/1: MILITARY VS CIVIL EMC STANDARDS - COMPARISONS AND PROBLEMS

Chairman: CAPT. R. AZZARONE, *General Directorate TELEDIFE, Rome, Italy*

- D. DIMITROV, *Head Quarter Bulgarian Navy, Varna, Bulgaria: Provision of EMC in Bulgarian Navy and Harmonization of Naval and Civil E3 Standards* 791
- H. KLOK, *Royal Netherlands Navy, Oestgeest, Netherlands: Risk Analysis by the Use of Commercial Equipment in a Military Environment* 794
- A. LAVELL-SMITH, *Defence Evaluation and Research Agency, Portsmouth West, UK: Harmonization of EMC Standards for the Naval Environment - a United Kingdom Approach* 799
- F. STEWART, *U.S. Space and Naval Warfare Systems Command, San Diego, California, USA: Harmonization of E3 Standards* 804

NATO/2: STANDARD PROCEDURES FOR SIMULATION, PREDICTION AND MODELLING

Chairman: A. LAVELL-SMITH, *Defence Evaluation and Research Agency, Portsmouth West, UK*

- M. BANDINELLI, A. BENEDETTI, S. CHITI, R. CIONI, *IDS Company, Pisa, Italy: Numerical Prediction of Ship Antenna Performance in the Radar Band* 807
- R. CIONI, F. TETI, *IDS Company, Pisa, Italy: Prediction of E.M. Field Levels Inside Closed Structures by a Statistical Approach* 812
- S. DI LAURA, *Defence Evaluation and Research Agency, Portsmouth West, UK: Modelling of Microwave Electromagnetic Interference in a Complex Coupling Environment* 816
- G. MANARA, A. MONORCHIO, *University of Pisa, Pisa, Italy: Validation of a Time Domain MoM Simulator for EMC Standards Guidelines* 820

NATO/3: APPLICATIONS OF EXISTING STANDARDS IN EMC TESTING AND MEASUREMENTS

Chairman: DR M. KUKULKA, *Polish Navy HQ, Gdynia, Poland*

- M. AGOSTINELLI, *CISAM Center, Pisa, Italy: Applications of Civilian and Military Standards to Carry out Transient Electromagnetic Field Measurement at CISAM EMP Facilities* 825
- D. BEM, Z.M. JOSKIEWICZ, T.W. WIECKOWSKI, *University of Technology, Wroclaw, Poland: Alternative Methods for Radiated Emission Measurements* 829
- G. MISURI, V. PROCACCI, *Maritelradar Institute, Livorno, Italy: Applications of NATO Standards for Evaluating Bulkhead Shielding in the Operational Rooms on Board of Ships* 836
- F. USTUNER, I. ARAZ, M. YAZICI, *TUBITAK National Research Institute of Electronics and Cryptology, Kocaeli, S. PAZAR, TUBITAK National Research Institute of Electronic and Cryptology, Gebze, Turkey: Testing the EMP Effect on an Ordnance System* 841

NATO/4: ASPECTS, METHODS AND AWARENESS IN EMC STANDARDS IMPLEMENTATION

Chairman: F.M. STEWART, *U.S. Space and Naval Warfare Systems Command, San Diego, USA*

- K. DYMARKOWSKI, J.M. UCZCIWEK, R.P. ZAJAC, *R&D Marine Technology Centre, Gdynia, Poland*: **Implementation of Standardised EMC Criteria During the Warship Design Process in Poland** 846
- R. HARMS, *Daimler-Benz Aerospace AG, Bremen*, L. REVERMANN, *WTD 71 Dept. Communication-Navigation EMC, Eckernförde, Germany*: **Costs and Time Effective EMC Testing of Equipment Used in Safety Critical Environments** 850
- J. KAZIK, *Defence Evaluation Research Agency, Portsmouth West, UK*: **EMC Assessment Using the Transmission Line Matrix Method (TLM)** 854
- F. STEWART, *U.S. Space and Naval Warfare Systems Command, San Diego, California, USA*: **Electromagnetic Environmental Effects (E3) Awareness in the US Navy** 859

III

WORKSHOPS

EUROPEAN TELECOMMUNICATIONS STANDARDS INSTITUTE ACTIVITIES IN EMC AND RADIO SPECTRUM MATTERS

Chairman: O.J. WHEATON, *Radiocommunications Agency, London, UK*

- D. AUST, *NOKIA GmbH, Bochum, Germany*: **Automotive EMC Directive and the Use of Radio Products in Vehicles** 865
- E. BLIKSRUD, *Norwegian Post and Telecommunications Authority, Oslo, Norway*: **Maritime EMC and the International Community** 868
- G. DE BRITO, *CNET, ISSY-LES-MOULINEAUX, France*: **The Interface Between ETSI and the Spectrum Managers in the European Radiocommunications Committee (ERC) of the European Conference of Postal and Telecommunications Administration (CEPT)** 872
- M. SHARPE, *ETSI, Sophia Antipolis, France*: **Overview of ETSI Activities** 876
- O. WHEATON, *Radiocommunication Agency, DTI, London, UK*: **European Legislation Initiatives: the R&TTE Directive and SLIM Initiative** 881

THE SPECTRUM ENGINEERING ADVANCED MONTE CARLO TOOL (SEAMCAT)

Chairman: A. BENAMAR, *Centre de Recherche de Motorola, Paris, France*

- A. BENAMAR, P. MOORUT, D. BOSCOVIC, *Motorola Labs, Gif-sur-Yvette Cedex, France*: **The Spectrum Engineering Advanced Monte Carlo Analysis Tool (SEAMCAT)** 884

IV OPEN MEETING OF URSI COMMISSION E "EM NOISE AND INTERFERENCE"

Organizer/Chairman: R.L. GARDNER, *Comm. E Chairman, USA*

- R. GARDNER, *Spectral Synthesis Labs, Alexandria, USA: Commission E Open Meeting*..... 889
- R. STRUZAK, *Co-Chair, URSI WG, ITU RRB, Poland: URSI WG E1: Spectrum Management/Utilization and Wireless Telecommunications (WG E1 Report)*..... 890
- W. RADASKY, *Metatech Corporation, Goleta, USA, M.W. Wik, Defence Materiel Administration, Stockholm, Sweden: The Standardisation of High Power Electromagnetic Transient Phenomena in the IEC (WG E2 Report)*..... 893
- M. Wik, *Defence Materiel Administration, Stockholm, Sweden, W.A. RADASKY, Metatech Corporation, Goleta, R.L. GARDNER, Spectral Synthesis Labs, Alexandria, USA: Intentional Electromagnetic Interference - What is the Threat and What Can We Do about it? (WG E2 Report)* 896
- R. GARDNER, *Spectral Synthesis Labs, Alexandria, D.C. STOUDT, Naval Surface Warfare Center, Dahlgren, C.E. BAUM, Air Force Research Laboratory, Albuquerque, USA: Testing Strategies for Susceptibility Testing in High Power Electromagnetics (WG E3 Report)* 898
- E. HAMID, Z. KAWASAKI, R. MARDIANA, *Osaka University, Osaka, Japan: Impact of the 1997-98 El Nino Event on Lightning Activity over Indonesia (WG E4 Report)* 902
- M. IANOZ, *Swiss Federal Institute of Technology, Lausanne, Switzerland: EMC Problems Connected to the Use of the Low Voltage Power Network for Information Transmission (WG E5 Report)* 908
- H. KIKUCHI, *Institute for Environmental Electromagnetics, Tokyo, Japan: Gravito-Electrodynamics of Dust and its Applications to Pre-Earthquake Effects and Tornadoes (WG E7 Report)* 910
- M. HAYAKAWA, *University of Electro-Communications, Tokyo, Japan, R. PIRJOLA, Finnish Meteorological Institute, Helsinki, Finland: Geoelectromagnetic Disturbances and Their Effects on Technological Systems (WG E8 Report)* 915
- J. GAVAN, *Academic Institute of Technology, Holon, Israel: Radio Noise and Interference above 30 MHz (WG E9 Report)* 921



EMC 2000

Patron's Address

It is my great pleasure to greet the participants of the 15th Wroclaw Symposium on Electromagnetic Compatibility which takes place on the verge of the new millennium.

The coming age will be, do we want it or not, the age of Information Society for which the converging telecommunication, computing, and media are the cornerstones. Their proper and fast development is a prerequisite for the society's progress and welfare.

This development depends on favourable regulatory environment but to a great extent also on your ability to solve the growing EMC problems stemming from the convergence process, and from the ever-growing demand for new services and systems.

I sincerely appreciate your efforts to make all the elements compatible, and I wish you success in finding the most effective solutions.

Tomasz Szyszko
Minister of Posts and Telecommunications
of the Republic of Poland



EMC 2000

CHAIRMAN'S MESSAGE

Ladies and Gentlemen, dear Guest and Friends,

I have the honour to welcome you cordially to the 15th International Wroclaw Symposium and Exhibition on Electromagnetic Compatibility being held in the Jubilee Year 2000. As our electromagnetic environment keeps growing and becomes more complex, EMC is becoming more and more essential for the whole society. The future of our technical civilization depends on the ability of solving growing EMC problems.

The well reputed position of the Wroclaw EMC Symposium is to a great extent the merit of numerous individuals around the world, and of many international organizations and associations of electrical and electronic engineers from many countries. They are quoted in these Proceedings, and we extend our gratitude to all of them. We owe our reputation also to the Scientific Program Committee with Professor Frans Louis Stumpers, Member of the Royal Netherlands Academy of Arts and Sciences, and Doctor Honoris Causa of the Wroclaw University of Technology, who chaired it successfully for many years and now is the Honorary Chairman, and to Professor Ryszard Strużak – its present Chairman. Professor Strużak was the Chairman of the Wroclaw EMC Symposium in the years 1980 - 1984. I would like also to bring out the role of the Symposium Council with its Chairman Professor Władysław Majewski. The international flavour of the Symposium has been gained with the support offered by the International Union of Radio Science URSI. The auspices granted by the Committee of Electronics and Telecommunications of the Polish Academy of Sciences add to the scientific atmosphere of the event.

The Symposium would not be possible without the authors of the papers presented here who always play the most important role in such events, and I should specially mention the eminent specialists who have organized and chair

the invited sessions. Thank them all very much indeed for their contribution to the success of the Symposium.

The Symposium owes very much to the eminent patronage of Mr. Tomasz Szyszko, the Minister of Posts and Telecommunications of the Republic of Poland, and his kind personal support. From the very beginning the Symposium has enjoyed the patronage of the consecutive Ministers of Posts and Telecommunications, and this tradition is most valuable for us.

We are very grateful to our sponsors who are quoted in these Proceedings. Their financial support helped greatly to organize the Symposium.

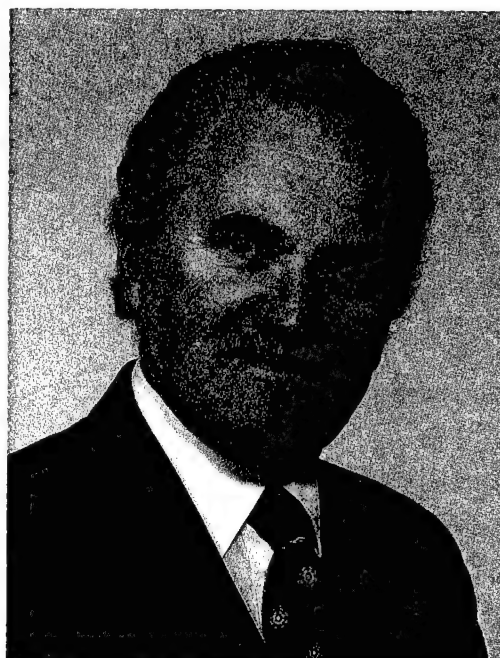
The objective of the Symposium is to bring together engineers and scientists who are interested in a better understanding of electromagnetic phenomena, and their influences on technical and biological systems. Our purpose in doing so is to become better mutually informed about our current work, to appraise the status of the field, to stimulate the future work, and, of course, to become better acquainted with each other.

It is up to you to decide to what extent this event and the information presented, will contribute to those aims.

Most of the preparation work we owe, traditionally, to Mr. Władysław Moroń, the Organizing Chairman, and to all the members of the Organizing Committee. Their endless efforts to make the Symposium a scientific and organizational successes, are appreciated.

I hope that the 15th Wrocław EMC Symposium will mark a new important step in promoting the development of EMC technology. I wish all the participants fruitful discussions and pleasant stay in beautiful Wrocław.

Prof. Daniel Józef Bem
Symposium Chairman



Welcome to EMC Wroclaw 2000

Almost thirty years ago, a few enthusiasts from the Wroclaw University of Technology and from the National Institute of Telecommunications (Wroclaw Branch) decided to organize a conference on electromagnetic compatibility (EMC), and the Wroclaw Symposium on EMC was born in 1972.

At that time, the concept of electromagnetic compatibility was already established in the United States, and EMC conferences were regularly being held there, but in Europe, divided by the cold-war iron curtain, there was no such event organized on a regular basis. Starting, we did not know whether we would have any support but the idea found wide appreciation, creating an international fraternity interested in the development of art and science of EMC.

At the beginning, the majority of participants came from Central and Eastern Europe, and the symposium proceedings were a chronicle of major achievements in EMC field in that region, but that pattern has changed with time. Every two years, Wroclaw has been gathering a number of individuals from around the world involved in research of electromagnetic interactions among natural and man-made systems. Thus, the Wroclaw Symposium proved to be the oldest regular European Conference in its field, with the Proceedings totalling more than 10'000 pages published until now.

During these years, we always tried to bring together individuals interested in various aspects of EMC, theory and practical applications, to enable their interaction, in the belief that new bright ideas often sparkle on the borders of different fields of activity.

As a result, Wroclaw became a meeting place of people involved in research of earth natural electromagnetic (EM) phenomena: people working in spectrum

engineering, management and monitoring; radioastronomers fighting for a clear spectrum for their observations people involved in the EMC measurements; people working in radio wave propagation and antenna theory; people involved in technical side of research of biological hazards of EM radiation; and people interested in counteracting the EM terrorism. Looking at the continuing interest evidenced by a wide participation, we believe that this approach has been welcomed by all.

The International Wroclaw Symposium on Electromagnetic Compatibility is a cooperative not-for-profit project that would not be possible without the support of numerous individuals and organizations. Having the privilege to be among the symposium founders, we would like to take this opportunity to express our deep gratitude to all of them.

Three persons deserve special tribute here. The late Professor Wilhelm Rotkiewicz created in fifties the Wroclaw Branch of the National Institute of Telecommunications that become later the national centre of EMC research and organisational base for the symposium. The late Professor Jan Holownia, first chairman of this symposium, was the main initiator of the symposium concept. Professor Frans Louis Stumpers played, as a Program Chairman, a crucial role in coordination with EMC initiatives in Western Europe and with the International Union of Radio Science (URSI), where he served as President and then Honorary President.

The years that have passed since the origination of the symposium witnessed many changes. About fifteen generations of electronic technologies appeared, according to the Moore's Law. Thirty generations of engineers/scientists left universities to start professional careers. The iron curtain has disappeared and European Union was born. The old millennium comes to the end, and the new millennium opens a new era marked by concepts of Global Information Society. All that reminds us that it is a time of change, and a time for change.

W. Moroń
Organizing Chairman

Prof. R. Strużak
Program Chairman

MODULATION OF AGW-INDUCED PLASMA INHOMOGENEITIES IN THE DISTURBED IONOSPHERE IN PERIOD OF EARTHQUAKE PREPARATION

N. Blaunstein

Department of Electrical and Computer Engineering, Ben-Gurion
University of the Negev, P.O.B. 653, Beer Sheva 84105, Israel
fax: 972-7-6472-949, e-mail: blaun@ee.bgu.ac.il

Abstract

Modulation of ionospheric plasma density by acoustic-gravity waves (AGW) is investigated. A rigorous electrodynamic model of the interaction of acoustic waves, generated by the lithospheric displacements during the seismic event preparation, with the cold dense ionospheric plasma in the presence of a magnetic field is constructed in conjunction with the actual height variations of the plasma particles' mobility and conductivity tensors in the ionosphere. A mechanism of creation of ionospheric inhomogeneities with different scales and with various degree of disturbance $\Delta N/N_0 = 10^{-4} - 10^{-5}$ (N_0 is the concentration of plasma electrons (ions) in background ionospheric plasma) is presented.

1. Mechanism of modulation of plasma density by AGW

During its movement through the ionospheric cold dense plasma, an acoustic-gravity wave (AGW) of frequency ω and wavenumber \mathbf{k} cause the neutral particle density N_m and the rate of ionization per unit volume $q(\mathbf{r})$ to vary as follows [1]:

$$\begin{aligned} N_m &= N_{m0} + \delta N_m \cdot \exp[i(\mathbf{k}\mathbf{r} - \omega t)] \\ q(\mathbf{r}) &= q_0 + \delta q \cdot \exp[i(\mathbf{k}\mathbf{r} - \omega t)] \end{aligned} \quad (1)$$

Here δN_m and δq are the disturbances of the neutral particle density and of the rate of ionization per unit volume due to AGW, respectively, \mathbf{r} is the position vector, and t is time. We estimate the changes in plasma concentration caused by the AGW.

1.1. Electrostatic case

In the D-layer and lower E-layer, the problem is electrostatic. At these altitudes, the ionization rate is as in

equation (1), but the recombination rate is of the form $\alpha_{eff} N_e^2$, where α_{eff} is the effective recombination coefficient, on the order of $(0.2 - 1.0) \cdot 10^{-6} \text{ cm}^3 \text{ s}^{-1}$. At these altitudes (50-100 km) ions move with the speed of neutral particles and both of them are less than the speed of AGW, i.e.,

$$V_m \approx V_i = 50 - 100 \text{ m/s} \ll V_{AW} \quad (2)$$

where V_{AW} is the speed of sound. In other words, the charged particle motion has no influence on the change of plasma concentration. In fact, for $V_m \approx 50 \text{ km}$ and $N_{0e} = N_{0i} = N_0 = 10^{10} \text{ m}^{-3}$, as well as for characteristic scale of quasiregular plasma inhomogeneities $\Lambda \approx 200 \text{ km}$, we obtain that the characteristic time of change of plasma density due to recombination

$$\tau_R = (\alpha_{eff} N)^{-1} \approx 100 - 500 \text{ s}; \quad (3)$$

and the characteristic time of charged particle transport

$$\tau_T = \Lambda / V_m \approx 4000 \text{ s}. \quad (4)$$

With $\tau_T \gg \tau_R$, we can ignore the movements of charged particles in the equation of conservation of particles

$$\frac{\partial N}{\partial t} = q - \alpha_{eff} N^2 - \text{div}(N \mathbf{V}_{e,i}) \quad (5)$$

and exclude the term $\text{div}(N \mathbf{V}_{e,i})$, i.e.,

$$\frac{\partial N}{\partial t} = q - \alpha_{eff} N^2 \quad (5a)$$

Here, as above, α_{eff} is the recombination coefficient, $N_e = N_i = N$ (plasma is quasi-neutral), $N = \delta N + N_0$, and $\delta N \ll N_0$, N_0 is the concentration of background ionospheric plasma. Introducing (1) in (5a) and linearizing, we find that the amplitude of plasma inhomogeneities due to AGW can be estimated as:

$$\delta N_{e,i} \approx \delta q \frac{2\alpha_{eff} N_{0e,i}}{\omega^2 + (2\alpha_{eff} N_{0e,i})^2} \quad (6)$$

Here $\delta q = q_0 \delta N_m / N_{0m} = q_0 \delta_{AW}$, δ_{AW} is the relative amplitude of AGW, and $q_0 = \alpha_{eff} N_{0e}^2 (N_{0e} + N_{0i})$. Using this notation, we finally have:

$$\delta N_{e,i} \approx \delta_{AW} \frac{2\alpha_{eff} N_{0e,i}^3}{\omega^2 + (2\alpha_{eff} N_{0e,i})^2} \quad (7)$$

For lower frequencies, $\omega \ll 2\alpha_{eff} N_{0e,i}$

$$\delta N / N \approx \delta_{AW} \quad (8)$$

Hence, for lower frequencies, the plasma disturbances are proportional to their source, i.e., to the amplitude of the AGW. For higher frequencies, $\omega \gg 2\alpha_{eff} N_{0e,i}$:

$$\delta N / N \approx \delta_{AW} F(\omega) \quad (9)$$

where $F(\omega) = (\alpha_{eff} N_0 / \omega)^2$. Because in the D-layer and lower E-layer $\alpha_{eff} N_0 = 0.002 - 0.01 \text{ s}^{-1}$, we have

$$F(\omega) \ll 1 \quad (10)$$

and $\delta N / N \ll \delta_{AW}$. Hence, for the AGW of high frequencies, plasma disturbances are weak, i.e., much less than the amplitude of the AGW.

1.2. Electrodynamic case

At altitudes of upper E-layer and F-layer ($h > 130$ -140 km) magnetic field is significant, and the problem of interaction between the AGW and the plasma is electrodynamic. For these altitudes, the amplitude of the moving plasma disturbances (MPD) depends on the orientation of the wave vector \mathbf{k} of the AGW relative the geomagnetic field \mathbf{B}_0 and relative to the plasma drift velocity \mathbf{V}_d . The amplitude of MPD is maximal when the condition of spatial resonance is "working" [2]:

$$\omega = \mathbf{k} \cdot \mathbf{V}_d \quad (11)$$

Here, because $v_{im} \sim N_m(T_m + T_i)$, the modulation of neutral particles (N_m and T_m) by the AGW according to (1) produces the same modulation of charged particles, i.e., the corresponding change of v_{im} and hence the corresponding change in the ion velocity \mathbf{V}_i . This modulation of \mathbf{V}_i causes the redistribution of plasma density N and the creation of MPD due to transport processes during interaction of charged particles with neutrals.

2. 3D-problem of MPD evolution

Let us consider that the plasma is isothermal, i.e., $T_e = T_i = T$, which is the case of ionosphere up to about 250 km, and choose a coordinate system $\{x, y, z\}$ in which the magnetic field \mathbf{B}_0 is elongated along z -axis. The particle movement is considered in a coordinate system $\{x, y, z\}$ which is at the rest with respect to average neutral flow.

The background plasma is quasi-regular and homogeneous. In this case the frequencies of interaction can be presented as periodic functions due to modulation cause by the AGW [3]:

$$v_{im} = v_{im}^0 + \delta v_{im} = v_{im}^0 \left\{ 1 + (\delta_A + \delta_T / 2) \exp[i(\mathbf{k}\mathbf{r} - \omega t)] \right\} \quad (12)$$

$$v_{ei} = v_{ei}^0 + \delta v_{ei} = v_{ei}^0 \left\{ 1 + (\delta_A + 3\delta_T / 2) \exp[i(\mathbf{k}\mathbf{r} - \omega t)] \right\}$$

where $\delta_A = \delta N_m / N_m = V_m / V_{ph}$ is the relative amplitude of the AGW, $V_{ph} = \omega / |\mathbf{k}|$ is the phase velocity of the AGW, $\delta_T = \delta N_m / N_m$ is the relative amplitude of the modulation of the temperature by the AGW. Because of the difference between \mathbf{V}_e and \mathbf{V}_i in the ambient magnetic (\mathbf{B}_0) and electric (\mathbf{E}_0) fields for electrons (e) and ions (i), the internal (ambipolar) field is created in plasma, i.e., $\delta \mathbf{E} = \mathbf{E} - \mathbf{E}_0 = \nabla \Phi$ (Φ is the potential of the ambipolar field), and also the changes of the tensors of charged particle mobilities:

$$\hat{\mathbf{M}}^a = \hat{\mathbf{M}}_0^a + \delta \hat{\mathbf{M}}^a, \quad a = e, i$$

$$(13)$$

where

$$\delta \hat{\mathbf{M}}^a = \frac{\delta v_a}{v_{a0}} \begin{pmatrix} M_p^a & 0 & 0 \\ 0 & M_p^a & 0 \\ 0 & 0 & -M_{||}^a \end{pmatrix} \quad (14)$$

Here, p denotes the Pedersen component of electrons ($a=e$) and ions ($a=i$) mobility (in direction of the electric field), and $||$ denotes the

mobility of charged particles along the magnetic field;

$$\mathbf{v}_e = \mathbf{v}_{em} + \mathbf{v}_{ei}, \quad \mathbf{v}_i = \mathbf{v}_{im} + \mathbf{v}_{ei}.$$

Finally, in the electrodynamic case we can present the disturbances of charged particle velocities as [4]:

$$\delta \mathbf{V}^a = q(\hat{\mathbf{M}}_0^a \delta \mathbf{E} + \delta \hat{\mathbf{M}}^a \mathbf{E}_0) + \frac{B_0}{Q_a} \hat{\mathbf{M}}_0^a \delta \mathbf{V}_m - \frac{D_a B_0}{Q_a} \hat{\mathbf{M}}_0^a \frac{\nabla \delta N}{N_0} \quad (15)$$

Here D_a is the coefficient of ambipolar diffusion of charged particles obtained in [5] for the case of quasi-homogeneous ionospheric plasma, $Q_a = \omega_{Hu} / v_a$, ω_{Hu} is the gyrofrequency of plasma particles in magnetic field. Because, as was shown by numerous experiments, disturbances of the plasma particles due to their modulation of AGW are weak, i.e., $\delta N / N_0 \ll 1$, we can in equation (5) exclude the ambipolar field. Linearizing equation (5) and taking into account equation (15), where the ambient electric field perturbation $\delta \mathbf{E}$ is also considered as weak, i.e., $\delta \mathbf{E} \ll \mathbf{E}_0$, an equation (5) can be solved and for longitudinal AGW, gives the relative amplitude of MPD:

$$\delta N = N_0 (\omega - \mathbf{k} \cdot \mathbf{V}_d) \times \frac{\delta_A k V_{ph} \cos^2 \chi + (\delta_A + \delta_T / 2) \left(\frac{\mathbf{k} \cdot \mathbf{E}}{Q_i B_0} \right)}{(\omega - \mathbf{k} \cdot \mathbf{V}_d)^2 + (D_a k_{\parallel}^2)}$$

(16)

where \mathbf{V}_d is the drift velocity of charged particles, $\mathbf{E} = \mathbf{E}_0 + \delta \mathbf{E}$, and χ is the angle between \mathbf{k} and \mathbf{B}_0 .

From (16) it follows that if

$$Q_i \frac{V_{ph}}{V_d} \cos^2 \chi \ll 1, \text{ then the influence}$$

of modulation exceeds the effects of interaction between the plasma and the neutral species. Expression (16) has a maximum for the AGW satisfying the "resonance" conditions

$$\omega - \mathbf{k} \cdot \mathbf{V}_d \approx D_a k_{\parallel}^2,$$

where k_{\parallel} is the component of vector \mathbf{k} along the magnetic field, and:

$$\delta N_{\max} = N_0 \times \frac{\delta_A k V_{ph} \cos^2 \chi + (\delta_A + \delta_T / 2) \left(\frac{\mathbf{k} \cdot \mathbf{E}}{Q_i B_0} \right)}{(D_a k_{\parallel}^2)}$$

(17)

The above analysis illustrates the principal possibility of the creation of plasma moving disturbances by longitudinal AGW and, finally, of the creation of plasma inhomogeneities.

References

1. Gossard, A. and Y. Huk, *Waves in the Atmosphere*, 1975.
2. Hines, C. O., *Can. J. Phys.*, vol. 38, 1960, pp. 1441-1481.
3. Martin, D. F. *Proc. Roy. Soc. Canada*, vol. A209, 1950, pp. 216-219.
4. Gel'berg, M. G., *Geom. and Aeronom.*, vol. 20, 1980, pp. 271-274.
5. Blaunstein, N., *Annales Geophysicae*, vol. 13, 1995, pp. 617-626.

ON THE CALCULATION OF GLOBAL QUASISTATIC ATMOSPHERIC ELECTRIC FIELD AND CURRENT

S.S. Davydenko

Institute of Applied Physics RAS, ul. Ulyanova 46, 603600 Nizhny Novgorod, Russia
fax: +7(8312)-384-385, e-mail: davyd@appl.sci-nnov.ru

A method of description of global electric field and current under inhomogeneous atmospheric conductivity is considered. As an example, the method is applied to the case of conductivity varying arbitrary with latitude and increasing exponentially with altitude. It is shown that under wide enough class of conductivity distribution the problem can be reduced to a set of ordinary differential equations describing an atmospheric electric potential. A method of the eigenvalue spectrum evaluation and properties of the appropriate eigenfunctions are described. To estimate responses of global atmospheric electric field and air-earth current to variations of latitude conductivity profile, a model of global electric circuit is constructed taking into account both a spatial inhomogeneity of the conductivity distribution and electric sources dealing with thunderstorms or with large-scale magnetospheric convection. Under model conductivity profile an exact general solution of the problem is obtained. It is shown that latitude variation of terrestrial atmospheric conductivity leads, in particular, to appearance of significant additional radial electric field in the lower atmosphere.

1. INTRODUCTION

It is known that an electric conductivity of terrestrial atmosphere depends substantially both on the geo-coordinates and altitude above the planetary surface. This dependence appears mainly due to variation of intensity of external ionization sources and differences in local meteorological conditions. Atmospheric conductivity at low heights, in the austasch layer, significantly depends on the atmospheric turbulence, surface properties, Earth's radioactivity and has a complex spatial distribution. When receding from the ground, a contribution of near-surface processes to the atmospheric conductivity decreases and cosmic rays become the main factor forming an exponential

growth of the conductivity with altitude and its large-scale latitude profile [1].

Generally, a spatial inhomogeneity of atmospheric conductivity leads to a significant complication in calculation of global circuit parameters. That is connected mainly with a change of eigenfunctions of the electrostatic problem: the eigenfunctions of homogeneous medium are not orthogonal under spatially inhomogeneous conductivity, and determining of the new set of eigenfunctions usually is a nontrivial problem. In some cases, however, one need to estimate an influence of the conductivity profile on a field and current distribution. It seems interesting, for example, under the terrestrial conditions, where atmospheric conductivity at the poles exceeds an equatorial conductivity more than a twice [1]. In the present work, we suggested a general method of calculation of electric field and current density assuming atmospheric conductivity to be a product of two functions depending on the altitude and latitude respectively.

2. BASIC EQUATIONS AND GENERAL SOLUTION

In a stationary problem electric potential δ , field \mathbf{E} and current density \mathbf{j} in a medium with conductivity $\sigma(r, \theta)$ can be described by the equation for a current density $\mathbf{j} = \sigma(r, \theta) \mathbf{E}$ and by the continuity equation $\text{div } \mathbf{j} = 0$. Here r is the radial distance and θ is the co-latitude in a spherical frame of reference. So far as the electric field is potential, one can reduce the above equations to the following second-order partial differential equation with respect to the electric potential δ :

$$\text{div} (\sigma(r, \theta) \nabla \delta) = 0. \quad (1)$$

In a case of arbitrary distribution of the conductivity $\sigma(r, \theta)$ it seems rather difficult to

obtain a general analytical solution of Eq.(1). However, if the conductivity can be presented as a product of functions depending on r and Θ :

$$\sigma(r, \Theta) = \sigma(r) \Lambda(\Theta), \quad (2)$$

one can present an electric potential in the form $\delta(r, \Theta) = F(r) G(\Theta)$ and separate variables in Eq.(1), reducing it to a set of the following ordinary differential equations:

$$(r^2 F'_r(r))'_r + r^2 \frac{\sigma_r(r)}{\sigma(r)} F'_r(r) - \lambda^2 F(r) = 0, \quad (3)$$

$$\begin{aligned} & ((1-x^2)G'_x(x))'_x + (1-x^2) \frac{\Phi'_x(x)}{\Phi(x)} G'_x(x) + \\ & + \lambda^2 G(x) = 0, \end{aligned} \quad (4)$$

where $x = \cos \Theta$, λ is a real separation constant.

A general solution of Eq.(4) can be presented as the power series

$$G(x) = \sum_{k=0}^{\infty} a_k (x-1)^k. \quad (5)$$

Substituting (5) into Eq.(4) and presenting the latitude profile of atmospheric conductivity in the form $\Phi(x) = \sum_{k=0}^{\infty} \phi_k (x-1)^k$ one can obtain

the following recursion relation for the power series coefficients:

$$\begin{aligned} a_k = -\frac{1}{k^2} \sum_{n=0}^{\infty} a_n \left\{ \lambda \left(-\frac{1}{2} \right)^{k-n} + \right. \\ \left. + n \left(\phi_{k-n}(k-n) - \left(-\frac{1}{2} \right)^{k-n} \right) \right\}. \end{aligned} \quad (6)$$

A general solution of Eq.(4) presents a set of eigenfunctions calculated by means of relation (6) for the corresponding eigenvalues Θ . To determine an eigenvalues spectrum one needs to use the known properties of the solution. In our case, this is a finiteness of eigenfunctions at the points $x = \pm 1$. For example, if a latitude profile of the conductivity is symmetrical with respect to the point $x=0$, eigenfunctions of Eq.(4) must be either even or odd. That possesses us to consider separately the conditions $G(0) = 0$ and $G'_x(0) = 0$ together with finiteness of the eigenfunctions at one of the points $x = \pm 1$ only. Taking into account the above properties, one can obtain a discrete eigenvalues spectrum λ_j , assuming free coefficient $a_0 = 1$ and solving the equations

$$\sum_k a_k (-1)^k = 0, \quad \sum_k k a_k (-1)^{k-1} = 0. \quad (7)$$

It should be pointed out that Eq.(3) has a continuous eigenvalue spectrum, so eigenvalues of the problem are determined namely by Eq.(4) under the above boundary conditions.

Using the obtained eigenvalues and relation (6) one can construct the appropriate eigenfunctions $G_j(x)$ of Eq.(4) and, in the similar way, general solutions $F_j(x)$ of Eq.(3). A set of these functions presents a general solution of Eq.(1) under conductivity distribution (2).

It is easily seen that in a case of uniform distribution of the conductivity over latitude the eigenfunctions $G_j(x)$ transform to the Legendre polynomials $P_j(x)$ of the second kind, belonging to the class of orthogonal polynomials. It is important to point out that the "modified Legendre polynomials" $G_j(x)$ also possess a specific weighted orthogonality:

$$\int_{-1}^1 G_j(x) G_k(x) \Phi(x) dx = 0$$

under $j \neq k$, that is one of their most important properties. As follows from the last relation, one can use $G_j(x)$ as a basis to expand into series a solution of the not uniform problem.

3. DESCRIPTION OF THE MODEL

To calculate global atmospheric electric field and current under terrestrial atmospheric conductivity in the framework of the above approach, we consider the following model problem. A planet of radius r_p and conductivity σ_p is surrounded by atmosphere of height h with conductivity

$$\sigma_s(r, \theta) = \sigma_{a0} \exp(r/H) \cdot \left(\frac{1+A}{\sin^4 \theta + A} \right)^{3/2}. \quad (8)$$

Here σ_{a0} is the conductivity at the planetary surface at the equator, H is the scale height of the conductivity variation, A is a dimensionless parameter. A comparison of the latitude profile (8) under $A \approx 1.15$ with recent observational results and with one of the known conductivity distribution models is presented in Fig. 1.

It should be pointed out that near the surface a conductivity of the terrestrial atmosphere significantly depends on the latitude and longitude, so the model (8) is only qualitatively reflects a real distribution of the conductivity.

First, we estimate responses of global atmospheric electric field and air-earth current

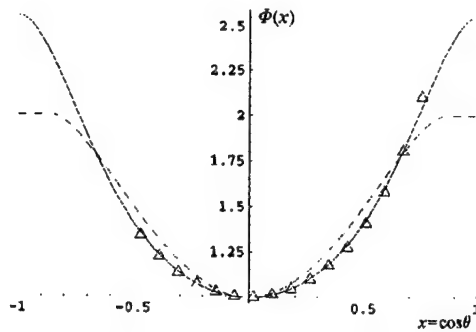


Fig.1. Measurements of a latitude distribution of the atmospheric conductivity [1] (triangles) as compared to the conductivity profile considered by Hays and Roble [2] (dashed line) and to the model distribution (8) under $A=1.14913$ (solid line).

to variations of latitude conductivity profile taking into account electric sources dealing with large-scale magnetospheric convection. These results appear general enough, and lower we qualitatively apply them to the case of thunderstorm electric generators in the global circuit. It is assumed that differential rotation of the well-conducted planetary plasma envelope provides the electric potential $U_a(\theta)$ at the upper boundary $r_a = r_p + h$ of the atmosphere. We are looking for a stationary solution, so the radial component of an electric current density must be continuous and the net current flowing through the upper atmospheric boundary must be zero. The above relations and a continuity of the electric potential at the boundaries of the atmospheric layer present boundary conditions of the problem.

Under the model latitude conductivity profile $\Phi(x) = \left(\frac{1+A}{\sin^4 \theta + A} \right)^{3/2}$ from (8) it is easy to determine two lowest eigenvalues of Eq.(4), $\lambda_0 = 0$ and $\lambda_2 = \sqrt{6}$. The appropriate latitude eigenfunctions are

$$G_0(x) = 1, \\ G_2(x) = P_2(x) - \left(\frac{231}{8}A + 11 \right)^{-1} \times \\ \times \left(\frac{33}{5} + \frac{27}{5}P_4(x) - P_6(x) \right), \quad (9)$$

where $P_k(x)$ are the Legendre polynomials of the order k . To determine the functions $F_0(r)$ and $F_2(r)$ one needs to substitute the radial conductivity profile $\sigma(r) = \sigma_{a0} \exp(r/H)$ from

(8) and the appropriate eigenvalue in Eq.(3). A general solution of Eq.(3) under $\lambda_0 = 0$ is

$$F_0(r) = A_0 + B_0 \int \xi^{-2} \exp(-\xi) d\xi, \quad (10)$$

and under $\lambda_2 = \sqrt{6}$ is

$$F_2(r) = A_2 F_{2,1}(r) + B_2 F_{2,2}(r), \quad (11)$$

where

$$F_{2,1}(r) = \xi^2 \left(\exp(-\xi) \xi^{-4} \right)'_r, \\ F_{2,2}(r) = \xi^2 \exp(-\xi) \left(\xi^{-2} \exp(\xi) \right)'''_{\xi\eta}. \quad (12)$$

Here A_0, B_0, A_2 and B_2 are constants depending on the boundary conditions, $\xi = r/H$.

Let us suppose that an external electric sources provides the electric potential

$$U_a(x) = D_0 G_0(x) + D_2 G_2(x) \quad (13)$$

at the upper boundary of the atmosphere [3], then a general form of the solution is

$$\phi(r, x) = F_0(r) G_0(x) + F_2(r) G_2(x). \quad (14)$$

Substituting expressions (9)-(12) in the formula (14) and taking into account the discussed above boundary conditions an exact distribution of the electric potential is obtained. Using known values of atmospheric conductivity $\sigma_{a0} = 4.5 \cdot 10^{-4} \text{ s}^{-1}$, total atmospheric height $h = 10^7 \text{ cm}$, scale height of the conductivity variation $H = 10^5 \text{ cm}$, Earth's interior conductivity $\sigma_p = 9 \cdot 10^6 \text{ s}^{-1}$ and the planetary radius $r_p = 6.37 \cdot 10^8 \text{ cm}$ [4], an exact solution (14) in the lower atmosphere ($z \ll h$) can be simplified and takes the form

$$\phi_a(z, x) \approx D_0 + D_2 G_2(x) (1 - \exp(-z/H)), \quad (15)$$

where $z = r - r_p$ is an altitude above the planetary surface. Using (15) one can obtain distributions of the vertical electric field E_{az} and current density j_{az} in the lower atmosphere:

$$E_{az}(z, x) \approx -D_2 G_2(x) \exp(-z/H) / H, \\ j_{az}(z, x) \approx -\sigma_{a0} D_2 \Phi(x) G_2(x) / H. \quad (16)$$

To clear up an influence of the latitude conductivity variations, let us consider the problem under the same boundary conditions assuming latitude independent atmospheric conductivity. In that case Eq.(4) reduces to the Legendre equation with the spectrum of eigen-

values $\lambda_j = j(j+1)$ and eigenfunctions $P_j(x)$. Using that eigenvalue spectrum it is possible to determine an asymptotic behavior of general solutions of Eq.(3) under $\xi=r/H \gg 1$:

$$\begin{aligned} F_{2k,1}(r) &\approx 1 + o[\xi^{-1}] \\ (F_{2k,1}(r))'_r &\approx k(k+1) \frac{\xi^{-2}}{H} + o\left[\frac{\xi^{-3}}{H}\right] \\ F_{2k,2}(r) &\approx (-1)^{2k+1} \exp(-\xi) \xi^{-2} + o[\xi^{-3}] \\ (F_{2k,2}(r))'_r &\approx (-1)^{2k} \exp(-\xi) \frac{\xi^{-2}}{H} + o\left[\frac{\xi^{-3}}{H}\right], \quad (18) \end{aligned}$$

where $o[\xi^{-1}]$, $o[\xi^{-3}/H]$ are small terms of the appropriate order of magnitude.

The electric potential at the upper atmospheric boundary can be presented as a linear combination of the lowest even Legendre polynomials:

$$U_a(x) = D_0 + D_2 \sum_{k=0}^j \alpha_{2k} P_{2k}(x),$$

where constants α_{2k} follow from the expression (9). Taking into account the above values of $\sigma_{a0}, \sigma_p, H, h, r_p$ and asymptotics (18) an exact distribution of electric potential in the lower atmosphere can be reduced to the following form:

$$\begin{aligned} \Phi_a^{(u)}(z, x) &\approx D_0 + D_2 \alpha_0 \exp(-z/H) + \\ &D_2 G_2(x) (1 - \exp(-z/H)) \quad (19) \end{aligned}$$

Distributions of vertical electric field and current density corresponding to the potential (19) are

$$\begin{aligned} E_{az}^{(u)}(z, x) &\approx D_2 (\alpha_0 - G_2(x)) \exp(-z/H) / H, \\ j_{az}^{(u)}(z, x) &\approx \sigma_{a0} D_2 (\alpha_0 - G_2(x)) / H. \quad (20) \end{aligned}$$

4. DISCUSSION OF THE RESULTS

As seen from the expressions (15), (19) for electric potential and (16), (20) for vertical electric field and current density, a variation of atmospheric conductivity with latitude leads to appearance of the additional latitude independent electric potential $\delta\Phi_a(z) = \Phi_a(z) - \Phi_a^{(u)}(z) \approx -D_2(\alpha_0 - G_2(x))$ and corresponding vertical electric field $\delta E_{az}(z) \approx E_{az}(z) - E_{az}^{(u)}(z) \approx D_2 \alpha_0 \exp(-z/H) / H$ (see Fig.2). As follows from the expression (9), the coefficient $\alpha_0 = (35A/8 + 5/3) \approx -0.15$, that is approximately equal to the ratio of the additional potential appearing near the ground

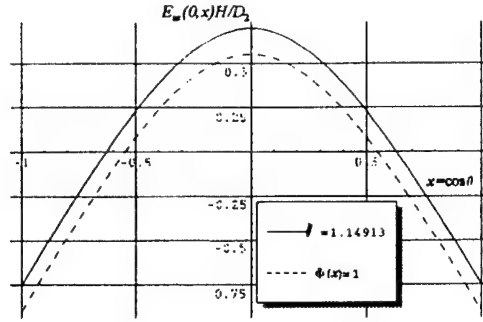


Fig.2. Vertical electric field near the ground in the cases of latitude-independent atmospheric conductivity (dashed line) and model latitude conductivity profile (8) under $A = 1.14913$ (solid line).

to the voltage D_2 applied to the upper boundary of atmospheric layer. Assuming the applied potential $U_a(x)$ is connected with a large-scale convection of the planetary plasma envelope, it is naturally to suppose that D_2 is of the order of unipolar potential $U = M\Omega/(r_p c)$, where M and Ω are the dipole magnetic moment and angular velocity of the planet, c is the velocity of light [3]. So far as under the terrestrial conditions $U \approx 10^5$ kV, it appears that $\delta\Phi_a \approx U\alpha_0 = 15$ kV.

Taking another value of A (as seen from (8), it is possible to accept $A < -1$ and $A > 0$) one can see that the similar effect appears clearly: in that case expressions (9), (15)-(16) and (19)-(20) are still valid. For example, under $A = -1.6$ the latitude conductivity profile (8) reaches a maximum at the equator, and under the same boundary conditions a sign of the additional electric field $\delta E_{az}(z)$ inverts (see Fig.2).

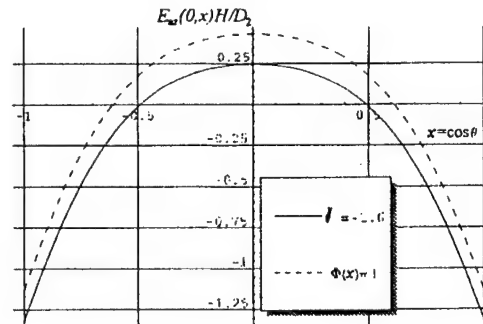


Fig.3. Comparison of vertical electric field at the ground in the cases of homogeneous (dashed line) and model latitude conductivity profile (8) under $A = -1.6$ (solid line).

The model can also take into account thunderstorms and other atmospheric electric sources as external currents with distributed magnitude in different regions of the atmosphere. It is naturally to present these currents in the thin enough atmospheric layer in the form

$$I_{ar}(r, \theta) = I(\theta) / r^2.$$

As seen, in that case a fundamental solution of non uniform problem coincides with eigenfunctions of Eq.(1) and is determined by conditions at the boundaries of the current layer and whole atmosphere. Performing calculations, one can see that the above results obtained under magnetospheric sources of atmospheric electricity are still valid: a latitude variation of atmospheric conductivity leads to a significant redistribution of vertical electric field at the ground. Under model terrestrial conductivity profile (8) that redistribution is of the order of 15% as compared to the case of latitude independent conductivity.

It should be also noticed that in the framework of the above approach more sophisticated models of atmospheric conductivity can be used. In particular, longitude dependence of atmospheric conductivity and existence of the auras layer can be naturally taken into consideration as well as the Earth's orography effect.

5. CONCLUSIONS

A method of description of a global electric field and current density under inho-

mogeneous atmospheric conductivity is elaborated. It is shown that the latitude conductivity variation leads to a significant redistribution of vertical electric field in the lower atmosphere, which is about 15% as compared to the case with the same boundary conditions (applied potentials and atmospheric external currents) under latitude independent conductivity of the atmospheric layer.

6. ACKNOWLEDGMENTS.

The work was supported by RFBR grants No.98-02-16236 and 00-02-17758.

7. REFERENCES

- 7.1. K.T. Driscoll, R.J. Blakeslee, J.C. Bailey and H.J. Christian, "Atmospheric Conductivity observations over a wide latitudinal range", Proceedings of 10th International Conference on Atmospheric Electricity, Osaka, Japan, 1996, pp.176-179.
- 7.2. R.B. Hays and R.G. Roble, "A quasi-static model of global atmospheric electricity. 1. The lower atmosphere", J.Geophys.Res., Vol.84, No.17, 1973, pp.3291--3305.
- 7.3. P.A. Bespalov, Yu.V. Chugunov and S.S. Davydenko, "Planetary electric generator under fair-weather conditions with altitude-dependent atmospheric conductivity", J.Atmos. Terr.Phys., Vol.58, No.5, 1996, pp.605-611.
- 7.4. H. Volland, "Electromagnetic coupling between lower and upper atmosphere", Physica Scripta, Vol.T18, 1987, pp.289-297.

GRAVITO-ELECTRODYNAMICS OF DUST IN ELECTRIC CUSPS AND ELECTRIC MIRRORS WITH ELECTRIC RECONNECTION AND ITS APPLICATIONS TO DIFFUSE DUST LAYERS IN THE TROPOSPHERE AND PRE-EARTHQUAKE ATMOSPHERIC AND IONOSPHERIC EFFECTS

Hiroshi Kikuchi

Institute for Environmental Electromagnetics
3-8-18, Komagome, Toshima-ku, Tokyo 170, Japan
Fax: +81-3-3917-9418; E-mail: hkikuchi@mars.dti.ne.jp

On the basis of 'Electrodynamics of Dust', it is shown that an electric cusp typically formed by a quadrupole constitutes 'electric mirrors' where uncharged and/or charged dust particles are reflected back and forth and trapped between conjugate mirror points. Such a quadrupole configuration really exists in the terrestrial atmosphere as a horizontal electrification of thunderclouds with their images onto the ground, for which an electric cusp-mirror model without or with gravity is applied. Results indicate that two kinds of diffuse dust layers could be expected below and beyond the mirror point by trapped dust grains and by escaping grains, respectively. Thus, the presence of dust and aerosols is thought to affect a whole population of the atmosphere and ionosphere, causing a variety of pre-earthquake effects observed from ground, balloons, and satellites. This could be attributed to roles of dust ejected from the earth's crust into the atmosphere and affected by electric cusps-mirrors of quadrupole-like thundercloud configurations.

1. INTRODUCTION AND SUMMARY

While electrodynamics or gravito-electrodynamics is concerned with the dynamics of a charged particle in an electromagnetic field or in an additional gravitational field, the so-called test particle approach has only been used, since the particle is usually considered a point charge and/or a material point. Accordingly, no electric but gravitational force only is exerted on uncharged particles. For this reason, conventional gravito-electrodynamics usually deals with the motion of charged particles only.

The situation is drastically changed, however, under some field configurations, typically when a particle is invading an electric cusp. Then, electric field merging toward the particle induces or polarizes tiny quadrupole-like charges on its surface or volume, thus electric forces being exerted on the grain. This is just *electric reconnection*

whose concept has already been introduced by the present author for more than a decade [1, 2].

In this paper, it is shown that the particle in an electric cusp can be greatly accelerated by electric reconnection and that electric-cusp configuration typically formed by a quadrupole constitutes *electric mirrors*, analogous to magnetic mirrors. Such a quadrupole configuration really exists in the terrestrial atmosphere as a horizontal electrification of thunderclouds with their images onto the ground, for which *dust electrodynamics* and *dust gravito-electrodynamics* are developed. Results indicate that two kinds of diffuse dust layers could be expected below and beyond the mirror point by trapped dust grains and by escaping grains, respectively. Thus, the presence of dust and aerosols is thought to affect a whole population of the atmosphere and ionosphere, causing a variety of pre-earthquake effects observed from ground, balloons, and satellites [3]. This could be attributed to roles of dust ejected from the earth's crust into the atmosphere and affected by electric cusps-mirrors of quadrupole-like thundercloud configurations.

2. ELECTRIC CUSP AND RECONNECTION

Electric cusp is an electrically neutral point, line or sheet, across which the electric field reversal occurs, and is thought to be a source-origin of *electric reconnection*, analogous to magnetic cusp for magnetic reconnection.

Electric reconnection is a phenomenon in which electric field lines in one direction tend to connect to other adjacent field lines in the opposite direction and by which energy stored in electric fields is released rapidly to be transferred to kinetic energy of particles in a *free-space*-like environment, causing particle acceleration.

2.1 Electric force exerted on a spherical dust in an electric cusp

A point-like uncharged particle in motion is not affected by electric forces but only by gravitational forces. The same is said for sizeable particles if they are so tiny that the so-called *test-particle approach* is feasible.

The situation is drastically changed, however, under some field configurations, typically when a dust particle is invading an electric cusp. Then, some of adjacent electric field lines of force in opposite directions tend to merge toward the particle, inducing or polarizing tiny quadrupole-like charges on its surface or volume, thus electric forces being exerted on the grain even when the particle is uncharged. Then, a total electric force exerted on the grain is a vector sum of contributions from quadrupole charges. Therefore, we start with the evaluation of the electric force between a spherical dust and a point charge.

2.1.1 Electric force exerted on a spherical dust by a point charge q

Consider the electric force between a point charge q and an isolated spherical conducting dust grain with radius a and total charge q_0 . Then, the electric field outside the grain is equivalent to the resultant field of the point charge q , two image charges on the sphere, q' and q'' , and dust charge q_0 , as shown in Fig. 1. Here

$$q' = -q'' = -(a/d)q \quad (1)$$

and q' is located at a distance $d' = a^2/d$ from the center of the sphere, while q'' is located at the center of the sphere.

Then, the electric force exerted on the spherical dust by a point charge q may be written as (e.g. [4])

$$f = -\frac{aq^2}{4\pi\epsilon} \left\{ \frac{1}{(d^2 - a^2)^2} - \frac{1}{d^4} \right\} + \frac{qq_0}{4\pi\epsilon d^2} \quad (2)$$

For $a \ll d$, this can be rewritten on Taylor's expansion, as

$$f \cong -\frac{a^3 q^2}{2\pi\epsilon d^5} + \frac{qq_0}{4\pi\epsilon d^2} \quad (3)$$

It is seen that an attractive electric force acts on the grain or object even if it is neutral or uncharged ($q_0 = 0$).

2.1.2 Electric force exerted on a spherical dust by a quadrupole

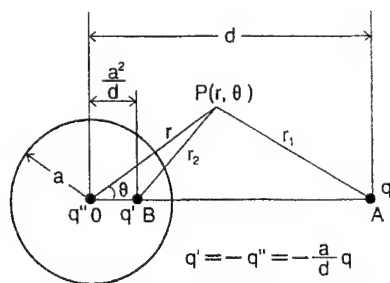


Fig. 1. Image charges of a point charge q for a spherical conducting grain.

We now consider the electric forces acting on an isolated conducting spherical dust in an electric cusp formed by a quadrupole with a rectangle of $2l$ and $2h$ as shown in Fig. 2. Then, a total electric force f exerted on the grain is a vector sum of each contribution from pole charges f_i ($i = 1, 2, 3, 4$), taking into account a given charge q_0 of the grain, namely

$$f = \sum_{i=1}^4 f_i = \frac{aq^2}{4\pi\epsilon} \sum_{i=1}^4 d_i \left\{ \frac{1}{(d_i^2 - a^2)^2} - \frac{1}{d_i^4} \right\} n_i - \frac{qq_0}{4\pi\epsilon} \sum_{i=1}^4 \frac{(-1)^{i-1}}{d_i^2} n_i, \quad (4)$$

where n_i is the outward unit vector normal to the spherical surface directed to each pole and d_i is the distance between the center of a spherical dust and each pole.

Now we proceed to the motion of a dust grain, whose rectangular and spherical coordinates are (x, y, z) and (r, θ, ϕ) with the origin at the cusp center, first near the cusp center, where $r, x, y, z \ll d_1, l, h$. Then we have

$$\begin{aligned} d_1^2 &\cong l^2 + h^2 - 2(lx + hy), & d_2^2 &\cong l^2 + h^2 + 2(lx - hy), \\ d_3^2 &\cong l^2 + h^2 + 2(lx + hy), & d_4^2 &\cong l^2 + h^2 - 2(lx - hy). \end{aligned} \quad (5)$$

Substituting Eqs. (5) in Eq. (4) and retaining the first order of $r/(l^2 + h^2)$, we obtain, after some manipulation,

$$f_x = \frac{2a^3 q^2}{\pi\epsilon(l^2 + h^2)^{3/2}} \left(\frac{6l^2}{l^2 + h^2} - 1 \right) x - \frac{3lhqq_0}{\pi\epsilon(l^2 + h^2)^{5/2}} y, \quad (6)$$

$$f_y = \frac{2a^3 q^2}{\pi\epsilon(l^2 + h^2)^{3/2}} \left(\frac{6h^2}{l^2 + h^2} - 1 \right) y - \frac{3lhqq_0}{\pi\epsilon(l^2 + h^2)^{5/2}} x, \quad (7)$$

where the first and second terms on the right-hand side are electric forces acting on the grain due to its induced and given charges, respectively. It is significant that the electric force exerted on the uncharged dust ($q_0 = 0$) by a quadrupole increases proportionally to its distance from the cusp center as long as it is still in a cusp zone, while for charged dust ($q_0 \neq 0$), the electric force on the grain is a sum of that on induced and given charges, its x - and y -component being proportional to y and x , respectively.

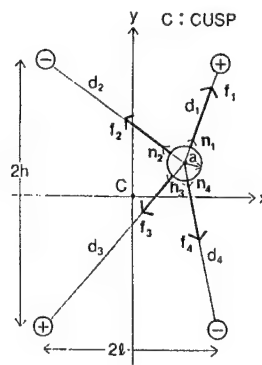


Fig. 2. An isolated spherical dust in or not in the ecliptic plane of a quadrupole with a rectangle of $2l$ and $2h$.

3. ELECTRODYNAMICS AND GRAVITO-ELECTRODYNAMICS OF DUST IN AN ELECTRIC CUSP OR MIRROR

Since the new kind of electric force on uncharged or even charged grains is usually not taken into account in the conventional dust dynamics, the present section is concerned with dust electrodynamics and dust gravito-electrodynamics in an electric cusp as an typical example.

3.1 Electrodynamics of uncharged dust near a cusp center in the ecliptic plane of a quadrupole

Based on the electric force on an uncharged dust obtained in the preceding section, we now proceed to dust electrodynamics in an electric cusp.

The equation of motion of an uncharged dust particle near a cusp center may be written, putting $q_0 = 0$ in Eqs. (6) and (7), as

$$m \frac{d^2 x}{dt^2} = f_x = \frac{2\alpha^3 q^2}{\pi \epsilon (l^2 + h^2)} \left(\frac{6l^2}{l^2 + h^2} - 1 \right) x = m\alpha^2 x, \quad (8)$$

$$m \frac{d^2 y}{dt^2} = f_y = \frac{2\alpha^3 q^2}{\pi \epsilon (l^2 + h^2)^3} \left(\frac{6h^2}{l^2 + h^2} - 1 \right) y = m\beta^2 y. \quad (9)$$

Integrating Eqs.(8) and (9) and putting the initial conditions of dust at $t = 0$: $x = x_0$, $y = y_0$; $u = dx/dt = u_0$, $v = dy/dt = v_0$, their solutions can be written as

$$x = x_0 \cosh \alpha t + \frac{u_0}{\alpha} \sinh \alpha t, \quad (10)$$

$$y = y_0 \cosh \beta t + \frac{v_0}{\beta} \sinh \beta t. \quad (11)$$

Accordingly, the velocity of dust leads to

$$u = \frac{dx}{dt} = \alpha (x_0 \sinh \alpha t + \frac{u_0}{\alpha} \cosh \alpha t), \quad (12)$$

$$v = \frac{dy}{dt} = \beta (y_0 \sinh \beta t + \frac{v_0}{\beta} \cosh \beta t). \quad (13)$$

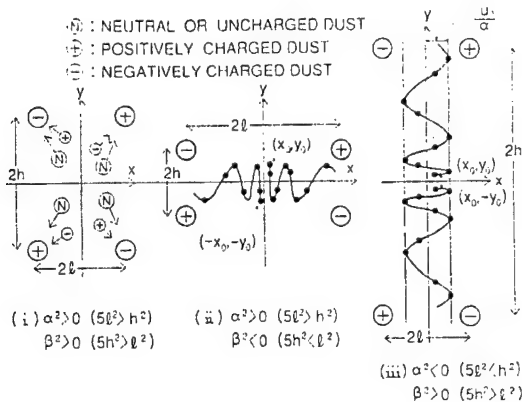


Fig.3. Schematic of charged and uncharged particle behavior in an electric cusp.

Fig.3 shows a schematic illustration of charged and uncharged particle behavior in an electric cusp with a quadrupole. In general, negatively and positively charged particles tend to enter the first or third quadrant and the second or forth quadrant, respectively and rapidly to go away from the cusp center. For the case (i) when $\alpha^2 > 0$ ($5l^2 > h^2$) and $\beta^2 > 0$ ($5h^2 > l^2$), uncharged particles are accelerated soon exponentially in both x and y directions. For the case (ii) when $\alpha^2 > 0$ (or $5l^2 > h^2$) but $\beta^2 < 0$ (or $5h^2 < l^2$), an uncharged particle is accelerated soon exponentially only in the x direction but is trapped in a zone around the x axis, oscillating sinusoidally in the y direction. The case (iii) when $\alpha^2 < 0$ (or $5l^2 < h^2$) but $\beta^2 > 0$ (or $5h^2 > l^2$) is the same as the case (ii) but the motion in the x and y directions is replaced.

3.2 Nonlinear electrodynamics of uncharged dust placed in a quadrupole: electric mirrors

We now consider the case when an uncharged dust is placed onto the midplane of a quadrupole ($x_0 = 0$) and in its ecliptic plane, choosing the cusp center for the origin of the rectangular coordinate, (x, y), but not only in a region of cusp ($-\infty < y < \infty$) and $a \ll d_1 = d_2$, $a \ll d_3 = d_4$, $\varphi = \pi/2$ (Fig.4). Then, the motion of dust is possible only on the y axis due to symmetry, and Eqs.(5) become

$$d_1^2 = d_2^2 = l^2 + (h-y)^2, \quad d_3^2 = d_4^2 = l^2 + (h+y)^2 \quad (14)$$

Therefore, Eq.(4) can be written, retaining up to the order (a^2/d_1^2) and (a^2/d_3^2) , as

$$f_y = \frac{\alpha^3 q^2}{\pi \epsilon} \left(\frac{h-y}{d_1^6} - \frac{h+y}{d_3^6} \right), \quad (15)$$

Then we have the equation of motion of dust

$$m \frac{d^2 y}{dt^2} = f_y = \frac{\alpha^3 q^2}{\pi \epsilon} \left(\frac{h-y}{d_1^6} - \frac{h+y}{d_3^6} \right). \quad (16)$$

This can be rewritten, putting $\rho = 3m/4\pi a^3$ (ρ : mass density of a spherical dust), as

$$\frac{d^2 y}{dt^2} = \frac{d\mathbf{v}}{dt} = \frac{3q^2}{4\pi^2 \rho \epsilon} \left(\frac{h-y}{d_1^6} - \frac{h+y}{d_3^6} \right) = \eta(q, \rho) D(y), \quad (17)$$

where

$$\eta(q, \rho) = 3q^2/4\pi^2 \rho \epsilon, \quad (18)$$

$$D(y) = \frac{h-y}{d_1^6} - \frac{h+y}{d_3^6} \quad (19)$$

is a geometrical factor to be determined by relative locations of the quadrupole and dust, and is also regarded as an acceleration (>0) or deceleration factor (<0).

It is noted that motion of uncharged dust does not depend on its size but only on its mass density.

Nonlinear differential equation (17) can be integrated exactly, referring to an initial condition, $y = y_0$, $v = v_0$ at $t = 0$, yielding

$$v^2 = v_0^2 + \frac{\eta(q, \rho)}{2} \left[\frac{1}{\{l^2 + (h-y)^2\}^2} + \frac{1}{\{l^2 + (h+y)^2\}^2} \right] y_0 \quad (20)$$

When $y = \pm h$, this can be written for $|y_0| \ll h$ as

$$v^2 = v_0^2 - \frac{\eta(q, \rho)}{(l^2 + h^2)^2} + \frac{\eta(q, \rho)}{2} \left[\frac{1}{l^2} + \frac{1}{(l^2 + 4h^2)^2} \right]. \quad (21)$$

This indicates that the particle velocity becomes maximum approximately at $y = \pm h$ where $D \approx 0$ from Eqs.(19) and (14), turning from acceleration to deceleration.

When an isolated dust particle was placed at the cusp center on the ground, $y_0 = 0$ at $t = 0$ with its initial velocity $v = v_0$, Eq.(20) may be written as

$$v^2 = v_0^2 - \frac{\eta(q, \rho)}{(l^2 + h^2)^2} + \frac{\eta(q, \rho)}{2} \left[\frac{1}{\{l^2 + (h-y)^2\}^2} + \frac{1}{\{l^2 + (h+y)^2\}^2} \right]. \quad (22)$$

When the particle starts moving upwards from the cusp center with a velocity of v_0 , it accelerates rapidly, gaining energy from the electrostatic energy of the environment until it reaches a point of $y \approx h$. Then the particle turns to abrupt deceleration, returning part of its kinetic energy to the field energy, and reaches a mirror point $y = y_M > 0$ where $v = 0$ and the particle tends to go back downwards in the exactly same way but changing the sign of v until it reaches the conjugate mirror point $y = -y_M < 0$ to be determined from Eq.(22). In such a way, a quadrupole constitutes an electric mirror as well as an electric cusp.

Since the third term (bracket) on the right-hand side is positive but rapidly decreasing with increasing $y > h$, a mirror point y_M should exist satisfying the relation:

$$v_0^2 < \frac{\eta(q, \rho)}{(l^2 + h^2)^2} = v_M^2 \quad (23)$$

This is the necessary condition required for the dust grain to mirror between conjugate points. Conversely, if $v_0 \geq v_M$, the dust grain tends to stop beyond the mirror point or to escape from the electric mirror, continuing to run upwards, so v_M may be termed as the *escape velocity*.

In particular, in an electric cusp, $0 < |y| \ll h$, retaining only the first order of y/h , Eq.(17) recovers Eq.(9) ($\eta D \rightarrow \beta^2$). Then, referring to $y_0 = 0$, we have from Eq.(13)

$$v^2 = v_0^2 + \beta^2 y^2 \quad \text{or} \quad (v^2 - v_0^2)^{1/2} = v_0 [(v/v_0)^2 - 1]^{1/2} = \beta y, \quad (v/v_0 > 1). \quad (24)$$

3.3 Gravito-electrodynamics of dust in an electric cusp: effects of gravity

So far we have neglected the gravitational force onto the dust grain. This subsection takes into account the effect of gravity, but for the nonrelativistic case and only under a constant gravitational force, focusing on how the

dust behavior in an electric cusp will be modified.

When an uncharged dust grain is placed on the mid-plane in a quadrupole, its motion is straight along the y -axis and is described exactly, referring to Eq.(17), by

$$\frac{d^2 y}{dt^2} = \frac{dv}{dt} = \eta(q, \rho) D(y) - g. \quad (25)$$

It is seen that the effect of gravity can be obtained simply from replacing the term ηD in Eq.(17) by $\eta D - g$, and consequently from replacing the term v^2 and v_0^2 in Eq.(20) or (22) by $v^2 + 2gy$ and $v_0^2 + 2gy_0$, respectively. Then, the mirror point with gravity can be obtained, putting $v = 0$, with the mirroring condition:

$$v_0^2 < \frac{\eta(q, \rho)}{(l^2 + h^2)^2} + 2gy_M = v_M^2 + 2gy_M = v_{MG}^2. \quad (26)$$

Here, the upper limit of v_0^2 increases by particle's gravitational potential energy, making easier the mirror effect, and a new escape velocity v_{MG} becomes higher.

3.4 Applications to dust dynamics under horizontal thundercloud electrification

Suppose two clouds of opposite polarities with charges $q = \pm 50$ Coulombs, facing each other horizontally at a height of $h = 1,000$ m with a horizontal distance of $2l = 10$ m which constitutes a quadrupole with their images onto the ground, and an electric cusp with its center on the ground surface. We now consider the motion of an aluminum dust grain of mass density $\rho = 2.69$ g/cm³ when it is launched from the cusp center to the atmosphere (dielectric constant $\epsilon = \epsilon_0$). Substituting these values into Eqs.(22) or (24), we have a height profile of the particle velocity as shown in Fig.4, where $\eta = 7.976 \times 10^8$ [m⁶/s²] from Eq.(18) and the solid and dashed lines represent the exact solution and its linear approximation without gravity. Its velocity increases with increasing height, more rapidly as it approaches the cloud height ($h = 1,000$ m), reaching a maximum as high as ~ 800 m/s, around which the effect of gravity no longer exists. Beyond this height,

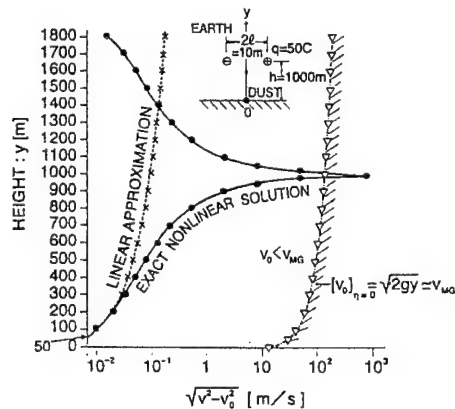


Fig.4. A height profile of uncharged dust velocity. It turns to abrupt deceleration. After the grain reaches a

mirror point where $v=0$ and if $v_0 < v_M$ without gravity or $v_0 < v_{MG}$ with gravity, the particle turns downwards falling to the ground where its downward speed goes back to its initial velocity v_0 , terminating half-turn's journey. Conversely, if $v_0 \geq v_M$ without gravity or $v_0 \geq v_{MG}$ with gravity, the dust grain tends to escape from the electric mirror, continuing to run upwards.

Consequently, dust grains with velocities beyond the escape velocity v_M or v_{MG} tend to be distributed or accumulated beyond the mirror point one after another in order of v_0 partly with the aid of collisions and/or pressure gradient, and partly due to additional electric fields, local and/or global, resulting in formation of a diffuse dust layer or dust distributions. This might occur beyond a height of $y > \sim 2h = 2,000$ m when $v_0 > v_{MG} \cong \sqrt{2gy}$ over a very wide range between the clouds and the ionosphere.

In addition, there may be a large amount of reflected and trapped dust grains within electric mirrors, part of which tends to form a diffuse dust layer just below the mirror point with the aid of collisions and/or pressure gradient. Accordingly, two kinds of diffuse dust layers could be expected below and beyond the mirror point by trapped dust grains and by escaping grains, respectively. Thus, the presence of dust and aerosols is thought to affect a whole population of the atmosphere and ionosphere, for instance as proved by a height profile of aerosol concentrations exhibiting a minimum around a height of ~ 5 km [5] which might correspond to a mirror point for dust particles. Thus, the presence of dust and aerosols is thought to affect a whole population of the atmosphere and ionosphere, causing a variety of pre-earthquake effects observed from ground, balloons as further discussed in the next section.

For a cloud-layer formation like a longitudinal sequence of quadrupoles with vertically periodic cusps, a dust grain will repeat acceleration and deceleration alternately every passing of a cusp center and quadrupole boundary, respectively, finally reaching a mirror point of the system like the case of a single quadrupole.

4. PRE-EARTHQUAKE ATMOSPHERIC AND IONOSPHERIC EFFECTS

Relevance of the electric cusp and reconnection model to pre-earthquake atmospheric and ionospheric effects has been indicated in an attempt to interpret a variety of those effects and to unite the processes in the earth's crust, atmospheric electricity, and ionosphere [2, 6]. They are phase variations of VLF signals and intensity variations of HF signals on passes over the epicenter of preparing earthquake, appearance or increase of E_s layers and additional layers, spread phenomena of bottom side ionograms, large-scale variations of electron density in F-layer, strong plasma density depletion within the upper atmosphere over the region of the preparing earthquake, and emanation of aerosol particle by the crust with a large content of metals before and some time after the earthquake. This could be explained by acceleration of

microparticles produced from fluidity of hard materials due electric reconnection of piezoelectric fields and by their injection into the atmosphere.

On the basis of Sec.3, it can be stated that the main causes of a variety of these pre-earthquake atmospheric and ionospheric phenomena are thought to be attributed to roles of dust produced in the earth's crust, ejected into the atmosphere, and affected by electric fields and space charges, in particular by electric cusps-mirrors of quadrupole-like thundercloud configurations.

If an additional vertical electric field is present, both uncharged and charged grains could gain energy from the field, increasing their kinetic energy continuously and resulting in overall acceleration. In particular, penetration of metallic ions and aerosols into the ionosphere [3, 6] might be attributed to such additional joint effects.

5. CONCLUSIONS

Exact and approximate solutions of dust dynamics in an electric cusp formed by a quadrupole reveal the following findings:

(1) A new kind of electric force is exerted on a dust particle, uncharged or charged, by electric reconnection, leading to particle acceleration in an electric cusp.

(2) A horizontal electrification of thunderclouds can form a quadrupole-like configuration and constitutes electric mirrors where uncharged and/or charged particles can be trapped, analogously to magnetic mirrors, although its mirror is influenced and modified with gravity.

(3) Two kinds of diffuse dust layers could be expected below and beyond the mirror point by trapped dust grains and by escaping grains, respectively under the influence of horizontal thunderclouds.

(4) The presence of dust and aerosols is thought to affect a whole population of the atmosphere and ionosphere, causing a variety of pre-earthquake effects.

(5) The main causes of a variety of these pre-earthquake atmospheric and ionospheric phenomena are thought to be attributed to roles of dust produced in the earth's crust, ejected into the atmosphere, and affected by atmospheric electric fields and space charges, in particular by electric cusps-mirrors of quadrupole-like thundercloud configurations.

6. REFERENCES

- [1] H. Kikuchi (ed.), *Dusty and Dirty Plasmas, Noise and Chaos in Space and in the Laboratory*, Plenum, New York, 1994, pp.535-544.
- [2] H. Kikuchi, *Physics and Chemistry of the Earth*, **21**, 549-557, 1996.
- [3] S.A. Pulinets et al., in [1], 1994, pp.545-557.
- [4] J.D. Jackson, *Classical Electrodynamics* (2nd edition), Wiley, New York, 1975, pp.54-62.
- [5] E.A. Mareev, in *XXVIth URSI GA-99 (Abstracts)*, E3, 1999.
- [6] S.A. Pulinets et al., in *XXVIth URSI GA-96 (Abstracts)*, HEG.6, 1996, p.669.

A MODEL OF FIREBALL OR PLASMOID PRODUCED BY A SUPERSONIC GAS FLOW IN THE LABORATORY AND BY INTER-CLOUD AND AIRPLANE DISCHARGES IN THE ATMOSPHERE BASED ON CONCEPTS OF CRITICAL IONIZATION VELOCITY AND ELECTRIC RECONNECTION

Hiroshi Kikuchi

Institute for Environmental Electromagnetics

3-8-18, Komagome, Toshima-ku, Tokyo 170, Japan

Fax: +81-3-3917-9418; E-mail: hkikuchi@mars.dti.ne.jp

While atmospheric and laboratory fireballs can be classified in general into two types in mechanism: continuing external source and self-sustaining internal source model, it is shown that the former type can be renovated to a rather simple physical form, based on two novel concepts of 'electric reconnection' and 'critical ionization velocity'. Specifically, as its examples, an attempt is made to explain two kinds of plasmoid; one is long-lived laboratory fireballs produced in a cold supersonic gas flow in the laboratory and the other is airplane-associated ball lightning observed inside and outside the plane, based on two concepts mentioned above with the aid of additional effects of dusty materials involved such as diffuse metals (e.g. electrode material) and carbon-containing substances (e.g. insulator material).

1. INTRODUCTION

The general view that the appearance of ball lightning is usually associated with thunderstorm activity implies that the energy source of ball lightning, somehow, goes back to the electrostatic energy stored in thunderclouds. The problem is, therefore, how electrostatic energy is converted to the ball energy through various processes. In general, two types of mechanism have been postulated to account for the prolonged luminosity of balls: either some external source of energy provides a continuing input to maintain the object (an external input source mechanism) or the ball itself contains some source of energy to maintain its form and output (a self-sustaining mechanism) [1].

A number of continuing external energy-source models proposed so far for the former type have been renovated to a rather simple physical form, based on two novel concepts of 'electric reconnection' and 'critical ionization velocity' (e.g. [2]). Such a model with a se-

quence of processes is introduced briefly in Sec.2.

For applications of this model to specific problems, Sec.3 takes up a recent report of stable, long-lived laboratory plasmoids produced in a cold supersonic gas flow in a wind tunnel to be explained in terms of critical ionization velocity. In close relation to these laboratory fireballs, airplane-associated ball lightning observed in the atmosphere [3, 4] is explained on the basis of a general model described in Sec.2, using a scenario similar to the case of rocket-triggered lightning [5] in Sec.4.

2. A CONTINUING EXTERNAL SOURCE MODEL BASED ON ELECTRIC CUSP, RECONNECTION, AND CRITICAL VELOCITY

Electric cusp is an electrically neutral point, line or sheet, across which the electric field reversal occurs, and is thought to be a source-origin of *electric reconnection*, analogous to magnetic cusp for magnetic reconnection.

A simplest and idealized form of electric cusp can be obtained from a symmetrical quadrupole configuration as shown on the left panel (a) in Fig.1 and its center of diagonal forms an electric cusp around which a low electric field region is attained as indicated by a stippled area. The middle panel (b) in Fig.1 constitutes a dipole above a conducting plane or ground, and is equivalent to the left panel (a) for the electric fields on and above the ground plane which can be replaced by an image of the dipole. The right panel (c) in Fig.1 shows a monopole placed symmetrically between two intersecting conducting-half planes perpendicular each other and is also equivalent to the panels (a) and (b) for the electric fields on and between the two half-planes which can be replaced by three mirror images of the monopole. Thus, these three panels are essentially the same due to the symmetrical configurations.

Electric reconnection is a phenomenon in which

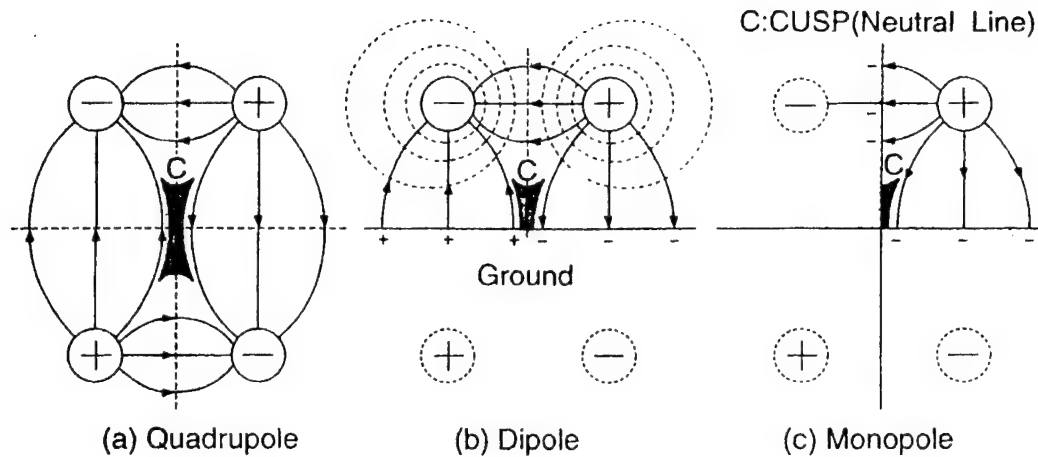


Fig. 1. The simplest form of an electric cusp. (a): quadrupole; (b): dipole; (c): monopole.

electric field lines in one direction tend to connect to other adjacent field lines in the opposite direction and by which energy stored in electric fields is released rapidly to be transferred to kinetic energy of particles or flow generation and ionization energy of the background gas, causing a critical ionization flow.

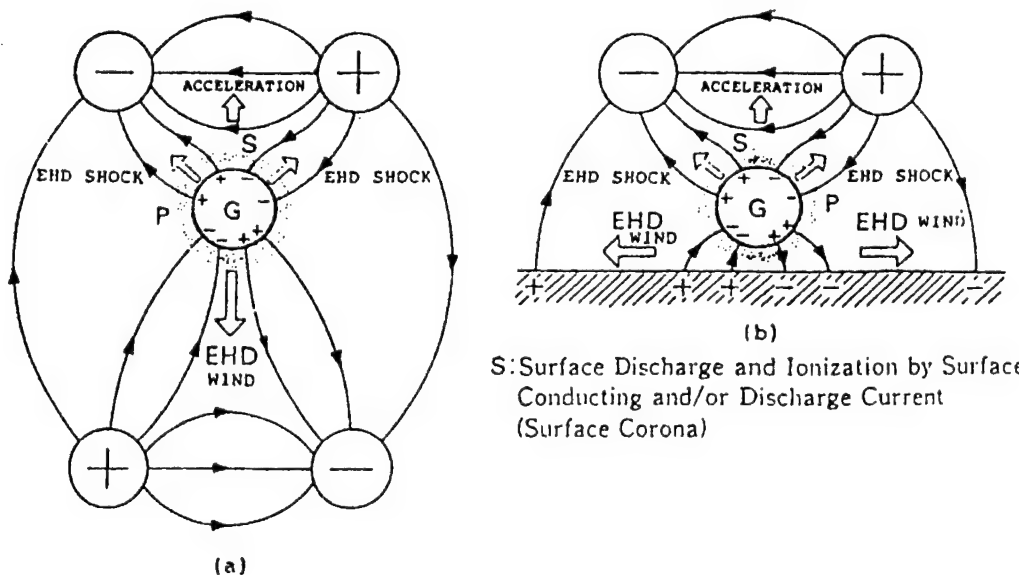
Critical ionization velocity is an upper limit of relative velocity of two counter-streams of charged particles or ionized and neutral gases, at which velocity a strong collective interaction occurs, causing ionization of neutral gas, regardless of gas pressure.

When a dust grain (uncharged or charged) is placed in an electric cusp, the electric field configuration around the particle or object changes drastically nearly from zero to infinite (very high) field intensity in such a way that electric field fluxes in both directions (opposite to each

other) tend to merge the particle inducing or polarizing tiny quadrupole-like charges in it, naturally leading to dust related-electric reconnection. This produces strong local electric fields, and if it is high enough, causing gas breakdown and surface discharge. Consequently, electrons and ions in the surface corona are first quickly accelerated in the form of radial EHD shock, gaining kinetic or flow energy from electrostatic energy in the environment by electric reconnection and subsequent energy conversion processes. As soon as preceding electrons and/or ions reach their critical ionization velocities, their kinetic or flow energy goes abruptly to ionization energy. As a result, electrons and/or ions are forced to stop, forming a spherical plasma layer around a nucleus of the dust grain or aerosol. Then, electric field lines are frozen-in to the solid particle or dust grain as long as the elec-

P: Plasmoid (Atmospheric) or Fire Ball

G: Conducting or Dielectric Body (Grain)



S: Surface Discharge and Ionization by Surface Conducting and/or Discharge Current (Surface Corona)

Fig. 2. Schematic of ball lightning formation.

trostatic energy of the environment is available for providing the ball with a continuing power source and tend to remain unchanged, resulting in the steady supply of energy necessary for sustaining a fireball-plasmoid for a long time. Such a whole process of fireball formation is illustrated schematically in Fig. 2.

There are, however, a couple of modifications to the standard process just described. One of them is the case when a sizeable object is inserted in an electric cusp instead of a small particle as discussed in Sec. 4. Then, the location of possible fireball formation becomes a leader head where its velocity reaches the critical velocity of the background gas.

Another modified case is the more basic one of two counter streams of charged particles or ionized and neutral gases. Then, the location of possible fireball formation becomes a point where the velocity of charged particle or plasma flow reaches the respective critical velocity, namely electron, ion, and atom critical velocities which are defined together as

$$\frac{1}{2} m_v v_{vc}^2 = eV_i \quad (v = -: \text{electron}, +: \text{ion}, \text{ and } a: \text{atom}) \quad (1)$$

where m_v and v_{vc} are the mass and critical velocity of species v , e the electronic charge, and V_i is the ionization potential of the neutral component; v_{-c} , v_{+c} , and v_{ac} represent electron, ion, and atom critical velocities, respectively.

In discharge physics, it is well known that electron and ion drift velocities are generally expressed as a monotonically increasing function of a parameter E/p , where E is the electric field and p is the gas pressure, and which may be termed the relative electric field intensity. In general, both drift velocities are proportional to E/p at relatively low electric field intensities, but they tend to be proportional to $(E/p)^{1/2}$ with increasing relative field intensity, transferring from elastic to inelastic collisions with the background gas and eventually tend to saturate to certain values, since particle's kinetic energy is converted to excitation and/or ionization energy.

Consequently, both electron and ion drift velocities

tend to saturate, most likely approaching their critical velocities at certain values of E/p .

Combining a new critical-velocity model described above with a conventional drift-velocity model, one can write as

$$v_{\pm d} = \mu_{\pm} E/p \quad \text{for } v_{\pm d} < v_{\pm c} \quad \text{and} \quad (2)$$

$$\frac{1}{2} m_{\pm} v_{\pm d}^2 = \frac{1}{2} m_{\pm} v_{\pm c}^2 = eV_i \quad \text{for } v_{\pm d} = v_{\pm c}, \quad (3)$$

where v_d and v_c are the drift and the critical velocity, respectively, μ the mobility, e the electronic charge, m and V_i the mass and ionization potential of the neutral gas, + and - refer to ions and electrons.

For example, electron and ion drift velocities transfer to electron and ion critical velocities, $[v_{-c}]_O = 2.18 \times 10^6$ m/s at $E/p \sim 2.5 \times 10^8$ V/m·atm and $[v_{+c}]_O = 1.27 \times 10^4$ m/s at $E/p \sim 4 \times 10^7$ V/m·atm for oxygen and $[v_{-c}]_N = 2.26 \times 10^6$ m/s at $E/p \sim 1.3 \times 10^8$ V/m·atm and $[v_{+c}]_N = 1.41 \times 10^4$ m/s at $E/p \sim 4.7 \times 10^7$ V/m·atm for nitrogen. This is explained in Figs. 3 and 4 in terms of a E/p dependence of drift velocities, unifying low and high pressure gases in relation to critical velocities.

Going back to plasmoid formation, there may be additional effects for sustaining fireballs in the presence of dusty particles, aerosols, and other materials. In this case, a dust grain or aerosols at leader space-charge head could become a nucleus of plasmoids, as discussed specifically in the following sections.

3. LABORATORY FIREBALLS IN A SUPERSONIC GAS FLOW IN A WIND TUNNEL

In this section, an attempt is made to explain stable, long-lived laboratory fireballs or plasmoids produced in a cold supersonic gas flow ($M \sim 2$, $T_{st} \sim 150^\circ\text{K}$) by Klimov-Bychkov, using three types of methods: high-frequency Tesla (HF) generator; microwave (MW) generators; and erosive high voltage pulse discharge in a wind tunnel [6].

High energetic long-lived non-equilibrium ball-type

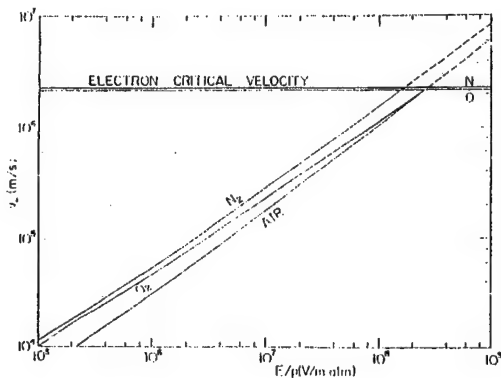


Fig. 3. Electron drift velocity and electron critical velocity in gases.

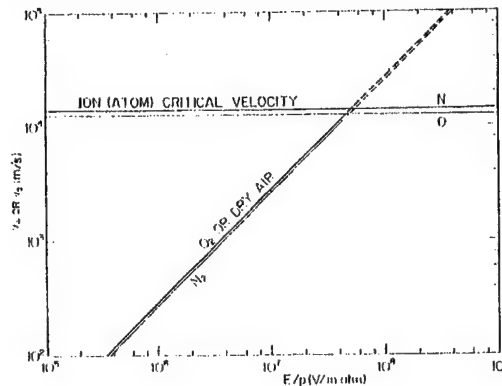


Fig. 4. Ion drift velocity and ion critical velocity in gases.

plasmoids created by HF and MW methods have two different types: diffuse and structural filament plasmoids, while high energetic long-lived non-equilibrium cluster plasma jets and cluster plasmoids (CP) were generated by erosive high voltage pulse discharge.

According to laboratory observations, the velocity of plasma precursor preceding a cold supersonic gas flow could be as high as ~ 10 km/s in the presence of an external electric field. It is inferred that this value of velocity may correspond to the atom critical velocity of the background gas or air, typically $\sim 10^4$ m/s (1.27×10^4 m/s at $E/p \sim 4 \times 10^4$ V/m·atm for oxygen and 1.41×10^4 m/s at $E/p \sim 4.7 \times 10^4$ V/m·atm for nitrogen), and when the relative velocity of two fluids between the precursor plasma and background gas or air reaches its critical velocity, a strong interaction between two fluids takes place, leading to collective avalanche ionization of the neutral gas, the so-called 'critical ionization' as described in Sec.3.

A new cluster plasma thus produced by critical ionization may be cooled by the following cool supersonic gas flow, liquid nitrogen and other dusty components, leading to 'plasma condensation' effective for a long-lived non-equilibrium state, and to creation of plasma structures like 'streamers' by applying charged molecular clusters, aerosols, dusty particles, and other methods. This may also provide the plasmoid with its nucleus, making its life time longer considerably.

Although various processes associated with cooling effects and long stability of fireballs or plasmoids are still largely open problems for further investigations, it is claimed that the source-origin or main cause of fireballs, somehow, could be attributed to a manifestation of 'critical velocity effect' between two fluids of a precursor plasma and a background gas, and then additional effects lead to different types of plasmoid as mentioned above.

Another interesting observation is plasmoid's motion through a thin channel, tube or hole of several mm in

diameter with a long length (upto 1 m), exhibiting its soap-bubble-like compressibility and deformability. Such a behavior of plasmoid is thought to be caused by the properties of containing substances such as metals and polymers [7]. These laboratory observations could apply to an explanation for fireballs observed inside airplanes, as described in the next section.

In addition, there are some other effects associated with ball production. One of them is generation of excited molecules with high concentration, e.g. $n^* > 10^{15}/\text{cm}^3$ in a large volume $V > 1,000 \text{ cm}^3$ [6]. This is because collisions between a plasma beam and background gas become inelastic already, causing dissociation, i.e. molecular excitation of the background neutral gas before the relative velocity reaches the critical velocity and ionization takes place.

4. AIRPLANE-ASSOCIATED BALL LIGHTNING

This section attempts to apply a general model of ball lightning based on electric reconnection and critical velocity specifically to airplane-associated ball lightning outside in the atmosphere and/or inside the plane. To effect this, relative locations of the airplane and cloud charges may play a key role in making the basic model feasible. In order to make an electric reconnection concept feasible, the airplane must be moving horizontally between two clouds with opposite polarities or more generally be invading an electric cusp formed by a horizontal dipole-like cloud charges with their images onto the ground, thereby forming a quadrupole, similar to the case of rocket-triggered lightning [5]. This can be proved by referring to a good correlation between frequency of fireball observations outside airplanes during a year and frequency of flash observations in 'stratified clouds' during a year, obtained by Amirov and Bychkov [8]. In this connection, there are many possibilities of leaders starting from a sharp portion of the airplane, typically its

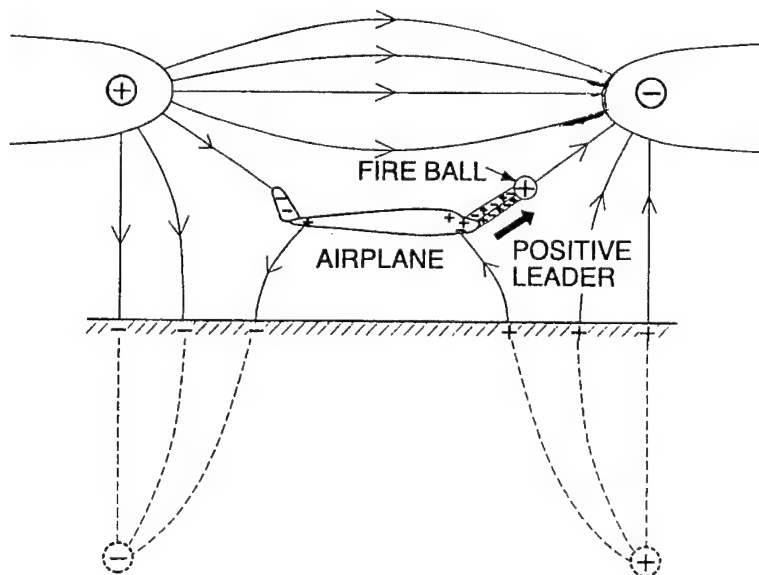


Fig.5. Airplane-associated ball lightning.

front tip or tail and advancing toward one of the clouds. The leaders can be positive or negative, moving toward the negative or positive clouds, respectively. Then, there may be a chance for leaders to be forced to stop as a result of conversion of kinetic or flow to ionization energy and no continuing energy supply sufficient for further advancement. Thus, space charges at leader head could create a fireball, possibly with a nucleus of dust grain, rather close to the airplane. With the aid of dust substances (e.g., emanated from a plane-tip) contained in the leader, the ball tends to remain there longer as long as partial energy supply for sustaining the ball still lasts, as indicated by laboratory fireballs.

A possible scheme with a whole process for airplane-associated ball lightning is schematically shown in Fig. 5, where the airplane is moving horizontally, invading an electric cusp of a quadrupole-like configuration formed by horizontal thundercloud charges and their images onto the ground. A positive leader initiated from the tip of the plane, and moved toward the cloud with negative polarity with a velocity of $\sim 10^4$ m/s (Secs. 3 and 4) upto a point between the plane tip and the cloud where the leader was forced to stop, losing its kinetic energy which was converted partly into ionization energy for the air, and partly ball energy, possibly with a nucleus of dust around the leader head. Similarly, it may be possible for a negative leader to start from a plane tip or tail when facing a positive cloud and to form a plasmoid in the same way.

Consequently, fireballs observed outside airplanes could be explained as a manifestation of joint effects of 'electric reconnection' and 'critical ionization velocity', similar to the case of rocket-triggered lightning [5], and further with additional effects of dust substances.

We next proceed to an explanation for fireballs inside airplanes. As stated in the preceding section, a plasmoid can get through a thin channel, tube or hole with a long length, exhibiting its soap-bubble-like compressibility and deformability with the aid of containing dust substances. There may be a number of thin channels or hole spaces connecting outside and inside a plane, through which a fireball produced outside the plane can invade inside the plane rather easily as proved by basic laboratory experiments described in Sec. 3.

5. CONCLUSIONS

A continuing external source model of ball lightning, based on concepts of 'critical ionization velocity' and 'electric reconnection' has been applied specifically to two kinds of fireballs; one is long-lived laboratory plasmoids observed in a cold supersonic gas flow and the other is airplane-associated ball lightning inside and outside the plane.

Explanations for them are summarized below:

(1) Stable long-lived laboratory fireballs are thought to be produced by combined effects of critical ionization velocity and plasma condensation between two fluids of precursor plasma and a supersonic gas flow and by

additional effects of dust components involved, such as aerosols, diffuse metals, carbon- or polymer-containing substances

(2) Observed plasmoid's motion through a thin channel, tube or hole with a long length could be attributed to its soap-bubble-like compressibility and deformability due to dust components involved in ball formation.

(3) Airplane-associated ball lightning outside the plane is thought to be produced by joint effects of electric reconnection and critical ionization velocity when an airplane is invading an electric cusp formed by a quadrupole-like configuration of horizontal thundercloud charges with their images onto the ground and by additional effects of dust components.

(4) Ball lightning observed inside the plane is inferred to be reappearance of a plasmoid produced outside the plane and getting through a thin channel or hole space connecting the inside and outside the plane, due to its soap-bubble-like compressibility and deformability, as proved by laboratory experiments.

References

- [1] H. Kikuchi, Ball Lightning, in *Handbook of the Atmospheric Electrodynamics*, H. Volland (ed.), Vol. I, Chap. 7, Boca Raton, 1995, pp. 167-187.
- [2] H. Kikuchi (ed.), *Environmental and Space Electromagnetics*, Springer-Verlag, Tokyo, 1991, pp. 561-575.
- [3] R.C. Jennison, *Nature*, **224**, 895, 1969.
- [4] R.C. Jennison, *Nature*, **245**, 95, 1973.
- [5] H. Kikuchi (ed.), *Laboratory and Space Plasmas*, Springer-Verlag, New York, 1981, pp. 331-334.
- [6] A.I. Klimov and V.L. Bychkov, *Proc. 6th ISBL (International Symposium on Ball Lightning)*, 1999, pp. 212-215.
- [7] V.L. Bychkov, A. Yu. Gridin, and A.L. Klimov, *On the Nature of Artificial Ball Lightnings*, High Temperature, **32**, No. 2, MAHK Hayka/ Interperiodica Publishing, 1994, pp. 179-183.
- [8] A.K. Amirov and V.L. Bychkov, *Proc. 6th ISBL*, 1999, pp. 34-37.

BIOGRAPHICAL NOTES

Hiroshi Kikuchi received Ph.D. degree from University of Tokyo in 1959 and was Chief, Ultramicrowave Laboratory of Electrotechnical Laboratories, Ministry of International Trade and Industry until 1961. Before his return to Japan as Professor of Nihon University, Tokyo in 1973, he worked with University of Oxford, Max-Planck Institute for Aeronomy, NASA/Goddard Space Center, as a Senior Research Scientist. He was a guest-professor at New York University, Max-Planck Institute, Nagoya University, and University of Oxford. He was Chairman, URSI Commission E (1987-1990) and is Life Fellow of IEEE. In 1999, he established the Institute for Environment Electromagnetics in Tokyo.

DUSTY PARTICLES EFFECTS ON TERRESTRIAL ELECTROMAGNETIC ENVIRONMENT AND THEIR EHD DESCRIPTION

Eugene A Mareev

Institute of Applied Physics, Russian Academy of Science,
46 Ulyanov str., 603600 Nizhny Novgorod, Russia

Phone: +7-8312-384-292, Fax: +7-8312-362-061, e-mail: mareev@appl.sci-nnov.ru

1. INTRODUCTION

Modification of terrestrial electromagnetic environment due to dusty particles and particularly due to their collective interaction is topics of intensive research efforts recently [1]. In the present paper we shortly review different ways of dust (aerosol) particle influence on the terrestrial electromagnetic environment and modern methods of their theoretical treatment. Special attention is paid to the basic ideas and applications of electrohydrodynamic (EHD) description of weakly conducting media with the presence of aerosols and highly charged hydrometeors. Electrical implications of active large-scale processes in the atmosphere (thunderstorms, mesoscale convective systems, dust and snowstorms, volcanic eruptions) are of great importance. In this connection we present a short summary of experimental data and give some basic physical ideas of their theoretical treatment. In particular, we consider the inductive charging of aerosol particles in a weakly conducting medium and note its high efficiency for electric field structures formation.

2. ELECTRIC STRUCTURE OF THE ATMOSPHERE

It is well known, that the ionosphere has a potential of several hundred thousand volts with respect to the Earth's surface. According to the classical picture of the global atmospheric electric environment [2], this potential, supported primarily by the thunderstorm activity all over the world, drives a vertical electric conduction current downward from the ionosphere to the ground in the fair weather regions. The fair weather current depends upon the ionospheric potential and the columnar resistance between the ionosphere and the ground. Horizontal currents flow freely along the highly conducting Earth's surface and in the ionosphere. A current flows upward from a

thunderstorm cloud top toward the ionosphere and also from the ground into the thunderstorm generator, closing the circuit.

Rather simple quasi-stationary picture, described above, is referred usually as a "global electric circuit". When treating the electrical phenomena in the atmosphere and coupling between them, this simplified concept is often helpful as a "zero" approach to the real nonequilibrium Earth's electrical system. Over the recent decade many efforts have been undertaken both in observation and theoretical modelling providing substantial progress in understanding the dynamics and structure of the global circuit. Now the global electric circuit, treated in a generalized sense as a complicated dynamical system, is considered as an important link of geospheric shells coupling, which should be taken into account when considering the modification of the terrestrial electromagnetic environment in the presence of dust and aerosol particles. It is evident now that aerosol distributions (including water droplets and ice crystals) in the troposphere and lower stratosphere substantially influence the main parameters, characterizing quasi-equilibrium state of the global circuit – atmospheric conductivity (and therefore the columnar resistance), air-earth current and electric field. Layers of an increased aerosol density can significantly reduce the atmospheric conductivity due to attachment of small ions to this aerosol particle [3].

Volcanic eruptions, forest fires, biomass burning and large dust storms can temporally disturb the character of upper tropospheric aerosols and therefore electrical variations. The raising of the dust particles from the ground is known to produce large electrical effects, which considerably alter the fair weather electrical state of the atmosphere [4]. Recent field observations performed during dust storms in the semi-deserts of California and Kalmykia showed electric field change from positive values 100-400 V/cm (which

exceeds more than two orders the mean value of the fair weather field strength) at the distance 2-8 km from the dust source, to the negative values - 100-200 V/cm at the distance 30-80 km [5]. It may be explained by the contact electrification of the surface loess-like soils during their intense wind erosion.

The most spectacular manifestations of permanent electrical activity in the atmosphere as connected to aerosol (hydrometeors) particle implication are related to thunderstorm activity. Some others are coupled to fair weather electricity as the inherent part of the global atmospheric electric circuit. Both them can be properly analysed under electrohydrodynamic (EHD) approach [1,6].

A thunderstorm as a generator of the global circuit is a key element in the field. In fact, it is a distributed EHD generator, based on the charge separation on colliding aerosol particles and their redistribution by an air flow [7]. A number of recent studies were devoted to the experimental investigation of severe thunderstorms and mesoscale convective systems, including the fine structure of electric field, the generation of abnormally great space charges, their distribution and dynamics over the cloud, electric field evolution before a cloud-to ground lightning flash and just after, conditions of an anvil formation etc. (see [8] for a detailed review). Now the active methods for thundercloud investigation, like the artificially triggered lightning, are widely used and give substantial information. Some new ideas concerning active diagnostics of severe thunderstorms are suggested.

Lightning induced transient luminous events in the lower ionosphere should be noted as the most intriguing phenomena of the recent decade [9]. The video observations have shown that certain types of lightning may create optical effects in the middle and upper atmospheres between the cloud tops of thunderstorms and the lower ionosphere. These observations have been obtained from the ground, from the space shuttle and from aircraft. At least two distinct types of optical effects have been documented: red sprites, large red luminous structures centered in the mesosphere, but possessing upward and downward appendages spanning the altitude range 40-95 km; blue jets, narrow, upward directed cones of blue light emanating directly from the tops of active thunderstorm systems and propagating upward to altitudes of approximately 40 km. Up to now a number of different theoretical models for blue jets and red sprites generation has been devoted, including the runaway air breakdown mechanism [9]. The latter is considered also as a mean to explain the measured X-ray emissions, associated with lightning and perhaps producing the occasional gamma-ray bursts. Whatever the mechanism is analysed, the penetration of

quasistatic electric field in the lower ionosphere is the most important stage, which is far from completion now. It is clear, however, that this process depends substantially on the charge distribution in a thundercloud and the features of the cloud-to-ground lightning channel development [10]. Further progress in understanding the terrestrial electromagnetic environment requires the study of the role of lightning induced transients in the global circuit dynamics.

A major goal in studying atmospheric electricity has long been the separation of local effects in order that the pattern of global scale might emerge. During the past decade new results concerning local processes recognition and their influence on the electrical structure of the global electric circuit have been derived. ULF pulsations of electric field and electric current in the surface atmospheric layer were investigated under fair weather conditions. A new method of structural-temporal analysis has been firstly applied to the study of spatio-temporal structures of the electric field [11]. This analysis allowed the quantitative estimations of spatial scales 0.5-1 km and life time not less than 10-20 min for respective elements, which have been called the "aeroelectric structures" (AES) [11,12]. Quasi-periodical sequences and high-amplitude solitary AES have been recognized.

3. MODELING OF DUSTY PLASMA ELECTRODYNAMICS

There are different levels of strictness in dusty plasma modeling. Comprehensive analysis requires formulation of kinetic equation for dust particles charge and velocity distribution. But usually the difficulties of kinetic description compel us to restrict analysis by the frame of hydrodynamic approach. Nevertheless, we are able to take into account at least partially strong correlation between highly charged particles [13].

Collective interaction accompanied by effective generation of large scale electric field (electric dynamo) and small scale structures in dusty plasmas is connected often with the charge exchange of colliding particles, as it occurs in clouds and dust storms.

Usually there is a possibility to distinguish a few fractions of aerosol particles with well-determined different macroscopic characteristics (such as the mean grain size, mass, velocity, and charge), in the simplest case - two fractions. Collective processes associated with the charge transfer can be analyzed then within the two-fluid hydrodynamic model for aerosol [14]. Let us consider two flows of charged aerosol grains moving in the conducting medium in the gravitational field g and in the uniform electric field E with the relative velocity U . We neglect the

processes of the growth, coalescence, and decay of grains; i.e., we assume that one flow consists of the heavy grains with mass M , and the other flow consists of the light grains with mass m . The velocities of the directional motion of the aerosol grains, which exchange their charges, are much higher than their thermal velocities. When the grains of different species collide, they exchange the charge δq that depends on the relative velocity of grains and the value of the electric field at the point at which the grains come into contact.

A number of specific mechanisms for the charge separation are discussed in the literature (see, for example [8]). These mechanisms depend on many factors, in particular, on the temperature distribution, phase composition, and size spectrum of aerosol grains in the cloud. However, we will not discuss in detail the microphysics of the charge separation. The dependence of the charge δq transferred in a single collision on the electric field is of primary importance for this problem. With respect to this parameter, all the mechanisms for the charge separation are divided into the inductive and noninductive mechanism [8].

For the mechanisms of the first type, the charge $\delta q = \delta q_i$ depends on the value and direction of the external electric field \mathbf{E} and is associated with the polarization of the interacting grains. Assuming the grains to be spherical in shape with diameters $D \gg d$ (where D and d are the diameters of the large and small particles, respectively) and averaging over the angle θ between the line passing through the centers of the grains and the direction of the electric field at the instant of collision ($-\pi/2 < \theta < \pi/2$), the charge δq_i can be expressed as [14]:

$$\delta q_i = \xi \cdot \frac{d^2}{4|\mathbf{U}|} \mathbf{E} \mathbf{U}, \quad (1)$$

where $\mathbf{U} = \mathbf{u} - \mathbf{v}$ is the relative velocity; \mathbf{u} and \mathbf{v} are the velocities of the heavy and light aerosol grains, respectively; and the quantity ξ is determined by the contact duration and the particle conductivity. Note that the scalar product $\mathbf{E} \mathbf{U}$ in formula (1) is only used to define the sign of the transferred charge in a one-dimensional problem.

The noninductive charging occurs due to the difference in both the chemical potentials and mass exchange between the interacting aerosol flows. Thus, the charge $\delta q = \delta q_s$ transferred to the ice crystal in a single collision with the heavier hailstone can be expressed as

$$\delta q_s = \left| \frac{\mathbf{U}}{U_0} \right|^p A_s(d, D, T), \quad (2)$$

where $p \approx 2 \div 3$, $U_0 \approx 3 \text{ m/s}$, $A_s(d, D, T)$ is the empirical function describing the dependence of δq_s on the characteristic sizes of hailstones and ice crystals and the air temperature. If the air temperature is lower than a certain critical temperature T_c , the hailstones acquire the negative charge and the ice crystals acquire the positive charge; for the air temperatures higher than the critical one, the situation is quite the reverse. The temperature T_c depends on the absolute humidity of air; usually, it lies between -15°C and -20°C . Although inductive and noninductive charging mechanisms are different in nature, such a dividing becomes somewhat vague at high external fields, when the relative velocity of charged grains begins to depend on the electric field.

Strictly speaking, formulae (1) and (2) are valid for the collisions between neutral grains. When the grains are charged, the transferred charge is governed by the electric field at the point at which the grains come into contact; this field, in turn, depends on the grain charges. In this case, the charge transferred in the collision can be expressed as

$$\tilde{\delta q}_{i,s} = \delta q_{i,s} - \eta_{i,s} d^2 (Q/D^2 - q/d^2), \quad (3)$$

where q and Q are the charges of the small and large particles, respectively, and the coefficient $\eta = \eta_i + \eta_s \approx (0.5 \div 5)\xi$. Note that the first and second terms on the right-hand side of formula (3) are opposite in sign.

Using the charge transfer parameterization assigned by the expressions (1)-(3) and respective rather complicated set of EHD equations, we have analyzed a thundercloud as a distributed EHD generator, taking into account aerosol charging effects, small ions dynamics due to their attachment to aerosols and corona processes as well as the aerodynamic flow and its dependence on the generated electric field [15]. The generation of great-scale and small-scale electric field structure has been considered. Our hypothesis, confirmed by the results of in-situ measurements in thunderclouds, is that multi-flow aerosol system encourages the development of small-scale instabilities and electric cell formation. For typical conditions of thundercloud estimations and numerical calculations give the characteristic size of these cells of order of some tens of meters.

We have considered also dusty plasma collective interaction under fair weather conditions. The nonequilibrium system has been investigated, which includes positive and negative light ions moving in electric field, and aerosol particles. Ion-

aerosol attachment coefficients are assumed to depend on the electric field strength. A characteristic scale of structures formed depends on the drift velocity of light ions, the air conductivity and the stationary concentration of neutral aerosol particles. A model can explain recently observed [11,12] meso-scale structures formation in the surface atmospheric layer as a result of a dynamic instability development.

5. CONCLUSIONS

Unlike other atmospheric subsystems, the electrical one provides a unique scalar index of the global status of the atmosphere. The electric state of the atmosphere is characterized by the stationary distribution of electric field, conductivity and electric current density, as well as by the presence of EHD structures of global, regional and local scales. Many natural processes (energetic particle precipitations, radioactive emanation, volcanic eruptions) and anthropogenic phenomena (aerosol releases due to man-made activity, radioactive pollutions, large-scale explosions and fires) eventually disturb the distribution of electric conductivity and change substantially the state of the global circuit. Significant recent investigations were devoted to possible implications of the global temperature change and global lightning distributions. Another important field of relevant research is stimulated by the looking for mechanisms of earthquake electromagnetic effects.

Further progress in the terrestrial electrical environment research is impossible without close link of observations and theoretical modelling. Now one of the main instruments for theoretical investigation of inherent electric processes in the atmosphere is suggested to be electrohydrodynamics of weakly conducting medium generalized in terms of aerosol particulate allowance. EHD approach has been proved to be a powerful method for the analysis of wave perturbations, turbulence, dissipation instabilities and structures in the atmosphere. basic ideas and applications. In particular, it is a mean for adequate analysis of active processes in the middle atmosphere and explanation of respective rocket measurements indicating the existence of large electric fields of unknown origins, correlated with abnormally high aerosol density occurrence. On the base of EHD approach a problem of turbulent electric dynamo is being formulated and studied as applied to large-scale electric field generation during thunderstorms and dust storms.

Acknowledgements. This work has been supported by the Russian Fund for Basic Research (grant N00-02-17758) and INTAS grant N 97-1372.

6. REFERENCES

- 5.1 "Dusty and dirty plasmas, noise and chaos in space and in the laboratory". Ed. by H.Kikuchi, Plenum Press, New York, 1994.
- 5.2 E.A. Bering III, A.A. Few, and J.R. Benbrook, "The global electric circuit", *Physics Today*, V.51, October 1998, pp.24-30.
- 5.3 W. Gringel, J.M. Rosen, and D.J. Hofmann, "Electrical structure from 0 to 30 km". In: *The Earth's Electrical Environment*. Ed. by E.P. Krider and R.G. Roble, National Academy Press, Washington, D.C., 1986, pp.166-182.
- 5.4 A.K. Kamra, "Experimental study of the electrification produced by dispersion of dust into the air", *J. Appl. Phys.*, Vol.44, No.1, 1973, pp. 125-131.
- 5.5 V.V. Smirnov, "Electric field of dust streams" (in Russian), *Izvestiya, Atmospheric and Oceanic Physics*, Vol. 35, No.5, 1999, pp. 616-623.
- 5.6 E.A. Mareev and V.Yu. Trakhtengerts, On the problem of electric dynamo, *Radiophysics and Quantum Electronics*, Vol.39, No.6, 1996, pp. 797-814.
- 5.7 E.A. Mareev, "Turbulent electric dynamo in thunderstorm clouds", *Proc.11th Int. Conf. on Atmos. Electr.*, Huntsville, USA, MSFC, 1999, pp.272-275.
- 5.8 D.R. MacGorman and W.D. Rust, "The electrical nature of storms", Oxford University Press, New York - Oxford, 1998, 422 p.
- 5.9 Journal of Atmospheric and Solar-Terrestrial Physics, Special Issue: "Effects of thunderstorm activity on the upper atmosphere and ionosphere", V.60, N 7-9, May-June 1998.
- 5.10 E.I. Smirnova, E.A. Mareev and Yu.V. Chugunov, "Modeling of lightning-generated electric field transitional processes", submitted to *GRL*, 2000.
- 5.11 S.V. Anisimov, E.A. Mareev and S.S. Bakastov, "On the generation and evolution of aeroelectric structures in the surface layer", *J. Geophys. Res.*, V.104, 1999, pp. 14359-14367.
- 5.12 S.V. Anisimov and E.A. Mareev, "Aeroelectric structures in the atmosphere" (in Russian), *Dokl. Acad. Nauk*, V.371, 2000.
- 5.13 E.A. Mareev and G.F. Sarafanov, "On spatial structures formation in dusty plasmas", *Physics of Plasmas*, Vol.5, No.5, May 1998, pp. 1563-1565.
- 5.14 E.A. Mareev, A.E. Sorokin and V.Yu. Trakhtengerts, "Collective charging effects in thunderstorm clouds", *Proc.10th Int. Conf. on Atmos. Electr.*, Osaka, Japan, 1996, pp.544-547.
- 5.15 E.A. Mareev, A.E. Sorokin and V.Yu. Trakhtengerts, "Collective charging effects in multi-vol aerosol plasma", *Plasma Physics Reports*, Vol.25, No.3, 1999, pp. 289-300.

THE ANOMALY UNSTABLE POLARIZATION FADING OF HF WAVE PROPAGATION APPEARED AT THE EARTHQUAKE IN TURKEY OF 1999

Umolk Dinan

(Ionosphere Monitoring Labs.)

(Univ. of Ankara)

Now he is in Fukui Univ. of Tech. Fukui, Japan.

Takeo Yoshino

Fukui University of Technology

2-36-22 Zempukuji, Suginamiku, Tokyo 167-0041, Japan.

Tel/Fax: +81-3-3397-5577, e-mail: yoshinot@nisiq.net

Abstract: The western Turkey had attacked a major earthquake of $M = 7.4$ at 00:01:39.80 UT of August 17 in 1999, along the North Anatolian fault. And the epicenter of this earthquake was located on the Kocaeri village which only few km south of Izmit city in the western end of Asian Turkey. Next major earthquake was following occurred at 16:57:20 UT of November 12, 1999 in the eastern Turkey. The epicenter location of second earthquake is 70 km east of Adapazari and 170km northwest of Ankara city. The magnitude was $M = 7.2$ and the focus is also locate on the north Anatolian fault. About 5 days prior to 2 hrs after of main shock of both earthquakes, the multi-frequency polarization fading detectors installed in the Ionosphere Monitoring Labs. of Turkey P.T.T. and Ankara University recorded the anomaly unstable fast fading signal, it seems to generated by the quick rotation of the polarization at the ionosphere disturbance. This paper describe the observation results and some discussion about the mechanism of this phenomena in the physically relation between the earthquake activity and the increasing of ordinary and extraordinary wave

activity in the ionosphere of the top area of epicenter.

INTRODUCTION

The $M = 7.4$ earthquake that struck western Turkey at 00:01:39.80 UT on August 17, 1999 occurred on one of the world's longest and best studied strike-slip faults: the east-west trending North Anatolian fault. The epicenter location of this earthquake is on the Kocaeli town that only few km southern of Izmit city center. Epicenter location is 40.702°N and 29.987°E , Depth of Focus is 17 km, and this location is in the western end of Asian portion of Turkey. About 3 months after Izmit earthquake, The $M = 7.2$ major earthquake occurred 70 km east of Adapazari or 170 km northwest of Ankara city, at 16:57:20 UT November 12, 1999. This earthquake is located about 110 km east along the Anatolian fault of the magnitude 7.4 main-shock on August 17, and the detailed location is near Duzce of Bolu districts. Epicenter location of this earthquake is 40.79°N And 31.11°E , and the depth of focus is about 10 km. The authors used all these data obtained from

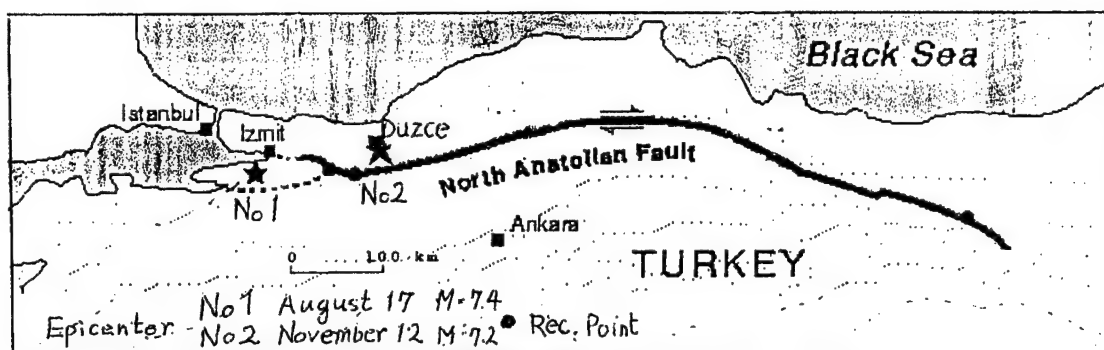


Fig. 1. The location of epicenters of IZMIT earthquake (August 17, 1999, $M = 7.4$) and Duzce earthquake (November 12, 1999, $M = 7.2$) on the east portion of North Anatolia Fault in the Turkey.

Kandili Observatory of Bogazici University, Turkey.

The map and locations of these earthquakes and Anatolian fault are shown in Fig. 1.

The multi-frequency polarization fading detector installed in the observatory of Ionosphere Monitoring Laboratory of Turkey P.P.T. and operated by University of Ankara had been observed frequently several anomaly unstable fast polarization fading signals about 5 days prior to 2 hours after main shock at both earthquakes. The fast fading signals are coming from northern side across North Anatolian fault. And the location of this observatory is located about 120 km south suburbs of Ankara city. The carrier frequencies of these quick polarization fading signals were spread between 6 MHz to 12 MHz HF signals. At the August earthquake, the locations of transmitting stations spread over the northwest direction from the receiving point in the central Hungary, for example, the stations of Sofia, Stara Zagora and etc. At the November earthquake, the location of transmitting stations spread over the north direction from the receiving point around Hungary and west Ukraine. This is a very interesting point that these HF signals are coming from northern side of North Anatolian fault and all their path are across on the top of epicenter area. It seems to produce of the quick rotation of polarization of radio waves by the

ionosphere disturbances with the unknown effects of the earthquakes. In fact that these radio signals had never appeared usually such quick polarization fading except only very short times of sunrise or sunset. Fig.2 shows the locations of observation point, the radio transmitters area for August earthquake by \bigcirc mark and for November earthquake by \triangle mark of northern side of the North Anatolian fault. As shown in this figure, the radio wave orbits at both earthquakes have a good correspondence to crossing over the epicenter areas.

POLARIZATION

By the generalized magnetoionic theory (today's plasma physics), when the electromagnetic wave propagating in the plasma (ionized gas) media, the wave are separated two waves which have different phase velocities each other according to the Appleton formula, named as ordinary wave (O-wave) and extraordinary wave (X-wave).

The O-wave and X-wave are always rotate to contrariwise each other on the wave front plane of the wave normal along the axis of propagation direction in the Plasma media.

The rotation velocities and direction of wave normal are determined by the directions of the wave normal

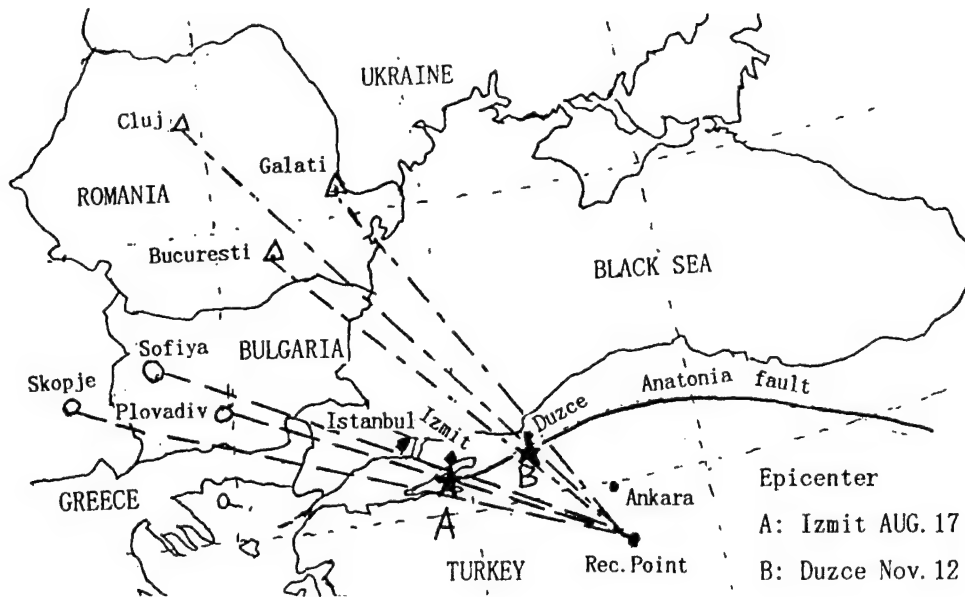


Fig. 2 Locations of transmitters which observed the Fast Polarization Fading the earthquakes of 1999 in Turkey. ○ (Izmit August 17, 1999) △ (Duzce November 12, 1999)

direction of incident wave and the direction of geomagnetic flux in the ionosphere, the ratio between plasma frequency (f_n) and frequency of carrier wave (f) and carrier wave frequency is higher or lower than the gyro frequency (f_h) and etc.

The polarization of radio wave front is generated by the interaction between the electric fields of O-wave and X-wave, which rotated to contrariwise direction. In the quiet ionosphere, the rotation speed of O-wave and X-wave is rotated with almost similar angular velocity, then the compound wave front of receiving wave seems to be rotate with very slowly and stable. Usually, the appearance of the fast polarization Fading will be very rare case in the low latitude and the short distance ionosphere propagation within 1000 km of the lower HF frequency wave as in the regions of Middle East. When the appearance of quick or fast polarization fading, the rotation velocities between O-wave and X-wave will be very different value, one is fast and other is slowly toward inverse direction. The anomaly phenomena occur to the electric field of wave normal of O-wave (X-wave)

takes quasi parallel to local geomagnetic field in the lower ionosphere, and X-wave (O-wave) of electron motion in a plane quasi perpendicular to the magnetic field by the anomaly variation of magnetic field in the ionosphere.

OBSERVATION RESULT OF FAST POLARIZATION FADING

Fig. 3 shows one of the examples of observation result of fast polarization at Izmit earthquake of August 17, 1999. The data recorded at receiving point of Ionosphere Monitoring Labs. About 5 days prior to earthquake, the signals came from northwest will be started the polarization fading. The fading range was gradually increased from 2 rotations per minute and until one rot/sec at main shock. Fig. 4 shows the occurrence data of fast polarization fading at Duzce earthquake of November 12, 1999. The data obtain very similar characteristics on the data at Izmit earthquake as shown in these figures.

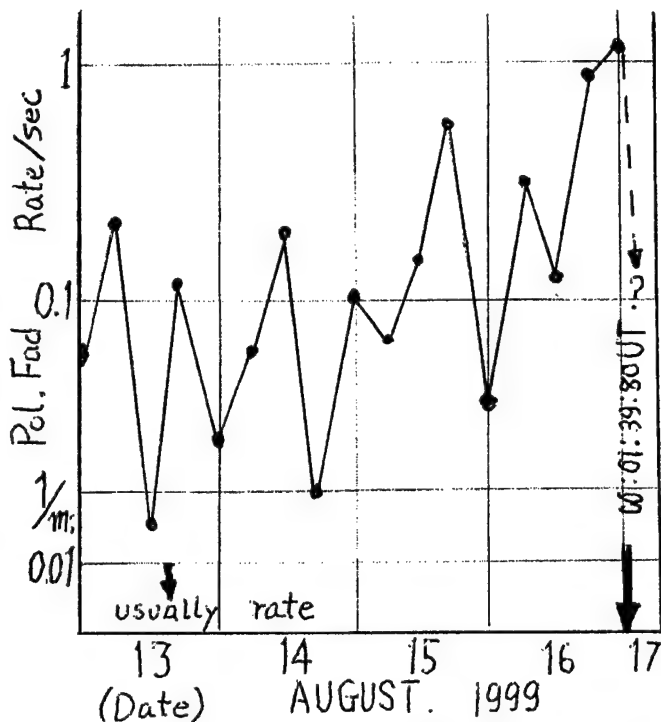


Fig. 3 Polarization Fading Rate at Izmit.

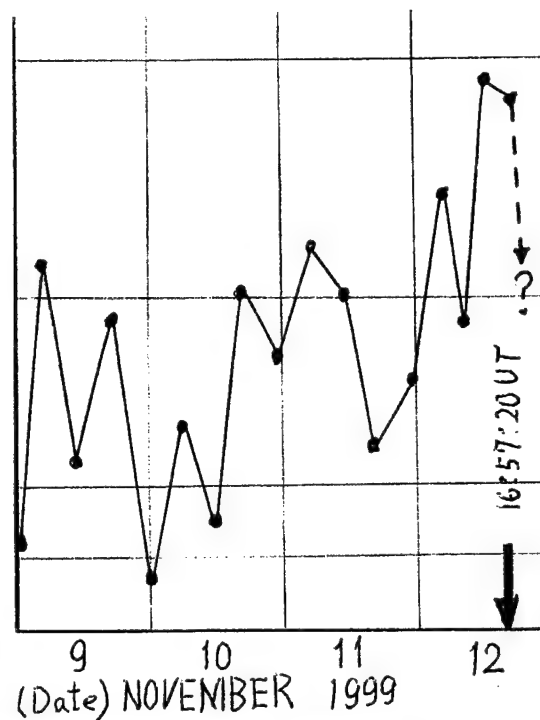


Fig. 4 Polarization Fading Rate at Duzce earthquake.

CONCLUSION

The authors possibly found a new ionosphere disturbance phenomena related by the pre-seismic effects at Izmit earthquake ($M = 7.4$) of August 17, 1999 and at Duzce earthquake ($M = 7.2$) of November 12, 1999 in Turkey. Both earthquakes occurred on the North Anatolia fault and the epicenter of Izmit earthquake was located western end of Asian continent, and Duzce earthquake was located only 110km east of the epicenter of Izmit earthquake. At both cases, the polarization wave measurement facility of Ionosphere Monitoring Labs. of Turkey P.T.T. observed anomaly fast polarization fading of lower HF band signals arrived across the North Anatolian fault from 5 days prior to main shock. Polarization fading speed were started slowly (2 rotations per minute) and finally increased to one rotation per second. The signals transmitted about 1000 km far and their frequency

range was spread between 5 MHz to 12 MHz at both cases. The directions of transmitting points spread north-western region at Izmit earthquake and north-eastern region at Duzce earthquake as shown in Fig. 2. These observation results suggest the pre-seismic effects will effected to the electric or magnetic field variation which produced the polarization anomaly to gave the different effect to O-wave and X-wave propagation characteristics. Now authors only detected the data, but we have not any distinctly the source mechanism of the phenomena. The authors wish to continue the clear of investigation of mechanism based on the observation data. And finally the author have to clear physically the source mechanism, what kinds of energy have generated at focus of earthquake and how this energy is transmit through soils to ground surface of epicenter area. And how to convert the penetrate mode energy to the electromagnetic noise wave radiation around the ground surface or emitted the EM wave at the bottom of ionosphere.

PLASMASPHERIC LOW-FREQUENCY EMISSION INTENSITY and SPECTRUM VARIATIONS over PREPARATION ZONES of QUICK (SEISMOGENOUS) and SLOW GEODYNAMIC PROCESSES in the EARTH CRUST

Larkina V.I., Ruzhin Yu. Ya.

IZMIRAN, Troitsk town, Moscow Region, 142092. Russia

larkina@izm-iran.rssi.ru

Results the last of satellite researches of electromagnetic signals in near-Earth space have shown that an ionosphere, as a whole, and the phenomena proceeding in it are a indicator of certain (determined) processes in the lithosphere. Presented below results of data processing, received on "Intercosmos 19" satellite give additional acknowledgement existence electromagnetic manifestations of lithospheric processes in top ionosphere. Thus revealed in given work electromagnetic processes are unequivocally connected not with catastrophic manifestation of seismic activity (such as earthquakes), and to current processes, while not clearer, occurring in the lithosphere.

Variations of low-frequency emissions and accompanying electromagnetic effects above deep faults of Baltic-Barents region.

Onboard "Intercosmos 19" satellite at its flight above deep faults of lithosphere in Barents-Kara sea region bursts of low-frequency emission intensity were discovered.

The amplitude of bursts exceeded a level of own noise, usually observable on these latitudes. The bursts of noise are reasonably located. Maximum frequency in spectra of observable signals 140-450 Hz. And it is possible and below (frequency 140 Hz - bottom frequency of a equipment). The amplitude of bursts of emissions essentially depends on thickness of earthly crust, on thickness of a sedimental cover and etc. [1].

Correlation analysis has shown, that the observable emissions have electromagnetic character. A correlation coefficient of curve of bursts of magnetic and electrical components of emission fields is 0.6 - 0.72. Simultaneously with bursts of emission intensity abnormal changes of temperature of environmental plasma were registered flows of low energy electrons ($E_e \sim 50$ eV and $E_e \sim 120$ eV). Unfortunately, on latitudes of Barents-Kara sea region ($L \geq 6$) flows of quasitrapped electrons ($E_e \geq 40$ keV) very weak. Nevertheless, occasionally, in a disturbed time they are observed (for example, [1]).

Results of observations of low-frequency emission over Middle Asia deep fault.

The results of observations of low-frequency emission intensity variations above deep fault of Black-Sea - Middle Asia differ from similar results, received in Barents-Kara Sea Region. By us follow abnormal changes of fields of noise above deep fault of lithosphere, taking place on a line Ashkhabad - Nebit - Dag - Krasnovodsk - Taman. It was revealed, that the observable emissions has electrostatic character, bursts of a electrical components of emission fields prevail. The correlation analysis it has confirmed. The correlation coefficient of bending around bursts of a magnetic and electrical components of noise field has compounded 0.15-0.2 Maxima in a noise spectrum was registered on frequency 4650 Hz.

Variations of low-frequency emissions and quasitrapped electrons close deep fault of lithosphere in northern part Pacific Ocean

At flight "Intercosmos 19" satellite close above deep fault of lithosphere in northern part of the Pacific ocean the bursts of intensity of a magnetic and electrical component of emission field were observed. Correlation analysis has confirmed, that observable emissions are electromagnetic, the correlation coefficient has compounded 0.6 - 0.75 Maxima in a spectrum of noise was registered on frequencies below 1 kHz.

Simultaneously with abnormal changes of intensity of noise bursts of density of a quasitrapped electrons (Ee

≥ 40 keV) flows were registered. It is interesting to note, that above fault of northern hemisphere abnormal noise bursts and particles are observed simultaneously, in the same place of a projection of a satellite orbit, and in southern, magneto-conjugated hemisphere, the bursts of noise and particles were take to the space. The bursts of particles were observed on the same L-shell, as in northern hemisphere (L~2), and bursts of waves were observed a little souther (L~2-2,2).

Conclusions:

There are considered variations of low-frequency emissions, electron flows and plasma parameters above deep faults of the lithosphere in three geographical regions:

- Barents - Kara Sea,
 - Black sea - Average Asia,
 - Northern part of the Pacific ocean.
1. Above deep faults of earthly crust abnormal bursts low-frequency emissions intensity are observed.
 2. The spectrum of noise above faults has a characteristic maximum, which will be quite agreed with latitudes of supervision.
 3. Above faults bursts of temperature of an environmental plasma are observed.
 4. Above deep faults of earthly crust abnormal bursts of electron flows, energy of registered particles differs for various regions are observed.
 5. The observable effects (of intensity variation of ones) depend on a site faults: on a land, on the sea.

Reference:

1. Larkina V.I., Sergeeva N.G., Senin B.V. (in present volume).

ANOMALIES OF IONOSPHERE TEC ABOVE THE TURKEY BEFORE TWO STRONG EARTHQUAKES AT 1999.

Oraevsky V.N., Ruzhin Yu.Ya., I.I.Shagimuratov
IZMIRAN, Troitsk-town, Moscow region, 142190 RUSSIA
E-mail: ruzhin@izmiran.rssi.ru

ABSTRACT

The present status of seismoionosphere precursors and the importance of presented pre-earthquake TEC Turkey anomalies are discussed.

1. INTRODUCTION

For today the space plasma precursors are known as electromagnetic disturbance [1,2] and as ionosphere plasma density structure [3-5] of different spatial and time scale behaviour. Possibility to use such anomalies for earthquake prediction is discussed more than 15 years (see [6] and reference therein). But up to now the main problem is limited experimental data due to complex space plasma images which varies in dependence of local time and very sensitive to geographic position [7,8]. Thus the sequence of the two Turkish earthquake of 1999 (August 17 and November 12) with magnitude more than 7.0 which occur practically at the same localisation (only 100km difference) could be as rare object of intensive investigation by involving all possible experimental data of classic seismomonitoring as well as some kind of atmosphere and ionosphere available data. Here we start to present some ionosphere or space plasma anomalies which appear as specific variation of total electron content (TEC) above the epicentre area on the eve of destructive earthquakes. This data is result of analyses of GPS data base of global net [9,10].

2. EXPERIMENTAL CONDITIONS.

Seismotectonic Summary

For the Turkish Earthquake of Aug. 17, 1999 (see later as EQ1) the initial preliminary magnitude, of 7.8, was based on recordings of seismic waves from a limited number of global stations that rapidly transmit data to the U.S. Geological Survey's National Earthquake Information Centre (NEIC) in Golden, Colo. The Izmit earthquake occurred at 00:01:39.80 UT (3:01 a.m. local time), and was centred at 40.702 N., 29.987 E., which places the epicentre about 11 kilometres Southeast of the city of Izmit. This location indicates that the earthquake occurred on the

northernmost strand of the North Anatolian fault system. The earthquake originated at a depth of 17 kilometres and caused right-lateral strike-slip movement on the fault. Preliminary field reports confirm this type of motion on the fault, and initial field observations indicate that the earthquake produced at least 60 kilometres of surface rupture and right-lateral offsets as large as 2.7 meters. Rupture from west to east, in two rupture events. Duration of strong shaking 37 seconds; maximum fault displacement 5 meters. The 900 km-long North Anatolian fault has many characteristics [11] similar to California's San Andreas fault. These two faults are right-lateral, strike-slip faults having similar lengths and similar long-term rates of movement.

The second earthquake (EQ2) with magnitude of 7.5 occurred at November 12, 1999 (16:57:19 UT) on the short distance (less of 100km) from EQ1 epicentre and was centred at 40.8N, 31.2E.

Ionosphere pre-earthquake disturbances in TEC around Ankara

As introduction of disposition geometry on FIG.1 the map of events for earthquake of 12th November (EQ2) is presented with foreshocks and aftershocks. The EQ1 of 17th august appears without foreshocks. The positions of base station Ankara of GPS ground net and epicentre of EQ1 are marked also. Let's note that more important information is received from GPS/Glonass satellites which tracks of subionosphere points are around the epicentres of both EQ. The all horizontal tracks of such satellites which intersect the epicentre area for EQ1 are shown on FIG.1 with corresponding the satellite number (GPS-3, GPS-14, GPS-15 and GPS-30). This orbit tracks are responsible for day time period when the anomalies of 'min' type (see Fig.2) or pre-earthquake plasma trough appear less than one day before the EQ1.

GPS NAVSTAR [9] is complete today and the Russian system GLONASS is nearly too. GPS consists of 24 satellites with 12-hour orbits at altitudes of 20000 km, having orbital inclinations about 55°. The number of satellites simultaneously seen in any point of the earth and in any moment of a time is more than 6, so GPS provides superior sky coverage (that enables realisation of continuous

ionosphere monitoring in several space sectors simultaneously). The GPS-receiver makes measurements [12] of group delay of a signal on P- and CA-codes and phase bearing on L1 (1.575 GHz) and L2 (1.227 GHz). The system GPS permits to measure not only phase, but also group delay of signals, propagated through ionosphere. Opportunity to measure the group delay and therefore to conduct measurements of the absolute electron contents (along a ray of sounding radiowave) eliminates a problem [12] of unknown initial phase always existing for phase measurements of TRANSIT type satellite system (frequency 150/ 400 MHz).

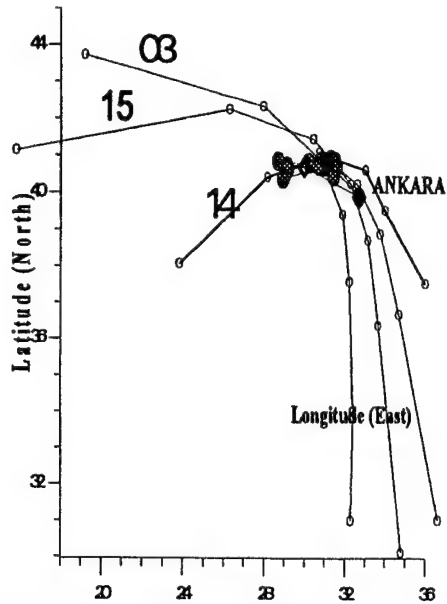


Fig.1. Geometry of main discussed points. 03,14,15 and 30 are subionosphere tracks of GPS satellites.

On Fig.2. the sequence of two plots of $DTEC = TEC_{corr} - TEC_{med}$ over Ankara area are derived from GPS/ISG data station measurement during the ionosphere perturbation on August and November 1999. DTEC is measured in units of $10E16m^{-2}$ or TECU. Here TEC_{corr} is corrected value of TEC and TEC_{med} is monthly median for Ankara station of GPS measurements.

We can surely see the specific positive-negative (or "max-min" structure) variations DTEC on eve the both earthquakes which can be as precursors of these EQs. The positive part of preseismic TEC variation as well as following negative bay begin to develop at sunrise time and are the day (sunlit time) events (see Fig.3a also). This is obvious difference of TEC precursor anomalies from preseismic plasma density or f_oF2 variations which is usually nocturnal one [3,4,5]. It is possible to characterise the ionisation of the F2-layer with a single parameters by the so-called critical frequency (maximal plasma frequency f_oF2) which is connected with the maximal electron density N_{max} that $(f_oF2)^2 = 80.6 * N_{max}$. So the main parameters of the ionosphere F2 layer displays the precursor type plasma anomalies by different ways. During time of

EQ1 preparation appear the possibility to observe in TEC of Ankara the action of Moon shadow on earth ionosphere (August 11,1999) as known source of ionosphere ionisation.

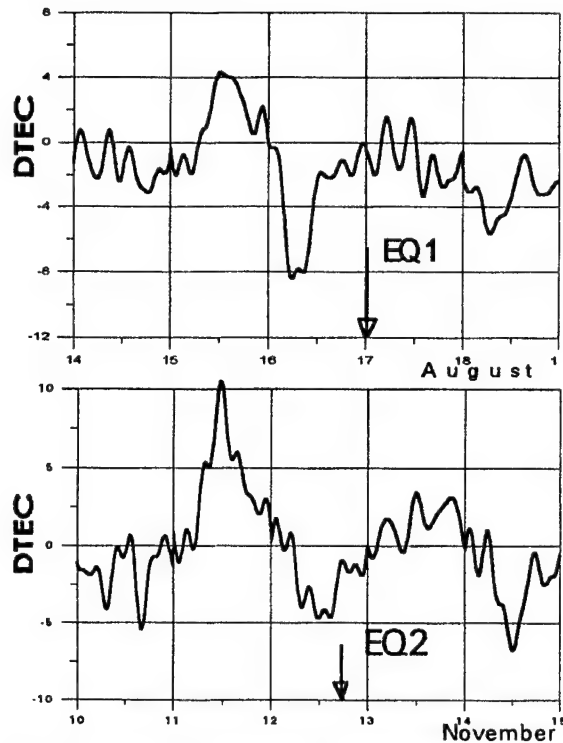


Fig.2. Preseismic ionosphere disturbance as GPS DTEC variations.

The "min" part of pre-EQ variations are shown in comparison with similar negative DTEC bay due to Solar eclipse action on Fig.3 for both earthquake. The deep plasma trough (a few TECU) in GPS derived DTEC data is observed which is caused by Moon shadow action on ionosphere above the Turkey area of future EQs. It is good chance to compare these TEC data for estimation of the effectivity of EQs as source of ionosphere disturbances.

3. DISCUSSION

The plasma anomalous structures at the ionosphere (N_{max} or maximal plasma frequency f_oF2) as kind of earthquake precursors are usually nocturnal ionospheric anomalies in plasma density distribution which appear over the preparation region some days before the earthquake and can be caused by local preseismic changes of the electrical parameters of the spherical condenser (capacitor) formed by the two high conductive shells: Earth's surface and lowest ionosphere boundary [3,5].

Such variations of the atmosphere electricity cause appropriate electric field at the ionospheric heights, which being added to existing natural field may both increase or decrease its action [8] on the ionospheric plasma characteristics: drifts, aeronomy, plasma chemistry, ion composition etc. Anomalous variations

appear inside whole ionosphere volume from the lowest boundary of Earth's plasma shell (80-100 km) up to 1000km and higher. Under fortunate coincidence precursor electric field can generate natural phenomena, 'fountain-effect' for example [5] leading to Appleton anomaly in the equatorial ionosphere over future earthquake position. The precursor horizontal size at ionosphere can reach value determined by a

future earthquake magnitude[3,5]. Both the preparation zone form in the lithosphere and the natural processes in the ionosphere depended on [8] the epicentre latitude, observational place, time, season and/or gelio-geophysical activity can influence on the concentricity and final dimension of plasma anomaly in horizontal plane.

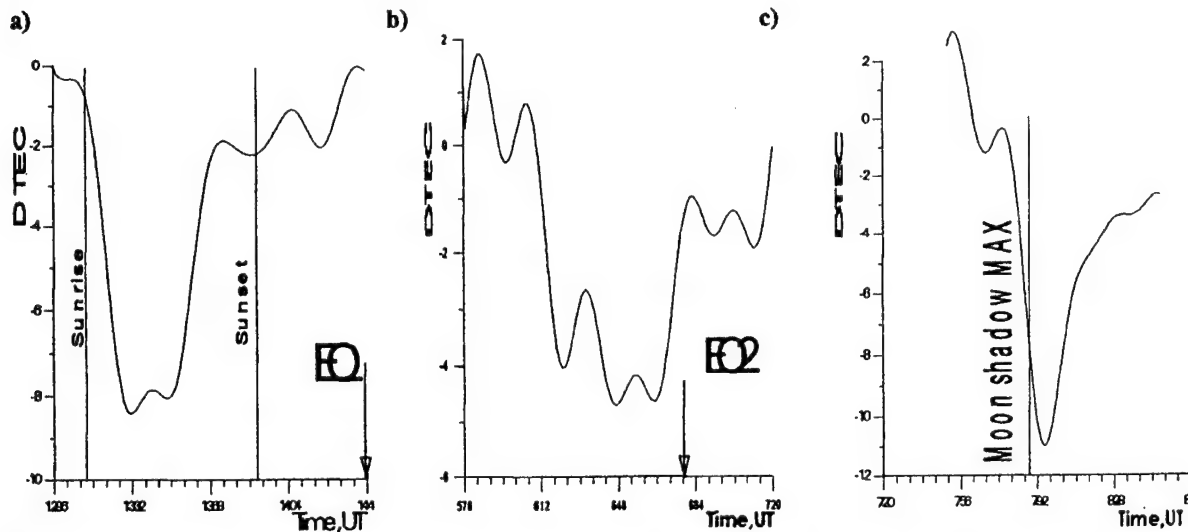


Fig.3. The three plots presents negative bays (or "min" of precursor structure) in DTEC for the EQ1-EQ2 and Solar eclipse effect in ionosphere above the Ankara. The time duration (horizontal axes) is one day or 24hrs (from midnight to midnight, Greenwich time)

The other way to characterise the ionisation of the F2-layer with a single parameters is to use the vertical total electron content (TEC) [13] which correspond to the integral of electron density over the height from the bottom to upper boundary or transmitting satellite orbit. As base of TEC measurements the radio-beacon on board of satellites have played an important role [13] in the study of the temporal and spatial structure of the ionosphere over nearly three decades.

Maximum electron density and TEC are connected over equivalent slab thickness τ : $TEC = N_{max} \cdot \tau$. Because the variability of the equivalent slab thickness is much smaller than that of TEC or that of the maximal electron density the long-term behaviour of TEC and N_{max} and also TEC and f_oF2 is often similar.

But in case of pre-earthquake anomalies it is a quiet different. The DTECU variations before the EQ (see Fig.2) occurs as combination or consequence of positive-negative variations. So it is necessary separately to examine the dependence of $TEC = N_{max} \cdot \tau$ during such ionosphere disturbances with maximum attention. The physical mechanism of the pre_EQ TEC behaviour is not yet fully understood. Obviously that it is physically related to the lithosphere area which involved in preseismic activity. Since the EQ TEC is characterised by the world wide deepest ionisation level (a few TECU) it provides a good check for the quality of GPS derived TEC data. It is évident [10] that the GPS/IGS data cannot reach

the spatial resolution of NNSS (TRANSIT) observations. However, the pre-EQ TEC is also well reflected in the GPS/IGS data. So its occurrence and movement may be studied by GPS techniques.

4. CONCLUSION

Precursors type of ionosphere total electron content anomalies for two destructive earthquakes in Turkey (at 1999) is analysed on base of TEC of GPS net.. We found the ionosphere anomalies which well pronounced one-two days before the two well known Turkey earthquakes of 1999 with magnitude more than $M=7.0$. For statistical purposes the number of these cases is negligible but for both earthquakes the ionosphere plasma TEC anomalies are very similar in form and dynamic. In comparison we use the TEC anomaly which is result of Sun shadowing of ionosphere by Moon in this region some days before the first destructive Turkey earthquake of 17th August of 1999. It is supported by existed in IZMIRAN classification of space plasma anomalies which appear to be as the seismoprecursors for existed system to improve the forecast of imminent earthquakes. It is proposed that the space plasma TEC anomalies could be as precursors for earthquake prediction

5. REFERENCES.

1. Larkina V.I., Migulin V.V., Nalivaiko A.V. et al. *Observation onboard the "Intercosmos 19" satellite of VLF emissions associated with seismic activity* // Geomagn. i Aeronom. 1983. V.23, N 5. P. 842-845
2. M.Parrot, J.Achache, J.J.Berthelier, E.Blanc, A.Deschamps, F.Lefeuvre, M.Menvielle, et al *High-frequency seismo-electromagnetic effects*, Phys. Earth Planet. Inter., 77, 65-83, 1993
3. Oraevsky V.N., Yu.Ya. Ruzhin, A.Kh.Depueva, *Seismoionospheric Precursors and Atmospheric Electricity*, Tr. J.of Physics, 18. '11. p.1229-1234, 1994
4. Pulinets S.A., Legen'ka A.D., Alekseev V.A. *Pre-earthquakes ionospheric effects and their possible mechanisms*, In Dusty and Dirty Plasmas, Noise and Chaos in Space and in the Laboratory: New-York: Plenum Publishing, pp.. 545-557,1994..
5. Ruzhin Yu.Ya., Depueva A.K., *Seismoprecursors in space as plasma and wave anomalies*, Journal of Atmospheric Electricity, vol.16, no.3, pp.271-288. 1996
6. *Electromagnetic Phenomena Related to Earthquake Prediction*, ed.M.Haiakawa and Y.Fujinawa, TERRAPUB,Tokyo, pp.159-174, 1994
7. Ruzhin Yu.Ya., V.I.Larkina, and A.Kh.Depueva *Earthquake precursors in magnetically conjugated ionosphere regions*. Adv. Space Res.Vol.21, No.3, pp. 525-528, 1998
8. Ruzhin Y.Y., A. Depueva, *Regional (Local) Manifestation of Seismoprecursor Space Anomalies* Proceed.14th Wroclaw EMC Symposium (URSI) , pp.. 582-585, 1998
9. Calais E.,and J.B.Minster, *GPS detection of ionospheric perturbations following the January,17,1994,Northridge earthquake*, Geoph.Res.Lett.,22.1045-1048,1995
10. <http://www.grdl.noaa.gov/cgi-bin/tecmap.p>
11. Ross S. Stein , Aykut A. Barka and James H. Dieterich *Progressive failure on the North Anatolian fault since 1939 by earthquake stress triggering*. Geophysic. Journ. International, VOL 128, pp. 594-604, 1997
12. Ruzhin Yu.Ya., Shagimuratov I.I., Kunitsyn V.E., et al. *GPS-based tomographic reconstruction of the ionosphere*. Adv.Space Res., 21, No.3, pp.521-524, 1998
13. Evans J.V. *Satellite Beacon Contribution to Studies of the Structures of the Ionosphere*. Rew.Geoph.&Space Phys. Vol.15, No.3, p p.325-349, 1977

HIGH FREQUENCY SEISMOPRECURSOR EMISSIONS

Yu. Ruzhin (1), C. Nomicos (2), F. Vallianatos (3)

1- IZMIRAN, Moscow, Russia; 2- TEI of Athens, Greece; 3- TEI, Crete, Greece

E-mail: ruzhin@izmiran.rssi.ru

ABSTRACT

In the present work we are focusing our interest on the HF precursors recorded by the four electromagnetic stations a few days prior the event associated with earthquakes with magnitude more than 5.0 and located in the vicinity of Crete island. Some new peculiarity is found. This is underhorizon epicenter position for main part of events under question. The another unusual result is that such preseismic signals are responsible for seaquakes. In result, we made conclusion about existing of some thunderstorm type activity before the seismic event. It means that above sea (up to 3-8 kilometers) the space charge cloud would be generated at one-three days before the active seismicity. Additional experimental facts and mechanism are discussed to explain this HF seismoprecursor signals generation.

1. INTRODUCTION AND STATEMENT OF THE PROBLEM

Many electromagnetic phenomena in various ranges of frequencies are known which are connected to displays of seismic activity [1-3]. The electromagnetic precursors of earthquakes (EQ) in a ULF-range registered even on satellite orbits in the ionosphere [3,4]. A number of recent papers on earthquake electromagnetic effects, together with the literature on this subject, can be found in Special Issue [5]. Here we focus interest on a new kind of electromagnetic precursors of earthquakes - precursors in high frequency (HF) range, which were registered by four stations of a network on an island Crete [6,7]. The island Crete is located in a southern part of Hellenic arch and since 1992 for research of electromagnetic precursors on an island the special network of telemetering stations is developed [6]. Among other parameters the measurements of HF noise on two frequency 41 and 53 MHz are conducted, which nature is now actively investigated. It is shown, that HF signals or the candidate in precursors occurs at some days before the first displays of earthquakes occurring in Crete island vicinity. The aim of the present paper is to continue discussions on the possible relation between seismic activity and preceding HF radioemissions, started by Nomicos et al. [6].

3. THE ANALYSIS OF EXPERIMENTAL DATA

In the present work we carry out the analysis of the data on HF radioemission, which were received by a network of reception stations on an island Crete during three years (1992-1995) for earthquakes with magnitude M more than 5.0. In the Table the list of all earthquakes and their data for this period is given. Here h is depth of EQ epicentre (km). The preliminary analysis of these data carried out in works [6,7] gives us such sequence of events. HF signal probably connected with EQ, occurs 1-3 days prior to event, but after signals (3 and 10 kHz) of ULF range. The long existence of signals (see Fig.1) from several hours up to one day was marked also. Let's note at once, that the island Crete is removed from industrial interference of Greece and Turkey and is an ideal place for reception seismoeffective electromagnetic HF radio emission. The amplitude of registered signals of radioemission is rather enough intensive to take in attention the astronomical radio-sources.

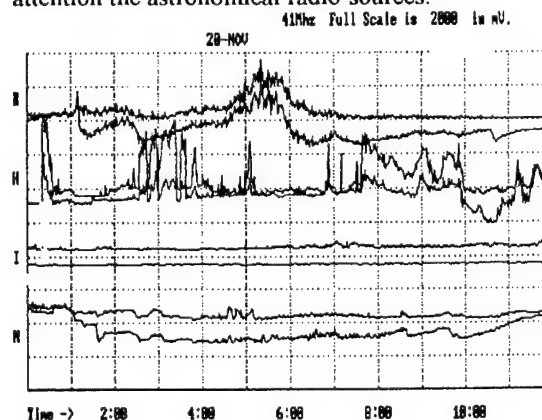


Fig1. The seismogenic HF signals for earthquake N1 of Table. N, I, H and D are the Crete stations symbol (Nipos, Heraklio, Ierapetra and Drapania)

The basic relation for the analysis

For HF range on distances $R > 2\pi\lambda$ (length of a wave $\lambda = 6-7.5\text{m}$) condition of optical propagation is satisfied. As result for distances 50-300 km the reception of signals is possible, if a source of radiation or/and the reception aerial are lifted above the ground

(sea level). If on ways of propagation there is an obstacle and the receiver gets in a zone of a radio-shadow, in case of absence of signals it is possible to calculate height where the source already is absent, and in case of presence of signals it is possible to estimate minimal height of radiation taking place above an obstacle. First step in our analysis was an estimation of horizon position for each of station of measurements (see Table) on the formula:

$$R = 3.55\sqrt{h_{ant}}, \quad (1)$$

(here R - distance up to horizon in km, and h_{ant} - height of the reception aerial in meters).

This parameter R is given in the Table under the appropriate name of each station. Let's note, that the account of refraction influence on HF propagation in troposphere gives a variation of R in some percents. The distance D for each station (to epicenter) before the appropriate earthquake was calculated as length of an arch of the big circle intersected through two points. It is determined by the appropriate central angle α_i which in geographical system of coordinates calculated under the formula:

$$\cos \alpha_i = \sin \varphi_1 * \sin \varphi_0 + \cos \varphi_1 * \cos \varphi_0 * \cos \Delta\lambda \quad (2)$$

Here φ_0 and φ_1 - latitudes of earthquake and reception station and $\Delta\lambda = \lambda_1 - \lambda_0$ - difference of its longitudes.

Comparing the ranges up to horizon and up to epicenter for each of stations, we find out, that always $D > R$ (see. Table) and actually all earthquakes are below the horizon. Taking into account, that the frequencies 41 and 53 MHz are not reflected from ionosphere, the superhorizon propagation is possible only if radiating and/or reception points are lifted above ground to heights H and h_{ant} accordingly. Proceeding from this geometry were calculated the minimal heights H_i of radiating points above epicenters of the future earthquakes for each station under the formula:

$$H_i = R_e / \cos(\alpha - \alpha_{ant}) \quad (3)$$

Where R_e - radius of the Earth ($R_e = 6372 \text{ km}$), and α_{ant} is determined by a ratio $\cos \alpha_{ant} = R_e / (R_e + h_{ant})$ and depends on height of the accepting aerial above a sea level.

Results of the analysis.

In Table the calculated H_i heights of radiation are allocated with a bold font only for those cases, when at concrete station the signals for both frequencies simultaneously are found out. On FIG.2 the results of the analysis for all cases of signals reception (distance more 100km) are submitted: range (D) - height (H). It is well visible, that radiating points of the radio-frequencies 41 and 53 MHz are in a range of heights from hundred meters up to several kilometers above a sea level. This unexpected conclusion is basic for an establishment of a nature of such signals generation mechanism. The following important fact is that practically all earthquakes for which are found out HF signal- precursors are seaquakes, i.e. them epicenters are under bottom of the sea. From the Table it is visible, that for full period of observation only for 4

earthquakes (N3; N8; N12; N16) the HF signals was not registered on any of stations. It is an occasion for the further research.

At the detailed analysis of absence of signals for other events by calculating azimuths of directions on appropriate epicenters by us was established, that the majority of the misses in the Table (absence of a signal at concrete station of a network) can be explained as screening (effect of a shadow) appropriate direction on a source by mountain, island or losses due to range increase. Not stopping on details, we shall note, that we could find a reasonable explanation of signal absence (proceeding from the analysis of concrete local conditions) for all events from the Table.

Let's result some most obvious examples. So for earthquake N3 a signal absent only at station Heraclion. It is established that in a direction on epicenter there was a mountain of height in 2000 meters, which provided shadow of radiation heights up to 12 km above epicenter. Similarly for a case N10 and Ierapetra: the shadow of emission height reached 19 km! Absence of a signal for event N19 at three stations could be result of attenuation of a signal by longer distance or shadow from islands. It is possible to note after such analysis for all events of the Table that the source seismogenic radioemission was more often at heights more 1-3 km (for events 11, 17 and 18 the heights are lower of 2,7 km).

For the more thin analysis further it is necessary to take into account, that the absence of a signal or its attenuation on occasion could be also connected to feature of used aeriels (horizontal halfwave dipole). So the horizontal polarization of antenna could not coincide with polarization coming EME of a wave, and the presence of a dead zone of reception along an axis of dipole could too affect on quality of signals reception.

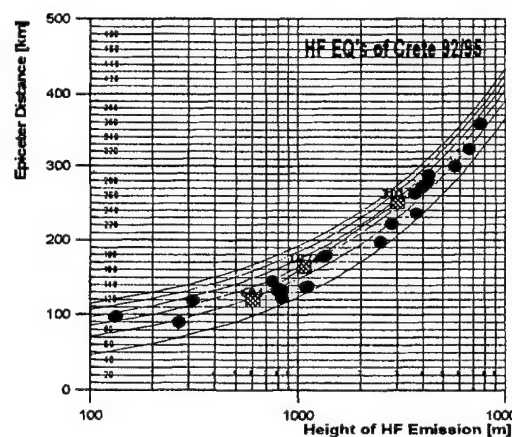


Fig.2. The minimum emitting heights .

4. DISCUSSION

The natural radioemission in HF range is very anomalous phenomenon and sometime can be observed as result of auroral activity [8,9] or artificial beam-plasma injection [10]. More realistic source of

broadband radioemission are thunderstorm [11-13] or lightning sources. First of all we examine all events of Table by this criteria (or meteorological processes) in map area and do not find any direct coincidence. More over such kind of HF range emission must eliminate the fine correlation in form and temporary behavior with ELF but it is absent for our data of analyses [6,7]. On the data of IZMIRAN station of solar storm radioemissions we have not found any event in HF range corresponded to items of our Table. The analysis of geomagnetic activity in the specified periods has shown complete absence of interrelation too. The meteoric radiopropagation could be a source of HF noise too at reception on a network of Crete stations. But, taking into account specificity of this way or sharp angle sensitivity (the condition orthogonality at height 90-100 km), and real orientation of a magnetic field vector (in area of the Mediterranean sea), has appeared impossible to ensure simultaneous registration at 3-4 stations of our network, that contradicts to the data of measurements. Besides practically all of monitored signals occurred irrespective of known regular meteoric flows. It is important also that the signals were not observed during the raised meteoric activity. Therefore, on all visibility the accepted signals on the nature are seismogenic. In this case they obviously differ from two known before cases [14,15] - where the individual bursts from the super-power earthquake ($M > 7.0$) were registered.

We can list now all than Crete HF preseismic radioemissions are differed from known [14,15] ones:

- The found out signals concerned to earthquakes of moderate energy (magnitude did not exceed 6.0 on a Richter scale)
- HF signal is received for the large number of earthquakes at a continuous number of the data, received almost for three years of observation
- HF a signal was registered on two frequencies of HF range 41 and 53 MHz and at several stations simultaneously.
- The spectrum of radiation exceeded 10MHz.
- The area of HF radiation (source of preseismic HF emissions) was under radiohorizon and the range of distances sometimes reached 300-350 km
- A signal was observed 1-3 days prior to earthquake and did not depend on a situation of the Sun, to be existed both at day and night. The time of its existence was some hours and sometimes reached more than one day duration
- The epicenter of earthquakes was under sea bottom, i.e. under thickness of water, and radiating source was above the sea in an atmosphere

The preconditions for model of HF precursors generation.

Radio emissions related to earthquake events are not yet well understood, either observationally or theoretically. Many different emission mechanisms have been suggested, including piezoelectricity,

triboelectricity, electrofiltration, and electrical discharges, as discussed in review by Parrot et al. [3].

To discuss the probable generation mechanism of HF radiation before earthquakes we shall present some results of radio-physical measurements of the abnormal phenomena in an atmosphere on the eve of Spitak earthquake [14]. By the authors with the help of weather radar is established, that for 1-3 days in an atmosphere above the epicenter there were charging structures similar thunderstorm, but considerably distinguished from them on duration and height of detection. The duration of existence (life time) made some hours whereas for thunderstorm activity the characteristic time does not exceed one hour. Unusual were also height and effective reflecting surface. Height made 5-30 km, and the area of reflection exceeded almost in 10 times similar for thunderstorms. By the Japanese group of the researchers [16-18] was informed in electromagnetic radiation (ELF range) from a surface of the sea as for earthquakes and volcanic activity in a zone of underwater breaks. The measurements a magnetic component of radiation and, hence were carried out, on which it is possible easily to locate a source of radiation. Large volume of an experimental material (it is received during a few years and on 8 stations network) has allowed (due to morphological attributes) to make a conclusion about importance of a gas phase during preparation of earthquakes (presence of gas bottom outflow). So this authors discovered that large scale radiation of ELF band which a mystery of its origin was owing to sea area and that the radiation might be owing to degas from the deep earth and be related to earthquake and volcanic eruption. For us the intermediate result, received by them, is important. It is an occurrence in air (at a surface of the sea) of an electrical charge. The formation of electrical charges in air occurs as a result of electrochemical interaction [18] with an atmosphere the products of degassing of terrestrial core, which injected to sea water before earthquake.

About the mechanism of generation HF radioemissions

It is known, that the optical luminescence of an atmosphere and lightning (thunder) are the usual phenomenon connected to forthcoming earthquake [19,20]. So, on the eve of powerful earthquake ($M = 7.3$) in China, which was successfully predicted, a many people observed a luminescence of the night sky [21] on remote distance of 100-200 kilometers from epicenter of the future earthquake. From FIG.2 follows, that height of seismogenic luminescence in this case could be as 1-2 km and above. It well supports the radar-tracking data on Spitak earthquake, where the anomalous charged clouds in an atmosphere are registered. Proceeding from this and being based on the received above results of our analysis of a number of continuous observation on a network of Crete island we can assume, that in our case in an atmosphere above the sea on the eve of earthquake at

heights of 0.1-10 km occur the charged clouds and, in a result, the conditions for the electrical discharges in an atmosphere are created which can serve a source of HF radio-emission registered on Crete.

Indirect confirmation of it can be the experimental works of the Japanese authors [16,17] in which is shown, that the source abnormal electromagnetic emission (EME) is located on a surface of the sea above a zone of the future earthquake. Let's note, that the magnitude range of these earthquakes corresponded to our : $M = 5.0-6.0$. As a source for such electromagnetic generator on a surface of the sea by them the model is offered [18], which basis is the injection of gases by bottom of the sea (in a zone of high pressure, arising by earthquakes preparation) which, reaching a surface of seawater, electrochemical interact with oxygen of an atmosphere with formation of positive ions (generation of charges at a surface of water) or/and them clusters.

By accepting it in attention and the assumption made by us above for an explanation of our results, we come to necessity whether to transport electrical charges from a surface of the sea (their occurrence on model of the Japanese) on height in some kilometers, whether to generate and to redistribute them at height in an atmosphere. This task is close on mechanism to generation of thunder activity in a nature [22]. One of known mechanisms of thunder electricity generation is the model of convection carry started in an atmosphere by a horizontal gradient of temperature

In our case the convective movement can be organized as follows. At the expense of increase of bottom temperature there is heating water, which rises as well as gases to a surface and creates necessary for convection a horizontal gradient of water temperature above epicenter of the future earthquake. The conditions for free thermal convection (termic) are created. Termic can arise or as separate volume - a bubble, or as a jet (fountain). Temp of bubble lift it is possible to define [22] by balance the force of resistance F and the force of bubble buoyancy:

$$F = (C_x/2) \rho' S \omega^2 = g(\rho' - \rho)V \quad (4)$$

as result:

$$\omega = \sqrt{\{(8/3 C_x) * g * r * (T' - T) / T\}} \quad (5)$$

Where r -radius, S - section, V - volume of a bubble, $C_x/2$ - const of air friction resistance (for sphere = 0.92), the meanings T , ρ concern to a bubble and T' , ρ' - to a neighboring atmosphere.

The size of thermal convective cell is determined by the basic gradient of temperature and can vary from hundreds meters up to tens kilometers. For typical radius of convective cloudiness by size in 1km and difference of temperatures in 0.5°C the estimation gives a lifting speed equal 7.5 m/s. Thus, through thermal convection the substance / charge/cluster from a sea surface can be transported up to height of 2-2.5 km for 5 minutes.

In our model due to convective carry of charges the local conditions promoting to generation of thunder electricity are created, the occurrence and time life of

which is defined by processes both in lithosphere and in an atmosphere. Thus, the occurrence of electrical charges in a surface of the sea and transportation them further on height up to 10 km in our model occurs due to energy allocated with bottom of the sea as gases and heat.

Set of processes in offered model

Let's present a sequence of key processes in our model of generation of seismogenic HF radiation:

- Gaseous injection occurring casually from the sea bottom in a zone of preparation of earthquake.
- Carry of gas from the bottom to a surface of the sea
- Oxidation of gas and formation of ions (charges) on border of sea water and air of atmosphere
- Local water heating within the limits of a zone of preparation of earthquake
- Convective transportation of electrical charges (ions) in troposphere and formation of structures of volume charges at atmosphere heights up to 10 km
- The electrical discharges in an atmosphere with radiation EME (in HF range including)

Let's note in addition, that as the small size of a nearby island results in formation of a shadow, it enables to carry out an independent estimation of the characteristic size of radiating volume in an atmosphere. That is it should be that of scale, as island (or its shadowing elements). It is well supported by the theory of convective cell [22]. So maximal height achievable by a cell, should be compared to its horizontal scale (can reach meaning 5-10km), that is close the sizes of shadow objects.

5. CONCLUSION

As the monitoring preseismic HF signals was carried out continuously and long time, the material is received for all possible events which were having place almost for the three-years period of observation. It is shown, that the area of generation of a seismic - precursors (HF radioemissions) is in an atmosphere (above the sea surface) at heights of 0.1-10 km. It is offered and proved the model of generation of a high-frequency earthquakes precursor which based on reasonable assumption of formation of the charged clouds in an atmosphere above a zone of preparation of earthquake and subsequent an electrical discharges serving a source EME in HF a range. So the gaseous emission from the earth may be as main source of preseismic electromagnetic precursor of earthquake. Further detailed studies were useful for analyzing the mechanism by which electromagnetic wave radiation associated with localized volcanic and earthquake activity is generated.

6. REFERENCES

1. M.B.Gohberg, V.A.Morgunov, T.Yoshino et al
Experimental measurement of electromagnetic emissions possibly related to earthquakes in Japan. J. Geophys. Res. 87, B9, 7824-7828, 1982

2. **A.C.Fraser-Smith, P.R.Bernardi, P.R.McGill, M.E.Ladd, B.A.Helliwell and O.G.Villard.** *Low frequency magnetic field measurements near the epicenter of the 7.1 Loma Prieta earthquake*, Geophys. Res. Lett., 17, 1465-1467, 1990
3. **M.Parrot, J.Achache, J.J.Berthelier, E.Blanc, A.Deschamps, F.Lefevre, M.Menvielle, et al** *High-frequency seismo-electromagnetic effects*, Phys. Earth Planet. Inter., 77, 65-83, 1993
4. **Yu.Ruzhin and A.Depueva.** *Seismoprecursors in space as plasma and waves anomalies*, Journ.Atmosph. Electricity, Vol.16, No.3, pp.271-288, 1996
5. **Special Issue: Seismo-Electromagnetic Phenomena.** Journal of Atmospheric Electricity, 16, N3, 288pp
6. **K.Nomikos, F.Vallianatos, J.Kalliakatos, S.Sideris and M.Bakatsakis.** *Latest aspects of telluric and electromagnetic variations associated with shallow and intermediate depth earthquakes in South Aegean*. Annali di Geophysica, X1/2, 361- 375, 1995
7. **F.Vallianatos and K.Nomikos.** *Sesmogenic Radioemissions as Earthquake Precursors in Greece*. Phys.Chem.Earth, Vol. 23, No. 9-10, pp.953-957, 1998
8. **L.Harang.** *Radio Noise From Aurora*, Planetary Space Sci., Vol.17, pp.869-877, 1969
9. **A.V.Dudnik, V.M.Kartashev, A.V.Lazarev et al.,** *The day variations of sporadic space radioemission at middle latitudes*, Geomagnetism & Aeronomy, Vol.28, No.1, pp.82-86, 1988
10. **V.N.Oraevsky, Yu.Ya.Ruzhin and A.S.Volokitin;** *High Frequency Electromagnetic Radiation in CRRES injection*, Advance Space Research, Vol.15, No.12, pp. (12)99-(12)102, 1995
11. **D.E.Proctor.** *VHF Radio Pictures of Cloud Flashes*, Journ. Geophys.Res., Vol.86, No.C5, pp.4041-4071, 1981
12. **James W. Warwick, C.O.Hayenga and J.W.Brosnahan,** *Interferometric Directions of Lightning Sources at 34 MHz*, Journ. Geophys.Res., Vol.84, No.C5, pp.2457-2467, 1979
13. **Waldteufel, P.Metzger, J.-L. Boulay et al.** *Triggered lightning Strokes Originating in Clear Air*, Journ. Geophys.Res., Vol.85, No.C5, pp.2861-2868, 1980
14. **V.V.Voinov, I.L.Gufeld, V.V.Kruglikov et al.,** *Effects in the ionosphere and atmosphere before the Spitack earthquake*, News of USSR Academy, Fizika Zemli (in Russian), No.3, pp.96-101, 1992
15. **Koitiro Maeda and Noritaka Tokimasa,** *Decametric Radiation at the time of the Hyogo-ken Nanbu Earthquake near Kobe in 1995*, Geoph. Research Lett., vol.23, no.18, pp.2433-2436, 1996
16. **M.Hata and S.Yabashu;** *Observation of ELF Radiation Related to Volcanic and Earthquake Activities in: Electromagnetic Phenomena Related to Earthquake Prediction*, ed.M.Haiakawa and Y.Fujinawa, TERRAPUB,Tokyo, pp.159-174, 1994
17. **M.Hata, X.Tian, I. Takumi et al.,** *ELF Horizontal Flux Precursor of Moderate Yamashi 96 Earthquake*, Journ.Atmosph. Electricity, Vol.16, No.3, pp.199-220, 1996
18. **M.Hata, I. Takumi and S.Yabashu;** *A model of earthquake seen by electromagnetic observation - gaseous emission from the Earth as main source of pre-seismic electromagnetic precursor and trigger of followed earthquake*, Ann. Geophysicae Supplement to Vol.16, p. C1188, 1998
19. **D.Finkelstein and J.Powell,** *Earthquake lightning*, Nature, Vol.228, No.5270-5273, pp.759-760, 1970
20. **D.Finkelstein, R.D.Hill, and J.Powell,** *The piezoelectric theory of Earthquake lightning*, Journ. Geophys.Res., Vol.78, No.6, pp.992-993, 1973
21. **Y.Zhao and F.Qian,** *Earthquake lights: a very convincing evidence for energy transfer from earth to air*, Intern.Workshop on Seismo_Electromagnetic (Abstracts), NASDA,Tokyo, p.242, 1997
22. **A.H.Hrgian.** *Physics of Atmosphere*. Moscow, MSU, 328p., 1986

TABLE

Earthquake (Sequake) M \geq 5.0 (1992-1995)						Drapania (32.2km)		Nipos (43.4km)		Heraklio (55.6km)		Ierapetra (18.9km)	
'	Date	ϕ .	λ .	M	h	H	D	H	D	H	D	H	D
1	21.11.92	35.58	22.39	6.0	70	590	119	1132	164	3007	251		305
2	27.01.93	36.02	22.36	5.4	120	821	134	1444	179		265		319
3	1.06.93	34.07	26.25	5.2	1		280		237		170		116
4	29.06.93	35.39	27.07	5.5	1	5641	300	3768	263		175		135
5	18.08.93	35.15	26.11	5.2	72	2805	221	1421	178	87	89		43
6	1.10.93	36.64	24.01	5.4	109	786	132	804	145		181	3692	236
7	23.05.94	35.48	24.7	6.0	66	262	90	23	50		46		103
8	3.02.95	34.35	24.97	5.0	38		172		133		107		97
9	16.02.95	34.46	26.59	5.0	28	OFF	162	3110	243	OFF	161	OFF	103
10	7.03.95	36.90	27.67	5.0	5	OFF	389	7781	358	4242	288		278
11	30.03.95	34.33	24.61	5.1	1	OFF	152	OFF	120	315	119	839	122
12	5.04.95	34.53	27.88	5.0	35		207		353		264		208
13	29.07.95	34.46	27.03	5.0	1	6667	324	4364	279		196	1111	138
14	22.08.95	36.62	26.74	5.4	179		301	4080	271		205		205
15	19.09.95	34.56	26.25	5.0	148		254		209		130	224	72
16	30.11.95	36.60	27.14	5.3	136		333		301		230		221
17	7.12.95	34.97	24.17	5.1	22	OFF	73	0	42	133	97	1090	137
18	10.12.95	34.93	24.17	5.4	24	OFF	74	12	47	140	98	1090	137
19	18.12.95	35.54	27.73	5.1	1		356		324		236	2485	197

THE STUDY OF ENERGY CORRESPONDENCE BETWEEN BOTTOM IONOSPHERE AND EARTHQUAKE FOCUS FOR SEISMOGENIC EM EMISSION

Takeo Yoshino and Masashi Ohtsuka

Fukui University of Technology
2-36-22 Zempukuji, Suginamiku, Tokyo Japan
Tel/Fax: +81-3-3397-5577
e-mail: yoshinot@nisiq.net

Abstract: In December 19, 1997, at 22:09 (JST 9 hours ahead of UT), an earthquake ($M = 4.6$, Depth = 10 km) were occurred at the sea bottom of northern off-shore of Fukui and Ishikawa prefecture. Prior to this main shock, a VLF sensor of Awara observatory received the cross-talk signals of MF broadcasting stations of Kanazawa area which located about 100km north of Observation point. We succeed the theoretical analysis to explain using a similar theory of the 'Luxembourg' effects.

INTRODUCTION

The Authors have constructed a facility for receive the space science and the radio signal emissions are associated with earthquake phenomena named as SEE (Seismogenic EM Emission). "The Awara Space Radio Observatory of Fukui University of Technology" is located in Awara Town of northern Fukui prefecture and the sensors and facilities are built on a small peninsula in the large Kitakata Lagoon (36.138N, 136.149E). The background noise levels through VLF and MF range around the observatory is one of the most low level areas in Honshu.

The December 19, 1997 at 22:09 JST an earthquake ($M = 4.6$, Depth = 10km) were occurred at the sea bottom of northern off-shore of Fukui and Ishikawa prefectures. The distance between epicenter and Awara observatory is approximately 10 km. The VLF observation sensors detected clearly the anomalous audio fre-

quency cross-talk signals of three broadcasting station of Kanazawa area about 100 km north of observatory. The map of the relations between both points shows in Fig. 1. The occurrence of above mentioned cross-talk phenomena was often appeared from about two days before and until few minutes prior to main shock as shown in Fig. 2. The authors made an attempt at analysis of the phenomena, and obtained a clear estimation results as one of the similar effects of "Luxembourg phenomena" in the bottom portion of ionosphere on the top of the earthquake epicenter.

CROSS-TALK ANALYSIS OF MF BROADCASTING SIGNALS INTO THE VLF RECEIVER

The estimation is due to by using of "Luxembourg phenomena". The seismogenic EM emission wave will be generated at the top of epicenter area in the disturbed the electron densities of the bottom of ionos-

phere by the earthquake energy. And the AM broadcasting signals will be modulated the electron density according to the program of modulation signals. When the SEE wave will be modulated by the electron density variation according to the modulation of broadcasting signals.

At 22:09 JST of December 19, 1997, an earthquake was occurred under the sea bottom of off-shore at northern Fukui prefecture. The location of Awara observation point, the epicenter location of this earthquake and the location of the transmission antenna of Broadcast station at Kanazawa is as shown in Fig. 1. The distance between observatory and the transmission antenna in Kanazawa is about 75 to 80 km towards northeast from observatory.

About 5 hours prior to this earthquake, the VLF receiver of Awara observatory begins the record of the quite strange cross-talk of audio voice and music signals

with overlapped three MF broadcast programs transmitting from Kanazawa area. The interference level was increased gradually and erased after 10 minutes of main shock as shown in Fig.2.

Fig. 3 shows the results of the FFT frequency and intensity spectrum of the noise characteristics: (a) shows the usual back-ground noise conditions. (b) Shows a typically FFT spectrum of the cross-talk interference of 42 minutes prior to the earthquake at November 19, 1997. The back ground noise level is higher than usually conditions, and many short harmonics structures are striking in the FFT picture. These are shown the typically voice and music voiceprint spectrums. (3) In this FFT spectrum, the interested rising-tone and the falling-tone voiceprint appears by the analyzing result of very low-frequency range below 600 Hz and longer timing analysis over 10 second or more. The time domain of these strange emissions has over 1 and few seconds, and the occurrences of these emissions are well correspondence with nearly equal to the impulsive domains of each seismogenic emissions. These three observation results suggests the usefully trace of investigation of the emission mechanism of seismogenic electromagnetic emission.

Fig. 4 illustrates a geometry profile of the vertically relationship between the energy transmission path of MF broadcasting stations from Kanazawa, location of Bottom of ionosphere, focus and epicenter of earthquake and the location of Awara observatory. Location of Awara observatory is only 10 km from epicenter, and the path of BC signals and the path of seismogenic waves are also shown in Fig. 4.

On the assumption that the free electrons in the lower ionosphere are as follows; (a) the mean free path is constant, (b) the collision frequency is very smaller than the wave frequency $\nu \ll \omega$, (c) no geomagnetic field. Power of incident MF (BC) wave ϖ is;

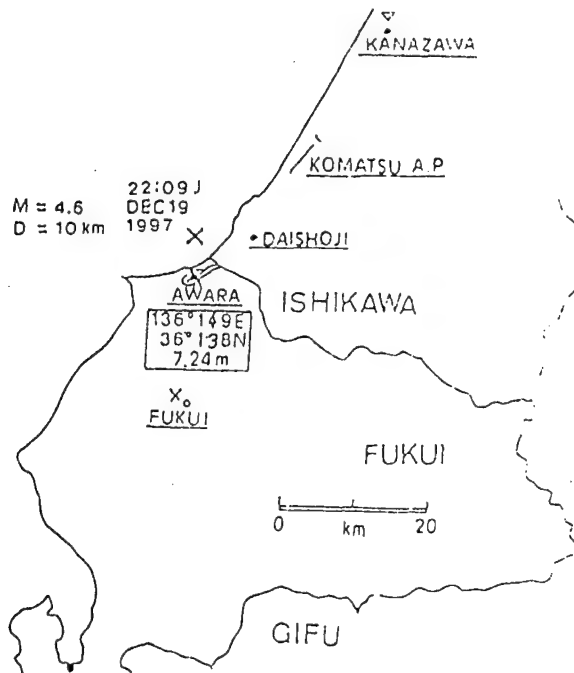


Fig. 1 The position of Awara observation point and epicenter of the earthquake at 22:09 JST of December 19th, 1997

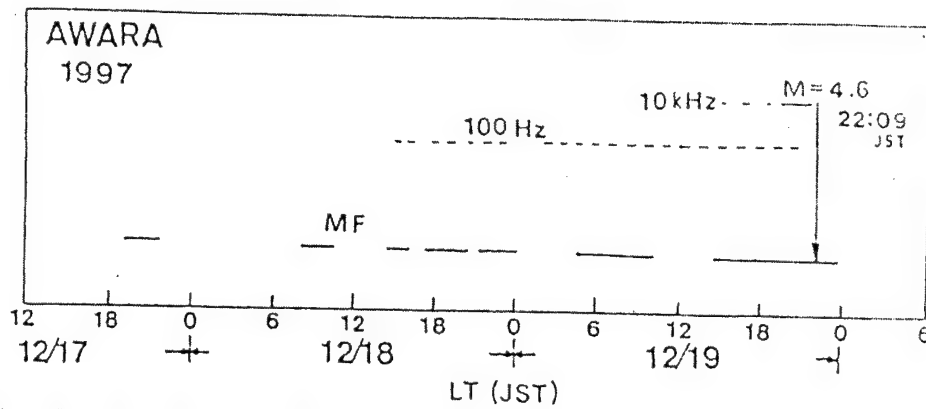


Fig. 2. The time of appeared the cross-talk signal of MF broadcast stations observed at Awara of the earthquake of December 19th in 1997. Black line shows the duration of cross-talk appearance, and the dotted line shows the time of background noise level.

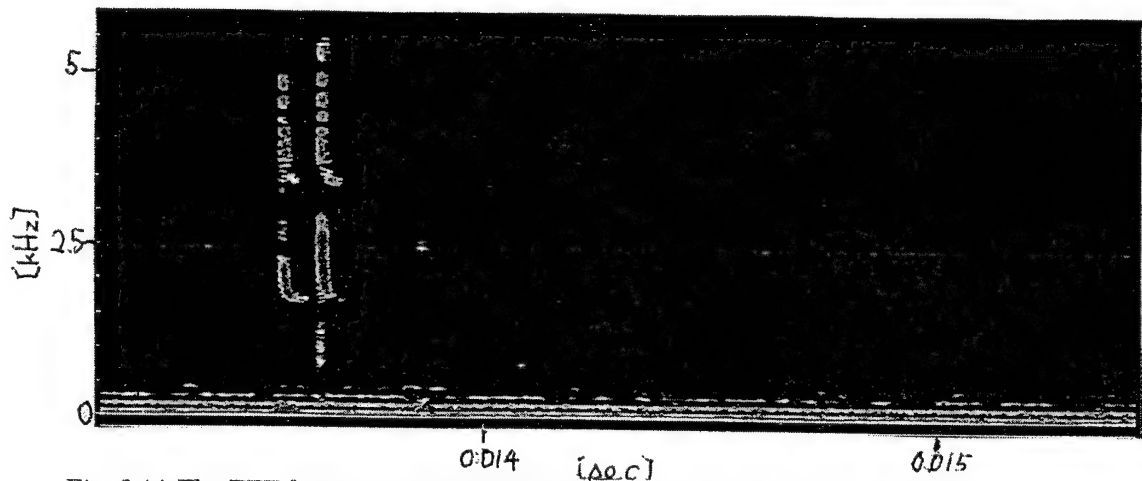


Fig. 3 (a) The FFT frequency and intensity spectrum of the noise characteristics at the usual Background noise conditions.

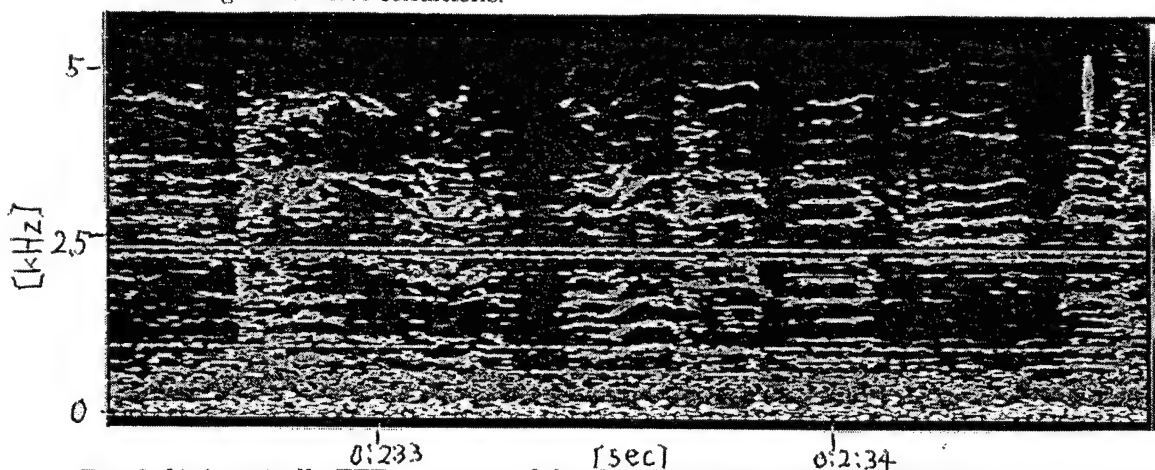


Fig. 3 (b) A typically FFT spectrum of the CROSS-TALK INTERFERENCE of 42 minutes prior to the earthquake at December 19, 1997. The background noise level is higher than usual condition. The typically voice and music harmonics structures are striking in picture.

$$\dot{m} = \int eE dx \quad (1)$$

where E is electric field strength of BC incident wave. The kinetic equation of charged particle at lower ionosphere is;

$$m\ddot{x} = eE = \sqrt{2} eE_e \sin \omega t \quad (2)$$

where E_e is electric field for electron and ω is angular frequency of incident wave. We obtain dx from (2),

$$dx = -\sqrt{2} (e/m\omega) E_e \cos \omega t dy$$

the loss of kinetic energy during dt is; $g(1/2 mx^2) \nu dt$,

the increase of Kinetic energy during dt ; $g(1/2 mx^2) =$

$mx dx$

$$m \nu dt = mx dx + g(1/2 mx^2) \nu dt \quad (3)$$

$$\text{put } x = I \nu \text{ in (3); } dv/dt + 1/2 g \nu^2 = a E_e^2 \quad (4)$$

where: $a = \alpha / m I^2$, g , ν and ν to be constant and $d\nu/dt = 0$, then

$$1/2 g \nu^2 = a E_e^2. \quad (5)$$

On the assumption that E_e is modulated by fm ,

$$E_e = E_0 (1 + M \sin 2\pi fm t) : M \ll 1 \quad (6)$$

where fm is a modulation frequency of an incident wave.

ν is vibrated with the small amplitude

$\delta \nu$ around ν_0

$$\nu = \nu_0 + \delta \nu : |\delta \nu| \ll \nu_0 \quad (7)$$

then $d(\delta \nu)/dt + R \delta \nu = 2a M E_0^2 \sin 2\pi fm t$,

where $R = d/d\nu_0 (1/2 g \nu^2)$

then we obtain the value of $\delta \nu$ is;

$$\delta \nu = 2a M E_0^2 / \sqrt{4\pi^2 fm^2 + R^2} \cdot \sin(2\pi fm t - \phi)$$

$$\tan \phi = 2\pi fm / R. \quad (8)$$

When the seismogenic wave is generated in the

Effectuated area[1] modulated by the incidence wave.

E' is the electric field intensity of SEE.

$$E' = E(\nu_0 + \delta \nu) = F(\nu_0) + dF(\nu_0)/d\nu_0 \delta \nu$$

After Taylor Expansion, and inserted into (7) of

this results,

$$E' = E_0 \{1 + M' \sin(2\pi fm t - \phi)\} \quad (9)$$

Then modulation index of second emitted wave

(seismogenic wave) M' is obtained by following

equation.

$$M' = BE_0^2 M / \sqrt{4\pi^2 fm^2 + R^2} \quad (10)$$

From these calculation results obtain to the seismo-

genic emission wave E' has same modulation fre-

quency fm of incidence wave E , and the modulation

index of seismogenic emission wave is shown as M' is;

$$M' = k \left\{ (f^2 + fh^2) \nu_0^2 E_0^2 M / (f^2 - fh^2)^2 \sqrt{4\pi^2 fm^2 + R^2} \right\} \quad (10)$$

Where

f : carrier frequency of incidence wave

fh : electron gyro-frequency in the ionosphere.

(2) Cross-talk characteristics of seismogenic emission

wave to an modulated incidence wave interaction.

We obtain the following characteristics from (10).

- ① $M' \propto M$: M' is in proportion to the modulation index of incidence wave.
- ② $M' \propto \nu_0^2$: Cross talk level increases in the lower altitude of ionosphere.
- ③ $R^2 \propto 4\pi^2 fm^2$: M' becomes to the modulation frequencies of incidence wave.
- ④ M' decreases in accordance with higher frequency.
- ⑤ M' increases when the f of incidence wave is closes into fh .
- ⑥ M' takes equal value to the modulation index M of incidence wave.

(3) Frequency effect on the interaction between modulation index.

As the denominator of (10)', the maximum cross-talk

level obtain at the gyro-frequency fh . The fh in the

winter season of Kanazawa area is approximately

1.25 MHz. The frequency and output power of the MF

band BC station at Kanazawa area is as following

Table, and the frequencies in Kanazawa area are

Very close to electron gyro-frequency fh as shown in

the Table.

Name of Station	Call	ANT. Power	Frequency
Hokuriku B. S.	JOMR	5 kW	1107 kHz
NHK 1 Kanazawa	JOJK	10 kW	1224 kHz
NHK 2 Kanazawa	JOJB	10 kW	1386 KHz

Table. 1 The transmission frequency of 3 broadcasting stations of Kanazawa.

CONCLUSION

By the estimation results by using the following modulation hypothesis, the author obtains the following modulation characteristics of SEE wave of modulated incidence wave interaction are;

1. Modulation Index of VLF wave is in proportion to the modulation index of incident AM wave.
2. Cross-talk level increases to the lower altitude of ionosphere.
3. Modulation index of VLF wave increases when the frequency of the incident MF wave is closer to gyro frequency at bottom ionosphere.

Reference

Yoshino, T., I. Tomizawa and Sugimoto, "The results of statistical analysis of seismogenic emissions as precursors to the earthquake and volcanic eruptions." Phys. of Earth and Planet. Interiors, 77, 21- 31, 1993.

CELLULAR AUTOMATON MODEL OF LIGHTNING DISCHARGE PRELIMINARY STAGE

M. Hayakawa¹⁾, D.I. Iudin^{1,2)}, N.V. Korovkin^{1,4)}, V.Y. Trakhtengerts³⁾

(1) The University of Electro-Communications, 1-5-1 Chofugaoka, Chofu Tokyo 182 - 8585, Japan

fax: +81-424-43-5783, e-mail: hayakawa@whistler.ee.uec.ac.jp,

(2) Radiophysical Research Institute, 25/14 Bolshaya Pecherskaya st., Nizhny Novgorod, 603600, Russia,

(3) Institute of Applied Physics, Russian Academy of Science, 46 Ulyanov st., Nizhny Novgorod, 603600, Russia,

(4) Saint Petersburg State Technical University, Polytechnicheskaya st., 29, St. Petersburg 125251, Russia,

fax: +81-424-43-5783, e-mail: korovkin@whistler.ee.uec.ac.jp, nv@caro.spb.ru.

Abstract: Traditional thundercloud models, which are based on continuous electrodynamics, cannot explain the great diversity of lightning discharges and all their features. Understanding the processes that define the preliminary stage of lightning discharge has been a major problem. A fractal cellular automaton model is developed, which describes the dynamics of the electrical charges in a thunderstorm cloud in its mature stage. Two key assumptions form the model basis: The first one suggests the small-scale electric structure of a cloud, originating from dissipative beam-plasma instability in the thundercloud. This instability is accompanied by a small-scale electrical stratification of the cloud. The second assumption is that the growth of an electric field in cells is restricted by an electric breakdown between maxima and minima of the electrostatic wave. The small-scale discharges initiate the spread of "breakdown infection". The process manifests itself as a self-maintaining chain reaction and may be considered as a self-organised critical (SOC) phenomenon. We obtain the power-law exponent for the ignition size distribution that confirm critical behaviour of the model. We also show that our results are substantiated by observations.

1. INTRODUCTION

The thunderstorm electricity problem is extremely diverse one, and includes a number of key questions. It begins with cloud electrification mechanisms, and ends with flash shaping final stage, when a stepped leader arises and a return stroke is established as the lightning discharge's most powerful manifestation. Considerable progress has been made recently in the understanding and modelling of elementary processes of cloud particles electrification [1]. Advances have been made in model development of the flash channel formation, when the channel formation is accompanied by a leader and return stroke progression [2,3,4].

Understanding the processes that define the preliminary stage of lightning discharge has been a major problem. In its most developed phase, this stage lasts

approximately one tenth of a second, and consists of numerous (up to 10,000) relatively weak discharges [4-8]. Widespread experimental efforts have demonstrated several peculiarities at the preliminary stage, proving it to be a very complex and puzzling phenomenon: Firstly, two subintervals (of approximately equal duration) may be selected in the preliminary breakdown stage. The first subinterval contains very high frequency pulses (VHF) which appear without any visible DC field changes. A gradual DC field change accompanies VHF during the second subinterval, and closely connects with leader progression.

Secondly, the results obtained with the VHF source location systems reveal pulse duration changes, which are connected with Doppler effect to the radiation of a fast (up to 10^7 m/s) moving source. [6; 9]. Sometimes VHF emission is observed as a consequence of coherent signals [10]. Thirdly, the precursor activity spreads VHF sources throughout much of the cloud. Finally, the universality of the frequency spectrum of electromagnetic signals emitted by the discharges was also established [11].

The question is what physical mechanism could result in the occurrence of such an intricate preliminary dynamic? It is particularly difficult to answer this question, since the median electric field strength in a cloud is of order of magnitude below the typical fields generating sparks in laboratory experiments.

2. SMALL-SCALE ELECTRICAL STRUCTURE

The principal aim of this paper is to raise the idea that the preliminary stage of lightning discharge is closely related to the fine electrical structure of a thundercloud. The multi-layered cellular electrical structure has been detected in practically all *in-situ* experiments [1, 12].

There is considerable physical evidence to support the existence of such a small-scale electrical structure in a thunderstorm cloud. The idea is that a mature thundercloud becomes similar to a plasma-like multi-flow system. The combined effect of gravity and uprising convective flow creates interpenetrative streams of charged heavy (large drops and hailstones) and light

(ice crystals and the fine drops) components. At the observed velocities $u = 5 \sim 20 \text{ m/s}$ of the uprising streams the large particles (with mass $M \sim 10^{-5} \text{ kg}$) are suspended in the stream. They fill the lower part of a cloud, while the light fraction is carried away by the stream into the upper regions of the cloud. Trakhtengerts [13] showed that this multiflow system becomes unstable due to electrostatic waves with the electric field $E \sim \exp(-i\omega t + i\vec{k}\vec{r})$, where \vec{r} and t are the space coordinate and time. In the simplest case of monodispersed charged hailstones and ionized air flow the frequency ω and the wave vector \vec{k} satisfy the dispersion equation [13]

$$1 - \frac{\Omega^2}{\omega(\omega + i\nu)} + \frac{4\pi i\sigma}{\omega - \vec{k} \cdot \vec{u}} = 0,$$

where $\Omega^2 = 4\pi q^2 N / M$, is the square of the "large particle gas" plasma frequency, q , N and M are the charge, density and mass of hailstones, $\nu \sim g/u$ is the effective collision frequency, g is acceleration due to gravity, \vec{u} and σ are the air flow velocity and conductivity. The instability threshold is given by the condition $(\Omega/\nu)^2 \geq 1$ and the instability growth rate is derived as $\gamma \approx 2\pi\sigma(\Omega/\nu)$ for the optimal spatial period $a \sim \pi/k \approx \pi u/\Omega$. For particle radius $\sim 0.5 \text{ cm}$ and $N \sim 10^3 \text{ m}^{-3}$ the instability threshold is achieved for $q \sim 10^{-10} \text{ Q}$. Putting $u \sim 10 \text{ m/s}$ and $\Omega \sim 2 \text{ v}$, we find $\nu \sim 1 \text{ s}^{-1}$, $a \sim 10 \text{ m}$ and $\gamma \sim 4\pi\sigma \sim 1 \text{ s}^{-1}$ ($4\pi\sigma \sim \nu$). Further research [14] on the charge exchange between the particles has shown this instability is universal in a wide range of the cloud parameters. At the nonlinear stage, a small-scale electric field amplitude is determined by a balance between the electric force and the force of gravity that are superimposed on a large particle $E \sim Mg/q \sim 10^6 \text{ V/m}$. Hence the small-scale electric field amplitude can exceed the median field amplitude quite considerably.

3. CLOUD METALLIZATION MODEL

We suppose that the small-scale electric field development is restricted by a breakdown between maxima and minima of the electrostatic wave. Given the necessary conditions, such an elementary (essentially spark) discharge in an arbitrary cell of our charge density grid should be able to cause discharges in its nearest neighbours. We may consider a situation when "breakdown infection" spreads all over the cells where the local electric field amplitude exceeds some activation level that is smaller than critical one. (We draw an analogy here with a laser triggered discharge experiment, where the electric field necessary for initiating a streamer is greatly scaled down [15]). Single cell breakdown leads to the "metallization" throughout all of the activated zone (a network of the closest neighboring cells where the electric field amplitude exceeds the activation level). Ionization propagates through the activation network by means of a "domino" effect.

With the above prescription, we maintain a two-

dimensional cellular automaton (CA) "breakdown spreading" model. In this study we use automaton grid of 500×500 cells. Each cell is characterised with a voltage drop U between maxima and minima of the electric wave. The voltage drops increase over time. To describe the voltage drop growth we use random deposition algorithm [16]. When the voltage drop amplitude reaches some critical value U_c there is a breakdown in the cell and the conductive lattice site with a short lifetime appears. At this point, voltage drop disappears and then goes up again (see Figure 1).

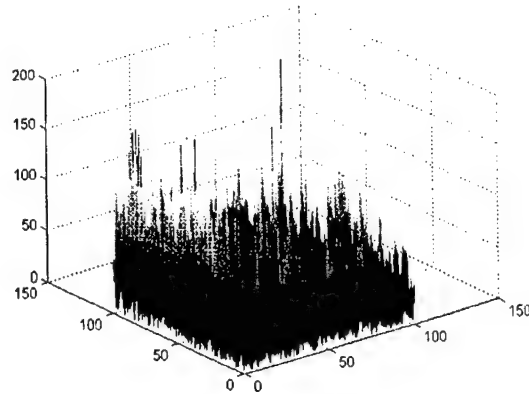
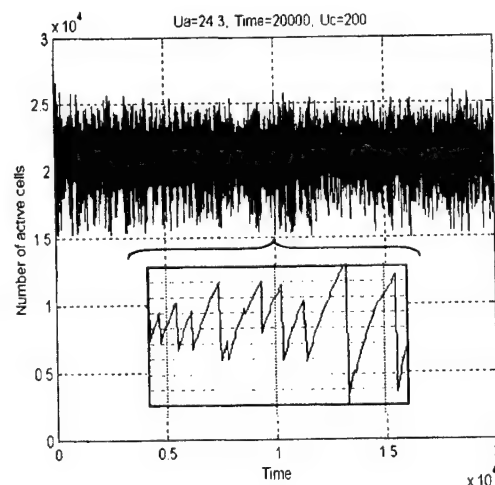


Figure 1.

We enter a cumulative distribution function of cells $f(U)$ over this voltage drops, such that $f(U)dU$ characterises specific fraction of cells where the voltage drops amplitude U hitting in an interval $[U, U+dU]$. It is obvious that $\int_0^U f(U)dU = 1$. A lattice site where the voltage drop exceeds some activation level U_a will be referred to as 'activated cell'. $p = \int_{U_a}^U f(U)dU$ is specific volume of the activated cells. We assume that a separate site breakdown causes breakdowns in neighboring cells, if the corresponding voltage drop exceeds the activation level and the single cell breakdown tends to the 'metallization' throughout the activated cluster.



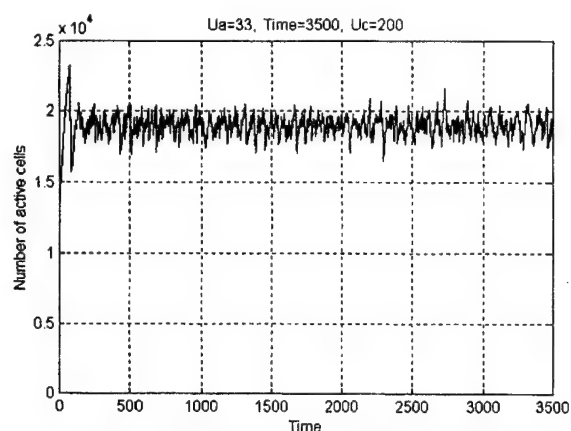


Figure 2. Active cells temporal evolution

In that way, each site of the lattice can be in one of three different states: the cell can be activated; the cell can be inert; the cell can be metallized. The lattice is updated in parallel according to the following algorithm: (i) a site occupied by a conductive cell becomes inert in the succeeding time step; (ii) an inert site becomes activated when correspondent value of U exceeds U_a ; (iii) an activated site becomes conductive

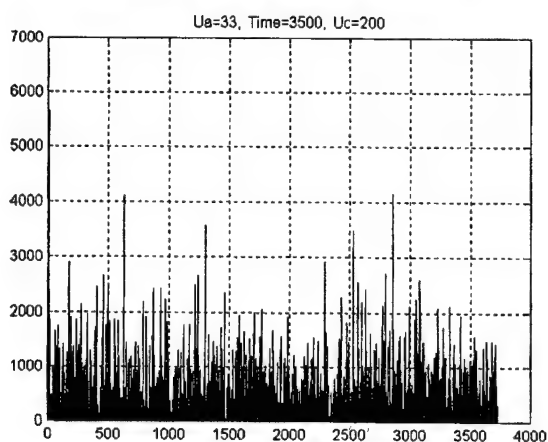
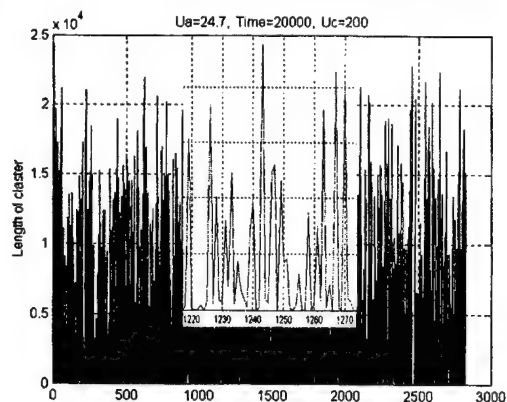


Figure 3. Metallized cluster size as function of time.

if correspondent value of U becomes equal to U_c or if it belongs to the activated cluster that contains such a critical site. So, the ionization is implied passing acti-

vated cluster in one time period step in the model. We choose the voltage drop growth rate so small ($\gamma \approx 1-10s$) that even the largest cluster "burns down" rapidly, before new activated bond grows at its edge.

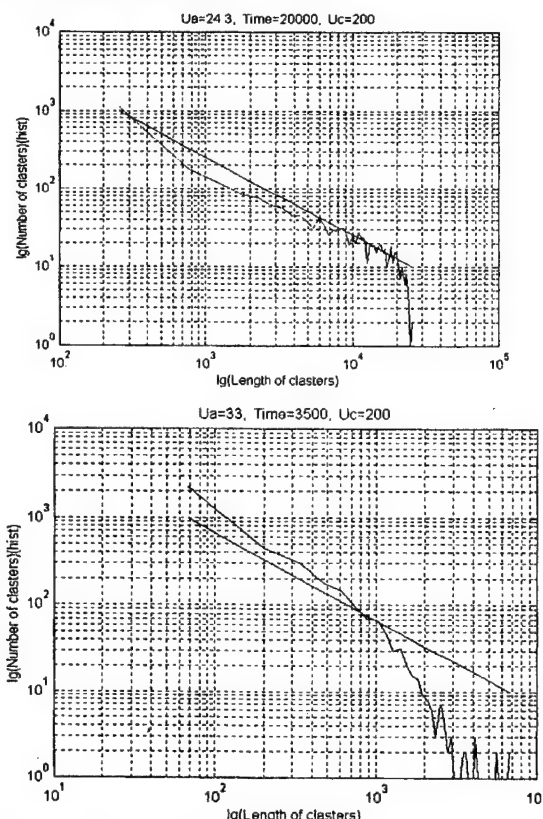


Figure 4. Power spectrum of the activated cells number.

Temporary fluctuations in the breakdown ignitions are shown in Figure 2 for two different values of U_a/U_c . Correspondent mean number of active cells $\langle p \rangle = \int_{U_a}^{U_c} f(U) dU$ having been calculated, we obtain

that fluctuation amplitude increases when $\langle p \rangle$ tends to some critical value $p_c \approx 0.59$ (see below). We construct a temporal record $S(t)$ of the "breakdown spreading" in the model. We define $S(t)$ in the following way. The signal is always zero except at those instances when breakdowns occur, in which case $S(t)$ is equal to the size of the cluster metallized at t . That is (as depicted in Figure 3), the signal $S(t)$ consists of a set of delta spikes of height equal to the metallized cluster size. Figure 4 shows the power spectrum for activated cells number that reveals scaling properties of the metallization process in vicinity of percolation threshold. Figure 5 shows numerical result for cumulative distribution functions $f(U)$

Our model of the breakdown spreading is very similar to a class of models referred to as 'forest-fire models' [17]. Cluster metallization in thunderclouds corresponds to the trees that catch fire spontaneously in the forest-fire models. A fire burns the very same cluster of trees where it started. Forest-fire models also exhibit SOC [17].

One way of looking at the breakdown infection

spreading is in terms of the percolation theory [18; 19].

The description is "mean field" in the sense that spatial correlations are ignored, and activated bonds are considered to be randomly distributed all over the lattice at a density equal to p . In this approximation, the sizes of burned-out clusters are simply given by the expression in percolation theory for the sizes of connected clusters: $R \equiv (2\pi/k) \left((p_c - p)/p_c \right)^v$, where p_c is threshold concentration, and v is the correlation radius critical exponent. Figure 6 shows the cluster size power depression, that confirms theoretical result $N \sim R^{d_f} \sim (p_c - \langle p \rangle)^{-v_{df}}$.

Thus the external driving of the system connected with the electrostatic streaming instability is obviously much slower than the internal relaxation processes connected with the small-scale electric discharges. The fine thundercloud electrical structure is built up on the scale of seconds, whereas the fine-scale electrical energy is released in a few microseconds during microdischarges.

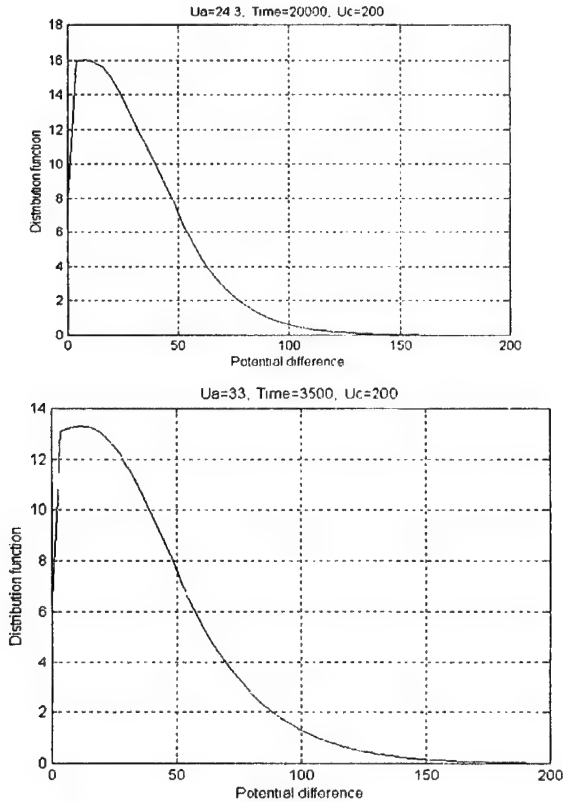


Figure 5. Cumulative distribution functions.

This is the separation of time scales that turns our system into the SOC-like dynamical state [22,23]. The separation of time scales is closely connected with the existence of the breakdown threshold. The fine-scale electrical field has to build up enough to pass a certain critical value. This occurs over a much longer period of time than the short breakdown time interval.

The model discussed allowed us to estimate the ap-

pearance rate F of microdischarges (activated cells discharges). This rate is determined by the relation

$$F \equiv \gamma \frac{V}{a^3} p,$$

here γ is the growth rate, and V is the volume of the thundercloud active part, where the instability takes place. On preliminary breakdown stage, when the activated cluster length is large enough for the leader progression, we have $p \sim p_c$. Putting $V \sim 10^{10} \text{ m}^3$ and $a \sim 10 \text{ m}$, $\gamma \sim 0.1 \text{ s}^{-1}$, we find: $F \sim 2.5 \cdot 10^5 \text{ s}^{-1}$; this is in good qualitative agreement with experiment [20].

4. DISCUSSION

Summarising the above results, we can conclude that exploration of short-scale electrical structure of a thundercloud is very promising for understanding the preliminary stage of a lightning discharge. The small-scale electrical stratification is caused by a thundercloud free energy, which is stored in the multiflow motion of the cloud media. Small-scale breakdown spreading leads to the formation of a stepped leader at the final stage.

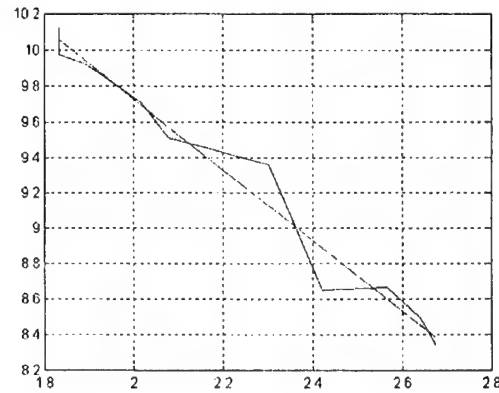


Figure 6. Numerical illustration of how the metallized cluster size is uniformly depressed when $(p_c - \langle p \rangle)$ increases.

It is already known that at the preliminary stage the long leader initiation requires a high ionization degree of the head gas, along with an energy supply necessary for heating it to "arc temperatures" and for compensation of heat losses [21]. An ordinary streamer mechanism of energy supply, inherent in a discharge in free gas, reduces the incorporation of electrical charge into the leader cover. The streamer mechanism is power consuming, since streamer development requires a strong electric field over the whole streamer zone. In our case, the ionization process penetrates the intra-cloud volume, that is already 'saturated' with energy and charge due to the beam plasma instability. The process manifests itself as a self-maintaining chain reaction and may be regarded as SOC phenomenon.

As a system will evolve into a SOC dynamical state, a separation of time scales is required. The process connected with the external driving of the system needs to be much slower than the internal relaxation processes.

That is the situation we deal with in the preliminary stage of lightning discharge. The fine thundercloud electrical structure is based on a time scale in seconds, owing to the electrostatic streaming instability. This occurs over a time scale much longer than the short breakdown time interval. During the built-up phase, energy is gradually stored in the fine electrical structure. This energy is then dissipated almost instantaneously at the moment the activated cluster metallizes.

A very diverse group of phenomena in science have been claimed to exhibit SOC behaviour. It started out with sandpiles, earthquakes, and forest fires. Next came motion of magnetic flux lines in superconductors, water droplets on surfaces, dynamics of magnetic domains, and growing interfaces. We believe that thundercloud activity should be added to this group. On the other hand, ideas about SOC should considerably affect thundercloud physics.

We have found encouraging results in the similarity between temporary variations in the number of cluster breakdown ignitions predicted by the model discussed, and the experimental temporary VHF records of the preliminary breakdown process. The well-known VHF radiation spectrum also confirms the power-law cluster distribution discovered here.

We hope that the suggested model may shed some light on the burst-like space-time fluctuations observed in the preliminary breakdown stage, and will stimulate more detailed examination of the thundercloud fine structure.

REFERENCES

1. D.R. MacGorwan, W.D. Rust, "The electrical nature of storms" (in English), Oxford Un. Press 1998.
2. A.A. Dulzon, M.D. Noskov, W. Lopatin, P.V. Shelukin, "The strike points distribution from fractal model of the stepped leader" (in English), Proc. 10th Intern. Confer. On Atmos. Electricity, 260, Osaka, 1996.
3. G. Labanne, P. Richard, A. Bondion, "El-m. properties of lightning channels formation and propagation" (in English), Lightning Electromagnetics, Ed. Robert L. Gardner, 1987.
4. V.A. Rakov, M.A. Uman, "K and M changes in close lightning ground flashes in Florida" (in English), J. Geophys. Res., D 11, 18,631-18,647, 1990.
5. M.A. Uman, "The Lightning Discharge" (in English), Internat. Geophys. Series, 39, 377, 1987.
6. D.E. Proctor, R. Uytenbogaart, B.M. Meredith, "VHF radio pictures of lightning flashes to ground" (in English), J. Geophys. Res., 93, D 10, 12,683-12,727, 1988.
7. J.P. Moreau, P.L. Rustan, "A study of lightning initiation based on VHF radiation, Lightning El.-magnetics" (in English), Ed. R.L. Gardner, 1987, p. 257.
8. M. Mazur, P.R. Krehbiel, X.M. Shao, "Correlated high-speed video and radio interferometric observations of a cloud-to-ground lightning flash", J. Geophys. Res., 100, 25,731-25,753, 1995.
9. D. E. Proctor, "Lightning and precipitation in a small multicell thunderstorm" (in English), J. Geophys. Res., 88, 5,421-5,440, 1983.
10. J. W. Warwick, "A new model of lightning, Dusty and Dirty Plasmas, Noise and Chaos in Space and in the Laboratory" (in English), Edited by H. Kikuchi, 284-293, N.Y., Plenum Press, 1994.
11. M. Boulch, J. Hamelin, C. Weidman, "UHF-VHF Radiation From Lightning" (in English), in "Lightning Electromagnetics, Ed. R.L. Gardner, 1987.
12. T.C. Marshall, W.D. Rust, "Electric field soundings through thunderstorms" (in English), J. Geophys. Res., 96, 22,297-22,306, 1991.
13. V.Y. Trakhtengerts, "Nature of electrical cells in thundercloud" (in English), Proc. 9th Intern. Confer. On Atmos. Electricity, 2, 416, St.-Petersburg, Russia, 1992.
14. E.A. Mareev, Sorokin A.B., Trakhtengerts V.Y., "Cloud collective charging effects in multi-flow aerosol plasma" (in English), Plasma Physics, 1999, 3, p. 123
15. D. Wang, Y. Shimada, S. Uchida, E. Fujiwara, Z.-I. Kawasaki, K. Matsuura, Y. Izaka, C. Yamanaka, "Fundamental Experiments Concerning Laser Triggered Lightning, Dusty and Dirty Plasmas" (in English), Noise and Chaos in Space and in the Laboratory, Ed. by H. Kikuchi, 313-322, N.Y., Plenum Press, 1994.
16. J.F. Gouyet, M. Rosso, B. Sapoval, "Fractal Surfaces and Interfaces, in Fractals and Disordered Systems" (in English), ed. A. Bunde and S. Havlin, Springer-Verlag, Berlin 1996.
17. Clar S., B. Drossel, F. Schwabl, "Scaling laws and simulation results for the self-organized critical forest-fire model" (in English), Phys. Rev. E, 50, 1009, 1994.
18. A. Bunde, S. Havlin, "Fractal and disordered systems" (in English), Sp.-Verlag, 1996.
19. D. Stauffer, "Introduction in Percolation Theory" (in English), Taylor and Francis, London 1985.
20. J.E. Nanevich, E.F. Vance, J.M. Hamm, "Observation of lightning in the frequency and time domains" (in English), Lightning Electromagnetics, Ed. R. L. Gardner, 1987, p. 191.
21. E.M. Bazelyan, Yu.P. Raizer, "Spark Discharge" (in English), N.Y., CRC Pr., 1998.
22. P. Bak, C. Tang, K. Wiesenfeld, "Self-Organized Criticality: An Explanation of 1/f Noise", Phys. Rev. Letters, 59, 381, 1987.
23. P. Bak, C. Tang, K. Wiesenfeld, "Self-Organized Criticality" (in English), Phys. Rev. A, 38, 364, 1988.

Masashi Hayakawa is now a professor of department of Electronic Engineering, The University of Electro-Communications (UEC), Tokyo Japan. He graduated from Department of Electrical Engineering, Nagoya University, and obtained B. Eng., Master of engineering and Doctor of engineering, all from Nagoya University. He worked at Research Institute of Atmospheric electricity. After moving to the present university, he extended his work very much, including EMC general problems, inverse problems, seismo-electromagnetics.

Nicolay Korovkin is now a professor of department of Electronic Engineering, UEC, Tokyo Japan. He graduated St. Petersburg State Technical University (SPSTU) 1977, Russia. He obtained M. S. electrophysics 1975, Ph. D. 1984 and Doctors degree 1995 theoretical electrical engineering, all from SPSTU. He is a member of International Power Academy, St. Petersburg Division.

Dmitry Iudin is now an assistant professor of Department of Electronic Engineering, UEC, Tokyo Japan. He graduated from Radiophysical Department, Nizhny Novgorod State University (NNSU) 1986. In 1999 he obtained Ph.D., radiophysics.

Victor Trakhtengerts is now a professor of Radiophysical Department, NNSU, Russia. He graduated from Radiophysical Department, NNSU. He obtained B. Eng., Master of radiophysics and Doctor of radiophysics, all from Institute of Applied Physics. He is a chief researcher in Institute of Applied Physics, Russian Academy of Science. In 1999 he was awarded of title of Honoured Worker of Science.

HURST EXPONENT DERIVED FOR NATURAL ELF ELECTROMAGNETIC NOISE

A.P. Nickolaenko

*Usikov's Institute for Radio Physics and Electronics
Ukrainian National Academy of Sciences, Kharkov, Ukraine
fax: +38 (0572) 44-1105, e-mail: sasha@vlf.kharkov.ua*

and

D. D. Iudin¹

*The University of Electro-Communications
1-5-1 Chofugaoka, Chofu-city, Tokyo 182-2525, Japan*

Abstract

Natural electromagnetic radio signal in the extremely low frequency (ELF) band is usually regarded as a random noise. It is a linear superposition independent EM pulses that had originated at remote global thunderstorms and traveled to an observer through the Earth-ionosphere cavity. The process of forming an electromagnetic response (ringing) of a resonant system to the pulsed excitation has much in common with the well-known Brownian motion (BM). The first distinction is that in Brownian motion the impacts of individual molecules are integrated by a moving particle having a great mass: this is an equivalent to a low-pass filtering of the random noise. Actually, the Earth-ionosphere cavity plays rather a role of the band-pass filter instead of LPF. The second difference from the Brownian motion is that the time delay between pulses and the time constant of the cavity are approximately the same, while in a classical case they are separated by many orders in magnitude. The Hurst exponential is often used when studying random and chaotic dynamic

signals. We present the first results of special processing of natural ELF radio noise for obtaining the Hurst exponent of the noise.

1. Introduction

Properties of natural radio signals strongly depend on their origin. Therefore, their features are of great importance when we study fundamental characteristics of terrestrial radio noise: e.g., we want to know whether the stochastic signal is a noise or a dynamic chaos. In the present work, we apply the Hurst exponent to study the nature of extremely low frequency (ELF) radio noise produced by electromagnetic (EM) radiation of thunderstorms from all over the world. The Hurst exponent is applied for the first time to this kind of signals, as far as we know. The standard statistical properties of the ELF radio noise were studied in 70s and published in literature (see for instance *Evans and Griffiths*, 1974).

To check the workability of the algorithm and of the approach itself, we used the radio

¹ On leave from the Institute of Applied Physics of Russian Academy of Sciences, 25, Bolshaya Pecherskaya st., Nizhnii Novgorod, 603000, Russia.

signals recorded with two orthogonal horizontal magnetic antennas in the frequency range of Schumann resonance band from 4 to 40 Hz (a courtesy from Dr. C. Price). Natural electromagnetic noise had been recorded at the Mitzpe Ramon field site of Tel Aviv University at Negev desert (30°N and 34°E). We used the waveforms of NS and EW outputs recorded during 5 min intervals each hour of a day. We demonstrate here results of processing of the data collected during a few days of March 1998.

2. Results of data processing and interpretation

The Hurst exponent (Hu) is defined for the random series $x(t_k) = x_k$ by the following formula (Turcotte, 1997):

$$\left(\frac{R_N}{S_N}\right)_{AV} = (N)^{Hu} \quad (1)$$

Here x_k is the discrete data set with the index $K \in [1; N]$, the range of random variable equals:

$$R_N = (x_{\max}) - (x_{\min}) \quad (2),$$

its standard deviation (or RMS value) and mean value are found from

$$S_N = \left[\frac{1}{N-1} \sum_{K=1}^N (x_K - \bar{x}_N)^2 \right]^{\frac{1}{2}} \quad (3)$$

$$\bar{x}_N = \frac{1}{N} \sum_{K=1}^N x_K \quad (4).$$

The R/S analysis was applied to river discharges and lake levels, thickness of tree rings, variations of atmospheric temperature, sunspot numbers, etc. Generally, $Hu \in [0.7; 0.8]$. When $Hu \in [0.5; 0.1]$, we speak that the process contains persistence (its current amplitude depends on the pre-history), while $Hu \in [0; 0.5]$ implies anti-persistence. For the Gaussian white noise the tilt of the line equals $Hu = 0.5$. So, the Hurst exponent describes the randomness of the statistical data set.

We had included the number of samples into analysis that satisfies the binary condition $M = 2^I$. This allows us to divide the data in two parts and compute the R and S values for each part, find their ratio and average it. Then, the

series is broken into four parts, and the computational procedure is repeated once again resulting in a new averaged ratio. Finally, the elementary data slice contains two points, and we have in this case, see (2-4) $R_2 = (2)^{\frac{1}{2}} \cdot S_2$ so that $R_2/S_2 = (2)^{1/2}$.

Current values of $\log_2 \left(\frac{R_N}{S_N} \right)_{AV}$ are

plotted against $I = \log_2(N)$, and the best fit straight line gives the Hu value (1), see Fig. 1 for illustrations.

The figure depicts two columns of plots related to computations of Hu . The left column represents the data obtained for the record performed around 09 UTC on March 17, 1998. The right frames display the signal recorded at 06 UT, March 21. In the data set processed, the left column corresponds to the highest level of the Hu values and the right one represents its lowest values.

The upper pair of plots in Fig. 1 shows that there exists an 'inertia' interval $I \in [7-12]$ where a stabilization of accumulated RMS amplitude takes place. This parameter becomes practically independent of the element length N (see Rytov, 1976). We also indicated the level $I=10$ in the figure using vertical arrows to demonstrate its optimal position and applicability for further use in signal processing: the RMS stabilization already had occurred at this level, while the signal range R still remains unsaturated (see the middle pair of the plots). Saturation of range estimate comes into view when $I \geq 12$. It is probably caused by the finite dynamic range of the equipment. The middle pair of plots illustrates that signal range initially grows as I^2 , and finally approached the \sqrt{I} dependence. Saturation corresponds to $R = x_{\max} - x_{\min} = 20$ (this is the maximum $\pm 10 V$ value of analog-digital converter), and we see a slanting Hu dependence in the lowest frames. Further growth of the RMS amplitude may even reduce the Hurst exponent. One may see from Fig. 1 that inertia interval with 1/4 slope occupies from 7 to 10 octaves. The level $I=10$ recommended for further applications in the analysis always remains within inertia interval regardless the two-fold increase of signal RMS amplitude (a four time increase in intensity) we had illustrated in Fig. 1.

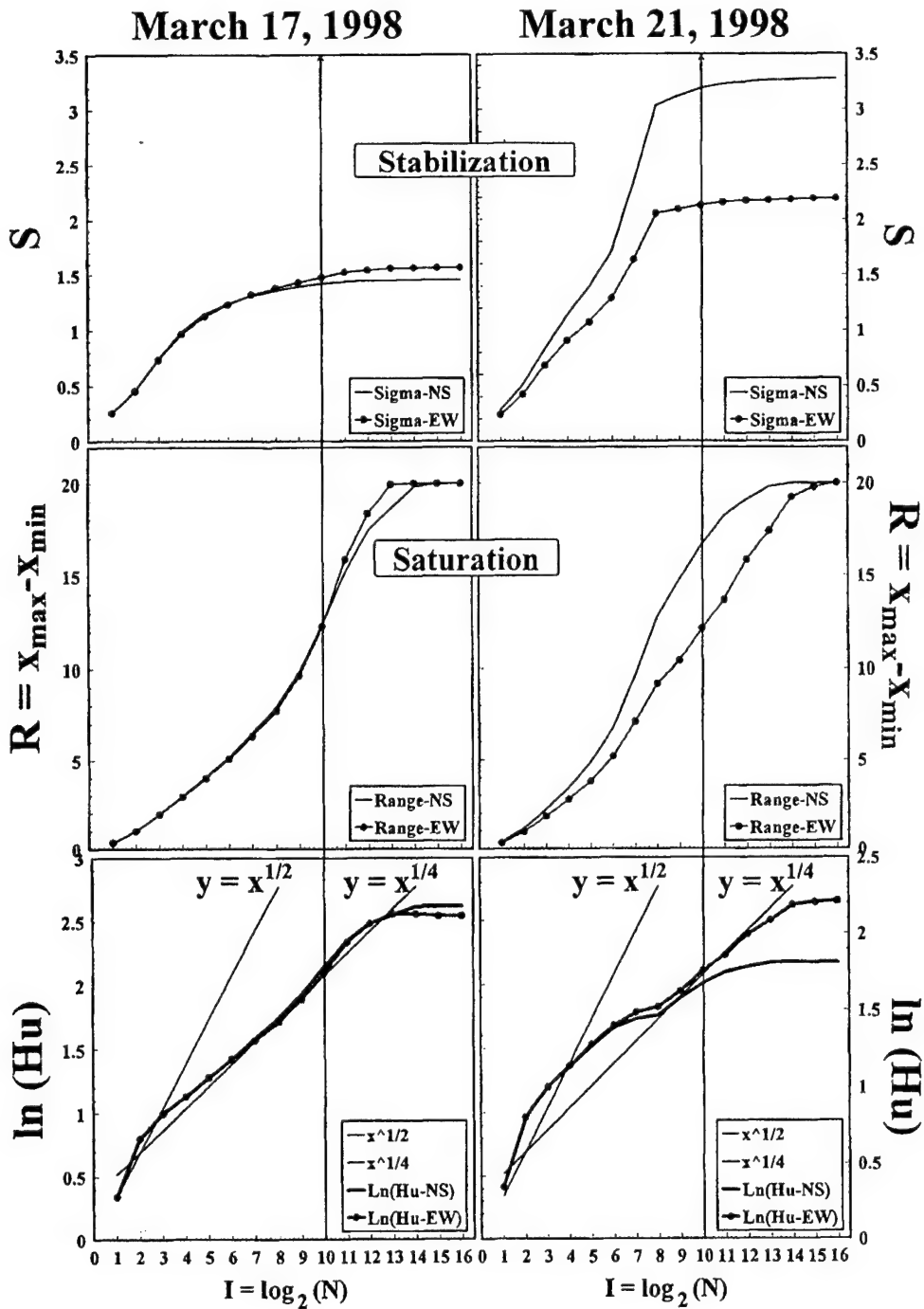


Fig. 1. Illustration of the functional dependence of the parameters involved in the Hurst exponent computations. Upper frames demonstrate the RMS amplitude stabilization for the lowest (left) and highest (right) signal levels. The middle frames depict how the saturation of signal range occurs. The lowest pair of plots shows resulting Hurst exponent. Vertical arrows indicate the $I = 10$ level we recommend for the further analysis when studying the temporal variations.

Inertia interval having the $1/4$ slope starts from the 'knee' area $I \in [2, 3]$ see Fig. 1. The knee position probably depends on the median interval between individual EM pulses. The pulses are still 'resolved' and independent at short segments of the signal, and the S , R and Hu values rapidly vary when I is small. For the fragments greater in duration, many independent pulses take part in forming the signal, stabilization occurs that is explained by the Central Limiting Theorem. As a result, we obtain a typical anti-persistent noise.

When the pulse rate grows, the RMS amplitude increases, and the inertia interval starts from lower values of I . Hence, the whole line of $1/4$ slope has to shift downward.

The fact that $Hu = 0.25$ indicates that the natural signals in Schumann resonance band should be regarded as an anti-persistent noise. A physically significant conclusion must be readily made. Since the signal is a composition of individual pulses arriving from the worldwide thunderstorm activity, and the resulting noise is normal, we have to conclude that no interaction is possible between individual pulses.

The above assumption about the pulse rate that drives variations in the Hurst exponent may be physically justified: variations of the pulse rate directly modulates the RMS noise level and its range. From the formal point of view, one may suppose that variations in the noise intensity are caused by pure alterations in the amplitude of arriving pulses. Validity of such an assumption is doubtful from the physical point of view because a lightning stroke in the atmosphere initiates after the electrostatic field reaches a 'standard' level.

An increase in the air convection and cloud electrification will result in an increase of the stroke number per unit time rather than their amplitude.

3. Conclusion.

Analysis performed in the present study allows to conclude the following.

1. The workability of the algorithm and that of approach had been proven for the natural radio signals in the ELF band.
2. Natural ELF radio signal in the frequency range of Schumann resonance should be regarded as an anti-persistent noise.
3. Indications had been found towards diurnal variations of the Hurst exponent that may be considered as a replica of daily changes in the electromagnetic pulse rate. This conclusion needs further investigation.

Acknowledgments: This work had been supported in part by the INTAS grant No. 1991-96.

References

- Evans, J.E. and A.S. Griffiths, Design of Sanguine noise processor based upon worldwide extremely low frequency recordings, *IEEE Trans.*, **Com-22**, No. 4, 528-539, 1974.
- Rytov, S. M., *Introduction to Statistical Radio Physics, Part 1: Random Processes*, Moscow, Nauka, 1976, pp. 204-210 (in Russian).
- Turcotte, D.L., *Fractals and Chaos in Geology and Geophysics*, Second edition, Cambridge University Press, Cambridge, 1997.

A COMPACT SOLUTION FOR NATURAL ELF PULSE IN TIME DOMAIN

A.P. Nickolaenko

*Usikov's Institute for Radio Physics and Electronics
Ukrainian National Academy of Sciences, Kharkov, Ukraine
fax: +38 (0572) 44-1105, e-mail: sasha@vlf.kharkov.ua*

and

L.M. Rabinowicz

*Radioastronomical Institute, Ukrainian National Academy of Sciences
Kharkov, Ukraine*

Abstract

We present an analytical time domain solution for the ELF electromagnetic wave propagating in the Earth ionosphere cavity. The workability of the formula obtained is demonstrated by computations of the pulse waveforms originating from a point vertical electric source.

1. Introduction

Natural electromagnetic radio signal in the extremely low frequency (ELF) band is a random succession of discrete pulses arriving from the global thunderstorm activity. Lightning strokes are the sources of ELF waves propagating as the TEM mode in the spherical cavity formed by the surface of the Earth and lower edge of ionosphere. Changes in the waveform occur due to dispersion and attenuation in the ionosphere. Therefore, initial delta-pulse arrives to a remote observer as an atmospheric having a sharp onset followed by a low frequency tail. The Earth-ionosphere cavity and Schumann resonance play the role of the low frequency band-pass filter in radio propagation.

When computing the fields, one applies the Fourier transform of the frequency domain field components [Nickolaenko and Hayakawa, 1998].

First, the fields are found using the mode theory [Wait, 1962], and then, the time domain solutions are computed numerically (Fourier transform).

We had construct an analytical time-domain solution for the pulsed ELF radio wave in the spherical Earth-ionosphere cavity in our previous work [Nickolaenko et al., 1999]. Now, our goal is in obtaining a compact form for the time domain presentation.

2. Model

A point vertical electric dipole is the source of the radio wave. We suppose the radiation moment of the source to be the delta-pulse in the time domain $M_c(t) = M_0 \cdot \delta(t)$. Therefore, our solution is the Green's function of the EM problem. Formal representation for such a solution in the frequency domain is well known:

$$E(\omega) = E_0 \sum_{n=0}^{\infty} \frac{(2n+1)P_n(\cos \theta)}{n(n+1) - \nu(\nu+1)} \quad (1)$$

$$E_0 = \frac{i\nu(\nu+1)M_c(\omega)}{4\pi\omega\epsilon ha^2} \quad (2)$$

$$H(\omega) = M_c(\omega) H_0 \sum_{n=0}^{\infty} \frac{(2n+1)P_n^1(\cos \theta)}{n(n+1) - \nu(\nu+1)} \quad (3)$$

$$H_0 = \frac{M_c(\omega)}{4\pi hac^2} \quad (4)$$

We use the polar spherical coordinate system $\{r, \theta, \varphi\}$ with the origin at the center of the Earth. The $\theta = 0$ axis points to the source, E_0 denotes the amplitude of vertical electric field $E_r(\omega)$ measured in $V \text{ sec/m}$, $H(\omega)$ is the full horizontal field component in $A \text{ sec/m}$, ω is the circular frequency, a is the radius of the Earth, h is effective ionosphere height, ϵ is the dielectric constant of the vacuum, θ is the angular distance $P_\nu[\cos(\pi - \theta)]$ and $P_\nu^1[\cos(\pi - \theta)]$ are the Legendre and associated Legendre functions that depend on the source distance, $\nu(\omega)$ is the propagation constant of the ELF radio wave,

integrand are situated found from the following equation:

$$n(n+1) - \nu(\omega)[\nu(\omega) + 1] = 0 \quad (6)$$

We use in this work the linear heuristic $\nu(f)$ dependence that corresponds to experimentally observed Schumann resonance frequencies of 8, 14, 20, etc., Hz [Nickolaenko *et al.*, 1999]: $\nu(\omega) = A\omega + B$ with $A = 1/12\pi - i/200\pi$ and $B = -1/3$.

We should note here that any spectral function $F(\omega)$ satisfies the Hermitic symmetry condition:

$$F(-\omega) = F^*(\omega) \quad (7)$$

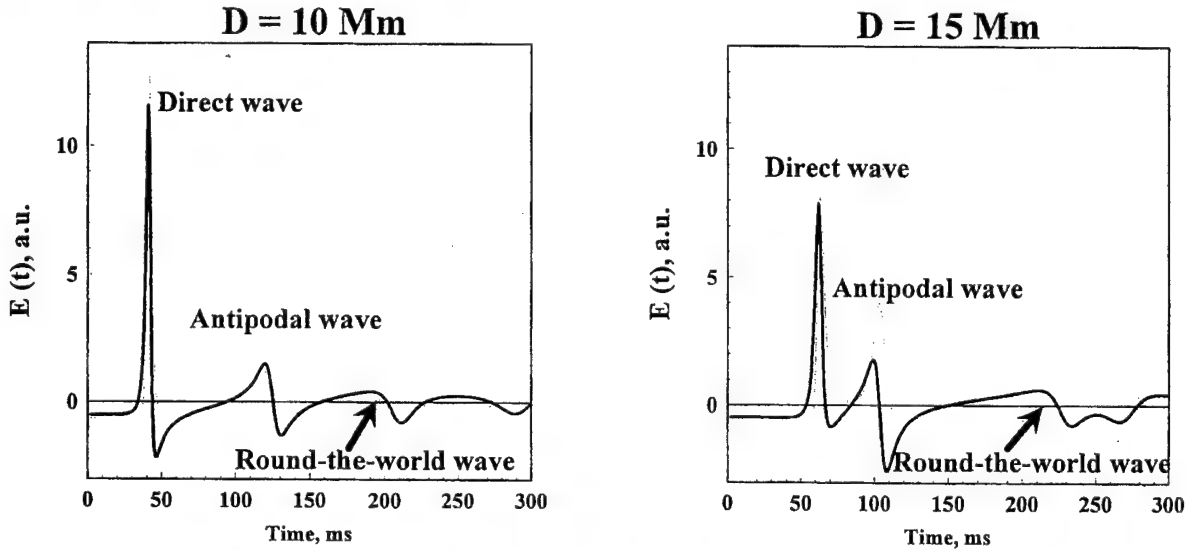


Fig. 1. Sample of computed pulse waveforms $E(t)$ at 10 and 15 Mm distance. Solid lines in the plots demonstrate dependence (16), while dashed lines depict results computed using sort (18) form.

Since $\text{Re}\{\nu\} > 0$ and $\text{Im}\{\nu\} < 0$, the traveling ELF radio waves attenuate with distance. The time domain solutions are obtained after Fourier transformation, e.g.,

$$E(t) = \frac{1}{2\pi} \int_{-\infty}^{\infty} E_r(\omega) e^{i\omega t} dt \quad (5)$$

The fields are presented in the time domain as a sum of residuals over the poles positioned in the upper half of the complex frequency plane:

The integration path in 'omega plane' is closed into upper half-space where the poles of

$$E(t) = A_E \sum_{n=-\infty}^{\infty} \frac{n(n+1)P_n(\cos \theta)}{\Omega_n \left. \frac{d\nu}{d\omega} \right|_{\omega=\Omega_n}} e^{i\Omega_n t} \quad (8)$$

and

$$H(t) = A_H \sum_{n=-\infty}^{\infty} \frac{P_n^1(\cos \theta)}{\left. \frac{d\nu}{d\omega} \right|_{\omega=\Omega_n}} e^{i\Omega_n t} \quad (9)$$

with the time domain amplitudes

$$A_E = \frac{M_0}{4\pi ha^2 \epsilon} \text{ and } A_H = \frac{M_0}{4\pi hac^2}.$$

We demonstrate below that the time domain series (8) and (9) are transformed into compact analytical expressions describing propagation of an ELF pulse. The linear frequency dependence of propagation constant plays an important role in obtaining compact formulas. In this case the poles become equidistant and are placed symmetrically in respect to the ordinate. This allows obtaining of the following simple relations:

$$E(t) = 2A_E \operatorname{Re} \left\{ \sum_{n=1}^{\infty} \frac{n(n+1)P_n(\cos \theta)}{n-B} e^{it \frac{n-B}{A}} \right\} \quad (10)$$

$$H(t) = 2A_H \operatorname{Im} \left\{ \frac{1}{A} \sum_{n=1}^{\infty} e^{it \frac{n-B}{A}} P_n^1(\cos \theta) \right\} \quad (11)$$

One may see that each term in (10) and (11) contains the factor that exponentially decays in time (parameter A is a complex value). These factors become unity when $t = 0$, and the series diverge at the source point $\theta = 0$. Both the series converge uniformly and absolutely within the whole Earth-ionosphere cavity for an arbitrary time $t \geq 0$, including the point where the lightning discharge was situated. When the time t increases, the exponential factors rapidly decay for higher mode numbers n . Hence, a smaller amount of terms is necessary to provide the same accuracy of the sum computations.

3. Accelerating convergence

To accelerate the convergence of series (10) and (11) we apply the technique used in frequency domain (Nickolaenko and Rabinowicz, 1974). Consider the generating function for the Legendre polynomials:

$$R_0(g, x) = \sum_{n=0}^{\infty} g^n P_n(x) = \frac{1}{(1-2gx+g^2)^{1/2}} \quad (12)$$

where $g = e^{it/A}$ and $x = \cos \theta$.

Series (12) converges uniformly and absolutely within the unit circle. After differentiating (12) in respect to g inside this circle we may obtain:

$$R_{-1}(g, x) = \sum_{n=0}^{\infty} (n+1)P_{n+1}(x)g^n \quad (13)$$

From the other hand, series (13) equals:

$$R_{-1}(g, x) = g \frac{\partial R_0(g, x)}{\partial g} + R_0(g, x) - 1 = \frac{1-xg}{(1-xg+g^2)^{3/2}} - 1 \quad (14)$$

We obtain an additional series using term by term integration in respect to g :

$$R_1(g, x) = \int_0^g R_0(s, x) ds = \sum_{n=1}^{\infty} \frac{g^{n+1} P_n(x)}{n+1} = \ln \frac{g-x+(1-2gx+g^2)^{1/2}}{1-x} \quad (15)$$

We have after substituting equations (12)-(15) into (10):

$$\frac{E(t)}{2E_A} = \operatorname{Re} \left\{ g^{-B} \left[R_{-1} + B(R_0 - 1) + B(B+1) \left(\frac{R_1 - g}{g} \right) + B(B+1)^2 \sum_{n=1}^{\infty} \frac{g^n P_n(x)}{(n+1)(n-B)} \right] \right\} \quad (16)$$

Expression for the magnetic field component is even more compact:

$$\frac{H(t)}{H_A} = \operatorname{Im} \left\{ \frac{1}{A} \frac{g^{(1-B)} (1-x^2)^{1/2}}{(1-2xg+g^2)^{3/2}} \right\} \quad (17)$$

4. Discussion of the results

We see that ELF pulsed signals are described in a clear compact way. In case of direct proportionality, namely, when parameter $B = 0$ and $A \neq 0$, analytical formulae become extremely simple:

$$E(t) = E_A \cdot \operatorname{Re} \left\{ \frac{1-xg}{(1-2xg+g^2)^{3/2}} - 1 \right\} \quad (18)$$

$$H(t) = H_A \operatorname{Im} \left\{ \frac{1}{A} \frac{g (1-x^2)^{1/2}}{(1-2xg+g^2)^{3/2}} \right\} \quad (19)$$

Computed waveforms for the electric pulses are shown in Fig. 1 obtained at 10 and 15 Mm distances. Time delay from the stroke is shown along the horizontal axis of the plots in ms. Pulse amplitude is depicted in arbitrary units on the ordinate. Solid lines in this figure show the solution (16), and dashed line represents equation (18). One may see an increase of the pulse delay with the distance. Antipodal and round-the-world waves are clearly seen in the plots.

5. Conclusion

To conclude the report we repeat the main results.

1. The compact analytical time domain solutions were obtained for both ELF field components.
2. The form of solution depends on the eigenvalue positions in complex frequency plane.
3. We constructed the accelerating procedure for the time domain solution obtained in the linear heuristic $\nu(\omega)$ dependence.
4. Formulae become extremely compact when $\nu(\omega)$ is directly proportional to frequency.
5. Computations show that all specific features of the ELF radio pulses are pertinent to the compact solutions.

Acknowledgments: This work had been supported in part by the INTAS grant No. 1991-96.

References

- Wait, J.R., *Electromagnetic waves in stratified media*, Pergamon Press, Oxford, New York, Paris, 1962.
- Nickolaenko and Rabinowicz, Speeding up the convergence of zonal harmonic series in the Schumann resonance problem, *J. Atmos. Terr. Phys.*, **36**, 979-987, 1974.
- Nickolaenko, A.P. and M. Hayakawa, Natural electromagnetic pulses in the ELF range, *Geophys. Res. Lett.*, **25**, 3103-3106, 1998.
- Nickolaenko, A. P., M. Hayakawa, I.G. Kudintseva, S.V. Myand, L.M. Rabinowicz, ELF sub-ionospheric pulse in time domain, *Geophys. Res. Lett.*, **26**, 999-1002, 1999.

BIOGRAPHICAL NOTES



A. P. Nickolaenko was born in Kharkov, Ukraine on June 08 1944. He graduated from the Kharkov state University in 1966 and joined the Institute of Radio Physics and Electronics of the Academy of Sciences of the Ukraine (IRE). In 1972, he got the degree of Candidate in Phys-Math Sciences (an equivalent of Ph.D.) from the Kharkov State University. In 1974 he was elected as a Senior Scientist of IRE. In 1988, A. P. Nickolaenko got the degree of Doctor in Phys-Math Sciences from Kharkov State University. In 1985-1996, A.P. Nickolaenko was a Senior and Leading (since 1988) Scientist of the Radio Astronomical Institute. In 1996 he returned to the Institute of Radio Physics and Electronics of NASU as a Leading Scientist. Dr. A.P. Nickolaenko took part in 34-th Soviet Antarctic Expedition (1988-1989) as a member of season stuff at the 'Bellinshausen' station. In 1995 and 1998-1999, Dr. A.P. Nickolaenko worked for the University of Electro-Communication as invited professor (Department

of Electronic Engineering, laboratory of Prof. M. Hayakawa)



L. M. Rabinowicz was born in Kharkov, Ukraine on June 02, 1948. He graduated from the Kharkov state University in 1972. Since 1966, L.M. Rabinowicz

worked for the Institute of Radio Physics and Electronics of the Ukrainian Academy of Sciences (IRE). He got the degree of Candidate in Phys.-Math. Sciences (an equivalent of Ph.D.) from the Kharkov State University in 1989. Since 1986, Dr. L.M. Rabinowicz works as the Research Fellow for the Radio Astronomical Institute of National Academy of Sciences of the Ukraine.

THREE DIMENSIONAL RAY-TRACING FOR VERY LOW LATITUDE WHISTLERS, WITH CONSIDERING THE LATITUDINAL AND LONGITUDINAL GRADIENTS OF THE IONOSPHERE

Kenji Ohta and Hiroshi Kanzaki

Department of Electronic Engineering, Chubu University, Kasugai Aichi, 487-8501 Japan
(e-mail:ohta@isc.chubu.ac.jp)

Masashi Hayakawa

Department of Electronic Engineering, The University of Electro-Communications, Chofu Tokyo
182-8585, Japan (e-mail:hayakawa@aurora.ee.uec.ac.jp)

Abstract

Propagation mechanism of very low latitude, less than geomagnetic latitude 20° , whistlers is poorly understood, and this paper examines the propagation characteristics of non-ducted propagation at very low latitudes by using 3-D ray tracing for realistic ionosphere /magnetosphere models with latitudinal and longitudinal gradients and IGRF magnetic model. By making full use of systematic analyses of ionospheric parameters, we conclude that Local Time (L. T.) the dependence of occurrence rate of whistlers at very low latitudes can be accounted for by means of the latitudinal gradient of the ionosphere.

1. Introduction

As is summarized in our review papers [1] [2] the propagation mechanism of whistlers at

very low latitudes (geomagnetic latitude, less than 20°) is very controversial, because both ducted and non-ducted propagations have been proposed. However, in our previous paper [3] we have investigated the non-ducted propagation in the three dimensional (3-D) situation with including both the latitudinal and longitudinal gradients of the ionosphere. And we have succeeded in explaining even the presence of echo-train whistlers [4] at geomagnetic latitudes $10-15^\circ$ by this non-ducted propagation.

This paper is a further extension of our previous paper [5], and we try to explain the L. T. dependence of very low latitude whistlers by above non-ducted propagation mechanism. We made the simultaneous whistler measurements in South China, Zhanjiang (geomag. lat. 10.0°N). Based on our observation and the results by Chinese colleagues [6], the occurrence of very low latitude whistlers is extremely limited to the

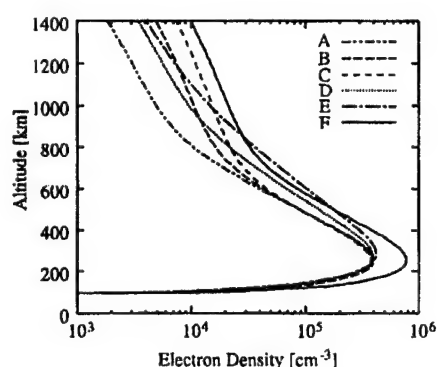


Fig.1 Profiles of background magnetospheric electron density

L. T. interval from 0h to 4h.

2. Ray-tracing in 3-D model

2.1 Ray-tracing model (electron density and magnetic field)

The electron density model of the ionosphere/magnetosphere (N_e) is expressed by the following equation [5].

$$N_e(r, \theta, \phi) = N_{DE}(r) N_l(r) N_g(r, \theta) N_L(\phi) \quad (1)$$

where $N_{DE}(r)$ is the diffusive equilibrium model, $N_l(r)$ is the modification factor due to the lower ionosphere, $N_g(r, \theta)$ is the latitudinal gradient, $N_L(\phi)$, longitudinal gradient, and (r, θ, ϕ) (geocentric distance, geographic colatitude, geographic longitude). The effect of the equatorial anomaly is included in the following way. The geographic latitude can be related to the geomagnetic latitude when we specify the longitude to be that of China because the latitudinal density gradient is expressed in terms of the following Singh[7]'s expression.

$$N_g' = 1 + C(r) \exp[\alpha(\sin \theta' - \sin \theta_0')] \quad (2)$$

where θ' is the geomagnetic latitude,

α and $\sin \theta_0'$ refer to the parameters in modeling the latitudinal gradient. The formula for $C(r)$ is already given in Ohta et al.[3]. Then, the longitudinal gradient is given by Zhou et al. [8],

$$N_L(\phi) = 1.0 + LG(\pi/180)(\phi - \phi_0) \quad (3)$$

where LG is the factor of longitudinal gradient, and ϕ_0 is the reference geographic longitude.

2.2 Ray tracing results

The information on the nighttime winter ionosphere parameters during 1978-1980 are based on the ISS-b satellite. Fig. 1 is the summary of the possible profiles (A~F) at low latitudes. Figs. 2 and 3 show the results of 3-D ray-tracing computations ($f = 5\text{kHz}$) indicating the final arrival point ($h = 120\text{km}$) and the final wave normal angle there for Model A and for Model F, respectively, when the two parameters, α and LG are widely changed. The reference values for α and LG are estimated by the observational results based on the NSSDC data at the height of 120km at L. T. = 0h on January 5th, 1988 on which day we could observe the largest number of whistlers at Zhanjiang. Launching position is determined that the final position in the Northern hemisphere is closest to Zhanjiang and also the final wave normal is closest to the vertical to the ionosphere.

Fig. 3 is the corresponding results for Model F. Model F is very difficult to generate ground whistlers, such that we can expect the reception of ground whistlers only for $\alpha \geq 13.55$ (in the top panel of Fig. 3).

2.3 Local time dependence of whistler occurrence rate

Examination of NSSDC data (on the

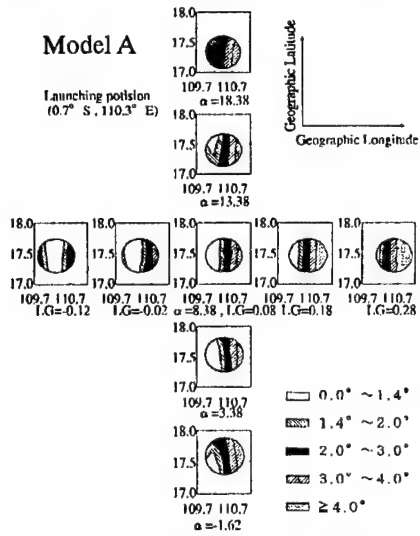


Fig.2 Final locations and incident angle, when parameters of α and LG change (model A)

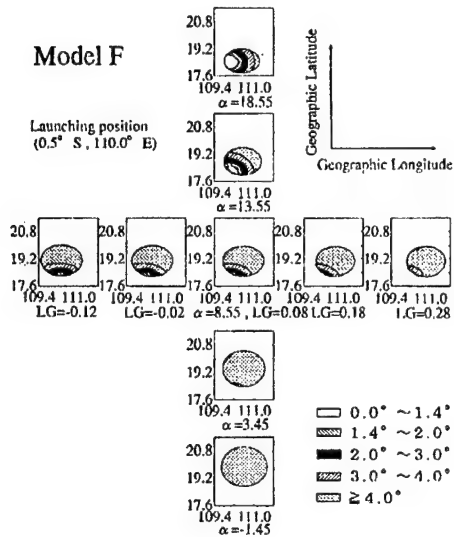


Fig.3 Final locations and incident angle, when parameters of α and LG change (model F)

ionospheric density profile) during midnight shows that there is a very small temporal

variation in LG, and so we will examine the effect of α (latitudinal gradient).

Fig. 4 is the result of temporal variation of α of the lower ionosphere ($h=120\text{km}$) in the Southern hemisphere (geographic coordinates, 0.5°S , 110.0°E) on Jan. 5th, 1988, which was

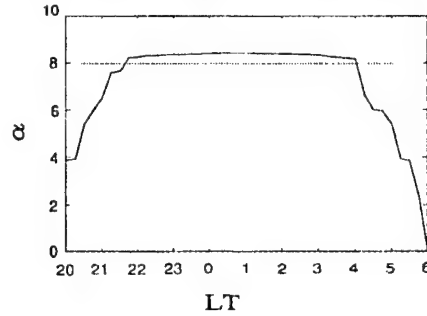


Fig.4 Variation of α with LT.

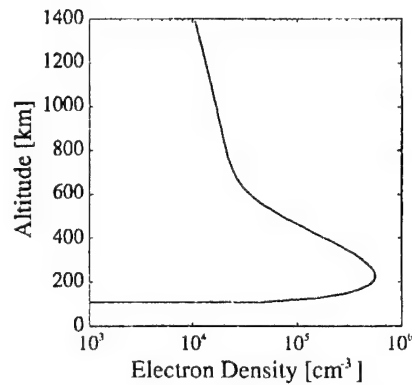


Fig.5 Profile of background magnetospheric electron density (model X)

estimated from the NSSDC data. This figure shows that α takes the largest value for about 6 hours from L. T. = 22h to L. T. = 4h. This behavior is easily expected by considering the spatial and temporal evolution of the equatorial anomaly. This time interval is nearly consistent with the observational fact that whistler occurrence is limited to these L. T. intervals.

Then, we have developed a particular profile based on the NSSDC data, in which the whistler is observable for $\alpha > 8$. This profile X is given in Fig. 5, which is closer to Model F, whose important characteristic is a sharp transition layer at lower altitude (~ 600 km).

Fig. 6 illustrates the corresponding result for Model X with changing α and LG. Then, the rays with the final wave normal angle less than 1.4° (indicated as a white area) are able to

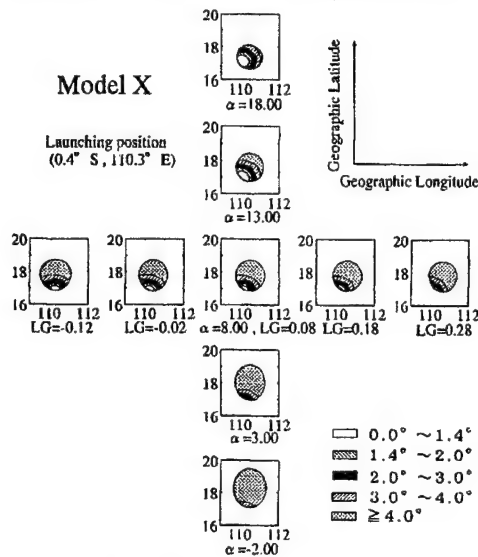


Fig. 6 Final locations and incident angle, when parameters of α and LG change (model X)

penetrate through the ionosphere onto the ground. This area exists only at the left bottom of the middle panel. However, with the increase in α and decrease in LG, the area of the ground reception is found to be widened.

3. Conclusion

This 3-D non-ducted propagation with a scatter in the initial wave normal angle in the Southern hemisphere, is used to explain the limited occurrence of very low latitude whistlers in the L. T=0h to 4h. We can summarize the present studies as follows.

- (1) The propagation of very low latitude whistlers can be explained and determined by the propagation characteristics in the ionosphere, not by the lightning activity.
- (2) The 3-D non-ducted propagation with taking into account a plausible small scatter in the initial wave normal angle, is very likely to explain the propagation characteristics of very low latitude whistlers. The ground reception is found to be strongly dependent on the ionospheric latitudinal gradient.
- (3) The L. T. dependence of the occurrence of very low latitude whistlers can be explained by the L. T. dependence of the latitudinal gradient of the ionosphere.
- (4) Then, the L. T. dependence of the occurrence of whistlers may be used to infer the possible magnetospheric /ionospheric profile (especially information on the transition layer) and a latitudinal gradient.

4. References

- [1] Hayakawa, M. and Y. Tanaka, On the propagation of low latitude whistlers, *Rev. Geophys.*, **16**, 111, 1978.
- [2] Hayakawa, M. and K. Ohta, The propagation of low latitude whistlers: A review, *Planet. Space Sci.*, **41**, 1339, 1992

- [3] Ohta, K., Y. Nishimura, T. Kitagawa and M. Hayakawa, Study of propagation characteristics of very low latitude whistlers by means of three-dimensional ray-tracing computations, *J. Geophys. Res.*, **102**, 7537, 1997.
- [4] Hayakawa, M., K. Ohta and S. Shimakura, Spaced direction finding of nighttime whistlers at low and equatorial latitudes, *J. Geophys. Res.*, **95**, 15091, 1990.
- [5] Ohta, K., M. Hayakawa and S. Shimakura, Occurrence rate of whistlers at low latitudes and the lightning activity in the conjugate hemisphere, *Trans. Inst. Electr. Inform. Comm. Engrs. Japan*, **J74-B-II**, 276-284, 1997 (in Japanese).
- [6] Liang, B. X., T. Bao and J. S. Xu, Propagation characteristics of nighttime whistlers in the region of equatorial anomaly, *J. Atmos. Terr. Phys.*, **47**, 999-1007, 1985.
- [7] Singh, B., On the ground observation of whistlers at low latitudes, *J. Geophys. Res.*, **81**, 2429-2432, 1976.
- [8] Zhou, H. B., J. S. Xu and M. Hayakawa, On the longitudinal effect in whistler propagation characteristics at low latitudes, *Planet. Space Sci.*, **36**, 833-839, 1988.

BIOGRAPHICAL NOTES

Kenji Ohta graduated from Department of Communication Engineering, Shinshu Univ. in 1966 and received the Doctor of Engineering from Nagoya Univ. in 1987 and he is Professor of Chubu University. He is member of the Society of Atmospheric Electricity of Japan and was awarded its Society Prize in 1991.

Masashi Hayakawa was graduated from Nagoya Univ. in 1966, where he obtained a Dr. of Eng. Degree and become a Professor of The Univ. of Electro Communication in 1990. In 1983 he was awarded the Tanakadate Prize, and in 1988 awarded the prize of The Society of Atmospheric Electricity of Japan.

WORLDWIDE LIGHTNING MAPPING WITH ELF TOMOGRAPHY

A. V. Shvets

Usikov Institute for Radiophysics and Electronics of the National Academy of Sciences of Ukraine,
12, Akad. Proskury St., Kharkov, 61085, Ukraine. Fax: 38 (0572) 441 105, E-mail: larisa.nipi@ugp.viaduk.net

A technique of tomographic reconstruction of the worldwide lightning activity is proposed. The technique is based on measurement of average Schumann Resonance (SR) spectra from different distant receiving stations distributed over the globe. Distance profiles of lightning intensity recovered from average spectra measured at each station are used for tomographic reconstruction. An effective algorithm for tomographic reconstruction has been developed to reduce required computational resources. It is shown that characteristic structure presented by the world thunderstorm centers can be resolved by only few distant optimally placed observation stations. A possibility of reconstruction of global lightning spatial distribution by application data from existing SR field sites is numerically studied.

1. INTRODUCTION

Radio waves in the lower end of ELF band propagating within the Earth-ionosphere waveguide exhibit very low attenuation. In the result of interference between radio waves repeatedly passed the globe circumference a phenomenon known as Schumann Resonances [1, 2] is observed in spectra of natural electromagnetic emissions. It is commonly assumed that the observed SR are excited by lightning discharges and their amplitudes supply information about global thunderstorm activity concentrated mainly in tropic belt over land areas. Interest to the SR as indicator of global environmental changes was stimulated last years after Williams's work [3], in which strong correlation between amplitude of the 1st mode of SR and anomalous changes in average tropical temperature was revealed during a 6-year time span. Recent works employ SR measurements for inferring global thunderstorm activity and its spatial reconstruction by using model of the world thunderstorm centers [4-9].

A simplified consideration employing a point source model placed on the Earth surface at some distance from an observer determines two characteristic ranges. The first is the globe circumference that determines basic SR frequencies. The second is a difference between direct and passed trough the antipodal to an observer point path lengths. Direct and antipodal waves come to an observation point with phase difference determined by source-observer range

and interfere "pure" SR producing a distance signature in field spectra.

Apart from horizontal magnetic or vertical electric field spectra of SR their combinations emphasizing the distance signature are employed for locating of lightning at great distances [10-13].

Observed SR signal morphologically consists of background formed by overlapping pulses from lightning discharges non-uniformly distributed all over the globe occurred with rate of about 100 s⁻¹ and so-called Q-bursts excited by "super"-discharges [14]. Q-bursts exceed a background amplitude by a few times, and interval between them is from few seconds to few minutes. While Q-bursts are isolated events and their sources may be located by techniques mentioned above for analysis of spatial structure of the global lightning a simple model of world thunderstorm centers is employed usually.

In this paper we introduce a technique of tomography reconstruction of the worldwide lightning activity structure based on decomposition of average SR spectra measured at different spaced receiving stations. Results of numerical simulation of tomography reconstruction are discussed.

2. PRINCIPLES OF THE WORLDWIDE LIGHTNING TOMOGRAPHY

Tomography methods are based on reconstruction of internal structure of a studied object from integral quantities measured along various paths through an object of interest. A tomographic projection is formed by grouping values measured along parallel paths under some angle in a cross-section of an object. Having a number of projections measured under different angles a desired two-dimensional distribution may be reconstructed on the base of the central slice theorem. Another approach used e.g. in the ionospheric tomography employs "pixel" method in which there is no necessity to form projections and tomography reconstruction is performed on a base of mathematical treating of an equation system relating integral quantities measured along different paths and pixel values exhibiting desired two-dimensional distribution. The second approach is employed for the aim of global lightning distribution in the present work.

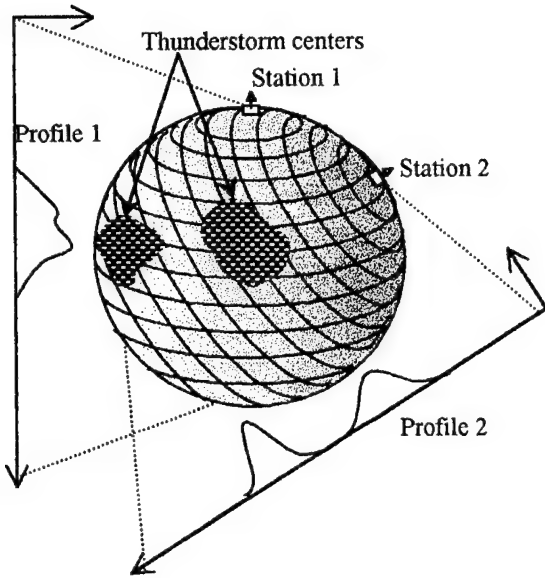


Fig. 1. Experimental setup for the worldwide lightning tomography.

Consider integral lightning intensity within annular concentric stripes on the Earth surface with center at an observation point as shown in Fig. 1. Lightning discharges within particular annular stripe are approximately equidistant from an observation point and form the same distance signature in measured SR spectra. Shvets [13] has proposed a technique for decomposition of average power SR spectra measured at a single site into distance lightning intensity profile. Each point in such a distance profile represents an integral value of lightning intensity within partial annular stripe. Different distant receiving points allow us to look on global lightning under various "angles of view" (see Fig. 1) and provide different distance profiles for the global lightning, which may be considered as tomographic projections in a certain sense. Mathematical treating of a set of such profiles supplies reconstruction of the global lightning over the Earth surface. Experimental setup for the worldwide lightning tomography is presented in Fig. 1. For simplicity only two receiving stations are shown. We can see that model spatial distribution consisting of two thunderstorm areas produce different distance profiles at the stations.

Thus, the problem of the global lightning mapping with ELF tomography consists of two-stage inverse problem. The first includes decomposition of measured average SR spectra at a number of stations distributed over the planet. The second includes reconstruction of a surface distribution of the global lightning activity from a set of distance profiles. Both of these stages are ill posed problems with constrictions dictated by physical sense of desired nonnegative quantities of lightning intensity and must be solved by the regularized least squares method (see e.g. 15, 16).

3. DISTANCE PROFILING OF THE WORLDWIDE LIGHTNING

The background SR signal is formed by incoherently overlapping pulses from lightning discharges non-uniformly distributed over the Earth surface, which occur at arbitrary and uncorrelated moments with Poisson interval distribution. Thus, after averaging of current lightning moments within partial distance intervals, we can write an approximate relation for the total energy of the signal postulating incoherent summation of energies of pulses produced by each lightning stroke [13]:

$$|E_r(\omega)|^2 = |\bar{M}|^2 \sum_{i=1}^N S_i |e(\omega, D_i)|^2 \quad (1)$$

where $E_r(\omega)$ is measured vertical electric component, S_i is a number of discharges from i^{th} distance interval (annular stripe), N is a number of distance intervals, $|\bar{M}|$ is a mean lightning current moment, $e(\omega, D_i)$ is a frequency response of the Earth-ionosphere cavity on vertical electric discharge from distance D_i (see Wait, 1970 17; Galejs, 1972 18; Bliokh et al., 1980 19). We suppose that field spectra of the sources within i^{th} interval are the same, each interval is represented by ensemble of strokes enough for statistical averaging, and a mean current moment $|\bar{M}|$ is independent of distance. We also suppose propagation parameters and frequency dependence of $|\bar{M}|$ being known (see e.g. Ishaq and Jones, 1977; Bliokh et al., 1980; Jones and Burke, 1992). Eq. 1 can be presented in operator form:

$$\hat{A} \vec{x} \approx \vec{b}, \quad x_i = S_i \geq 0, \quad b_j = |E_r(\omega_j)|^2, \quad (2)$$

$$A_{ij} = |\bar{M}|^2 |e(\omega_j, D_i)|^2; \quad i = 1..N, \quad j = 1..P.$$

where \vec{x} is an unknown vector, P is a number of discrete points in an analyzed spectrum. The task can be also resolved if we use measured orthogonal magnetic components instead of the vertical electric component by the same way. As was shown by Shvets [3] a linear combination of electric and full magnetic power spectra emphasizing a distance signature may be constructed and can be used for recovering of distance profile of lightning intensity.

4. TOMOGRAPHY RECONSTRUCTION PROCEDURE

Laying on the Earth surface a net with M discrete ordered points and assigning them unknown values of lightning intensity we get an unknown M -dimensional vector \vec{s} . Sum of elements of \vec{s} matching i^{th} annular stripe centered at k^{th} observation point is equal to i^{th} value of k^{th} distance profile. From this condition the next equation system can be constructed:

$$S_{ki} = \sum_{j=1}^M W_{kij} s_j; \quad k = 1..K, \quad i = 1..N, \quad j = 1..M \quad (3)$$

where S_{ki} is an integral lightning intensity within i^{th} distance interval as measured from k^{th} observation point,

W_{kij} is a system matrix determined by geometry of the observation points distribution, s_j is a number of lightning strokes at j^{th} discrete point of the Earth surface, K is a total number of the observation stations. The system matrix W_{kij} has $K \cdot N$ rows and M columns. The row elements of the system matrix can be unit or zero. Only row elements matching an interior of partial annular stripe are equal to unity while all other elements in corresponding row are zeros. So, geometry of observation points distribution and type of a discrete net determine the system matrix. It is simply to show that the system matrix is essentially sparse. Approximate estimation of part of nonzero elements in a matrix row can be evaluated from ratio between area of a partial spherical annular stripe of width Δ and total area of the Earth surface.

Solving algorithm for tomographic reconstruction from Eq. 3 requires considerable computational resources both for memory and processor speed because of relatively large size of a system matrix and can take much time. Possible acceleration of a solving algorithm can be based on natural supposition that some points in a distance profiles takes zero or very small values due to essential non-homogeneity of a global lightning distribution. Such zero points in distance profiles supply immediate finding of zero elements of unknown vector \vec{S} and excluding of corresponding columns from Eq. 3.

Geometrical sense of this operation is finding of intersection areas between nonzero parts of all distance profiles. Tomographic reconstruction then is performed on essentially reduced intersection areas.

5. RESULTS OF MODELLING

Two basic questions arise when we start thinking about practical realization of the technique proposed.

- How many observation points it is need for reliable reconstruction of lightning distribution?
- How they should be arranged on the Earth surface?

Both of these questions we will clarify here by means of numerical simulation. Some reasons for optimizing of observatories' arrangement could be taken from known features of the world thunderstorm distribution. As was mentioned above thunderstorms mainly are concentrated in the world thunderstorm centers situated predominantly in tropic belt over land areas. To resolve different thunderstorm zones we have to require them to be distinguishable one from other in distance profiles recovered from different prospective observation sites. For that their positions should be chosen at points differently distanced from various thunderstorm centers, i.e. in tropics.

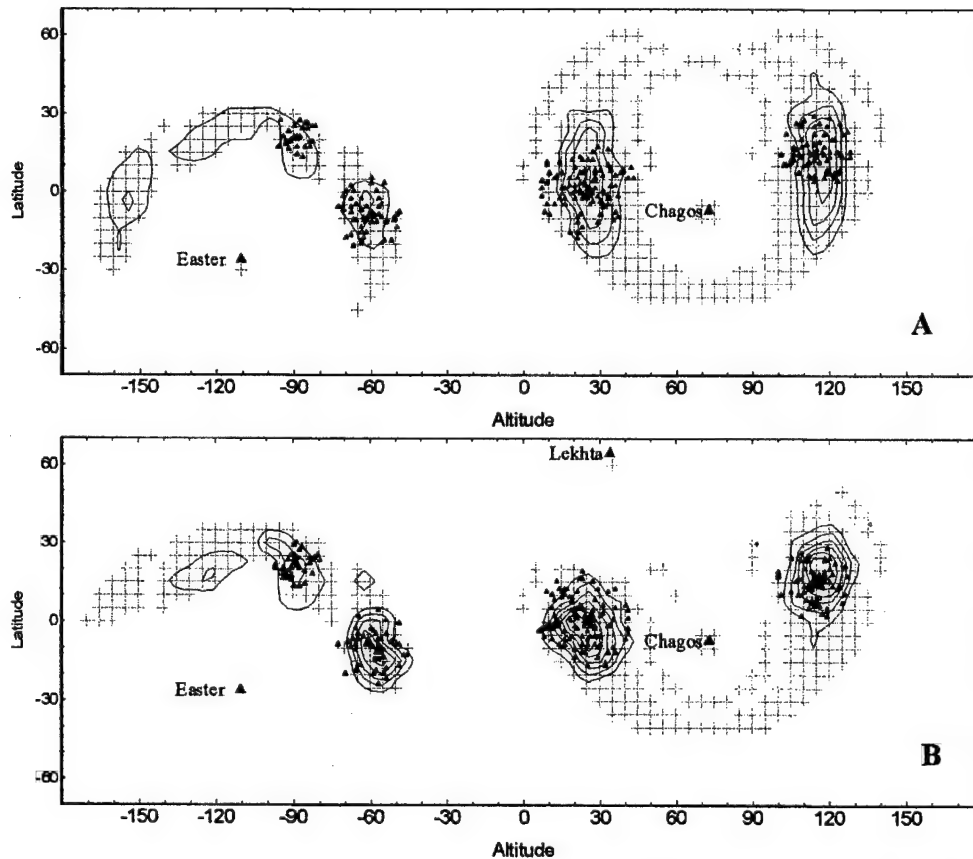


Fig. 2. Results of reconstruction of a model lightning distribution. A – two field sites placed within tropics. B – two field sites placed in tropics combined with high latitude station that allows increasing latitudinal resolution.

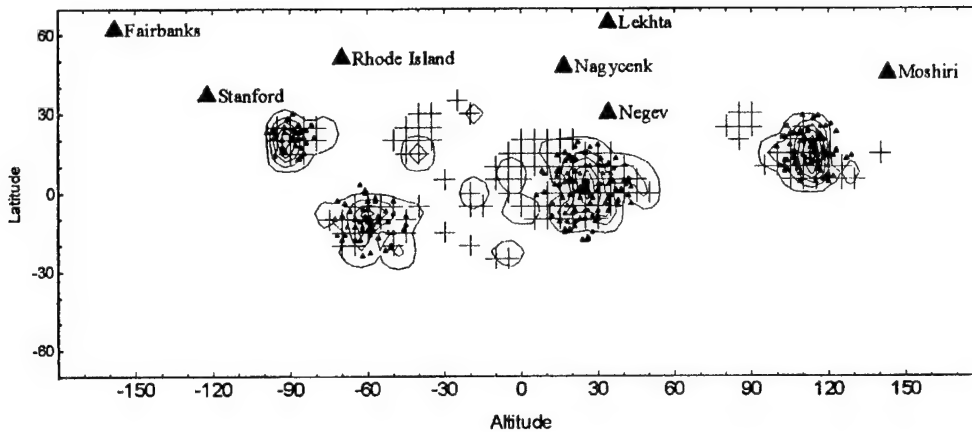


Fig. 3. Tomography reconstruction of a model lightning distribution with using existing SR sites.

For numerical simulation four circle zones of different sizes covered approximately the world

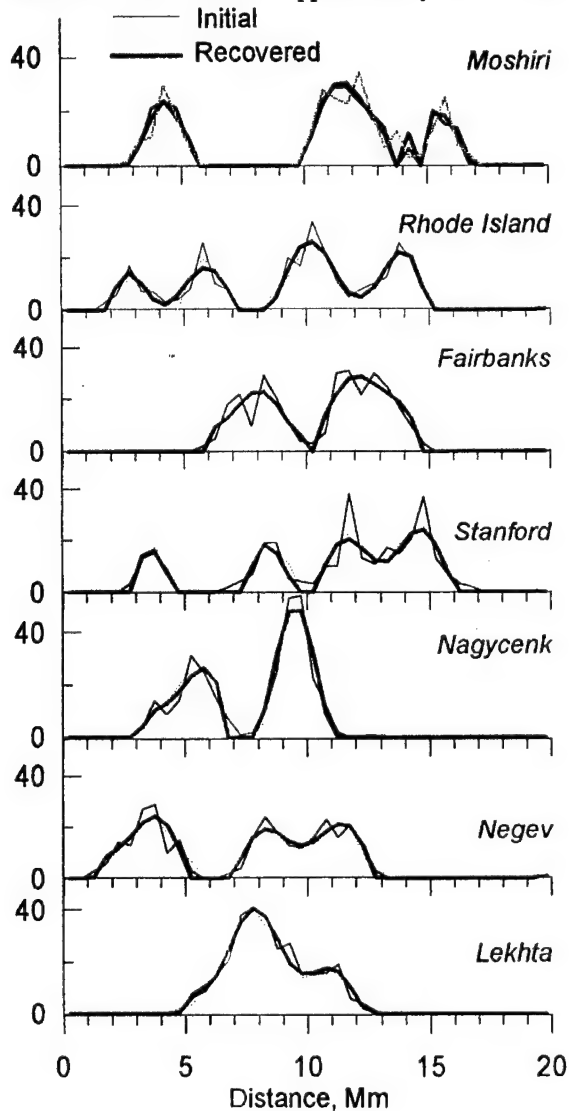


Fig. 4. Distance profiles recovered from average power spectra formed at the SR field sites by model source distribution.

thunderstorm centers were used. Co-ordinates of model standard lightning discharges were calculated to fill stochastically these areas. The simulated spatial distribution was used for calculation of average power field spectra for each observation station. These spectra together with field site co-ordinates are input parameters for tomographic reconstruction procedure.

Results of tomographic reconstruction of the model lightning distribution for optimized arrangement of prospective ELF receiving stations are presented in Fig. 2. Co-ordinates of lightning discharges are marked by small filled triangles. The reconstruction task is solving on a sufficiently reduced point set formed by intersection between all distance profiles. Crosses mark these intersection points in the figures. Co-ordinates of field sites are marked by large labeled solid triangles. Contour level lines in these figures present reconstructed lightning distributions. We can see that with optimized arrangement for concentrated in tropics sources the only few observation sites allow us to estimate spatial structure of the global thunderstorm activity.

Reconstruction result with existing SR observation sites is shown in Fig. 3. Some minor phantom sources appear for such combination of stations and lightning distribution. Comparisons between initial and decomposed distance profiles for a number of operating at present or in the past SR field sites are presented in Fig. 4.

6. CONCLUSIONS

1. A technique of tomographic reconstruction of the worldwide lightning activity was proposed.

2. The technique is based on measurement of average SR spectra from different distant receiving stations situated over the globe. Distance profiles of lightning intensity are recovered from the average spectra measured at each station and used for tomographic reconstruction.

3. An effective algorithm for tomographic reconstruction has been developed to reduce required computational resources.

4. It is shown that characteristic distribution of the world thunderstorm activity concentrated within the world thunderstorm centers can be resolved by only few distant optimally placed observation stations.

5. Results of numerical simulation of tomographic procedure show satisfactory reconstruction of global lightning distribution by application existing SR field sites.

Acknowledgement. This research is supported in part by a grant #96-1991 from INTAS.

REFERENCES

1. Schumann W.O., "Über die Strahlungslosen Eigenschwingungen einer leitenden Kugel die von Luftschicht und einer Ionosphärenhülle umgeben ist", *Z. Naturforsch.*, Vol. 7a, 1952, pp. 149-154.
2. Balser M., Wagner C.A., "Observation of Earth - Ionosphere Cavity Resonances", *Nature*, Vol. 188, 1960, pp. 638-641.
3. Williams, E. R., "The Schumann Resonance: A global tropical thermometer", *Science*, Vol. 256, 1992, pp. 1184-1187.
4. Nickolaenko A. P., Hayakawa M., and Hobara Y., "Temporal variations of the global lightning activity deduced from the Schumann resonance data", *J. Atmos. Solar-Terr. Phys.*, Vol. 58, 1996, pp. 1699-17109.
5. Fullekrug, M. and A.C. Fraser-Smith, "Global lightning and climate variability inferred from ELF magnetic field variations", *Geophys. Res. Letters*, Vol. 24, No. 19, 1997, pp. 2411-2414.
6. Heckman, S.J., E. Williams, and R. Boldi, "Total global lightning inferred from Schumann resonance measurements", *J. Geophys. Res.*, Vol. 103, 1998, pp. 31775-31779.
7. Nickolaenko A.P., Satori G., Zieger B., Rabinowicz L.M., and Kudintseva I.G., "Parameters of global thunderstorm activity deduced from the long-term Schumann resonance records", *J. Atmos. Solar-Terr. Phys.*, Vol. 60, 1998, pp. 387-399.
8. Satori, G., and B. Zieger, "Anomalous behavior of Schumann resonances during the transition between 1995 and 1996", *J. Geophys. Res.*, Vol. 103, No. D12, 1998, pp. 14147-14155.
9. Belyaev, G.G., A. Yu. Schekotov, A. V. Shvets, A. P. Nickolaenko, "Schumann resonances observed using Poynting vector spectra", *J. Atmos. Solar-Terr. Phys.*, Vol. 61, 1999, pp. 751-763.
10. Kemp D. T., and Jones D. Li, "A new technique for the analysis of transient ELF electromagnetic disturbances within the Earth-ionosphere cavity", *J. Atmos. Terr. Phys.*, Vol. 33, 1971, pp. 567-572.
11. Ishaq M., and Jones D. Li., "Method of obtaining radiowave propagation parameters for the Earth-ionosphere duct at ELF", *Electronic Letters* Vol. 13, 1977, pp. 254-255.
12. Nickolaenko A.P. and Kudintseva I.G., "A modified technique to locate the sources of ELF transient events", *J. Atmos. Terr. Phys.*, vol. 56, 1994, pp. 1493-1498.
13. Shvets A.V., "A technique for reconstruction of global lightning distance profile from background Schumann resonance signal", *J. Atmos. Solar-Terr. Phys.*, 2000, submitted.
14. Ogawa, T., Tanaka, Y., Miura, T., Yasuhara, M., "Observations of natural ELF and VLF electromagnetic noises by using the ball antennas", *J. Geomagnetism and Geoelectricity*, Vol. 18, 1966, pp. 443-454.
15. Lawson, C. L., and R. J. Hanson, "Solving Least Squares Problems", Prentice Hall, ch. 23, 1974, p. 161.
16. Tikhonov, A., and V. Arsenin, "Solutions of ill-posed problems", Wiley, New York, 1977.
17. Wait J. R., 1970. *Electromagnetic Waves in Stratified Media*. Pergamon Press, Oxford, (2-nd Ed.).
18. Galejs, J., "Terrestrial propagation on Long Electromagnetic Waves", Pergamon Press, New York, 1972.
19. Bliokh, P.V., Nickolaenko, A.P., Filippov, Yu. F., "Schumann resonances in the Earth-ionosphere cavity", In: *IEE Electromagnetic Waves Series 8*. Peter Perigrinus Ltd, Stevenage, 1980.

BIOGRAPHICAL NOTE



Alexander V. Shvets received the B.S., M.S. and Ph.D. degrees all from Kharkov University in 1980, 1982, and 1994, respectively. He worked in the Institute of Radio Astronomy as

Junior Fellow and Research Associate. He is now a senior researcher at the Usikov Institute for Radiophysics and Electronics of the National Academy of Sciences of Ukraine. From January to August of 1997 he was an invited scientist at the Earth Observation Research Center of the National Space Development Agency of Japan. His main research interests include experimental studies of ELF-VLF radio waves propagation within the Earth-ionosphere cavity, inverse problem, and seismogenic emissions.

ULF ELECTROMAGNETIC PRECURSORS FOR AN EARTHQUAKE AT BIAK, INDONESIA ON FEBRUARY 17, 1996

Masashi Hayakawa ^{1,2)}, Tetsuya Itoh ¹⁾, Katsumi Hattori ³⁾, and Kiyohumi Yumoto ⁴⁾

1. Department of Electronic Engineering, The University of Electro-Communications, 1-5-1 Chofugaoka, Chofu Tokyo 182-8585, Japan fax: +81 (0)424 43 5783 e-mail: hayakawa@whistler.ec.ucc.ac.jp
2. EORC, NASDA (National Space Development Agency of Japan), 1-9-9 Roppongi, Minato-ku, Tokyo 106-0032, Japan
3. The Institute of Physical and Chemical Research (RIKEN), 3-20-1 Orido, Shimizu, Shizuoka 424-8610, Japan e-mail: hattori@iord.u-tokai.ac.jp
4. Department of Earth and Planetary Sciences, Kyushu University, Fukuoka 812-8581, Japan e-mail: yumoto@geo.kyushu-u.ac.jp

ULF electromagnetic emissions associated with a large earthquake occurred at Biak Island, Indonesia at 5h 59m UT on February 17, 1996 (magnitude (M_w) = 8.2 and depth = 20 km from USGS catalog), have been investigated on the basis of ULF magnetic observations at two stations, Biak and Darwin in Australia (about 1,200 km apart). Though a simple analysis of magnetic field intensity (horizontal and vertical magnetic field components) at both stations was found to be closely correlated with geomagnetic ΣK_p activity, a detailed analysis of the difference of H and Z components at the two stations, the polarization analysis (Z/H) and fractal analysis (frequency spectrum slope) at these two stations has yielded that the ULF emissions (in the frequency range from 5 mHz to 30 mHz) about 1.5-1.0 months before the quake are likely to be a precursory signature of the quake with its intensity on the order of 0.2-0.3 nT.

1. INTRODUCTION

Electromagnetic phenomena are recently considered as a promising candidate for short-term earthquake prediction (e.g. Hayakawa and Fujinawa, 1994 [1]; Hayakawa, 1999 [2]), and since the paper by Gokhberg et al. (1982) [3] there have been accumulated a lot of evidence of precursory signals in a very wide frequency range from ULF to HF. Especially, the ULF range is promising, because there have been reported convincing evidences of ULF signature for recent large earthquakes (Kopytenko et al., 1990 [4]; Fraser-Smith et al., 1990 [5]; Molchanov et al., 1992 [6]; Hayakawa et al., 1996 [7]; Kawate et al., 1998 [8]). However, more data on the presence of ULF signature of earthquakes need to be accumulated.

The earthquake we will analyze, took place in Biak Island, Indonesia at 5h59m U.T. on February 17, 1996 (Geographic coordinates, 0.27°S, 136.54°E; D=20km, and M=8.0). The magnitude of this earthquake is larger than that of Spitak and Loma Prieta [4, 5, 6], but is very close to that of Guam earthquake [7]. In this

paper we will report on a precursory signature of this earthquake in ULF emissions on the basis of the conventional analysis of intensity, and polarization and fractal analysis at two remotely separated stations (Biak and Darwin in Australia) as shown in Fig. 1.

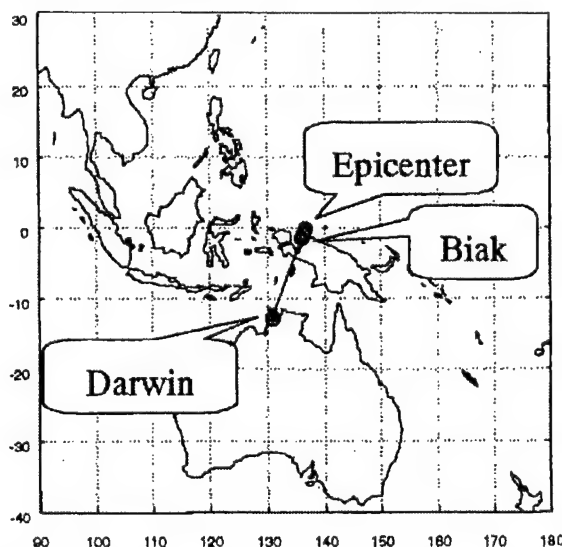


Fig.1 The relative location of two ULF observing stations (Biak, Darwin) and the earthquake epicenter.

2. ULF MAGNETIC FIELD MEASUREMENTS, EXPERIMENTAL RESULTS AND DISCUSSION

The ULF magnetic field observation has been performed at two magnetic observatories, (1)Biak (geographic coordinates: 1.08°S, 136.05°E; geomagnetic coordinates: 12.02°S, 206.94°E; L=1.05) and (2)Darwin (Australia) (about 1,200km apart from Biak) (Fig. 1). The ULF magnetic fields at each station are measured by three ring-core-type fluxgate magnetometers (H(NS), D(EW) and Z (vertical)), and data were digitized at 1sec sampling rate, which limits the upper analyzable frequency to be about 0.4Hz. Some more details on

the measurement equipment and data acquisition methods are given in Yumoto et al. (1996) [9]. The data used in this report cover the period from November 1, 1995 to March 16, 1996. Unfortunately, the data just after the earthquake (Feb. 18 to March 1) are missing. The distance between Biak observatory and the epicenter is about 100km.

As in the paper by Hayakawa et al. (1996) [7], we have used the midnight period of 6 hours from L.T.=22h-04h because the variability of the data at night is already known to be smaller than at daytime (Saito, 1969 [10]) and also we expect much smaller artificial noises. The waveforms of three field components during each interval of 30 minutes were subjected to an FFT analysis, and the data for one day consist of 12 frequency spectra during each 30 min. intervals. The frequency spectrum of the magnetic field intensity for each 30 min. interval is compared with the average (m) and the standard deviation (σ) over the whole period (excluding the period of no measurement). After looking at many frequency spectra, we have chosen the frequency range from 5mHz($T=200s$) to 30mHz($\sim 30s$), where ULF activity is generally enhanced. In order to estimate the wave activity, we define the following quantities: When the signal intensity (either H or Z)

exceeds its corresponding level ($m+\sigma$) at each 30 min. interval, we make the integration ($H(\text{or } Z)(f)-m(f)$) over the frequency. These values (for H and Z) are plotted as a function of day in the top two panels (Biak and Darwin) in Fig.2. The bottom panel indicates the corresponding temporal evolution of geomagnetic activity expressed by the daily sum of 3 hours Kp index (ΣKp). A simple glance on the comparison between the ULF activities at Biak and Darwin, shows that the temporal evolutions at both stations exhibit a general resemblance, and also the comparison of those H and Z variations at those stations with ΣKp , indicates that when we observe a peak in ΣKp , we can identify the corresponding enhanced activities in ULF a few days delayed from the peak as is known in the pulsation study (Saito, 1969 [10]). This overall correlative study may suggest that ULF activity is mainly dominated by geomagnetic pulsation activity. This kind of simple correlation study does not seem to have yielded any conspicuous effect in ULF in good contrast to the case of Guam earthquake (Hayakawa et al., 1996 [7]) for which even this kind of simple analysis has suggested a significant seismo-effect in ULF. This is because the epicentral distance in the present case is relatively large, about 100km.

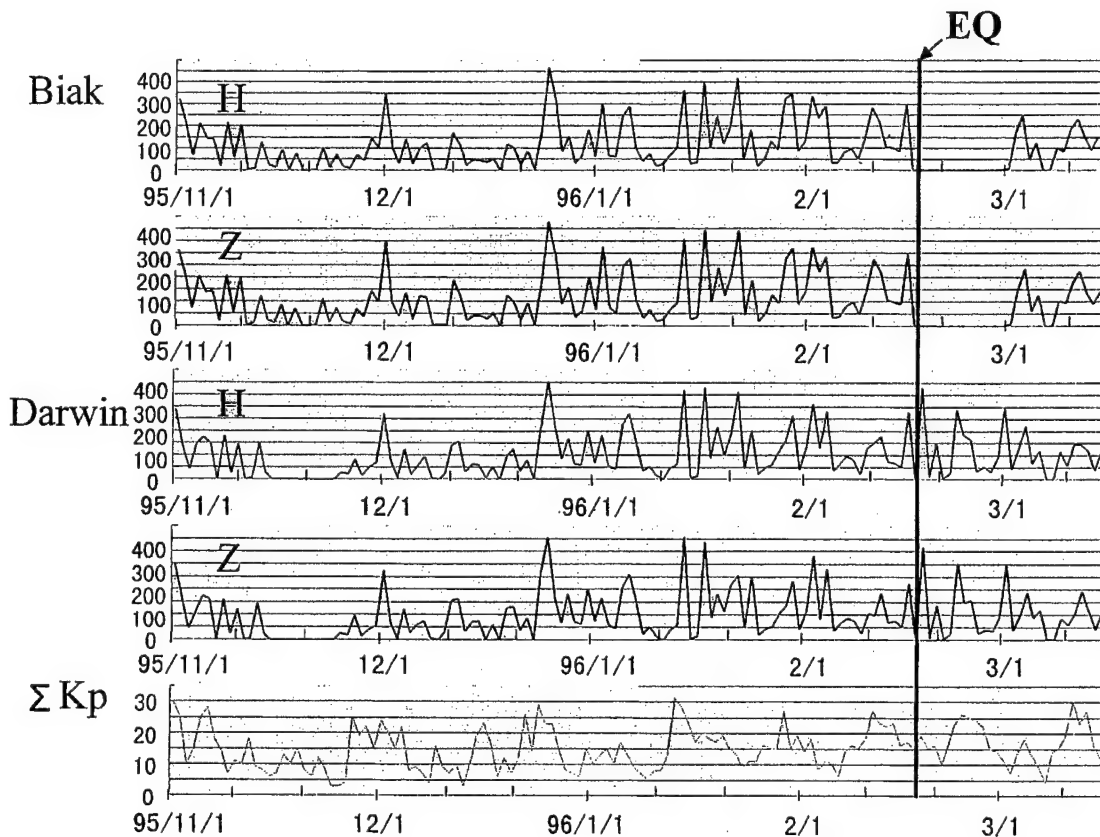


Fig.2 The temporal evolutions of ULF wave activity integrated over (0.005Hz-0.03Hz) observed at Biak and Darwin, and also that of ΣKp .

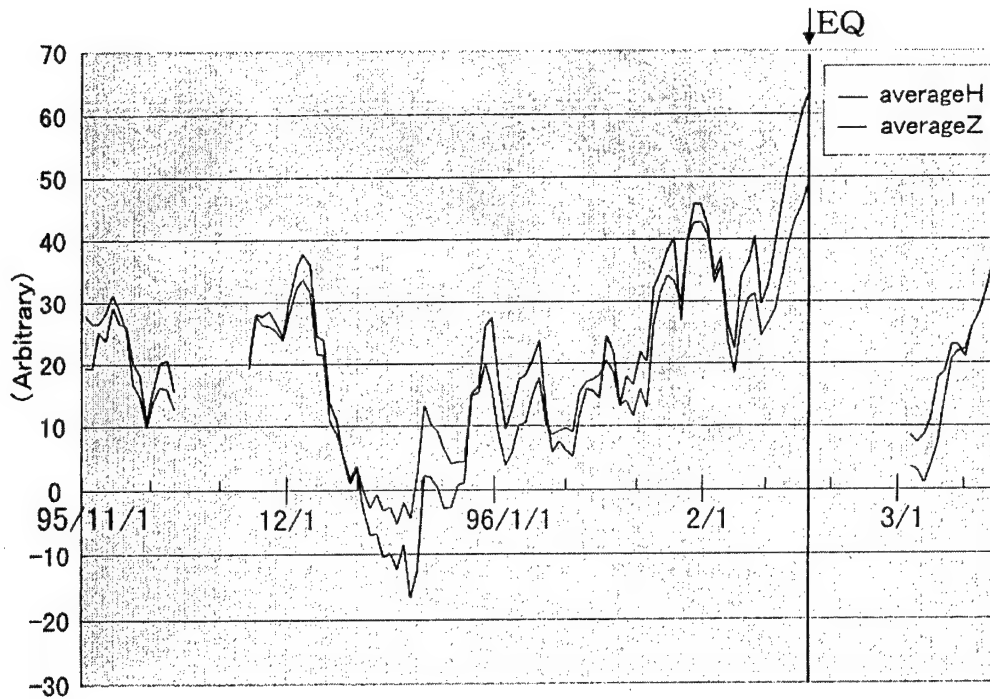


Fig.3 The temporal evolution of the difference in ULF activities at the two stations (Biak and Darwin). The difference of ULF (Biak) – ULF (Darwin) is plotted.

As a next step, we plotted the difference of ULF activities at the two stations in Fig.3. The most important point in Fig. 3 is that the ULF activity (both Z and H) at Biak is very much enhanced (as compared with that at Darwin) from about 1.5 months before the quake, though space ULF wave activity is found to decrease generally with decreasing latitude (Saito, 1969 [10]) and this enhancement shows a maximum just before the quake. Especially, we find a more significant increase in Z than H. However, the behavior after the quake looks like that prior to the quake, though we cannot say anything definite due to the limited data set. As the whole, it seems that the Z component observed only at Biak is more enhanced before the quake, which may indicate a possibility of the presence of seismo-ULF emissions.

Next, we present an analysis of polarization (Z/H) as developed by Hayakawa et al. (1996) [7], and its temporal evolution is shown in Fig. 4. The curves indicate the daily value and the running average over a time window of 10 days. We used only the magnetic data whose intensity (either in H or Z) in our frequency range exceeds its corresponding $m+\sigma$. As is clearly seen from Fig.4, we find no significant change in Z/H at Darwin, but we notice a very significant change in Z/H at Biak, such that a conspicuous peak in the ratio (Z/H) is found about 1.5-1.0 months before (Jan. 1 ~ Jan. 15) and a small peak two weeks before (Feb. 1 ~ Feb. 17) the quake. The curve with variable changes indicates the daily value (average over one day), and the smooth curve indicates the running average over ± 5 days. These enhancements are highly likely to be considered as a precursory signature in ULF emissions of the quake

(as is found in Hayakawa et al., 1996 [7]).

The previous polarization analysis seems to show convincing evidence on the reception of precursory seismo-ULF emissions about 1.5-1.0 months before the quake. This is furthermore confirmed by a fractal analysis (Hayakawa et al., 1999 [11]; Smirnova et al., 1999 [12]) based on the self-organized criticality concept. As is known, the spectrum of emissions exhibits a power-law behavior f^β , which is typical for self-organized critical dynamics. In this sense, the temporal variation of this β is examined, based on the spectrum in the frequency range from $10^{-3.5}$ to $10^{-0.5}$ Hz. Fig.5 illustrates the temporal evolutions of β at both stations at L.T.=12:00-13:00 (daytime), which indicate that a similar tendency was found in a different time window as well because the previous figures were concerned only with nighttime data. Fig.5 indicates that the value of β approaches unity for about two weeks (Dec. 23 ~ Jan. 10), that is, about 1.9-1.0 months before the quake. This period with $\beta \sim 1$ seems to be coincident with the period of enhanced polarization in Fig. 4. Because the principal feature of self-organized criticality is fractal organization of different parameters both in space (scale-invariant structure) and in time (flicker noise or $1/f$ noise), when the focal region becomes a super-critical state, β decreases down to unity (Hayakawa et al., 1999 [11]; Vallianatos and Tzanis, 1999 [13]). $\beta \sim 1.0$ means that higher frequency components are generally being generated, perhaps due to the generation of smaller-scale cracks as suggested by Molchanov and Hayakawa (1995) [14] and Vallianatos and Tzanis (1998) [15].

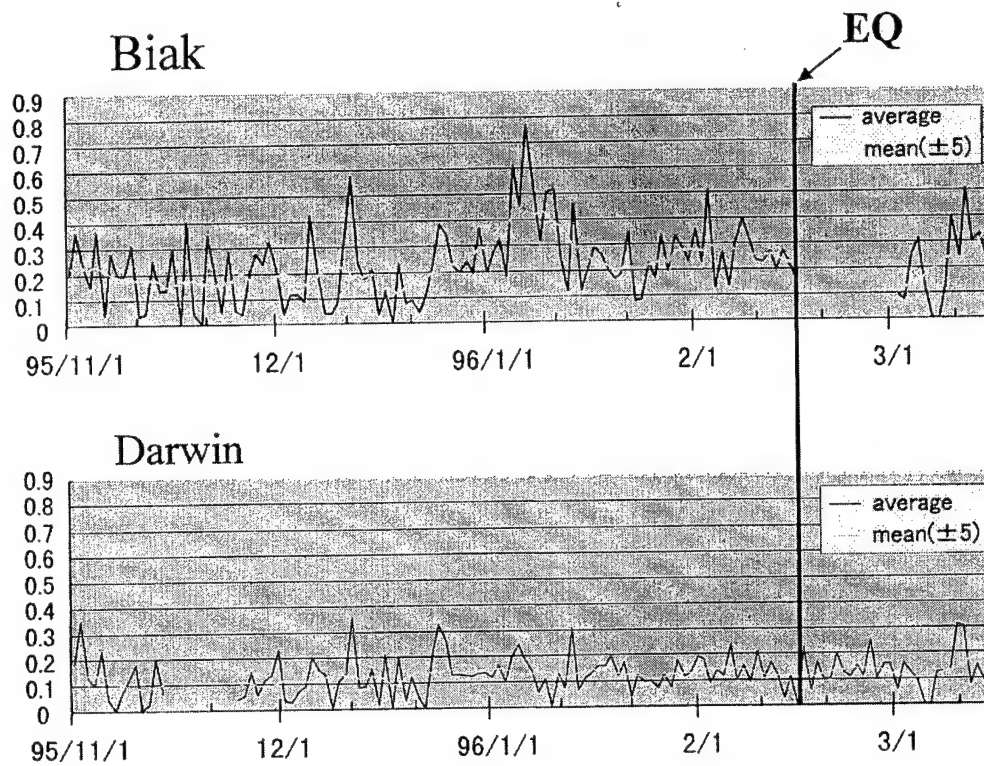


Fig.4 The temporal evolution of the polarization ratio (Z/H) at Biak and Darwin.

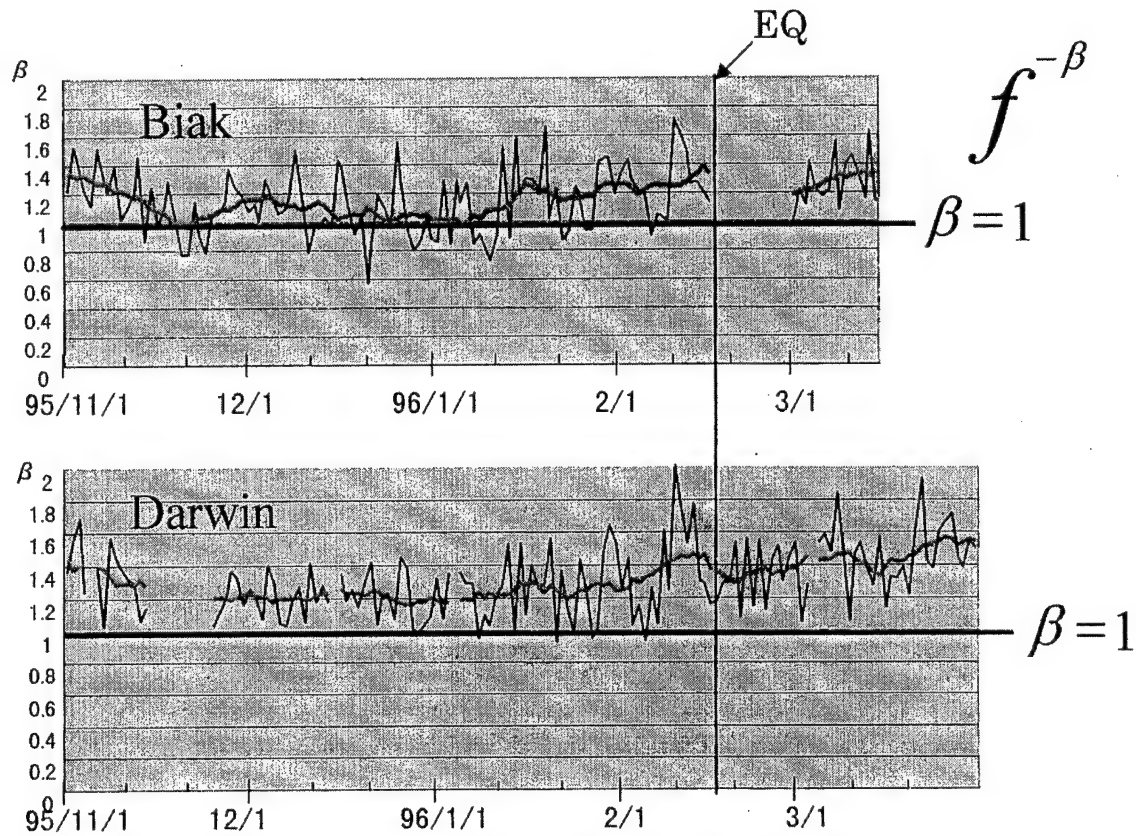


Fig.5 The temporal evolution of spectrum slope (β) at both stations.

3. CONCLUSION

Longer data base is, of course, required, but the length of 3.5 months before the quake used in this paper is considered to be acceptable, because the results for three previous events (Spitak, Loma Prieta and Guam earthquakes) have suggested the occurrence of ULF precursors within one month before the quake. We have examined the ULF magnetic data at Biak and Darwin in order to detect any precursory signature of the earthquake occurred at Biak. Together with the intensity variation (Fig.3), the polarization ratio (Z/H) (Fig. 4) and fractal analysis (Fig. 5), we can conclude that ULF emissions observed about 1.5-1.0 months before the quake are likely to be a precursory signature of the quake. The intensity during 1.5-1.0 months before the quake in the frequency range from 5 mHz to 30 mHz is found to be 0.3 nT at maximum for H and 0.16 nT for Z.

We are grateful to the Magnetic Observation Group of IRDC, Bandung LSPSN; Mr. Sukmadradjat, Biak Aerospace Observation Station, Mr. S. Wilson and Mamat Ruhimat, Bandung LAPAN for their ceaseless support.

4. REFERENCES

- 4.1. M. Hayakawa and Y. Fujinawa, Editors, "Electromagnetic Phenomena Related to Earthquake Prediction", Terra Sci. Pub. Co., Tokyo, 1994, pp. 677.
- 4.2. M. Hayakawa, Editor, "Atmospheric and Ionospheric Electromagnetic Phenomena Associated with Earthquakes", Terra Sci. Pub. Co., Tokyo, 1999, pp. 996.
- 4.3. M. B. Gokhberg, V. A. Morgunov, T. Yoshino and I. Tomizawa, "Experimental measurements of electromagnetic emissions possibly related to earthquakes in Japan," *J. Geophys. Res.*, 87, 1982, pp. 7824-7828.
- 4.4. Yu. A. Kopytenko, T. G. Matiashvili, P. M. Voronov, E. A. Kopytenko, and O. A. Molchanov, "Ultra low frequency emission associated with Spitak earthquake and following aftershock activity using geomagnetic pulsation data at observatories Dusheti and Vardziya," Preprint of IZMIRAN, N3(888), Moscow, January, 1990.
- 4.5. A. C. Fraser-Smith, A. Bernardi, P. R. McGill, M. E. Ladd, R. A. Helliwell and O. G. Villard, Jr., "Low-frequency magnetic field measurements near the epicenter of the Ms 7.1 Loma Prieta earthquake," *Geophys. Res. Lett.*, 17, 1990, pp. 1465-68.
- 4.6. O. A. Molchanov, Yu. A. Kopytenko, P. M. Voronov, E. A. Kopytenko, T. G. Matiashvili, A. C. Fraser-Smith and A. Bernardi, "Results of ULF magnetic field measurements near the epicenters of the Spitak ($M_s=6.9$) and Loma Prieta ($M_s=7.1$) earthquakes: Comparative analysis," *Geophys. Res. Lett.*, 19, 1992, pp. 1495-98.
- 4.7. M. Hayakawa, R. Kawate, O. A. Molchanov, and K. Yumoto, "Results of ultra-low-frequency magnetic field measurements during the Guam earthquake of 8 August 1993," *Geophys. Res. Lett.*, 23, 1996, pp. 241-244.
- 4.8. R. Kawate, O. A. Molchanov and M. Hayakawa, "Ultra-low-frequency magnetic fields during the Guam earthquake of 8 August 1993 and their interpretation," *Phys. Earth Planet. Inter.*, 105, 1998, pp. 229-238.
- 4.9. K. Yumoto and 210° MM Magnetic Observation Group, "The STEP 210° magnetic meridian network project," *J. Geomagn. Geoelectr.*, 48, 1996, pp. 1297-1309.
- 4.10. T. Saito, Geomagnetic pulsations, *Space Sci. Rev.*, 10, 1969, pp. 319-412.
- 4.11. M. Hayakawa, T. Ito and N. Smirnova, "Fractal analysis of geomagnetic ULF data associated with the Guam earthquake on August 8, 1993," *Geophys. Res. Lett.*, 26, 1999, pp. 2797-2800.
- 4.12. N. Smirnova, V. Troyan, M. Hayakawa, Th. Petersen, and Y. A. Kopytenko, "Natural disasters in relation to cosmo-helio-geophysical factors and geomagnetic disturbances," *Natural Hazards*, in press, 1999.
- 4.13. F. Vallianatos and A. Tzanis, "On possible scaling laws between electric earthquake precursors (EEP) and earthquake magnitude," *Geophys. Res. Lett.*, in press, 1999.
- 4.14. O. A. Molchanov, and M. Hayakawa, "Generation of ULF electromagnetic emissions by microfracturing," *Geophys. Res. Lett.*, 22, 1995, pp. 3091-94.
- 4.15. F. Vallianatos and A. Tzanis, "Electric current generation associated with the deformation rate of a solid: preseismic and coseismic signals," *Phys. Chem. Earth*, 23, 1998, pp. 933-938.

BIOGRAPHICAL NOTE

Masashi Hayakawa is now a professor of Department of Electronic Engineering, The University of Electro-Communications, Tokyo Japan. He graduated from Department of Electrical Engineering, Nagoya University, and obtained B. Eng., Master of engineering and Doctor of engineering, all from Nagoya University. He worked at Research Institute of Atmospherics, Nagoya University and studied space physics and atmospheric electricity. After moving to the present university, he extended his work very much, including EMC general problems, inverse problems, seismo-electromagnetics in addition to the previous works (space physics, atmospheric electricity).

NATURAL LOW-FREQUENCY EMISSIONS as a TOOL of RESEARCH of PROCESSES OCCURRING in the PLASMASPHERE

V.G. Larkin, V.I. Larkina

IZMIRAN, Troitsk town, Moscow Region, 142092, Russia
Fax: 007(095)3340124; E-mail: larkina@izmiran.rssi.ru

Magnetosphere is gigantic natural laboratory, in which diverse geophysical processes occur. In a magnetospheric plasma are present electrical and electromagnetic (geomagnetic) fields. Magnetosphere plasma presents a mix of various energy particles from thermal up to highly and super highly energy particles. Besides in a plasma, by certain (determined) conditions, are excited electromagnetic and electrostatic waves and they interact with particles of a plasma, resulting to evolution of the various geophysical phenomena on an earthly surface and in magnetosphere of the Earth. Thanking all this, the magnetospheric plasma differs from a laboratory plasma, where it is possible serially to enter particles, to change fields, "warm up" of a plasma and etc..

In the last years interest to quantitative and qualitative researches of radio noises as natural, so and artificial origin, in the various areas of the near-Earth space in a extensive range of frequencies, in a volume of low-frequency (0,1 - 20 kHz) has considerably increased.

Detailed investigations of the space-temporary and spectral characteristics of low-frequency emissions and their communications (connections) with different geophysical phenomena permits to use their property for means of diagnostics and study of dynamic processes in magnetosphere. The low-frequency emissions bear the information on parameters environment, in which they are excited and spreaded, about flows of energy particles, penetrating in various areas of spaces and causing to excitation of these emissions and by that the items of information about conditions of a space plasma and about flows of particles, diving through this space give. Detailed study of low-frequency emissions and their connections with various parameters of environment in various conditions of geomagnetic disturbances permits to judge about from unsteady (changeable) of a property plasma and flows of particles at change of geomagnetic activity and gives the information on magnetosphere-ionosphere interrelation.

The level of natural low-frequency emissions in magnetosphere and external ionosphere considerably changes in dependence and from a condition of a magnetospheric plasma. These changes are the most essential in a time of geomagnetic

storms: a position (situation) of plasmopause and in this connection changes redistribution of flows of electrons and ions occurs, essentially distribution electrons of average energy varies.

Variations of low-frequency emissions intensity and the density of a vigorous electron flow

Earlier in [1] us is established, that in a time of geomagnetic disturbances a level of low-frequency noise intensity grows, the amplitude of noise changes proportionally Dst-variations and the maximum of emission intensity during magnetic disturbances is moved on more low a L-shell. Also earlier in [2] communication (connection) between changes of low-frequency emission intensity and level disturbances is shown. As a quality of a parameter of a level disturbances of a magnetic field in average latitudes (in the region of closed lines of magnetic field) was used Dst-variations.

Figure 1 are illustrates the position variations of L-shell, where intensity of low-frequency emission field (L_{max}) on frequency 500 Hz was maximum Dst during geomagnetic storms and disturbances. On horizontal axes sizes Dst-variations are in main and recovery phases of several geomagnetic storms (continuous line). Simultaneously, on it a drawing (the shaped line) are put changes (L'_{max}), where maximum density of a vigorous electron flow it (40 keV) is registered.

The left-hand part of the figure depicts the events during the main phase of the storm, right – the position during the recovery phase. The variations of L_{max} , where the noise amplitude is a maximum are given for frequency of 500 Hz. The result obtained for other frequencies are similar. The data are received during the storms: on August 16, 1970 (SSC at 16.04 UT), on December 16, 1971 (SSC at 19.06 UT), on January 21 and 28, 1972 and on February 24, 1972 (SSC at 06.42 UT). The data on emissions ($f = 500$ Hz) marks by points for storm on August 16, 1970, by rhombus for storm on December 16 1971, by circles for storms on January 21 and 28, 1972, direct crosses for storm on February 24, 1972. Items of information on flows are designated for storm on December 16, 1971 - by triangles, for storms on January 21 and 28,

1972 - squares, for storm on February 24, 1972 - by crosses.

From a drawing it is visible, that the points for separate storms are by small heap and on it it is possible to conduct average resulting curve. As it is visible, in a active phase of storm L_{max} and L'_{max} decrease. Besides speed of reduction L_{max} in a main phase of storm more, than speed of reduction L_{max} in a recovery phase.

Table 1

Parameter	Phase of	Storms
	Main, γ^1	Recovery, γ^1
$\Delta L_{max}/\Delta D_{st}$	$-4 \cdot 10^{-2}$	$3 \cdot 10^{-3}$
$\Delta L'_{max}/\Delta D_{st}$	$-3 \cdot 10^{-2}$	$3 \cdot 10^{-3}$

Table 1 shows the value of $\Delta L_{max}/\Delta D_{st}$ and $\Delta L'_{max}/\Delta D_{st}$ during the main and recovery phases of the storms. The value $\Delta L_{max}/\Delta D_{st}$ is somewhat greater than that of $\Delta L'_{max}/\Delta D_{st}$ in the main phase, but the values are equal in the recovery phase. Hence, as the storm develops, the maximum of the electron flux density (dashed line in fig. 1) moves at a slower rate than the maximum of the noise amplitude. For $D_{st} \sim -40$ nT, the maxima of intensity are shifted relative to each by 0.5L. Note that the values of $\Delta L_{max}/\Delta D_{st}$ and $\Delta L'_{max}/\Delta D_{st}$ in the main phase are one order of magnitude greater than those in recovery phase. Since the main phase is generally shorter than the recovery phase, it follows from fig. 1 and table 1 that the emission intensity may return to its quiet-time level in a time equal to, or less than, that of recovery phase.

A similar consideration of the variation with other indices of geomagnetic activity such as Kp and AE does not give such consistent results, as those obtained with Dst. The reason for this is probably that Dst is the best measure of geomagnetic disturbance in the region of magnetosphere, where plasmaspheric noise are generated.

Low-frequency emissions and density of a plasma on satellite heights

In this section communication (connection) between concentration of a plasma particles and exciting and extending in it low-frequency waves is shown.

The known relation between the amplitudes of the magnetic and electrical noise field components in case of quasilongitudinal wave propagation:

$$b/e = 3.336 n_0(\theta) \cdot \varphi(\theta) \quad (1),$$

where b is induction of the magnetic field in nT/ $\sqrt{\text{Hz}}$ and e is the intensity of the the wave electrical field in V/m/ $\sqrt{\text{Hz}}$, $n_0(\theta)$ is refraction index:

$$n_0(\theta) = \omega_{ce} [\omega(\omega_{Be} \cos \theta - \omega)] \quad (2),$$

θ is angle between a wave front normal (wave vector k) and the geomagnetic field vector B_0 , ω_{ce} is a plasma frequency ($\omega_{ce} = 4\pi e^2 N_e/m$), ω is frequency of a wave, ω_{Be} is electron gyrofrequency ($\omega_{Be} = eB_0/mc$), e and m - charge and mass of electrons, $\lambda = \omega/\omega_{Be}$ is normalised wave frequency, $\varphi(\theta)$ is some function, connecting normalized wave frequency to wave vector orientation:

$$\varphi(\theta) = \sqrt{2(1-\lambda)(\cos \theta - \lambda)} / (1 + 2\lambda^2 + \cos^2 \theta - 4\lambda \cos \theta) \quad (3)$$

The directional pattern of the Intercosmos 19 antennas is sufficiently wide; therefore, the received

frequency 500 Hz $E_q \approx 40 \text{ keV}$

16 January 1970 •

16 December 1971 ◊ Δ

21 and 28 January 1972 ◻ □

24 February 1972 + x

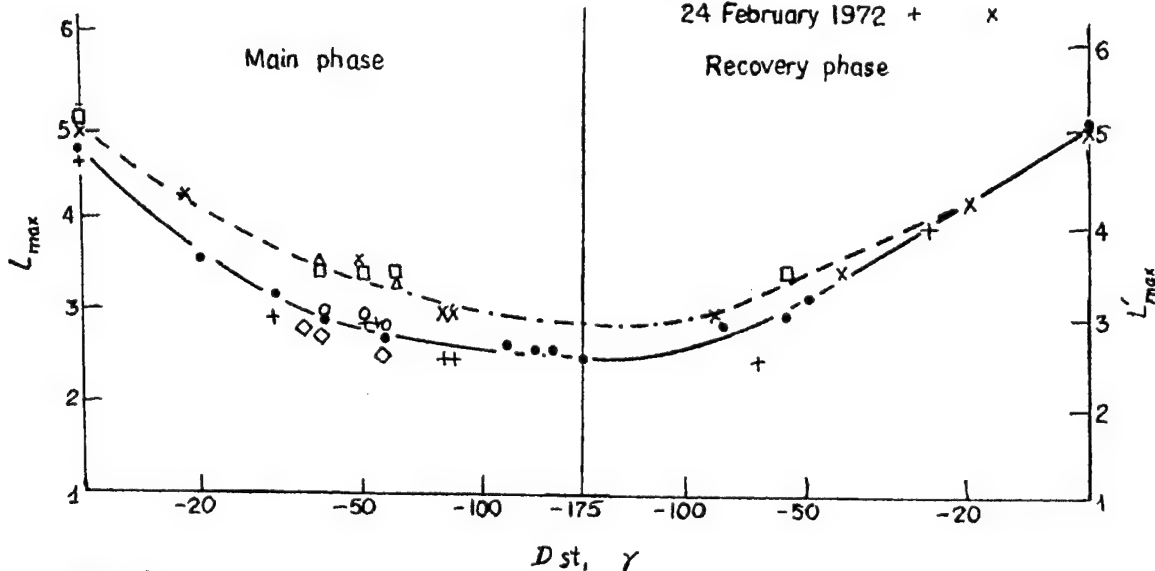


Fig. 1

signal level was in practice the same within a sufficiently large solid angle of the antennas. Thus, as a first approximation, the values of the electrical and magnetic components e_y and b_x , of the noise fields measured on Intercosmos 19 may be considered to coincide approximately with the field amplitude.

Figure 2 shows the variations of the plasma ion number density N_i in cm^{-3} along a night-time portion of "Intercosmos 19" orbit on March 5, 1979 from near-equatorial to near-polar latitudes. The night-time results have been chosen in order to avoid the possible (probable) contribution from effect of day-time excitation of emissions at heights 200-400 kms. On fig. 2 changes of intensity of magnetic (b) in $\gamma/\sqrt{\text{Hz}}$ and electrical (e) in $\text{mkV}/\text{m}\sqrt{\text{Hz}}$ components of emission field at selected frequency 450 Hz are indicated. We shall notice, that the ion number density at the "Intercosmos 19" orbital altitudes practically equal to the electron one. In distribution of particle density well see all characteristic change of concentration: main ionospheric trough, a auroral peak, auroral trough and etc.. The small-scale 2-4-s periodic fluctuations of the number density were observed at auroral trough and polar-peak.

A top of a figure present the changes of $\cos \theta$ lengthways orbit depending on invariant latitude Φ . For latitudes less 50° $\cos \theta = 1$, for $\Phi = 50^\circ - 60^\circ$ $\cos \theta \approx 0.9$ and for $\Phi = 70^\circ$ $\cos \theta \approx 0.8$ are indicated. The results are similar for frequency measured on satellite and are distinguished only in the fourth mark of function $\cos \theta$.

The bottom part of a drawing contains the items of information on changes of amplitude magnetic (b)

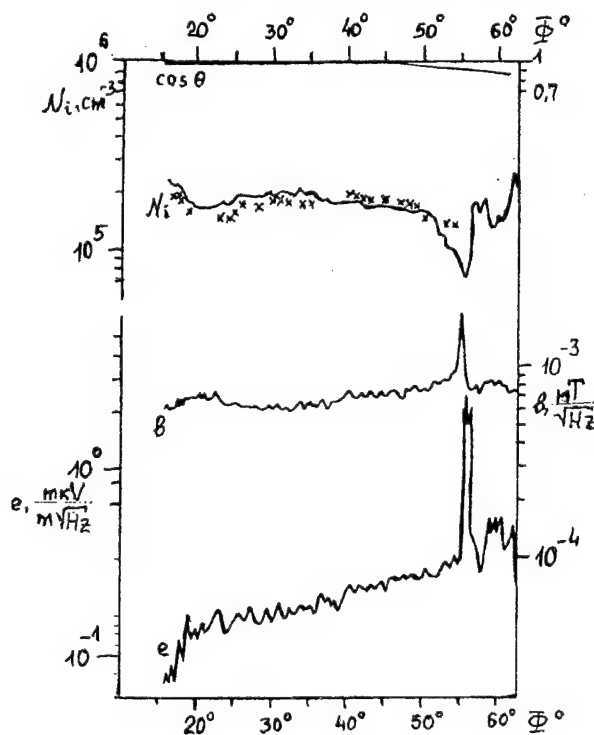


Fig. 2

and electrical (e) field component of emissions along considered orbit for frequency 450 Hz. The amplitude of emissions grows with a increase invariant latitude Φ . The significant gradient $\Delta b/\Delta \Phi$ и $\Delta e/\Delta \Phi$ is observed on latitudes $\Phi = 15-20^\circ$ and $\Phi = 54-56^\circ$, that is in the region of internal radiation belt and in the field of main ionospheric trough, thereby confirming the hypothetical generation of the ELF and VLF waves in the region of the main ionospheric trough at high number gradients [3].

After a output (exit) of satellite from trough the amplitude of noise has decreased. In the auroral areas are registered diverse variations of density and each time at the reduction N_i amplitude of emissions increased, for example, on $\Phi = 58^\circ - 62^\circ$, $\Phi = 63^\circ - 64^\circ$, $\Phi = 65^\circ - 66^\circ$.

As in low and average latitudes $\cos \theta \rightarrow 1$, in these areas of the space the formula (2) can be recorded in a simplified kind:

$$n_0(\theta) = \omega_{ce}[\omega(\omega_{pe} - \omega)] \quad (3).$$

Then from (1) and (2), knowing b and e, we have defined N_i for happen (case) of longitudinal distribution of waves.

In a top part of fig. 2 (near N_i) of cross settlement significances of concentration are put. The settlement significances (data) differ from real on $\pm 10\%$. Fluctuations of settlement sizes of significances more, than real. It was possible is to explained by that the real significances N_i on graph are middled and, in second, by (with) amplitude of a electrical components appreciably are fluctuated. The significances N_i , received on a data of registered of emissions on frequencies 140, 450 and 800 Hz are very close. Thus, the accounts have shown, that on average latitudes $\Phi \leq 50^\circ$ on all frequencies of the ELF wave range are distributed quasilongitudinal, that is the low-frequency waves, arising in equatorial region at plasmasphere heights, are distributed practically along of the magnetic field lines. In quiet conditions at absence of measurements of concentration for its definition (determination) on average latitudes it is possible and use of measurement of magnetic and electrical making fields of low-frequency emissions. The valuation of concentration mistake did not exceed 10-15%.

Low frequency emissions previous earthquakes

In the eighties the investigations of electromagnetic effects related to earthquakes at ionosphere altitudes with the use of satellite measurements were initiated. It was discovered [4]:

- increase of intensity of low-frequency emissions 3-6 hours before and 3-6 hours after strong earthquakes ($M > 5.5$), when the satellite was flying, near the epicentre;
- dimension of burst observation zones $\pm 3^\circ$ along latitude and $\pm 60^\circ$ along longitude. These are the so-called "noise belts";

-amplitude of noise bursts increase when satellite is moving to the epicentre along longitude, to the moment of the main shock - along time;
 -before the earthquake electric and magnetic components of emission field were observed, after the earthquake there was . observed only electric component;
 -reliability of the observed effect, calculated on the basis of experimental data processing made up 85-90%.

Earlier we received the global space-temporary distribution of the natural low frequency emission intensity (daily allowances, latitudinal and altitude variations in absolute units) in different conditions of the geomagnetic disturbances. The following drawing demonstrates the reliability of distinguish of signals connected with development seismic processes. Fig. 3 is submitted middle latitudinal dependence of the low frequency noise intensity on frequency 4,65 kHz for various geomagnetic activity conditions. These results have received in four months of a "Intercosmos" satellite function: 2 months - "Intercosmos 5" and 2 months - "Intercosmos 19" and specified (I) root-mean-square spread of data. The separate badges, as an example, show the noise intensity burst size, registered on channel outputs during earthquake preparation, results received after earthquake for the same data is denoted by circles. From a drawing it is clearly visible, that the emission intensity bursts, connected with development seismic activity, obviously exceeds emission levels, usually observable in give space area. We were analysed not only individual events by "Intercosmos 19" satellite data, but we are received also statistical characteristics by formalism of the data processing process help on modern computind means.

The processes of earthquake preparation are accompanied by simultaneous changes:

- of low frequency emissions intensity (magnetic and electric componements),
- of concentration and temperature of a plasma environmental by Earth and
- vigorous electron precipitation.

It was established (installed) the space-temporary sizes of ones manifestation zone. Thus, we can see variety of change of near-Earth space plasma parameters over the earthquake epicentres. Everything are additional attributes, indicative local disturbances of the magnetosphere parameters by effects of seismic activity and can be used as short-term earthquake prediction together with whole complex other satellite and, certainly, ground result of supervision.

By results of registration of intensity low-frequency emissions, flows vigorous electrons and plasma density traced (followed) the processes developed in plasmasphere above epicentre of the future earthquake, development of the seismic phenomena in a time and in the space. Zones of changes of parameters of a plasma: intensity of fields of low-frequency noise, flows of vigorous particles and density of a plasma are determined.

Table 2

The sizes of a zone of supervision seismoionospheric anomalous on the upper ionospher heights.

Parameter	Range	Size of zone	Time (before)
Waves	ELF/VLF	$\Delta\phi \pm 3^\circ$ $\Delta\lambda \pm 60^\circ$	Some Hours
Electrons	≥ 40 keV	0,1 L	2,5-3 hours
Plasma Density		$\pm 3^\circ$	Day

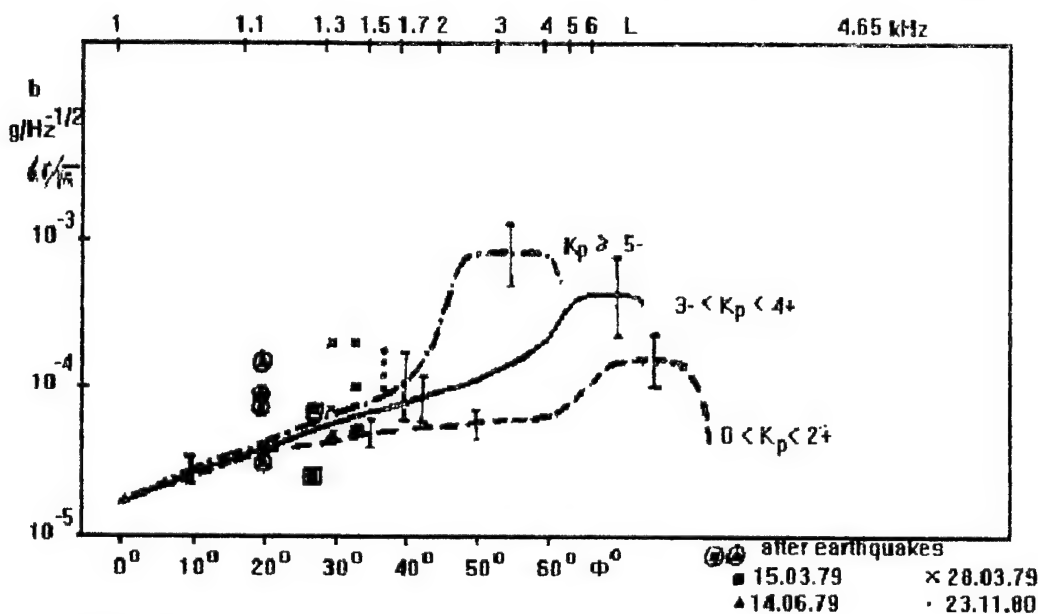


Fig. 3

In IZMIRAN some years ago we suggested a method of selecting, obtaining and using of data for Earthquake prediction. Earthquake prediction program according to the methodics was elaborated and adopted in IZMIRAN.

In the last time it was recently found out, that over deep fault zones of earthly crust bursts of intensity low-frequency emissions, thermal electros and temperature of an environmental plasma are observed. In our days we created the method of detection of lithosphere zones of variable geodynamic activity.

The research of low-frequency emissions has application meaning (importance) for the solution of problems of forecasting (prediction) geomagnetic disturbances and, specially, earthquakes.

1. Knowing value of intensity of low-frequency emissions, it is possible to define(determine) expected values Dst of variations, it is possible to define(determine) an expected level geomagnetic disturbances.

2. Knowing a spatial distribution of intensity ELF/VLF emissions, it is possible to place(install) (to compute) a spatial distribution of cathode rays of mean energies.

3. In quiet and moderately - perturbed conditions at lack of gaugings of density for its definition it is possible to utilize observed datas of magnetic and

electrical components of a field of low-frequency emissions. Thus the mistake of an estimations of density does not exceed 10-15%.

4. On variations of low-frequency emissions with a high scale of veracity it is possible to do (make) the forecast of seismic activity (hazard).

References:

1. Larkina V.I., Likhter Ja.I. Storm-time variations of plasmaspheric ELF hiss //J. Atm. Terr. Phys. 1982. V.44, N 5. P.415-423
2. Larkina V.I. Low frequency Emissions on board "Intercosmos" satellites related to ring current space variations //Fourteenth International Wroclaw Symposium and Exhibition on Electromagnetic Compatibility. Poland. Wroclaw. 1998. P.535-539
3. Гдалевич Г.Л., Лихтер Я.И., Ларкина В.И. и др. Экспериментальное доказательство возбуждения волн КНЧ-ОНЧ диапазона в авроральных областях внешней ионосферы //Низкочастотные излучения в ионосфере и магнитосфере Земли. Апатиты. КФ АН СССР. 1981. С.58-62
4. Larkina V.I. Seismogenic electromagnetic emissions in the upper ionosphere: experimental evidence //Eleventh International Wroclaw Symposium on Electromagnetic Compatibility. Poland. Wroclaw. 1992. P.611-615

IONOSPHERIC ELECTROMAGNETIC EFFECTS above VARIOUS EUROASIA ARCTIC TECTONIC AREAS

V.I. Larkina

IZMIRAN, Troitsk, Moscow Region, 142092, Russia, E-mail: larkina@izmiran.rssi.ru, FAX: (095)334-02-91

N.G. Sergeeva

Polar Geophysical Institute, Murmansk, 183010, Russia, E-mail: sergeeva@pgi.ru, FAX: (815-2)56-03-37

B.V. Senin

SOYUZMORGEO, Gelendzhik, Krasnodar Region, E-mail: smg@gelon.ru

The variations of the intensity of low-frequency emissions (0.1-20 kHz), the density of the low-energetic electrons flux and the temperature of the plasma by measurements on the «Intercosmos 19» satellite above deep faults of the Norwegian Sea, the Baltic Shield, the Barents and Kara Seas and the West Siberian Lowland have been considered. These regions represent a consecutive change of the Earth crust structure and its geodynamic mode in the zone of the transition from the Euroasian continent to the Arctic ocean. The experimental data on five flights of the satellite have been thoroughly investigated.

THE EXPERIMENTAL DATA

Two flights of the «Intercosmos-19» satellite with approximately identical orbits have been chosen, their height: ~950 km: November 20, 1980 (orbit 9147) and November 23, 1980 (orbit 9190) and the third orbit on March 15, 1979 (orbit 231) with the height ~580 km. The trajectory 231 has passed between the trajectories 9190 and 9147. Besides, two orbits 9148 (November 20, 1980) and 9191 (November 23, 1980) have been chosen. We have united the flights in two groups, in which trajectories have passed close to each other (see table). Fig.1 shows the projections of the orbits to the surface Earth, in each group

of orbits of the projections of the orbits have crossed the same tectonic structures.

Geophysical conditions for orbits 9147 and 9190 have been the following. The intensive positive disturbance of the interplanetary magnetic field (IMF) has begun at 8.30 UT on November 15, 1980. The high activity has been kept till November 20, up to the end of the positive IMF. Then, the inclusion of the short site of the negative IMF has had an effect on the activity downturn up to November 24 [1]. The days November 20 and 23, 1980 have been moderately disturbed ($K_p = 4$ and $K_p = 3$, accordingly). The geophysical conditions for orbit 231 have been a little different. The sudden storm has begun on March 9, 1979 at 8.08 UT, its active period has been on 10÷11 March. The period of the positive IMF (followed after the storm) has been accompanied by the appreciable decrease of the geomagnetic activity up to March 17 [2]. March 15, 1979 - $K_p = 3$.

Fig.2 shows the bursts envelope of the low-frequency emissions intensity for two components (electrical and magnetic) on frequencies 140, 450, 800 and 4650 Hz. For the frequency of 15000 Hz the envelope of the signal of the field magnetic component

Table. Characteristics of orbits and measured ionospheric parameters on board satellite «Intercosmos-19»

Orbit	Date	height satellite, km	Ionospheric parameters	Index of disturbance	Universal time
9147	20.11.1980	~950	Electromagnetic emission, temperature of the plasma T_n	$K_p = 4$	17.54 - 18.00
9190	23.11.1980	~950	Electromagnetic emission, temperature of the plasma T_n	$K_p = 3$	17.02 - 17.08
231	15.03.1979	~580	Low energetic flux $E_e = 120$ eV	$K_p = 3$	15.24 - 15.30
9148	20.11.1980	~950	Electromagnetic emission, temperature of the plasma T_n	$K_p = 4$	19.35 - 19.44
9191	23.11.1980	~950	Electromagnetic emission, temperature of the plasma T_n	$K_p = 4$	18.43 - 18.52

Figure 1 displays electromagnetic emission data and a geological cross-section for Orbit 9147 on 21.11.1980.

The top section shows five frequency bands of electromagnetic emission (dB) over time (UT):

- 15000 Hz
- 4650 Hz
- 300 Hz
- 50 Hz
- 10 Hz

The bottom section is a geological cross-section (km) showing various tectonic and geological features:

- Scandinavian Peninsula, Baltic Shield
- Barents Sea
- South-Barents Basin
- Novaya Zemlya, Novaya Zemlya Group of islands
- Kara Sea
- South-Kara Basin
- Finmark Dikection Zone
- Lapland Massif
- Novaya Zemlya Massif (microplate)

Legend:

- Conditional marks:
 - sedimentary cover
 - Earth crust
 - faults zones: a) local; b) regional
 - dislocation zone
 - water

Fig. 2. Experimental data of the electromagnetic emission and tectonical structures of the lithosphere (orbit 9147).

has been shown, the electrical component has not been registered due to a technical reason. In the top part of figures of the envelope bursts, of the temperature variations, of plasma (T_e) at height of the «Intercosmos-19» satellite have been shown. In the bottom part a tectonic section along the orbit projection to the Earth surface has been shown.

Let us consider general regularities of the variations of the low-frequency emission intensity on orbits 9147 and 9190 when the satellite has been crossed above the deep faults. In the Baltic Shield region the variations of the low-frequency emission intensity on all frequencies of 140÷15000 Hz above the regional seismogenic zones along the contact of rather rigid blocks (Norbotten and Lapland), and also along the borders of these blocks with wide dislocation zones (zone 1 and 2) have been observed. It can be explained by the increased mobility and, accordingly, jointing and permeability of the zones dividing parts of the Earth crust with the various physical characteristics.

Above the region of transition from the Baltic Shield to the mobile platform the variations of the low-frequency emission intensity on all frequencies (zone 3) have been observed as well.

The new burst of the low-frequency emission intensity on all frequencies has been observed above the east restriction of the central hollow of the South-Barents basin and probably with the regions of the most thinned and sometimes along the separate zones of the broken Earth crust (zone 4).

To northeast from the central hollow of the South-Barents basin the variations of the low-frequency emission intensity with the large amplitude have been observed above the central and rear systems of the Novaya Zemlya faults (zone 5).

We can see the distinctions in the variations of the low-frequency emission intensity above the deep faults on two orbits as well. On orbit 9147 above the active zone of the frontal overlap of the Novaya Zemlya orogenic belt the high amplitude variations of the low-frequency emission intensity have not been observed. It can be connected to a different nature of the regional faults. If the central and rear zones have been represented by fault infringements reflecting stretching conditions, the frontal zones here are overfaults and overfault-overlaps, occurring in compression conditions. On orbit 9190 unlike orbit 9147 the high amplitude variations of the low-frequency emission intensity have been observed above the Novaya Zemlya frontal faults. It has been connected to the fact that the trajectory 9190 has passed above the knot of crossing frontal overlap zone with powerful cross shear-fault zone, which has crossed the Novaya Zemlya in the northwest direction. On the basis of the structural-geological attributes it has

been supposed, that at this area the conditions of the submeridional stretching have prevailed over the conditions of the sublatitudinal compression. On orbit 9190 the bursts of the low-frequency emission intensity on all frequencies have been well expressed in the area of transition from the continental area to the mobile marginal platform. It has been connected to the high degree of isolation of the Earth crust blocks and the faults zones, dividing them. Above the blocks of the Baltic Shield ancient crust (the block Vasa, the Karelian massif) the quiet field of the low-frequency emission has been observed.

Fig.3 shows the bursts envelope of the low-frequency emissions intensity for two components (electrical and magnetic) on frequencies 140, 450, 800 and 4650 Hz for orbit 9191.

Orbits 9148 and 9191 have been the most interesting ones from the point of view of the estimation of the connection between the structure of the electromagnetic emission and the tectonic features of the Earth crust in the zone of transition from the continent to the ocean and the zone of transition from the Kara Sea to the West Siberian Lowland. The variations of noise emissions above the faults from the Norwegian Sea up to the Kara Sea on these orbits have not been considered, as the regularities of the variations [3] have coincided with the variations on orbits 9147 and 9190. In the region of the transition from the Kara Sea to the West Siberian Lowland (the zone k) the sharp jump of the field intensity on frequencies 450, 800 and 4650 Hz has been observed, it is most appreciable in the electrical component of the emissions field. In the Yuribey dislocation zone the weak variations of the noise intensity (zone l) on all frequencies have been noticed. With transition from the Yuribey zone to the Enisey-Khatanga trough the jump of the intensity on all frequencies above the tectonic border of the internal zone of the Enisey-Khatanga trough (zone m_1) has been observed. The trough has been characterised by weak fluctuations of the emissions intensity. Further, the next border of this trough with the ancient Siberian platform has been marked by sharp jumps of the intensity (zone m_2), which has been differently expressed on various frequencies. Above the PriEnisey block the amplitude of the variations on all frequencies both in the magnetic, and in the electrical component of the noise emissions field considerably has increased. The same regularities of the noise variations have been observed in the zone of transition from the Kara Sea to the West Siberian Lowland on the other orbit (9148). The general appropriateness for these two orbits is the presence of the local disturbances of the low-frequency emission above the tectonic zones (above the regional and deep faults), which have divided large tectonic elements.

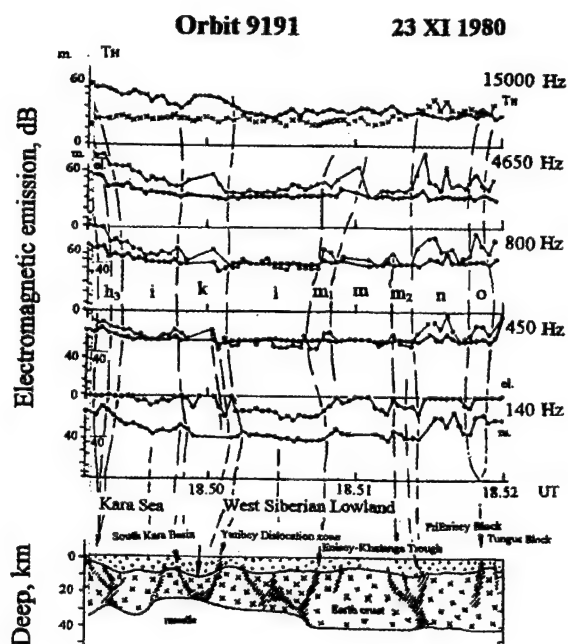


Fig. 3. Experimental data of the electromagnetic emission and tectonical structures of the lithosphere (orbit 9191).

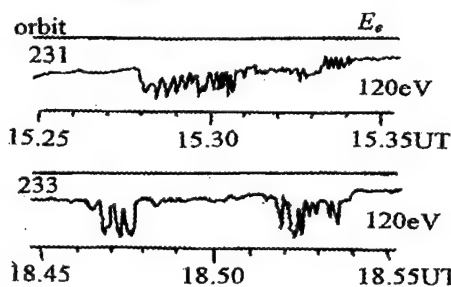
Thus, along the trajectories 9147 and 9190, 9148 and 9191 the conformity of the maxima of the low-frequency emission intensity to the regional faults zones has been most characteristic, for which is established or the prevailing mode of the stretching is supposed on structural features. The presence of the thick (more than 15-18 km) sedimentary cover has not been probably a handicap for the occurrence of the variations of the low-frequency emission intensity above the stretching zones, in case of a significant thinning or complete break of the crystal Earth crust, as it has been observed in the central hollow of the South-Barents basin.

The variations of the density of the electrons flux with the energy $E_e = 120$ eV at 15.28-15.30.28 UT with two characteristic of the fluctuations regions have been observed by the «Intercosmos-19» satellite above the South Barents basin and the Novaya Zemlya orogenic belt on orbit 231 on March 15, 1979. In one part of the flux above the South-Barents basin and the Novaya Zemlya at 15.28 ÷ 15.29.30 UT the periods of fluctuations equal to 12.5-17 seconds have prevailed. In the other part of the flux above the Kara Sea the period of fluctuations has decreased to 7.5-5 seconds (Fig.4). Above the deep faults of the same region the fluxes of the low-energetic particles of different energies 120 eV and 50 eV with periods of fluctuations equal to 20-25 seconds had been registered earlier [4]. One can state the assumption, that the simultaneous bursts of the low-

frequency emissions intensity observed in the South-Barents basin and the fluxes of the low-energetic electrons can be connected to the allocation of radon, as it follows from the recently published work [5]. It is necessary to state, that direct measurements of the radon contents in the South-Barents basin, as far as it is known, had not been carried out. At the same time on rather small amounts of tests the concentration of radioactive elements [6] were investigated which can be a source of radon to some extent.

«Intercosmos-19»

March 15, 1979



July 14, 1979

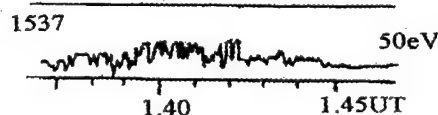


Fig. 4. Variations density of the low-energetic electrons fluxes.

Let us consider variations of the plasma temperature at heights of the satellite T_e on two orbits 9147 and 9190 (Fig.2). One can see the increase of the temperature on both orbits in ~1.6 time in comparison to the background level of the temperature above the seismoactive faults of the Baltic Shield zone, and above the faults of the South-Barents basin ~1.3 time and the South Kara basins in ~1.4 time. The increase of the temperature in ~1.2 time has been observed above the faults of the seismoactive zone of the Baltic Shield [7]. It has confirmed the conclusion on the spatial stability of the observed effects above the deep faults once more [4, 7].

THE RESULTS OF THE CORRELATION ANALYSIS

The correlation analysis of the simultaneous bursts of the intensity of the magnetic and electrical components of the emissions field for the Barents-Kara region has been executed. The Barents-Kara region has been divided into three areas: the Barents Sea, the Novaya Zemlya and the Kara Sea. Their size has been chosen so that the number of points participating in the correlation analysis would have been identical.

The correlation analysis has shown, that the observed low-frequency emissions have been electromagnetic, the correlation coefficients have been $R_{m,el} = 0.66 \pm 0.91$ for orbit 9147 and $R_{m,el} = 0.54 \pm 0.98$ for orbit 9190. Above the Novaya Zemlya (above the knot of crossing of the frontal overlapping zone with powerful cross of the shear-раздвиговой zone) on orbit 9190 the coefficients correlation on all frequencies have been higher: $R_{m,el} = 0.81 \pm 0.98$. Unfortunately, to execute the correlation analysis of the simultaneous bursts of the low-frequency emissions intensity for the magnetic and electrical components of the field and the density of the low-energetic particles flux observed on orbit 231 has been impossible because of a telemetric error. The correlation analysis between the electrical components of the field, the envelope bursts, of the field of the low-frequency emission on orbits 9147 and 9190 and the envelope bursts of density of the electrons flux with energy $E_e = 120$ eV on orbit 231 above the same region has been executed. As the heights of the orbits have been different ($h_{9147,9190} \sim 950$ km and $h_{231} \sim 580$ km), the correlation coefficients $R_{el,e}$ have been less than 0.5. Because of the difference of the satellite heights the variations of the low-frequency emission intensity have been moved in space in relation to the variations of the density of the low-energetic particles flux.

CONCLUSIONS

As a result of the analysis of all experimental data it is possible to make the following conclusions:

1. The steady variations of the low-frequency emission intensity on all frequencies 140÷15000 Hz have been observed above the zones of the deep faults of the lithosphere. The stretching mode has been characteristic for these zones. The frontal zones of the Novaya Zemlya orogenic belt, which are overfaults and overfault-overlaps, occurring in the conditions of compression have been exception;

2. The increase of amplitudes in the electrical and magnetic components of the field of the low-frequency emission has occurred above the zones with the high gradient of thickness of the Earth crust at transition from the oceanic crust to the continental one, from the deep hollow of the basement to the orogenic belt. The most active, frequently seismogenic systems of faults have been connected to these zones, as a rule;

3. The significant decrease of the amplitude of the variations of the low-frequency emission intensity or the complete absence of the variations has been observed above the faults zones, which have been buried under the powerful sedimentary cover and have not had obvious attributes of the tectonic activity;

4. Above the Barents-Kara mobile marginal-continental platform the variations of the low-frequency emission intensity and the increase of the plasma temperature at heights of the satellite (~ 950 km) in 1,3 time have been observed, as well as the variations of the density of the structured electrons flux with energy $E_e = 120$ eV, which have been divided into two parts on fluctuations periods;

5. Above the Siberian Lowland the jumps in changes of the amplitude of the low-frequency emissions above the tectonic borders of the structures have been observed: above the border of the internal zone of the Yenisey-Khatanga trough and above its border with the ancient Siberian platform, in particular;

6. The simultaneous bursts of the low-frequency emissions intensity observed in the South-Barents basin region and the low-energetic electrons fluxes can be connected to the radon allocation and to technogenic pollution of this region by the radioactive elements of nuclear explosions.

Acknowledgments. The authors would like to thank academician V.V. Migulin for fruitful discussions during the course of this work and S.V. Tolochkina and N.I. Lomakina for design this paper.

REFERENCES

1. «The auroral phenomena 80» (in Russian), ed. Brunelli B.E., Kola Science Centre, Apatity, 1984.
2. «The auroral phenomena 79» (in Russian) ed. Brunelli B.E., Kola Science Centre, Apatity, 1982.
3. Acad. Migulin V.V., Larkina V.I., Sergeeva N.G. and B.V. Senin, Regional structure reflection of lithosphere in the satellite observations of electromagnetic emission (in Russian), *Docl. Akad. Nauk*, v.357, № 2, 1997, pp.252 - 254.
4. Larkina V.I., Acad. Migulin V.V., Sergeeva N.G. and B.V. Senin, Electromagnetic emissions over the deep lithosphere faults by satellite measurements, *Docl. Akad. Nauk*, v.360, № 6, 1998, pp.814 - 818.
5. Pulincts S.A., Alekseev V.A., Boyarchuck K.A., Hegai V.V. and V.Kh. Depuev, Radon and ionosphere monitoring as a means for strong earthquakes forecast // *IL NUOVO CIMENTO*, v.22C, N 3-4, 1999, pp.621-626.
6. Matishov G., Matishov D., Shchipa E. and K. Rissanen, Radionuclides in ecosystems of the region of the Barents and Kara Seas (in Russian), Kola Science Centre Russian Academy Science, Apatity, 1999, 237 P.
7. Larkina V.I., Acad. Migulin V.V., Sergeeva N.G. and B.V. Senin, Ionospheric electromagnetic effects over the Baltic Shield by satellite measurements, *Docl. Akad. Nauk*, v.367, № 6, 1999, pp.815-819.

ON THE ASSOCIATION OF ANOMALIES IN SUBIONOSPHERIC VLF PROPAGATION AT KASUGAI WITH EARTHQUAKES AT THE CENTER OF JAPAN

Kenji Ohta and Kazuyuki Makita

Department of Electronic Engineering, Chubu University, Kasugai Aichi, 487-8501
Japan (e-mail:ohta@isc.chubu.ac.jp)

Masashi Hayakawa

Department of Electronic Engineering, The University of Electro-Communications,
Chofu Tokyo 182-8585, Japan (e-mail:hayakawa@aurora.ee.uec.ac.jp)

Abstract.

The subionospheric VLF signals transmitted from NWC VLF transmitter ($f=19.8\text{kHz}$) in Australia, have been monitored at Kasugai in Japan in order to find out the ionospheric perturbations associated with earthquakes. The period of seven months from Jan. to July 1998 when the observation was stable was chosen for the analysis. The terminator times (the times when a minimum appears in the diurnal variation of amplitude and/or phase around sunset and sunrise) are used to identify the VLF subionospheric propagation anomaly, in order to make correlation with the earthquakes at the center of Japan with magnitude greater than 3.5.

1. Introduction

Electromagnetic phenomena are recently considered to be a very promising candidate for short-time earthquake prediction [1][2] and both passive and active methods have been proposed. As an active radiosounding method, the use of subionospheric VLF transmitter signals has been suggested to study the ionospheric perturbations associated with earthquakes [3]. Hayakawa et al. have found a convincing precursory anomaly in the subionospheric propagation between Japan Omega at Tsushima and Inubu observatory (distance is $\sim 1\text{Mm}$) before 5-11 days for the Kobe earthquake [4][5].

NASDA's Earthquake Remote Sensing Frontier Project started in 1996,

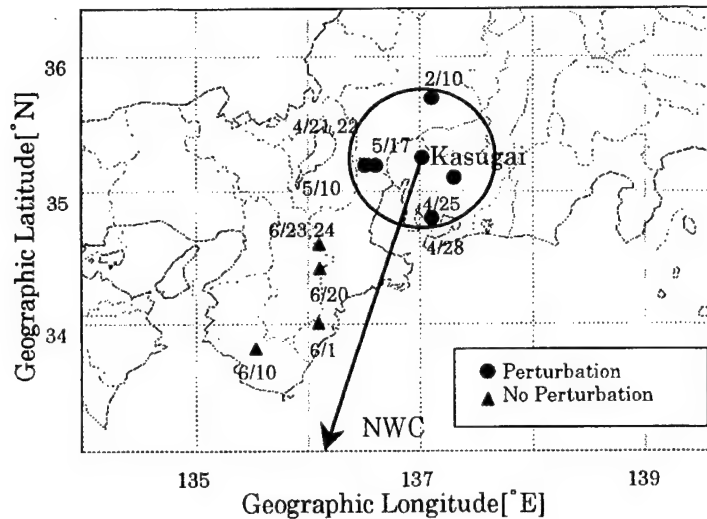


Fig. 1 Locations of the observing station, Kasugai and the epicenters of earthquakes (with $M \geq 3.5$) in the Tokai area. NWC-Kasugai is illustrated and a circle with radius of 60 km.

and the use of subionospheric VLF signals is considered as the most important observation item. Two key stations are established; one is Chofu (Univ. of Electro-Communications) and the second is Kasugai, Aichi (Chubu Univ.) and at both stations we receive several VLF transmitter signals simultaneously. Data are being collected, but in this report we will report on the recent results observed at Kasugai, Aichi.

2. Observation of subionospheric VLF signal at Kasugai

On the roof of Department of Electronics Engineering of Chubu University at Kasugai, we have been receiving several subionospheric VLF

transmitter signals by means of the so-called Omnipal receiving system [6]. In this paper we use only the data from NWC (Australia) (frequency is 19.8 kHz), and this continuous observation has started in August 1997. The receiving system consists of VLF vertical antenna, pre- and main-amplifiers, GPS antenna etc., and it can monitor the signal amplitude and phase every 0.1s (100ms). Fig. 1 shows the location of receiving station at Kasugai with radius of 60 km and the propagation path of NWC VLF transmitter.

3. Observational Results

The terminator times is defined as the time when there is observed a local minimum around sunrise and sunset.

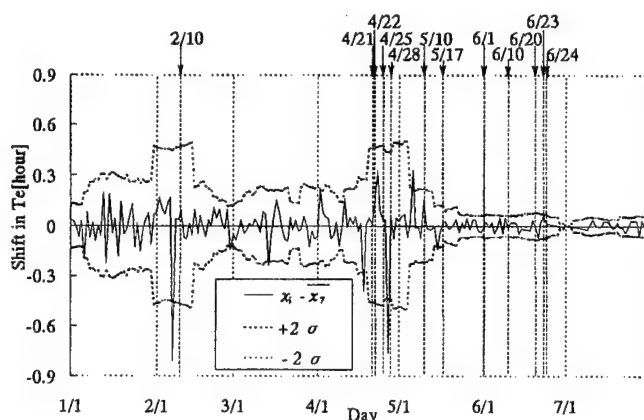


Fig. 2 The temporal evolution of the shift in the terminator time (Te) in the amplitude. 0 means the running mean, and $\pm 2\sigma$ lines are also illustrated. The times of earthquakes are given by vertical lines.

Though Kasugai-NWC is a long distance (distance; more than 6Mm) propagation, we use this "terminator time" method for the analysis as for the short-distance propagation in order to find the propagation anomaly.

Based on the continuous observation of subionospheric VLF signals, we estimate the Tm (morning terminator) and Te (evening terminator) every day, and try to find out anomalous behaviors in these Tm and Te. As the objective criterion to find an anomaly, we use the 2σ (σ : standard deviation) criterion as defined below,

$$\sigma = \sqrt{\frac{1}{n} \sum_{i=1}^n (x_i - \bar{x}_{i7})^2}$$

where x_i is the value on each day, \bar{x}_{i7} is the running average over ± 7 days around that day, and n is the number of data. Since anomalies for Tm are not so clear as for Te, we deal with the

characteristics of Te only.

Fig. 2 illustrates the temporal evolution on the shift in Te on the amplitude record during the analyzed whole period of 7 months from January to July 1998. The times of earthquakes are indicated by vertical dot-broken lines and their corresponding dates are given on the top of the figure. Table 1 is the summary of those earthquakes (time of occurrence, magnitude, place, its geographic coordinates, depth, VLF perturbation), which took place in the Tokai area around Nagoya (Aichi, Gifu, Mie and Wakayama Prefectures) with magnitude greater than 3.5. In Fig. 2 the zero line means the running mean, and broken lines indicate the $\pm 2\sigma$ curve. Let us look at significant deviations in Fig. 2 one by one. Since the earthquake on Feb. 10 is an isolated one ($M=4.3$, $d=10\text{km}$), we can notice a very conspicuous deviation on Feb. 7, which

Table 1 Parameters of earthquakes (with $M \geq 3.5$) in the Tokai area

No.	Date (M,D)	Magni- tude	Epicenter (Place)	Geographic Coordinates	Depth (km)	Precursory Effect (M,D)
1	2.10	4.3	Hida, Gifu-Pref	35.7, 137.1	10	2.07
2	4.21	3.6	Mino Middle-West, Gifu-Pref	35.2, 136.6	10	4.18
3	4.22	5.2	"	"	10	4.18
4	4.22	3.5	"	"	10	4.18
5	4.25	3.9	East, Aichi-Pref	35.1, 137.3	40	4.18 or 4.23
6	4.28	3.7	West, Aichi-Pref	34.8, 137.1	40	4.27
7	5.10	3.6	North, Mie-Pref	35.2, 136.5	10	5.06
8	5.17	3.9	Mino Middle-West, Gifu-Pref	35.2, 136.6	20	5.15
9	6.01	5.9	South, Mie-Pref	34.0, 136.1	400	no
10	6.10	4.3	North, Wakayama-Pref	33.9, 135.4	60	no
11	6.20	3.6	Middle, Mie-Pref	34.4, 136.1	10	no
12	6.23	4.4	"	34.6, 136.1	40	no
13	6.24	4.0	"	34.6, 136.1	40	no

took place three days before the earthquake. So that, this propagation anomaly is higher likely to be precursory to the earthquake. Next, when we look at Table 1, the quake Nos. 2~4 occurred at the same position, which means that these quakes should be treated as a group (as a swarm). The depths of the earthquakes (Nos. 1~8) is relatively small, less than 40km. This may be the reason why precursory ionospheric perturbations are clearly identified. The earthquake (No. 9) has an extremely large depth (400km), which may be associated with the absence of the ionospheric perturbations for this earthquake. Then, we have to describe the characteristics of the subsequent earthquakes (Nos. 9,10,12,13). Though the quake No. 11 is very shallow, others have relatively larger depths. However, the reason why there are no ionospheric perturbations associated with those quakes, is very unclear, though one reason is that many of them occurred at

deeper depths.

4. Summary and conclusion

As in the case of short distance propagation [4], the abnormal change in the terminator time (T_e in this paper) in the diurnal variation of subionospheric propagation (amplitude and phase) is used to identify the seismo-ionospheric perturbations. Unlike the short distance case, the anomalous shift in T_e is found to be positive on some occasions, and negative on other occasions (this needs a theoretical interpretation). By using the 2σ criterion, we have investigated the correlation of propagation anomaly (ionospheric perturbations) with an earthquake. In the case of an isolated earthquake with moderate magnitude ($M \geq 3.5$) and with smaller depths ($d=10-20\text{km}$), we could succeed in identify a propagation anomaly, mainly before the quake (probably as a precursor). There was also observed an anomaly in propagation before a series of quakes,

but no anomalies are found to be associated with earthquakes with larger depths.

5. References

- [1] Hayakawa, M. and Y. Fujinawa (Editors), *Electromagnetic Phenomena Related to Earthquake Prediction*, Terra Sci. Pub. Co., 667., Tokyo, 1994
- [2] Hayakawa, M. (Editor), *Atmospheric and Ionospheric Electromagnetic Phenomena Associated with Earthquake*, Terra Sci. Pub. Co., 997, Tokyo, 1999.
- [3] Gokhberg, M. B., I. L. Gufeld, A. A. Rozhnoy, V. F. Marenko, V. S. Yampolsky, and E. A. Ponomarev, Study of seismic influence on the ionosphere by super long-wave probing of the Earth-ionosphere waveguide, *Phys. Earth Planet. Inter.*, pp.57-64, 1989.
- [4] Hayakawa, M., O. A. Molchanov, T. Ondoh, and E. Kawai, The precursory signature effect of the Kobe earthquake on VLF subionospheric signals, *J. Comm. Res. Lab.*, 43, pp.413-418, 1996.
- [5] Molchanov, O. A. and M. Hayakawa, Subionospheric VLF signal perturbation possibly related to earthquakes, *J. Geophys. Res.*, 103, 17, pp. 489-504, 1998.
- [6] Dowden, R. L. and C. D. D. Adams, Phase and amplitude perturbations on subionospheric signals explained in terms of echoes from lightning-induced electron precipitation ionization patches, *J. Geophys. Res.*, 93, 11, pp.543-550, 1988.

BIOGRAPHICAL NOTES

Kenji Ohta graduated from Department of Communication Engineering, Shinshu Univ. in 1966 and received the Doctor of Engineering from Nagoya Univ. in 1987 and he is Professor of Chubu University. He is member of the Society of Atmospheric Electricity of Japan and was awarded its Society Prize in 1991.

Msashi Hayakawa was graduated from Nagoya Univ. in 1966, where he obtained a Dr. of Eng. Degree and become a Professor of The Univ. of Electro Communication in 1990. In 1983 he was awarded the Tanakadate Prize, and in 1988 awarded the prize of The Society of Atmospheric Electricity of Japan.

ESTIMATION OF ATTENUATION CHARACTERISTICS OF FEED-THROUGH TYPE EMI FILTERS USING Fe-Si ALLOY FLAKE-POLYMER COMPOSITE

Tadaharu Akino Shinichi Shinohara Risaburo Sato
Electromagnetic Compatibility Research Laboratories Co., Ltd.
6-6-3, Minami-Yoshinari Aoba-ku, Sendai, 989-3204 Japan
Fax: +81 22 279 3640 E-mail: akino@emc-l.co.jp

The authors have constructed a prototype feed-through type EMI filter by filling the hollow portion of a coaxial structure having an outer diameter of 7.00 mm and an inner diameter of 3.04 mm with composite magnetic material made up of Fe-Si alloy flakes and polyphenylene sulfide resin. Insertion losses were measured in the frequency range from 100 MHz to 20 GHz for filter specimens containing different length of composite magnetic material, and an insertion loss of 10 dB and greater was observed from 1 GHz to 20 GHz in the case of 20 mm. In addition, using material constants of the composite magnetic material measured beforehand, insertion losses were calculated, and it was found that the results of calculation agreed relatively well with the above measurements.

On the basis of the above, the authors have been able to clarify how the material constants of the composite magnetic material affect insertion loss.

1. INTRODUCTION

As processing speeds of information and communication devices become increasingly faster, the internal operating frequency of system LSIs have been reaching several hundred MHz while that of ICs on circuit boards 100 MHz [1]. This rise in operating frequency causes electromagnetic interference (EMI) affecting frequencies up to the GHz band. As a means of suppressing such high-frequency EMI, a method based on the concept of "zone separation" has been considered effective [2]. In this method, a circuit generating the EMI is shielded, and power is supplied to and signals are transferred to and from the interior of such a shielded circuit via a feed-through type EMI filter.

Conventionally, feed-through type EMI filters used for zone separation have been configured as low-pass

filters in which a feed-through type capacitor in a metallic cylindrical case is connected to a choke coil (or ferrite beads) in an L-, T-, or π -circuit. When applied to the GHz band, however, this type of EMI filter suffers from dispersion in insertion loss due to variation in constituent elements, and decrease in insertion loss due to the effects of parasitic elements on frequency characteristics. This latter drawback is manifested as degraded suppression of conductive EMI in the GHz band.

With the aim of solving the above technical problems possessed by conventional feed-through type EMI filters, the authors have been researching methods of configuring this type of filter with particular attention placed on insertion loss obtained by filling the hollow portion of a coaxial structure with composite magnetic material [3]. In this regard, we have previously constructed feed-through type EMI filters using composite magnetic material consisting of Ni-Zn ferrite powder and polyester resin, measured their insertion losses, and examined the effects of material constants (complex relative permeability (μ_r) and complex relative permittivity (ϵ_r) on insertion loss [3].

In this paper, we report on the construction of a feed-through type EMI filter using composite magnetic material made up of Fe-Si alloy flakes and polyphenylene sulfide (PPS) resin. We describe the results of measuring insertion loss in the frequency range from 100 MHz to 20 GHz, and present a method for estimating attenuation characteristics from the material constants of this composite magnetic material.

2. TEST SPECIMENS

2.1 Composite magnetic material

For the magnetic portion of the composite magnetic

material, we took Fe-Si alloy particles of about $6\text{ }\mu\text{m}$ in diameter and formed them into flakes about $0.3\text{ }\mu\text{m}$ thick and $50\text{ }\mu\text{m}$ long. An electron micrograph of these processed flakes is shown in Fig. 1. As a binder, we used PPS resin, which is known to have good affinity with magnetic powder.

The above magnetic flakes and binder were combined at a ratio of 80:20 (weight-%) and a material suitable for molding was prepared.

Next, using a plastic mold, this material was formed into seven types of cylindrically shaped specimens having outer/inner diameters of 7.00 mm/3.04 mm suitable for a 7-mm coaxial structure, and lengths of 0.5, 1, 2, 5, 10, 20, and 40 mm. An electron micrograph of a lengthwise cross-section of the 20 mm specimen is shown in Fig. 2.

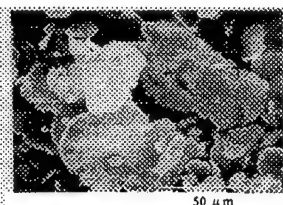


Fig. 1 Photograph of Fe-Si alloy flake's shape.

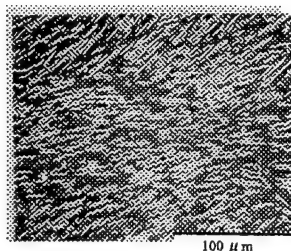


Fig. 2 Photograph of center-lengthwise cross sectional structure of Fe-Si alloy flake-polymer specimen.

2.2 Feed-through type EMI filter

The coaxial structure was made of brass, and the outer diameter of the center conductor and the inner diameter of the outer conductor were set to 3.04 mm and 7 mm, respectively, in accordance with the characteristic impedance ($50\text{ }\Omega$) of the measurement system. The lengths of the center conductor and outer conductor were set to 5, 10, 20, and 40 mm based on the lengths of the cylindrically shaped molded specimens.

The feed-through type EMI filter shown in Fig. 3 was constructed by filling the hollow portion of this coaxial structure with the cylindrically shaped molded specimens of the composite magnetic material.

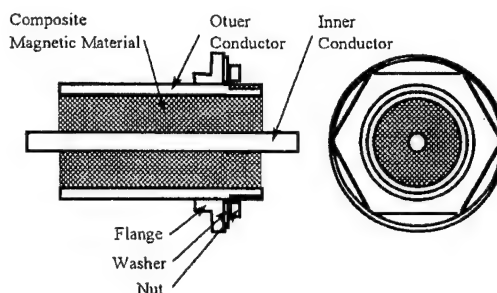


Fig. 3 Structure of feed-through type EMI filter.

3. MEASUREMENT METHOD

3.1 Material constants

Using a network analyzer (Agilent Technologies 8720D), S parameters (S_{11} , S_{21}) were measured from 50 MHz to 20 GHz for a cylindrically shaped 5 mm long molded specimen inserted in the 7-mm coaxial structure. Using these S parameters, the material constants of complex relative permeability (μ_r) and complex relative permittivity (ϵ_r) were calculated by the Nicolson-Ross, Weir method [4].

3.2 Insertion loss and reflection loss

The system for measuring insertion loss and reflection loss of a feed-through type EMI filter is shown in Fig. 4. In this $50\text{-}\Omega$ system, insertion loss and reflection loss were measured from 100 MHz to 20 GHz by the 2-port method using a network analyzer (Agilent Technologies 8720D).

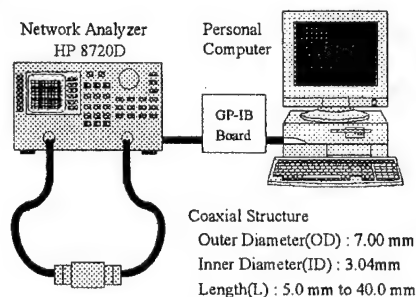


Fig. 4 System for measuring insertion loss and reflection loss.

4. MEASUREMENT RESULTS

4.1 Material constants

The results of measuring and calculating the material constants of the composite magnetic material are shown in Fig. 5. At the lower measurement limit of 50 MHz, the frequency dispersion phenomenon of μ_r , the real part of complex relative permeability, already appears,

and its value drops to 1 at 3 GHz. On the other hand, μ_r'' , the imaginary part of complex relative permeability, exhibits a maximum value at 2 GHz due to magnetic resonance phenomena.

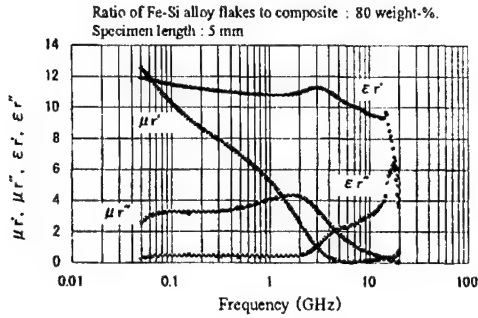


Fig. 5 Frequency characteristics of material constants of composite magnetic material.

The results of calculating the loss coefficient ($\tan \delta$) for μ_r and ϵ_r are shown in Fig. 6. While $\tan \delta$ of μ_r ($= \mu_r'' / \mu_r'$) shows a value near 70 at a frequency of 6 GHz, $\tan \delta$ of ϵ_r ($= \epsilon_r'' / \epsilon_r'$) is less than 1 within the entire measurement frequency range.

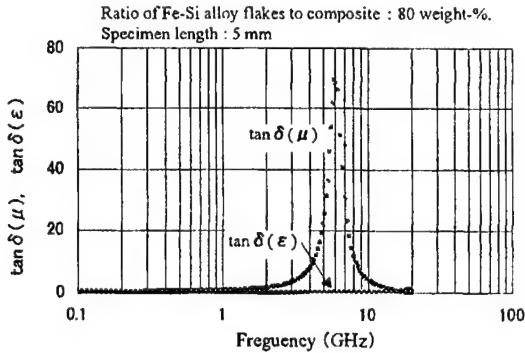


Fig. 6 Frequency characteristics of $\tan \delta$ of composite magnetic material.

4.2 Insertion loss

The results of measuring insertion loss from 100 MHz to 20 GHz for feed-through type EMI filters filled with cylindrically shaped molded specimens of seven different lengths are shown in Fig. 7. As shown, insertion loss is roughly proportional to length up to about 5 GHz. However, for the 40 mm long specimen, insertion loss climbs above 100 dB from a frequency of 3 GHz, exceeding the limit (100 dB) of the measurement system and preventing valid values from being obtained.

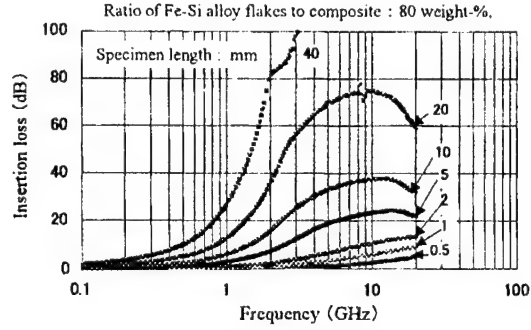


Fig. 7 Frequency characteristics of insertion loss of feed-through type EMI filter.

4.3 Reflection loss

The results of measuring reflection loss for the same seven specimens used the measurement of insertion loss are shown in Fig. 8. As shown, reflection loss is roughly inversely proportional to length up to about 300 MHz. In the case of specimen lengths 5 to 40 mm, measured values behave similarly from a frequency of 1 GHz. However, for the specimen lengths 0.5 to 2 mm, reflection loss is roughly proportional to length up to about 10 GHz.

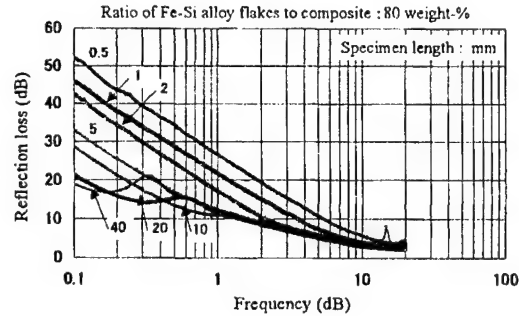


Fig. 8 Frequency characteristics of reflection loss of feed-through type EMI filter.

5. RESULTS OF CALCULATING INSERTION LOSS

5.1 Calculation model

The model used for calculating insertion loss when filling the hollow portion of a coaxial structure with composite magnetic material is shown in Fig. 9.

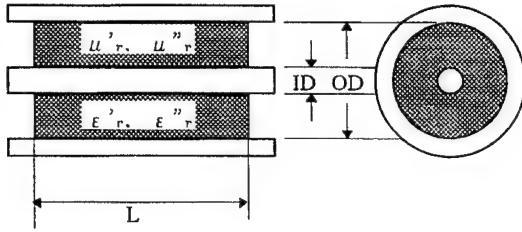
The complex relative permeability (μ_r) and complex relative permittivity (ϵ_r) of an inserted specimen are given by Eqs. (1) and (2), respectively.

$$\mu_r = \mu_r' - j \mu_r'' \quad (1)$$

$$\epsilon_r = \epsilon_r' - j \epsilon_r'' \quad (2)$$

Now, given that the length of the coaxial structure is

infinite and μ_r and ϵ_r inside the coaxial structure are uniformly distributed, the propagation constant ($\dot{\gamma}$) can be expressed as shown in Eq. (3), for electromagnetic waves propagating in TEM mode [5]:



OD : Outer diameter of composite magnetic material

ID : Inner diameter of above

L : Length of above

Fig. 9 Model of feed-through type EMI filter.

$$\begin{aligned}\dot{\gamma} &= \alpha + j\beta \\ &= j\omega\sqrt{\mu_0 \cdot \epsilon_0 \cdot \mu_r \cdot \epsilon_r} \\ &= j\frac{\omega}{c}\sqrt{(\mu_r' - j\mu_r'')(\epsilon_r' - j\epsilon_r'')} \quad (3)\end{aligned}$$

The symbols used in this equation are explained below:

- α : Attenuation constant,
- β : Phase constant,
- μ_0 : Permeability in vacuum,
- ϵ_0 : Permittivity in vacuum,
- ω : Angular frequency,
- c : Speed of light.

Next, reorganizing Eq. (3) with respect to α (neper/meter) and using GHz as unit of frequency, attenuation in dB per centimeter can be given by Eq. (4). Consequently, if the material constants and length of the composite magnetic material are known, this equation can be used to estimate insertion loss at any frequency.

$$\begin{aligned}Att &= 1.286 f \sqrt{\mu_r' \times \epsilon_r'} \\ &\times \left\{ \sqrt{\left[\left(\frac{\mu_r''}{\mu_r'} \right)^2 + 1 \right] \left[\left(\frac{\epsilon_r''}{\epsilon_r'} \right)^2 + 1 \right]} + \left(\frac{\mu_r''}{\mu_r'} \right) \cdot \left(\frac{\epsilon_r''}{\epsilon_r'} \right) - 1 \right\}^{1/2} \\ &[\text{dB/cm}] \quad (4)\end{aligned}$$

5.2 Calculation results

Using the material constants (μ_r and ϵ_r) calculated earlier by the Nicolson-Ross, Weir method from the S parameters (S_{11} , S_{21}) measured by a network analyzer, insertion loss was calculated from Eq. (4). Calculated and measured values for insertion loss are compared in Fig. 10 for specimens of lengths 5, 10, and 20 mm.

While calculated and measured values behave similarly for all three specimens, measured values are greater than calculated values in all cases, and the difference between them becomes larger as frequency increases.

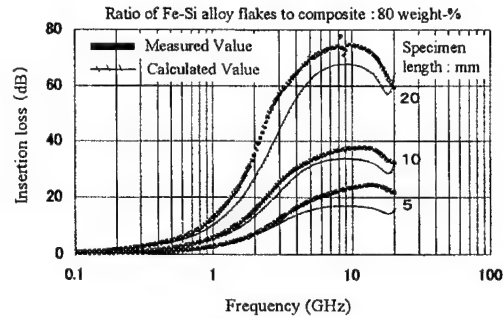


Fig. 10 Comparison between calculated and measured insertion loss of feed-through type EMI filter (Specimen lengths : 5, 10, and 20 mm).

Next, calculated and measured values for insertion loss in the case of specimen lengths 0.5, 1, and 2 mm are compared in Fig. 11.

Here, calculated values are greater than measured values for the three specimens up to the frequency where calculated and measured values cross. After this frequency, however, calculated and measured values diverge significantly.

The reason for this behavior is thought to be that multiple reflection modes occur inside specimens as the specimen length shortens (refer to Fig. 8), and that the orientation of Fe-Si alloy flakes in the composite magnetic material participate in shape magnetic anisotropy (refer to Fig. 2).

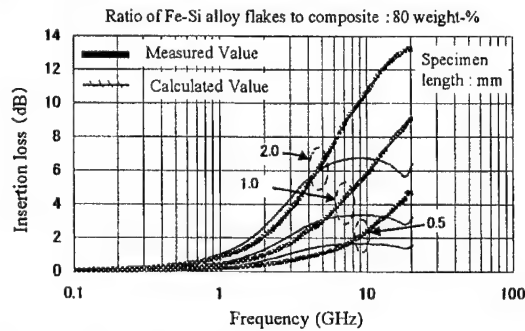


Fig. 11 Comparison between calculated and measured insertion loss of feed-through type EMI filter (Specimen lengths : 0.5, 1, and 2 mm).

To examine the attenuation characteristics of the feed-through type EMI filter, we calculate the two terms in Eq. (4) and the product of Eqs. (5) and (6) below from

the values of $\dot{\mu}_r$ and $\dot{\epsilon}_r$ (see Fig. 5):

$$K = \sqrt{\dot{\mu}_r \times \dot{\epsilon}_r} \quad (5)$$

$$L = \left\{ \left[\left(\frac{\mu_r''}{\mu_r'} \right)^2 + 1 \right] \left[\left(\frac{\epsilon_r''}{\epsilon_r'} \right)^2 + 1 \right] + \left(\frac{\mu_r''}{\mu_r'} \right) \cdot \left(\frac{\epsilon_r''}{\epsilon_r'} \right) - 1 \right\}^{1/2} \quad (6)$$

The results of these calculations are shown in Fig. 12. As we can see, attenuation is governed by characteristics determined by Eq. (5) for low frequencies under 3.5 GHz, and by those determined by Eq. (6) for high frequencies above 3.5 GHz. In addition, frequency characteristics of Eq. (6) behave similarly to those of $\tan \delta$ of $\dot{\mu}_r$ (see Fig. 6), leading us to surmise that insertion loss at frequencies exceeding 3.5 GHz depend on $\tan \delta$ of $\dot{\mu}_r$.

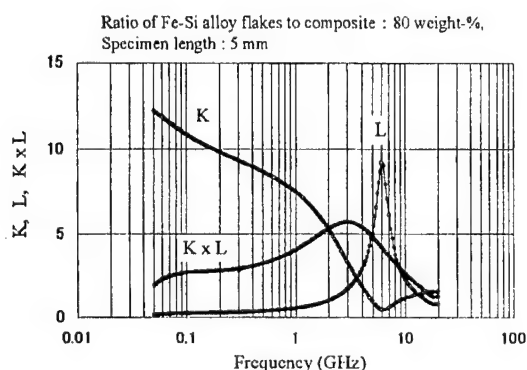


Fig. 12 Analysis of factors governing attenuation characteristics of feed-through type EMI filter.

6. CONCLUSIONS

This paper has described the construction of a feed-through type EMI filter by filling the hollow portion of a coaxial structure with composite magnetic material composed of Fe-Si alloy flakes and PPS resin, and the measurement of insertion loss for filter specimens of various lengths. It was found that an insertion loss of 10 dB and greater could be obtained in the range from 1 to 20 GHz for 20 mm in length.

In addition, calculations of insertion loss were performed using the propagation constant for an infinitely long coaxial line and the $\dot{\mu}_r$ and $\dot{\epsilon}_r$ of composite magnetic material composed of Fe-Si alloy flakes and PPS resin. Calculated values were found to generally agree with insertion loss measured by the 2-port method using a network analyzer for specimens 5 mm and greater in length.

In future studies, the authors plan to clarify further the reason why differences appear between measured and calculated values for insertion loss.

7. REFERENCES

- [1] J. Silberman, et al. "A 1.0GHz Single-Issue 64b Power PC Integer Processor", IEEE International Solid-State Circuits Conference 1998, Digest of Technical Papers, IEEE Press, 1998, pp.230-231
- [2] F. Edward Vance. "Electromagnetic Interference Control", IEEE Transactions, Vol. EMC-22, No.4, 1980, p.321
- [3] T. Akino, S. Shinohara, R. Sato, "Effect of Magnetic Properties of Ferrite-Resin Composite on Attenuation Characteristics in GHz Band" (in Japanese), Technical Report of IEICE, EMCJ98-15, 1998, pp.35-40
- [4] A. M. Nicolson and G. F. Ross, "Measurement of the intrinsic properties of materials by time domain techniques", IEEE Transactions, Instrum. Meas. vol. IM-17, 1974, pp.33-36
- [5] R. Sato, "Transmission circuits", (in Japanese), Corona Co.

BIOGRAPHICAL NOTES

Tadaharu Akino received the B. degrees from Kogakuin University, Tokyo, Japan, in 1962. He worked in TDK Corporation, and was engaged in development of EMI countermeasure components. Since 1996, he has been a chief researcher at Electromagnetic Compatibility Research Laboratories Co., Ltd. Presently he is engaged in research on countermeasures technology on EMC.

Shinichi Shinohara received the M.E. degrees from University of Electro-Communications, Chofu, Japan, in 1972. He worked in the NTT's Laboratories, and was engaged in development of telephone System. He joined Sony Corporation in 1998. Since 1996, he has been a general manager at Electromagnetic Compatibility Research Laboratories Co., Ltd. Presently he is engaged in research on countermeasures technology on EMC.

Risaburo Sato received the Ph.D. degrees from Tohoku University, Sendai, Japan, in 1952. From 1961 to 1984, he was a Professor at Tohoku University. From 1984 to 1999, he was Dean of the Faculty of Engineering of Tohoku Gakuin University, Tagajo, Japan. He is a life member of IEEE of USA and the president of Electromagnetic Compatibility Research Laboratories Co., Ltd.

RESEARCH AND DESIGN OF GYROMAGNETIC MEDIA AND DEVICES ON THEIR BASE FOR EMC AND ECOLOGY PROBLEMS

L. Mikhailovsky, A. Kitaytsev, M. Koledintseva*, V. Cheparin

Moscow Power Engineering Institute (Technical University), Krasnokazarmennaya, 14
111250 Moscow RUSSIA, fax: +7-095-362-89-38; kitaitsev@b14s1nt.mpei.ac.ru; marina@ieee.org

A number of problems of EMC on microwaves-detection and measurement of power (spectrum) parameters of signals and suppression of unwanted radiation - can be solved using unique properties of gyromagnetic media. Hexagonal ferrites with high internal field of magnetic anisotropy allow their operation without intense external magnets. Approaches to the study of interaction of gyromagnetic media with electromagnetic field and ways of modeling microwave frequency-selective measuring devices, absorbing coatings and all-mode filters of harmonics are discussed.

1. INTRODUCTION

EMC of electronic equipment and electromagnetic ecology at microwaves need methods and devices for detection, spectrum analysis, measuring of signal parameters, as well as coatings and filters suppressing unwanted radiation. The elaborated equipment must operate in wide frequency band and range of power, satisfy demands on reliability, low cost, and technologically simple and repeatable manufacturing. It's necessary to underline that only frequency-selective methods allow getting the most full and adequate information on the radiation under investigation.

All the mentioned above problems can be solved using microwave gyromagnetic media due to their unique frequency-selective physical properties. Gyromagnetic media exhibit frequency-selective absorption of electromagnetic energy at ferromagnetic (or anti-ferromagnetic) resonance. In the vicinity of FMR and power level less than that of spin wave instability excitation stable non-linear effects take place.

Due to pure spin mechanism of this interaction (Lande factor $g=2$) such media could be considered as "non-current", because their conductivity current losses turn out to be negligible. Permeability of these media in general

case has tensor character, they exhibit non-reciprocal interaction with electromagnetic waves of various polarization.

In the past years the significant success in basic and applied research of gyromagnetic media at microwaves is achieved in the Ferrite Laboratory of Moscow Power Engineering Institute (Technical University). Main research and development topics directly aimed at the solution of the problems of EMC and ecology, are the following:

- A. Physical bases of elaboration of frequency-selective methods and devices for microwave signals detection, spectrum analysis and power parameters measuring using monocrystalline garnet and hexagonal ferrite resonators;
- B. Elaboration of technology of composite absorbing materials, study of their chemical and physical properties. Research of physics of their interaction with microwaves, and design of coatings and devices - filters of harmonics on base of dispersed (powder) polycrystalline hexagonal ferrites.

2. FREQUENCY-SELECTIVE MEASURING DEVICES ON BASE OF FERRITE RESONATORS

The development of the first topic (A) mainly uses the classical approach to the description of interaction of gyromagnetic media with microwaves. This approach is based on phenomenological model of the magnetization vector precession [1]. Its mathematical language employs continuous harmonic functions used in classical field theory. Operation of the elaborated devices (magnetic detector, cross-multiplier, gyromagnetic converter, ferrite-diode converter, filter-preselector, ferrite mixer) is based on stable non-linear resonance effects in ferrite high-quality monocrystalline resonators, regimes of resonance detection and cross-multiplication of the magnetic

detector invented in 60-ies by L.K.Mikhailovsky [2]. The scheme of non-heterodyne gyromagnetic converter (GC) is shown on fig.1. The "panoramic" measurer of power parameters of 10^{-3} - 10^3 W (spectrum power density, width of spectrum; integral power of wide-band signals, and peak power of pulsed signals) was elaborated in MPEI (TU) (fig.2). This device was produced in industry in small series for testing spectrum power parameters of intense wide-band noise signals. The measurer uses a GC with monocrystalline ferrite (YIG, Ca-Bi-Va garnet) resonator as a stable non-linear resonance scanning element (for the frequency range 300 MHz- 30 GHz) [3]. Another device using GC is wattmeter of peak and average power of pulse signals of microsecond duration (fig.3) which can operate at up to 1 MW power level [4]. The devices on base of GC exhibit stable functioning at high power levels admissible for the transmission line path. Frequency selectivity of the devices is determined by the width of FMR of the employed ferrite resonator, usually 1-10 MHz.

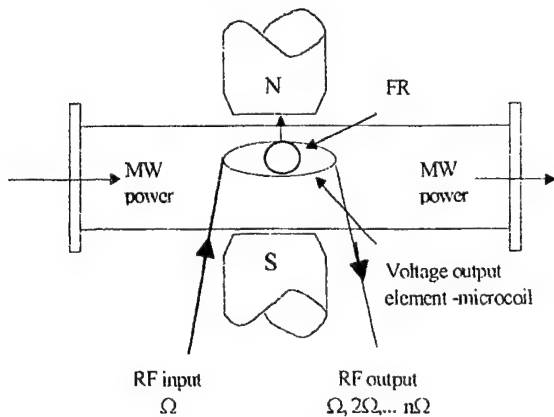


Fig.1. Gyromagnetic converter.

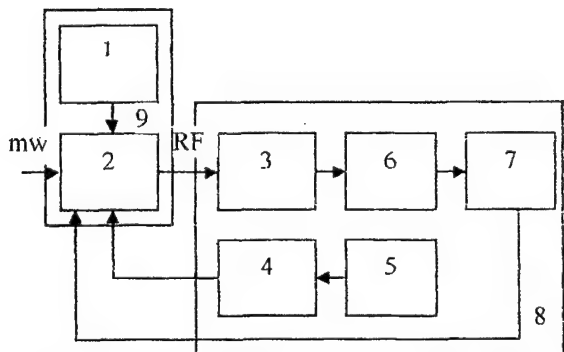


Fig.2. Functional scheme of microwave measurer of power parameters:

1- magnetic system; 2- magnetic detector; 3-high-pass filter; 4-low-pass filter; 5-RF modulating oscillator; 6- amplifier of converted signal; 7-scanning and displaying block; 8- measuring block; 9-gyromagnetic converter.

Application of monocrystalline hexagonal ferrite resonators (HFR) prolongs the frequency range of this measurer to mm-waveband (30 – 75 GHz) without intense and massive external magnetization field [5]. Modernization of the measurer allows providing additional function: detection of low-intensity harmonic signals on background of the wide-band noise, it gives more adequate information on the contents of microwave spectrum under investigation [6].

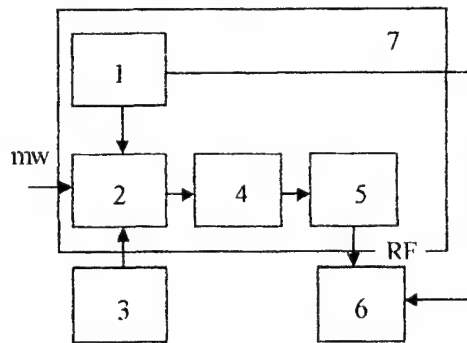


Fig.3. Functional scheme of microwave wattmeter of pulse signals:

1- magnetic system; 2- magnetic detector; 3- RF modulating oscillator; 4- attenuator; 5-crystalline detector; 6- scanning and displaying block; 7- ferrite-diode converter

3. GYROMAGNETIC ABSORBERS AND FILTERING TECHNIQUES

The second topic (B) uses both classical approach operating with averaged in space constitutive parameters of media – ϵ and μ , and non-classical approach based on axiomatic quantum field theory and its mathematical language – gyrovector formalism with discrete counting out in space-time for quantification of both electromagnetic field and gyromagnetic media [7]. Gyromagnetic particles are represented as "point" centers of absorption and radiation (CAR) of electromagnetic energy, where spin moment turns over, and instantaneous transition from one discrete energy level to the other with absorption or radiation of the corresponding energy quantum takes place. This theory forms the novel trend in microwave electronics - Spin-Electronics and Non-Phase Electrodynamics (see, for example, review [8, 9]).

Non-classical approach clears up the picture of interaction at microcosm level, while classical approach allows by introducing effective constitutive parameters of composite absorbing materials to deal with them as homogeneous

media and apply modern means of computational electromagnetics for the design of the devices on their base [10]. Wide-band composite gyromagnetic materials (CGM) using high-anisotropy hexagonal ferrite powders of various chemical formulae are elaborated [11]. Due to the phenomenon of natural ferromagnetic resonance in hexagonal ferrite particles with high field of crystallographic anisotropy, it is possible to design coatings and devices operating without external magnets. Desirable frequency characteristic of the absorption could be formed (see, for example, fig.4), and filters of harmonics with the necessary parameters could be designed by varying the contents of the composite material, geometry and position of CGM layers [12]. Such materials were used, for example, for suppressing the 5th harmonic of magnetron radiation of microwave oven that falls into the frequency band of telecommunication systems (fig.5) [13].

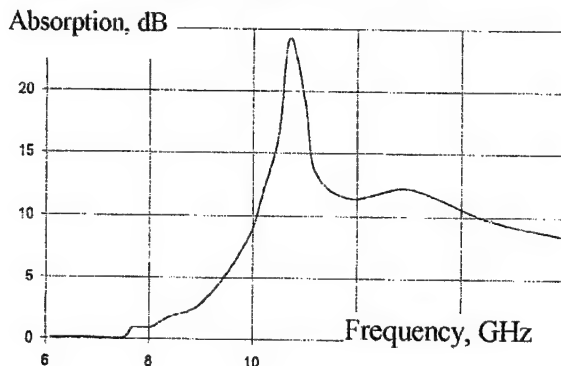


Fig.4. Absorption characteristic of composite gyromagnetic material with doped hexagonal ferrites as a filler and polymeric (hermetic) base.

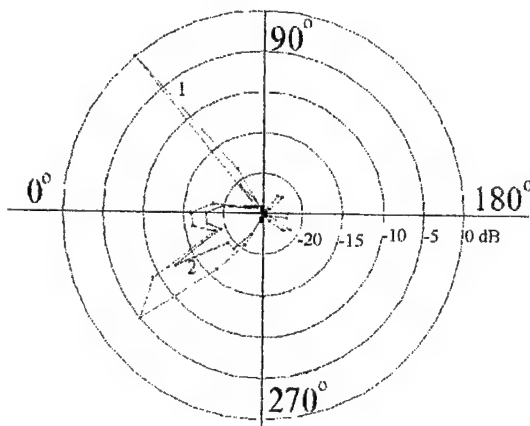


Fig. 5. Radiation diagram from the microwave oven; 1- without absorber; 2- with absorber. 0° corresponds to the direction normal to the microwave oven door.

4. APPLICATION OF GYROMAGNETIC MATERIALS AND DEVICES

Developed materials and devices could be used:

- In all the branches of industry using microwaves for harmful radiation suppression;
- In radio electronics for EMC problems that require the suppression of spurious radiation in transmitting devices, and that require noise immunity in receiving devices; one example would be suppression of the 5th harmonic in microwave oven radiation, which causes interference in satellite telecommunication systems;
- For domestic (everyday) life to protect people from harmful radiation (microwave ovens, medical equipment; portable hand-phones);
- For protection of human beings in outer space conditions;
- For optimal design of modern computers that have microprocessors operating at near-microwave frequencies.

5. CONCLUSION

Basic and applied research in the field of gyromagnetic media carried out in recent years in MPEI (TU) yielded in the design of microwave equipment having new principles of functioning and construction. The "panoramic" equipment aimed at testing and measuring power parameters of microwave signals operates in the frequency band 0.3-75 GHz. Due to frequency selectivity at FMR and low "current" conductivity losses in gyromagnetic media the devices are resistant to high-power overload. All-directionally matched with free space spin (non-current) absorbing materials have been elaborated and tested. All-mode waveguide filters of harmonics of intense sources of microwave radiation using gyromagnetic composite films have been designed. The elaborated devices and coats can be used for the solution of various problems of electromagnetic compatibility and ecology.

6. REFERENCES

- [1]. L.D. Landau, E.M. Lifshits "Theoretical Physics. Electrodynamics of Continuous Media" (Russian). V.8, Moscow, Ed. 'Nauka', 1992. - 664 pp.
- [2]. L.K. Mikhailovsky "Cross-non-linear properties of gyromagnetic detectors" (Russian). Conference Transactions 7 International conference on microwave ferrites Smolence, CSSR, Sept.17-22,1984, s.4.

- [3]. A.A. Kitaytsev et. al. "Panoramic Measurer of Power Parameters." (Russian). Transactions of Moscow Power Engineering Institute No 241. Moscow, Ed. MPEI, 1991, pp. 40-47.
- [4]. V.F. Balakov et.al. "Measurers of microwave signal parameters based on ferrite monocrystals" (Russian). Trans. of Moscow Power Engineering Inst. No 464, Moscow, Russia, 1980, pp. 46-49.
- [5]. A.A. Kitaytsev, M.Y. Koledintseva "Physical and technical bases of using ferromagnetic resonance in hexagonal ferrites for electromagnetic compatibility problems" (English) IEEE Trans. EMC, Vol. 41, No 1, Feb. 1999, pp.15-21.
- [6]. A.A. Kitaytsev, M.Y. Koledintseva, V.A. Konkin, "Reproduction of spectrum envelope of microwave wideband noise and detection of a narrowband signal in it" (Russian, English). Proc. 9 Int. Conf. "Microwave Engineering and Telecommunication Technology", CriMiCo'99, Sevastopol, Crimea, Ukraine, 13-17 Sept., 1999, presentation No 7.9.
- [7]. L.K. Mikhailovsky Gyromodel (Multitime gyrovector formalism) in the theory of electromagnetic field interaction with gyromagnetic medium (The Review). Proceedings of the 12th International conference on microwave ferrites. Gyulechitsa, Bulgaria, 19-23.09.1994. P.38-57.
- [8]. L.K. Mikhailovsky "Spin-Electronics and Non-phase Electrodynamics" (Russian). Proc. 14 Int. Conf. On Gyromagnetic Electronics and Electrodynamics (Microwave Ferrites) ICMF'98, Section "Spin-Electronics", Nov. 13-16, 1998, Moscow, Russia, V. 2, pp. 21-29.
- [9]. L.K. Mikhailovsky, E.P. Chigin "Currentless" Spin-Electronics & Non-Phase Electrodynamics" (review). Proc. 43 Scientific Colloq. Ilmenau TU, 20-25 Sept. 1998, Germany.
- [10]. A.A. Kitaytsev, M.Y. Koledintseva, V.P. Cheparin, A.A. Shinkov "Electrodynamic parameters of composite gyromagnetic material based on hexagonal ferrites". Proc. URSI Symposium on Electromagnetic Theory EMT'98, Greece, Thessaloniki, V.2, p.790-793.
- [11]. V.N. Karpov, A.A. Kitaytsev, L.K. Mikhailovsky, N.I. Savchenko, V.P. Cheparin. "Application of natural ferromagnetic resonance in dispersed hexaferrite for the solution of electromagnetic compatibility problems", Proc. Int. Conf. on Currentless Spin Electronics (ICCSE), Moscow, Russia, Ed. Moscow Power Engineering Inst., 1995, pp. 97-101.
- [12]. A.A. Kitaytsev, M.Y. Koledintseva, A.A. Shinkov "Filtering of unwanted microwave radiation by means of composite gyromagnetic thick films". Proc. 14th Int. Wroclaw Symp. And Exhibition on Electromagnetic Compatibility EMC'98, June 23-25, 1998, Wroclaw, Poland, p. 385-387.
- [13]. A.A. Kitaytsev, M.Y. Koledintseva, V.A. Konkin, V.P. Cheparin, A.A. Shinkov "Application of

composite gyromagnetic materials for absorbing radiation produced by microwave oven". Proc. Int. Symp. on Electromagnetic Compatibility EMC'99 Tokyo, May 17-21, 1999, paper 19P204, pp. 405-407.

BIOGRAPHICAL NOTES

Leonard K. Mikhailovsky, Dr.Sc., Prof. was born in 1927. M.Sc. – 1950, Ph.D. – 1956, D.Sc. – 1985 (Moscow Power Engineering Institute). In 1962 he organized the Ferrite Laboratory of Moscow Power Engineering Institute. Since 1969 he was among organizers of Int. Conf. on Microwave Ferrites. In 1967 he organized National Bureau on Gyromagnetic Electronics and Electrodynamics. He is a founder of a new scientific branch - Spin Electronics and Non-phase Electrodynamics (Gyrovector Electrodynamics), and since 1992 he is a Chairman of annual Int. Conferences with the same title.

Alexander A. Kitaytsev, Ph.D., Head of the Lab. Was born in 1941. M.Sc. – 1965, Ph.D. – 1972. (Moscow Power Engineering Institute). Works in the Ferrite Lab of MPEI (TU) since 1962. Since 1984 he is the Head of the Ferrite Lab of MPEI (TU). Scientific interests - theoretical analysis and experimental research of interaction of gyromagnetic media with microwave radiation, elaboration of equipment for measuring power parameters of microwave signals and noise.

Marina Y. Koledintseva, Ph.D., Senior researcher, Associate Prof., was born in 1961. M.Sc. (honors) – 1984, Ph.D.-1996 (Moscow Power Engineering Institute). Works in the Ferrite Lab of MPEI (TU) since 1979. Since 1996 – Member of IEEE (AP, EMC). Scientific interests - theoretical analysis and experimental research of interaction of gyromagnetic media with microwave radiation. Development of methods of the gyromagnetic composite media characteristics calculation and measuring.

Vladimir P. Cheparin, Ph.D., Doctor of Electrical Engineering of Russian Academy of Electrotechnical Sciences, Professor, Deputy Head of the Chair of Electrotechnical Materials of MPEI (TU). Was born in 1940. M.Sc. – 1964, Ph.D. – 1971, Doctor of EE – 1994 (Moscow Power Engineering Institute). Scientific interests - research and design of formulae and technology of the doped hexagonal ferrites manufacturing with various inner magnetic crystallographic field values for operating in the range 2-200 GHz.

Transmission link radiation And common current generation by 15 pin D connector

P. Nadeau, A. Reineix, , B. Jecko.

IRCOM

Electromagnetism Department

UMR au CNRS n°6615

123, Rue Albert Thomas

87 060 Limoges Cedex - France

Phone : (33)05.55.45.73.56 Fax : (33)05.55.45.75.15 Email :nadeau@alpha1.unilim.fr

Abstract : Norms impose the limitation of electromagnetic radiation of numerical links between equipment, in the frequency range 100 MHz – 1GHz. This radiation is caused mainly by common mode current. This paper describes with the Finite Difference in Time Domain (FDTD) method, the asymmetry of the transmission line created by different termination for 15 pin D connector. This asymmetry has a direct impact in the level of transmission link radiation.

1. INTRODUCTION

In the following scheme (fig.1) 15 pin D connector realises the mechanical link between cables and boxes, and assumes the propagation of electric signals. The cable-connector interface modifies the propagation mode. We will present the effects of this additional element on the parasitic radiation. In our simulations, the transmission line is symmetrical, so only differential mode current flows out the line. The aim of this simulations is to determine if the connector can be able to disturb this symmetry and to generate a common mode radiation.

Therefore, different terminations for 15 pin D connector will be evaluated. The use of pins 6 and 7 of the connector (fig. 4) will be compared to the use of pins 8 and 9. This evaluation will be done in two cases 1)all others opened and 2) all others shorted to the box.

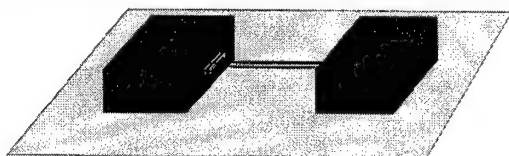


fig. 1 : Numerical link between two boxes with 15 pin D connector

2. THEORETICAL SIGNIFICANT PARAMETER

2.1. Total radiated power

Before knowing the favoured parasitic radiation directions of the system, we will interest ourselves in the total radiated power in all the space normalised by the accepted power line. This calculation uses a Huygen's surface around the studied problem.

$$\eta = (P_{rad})/(P_{acc.}) = \left(\frac{1}{2} \iint \vec{E} \wedge \vec{H} \cdot d\vec{S} \right) / \left(\frac{1}{2} \Re \{ \vec{V} \cdot \vec{I} \} \right) \quad (1)$$

2.2. Differential and common mode currents

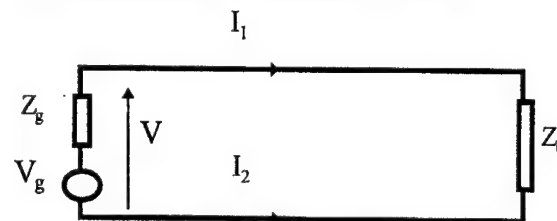


fig.2 : Transmission line.

On a transmission line, the common and the differential mode currents are computed with two transient contributions. The following simple transmission line shows this calculation :

$$I_c = \frac{I_1 + I_2}{2} \quad (2)$$

$$I_d = \frac{I_1 - I_2}{2} \quad (3)$$

The voltage supply uses a gaussian impulsions with an amplitude voltage of 1Volt and an 0.5ns rise time to cover the frequency range (100MHz – 1GHz). The line

length is 30 cm, adapted on his characteristic impedance.

3. SIMPLE TRANSMISSION LINE RADIATION AND PROPAGATION MODES

C.R.Paul works [1] have showed the unequal contribution of the common and differential mode on the parasitic radiation. First we consider a simple transmission line (fig. 2) without connectors and boxes.

The radiated power (fig. 3) of this symmetry line shows only the differential mode effect. The level of the radiated power is characterised by the level of the differential-mode current and the distance between the wire of the transmission line. In our case the wires are separated by 1.5cm.

A way to add common mode effect on this simple structure is to cut down symmetry with a discrepancy of the supply position. In this case the common mode current is about $10\mu\text{A}$ whereas the differential mode current is round 1mA .

The resulting radiated power is the sum of the differential and the common effect. The fig. 3 compares the maximum of the radiated power with the magnitude of the common mode current in frequency domain. The same resonance frequencies are observed. So the common mode directly influences the level and the resonance of the radiated power. The power peak are depending on the resonance frequencies of the lines.

So the prediction of the radiated emission has to take into account the presence of the common-mode current otherwise radiated emission will be severely under-predicted.

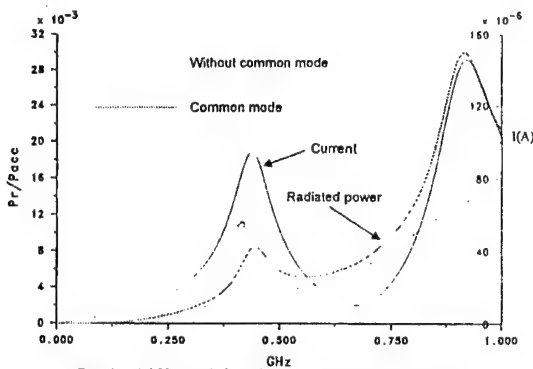


fig. 3 : Differential and common mode influence

4. TRANSMISSION LINK RADIATION AND 15 PIN D CONNECTOR MODELLING

The D connector has gained a tremendous popularity in most of industrial applications. For this reason, its performances will be evaluated. Two types of connectors will be modelled 1) shielded and 2) unshielded.

4.1. Characteristics of the global structure

4.1.1 Dimensions of the global structure

The geometry of the problem is presented in fig.1 : it consists of a 30 cm transmission line (two parallel wires), two boxes and D connectors.

The main characteristics are :

Box dimensions 4 cm*4cm*4cm

Line, generator and charge impedance 530Ω .

The load and generator resistance of this structure are chosen to provide a matched load.

4.1.2. Characteristics of 15 pin D connector

The fig. 4 presents the classical 15 pin D connector geometry.

In this part, shielded and unshielded connectors and termination influences will now be studied in the different configurations described in the introduction .

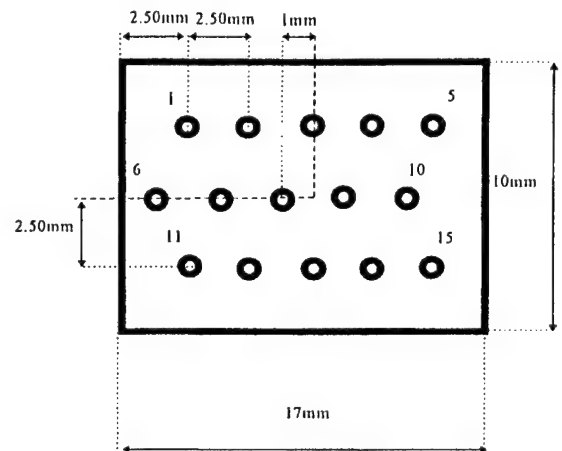


fig.4 Geometry of 15 pin D connector

4.2. Opened non used pins

4.2.1. Shielded 15 pin D connector

Common-mode current generation is caused by ground-noise and symmetries. In our simulations ground-noise will not be considered, so the transmission line has no connection with the metallic boxes. Asymmetry in 15 pin D connector may be caused by his shield and the used of 6 and 7 pins (fig.4) for the transmission line.

We compare on fig.5 this case with the following one which is : The transmission line is positioned in the middle of the connector pins 8 and 9 (fig.4). A common-mode current of $8\mu\text{A}$ appears, if the line connections are placed on the border part of the connectors (transmission line pins position 6 and 7 on fig. 4). On this other case the radiated power is only due to differential-mode current.

So the radiated power of a transmission link between equipment will be directly influenced by the choice of the terminations of the connector.

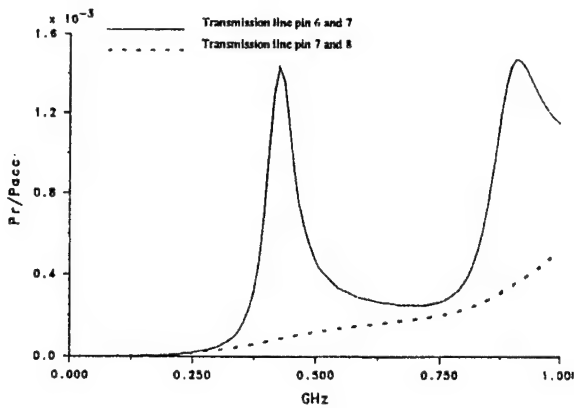


fig. 5

4.2.2 Unshielded connector

In the last paragraph, it has been showed that the presence of a shielded connector can be at the origin of a common-mode current. In the case of unshielded connector, asymmetry may be caused by the metallic border of the boxes.

The fig.6 compares the radiated power when the transmission line uses 6 and 7 pins (fig.4) but with a shielded and unshielded connector. This figure shows that the level of the radiated power is more influenced by the presence of the shielded connector than by the border part of the boxes.

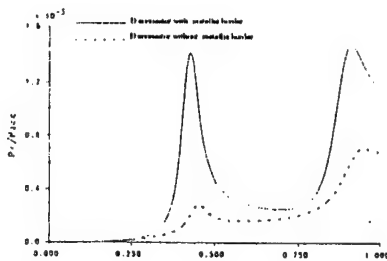


fig.6

4.3 Non used pins shorted to the electric ground

In most cases, industrial methods chose that all the non used pins are shorted to the electric ground of the box or the PCB border. It was a real important and difficult operation because in all our simulations this act increases the common mode current. The fig. 7 precises the metallic ground connections in two different cases (case 1 and case 2). Influences of this connections will be only evaluated when the connectors generate common-mode current (Use of pins 6 and 7 for the transmission line).

4.3.1. Shielded connector

On case 1 and 2 the common mode current is about $28\mu\text{A}$, whereas it is round $8\mu\text{A}$ when the pins are opened. The additional common mode increases significantly the radiated power in different thin frequency bands (fig. 8). The common mode currents have exactly the same frequency dependence. But the total radiated power presents a resonant frequency which does not depend of the line length. The common-mode current interacts with the ground-wires and therefore has current induced in it. The non used pins of the connector and the ground wires are equivalent to a R.L.C circuit. This circuit is described on fig. 9.

So the current induced has a resonant frequency which depends of the physical characteristics of the wires and pins (Inductance and mutual capacitance between pins and shield of the connector).

When the line carries only differential-mode current, this phenomena has not been observed.

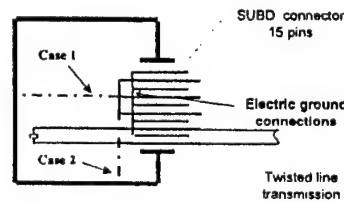


fig. 7

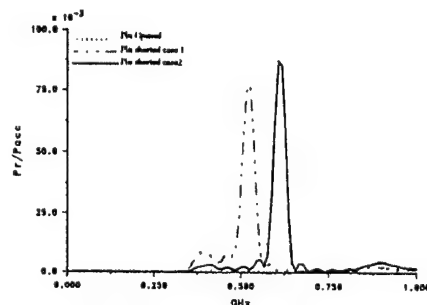


fig. 8 Total Radiated Power

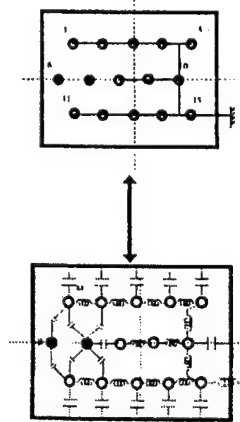


fig. 9 Equivalent circuit

4.3.2 Unshielded connector

In this case, the mutual capacitance are reduced so the resonant frequency increases. It is confirmed on the fig.10 which compares the total radiated power with shielded and unshielded connectors in case 1 (fig.7).

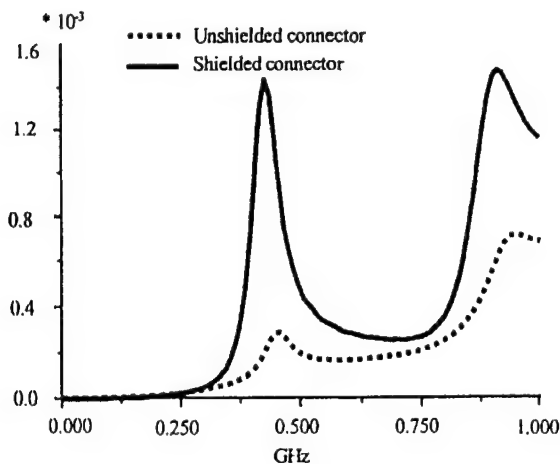


fig.10

4.3.3 Remarks

This last numerical results must be confirmed by experiment. The resonant frequency is depending of the radius of the pins and wires. In our simulations, they are

modelled by Holland formalism [2] which limits their radius at 1/10 of elementary finite-difference cells. So the resonant frequency will be certainly translated outside the frequency range of 100MHz-1Gz.

5..CONCLUSION

The radiation level of a transmission line between equipment is depending of the termination of the connector. The 15 pin D connector can be able to generate an asymmetry which is at the origin of this current. This asymmetry has a direct impact on the common-mode current amplitude. But we can limit this amplitude if an unshielded connector is associated with an unshielded cable.

Concerning the resonant peak on the radiated power when the non used pins are shorted to the electric ground of the box, the numerical results must be confirmed by the experiment.

6. REFERENCES

- 3.[1] C.R PAUL , 'A comparison of the contributions of common-mode and differential currents in radiated emission', *IEEE Transactions on Electromagnetic Compatibility*, Vol. 31,No.2 May 1989
- 4.[2] R. HOLLAND, L. SIMPSON , 'Finite Difference Analysis of EMP Coupling to the thin struts and wires'. *IEEE Transactions on Electromagnetic Compatibility*. Vol. EMC 23,No.2 May 1981

Pascal Nadeau was born in Libourne, France, in 1969. He received the Diplôme d'Etude Supérieure Spécialisée in Micro-Electronic. He is presently PhD student in Electronic from the University of Limoges, Limoges, France, in the laboratory of Electromagnetism of the Institut de Recherche en Communications Optiques et Microondes (IRCOM). He is now engaged on electromagnetic compatibility on unshielded connectors.

Alain Reineix was born in Neuvis Entier, France, in 1961. He received the doctorat in Electronic from the University of Limoges, France, in 1986. He currently CNRS researcher at the Institut de Recherche en Communications Optiques et Micro-ondes (IRCOM) of the university of Limoges. His main interest domains concern the development of time domain numerical tools for solving electromagnetic problems, particularly the FDTD approach. The domain of application are the antennas, the Electromagnetic Compatibility, the radar Cross Section.

Bernard Jecko was born in Trelissac, France, in 1944. He received the Doctorat Third Cycle and the Doctorat es Sciences degrees from the University of Limoges, Limoges, France, in 1971 and 1972, respectively. He is currently a Professor at the University of Limoges and leads the Electromagnetic Team of the Institut de Recherche en Communications Optiques et Microondes (IRCOM). His research interest is in the area of electromagnetic wave diffraction theory, particularly in the time domain.

NEW GENERATION OF ABSORBING MATERIALS

Andrzej A. Vogt, Hubert A. Kołodziej
University of Wrocław, Faculty of Chemistry
50-383 Wrocław, Poland
E-mail: HAK@wchuwr.chem.uni.wroc.pl

Andrzej E. Sowa
Wrocław University of Technology
Institute of Telecommunication and
Acoustics
50-370 Wrocław, Poland

1. ABSTRACT

A group of new low reflectivity absorbing electromagnetic energy materials has been developed at the University of Wrocław, Department of Chemistry. These are composite materials showing synergetic effect for magnetic properties. The complex permeability of these materials performs in a broad band of absorption and dispersion starting as low as from 1MHz. The physical properties of these materials are revolutionary in comparison to ferrites. These materials can be hard, elastic and can be plastic as well. The materials can serve even as a gap filler (for hard tiles). The consistency of the material does not affect its magnetic properties. The materials exhibit good temperature and time stability. The manufacturing cost of these materials is reasonable.

At present, one of the materials is being used in the cable industry for coating specialist EMC cables. The most labour intensive and time the new materials. consuming work is now devoted to the development of the other practical use of new materials.

2. INTRODUCTION

Electromagnetic energy absorbers are of great importance for EMC. Absorbers are necessary to solve many EMC problems. Absorbers are necessary to cover reflecting surfaces where the presence of electromagnetic radiation is undesired. Amongst others places, it is used to line the walls of electromagnetic test chambers to simulate conditions of free space or open area test sites and even to cover the outside walls of buildings. On the other hand, absorbers can be used in EMC cables to break the unwanted RF currents flowing in a cable or in its

screen and it is used in the absorbing elements of filters. The area is still growing where the absorber cannot be substituted by another measure to limit the unwanted presence of RF energy. EMC absorbers have been around for more than 60 years [1,2].

For more than 30 years the majority of low reflectivity broadband absorbers have been made from two layers of materials: the first layer is polyurethane foam loaded with graphite, the second layer is made of sintered ferrite. The absorbers are especially shaped to minimise their reflectivity. The foam absorbers are shaped into pyramids or wedges - which guarantees low reflectivity even for incidence angles away from the normal. The thickness of the absorber (the height of pyramids) lining an anechoic chamber must be at least $\lambda/4$ for EMC applications. This is equivalent to approximately 2.5m. at 30MHz. The absorbers of the first layer are broadband absorbers - their effectiveness increases proportionately to their height. For higher frequencies, foam absorbers can be made from flat foam sheets with tapered carbon loading.

The ferrite absorbers can be in the form of solid tiles or grids. The latter increases the useful bandwidth. The best reflectivity occurs at normal incidence angles and worsens significantly for angles away from the norm. The thickness of the solid ferrite absorber lining an anechoic chamber is usually between 6 and 7mm. In the case of the grid - about 20mm.

The reflectivity level offered by the solid ferrite absorber is usually low enough for emission and immunity measurements according to the applicable EMC standards in the range 30 to about 600MHz [2]. The range above 600MHz (to 1000MHz) calls for special measures - multilayer designs. These hybrids can be of 2 or more layers. The most popular hybrid is made of a ferrite layer at the bottom (shielding side) and a pyramidal foam absorber at the top. To fulfil emission

site requirements, the hybrid height should be between about 0.5m to 1 m for the higher performance absorber. The performance of the above mentioned hybrid can be further improved by additional layers of dielectric material (usually plywood) placed between metal (shield) and ferrite layer or between ferrite layer and foam absorber.

Another solution is a hollow absorber. At the bottom, layers of ferrite and dielectric are placed and the top is made of hard foam absorber plates. The required total height for the high performance absorber is about 1m. This solution containing a foam absorber at the top, results in a very high bandwidth.

Low reflectivity in a more restricted bandwidth (but satisfying the EMC standards requirements) can be obtained with a multilayer design consisting of ferrite, dielectric and e.g. ferrite rubber layer. A ferrite grid can be another interesting alternative.

Another area of the use of foam and ferrite absorbers is the reduction of cavity Qs in shielded enclosures (e.g. computer housings), suppression of unwanted RF surface currents flowing in any shape metallic surfaces and RF currents flowing in cables or their screens (coaxial cables). These absorbers can reduce reflectivity as well. Flat foam sheet can be loaded with carbon or magnetic material (eg. powdered ferrite or carbonyl iron). Practical reasons call for the use of absorbers made of silicone rubber, polyurethane rubber, elastomer or other elastic polymer base and a ferrite powder as a loader. These absorbers can be in a form of flat thin sheets, sleeves or coats as well as other shapes. Absorbing paints can also be included. Ferrite loader is the best, but it must be emphasised that the ferrite powder absorbing properties are very poor in comparison to solid sintered ferrites.

Summing up:

Foam absorbers are very broadband but they are very thick at lower frequencies.

Ferrite absorbers are characterised by their smaller bandwidth and their thinness. They are rigid, extremely hard and very sensitive to any gaps existing between adjacent tiles.

Elastic absorbers containing ferrite powders are characterised by very poor parameters in comparison to the solid sintered ferrite, even for the greatest saturation of ferrite (e.g. more than 90% wt.).

The purpose of this paper is to present a group of new absorptive materials with unique properties, developed at the University of Wroclaw, Faculty of

Chemistry which will open new horizons for EMC absorbers designers.

3. EXPERIMENTS AND RESULTS

3.1 Synthesis and electromagnetic results

We have synthesised several broad band absorptive materials with high and low DC electric conductivity. The synthesis of the main component was performed by means of the wet method at room temperature. All of these materials are multi-composite systems and can be obtained in several forms (consistency) starting from hard solid state and ending at putty like materials. In all cases we observed a synergetic effect especially for complex magnetic permeability where the value of each component itself was several times lower than that of the final product.

Fig.1 shows the complex electric permittivity for one of our materials with very high DC conductivity and very substantial contribution of electric conductivity up to 30

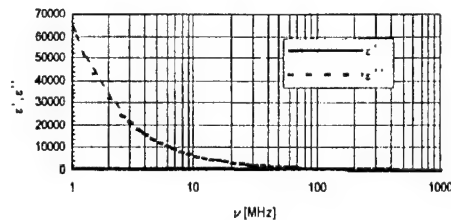


Fig.1 Real and imaginary part of electric permittivity of CEF material.

The complex magnetic permeability is shown in fig.2. The imaginary part (μ'') is almost constant in the range of 1 MHz to 100 MHz then gradually goes down to the value 2.5 at 1000MHz.

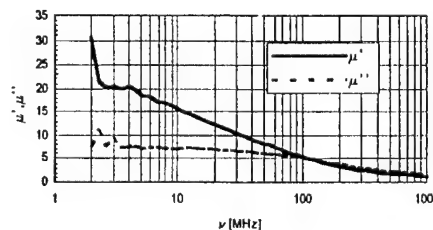


Fig.2 The complex magnetic permeability vs. frequency for CEF material.

Knowing that $\gamma = \alpha + j\beta = j2\pi/\lambda(\mu\epsilon^*)^{1/2}$ one can calculate α being the relative attenuation of the material under test.

The values of the relative attenuation vs. frequency for CFE material are presented in Fig.3

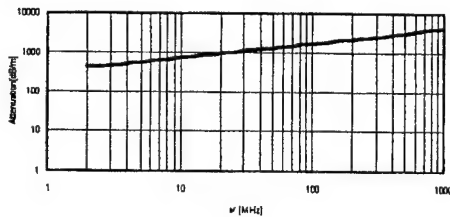


Fig.3 Relative attenuation for CEF material

Another group of our materials are low DC conductive materials with the specific resistance of about $5000 \Omega \cdot m$, which appears to be of great interest to EMC cables manufacturers. The most typical for this group developed in our laboratory is a material named KWE. The electromagnetic parameters as a function of frequency are presented in figs.4, 5 and 6.

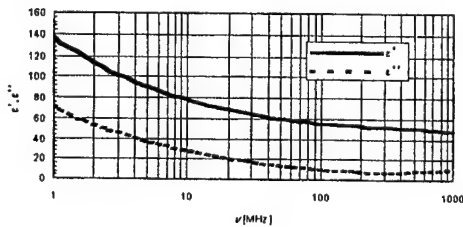


Fig.4 The complex electric permittivity vs. frequency for KWE.

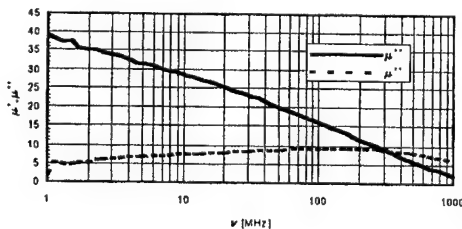


Fig.5 The complex magnetic permeability vs. frequency for KWE.

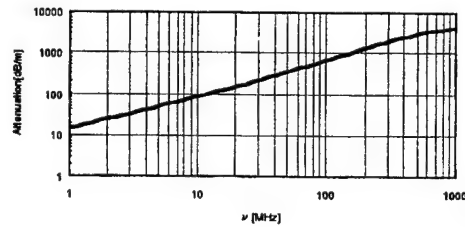


Fig.6 Relative attenuation for KWE material

All the materials of the type KWE are easily extrudable at certain temperatures and pressures. The MFI (melt flow index) is suitable for cable production.

The next group of absorbing materials developed in our laboratory is REC. This group of materials is nonextrudable, but can be formed into plates, rods, pellets and any other shapes, or even paint. The consistency of this material can be varied from hard solid state to very soft putty. The most typical representative of these materials is REC-65.

The electromagnetic parameters vs. frequency are shown in figs.7, 8 and 9.

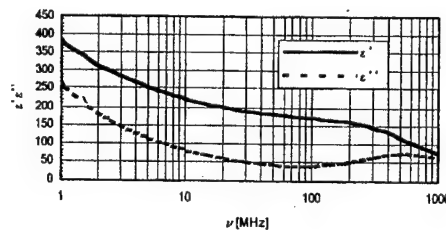


Fig.7 Complex electric permittivity vs. frequency for REC-65 material.

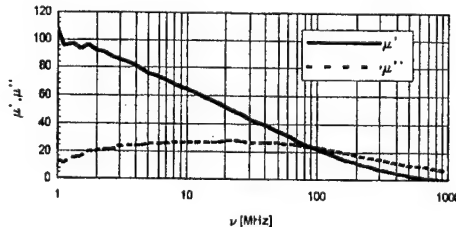


Fig.8 The complex magnetic permeability vs. frequency for REC-65 material.

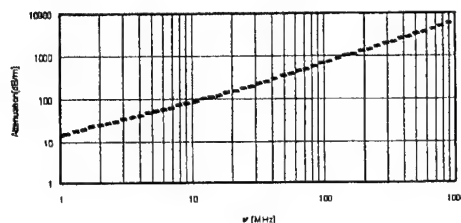


Fig.9 Relative attenuation for REC-65 material.

3.2 Measurement methods

The electric permittivity measurements were performed by means of the lumped-capacitance method [4,5] using a HP-4191A RF impedance analyser. The complex input impedance of the capacitor is described by the following equation:

$$Z(r) = \frac{d\omega}{i2\pi} \frac{J_0(k\sqrt{\epsilon^*}r)}{k\sqrt{\epsilon^*}rJ_1(k\sqrt{\epsilon^*}r)}$$

where: r is the radius the cylindrical sample, $k = 1/\lambda$, d is the thickness of the sample and $\epsilon^* = \epsilon - j\epsilon''$.

The complex magnetic permeability measurements were performed by means of the inductance method. The inductance method is derived from the permeability of the self-inductance and resistance of magnetic materials. First, the inductance value L of the sample holder is measured without the sample. Then, the sample is put into the sample holder and measured for the inductance value again. Relative permeability is calculated from the following relationship [6]:

$$\mu' = \frac{L_s - L_0}{\mu_0} \frac{2\pi}{h \ln\left(\frac{a}{b}\right)}$$

where L_s and L_0 are the inductance of the sample holder with and without sample, respectively, μ_0 is the magnetic permeability of free space, h , a and b are the dimensions of the toroidal - like sample. All the measurements of inductance and dissipation factor ($\tan\delta_\mu$) were performed using the HP-4191A RF impedance analyser. The average accuracy of inductance measurements was $\pm 3\%$ and for $\tan\delta_\mu$ was $\pm 5\%$.

4. CONCLUSION.

The properties of the materials presented allow us to consider them as unique new proposals for the designers of EMC absorbers.

They can replace classical absorptive materials or enhance their performance in complex absorbing structures.

The mechanical properties, such as high plasticity, elasticity, adhesivity and extrudibility (if required), give a very broad field of applications. The additional advantage of these materials is that their specific weight is almost half that of solid ferrites.

These materials can be easily formed into plates, pellets, rods and other much more complex shapes.

They can also be manufactured as paints, putties, fillers and magnetic fluids.

It appears that these materials will open new perspectives for EMC absorbing facilities and EMC cables manufacturers.

5. REFERENCES

- 5.1 Emerson W.H., "Electromagnetic wave absorbers and anechoic chambers through the years", IEEE Trans. on Antennas and Propagation, vol. AP-21, No.4, July 1973, pp.484-490
- 5.2 Holloway Ch.L., DeLyser R.R., German R.F., McKenna P., Kanda M., "Comparison of electromagnetic absorber used in anechoic and semi-anechoic chambers for emission and immunity testing of digital devices", IEEE Trans. on EMC, vol.39, No.1, Feb. 1997, pp.33-47
- 5.2 Freundlich, P., Kolodziej, H. A., Narewski, E. An algorithm to be used in lumped capacitance method for measurements of complex electric permittivity in systems with large $\tan\delta$ from 100MHz to 18 GHz. (English) J.Phys.E.14 1045 1981
- 5.3 Kolodziej, H. A., Pajdowska, M., Sobczyk, L. Lumped-capacitance method Applied to the measurements of complex permittivity measurements in polar liquids from 100 MHz to 3 GHz, (English). J.Phys.E.11 752 1979
- 5.4 The measuring complex permittivity and permeability at RF and microwave frequencies. Symposium Paper, HP Lit No 5952- 2385(D), Sept 89

ELECTROMAGNETIC RADIATION OF MULTIPAIR BALANCED CABLES WITH DOUBLE TWISTED CONDUCTORS

Liudmyla Dikmarova, Vitalij Nichoga

Karpenko Physico-Mechanical Institute of National Academy of Sciences of Ukraine, Ukraine, 79601, Lviv,
5 Naukova St., tel.: +380 (322) 65-42-92, fax: +380 (322) 64-94-27, e-mail: nich@ah.ipm.lviv.ua

When determining parasite radiation and levels of interference, created by conductive communication lines, it is necessary to know allocation and intensity of their exterior electromagnetic fields. For this case on the basis of a solution of the electrodynamics problem the weak radiation of a multipair cable is considered and some effects, which are not taken into account in the theory of signal transmission by communication lines, are studied.

1. INTRODUCTION

In contradistinction to known solutions for a two-wire line twisted in group and in winding [1] our physical and mathematical model for determining external field takes into account oscillatory character of co-ordinate of point of a helical line, formed by pair of multicore cable, each pair of which has pitches of strand in group h and in winding H . In the majority of modern cables a group consists of two wires, while a winding can consist of two and more groups.

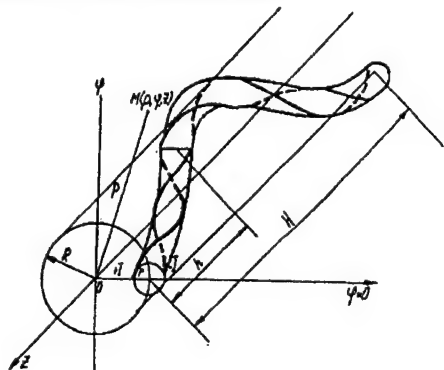


Fig. 1. Model of a line with double twisted wires

Taking into account that in the majority of multipair balanced cables low enough frequencies are used the delivered problem is solved in a quasistatic approximation with the conjecture, that wires are rather thin. Fields components of a cable with double strand of conductors are found with the help of a vector potential in a cylindrical co-ordinate system (ρ, φ, z) , z axis of which coincides an axis of a cable.

2. MATHEMATICAL MODEL OF CABLE FIELD

As a result of a solution of the electrodynamics problems the algorithms for determination of separate components of electrical and magnetic fields of a cable are obtained with feeding currents $+I$ and $-I$ in a separate pair. Thus it is shown, that the external field of each pair of a multipair cable with double strand of conductors has 6 components: 3 magnetic H_φ, H_ρ, H_z and 3 electrical E_φ, E_ρ, E_z . Thus expressions for field components are rather complicated [1]. In engineering practice the approximated formulas can be used, which are correct when $R \ll H$ and $r \ll h$:

$$H_\rho = 2I \sum_{n=-\infty}^{\infty} \sum_{k=\pm 1, \pm 3, \dots} \left[\frac{nK_n(g\rho)a_{nk}}{2\pi\rho} + K_{n+1}(g\rho)b_{nk}|g| \sin F \right],$$

$$H_\varphi = 2I \sum_{n=-\infty}^{\infty} \sum_{k=\pm 1, \pm 3, \dots} \left[K_{n+1}(g\rho)b_{nk}|g| - \frac{K'_n(g\rho)|g|a_{nk}}{2\pi} \right] \cos F,$$

$$H_z = 2I \sum_{n=-\infty}^{\infty} \sum_{k=\pm 1, \pm 3, \dots} \left[\frac{n+1}{\rho} K_{n+1}(g\rho) + K'_{n+1}(g\rho)b_{nk}|g| \right] \cos F,$$

$$E_\rho = -2j\omega\mu_0 I \sum_{n=-\infty}^{\infty} \sum_{k=\pm 1, \pm 3, \dots} K_{n+1}(g\rho)b_{nk} \sin F,$$

$$E_\varphi = -2j\omega\mu_0 I \sum_{n=-\infty}^{\infty} \sum_{k=\pm 1, \pm 3, \dots} K_{n+1}(g\rho)b_{nk} \cos F,$$

$$E_z = -\frac{j\omega\mu_0 I}{\pi} \sum_{n=-\infty}^{\infty} \sum_{k=\pm 1, \pm 3, \dots} K_n(g\rho)a_{nk} \cos F,$$

where $a_{nk} = I_{n+k}(gR) \cdot I_k(g\rho)$,

$$b_{nk} = \frac{R}{H} I_{n+k+1}(gR) \cdot I_k(g\rho) + \frac{r}{h} I_{nk}(gR) \cdot I_{k-1}(g\rho),$$

$$g = \frac{2\pi m}{H} + 2\pi k \left(\frac{1}{H} - \frac{1}{h} \right), \quad F = -n\varphi + gZ - k\delta_0.$$

the pitch of strand in group $h=22$ cm and the pitch of winding $H=44$ cm is shown in Fig. 4.

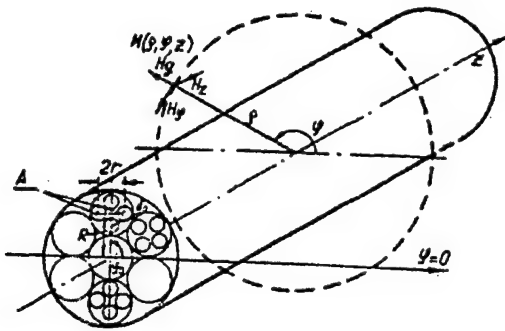


Fig. 4. Attitude of measuring point $M(\rho, \varphi, z)$ near a cable

Measurements of components H_φ , H_ρ , H_z has been carried out with the help of "point" inductive sensors assembled in the special box, located on the measuring installation platform. The scheme of measurements is shown in Fig. 5.

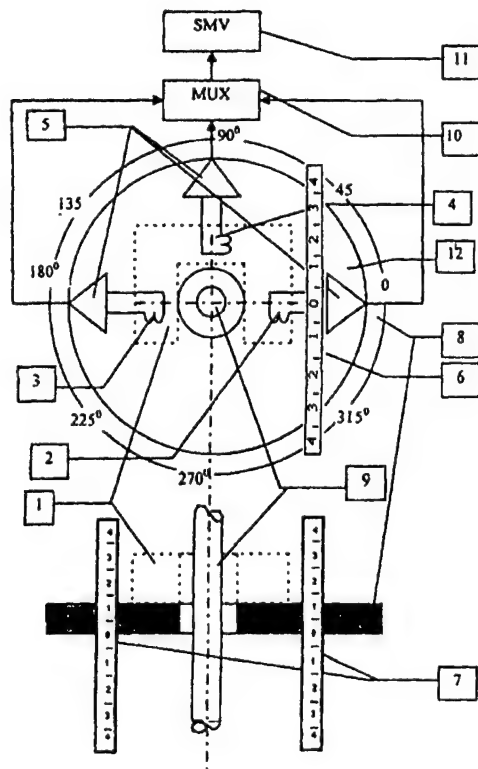


Fig. 5. Instrument installation scheme: 1 - box with "point" sensors; 2, 3, 4 - "point" induction sensors; 5 - preamplifiers of sensors; 6 - measuring ruler for component H_ρ ; 7 - measuring ruler for component H_z ; 8 - measuring limb for component H_φ ; 9 - investigated cable; 10 - sensor commutator; 11 - selective microvoltmeter; 12 - movable measuring table.

The installation allows to displace sensors on azimuth (H_φ), on radius (H_ρ), and length of a cable (H_z). Each of three sensors (2, 3, 4 in Fig. 5) is located in the special mobile box (1) on identical distances from an axis of a cable (9) and has different spatial orientation. "Point" sensors consist of diminutive induction coils with diameters that equal 5 mm, which are connected to the pre-amplifiers (5). The output signal of each amplifiers goes to the commutator of signals MUX (10) and then to the selective microvoltmeter SMV (11). The box (1) with sensors has a possibility to be rotated on movable measuring table (12) of the installation. Thus its position is fixed with the help of measuring ruler (6). The position of sensors on azimuth is accomplished by rotation of mobile measuring table (12) around the measuring limb (8) that surrounds a cable (9). Displacement of the sensors along a cable is fixed by measuring ruler (7).

5. RESULTS OF MEASUREMENTS

The experimental measurements have shown, that theoretical calculations give the overstated level of magnetic field components, especially immediately near a cable, where results can differ on the order and more.

It was revealed that a medium, in which a cable is located, does not influence practically on magnetic field components values on distance up to 0.5 m. It completely confirms conclusions, which were made in [3, 4] by examination of medium effect on field of a two-wire line in immediate proximity from it.

The spatial pictures of external magnetic field near the cable with only one pair connected to the signal source are shown in Fig. 6 and Fig. 7.

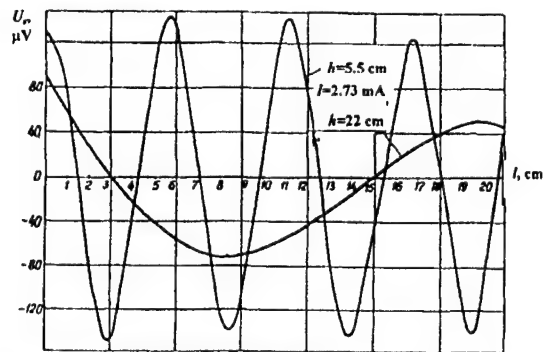


Fig. 6. Variation of output signal level of the "point" induction sensor when moving along surfaces of the cables with $h=5.5$ cm and $h=22$ cm

In Fig. 6 variation of the output signal of the "point" magnetic sensor, which is oriented for registration of magnetic field component H_φ and moves along the one-quadded cable with $h=5.5$ cm and the seven-quadded cable with $h=22$ cm are presented.

In Fig. 7 the experimentally obtained dependencies, (curves 1, 2, 3), which characterise variations of components H_φ , H_ρ , H_z upon radial distance from cable axis, are given. These measurements were carried out at fre-

Here δ_0 - initial angle of radius r of rotation around the line $\varphi=0$ (when $z=0$) (see Fig. 1), I_m, K_m, K'_m - modified Bessel functions of m order and their derivatives.

Character of field distribution around a cable is rather complicated and essentially depends on distance from an observation point to a cable axis.

3. CALCULATION RESULTS

The calculating algorithms for field components was obtained as series and are rather complicated and consequently those terms of series are used only, which ones give greater contribution to field magnitude.

As numerical analysis showed, bigger terms are that in which values of g are lower. In this case it is sufficient to consider that members only, for which $|n|+|k|\leq 5$.

In Fig. 2 the results of calculations of the polar diagrams for components of the magnetic field of the two-wire line with double twisting of wires ($R=5$ mm, $r=2$ mm, $H=200$ mm, $h=100$ mm, $I=1$ A, $\delta_0=0$, $f=10^5$ Hz near the cable for $\rho=0.03$ m (Fig. 2a) and for considerable distance $\rho=0.5$ m (Fig. 2b).

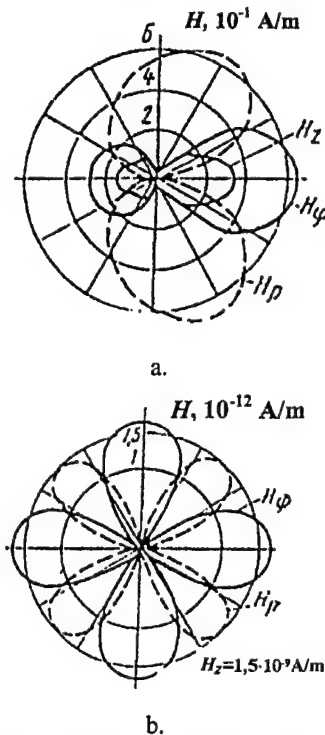


Fig. 2. The polar diagrams of magnetic field components

As it is visible from given data near to a cable the components H_φ and H_ρ predominate and the picture of a field is similar to structure of a field of a two-wire not twisted cable. When distance from a cable increases, component H_z becomes greater (Fig. 2b) than H_φ and H_ρ or has the same order, and the polar diagram becomes more complicated. The magnetic field near cable attenuates approximately as ρ^{-5} . When distance from cable increases the field attenuates weaker.

Periodical variation along a cable axis is a characteristic feature of this field. Thus the period of variation of field components near a cable is equal to a pitch h of strand of conductors in group, on large distances the periodicity has more complicated character and depends on a relation h/H .

The character of variation of magnetic field components along z axis of a cable with the same parameters of pitches of strand in group h and in winding H is presented in Fig. 3. As calculations have shown, near to a cable ($\rho=0.03$ m, Fig. 3a) the components of a field change the sign with periodicity, which equals $0.5 h$ (≈ 50 mm), and on large distances ($\rho=0.5$ m, Fig. 3b) the periodicity has more complicated character and depends on a relation h/H . In this case, when h and H are selected, this periodicity equals h , that is $H/2=100$ mm.

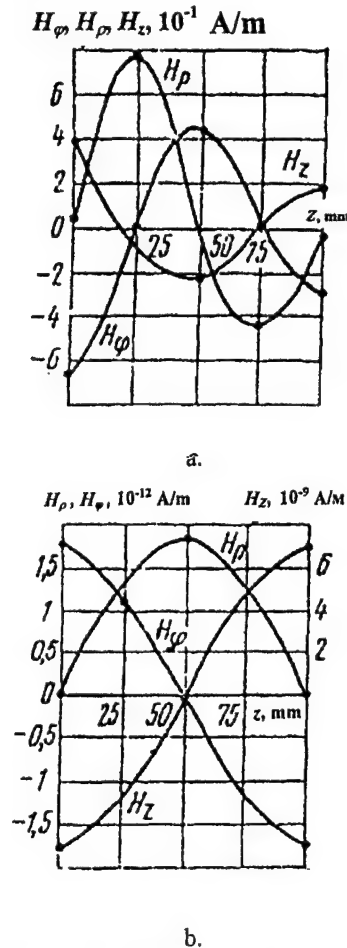


Fig. 3. Periodicity of magnetic field along the cable

4. EXPERIMENTAL INVESTIGATIONS

Experimental investigation of structure and character of magnetic field components of a two-wire cable with double twisting of wires has been carried out on cuts of cables of different types with feeding a testing signal in one of pairs. Attitude of measuring point $M(\rho, \varphi, z)$ concerning the pair A of the multipair cable with

quencies 1 and 30 kHz by the "point" sensor when current in a cable pair $I = 1$ A. On both frequencies the levels of measured signals were identical in error limits of experiment. In the same Fig. the calculated dependency of component H_φ (curve 6) for the same cable is shown.

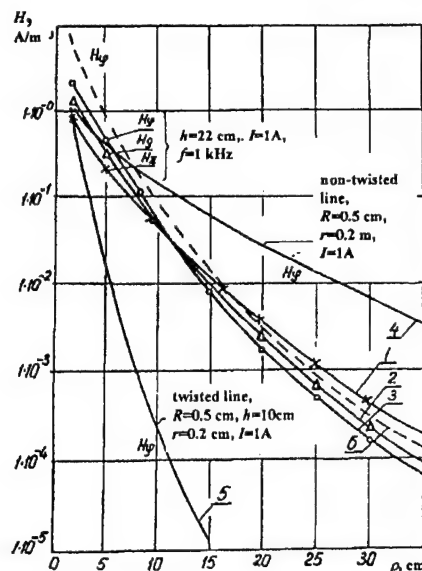


Fig. 7. Dependency of magnetic field components on distance ρ for twisted pair with $h=22$ cm (curves 1, 2, 3 - experiment, curve 6 - calculation)

For comparison of dependency of component H_φ on distance from non-twisted and twisted pairs ($h = 10$ cm) lines the extreme curves (Fig. 7, curves 4 and 5 correspondingly) are presented.

6. CONCLUSIONS

1. The components of an exterior magnetic field of two-wire pairs of a cable with double twisting of conductors depend on pitches of strand in group h and in winding H , and also on a relation r/ρ .

2. When distance from a cable increases the attenuation of field components augments with a diminution of a pitch of strand in group h .

3. Magnetic components of cable with double twisting of wires in the 1-30 kHz frequency band does not depend on frequency.

7. REFERENCES

- 7.1. I.I. Grodnev, I.L. Shulga, V.P. Chulyk, "Electromagnetic field of twisted cable circuit" (Russian), Telecommunication, No. 5, 1973, pp. 11-16.
- 7.2. L.P. Dikmarova, R.P. Pavliuk, "Electromagnetic field of twisted in group and in повив of a two-wire line" (Russian), Telecommunication, No. 3, 1984, pp. 48-51.
- 7.3. L.P. Dikmarova, P.B. Dub, V.O. Nichoga, "Investigation of parasite radiation of communication balanced cable" (Ukrainian), Proceedings of the Conference on legal, normative and metrological assurance of information protection systems in Ukraine, Kyiv, Ukraine, June 9-11, 1998, pp. 178-184.
- 7.4. V.O. Nichoga, P.B. Dub, "Magnetic field of aerial double wire lines with taking into account ground conductivity" (Ukrainian), Selection and Processing of Information, 1997, Vol. 11 (87), pp. 7-10.

BIOGRAPHICAL NOTES

Vitalij Nichoga is a leading scientific researcher and the manager of laboratory of primary measuring transducers of Karpenko Physico-Mechanical Institute of National Academy of Sciences of Ukraine. He graduated Radio Engineering Faculty of State University "Lvivska Politechnika" in 1960, obtained his Dr. eng. degree in 1966 and Dr. hab. degree in 1996. Investigation of electromagnetic fields and manufacturing of instrumentation for their measuring are his main scientific interests.

Liudmyla Dikmarova is a senior scientific researcher of Karpenko Physico-Mechanical Institute of National Academy of Sciences of Ukraine. She graduated Electric Engineering Faculty of State University "Lvivska Politechnika" in 1950, obtained his Dr. eng. degree in 1954 and Dr. hab. degree in 1989. Investigation of electromagnetic fields concerning geophysics, communication lines and testing of underground pipelines corrosion are her main scientific interest.

LINEAR FILTRATION OF RANDOM PROCESSES IN EMC MODELS: THE "PARTIAL REACTION" METHOD

Eduard G. Kourennyi*, Victor A. Petrosov**, Lidiya V. Chernikova*

*Chair of EPG, The Donetsk State Technical University, Artema St., 58, Donetsk 83000 Ukraine,
led@dgtu.donetsk.ua, lida@elf.dgtu.donetsk.ua

**Chair of EPP, The Priasovsk State Technical University, Republic alley, 7, Mariupol 87500, Ukraine

The task of determination of random process characteristics on linear filter output is considered and unified calculation method is suggested. It is based on representation of linear system in form of linear aperiodic links connected in parallel. This method allows to unify and simplify solution of linear filtering problem. The effectiveness of method is illustrated by EMC estimation of lighting facilities by dose of voltage oscillations.

1. PROBLEM DESCRIPTION

Linear filter is a component in the dynamic EMC model. The filter models the reaction $Y(t)$ of an object to the interference $X(t)$. The problem consists of the determination of probabilistic reaction characteristics from the known interference characteristics. Generally, this problem is solved within the bounds of correlation theory of random processes. For simplicity, let us limit the problem to finding the reaction dispersion $D_Y(t)$ from the influence of stationary random interference on an object. We assume that the correlation function $K_X(\tau)$ and the spectral density $S_X(\omega)$ do not depend on time t .

After feeding stationary interference to the object input, the transitional random process starts to proceed at the object output, and for $t \rightarrow \infty$ the steady state sets in. For the steady state, the reaction dispersion can be calculated by well-known formulas (e.g. [1]):

$$D_Y = \int_0^\infty \int_0^\infty g(v)g(u)K_X(v-u)dvdu = \int_0^\infty A^2(\omega)S_X(\omega)d\omega \quad (1)$$

where $g(t)$ is the weight or impulse function of the filter, $A(\omega)$ is the amplitude-frequency function of the filter, and v and u are variables of integration.

The usage of these formulas, however, entails cumbersome computations. First, the filter should be described by linear differential equation of the n^{th} degree (n is high), making the expression for $g(t)$ and $A(\omega)$ quite complicated. For example, for the flickermeter filter $n=4$ [2]. Second, it is necessary to fulfil double integration in each new task.

The purpose of the paper is to work out a unified calculation method that would allow solution of the problem by algebraic transformation without integration. There are two types of the problem: in the first type the unification is realized partially for every type of the interference correlation function; in the second type the total unification is realized.

2. PROBLEM OF THE FIRST TYPE

The idea of the suggested method is that the filter with complex structure is represented in the form of linear aperiodic links connected in parallel (Fig. 1).

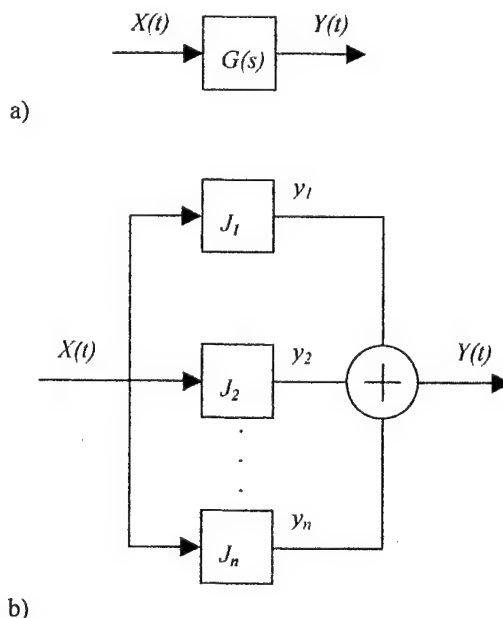


Figure 1.

The decision reaction equals to the sum of "partial" reactions $y(t)$ of each link to interference. Transfer coefficients a and time constants J of the links are determined from the condition that the transfer function $G(s)$ of the filter must be equal to the sum of transfer functions of the links.

The transfer function of the filter is equal to the ratio of two polynomials $f(s)$ and $z(s)$. This ratio is expressed by means of simple roots s_1, s_2, \dots, s_n of equation $z(s)=0$. This allows determination of characteristics of any link i :

$$a_i = \frac{f(s)}{T_n^n \cdot \prod_{l=1}^n (s-s_l)} \cdot (s-s_i) \Big|_{s=s_i} ; J_i = -\frac{1}{s_i}, \quad (2)$$

where T_n^n is the coefficient of s^n in the polynomial $z(s)$. For $s=s_i$, the value of a_i is not zero because the multiplier $(s-s_i)$ is cancelled by the same multiplier in denominator. The values of link parameters can be complex, however the imaginary quantities are absent in final expressions.

The same process $X(t)$ is fed to the inputs of links, thus the "partial" reactions are correlated variables. Therefore, in addition to "partial" dispersion D_y , it is necessary to take into account the intercorrelation moment k_{ir} . Intercorrelation moment between i and r "partial" reactions is calculated by formula

$$k_{ir} = \int_0^\infty \int_0^\infty g_i(v) g_r(u) K_X(v-u) dv du \quad (3)$$

The decision dispersion of reaction is

$$D_Y = \sum_{i=1}^n D_{yi} + 2 \sum_{i \neq r} k_{ir} \quad (4)$$

For each type of correlation function, D_y and k_{ir} were calculated by means of using $g(t) = \gamma \cdot a \cdot e^{-\gamma t}$ as weight functions in formulas (1) and (3), with $\gamma=1/T$. For instance, for exponential correlation function with dispersion D_X and parameter α we will have

$$D_y = D_X \cdot \frac{a^2 \gamma}{\alpha + \gamma}, \quad k_{ir} = D_X \cdot \frac{a_i a_r \gamma_i \gamma_r (\gamma_i + \gamma_r + 2\alpha)}{(\gamma_i + \gamma_r) \cdot (\alpha + \gamma_i) \cdot (\alpha + \gamma_r)} \quad (5)$$

Correlation functions of reactions are found similarly.

Thus for users this task comes to determination of roots s_i and to algebraical calculations by formula (4). Unification of computations means that the same expressions for D_y and k_{ir} are used for filters of different structure.

In this case unification is not total because quantities D_y and k_{ir} are different for different correlation functions. However fundamental advantage of such unification is that it can also be applied to nonstationary processes $X(t)$ and $Y(t)$.

3. PROBLEM OF THE SECOND TYPE

Total unification of calculations is only possible for the steady state processes (indicated by tilde, \sim). It is well known that stationary process $X(t)$ is a result of passing white noise $\xi(t)$ through a linear system with transfer function $G_X(s)$ (Fig 2), the parameters of which depend on interference correlation function type. For example, for exponential correlation function the linear system is an aperiodic link with parameters

$$a_X = \sqrt{\frac{2D_X}{\pi \cdot c \cdot \alpha}}, \quad T_X = \frac{1}{\alpha}, \quad (6)$$

where the constant c is spectral density of white noise.

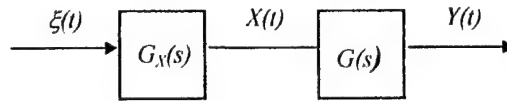


Figure 2.

As a result, the filter can be represented as the combined system with transfer function $G_c(s) = G_X(s)G(s)$. If m is the degree of the polynomial in denominator $G(s)$, then the system has $n+m$ degree.

Instead of interference, white noise is fed to the input of the combined system. Using the "partial reactions" method for this system, one can obtain $n+m$ linear aperiodic links connected in parallel. Parameters \tilde{a} and \tilde{J} of these links are determined by formulas (2), but for $n+m$ roots. Spectral density of white noise is equal to the constant c and the correlation function of white noise is expressed through delta-function:

$$k_X(\tau) = \pi \cdot c \cdot \delta(\tau) \quad (7)$$

Using these values in formulas (1) and (2) yields simple expressions after integration:

$$\tilde{D}_y = \frac{\pi \cdot c \cdot \tilde{a}^2}{2\tilde{J}}, \quad \tilde{k}_{ir} = \frac{\pi \cdot c \cdot \tilde{a}_i \cdot \tilde{a}_r}{\tilde{J}_i + \tilde{J}_r} \quad (8)$$

Decision dispersion is calculated by formula (4). In the final expression, the constant quantity πc is canceled out. Therefore we can put $\pi c=1$. Unification of calculation is total since formulas (8) are independent on the type of correlation function and $G(s)$.

4. EXAMPLE

The dose ψ of voltage oscillation is standardized in standard [3]. This dose is equal to the dispersion of a process on the filter output, which is completely analogous to flickermeter filter [2]. The following values of the dose are allowed: $0.018 (\%)^2$ and $0.034 (\%)^2$ for incandescent lamps for work with significant visual effort and in normal conditions, respectively; and $0.079 (\%)^2$ for fluorescent lamps. Let us estimate acceptability

of fast voltage fluctuations with exponential correlation function for $D_X = 2 (\%)^2$ and $\alpha = 0.7 s^{-1}$.

Expression for filter transfer function from [2] can be represented as

$$G(s) = \frac{b \cdot T_1 s \cdot (T_2 s + 1)}{(T_1^2 s^2 + T_3 s + 1) \cdot (T_3 s + 1) \cdot (T_4 s + 1)} \quad (9)$$

where $b = 1.748$, $T_1 = 0.017 s$, $T_2 = 0.07 s$,

$T_3 = 0.013 s$, $T_4 = 0.00726 s$, $T_5 = 0.015 s$.

As the dose is estimated for steady state conditions, we can solve the problem two ways.

The first way corresponds to the problem of the first type. Let us determine the denominator roots in formula (9):

$$s_{1,2} = -\lambda \pm j\beta = -25.51 \pm j51.556 s^{-1},$$

$$s_3 = -\gamma_3 = -7.699 s^{-1},$$

$$s_4 = -\gamma_4 = -137.6 s^{-1},$$

$$\text{where } \lambda = \frac{T_5}{2 \cdot T_1^2}, \quad \beta = \frac{\sqrt{4T_1^2 - T_5^2}}{2 \cdot T_1^2}, \quad \gamma_{3,4} = 1/T_{3,4};$$

$$j = \sqrt{-1}.$$

Numerically,

$$a_1 = 0.296 + j0.482 s, \quad J_1 = 0.007 + j0.016 s.$$

Parameters a_2 and J_2 are calculated similarly:

$$a_2 = 0.296 - j0.482 s, \quad J_2 = 0.007 - j0.016 s,$$

and so on.

For first and second links by formulas (5):

$$D_{y1} = D_U \cdot \frac{a_1^2 \gamma_1}{\alpha + \gamma_1^2} = -0.282 + j0.57 (\%)^2,$$

$$D_{y2} = D_U \cdot \frac{a_2^2 \gamma_2}{\alpha + \gamma_2^2} = -0.282 - j0.57 (\%)^2,$$

$$k_{12} = D_U \cdot \frac{a_1 a_2 \gamma_1 \gamma_2 (\gamma_1 + \gamma_2 + 2\alpha)}{(\gamma_1 + \gamma_2) \cdot (\alpha + \gamma_1) \cdot (\alpha + \gamma_2)} = 0.65 (\%)^2.$$

After calculation of the parameters for other links by formula (4) we can find the decision dose of voltage oscillations as:

$$\Psi = \sum_{i=1}^4 D_{yi} + 2 \cdot (k_{12} + k_{13} + k_{14} + k_{23} + k_{24} + k_{34});$$

$$\Psi = 0.028 (\%)^2.$$

The second way corresponds to the problem of the second type. As the dose has the largest value at steady state conditions, we will use formulas (8) with the assumption that $\pi \cdot c = 1 (\%)^2 s$.

According to formula (6), the inertial link with parameters $a_X = 0.954 s$ and $T_X = 1.429 s$ is added to the filter. In this case, the combined system will have the following transfer function:

$$G_c(s) = \frac{a_X b T_1 s (T_2 s + 1)}{(T_1^2 s^2 + T_3 s + 1)(T_3 s + 1)(T_4 s + 1)(T_X s + 1)}$$

In the denominator, the polynomial in the first brackets has complex roots:

$$s_{1,2} = -25.51 \pm j51.556 s^{-1} \quad (\text{for } j = \sqrt{-1}),$$

and other roots are real:

$$s_3 = -7.699 s^{-1}, \quad s_4 = -137.6 s^{-1}, \quad s_5 = -0.7 s^{-1}.$$

Taking into account that the multiplier of s^5 in the denominator of $G_c(s)$ is equal to $T_1^2 T_3 T_4 T_X$, we can determine the parameters of the first link by formula (8):

$$\tilde{a}_1 = \frac{-a_X \cdot b \cdot (T_2 s + 1)}{T_1 T_3 T_4 T_X \cdot (s_1 - s_2) \cdot (s_1 - s_3) \cdot (s_1 - s_4) \cdot (s_1 - s_5)}$$

$$\tilde{a}_1 = 0.0036 - j0.0055 s \quad \text{and} \quad \tilde{J}_1 = 0.0077 + j0.016 s.$$

Parameters of other links are calculated likewise. Time constants of the three links are real and equal to T_3 , T_4 and T_X , while their transfer coefficients are complex.

For the first and second links, formulas (8) give

$$\tilde{D}_{y1} = -7.86 \cdot 10^{-3} - j0.26 \cdot 10^{-3} (\%)^2,$$

$$\tilde{D}_{y2} = -7.86 \cdot 10^{-3} + j0.26 \cdot 10^{-3} (\%)^2,$$

$$\tilde{k}_{12} = 8.865 \cdot 10^{-3} (\%)^2.$$

The decision dose of voltage oscillation

$$\tilde{\Psi} = \sum_{i=1}^4 \tilde{D}_{yi} + 2 \cdot (\tilde{k}_{12} + \tilde{k}_{13} + \tilde{k}_{14} + \tilde{k}_{23} + \tilde{k}_{24} + \tilde{k}_{34});$$

$$\tilde{\Psi} = 0.028 (\%)^2.$$

By comparing of this value with the acceptable ones we can conclude that voltage oscillations in this example are only inadmissible for work under incandescent illumination, which would require significant visual effort.

5. CONCLUSION

It is recommended that determination of the process characteristics after linear filtering in EMC models is done using "partial reactions" method, which unifies and simplifies the calculations.

6. REFERENCES

- 6.1 A.K. Shidlovskiy, E.G. Kourennyi "Introduction in statistical dynamics of power supply systems" (in Russian), Naukova dumka, Kiev, 1984, pp. 56-57.
- 6.2 "Flickermeter. Functional and design specifications" (in English), IEC, Publication 868, Geneva, 1986, p. 19.
- 6.3 GOST 13109-87 "Electrical energy. Requirements for quality of electrical energy in general-purpose electrical networks" (in Russian), Moscow, brought to use at 01.01.89, pp. 2-3.

BIOGRAPHICAL NOTES



Eduard G. Kourennyi. M. Eng. (The Novochoerkask Polytechnical Institute), Doctor of Sciences, Professor of the Department of Electrical Supply of Industry and Sities (ESIS) of the Donetsk State Technical University (DSTU), Expert of the Ukraine Superior Certifying Commission, S. A. Lebedev Award of Ukrainian Academy of Sciences, Consulting of the joint-stock company "Stirol" (Ukraine), Member of IAEE. Scientific interests: ESIS, EMC, electrical saving, statistic dynamics of energy systems.



Victor A. Petrosov. M. Eng. (The Priazovsk State Technical University), Ph. D, deputy mayor of Mariupol (Ukraine). Scientific interests: EMC, electrical saving.



Lidiya V. Chernikova. M. Eng. (DSTU), postgraduate student of the Department of ESIS of the DSTU. Scientific interests: EMC, statistic dynamics of energy systems.

MAINS RFI-FILTERS DESIGN METHODOLOGY

T. Kurowski*, V. Pilinsky**, M. Rodionova**, A. Rybin**.

*Technical University of Zielona Gora, Institute of Industrial Electrical Engineering,
50, Podgorna, 65246, Zielona Gora, Poland; Ph. (+4868) 325-48-31,
fax (+4868) 325-46-16, E-mail: kurowski@iep.pz.zgora.pl

**National Technical University of Ukraine, "Kiev Polytechnic Institute",
(NTUU "KPI"), Electronics Department
Prospect Peremohy, 03056, Kiev, Ukraine; Ph. (+380 44) 441-18-80,
fax (+380 44) 247-59-32 E-mail: pilinsky@ztri.ntu-kpi.kiev.ua

To decrease interferences in the Mains and EMC demands accomplish the Power Lines RFI Filters are used. For these Filters design it's necessary to know the impedances of the Mains - as conductive electromagnetic interference (EMI) receptor - and of the Power Supply Mains terminals - as EMI source.

Mains impedance may be considered standard, but Switched Mode Power Supply (SMPS) impedance - is a problem!

The methodic of Power Supply Mains terminal impedance simulation taking into account non-linear nature of SMPS as EMI source is suggested.

In the paper the methodology of RFI-Filters designing is suggested to provide filters synthesis for given SMPS, subject to rated and parasitic component's parameters.

1. INTRODUCTION

EMC Directive 86/339 EEC introduction forces engineers to take measures on EMC accomplishing. RFI-filters are the most effective means of EMI suppression are RFI-filters. All filters characteristics in reference books are given for fixed impedances - 50 Ω - for the EMI source and receptor. However, if it's possible to agree with such receptor impedance, but for the EMI source it isn't correct.

Nowadays switched mode power supplies are the most widespread EMI sources. Conductive EMI, produced by SMPS, exceed normative levels essentially.

RFI-filters design is complicated by frequency dependence of impedance of SMPS as viewed from the Mains terminals. Moreover, filters' attenuation is influenced by the components' parasitic parameters because of high frequency range - from tens kilohertz to ones gigahertz. Therefore the process of designing of RFI-filters with predicted attenuation for specific SMPS is rather difficult.

Principle characteristics of the SMPS Mains RFI-filters design and simulation are considered in [1...3], but problem remains actual.

For correct RFI-filters design it's necessary to take into account the internal input impedances of SMPS as the EMI source and Mains as the interferences receptor.

Usually Mains is simulated as an equivalent voltage source with Line Impedance Stabilization Network (LISN), so the problem consists in SMPS input impedance simulation. The authors suggest the conception of the system "Mains - RFI-filter - SMPS" simulation which gives possibility to design the filter properly.

The system "Mains - RFI-filter - SMPS" must be simulated as linear-parametric circuit where the internal resistances of the active switching components are the parameters [4].

The model of the system is presented as number of an equivalent circuits which topology is defined by the processes of active components switching.

Analysis in time domain is based on the Laplace transform and modified method of fitting. Then the amplitude-frequency characteristics (AFC) of the solution matrix elements are calculated and their forms are taken as the criterion of EMC accomplishing. For the first time this procedure is carried out for the SMPS only, then RFI-filter is taken into account.

New meanings of the solution matrix elements are calculated in according with the modification method [5]:

$$[Y_m(p)]^{-1} = [Y_{m-1}(p)]^{-1} - g[A] / (1 + g\xi), \quad (1)$$

where m - number of the modification of the solution matrix; g - conductivity; ξ - mutual derivative, which is calculated on $(m-1)$ modification of the solution matrix:

$$\xi = Z_{aa} - Z_{ab} - Z_{ba} - Z_{bb},$$

where a, b - numbers of the nodes of conductivity g connection; $[A_{m-1}]$ - matrix of increment:

$$[A] = [\xi_{zo}] \cdot [\xi_{oz}],$$

$$[\xi_{zo}] = [(Z_{a1} - Z_{b1}) (Z_{a2} - Z_{b2}) \dots (Z_{an} - Z_{bn})],$$

$$[\xi_{oz}]^T = [(Z_{1a} - Z_{1b}) (Z_{2a} - Z_{2b}) \dots (Z_{na} - Z_{nb})]^T,$$

n - order of matrix $[Y_m]^{-1}$, T - the symbol of transposition; all z_{ij} are the elements of $[Y_{m-1}]^{-1}$.

Suggested method of simulation makes it possible to design the RFI-filter and to accomplish EMC demands in the system "Mains - Filter - SMPS".

2. SYNTHESIS OF RFI-FILTERS

The procedure of SMPS Mains RFI-filters synthesis may be represented by next algorithm.

1. To calculate current $i^1(t)$ and voltage $u^1(t)$ meanings in SMPS Mains input (Fig. 1) taking into account Mains internal impedance as that of linear stabilization network (LISN).

Here the model of SMPS presentation is important. As it was shown in [4,5], it's expediently to use parametrical SMPS model with linearization in time intervals. This one allows to reflect the process of EMI generation caused by active SMPS components switching.

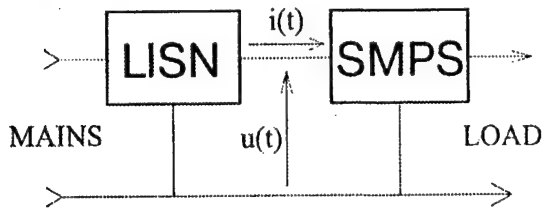
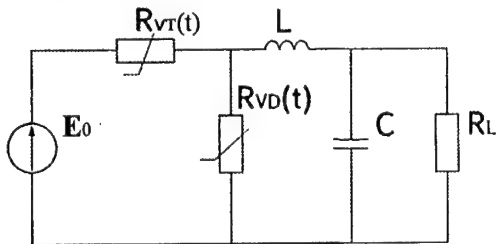


Fig. 1

An example of the model of SMPS on the basis of switched mode voltage regulator is presented in Fig. 2,a, where the regular components parameters are taken into account only. The changing parameter is SMPS switches internal resistance R_{sw} (Fig. 2,b).



a)

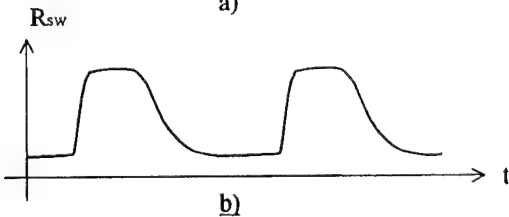


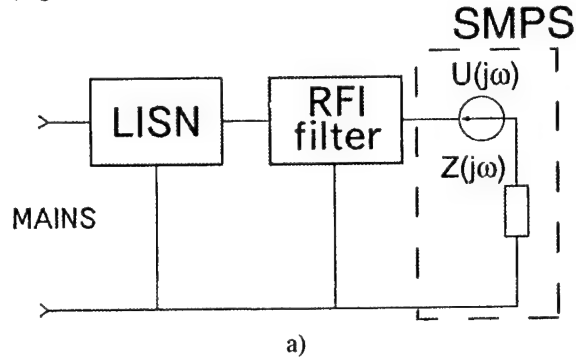
Fig. 2

To calculate currents and volages it's used modified method of filling [5].

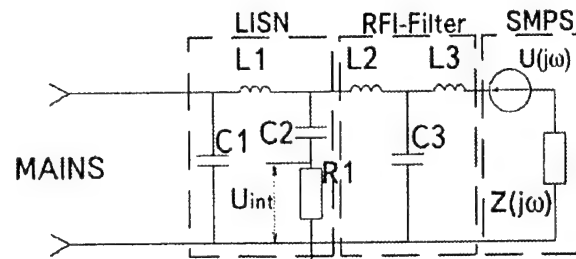
2. To find Fourier – images of $i^1(t)$, $u^1(t)$. With this purpose it's possible to use one of the well-known programs – for example, Mathcad or Matlab. Then the

ratio $U^{(1)}(j\omega)/I^{(1)}(j\omega) = Z^{(1)}(j\omega)$ gives input impedance of SMPS.

3. To put into the model (Fig. 1) RFI-filter with prescribed meanings of L and C (Fig. 3,a) and calculate voltage drop $u_{int}(\omega)$ across LISN active resistor R1 (Fig. 3,b)



a)



b)

Fig. 3

If this voltage level is more then limited normative one, parameters of RFI-filter components must be changed.

4. To calculate new meanings $u^{(2)}(t)$, $i^{(2)}(t)$ in the circuit (Fig. 4) and to find $Z^{(2)}(j\omega) = U^{(2)}(j\omega)/I^{(2)}(j\omega)$ – new condition for RFI-filter calculation.

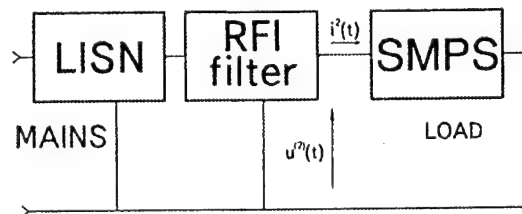


Fig. 4

5. To calculate new parameters of RFI-filter elements on the basis of model (Fig. 3) with new meanings of current and voltage.

6. To check the interference voltage level on R1 once more.

Thus the procedure of RFI-filter design taking into account internal SMPS impedance as viewed from the Mains terminals is iterative: if the iteration coversges, the designing is over. Otherwise it's necessary to change filter's circuit. It should be noted, that RFI-filter introduction in the circuit (Fig. 3) may results in EMI

increasing – this is explained by parametrical character of SMPS.

As an example, let us examine model (Fig.5). When the switch SW is opening, current i_L can't be changed abruptly in the moment of commutation.

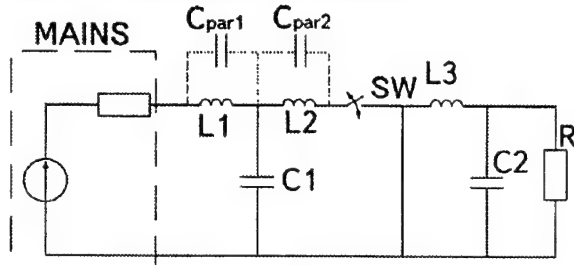


Fig. 5

Therefore current in the system «Mains-Filter-SMPS» is the same as before the commutation moment, i.e. δ -pulse of the voltage is arised. So the filter is the source of additional interferences. The situation becomes much more complicated when parasitic parameters of the filter components C_{par} are taking into account. They form the ways of δ -pulses propagation to the Mains.

3. CRITERION OF EMC ACCOMPLISHING

The procedure of Mains RFI-filters design may be simplified essentially: it's possible to evaluate the influence of the filter's and Mains' parameters throughout the designing of filter directly. Such a possibility the modifications method [5,6] gives.

It's based on division of complicated circuit on subnetworks by breaking of the conductances – links. This is resulted in transformation of the matrix of nodal admittances $[Y(p)]$ and it's reverse matrix $[Y(p)]^{-1}$ to the block-diagonal form. Step-by-step «growing» of the breaking links results in forming of the matrix of analysed circuit (1).

Modifications method gives the possibility of evaluation of every parasitic parameter influence after calculation of the matrix (1) in frequency domain at the steady-state process analysis:

$$[Y_m(j\omega)]^{-1} = [Y_{m-1}(j\omega)]^{-1} - \frac{j\omega_i C_{par}}{1 + j\omega_i C_{par} \xi} \cdot [A], \quad (2)$$

where $[Y_{m-1}]^{-1}$ is the initial reverse matrix on the frequency ω_i of imaginary component of the pole.

It is obvious that changing of the meanings of the matrix $[Y_m]^{-1}$ elements to a great extent is possible

only when the coefficient $\frac{j\omega_i C_{par} \xi}{1 + j\omega_i C_{par} \xi}$ is changed

sufficiently. Consequently, those meanings of C_{par} , that result in sharp variation of this coefficient, affect the matrix's elements appreciably. Thus, making the denominator of this coefficient approach to zero, it's

possible to calculate so-called critical meaning C_{cr} of parasitic parameters:

$$j\omega_i C_{cr} = 1/\xi. \quad (3)$$

Degree of approximation of amplitude – frequency characteristics of the matrix $[Y_m]^{-1}$ elements to the initial ones, which are calculated without parasitic parameters, is interpreted as indirect criterion of EMC: reduction of AFC results in EMI decreasing. Interconnection between AFC of the elements of solution matrix (a, c, e) and process in time domain (b, d, f) is illustrated in Fig. 6.

Indirect criterion of EMC makes it possible to take into account interferences, dealt with δ -pulses propagation: if AFC of matrix elements have no «direct component», δ -pulses in time domain are absent.

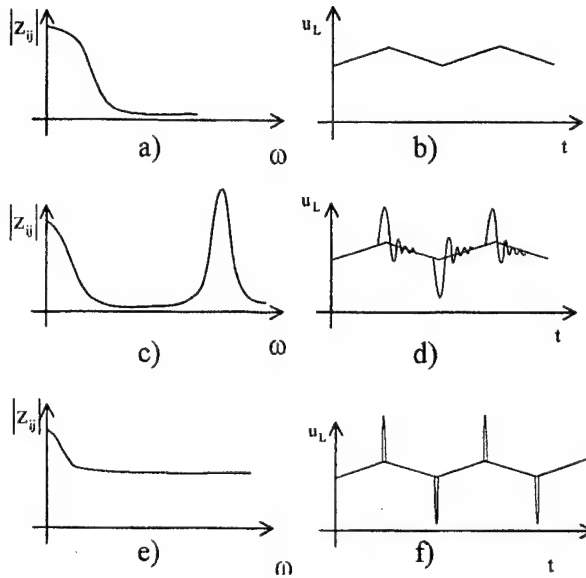


Fig. 6

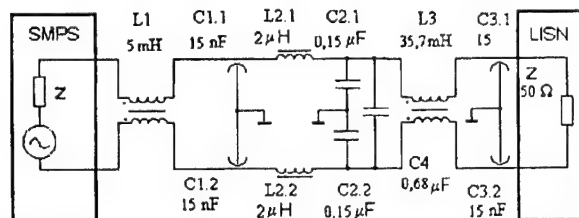
4. REALIZATION OF ALGORITHM OF RFI-FILTERS DESIGN

Methodics of RFI-filters design allowing Mains and SMPS properties consists of three principal blocks:

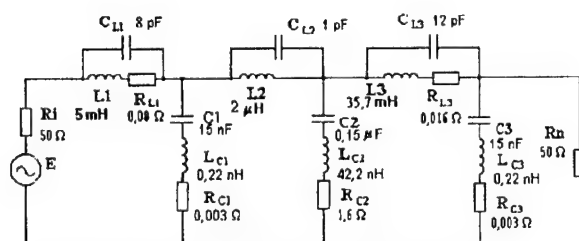
1. Time domain analysis of initial SMPS to check it's correspondence to the specification demands;
 - formation of SMPS models in time intervals of linearization without parasitic parameters;
 - formation of the nodal conductivities matrixes and matrixes of nodal capacitances;
 - formation of the solution matrixes;
 - calculation of initial AFC of the solution matrixes elements;
 - transition from a transform of the solution matrixes elements to the original time functions;
 - substitution of time intervals duration and calculation of matrixes of coefficients;
 - calculations of steady state nodal voltages;
 - calculation of SMPS characteristics;

2. Frequency domain analysis to take EMC demands into account on indirect EMC criterion:
 - change of SMPS models by introduction of parasitic parameters;
 - determination of influencing parasitic parameters;
 - calculation of the critical meanings of parasitic parameters;
 - calculation of the solution matrixes elements taking into account influencing parasitic parameters;
 - calculation of real AFC of the solution matrixes elements;
 - checking of correspondence of initial and real AFC on indirect criterion;
 - changing of SMPS models by introduction EMI suppression means (RFI-filters);
3. Time domain analysis of the system "Mains – RFI-filters – SMPS" to check the propriety of the design procedure:
 - calculation of steady - state nodal voltages;
 - calculation of SMPS characteristics;

Filter's circuit with parasitic parameters and it's model for asymmetrical interferences in accordance with [7] are shown in Fig. 7, a, b.



a)

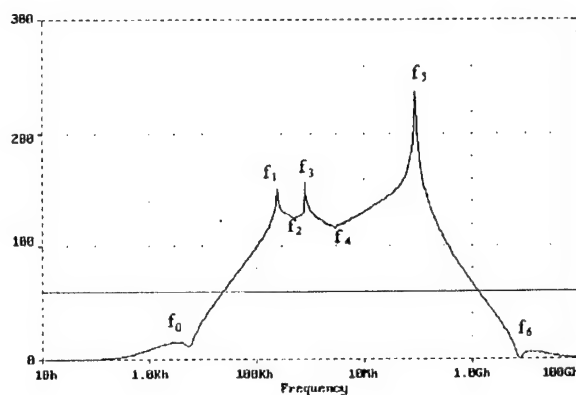


b)

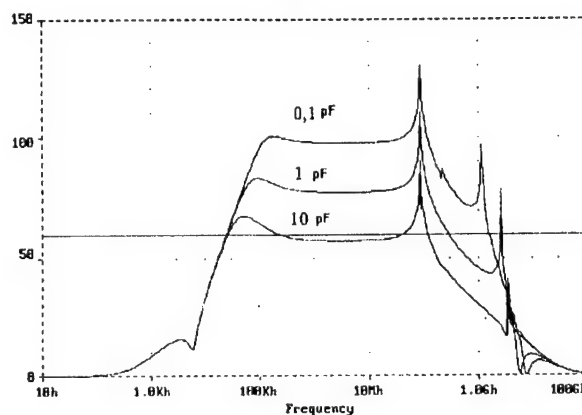
Fig. 7

Frequency response of the filter's attenuation is represented in Fig. 8, a. Frequencies of extremums are conditioned by rated and parasitic parameters of the filter (f_0 : L1, L3, C2; f_1 : L3, C1; f_2 : L1, L3, C1, C2; f_3 : L1, C1; f_4 : L2, C2; f_5 : L2, C1, C2; f_6 : C1, C2; f_7 : C1, C2).

Variation of this frequency response at changing of the parameter which is modelling filter's capacitance "input-output" is shown in Fig. 8 b. Results obtained show influence of the filter's construction on filter's attenuation.



a)



b)

Fig. 8

5. CONCLUSION

Methodology of Mains RFI-filters design in the system "Mains – Filter – SMPS" has been described, which has applied to rational choice of means of EMC ensuring. The principle advantage of the methodology suggested is correct consideration of Mains terminals SMPS impedance. It is also shown joint influence of rated and parasitic filter's parameters on filter's attenuation. It's hoped to be able to exploit the results and methodics described to further improvement of RFI-filters design procedure.

6. REFERENCES

1. R. D. Middlebrook, "Input Filter Considerations in Design and Application of Switching Regulators", IEEE Power Electronics Specialists Conference Records, 1977, pp. 36-57.
2. R. B. Ridley, "Secondary LC – filter analysis and design techniques for current – mode – controlled converters", IEEE Trans. Power Electron., 1988, vol.3, №4, pp. 499-507.
3. D. M. Mitchell, "DC-DC Switching regulator analysis small – signal MathCAD design aids", Cedar Rapids, - Iowa, 1992.

4. V. Pilinsky, M. Rodionova, A. Rybin, "Methodics of electromagnetic interferences prediction based on indirect criterion" (Russian), Proceedings of International Wroclaw Symposium on Electromagnetic Compatibility EMC-90", pp. 425-430.
5. A. Rybin, M. Rodionova, "Analysis of the parametric circuits on the basis of modifications method" (Russian), Radioelectronics, 1990, vol. 33, №6. pp. 38-42.
6. V. Pilinsky, M. Rodionova, V. Temnikov, V. Shvaichenko, "SMPS Interferences: Prediction and Suppression", Proceedings of International Conference on Electrical Drives and Power Electronics, Kosice (Slovakia), 1996, vol.2, pp. 479 - 483
7. CISPR 17. Methods of Measurement of the Suppression Characteristics of Passive Radio Interference Filters and Suppression Components, pp.46
8. V. Pilinsky, V. Pervoj, M. Rodionova, A. Janushevsky, "Simulation of Mains RFI Protecting Filter" (Russian), Juridical, Regulated and Metrological Accomplishing of the System of Information Protection in Ukraine, Kiev, 2000, pp. 170-174.
9. V.V. Pilinsky, V.S. Kotelchuk, "Design procedure of the Mains EMI filters", Proceedings of International Conference on Electrical Drives and Power Electronics, High Tatras, (Slovakia), 1999, pp. 314-318.

BIOGRAPHICAL NOTES

Rodionova Mariya received the degree in electrical engineering from the Faculty of Electroacoustics in National Technical University of Ukraine «Kiev Polytechnic Institute» in 1972. Currently she is a senior lecturer in NTUU «KPI», Department of Acoustics and Acoustoelectronics. Her research interests include power electronics, electromagnetic compatibility of electronics with special attention to analysis and simulation with EMC providing. She has published as author and coauthor more than 70 papers and 2 books. In research she has cooperated with Technical Universities of Wroclaw and Zielona Gora (Poland).

Tadeusz Kurowsky was born in Wylany (Poland) in 1941. He received the degree and the Ph. D degree, both in electrical engineering, from Technical University of Wroclaw, Poland, in 1964 and 1975 respectively. In 1991 he received the Dr. Sc degree on research results of electromagnetic compatibility of Power Converters. Presently he is professor in Technical University of Zielona Gora. His research interests are mainly in electrical drivers and electromagnetic compatibility in power electronics. Mr. Kurowsky has authored or coauthored more than 80 papers in this area including 4 books, 5 patents. He has cooperated in research with Kiev Polytechnic Institute (Ukraine).

Pilinsky Vladimir was born in Saint-Petersburg in 1941. Main scientific interests are: power electronics & telecommunication (Switched-mode Power Supplies for Electronics, Electromagnetic Compatibility of Radioelectronics). In 1963 he graduated from Kiev Polytechnic Institute. In 1973 he obtained Ph. D. degree in electrical engineering. 1963 till 1980 he was assistant, lecturer, docent in KPI. From 1980 till 1986 he was the Head of the Technical Universities Department at Ministry of Education of Ukraine. From 1986 till now he is the full professor (1993) in KPI and the Head of the EMC Center. He is the author and coauthor of more than 220 published works, including 8 books. He has cooperated in research with Technical Universities of Wroclaw and Zielona Gora (Poland).

Alexander Rybin was born in Kiev in 1948. He received the degree and the Ph. D Degree, both in electrical engineering, from Kiev Polytechnic Institute, in 1972 and 1981 respectively. Presently he is associate professor in NTUU KPI. His research interests are mainly in fundamental electromagnetic theory, signal processing, medical electronic equipment.

Mr. Rybin has authored or coauthored more than 170 papers include 8 books. He has cooperated in research with Technical Universities of Prague and Brno (Czech Republic).

HIGH FREQUENCY SPURIOUS RESPONSE OF RECTANGULAR WAVEGUIDE COMPONENTS

Vladimir Lenivenko

EM Solutions Pty. Ltd., Unit 7, 35 Ethel St., Yeerongpilly QLD 4105 Australia,
fax: (617) 33926400, e-mail: vladl@powerup.com.au

This paper presents a review of waveguide components with respect to their inherent features having crucial influence to the spurious and out-of-band emission of communication systems in the broad frequency range. Problems of mode conversion, stop band performance, interchannel isolation and other factors that define EMC characteristics considered with extensive use of proven rigorous modelling approach – mode matching technique (MMT) and generalized S-matrix formulation.

Experimental verification was conducted using modern precise CNC-machined waveguide components. Considerable number of experimental plots presented and discussed in order to illustrate and verify all theoretical results, so component of every type is sufficiently characterised from the point of view of its EMC performance.

1. MODELLING APPROACH

1.1. Spurious response

ITU Recommendations define spurious emission of radio-relay system as emission on a frequency or frequencies, which are outside the necessary bandwidth and the level of which may be reduced without affecting the corresponding transmission of information [1]. Since the impact of passive RF network on the overall spurious emission is crucial, investigation of spurious frequency response of waveguide components become of great interest. As far as EMC regulations consider typical interference scenario as a whole, including all possible passes to a victim, complete prediction of spurious and out-of band radiations ultimately require rigorous analysis of passive waveguide components configured into a network dedicated to particular purpose. Multimode nature of EM fields create multiple virtual channels associated with particular propagating or evanescent modes, actually converting 2-port devices into multiport ones providing additional passes for interference. Example of such network might be RF front end of digital radio-relay system, including waveguide transitions, bends, filters and diplexer, connecting receiver, transmitter and antenna into a single system. RF specification and EMC properties of the front end actually define the EMC specification for the entire system.

1.2. Rigorous 3D EM simulation

Rigorous 3D EM simulation of waveguide components has been performed to investigate out-of-band and spurious response. Based on the MMT approach, the simulation takes into account step discontinuities including E-plane and H-plane steps, coupling irises having finite wall thickness, symmetrical and asymmetrical waveguide junctions, distinctly overmoded regions with higher order mode conversion and mode interaction between all discontinuities as well as effects of polarization conversion. Simulation models for components can be built by decomposition of complex waveguide structures into basic key building blocks. Fig. 1 shows two types of key building blocks suitable for this purposes and allowing to cover broad variety of components.

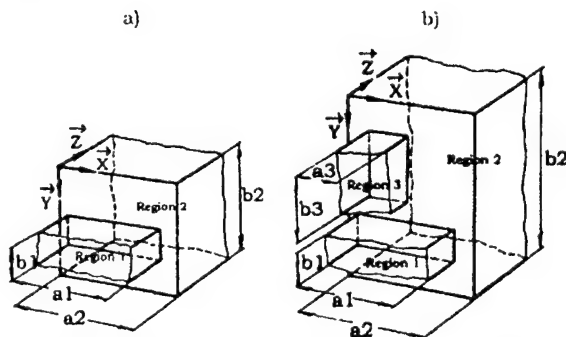


Fig. 1. Two-port (a) and three-port (b) building blocks

These are two-port junction (fig. 1a) and generalized three-port junction (fig. 1b) formed by rectangular waveguides of arbitrary dimensions. Modal analysis of such junctions presented in the literature [2]. Electromagnetic fields on either side of the bifurcation are treated as superposition of waveguide eigen modes. Application of the conditions of continuity to the fields at the interface results in a system of integral equations which can be converted to a system of linear algebraic equations using method of Galerkin, yielding generalized S-matrix of the building block. Generalized S-matrices of building blocks computed and stored and later used for junction-by-junction assembly of entire complex waveguide structure [3]. Unlike traditional design and analysis methods this technique allows accurate prediction of spurious response.

2. WAVEGUIDE TRANSITION

The waveguide transition shown in Fig. 2 is designed to match standard WR112 waveguide to a square waveguide 28.5x28.5 mm covering 7 – 10 GHz.

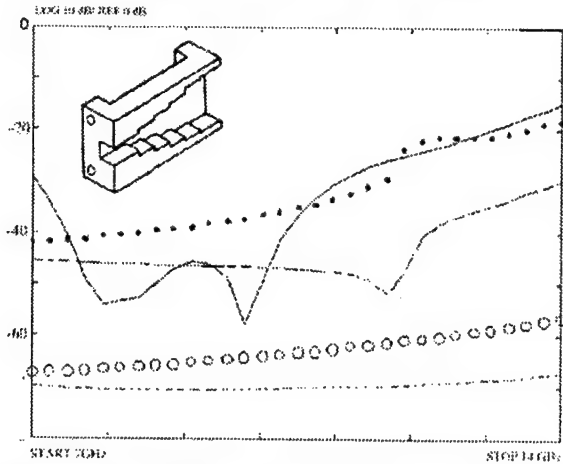


Fig. 2. Waveguide transition and its multimode response in 2:1 frequency range

The input port, as it supposed to be, supports the only propagating mode TE_{10} . As far as cross-section of the transition is gradually increasing towards the square one, the output port supports already three propagation modes: TE_{10} , TE_{11} , TM_{11} . In general, transition having rectangular cross section and arbitrary profile in z direction would generate all possible modes. If only modes having f_c below or equal to 40GHz to be considered, then port 1 would get 42 modes (up to TM_{42} having $f_c = 39.526$ GHz), and port 2 would get 88 modes (up to TM_{27} having $f_c = 38.441$ GHz), causing multimode excitation of the output waveguide within the entire pass-band, as well as generation of depolarised wave, since H_{01} mode has $f_c = 5.2632$ GHz in the port 2 region. Meanwhile, in most practical cases it is desirable to maintain single mode operation. Fortunately, there is a possibility to suppress considerable part of the higher modes effectively using well-known properties of symmetry. Evaluating the expressions for coupling coefficients, describing coupling between H_{mn} , E_{mn} modes in each building block, it's possible to see that for structures having E-plane symmetry all coupling coefficients for odd numbers $n = 1, 3, \dots$ become equal to zero indicating that modes H_{mn} , E_{mn} , having $m = 1, 2, 3, \dots$ won't be present. Furthermore, as far as this transition has constant dimension a , coupling coefficients for all modes having $m = 0, 2, 3, 4, \dots$ become equal to zero and only waves H_{10} , H_{1n} , E_{1n} , $n = 2, 4, 6, \dots$ will be present. Table 1 shows modal content of EM fields in the regions of input and output ports. Fig. 2 shows reflection and mode conversion effects. Reflection coefficient $|S_{11}|$ of dominant mode at the input port is shown by solid line. Mode conversion is characterised by coefficients $|S_{21}|$ for several different modes (dashed line for H_{12} , dotted line for E_{12} , dash dot for H_{14} , o-mark for E_{14}) obtained in assumption that input port is excited by only dominant H_{10} mode (0 dB level). Plotted values of mode conversion coefficients for modes under cut-off show relative amplitudes of evanescent modes in the refer

ence plane located at the output port of the transition. The first higher mode for this type of structure (E_{12}) is the most pronounced one and become propagating over 11.8 GHz with amplitude more than -20 dB.

Table 1

Region	Mode	Cut-off frequency, GHz
Port 1	H_{10}	5.2632
	H_{12} , E_{12}	24.347
Port 2	H_{10}	5.2632
	H_{12} , E_{12}	11.802
	H_{14} , E_{14}	21.772
	H_{16} , E_{16}	32.124

3. WAVEGUIDE BEND IN E-PLANE

Geometry of the waveguide bend is shown in Fig. 3. This structure is designed for WR62 waveguide and supposed to be transparent in the vicinity of 15GHz with reflection loss below 20 dB within 14.75 – 15.25 GHz. Table 2 shows modal content of electromagnetic field at the transition ports. Eigenmodes with cut-off frequencies up to 50 GHz presented in the table. Both ports are identical, dimension a of the waveguide is changed inside the bended section forming step in H-plane. Since the step is symmetrical in H-plane it suppresses eigenmodes having even numbers $m = 0, 2, 4, \dots$. As far as no symmetry in the E-plane, full range of n values to be considered: $n = 0, 1, 2, 3, \dots$. Fig. 3 shows plotted values of reflection $|S_{11}|$ (diamonds for calculated and solid line for experimental results), as well as mode conversion coefficients $|S_{21}|$ for H_{11} (dashed line), E_{11} (dotted line).

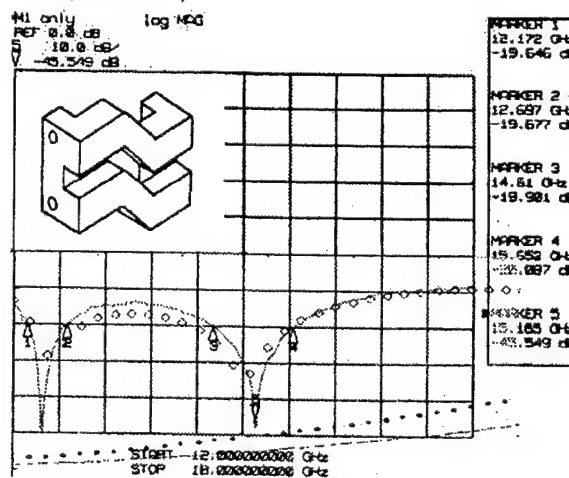


Fig. 3. Waveguide bend in E-plane and its multimode response

Since the cross-sections of both two ports of this structure are identical, no other propagating modes appear, and amplitudes of evanescent modes depend on the position of reference plane regarding to output port. Close proximity to the output port (short regular waveguide section attached to the port) may cause quite significant values of evanescent modes couple to the next following component in the network.

Table 2

Region	Mode	Cut-off frequency, GHz
Port 1,2	H ₁₀	9.4937
	H ₁₁ , E ₁₁	21.228
	H ₃₀	28.481
	H ₃₁ , E ₃₁	34.23
	H ₁₂ , E ₁₂	39.143
	H ₅₀	47.468
	H ₃₂ , E ₃₂	47.468

4. LOW PASS FILTER

Fig. 4 shows geometry and performance of the low pass filter (LPF) designed for suppressing the second harmonic response of the HPA. This typical application requires low loss in the pass band and high attenuation in the stop band, as well as high power handling capability. High frequency performance is prone to spurious responses causing deterioration of stop band and consequent degradation of overall system performance. For this particular example the spec is as following: pass band 5.6 – 6.4 GHz, stop band 11.2 – 12.8 GHz, stop band attenuation greater than 60 dB is required (see Fig. 4b for measured performance).

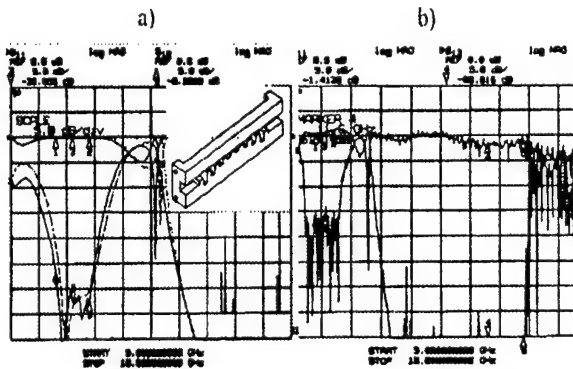


Fig. 4. Pass band (a) and stop band (b) of the LPF

This structure is designed for standard WR137 waveguide using Ahiezer-Zolotarev prototype as an initial point for direct CAD optimisation. Both input ports are identical, dimension *a* may be slightly changed inside filter in order to fine-tune exact stop band location, but in this particular example it's constant. As far as no symmetry in the E-plane observed, modal structure is quite similar to the one for E-plane waveguide bend, with pronounced TM_{1n} part of the modal content. Computed values of $|S_{11}|$ and $|S_{21}|$ for dominant mode shown in Fig. 4a (dashed and dash-dot lines respectively; measured performance is plotted with bold solid lines). Fig. 4b presents only experimental plot measured in 3:1 frequency range. It shows complicated spurious response. Intensive conversion of dominant mode into E₁₁ occurs immediately as E₁₁ become propagating causing two different things: converted energy passes the filters in the form of E₁₁ propagating wave; con-

verted energy reflects from the input port causing strong reflected wave almost entirely of E₁₁ content. Reflection of dominant mode in this point is considerably lower since it is almost completely consumed while converting into other modes. Due to wide frequency range (3:1) it's impossible to use standard calibrations kit for WR137. Alternatively, calibration using coaxial cal kit allows to cover frequency range but affected by waveguide adapters response. So far, the accuracy of measurements significantly degraded and measured results may be used just as indicative ones. Computed results presented in Fig. 5 allow to see much more detailed picture. Following values shown in Fig. 5: reflection $|S_{11}|$ (depicted by diamonds) and insertion loss $|S_{21}|$ (squares) for dominant mode, as well as mode conversion coefficients $|S_{21}|$ for H₁₁ (dashed line), E₁₁ (bold dots), and for E₁₂ (dash-dot line). Normalized amplitude of reflected E₁₁ is depicted by dotted line.

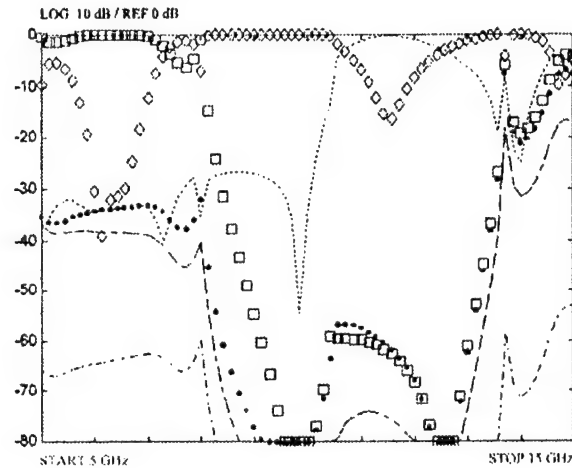


Fig. 5. Spurious response of LPF in 3:1 frequency range

Reduced reflection of dominant mode occurs in the vicinity of 10.6 GHz, (as measured) and accompanied with high level of reflected E₁₁ propagating backwards (from the input port to generator), as well as pronounced E₁₁ content of forward propagating wave after the filter.

5. BAND PASS FILTER

Direct coupled waveguide band pass filter (BPF) was analysed. Geometry of this structure is shown in Fig. 6. Filter is formed by six resonators coupled through the inductive irises. The structure has symmetry in the H-plane, so only odd indexes $m = 1, 3, 5, 7, \dots$ to be taken. Since no changes occur along the Y-axis, there is no mode conversion and unique index $n = 0$ to be taken. These symmetry features allow great reduction in computation time since only few modes supported by the structure. The filter is designed for 23 GHz band using Chebyshev prototype as an initial point for direct CAD optimisation, with actual spec as following: pass band 23.24 – 23.44 GHz, rejection at 22.2 GHz is 70dB.

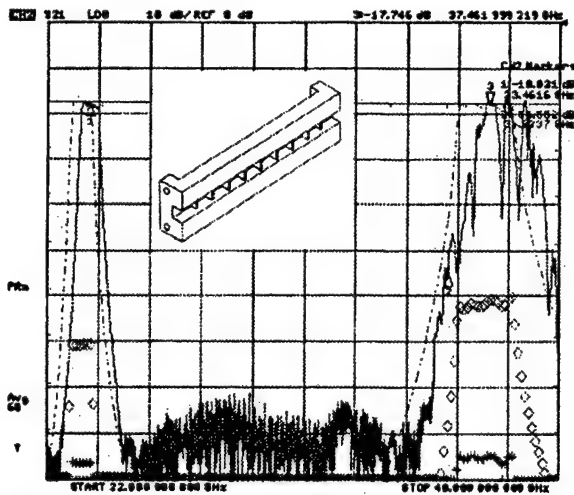


Fig. 6. Stop band performance of BPF

Fig. 6 shows plotted values of insertion loss $|S_{21}|$ for dominant mode (dash-dot line for calculated and solid line for experimental results), as well as mode conversion coefficients $|S_{21}|$ for TE_{30} (diamonds), TE_{50} (stars) showing normalized amplitudes of the first two higher modes as they appear at the output port.

6. DIPLEXER

Two band pass filters coupled to a common port constitute a diplexer. Diplexer configuration shown in Fig. 7 is typical for RF front-end design of microwave radio.

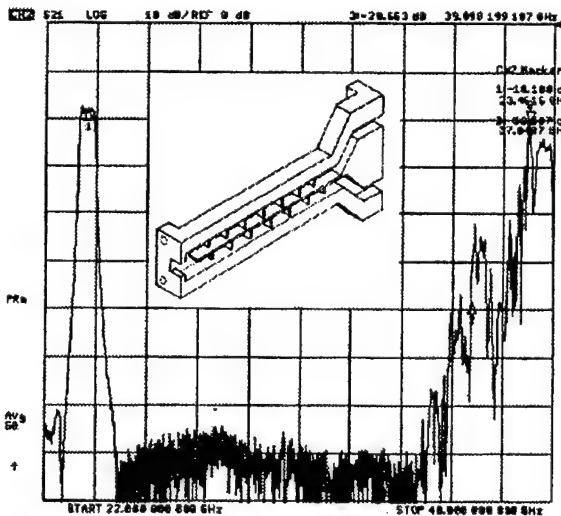


Fig. 7. Stop band performance of diplexer

Diplexer's operation and design approach were published in [4]. Here we'd rather be interested to illustrate the influential factors affecting its spurious response. The structure of eigenmodes is obviously very much defined by band pass filters with the addition of the common port coupling section and waveguide bends, if included. Fig. 7 shows measured stop band response of the 23 GHz diplexer.

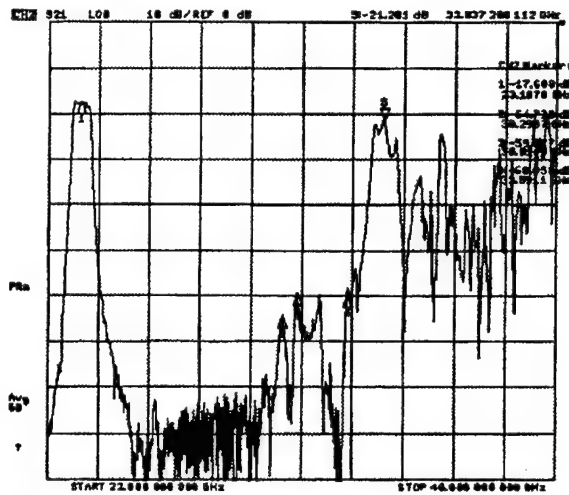


Fig. 8. Stop band performance of tuned diplexer

This result achieved with BPF like the one discussed above. Appropriate stop band characteristics are very similar except the second band at high frequency end is somewhat suppressed. As shown above, E-plane bends have modal structure very similar to a LPF, causing additional attenuation at the high frequency end.

Following comparison shows that slight changes in a symmetry order might crush the stop band performance. Fig. 8 shows high frequency response of a diplexer designed to that same specification and using that same structural configuration. The only difference: it's tuned using E-plane tuning screws inserted in the middle of each resonator. Tuning screws enrich the eigenmode structure of BPF causing significant degradation of stop band performance.

7. POWER COMBINER / DIVIDER

Geometry of the 3-dB H-plane power combiner/divider is shown in Fig. 9. It's designed for Ku-band satcom applications to a following specification: frequency band 14.0 – 14.5 GHz, two way equal coupling: 3.01 dB, insertion loss 0.15 dB. Return loss 20 dB min. This structure doesn't introduce changes in the waveguide's b dimension yielding reduced and simplified mode structure shown in Table 3.

Table 3

Region	Mode	Cut-off frequency, GHz
Ports 1-4	H_{10}	7.8947
	H_{20}	15.789
Cavity	H_{10}	2.5283
	H_{20}	5.0565
	H_{30}	7.5848
	H_{40}	1.0113
	H_{50}	12.641
	H_{60}	15.17
	H_{70}	17.698

Eigenmodes with cut-off frequencies up to 20 GHz presented in the table. Table depicts eigenmodes for two regions of the structure: the input port region and common internal cavity of the combiner.

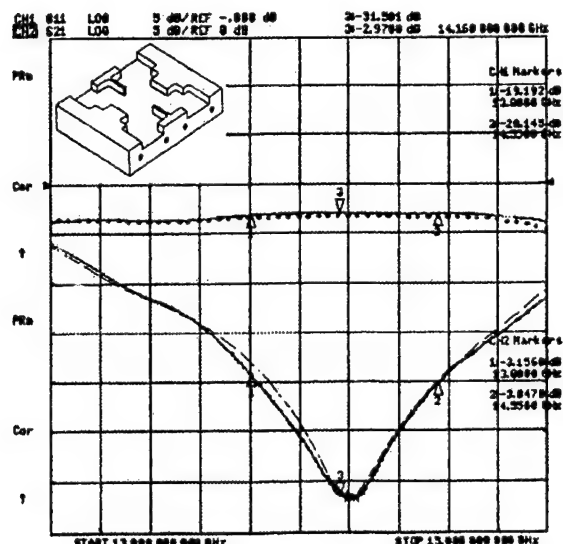


Fig. 9. Pass band performance of 3-dB combiner

Fig. 9 shows in-band performance of the combiner. Measured reflection $|S_{11}|$ and insertion loss $|S_{21}|$ for dominant mode plotted by solid lines while theoretical response is shown by dash-dot and dotted lines respectively. Spurious response is presented in Fig. 10. It was measured for frequency range 13 – 20 GHz and plotted (solid line). As discussed, measured data cannot be used for quantitative comparison but rather as an indication.

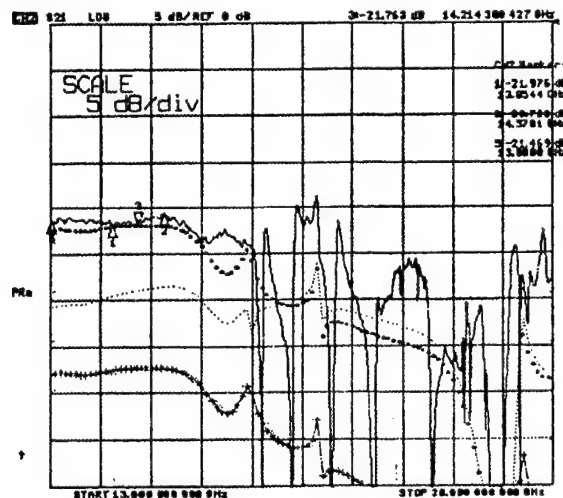


Fig. 10. Spurious response of 3-dB combiner

Theoretical results presented in Fig. 10 showing $|S_{21}|$ for dominant mode (bold dots), and the first two higher modes: H_{20} (dotted line) and H_{30} (line with stars) in the assumption of a single mode excitation of the input port.

8. CONCLUSIONS

Review of the spurious performance of several commonly used waveguide components was done using

MMT-based full-wave modelling and experimental investigation. Symmetry of the waveguide structure is the main feature influencing the spurious response of the component. For given electrical dimensions structures having higher order of symmetry get less number of eigenmodes. Their spurious response is more correlated with the dominant mode response. Structures having lower order of symmetry tend to show much more complicated spurious response with more pronounced mode conversion effects.

Measuring of actual spurious performance is complicated by difficulties of performing calibration in a very broad frequency range and for higher modes at the ports of Vector Network Analyser.

Practical difficulties in experimental investigation of spurious response make theoretical prediction increasingly valuable.

Reduction in number of eigenmodes leads to significant increase in the efficiency and accuracy of computation, actually allowing use of personal computers for accurate MMT modelling of spurious performance.

Specification for passive components is usually written for dominant mode only. Multiple examples considered above show it is not sufficient for controlling spurious response.

9. REFERENCES

- 9.1. Recommendation ITU-R F.1191-1, "Bandwidths and unwanted emissions of digital radio-relay systems".
- 9.2. W. Hauth, R. Keller, U. Papziner, R. Ihmels, T. Sieverding, and F. Arndt "Rigorous CAD of multiport coupled rectangular waveguide components", Proc. 23rd European Microwave Conf., Madrid, Spain, Sept. 1993, pp. 611 – 614.
- 9.3. V.V. Nikolskij et al., "Decomposition approach to the problems of electromagnetics" (Russian), Nauka Press, Moscow, 1983, ch. 1.5, pp. 30 – 32.
- 9.4. J. Ditloff, and F. Arndt, "Rigorous field theory design of millimetre-wave E-plane integrated circuit multiplexers", IEEE Trans. on MTT, vol. MTT-37, No. 2, Feb. 1989, pp. 340 – 350.

BIOGRAPHICAL NOTE

Vladimir A. Lenivenko received his MS and PhD degrees from Kiev Polytechnical Institute in 1983 and 1989. Currently he is Senior Engineer at EM Solutions Pty. Ltd. and involved in R&D and production of communication systems. His areas of interests include antennas, filters and waveguide structures with applications in microwave engineering and EMC. He is the author of more than 20 publications presented in international and national conferences.

CONDUCTED ELECTROMAGNETIC INTERFERENCE PROPAGATION THROUGH THE POWER TRANSFORMER

Jaroslav Luszcz
Technical University of Gdansk
PL 80-216 Gdansk, Sobieskiego 7, Poland,
tel (+48 58) 3472534, fax (+48 58) 3410880, e-mail jlusz@ely.pg.gda.pl

ABSTRACT

The aim of this paper is to present an experimental method to obtain a wide frequency range equivalent circuit of two windings transformer. Presented method allows to determinate especially stray capacitance of wound components. A developed equivalent circuit consists of among others ten capacitance which represents an electrostatic interaction between the windings and other elements of transformer electrically connected with earth. An experimental verification of the calculated levels of the attenuation of transformer for the voltages and currents of EMI is also presented.

Key words:

*electromagnetic compatibility EMC,
electromagnetic interference (EMI),
conducted emission, transformers*

1. INTRODUCTION.

The operation of electrical and electronic equipment usually is accompanied by effects of generation of electromagnetic interference. This interference includes:

- symmetrical voltage and current components,
- unsymmetrical voltage and current components,
- electrical field components,
- magnetic field components.

Interference can make a bad influence on other equipment's which are operated in the same electromagnetic environment. The strength of this bad influence depends on many parameters associated with every elements which are taking part in this interaction between the source of interference and the influenced receiver. We can

distinguish same general features which are determining this interaction.

This parameters are:

- level of emissivity of the source of interference,
- the quality of propagation between the source and the receiver,
- level of the susceptibility of the influenced receiver of interference.

There are two different kind of ways of interference propagation:

- by symmetrical and unsymmetrical components of the voltages and currents existing in electrical circuits (conducted RFI),
- by electrical and magnetic field components (radiated RFI).

The electric power system is the main way for transmitting symmetrical and unsymmetrical components of conducted interference. In the electric power system there are many transformers which are taking part in interference propagation. This paper will be present a method how to find out parameters of two winding transformers which is useful for calculating the attenuation level of transformers for conducted EMI.

2. A LUMPED COMPONENT EQUIVALENT CIRCUIT OF TWO WINDING TRANSFORMERS.

In Fig. 1. are shown two different kind of couplings existing in real transformers. This coupling exist between the primary winding, secondary winding and also between each winding and earth.

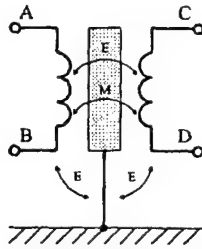


Fig. 1. Electrical and magnetic coupling existing in transformers.

A - B primary winding,
C - D secondary winding.

Proposed lumped component equivalent circuit is shown in Fig. 2. This equivalent circuit includes ten lumped capacitance which represents electrical couplings and magnetic coupling (η , k).

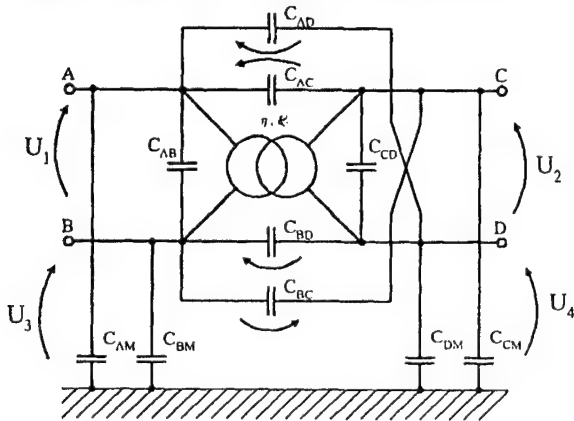


Fig. 2. Equivalent circuit of two windings transformer used to calculate wide range frequency characteristic.

C_{AB} , C_{CD} - stray capacitance of primary and secondary windings,

$C_{AM}, C_{BM}, C_{CM}, C_{DM}$ - stray capacitance between windings and ground,

$C_{AD}, C_{BD}, C_{AC}, C_{BC}$ - inter winding stray capacitance,

U_1, U_2 - primary and secondary symmetrical voltage,

U_3, U_4 - primary and secondary unsymmetrical voltage.

3. A METHOD OF DETERMINATION THE LUMPED PARAMETERS OF THE EQUIVALENT CIRCUIT.

To determinate stray capacitance is enough to measure wide range frequency characteristics of transformer with additional wire connection between windings ports A, B, C, D and ground. In Fig. 3. are shown six different primary and secondary windings connection.

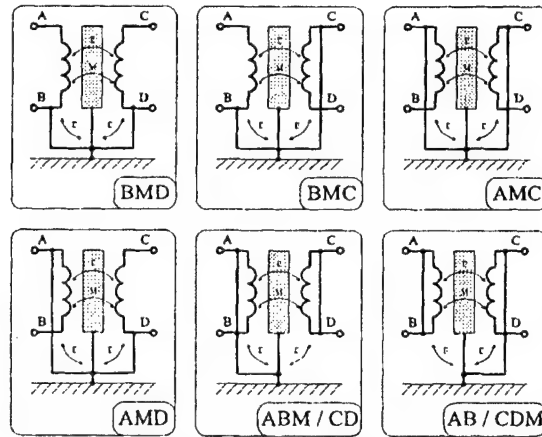


Fig. 3. Connection between windings used for measurement impedance characteristics.

For connection BMD, BMC, AMC, AMD it is possible to measure open circuit impedance characteristic ZOC and short circuit impedance characteristic ZSC. For calculating all capacitance we have to measure additionally two more characteristic for connection ABM/CD and AB/CDM. These all-additional connections allow eliminating some of the capacitance and make easier to determinate the other ones. The reduced by the additional inter-windings connection model is much simpler (Fig. 4.).

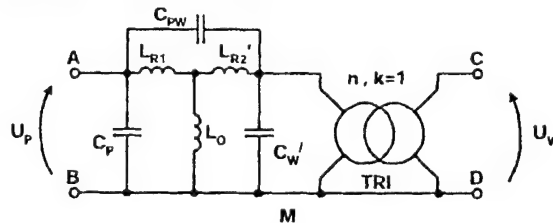


Fig. 4. Circuit model of transformer for the connection type AMD.

For the reduced transformer we can measure four different impedance characteristics:

$Z_z(f)$ - primary impedance characteristic with the secondary windings short circuit,

$Z_o(f)$ - primary impedance characteristic with the secondary windings open,

$Z_z'(f)$ - secondary impedance characteristic with the primary windings short circuit,

$Z_o'(f)$ - secondary impedance characteristic with the primary windings open.

In the reduced model (Fig. 4.) we can distinguish four different resonance circuits which are clearly noticeable on the measured impedance characteristic (Fig. 5.). By the analysing the resonance circuits and the measured characteristics it is possible to determinate the tree strays capacitance existing in the reduced model. The values of all capacitance of the full transformer model are possible to calculated

based on the analysis of the math relation between the all equivalent capacitance determined in all configuration of the different reduced models. Results of measuring ten different impedance characteristic allows to calculate ten lumped capacitance by analysing resonance frequencies. Comparison between real measured impedance characteristics and calculated by using presented equivalent circuit are shown in Fig. 5.

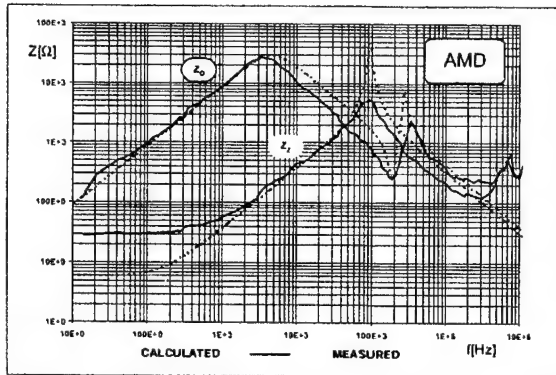


Fig. 5. An example of Z_{oc} and Z_{sc} impedance characteristic for AMD connection of transformer.

4. AN EXPERIMENTAL VERIFICATION OF CALCULATED EMI ATTENUATION LEVELS.

Based on the evaluated high frequency circuit model of transformers it is possible to calculate the attenuation of transformer for EMI (voltages and currents). The block diagram of the evaluated experimental models for EMI currents and voltages is presented in Fig. 6 and 7.

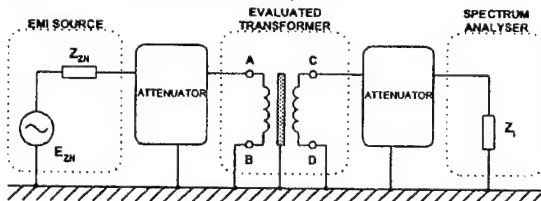


Fig. 6. Evaluated experimental model for EMI voltages attenuation measurement.

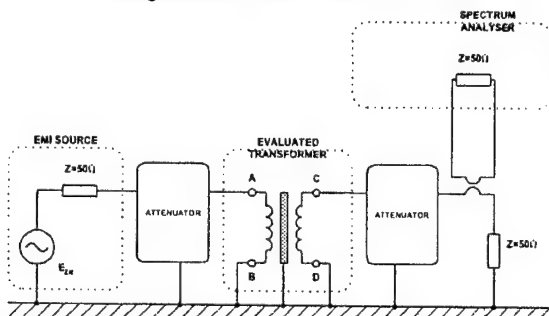


Fig. 7. Evaluated experimental model for EMI currents attenuation measurement.

The calculated and measured attenuation characteristic of evaluated transformer for EMI currents and voltages is presented in Fig. 8 and Fig. 9.

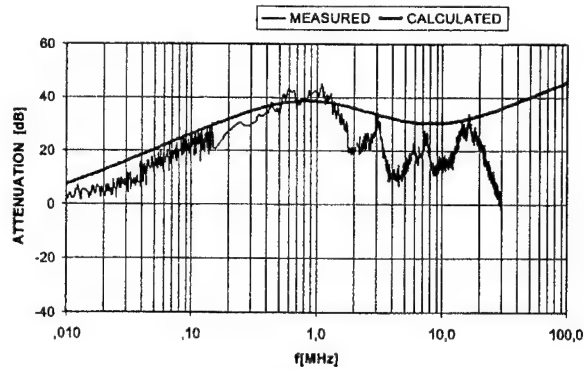


Fig. 8. Calculated and measured transformer attenuation (EMI voltages).

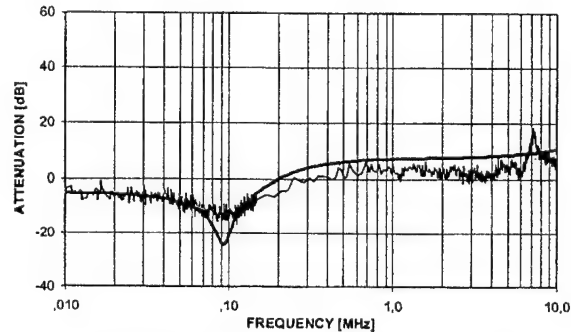


Fig. 9. Calculated and measured transformer attenuation (EMI currents).

5. CONCLUSION

Presented equivalent circuit is accurate enough to calculate wide frequency range current and voltage characteristics of transformers. Presented method allows to recognise EMI propagation process in transformer and predict the suppression level. This equivalent circuit is also useful for studying interwinding capacitive currents and their influence on the final EMI suppression frequency characteristic of transformers. The attenuation level of transformers for conducted EMI depends on the stray capacitance of the windings existing in real transformer. This capacitance determine the resonance frequencies existing in transformer which have the main influence on the EMI propagation.

6. REFERENCES

- [1] Alber F.: Distribution Transformers and EMC. *Elektromagnetische Zeitschrift* vol.115, no. 20, Oct. 1994.
- [2] Apeldorn O., Kriegel K.: Optimal Design of Transformers for High-Power High-Frequency Applications. EPE Conference. Sevilla 1995.
- [3] Baccigalupi P., Daponte P., Grimaldi D.: On Circuit Theory Approach to Evaluate the Stray Capacitances of Two Coupled Inductors. *IEEE Transaction on Instrumentation and Measurement*, Vol. 43, No. 5, October 1994.
- [4] Bastard P., Bertrand P., Meunier M.: A Transformer Model for Winding Fault Studies. *IEEE Transaction on Power Delivery*, Vol. 9, No. 2, April 1994.
- [5] Cagitore B., Keradec P. J.: The Two Winding Transformer: An Experimental Method to Obtain a Wide Frequency Range Equivalent Circuit. *IEEE Transaction on Instrumentation and Measurement*, Vol. 43, No. 2, 1994.
- [6] Degeneff R.C., Gutierrez M., McKenny P. J., Schneider J. M.: Nonlinear, Lumped Parameter Transformer Model Reduction Technique. *IEEE Transaction on Power Delivery*, Vol. 10, No. 2, April 1995.
- [7] Dellago E., Sassone G.: High frequency power transformer model for circuit simulation. *IEEE Trans. on Power Electronics* vol.12, no 4, 1997.
- [8] Francheck M. A., Mc Whirter J. H., Malewski R.: Experimental Validation of a Computer Model Simulating an Impulse Voltage Distribution in HV Transformer Windings. *IEEE Transaction on Power Delivery*, Vol. 9, No. 4, Oct. 1994.
- [9] Francisco de Leon, Semlyen A.: Complete Transformer Model for Electromagnetic Transients. *IEEE Transaction on Power Delivery*, Vol. 9, No. 1, January 1994.
- [10] Francisco de Leon, Semlyen A.: Complete Transformer Model for Electromagnetic Transients. *IEEE Transaction on Power Delivery*, Vol. 9, No. 1, January 1994.
- [11] Gutierrez M., Degeneff R.C., McKenny P. J., Schneider J. M.: Linear, Lumped Parameter Transformer Model Reduction Technique. *IEEE Transaction on Power Delivery*, Vol. 10, No. 2, April 1995.
- [12] Krasucki F.: *Electromagnetic Compatibility in Underground Mining - Selected Problems*. Warszawa, PWN 1993.
- [13] Lin C. E., Yeh C. J., Huang L. C., Cheng C. L.: Transient Model and Simulation In Three-Phase Three-Limb Transformers. *IEEE Transaction on Power Delivery*, Vol. 10, No. 2, April 1995.
- [14] Luszczyński J.: The influence of the selected transformers on the electromagnetic interference propagation. (in Polish, not published)
- [15] Luszczyński J.: Electromagnetic interference suppression in transformers. IX Oin PEC'98 Białystok - Kaunas 1998.
- [16] Massarini A., Kazimierczuk K.: Self-capacitance of inductors. *IEEE Transaction on Power Electronics* vol.12, no 4, 1997.
- [17] Morrill A. M., Caliskan A. V., Lee C. Q.: High frequency planar power transformers. *IEEE Transaction on Power Electronics*, Vol. 7, No. 3, July 1992.
- [18] Ngo T. D. K., Lai R. S.: Effect of height on power density in spiral wound power pot core transformers. *IEEE Transaction on Power Electronics*, Vol. 7, No. 3, 1992.
- [19] Nuns J., Foch H., Metz M., Yang X.: Radiated and conducted interference in induction heating equipment: characteristics and remedies. EPE Conference. 1993.
- [20] Paap G. C., Alkema A. A., Lou van der Sluis: Overvoltages in Power Transformers Caused by No-Load Switching. *IEEE Transaction on Power Delivery*, Vol. 10, No. 1, January 1995.
- [21] Papadakis B. C., Hatziaargyriou N. D., Bakopoulos J. A., Prousalidis J.M.: Three Phase Transformer Modelling for Fast Electromagnetic Transients Studies. *IEEE Transaction on Power Delivery*, Vol. 9, No. 2, April 1994.
- [22] Scheich R., Roudet J., Bigot S., Ferrieux J. P.: Common mode RFI power converter phenomenon, its modelling and its measurement. EPE Conference. Brighton 1993.
- [23] Yanada T., Matsuda T., Ichinokura O., Jinzenji T.: Performance and Noise Attenuation Mechanism of Noise Reduction Transformer. *IEEE Transaction on Magnetics*, Vol. 30, No. 6, Nov. 1994.

MULTIPLE - KNIFE - EDGE DIFFRACTION LOSS ESTIMATION BY THE LOGARITHMIC - CELL - SIMULATION METHOD

V.A.Aporovitch

Scientific Research Institute of Automation Facilities, F.Skorina ave., 117,
Minsk, 220600, Belarus, Fax. (375-17)264-24-50,
e-mail: lab9002@niisa.belpak.minsk.by

Radiowave propagation distances to 100...200 km are most important for EMC now. Diffraction factor is dominant on this distances. The paper proposes new heuristic Logarithmic-Cell-Simulation computer method for multiple-knife-edge diffraction loss estimation on such distances. It realized compare of results by this method and experimental results. Method provides quality which is better then quality of analytic methods.

1. INTRODUCTION

Some years ago distances of radio interference propagation in many hundreds of kilometers was actual. Modern situation characterizes by extremely growth of mobile and fixed telecommunications services. The density of such services grows too. Then, distances of radio interference propagation to 100...200 kilometers became the most important. But diffraction factor is a dominant one on this distances. Creation of new precise methods of diffraction loss calculation is actual. Now we can see two group of such methods. The first one is a group of analytic methods, for example Deygout's method [1] or ITU-R Recommendation [2]. The second group includes numerical methods of computer simulation, which are described in [3]. The first group uses theoretical approximations of obstacles, then the precision of calculations is not very good. The second group can give good precision, but in limited distances. The reason of this situation is the limitations on computer memory and processor's speed. For example, we want to use Transmission Line Matrix Method (TLM) [3] for propagation path with distance 100 km, height 2 km and wavelength 0.1m. We need some means of electromagnetic field strength and information on properties of space in every cell of space. (Cell is wavelength on wavelength). For example, we need 20 bytes for information on cell. Volume of the computer memory will be:

$$V_{\text{RAM}} = \frac{100000[\text{m}]}{0.1[\text{m}]} \cdot \frac{2000[\text{m}]}{0.1[\text{m}]} \cdot 20[\text{byte}] = 4 \cdot 10^{11}[\text{byte}],$$

which is impossible now.

This paper propose new Logarithmic - Cell-Simulation Method (LCSM) which includes features of the first and the second group.

2. MAIN FEATURES OF THE LCSM

We used process which is similar as wave propagation. Process is in the 2-D working space (WS) consisting of square cells. There are two kinds of cell. The first kind consists of cells, the condition of which can be change. Such cell can be in three conditions: "active", "not active" and "occupied". Every cell has 8 cell-neighbors. On every step of process we use following rules:

1. Cell is not active. The cell becomes active, if it has 3,4,5 or 6 active cell-neighbors. It remains not active in other events.

2. Cell is active. It remains active, if it has 3,4,5, or 6 active cell-neighbors and it becomes occupied in other events.

3. Cell is occupied. It remains occupied in every events.

The second kind of cells includes ones, which can not be change. Such cells need for absorbing border of WS and absorbing obstacles formation. They are always "occupied".

Initial WS has absorbing border and obstacles. There is cross of active cells - see view of WS on Fig.1. Other cells are not active.

There are cells of "transmitter" (it is center of cross) and "receiver". At the first step of process, accordance to rules 1-3, cells-neighbors of cross become active. At the second step cells-neighbors of new active cells become active, and cells of cross become occupied and so on.

If we start process, active cells and occupied ones begin to cover WS from step to step, as it shown on Fig.2. When the cell of receiver becomes active process stops.

Process is similar as radio-wave propagation with diffraction. We can use it for computer simulation.

The task is to create analytic dependencies and algorithm of this heuristic method.

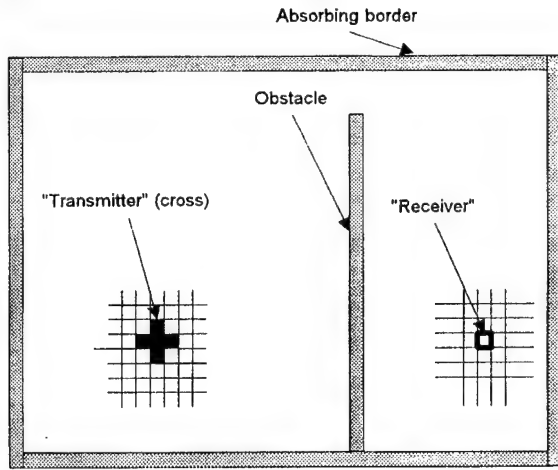


Fig. 1. View of WS

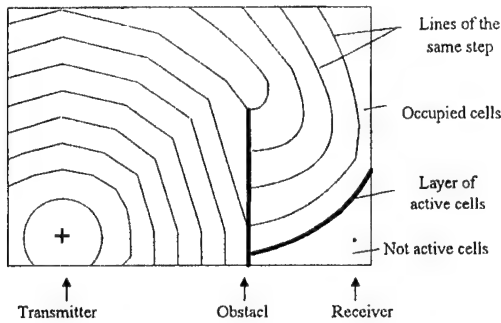


Fig. 2. View of process on WS

3. ALGORITHM OF THE LCSM

Research of proposed above process helped us to create LCSM and its algorithm.

We can define radiowave propagation loss L for isotropic loss-free antennas in dB as

$$L = L_0 + F, \quad (1)$$

where L_0 is free space loss (dB), F is an additional factor (dB). Our task was to estimate factor F by LCSM.

3.1. Diffraction on one obstacle.

Event with one obstacle and its representation on WS are shown on Fig. 3.

Parameters:

$$A = K_1 \log \left(K_2 \frac{a}{\lambda} + \sqrt{K_2 \frac{a}{\lambda} + 1} \right); \quad (2)$$

$$A + B = K_1 \log \left(K_2 \frac{a+b}{\lambda} + \sqrt{K_2 \frac{a+b}{\lambda} + 1} \right); \quad (3)$$

$$H = K_1 \log \left(K_2 \frac{h}{\lambda} + \sqrt{K_2 \frac{h}{\lambda} + 1} \right) - \frac{A - D_3}{K_3}; \quad (4)$$

where: a, b, h are parameters of obstacle from Fig 1;

A, B, H are representations of a, b, h on WS;

λ is wavelength;

k_1, k_2, k_3 and D_3 are any constants.

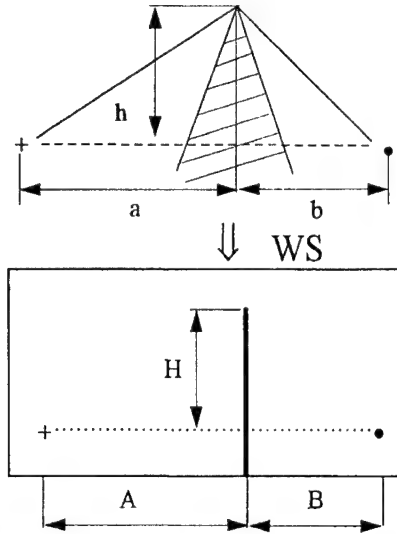


Fig. 3. Event with one obstacle and its representation on WS

Obvious,

$$F \approx T - T_0, \quad (5)$$

where T is period (in steps) from the beginning of the process on WS to moment of activation of receiver cell (Fig. 1,2) on path with obstacle (obstacles);

T_0 is a period (in steps) from the beginning of the process on WS to moment of activation of receiver cell without obstacles on the path (i.e. "free space").

When we use heuristic constants from Table 1:

$$F_L = \frac{T - T_0}{10}, \quad (6)$$

where F_L is estimation of factor F by LCSM in dB. The mean of T we can get by computer simulation of the propagation process on WS. The name "logarithmic" in LCSM appeared from formulas (1-3).

Table 1

K_1	K_2	K_3	D_3
2	50	2.1	104

Limitations are: $\frac{a}{h} \geq 10$; $\frac{b}{h} \geq 10$; $a \geq b$.

They are normal in practice. When $a < b$, we have to exchange the places of transmitter and receiver. Results of computer simulation showed a very good agreement with Fresnel formula for knife-edge obstacle [4] and its approximations [2, 5].

3.2. Diffraction on multiple (two or more) obstacles

Event with two or more knife-edge obstacles needs to prepare WS accordance with following main algorithm (see Fig.4).

1. Prepare the profile of path.
2. Find two main obstacles.
3. Find another obstacles.
4. Group obstacles in the first group near first main obstacle.
5. Group obstacles in the second group near second main obstacle.
6. Represent the second group on WS with accordance to formulas (2-4).
7. Represent the first group on WS with accordance to formulas (2-4) with assumption transmitter and receiver place exchange.
8. Correct a representation of a distance between main obstacles.
9. Build a screen between main obstacles.

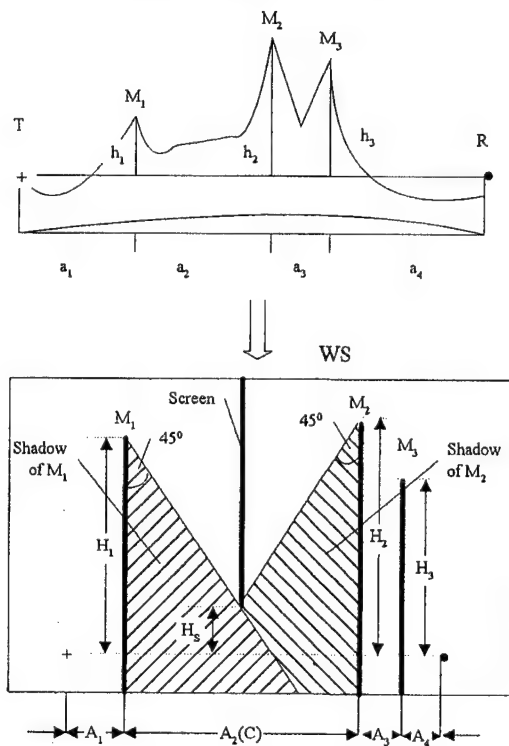


Fig. 4. Preparation of WS

We can see an example of WS preparation on Fig. 4. The real path is shown on a top. We can see 3 obstacles M_1 , M_2 and M_3 with heights h_1 , h_2 and h_3 . Distances are a_1 , a_2 , a_3 and a_4 . We define M_1 and M_2 as main obstacles and M_3 as another one. The first

group includes M_1 , the second group includes M_2 and M_3 . We represent M_2 on WS (second group) with accordance to formulas (2-4), where $a = a_1 + a_2$, $b = a_3 + a_4$, $h = h_2$, $A = A_1 + A_2$, $A + B = A_1 + A_2 + A_3 + A_4$. We represent M_3 on WS (second group), where $a = a_1 + a_2 + a_3$, $b = a_4$, $h = h_3$, $A = A_1 + A_2 + A_3$. We represent M_1 on WS (first group), where $a = a_2 + a_3 + a_4$, $b = a_1$, $h = h_1$, $A = A_2 + A_3 + A_4$. Distance between main obstacles on WS has to be:

$$C = K_1 \log(K_2 \frac{c}{\lambda}), \quad (7)$$

where c is a distance between main obstacles. Here $c = a_2$.

We have to change A_2 on C .

Screen is need to separate group of obstacles, because a shadows of them are not the same, as in real linear (non-logarithmic) space. Here shadow has a 45° behind the obstacle. And there can not be the propagation straight from M_1 to M_2 on WS. The height of screen H_s is defined by the point of shadows cross-see Fig. 4. At first we calculate H_{s1} as point of shadows cross. If $H_{s1} < 0$ then we correct it. For two obstacles $H_s = -H_{s1}$. For more then two ones $H_s = 0$.

Configuration of WS fully define the character of process. Then we begin process step by step, and can have T and F_L (16) when process achieves the point of receiver.

4. COMPARISON WITH MEASURED RESULTS

For comparison with measured results we use some paths with multiple-knife-edge obstacles. Results of comparison are in Table 2, where F_D is a loss factor, which was calculated by Deygout's method [1], F_E is a experimentally measured loss factor. N_M is amount of obstacles. The range of N_M is 2-5, the range of λ is 0.032-14.6 m.

The average means $m(F_D - F_E)$ and root-mean-square $\sigma(F_D - F_E)$, $\sigma(F_D - F_E)$ are in Table 3. We can see, that LCSM have the same or better quality, which allows practically applications.

5. CONCLUSIONS

1. For multiple-knife-edge diffraction LCSM has the same or better quality of loss estimation than analytic methods. So we can use LCSM for estimation level of interference for distances to 100...200 km.

2. We can calculate diffraction loss of all paths on modern computers, because we use logarithmic representation. Then WS is not large. It does not need large computer memory and time of processing. Really, WS volume in computer memory was not larger then 256 KB.

3. LCSM gives possibility to develop this method in directions of taking into account the shape of obstacles, absorbing and reflection properties of the ground and so on.

Table 2

N	Reference	N_M	λ , m	$F_D - F_B$, dB	$F_L - F_B$, dB
1	[6], Fig.1, path 8	5	3.88	-4.2	2.4
2	[6], Fig.1, path 24	5	6.03	11.7	-3.5
3	[6], Fig.1, path 36	4	3.88	7	-4.9
4	[7], Fig.1	3	0.36	-13	1.4
5	[7], Fig.2	4	0.36	2.8	-4.3
6	[1], Fig.10	2	0.162	0.5	4.8
7	[1], Fig.11	2	0.167	1	1.4
8	[1], Fig.12	2	0.167	-2	-0.6
9	[1], Fig.13	3	0.162	0.5	-4.4
10	[1], Fig.14	5	0.167	-3	5.3
11	[1], Fig.15	2	1.875	-0.5	-4.0
12	[1], Fig.16	2	0.122	-3	3.2
13	[1], Fig.17	2	0.122	0.5	1.3
14	[1], Fig.18	2	0.122	1.5	7.6
15	[1], Fig.19	2	0.122	5	-1.6
16	[8], Fig. 4.1	3	1.44	4	-9.6
17	[9], Fig. 34 a)	3	14.6	-5.3	-7.0
18	[9], Fig.35 a)	3	14.6	-11.7	-1.3
19	[9], Fig. 36 b)	2	10.7	-7.3	-0.2
20	[10], Fig. 3, b=10m	2	0.032	6.2	0.1
21	[10], Fig. 3, b=30m	2	0.032	4.4	-3.2
22	[10], Fig. 3, b=60m	2	0.032	5.3	-6.1
23	[11], path 9	3	6.03	4.5	2.2
24	[11], path 13	3	3.88	-2	4.6

Table 3

N_M	$m(F_D - F_B)$, dB	$m(F_L - F_B)$, dB	$\sigma(F_D - F_B)$, dB	$\sigma(F_L - F_B)$, dB
2	0.97	0.23	4.25	3.9
>2	-1.89	-1.59	3.64	3.61
Total	-0.46	-0.68	5.67	4.23

6. REFERENCES

1. J.Deygont, "Multiple Knife-Edge Diffraction on Microwaves", IEEE Trans., Vol.AP-14, NO.4, pp. 480-489.
2. ITU-R Recommendation PN.526-3, "Propagation by Diffraction", International Telecommunication Union, Geneva, 1995, 1994 PN Series Volume, pp. 129-149.
3. Jose Perini, "Numerical Methods in EMC - an Update", Proceedings of Zurich Symposium on Electromagnetic Compatibility, March 7-9, 1995, pp.3-19.
4. M.P.Doluhanov, "Radio Wave Propagation", "Sviaz", Moscow, 1972 (Russian).
5. M O Al-Nuaimi, "Interference Reduction at Microwave Radio Terminals Using Site Shielding", Proceedings of International Wroclaw Symposium on Electromagnetic compatibility EMC-92, Wroclaw, Poland, pp.698-702.
6. V.V.Kuznetsov, E.V.Zubricki, "Experimental Research of TV-Signal Passing on Mountain Paths" (Russian), Proceedings of Buriat Institute of Natural Sciences, Issue 1, Physical Series, "Propagation of Microwave in Mountain Locality Conditions", Academy of Science, Siberian Section, Ulan-Ude, USSR, 1968, pp.116-138.
7. V.N.Troicki, "Diffraction of Microwave on Mountain Ranges", (Russian), Academy of Science of the USSR, Institute of Radioengineering and Electronics, Collection "Radiowave propagation", Moscow, "Nauka", 1975, pp.154-186.
8. Ch.C.Cidipov, "Microwave propagation in Mountain Locality", "Nauka", Novosibirsk, 1977 (Russian).
9. U.I. Davidenko, N.T.Nechaev, "Features of VHF Radiowave propagation", Ministry of Defense of the USSR Publisher, Moscow, 1960 (Russian).
10. T.Orozobakov, "Diffraction propagation of Microwave Behind Two Obstacles" (Russian), Academy of Science, Institute of Physics and Mathematics, Collection "Microwave propagation in Mountain Locality", "Ilim", Frunze, USSR, 1971, pp.20-29.
11. Ch.C.Cidipov, V.N.Abarikov, V.I.Gorjachkin, V.V.Kuznetsov, "Investigation of TV-Transmitter Field Strength Behind Line-of-Site", (Russian), "Electrosviaz", No2, 1963, pp.16-21.

BIOGRAPHICAL NOTE

V.A.Aporovitch works as chief Specialist of Research Institute of Automation Facilities in Minsk (Belarus). Doctor of Science (1984). Main scientific interests are EMC and digital information processing. He is author of 49 papers and inventions.

FREQUENCY-DOMAIN AND PULSE RADIATION OF BROADBAND MATCHED ANTENNA ARRAY

Gennadij G. Chavka, Maciej Sadowski

Technical University of Białystok, Grunwaldzka str. 11/15

15-893 Białystok, Poland, fax: (085) 742 16 57, e-mail: ggc@cksr.ac.bialystok.pl

This paper deals with the mathematical model of the multiport broadband matching problem and results of frequency-domain and pulse simulation of matched antenna array. It is used a complex normalized scattering matrix for multiport network connection. The power parameters are based on the singular expansion of the multiport scattering matrices and may be used for the matching network optimization and EMC time-frequency analysis of antenna array.

1. INTRODUCTION

The EMC problem of phased antenna arrays are closely connected with antenna broadband matching problems and an analysis of time and frequency-domain power and propagation characteristics. The solution of this problem may be carried out by use of the scattering matrices normalized to complex impedance's [1,2].

This paper presents the mathematical model and results of frequency-domain and pulse simulation of matched antenna array. The power parameters based on eigenvalues of the dissipation matrices of the antenna array are introduced. These parameters allow to estimate the power transmitter properties, as well as the radiation directivity of the antenna arrays without and with optimal broadband antenna matching networks.

2. SCATTERING MATRICES OF DOUBLE-SIDE AND CASCADE CONNECTION OF MULTIPORTS

Complex incident and reflected waves and block relations of the scattering matrix S_N of double-side multiport network normalized to separate complex internal source impedance's z_α and z_β for ports "α" and "β" are given by [3,4] (Fig. 1,a):

$$\begin{cases} 2R_{\alpha,\beta}^{0.5} \mathbf{a}_{\alpha,\beta} = \mathbf{U}_{\alpha,\beta} + \mathbf{z}_{\alpha,\beta} \mathbf{I}_{\alpha,\beta}, \\ 2R_{\alpha,\beta}^{0.5} \mathbf{b}_{\alpha,\beta} = \mathbf{U}_{\alpha,\beta} - \mathbf{z}_{\alpha,\beta}^* \mathbf{I}_{\alpha,\beta}, \end{cases} \quad (1)$$

$$\begin{bmatrix} \mathbf{b}_\alpha \\ \mathbf{b}_\beta \end{bmatrix} = \begin{bmatrix} S_{\alpha\alpha} & S_{\alpha\beta} \\ S_{\beta\alpha} & S_{\beta\beta} \end{bmatrix} \begin{bmatrix} \mathbf{a}_\alpha \\ \mathbf{a}_\beta \end{bmatrix}, \quad (2)$$

where $\mathbf{U}_{\alpha,\beta}$ and $\mathbf{I}_{\alpha,\beta}$ - voltage and current vectors; $\mathbf{R}_{\alpha,\beta}$ - real parts of diagonal matrix of impedance's $\mathbf{z}_{\alpha,\beta}$; superscript (*) denotes the complex conjugate value.

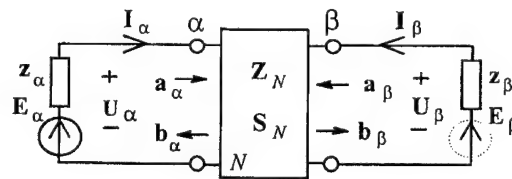


Fig. 1. Complex normalization of scattering matrix of double-side n -port.

For reciprocal coupling network N :

$$S_{\alpha\alpha} = S_{\alpha\alpha}^t, S_{\beta\beta} = S_{\beta\beta}^t, S_{\alpha\beta} = S_{\beta\alpha}^t \quad (3)$$

and for lossless network scattering matrix S_N is unitary:

$$S_N S_N^+ = 1, \quad (4)$$

superscript (+) denotes the hermit conjugate value.

The scattering matrix S_N of the coupling network is connected with impedance matrix Z_N by:

$$S_N = R_o^{-0.5} (Z_N - Z_o^*) (Z_N + Z_o)^{-1} R_o^{0.5}, \quad (5)$$

where $R_o = \text{Re} Z_o$, $Z_o = \{z_\alpha, z_\beta\}$ - diagonal matrix of impedance's (Fig. 1). For one-side excitation ($\mathbf{a}_\beta = 0$):

$$\mathbf{b}_\alpha = S_{\alpha\alpha} \mathbf{a}_\alpha, \mathbf{b}_\beta = S_{\beta\alpha} \mathbf{a}_\alpha, \mathbf{a}_\alpha = 0.5 R_\alpha^{0.5} \mathbf{E}_\alpha. \quad (6)$$

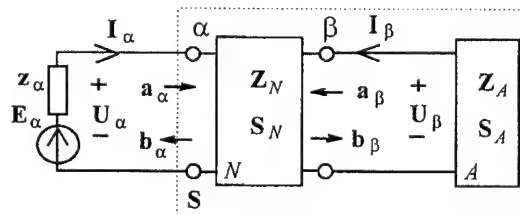


Fig. 2. Cascade connection of multiport networks.

For the cascade connection of multiport networks (Fig.2) **broadband matching problem** is **synthesis** of optimal coupling network N for a **maximization** of the total average power absorbed by n -port antenna in the given frequency band. In this case complex incident and reflected waves for ports " β " are connected by the scattering matrix of the given n -port antenna:

$$\mathbf{a}_\beta = \mathbf{S}_A \mathbf{b}_\beta, \quad (7)$$

\mathbf{b}_β - incident, \mathbf{a}_β - reflected waves for antenna; \mathbf{S}_A - scattering matrix of n -port antenna, normalized to diagonal matrix of *complex conjugate* impedance's \mathbf{z}_β^* :

$$\mathbf{S}_A = \mathbf{R}_\beta^{-0.5} (\mathbf{Z}_A - \mathbf{z}_\beta) (\mathbf{Z}_A + \mathbf{z}_\beta^*)^{-1} \mathbf{R}_\beta^{0.5}. \quad (8)$$

Then the total scattering matrix of the cascade connection of multiport networks is given by:

$$\mathbf{S} = \mathbf{S}_{\alpha\alpha} + \mathbf{S}_{\alpha\beta} \mathbf{S}_A (\mathbf{1} - \mathbf{S}_{\beta\beta} \mathbf{S}_A)^{-1} \mathbf{S}_{\beta\alpha}. \quad (9)$$

The total normalized average power absorbed by the whole multiport network (Fig.2) for the given excitation vector \mathbf{a}_α is given by **Rayleigh ratio** [3,4]:

$$\frac{P}{P_{\max}} = \frac{\mathbf{a}_\alpha^+ (\mathbf{1} - \mathbf{S}^+ \mathbf{S}) \mathbf{a}_\alpha}{\mathbf{a}_\alpha^+ \mathbf{a}_\alpha} = \frac{\mathbf{a}_\alpha^+ \mathbf{D} \mathbf{a}_\alpha}{\mathbf{a}_\alpha^+ \mathbf{a}_\alpha}, \quad (10)$$

where $\mathbf{D} = \mathbf{1} - \mathbf{S}^+ \mathbf{S}$ - **dissipation** matrix of whole network. It is **hermetian** matrix $\mathbf{D} = \mathbf{D}^+$ and **unitary similar** to diagonal **positive real** matrix of its **eigenvalues** d_i :

$$\mathbf{D} = \mathbf{V} \{d_i\} \mathbf{V}^+, \quad d_i = d_i^*, \quad \mathbf{V} \mathbf{V}^+ = \mathbf{1}, \quad (11)$$

where \mathbf{V} - complex **unitary** matrix (called the **modal**) of the **eigenvectors** of the matrix \mathbf{D} .

It is known, that the Rayleigh ratio has stationary values equal to the eigenvalues of the corresponding hermetian matrix; this means that the normalized total average power P/P_{\max} is limited by the **minimum** and the **maximum** eigenvalues of the dissipation matrix:

$$d_{\min} \leq \mathbf{a}_\alpha^+ \mathbf{D} \mathbf{a}_\alpha / \mathbf{a}_\alpha^+ \mathbf{a}_\alpha \leq d_{\max} \quad (12)$$

and then the **optimization** and the **matching** problem is synthesis of $2n$ -port optimal coupling network for **maximization** of the **minimum** or **maximum** eigenvalues of the dissipation matrix \mathbf{D} at the given frequency band.

There are very kinds of solutions of this task; in this paper it is used one of these - synthesis of $2n$ -port coupling network as n two-port **optimal broadband matching networks** for given excitation vector \mathbf{a}_α .

Before the eigenvalues the main power parameters of the multiport broadband matched antenna array are:

- **partial antenna input impedance's** z_{Ai} and **partial traveling-wave ratio**:

$$z_{Ai} = U_{\beta i} / I_{\beta i}, \quad s_{Ai} = \frac{z_{Ai} - z_{\beta i}^*}{z_{Ai} + z_{\beta i}}, \quad TWR_{Ai} = \frac{1 - |s_{Ai}|}{1 + |s_{Ai}|}; \quad (13)$$

- an **equivalent traveling-wave ratio**:

$$TWR_{eq} = \frac{1 - |s_{ekv}|}{1 + |s_{ekv}|}, \quad |s_{eq}|^2 = 1 - P/P_{\max}, \quad (14)$$

- an antenna **directivity**

$$D_{ant} = |e_{ant}|^2 r^2 / 60 P_{ant} \quad (15)$$

- and an **equivalent isotropic radiated power** (EIRP) of the antenna array:

$$P_{efant} = P_{ant} D_{ant}. \quad (16)$$

The introduced power parameters are used for the computer simulation of broadband matched antenna array.

3. POWER PARAMETERS OF BROADBAND MATCHED ANTENNA ARRAY

Consider the power parameters of 8-port linear antenna array without and with optimal broadband lossless matching networks to operate as a base station of system GSM in frequency band 890-960 MHz (Fig.3). Let a length of radiators equal to 13cm., a diameter - 5mm., a length of the array - 70cm, distance to reflector - 8cm; the reflector consists of 46 grounded monopoles.

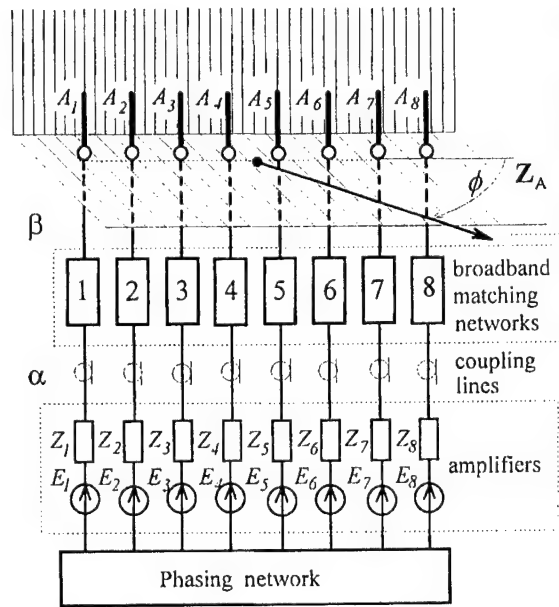


Fig.3. Structure of broadband matched antenna array.

In this paper, a computer simulation of time and frequency-domain characteristics of this antenna array for given 8 excitation amplifiers (1W every) is carried out.

The computation method is based on the frequency-domain mixed-potential electric field integrals combined with the method of moments for a polynomial approximation of the current distribution in all elements of the antenna array [5]. It has been taken into account also a radiation of distributed and „lumped” elements of the optimum matching device for the given array. The influence of array radiation and the mutual coupling between array's elements is taken into account automatically during of the integral equation formulation.

Partial input impedance's and corresponding TWR characteristics (13) for in-phase excitation of the antenna arrays are shown in Fig.4,5. We see that input impedance's are similar. The 1st and 8th dipoles (external) have the most change of the input impedance: a resistance about 250Ω and a reactance about -150Ω in frequency band. For others dipoles average values amounts: the resistance about 200Ω and the reactance about -100Ω .

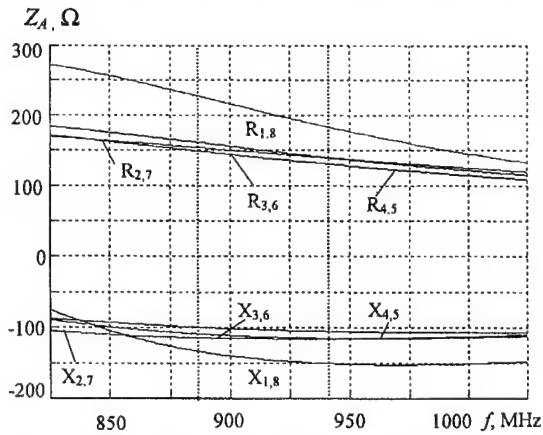


Fig.4. Partial impedance of input ports antenna array.

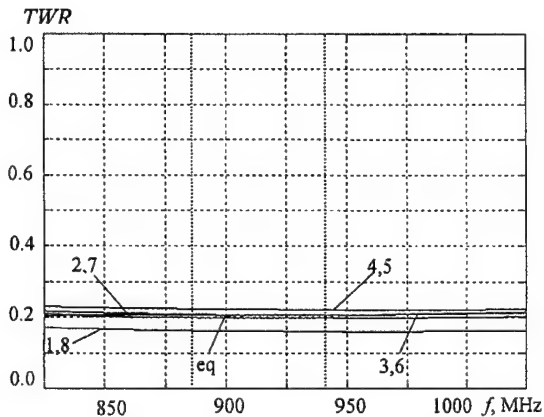


Fig.5. TWR characteristics of antenna array.

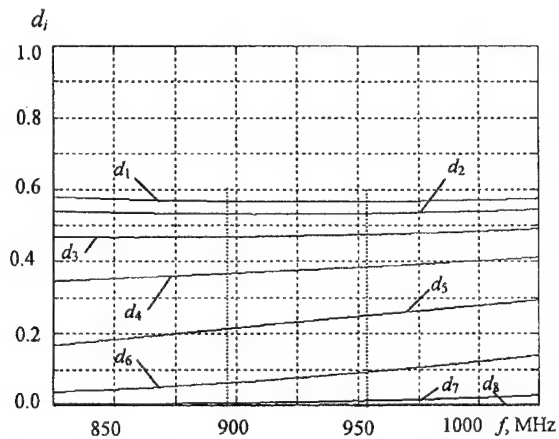


Fig.6. Eigenvalues characteristics of antenna array.

Partial and equivalent (14) TWR characteristics in Fig.5 have values about 0.2 in the given frequency band. It's mean that the almost half of delivered power to antenna array without of the broadband matching is reflected back to generators (see (14), Fig.9).

Eigenvalues characteristics of the dissipation matrix (11) of the antenna array without of the broadband matching are presented in Fig.6. We see that the highest eigenvalues has values about 0.6 and the smallest it - about 0. It's means that the normalized total average power is limited by these values (see formula 12, Fig.9).

Optimal matching networks have been synthesized for the partial impedance's (Fig.4) of the antenna array (four pair networks because of an array symmetry, Fig.3). They are 2nd order Fano matching circuits synthesized by use of a program DIASP realizing conjugate gradient methods [6]. Characteristics of TWR, power and eigenvalues become improved after include of the matching networks between dipoles and generators.

These characteristics with optimal broadband matching are presented in Fig.7,8,9. As evident from Fig.7 TWR values are situated between 0.9 and 1.0 in given frequency band; values of TWR are raised as compared with characteristics without of matching network.

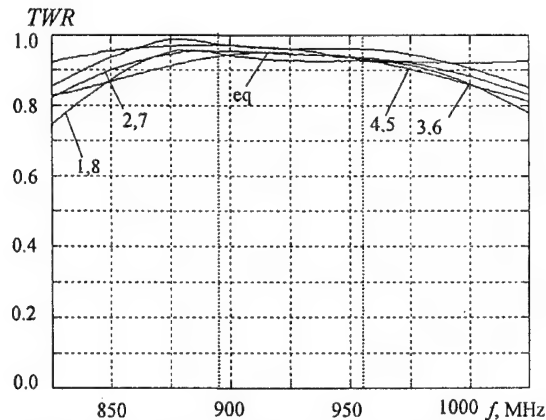


Fig.7. TWR characteristics with matching network.

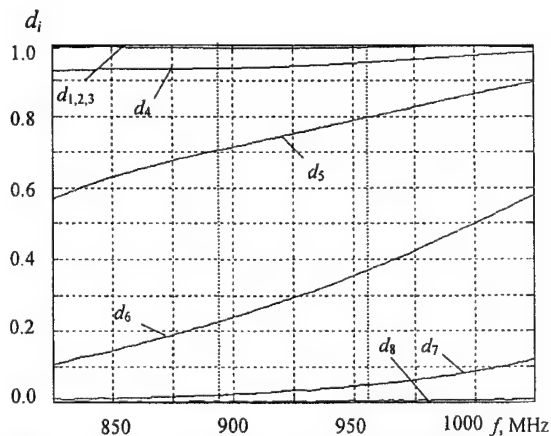


Fig.8. Eigenvalues characteristics with matching networks.

The eigenvalues characteristic of the dissipation matrix of the cascade connection of the eight matching networks with given antenna array (11) (Fig.3) are presented in Fig.8. We can see that eigenvalues characteristics raised too, as compared with the characteristics without matching networks. The three highest eigenvalues are almost the same and nearly equal 1. It's mean that we can achieve the total normalized average power absorbed by the whole multiport network in the given frequency band nearly equal 1 too by use of corresponding excitation eigenvector. Detail analysis shows that an in-phase excitation vector corresponds to the maximum eigenvalue d_1 of the dissipation matrix of the antenna array. It is remind that optimal matching networks are synthesized really for the in-phase excitation of the antenna array. Then for the lossless matching networks the total normalized average power of the antenna array is equal near 1 for this in-phase excitation.

Frequency characteristic of the total average power of the antenna array are showed in Fig.9. The summary antenna power with the matching networks is highest near 2 times and achieve value $8 \cdot 1W = 8W$ then without its. This result follows directly from eigenvalues characteristics (Fig.6,8 and formula 12).

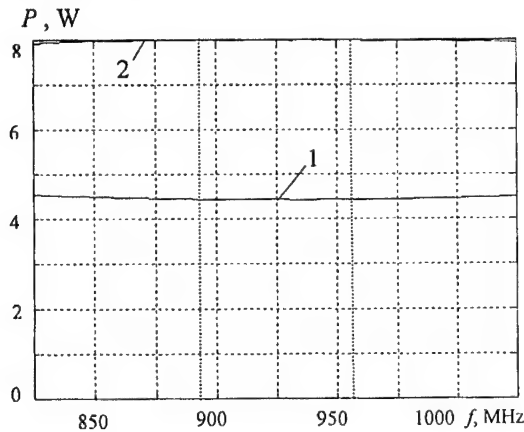


Fig.9. Summation power characteristics of antenna array without (1) and with matched networks (2).

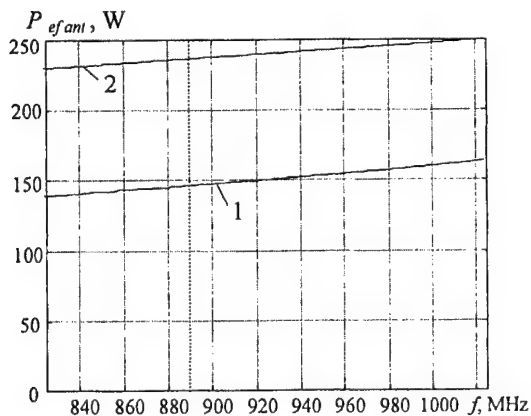


Fig.10. EIRP characteristics without (1) and with (2) matching networks.

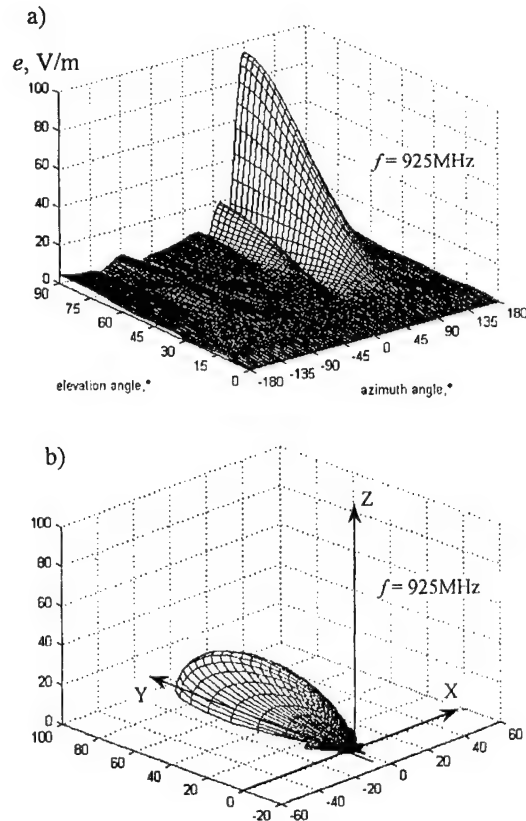


Fig.11 3D radiation pattern of antenna array: a) Cartesian coordinates, b) spherical coordinates.

In Fig.10 it is shown characteristics of the equivalent isotropic radiated power (EIRP) of the antenna array without and with optimal matching networks (16). The antenna directivity (15) is equal 30 (~15dB) and value of EIRP achieves 240W (!) with use of eight amplifier 1W every. This is a consequence of the optimal matching of the antenna array.

3D radiation patterns of the antenna array for excitation frequency 925MHz for Cartesian and spherical coordinates are shown in Fig.11. We can see a whole form of the radiation patterns and determine a side- and back-lobe levels; a main-lobe beamwidth is near 20° .

4. PULSE RADIATION OF ANTENNA ARRAY

Pulse radiation analysis of the antenna array in time-domain is executed. The radio-impulse is used in form of a rectangular cosine wave on frequency 925 MHz. The period of the pulses is 100ns, the time of cosine wave is 25ns. The analysis is carried out for 90° elevation and two azimuth directions: 90° and 45° . At first it was computed a spectrum of the radio pulse, next it was executed a product of the radio pulse spectrum and electromagnetic field intensity at the given azimuth direction. Finally an inverse Fourier transform was calculated. Results are shown on Fig.12, 13.

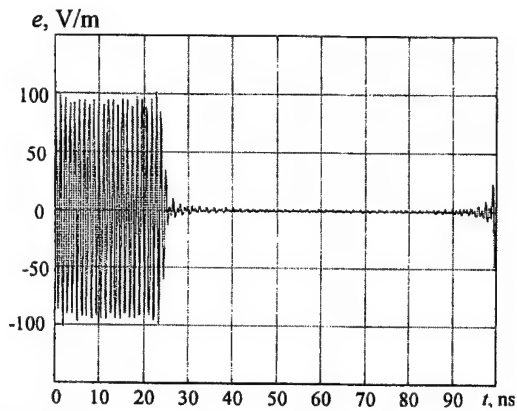


Fig.12. Time-domain response for radio pulse, $\phi = 90^\circ$

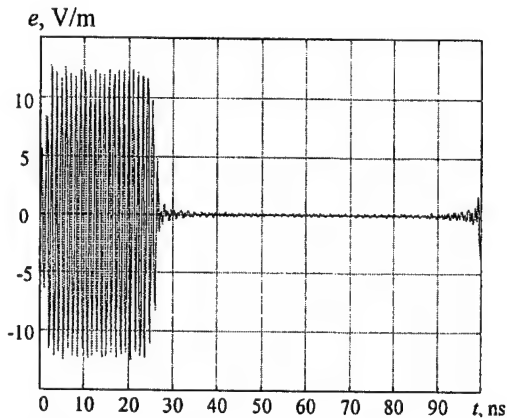


Fig.13. Time-domain response for radio pulse, $\phi = 45^\circ$

For 90° azimuth direction time-domain pulse enough precisely corresponds with original radio pulse. On 45° azimuth direction we can see distortion of radio pulse, especially on the first five ns. The high changes of electromagnetic pulse intensity on this direction are reason of this shape of the pulse. On direction main lobe (azimuth 90°) time-domain field pulse has very high level - about 100V/m; for direction 45° field pulse level is small as it is shown on Fig.12, 13.

5. CONCLUSIONS

This paper presents two aspects: a new approach to broadband matching of phased antenna array; time - and frequency-domain power and radiation characteristics of matched arrays. The proposed power parameters are based on the singular expansion of the dissipation matrix of the antenna array and a whole multiport subsystem. They may be used for the matching network optimization and EMC time-frequency analysis of antenna array.

The work was partially supported under the rector's project by Technical University of Białystok.

6. REFERENCES

1. W.K.Chen, "Broadband Matching: Theory and Implementations" (English), World Scientific Publishing Co. Pte. Ltd., 1988.
2. R.W. Newcomb, "Linear Multiport Synthesis", McGraw Hill Book Co., New York, 1966.
3. G.Chavka, "Power Parameters of the Scattering Matrix Normalized to Complex Loads" (English), 2nd International Conference on Advanced Methods in the Theory of Electrical Engineering, AMTEE '95, Plzeň, Czech Republic, 1995, pp.197-200.
4. G.Chavka, "Broadband Matching of Complex n-Port Loads", Proceedings of European Conference on Circuit Theory and Design, ECTTD'99, vol.1, pp.623-626, Stresa, Italy, 29.08-2.09.1999.
5. A.R. Djordjević, M.B. Baždar, T.K. Sarkar, R.F. Harrington, "Analysis of Wire Antennas and Scatterers: AWAS for Windows", Artech House, 1995.
6. O.V. Alekseev, A.A. Golovkov, G.G. Chavka, "Computer aided design of radio transmitters" (Russian), Radio and communication, Moscow, 1987.

BIOGRAPHICAL NOTE



Gennadij G. Chavka was born in Russia in 1942. He received M.Sc., Ph.D. and D.Sc. degrees from Saint-Petersburg State Electrotechnical University, Russia in 1965, 1969 and 1987 respectively. Since 1988 he is Professor of St.-Petersburg State Electrotechnical University, Department of radio electronic equipment,

and since 1993 he is Professor of Electrical Engineering, Technical University of Białystok too. He is a member of Institute of Electrical and Electronics Engineers, USA. The main interests are: radiocommunication, antennas and antenna arrays, network synthesis, broadband radio transmitters, multiport transmitting and receiving subsystems, CAD of radio equipment. He is the author of 5 books, 25 patents, over 150 papers and conference presentations.



Maciej Sadowski was born in Białystok, Poland in 1971. He received M.Sc. degree from Technical University of Białystok 1996. Since 1996 he is assistant in Technical University of Białystok. The main interests are: radiocommunication, antennas and antenna arrays, CAD of antenna beam former.

RECEPTION CONDITIONS OF COMMUNICATION SATELLITE IN POLAND

Wojciech J. Krzysztofik

Wroclaw University of Technology,
Institute of Telecommunication & Acoustics, The Radio Department
Wybrzeże Wyspiańskiego 27, 50-370 Wrocław, POLAND
Email: wojka@zr.ita.pwr.wroc.pl

An extensive set of measurements, for the purpose of mapping of the satellite EM-field coverage over the Poland was done. The power level and SNR of signals (beacon and communication – TVSat) received from a few satellites (EUTELSAT, ASTRA, INTELSAT) were monitored and collected on two measuring setups, fixed - situated in Wrocław, and mobile one used all over the Poland territory. Measuring setups are fully automatic, it means the setup control, data acquisition and storing are controlled by PC computer. Trace of a trip and a geographical position of the measuring point was determined by GPS navigational terminal. The measured power levels are compared with EIRP footprints published by satellite system administrations. Obtained results of SNR ratio permit to qualify the satellite television signals reception, especially that which are well popular in the Poland.

1. INTRODUCTION

During the last decade there was a tremendous increase in the number of satellite communication users in Poland. Most popular satellite service became direct – satellite-television (DBS), other – satellite navigation GPS, many VSAT system clients, and recently global telephony via IRIDIUM or GLOBALSTAR satellite systems. The field strength specifications associated with modern communications devices are steadily approaching the limits of radio design capabilities. Consequently, there is a demand for radio test engineers to measure field strength performance of increasingly higher accuracy. Information available on common market, concerning most satellites are insufficient for systems designer. The World Satellite Almanac does not guarantee that the values expressed therein will necessarily correspond to performance levels found in the field. So, more data have been still needed to characterize the propagation impairments for satellite systems planning. Broadcasting by satellites leads to propagation considerations that are not entirely comparable with those occurring in the fixed-satellite

service. Attenuation data for space-to-Earth direction are needed in the form of statistical averages and/or contour maps of attenuation and depolarization for large areas [1]. Specific coordination problems may arise at the margin of the service area between satellite broadcasting systems and terrestrial or other space services [2]. In the case of space-to-Earth paths for broadcasting systems, several propagation effects (e.g. tropospheric absorption, attenuation, and depolarization; and ionospheric scintillation and Faraday rotation; local environmental effects, including attenuation by buildings and vegetation) may require consideration. Each of these contributions has its own characteristics as a function of frequency, geographic location and elevation angle. This paper discusses some of these effects and refers them to experimental results were done.

2. TASK AND MEASUREMENTS TO BE PERFORMED

The object of the monitoring at present day is classified into the two classes of geostationary and low altitude satellites. Considering the importance in space telecommunications, geostationary satellites are taken as the primary object of monitoring. In principle, the tasks entrusted to radio monitoring station for space services do not differ from those of terrestrial radio monitoring station. However, they are performed under dissimilar conditions, which result from the fact that a space station revolves as a satellite of the Earth and a basic knowledge of its orbit is a prerequisite for any observations and measurements. The functions of the radio monitoring station for space services can be outlined as follows:

- regular and systematical observation of the radio-frequency spectrum with the aim of detecting and identifying space station emissions;
- determination of occupancy and percentage use of transponders;
- measurements and recording of the characteristics of space station emissions;

- investigation and elimination of harmful interference caused by space stations, if appropriate, in cooperation with terrestrial and other space monitoring stations;
- performance of measurements and recordings in context of technical and scientific projects.

There are number of factors in providing the above-mentioned capabilities which must be balanced against cost, frequency coverage, system sensitivity, antenna slewing rate, degree of sophistication of signal analysis instrumentation, and degree of automation of measurements.

3. EQUIPMENT AND FACILITY

In general, as in more conventional monitoring surveillance, equipment for monitoring signals from spacecraft must have adequate flexibility to cover a wide range of frequencies, in contrast to the spot frequency coverage that suffices for the needs of research or operating space agency. The location of the monitoring station should be such that interference from man-made signals and noise is at a minimum.

A highly automated and sophisticated satellite monitoring system, fully steerable, with continuous frequency coverage across the 11 to 12.5 GHz spectrum, and sensitive enough to give carrier-to-noise ratios of at least 26 dB on all signals of interest was designed [4].

3.1. Antennas

Primary feed parabolic reflectors of 1.8 m and 1.3 m in diameter are used on fixed and mobile measuring setups, respectively. Because of quite sharp directivity of such high-gain (44 dB) antennas, considerable care is required in acquiring and tracking the signals from spacecraft. Variations in the polarization of the received field occur owing to the rotation of the spacecraft and to effects on the propagation path (Faraday effect). The orientation of the polarization plane of a linearly polarized signal transmitted by a geostationary space station relative to the horizontal plane of the observation point depends on the geographical location of the latter relative to the satellite. The antenna can be pointed in azimuth within the limits $\pm 90^\circ$ and in elevation within the limits $0 - 90^\circ$, roughly to start with, by means of the antennas manual system.

3.2. Receiver

For economic reasons and because a general coverage receiver is required at monitoring station, the extremely low noise figures possible for fixed-frequency receiver used for space research and operational purposes are not equaled by available monitoring receivers. However, the receiver should have a relatively low noise figure and be capable of receiving signals in the order of a few hundredths of microvolt or less at the receiver input.

Receiver should have a wide range of adjustable bandwidth to permit reception of both wide-band (communication signals) and narrow-band (beacon)

transmission from spacecraft. The figure of merit for measurement apparatus with an antenna diameter of the order 1.8 m may attain 20 dB/K at frequency of 11 GHz. The sensitivity of such an earth monitoring station is adequate for analyzing the emission characteristics of most existing and notified satellites.

To facilitate "acquisition" of the signal from spacecraft, it is desirable to be able to sweep a narrow band of frequencies automatically and to record the received signals.

A block diagram of a small earth monitoring station is shown in Fig. 1.

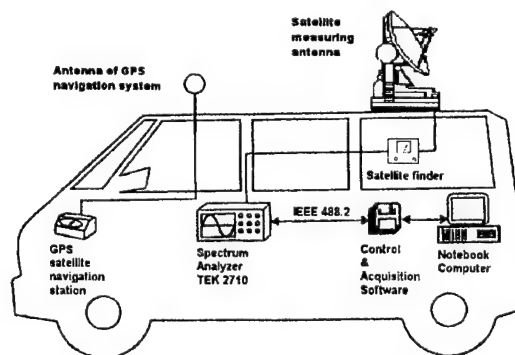
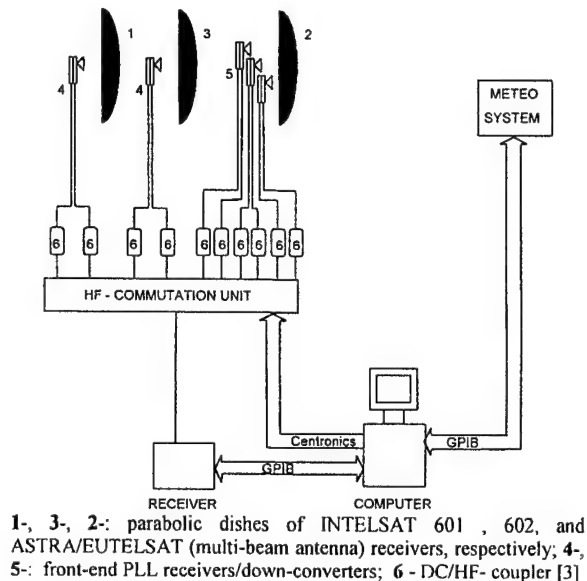


Fig. 1. Block diagram of the satellite monitoring systems: a) ground station situated in Wroclaw, and b) mobile equipment

Details concerning the fixed ground station are available in [3],[4],[5].

The satellite-measuring vehicle breaks new ground in mobile monitoring systems [6]. At last, a vehicle is available fully equipped with both self-energizing measuring set-up with receiver, computer, antenna and AC power supply or fly-away single reception system capable up to -60 dBW of EIRP in compliance with all satellite system regulations. Mobile measuring set-up can be easily transported using a mini-van or limousine

car and can be rapidly deployed for action by one operator. Irrespective of location and conditions, the collapsed measuring antenna can be deployed in either vehicle roof mount or flyaway ground mount situations.

4. SATELLITE LINK BUDGET

Prior to the establishment of a satellite link an essential preliminary step is the calculation of signal levels through the system, to ensure that they are adequate to provide the quality of service required. When computing link budgets, account must be taken of the form of modulation and coding (if used) and atmospheric/propagation losses, which are dependent on the frequencies, as these determine service availability (i.e. the percentage of time that the link provides acceptable service).

The system signal-to-noise performance for satellite receive terminal is directly related to the carrier-to-noise power ratio (CNR) defined by the following equation

$$\text{CNR} = \text{EIRP} - L_o - L_m + G - 10 \log kTB \quad (1)$$

where EIRP [dBW] is isotropic radiated power transmitted by satellite, $L_o = (4\pi R/\lambda)^2$ is the free-space loss, R is the propagation path length, L_m is the loss due to atmospheric absorption, G is a gain of receive antenna, and last component represents noise introduced by the antenna, LNB and system components.

For the sake of completeness, the preliminary Ku-band propagation effects are listed below:

1. *Rain attenuation.* Signal attenuation due to rain is the most severe propagation effect at Ku-band. This kind of loss can exceed 5 dB for small percentages of time.
2. *Gaseous absorption.* A loss close to 1 dB can be associated with oxygen and water vapour absorption.
3. *Cloud attenuation.* Clouds attenuation along the propagation path can attenuate Ku-band frequencies. Typical values are in order of 1 dB or more.

The rain attenuation is the dominant effect at frequencies above 10 GHz. As attenuation increases, so does emission noise. For earth stations with low-noise front-ends, this increase of noise temperature may have a greater impact on the resulting CNR ratio than attenuation itself.

The atmospheric contribution to antenna noise in a ground station may be estimated with the equation

$$T_s = T_m (1 - 10^{-L_m/10}) \quad (2)$$

T_s is a sky-noise temperature as seen by the antenna, L_m is a path attenuation, and T_m is the effective temperature of the medium.

The effective temperature is dependent on the contribution of scattering to attenuation and on the physical extent of clouds and rain cells on vertical variation of physical temperature of the scatterers, to a lesser extent, on antenna beamwidth. The effective temperature of medium has been determined to lie in

range 260-280 K for rain and clouds along the path at frequencies between 10 and 30 GHz.

A broadcasting satellite must serve a large area, preferably with the same quality of service throughout for the same time percentage [2]. However, portions of the service area (e.g. within different climatic zones) may be affected differently by certain propagation effects. Such differences can be characterized with coordinated measurements performed at several locations distributed over the service area. Such data are useful both for evaluating subscriber equipment requirements and for determining interference conditions at the borders of the service area, but these data are scarce.

Reliable statistics are needed to predict the above effects for slant-path applications. Note that each effect is not only a function of frequency, but also of location, path elevation angle and season (time). Since it is not possible to make observations at every location, the region of interest can be divided into several rain and atmospheric climate zones that have a certain statistical attribute. The carefully planned experiment can lead to a wealth of well qualified propagation statistics which will allow a validation of propagation prediction models that are needed for the planning of new satellite services.

5. SOME MEASURED DATA

5.1. Long-term satellite signal observations

The Radio Department of Wrocław University of Technology has been carrying out a systematic measurements and monitoring of the communication satellite signals both in fixed place in Wrocław [3], [4], [5], [7], and in different locations, uniformly distributed all over the Poland since 1994 [6].

Table 1 shows the eleventh signals collected during experiment and their corresponding data rates.

Table 1. Signals observed during Wrocław campaign

Satellite	Pol	f [MHz]	Signal	Az [°]	EI [°]	Pol. Incl [°]	Expec EIRP dBW
Intelsat 602	H	11452	BEACON	126.98	17.58	30.3	7
Intelsat 602	H	11468	TV RETE 4	126.98	17.58	30.3	40
Astra 1D	H	11447,5	BEACON	177.24	31.43	1.7	45-52
Astra 1C	H	10964	TV ZDF	177.24	31.43	1.7	45-52
Astra 1C	V	10979	TV UK Living	177.24	31.43	1.7	45-52
Eutelsat II F1	H	11451,1	BEACON	185.20	31.34	3.3	9
Eutelsat II F1	H	11471	TV Polonia	185.20	31.34	3.3	50.5
Eutelsat II F1	V	11489	TV RTL-7 Poland	185.20	31.34	3.3	50
Eutelsat II F3	V	11658	TV RTT Tunisia	181.35	31.46	0.8	45
Intelsat 601	V	11198	BEACON	231.66	18.31	29.7	7
Intelsat 601	V	10995	TV BBC	231.66	18.31	29.7	41

Notice: H/V – horizontal/vertical polarisation, respectively

Some statistics of results obtained from fixed site are presented in Fig. 2 and Fig. 3.

The cumulative statistics of atmospheric attenuation were proceeded both for the average year and worst month. Figure 2 shows an example of comparison of measured and predicted, according to ITU method [1], [2], attenuation statistics at Ku-band

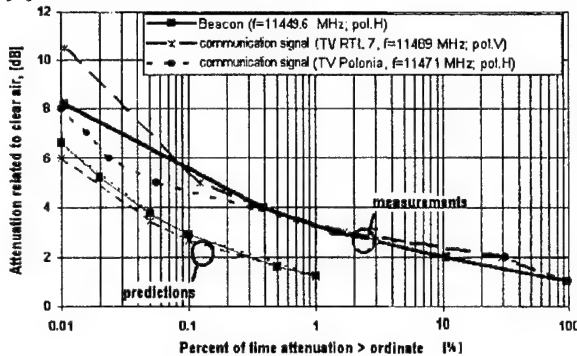


Fig. 2. Cumulative distributions of atmospheric attenuation exceeded in percent of total time of campaign duration in Wrocław for EUTELSAT Hot Bird satellite signals [4], [5], [7].

The impact of various types of impairments on the TV-picture quality is evaluated in a five-grade scale, taking into account of a CNR of the received satellite signal, according to ITU-R Recommendation S. 483-3 [8]. Cumulative results of observations are shown in Fig. 3.

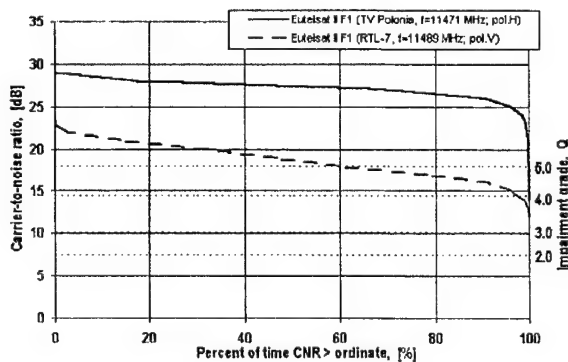


Fig. 3. CNR and related impairment grades of the Ku-band communication satellite signals, estimated in Wrocław [4], [5], [7]

Quality of different TV-sat signal can be different, even they are transmitted from the same satellite. In general, achieved grades are good or better for 99 % of the measured period of time.

5.2. Some results of mobile measurements

Measurements on the area of Poland were done during June-July 1997, along the track (all about 4456 km) shown in Fig. 4. The twenty six measuring points were uniformly distributed one degree apart (i.e. 59.6 km) in

longitude, between 14° and 24° meridians, at four latitudes, namely 54° , 52.5° , 51° and 50° . The route trace for a day measuring session was introduced into database of on board GPS satellite navigation system. Each measuring point was indicated by means of GPS system and verified on in scale 1:10000 a geographic map.

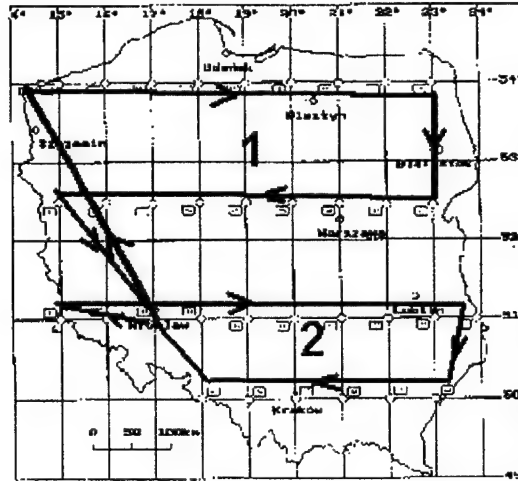


Fig. 4. Measuring track all over the Poland

At each point transmissions from ASTRA and EUTELSAT (see Table 1) satellites were monitored, including communication signals (TVSat programmes) and telemetric signals (beacons). In Fig. 5 the EIRP coverage of ASTRA 1C transmission is shown. It is worth to mention that footprints from the operator, Societe Europeenne des Satellites, Chateau Betzdorf, Luxembourg [9], are only coarse, and are shown on a map without geographical grid of coordinates. Comparison of two sets in Fig. 5a [8] and 5b shows some discrepancies. Estimated differences in EIRP levels are about 3 dB or less.

Provided that in a direct broadcast satellite (DBS) system the dish is accurately pointed, a good reception quality is achieved on EIRP contours (using dish of corresponding diameters, and a LNC of 1.2 dB noise figure) as follows: 51 dBW (60 cm), 49 (75 cm), 47 (90 cm), and 45 (120 cm), respectively. So, looking on our experimentally verified footprints antenna diameters for good reception should be increased of about few tenth cm, depending on geographical .

6. SUMMARY AND CONCLUSIONS

This paper described an experimental campaign for collecting Ku-band propagation data using ASTRA, EUTELSAT, and INTELSAT satellites. The objective to the experiment is to characterize satellite communication channels received in Poland. The campaign consists of a single fixed (on the roof of the Wrocław University of Technology) measuring site, and the mobile terminal. The site began collecting data in March 1997 and data analysis began late 1998 year. Sample

measurements and preliminary results have reported in Figures 2 to 5.

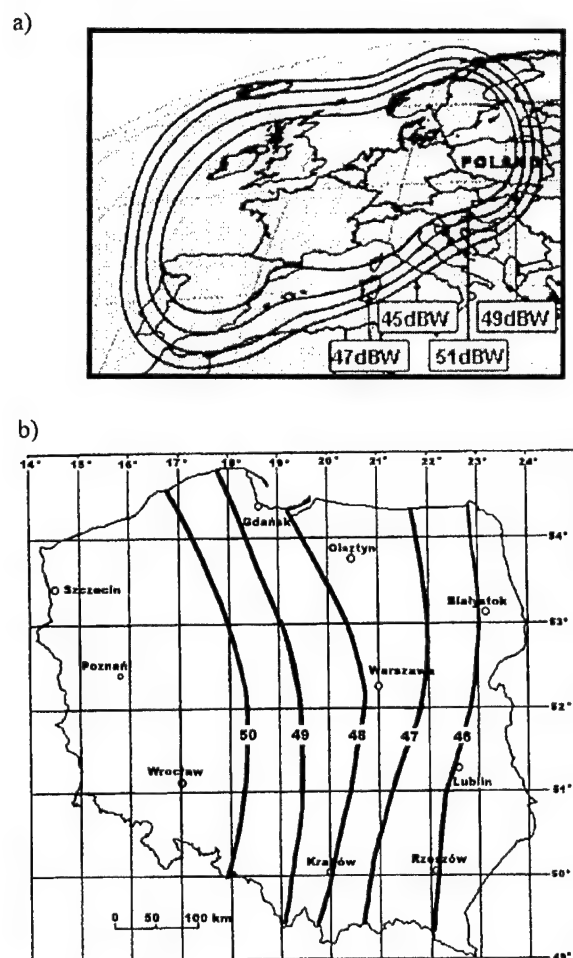


Fig.5. Transmit coverage satellite ASTRA 1C, horizontal polarization Mode 1 published by operator [9] (a), and verified experimentally at $f=10964$ MHz for transponder No. 33 (b)

Basing on the collected data, up to date many refined statistics and results that have never been done in Poland before, are developed.

A number of years of observations are needed for a single path to provide a reliable estimate of actual attenuation distribution. To obtain an uncertainty of less than 10% r.m.s., a minimum of four years of observation are needed. The variation from year-to-year of the measured path attenuation from the long-term average is of interest to system designers if additional margin (or safety factor) is required to perfect sensitive links that require extremely high availability, such as telemetry, command, control, monitoring functions, and e.g. in VSAT systems

ACKNOWLEDGMENTS

This work was supported by the State Committee for Scientific Research (KBN), under contract No. PB 1172/Z6/93/04.

7. REFERENCES

- [1] ITU-R Section 5F, „Propagation Data and Prediction Methods Required for Earth-Space Telecommunication Systems”, Report 564-4, Geneva, Switzerland, 1990
- [2] ITU-R Section 5F, „Propagation Data for Broadcasting from Satellites”, Report 565-4, Geneva, Switzerland, 1990
- [3] W.J. Krzysztofik, D.J. Bem, J. Skrzypczyński, „Some results of long-term satellite radio-signals monitoring in Poland, Proceedings of XIVth International Wrocław Symposium on Electromagnetic Compatibility, EMC-98, June 23 25, 1998, pp. 46- 50
- [4] W.J. Krzysztofik, M. Rotko, „Research of satellite signal reception conditions in Wrocław”, (in Polish), Proceedings of National Conference on Radio Broadcasting & Communication, KKRR'99, May 18-20, 1999, pp. 125-8
- [5] M. Rotko, „The communication satellites signals observations and analysis”, (in Polish), Master of Science Thesis, Wrocław University of Technology, Institute of Telecommunications & Acoustics, Wrocław, Poland 1999
- [6] W.J. Krzysztofik, „Mobile Measurements of Satellite Signals all over the Poland Territory”, Report, Report, Wrocław University of Technology, Wrocław, Poland, 1998
- [7] W.J. Krzysztofik, Long-term communication satellite signal monitoring in Wrocław-POLAND, Millennium Conference on Antennas & Propagation, Davos, Switzerland, 9-14 April, 2000 (in print)
- [8] ITU-R S.483-3, Maximum permissible level of interference in a television channel of a geostationary-satellite network in the fixed-satellite service employing frequency modulation, caused by other networks of this service, Geneva, Switzerland, 1997
- [9] www.astra.lu

BIOGRAPHICAL NOTE



Wojciech J. Krzysztofik was born in Świdnica, Poland on March 28, 1949. He received the M. Sc., and Ph.D. degrees from Wrocław University of Technology, Wrocław, Poland, both in electrical engineering, in 1974 and 1983, respectively. Since 1974 he has been a member of the Department of Electronics Engineering, the Institute of Telecommunications & Acoustics of the Wrocław University of Technology, where he is currently an Assistant Professor.

In 1988 he was a Visiting Professor at the Chalmers University of Technology, Sweden. Since 1988 to 1990 he was engaged as a Professor of Telecommunications at the College of Engineering of Mosul University, Iraq.

His research interest are in microwave remote sensing, and microwave application in communication, the electromagnetic theory of numerical methods applied to scatterers and antennas of arbitrary shape in complex environments. Recently he was a manager of a project entitled „Investigation of Satellite Signal Reception in Poland” supported by the Polish Council of Scientific Research.

FINE TUNING OF THE OKUMURA-HATA PROPAGATION PREDICTION MODEL USING THE MINIMUM SQUARES METHOD AND FUZZY LOGIC APPROACH

Arturas Medeisis

State Radio Frequency Service, Algirdo str. 27, LT-2006 Vilnius, Lithuania

Telefax: +370 2 26 15 64 E-mail: medeisis@ieee.org

The paper presents a simple approach of the fast validation and tuning of empirical propagation model in specific environment. It shows how the necessary changes may be introduced into selected model in order to improve its accuracy.

Further improvement of a model may be achieved using the Fuzzy Logic for better classification of empirical model parameters. Several fuzzy sets are proposed with their associated membership functions.

It is believed that so improved empirical model may serve better in establishing proper frequency-distance separation constraints to ensure compatibility of dense land mobile radiocommunication networks.

1. INTRODUCTION

It is very important to have a suitable tool for the accurate prediction of propagation of radio waves in the VHF and UHF bands (30-3000 MHz), that would suit the needs of land mobile radiocommunication services. Indeed, these frequencies are heavily used today for various networks in the land mobile service, therefore proper selection of operating frequencies is necessary to ensure the intra-service electromagnetic compatibility of neighbouring radio stations. This is usually achieved by applying the established rules of frequency-distance separation, where accurate propagation prediction tool becomes of crucial importance.

Several solutions are known today to calculate the RF field by deterministic or nearly deterministic methods. However all of these methods require availability of detailed information on the profile of terrain along the modelled path, as well as database of vegetation, buildings etc. Also these models usually require an extensive computational power to run. All this often renders such models to be too expensive for use by many potential users.

At the same time, very often comparatively good approximation of the RF field may be obtained using simple and universal empirical models, such as Okumura-Hata [1, 2, 3], Lee [4], ITU-R Rec. P.370 [5]

and some others. These models were developed based on the statistical analysis of extensive measurement data and have a very simple form, are easy to calculate and require only general knowledge about the environment of radio coverage area in question. However, the widespread acceptance of such empirical models is sometimes hampered by their poor performance in some cases. This happens because these universal models were derived from experimental data gathered in usually one country, region or even single urban area. Then notable deviation of modelling results from real values may occur when employing such model in country, where topographic environment, building practice and vegetation density differ significantly from those in the country of model's origin.

Therefore it may be concluded that before using any of such empirical models in another country or region they ideally must be thoroughly validated and adapted to the particular environment. In this paper we show how the empirical Okumura-Hata model was tested in Lithuania and how necessary changes were introduced into it. We also suggest a novel approach for better classification of propagation environment by means of applying certain "fuzzy logic approximation".

2. RESULTS OF TESTING VARIOUS MODELS

The following study is based on the results of testing of three well-known empirical models - ITU-R Rec. P.370, Lee and Okumura-Hata models in the environment of Lithuania. For this purpose the measurement campaign was carried out in the summer of year 1999 in various regions of Lithuania. During that campaign RF field strength was measured in coverage areas of some 30 radio stations in the land mobile service, working in the frequency bands 160 MHz, 450 MHz, 900 MHz and 1800 MHz.

Results of this validation reveal that while some of the models provided fairly close approximation in some cases, none of them performed equally well across all frequency bands and propagation environments. Few examples from this measurement campaign [6] are presented below in Fig. 1-4.

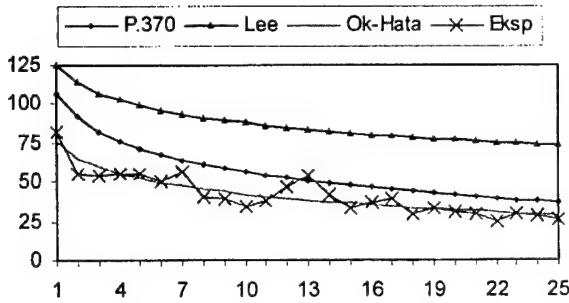


Fig. 1. Measurement results in Vilnius district (160 MHz). Here and below - R , km, vs. E_R , dB(μ V/m)

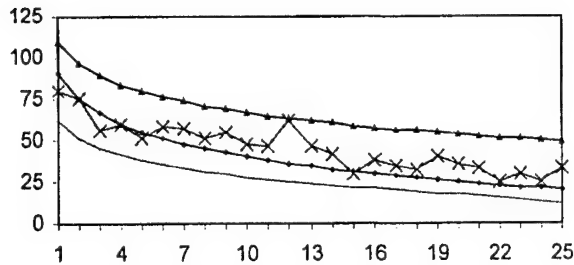


Fig. 2. Results in Pasvalys district (450 MHz)

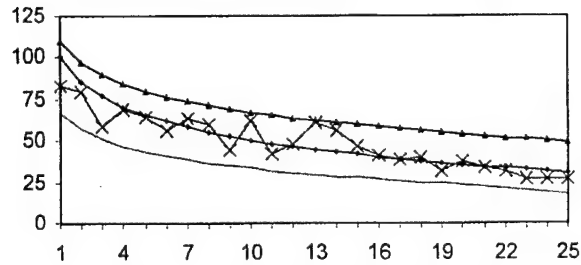


Fig. 3. Results in Birzai district (900 MHz)

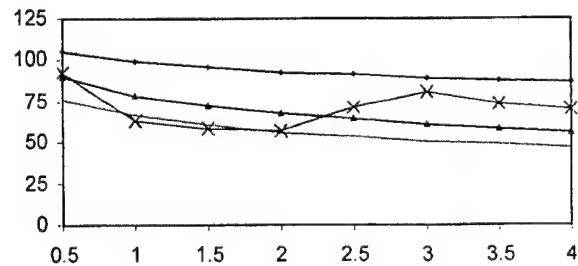


Fig. 4. Results in Vilnius city (1800 MHz)
(here free-space curve is used instead of P.370)

Even from these limited results it may be seen how differently well various models performed in different coverage areas. In order to determine the most appropriate model, it was suggested to use a least squares criterion. By applying this criterion to measurement results, as described in [7], it was found that the Okumura-Hata model more often proved to be a better fit of experimental results. Therefore the following studies addressed the possibilities to improve further applicability of this model for environmental conditions of Lithuania.

3. EMPIRICAL OKUMURA-HATA MODEL

This empirical propagation prediction model was first published by Y. Okumura et al in 1968 [1] and was based on measurement results in various districts of Tokyo, Japan. Initially it was presented in [1] as a set of empirical curves, classified for various frequencies and area types. Later, M. Hata [2] further developed this model and approximated original Okumura curves with certain mathematical expression, which then became widely known as the Okumura-Hata model [3].

The Okumura-Hata model was formally recognised by ITU-R in the Recommendation P.529 [3], which suggested to use the following expression for the received electric field strength E_R , dB(μ V/m):

$$E_R = 35.55 + P_{BS} - 6.16 \log f + 13.82 \log h_{BS} + \\ + a(h_{MS}) - (44.9 - 6.55 \log h_{BS}) \log R^\gamma. \quad (1)$$

Where:

P_{BS} - radiated power of the transmitter, dBW;
 f - operating frequency, MHz;
 h_{BS} - effective height of the transmitter antenna, m, above average terrain in the range 3-15 km;
 h_{MS} - height of receiver antenna, m;
 $a(h_{MS}) = (1.1 \log f - 0.7) h_{MS} - (1.56 \log f - 0.8)$;
 R - distance from the transmitter, km;
 $\gamma = 1$, for $R \leq 20$ km;
 $\gamma = 1 + (0.14 + 1.87 \cdot 10^{-4} f + 1.07 \cdot 10^{-3} h_{BS}) \cdot (\log(R/20))^{0.8}$, for $20 \leq R \leq 100$ km.

For the purposes of model tuning it could be useful to define two basic elements in the Okumura-Hata model (1). First of them is the initial offset parameter, let us mark it as E_0 , which for the given Okumura-Hata model equals:

$$E_0 = 35.55 \text{ dB}(\mu\text{V/m}). \quad (2)$$

The slope of model curve in the Okumura-Hata model is also constant for a given system installation and may be expressed from (1) as follows:

$$\gamma_{SYS} = -\gamma \cdot (44.9 - 6.55 \log h_{BS}). \quad (3)$$

Thus it may be suggested, that for the tuning of the model two parameters may be used – initial offset parameter E_0 (2) and slope parameter γ from the overall slope expression (3). It seems that other functions of the model, which deal with the system design parameters (height of antennas, frequency), should not be subject of tuning, because it is unlikely that the functional dependability of field strength from these parameters may change from area to area.

4. TUNING OF THE MODEL

As described in previous section, the tuning of the Okumura-Hata model may be achieved by proper adjustment of parameters E_0 and γ in the model. The most appropriate tool for such tuning may be the well-known statistical method of minimum (least) squares. In accordance with it, the best fit of the theoretical model

curve with a given set of experimental points would be achieved if the sum of deviation squares is minimum:

$$S(a, b, c, \dots) = \sum_{i=1}^n [y_i - E_R(x_i, a, b, c, \dots)]^2 = \min. \quad (4)$$

Where:

y_i - measurement result at the distance x_i ;
 $E_R(x_i, a, b, c, \dots)$ - modelling result at the x_i ;
 a, b, c - parameters of the model;
 n - volume of the experimental set.

It may be noted, that equation (4) shall be satisfied if all partial differentials of the S function are equal zeros:

$$\begin{cases} \partial S / \partial a = 0; \\ \partial S / \partial b = 0; \\ \dots \end{cases} \quad (5)$$

The solution of system (5) for the given Okumura-Hata model is described in detail in [8]. It is shown there that the empirical parameters E_0 (2) and γ (3) of the model may be calculated as follows:

$$\begin{aligned} \tilde{E}_0 &= \tilde{a} - E_{SYS}; \\ \tilde{\gamma} &= -\frac{\tilde{b}}{44.9 - 6.55 \cdot \log h_{BS}}. \end{aligned} \quad (6)$$

Where statistical estimates of the intermediate parameters a and b are derived from the set of experimental measurements $\{(x_i = \log R_i; y_i)\}_{i=1 \dots n}$ using the following expressions:

$$\begin{aligned} \tilde{a} &= \frac{\sum x_i^2 \cdot \sum y_i - \sum x_i \cdot \sum x_i y_i}{n \cdot \sum x_i^2 - (\sum x_i)^2}; \\ \tilde{b} &= \frac{n \cdot \sum x_i y_i - \sum x_i \cdot \sum y_i}{n \cdot \sum x_i^2 - (\sum x_i)^2}. \end{aligned} \quad (7)$$

Further analysis performed with the results of aforementioned measurement campaign in Lithuania [6] through application of expressions (6) and (7), gave a set of E_0 and γ parameters for different environments and frequency bands. Grouping those results according to their urban or rural origin and frequency band allowed to calculate average values for the empirical model parameters, which are given below in Table 1.

Table 1. Calculated empirical parameters for the Okumura-Hata model (1)

	160 MHz		450 MHz		900 MHz	
	Urban	Rural	Urban	Rural	Urban	Rural
E_0	40	40	40	50	35	60
γ	1.25	1.20	1.30	1.20	1.00	1.25

Modified empirical parameters given in the Table 1 allow to improve precision of the Okumura-Hata model. It is obvious, that these modified empirical parameters should be, first of all, applicable to the propagation conditions met in Lithuania and other

neighbouring countries of a region. However, for urban propagation at 900 MHz (which is a standard option for the Okumura-Hata model) the calculated parameters in Table 1 are the same as those of original model (1). Therefore it is suggested that other values, especially those for rural areas, may be also valid on a wider scope than just regional modification [8].

5. USE OF FUZZY LOGIC

5.1. Fuzzy logic concept

For further fine tuning of empirical model the concept of fuzzy logic approximation may be used. This approach was suggested recently by S. Faruque in his paper [9]. For classification of propagation environments he proposed to use certain fuzzy sets, which are linked to the relevant empirical parameters of the model through the membership functions of those fuzzy sets. So Faruque proposed to use the triangular membership function (see Fig. 5 below) to describe dependence of the model's parameter on the building clutter in coverage area.

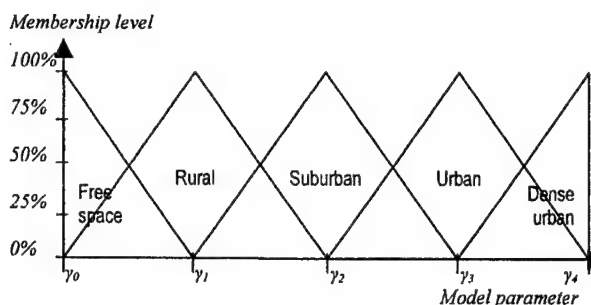


Fig. 5. Classification of propagation environment by means of fuzzy sets (from S. Faruque [9])

Basically, fuzzy sets described by Fig. 5 allow to make a classification decision when the coverage area does not clearly belongs to one typical state. For example, when the area may be characterised as something between the typical urban and typical suburban, in terms of fuzzy logic it may be described as 50% urban and 50% suburban. Then the desired value of empirical parameter for model tuning may be obtained from Fig. 5 as $\gamma^* = 0.5 \gamma_2 + 0.5 \gamma_3$. Similarly, the desired value of model parameter may be obtained for area considered to be e.g. 75% typical urban and so on.

5.2. Fuzzy sets and propagation modelling

It may be assumed that the use of such flexible tool for better classification of propagation environment might be very useful. Indeed, it should be recognised that the definition of propagation areas as "urban", "suburban", etc. is in itself not very clear, because it presumes some kind of human subjective judgement. Therefore the fuzzy logic with its flexible assignment of membership values tends itself towards that subjective assessment of type of coverage area.

However, it may be also assumed, that the accurate selection of empirical parameters through the

fuzzy sets will depend on establishing proper membership functions for those fuzzy sets. Faruque proposed to use the triangular functions (see Fig. 5). At the same time it appears that the membership functions of fuzzy sets may be anything between equal distribution rectangular and δ -function [10].

Other issue, which deserves attention, is a possibility to describe by fuzzy sets not only the building density (urban vs. rural areas) but also some other area characteristics. In this study it was suggested to establish two more families of fuzzy sets, which would describe vegetation density (forested vs. open areas) and terrain irregularity (hilly vs. flat areas). Therefore the following section attempts to propose the membership functions for all these three types of fuzzy set families.

5.3. Selection of membership functions

Previous section offered to use three families of fuzzy sets to characterise the propagation environment. These three families describe building density, vegetation density and terrain irregularity.

It is therefore suggested that in each of those families the proper classification of environment may be achieved by assigning a certain membership value between two contrary boundaries. Those boundaries may be "dense urban" - "rural", "dense forest" - "open" and "very hilly" - "flat" for those three fuzzy families respectively. It was deliberately decided not to use the proposed by Faruque [9] intermediate sets "suburban" and "urban" in the building density category, because it was felt that they may be anyway described as a fractions of those boundary categories "rural" and "dense urban".

Trying to establish the membership functions for those three fuzzy sets, it was decided to use the experimental set-up with human expert, as suggested in some of the works in [11]. The essence of that experiment is that human expert saw the particular coverage areas in which the aforementioned measurements [6] were carried out. Every time expert was asked to classify the environment in terms of percentage of those three fuzzy sets: "dense urban" - "rural", "dense forest" - "open" and "very hilly" - "flat". So obtained fuzzy grades were recorded against the values of the empirical model parameters E_0 and γ , calculated for that coverage area.

One example resulting from that experiment is shown in Fig. 6 for the case of E_0 parameter in areas with different clutter density between "dense urban" and "rural". The same figure shows a proposed approximation for the membership function. It may be seen from example in Fig. 6, that the spread of experimental points is quite significant. However, it is clear that the triangular shape would not be suitable to approximate the membership function.

Therefore, based on the results of this experimental research, it is proposed to consider using

logarithm functions for approximation of the shape of membership functions of fuzzy sets that describe the environmental features of coverage areas. It is believed that the logarithm form is more appropriate because of subjective difficulty to distinguish clearly such ultimate parameters as density of urban or density of forest, etc.

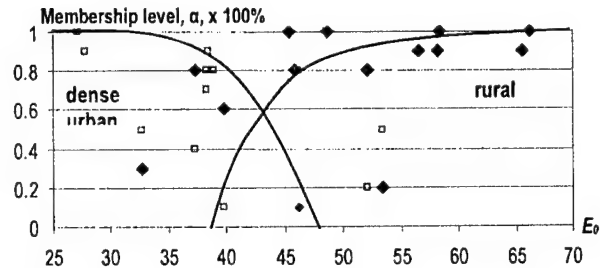


Fig. 6. Experimental analysis of E_0 parameter for different grades of fuzzy set "dense urban - rural"

Based on this reasoning the membership functions for three aforementioned fuzzy sets ("urban vs. rural areas", "forested vs. open areas", "hilly vs. flat areas") were suggested for use with modified Okumura-Hata model (1). The marginal absolute values were selected based on results in Table 1 and shape of the membership functions followed the log function. Below Fig. 7-8 show the proposed membership functions for parameters E_0 and γ of the Okumura-Hata model. These are given for the fuzzy set "urban vs. rural areas".

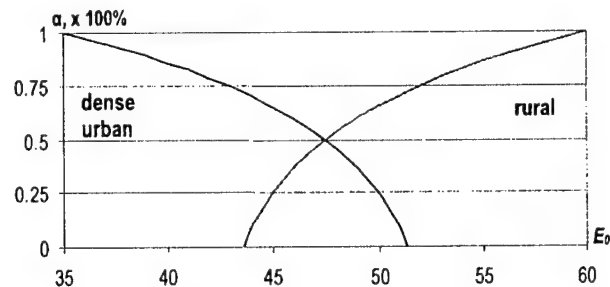


Fig. 7. Proposed fuzzy membership function to describe parameter E_0 in urban vs. rural areas

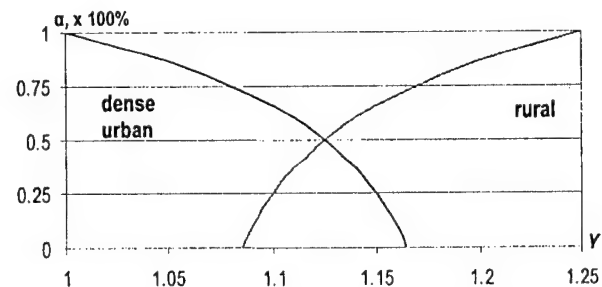


Fig. 8. Proposed fuzzy membership function to describe parameter γ in urban vs. rural areas

It is believed, that the "urban vs. rural" feature is the most important and therefore should be considered first in selection of empirical model parameters. The density of vegetation and terrain irregularity are seen as secondary options, because they

may be used to modify the primary parameter. This would then mean that the "urban" may become "dense urban with a lot of vegetation in the streets" or "dense urban across the hilly terrain", or both of above in various combinations.

Therefore, it is suggested that account of "forested vs. open" and "hilly vs. flat" features is taken as a modification of primary empirical parameters, selected based on "urban vs. rural" parameter from Fig. 7-8. The membership functions are thought to be identical for both fuzzy sets and are shown Fig. 9-10.

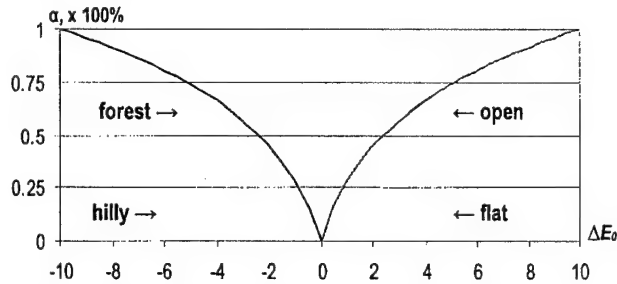


Fig. 9. Proposed fuzzy membership function to describe change of parameter E_0 in forested vs. open areas and hilly vs. flat areas

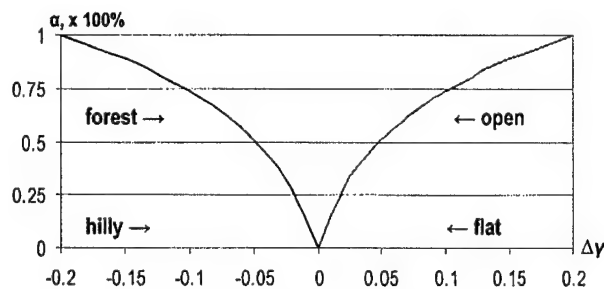


Fig. 10. Proposed fuzzy membership function to describe change of parameter γ in forested vs. open areas and hilly vs. flat areas

So, when applying the proposed "fuzzy logic" approach for tuning of the empirical propagation model (1), the following procedure should be followed. First, the initial model parameters E_0 and γ should be selected from Fig. 7 and 8 respectively, based on evaluation of coverage area in terms of its likeness to urban vs. rural. Then, if the coverage area exhibits notable abnormalities (for that region) in terms of vegetation density or terrain irregularity, then the selected E_0 and γ parameters should be modified from the Fig. 9 and 10, following the principle:

$$\begin{aligned} E_i &= E_0 + \Delta E_0; \\ \gamma_i &= \gamma + \Delta \gamma. \end{aligned} \quad (8)$$

If the coverage area may be characterised both in terms of vegetation density and terrain irregularity, then the resulting for each class parameters ΔE_0 and $\Delta \gamma$ may be summed before applying in (8).

6. CONCLUSIONS

The paper shows a simple approach to the fast validation and tuning of empirical propagation prediction model in the specific environment. Using a particular example of the Okumura-Hata model [3], the paper describes how the minimum necessary changes may be introduced to improve accuracy of the model.

For a further, more finer tuning of the model it is proposed to use three "fuzzy sets" that allow better classification of building density, terrain irregularity and vegetation density in the coverage area. The corresponding fuzzy membership functions are proposed, based on the results of experimental research.

7. REFERENCES

- 7.1. Y. Okumura, E. Ohmori, T. Kawano, and K. Fukuda, "Field strength and its variability in VHF and UHF land-mobile service," *Rev. Elec. Comm. Lab.*, vol. 16, No. 9-10, pp. 825-873, 1968.
- 7.2. M. Hata, "Empirical formula for propagation loss in land mobile radio services," *IEEE Trans. Veh. Tech.*, vol. 29, No. 3, pp. 317-325, 1980.
- 7.3. "Prediction methods for the terrestrial land mobile service in the VHF and UHF bands"// ITU-R Recommendation P. 529-2. Geneva: ITU, pp. 5-7, 1995.
- 7.4. Lee W., "Mobile communications design fundamentals" - New York: Wiley, 1993.
- 7.5. "VHF and UHF propagation curves for the frequency range from 30 MHz to 1000 MHz. Broadcasting services," ITU-R Recommendation P.370-7. Geneva: ITU, 1995.
- 7.6. A. Medeisis, "Experimental research and modelling of propagation of radio waves in the land mobile services" (in Lithuanian), *Elektronika ir Elektrotechnika* (Kaunas), Vol. , No. 1, in press.
- 7.7. A. Medeisis, A. Kajackas, "Adaptation of the universal propagation prediction models to address the specific propagation conditions and the needs of spectrum managers," *Antennas & Propagation (AP 2000)*, Proc. Conference on, 9-14 April 2000, Davos, in press.
- 7.8. A. Medeisis, A. Kajackas, "On the use of the universal Okumura-Hata propagation prediction model in rural areas," *Vehicular Technology (VTC2000 Spring)*, Proc. IEEE Conference on, in press.
- 7.9. S.Faruque, "Propagation prediction based on environmental classification and fuzzy logic approximation," *Communications, 1996 (ICC'96)*, Proc. IEEE International Conference on, 23-27 June 1996, Vol. 1, p.p. 272-276.
- 7.10. J. Mendel, "Fuzzy logic systems for engineering: a tutorial", *Proceedings of the IEEE*, Vol. 83, No. 3, March 1995, pp. 345-377.
- 7.11. "Fuzzy sets and possibility theory. Recent developments" / Editor R. Yager - Pergamon Press, 1982.

BIOGRAPHICAL NOTE

Arturas Medeisis received B.S.E.E. degree from the Vilnius Technical University in 1995 and M.Sc. degree in Telecommunications engineering from Kaunas University of Technology (KTU) in 1997. Since 1995 he works as radiocommunications engineer with the State Radio Frequency Service of Lithuania. Currently he is also a PhD student at the KTU.

INTERFERENCE DUE TO SUPERREFRACTION AND DUCTING IN THE VHF BAND IN A TROPICAL LOCATION IN NIGERIA.

O. A. Aboaba

Department of Electronic and Electrical Engineering,
Obafemi Awolowo University, Ile-Ife
Nigeria.

Email: oaboaba@oauife.edu.ng

Interference between stations working within the same frequency band or stations sharing the same frequency has been a major constraint in the planning of radio services. This article describes the findings of a research made in the southwestern part of Nigeria. Earlier in this region, statistical characteristics of anomalous propagation effects were studied in over-the-horizon radiowave propagation [4.1]. However, issues related to seasonal and diurnal signal level variations were not dealt with. The result shows that the seasonal and diurnal signal level variations were significantly high, indicating a high occurrence of superrefractivity and ducting in the region.

1. INTRODUCTION

A major task for the radiocommunication engineer in designing a communication system is to be able to predict the behaviour of the radio signal from the point of transmission to the receiving point. Preliminary calculations before the system design is embarked upon involve the signal strength expected at the receiving point, its behaviour with time, and the probability of interference between a given system and another system operating on the same or adjacent frequency channel.

The parameters involved fall into two categories. The first category are parameters within the control of the design engineer, such as the transmitter power, frequency, type of signal modulation, type of aerial structure, and the sites of the transmitter and receiver. The second category are parameters that are usually not within his control, such as the nature of the terrain over which the propagation is to be made, and the nature of the propagation medium. A reliable communication system can only be obtained after all relevant parameters are known, and this, therefore, calls for proper preliminary survey of the path during the design state.

Communication links operating at frequencies within the VHF, right up to microwaves, depend very much on the propagation conditions of the earth's lower atmosphere (i.e. the troposphere), since the geometry of

the path travelled by the radiowave depends mostly on the vertical distribution of the atmospheric refractive index.

The signals from a "wanted" transmitter operating in the VHF band would typically travel over paths of 50km or less, while signals from a potentially interfering station would travel from far greater distances. For most of the time therefore, signals from potentially interfering stations would not be received because of the large distances involved. However, there are occasions when the vertical distribution of the atmospheric refractive index cause radio signals to travel to far greater distances than normal and arrive in another service area with sufficient strength to cause interference to the wanted service.

2. INTERFERENCE DUE TO SUPERREFRACTION AND DUCTING IN ILE-IFE.

Ile-Ife lies in the southwestern part of Nigeria and located between latitudes 7°N and $7^{\circ}35'\text{N}$, longitudes $4^{\circ}20'\text{E}$ and $4^{\circ}45'\text{E}$, covering an area of 1846km^2 [4.4]. The geographical location is shown in fig.1. Its climate is tropical. i.e.hot and humid with two main seasons: rainy season and dry season. The dry season is dominated by hot, dry harmattan winds.

Superrefraction is an anomalous propagation which occurs when the lapse rate of earth's refractive index exceeds 40N/km causing the radio signal curvature to increase, extending the radio horizon and increase path clearance. Ducting occurs when the lapse rate of earth's refractive index exceeds 157N/km , causing the radio signal to bend towards the earth more rapidly than the earth's curvature. This can cause rays to propagate to extremely long ranges beyond the normal horizon. These abnormal propagation effects, which are often prevalent in the West African tropical sub-region, is a major cause of interference between stations working in the same band or stations sharing the same frequency in the region. Whilst this is a well-documented propagation mechanism [4.1], interference prediction

methods, which are used in broadcasting, do not model this effect very well.

2.1 Methodology

To simulate a potentially interfering situation, the distance from the transmitter source to the receiver point should be beyond the visible horizon, and distances between about 200km and 400km are often considered suitable. As a result an FM transmitting station located at a radio distance of 200km from Ile-Ife was utilized for this study.

The frequency of operation is 100.50MHz while the transmitter height is about 280m with an effective radiated power of 30kw. The computer controls the acquisition of data using RS232 commands sent to the



Fig. 1 Geographical Location of Receiving Station.

radioreceiver and data logger respectively. Measurements were taken for 24 hours each day.

2.2 Results

The results obtained from several months of continuous measurements have shown large variation in the received field strength. Fig.2 shows a situation where the received signal level exhibits quite frequent deep and relatively short duration fades. A situation of complete fade-out (or dropout) which may be from a few minutes to a number of hours is also observed during this period. This is as a result of tropospheric radio ducts associated with temperature inversions at or near the earth's surface. The principal cause of fade-out in the duct regions can be associated with the condition where one or both aerial terminals of the link move into or out of a radio duct due to the duct region changing its position. The formation of a duct along the path makes the signal level to propagate over long distances and cause interference in nearby stations.

3. CONCLUSIONS.

It has been observed that high values of field strength were obtained during the dry months of Nov. – March. This indicates a high incidence of anomalous propagation in the area during these dry months.

The knowledge of the statistical characteristics of these received signals may be used in assessing the potential for interference between stations working in the same band or stations sharing the same frequency.

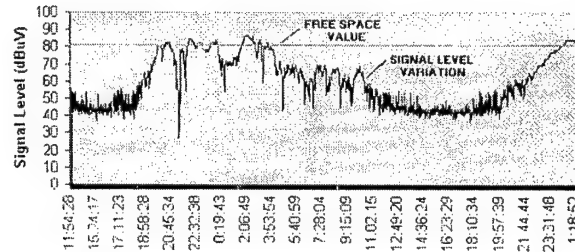


Fig.2 Diurnal Signal Level Variation.

4. REFERENCES

- 4.1 I.E. Owolabi and G.O. Ajayi, "Superrefraction conditions and their implications for tropospheric radiowave propagation in West Africa", 1976.
- 4.2 J. Griffiths, "Radiowave Propagation and Antennas; An Introduction", Prentice-Hall International, 1987, pp5-22.
- 4.3 W.G. Burrows, "VHF Radiowave Propagation in the troposphere", International Textbook Company Ltd., Intertext House, Parkgate Road, London, 1968, pp1-8.
- 4.4 O.A. Aboaba, "Experimental Studies in the VHF/UHF Frequencies in a Tropical Climate", presented at URSI'99, Toronto, Canada. August 1999.

BIOGRAPHICAL NOTE

Full name of Author: Olusegun Abiola ABOABA
 Affiliation: Department of Electronic & Electrical Eng.
 Obafemi Awolowo University, Ile-Ife,
 Nigeria.
 Educational Qualification: B.Sc (Elect. & Elect. Eng.)

Fluctuations of VHF/UHF Signal Level in Distant Tropospheric Propagation over the Far-Eastern Region of Russia

E.V. Batueva., D.D. Darizhapov.

Siberian Branch of RAS, Buryat Scientific Center Department Of Physical Problems
8, Sakhyanova st., Ulan-Ude, 670047
Tel: (3012)332841, Fax: (3012)332841, E-mail: dari@bsc..buryatia.ru

Owing to complex non-stationary processes occurring in border atmospheric layers the study of tropospheric propagation of radio waves in VHF/UHF range calls for further accumulation and generalization of experimental data determining fluctuation characteristics of the radio signal and their formation under radio meteorological conditions of air currents prevailing in different physical and climatic regions of Russia [1]. Fairly comprehensive results have been obtained to-date in similar studies made in regions with sharply continental climate [2], in extremely severe climatic zones [3], as well as in Arctic Sea coastal area [4].

This article describes the findings of the research made in the far-eastern coastal regions where a complex climate-forming process is at work on "land-ocean" border line. Earlier in this region statistical characteristics of the signal were studied in over-the-horizon radio wave propagation [5, 6], however, the issues related to seasonal and diurnal signal variations, as well as radio meteorological factors in forming their peculiar features were not dealt with. It should be noted that similar study in this region was made in the area of far-eastern seas [7]. As it was expected the comparison between these two groups of findings showed a marked difference between the characteristics of UHF/UHF fluctuations on tropospheric paths of comparable extension, caused by differences in underlining environments. The article presents the main radio meteorological factors and physical mechanisms contributing to the specific fluctuation of the signal in various seasons and hours.

Keywords: troposphere, radio wave propagation, distant tropospheric propagation

1. Conditions of experiments, radio line characteristics

Two paths of radio relay line for VHF/UHF distant tropospheric propagation (DTP) were examined with a common receiver at the intermediate station near the town of Magadan. Lengthwise profiles of the paths 1 and 2 are shown in Fig. 1 a, b. The geographical extension of path 1 is 204.66 km, and path 2 – 415.3 km. The equivalent distances are 167.1 km and 383.7 km respectively. Scatter angles in these intervals under normal atmospheric refraction ($a = 8500$ km) are 19.7 and 45.1 mrad accordingly.

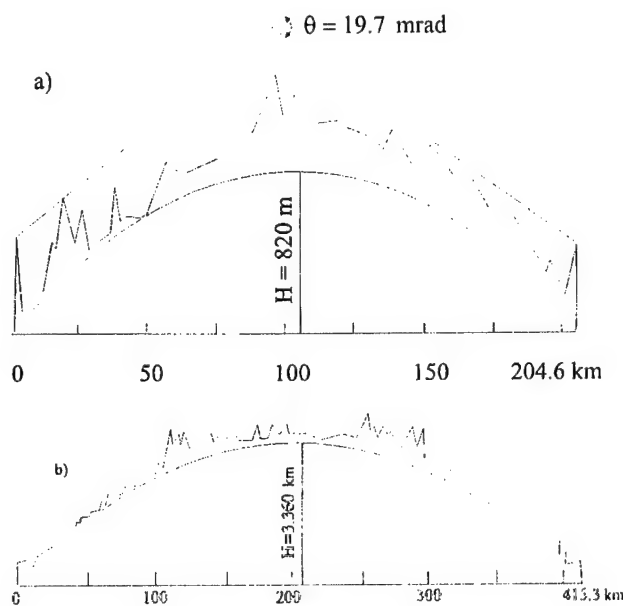


Fig. 1

Both paths run over rugged mountainous terrain along the coast of the Sea of Okhotsk. Path 1 is laid over the peninsula, with an over-radiating portion of the troposphere located about 100 km off the coast and blocked from the ocean by a mountain chain system; path 2 runs near the coast.

In the intervals under study a standard tropospheric radio relay station "Horizont-M" was utilized equipped with parabolic antennas 20×20 m (path 1) and 30×30 m (path 2) in dimensions and operating on fourfold receiving scheme and on 36 cm wave length. Coefficients of receiver-transmitter antennas on path 1 were 41.5 and 42.0 dB, and 46 and 46.5 dB on path 2 respectively.

Continuous round-the-clock registration of slow variations of the signal was performed with a fast recorder H-338/3. Registration of quick fading of the signal was made every three hours during the interval of 5...50 minutes with the integrating condensator disconnected from the recording circuit. The recording interval of quick sinking was established in accordance with the

character of fluctuations and was sufficiently long "to encompass" several dozens of auto-correlation radii. Recording time constant in this case equaled 50 ms. Calibration of measuring devices was done with a G4-76A generator. Absolute error in measuring the signal level was 1.5 dB.

2. Radiometeorological conditions of the area under study

The relationship between the signal level and radio meteorological parameters was studied on over-the-horizon paths on the western coast of the Sea of Okhotsk through comparing the 6-hourly median levels with the data of aerological sounding gathered at the stations of Magadan and Okhotsk in 1991-1992 in following atmospheric layers: 0÷900, 300÷600 and 600÷900 m [8].

Fig. 2 a,b,c,d shows distribution histograms of ground signal values N at Magadan station in winter, spring, summer and autumn respectively; maximum median value of N is registered in summer, minimum – in winter.

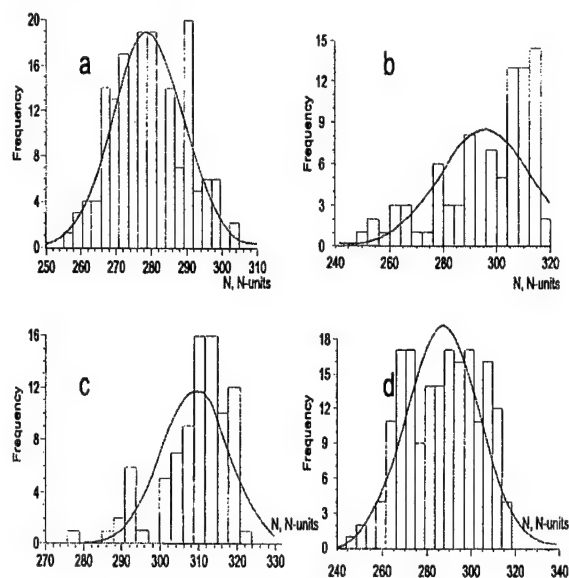


Fig. 2

3. Seasonal and diurnal variations of slow signal fading

Due to the occurrence of non-stationary DTP processes on the studied path the fadings of different types of signal were registered – quick fluctuations ranging from a fraction to dozens of seconds in duration were superimposed on slow variations of signal level ranging from several minutes to dozens of minutes. Such a manner of signal fluctuation necessitates a provisional division into quick and slow fading.

Integrated statistical data on distribution of slow fluctuations of the tropospheric signal based on the results of seasonal measurements on paths 1 and 2 are shown on Fig. 3 respectively. The mentioned distributions of the signal are based on hourly median values of the signal in each season of the year. It follows from the figures that maximum median levels of the signal on path 1 occurs in autumn and on path 2 in summer. Minimum median signal levels on both paths occur in winter, which is caused by

seasonal variations of radio and meteorological conditions of the period under study. Besides, the graphs show that the amplitude of seasonal variation of the signal on median levels of path 1 makes 9.4 dB, on path 2 – 14.8 dB. The dispersion of seasonal distribution of the signal on path 2 considerably exceeds the dispersion observed on path 1. This regularity can be explained by special positioning of the studied path with respect to coastline.

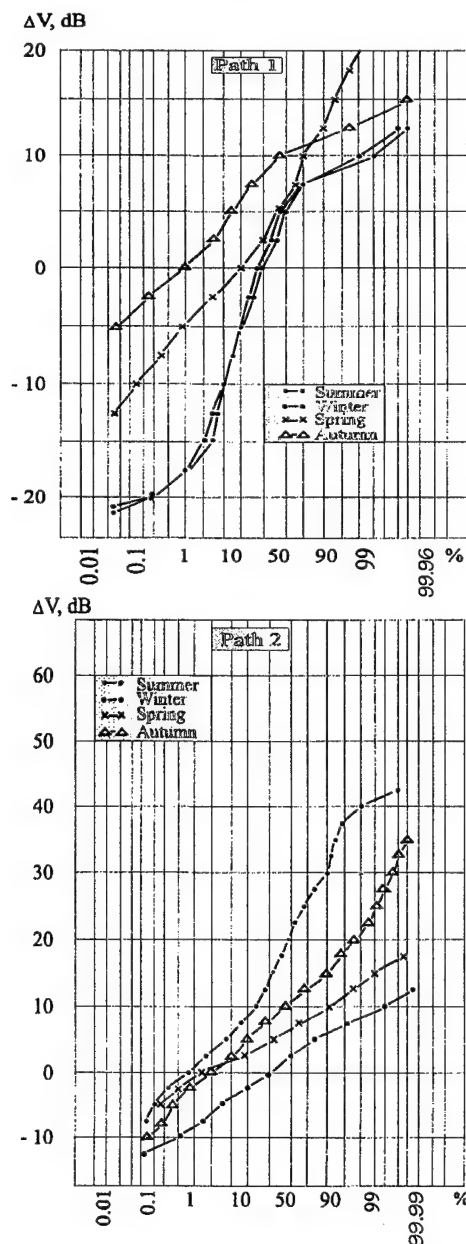


Fig. 3

As noted above path 2 unlike path 1 runs along the coastline causing considerably greater variability in radio meteorological conditions both throughout the entire layer of troposphere and in the overradiating volume. Other things being equal the standard deviation for approximating logarithmically correct law of distribution will diminish with an increase of path extension. This can be explained by an increase in the height of the overradiating volume in which the intensity, dimensions and

form of irregularity is more stable [1]. However, in spite of relatively greater extension of path 2, the amplitude of seasonal signal variation and the dispersion of seasonal distributions turned out to be substantially in excess of analogous statistical parameters of path 1.

Consequently, the tropospheric processes occurring near the "land-ocean" border play the dominant role in forming the fluctuation regime on the coastal path. Change of directions in a breeze circulation in a fairly powerful vertical current brings about, depending on hour and season, radio meteorological conditions of opposite polarity, which play an essential role in forming a fluctuation regime.

Judging by integrated distributions autumn season is characterized by the greatest stability of the signal on path 1, and winter and spring season – on path 2. Apparently, this regularity is conditioned by seasonal interrelationship between the structure variables, dynamics, intensity and form of tropospheric irregularities. These irregularities are stabilized in the troposphere on a coastal path 2 in winter and spring when the underlying surface becomes uniform after the Sea of Okhotsk becomes frozen.

The diurnal cycle of median values of the signal in all seasons on the studied paths shows its maximum at night and in the morning hours and minimum value – in the day time.

Unlike the discovered correspondence of the statistical parameters of seasonal signal variations on the experimental paths, diurnal variations of the signal are characterized by the opposite relationship. Table 1 presents diurnal amplitude variations of the signal registered on the

studied paths in different seasons. The shorter path 1 shows the greatest amplitude of diurnal variation of a median signal level in summer and equals around 13 dB, while on path 2 this parameter equals 3.5 dB only.

Night and morning hours of summer when the temperature near the ground level drops to lowest levels the intensity of temperature inversion in the border layers of atmosphere increases. As a result the height of the over-radiating volume of the troposphere and radio wave scatter angle diminishes. Consequently, such a variation in a radio meteorological structure of the troposphere brings about higher signal level. It should be noted that while the volume of overradiating troposphere, "cut-out" by crossing of orientation diagrams of receiver-transmitter antennas, occupies a fairly substantial range of heights vertically on the studied paths, only the lower part of this volume makes an essential contribution to forming of DTP field [9, 10].

Table 1

Seasons	Amplitude of diurnal variation of signal level, dB	
	path 1	path 2
Winter	1.5	2.0
Spring	4.0	3.0
Summer	13.0	13.0
Autumn	2.5	2.5

Table 2

Station	Season	Time, Hours	Correlation coefficient r for						
			N_0	$g_n(0 \div 100 \text{ m})$	$g_n(0 \div 300 \text{ m})$	$g_n(0 \div 600 \text{ m})$	$g_n(0 \div 900 \text{ m})$	$g_n(300 \div 600 \text{ m})$	$g_n(600 \div 900 \text{ m})$
Magadan	Winter	0	0.26/0.30	0.58/0.45	0.28/0.01	0.09/0.20	0.50/0.32	0.38/0.52	0.69/0.27
		12	0.06/0.18	0.55/0.55	0.59/0.63	0.62/0.70	0.28/0.66	0.52/0.71	0.20/0.36
	Spring	0	0.84/0.43	0.76/0.74	0.78/0.72	0.72/0.79	0.77/0.74	0.66/0.83	0.85/0.64
		12	0.99/0.93	0.91/0.99	0.93/0.99	0.87/0.98	0.82/0.96	0.73/0.91	0.67/0.87
	Summer	0	0.01/0.61	0.60/0.99	0.98/0.74	0.97/0.36	0.92/0.66	0.98/0.99	0.90/0.35
		12	0.37/0.06	0.73/0.95	0.49/0.82	0.29/0.14	0.06/0.37	0.65/0.25	0.11/0.54
	Autumn	0	0.23/0.62	0.41/0.67	0.38/0.42	0.38/0.19	0.61/0.09	0.64/0.01	0.67/0.01
		12	0.13/0.66	0.41/0.14	0.13/0.00	0.13/0.13	0.25/0.25	0.10/0.35	0.37/0.42
Okhotsk	Winter	0	0.16	0.69	0.78	0.69	0.71	0.05	0.54
		12	0.18	0.75	0.59	0.31	0.15	0.43	0.57
	Spring	0	0.46	0.19	0.40	0.66	0.65	0.99	0.72
		12	0.97	0.89	0.92	0.80	0.10	0.03	0.93
	Summer	0	0.67	0.71	0.88	0.85	0.73	0.62	0.37
		12	0.42	0.86	0.93	0.97	0.89	0.88	0.32
	Autumn	0	0.45	0.69	0.58	0.50	0.33	0.64	0.02
		12	0.07	0.02	0.15	0.20	0.05	0.20	0.35

The reason why this happens is, firstly, the scatter angle from this part of the volume is relatively small, secondly, the intensity of tropospheric irregularities in the lower volume is much greater due to its proximity to the earth surface. Besides, the troposphere zone located below the mentioned volume can play an appreciable role in the mechanism of signal transmission of DTP due to weak diffraction caused by screening of radio waves by the earth surface[10].

4. The study of correlation between DTP signal level and radio meteorological parameters

Table 2 shows the findings of the research into statistical relationship between median values of the multiplier of signal V weakening and radio meteorological parameters (refractivity N near the ground and the vertical gradient of refraction index g_n) obtained at aerological radio sounding stations of Magadan and Okhotsk located near the linked points.

As shown by these tables the correlation coefficient r between the corresponding values of the multiplier of DTP signal weakening, refraction index N near the ground and its vertical gradients ranges widely from 0 to 0.99.

In spring-autumn season the correlation index increases as compared with the other seasons and basically falls within the range of 0.65 ... 0.99 which can be attributed to considerably less contrast conditions of atmospheric circulation in a warmer period, rather than in a cold one.

Correlation of signal level with radio meteorological parameters was made through comparison of mean values over three days.

The correlation index between the signal level and index gradient of air refraction is higher than that between the signal level and refraction index near the surface of the earth. Correlation between V and g_n is stable in the near-the-surface layer 900 m thick in all seasons and at all times diurnally. Only in daytime in summer at Magadan station r decreases with an increase of thickness of layer: on path 1 from 0.71 in the lower 100 m thick layer near the surface to 0.06 in 0...900 m layer and on path 2 from 0.95 to 0.25 accordingly which is conditioned by vertical distribution of air moisture in the border layer of atmosphere. The correlation between V and g_n does not depend on the height of the lower boundary of the layer in question and is stable in layers 0...300, 300...600 and 600...900 m in thickness.

5. Conclusion

The seasonal variations of the mean signal components on over-the-horizon tropospheric paths in the far-eastern coastal area of Russia reveal one maximum value in summer or autumn depending on location of radio paths under study and one minimum value in winter.

The maximum signal value is registered in autumn on the path running along the ocean coast, and on the path running at a distance from the coast in summer, which is

explained by peculiarities of tropospheric processes occurring near the "land-ocean" border.

The seasonal variations of median signal level on the studied paths correspond to a considerable degree to the variations of radio meteorological parameters in the far-eastern troposphere. In spring-autumn as compared with the other seasons an increase was observed in correlation coefficient of signal level with radio meteorological parameters. In the lower 900 m thick layer of atmosphere the correlation link between the signal level and radio meteorological parameters throughout the year is stable at all heights and decreases with an increase of thickness of the layer during the day in summer.

6. References

- 6.1. A.I.Kalinin, V.N.Troitsky, A.A.Shur, "The study of distant tropospheric propagation of VHF/UHF", Radio wave Propagation. M., Nauka Publishers, 1975, pp. 127-153.
- 6.2. D.D.Darizhapov, G.S.Zhamsueva, D.Z.Tsydypov, N.B.Chimitdorzhiev, "Radio signal characteristics in diffractive-tropospheric propagation", Radio Technics and Electronics, vol. 31, 1986, pp. 1481-1486.
- 6.3. D.D.Darizhapov, G.S.Zhamsueva, D.Z.Tsydypov, N.B.Chimitdorzhiev, "VHF/UHF fluctuation in tropospheric propagation under extreme climatic conditions", Radio Physics, vol. 33, 1990, pp. 1027-1032.
- 6.4. D.D.Darizhapov, G.S.Zhamsueva, D.Z.Tsydypov, N.B.Chimitdorzhiev, "Slow fluctuations of radio signal on high latitudinal tropospheric paths", Radio Technics and Electronics, vol. 36, 1991, pp. 641-647.
- 6.5. V.N.Troitsky, "Research into propagation of decimeter radio waves in high latitudes", *Electrosvyaz* (Electrical Communications), No 6, 1984, pp. 39-41.
- 6.6. A.A.Shur, "Climatic influences on VHF/UHF distant propagation", *Electrosvyaz* (Electrical Communications), No 5, 1976, pp. 10-12.
- 6.7. G.S.Sharygin, "Statistical structure of over-the-horizon VHF/UHF field". M.: Radio and Communications, 1983, 140p.
- 6.8. E.V.Batueva, D.D.Darizhapov, "Variations of radio meteorological parameters in the troposphere of the far-eastern regions of Russia", *Izvestiya* (Proceedings) of Russian Academy of Sciences. Physics of Atmosphere and Ocean, vol. 32, No 3, 1996, pp. 359-363.
- 6.9. Yu.I.Davydenko, "VHF/UHF propagation and radio relay lines", M.: Voenizdat Publishers, 1963, 136p.
- 6.10. A.V.Kukushkin, V.D.Freilicher, I.M.Fucs, "VHF/UHF over-the-horizon propagation at sea", *Izvestia* (Proceedings) of universities. Radio Physics, vol. 30, 1987, pp. 811-839.

Darizhapov Dashi D. – Head of Radio Cosmic Physics Laboratory, Specialist in domain radio wave propagation.

Batueva Elizaveta V. – Research Worker of the Radio Cosmic Physics Laboratory, specialist in domain radiometeorology.

REDUCING LEVEL OF SIDE RADIATION OF VIBRATOR AND MICROSTRIP ANTENNAS IN DEFINITE DIRECTION

N.N.Gorobets, N.P.Yelisseyeva

Kharkiv National University, 4 Svobody Sq., Kharkiv, 61077, Ukraine,

E-mail: Nadezhda.P.Yelisseyeva@univer.kharkov.ua

Using the uniform geometrical theory of diffraction the radiation levels of the electric vibrator above a metal rectangular screen in separated definite directions in far field zone have been calculated when changing sizes of the screen over wide ranges. It is shown that the interference oscillations of the lateral radiation amplitude take place when the side screen ratio values are in definite interval, depending on a given observation direction. There were worked out algorithms and programs of calculating the dependencies of field amplitudes in the given observation directions on the ratio screen sides for fixed size of one of them. Normalized amplitude directive patterns were calculated under the rectangular screen having optimum sizes at different distances between the vibrator and screen.

1. INTRODUCTION

The problem of radiation suppression in definite separated direction is actual and important for providing noiseless and EMC RES of different frequency bands and of different functional operations. Based on the uniform geometrical theory of diffraction (UGTD) method, we have worked out in detail a calculation technique for the spatial field distributions in the far zone of a vibrator antenna with finite-size metal flat or corner screens of arbitrary apex angle [1,2]. The fast-acting algorithms of account by this method allows to carry out the numerical analysis of radiation in any direction of observation in dependence on two sizes of the screen and situation of the vibrator concerning it. The developed algorithms yields reliable results beginning with screen-sizes of the order of the wave length for the vibrator in this case at a distance from the screen of not more than 0.3λ . With increasing the screen-sizes, accuracy sufficient for practice is provided even for a greater distance of the vibrator from the screen. Analysis of the Front to Back Ratios of the radiating system vibrator-screen in [3-5], when changing sizes of the screen over wide ranges, has proved possibility of sufficient decreasing levels of the back radiation by means of choosing an appropriate ratio of

screen sides. Using the UGTD method we analyze now a physical possibility of the radiation suppression in arbitrary definite direction of shadow half-space by varying the screen sides ratio.

2. METHODOLOGY

As a theoretical model of the radiating system we use a metal infinitely thin rectangular screen, excited by electric dipole located on the height h over the screen center and oriented parallel to the one of the screen edges. Z-axis is directed along the screen normal while X- and Y- axes are directed along W and L screen sides, correspondingly. The angle θ is measured from the screen normal and the angle φ lies in the screen plane. Within the frame of UGTD method the field in arbitrary direction is determined as a superposition of geometrooptical (GO) and diffracted on the screen edges fields:

$$E(\theta, \varphi) = E_{go} + E_{dif},$$
$$E_{dif} = E_{1,2} + E_{3,4} + E_{12} + E_{21} + E_{34} + E_{43}. \quad (1)$$

Here $E_{1,2}$ and $E_{3,4}$ - singly diffracted waves excited under diffraction of the incident and reflected waves on each of the four edges of the screen, and E_{12} , E_{34} , E_{21} , E_{43} - twicely diffracted waves on its parallel edges.

The spatial radiation-patterns are defined by boundaries "light-shadow" of each of the field components depending on screen sizes and vibrator positions. In the shadow region of the GO dipole field, for a general case in each cross-section $\varphi = \text{const}$ there are the angle θ sectors (I), where the field is contributed by the waves diffracted only on the edges (1,2), which are parallel to the dipole; sector II, where the field is contributed by the waves diffracted only on the edges (3,4), which are transverse to the dipole; and sector (III), where the field is a superposition of all edge fields. The diffracted on the 1,2 edges fields do not depend on the lengths W . From physical points of view is clear that we may minimize the radiation in definite direction of angle

sectors II and III, when electromagnetic fields diffracted on the transversal or orthogonal screen-edges are opposite in phase having equal amplitudes. The diffracted on the screen edges field's form the shadow cones with apex angle β which are determined by the screen side's ratio and dipole distance from the screen.

$$\beta_{1,2} = \arctg \left[\sqrt{\left(h^2 + (L/2)^2\right) / (W/2)^2} \right]$$

$$\beta_{3,4} = \arctg \left[\sqrt{\left(h^2 + (W/2)^2\right) / (L/2)^2} \right]. \quad (2)$$

Each defined direction of observation θ corresponds to the light and shadow boundary of the edges (located on its shadow cone surface) for fixed dipole location relatively to the screen for definite screen sides ratio $(W/L)_b$. It means that in definite direction the diffracted on 1,2 edges field contributes the whole field only for $W/L > (W/L)_{b1,2}$. The diffracted on the 3,4 edges fields contribute when $W/L < (W/L)_{b3,4}$. From (2) for fixed h and L the following condition should be satisfied:

$$W_{b1,2} = \frac{\sqrt{4h^2 + L^2 \cos^2 \varphi \sin^2 \theta}}{\sqrt{1 - \cos^2 \varphi \sin^2 \theta}} \quad (3)$$

$$W_{b3,4} = \sqrt{L^2 \frac{(1 + \sin^2 \varphi \tg^2 \theta \cos^2 \varphi \sin^2 \theta)}{(1 - \cos^2 \varphi \sin^2 \theta) \sin^2 \varphi \tg^2 \theta} - 4h^2}.$$

So the whole field is determined in sectors I, II by interference of the fields diffracted on the 1,2 or 3,4 edges only, and in sectors III by interference of the fields diffracted on the all screen edges.

$W/L > (W/L)_{b1,2}$ sector I ($E_{1,2}$);

$W/L < (W/L)_{b3,4}$ sector II ($E_{3,4}$)

$(W/L)_{b1,2} < W/L < (W/L)_{b3,4}$ sector III ($E_{1,2}, E_{3,4}$).

3. ANALYSIS OF THE CALCULATION RESULTS

Efficient algorithms and computer codes for calculation and analysis of directional properties of dipole antennas with the plane screen have been worked. Fig. 1 shows the radiation levels dependencies $V = 20 \lg (|E(\theta, \varphi)| / |E(0, 0)|)$ on the screen sides ratio W/L in the plane $\varphi = 0^\circ$ in the directions $\theta = 120^\circ$, $\theta = 150^\circ$, $\theta = 170^\circ$, $\theta = 180^\circ$ for various values L . For defined angle θ the ratio $(W/L)_b$ from (3) stays constant when changing L (for $L > 1$). For directions $\theta = 120^\circ$, $\theta = 150^\circ$, $\theta = 170^\circ$ the values $(W/L)_{b1,2}$ are equalled 1.9; 0.96; 0.18, correspondingly. So in these directions for $W/L < (W/L)_{b1,2}$ the whole field is determined by the field diffracted on the edges 3,4 only and for large W/L

by interference of the field diffracted on the all edges. In direction $\theta = 180^\circ$ the field amplitude equalled to the whole diffracted field amplitude at any W/L .

The calculated normalized radiation patterns of the main radiation field component in the plane $\varphi = 0^\circ$ are shown in Fig. 2 for the screen $L = \lambda$ at the dipole distance $h = 0,05\lambda$ (the curves 1,2,3) and $h = 0,25\lambda$ (the curves 4,5,6) for the screen sides ratios $(W/L)_{opt}$, which provide minimal radiation for the observation angles $\theta = 120^\circ, 150^\circ, 180^\circ$. There are $(W/L)_{opt} = 1.66$ for $\theta = 120^\circ$ (the curves 1, 4), $(W/L)_{opt} = 1$ for $\theta = 150^\circ$ (the curves 2, 5), $(W/L)_{opt} = 1.9$ for $\theta = 180^\circ$ (the curves 3,6).

4. CONCLUSIONS

There have been worked out algorithms and programs allowing investigating radiation characteristics of the vibrator antennas having screens with high accuracy at any observation direction. The calculated dependencies of the radiation level for the dipole above the screen in dependence on the screen sides ratio W/L prove a possibility of the radiation suppression in shadow half - space for the arbitrary direction θ , φ , when the whole field in this direction is determined by interference of the fields diffracted on the all screen edges. It takes place when the side screen ratio values are in definite interval, depending on a given observation direction.

5. REFERENCES

1. Gorobets N.N., Yeliseyeva N.P. "Directional and Polarization Characteristics of the Radiation of Finite - Size Corner Antennas with an Arbitrary Aperture Angle", Journal of Communication Technology and Electronics, 1993, Vol.38, N6, pp.99-108.
2. Yeliseyeva N.P. "Pattern Analysis of an Arbitrarily Oriented Oscillator Placed above a Flat Screen", Telecommunications and Radio Engineering, 1999, Vol. 53, N 1, pp. 43-53.
3. Gorobets N.N., Yeliseyeva N.P. "Decreasing levels of lateral and back radiations of vibrator and microstrip antennas", Proceedings of the 12-th International Wroclaw Symposium on Electromagnetic Compatibility, Wroclaw, Poland, 1994, pp.30-34.
4. Gorobets N.N., Yeliseyeva N.P. "Optimizing radiation of microstrip and vibrator antennas by means of choosing form of the screen", Proceedings of Ninth International Conference on Antennas and Propagation, Eindhoven, The Netherlands, 1995, Vol.1, pp. 295-298.
5. Gorobets N.N., Yeliseyeva N.P. "Influence of Diffraction Effects on Radiation Characteristics of a Wire Antenna with Finite-Size Plane and Corner Reflector of Arbitrary Apex Angle", Proceedings of VIIth International Conference on Mathematical Methods in Electromagnetic Theory, Kharkov, Ukraine, 1998, Vol.2, pp. 568-570.

BIOGRAPHICAL NOTES

Nikolai N. Gorobets was born in Zhitomir in 1940. In 1962 he graduated from the Radiophysics Department of Kharkov State University. From 1971 up to now he works as Head of the Applied Electrodynamics Department of Kharkov State University. In 1984 he got a Doctor of Phys. & Math. Sci. degree. His research interests are in the areas of developing and applying of the theory electromagnetic wave radiation with the circular and elliptical polarization.

Nadezhda P. Elisseyeva was born in 1947 in Odessa. In 1970 she graduated from the Radiophysics Department of Kharkov State University. She works in the Applied Electrodynamics Department as a senior res. fellow. In 1990 she got a Ph.D. degree. Her research interests are connected with the scattering and radiation of electromagnetic waves.

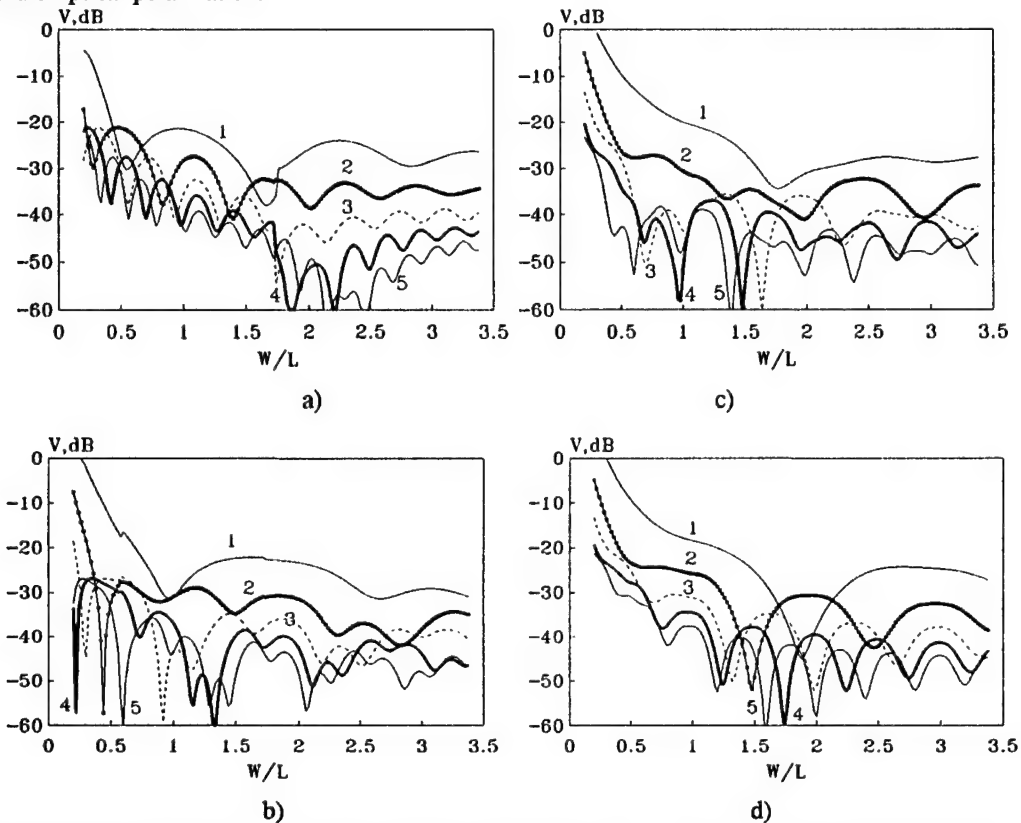


Fig.1. Dependencies of V on the screen sides ratio W/L in the plane $\varphi = 0^\circ$ in the directions $\theta = 120^\circ$ (a), 150° (b), 170° (c), 180° (d), when $L = \lambda, 2\lambda, 3\lambda, 4\lambda, 5\lambda$ (correspondingly the curves 1,2,3,4,5) and $h = 0,05\lambda$.

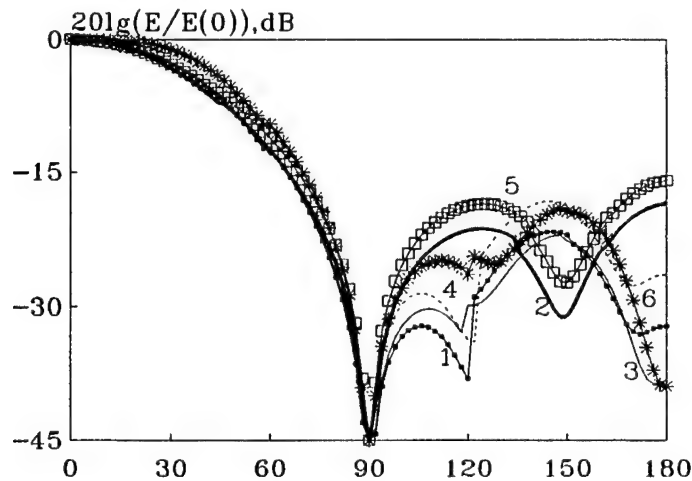


Fig.2 Normalized amplitude directive patterns in optimum cases.

STATISTICAL STUDIES OF VHF AND UHF RADIO WAVES PROPAGATION IN THE SOUTH BALTIC AREA

Wiktor Pawłowski

Technical University of Gdańsk

ul.G.Narutowicza 11/12, PL-80-952 Gdańsk, Poland

Phone: +48 58 3471588, 3472562, Fax: +48 58 3416132, e-mail: radio@pg.gda.pl

The subject of the paper are results of investigations of the influence of the atmospheric refraction and the synoptic situation on the propagation conditions of VHF and UHF radio waves in the south Baltic area and the coastal region of Poland. The obtained results show that the atmospheric circulation affect the correlation between the field strength and the radio refractive index substantial. This phenomena was analyzed having in view its utilization by forecast of propagation conditions of radio waves in the region of south Baltic. The influence of air mass was of less importance.

1. INTRODUCTION

A great importance for the analysis of fulfilling of EMC conditions in radio communication systems in the VHF and UHF bands has the distribution of the atmospheric refraction in the region of interest [1]. The atmospheric refraction affect the propagation conditions in the above mentioned frequency bands, especially at the sea and in coastal regions [2],[3].

To obtain data, suitable for the coastal region of Poland, a comprehensive study of the radio climate of that region has been carried out at the Technical University of Gdańsk. The obtained results, which related to problems connected with the time distribution of the radio refractivity of the atmosphere, as well as of the gradient of the radio refractive index in a thin near the ground layer of the atmosphere, has been soon presented in detail [4].

An important part of the related here study are investigations of propagation conditions of m- and dcm-waves in the south Baltic area. An attempt had been undertaken to examine the regression and the correlation between statistical parameters describing the field strength records and the parameters characterizing the atmosphere refraction at the same time. The aim of this paper is to present some results of the study, from this point of view.

2. THE RESEARCH METHOD

The presented in this paper results were obtained analyzing records of the field strength of a radio broadcasting station in south Sweden at the frequency 96.7 MHz. The propagation path Emmaboda-Gdańsk of 320 km length is a transhorizon path, in majority a sea path [5].

The records, each 30 minutes long in time, originate from the summer season because of the large variability of the distributions of the atmospheric refraction in that period. Each record was the subject of a statistical analysis. The mean value and the standard deviation of the course of field strength of the 30-minutes records were calculated. The fluctuation of the field strength was examined, too. In the field strength records the number of passages of the course of the field strength through its mean level was elaborated.

On the other hand, parameters characterizing the atmospheric refraction were used. The value of the radio refractive index at the surface N , and its wet term W , were applied. They were defined as follows. The refractive index N is given by the well known formula [2]

$$N = \frac{77,6}{T} \left(p + 4810 \frac{e}{T} \right) \quad (1)$$

where:

p - the atmospheric pressure in [hPa],

T - the air temperature in [K] and

e - the partial pressure of water vapor [hPa].

The refractive index N can be expressed as the sum given below

$$N = D + W \quad (2)$$

where:

$$D = 77,6 \frac{p}{T}, \text{ the dry term of } N \quad (3)$$

and

$$W = 3,73 \cdot 10^5 \frac{e}{T^2}, \text{ the wet term of } N. \quad (4)$$

For each field strength record the corresponding defined above N -values and W -values were calculated. This calculation was based on data originating from the Polish Meteorological Service.

The correlation between, on the one hand, the mean of the field strength or the field fluctuation frequency and on the other hand, and the N -value or the W -value was analyzed.

Furthermore, the mentioned above data were applied in a regression analysis of the field strength parameters relative to the N -values and the W -values. It was assumed that the N -values and the W -values are independent variables.

For the estimation of regression coefficients the least square method was applied. The employed equations, which present straight lines can be described by the following expression

$$Y = \bar{y} + b(x - \bar{x}) \quad (5)$$

where:

\bar{y} - the mean value of the dependent variable,

\bar{x} - the mean value of the independent variable,

b - the slope of the straight line.

The coefficient b represent the mean change of the dependent variable when the independent variable changes by one unit. Therefore, for propagation analysis reasons, it was useful to assume that the dependent variables are parameters describing the field strength record and that the independent variables are parameters characterizing the atmospheric refraction.

The regression analysis were carried out taking into account, on the one hand, the field strength measurement hours of 6⁰⁰, 12⁰⁰ and 18⁰⁰ UT and on the other hand, - the synoptic situation. The synoptic situation was classified taking into consideration the so called character of the atmospheric circulation and the air mass.

The character of the atmospheric circulation depends on the location of the main atmospheric circulation areas, i.e. the anticyclone and the cyclone in relation to the propagation path. Following 3 characters of the atmospheric circulation were used:

- AA - the region of the propagation path is covered by the center of a anticyclone,
- A - the propagation path is under the influence of an anticyclone area and
- C - the propagation path is under the influence of anticyclone area or is covered by the center of a cyclone.

The classification of air masses used by the Polish Meteorological Service was applied. The following air masses were observed mostly in the measurement period:

PPm - polar maritime air,

PPm_s - the old polar maritime air

PPm_c - the warm polar maritime air.

3. CORRELATION OF THE FIELD STRENGTH AND THE RADIO REFRACTIVE INDEX

The correlation between the statistical parameters of the field strength and the N -value or the W -value had been carried out for different measurement hours. The values of correlation coefficient at 6⁰⁰, 12⁰⁰ and 18⁰⁰ UT equaled 0,27, 0,39 and 0,52, respectively. These values are very small and practical insignificant.

Therefore, the influence of the synoptic situation on the correlation between the field strength and radio refractive index was investigated, with the aim to form more homogenous populations of data.

The influence of the character of the atmospheric circulation and the air mass on the correlation coefficients had been examined. The obtained results are shown in Table 1, for the character of atmospheric circulation, and Table 2, for the air mass.

Table 1 Influence of the character of the atmospheric circulation

hour	character of atmospheric circulation		
	AA	A	C
6 ⁰⁰	0,60	0,41	0,01
12 ⁰⁰	0,25	0,36	0,43
18 ⁰⁰	0,14	0,48	0,50

Table 2 Influence of the air mass

hour	air mass		
	PPm	PPm _s	PPm _c
6 ⁰⁰	0,09	0,10	0,18
12 ⁰⁰	0,44	0,15	0,05
18 ⁰⁰	0,53	0,45	0,22

The significant correlation coefficients, at least at significant level 0.05, are given in bold digits.

Comparison of data in Table 1 and Table 2 lead to the conclusion that the usefulness of the character of atmospheric circulation as classification criterion, when forming the object populations of data, should be analyzed. Therefore, in the related below results of the study the attention was fixed on this aspect. Results obtained for air mass population are not discussed because its insubstantial influence on the correlation coefficients, as seen from Table 2.

4. REGRESSION COEFFICIENTS

4.1. The influence of the character of the atmospheric refraction on the regression of the field strength mean relative to N and W

The influence of the atmospheric circulation on values of the regression coefficient of statistical parameters of the field strength records relative to

the N -values and the W -values had been investigated for all measurement hours

The obtained object regression coefficients of the mean field strength relative to the N -value and W -value are given in Table 3. The significance of object regressions was examined by means of statistical tests. Regression coefficients significant at least at the significant level of 0.05 are given in bold digits. They are given in dB/N-unit.

Table 3. Regressions coefficients - field mean relatively N and W taking into account the character of the atmospheric circulation

hour	character of atmospheric circulation	field strength mean	
		N	W
6 ⁰⁰	AA	0,6	0,5
	A	0,4	0,3
	C	-0,1	0,1
12 ⁰⁰	AA	0,2	0,1
	A	0,3	0,3
	C	0,3	0,2
18 ⁰⁰	AA	0,1	0,1
	A	0,4	0,4
	C	0,2	0,2

The differentiation of data contained in Table 3 had been examined by means of the covariance analysis. The question was: is one allowed to use object regression straight lines or should he construct a common straight line basing on all data, i.e. the general population. This investigation were carried out by means of F-tests. The obtained results are given below in Table 4.

Table 4 Calculated and tabulated F-test values (the field strength mean)

hour	character of atmospheric circulation			
	N-value		W-value	
	calculated	tabulated	calculated	tabulated
6 ⁰⁰	3,44	3,13	3,13	3,13
12 ⁰⁰	0,09	3,13	0,36	3,13
18 ⁰⁰	0,42	3,16	1,25	3,16

The comparison of calculated and tabulated F-test values show that for measurement hour 6⁰⁰ the influence of the character of atmospheric circulation is substantial in the light of statistical tests. The examination regression coefficients by statistical tests show that they are substantial at least at significance level of 0,05 for character of circulation AA and A - at 6⁰⁰ UT, and for circulation character A and C - at 12⁰⁰ and 18⁰⁰ UT.

The values of regression coefficients for all measurements hours and different air masses are given in Table 5. The comparison of these data with data in Table 3 confirm the mentioned above

conclusion that the classification according to the air mass is inadvisable, because the most regression coefficients are insubstantial in the light of statistical tests.

Table 5. Regressions coefficients - field mean relatively N and W taking into account the air mass

hour	air mass	field strength mean	
		N	W
6 ⁰⁰	PPm	0,1	0,1
	PPm _s	-0,1	-0,2
	PPm _c	0,2	-0,7
12 ⁰⁰	PPm	0,4	0,3
	PPm _s	0,2	-0,1
	PPm _c	-0,1	0,1
18 ⁰⁰	PPm	0,3	0,3
	PPm _s	0,6	0,2
	PPm _c	0,2	0,2

The regression of the standard deviation of the field strength relative to the N -value and the W -value was not analyzed. This was a consequence of results of investigations of the influence of the character of the atmospheric circulation on the standard deviations of field strength. This influence is not substantial in the light of variance analyses [5].

4.2. The influence of the character of the atmospheric refraction on the regression of field strength fluctuations relative to N and W

The regression of the fluctuations of the field strength relative to the N -value and W -value was examined in a similar way, as in the case of the mean of the field strength. The obtained results are put together in Table 6. The regression coefficients are given in cycles pro hour and pro N -unit.

Table 6. Regressions coefficients - field strength fluctuations relatively N and W taking into account the character of the atmospheric circulation

hour	character of atmospheric circulation	field fluctuation	
		N	W
6 ⁰⁰	AA	- 0,5	- 0,3
	A	- 1,9	- 1,3
	C	1,6	1,3
12 ⁰⁰	AA	0,6	0,5
	A	- 1,3	- 0,7
	C	- 0,6	- 0,4
18 ⁰⁰	AA	0,3	0,2
	A	- 0,5	- 0,4
	C	- 1,7	- 1,5

The differentiation of regression coefficients in Table 6 was examined only for 6⁰⁰ and 12⁰⁰ UT only, because the 18⁰⁰ UT regression coefficients are insubstantial. The obtained results are shown in Table 7. It was obtained that the influence of the character of atmospheric circulation on the differentiation of regression coefficients is insubstantial.

Table 7 Calculated and tabulated F-test values (the field strength fluctuation)

hour	character of atmospheric circulation			
	N-value		W-value	
	calculated	tabulated	calculated	tabulated
6 ⁰⁰	2,78	3,13	2,05	3,13
12 ⁰⁰	0,32	3,13	0,22	3,13

5. FINAL REMARKS

The comparison of values of regression coefficients obtained in both cases: in the first case, taking the *N*-value as the independent variable and the second case - the *W*-value as the independent variable, show that the *N*-value and the *W*-value have similar features, from the radiometeorological point of view.

The calculated values of the regression coefficients are similar. Furthermore, the regression coefficients in both mentioned above cases are significant for the same objects, in the light of examination by means statistical tests. And, on the end, the influence of the character of atmospheric circulation on the differentiation of the object regression coefficients taking the *N*-value or the *W*-value as independent variables, is similar, too.

The presented results show that the *N*-value and *W*-value can be taken interchangeably, when analyzing propagation conditions of radio waves in the VHF and UHF bands in the south Baltic area.

A part of the object regression coefficients is insubstantial in the light of statistical tests. An effect to this result have that that in the related study data originating from individual records have been

statistical tested. This was necessary because the relative short time of the propagation measurements. Using month mean obtained in a suitable long time (in place of single record means) the annual cycle of the described phenomena could be recognized. In this way obtained knowledge about the radiometeorology of a region of interest is important for the fulfilling of EMC conditions when planning radiocommunication systems.

6. REFERENCES

- 6.1. K.H.Craig, „Refractivity parameters and prediction modeling”, Proc. of the XXIVth General Assembly of URSI Symp., Kyoto, 1993, F8-3, p.251
- 6.2. ITU-R, Rep.563, „Radiometeorological data”
- 6.3. ITU-R, Rec.470, „VHF and UHF propagation curves for frequency range from 30 to 1000 MHz”
- 6.4. W.Pawłowski, „Radio climate of the coastal region of Poland”, Proc. of the XIVth Wrocław EMC Symp. on Electromagnetic Compatibility”, Wrocław, Poland, 28.06.-01.07., 1994, pp. 53-57
- 6.5. W.Pawłowski, „Propagation conditions in the VHF and UHF bands in the coastal region of Poland”, Proc. of the XVIth Wrocław EMC Symp. on Electromagnetic Compatibility”, Wrocław, Poland, June 23-25, 1998, pp. 68-71

BIOGRAPHICAL NOTE

Wiktor Pawłowski was born 1933. He graduated at the Technical University of Gdańsk 1957 and received the Dr.Ing. degree in Electronics from the Technical University of Warsaw in 1966. Since 1957 he is with the Technical University of Gdańsk, working on radiocommunication with special interest in propagation of radio waves in non-ionized media.

EXCITATION OF THE INFINITE PERFECT CONDUCTING NONLINEAR LOADED CIRCULAR CYLINDER COATED WITH THE DIELECTRIC

Diana V. Semenikhina, Andrey A. Beletsky

State Radio Engineering University, Taganrog, 347924, Russia, airpu@tsure.ru

Two-dimensional problem of the perfect conducting nonlinear loaded circular cylinder coated with the dielectric exciting is solved with the integral equations' method. It's shown that dielectric coating, which depth and dielectric permittivity correspond to the surface wave exciting at the harmonic's frequency, changes the cylindrical nonlinear radiator's pattern and raises electromagnetic field (EMF) level at the harmonic's frequency.

1. INTRODUCTION

Spurious nonlinear loaded antennas' radiation and nonlinear scattering research is usually limited to the short distance to the receiving system because of small radiated at harmonic's frequencies EMF levels relative to fundamental frequency one. As a rule, electromagnetic compatibility (EMC) problems' urgency rises only as receiving device energy characteristics increases. From earlier researches it follows that harmonic levels of EMF radiated by nonlinear loaded antenna increases with either exciting source amplitude increasing or changing nonlinear load parameters by moving the working point to the steeper section of the voltage-current characteristic (VCC).

In the last case electro-physycal parameters of loads founded may only be recommended for synthesizing of appropriate semiconducting devices.

We found another one reason of the harmonic's frequency spurious radiation for nonlinear loaded antennas and scatterers with circular cylindrical shape and dielectric coat when EMF source and nonlinear loads' parameters are invariant. It hides in the known dispersion properties of the dielectric coated cylinder [3].

Electrodynamics problem analysis of the excitation of the perfect conducting dielectric coated cylinder loaded with nonlinear narrow slots parallel with the cylinder's element is carried out in two steps. At first the EMF radiation problem of the magnetic current filament on the surface of perfect conducting dielectric coated cylinder is posed (filament is used as a model for secondary current in the nonlinear load). It permits us to find the coat with the greatest ratio of the EMF levels' at harmonic frequencies. It's the best conditions for radiation of field harmonic generated on radiator nonlinear loads. We solve then the excitation problem of the cylindrical nonlinear loaded dielectric coated radiator. At last we can find pattern and scattering pattern (SP) of the nonlinear radiator with given coat parameters. Analysis of the pattern and SP changings and possibilities of radiated EMF harmonic level increasing is of a practical interest.

2. BOUNDARY PROBLEM

We have infinite perfect conducting circled cylinder of a radius. On the surface S_1 of the cylinder there are M nonlinear parallel with the cylinder's element homogeneous loads having in cylindrical co-ordinate system (CCS) $(a, \Delta\varphi_q)$ co-ordinates (fig.1), $q = 1...M$, where $\Delta\varphi_q$ is an angular load width. Let's consider loads to be narrow nonlinear slots. Loads' parameters are defined with the following polynomial VCC:

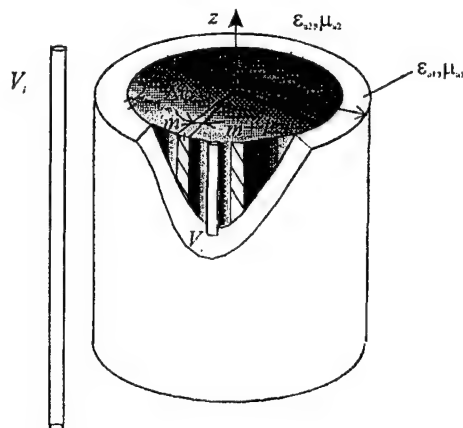


Fig. 1

$$i^e(t) = \sum_{v=0}^Q (a_v u^v(t) + b_v du^v(t)/dt).$$

Here VCC parameters a_v, b_v link the current i^e which flows throw the nonlinear load (transversely the slot) with the voltage u on the slot's edges.

Cylinder is coated with the dielectric layer with b ($b > a$) external radius and $\tilde{\epsilon}_{a1}, \mu_{a1}$ parameters. Let's call $r=b$ surface as S . Primary source at ω frequency is placed in the homogeneous on z co-ordinate V_1 volume.

The problem is to find the EMF at fundamental and harmonic frequencies in the observation point p for the given external source with given object present considering exterior volume with homogeneous $\tilde{\epsilon}_{a2}, \mu_{a2}$ parameters.

Volume inside the dielectric coat is indicated as V_1 and outside it as V_2 . Let's put the primary source in V_1 . Taking into consideration that the problem is two-dimensional we can obtain for observation points $p_2 \in V_2$ following integral relations for EMF at $n\omega$ frequency:

$$\bar{b}_2 \bar{H}_n(p_2) = - \int_{\Phi'} (\bar{J}_n^e \bar{E}_{n2}^m - \bar{J}_n^m \bar{H}_{n2}^m) b d\varphi', \quad (1)$$

where integration on φ' is performed on surface S , $\bar{E}_{n2}^m, \bar{H}_{n2}^m$ stands for auxiliary fields of elemental 2-D magnetic radiator at $n\omega$ frequency (n is a harmonic number) placed in the point $p_2 \in V_2$, $\bar{J}_n^{e,m}$ are surface currents on S when $r=b+0$.

In V_1 volume we have:

$$\begin{aligned} \bar{b}_1 \bar{H}_n(p_1) = & - \int_{S_j} (\bar{J}_n^{e,p} \bar{E}_{n1}^m - \bar{J}_n^{m,p} \bar{H}_{n1}^m) dS' - \\ & - \int_{\Phi'} (\bar{J}_n^e \bar{E}_{n1}^m - \bar{J}_n^m \bar{H}_{n1}^m) b d\varphi' - \int_{\Phi'} \bar{J}_n^m \bar{H}_{n1}^m a d\varphi'. \end{aligned} \quad (2)$$

where in the second addend we perform integration on the surface S and in the third one on S_1 ; $\bar{E}_{n1}^m, \bar{H}_{n1}^m$ stands for auxiliary fields of the elemental 2-D magnetic radiator placed in the point $p_1 \in V_1$; $\bar{J}_{n1}^{e,m}$ are surface currents on surface S when $r=b$ and \bar{J}_n^m are surface currents on nonlinear loads.

Auxiliary fields $\bar{E}_{n1}^m, \bar{H}_{n1}^m$ are chosen to comply the boundary conditions on the perfect conducting cylinder surface with $r=a$ radius.

Let's take into account continuity conditions for tangent field vectors' components on surface S when $r=b$. Besides surface currents $\bar{J}_{n1}^{e,m}$ and $\bar{J}_{n2}^{e,m}$ in (1) and (2) are equal but have different directions. Calling $\bar{J}_{n12}^{e,m} = -\bar{J}_{n1}^{e,m} = \bar{J}_{n2}^{e,m}$, choosing $\bar{b}_1 = \bar{b}_2 = \bar{b}$ and putting observation point on the surface S we obtain:

$$\int_{S_j} (\bar{J}_n^{e,p} \bar{E}_{n1}^m - \bar{J}_n^{m,p} \bar{H}_{n1}^m) dS' = \int_{\Phi'} (\bar{J}_{n12}^{e,m} (\bar{E}_{n1}^{m,a} + \bar{E}_{n2}^{m,a}) - \bar{J}_{n12}^m (\bar{H}_{n1}^{m,a} + \bar{H}_{n2}^{m,a})) b d\Phi' + \int_{\Phi'} \bar{J}_n^m \bar{H}_{n1}^{m,a} ad\Phi', \quad (3)$$

where assumed that due to narrow of slots on Φ co-ordinate magnetic current flows only along z co-ordinate the last integral may be represented as sum of integrals:

$$\int_{\Phi'} \bar{J}_n^m \bar{H}_{n1}^{m,a} ad\Phi' = \sum_{\mu=1}^M \int_{\Delta\Phi_\mu} J_{n1z}^m H_{n1z}^{m,z} ad\Phi', \quad q=1 \dots M.$$

Putting the observation point p_2 on the nonlinear load surface with number q and choosing $\bar{b}_2 = \bar{b}$ we get from (2):

$$\begin{aligned} -J_{nq\Phi}^p &= - \int_{S_j} (\bar{J}_n^{e,p} \bar{E}_{n1}^m - \bar{J}_n^{m,p} \bar{H}_{n1}^m) dS' + \\ &+ \int_{\Phi'} (\bar{J}_{n12}^{e,m} \bar{E}_{n1}^{m,z} - \bar{J}_{n12}^m \bar{H}_{n1}^{m,z}) b d\Phi' + \\ &+ \sum_{\mu=1}^M \int_{\Delta\Phi_\mu} J_{n1z}^m H_{n1z}^{m,z} ad\Phi', \quad q=1 \dots M. \end{aligned} \quad (4)$$

Or using nonlinear boundary conditions (that can be obtained with the method given in [5]) on the q nonlinear load's surface and doing the same procedure for M loads we obtain M equations of such type:

$$\begin{aligned} \Delta\Phi_q A_{nq} J_{nqz}^m - \Delta\Phi_q^2 a^2 B_{nq} \sum_{s=-\infty}^{\infty} J_{sqz}^m J_{n-sqz}^m + \\ + C_{nq} a^3 \Delta\Phi_q^3 \sum_{\xi=-\infty}^{\infty} J_{n-\xi qz}^m \sum_{s=-\infty}^{\infty} J_{sqz}^m J_{\xi-sqz}^m = \\ = \int_{\Phi'} (\bar{J}_{n12}^{e,m} \bar{E}_{n1}^{m,z} - \bar{J}_{n12}^m \bar{H}_{n1}^{m,z}) b d\Phi' + \sum_{\mu=1}^M \int_{\Delta\Phi_\mu} J_{n1z}^m H_{n1z}^{m,z} ad\Phi' - \\ - \int_{S_j} (\bar{J}_n^{e,p} \bar{E}_{n1}^m - \bar{J}_n^{m,p} \bar{H}_{n1}^m) dS', \quad q=1 \dots M, \end{aligned} \quad (5)$$

where A_n, B_n, C_n are coefficients defined by nonlinear load parameters as $A_n = a_1 + in\omega b_1$, $B_n = a_2 + in\omega b_2$, $C_n = a_3 + in\omega b_3$.

Equations (3), (5) are the system of nonlinear integral equations (SNIE) about unknown surface currents on S and S_1 .

When the cylinder is exciting with the primary source placed in V_2 in a similar manner we get the following system of integral equations:

$$\begin{aligned} - \int_{S_j} (\bar{J}_n^{e,p} \bar{E}_{n2}^{m,a} - \bar{J}_n^{m,p} \bar{H}_{n2}^{m,a}) dS' = \int_{\Phi'} (\bar{J}_{n12}^{e,m} (\bar{E}_{n1}^{m,a} + \bar{E}_{n2}^{m,a}) - \\ - \bar{J}_{n12}^m (\bar{H}_{n1}^{m,a} + \bar{H}_{n2}^{m,a})) b d\Phi' + \int_{\Phi'} \bar{J}_n^m \bar{H}_{n1}^{m,a} ad\Phi'. \end{aligned} \quad (6)$$

$$\begin{aligned} \Delta\Phi_q A_{nq} J_{nqz}^m - \Delta\Phi_q^2 a^2 B_{nq} \sum_{s=-\infty}^{\infty} J_{sqz}^m J_{n-sqz}^m + \\ + C_{nq} a^3 \Delta\Phi_q^3 \sum_{\eta=-\infty}^{\infty} J_{n-\eta sqz}^m \sum_{\eta=-\infty}^{\infty} J_{sqz}^m J_{\eta-sqz}^m = \\ = \int_{\Phi'} (\bar{J}_{n12}^{e,m} \bar{E}_{n1}^{m,z} - \bar{J}_{n12}^m \bar{H}_{n1}^{m,z}) b d\Phi' + \\ + \sum_{\mu=1}^M \int_{\Delta\Phi_\mu} J_{n1z}^m H_{n1z}^{m,z} ad\Phi', \quad q=1 \dots M. \end{aligned} \quad (7)$$

For the auxiliary field $\bar{E}_{n1}^{m,z}, \bar{H}_{n1}^{m,z}$ we take the field of in-phase magnetic current filament placed between two coaxial perfect conducting cylinders of a and b radiuses when the space between cylinders is filled with the dielectric with parameters $\tilde{\epsilon}_{a1}, \mu_{a1}$. For the auxiliary field $\bar{E}_{n2}^{m,z}, \bar{H}_{n2}^{m,z}$ we take the field of in-phase magnetic current filament with perfect conducting cylinder of b radius (in CCS center) present placed in the space with parameters $\tilde{\epsilon}_{a2}, \mu_{a2}$ [6]. Taking into consideration auxiliary field components the first integral in the right side of (3) contains only addend $-J_{n12z}^m (H_{n1z}^{m,z} + H_{n2z}^{m,z})$ and the first integral in the right side of (5) contains only addend $-J_{n12z}^m H_{n1z}^{m,z}$. In the same manner (6), (7) are transformed.

With chosen auxiliary fields systems of nonlinear integral equations are solved about z component of magnetic currents on cylinder with $r=b$ and nonlinear loads.

Auxiliary field in V_1 volume that is the field of in-phase magnetic current filament placed between two coaxial perfect conducting cylinders of a and b radiuses and in parallel their axis must satisfy the boundary conditions for tangent component of \bar{E} vector when $r=a, b$. It can be written as follows:

$$\begin{aligned} H_{z1}^{m,z}(r, \Phi, r', \Phi') = -\frac{k_1}{4W_1} \times \\ \times \sum_{m=-\infty}^{\infty} \frac{e^{im(\Phi-\Phi')}}{J'_m(k_1 a) H_m^{(2)}(k_1 b) - H_m^{(2)}(k_1 a) J'_m(k_1 b)} \times (8) \\ \times \begin{cases} (J_m(k_1 r') H_m^{(2)}(k_1 b) - H_m^{(2)}(k_1 r') J'_m(k_1 b)) \times \\ \times (J_m(k_1 r) H_m^{(2)}(k_1 a) - H_m^{(2)}(k_1 r) J'_m(k_1 a)) & a < r < r'; \\ (J_m(k_1 r) H_m^{(2)}(k_1 b) - H_m^{(2)}(k_1 r) J'_m(k_1 b)) \times \\ \times (J_m(k_1 r') H_m^{(2)}(k_1 a) - H_m^{(2)}(k_1 r') J'_m(k_1 a)) & r' < r < b; \end{cases} \end{aligned}$$

Here as further we use $k_{1,2}, W_{1,2}$ for propagation coefficient and characteristic impedance in $V_{1,2}$ volume and $J_m(x), H_m^{(2)}(x)$ for Bessel and Hankel functions.

Let's consider the solution of the SNIE with the moment method. Base functions for unknown currents can be taken in the form of piece constant functions (we consider the current on the each nonlinear load to be constant on the whole load

and current on the surface $r = b$ to be uniform on sections $\Delta\varphi$ ($\Delta\varphi b \ll \lambda_n$). For the test functions we take δ -functions. Then from (3), (5) we obtain the following system of nonlinear algebraic equations (SNAE):

$$\begin{cases} \sum_{v=1}^N J_{n12vz}^m \rho_{nvq}^{bb} - \sum_{\mu=1}^M J_{n\mu z}^m \rho_{n\mu q}^{ab} = -F_{nq}^{1,b}, & \eta = 1 \dots N_\varphi \\ \Delta\varphi_q a A_{nq} J_{nqz}^m - \Delta\varphi_q^2 a^2 B_{nq} \sum_{s=-\infty}^{\infty} J_{sqz}^m J_{n-sqz}^m + \\ + \Delta\varphi_q^3 a^3 C_{nq} \sum_{\xi=-\infty}^{\infty} J_{n-\xi qz}^m \sum_{s=-\infty}^{\infty} J_{sqz}^m J_{\xi-sqz}^m - \sum_{\mu=1}^M J_{n\mu z}^m \rho_{n\mu q}^{aa} + \\ + \sum_{v=1}^N J_{n12vz}^m \rho_{nvq}^{ba} = -F_{nq}^{1,a}, & q = 1 \dots M, \end{cases} \quad (9a)$$

and from (6), (7) we get SNAE:

$$\begin{cases} \sum_{v=1}^N J_{n12vz}^m \rho_{nvq}^{bb} - \sum_{\mu=1}^M J_{n\mu z}^m \rho_{n\mu q}^{ab} = F_{nq}^2, & \eta = 1 \dots N_\varphi, \\ \Delta\varphi_q a A_{nq} J_{nqz}^m - \Delta\varphi_q^2 a^2 B_{nq} \sum_{s=-\infty}^{\infty} J_{sqz}^m J_{n-sqz}^m + \\ + \Delta\varphi_q^3 a^3 C_{nq} \sum_{\xi=-\infty}^{\infty} J_{n-\xi qz}^m \sum_{s=-\infty}^{\infty} J_{sqz}^m J_{\xi-sqz}^m - \sum_{\mu=1}^M J_{n\mu z}^m \rho_{n\mu q}^{aa} + \\ + \sum_{v=1}^N J_{n12vz}^m \rho_{nvq}^{ba} = 0, & q = 1 \dots M. \end{cases} \quad (9b)$$

with the following coefficients:

$$\begin{aligned} \rho_{n\mu q}^{aa} &= \int_{\varphi_\mu - \Delta\varphi_\mu/2}^{\varphi_\mu + \Delta\varphi_\mu/2} H_{nz1}^{m,z}(a, \varphi_q, a, \varphi') a d\varphi' = \\ &= -\frac{\Delta\varphi_\mu}{2i\pi W_{n1}} \sum_{m=-\infty}^{\infty} \text{sinc}(\Delta\varphi_\mu m/2) \frac{e^{im(\varphi_\mu - \varphi_q)}}{Z_{1mn}} \times \\ &\times \left(J_m(k_{n1}a) H_m^{(2)}(k_{n1}b) - (J'_m(k_{n1}b) H_m^{(2)}(k_{n1}a)) \right) \\ \rho_{nvq}^{ba} &= \int_{\varphi_v - \Delta\varphi_v/2}^{\varphi_v + \Delta\varphi_v/2} H_{nz1}^{m,z}(a, \varphi_q, b, \varphi') b d\varphi' = \\ &= \frac{\Delta\varphi_v}{\pi^2 W_{n1} k_{n1} a} \sum_{m=-\infty}^{\infty} \text{sinc}(\Delta\varphi_v m/2) \frac{e^{im(\varphi_v - \varphi_q)}}{Z_{1mn}} \\ \rho_{nv\mu}^{bb} &= \int_{\varphi_\mu - \Delta\varphi_\mu/2}^{\varphi_\mu + \Delta\varphi_\mu/2} (H_{nz1}^{m,z}(b, \varphi_\mu, b, \varphi') + H_{nz2}^{m,z}(b, \varphi_\mu, b, \varphi')) b d\varphi' = \\ &= -\frac{\Delta\varphi_v}{2i\pi W_{n1}} \sum_{m=-\infty}^{\infty} \text{sinc}(\Delta\varphi_v m/2) e^{im(\varphi_v - \varphi_\mu)} \times \\ &\times \left(\frac{(J_m(k_{n1}b) H_m^{(2)}(k_{n1}a) - (J'_m(k_{n1}a) H_m^{(2)}(k_{n1}b)))}{Z_{1mn}} - \right. \\ &\left. - \frac{\Delta\varphi_v}{2i\pi W_{n2}} \sum_{m=-\infty}^{\infty} \text{sinc}(\Delta\varphi_v m/2) e^{im(\varphi_v - \varphi_\mu)} \frac{H_m^{(2)}(k_{n2}b)}{H_m^{(2)}(k_{n2}b)} \right) \\ \rho_{nvq}^{ba} &= \rho_{nvq}^{ab} \end{aligned}$$

where $\text{sinc}(x) = \sin(x)/x$.

When the system is excited with the magnetic current filament with co-ordinates (r_0, φ_0) we have:

$$\begin{aligned} F_{n\mu}^{1a,b} &= - \int_{S_j} \bar{J}_n^{m,p} H_{nz}^{m,z} dS' = \delta_n^{\pm 1} \frac{I_0^m}{2i\pi W_1} \sum_{m=-\infty}^{\infty} \frac{e^{im(\varphi_\mu - \varphi_0)}}{Z_{1m}} \times \\ &\times \left\{ \frac{1}{a} \left(J_m(k_1 r_0) H_m^{(2)}(k_1 b) - J'_m(k_1 b) H_m^{(2)}(k_1 r_0) \right) \text{at } r = a; \right. \\ &\left. \frac{1}{b} \left(J_m(k_1 r_0) H_m^{(2)}(k_1 a) - J'_m(k_1 a) H_m^{(2)}(k_1 r_0) \right) \text{at } r = b. \right. \end{aligned}$$

$$\begin{aligned} F_{vn}^{2a,b} &= - \int_{S_j} \bar{J}_n^{m,p} H_{nz}^{m,z} dS' = \\ &= \delta_n^{\pm 1} \frac{I_0^m}{2i\pi b W_2} \sum_{m=-\infty}^{\infty} e^{im(\varphi_\mu - \varphi_0)} \frac{H_m^{(2)}(k_2 r_0)}{H_m^{(2)}(k_2 b)} \end{aligned}$$

The solution of the SNAE (9) gives us unknown harmonic values of the magnetic surface currents on loads and on the dielectric.

3. PATTERNS AND SCATTERING PATTERNS

For considering problem fields in V_2 volume may be found by two ways: 1) as a sum of fields of primary source and fields of secondary sources which are magnetic surface currents on nonlinear loads with the help of auxiliary field for the dielectric coated cylinder; 2) using equivalent surface current theorem for surface currents on the dielectric layer founded from the SNAE solution; in this case for the auxiliary field we must take field of a perfect conducting cylinder of radius b .

In the first case we can look on founded nonlinear loads' magnetic currents as being magnetic currents' sheets on the surface of cylinder $r = a$. So we have:

$$\bar{b}H(p) = \int_{S_j} \bar{J}_n^{m,p} \bar{H}_n^{m,a} dS' + \sum_{q=1}^M J_{nqz}^m \int_{\Delta\varphi_q} H_{nz}^{m,a} a d\varphi', \quad (10)$$

where the auxiliary field determined as field of the magnetic current filament on the dielectric coated cylinder is:

$$\begin{aligned} H_z^{m,z}(r, \varphi, r', \varphi') &= -\frac{k_1}{4W_1} \sum_{m=-\infty}^{\infty} e^{im(\varphi - \varphi')} \times \\ &\times \frac{(J_m(k_1 r') H_m^{(2)}(k_1 a) - H_m^{(2)}(k_1 r) J'_m(k_1 a))}{H_m^{(2)}(k_1 a) H_m^{(2)}(k_2 b)} \times \\ &\times \left\{ H_m^{(2)}(k_1 b) + \frac{(J_m(k_1 b) H_m^{(2)}(k_1 a) - H_m^{(2)}(k_1 b) J'_m(k_1 a))}{Z_{1m}} \right. \\ &\times \left. \left(H_m^{(2)}(k_1 b) H_m^{(2)}(k_2 b) - \frac{W_2}{W_1} H_m^{(2)}(k_1 b) H_m^{(2)}(k_2 b) \right) \right\} \times \\ &\times H_m^{(2)}(k_2 r), \quad r > b; \end{aligned}$$

where

$$\begin{aligned} Z_{1m} &= \frac{W_2}{W_1} H_m^{(2)}(k_2 b) (J_m(k_1 b) H_m^{(2)}(k_1 a) - \\ &- H_m^{(2)}(k_1 b) J'_m(k_1 a)) - H_m^{(2)}(k_2 b) \times \\ &\times (J'_m(k_1 b) H_m^{(2)}(k_1 a) - H_m^{(2)}(k_1 b) J'_m(k_1 a)). \end{aligned}$$

Let's perform the integration in (10) in the case of excitation by the filament of the magnetic current (with I_0^m amplitude) flowing along z co-ordinate and find pattern of the structure when $r \rightarrow \infty$. The expression is normalized to $I_0^m \sqrt{2/\pi k_2 r} e^{-i(k_2 r - \pi/4)}$ that allows us to compare patterns

of n 's EMF harmonics for equal physical distances to observation point. We get

$$F_{nz}^p(r, \varphi) = \delta_n^{\pm 1} \left\{ \frac{i}{2\pi b W_1} \sum_{m=0}^{\infty} \varepsilon_m \cos(m(\varphi - \varphi_0)) e^{im\pi/2} \times \right. \\ \left. \frac{(J_m(k_1 r_0) H_m^{(2)}(k_1 a) - J_m'(k_1 a) H_m^{(2)}(k_1 r_0))}{Z_m} \right\} + \\ + \frac{e^{-i(k_{n2} - k_2)r}}{I_0^m W_1 \pi^2 k_{n1} b \sqrt{n}} \sum_{q=1}^M J_{nqz}^m \Delta \varphi_q \times \\ \times \sum_{m=0}^{\infty} \frac{\varepsilon_m \cos(m(\varphi - \varphi_q)) e^{im\pi/2} \text{sinc}(\Delta \varphi_q \frac{m}{2})}{Z_{mn}} \quad (11)$$

where J_{nqz}^m values are determined by the solution of the system (9), $\delta_n^{\pm 1}$ is the Kronecker symbol.

Let's find SP of the nonlinear loaded dielectric coated cylinder. Assume that the external magnetic current filament is placed at infinity ($r_0 \rightarrow \infty$). As in the case of patterns there are two ways to find SP. When $r \rightarrow \infty, r_0 \rightarrow \infty$ we take SP at fundamental frequency as:

$$F_{1H}^s(\varphi) = \frac{H_{1z}(r, \varphi) - H_{1z}^f(r, \varphi)}{\sqrt{2/\pi k_2 r} e^{i\pi/4} e^{-ik_2 r} H_0} \quad (11a)$$

and at harmonics' frequencies as:

$$F_{nH}^s(r, \varphi) = \frac{H_{nz}(r, \varphi)}{\sqrt{2/\pi k_2 r} e^{i\pi/4} e^{-ik_2 r} H_0}, \quad (11b)$$

where $H_{1z}^f(r, \varphi)$ is strength of magnetic field fallen on the cylinder, $H_0 = -\frac{I_0^m k_2}{4W_2} \sqrt{\frac{2}{\pi k_2 r_0}} e^{-ik_2 r_0} e^{i\pi/4}$. We use (10) when we find EMF in the first way. Performing the integration in the first addend of the right side for $r > r_0 > b$ we obtain:

$$F_{1H}^s(\varphi) = \sum_{m=0}^{\infty} \varepsilon_m \cos(m(\varphi - \varphi_0)) (-1)^m \times \\ \times \left\{ J_m'(k_1 b) H_m^{(2)}(k_1 a) - J_m'(k_1 a) H_m^{(2)}(k_1 b) \right\} J_m'(k_2 b) - \\ - \frac{W_2}{W_1} (J_m(k_1 b) H_m^{(2)}(k_1 a) - J_m(k_1 a) H_m^{(2)}(k_1 b)) \times \\ \times J_m'(k_2 b) \Big/ Z_m + \frac{1}{W_1 \pi^2 k_1 b H_0} \sum_{q=1}^M J_{1qz}^m \Delta \varphi_q \times \\ \times \sum_{m=0}^{\infty} \varepsilon_m i^m \cos(m(\varphi - \varphi_q)) \frac{\text{sinc}(\Delta \varphi_q m/2)}{Z_m}; \quad (12a)$$

$$F_{nH}^s(r, \varphi) = \frac{1}{\sqrt{n}} e^{-i(k_{n2} - k_2)r} \frac{1}{W_1 \pi^2 k_{n1} b H_0} \times \\ \times \sum_{q=1}^M J_{nqz}^m \Delta \varphi_q \sum_{m=0}^{\infty} \varepsilon_m i^m \cos(m(\varphi - \varphi_q)) \frac{\text{sinc}(\Delta \varphi_q m/2)}{Z_{nm}} \quad (12b)$$

If we introduce in (12) the equal normalization it allows us to compare SP of the scattered field at the equal distance r . In that case scattered field's relative level not only determined by distance but also dependence of the J_{nqz}^m / H_0 ratio on H_0 which is nonlinear.

4. NUMERICAL RESULTS

At first let's analyze patterns for cylinder without loads. The aim is to determine parameters of the dielectric coat for the best EMF radiation for the source on the perfect conducting cylinder's surface at multiple frequencies. That is we find parameters of the dielectric for which field strengths' ratio at the multiple frequencies has a maximum. For the coat with $(a-b)/a \leq 10\%$ ($a = 3$ cm, $b = 3.3$ cm) dependencies of the EMF of identity magnetic current filaments on the cylinder surface on dielectric permittivity ε shown on the fig.2 for current frequencies of 3,125 GHz, 6,25

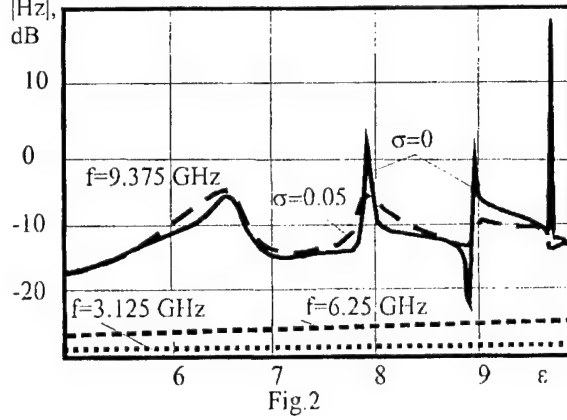


Fig.2

GHz and 9,375 GHz (layer conductivity $\sigma=0$ and 0.05). There are several extrema at 9,375 GHz that correspond for maximum differences of field levels at frequencies of 3,125 GHz and 9,375 GHz. As known [3,4] the reason of field increasing at extremum points may be surface delayed waves appeared on the dielectric layer which in the observation point produced addition radiation; or it may take place due to damp out of the surface waves when there are losses in the dielectric. Indeed, from fig.2 we can see that in presence of loss ($\sigma=0,05$) peaks in extremum points are cut relative to the no loss case. In the same time other graph parts are invariant because the field on them doesn't caused by surface waves radiation. Calculated surface current amplitude and phase patterns at $\varepsilon=9,888$; 8,962; 7,928 ($a=3$ cm, $b=3,3$ cm) in extremum points show that two waves propagated from the source in opposite directions appear. Superposed on one another they give standing wave on the layer surface. Surface wave slowness factors are 1,834; 1,69; 1,53 respectively.

Nonlinear loaded dielectric coated cylinder's patterns which is excited by the magnetic current filament placed in the dielectric with parameters $\varepsilon=7,928$ and 9,888 (this values correspond with the extremum points of EMF dependence on ε at frequency of 9,375 GHz) are shown on the fig.3. Primary current frequency is 3,125 GHz, current amplitude is 0,05 V. Nonlinear load with cubic VCC was used and thus EMF was determinated only on first and third harmonic frequencies. There is also patterns of cylinder with the same nonlinear load but without coating on the fig.3 (the pattern for $\varepsilon=1$ is indicated by the dashed line). Patterns for coated cylinder are compared with them. We notice from the fig.3 that at first radiation field at third harmonic frequency is determined by surface waves excited on the layer. At second field amplitude in directions of maximum of pattern's lobes exceeds the same one for cylinder without coating by 8...20 dB in the backward direction and more than 10...30 dB in the shadow area. Relative level of the EMF at third harmonic frequency compared to fundamental frequency one increases. At third EMF level relative increasing (for example for $\varphi=0^\circ$) when ε is given compared to the EMF for $\varepsilon=1$ is much less than it may be assumed from the comparing field levels on fig.2. It takes place because at ε changes EMF radiation conditions and secondary currents on nonlinear load excitation conditions are change also. Amplitudes of currents on the load at harmonic frequency when ε has values mentioned above are much less

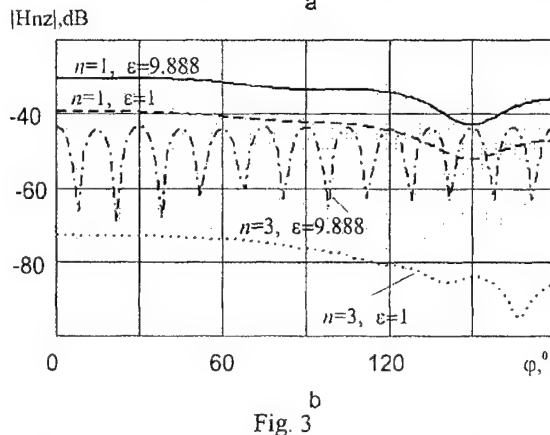
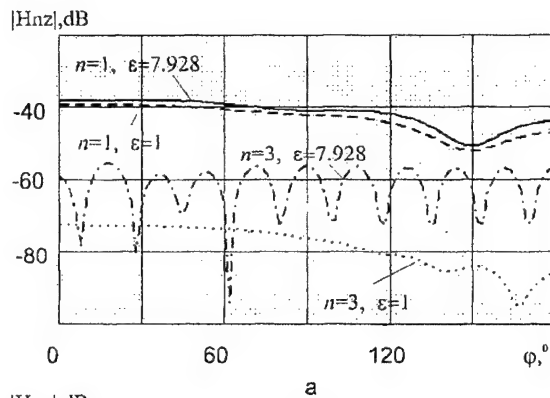


Fig. 3

then for $\epsilon = 1$. Consequently EMF amplitude essentially (more than 10 dB) decreases when small losses exist in the layer (fig. 4: $\epsilon = 7.928, \sigma = 0.05$).

Field increasing at third harmonic compared to uncoated cylinder case and field level changing compared to the field at the fundamental frequency are influenced by the layer depth and the primary source position relative to the nonlinear load (when other cylinder and coat's parameters are invariant). The closer the primary source to nonlinear load the more field increasing at harmonic frequency and the less one at ω frequency. Thus coating the perfect conducting cylinder with dielectric layer which depth and ϵ correspond to excitation of the surface waves at harmonic frequency on the layer surface effects cylindrical nonlinear radiator's patterns changes and EMF level at harmonic frequency increasing. Under these conditions essentially uniform radiation at harmonic frequency for any observation angles is taken place (when radius b is small in comparison with λ) and patterns shape at the fundamental frequency doesn't change a lot.

Let's consider now scattering patterns of the nonlinear loaded dielectric coated cylinder with the same ϵ parameter as it was for patterns. Scattering patterns for these cases and ones for cylinder without coat are shown on fig. 5.

Investigations show that coating the cylinder with dielectric layer produces secondary surface current density at harmonic frequency decreasing. It takes place due to exciting EMF level decreasing near the load for $\epsilon > 1$. In EMF scattering case on the structure with $\epsilon > 1$ decreasing of the density of the secondary current on the load exceeds the exciting case one by tens dB for equal ϵ (because in this case the source is placed far from the load). Thus the scattering field at harmonic frequency ($3f = 9.375$ GHz) in the most cases is less than one for cylinder without coating by tens dB in the backward direction and has comparable level in the shadow area even for ϵ corresponded maximum EMF radiation levels at frequency of 9.375 GHz.

Consequently as a rule the dielectric layer decreases (shields) scattering field at the third harmonic frequency. In the same time the scattering field at the fundamental frequency

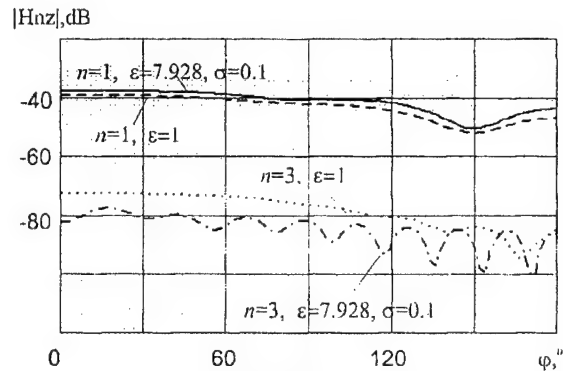


Fig. 4

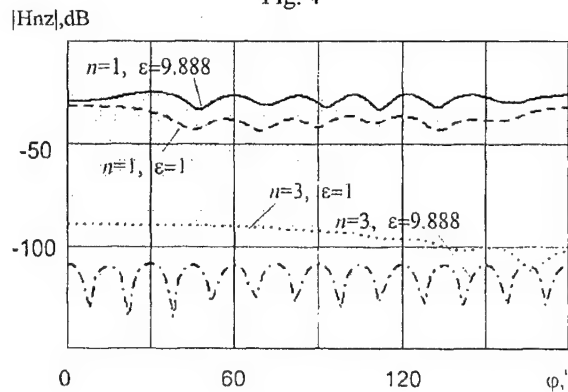


Fig. 5

increases: in backward direction about several dB (up to 5 dB) and in angles sector $20^\circ \dots 170^\circ$ by 5...10 dB.

5. REFERENCES

1. Petrov B.M., Semenikhina D.V. «Electromagnetic waves scattering by the nonlinear loaded semiplane» (in russian), Radioelectronics. V.34, N11, 1991, pp.98-100.
2. Petrov B.M., Semenikhina D.V., Panichev A.I. «Nonlinear scattering effect (monograph)» (in russian), Taganrog, TSURE, 1997.
3. Uberall H., Gaunavid G.C. «Relation Between the Ringing Resonances and Surface Waves in Radar Scattering», IEEE Trans. Antennas and Propag., V.32, N10, 1984, pp.1071-1079.
4. Mao Zhiji, Wu Jianxiang. «The Pattern of Magnetic-Source of the Surface of the Infinite Length Conducting Circular Cylinder Coated with a Dielectric», Antennas and Propag., AP-S Int. Symp. Syracuse, N.Y., June 6-10, 1988, Dig. Vol. 3. New York (N. Y.), 1988, pp.1078-1081.
5. Petrov B.M., Semenikhina D.V., Panichev A.I. «A New Analysis Method of Nonlinear Scattering for Solution EMC Problems», 11 Internat. Wroclaw Symp. on Electromag. Compat., 1992, Part I, pp.45-49.

BIOGRAPHICAL NOTES

Diana V. Semenikhina was born in Taganrog, Russia, in 1962. She graduated from Taganrog Radio Engineering Institute in 1985. In 1990 she received the scientific degree of the candidate of technical sciences. From 1991 to 1997 she worked as Senior Lecturer in Antennas & Radiotransmitter devices' Dept. of Taganrog State University of Radio Engineering. From 1997 she working toward Ph. degree dissertation.

Andrey A. Beletsky was born in Taganrog, Russia in 1976. He graduated from Taganrog State University of Radio Engineering in 1998. Now he is an post-graduated student of Antennas & Radiotransmitter devices' Dept. of Taganrog State University of Radio Engineering.

NUMERICAL COMPUTATION OF THE NEAR-FIELD OF TYPICAL AMATEUR RADIO ANTENNAS AND COMPARISON WITH APPROXIMATE RESULTS OF FAR-FIELD FORMULAS APPLIED IN THE NEAR-FIELD REGION

Ulrich Jakobus, DG6SHF

Institut für Hochfrequenztechnik, University of Stuttgart
Pfaffenwaldring 47, 70550 Stuttgart, Germany
Fax +49 (0)711/685-7412, Phone +49 (0)711/685-7420
E-Mail u.jakobus@ieee.org

In order to assess the possible exposure in the near-field of amateur radio antennas, it is important to have approximate formulas at hand. This paper discusses the application of far-field formulas in the near-field region, and compares the results to a rigorous near-field analysis using numerical techniques.

1 INTRODUCTION

It is important for radio amateurs to be aware of the field strength level in the near-field region of their transmitting antennas in order to ensure the conformity to safety limits defined in national and international EMC standards e.g. concerning the field exposure of humans in the close vicinity of antennas.

For the far-field region of an antenna radiating in free-space, relatively simple formulas exist so that the electric or magnetic field strength can be computed from the radiated power, the antenna directivity in a specific direction, and from the distance of the observation point to the antenna.

The situation is much more complicated for the near-field region, even when effects such as buildings, ground etc. are ignored. No simple formulas exist for general antennas, so the only choice a radio amateur has is either to perform measurements or to apply numerical techniques. It would be desirable to have simple formulas at hand, at least in the sense of a worst-case approximation, to ensure that safety limits are not exceeded.

In the present paper the near-field of some typical amateur radio antennas (half-wave dipole, 15-element Yagi Uda antenna, and magnetic loop antenna) is computed numerically. The far-field formulas are applied also for distance ranges in the near-field, and the resulting field strength values are com-

pared to those obtained by the rigorous numerical method. It is discussed under which circumstances the application of the far-field formulas in the near-field is justified as a worst case approximation in order to obtain an upper bound for the field strength level to be expected.

2 THEORETICAL CONSIDERATIONS

2.1 Exact near-field computations

Using a computer model of an antenna and numerical techniques, it is possible to accurately predict the near-field, e.g. the electric field strength E^{NF} at any arbitrary point in space (the index NF indicates the near-field). Here in this paper, the method of moments as implemented in the computer code FEKO [1] is used for this purpose.

Once E^{NF} has been computed, it is normalised according to

$$\Gamma^{\text{NF}} = \frac{\lambda \cdot E^{\text{NF}}}{\sqrt{P_t \cdot Z_{F0}}} \quad (1)$$

with the wavelength λ , the radiated power P_t and the free-space impedance $Z_{F0} \approx 376.73 \Omega$, so that the dimensionless figure Γ^{NF} can be used to characterise the near-field of an antenna, independent of the operating frequency or the transmitted power.

2.2 Approximate far-field formulas

The well-known formula

$$E^{\text{FF}} = \sqrt{\frac{P_t \cdot Z_{F0} \cdot D}{4\pi r^2}} \quad (2)$$

represents a relation to compute the electrical field strength E^{FF} (RMS value) of an antenna in the

main-beam direction in the far-field, indicated by the index FF. P_t denotes the transmitted power, $Z_{F0} \approx 376.73 \Omega$ is the wave impedance of free space, and D represents the directivity of the antenna under consideration as compared to an isotropic point source. Finally, r in eqn. (2) is the distance of the observation point to the antenna.

The expression (2) can be extended to directions other than the main beam direction by introducing the normalised field pattern $C(\vartheta, \varphi)$, leading to

$$E^{FF}(\vartheta, \varphi) = \sqrt{\frac{P_t \cdot Z_{F0} \cdot D}{4\pi r^2}} \cdot C(\vartheta, \varphi) \quad (3)$$

Also normalising the far-field (3) according to eqn. (1) leads to the simplified representation

$$\Gamma^{FF}(\vartheta, \varphi) = \frac{\lambda \cdot E^{FF}}{\sqrt{P_t \cdot Z_{F0}}} = \sqrt{\frac{D}{4\pi}} \cdot \frac{\lambda}{r} \cdot C(\vartheta, \varphi) \quad (4)$$

2.3 Distance definitions

The far-field formulas (3) and (4) depend on the distance r of the observation point to the antenna. In the far-field with distances r much larger than the typical antenna dimensions, there are no ambiguities with respect to distance measurement.

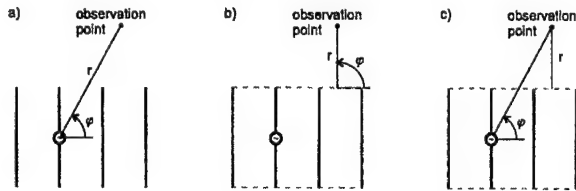


Fig. 1: Possible definitions for the distance r of an observation point to an antenna.

When applying the far-field formulas also for observation points in the near-field, then one faces the problems of having a unique definition for the distance r . Several options are indicated in Fig. 1.

If the far-field formulas shall be applied in a worst-case sense, so that the actual near-field will not exceed that far-field value, then the smallest value of r should be used in eqn. (3). This corresponds to Figs. 1 b) and c), where the distance is measured with respect to the closest antenna element. The difference between the definitions b) and c) is that in b) also the angles ϑ, φ are measured with respect to this point, whereas in the definition c) the angles are measured with respect to the phase centre of the antenna. This definition c) is the preferred one, since then the normalised field pattern $C(\vartheta, \varphi)$ is based on more useful angles.

3 NUMERICAL RESULTS

3.1 Results for a 15-element Yagi-Uda antenna

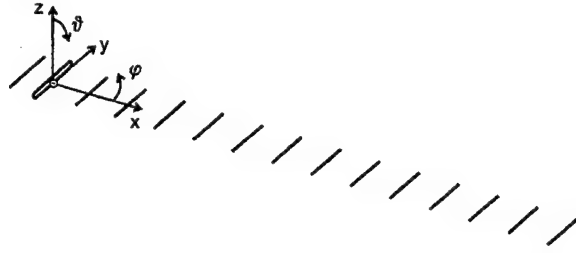


Fig. 2: 15-element Yagi Uda antenna with co-ordinate system.

As a first example, the 15-element Yagi-Uda antenna according to Fig. 2 shall be considered. The antenna consists of a reflector of length 0.475λ (λ is the free-space wavelength), a folded $\frac{\lambda}{2}$ -dipole at the distance 0.2λ to the reflector, and 13 further directors with mutual distances 0.308λ . The diameter of all wires is 0.0085λ , and the length of the directors can be found in [2, Table 9.6] or [3, Table 5-4]. The computed far-field directivity is $D = 34.9$, corresponding to 15.4 dBi.

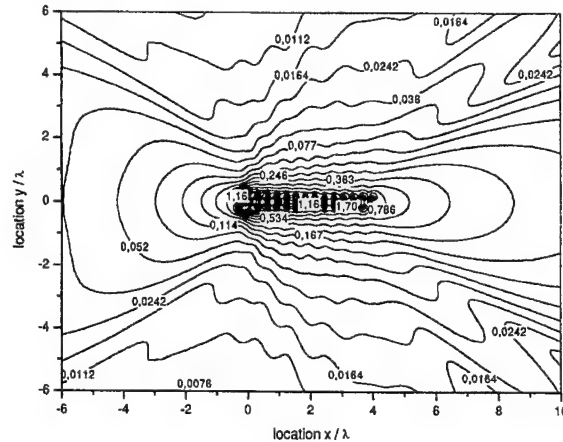


Fig. 3: Computed electric near-field for the 15-element Yagi-Uda antenna, normalised values according to eqn. (1).

The electric near-field E^{NF} (RMS value including all vector components) in the vicinity of the antenna is shown in Fig. 3. The values have been normalised according to eqn. (1).

One can now also apply far-field formulas in the near-field region, and define at every observation point the ratio

$$v = \frac{E^{NF}}{E^{FF}} = \frac{\Gamma^{NF}}{\Gamma^{FF}} \quad (5)$$

of the electric field strength based on the exact near-field computation (NF) and the approximate far-

field formulas (FF). For regions with $v < 1$, the near-field is smaller than the value based on the far-field approximation, so from a worst-case point of view, it is then safe to apply the far-field formulas in order to verify the conformity of an antenna to safety limits.

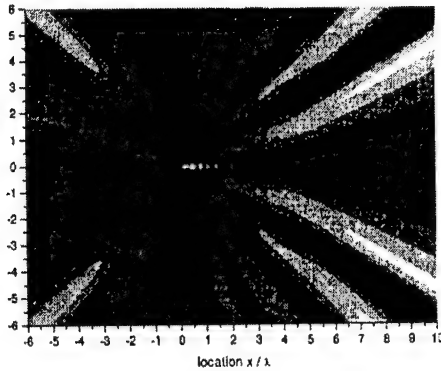


Fig. 4: Ratio v according to eqn. (5) for the 15-element Yagi-Uda antenna for a distance definition according to Fig. 1 a).

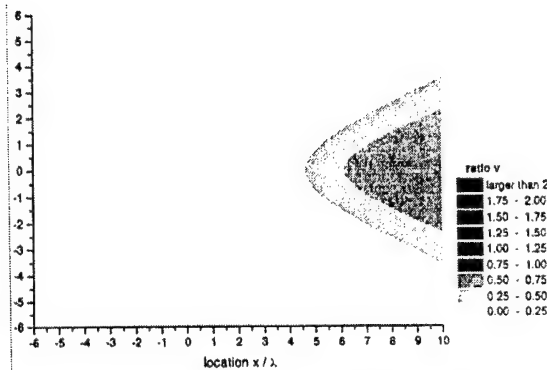


Fig. 5: Ratio v according to eqn. (5) for the 15-element Yagi-Uda antenna for a distance definition according to Fig. 1 c).

For the 15-element Yagi-Uda antenna, this ratio v based on a distance definition according to Fig. 1 a) is depicted in Fig. 4. Obviously there are regions with $v > 1$, but by simply redefining the distance definition according to Fig. 1 c) and assuming a worst case directivity as in the main-beam direction for all directions, one obtains the graph in Fig. 5. For all points in the considered plane, one realises that $v < 1$, so that the far-field formulas can be applied in the near-field region in order to obtain a worst case approximation.

3.2 Results for a $\frac{\lambda}{2}$ -dipole antenna

In this section a similar investigation shall be conducted for a simple $\frac{\lambda}{2}$ -dipole antenna with a wire diameter of 0.002λ . The electric near-field of the

antenna, which is aligned parallel to the y -axis, is depicted in Fig. 6, again it has been normalised with the help of eqn. (1).

The ratio v according to eqn. (5) for this antenna is shown in Fig. 7. Again it can be observed that everywhere in space the far-field formulas yield lower field strength values than the actual near-field, provided that a distance definition according to Fig. 1 c) is used and the angular dependency of the relative field pattern $C(\vartheta, \varphi)$ is neglected.

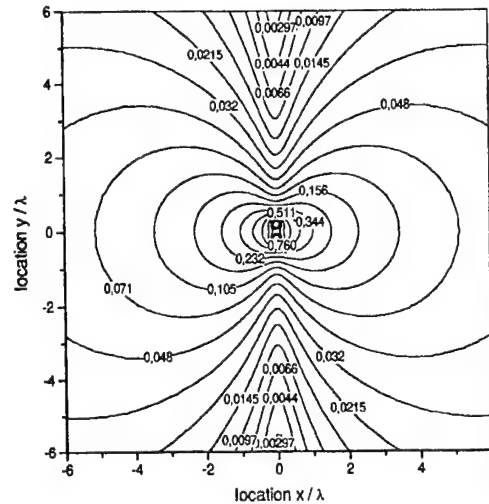


Fig. 6: Computed electric near-field for the $\frac{\lambda}{2}$ -dipole antenna, normalised values according to eqn. (1).

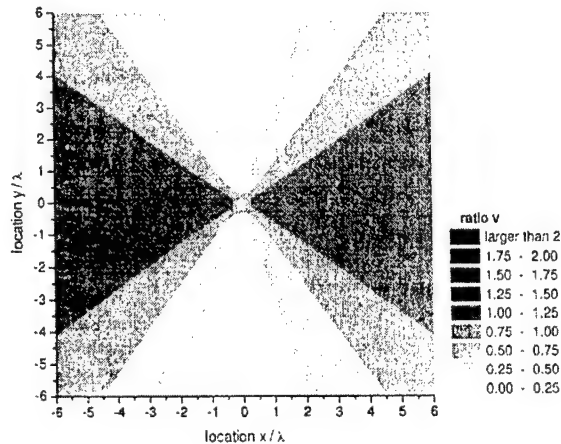


Fig. 7: Ratio v according to eqn. (5) for the $\frac{\lambda}{2}$ -dipole antenna for a distance definition according to Fig. 1 c).

3.3 Results for a magnetic loop antenna

Quite popular amongst radio amateurs are also magnetic loop antennas, and hence such an antenna shall be considered as well.

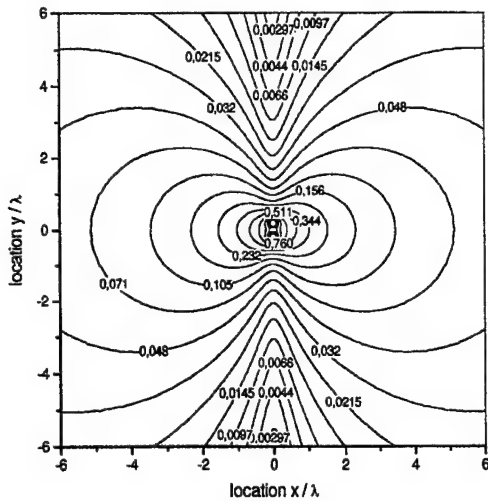


Fig. 8: Computed electric near-field for the magnetic loop antenna, normalised values according to eqn. (1).

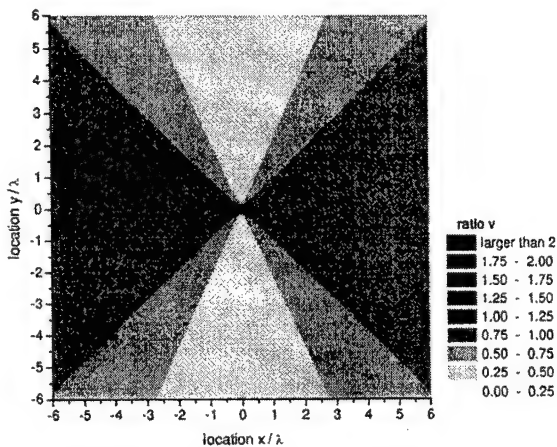


Fig. 9: Ratio v according to eqn. (5) for the magnetic loop antenna for a distance definition according to Fig. 1 c).

The magnetic loop considered here is located in the xz -plane, has a diameter of $\frac{\lambda}{20}$, and a wire radius of 0.002λ .

The computed near-field is depicted in Fig. 8, and the ratio v is plotted in Fig. 9.

4 CONCLUSIONS

For three typical amateur radio antennas, the electric near-field has been computed by applying rigorous numerical techniques. In order to assist radio amateurs in estimating the field strength level using approximate formulas, it was shown that an application of the far-field formulas in the near-field can be used as a worst case approximation, provided that the distance definition according to Fig. 1 c) is used and the angular dependence of the radiation pattern is neglected.

REFERENCES

- [1] Electromagnetic Software & Systems (EMSS), Stellenbosch, South Africa, *FEKO User's Guide*, 1999. URL <http://www.feko.co.za>.
- [2] C. A. Balanis, *Antenna Theory: Analysis and Design*. New York: John Wiley & Sons, 1982.
- [3] W. L. Stutzman and G. A. Thiele, *Antenna Theory and Design*. New York: John Wiley & Sons, second ed., 1998.

BIOGRAPHICAL NOTE

Ulrich Jakobus received the Dipl.-Ing. and Dr.-Ing. degrees in electrical engineering from the University of Stuttgart, Germany, in 1991 and 1994, respectively. He completed his Habilitation in 1999 and became Privatdozent at the same university.

Since 1991 he is with the Institut für Hochfrequenztechnik, University of Stuttgart. There his main areas of research include numerical techniques in electromagnetics, antennas, electromagnetic compatibility, and bioelectromagnetics.

EM RADIATION HAZARD IN RESIDENTIAL AREAS

Wojciech Klosok¹ and Hubert Trzaska²

1. Polish Amateur Radio Union
P.O.Box 131, 44201 Rybnik, Poland
E-mail: WKLOSOK@RSI.PL

2. EM Environment Protection Lab., ITA
Technical University of Wroclaw
Wyspianskiego 27, 50-370 Wroclaw, Poland
E-mail: HUTRZ@ZR.ITA.PWR.WROC.PL

Abstract: The work deals with problems faced by inhabitants of residential areas, potentially exposed to a hazard created by sources of EM radiation. Cases of paranoiac character, exposure created by unidentified sources as well as power line frequency and RF sources are analysed. It is shown that presently in the discussed cases a hazardous exposure is rather exceptional. However, almost any potential source of radiation creates negative countermeasures of inhabitants in the area where an investment is planned. The countermeasures are especially bothersome for operators of the Amateur Radio Service.

1. INTRODUCTION

The Electromagnetic Environment Protection Lab has been involved, among others, in EM field measurements. The majority of Polish inspection services (The National Radiocommunication Agency, The National Sanitary Inspection) have been supplied with EM field meters designed and currently recalibrated in the Lab. As a result the Lab has the widest metrological possibilities within the country. Because of this and due to a long-time experience of the Lab in the field in cases of doubts or troubles in measurements and the measurements' results interpretation the Lab is usually invited to consult for the services mentioned and to other institutions and persons involved. Similarly, the Lab plays a role of an independent 'mediator' if inspected institutions or single persons are not satisfied with the results of measurements performed by governmental services. In the case of unusual metrological needs or situations we are usually shown as the place where any help may be found. It resulted in many visits of people convinced that they are victims of the exposure to intentional or unintentional EM radiation. We always try to do everything possible to help the miserables (in relation to individual persons it is done on a voluntary basis).

Each of the cases is approached with full forbearance and confidence (although the latter is sometime abused because we sometimes make a use of the collected material in our publications, but it is never done without an agreement of a person involved, especially while a publication makes it possible to identify the person). Our engagement is related to several groups of problems; the Amateur Radio Service (ARS) and its role in the EM environment pollution in residential areas is one of them.

2. 'MARTIANS'?

This group of 'victims' experience feelings of sensations related to real or imagined EM irradiation. People complain about EM radiation from a BC or TV station, mysterious generators installed in the neighbourhood and used intentionally or unintentionally to annihilate them, microwave ovens, satellite TV (receiving) antennas or, even, coffee mills. Such wild notions as security or/and intelligence services, police, neighbours or family members looking for their lives and property or even small green men are said to be responsible for their problems. Below we will present several selected cases of the exposure. They seem to be the most specific ones.

1. MI-5?

A high school professor from a small town, after her visit to Australia, has been discovered as a candidate to the British throne. Because of this the British secret services followed her every step and supervised her life to protect her against any undesirable escapades that would humiliate the Royal Family. An implanted (into her body) radio transmitter enabled round the clock observations. Apart from breaking her privacy the transmitter affected her health. It caused troubles usually associated with the exposition to the EM waves. After many talks and explanations that any transmitter

should have a power source we suggested that she should have her whole body X-rayed. It was done and the results (with consultation of a radiologist) have allayed her misgivings. Consulting the case with doctors we came to a supposition that her problems could be connected with her climacteric.

2. A BC station?

A master-builder, resident of a small town, near a FM&TV transmitting center, complained of 'hearing' AM & FM BC programs while staying at home and during walks near transmitting centers. At the same time he was feeling the headaches, exasperation, anxiety. The 'hearing', however, was not correlated with the stations' programs. Laboratory tests did not confirm his sensitivity to FM or AM modulated fields. After several talks and laboratory experiments we suggested that he should have screened his head with, for instance, a bucket. After that he logically asked if the bucket should be enamelled or zinc plated (he had no doubt that it should be a metallic one). The therapy was successful, a couple of months after that he came to the ITA director's office and extolled us to the skies as we helped him like nobody before. Since that time our colleagues have had a subject for jokes about us.

3. A μ -wave oven?

A university professor (sic!), highly qualified dowser (as a hobbyist), complained of EM fields radiated by a microwave oven. He claimed he was able to sense some kind of discomfort just at the moment when the oven was turned on. Performed measurements showed good performance of the device and the field levels well below limits. His wife said he was able to sense even when the oven was not working. In his opinion the feelings could be caused by other ovens used by their neighbours in the apartment house.

4. A coffee-mill?

A newspaper reporter during an interview with us reported to us that she had irritating feelings even when she was using an electric coffee-mill. Thus, the alarm clocks were not a new discovery of the British reporter [1]. One may notice here that these fields are several orders below those of a hair-dryers [2], however, they are generated in a wide frequency spectrum.

5. The neighbours?

The subject of complains are usually health problems (headaches, physical or mental shocks, pain in different parts of the body, heat or/and cool) caused by EM field generators installed by neighbours (all the studied cases took place in apartment houses). These generators that are small-sized devices brought from the West (what an indirect appreciation of Western technology!), especially to persecute or annihilate the neighbours. Sometime the complaints were justified by EMI observed on the screen of a TV receiver or similar phenomena and caused by equipment installed in another flat (medical devices like EEG, EKG,

sonograph or diathermy, microwave ovens mentioned or video-recorders and sets for video-tapes copying).

In these cases a police was usually involved. But, in our opinion, in the majority of the cases the problem here is in jealousy or variances with the neighbours. EM field is more or less perfidiously called here because of its' mystery and, in beliefs of the involved persons, impossible to check.

We cite these sometimes humorous cases to illustrate the scale of the problem. Although in the majority of them no evident connection with the EM field may be found, in some of the cases the hypersensitivity to EM field may play a certain role [3].

2. 50Hz

Contrary to the cases presented above, where it was impossible to identify a radiation source, we will start now a presentation of cases in which a source may be easily found. The latter does not mean that the source is really responsible for sensations and feelings of a victim.

Apart from HV power-lines the problem is caused by the local power substations. Up to now the substations were located on the ground floor of apartment houses (now it is prohibited). People located above or/and close to a substation compartment often explained to themselves their life troubles, physical and emotional sensations or diseases as associated with 'the dangerous neighbourhood'. Measurements performed have confirmed only very few cases in which the magnetic field exceeded the typical floor values for quarters equipped with the AC power installation (The Polish environmental standard allows 80 A/m at 50 Hz) whereas E-field measurements have never shown any influence of the local substation on the electric field intensity as compared to the typical floor of 50 Hz, 220 V home power-installation (environmental limit is here 10 kV/m).

It is impossible to judge here if the feelings of the people are true, based on EM phobia or results from hypersensitivity. The presence of the phobia may be concluded from creation of local committees fighting against The International Strong Magnetic Fields Lab in Wroclaw, a DC submarine cable from Poland to Sweden, etc. The author would have never seen the paper on 'We've found cancer link to pylons, say scientists' published in Daily Mail (Feb.14, 1996) if it weren't for the letters received by him from frightened people. The subtitle of the paper warns: 'Some experts say pylons, and even alarm clocks, may have the power to cause cancer [4].

3. COMMUNICATION DEVICES

We would not like to discuss here an imaginary exposure from satellite receiving antennas, radio-receivers, tape-recorders and similar devices which may be responsible for EM interference, but not for exposure exceeding standards in law.

3.1. A FM BC station

The station, located on the top of a hill, in a suburban residential area, contains transmitters for several TV and FM programmes. As usually, on the top of its antenna tower are located antennas for IV-th TV band, below them antennas for III-rd TV band and at the lowest level were installed antennas for FM bands. Inhabitants of that area, that make a match of their health problems with emissions from the station, invited us to measure the EM field around and inside their houses. The measurements lead us to the following conclusions:

- nowhere (in open space) the measured values exceeded levels permitted for general public (7 V/m); the maximal measured values, at a distance from the antenna tower, were around 5 V/m,
- the fields exceeding the limits could be found only in close proximity of conducting bodies due to standing waves and resonant phenomena,
- the standing wave measurements allowed to indicate a source responsible for the radiation, these were FM transmitters,
- probably because of the beam inclination the fields exceeded (at FM frequencies) 1 V/m within quite a large radius (while near the antenna the field was well below 1 V/m).

As in the cases presented above, the residents were round the clock irradiated by the station. Their health was never investigated, nor any protection measures were proposed by the station operator. During our talks there, the Director of the school mentioned that in her opinion the children are more sickly and dulled compared to previous generations. As no medical investigations could support the point one may suppose that these disadvantageous health variations have been caused by less and less time spend playing in the open air in favour of watching TV, video-tapes and computer games.

Similar problems appear in the proximity of several AM and FM BC stations. It may be summarised as: round the clock and not exceeding permitted levels. Doubts may arise in the relation to a hazard created by the permanent exposure and a role played by the modulation (especially in the case of AM).

3.2 Radiotelephone base stations

As a rule the radiotelephone base stations are located on roofs of tall buildings, steeples, antenna towers or other natural or artificial heights. Due to directional properties of antennas applied as well as radiated power in an area the field intensity exceeds that permitted by environmental standard (0.1 W/m²). However, the area is focused in the horizontal direction and its range does not exceed 20 m [5]. An excessive exposure may take place only on the roof of the building, in close proximity of the antennas. EM Environment Protection Lab was involved in many theoretical estimations and EMF measurements near the stations (along with requirements of Polish standards) and in no case the EMF intensities,

exceeding those permitted, were found at places where inhabitants may appear. With no regard to it in almost any case, while a station was planned and then installed, the investment was followed by strong activity of the inhabitants creating protest committees, then writing letters to the highest bodies and, even, damaging the installed devices.

The case leads to the following comments:

- it is very interesting that doubts and protests are caused by base stations while the use of portable devices is widely accepted,
- beneficial in any aspect large antennas' installations seem to be impressive and rather their sizes than fields generated by them are the matter of protests; the point may be supported by strong protests against large DBS receiving antennas several years ago,
- a similar doubt may be formulated as above: what is the role of a long-term low-level exposure; however, the question seems to be the most absorbing for investigators world-wide now.

3.3. The Amateur Radio Service

The service was always located within residential areas. It has already been shown that the service may create some problems while long-wire type antennas are applied. Other possibilities are fields generated by high gain, directional antennas at a distance, while the beam of the antenna illuminates an object. Although hams' stations may generate fields exceeding those of professional services their work is usually very irregular and, sometimes, their activity is broken for longer periods of time [6].

Similarly as in other services in the case of the ARS the most 'controversial' seem to be their antennas. We'll illustrate it with two examples.

a. SP6TPF

A ham's station located in an apartment house in Opole. Equipped with a 100 W transceiver and two antennas: a W3DZZ multiband dipole and a directional one (cubical quad). The neighbours accused the operator of interference in radio- and TV reception as well as in video-tape watching and of hazardous affecting their health. The case was taken to a court. As a result series of investigations and measurements were performed. Among others our Lab was involved in a part of them. It was discovered by inspectors that home entertainment devices applied by the neighbours and their installation are out of order (mismatched antennas, non-linear heads of active antennas, ungrounded installations, devices without necessary homologation, etc.). On the other hand, the station was investigated in every aspect. Even an expert in civil engineering was engaged to find if the construction of the quad antenna may create a possibility to damage the chimney top to which the antenna was partly fastened. Of course no EMF levels exceeding both the EMI and the environment protection standard were found.

The end of the case looks likes a comedy. The court was unable to find any formal reason to stop the activity

of the station. However, the operator has ordered to remove a reflector of the antenna that overlooks the next house - where his adversaries reside.

b. SP9PT

DX-man active for over forty years, after moving in 1987 to a dwelling house in a suburban area, has become 'an enemy' of the local community. His shack from very beginning included a TS950S 100 W multiband transceiver and antennas: 3 element beam for 18 and 24 MHz bands and GP and inverted V for the others. Strictures of his neighbours were similar as in the previous case. They were focused on EMI and a hazard created to them (it included cases of the cancer due to unwanted exposure to the ham's emissions). The next steps were almost identical as above and they involved any available bodies and commissions. Again, as in the previous case any investigations gave similar results. Inappropriate installations of TV antennas, old type home entertainment electronic devices and no fields exceeding those permitted by the protection standards. The ham, at his own expense, modernised antenna's installation in the nearest house and offered RFI filters and a change of an old TV receiver to a better one, the latter was not accepted by the family active involved in the protests.

Although emissions of the ham are limited to ten or so minutes a day his neighbours, after reading a paper in a journal (the paper was devoted to hazards created by the former 2 MW LW Central BC station, working round-clock, and protest against it by the local community) and unfavourable for them results of any investigations, started making phone calls to the ham with abuses. Finally he was informed that as he is responsible for destroying his lives, he and his family would be an object of similar response. As a result of the threat a prosecutor initiated an investigation which was then closed because the case did not include 'evident symptoms of an offence'.

4. CONCLUSION

The problem of potential hazard created in residential areas was illustrated with some examples. They may lead to three reasons of negative feelings of the persons involved:

- schizophrenia or/and other mental diseases,
- an EM phobia,
- a hypersensitivity.

The above does not include any hazard understood as an exposure exceeding levels permitted by the Polish protection standards. Not to mention about less restrictive standards of the Western World. The exposure was measured or estimated in any presented case and in no case it was above limits (if any measurable EM levels were found).

Although the phobia may be considered as a kind of mental disease in our studies we differentiate them with the use of a primitive criterion: in cases of phobia usually there was a reason for it (a source of radiation,

e.g.: antennas, transformers) while in the other ones the reason was unnecessary. These cases require a treatment in the form of a medical cure (mental diseases) or an information (phobia).

The last case requires a bit more care. Presented materials show that in some cases the presence of a hypersensitivity can not be excluded. On the one hand we may ask why 'an allergy' must not exist in the area of EMF while it is well confirmed in cases of many other physical and chemical factors. On the other hand, however, it may be confirmed by the personal feelings of the authors. In their opinion their health problems may be associated with the long term exposure to relatively weak EMF. Fortunately, the problem of hypersensitivity has been intensively studied lately.

A hazard created by a permanent, low-level exposure may lead to a necessity to lower the valid standards. The present ones seem to be rather satisfying, representing better financial possibilities, circles of business than the general public. With no regard to it the standards require a simplification, in order to be in a correlation with present knowledge [7].

REFERENCES

1. A. Kent - A hidden danger in our homes? Daily Mail, June 7, 1994.
2. D. Wu, O. P. Ghandi, J. Y. Chen - Electric field and current density distributions induced in a millimeter-resolution model of the human head and neck by magnetic fields of a hair dryer and an electric shaver. Sixteenth Annual Meeting of the BEMS, Copenhagen 1994, paper nr.C-1-4.
3. H. Trzaska - Hypersensitivity? Proc. of the COST 244 Meeting on Electromagnetic hypersensitivity, Graz 1994, pp.106-117.
4. H. Trzaska - EM environment in apartment houses. proc. 1988 Intl. EMC Symp. Wroclaw, pp.471-474.
5. H. Aniolczyk - EMF distribution around GSM base-stations (in Polish). In Proc. 1-st Natl. Conf. GSM and Human and Environment Protection, Warsaw 1998.
6. H. Trzaska - ARS and EM-radiation hazard. Proc. 1994 Intl. EMC Symp. Sendai, pp.191-194.
7. WHO Intl. EMF Project. Intl. Round Table on World EMS Standards Harmonization, Zagreb 1998.

BIOGRAPHICAL NOTES

Mr. W. Klosok was born in 1942 in Radlin (Upper Silesia). Has completed his M.Sc. in mining geodesy at the Mining and Metallurgical Academy in Cracov in 1967. Retired staff member of the Rybnik Mining Company. Judicial and governmental expert in mining. Active ham radio SP9PT.

Prof. H. Trzaska was born in Wilno (Poland) in 1939. His. M.Sc., Ph.Dr. and D.Sc. degrees completed at the Techn. Univ. of Wroclaw in 1962, 1970 and 1988 resp. Head of the EM Env. Prot. Lab., involved in labour safety and environment protection against EMF. Active ham radio SP6RT.

VERY HIGH POWER SCIENTIFIC RADIO EMISSIONS AS EMI SOURCES TO RADIO AMATEUR SERVICE

Antero Väänänen

Vaasa Polytechnic University, Wolffintie 30, FIN-65200 Vaasa, Finland; now at
Sodankylä Geophysical Observatory, Tähteläntie 112, FIN-99600 Sodankylä, Finland

Fax: +358 16 615529, Tel: +358 16 619829, E-mail: av@sgo.fi

Radio transmissions of very high effective radiated power are used for many different scientific purposes. Most of the transmissions have the nature of a radar system, and many of them operate on or near the frequency bands which are available to radio amateur use. Some of these systems, having the potential to cause EMI problems to radio amateurs, are presented.

1. INTRODUCTION

Research on the state and properties of the atmosphere with all its different layers can be made, for scientific and everyday purposes, with the help of radar-type systems transmitting high power radio waves. Some methods employ also artificial modification of some properties of the investigated volume of the ionosphere by the use of high power radio waves. In some cases these transmissions employ frequencies even inside the frequency bands allocated exclusively for radio amateur use, and in very many cases the operation is on frequencies very near to amateur radio frequency bands. This leads to several possible types of EMI problems for radio amateurs. For the most part it is quite probable that an average radio amateur does not know the existence of these scientific rf systems, and so the cause of the problems may remain unsolved. The purpose of this presentation is to give an overview of these systems, which could maybe be helpful information for solving EMI mysteries.

2. IONOSONDES

An ionosonde is a radar-type system for measuring the height and other properties of the ionospheric layers. The most common type is the directly upwards-transmitting Vertical Incidence Sounder. Oblique-incidence sounders were somewhat less rare 20-30 years ago than nowadays. Most ionosondes transmit pulses, either simple or coded, but there is also a variant using continuous frequency-sweepped signal. The pulse may be repeated (typically 2-16 times) on a certain frequency, and then the transmission is moved to the next frequency. Pulse length is often 40-70 μ s, and pulse repetition frequency 50, 100 or 200 Hz, for

example. In the simplest ionosonde the apparent height of the ionospheric layer is determined from the delay time between the leading edges of the transmitted pulse and its returned echo. The more advanced ionosondes may measure also the frequency, doppler shift and its spread, amplitude, phase, angle (direction) of arrival and polarization of the returned signal. A product of these measurements interesting to radio amateurs is the critical frequency, which is the highest frequency that is still reflected back to the earth. The maximum usable frequency for ordinary radio contacts is approximately three times this vertical critical frequency. The frequency range of ionosonde measurements starts usually at 0.5 or 1 MHz and goes to 16-20 MHz in the VIS systems, but may reach even 45 MHz in oblique sounders. The frequency can be stepped in many different ways, linearly or logarithmically. A basic system could be a logarithmic sweep of 100 or 200 frequency steps per octave. A modern computer-controlled system could leave gaps in the sweep, but most ionosondes do not, and thus their pulse trains can be heard very often also on radio amateur bands. The soundings are made at least every hour and half-hour, but at many locations with shorter intervals down to 5 minutes. The sounding itself may last from some seconds to several minutes, depending on the frequency resolution and number of pulse repetitions. Many ionosonde transmitters have output powers from some kW to some tens of kW. The most modern "digital" or chirped CW/FM versions use less power, down to 100-600 W, due to their more sophisticated principles (coded pulses etc). Transmitting antenna in a VIS is pointed upwards and is usually a delta loop (made somehow to have the required bandwidth), rhombic or log-periodic. The tx antennas are usually not very effectively directive on the lowest frequencies, and also due to the reflection from the ionosphere, the transmitted signal spreads to a not very small area. In the near field an ionosonde is an extremely nasty neighbour to a radio amateur or a swl. The pulses have a broad spectrum compared to normal signals, and often the harmonic overtone attenuation is not good inside the swept frequency range. Attenuation of spurious components outside the

swept range is better. The total number of ionosondes in operation is probably at least over one hundred units, and they are not, unfortunately, all located in isolated uninhabited places.

3. IONOSPHERIC HEATERS

An ionospheric heater is a very powerful lower HF transmitting facility with a vertically radiating antenna system. The purpose is to modify the properties of a certain volume of the ionosphere by heating it with a high-power electromagnetic wave which is absorbed by this volume, in order to be able to measure its physical parameters in new or better ways with the help of this modification. The frequency range which can be used for this purpose is usually (due to the basic physical properties of the ionosphere itself) approximately from 2 to 10 MHz. Transmitter output powers are up to MW class and antenna system gains around 20-30 dB, leading to ERP's of over 1 GW (see

Tables 1 and 2 for some details). The transmitted signal may be CW or pulsed or modulated with a broad range of frequencies from mHz's to kHz's. With pulse modulation the transmitted signal can occupy a surprisingly broad bandwidth. Fig. 1 is an example of EISCAT heater signal with pulse modulation, recorded from an ionospherically propagated signal 95 km away from the heater. When the carrier frequency is near the edge of a radio amateur band, this kind of a signal may cause several difficulties to reception in amateur traffic (in this example making it totally impossible to listen to weak US DX signals below 4 MHz). The enormous ERP of the heater signal may also cause cross modulation and other nonlinear effects in the ionosphere. The total number of these installations in the world is, fortunately, a decade lower than the number of ionosondes, but we have some of these here in Europe, in northern Norway and in Russia.

Table 1. List of known ionospheric heaters.

Heater	Location	ERP	Freq. range	Notes
Arecibo	18°N, 67°W	300 MW	3 - 15 MHz	Operational 1971
EISCAT	69.6°N, 19.2°E	1200 MW	2.5/4-8 MHz	Operational 1980
HIPAS	64.9°N, 146.9°W	130 MW	2.8-4.9 MHz	Operational 1981
Platteville	40.2°N, 104.7°W	80 MW	2.8-10 MHz	Operational 1970-1978
HAARP	62.2°N, 145.9°W	>1000 MW	2 - 12 MHz	Operational 1996, Completed 2002
Gissar (Dushanbe)	38°N, 65°E	6-8 MW	4 - 6 MHz	Operational 1981, now in Tadzhikistan, not in use?
Kharkov	50°N, 36°E	15 MW	6 - 12 MHz	
Moscow	56°N, 38°E	1000 MW	1.35 MHz	Operational 1960
Sura, Nizhny Novgorod	56.3°N, 49.3°E	320 MW	4.5 - 9 MHz	Operational 1972
Monchagorsk	68°N, 35°E	10 MW	3.3 MHz	Operational 1976
Zimenki (near Sura)	56°N	20 MW	4.6-5.7 MHz	

Table 2. Some technical details of the EISCAT heater in Ramfjordmoen (near Tromsø), Norway.

Frequencies in use now kHz	4040, 4544, 4912.8, 5423, 6770, 6960, 7100, 7953
Earlier also	2759, 3324, 3515, 4440, 4800, 5250, 5730, 6970, 7305, 7350, 8190
Antenna systems	Array 1: 12 x 12 full-wave wideband cross dipoles for 5.5-8 MHz, 30 dBi Array 2: 6 x 6 full-wave wideband cross dipoles for 3.85-5.65 MHz, 24 dBi Array 3: 6 x 6 full-wave wideband cross dipoles for 5.5-8 MHz, 24 dBi
Field strength at 100 km height	Array 1: 2.5 V/m Arrays 2 and 3: 1.4 V/m
Field strength at 250 km height	Array 1: 1 V/m Arrays 2 and 3: 0.5 V/m
TX output power	1.2 MW

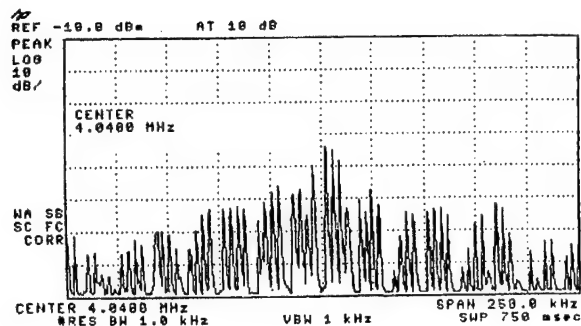


Fig. 1. Spectrum of pulse modulated EISCAT heater transmission.

One would wish that facilities like these (or high power LF-HF broadcast transmitting sites as well) should be constructed far from normal living and working areas, but that is again not the case. Nearest ham lives only 2 km away from the site in Norway, and that is certainly a very unpleasant situation.

4. AURORAL RADARS

The atmosphere of the polar regions is especially interesting to science. Several important phenomena occur only there, and many other things are more pronounced and more easily observable there than elsewhere. There are many ways to probe it. Auroral radars are a tool especially suited for looking at the magnetic field-aligned structures and phenomena. Because the field lines are almost vertical and VHF and higher frequencies propagate along straight lines but HF waves refract, it is possible to get much stronger echo signals back to radar on HF than on VHF or UHF.

4.1. HF Auroral Radars

First system of the currently used type of HF auroral radars was put up in Goose Bay in Labrador, Canada, in 1983. Since that there are also others up and coming, those nearest to us are situated in Finland and Iceland. These radars operate in synchronised pairs viewing the same area, and are together called the SuperDARN (Dual Auroral Radar Network). Table 3 gives locations of operational and considered sites. The system uses frequency range 8 – 20 MHz, divided in several narrower sub-ranges, and it automatically chooses a good quiet frequency inside a subrange that is most suitable at a certain time. Table 4 gives the frequency bands used at the Hankasalmi radar. The main antenna is a group of 16 log-periodic yagis with a feed system that gives 16 electronically formed switchable beams inside a 52 degree sector. The azimuthal resolution is 2.5° - 6°. A secondary group of 4 log-yagis is used only for reception to assist in

determining also the vertical arrival angle. A 600 W (500-800W) PA is feeding each TX antenna, total peak power being thus about 10 kW. The antenna system has a gain of 25 dB and so the ERP is about 3 MW. Transmitted signal consists of pulse groups (5-7 pulses, 200-300 μ s long) repeated at 10 Hz for 7 seconds in each beam, and the scan of the beams is repeated at 2-minute intervals. For frequencies near the radar frequency and amateurs in the radar beam area this pulse signal may cause same problems as the ionosondes: overloading of RX front end and upsetting the AGC system. The ERP is so high that also ionospheric nonlinearities can be generated. For example the pulse trains have been heard and recorded on VLF due to Ionospheric Envelope Demodulation in VLF measurement campaigns in northern Finland.

Table 3. Sites of SuperDARN radars.

Station	Status
Hankasalmi, Finland	Oper
Thykkvibær, Iceland	Oper
Stokkseyri, Iceland	Oper
Goose Bay, Canada	Oper
Kapuskasing, Canada	Oper
Saskatoon, Canada	Oper
Prince George, Canada	Not yet
King Salmon, Alaska	Not yet
Kodiak, Alaska	Oper
Halley, Antarctica	Oper
SANAE, Antarctica	Oper
Syowa South, Antarctica	Oper
Syowa East, Antarctica	Oper
Tiger, Australia	Not yet
Kerguelen	Not yet

Table 4. Frequency bands in kHz for SuperDARN radar at Hankasalmi, Finland. Some other bands have also been used earlier.

9040-9140	9900-9995	11075-11175
11550-11600	13440-13510	13870-13900
16210-16380	18030-18052	19415-19680
19800-19990		

4.1. VHF Auroral Radars

The original DARN network included also VHF auroral radars, the first of these being a pair called

STARE, Scandinavian Twin Auroral Radar Experiment. Its success led to the construction of other corresponding systems, including SABRE = Sweden And Britain Radar Experiment (on 153.2 MHz), DAR – Double Altitude Radar in Russian Karelia on 88 MHz and BARS, Bistatic Auroral Radar System. The STARE is still in operation, in a modernized configuration. Station sites are Midsandán in Norway, using 140.0 MHz, and Hankasalmi, Finland, where the frequency is very near to 2 m amateur band at 143.8 MHz. Transmitter peak power is 50 kW, and with a group of 8 long yagis the ERP is again in the MW class, capable of causing trouble to radio amateurs trying to use the 2 m band in the TX beam area.

5. IONOSPHERIC RADARS

The structures in the ionosphere which are probed with the auroral radars are said to generate coherent scatter, having dimensions in the scale of the radar wavelength. Another type of radars for ionospheric research is the incoherent scatter radar, which works with signals scattered back by individual electrons in the ionospheric plasma. These radars use still much higher TX powers and antenna gains than the former group. There are several representatives of this group, too, around the world. Maybe the best known in amateur circles is the Arecibo radar in Puerto Rico. Its antenna (the 1000-ft diameter dish) has been used also for amateur experiments, because the radar operates at 430 MHz and thus there are not difficulties due to large frequency differences. TX output power is about 2.5 MW. EISCAT has three radars in Norway: 224 MHz, 3 MW, 46 dB, and 931.5 MHz, 1.5 MW, 48 dB (near Tromsø), and 500 MHz, 1 MW, 45 dB (on Svalbard). The ERP's of installations like these seem to have an enormous potential of generating EMI. However, the antennas are usually directed at reasonably high elevations, and thus the highest field strength values are not experienced at ground level. The most experiences of EMI problems are with other objects than radio amateur stations. One part of the EMI potential comes from the fact at most sites there are several different high-power systems which can be operated simultaneously, and this can lead to generation of passive intermodulation at a substantial signal level. Another aspect is the still very high power level in antenna sidelobes - at 30 dB attenuation around 50 - 100 MW, and with about 45 dB attenuation still at the nominal output level, around 1-5 MW.

6. ATMOSPHERIC RADARS

Ionosphere is a part of the atmosphere, but the preceeding two radar types differ from the following radars in the respect that ionospheric and auroral radars measure mainly phenomena in the ionized plasma in

upper atmosphere, whereas the types presented next measure mainly the neutral atmosphere, and at lower heights. The division is not always clear, and one radar installation may be used for several types of observations in slightly different configurations.

6.1. MST, ST and MLT radars

This group is mainly used for research of turbulence, wave and wind phenomena, in height range of roughly 15 - 200 km, but can be adapted also to ionosphere or meteor studies. The largest subgroup uses frequencies around 50 MHz - near or inside the amateur band. About 2-3 MHz and UHF frequencies are found, too. Table 5 gives a summary of technical details of some radars in this group. As the typical antenna system is a large group of vertical yagis, these radars are, fortunately, not often a source of severe EMI to amateurs on a large scale. In the neighbourhood, due to antenna sidelobes, problems may arise, because the total peak ERP is again very high, and pulse transmissions are prone to cause interference.

Table 5. Some MST/ST/Meteor Radars.

Station	Freq. MHz	TX pwr kW	Ant. System yagis
Gadanki, India	53	2500	1024
MU, Japan	46.5	1000	475
Chung-Li, Taiwan	52	180	195
Aberystwyth, Wales	46.5	160	400
La Ferte Vidame, F	52.05	20	156
Esrang, Sweden	52	36+36	140+144
Longyearbyen, Norway	53.5	150	356

6.2. Wind profilers, boundary layer radars

These radars represent a new and growing group, specially intended for wind measurements, for heights of about 200 m to 20 km (vertical profile or distribution of wind speed, direction, and turbulence). ST/MST radars are not much different technically. There has been a search for frequencies for this new user, from three ranges: around 50 MHz, about 400-500 MHz and around 1 GHz. Some systems having frequencies near amateur bands are listed in Table 6. In addition to those, around 50 MHz, 915 MHz and 961 MHz are used at many sites (problems to GSM!?), and even 78.2 GHz and 95 GHz are mentioned. The frequencies on the 23 cm amateur band create a

potential EMI situation, and at least in Austria bad interference problems have been reported.

Table 6. Some Wind Profiler Radars with frequencies near Amateur bands, operating or tested.

Station	Frequency MHz
Lindenberg (nr Berlin), Germany	1290 & 482
Hamburg, Germany	1235
Payerne, Switzerland	1290
Zurich, Switzerland	1290
Graz, Austria	1280
Cabauw, Netherlands	1290
Paris/CDG Airport, France	1238
Rennes, France	1238
Spain, North coast	1000 (?)
Copenhagen, Denmark	400
USA, 31 station network	404

6.3. Meteor radars

This instrument is nearly same as a MST radar, and many MST radars are used also for this purpose in a modified configuration. Meteor radar records meteor trails, and because they can come from almost any direction, a meteor radar cannot have very directional antennas. Most suitable frequencies are in the range 20-60 MHz. Meteors can be a research subject as such, but most often this radar type is used for the same purpose as the MST radars, because the meteor trails drift due to upper atmosphere winds, and so these winds can be measured also in this way. Transmitter power in a basic system may be around 10 kW, TX antenna is a simple yagi and receiving array consists of a few more yagis. Many meteor and MST radars have frequencies inside or very near to the 50 MHz amateur allocation – a nuisance to a large area under good (high MUF) propagation conditions, and in every case an interference source to nearby hams.

6.4. Weather radars

This name is used for the "ordinary" weather radars which give mainly a picture of the rain situation of the area around them, using rotary scanning in the horizontal plane. In the U.S. the frequency allocation for these radars is 2700-2900 MHz, which should not cause problems to radio amateurs. Here in Europe the frequency allocation for this application is 5600-5650 MHz. Radio amateurs can use 5650-5850 MHz, but a weather radar is not a pleasant neighbour. Typical transmitter output powers are around 250-800 kW and antennas are 4-8 meter parabolic dishes, having 40-50 dB gain. Together these can make over GW ERP's.

Higher frequencies are used in some cases, and this same coexistence problem may arise at least at 24 GHz.

7. CONCLUSION

There are at least hundreds of high power radio transmitter-based systems for scientific purposes in use around the world, directly on or near the frequency bands which are allocated for amateur radio. Pulse type transmissions and high ERP levels very easily lead to EMI problems, which may remain mysteries, if the existence of these transmissions is not known. High signal levels lead to overloading and nonlinear distortion, if receiver does not have enough dynamic range and selectivity. Pulses easily upset AGC circuits. Intermodulation can be generated also as passive IM, outside the RX or TX involved, due to the very high power levels. Even ionospheric IM-type nonlinearity can shift signals to new, strange frequencies, caused by the very high signal power levels.

8. REFERENCES

- 8.1. "EISCAT European Incoherent Scatter Scientific Association Annual Report 1994-1995", EISCAT Headquarters, Kiruna, 1996
- 8.2. "EISCAT European Incoherent Scatter Scientific Association Annual Report 1996-1997", EISCAT Headquarters, Kiruna, 1999
- 8.3. B. Edwards, ed., "Proceedings of the seventh workshop on technical and scientific aspects of MST radar", Hilton Head Island, South Carolina, 1995
- 8.4. "European Commission Directorate General XII, Unit XII-B-1, Draft minutes of the sixth meeting of the management committee - COST Action 76. Development of VHF/UHF windprofilers and vertical sounders for use in European observing systems", Lindenberg, 1996
- 8.5. R.A. Greenwald et al., "DARN/SuperDARN, A Global View of the Dynamics of High-Latitude Convection", Space Science Reviews 71: 761-796, Belgium, 1995
- 8.6. E. Timofeev, Y. Miroshnikov, "Altitude Characteristics of Radar Aurora as Seen by a 90-MHz Double-Altitude Radar System Operated at Karmaselga, Karelia", J Geophys (1982) 51: 44-54
- 8.7. E. Nielsen et al., "STARE: Observations of a field-aligned line current", Geophysical Research Letters, Vol. 26, No. 1, 1999
- 8.8. A. Oikarinen, "VLF waves generated by Ionospheric Heaters" (in Finnish), thesis, University of Oulu, Oulu, Finland, 1997
- 8.9. J. Röttger, "Radar systems in ionospheric research", in M. A. Stuchly, ed., "Modern Radio Science", Oxford University Press, Oxford, 1999, pp. 213-247

EMC 2000

INTERNATIONAL WROCLAW SYMPOSIUM
ON ELECTROMAGNETIC COMPATIBILITY

EMC WORK IN IARU

Christian M. Verholt
IARU EMC Adviser & Chairman of Reg. 1 EMC WG
Lórkebakken 6, DK - 2400 Copenhagen NV, Denmark
E-mail: CMV@DS.DK

General: This presentation will present the status of the work within the International Amateur Radio Union - IARU - Region 1 EMC WG, and give views on the development in EMC, both in relation to technology and standards. It will present concerns related to radio amateurs and users of electronic equipment.

1. INTRODUCTION

1.1 The tradition and role of radio amateurs with respect to EMC:

As radio amateurs are heavy users of the radio spectrum, EMC problems have always been a major problem. Radio amateurs share the domestic environment with other users of electrical and electronic equipment and the compatibility problem includes both immunity and emission aspects.

This has been the case for more than 70 years giving the radio amateurs an outstanding experience with causes of interference, the social and physiological interactions, solutions of interference and the responses of authorities and manufacturers.

1.2 The organisation of EMC work within IARU:

The members of IARU are the national amateur radio societies all over the world. Most national societies have formed their own EMC group giving advice to the individual radio amateur. Furthermore, many societies publish magazines where amateur relevant technical information is presented including EMC relevant information.

The main task of the IARU EMC working group is to gather and distribute information and to influence legislation and standardisation at an international level. The IARU is a member of CISPR and is active in most EMC committees.

2. STATUS OF THE IARU WORK

2.1 Working process:

The work is concentrated in the EMC working group where 35 members from most countries in the region

participate. Some members are more active than others in distributing material and responses. The annual WG meeting is essential for keeping a reasonable coordination and focus. All documents and other information are distributed through the IARU office.

2.2 Examples of achievements:

One of the main tasks is to emphasize the existence of radio amateurs and their need for interference free spectrum and the need for immune electronics. This objective has been pursued and the result is e.g. visible in the work programme of the newly established CISPR H and in the emission documents for frequencies above 1GHz of CISPR G

2.3 Present work:

We are presently dealing with the emissions from power line transmission systems and emissions from lifts using power drives. The discussion on immunity of analogue telephones is of major concern too.

3. THE ELECTROMAGNETIC ENVIRONMENT

3.1. The noise floor is rising rapidly and it is often difficult to find a noise-free frequency. Individual equipment may emit at discrete frequencies, but the amount of equipment in residential houses with clocks and switched power circuitry is growing.

3.2. Some of the receivers have special features as e.g. Digital Signalling Processing (DSP), which can cope with part of the interference. Other receivers e.g. receivers used for the reception of digital signals (FSK-QPSK-GMSK) are rather susceptible to interference and the result of interference is fatal for the communication link. Comparing the result of interference between "analogue receivers" and "digital receivers" will lead you to the conclusion that the susceptibility is almost the same, but the consequence for a digital receiver is much worse.

3.3. Cordless telephones and low power devices (LPD') are used in large numbers and the usage influences the

environment greatly. The field strengths that other electronic devices must be immune to are higher and especially the levels at frequencies above 1GHz are different from what equipment was exposed to just a few years ago.

3.4 The fields from radio amateur transmitters are almost unchanged over the last 20 years, but a number of countries have raised the allowed maximum output power. This may lead to higher field strengths in the HF part of the spectrum. The planning restraints on outdoor antennas force some amateurs to use indoor antennas which result in rather high field strengths around electronic equipment. The ranges of field strengths from legal amateur transmitters both near field and far field are from 3V/m to 200V/m.

4. TRENDS IN TECHNOLOGY

4.1. The digital revolution is now leading to instalment of a lot of digital equipment in all environments. The technology is going to higher clock frequencies and faster equipment. The power consumption and the size of the equipment are decreasing. The usage of switched mode technologies in e.g. power supply, motor controllers and audio amplifiers are growing rapidly. There seems to be a general idea that anything (from water pipes to power leads), which can carry electrical signals in houses, can uncritically be used for high-speed data communication.

The use of SMD components improves the immunity of equipment because of their more ideal - non-parasitic - properties.

In reality - with respect to EMC - we gain some and we loose some.

5. TRENDS IN STANDARDISATION

5.1. The role and usage of international standards increases because of the change of legislation towards a more international regime which has shifted the setting of limits from national authorities to a forum dominated by manufacturers. We fear that this will result in standards where the level of protection offered to radio services is not adequate.

5.2. Emission limits are kept uniform for most equipment, but there is an increasing number of standards where exceptions in standards allow more or less free unwanted radiation. The Authorities have now identified this development and CENELEC have been asked to come up with a proposal for a solution. This work has been progressed in the newly established Strategic Review Panel.

5.3. Immunity requirements shall also be based on environmental considerations where the radio services used in the environment and the typical configuration e.g. protection distances are taken into account. Furthermore, the interference susceptibility of the receiving system should be taken into account. At present, the new digital radio services have not been evaluated properly and this work should be performed as soon as possible.

6. FUTURE WORK IN IARU

The IARU Region 1 Working Group will continue to:

- Monitor and participate in the EMC work
- Prepare technical information for both professionals and radio amateurs
- Support the EMC work in national societies
- Distribute technical information
- Give recommendations regarding acceptance of draft standards
- Be a forum within the radio amateur community for EMC related discussions

7. CONCLUSIONS

The radio amateurs have some real concerns with regards to the protection of radio services. We hope that the users of the radio spectrum together with the national authorities and manufacturers will acknowledge the need for adequate protection of radio services. We are especially concerned with the rapid introduction of high-speed telecommunication services on existing unshielded cables.

The work of the EMC WG is of great importance to the radio amateurs because of the international development of limits and regulation. Neither the individual radio amateur nor the national society can do this.

The IARU EMC WG shall continue to influence the professional and commercial EMC work to the benefit of radio amateurs.

The support from all WG members and National Societies is vital for the success of the work.

BIOGRAPHICAL NOTE

Christian M. Verholt. Radio amateur since 1970 as OZ8CY. Project manager of an EMC test lab in Jutland Telephone Company, Denmark, 1977 to 1990. Active in EMC standardisation since 1982 and member of IEC TC77, TC77B, TC85, TC106, CISPR (S, E, G, H); Cenelec TC210, SC210A TC211.

THE DETERMINATION OF THE COORDINATION AREA AROUND EARTH STATIONS

Gerald K. Chan
Communications Research Centre Canada
3701 Carling Avenue
Ottawa, Ontario, Canada K2H 8S2

ABSTRACT

The current Appendix S7 (28) of the International Telecommunication Union Radio Regulations on the method(s) for the determination of the coordination area around an earth station has been in existence for over 20 years. In view of the many new frequency allocations and new systems, the ITU recognised that there is a need to update the Appendix and has therefore established Task Group (TG) 1/6 in early 1997 to establish the technical basis for the World Radio Conference to study this urgent matter. This paper reports the work conducted in TG 1/6 which was completed in November 1999.

1. INTRODUCTION & BACKGROUND

The current Appendix S7 (28) of the International Telecommunication Union (ITU) Radio Regulations contains method(s) for the determination of the coordination area around an earth station in frequency bands between 1 GHz and 40 GHz shared between space and terrestrial radiocommunications services. Over the past 20 years, many new frequency allocations have been made to various radio services beyond this frequency range. As well, many new satellite systems have been proposed and introduced in operation.

The ITU recognised that there is a need to update the Appendix. As a result, ITU-R Study Group 1 established a Question [1] to study the technical procedures and propagation models that should be used in the determination of coordination areas around earth stations operating in frequency bands between 100 MHz and 105 GHz for coordination between:

- the earth station of a GSO (Geo-stationary Orbit) satellite network and a terrestrial station;
- the earth station of a GSO (Non-Geo-stationary Orbit) satellite in a slightly inclined orbit and a terrestrial station;

- the earth station of an NGSO satellite network and a terrestrial station;
- two earth stations of GSO satellite networks, when the two networks operate in opposite directions of transmission;
- two earth stations, one of which is part of a GSO satellite network and the other is part of an NGSO satellite network, when the two networks operate in opposite directions of transmission; and
- two earth stations of NGSO networks, when the two networks operate in opposite directions of transmission.

In order to conduct this work in an expeditious manner, the ITU established Task Group (TG) 1/6 in early 1997 to study this urgent matter. TG 1/6 began its work by creating a structure within the Task Group to address this difficult work. Three coordinators were appointed to lead the work which was organized in three categories: propagation models, system parameters, and procedures and methodologies. Reference was made to the existing Appendix S7, Recommendations ITU-R IS.847-1, IS.848-1, and IS.849-1. A close working relationship was established with Working Party (WP) 3M, WP 4/9S, and WP 4A. The output of this work is contained in the ITU-R Draft New Recommendation (DNR)-DOC1/1004 [2]. The following sections provide a brief outline highlighting these three categories of work.

2. PROPAGATION MODELS

2.1 Propagation model concepts and considerations

The determination of the coordination area is based on the concept of the permissible interference power at the antenna terminals of a receiving terrestrial or earth station. Hence, the attenuation required to limit the level of interference between a transmitting terrestrial or earth station and a receiving terrestrial or earth station to the permissible

interference power for p % of the time is represented by the "minimum required loss". The minimum required loss needs to be equal to or exceeded by the predicted path loss for all but p % of the time.

The determination of the predicted path loss is based on a number of propagation mechanisms which may be categorized in two modes as follows:

2.1.1 Propagation mode (1)

Propagation phenomena in clear air (tropospheric scatter, ducting, layer reflection/refraction, gaseous absorption and site shielding) are confined to propagation along a great-circle path and are described by the following mechanisms:

- Diffraction
- Tropospheric scatter
- Surface ducting
- Elevated layer reflection and refraction

2.1.2 Propagation mode (2)

Hydrometeor scatter can be a potential source of interference between terrestrial link transmitters and earth stations because it may act isotropically, and can therefore have an impact irrespective of whether the common volume is on or off the great-circle interference path between the coordinating earth station and terrestrial stations, or receiving earth stations operating in bidirectionally allocated frequency bands.

2.2 Extension of frequency bands

The existing Appendix S7 uses propagation models for the frequency band ranging from 1 to 40 GHz. TG 1/6, through collaboration with ITU-R WP 3M, has expanded the frequency band so that the entire frequency range from 100 MHz to 105 GHz is covered.

For the determination of the propagation mode (1) required distances corresponding to the minimum required loss, the applicable frequency range has been divided into three parts:

- For VHF/UHF frequencies between 100 MHz and 790 MHz and for time percentages from 1% to 50% of an average year: the propagation model is based on observational data and includes all of the propagation mode (1) mechanisms except site shielding (which is applied separately).
- From 790 MHz to 60 GHz and for time percentages from 0.001% to 50% of an average year: the propagation model takes account of tropospheric scatter, ducting and layer reflection/refraction. In this model, separate

calculations are made for each of the propagation mode (1) mechanisms.

- From 60 GHz to 105 GHz and for time percentages from 0.001% to 50% of an average year: the millimetric model is based upon free-space loss and a conservative estimate of gaseous absorption, plus an allowance for signal enhancements at small time percentages.

For the determination of the propagation mode (2) required distance corresponding to the required loss, interference arising from hydrometeor scatter can be ignored at frequencies below 1 GHz and above 40.5 GHz outside the minimum coordination distance. Below 1 GHz the level of the scattered signal is very low and above 40.5 GHz, although significant scattering occurs, the scattered signal is highly attenuated on the path from the scatter volume to the receiving terrestrial station or earth station. Site shielding is not relevant to propagation mode (2) mechanisms as the interference path is via the main beam of the coordinating earth station antenna.

2.3 Correction Factor

In determining the coordination area, the pertinent parameters of the coordinating earth station are known, but knowledge of the terrestrial stations or other earth stations sharing that frequency range is limited. Hence it is necessary to rely on assumed system parameters for the unknown terrestrial stations or the unknown receiving earth stations. Further, many aspects of the interference path between the coordinating earth station and the terrestrial stations or other earth stations (e.g. antenna geometry and directivity) are unknown.

The determination of the coordination area is based on unfavourable assumptions regarding system parameter values and interference path geometry. However, in certain circumstances, to assume that all the worst-case values will occur simultaneously is unrealistic, and leads to unnecessarily large values of minimum required loss, hence unnecessarily large coordination areas. For propagation mode (1) detailed analyses, supported by extensive operational experience, have shown that the requirement for the propagation mode (1) minimum required loss can be reduced because of the very small probability that the worst case assumptions for system parameter values and interference path geometry will exist simultaneously. Therefore a correction is applied within the calculation for the propagation mode (1) predicted path loss in the appropriate sharing scenario.

This correction applies to cases of coordination with the fixed service. It is frequency, distance and path dependent. It does not apply in the case of the coordination of an earth station with mobile stations

or with other earth stations operating in the opposite direction of transmission, nor in the case of propagation via hydrometeor scatter (propagation mode (2)). As well, it does not apply to wholly sea paths.

2.4 Distance limits

TG 1/6 also reviewed the concept of distance limits which currently is used in the existing Appendix S7 and was decided that it is appropriate to continue to use this concept. Hence the coordination distance, on any azimuth, must lie within the range between the minimum coordination distance and the maximum calculation distance.

3. SYSTEM PARAMETERS

As stated earlier, in the determination of the coordination area, the pertinent parameters of the coordinating earth station are known, but knowledge of the terrestrial stations or other earth stations sharing that frequency range is limited. Hence it is necessary to rely on assumed system parameters for the unknown terrestrial stations or the unknown receiving earth stations.

In this respect, Liaison Statements were sent out by TG 1/6 in the beginning of study program to all relevant ITU-R Working Parties with an objective to seek inputs from various WPs since a wide variety of radiocommunication services over the extended frequency bands, even for stations operating in bidirectionally allocated bands, are involved.

These parameters are captured in Tables 1-3 of the Annex 2 of the DNR. The system parameter values are required by the methods in the DNR to determine the coordination area around a coordinating earth station in the space services when the band is shared with terrestrial radiocommunication services or other earth stations operating in the opposite direction of transmission.

Table 1 in Annex 2 of the DNR is limited to those system parameter values required for the case of a transmitting earth station sharing the same spectrum with terrestrial services. Table 2 is limited to those parameter values required for the case of a receiving earth station sharing spectrum with terrestrial services. Table 3 is a new Table created by TG 1/6 and is limited to those parameter values required for the case of a coordinating transmitting earth station which is sharing spectrum in a bi-directionally allocated band with other earth stations operating in the opposite direction of transmission.

These system parameter Tables include primary allocations to the space and terrestrial services in

Article S5 of the Radio Regulations in all bands between 100 MHz and 105 GHz. Some of the columns in the Tables have incomplete information. In some cases, this is because there is no requirement to calculate coordination distances as pre-determined coordination distances apply. In other cases, the service allocations are new and the systems may not be introduced for some years. Hence, the system parameters are the subject of ongoing development within the ITU-R Study Groups.

4. PROCEDURES & METHODOLOGIES

The work in this category was largely focussed on providing new and updated methods to determine the coordination area around an earth station operating to non-geostationary space stations, including those operating in bidirectional bands.

For earth stations that operate to non-geostationary space stations and track the space station, the antenna gain in the direction of the horizon on any azimuth varies with time. Two methods are available to take this effect into account and are described in the sections below.

4.1 Time-Invariant Gain (TIG) Method

The TIG method uses fixed values of antenna gain based on the maximum assumed variation in horizon antenna gain on each azimuth under consideration. The values of horizon antenna gain are used for each azimuth to determine the propagation mode (1) required distances. They are derived from the antenna pattern and the maximum and minimum angular separation of the antenna main beam axis from the direction of the physical horizon at the azimuth under consideration.

The TIG method is used to determine the coordination contour. This method provides ease of implementation since it is not dependent on the availability of the distribution of the values for the horizon gain of the earth station antenna. As a consequence of this simplification, it usually overestimates the necessary distance. In order to reduce the coordination burden and on the basis of bilateral and multilateral agreements, administrations can use the TVG method (see below) to draw supplementary contours and obtain less conservative results.

4.2 Time-Variant Gain (TVG) Method

The TVG method requires the cumulative distribution of the time-varying horizon antenna gain of an earth station operating to a non-geostationary space station. This method closely approximates the convolution of the distribution of the horizon gain of the earth station antenna with the propagation mode

(1) path loss. This approach may produce slightly smaller distances than those obtained by an ideal convolution which cannot be implemented due to the limitations of the current model for propagation mode (1).

Hence, in comparison to the TIG method, the TVG method usually produces smaller distances, but requires greater effort in determining the cumulative distribution of the horizon gain of the earth station antenna for each azimuth to be considered.

The use of the TVG method is supported by ITU-R WP 4/9S and ITU-R WP 4A.

5. CONCLUSIONS

The work of TG 1/6, which spanned over about two and a half years, was completed during the fifth and final meeting which took place during November 1-5, 1999 in Geneva. All the major requirements identified in Question ITU-R 212/1 have been addressed and satisfied. The output of TG 1/6 was a Draft New Recommendation which, upon approval by the Radiocommunication Assembly, will form the basis for the World Radio Conference (WRC) 2000 to update Appendix S7 of the Radio Regulations.

The work of TG 1/6 was of much diverse complexity and difficulty. Its success was largely attributed to the hard working coordinators, delegates, all participating Administrations, the ITU-R counsellors, and in particular, the relevant WPs. These are WP3M, WP 4-9S, WP4A, WP 7B, WP 7C, WP 8A, WP 8B, WP 8D, WP 9B, WP 9D, and JWP 10-11S which provided valuable inputs and contributions during the entire course of the study.

A number of topics for future studies have also been identified. These are:

- Methods considering the cumulative impact in determining the coordination areas for high-density earth stations (fixed and mobile) or based on system parameters representing high density use (fixed and mobile).
- Methods to address the modeling of VHF/UHF frequencies for percentages of time below 1 %.
- Some system parameter values still missing from the parameter value Tables.
- Future consideration of suppression of Recommendations ITU-R IS.847-1, IS.848-1, and IS.849-1, since the material contained in these Recommendations has been updated and now contained in the new DNR. Future revision to Question ITU-R 212/1, now that the work of TG

1/6 has been completed. Future maintenance of the DNR considering that the propagation information contained in the DNR originated from Recommendation ITU-R P.620-4 which was a composite document bringing together material from a relatively large number of ITU-R P.Series Recommendations.

- The collection of experience in the future use of the Time Variant Gain (TVG) method.
- The development of equations for the Time Invariant Gain (TIG) method for non-circular orbit situations.

6. REFERENCES

- 6.1 Question ITU-R 212/1, "Development of method(s) for the determination of the coordination area around earth stations".
- 6.3 ITU-R Draft New Recommendation – DOC 1/1004, "Determination of the Coordination Area Around an Earth Station in Frequency Bands Between 100 MHz and 105 GHz".

BIOGRAPHICAL NOTE

Dr. Gerald K. Chan received his B.A.Sc. degree in Electrical Engineering from Queen's University, Kingston, Ontario, and his M. Eng. and Ph.D. degrees in Systems and Computer Engineering from Carleton University, Ottawa, Ontario. He is currently Vice President, Terrestrial Wireless Systems, at the Communications Research Centre Canada, an agency of Industry Canada, in Ottawa. Dr. Chan is international chairman of ITU-R TG 1/6, a Senior Member of the IEEE, and a member of the Association of Professional Engineers in the Province of Ontario.



WORK OF THE ITU-R TASK GROUP 1/5: UNWANTED EMISSIONS

Mohan S. Dhamrait

Radiocommunications Agency

14R/3B, Wyndham House, 189 Marsh Wall, London E14 9SX, UK

fax +44 207 2110021, e-mail dhamraitm@ra.gtnet.gov.uk

1. INTRODUCTION

In 1996, ITU-R Study Group 1 (Spectrum Utilisation and Monitoring) established Task Group 1/5 to study all unwanted emissions, the first meeting was held in Geneva in July 1997. The main objective of the study is to continue the work of an earlier task group, which considered only spurious emissions. The other important objectives are to produce:

- 'safety net' limits for out-of-band emissions;
- appropriate spurious emission limits for space systems;
- recommendations to protect safety and passive services from unwanted emissions, in particular from satellite systems;
- a definition of the boundary condition between spurious and out-of-band emissions;
- an interference analysis tool based on the Monte Carlo simulation method;
- revisions of existing recommendations SM.326, 328 and 329.

The Task Group has had six meetings to date and intends to conclude its work during the meeting scheduled for October 2000 in Geneva.

2. THE DEFINITION AND SCENE SETTING

From the definition given in the Radio Regulations, it can be seen that unwanted emissions consist of spurious emissions and out-of-band emissions. Spurious emissions include harmonic emissions, parasitic emissions, inter-modulation products and frequency conversion products. In recent years, spectrum sharing has become a very complex subject with the emergence of digital modulation techniques such as TDMA/CDMA, coupled with the introduction of new types of satellite

services, especially non-geostationary medium and low orbit (NGSO) satellite networks. The frequency allocation table in Article S5 of the Radio Regulations does not help the spectrum engineer, as allocations to high power satellite systems are often placed adjacent to services such as safety-of-life and radio astronomy that use sensitive receivers and require a high degree of protection from interference.

In making its recommendations, the Task Group has taken full account of spectrum efficiency objectives, together with the need to provide an acceptable level of protection for other services, and then attempt to find a careful balance with the requirement to foster the introduction of new telecommunication services without a prohibitive economic burden in reducing unwanted emission levels.

There has been conflict in the Task Group between members representing the different services. On one hand, some consider that their operations will be constrained unnecessarily if too stringent limits for unwanted emissions are specified for their services, even meeting the minimum, so called "safety net", limits can be costly. On the other hand, the scientific communities require their services to be fully protected, while some administrations see unwanted emission limits as an essential means to protect the spectrum for future new services.

3. WORKPLAN, METHOD OF WORKING AND PROGRESS

The Task Group has set up a number of drafting groups to make progress on the important objectives as specified in ITU-R Question 211/1 and ITU-R Decision 1/39. The Task Group needs the practical advice of experts from the different services, therefore it has been working very closely with other ITU-R study groups. Additionally, a good working relationship has

been established with CISPR to take account of the convergence between radiocommunications and information technology (IT) equipment.

Annex 1 gives details of the progress made so far for each area of work.

The following important tasks have still to be completed by the final meeting:

- Draft new recommendation on the "safety net" limits for the out of band emissions;
- Draft new report on the Monte Carlo spectrum management tool.
- Draft new recommendation on the protection of safety services from unwanted emissions
- Draft new recommendation on the protection of passive services from unwanted emissions
- Draft report on the boundary conditions between spurious and out-of-band of emissions this an agenda item for a future world radio conference

4. CONCLUSIONS

Since its first meeting, the Task Group has made excellent progress.

It has revised three existing recommendations:

- ITU-R SM.329 spurious emissions;
- ITU-R SM.328 spectra and bandwidth of emissions;
- ITU-R SM.326 determination and measurement of the power of the radio transmitters.

It has also produced the following documents:

- A new Report on production and mitigation of intermodulation products in the transmitter;
- A new Recommendation on determination and measurement of intermodulation products in transmitters using frequency, phase or complex modulations;
- in preparation for WRC2000, a contribution from TG1/5 has been accepted by the recent CPM for inclusion in Chapter 7 of the CPM Report. It deals with spurious limits for space systems and includes proposals for improvements to the text of the Appendix S3 of the Radio Regulations.
- A draft new Recommendation on "The protection of services from interference caused by out-of-band

emissions of transmitters operating at the outermost frequency of adjacent allocated bands".

Unwanted emissions are a form of pollution that can render the radio spectrum, a finite natural resource, unusable or difficult to use. It is therefore in the interests of all radio services to cooperate in the studies to reduce effects of unwanted emissions in the most effective and economical way possible. Otherwise, if the necessary measures are not taken now, then only a limited amount of spectrum will remain available for the introduction of future new technologies and services. In addition, there will be severe constraints on the use of the radio spectrum for the benefit of mankind through the pursuit of scientific knowledge and the effective management of the Earth's natural resources.

Finally, who benefits from the efficient use of the spectrum?

- Users/operators, since more spectrum is available for new services;
- Manufacturers, through selling more equipment;
- Regulators, due to increased revenue from additional licence fees and increased GNP.

BIOGRAPHICAL NOTE

Mohan S. Dhamrait, AMIEE, Senior Spectrum Engineer joined the UK Radiocommunications Agency in August 1965, worked in the Radio Investigation Service, Land Mobile, Satellite Communications and Fixed Services, before moving to the International Policy Unit of Branch 1 dealing with spectrum engineering and inter-service sharing issues. He is Chairman of ITU-R Task Group 1/5, and CEPT Chairman of WG Spectrum Engineering PT 21 on unwanted emissions and Chairman of Monte Carlo Management Committee on SEAMCAT



Annex 1: TG1/5 Workplan and progress in each area

	DG1	DG2	DG3	DG4	DG5	DG6	DG7	DG8	Rapporteurs Group 1
	CPM text	Intermodulation.	OOB limits	Protection of services from OOB emissions/boundary conditions	Rec. 329	Protection of Safety and passive services	CISPR issues	Monte Carlo	Definitions
	Mr Luther USA	Mr Loew Germany	Mr Rinaldo USA	Dr Murotani Japan	Mr Fournier France	Dr Baan Netherlands	Mr Olivier France	Dr Benamar Motorola	Mr Narasimham INMARSAT
Meeting 11-20 Jan 99 (fourth meeting)	Deliverable: Text for the draft CPM Report to WRC-00 on Spurious emission limits for Space services in response to agenda item 1.2 for WRC-00 and recommends 1 and 2 of Rec. 66 (Rev. WRC-97) March/April 1999, Deadline for input to draft CPM Report to WRC-2000.	Preliminary draft new Report on production and mitigation of intermod. products in the transmitter. Preliminary draft new Rec. on determination and measurement of intermod. products in transmitter using frequency, phase or complex modulations.	Working document towards preliminary draft new Rec. on maximum permitted levels of Out-of-band emissions including measurement methods and techniques.	Preliminary draft new Rec(s) ITU-R on protection of services from interference caused by OOB emissions of transmitters operating at the outermost frequency of adjacent allocated bands. Working document on boundary conditions	Working document towards preliminary draft revision of ITU-R Rec. SM.329-7.	Working document towards study on <i>recommends</i> 7 and 8 of Rec. 66 (Rev. WRC-97)	On-going liaison with CISPR Data on radiocommunications receivers supplied. Some definitions agreed i.e. for interconnect ed IT and Radio equipment.	Progress report on software given. Monte Carlo spectrum management tool named SEAMCAT (Spectrum Engineering Advanced Monte Carlo Analysis Tool)	

16-24 Aug. 99 (fifth meeting)	DG1 work is completed.	<p>Draft new Report on production and mitigation of intermodulation products in the transmitter.</p> <p>Draft new Recommendation on determination and measurement of intermodulation products in transmitter using frequency, phase, or complex modulations. DG2 Work is completed.</p>	Draft document towards Preliminary draft new Rec. on maximum permitted levels of Out-of-band emissions including measurement methods and techniques.	<p>Preliminary draft new Rec(s) ITU-R on protection of services from interference caused by OAB emissions. Working document on boundary conditions. DG4 Work is completed.</p>	Final draft revision of ITU-R Rec. SM.329-7. DG5 Work is completed.	Study on <i>recommends</i> 7,8 of Rec. 66 (Rev. WRC-97) 2 Preliminary draft new Recs. on the protection of safety of life and passive services from unwanted emissions.	On-going liaison with CISPR	"SEAMCAT" Monte Carlo Tool completed. Demonstration of software.	Report on definitions completed and sent to WP1A.
--	-----------------------------------	--	--	---	--	---	-----------------------------	--	---

6-14 Jan. 00 (sixth meeting)						Preliminary draft new Rec. on maximum permitted levels of Out-of-band emissions including measurement methods and techniques. Refinement on boundary conditions between spurious and OOB emissions and revision of the table dealing with applicability of the values of 6 and 26dB for the X dB points for various digital modulations in Rec. SM.443			Preliminary draft new Recs. on the protection of safety of life and passive services from unwanted emissions.	On-going liaison with CISPR	SEAMCAT software made available to TGI/5, ITU-R and MoU members. Working document towards a draft new Report on SEAMCAT. Future enhancements and development of software discussed.	Further work on definitions carried out. Report to WPIA up-dated.
23-31 October 2000						DG3 completes Draft new Rec. on maximum permitted levels of Out-of-band emissions including measurement methods and techniques. Final report on boundary conditions and Rec 443.			DG6 completes draft new Recs. On the protection of safety of life and passive services from unwanted emissions.	On-going liaison with CISPR	Final ITU-R Report on SEAMCAT. Progress report on the future development of the software.	Final report on definitions to WPIA and Study Group 1.

PREPARATION TO AND SOME RESULTS OF WRC-2000

Albert Nalbandian
ITU Radiocommunication Bureau, Study Group Department
albert.nalbandian@itu.int

The role of the ITU in the spectrum management is reviewed in this paper. The ITU has provided a forum for setting standards for radio systems since 1906 when the first edition of the Radio Regulations was approved. Today, the ITU Radio Regulations define 40 radiocommunication services, all depend on frequency allocations. In 1998, the ITU Plenipotentiary Conference approved Council Resolution 1130 to convene WRC-2000 in Istanbul (Turkey) from 8 May - 2 June 2000. The Agenda includes many difficult and important items on possible frequency allocations and necessary regulatory/procedural modifications, which will facilitate use of frequency bands up to 275 GHz by practically all radiocommunication services. The duties and functions of the Conference Preparatory Meeting are considered. The main results of WRC-2000 will be reported at the symposium.

1. INTRODUCTION

The future of many new radiocommunication services depends critically on availability of the frequency bands within radio-frequency spectrum. However, the spectrum is a resource limited by technology and management capability. As the demand on resources like spectrum/orbit grows, and as the complexity of radio systems increases, there is greater need for international cooperation. Each country should therefore work together with other countries to maximize its benefit.

The Agenda of the 2000 World Radiocommunication Conference (Istanbul, 8 May - 2 June 2000) included many difficult and important items. The Conference considered two sets of problems that are traditional for such conferences:

- ◊ possible frequency allocations to the radio-communication services; and
- ◊ necessary regulatory modifications which will facilitate the efficient use of spectrum.

At the international level, the ITU has provided a forum for such cooperation. An important element of that cooperation is setting standards for radio systems.

This activity has continued since 1906 when the limited nature of spectrum was recognized and the first international radio treaty provisions (the Service Regulations) were adopted. The scope of this recognition has since been extended to include the limited nature of the geostationary satellite orbit. The first allocation of radio frequencies to the various radio services was made in 1927. The Conference also created the CCIR (now the ITU-R Study Groups) to develop technical bases for efficient utilization of the frequency spectrum and to recommend performance standards for radio systems. Held in 1932, 1947, 1959 and 1979, the conferences completely revised the Radio Regulations (RR).

Today, the ITU work on radio is consolidated in the Radiocommunication Sector (ITU-R) with the aim to ensure rational, equitable, efficient and economical use of the spectrum/orbit resource by all radio services.

2. ITU ACTIVITY IN RADIOCOMMUNICATIONS

According to the ITU Constitution and Convention the Radiocommunication Sector works through:

- ◊ World Radiocommunication Conference (WRC);
- ◊ Radio Regulations Board (RR);
- ◊ Radiocommunication Assembly (RA);
- ◊ Radiocommunication Study Groups (ITU-R SGs);
- ◊ Radiocommunication Advisory Group (RAG);
- ◊ Radiocommunication Bureau (BR).

The legislative functions of the Sector, involving the revision of the RR, are the responsibility of World Radiocommunication Conferences. These are normally organized every two/three years, with Assemblies being associated in time and place with Conferences. The responsibility of Radiocommunication Assemblies is to provide the technical and operational basis for the rational, efficient, economical and equitable use of the spectrum/orbit resources by all radiocommunication services.

A WRC when revising the RR should:

- ♦ take into account technical progress and the requirements of radiocommunication services; and
- ♦ provide the basic tools which will enable countries to improve the utilization of the limited spectrum/orbit resources.

The following three approaches are used by WRCs to regulate spectrum utilization:

- ⇒ frequency band allocation to the terrestrial or space radiocommunication services, or the radio astronomy service (Table of Frequency Allocations);
- ⇒ allotment of a radio frequency or radio frequency channel to countries or geographical areas, for terrestrial or space radiocommunication services;
- ⇒ assignment of a radio frequency or radio frequency channel to a radio station.

The 1989 ITU Plenipotentiary Conference created a Voluntary Group of Experts (VGE) to study allocation and improved use of the spectrum and simplification of the RR. WRC-95 based on the VGE recommendations has reviewed and simplified the RR. The Radio Regulations, edition 1998 serve as the primary international agreement covering rules and procedures for operating a radio system and for resolving problems of interference. The Table of Frequency Allocations and the different Allotment and Assignment Plans are used as a basis for international and national spectrum utilization.

3. BACKGROUND

At WRC-97 a long list of items was proposed for inclusion to the Agenda of the next two Conferences. Among them there were eight items that could only be included in the agenda for WRC-2000 if the ITU Council can provide extra budgetary and conference resources. Many proposals from administrations have not been included and have been deferred to future conference agendas. The Council decided not to include these items to the agenda for WRC-2000 (see Resolution 1130).

Indeed, the WRC-2000 agenda includes many difficult and important items. The Conference will consider possible frequency allocations and necessary regulatory modifications that will facilitate the use of spectrum up to 275 GHz by practically all radiocommunication services, in particular:

- IMT-2000;
- maritime and aeronautical services;
- space science services;
- fixed service including high-density applications and high-altitude platform stations;
- radionavigation-satellite service; and

- broadcasting-satellite service.
- fixed-satellite service including non-GSO and GSO satellite systems;

In addition, the Conference will consider topics referred to it by the 1998 Plenipotentiary Conference such as:

- evaluation of the administrative due diligence procedure for satellite networks adopted by WRC-97;
- simplification of coordination and notification procedures for satellite networks;
- role of the notifying administration in the case of an administration notifying on behalf of a named group of administrations; and
- implementation of processing charges for satellite network filings and administrative procedures.

4. ORGANIZATION OF THE ITU-R STUDIES

According to the ITU Constitution the Radiocommunication Assembly provides the necessary technical bases for the spectrum management.

One of the tools to achieve the Sector's aim is the development of ITU-R Recommendations on the technical characteristics and operational procedures for radiocommunication services and systems. ITU-R Recommendations approved by the Member States contain the best currently available information on a topic and may be regarded as "standards".

Technical studies leading to the production of Recommendations are undertaken in the ITU-R Study Groups, each of which addresses a particular area of radiocommunications. The ITU-R Study Groups (ex-CCIR) terms of reference have periodically been reviewed and modified to follow the current needs of the participants, but studies of the efficient use of the radio frequency spectrum and the geostationary satellite orbit have always been included.

The ITU-R studies are focused on the technical and operational aspects of the spectrum management. Studies on spectrum management include:

- ⇒ studies of "General principles" which are common for all services defined by the RR;
- ⇒ "Service oriented" studies which concern requirements of the specific service or services.

"General principles" include:

- ◊ characteristics of the transmitted signals (necessary bandwidth, frequency tolerances, level of unwanted emission, etc.);
- ◊ propagation for the different frequency bands and geographic regions;
- ◊ general principles of sharing;
- ◊ avoidance of interference;

- ◊ noise levels;
 - ◊ spectrum control.
- "Service oriented principles" include:
- ◊ system characteristics;
 - ◊ sharing criteria;
 - ◊ interference criteria;
 - ◊ protection ratios.

The 1997 Radiocommunication Assembly adopted the work programs and the structure of the ITU-R Study Groups including Special Committee (SC) on regulatory/procedural matters and Conference Preparatory Meeting (CPM) (see Table 1):

Radiocommunication Study Groups	
SG 1	Spectrum Management
SG 3	Radio Wave Propagation
SG 4	Fixed-Satellite Service
SG 7	Science Services
SG 8	Mobile, Radiodetermination, Amateur and Related Satellite Services
SG 9	Fixed Service
SG 10	Broadcasting Service (Sound)
SG 11	Broadcasting Service (Television)
SC	Special Committee on Regulatory/Procedural Matters
CPM	Conference Preparatory Meeting

Table 1. Structure of the ITU-R Study Groups

In the 1997 – 1999 study period ITU-R Study Groups carry out studies on more than 400 Questions and manage around 800 ITU-R Recommendations.

5. THE ITU-R PREPARATION FOR THE WRC

The ITU-R Study Groups also carry out preparatory studies of the technical, operational and procedural matters to be considered by Radiocommunication Conferences. For such preparation the Assembly set up by its Resolution ITU-R 2 Conference Preparatory Meeting (CPM).

The purpose of the CPM is to develop and approve the CPM Report to a WRC. The CPM Report combines the technical report for the agenda items of a WRC and the regulatory/procedural advice prepared by the SCRPM. The CPM Report can be considered as a guide to administrations to assist in their preparations to a WRC. It is the purpose of the CPM Report to illustrate the possible methods to satisfy the agenda – both advantages and disadvantages. Therefore the CPM does not make the decision on how to resolve a WRC agenda item that is for the WRC itself. It is important that Administrations participate in the CPM process, to insure that all the technical issues pertaining to WRC agenda items are adequately reflected in the CPM Report.

For each WRC there are two-CPM sessions: CPM-1 and CPM-2. As the first CPM establishes the work program needed to prepare the final report it is essential that it be held as soon as possible after the preceding WRC has determined the agenda to be recommended for the next two WRC. It has normally been held in the week following a WRC, only two days in length. The CPM-2 usually meets six months before a WRC to prepare its Final Report to a WRC. Organization of the ITU-R conference preparatory work is shown in Figure 1.

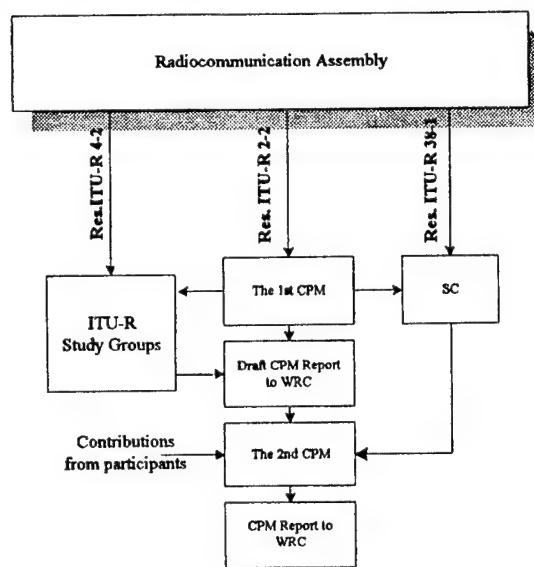


Fig. 1. Organization of the conference preparatory work

The 1997 Radiocommunication Assembly by its Resolution ITU-R 2-2 re-confirmed that preparatory studies for a WRC are to be carried out by a CPM and nominated Mr. T. Boe (Norway) as the Chairman of CPM-99, Mr. R. Barton (Australia) and Mr. E. Behdad (Islamic Republic of Iran) as the Vice-Chairmen. Mr. T. Boe, due to other obligations, was no longer available to chair the CPM. Consequently, following consultations with both Vice-Chairmen of the CPM, it was proposed that Mr. R Barton act as Chairman of the CPM for WRC-2000.

The first Conference Preparatory Meeting (Geneva, 26-27 November 1997) organized preparatory studies for WRC-2000 and identified studies for the following WRC. A structure for the CPM Report to WRC-2000 was agreed together with a preparatory process, working procedures and a chapter structure.

All WRC-2000 agenda items were grouped in the seven Chapters. The meeting appointed a Rapporteur for each Chapter to assist the CPM Chairman in managing the development and flow of draft report contributions. The meeting also decided that all appropriate regulatory/procedural studies on the relevant

agenda items would be carried out by the Special Committee and the results of the studies should be submitted as contributions to the work of CPM-2 in finalizing its report. The structure of the CPM Report

to WRC-2000 with indication of the Chapter Rapporteurs and the Assistant on regulatory/procedural matters is shown in Table 2.

Table 2. Structure of the CPM Report to WRC-2000

Chapter of the CPM Report to WRC-2000	Rapporteur	SC Assistant
Chapter 1. Mobile and radionavigation services	Mr. C. Van Diepenbeek (Netherlands)	Mr. R. Amero (Canada)
Chapter 2. Mobile-satellite and radionavigation-satellite services	Mr. S. Jones (United Kingdom)	Not required
Chapter 3. Non-GSO FSS issues	Ms. V. Rawat (Canada)	Mr. Ronald Davidson (USA)
Chapter 4. Space science services and radio astronomy	Mr. R. Jacobson (Australia)	Not required
Chapter 5. Appendices S30 and S30A	Mr. E. Behdad (Islamic Republic of Iran)	Mr. François Rancy (France)
Chapter 6. Fixed and Fixed-satellite services	Mr. H. Kimball (United States)	Mr. Alan Ashman (Australia)
Chapter 7. Other matters	Mr. N. Kisrawi (Syria)	Mr. Frank Williams (USA)
Chapter 8. Progress of studies for future conferences		Not required

All the necessary ITU-R studies were completed by 31 May 1999, as was agreed at the first CPM in 1997. On the basis of the available reports from ITU-R Study Groups, a draft CPM Report to WRC-2000 was prepared. For each Agenda item a Chapter contains summary of technical and operational studies, analysis of the results of these studies, and methods to satisfy the agenda item and their advantages and disadvantages.

CPM99-2 met from 15 to 26 November 1999, at that time the Report was finalized. The purpose of this CPM-2 was essentially to review, modify, and approve the CPM Report to WRC-2000. Administrations and organizations submitted input contributions with proposals to modify the Draft CPM Report. The Report prepared by the SC was merged with the technical content to provide a consolidated CPM Report.

The burden of preparation for future conferences is likely to increase. There is a need for overall interregional consultations and coordination. Regional preparations for WRCs are becoming more important in the whole process. Many regional telecommunication organizations have coordinated their preparations for WRC-2000. A number of common proposals have been submitted to this Conference from administrations participating in the regional telecommunication organizations. The consolidation of views at regional level, together with the opportunity for interregional discussions prior to the Conference, has eased the task of reaching a consensus during the Conference. There is consequently great benefit to the Member States of coordination of preparations at regional level. The success of future conferences will depend on greater efficiency of regional coordination and interaction at interregional level prior to future conferences.

6. CONCLUSIONS

Since its creation in 1993, CPM has become a key instrument for ITU Member States and Sector Members alike, as the results of its work on technical, operational, regulatory and procedural items enable administrations to move towards a consensus in many areas before the conference even begins.

Through a cooperative effort, a common position has been reached, satisfying all parties involved. Decisions on frequency allocations and inter-service sharing arrangements will be taken, largely by consensus, by the participating delegations at WRC-2000. The ITU-R preparation is the first step towards reaching such a consensus.

The results of WRC-2000 will be presented on the slides that will be prepared during and after the Conference.

BIOGRAPHICAL NOTE

Albert Nalbandian, Counsellor Radiocommunication Bureau (BR), is responsible for the work of ITU-R Study Group 1 "Spectrum management", ITU-R Study Group 7 "Science services" and CPM. In 1985 he joined to the ITU with 20 years of experience in satellite communication and broadcasting and radio engineering. He received his diploma in radio communications and broadcasting in 1965 from Moscow Telecommunication Institute. As ITU representative he participated (on behalf the CCIR or BR) in a number of the international conferences and symposia on radio.

He can be contacted at ITU, Radiocommunication Bureau Study Groups Department
Place des Nations
CH 1211 Geneva
albert.nalbandian@itu.int

SPECTRUM SHARING AND SPECTRUM FEES IN 2000

Alexandre PAVLIOUK

Radio Research and Development Institute (NIIR)
16, Kazakova str., 103064 Moscow, Russia
Tel. + 7 095 261-18-41; Fax: + 7 095 261-52-68,
E-m.: pavliouk@hotmail.com

Spectrum sharing and spectrum fees issues are considered in line with activities of Working Party 1B "Principals and techniques for spectrum planning, and sharing and utilization" of the Study Group 1 "Spectrum management", working within Radiocommunication Sector of the International Telecommunication Union (ITU-R). The major issues of relevant ITU-R Recommendations and Reports are commented and some suggestions concerning their possible improvements are presented for further considerations.

1. INTRODUCTION

Working Party 1B (WP 1B) "Principals and techniques for spectrum planning, and sharing and utilization" of the ITU-R Study Group 1 (SG 1) "Spectrum management" is working under direction of 10 Questions and 10 Recommendations assigned to its activities, as it is presented in Section 1B of the ITU-R SM Series Volume of 1997 [1]. One Recommendation, ITU-R SM.337-4 "Frequency and distance separation", exists since 1948 and during this period it was revised 8 times. The rest Recommendations were developed in the period since 1990 (some of them - on the basis of previous CCIR Reports). However, the majority of the Recommendations were developed since 1995. There is also one, newly approved by SG 1, Report ITU-R SM. 2022 "The effect on digital communications systems of interference from other modulation schemes". These Recommendations and the Report mainly concern:

- protection ratios for sharing investigations;
- definition of spectrum use efficiency of a radio system;
- techniques for aiding frequency assignment for terrestrial services in border areas;
- different spectrally efficient techniques and systems (multi-service ones, adaptive antenna, spread spectrum and digital techniques) and

their performance functions in various interference environments, etc.

Since 1995 WP 1B has been studying the new ITU-R subject – spectrum economic issues and in 1997 it developed the first ITU-R output document on the matter that is Report ITU-R SM.2012 "Economic aspects of spectrum management" [2].

Spectrum sharing and spectrum fees issues in their further development within WP 1B are shortly discussed in the paper. It is necessary to mention, that WP 1B covers only general principals and techniques of spectrum sharing but particular application issues, associated with exact radio services, are studied by other ITU-R SG-s. In this short paper it is not possible at all to analyse those numerous Recommendations on the subject developed outside WP 1B.

2. SPECTRUM SHARING

All issues covered by Recommendations presented in Section 1B of ITU-R Volume SM [1] and by Report ITU-R SM.2022 can be considered only as technical criteria for spectrum planning and sharing. However, up to 1995 there was no ITU-R Recommendation concerning general principals of spectrum sharing. The Recommendation on the matter, ITU-R SM.1132 "General principles and methods for sharing between radio services", was created only in 1995 but in [1] it was allocated to Section 1A of the Volume which is covered by WP 1A of SG 1.

Recommendation stated that utilization of the radio spectrum is dependent on frequency, time, spatial location and orthogonal signal separation. Any sharing of the spectrum will have to take into account one or more of these dimensions. Sharing can be accomplished in a straightforward fashion when any two of these dimensions are in common and the third and/or fourth dimension differs by a degree sufficient to ensure that all

the involved services (two or more) can operate satisfactorily. Sharing can also be accomplished when services have all four dimensions in common. In such cases, sharing is accomplished by applying technical conditions, which do not compromise the performance requirements of the services involved.

Then the Recommendation shortly described technical methods to facilitate sharing by implementation of these four dimensions as well as some sharing approaches applicable for particular services and radio systems including spread spectrum, packet radio, frequency agility etc.

In 1997 all matters concerning this Recommendation were transferred to WP 1B. At its last meeting in Assen, the Netherlands, August 1999, WP 1B has considerably amended this Recommendation by preparation of a new draft, whose title now reads: "General principles and methods for sharing between radio services or radio stations". The draft was adopted by SG 1 at its meeting which was held in Assen just after WP 1B meeting, and the draft is recently in the process of approval by ITU-R members by correspondence.

As it is seen from the new title, the scope of the Recommendation was extended to cover radio station sharing issues, i.e. matters of frequency planning through relevant frequency assignment. In this connection, the Recommendation states that in the case when services or stations have all four dimensions in common, service sharing rules can not ensure non-interference conditions and individual assignments must be made on the basis of the totality of assignments already made in all of the overlapping services, so that combinations of factors can be found for individual assignments that will not interfere with each other. Descriptions of technical methods to facilitate sharing through implementation of these four dimensions (the fourth one was extended from "orthogonal signal separation" to more general "signal separation") as well as descriptions of sharing approaches applicable for particular services and radio systems, were considerably detailed.

Commenting this Recommendation, it seems useful to mention one issue, which is not covered here yet. As it was shown in [3], increasing of spectrum use efficiency through implementation of spectrum sharing by two or several services is possible only under conditions, that each service, due to one or other reason, does not fully use the overall spectral resource, determined by above mentioned four dimensions, and there are free portions of the resource, related to one or several dimensions, that can be used by other service(s). If the whole network of stations belonging to one service uses the overall spectral resource in the most efficient way, i.e. completely

(as it is related to all four dimensions) there is no room at all for emissions of stations belonging to other service(s). It means that the sharing, as it is, can not create additional overall spectral resource, it leads only to distribution of existing one between radio services and their applications. This basic issue is a very important one for clear understanding of sharing significance and limitations.

Therefore, when considering more efficient spectrum utilization based on spectrum sharing concept, it is necessary to search for such combinations of services, which, due to one or other reasons, can not use the overall spectral resource effectively or fully enough leaving some non-used capacity that may be assigned to stations of other service(s) under specific conditions. These conditions, i.e. clearly defined complex of organisational and technical arrangements, should be worked out for each particular case [3].

In another words, possibilities of implementation of sharing concept significantly decrease with the increasing of spectrum use efficiency of each radio service. It is clearly demonstrated by several last ITU-R World Radiocommunication Conferences (WRC-s) that were unable to define sharing feasibility of some new radio services and their applications, which suppose to use spectrum more or less effectively (satellite digital broadcasting, satellite and terrestrial mobile services and their applications etc.).

It should be also taken into account that implementation of spectrum sharing concept leads to significant increase of difficulties related to practical frequency assignment process. Sharing implementation adds much more organisational (administrative) difficulties to usual technical ones related to frequency assignments within only one radio service. It is due to the fact that various radio services may belong to different governmental or commercial bodies and co-ordination process, concerning frequency assignments between these bodies, becomes much more difficult and lengthy in comparison with the case of one service belonging to only one body.

It seems would be useful to make further amendments in Recommendation ITU-R SM.1132 in line with above suggestions. It would lead to more clear understanding of sharing principal significance and practical substantial limitations.

It cannot be excluded, that, realizing difficulties in attempts to practically increase spectrum use efficiency through wide application of sharing concept (but such expectations took place rather widely in 80-th - beginning of the 90-th years), attention of the international telecommunication community is recently shifting to other promising possibility - implementation of spectrum redeployment (refarming) measures. This approach leads to employment of various administrative and technical measures resulting in reallocation of

some frequency bands and in their further step-by-step reassignment for the benefit of new, more effective, radio services (and their applications) and relevant stations, under terms of maintaining sharing conditions of new service(s) stations with stations of replaced service(s) during the whole transitional period.

Following these feelings, WP 1B in 1998 developed the draft new Question, which was later approved by ITU-R members as Question 216/1 "Spectrum redeployment as a method of national spectrum management". Answering this Question, WP 1B has initiated studies of spectrum redeployment (refarming) issues. At its last meeting in Assen WP 1B has developed working materials on the subject [4].

The Document [4] contains the following definition: "Spectrum redeployment (spectrum refarming) is a combination of administrative, financial and technical measures aimed at removing the existing frequency assignments either completely or partially from a particular frequency band. The frequency band may then be allocated to the same or different service(s). These measures may be implemented in short, medium or long timescales." It seems to be useful to amend this definition in future by saying that sharing conditions between stations of replaced and replacing services should be maintained during the whole process of the redeployment. Certainly, this provision is a rather obvious one, however it seems would not harm to stress that in the definition, much over that sharing conditions are mentioned in section 2.2. of [4]. Generally speaking, spectrum sharing can be considered as the first stage of the spectrum redeployment when only a part of the overall spectral resource is provided to other service(s).

The document [4] shortly considers a number of scenarios for redeployment of the spectrum that is currently used in Europe:

- migration at the expiry of the current license,
- migration at the end of the equipment's lifetime,
- forced migration to frequency bands within the tuning range of the equipment used,
- forced migration into other frequency bands,
- forced migration to achieve greater spectral efficiency.

As it is stated in [4], one of the major issues with spectrum redeployment is the use of a redeployment fund to aid its implementation. Although, whether a redeployment fund is actually essential to the operation of a spectrum redeployment policy is not obvious, especially as it would be generally undesirable for existing users to assume there was an automatic right to compensation, e.g., it could distort market values, promote spectrum hoarding. Further issues include spectrum redeployment's interaction with spectrum pricing,

spectrum management policies and tools. All these issues are shortly discussed in [4].

It can be noted that the first victim in the redeployment process is the fixed radio service because particularly this service, as the practice showed, has provided frequency bands for redeployment activities at the last ITU-R WRC-s. This process is a rather natural one because, as it was already shown many years ago (see for example [5]), particularly the fixed radio service is using the radio spectrum in the most non-rational way, as far as its objectives can be principally accomplished by other alternative telecommunication means, for example, by cable and/or fiber-optical links. On the contrary, objectives of some other radio services, such as mobile, radio navigation, radio astronomy, space operation and research, etc., principally cannot be accomplished by any other means except the radio ones. It seems that all redeployment processes should be strategically oriented on providing such benefits for the radio-communication services whose objectives principally cannot be accomplished by any other means except the radio ones.

Therefore, it seems be useful to clearly identify these objectives of spectrum redeployment in future ITU-R Recommendation(s) on the subject. In [4] this issue is mentioned in application to 1-3 GHz frequency band, which is very suitable for mobile services, but it is not stressed yet as a strategic orientation.

Without any doubts, document [4] creates a good basis for a draft new Recommendation on the subject which is planned to be developed at the next WP 1B meeting to be held in the end of 2000.

3. SPECTRUM FEES

More and more attention of telecommunication administrations of many countries, developed and developing ones, is recently paid to economic aspects of radio spectrum management. It is felt that, under circumstances of continuously increasing frequency band congestion, administrative and technical measures aimed to increase spectrum utilisation efficiency in the most developed countries have already basically exhausted, and at the recent evolution stage modern radio spectrum management is mainly associated with economic measures, rather than with administrative and technical ones [6]. Developing countries where significant frequency band congestion has not evinced yet, recently have also begun to display increased interest to economic aspects of spectrum management in expectations to find available sources for financing their programs of modern spectrum management development.

Following requirements of many countries to provide an international guidance on that important problem, ITU-R at its Radiocommunication Assembly in 1995 through SG 1 has launched a study program in this new field of activity. The program consists of three interrelated Questions:

- Question 206/1 Strategies for economic approaches to national spectrum management and their financing,
- Question 207/1 Assessment, for spectrum planning and strategic development purposes, of the benefits arising from the use of radio spectrum,
- Question 208/1 Alternative methods of national spectrum management.

SG 1 has charged these studies to WP 1B. In result of extensive work in that new area, WP 1B has managed to develop the first ITU-R material on the matter and to present it to the next ITU-R Radiocommunication Assembly held in 1997. It was a rather voluminous (more than 70 pages) Report ITU-R SM.2012 "Economic aspects of spectrum management". The Report concerned the following major issues:

- application of economic factors to spectrum management activities (Chapter 1),
- strategies for economic approaches to national spectrum management and their financing (Chapter 2),
- assessment of the benefits of using the radio spectrum (Chapter 3),
- alternative support for national spectrum management (Chapter 4).

The Report described various economic aspects with their application to spectrum management and its financing: traditional national budget financing, spectrum use fees, spectrum usage comparative hearings, lotteries and auctions. Advantages and disadvantages of these approaches are discussed in detail and some general suggestions on their practical implementation in different situations are presented. Issues of transferable and flexible spectrum rights implementations are also covered. Experiences of some telecommunication administrations in the field of practical implementation of these economic aspects of spectrum management are also given. Detailed review of the Report is presented in [7].

Since 1997 WP 1B has continued its studies in this promising area and at its last meeting in Assen the group has developed considerably amended and extended version of the Report. SG 1 later approved the draft developed by WP 1B at its Assen meeting in 1999, conducted just after WP 1B meeting, and the new version of the Report (it will be Report ITU-R SM.2012-1) is

planned to be presented at the next ITU-R Radiocommunication Assembly to be held in May 2000.

The volume of the Report was almost doubled. The major amendments concern the following issues.

May be due to the fact that previous expectations on great advantages of wide implementation of spectrum auctioning mechanisms (and it seems that auctioning issues were, generally speaking, the main orientation of the previous version of the Report) become somewhat restrained, as it can be concluded, for example, from [8], the major amendments to the previous version of the Report concern wide practical implementation of the very well known and convenient frequency license fees concept. These issues are major amendments of Chapter 2. This Chapter is also supplemented by a new section 2.5 "Managing a change in spectrum management funding" which concerns major objectives of a spectrum management authority, in legal and organizational aspects, under implementation of new approaches in funding national spectrum management activities through spectrum pricing mechanisms.

Section 4.5 "Implementation measures" of Chapter 4 was renamed as "Legal and administrative implementation measures" and supplemented by rather detailed subsections "Contracting /Privatization Options", "Contractable/Privatizable Functions" and by the table summarizing functions and activities of spectrum management staff that can be contracted and/or privatized with indication relevant reasons.

As far as it concerns Chapters 1 and 3, the first one contains only minor modifications while the second one was left without any of them.

Separate Chapter 5 was added which concerns detailed description of experiences of different Administrations in practical implementation of various economic measures in relation to the spectrum management process. This Chapter now combines all experience issues, which were previously presented in Chapters 2 and 3 of [2]. The majority of countries which experience(s) in implementation of spectrum pricing and/or alternative organizational issues (Australia, Canada, Germany, Israel, New Zealand, Russian Federation, United Kingdom and United States) have presented contributions on basis of which relevant sections of the new version of the Report were considerably extended. With a great satisfaction it can be noted, that experiences of two more countries are reflected in the new version. China presents its experience in the implementation of a license fees regime when fee levels depend on bandwidth used, coverage area and frequency. Kyrgyz Republic, on basis of a method described in [9] and [10], presents detailed description of its automated spectrum fees accounting system

aimed to cover the cost of the national spectrum management.

Unfortunately, great and very useful experiences of many other countries, developed and developing ones, in practical implementation of spectrum management economic mechanisms, which are known through other information sources, particularly through the INTERNET, are not reflected yet in this new version of the Report. It seems to be very beneficial for many ITU-R members to eliminate these shortages in the following next version of the Report, which is recently under development by WP 1B. All ITU-R members are kindly invited to contribute to the process through ordinary ITU-R working mechanism.

4. CONCLUSIONS

ITU-R through its GS 1, and particularly WP 1B, is carrying out significant studies in fields of spectrum sharing and spectrum fees issues. There is a room for further improvements of relevant ITU-R Recommendations and Reports. A new promising field of the WP 1B activity is the development of Recommendation(s) on spectrum redeployment (refarming) matters. This subject means implementation of various administrative and technical measures resulting in reallocation of some frequency bands for the benefit of a new, more effective, radio service and/or their applications, and in their further step-by-step re-assignment to stations of the new services (and/or their applications), under terms of maintaining sharing conditions of new service(s) stations with stations of replaced service(s) during the whole transitional period. First results of spectrum redeployment studies in form of ITU-R Recommendation(s) are planned to be available in the end of 2000.

5. REFERENCES

- 5.1 ITU-R Recommendations. Volume 1997. SM Series, Spectrum Management. ITU, 1998.
- 5.2 Report ITU-R SM.2012 "Economic aspects of spectrum management". Volume 1997. SM Series, Spectrum Management. ITU, 1997.
- 5.3 A. Pavliouk. Frequency Planning – the Basic Element of Spectrum Management. Proceedings of the 10-th International Wroclaw Symposium on EMC, 1990, pp. 1022 – 1929.

- 5.4 Documents of ITU-R Study Groups. Doc. 1B/TEMP/14, August 1999. Working Document Answering Question ITU-R 216-1 on Spectrum Redeployment.
- 5.5 A. Pavliouk. Criteria of Efficient Spectrum Use and Frequency Planning. Proceedings of the 9-th International Wroclaw Symposium on EMC, 1988, pp. 849-852.
- 5.6 W. Webb. Modern Radio Spectrum Management. 1997 International Forum on Spectrum Management, London, June 1997, pp. 1 – 13. (IBC Technical Services Ltd).
- 5.7 A. Pavliouk. International Studies of Economic Aspects of Spectrum Management. Proceedings of the 14-th International Wroclaw Symposium on EMC, 1998, pp. 609 – 613.
- 5.8 H. Shostek. The Political Drivers of Spectrum Value. Telecommunications, September, 1999, (www.telecommagazine.com).
- 5.9 Telecommunication Development Conference, Valletta, Malta, 1998 (WTDC-98). Doc. 37-E. Kyrgyz Republic. Development of Modern Telecommunications and Problems of State Regulation of Telecommunications in New Countries. (Draftsmen B. Nurmatov and A. Pavliouk).
- 5.10 B. Nurmatov, A. Pavliouk. Experience in Development of a Method for Calculating Spectrum Use Fees. Proceedings of the XXVI-th General Assembly of the International Union of Radio Science (URSI), Toronto, Canada, 1999, p. 285.

BIOGRAPHICAL NOTE

Alexandre P. Pavliouk received the Ph. D. degree from Radio Research and Development Institute (NIIR), Moscow, Russia, in 1972. Leading scientist of the NIIR. Many years he was a chief of the NIIR's EMC department. During 1978 – 1984 he worked as a Counsellor of the CCIR secretariat in Geneva being responsible for activities of GS 1 on spectrum utilization and monitoring, and SG 6 on propagation in ionized media. He is an expert in fields of radio measurements and monitoring, frequency planning, spectrum management and radiocommunications development. He is the author of about 150 various articles and papers on the above subjects, including about 50 contributions to different CCIR and recently ITU-R SG-s and their working organs. Recently he is a Vice-Chairman of the ITU-R SG 1 and Chairman of its WP 1B. ITU-D Senior Expert on spectrum management and radiocommunications development.

EMC 2000

INTERNATIONAL WROCLAW SYMPOSIUM ON ELECTROMAGNETIC COMPATIBILITY WORKSHOP

The Changing Role of Monitoring in the Spectrum Management Process

Jan J. Verduijn

Radiocommunications Agency

P.O. Box 450, 9700 AL Groningen, The Netherlands

e-mail: jan.verduijn@rdr.nl; telephone: + 31 294 25 8482; fax: + 31 294 25 8444

1. INTRODUCTION

The aim of this document is to give information of the role of the monitoring function in relation with the Spectrum Management Process and the activities performed within the ITU-R Study Group 1 Working Party 1C on Spectrum Monitoring matters.

The role of monitoring in the spectrum management process is significant changing as it was in the past. Reason for this change is the growing responsibility of the Regulatory Authority as a result of the enormous amount of money involved in the radiocommunications.

Also the topics to be handled in the ITU-R Study Group 1 Working Party 1C on monitoring matters are influenced by this changing role.

2. SPECTRUM MANAGEMENT

Spectrum Management is the combination of administrative, scientific and technical procedures necessary to ensure the efficient operation of radiocommunications equipment and services without causing harmful interference. Within this definition activities take place as frequency planning (frequency management), enforcement and monitoring.

The monitoring function can be described as giving assistance to both frequency management and enforcement departments.

3. ROLE OF MONITORING IN THE PAST

In the Spectrummanagement Handbook published by ITU you can read that monitoring is a tool to:

1. Ensure compliance with national spectrum management rules and regulations through the verification of proper technical and operational characteristics of transmitted signals, and the detection and identification of unauthorized transmitters;
2. Locate and resolve interference problems;
3. Determine channel and band usage, including assessment of channel availability and verification of the efficacy of the frequency assignment process and spectrum analytical methods.

In the Spectrum Monitoring Handbook also published by ITU is stated that monitoring serves as the eyes and ears of the spectrum management process.

The actual situation was, that in many countries hardly any work was done for the frequency management department and almost all-monitoring activities were related to enforcement purposes. Handling interference

cases was one of the main activities carried out in the daily monitoring work.

If activities were carried out on request of the frequency management department it was mostly done on an ad-hoc basis

4. ROLE OF MONITORING IN THE FUTURE

(Radio-)telecommunication is one of the most growing economic sectors in the world.

Now that telecommunications are evolving evermore rapidly and that the impact of telecommunications on national economy is growing, it is obvious that the Regulatory Authority has a major role to play. Operators are paying plenty of money for parts of the spectrum so that they can provide services to the public. Auctions, beauty contests or other instruments are often used for this purpose. These financial sources in most cases will go to the state budget and can be seen as an extra income for the government. Because spectrum use is highly priced, it is obvious that Telecoms operators demand a 'clean' and usable spectrum. This means that also the Regulatory Authority as being responsible for the control of the radiospectrum must be ready to carry out this task. Nowadays, Regulatory Authorities or Radio Communications Agencies are made liable in taking care of the spectrum.

High-quality Spectrum Management being a prerequisite, a mere theoretical frequency planning is not enough. More information about the current use of radio spectrum is needed to achieve successful Spectrum Management. This information can be obtained only through the Monitoring function.

5. RELATION BETWEEN FREQUENCY MANAGEMENT AND MONITORING DEPARTMENTS

As stated the theoretical frequency planning is not enough. A structured relation between the frequency management and monitoring departments is needed to realise a high quality spec-

trum management of the Regulatory Authority.

In the changing responsibility of the Regulatory Authority in controlling the radiospectrum both Frequency Management and Monitoring Departments are 'growing' in a structured relation to each other.

Where in the past activities carried out by the Monitoring Service were 70-30% in favour for enforcement activities, nowadays it is the opposite.

The relation between the Monitoring and Frequency Management Departments can be simply illustrated by Figure 1.

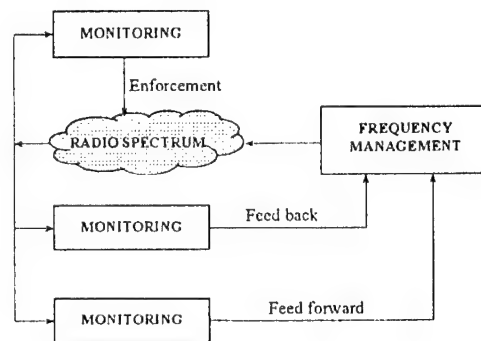


Figure 1. Spectrum Management Cycle

The explanation to this Figure 1.:

- The spectrum is used for all kinds of radio transmissions. Frequency Management is of overriding importance for the efficient and effective use of the radio spectrum. (Inter)National authorities are setting the rules for the use of the radio spectrum via assignments, licence parameters, etc.
- The Monitoring Service observes the radiospectrum and the monitoring operators have the duty to compare whether the use of the radiospectrum matches the policy of Frequency Management. Via this loop Monitoring gives **feedback** to Frequency Management.
- In observing the radio spectrum, Monitoring can also provide information to Frequency Management on (hitherto) unknown or new use of the radiospec-

trum. When Spectrum Management sets up an experiment for new services **before** a policy on that new service has been developed, Monitoring can observe the experiment and advise on it. That is why a **feed-forward** loop is appropriate.

- Monitoring can also address radio spectrum users directly in case of interference. The monitoring operators can give guidelines to the users to avoid interference, etc. This is called **Enforcement**. In this case, no direct line to Spectrum Management is needed.

To meet the requirements of high quality spectrum management in total, it is absolutely necessary that the Figure 1 scheme will be applicable.

6. ACTIVITIES IN WORKING PARTY 1C ON MONITORING MATTERS

The scope of ITU-R Study Group 1 is Spectrum Management (Spectrum planning, utilisation, engineering, sharing & monitoring).

As all Study Groups within ITU-R Study Group 1 is:

- a) Drafting Technical Bases for Radiocommunication Conferences;
- b) Developing Draft ITU-R Recommendations on technical characteristics of, and operational procedures for radiocommunications services and systems;
- c) Compiling Handbooks on spectrum management and emerging radiocommunications services and systems.

Within ITU-R Study Group 1 Working Party 1C deals with Monitoring matters.

To realise the tasks for both frequency management and enforcement sections and facing the fact of the rapidly development of telecommunications it is necessary to develop monitoring measuring protocols and procedures to meet these tasks.

Facing the same difficulties combined with the available technical knowledge spread all over the world is the base for the work in Working Party 1C.

Inventing the wheel by your selves is an outdated statement. Co-operation is the key word these days. Sharing knowledge and problems is the success of the work. So within WP1C representatives of administrations and manufacturers of monitoring equipment are working together for the benefit of both interest.

The advantage for administrations is support of international accepted Recommendations in their daily monitoring work.

The advantage for manufacturers of monitoring equipment is in making their equipment 'ITU compliant'.

Another example of such an international co-operation is CEPT Project Team 22 on Spectrum Monitoring, where monitoring experts of 21 European countries twice a year meet for the benefit of support of CEPT Working Group Frequency Management, solving mutual European enforcement problems, monitoring campaigns for CEPT and ITU, and development of European Recommendations in the field of Monitoring.

Within WP1C measuring protocols, working procedures between monitoring services etc. are laid down in Recommendations.

Due to the growing complexity of transmissions also the monitoring functions becomes more difficult to perform.

Because the sometimes very high licence-fees the Regulatory Authority wants to be informed whether license-holders are working in conformity of the licence-conditions. In the past such verification could often be done by listening and simple measurements. Nowadays within one transmission sometimes more than one service is the emitted. For this reason it is necessary to 'look' into the spectrum of such a transmission. In this respect transmission as DAB, DVB, cellular networks, satellitesystems can be identified.

The monitoring technique to realise such a task is Signal-analysis.

For the future development of the monitoring function, signal analysis will be one of the most important monitoring tools.

Due to the increasing use of (mobile) satellite systems, sharing of satellite services with terrestrial services also the monitoring function becomes more and more important.

The output of the Working Party 1C is of great importance for the developed and developing countries for the improvement of the national monitoring services.

7. SPECTRUM MONITORING HANDBOOK

At this moment one of the most important issues on the agenda of WP1C is the revision of the Spectrum Monitoring Handbook.

Due to the rapid development of telecommunications such as the introduction of digital techniques and the growing use of software in monitoring techniques it was necessary to take the decision to revise the present Handbook issued in 1995.

The high quality of this present Handbook could be reached by a great participation of sharing 'monitoring-knowledge' from all over the world. The success of the work done can be expressed by the fact that this present Handbook is the best seller of ITU-publications.

Nevertheless it was needed to revise the Handbook.

At his moment the work to come to a revised Handbook has already begun.

In April the first meeting took place in Paris, France. The second meeting will be held in January 2001 in Munich, Germany.

A third meeting is foreseen in June 2001.

Again participation from all over the world can be noted.

Therefore it is expected that also this revised Handbook will be on the top of the best sellers list of ITU publications.

BIOGRAPHICAL NOTES

J.J. Verduijn works within the Radiocommunications Agency of the Netherlands as Advisor International Projects of the Frequency Management, Infrastructure & Systems.

Within the Radiocommunications Agency he was working in the monitoring service for 24 years, responsible for the development of monitoring policy and contributing to the international monitoring policy. In this respect he was co-founder of CEPT Project Team 22 on Spectrum Monitoring. Presently he serves as vice-chairman of Working Party 1C of ITU-R Study Group 1.

PROBABILITY OF INTERMODULATION INTERFERENCE OF LAND MOBILE CELLULAR RADIO SYSTEMS

L.Sh.Alter

Radio Research and Development Institute (LONIIR),
Bolshoy Smolensky pr.,4, 193029 St.Petersburg, Russian Federation
Fax. (+7 812) 567 69 82; E-mail: alter @ loniir.ru

An analysis of 3rd order intermodulation interference (IMI) which are generated by 2 unwanted signals of mobile stations in victim base station receiver is performed. As a result we have obtained an equations of the interference zone radii and interference probability.

The calculations of IMI probability for NMT-450 cellular system as an example are given.

INTRODUCTION

It is known that two strong unwanted signals affecting a receiver can generate intermodulation interference. For planning network it is necessary to estimate signal reception quality. Interference probability in system is one of such important parameters.

Well known papers consider usually two-signal IMI [1-5,8]. This paper presents the method and results of IMI probability calculations which are caused by 2 unwanted signals. IMI probability is a function of transceiver, network, signals fading parameters and probability of unwanted mobile station position.

1. INTERFERENCES ZONE

1.1 Common equation

Let the service zone is a circle with radius R_0 and base station (BS) is disposed in its center. A scheme of IMI generating is shown in Fig.1.

The frequency and energy requirements [3,4,8] for 2-signal IMI of the 3rd order are :

$$2F_1 - F_2 \leq F_r \pm Br/2, \quad (1)$$

$$2P_1 + P_2 > 3W_2, \quad (2)$$

where F_1, F_2 = unwanted signal frequencies ; F_r = victim receiver frequency; Br = receiver bandwidth; P_1, P_2 = unwanted signals powers at receiver input, dBW;

W_2 = receiver susceptibility for 2-signal interference of the 3rd order, dBW.

The value W_2 is determined by 2 equal levels $P_1=P_2$ of unwanted signals which cause SINAD ratio decreasing by 6 dB at receiver output [6,12].

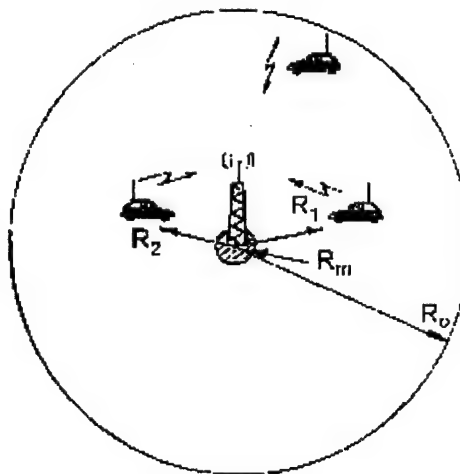


Fig.1 : A scheme of intermodulation interference generating.

Theoretical studies have shown - and this has been verified by experimental work - that magnitude W_2 is function of frequency diversity of unwanted and wanted signals $dF_{1(2)}$, level of wanted signal at the input of receiver P_s and receiver susceptibility parameters [4]. Results of W_2 measuring of BS receiver of NMT-450 cellular system are shown in Fig.2 and 3. Fig.2 presents the dependence W_2 from P_s where $dF_1 = 175$ kHz, $dF_2 = 350$ kHz. Fig.3 presents the dependence W_2 from dF_1 where $P_s = -100$ dBm.

At special case for cellular system when mobile station unwanted signals are in preselector band, i.e. $dF_{1(2)} < Brf$, where $dF_{1(2)} = [F_{1(2)} - F_r]$; Brf = preselector bandwidth, we can write :

$$W_2 = S_2 + P_{so} + d_2(P_s - P_{so}), \quad (3)$$

where P_{so} = receiver sensitivity, dBW; S_2 = receiver intermodulation (RIM) selectivity (RIM response rejection ratio) for 2-signal interference, dB; d_2 = parameter of RIM susceptibility model (d_2 show how W_2 vary in case of P_s varying). Amplitude requirement (3) in terms of field strengths is:

$$2E_1 + E_2 \geq 3[S_2 + E_{so} + d_2(E_s - E_{so})] \quad (4)$$

where E_1 , E_2 , E_s = unwanted and wanted signal field strengths at receiver antenna location, dBμV/m; E_{so} = wanted field strength which corresponds to P_{so} .

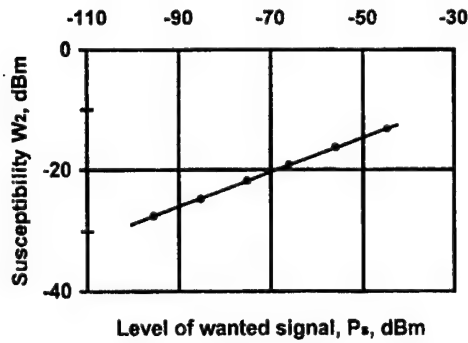


Fig.2 Dependence of receiver susceptibility W_2 on level of wanted signal at the input of receiver P_s .

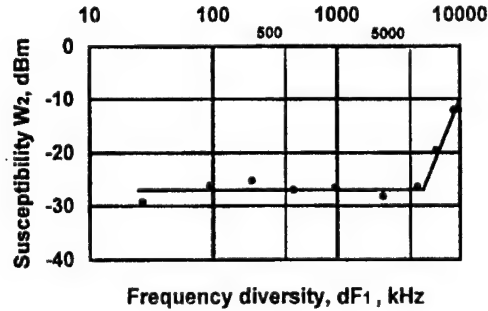


Fig.3 Dependence of receiver susceptibility W_2 on frequency diversity of unwanted and wanted signals dF_1 .

Then (4) can be represented as

$$2E_1 + E_2 - 3d_2 E_s \geq 3[S_2 + E_{so}(1 - d_2)], \quad (5)$$

To determine service and interference zones the wanted and unwanted signal path loss model is formed taking into account the fading with normal distribution law at measurement units in dB [3,10].

Left parts (5) are the sum of three independent random values with overall standard deviations:

$$\sigma_{2\Sigma} = \sqrt{4\sigma_1^2 + \sigma_2^2 + 9d_2^2\sigma_s^2}, \quad (6)$$

and median values:

$$E_{m2\Sigma} = 2E_{m1} + E_{m2} - 3d_2E_{ms}, \quad (7)$$

where σ_1 , σ_2 , σ_s , E_{m1} , E_{m2} , E_{ms} = standard deviations and median values of wanted and unwanted signals respectively.

Median values E_{m1} , E_{m2} , E_{ms} close to BS receiver antenna which is at the distance R to signal source are:

$$E_m = 107,2 + P_\Sigma - L(R) + 20\lg F, \quad (8)$$

$$P_\Sigma = P_t + G_t - B_t,$$

where P_t = transmitter power, dBW; G_t = antenna gain, dBi; B_t = antenna feeder path loss, dB; F = transmitter frequency, MHz; $L(R)$ = unwanted and wanted signal path loss at distance R , dB.

Interfering zone of mobile stations will be maximum in case of minimum wanted signal level. This takes place at the distance $R = R_0$ between mobile station and BS where R_0 is a radius of service zone.

Probability of interference appearing, i.e. eq.(5) requirement complying for two unwanted signals due to fading:

$$P_{pr} = 1 - \Phi(Z_2) \quad (9)$$

where $\Phi(Z_2)$ - probability integral;

$$Z_2 = \frac{3S_2 + 3E_{so}(1 - d_2) - E_{m2\Sigma}}{\sigma_{2\Sigma}}. \quad (10)$$

Using approximation of $\Phi(Z_2)$ we receive:

$$\Phi(Z_2) = 0,5[1 \pm \sqrt{1 - \exp(-0,619536 \cdot Z_2^2)}]$$

Substituting it into eq.(9) we get:

$$1 - P_{pr} = 0,5[1 \pm \sqrt{1 - \exp(-0,619536 \cdot Z_2^2)}]$$

Solving this equation for Z_2 we receive:

$$Z_2 = \sqrt{-1,6141 \cdot \ln[4P_{pr}(1 - P_{pr})]} \quad (11)$$

Denoting

$$A_1(P_{pr}) = \sqrt{-1,6141 \cdot \ln[4P_{pr}(1 - P_{pr})]} \quad (12)$$

and equating right parts of eq. (10) and (11) we receive:

$$\frac{3S_2 + 3E_{so}(1 - d_2) - E_{m2\Sigma}}{\sigma_{2\Sigma}} = A_1(P_{pr}) \quad (13)$$

Substituting $E_{m2\Sigma}$ from eq.(7),(8) to (13) we receive for unwanted signals:

$$2L_1 + L_2 \leq A_1(P_{pr}) \cdot \sigma_{2\Sigma} - 3[S_2 + E_{so}(1 - d_2) - 107,2 - P_\Sigma - 20\lg F + d_2E_{ms}], \quad (14)$$

where L_1, L_2 = unwanted signal path loss at frequencies F_1, F_2 , dB; P_{pr} = probability of interference appearing due to fading.

Equations (14) allow to calculate max path loss $2L_1 + L_2$ which correspond IMI formed by 2 unwanted signals with given probability P_{pr} .

1.2 Path loss

The median values of path loss L of wanted and unwanted signals are function of distance R . The calculation for a distance of $0.05 < R < 1.6$ km in large city was made using "Lee's model" [9]. In this case path loss L can be approximated

$$L = 114 + 41.5 \log R \quad (15)$$

for $F = 450$ MHz, BS antenna height $H = 40$ m and building density parameter $B = 0.33$.

1.3 Interference zone

Fading of the wanted and unwanted signals are approximated by normal distribution law with $\sigma = 10$ dB [10]. Assume that $\sigma_1 = \sigma_2 = \sigma_3 = 10$ dB. In this case $\sigma_{2\Sigma} = 24.5$ dB (see eq.6).

For calculation of interference zone let's use next parameters of NMT-450 system: $F = 450$ MHz; $P_t = 0.15$ W; $G_t = 5$ dB; $B_t = 1$ dB; $d_2 = 0.33$; $E_{so} = 9.3$ dB μ V/m (where E_{so} corresponds to sensitivity $P_{so} = -117$ dBm or $U = -4$ dB μ V emf); $P_{pb} = 0.1$; Here P_t is minimum transmitter power as P_t is controlled by BS.

Calculating interference zone as a function of IMI selectivity S_2 and median value of wanted signal field strength E_{ms} for a pair of unwanted signals F_1 and F_2 with substituting the NMT-450 parameters in (14) we receive:

$$2L_1 + L_2 \leq 480.8 - 3S_2 - E_{ms} \quad (16)$$

Let $S_2 = 70$ dB [7,12] and $E_{ms} = 25$ dB μ V/m.

When using eq.(15),(16) we get:

$$R_1^2 R_2 \leq C_2, \quad C_2 = 4.81 \cdot 10^{-3} \text{ km}^3. \quad (17)$$

2. INTERFERENCE PROBABILITY

2.1 Common equation

The IMI probability $P\{I_2\}$ is a function of set of random factors [11] such as: 1) probability $P\{T\}$ that simultaneously unwanted transmitters are transmitting and wanted signal is satisfactorily received in absence of unwanted energy simultaneously; 2) probability $P\{F\}$ of IMI frequency condition fulfilment (see eq.(1)); 3) probability $P\{I\}$ of energy condition fulfilment (see eq.(2)).

The receiver and transmitter parameters can be assumed as determine parameters with correct accuracy. Then IMI probability is:

$$P\{I_2\} = P\{T\} * P\{F\} * P\{I\}.$$

Assume that BS have N_{ch} channels which carriers are spaced with the same step. Then in Busy Hours all BS channels are active, mobile stations (which are transmit at F_1 and F_2) in service zone are active too

and so the frequency conditions of IMI are fulfilled. In this case $P\{T\} \cong 1$ and $P\{F\} \cong 1$. Let's determine $P\{I\}$.

2.2 Probability of existing single interference

Let unwanted MS with frequencies F_1 and F_2 are removed from BS at a distances R_1 and R_2 accordingly (see Fig.1). Locations of MS are random variables, so we have a pair of random variables. Domains of R_1 and R_2 are:

$$R_m < R_1 < R_o; \quad R_m < R_2 < R_o,$$

where R_m = minimum distance MS to BS. Let a area density of MS within service zone be constant.

Probability of interference in BS receiver (i.e. I_2 event, see eq. (14)) is:

$$P\{I_2\} = P\{R_1^2 R_2 < C_2\}. \quad (18)$$

Fig.4 shows the domain of random variables R_1 , R_2 and domain S in which IMI exists.

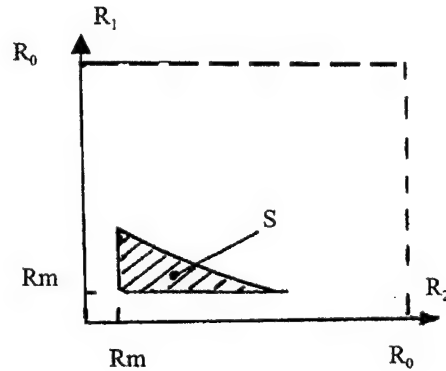


Fig.4 : Domain S in which IMI exists.

Probability of I_2 event is:

$$P\{R_1^2 R_2 < C_2\} = H_2 \iint_{(S)} f(R_1, R_2) dR_1 dR_2 \quad (19)$$

where $f(R_1, R_2)$ = distribution density of pair of variables; H_2 = normalizing coefficient.

Due to R_1 и R_2 are independent (random) variables we have:

$$f(R_1, R_2) = f_1(R_1) * f_2(R_2) \quad (20)$$

Density of distribution of random variables R :

$$f(R) = 2R / (R_o^2 - R_m^2).$$

Using eq.(20) in this case eq.(19) can be written as

$$P\{I_2\} = H_2 \int_{R_m}^{R^*} \left(\int_{R_m}^{R^{**}} R_2 dR_2 \right) R_1 dR_1, \quad (21)$$

$$R^* = \sqrt{C_2 / R_m}; \quad R^{**} = C_2 / R_1^2.$$

Normalizing coefficient can be received from following condition:

$$H_2 \int_{R_m}^{R_0} \left(\int_{R_m}^{R_0} R_2 dR_2 \right) R_1 dR_1 = 1;$$

$$H_2 = 4/(R_0^2 - R_m^2).$$

Calculating eq. (19) for $C_2=4.81 \cdot 10^{-3}$ and $R_m = 0.05$ km using programm Mathcat we receive:

$$P\{I_2\} = H_2 \cdot 2.195 \cdot 10^{-3}. \quad (22)$$

Calculation results of $P\{I_2\}$ for different R_0 are shown in table 1.

Table 1 : Probability of single IMI

R_0 , km	1.0	1.5	2.0
H_2	4.0	0.79	0.25
$P\{I_2\}$	$8.78 \cdot 10^{-3}$	$1.73 \cdot 10^{-3}$	$0.55 \cdot 10^{-3}$

2.3 Probability of existing intermodulation interference set

Let consider the affecting of IMI set to a receiver. Assume that BS has N_{ch} channels which carriers are spaced with uniform step. Then a number of IMI increases.

For exsample if BS has 16 channels then each receiver is affected by 7 interferences of $2F_1 - F_2$ form ($Q=7$) [1]. In this case the probability of BS receiver beeing attacted by at least one IMI is :

$$P\{I_{2\Sigma}\} = 1 - [1 - P\{I_2\}]^Q;$$

Calculation results of $P\{I_{2\Sigma}\}$ for different R_0 are shown in tables 2 for $Q=7$.

Table 2 : Total probability of IMI

R_0 , km	1.0	1.5	2.0
$P\{I_{2\Sigma}\}$	$6.0 \cdot 10^{-2}$	$1.2 \cdot 10^{-2}$	$0.38 \cdot 10^{-2}$

From data given in table 2 we see that probability of IMI is significant if $R < 1.6$ km. When the number of channels is more then the number of IMI increases and IMI probability increases too.

CONCLUSION

1. Experemental researches of susceptibility W_2 and IMI analysis allow to calculate the radii of interference zone and IMI probability of $2F_1 - F_2$ form as a function of MS, BS cellular system transceiver, network (E_{ms}, R_0, N_{ch}) and signals fading parameters, probability of unwanted mobile station position. When the number of channels increases then the number of IMI increases and IMI probability increases too.

2. For NMT-450 cellular system the IMI probability of $2F_1 - F_2$ form is significant (i.e. is more 0.01) in case when service zone radius $R_0 < 1.6$ km.

REFERENCE

- [1] Recommendation ITU-R M. 739 - 1.
- [2] ITU. Doc.1/1009 Intermodulation interference calculation in the land mobile service. 12 July 1995.
- [3] CCIR.1990. Report 655-2.
- [4] CCIR.1990. Report 522-2.
- [5] CCIR.1990. Report 842-2.
- [6] Recommendation ITU-R SM.332.
- [7] CCIR.1990. Recommendation 478-4.
- [8] G.K.Chan, S.Bartlett. Identification of land mobile denied spectrum due to radio interference. 10th International Zurich Symposium on EMC, 9-11 March, 1993, p.538.
- [9] W.Lee. Mobile Communication Design Fundamentals, Second Edition. John Wiley and Sons, Inc., N.Y., 1993.
- [10] Recommendation ITU-R P.1145.
- [11] CCIR.1990. Report 829.
- [12] European Telecommunication Standard ETS 300 086. Radio Equipment and System Land Mobile Service.

Leonid Alter - received the MS from St.Petersburg Telecom. University (1968) and PhD from Moscow Telecom. University (1987). He is a senior researcher, an expert in the field of radio system planning and system EMC simulation on base of PC, an author of 24 papers and patents.

GENERALIZED EMC ANALYSIS OF AIR NAVIGATION AND GSM NETWORKS IN BELARUS

Anatoly Budai: Belarus Ministry of Posts and Telecommunications, 10 F.Skorina av., Minsk 220050,
E-mail: dts@minsvaz.belpak.minsk.by, Fax: 375-17-2277559

Konstantin Kovalev, Victor Kozel, Vladimir Mordachev: Belarusian State University of Informatics and
Radioelectronics, 6 P.Brovka str., Minsk 220027, E-mail: nilemc@gw.bsuir.unibel.by, Fax: (375-17)-2310914
Victor Nikonov: Belarus State Supervisory Department for Telecommunications, 22 Engels str., Minsk 220030,
E-mail: nikonov@belgie.belpak.minsk.by, Fax: 375-17-2278624

This paper presents the results of electromagnetic compatibility (EMC) generalized analysis for Aeronautical Radionavigation Service network and GSM-900 mobile communication network on the territory of the Republic of Belarus. The analysis is based on evaluations of potentially usable spectrum (radiofrequency resource) that corresponds to the part of the general frequency band allocated for the GSM network that is potentially usable under the EMC conditions.

Keywords: GSM, Radionavigation, compatibility

Presence of a developed airdrome network equipped by 900 MHz navigation and landing systems in the Republic of Belarus substantially limits the possibilities of GSM mobile network frequency planning on Belarusian territory. Since the spectrum is shared by the Aeronautical Radionavigation Service (ARNS) and the GSM network, it is required to evaluate the spectrum bandwidth utilized by navigation systems and solve the efficient sharing problem for this frequency band. The spectrum occupied by the ARNS ground radio transmission equipment is fixed and cannot be used in the GSM network. The spectrum used by the on-board radioreceiving equipment is defined on the border of possible location of GSM network transmitters with the given power provided that the desired signal at the navigation receiver input within the beacon responsibility area exceeds the total GSM network transmitter signal by the protection ratio value.

In general, the radioelectronic system spectrum is defined as space volume or area where the given system operates multiplied by the bandwidth required for its operation [1,2]. The above definition characterizes a certain space-frequency volume occupied by a radio system, with consideration herewith that the problem of EMC with other systems (of the same or different type) does not exist or is already solved. Therefore this spectrum definition is unsuitable for evaluation of the potentially usable spectrum in the environment of electromagnetic collisions between

different radio systems that operate in concurrent or overlaid space-frequency areas.

In this connection, it is necessary in some cases to correct the analyzed spectrum definition so as to take account of the EMC problem when solving the problems of business planning and radio systems designing.

Since in this case the radio system (GSM-900 network) designing is carried out within the framework of frequency-territorial restrictions stipulated by already existing radio facilities of the ARNS network, the EMC problem is solved only by selection of the corresponding technical and regulatory decisions to be used in the designed system. It is considered a priori for the existing REF ARNS that the EMC problem will be eventually solved; hence the spectrum that these facilities occupy may be evaluated in accordance with the above definition. For system project elements, it is reasonable to introduce a notion of the potentially usable spectrum which relates to estimation of the part from the general frequency band intended to be used in the designed system that is potentially usable under the EMC provision conditions.

In particular, the potentially usable spectrum can be evaluated as follows:

$$PFR = \frac{1}{2\pi NM(P_{\max} - P_{\min})(h_{\max} - h_{\min})} * \sum_{i=1}^N \sum_{j=1}^M \int_{-\pi}^{\pi} \int_{h_{\min}}^{h_{\max}} \int_{P_{\min}}^{P_{\max}} S_{ij}(P, h, \lambda) dP dh d\lambda \quad (1)$$

where N is a number of assumed locations for designed system transceivers, M is the total number of frequency channels provided by the designed system standard; P, h, λ is the effective radiated power (ERP), the effective height and the azimuth of GSM network base station (BS) transmitting antenna's maximum radiation, respectively; $[P_{\min}, P_{\max}]$ is the range of nominal BS

ERP; $[h_{min}, h_{max}]$ is the variation range of the BS transmitting antenna's nominal efficient height; $S_{ij}(P, h, \lambda)$ is the relative coverage area of i -th designed system BS transceiver on j -th frequency channel, defined as follows:

$$S_{ij}(P, h, \lambda) = \frac{S_{ij EMC}(P, h, \lambda)}{S_{ij NOM}(P, h, \lambda)}, \quad (2)$$

where $S_{ij NOM}(P, h, \lambda)$ is the nominal coverage area of i -th transceiver of the designed system BS on j -th frequency channel; $S_{ij EMC}(P, h, \lambda)$ is the coverage area of i -th project system transceiver on j -th frequency channel when the transceiver parameters are changed to provide EMC with the existing radio facilities.

With reference to GSM regular network (ERP and antenna height are constant for all network elements) the expression for PFR can be reduced to the following form:

$$PFR = \frac{1}{124NL} \sum_{i=1}^N \sum_{j=1}^M \sum_{k=1}^L \frac{S_{ijk EMC}}{S_{NOM}}, \quad (3)$$

where L is the number of radiation sectors for a BS; S_{NOM} is the coverage area with typical BS parameters (ERP and antenna height). Taking into consideration that the BS coverage area is directly proportional to the square of its radius and the signal level at mobile station location is directly proportional to the base station ERP and is inversely proportional (at first approximation) to fourth power of distance between base and mobile stations, the relation (3) can be reduced to the following form:

$$PFR = \frac{1}{124NL} \sum_{i=1}^N \sum_{j=1}^M \sum_{k=1}^L \sqrt{\frac{P_{ijk EMC}}{P_{NOM}}}, \quad (4)$$

where P_{NOM} is the nominal BS ERP value accepted for the designed uniform GSM network; $P_{ijk EMC}$ is the ERP value of i -th BS in k -th radiation sector on j -th frequency channel that ensures that the EMC with 900 MHz ARNS systems is achieved ($P_{ijk EMC} \leq P_{NOM}$).

The expression under the square-root sign may be treated as a value which is inversely proportional to the value by which the interference impact on ARNS system exceeds the maximum tolerable level from k -th radiation sector of i -th BS on j -th frequency channel.

The degree by which the interference impact exceeds the maximum tolerable level may be determined comparing the level of interference created by i -th BS radiation in k -th sector on j -th frequency channel with the desired signal level from each ARNS beacon at the interference impact location (at the aircraft location). The comparison implies that the polarization and frequency selectivity of the

interference receptor, the total interference impact of several GSM transmitting facilities on the receptor, and protection ratios required for normal ARNS radio facilities operation are to be taken account of.

The calculation results of GSM equipment interference impact on on-board equipment of Belarusian ARNS for uniform GSM network segments located in regional centers and in Minsk are presented as histograms that illustrate the distribution of GSM frequency grid channels number based on the degree of impact on the aeronautical radionavigation service (see Fig.1-Fig.9).

The following characteristics of GSM network segments were assumed for the interference impact analysis:

- BS transmitter power - 40 dBm;
- mobile station transmitter power- 33 dBm;
- BS antenna gain factor - 17 dBi;
- width of BS Antenna Pattern - 90° horizontal and 7° vertical;
- BS antenna height - 50 m;
- base stations use single-sector coverage area with maximum radiation directions of 180°, 300° and 60° (Fig.1, Fig.2 and Fig.3 respectively) or three-sector coverage area with maximum radiation directions of 60°, 180° and 300° (Fig.4-Fig.9).

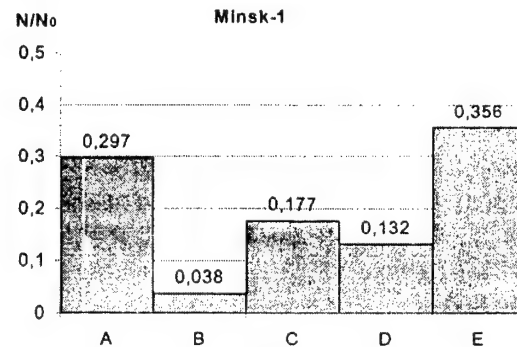


Fig.1.

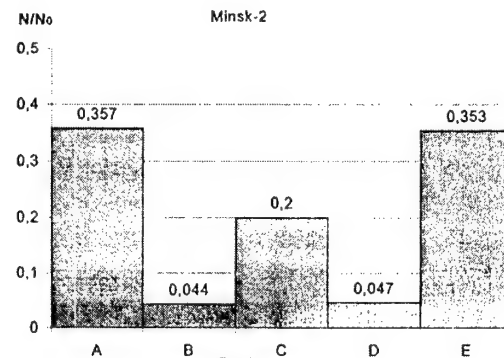
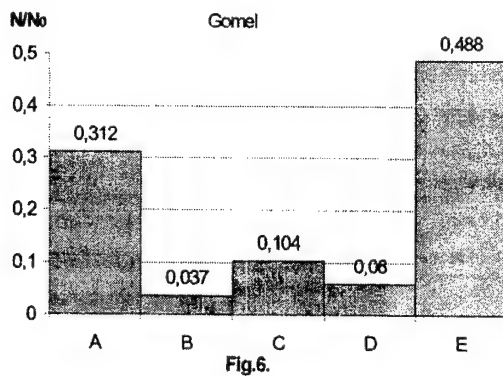
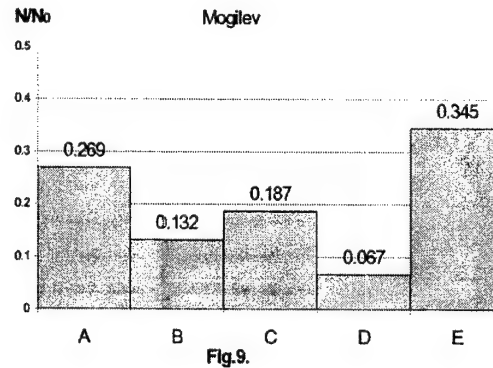
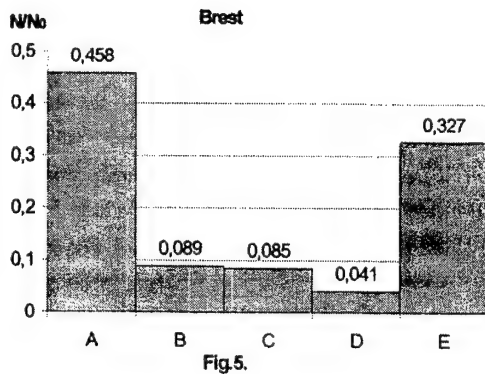
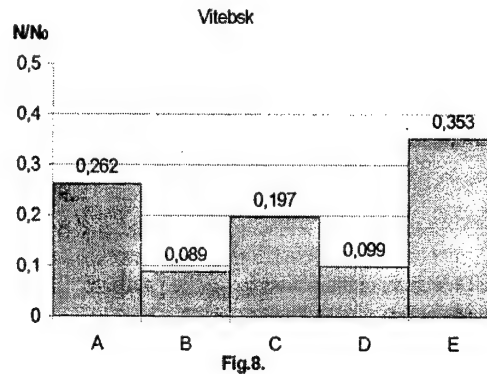
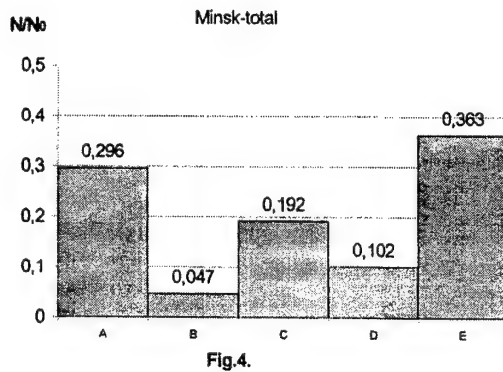
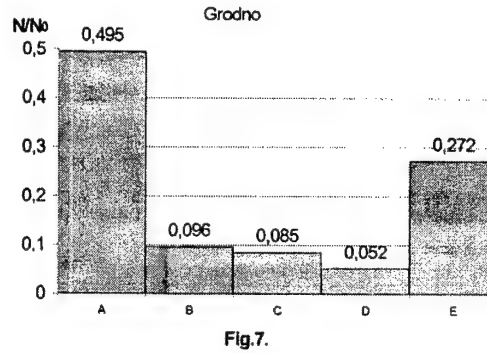
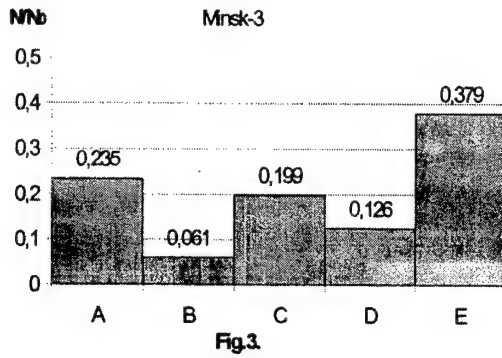


Fig.2.



Intervals of calculation data histograms correspond to the following interference margins (signal to interference ratio exceedance over the maximum tolerable level) and to the relative coverage area values of ARNS-equipment:

Interval	Interference margin, dB	Relative coverage area
A	$-\infty \dots -9$	0
B	$-9 \dots -5$	0.35
C	$-5 \dots 0$	0.56
D	$0 \dots +5$	1
E	$+5 \dots +\infty$	1

In accordance with received results, the potentially usable spectrum may also be interpreted as the relative coverage area of a GSM BS, averaged by degree of impact on ARNS radio facilities with provision for

GSM network channel allocation at the BS deployment point:

$$PFR = \sum_5 S_i N_i,$$

where S_i - the relative coverage area for GSM network channels that fall into i -th interference margin interval; N_i - the relative number of channels that fall into i -th interference margin interval.

Potentially usable spectrum estimation results for the considered segments of the uniform GSM network are detailed below.

GSM network segment	Potentially usable spectrum	Number of potentially usable GSM network channels
Minsk-1	0.60	74
Minsk-2	0.52	65
Minsk-3	0.63	79
Minsk	0.58	73
Brest	0.44	55
Gomel	0.62	76
Grodno	0.40	50
Vitebsk	0.59	73
Mogilev	0.56	69

The potentially usable spectrum definition used above (Eq.3,4) is invariant to the type of frequency-territorial limitations imposed on the designed system. In particular, the coverage area sizes (ERP values) of network base stations may be limited by usage conditions for the designed network frequencies in border regions.

For instance, taking into account the limitations imposed on the Grodno GSM segment by the ARNS as well as the limitations due to international agreements on frequency coordination in border regions leads to the following distribution of the GSM frequency grid channels according to the relative coverage area (see Fig.10).

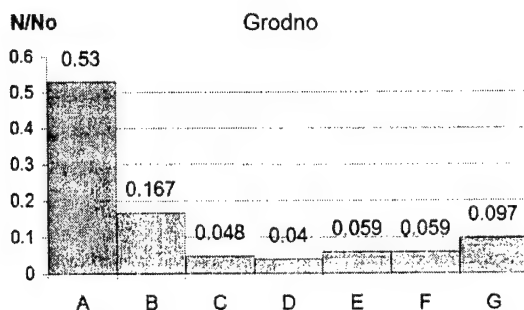


Fig.10

Histogram intervals correspond to the following relative coverage area values:

Interval	Relative coverage area
A	0
B	0.18

C	0.35
D	0.56
E	0.7
F	0.82
G	1.0

Thus, if we additionally take account of limitations stipulated by frequency usage regulations in border areas, the potentially usable spectrum for the Grodno GSM network is reduced to 0.25 (31 channel is potentially usable).

On the whole, the above results show that:

- On the average, 20-30% of GSM network frequency channels on the whole territory of the Republic may be considered as free from interference interaction with the ARNS network;
- There is a real danger of interference impact on ARNS for 40-50% of GSM-network channels subject to investigated point location on Belarusian territory, but this impact may in principle be eliminated by introducing additional requirements to antenna selectivity and orientation, as well as restrictions on transmit power of GSM network base stations in bands of the corresponding ARNS channels;
- 30-40% frequency channels in different sections of GSM frequency grid (subject to the geographical location of the populated area) cannot be used in GSM network due to substantial violation of EMC conditions.

The results of potentially usable spectrum analysis on the whole Belarusian territory are useful for clarification of real possibilities and prospects of GSM-900 network development as well as for frequency allocation coordination in border regions taking account of operation and upgrade plans for ARNS systems in Belarus and border states.

REFERENCES

1. «Definition of Spectrum Use and Efficiency of a Radio System», Rec. ITU-R SM.1046, 1994, pp.1-3.
2. A.A.Cashel, «About measurement and evaluation of Radio Frequency Spectrum Using» (in Russian), Radiotekhnika, Vol.27, No.11, 1972, pp.13-18.

BIOGRAPHICAL NOTES

Anatoly Budai is Belarus Posts and Telecommunications Vice-Minister, Victor Nikonov is Chief of Belarus State Supervisory Department for Telecommunications, Vladimir Mordachev (Ph.D) is Head of Research EMC Laboratory of Belarusian State University of Informatics and Radioelectronics (BSUIR), Victor Kozel (Ph.D) is ass.professor of BSUIR Radioelectronic Devices Department, Konstantin Kovalev is Researcher of BSUIR Research EMC Laboratory.

THE PROBLEM OF GENERATING FALSE ALERT SIGNALS WITH HELP OF DIGITAL SELECTIVE CALLING –
DSC IN THE GMDSS SYSTEM

Jerzy Czajkowski, Karol Korcz
Merchant Marine Academy Gdynia Poland
e-mail: czajkowski@post.pl

Abstract

In the recently introduced system of Global Maritime Distress and Safety System – GMDSS, the basic and at the same time the only way of sending alert signal with help of terrestrial communication is the digital selective calling – DSC. This system, however, during its seven years period of testing i.e. from 01.02.1992 to 01.02.1999 has caused and still creating many problems and much trouble during its exploitation at sea.

One of the most worrying and not clarified problems derives from the generation of false alert signals.

Two basic factors may certainly have some influence on the wrong work of the DSC system:

- *the human factor*
- *interferences resulting from applied solutions of radiocommunication, radionavigation and apparatus systems on seaships*

In this paper the author wishes to present his exploitation experiences of DSC in real conditions at sea carried out during first phase of introducing the GMDSS system and at the end of the seven years period of its full testing. The obtained results particularly those concerning the problem of generating false alert signals permit to formulate proper conclusions.

1. INTRODUCTION

In 1999 the implementation period of the distress system i.e. its introduction in the world the new Global Maritime Distress and Safety System (GMDSS) was completed.

In this system an important role has been given to an entirely new subsystem, i.e. to the Digital Selective Calling which will permit in the system, through terrestrial communication, the automatic creation of radiocommunication links, including also the establishing of communication of the distress, urgent, safety and routine type.

In the article the author presents the results of exploitation research of this system which have been carried out in real condition at sea during the exploitation of ships equipped with GMDSS devices.

From the acquired data it results that the DSC system, although with some reticence and difficulties, has been accepted in the world and in spite of complicated operational procedures fulfil the presupposed functions.

2. BACKGROUND

As known, the distress system used up to now at sea permitted to inform ships being in the vicinity of an accident about the necessity of affording help. The new Global Maritime Distress and Safety System – GMDSS changed in a basic way the execution of alarming by giving ships the possibility of transmitting the alarm on shore – to the Rescue Coordination Center by means of Digital Selective Calling – DSC. This system permits, without the intermediary of satellites, to send distress signals from ships to land and reversely also as well as between ships by using to that end specially allotted frequencies from sea bands in the VHF, MF and HF frequencies. These are contained in table 1.

Table 1. List of distress frequencies and in case of emergency in the GMDSS system

	DSC Distress Frequencies	Associated voice frequencies	Associated data frequencies
VHF	156,525 MHz (Ch. 70)	156,8 MHz	
MF	2187,5 kHz	2182 kHz	2174,5 kHz
HF	4207,5 kHz	4125 kHz	4177,5 kHz
	6312 kHz	6215 kHz	6268 kHz
	8414,5 kHz	8291 kHz	8376,5 kHz
	12577 kHz	12290 kHz	12520 kHz
	16804 kHz	16420 kHz	16695 kHz

3. INTRODUCTION TO THE DSC SYSTEM

The basic technical and systemic characteristics and the exploitation data of this system have been presented by the author in [1] [2]. We want to remind here only the most important ones. According to Recommendation ITU-R M.493-8 to send a DSC signal a synchronous system composed from a ten-bit error-detecting code has been used. It is based on the International Alphabet no 5 (ITA5 tab. 1.2) composed of $2^7=128$ sequences.

Draw. 1 presents as an example a 10-bit code sequence constitutes a calling sequence divided into an information and a check part.

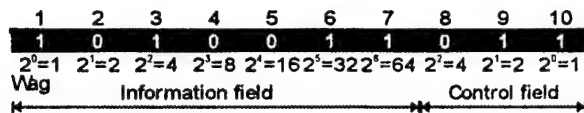


Fig. 1. Code sequence of a DSC

The detecting properties permitting to detect binary errors have been created by giving the number of 0 of the information field in a binary form.

General Format

The general format of a calling sequence is given in Table 2. This format is called general as the calling sequence can take various kinds of calling depending on its destination..

Table 2. General format of a calling sequence

Dot pattern	Phasing sequence	Format specifier	Address	Category
Self identification	Message 1	Message 2	Message 3	...
End of sequence				

Phasing sequence

A phasing sequence of a calling provides:

- information to the receiver to permit stop to further searching; this receiver, according to the characteristics of the GMDSS system carries out radio watch on frequencies destined to DSC calling
- information serving to reproduce precisely the position of particular bits and to univocally spot the position of code sequences forming the whole calling sequence

Format specifier

- The format specifier of calling sequence defines the form of the entire sequence, depending on the kind of calling. The symbol of the format specifier is transmitted twice in both the DX (Direct) and RX (Repetition) positions.

Address.

The address part of a calling sequence contains information defining the addressee of a given sequence. For a selective call or for a group of ships, in the address field we put the numeric or alphanumeric address of the calling station. The call of the group of ships in a given geographic area is defined by coding geographic coordinates according to the Mercator projection. In case of a distress call or all ships call the address is not given.

Category

The category information defines the degree of priority of the call sequence. For a distress call the priority is defined by the format specifier and the call sequence has no category information.

Self-identification

In the self-identification field a 9 digit identifier is transmitted - assigned to each station and coded as the address. It is used to identify the transmitting station.

Messages

As known the main task of a selective call is to transmit messages. The message in a call sequence consists of several elements and its form depends on the type of call. For distress calls the message concerning distress is contained in four elements.

- message 1 describes the nature of distress endangering a ship.
- message 2 is the "distress coordinates" message indicating the location of the ship in distress.
- message 3 is the time indication (UTC), when the coordinates were valid.
- message 4 is of a single character to indicate the type of communication (telephone or teleprinter) which is preferred by the station in distress.

End of sequence

The end of sequence character is transmitted three times in the DX position and once in the RX position. It is the of the three unique characters corresponding to symbols 117, 222 and 127.

- Symbol no 117 if the call requires acknowledgement (RQ)
- symbol no 122 if the sequence is an answer to a call that requires acknowledgement (BQ)
- symbol no 127 for all other calls.

Error-check character.

The error-check character is the final character transmitted and is the sign of error check. It serves to date at errors which are undetected by the ten-unit error detecting code and the time diversity employed.

The seven information bits of the error-check character shall be equal to least significant bit of the modulo-2 sums of the corresponding bits of all informations characters.

4. FALSE DISTRESS CALLS

After 8 years of GMDSS functioning it appears that false calls are the greatest problem connected with its implementation. According to the Radiocommunication Rules a false call is a call with distress priority sent by a station which is not in distress. This problem being monitored and analysed in detail under the auspices of IMO by many centers connected with domestic maritime administrations. A list, in the graphic form, of received false calls in DSC system by MRCC Bremen in the period from the beginning of GMDSS implementation till the middle of 1998 (also covering the period of DSC introduction) has been presented in the Fig. 2.

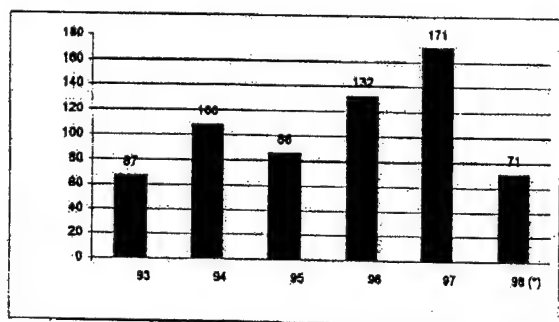


Fig. 2. Number of false DSC calls received by MRCC Bremen in the period of GMDSS implementation (*data FROM THE FIRST HALF OF 1998)

It can be seen from the list that the number of received false calls has been increasing what is confirmed by data from 1999. If the data showing that the percentage of received false calls constitutes 100% of all received calls are taken into consideration this is undoubtedly, annoying. The above presented data are also confirmed by other world centres including RCCs – (Rescue Coordination Centre)

A list illustrating share of different GMDSS subsystems responsible for distress calls in generation of false calls received also by MRCC Bremen in the same as above-mentioned period (Fig. 3) supplies interesting information.

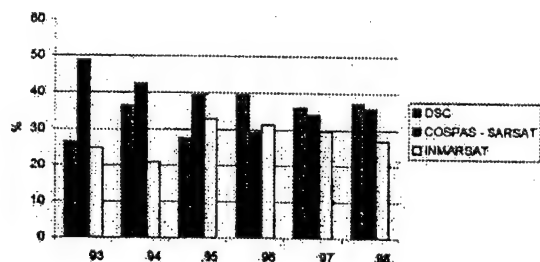


Fig. 3. Participation of different GMDSS subsystems in generation of false alerts

The data concerning INMARSAT organisation refer to all INMARSAT systems used in maritime communication, that is systems A, B, C and E. It can be concluded from the presented data that the problem of transmitting false distress calls, almost to the same degree concerns all 3 GMDSS subsystems fulfilling the function of alarming in distress that is DSC, INMARSAT and COSPAS/SARSAT. In the authors opinion it can indicate common reasons for false alarm generating and at the same time common methods of their elimination.

As it can be observed from the presented data (although not exhaustive) the problem of false distress calls is being profoundly examined. The results of this research are deeply analysed which allows to draw concrete conclusions both by international organizations (first of all IMO and ITU) and GMDSS users themselves.

Investigations of the DSC system operation in real conditions at sea during the first and last year of the GMDSS system application was conducted by the author with use of DSC equipment installed on the Polish ship M/V POLASIA – (MMSI – 261431370) and the training ship of Szczecin Maritime University – Poland M/V "Navigator XXI" (MMSI – 261187000). Some of the obtaining results are presented at Fig. 4.

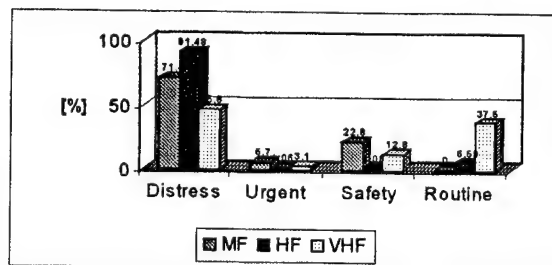


Fig. 4. Distribution of received DSC callings and frequency band in function of communication category.

Fig.4 shows the distribution of received DSC calling in frequency bands in function of communication categories. The comparison of achieved results with the results achieved six years earlier and presented on fig. 4 looks very interesting. It appears that the tendency to use DSC system to perform distress function on HF band, where was noted a small increase from 90% in 1993 to 91,48% in 1998 – was prevailing.

An increase in the number of distress callings in MF band, from 6,7% up to 71,4% was also noted – it was above 10 times increased, also in VHF band – from 19% in 1993 to 46,8% in 1998 – 2,5 times.

Hence we may assume, that in the last year of applying GMDSS system, the DSC system is admitted by users of the system to perform distress duties before all and this on frequencies of all three bands: VHF, MF and HF.

But we notice also a lot of examples of message corruption and information transposition especially with the HF DSC system. Furthermore we

observed that many DSC alerts are currently relayed and acknowledged – which can create false alerts and interferences.

5. RECAPITULATION

It results from the analysis of working DSC system particularly in the scope of distress alarming that generation of false calls constitutes the basic problem. Such a great percentage of false calls causes the necessity of continuous examination of the DSC system working in real conditions. The above problem causes serious consequences for the whole GMDSS system. The most important of them can be formed as follows:

- reducing readiness and efficiency by RCCs;
- high costs of RCC being on standby and performing false SAR actions;
- interfering the GMDSS working; and
- impairing users trust in GMDSS.

Thus, in the above aspect it seems essential to undertake measures leading to significant reduction (if not elimination) of false calls. International institutions responsible for the safety at sea IMO or ITU have undertaken such steps but in the authors opinion all centres active in this field should contribute to this end. It ought to be carried out in three coordinated training areas:

- administrative, performed by international and domestic organizations;
- technical, concerning manufactures of DSC equipment;
- training, being the domain of operators training centers.

It results from the analysis of efficiency and reliability of alarming methods used in the system DSC MF/HF/VHF that two basic factors influence their incorrect work:

- human;
- resulting from applied functional and equipment solutions.

Omitting the human factor, the problem concerns a possibility of committing errors in DSC transmission – as a result of accumulating a great number of radiocommunication, radionavigational, electronavigational and electrical devices or ship automation systems in the small space of ship bridge. Therefore, the problem of electromagnetic compatibility plays a very important role here as the interaction of systems and devices can influence generation of errors in DSC calling format (Tab 2).

The improvement of the existing state referring to the transmission of false distress calls, in the authors opinion can be achieved by:

- raising quality of training for GMDSS operators, system users,
- Rationalization (simplification and standardisation) of operational procedures in distress alarming,
- Designing user-friendly DSC devices; the use of unmistakably identified buttons, secured against

chance initialisation of alarm,

- Designing DSC devices requiring at least double confirmation to emit alarm signals.
- Examination of the influence of radioelectronic and natural interferences on the proper work of GMDSS devices and subsystems (including DSC).

6. BIBLIOGRAPHY

1. *Recommendation ITU-R M.541-7 OPERATIONAL PROCEDURES FOR THE USE OF DIGITAL SELECTIVE CALLING (DSC) EQUIPMENT IN THE MARITIME MOBILE SERVICE*
2. *Recommendation ITU-R M.493-8 DIGITAL SELECTIVE-CALLING SYSTEM FOR USE IN THE MARITIME MOBILE SERVICE*
3. *IMO GMDSS Handbook – 2nd Edition 1996*, London 1996
4. Czajkowski Jerzy "Exploitation Study of DSC System during the first period of GMDSS Application" *Conference CEPT Oslo 1999*
5. Czajkowski Jerzy "Exploitation Study of DSC System during the last year of applying GMDSS and final conclusions". *Conference CEPT Oslo 1999*.
6. Czajkowski Jerzy "Estimation of usefulness of Digital Selective Calling system in GMDSS". *Polish Maritime Research December 1999*.
7. *IMO COMSAR I/INF15 „Examples of DSC false alerts submitted by Norway” December 1995*
8. *IMO COMSAR 4/7 April 1999 „Emergency Radiocommunications: False Alerts and Interferences. Operational performance of the MF/HF DSC system. Submitted by Australia.”*

7. BIBLIOGRAPHICAL NOTES

Jerzy Czajkowski:

- Dr. Sc. (Radio Communication) of Gdańsk Technical University.
- Associate Professor – Head of GMDSS Training Centre.
- Lecturer in Radioelectronics at the Maritime Academy for 5 years.
- Vice-rector of Gdynia Maritime Academy from 1985 to 1990.
- Radioofficer with experience at sea.
- Author of several books on radioelectronics, teaching books for students and many articles on radiocommunication.
- Vice chairman of the national exam – commission for GMDSS certificates

Karol KORCZ began his work in Marine Radio Electronics Department in Gdynia Maritime Academy in 1984. His experience includes employment as Radioofficer and Radioelectronic on the seagoing ships. In the years 1993-1999 he was Deputy Dean of Faculty of Marine Electrical Engineering. His science interest includes the electromagnetic compatibility in ships and the radio marine regulations.

PROBLEMS OF UMTS NETWORKS EMC WITH RADIO RELAY SYSTEMS OF THE FIXED SERVICE IN RUSSIA

A. Gouliaev, P. Mamtchenkov, M. Selivanov, Dr. N. Smirnov

*Radio Research & Development Institute (NIIR),
16, Kazakova str., 103064, Moscow, Russia, Tel: + 7 095 267-4740, Fax: + 7 095 267-8430
e-mail: gulyaev@hotmail.com*

The paper deals with the topical for Russia problems of the 2 GHz band sharing aspects between the coming UMTS networks and radio relay systems of the fixed service. The EMC analysis is developed on the basis of modified Hata model of radio waves propagation in urban areas. Based upon the technical characteristics of the UMTS equipment which are being developed within 3GPP TSG RAN and ERC TGI and the typical characteristics of radio relay stations deployed on the territory of Russia the required cross-service frequency-distance separations are defined.

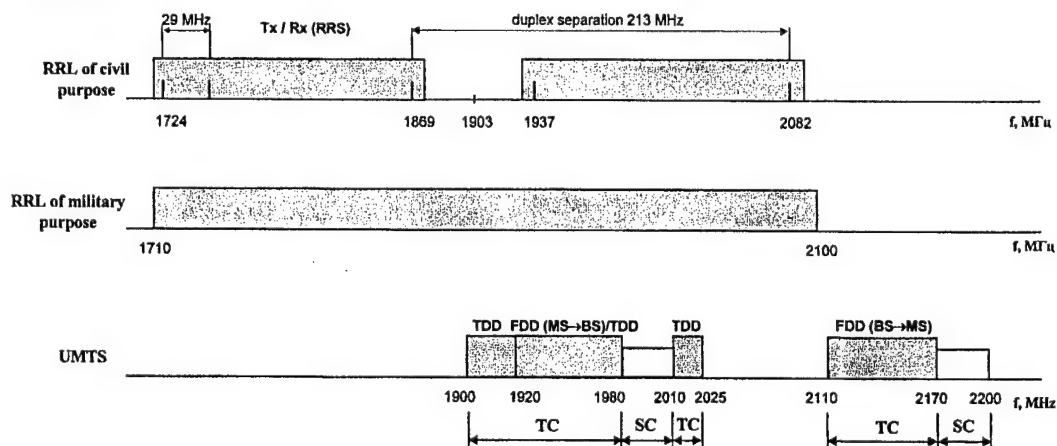
1. INTRODUCTION

Introduction of new technologies in Russia in the 2 GHz band under a deficit of a frequency resource leads to aggravation of intersystem EMC problems due to historically turned out frequency sharing in this band between civil and military radio relay links (RRL). In the majority of CEPT countries the activities on removing radio relays of the fixed service from the 2 GHz band are being conducted. In Russia this band can not be refarmed in an immediate manner in view of a number of economical reasons and necessity of its usage by RRL of military purpose. This fact is a substantial obstacle in the way of coming UMTS system implementation.

The chart (fig.1) illustrates frequency allocations to RRL of civil and military purpose and European frequency allocation to UMTS. As shown in fig.1, in Russia the main problem of frequency bands allocation to UMTS (particularly for terrestrial component) is connected with the necessity of its sharing with line-of-sight civil and military RRL of the fixed service.

2. PROCEDURE OF SHARING STUDY

The base of analysis is a calculation of the required frequency-distance separations between potentially incompatible transmitters and receivers for different orientations of their antenna patterns. Here, the criterion is ensuring the required wanted signal reception quality in the presence of unwanted interference. Calculated on the basis of the assumed radio waves propagation model results for the concrete radiocommunication equipment can be considered the upper limits of the required values. This is because of leaving out of account the path loss due to terrain constraints. In case of real separations exceed the calculated ones EMC between the systems is considered to be ensured. Otherwise, the additional limitations in radiated power, frequency offsets or antenna patterns orientations should be introduced.



Note: TC - terrestrial component, SC - satellite component.

Fig. 1

The required separations (taking into account multipath fading effect) are defined according to the following criterion:

$$P_S - P_I \geq A + (\sqrt{2} - 1)k\sigma, \quad (1)$$

where

P_S – receiver sensitivity (dBW);

P_I – interf. signal power at a receiver input (dBW);

A – protection ratio of a receiver (dB);

$(\sqrt{2} - 1)k\sigma$ – signal margin due to multipath fading;

k – coefficient accounting fading margin for a given percentage of time of intolerable deterioration of communication quality;

σ – standard deviation characterizing fluctuations in wanted and interfering signal levels; we assume that wanted and interfering signal power levels follow log-normal distribution at the receiver input (dB) (for medium cities σ is usually taken equal to 6 dB[2]);

$$P_I = P_T + G_T(\varphi_S) + G_S(\varphi_T) + U_T + U_S + N(\Delta f) - L(R) + \gamma_{pol},$$

where

P_T – interference signal transmitter power (dBW);

$G_T(\varphi_S)$ – interference signal transmit antenna gain in the direction (φ_S) of wanted signal receiver;

$G_S(\varphi_T)$ – wanted signal receive antenna gain in the direction (φ_T) of interference signal transmitter;

U_T, U_S – transmit and receive antennas feed loss (dB);

$N(\Delta f)$ – interference signal attenuation ratio in a receiver linear section (dB);

Δf – frequency offset (MHz);

γ_{pol} – interference signal attenuation ratio due to discrepancy in polarizations (dB);

$L(R)$ – path loss in the distance of R (km), (dB);

For the 2 GHz band the modified Hata Model [3,4] is applied for interference signal median value calculation.

$$L(R) = \alpha + \beta \cdot \lg(R) \quad (2)$$

Here, α, β – coefficients dependent on the frequency range and antenna heights, dB. In case of medium city for the range 1.5...2 GHz parameters α and β are as follows:

$$\alpha = 46,3 + 33,9 \cdot \lg(f) - 13,82 \cdot \lg(h_T) - a(h_R),$$

$$\beta = 44,9 - 6,55 \cdot \lg(h_T),$$

where

f – signal operational frequency, MHz;

h_T, h_R – transmit and receive antenna heights, m;

$$a(h_T) = (1,1 \cdot \lg(f) - 0,7) - (1,56 \cdot \lg(f) - 0,8), \text{ dB}.$$

Considering (1), (2) the formula for the required frequency-distance separations can be derived:

$$D = 10^{\frac{-1}{\beta}(Z + \alpha)}, \quad (3)$$

where

D – required distance separation, km;

Z – complex power parameter, dB.

Parameter Z in (3) is defined as:

$$Z = P_S - P_T - G_T(\varphi_S) - G_S(\varphi_T) - U_T - U_S - \gamma_{pol} - N(\Delta f) - A - (\sqrt{2} - 1)k\sigma \quad (4)$$

Parameter Z represents the difference between the minimal signal power at the receiver input (receiver sensitivity) and the radiated interference signal power in receiver bandwidth taking into account frequency offset, protection ratio of a receiver and multipath fading margin. The more this difference, the closer a receiver of wanted signal and a transmitter of interference signal can be installed on conditions that EMC is ensured.

3. SHARING CONDITIONS

The calculation of frequency offsets and distance separations for radioelectronic installations (REI) of UMTS system and fixed civil and military services was made for all potential combinations of mutual interferences.

Table 1 presents the assumptions for assessment concerning the 3-rd generation radioelectronic installations. The typical values of parameters for radioelectronic installations of fixed services were taken into account.

Fig. 2 presents the dependences of required separation distances of MS_{3G} , BS_{3G} (3rd generation mobile and base stations) and RRLs on parameter Z . These characteristics were obtained by means of modified Hata's path loss model on the basis of the formula (3). Sharp bend of $D(z)$ curve for BS_{3G} is due to transition at this point to a free space model (extreme case). Spectrum masks and receiver selectivity were approximated by linear-logarithmic functions (fig. 3). Fig. 4 and 5 show the dependences of interference attenuation ratio in receiver linear section for different cases of mutual interference of REI.

Table 1

Symbol	Unit	Parameter	BS_{3G}	MS_{3G}
P_R	DBW	Receiver sensitivity	-133	-129
P_T	dBW	Transmitter power	11	-9
G_R	dB	Receiver antenna gain	14,5	0
G_T	dB	Transmitter antenna gain	14,5	0
U	dB	Feed loss	0	
f	MHz	Operational frequency	2000	
A	dB	Protection ratio of Rx in the presence of co-channel interference	-21,6	-19,1
h_T	m	Transmitter antenna height	40	1,5
h_R	m	Receiver antenna height	40	1,5

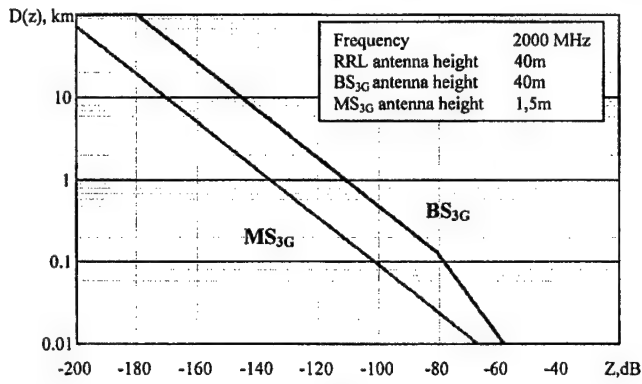


Fig. 2

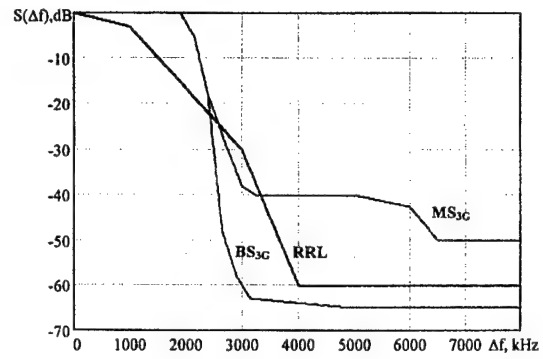


Fig. 3

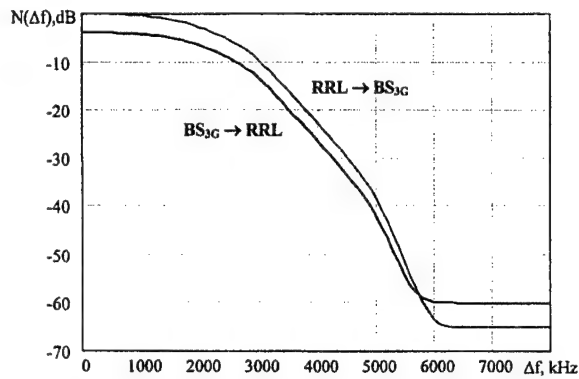


Fig. 4

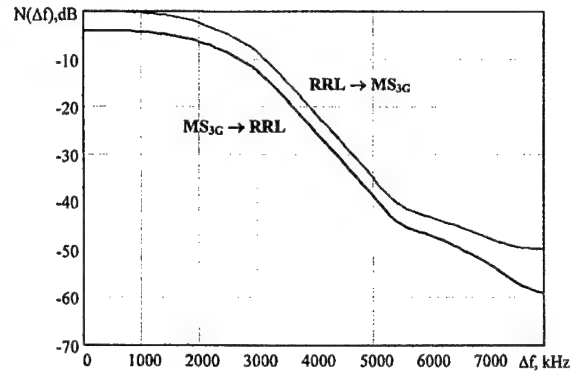


Fig. 5

The corresponding results of required separation distances calculation between radioelectronic installations for different frequency offsets and cases of mutual orientation of transmitter and receiver antenna patterns are presented in tables 2 and 3:

M-M — the influence direction from the main lobe of interference source to the main lobe of the interfered station;

M-S — the influence direction from the main lobe of transmitter to the side lobes of the receiver;
S-M — the influence direction from the side lobes of receiver to the main lobe of transmitter;
S-S — the influence direction from the side lobe of interference source to the side lobe of the interfered station.

Table 2

Tx RRL → Rx BS _{3G}					Tx BS _{3G} → Rx RRL				
Δf, MHz	D, km				Δf, MHz	D, km			
	M-M	M-S	S-M	S-S		M-M	M-S	S-M	S-S
0	27,4	7,2	3,67	0,96	0	> 100	43,9	85,1	11,5
2	22,3	5,87	3,03	78	2	> 100	35,7	70,2	9,39
4	5,87	1,54	0,78	0,21	4	71,1	9,39	18,2	2,47
6	0,35	< 0,1	< 0,1	< 0,1	6	7,65	1,04	2	0,27

Table 3

Tx RRL → Rx MS _{3G}					Tx MS _{3G} → Rx RRL				
Δf, MHz	D, km				Δf, MHz	D, km			
	M-M	M-S	S-M	S-S		M-M	M-S	S-M	S-S
0	2,05	2,05	0,27	0,27	0	5,99	0,81	5,99	0,81
2	1,8	1,8	0,24	0,24	2	5,25	0,71	5,25	0,71
4	0,5	0,5	< 0,1	< 0,1	4	1,67	0,22	1,67	0,22
6	0,12	0,12	< 0,1	< 0,1	6	0,34	0,05	0,34	0,05
8	< 0,1	< 0,1	< 0,1	< 0,1	8	0,14	0,02	0,14	0,02

Also the results of required separations between typical military line-of-sight RRL and UMTS MS and BS for different frequency offsets and cases of mutual antenna orientations are obtained (both for vertical and horizontal polarization of military RRL antennas).

4. RECOMMENDATIONS ON SHARING CONDITIONS BETWEEN RRL AND UMTS

Assuming typical values of REI characteristics for UMTS and RRL the crucial influence will be in direction from UMTS radio equipment to RRL ones.

In the case of BS_{3G} and RRL installations line-of-sight position and on conditions that antenna patterns are oriented by the main lobes simultaneous sharing is impossible.

In the case of absence of line-of-sight position in city environment the required distance separation between RRL of civil purpose REI and BS_{3G} which operate on the same channels depends on the mutual antenna patterns orientation and comes to 1...27.4 km. For RRL of civil purpose REI and MS_{3G} it comes to 0.1...2.05 km.

For providing sharing between UMTS and RRLs of the fixed service it is necessary to apply frequency or distance separations. On conditions that antenna patterns are oriented to each other by side lobes and with 6...8 MHz of frequency offset between RRL transmitters and MS_{3G}/BS_{3G} receivers sharing is possible.

The required distance separations between RRL of military purpose REI and BS_{3G} were calculated putting into consideration as the interference from RRL REI to BS_{3G}, as reverse influence. Analysis of these results for RRL installations of military purpose in the vertical polarization mode which operate simultaneously on the same channels with BS_{3G} in the 2GHz band and, on conditions that antenna patterns are oriented by the main lobes, shows that the required distance separation comes to 36.6...54.7 km.

The required distance separation between RRL of military purpose installations in the horizontal

polarization mode and BS_{3G} is 4...5 times less and comes to 7.2...10.6 km.

The required frequency offset between line-of-sight RRL of military purpose installations and BS_{3G} sharing the 2GHz band, comes to 6...12 MHz.

So, for ensuring EMC of military RRL REI with BS_{3G} it is necessary to apply distance separations putting into account antenna patterns orientation and polarization, as well as restrictions on frequency assignments.

5. CONCLUSION

The obtained values of the required frequency-distance separations between the mentioned systems are of great practical importance for the possibility estimation of frequency allocations to UMTS networks in the specific regions of the Russian Federation, particularly in urban area. Provisions from this paper can also be included into appropriate agreements between the Russian and neighboring countries administrations concerning the use of the frequency bands in the border areas.

The results obtained in the paper testify to the necessity of the further regulation of the national frequency management policy and making corresponding changes to the table of frequency allocations of the Russian Federation aimed on the step-by-step superseding the existing fixed service radio relays in the 2 GHz band by the coming 3rd generation UMTS system.

6. REFERENCES

1. Table of frequency allocations between 3 kHz and 400 GHz to the radio services on the Russian Federation, Moscow, 1996.
2. Michel D. Yacoub. Foundations of mobile radio engineering, CRC Press, 1993.
3. Hata M. Empirical formula for propagation loss in land mobile radio services IEEE Transactions on Vehicular Technology, vol. 29, №3, August, 1980.
4. EURO-COST 231 TD (91) 73. Urban transmission loss models for mobile radio in the 900 and 1800 MHz bands, — The Hague, September, 1991.

Compatibility Between Mobile Services and TV Broadcasting in the VHF Band. Practical experiences

Mirosław Pietranik, Wiktor Sęga, Ryszard Żarko
Instytut Łączności O/Wrocław, ul. Swojczycka 38, 510501 Wrocław
tel. (+71) 3483051, fax.: (+71) 3728878,
E-mail: mpie@il.wroc.pl, wseg@il.wroc.pl, rzar@il.wroc.pl

TV transmitters operated in the adjacent band to the radiocommunication mobile services (MS) may cause serious interference. The paper deals with such a situation when mobile services in the 164 ÷ 174 MHz band and TV transmitter in R6 channel are operated at the same area. The evaluation bases on the measurements of the TV signal spectrum and MS receiver immunity. In the paper the protection of the land mobile services from the broadcasting television is presented.

1. INTERFERING SIGNAL

Fig. 1 illustrates the signal of the TV transmitter from the channel R6. Special filters are used to form the main and vestigial sidebands of the TV signal. Their attenuation is normalised [1, 2]. For the TV D/K systems the attenuation of the vestigial sideband (at the frequencies 1,25 MHz below the video carrier) relative to the main sideband should be greater than 20 dB. Taking into account that the level of the main sideband relative to vision carrier is -35 dB in the result one may conclude that the difference between levels of vision carrier vestigial sideband is more than 55 dB.

Though the level of spectrum in the lower vestigial sideband is quite small even in the case of high power TV transmitter, but it may be high enough to interfere the RRL receivers.

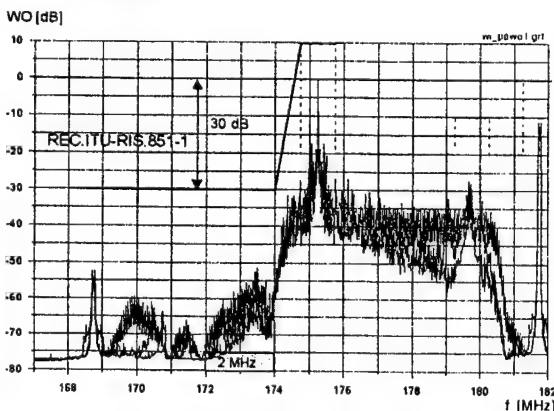


Fig. 1. An example of the TV signal

In the Fig.1 three spectra are presented; each of them is connected with modulation of the TV signal by its own (different from others) picture contents. The influence of the modulating picture content is obvious. Figs 2, 3, 4, 5 and 6 illustrate this influence more detail. The measured level and character of the TV signal depend also on the detector used and the resolution bandwidth of the measuring receiver. For example Figures 2 and 5 illustrate the influence of the detector used to measure TV signal spectrum. Influences of the resolution bandwidth illustrate Figures 2 and 4. Fig. 3 shows the nearest vicinity of one spectrum line. The character of the spectrum depends on the contents of the test pattern used to modulate TV signal. Measurements were carried out with the help of peak and rms detectors with receiver bandwidth resolution 10 Hz.

Distance between two adjacent lines of the spectra is 15625 Hz. This distance is comparable with channel separation used in mobile radiocommunication: 12,5 or 25 kHz.

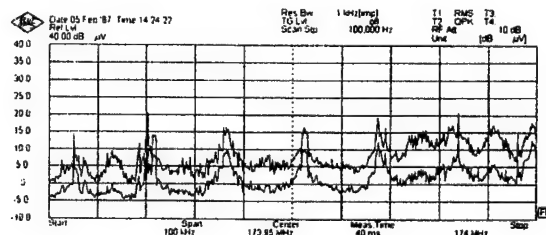


Fig. 2. Test pattern: H-sweep. Resolution bandwidth: 1 KHz. Detectors used: peak - upper curve; rms - lower curve

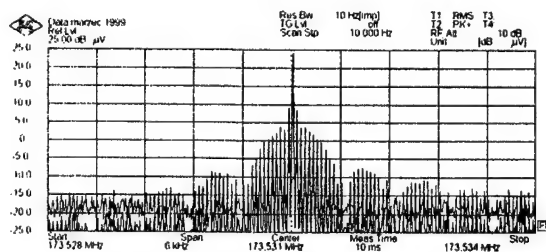


Fig. 3. Spectrum in the vicinity of one spectrum line

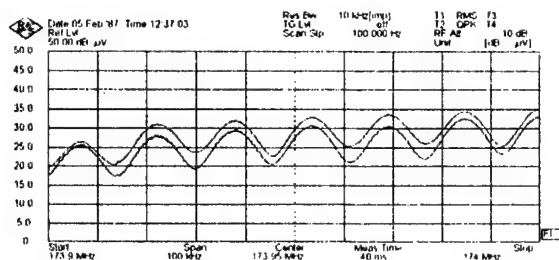


Fig. 4. Test pattern: H-sweep. Resolution bandwidth: 10 KHz

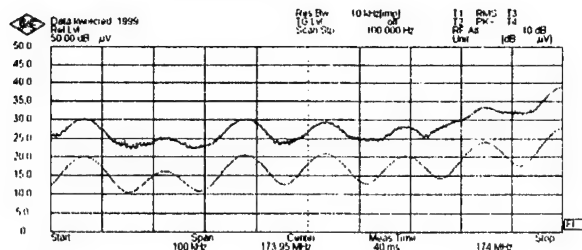


Fig. 5. Test pattern: Mire. Resolution bandwidth: 10 kHz. Detectors: peak - upper curve; rms - lower curve

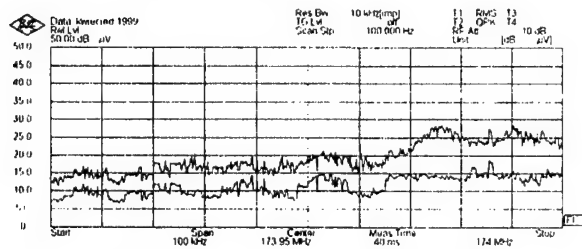


Fig. 6. Test pattern: movies from videorecorder. Resolution bandwidth: 10 KHz. Detectors: peak - upper curve; rms - lower curve

Generally the interference depends on the real attenuation of the vestigial sideband of the TV transmitter, content of the video picture and the modulation deep of the TV signal. The interference has pulse character. It arises from the AM modulation and linear scanning of the TV signal: see Fig. 2.

2. ASSESSMENT OF THE INTERFERING SIGNAL

Detectors

The appropriate detector should be used to obtain best correlation with subjective assessment of the RRL receiver interference due to character of TV interfering signal. In the case of mutual interference inside the radiocommunication mobile service, where interfered and interfering signals are FM modulated, the rms detector is preferred. But in the case of pulse interference or interfering signals AM modulated (the TV signal) the better one is quasi-peak detector followed by the psophometric filter [3]. The problem is very important because different detectors give different values of the $(S/I)_{AF}$ ratio in case of the same subjective assessment of the resulting interference. Appropriate results of measurement, conforming the above conclusion, are presented in the Figs 6 and 7. For that part of the TV signal spectrum which is in the band of

radiocommunication service the linear dependence between level of TV interfering signal and the level of useful radiocommunication signal is observed: see Fig. 7 and Fig. 9.

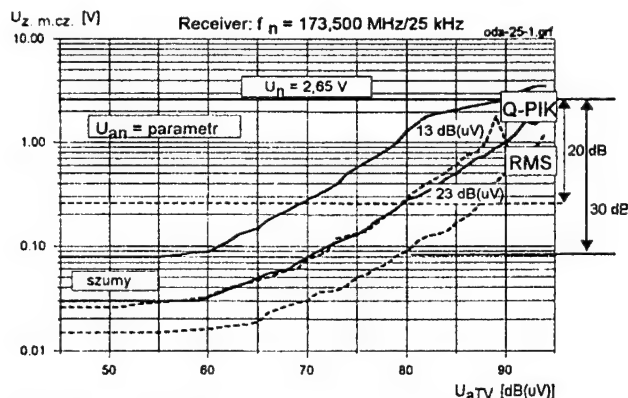


Fig. 7. Dependence between level of the TV vision carrier - U_{aTV} and useful radiocommunication signal - U_{an} measured at the input of the MS receiver.

Interfering spectral lines relative to the MS channel

Comparing the frequency of the spectral lines (connected with line frequency of the TV signal) and frequency of the MS channel one can see that for every 5th succeeding channel (starting from 174 MHz) they are the same. This causes the serious interfering problem in these channels. Practical measurements show that the same serious problem exist even if the frequencies of spectrum lines are slightly moved from central position, up to ± 3.125 kHz. For extreme positions the interference are even greater than for the central position of the spectral line in the channel considered. That means that for a given level of the interfering spectral line to receive the same intelligibility (the same value of the $(S/I)_{AF}$ ratio) the bigger useful signal should be applied (Fig. 8 illustrates that problem). For every channel three levels of useful signals are presented.

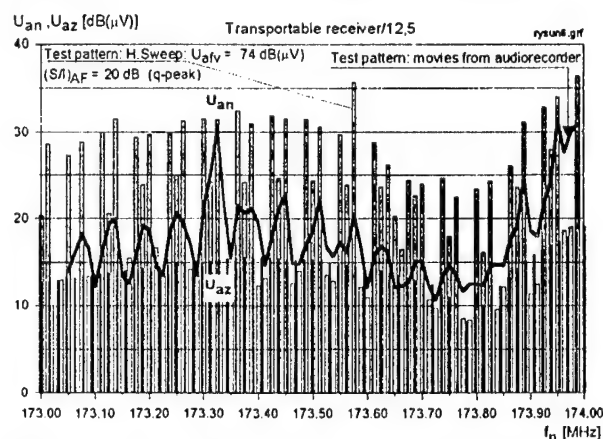


Fig. 8. U_{az} - spectrum lines of the interfering TV signal for the H-sweep test patterns- black columns; U_{an} - levels of useful signal - grey columns or curve.

They are connected with the interfering spectral line lying in the central position of the MS channel or detuned by ± 3.125 kHz. During measurements the level of interfering TV signal vision carrier was 74 dB(μ V) at the HF input of the tested MS receiver. The same level was

used for the TV signal modulated by the H-sweep test pattern or test pattern taken from videoplayer. In both cases the levels of useful signal - U_{an} was regulated to assure at the AF output of the MS receiver the ratio $(S/I)_{AF} = 20$ dB. Grey columns represent the useful signal connected with H-sweep test pattern, the curve responds to the test pattern taken from videoplayer. The frequencies of the useful signal were tuned with the step of 12,5 kHz, according to MS channel raster. The ratio $(S/I)_{AF} = 20$ dB was chosen, because in this case good audio quality (at the output of MS receiver) is observed. The limiting intelligibility is observed at $(S/I)_{AF} = 10$ dB.

Protection ratio - PR

The protection ratio (PR) is defined as a difference between level of the TV signal vision carrier and useful signal assuring the good intelligibility of the reception:

$$PR = (U_{aTV} - U_{an}) \text{ [dB]}$$

For example, for values shown in the Fig. 8 $PR = 49$ dB for $f_n = 173,975$ MHz and $PR = 56$ dB at $f_n = 173,500$ MHz,

The above expression, used to calculate the PR, is valid only in the range of linear behaviour of the MS receiver. At a certain level of the interfering signal the desensitisation can occur. In the Fig. 9 there are results of measurements for two-type tested receivers and two width of MS channels. The desensitisation occurs at 112 dB(μ V/m) for portable receiver (MC2100) and 90 dB(μ V/m) for mobile receivers (MT2100). The influence of channel width is rather small.

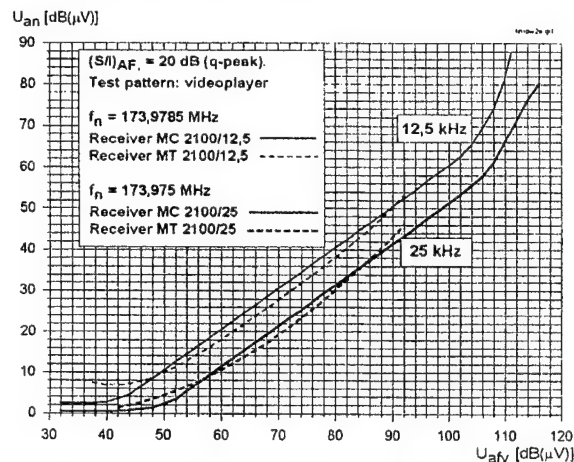


Fig. 9 Linearity and desensitisation of MS receivers

3. FIELD IMMUNITY OF THE MS RECEIVER

In the Figs 10 to 14 there are results of PR calculated basing on the measurements of the MS receivers immunity carried out in the GTEM cell. During investigations two test pattern modulating TV interfering signals and two channel width of the MS receivers: 12,5 kHz and 25 kHz were used. Comparing Figs. 10 and 11 or 12 and 13 the influence of the test pattern is can be observed.

The results presented in the Fig. 10 to 13 were received for the mobile MS receivers MT 2100. The same measurements were carried out for the portable receiver MC 2100 (Fig. 14), which are more immune than the mobile. The receivers with channel spacing 25 kHz

are also more immune (but not so much) than receivers with 12,5 kHz channel spacing.

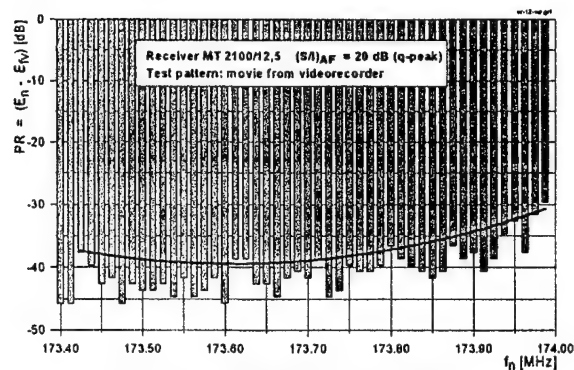


Fig. 10 Receiver MT 2100/12.5

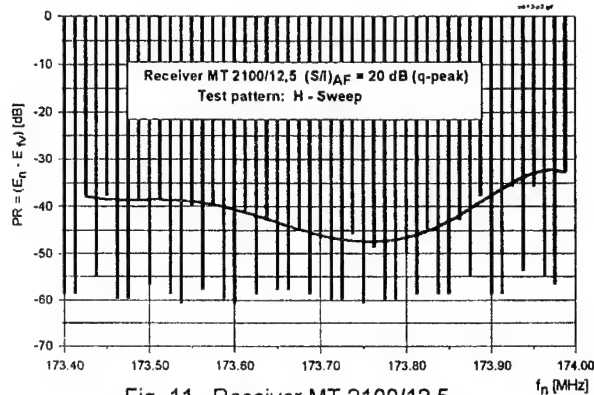


Fig. 11 Receiver MT 2100/12.5

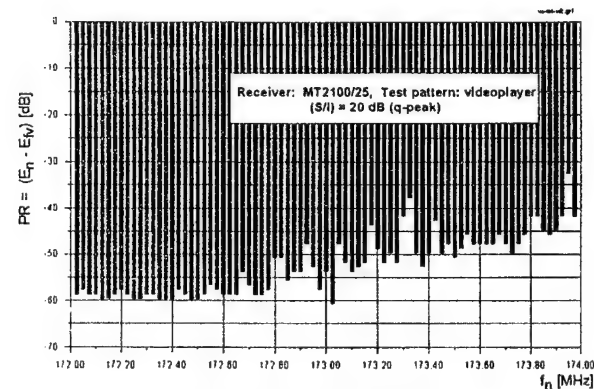


Fig. 12 Receiver MT 2100/25

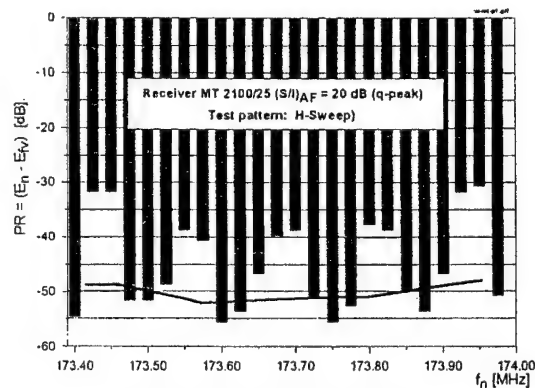


Fig. 13. Receiver MT 2100/25

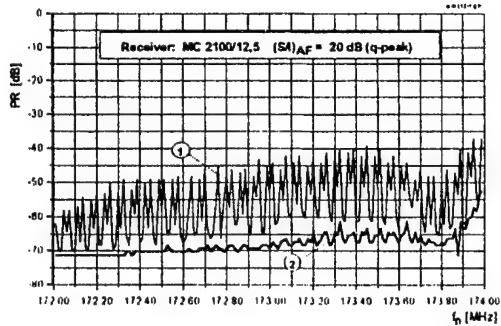


Fig. 14. Receiver MC 2100/12.5. 1) H-sweep test pattern, 2) test pattern from videoplayer

4. CONCLUSIONS

Values of the PR ratios depend on the frequency separation of the MS channel and the TV vision carrier. The influence of the TV programme contents (film or patterns with sharp edges like letters, tests etc) is also observed. Taking into account the worst case (from Figs. 10 - 14) the level of TV vision carrier E_{TV} , which will not cause interference to the MS reception, should fulfil following relations:

$$E_{TV} \leq E_n + PR \quad \text{dB}(\mu\text{V/m}),$$

where:

E_n – minimum median field strength to be protected (in the considered band 22 dB($\mu\text{V/m}$)),

PR – protection ratio (20-40 dB).

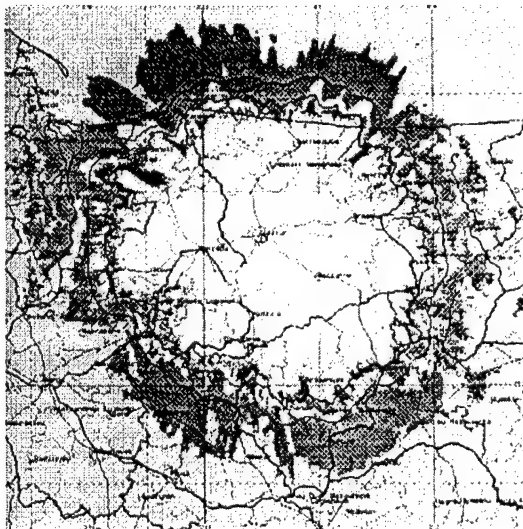


Fig. 15. An example of the computer simulation results

White - $E_{TV} > 62\text{dB}$, interference is most probably,
 Grey - $52\text{dB} < E_{TV} < 62\text{dB}$, interference may occur,
 Black - $42\text{dB} < E_{TV} < 52\text{dB}$, sharing MS and TV is feasible.

In the Figure 15 the results of the computer simulation of the interference to mobile radiocommunication services (in the band 172 – 174 MHz) caused by TV station in the channel R6 is presented.

5. REFERENCES

- [1] BN-71/3321-03, TV transmitters. Requirements – product standard (in Polish)
- [2] CCIR Rec. 624-3. Dubrovnik 1986. TV standards.
- [3] PN-EN 55013, Limits and methods of measurement of radio disturbance characteristics of broadcast receivers and associated equipment
- [4] Rec. ITU-R IS.851-1: Sharing between the broadcasting service and the fixed and/or mobile services in the VHF and UHF bands.
- [5] SE(96) TEMP 24: Compatibility between ERMES service and TV Channel R-6 (System D) in Hungary.
- [6] Preliminary Report. CEPT Project Team SE7: ERMES/TV Channel R-VI (system D) compatibility.
- [7] CEPT FM10/SE7(93)39: Final report of the CEPT FM/SE7 Joint Project Team studying the compatibility problems between certain radiocommunications systems operating in adjacent bands.

BIOGRAPHICAL NOTES

Mirosław Pietranik obtained his M.S. degree in 1961 from Technical University of Wrocław and his Ph.D. degree in 1974 from Warsaw National Institute of Telecommunications. His technical activity during whole professional life concerns EMI/EMC problems. He co-operates with CISPR working group SC A and SC F in the field of click measurements and mds clamp calibration and with the SC E in the field of immunity problems in radio and TV reception. He works in Wrocław branch of Warsaw National Institute of Telecommunications. and now he is head of EMC Measuring Apparatus Laboratory which received accreditation from Polish House of Measure.

Wiktor Sęga was graduated from the Technical University of Wrocław (Poland) in 1975, and then he joined the Institute of Telecommunications and Acoustics of this University. In 1979 he obtained a Ph.D. in telecommunications from the Technical University of Wrocław. Since 1979 he has been working in the National Institute of Telecommunications, Wrocław Branch. Dr W. Sęga is involved in preparation of engineering models and software for the computer-aided national spectrum management. He was responsible for elaboration of the digital terrain model for the territory of Poland. Since 1988 to 1989 he worked with Wireless Planning and Coordination Wing of the Ministry of Communications in India, as the UNDP/ITU expert. He is engaged in the ITU-R and CEPT studies. Dr W. Sęga is the Technical Program Coordinator of the International Symposium on EMC.

Ryszard Żarko received his M.S. degree in 1956 and Ph.D. degree in 1964 from Technical University of Wrocław, both in radio-engineering. Since 1956 he was with Technical University of Wrocław, lately as Assistant Professor in the Institute of Telecommunications and Acoustics. Now he co-operates with Wrocław branch of Warsaw National Institute of Telecommunications in the field of immunity problems in radio-communications.

ASSESSMENT OF THE INTERNATIONAL COORDINATION NECESSITY OF MICROWAVE RADIO RELAY LINKS

Wiktor Sęga, Wojciech Tyczyński

National Institute of Telecommunications ul. Swojczycka 38, Wrocław, Poland
wseg@il.wroc.pl, wtyc@il.wroc.pl

In the paper the assessment of the need of international coordination of microwave radio links is considered. In order to reduce as much as possible unnecessary coordinations the assessment is based on the results of calculations in the points located on the borderline. Additionally, to be absolute sure that a necessary coordination is not missed, calculations are performed in the "critical points" which are located on the hills or mountains inside the foreign country. The method can also be applied to reduce the number of foreign links stored in the database.

1. INTRODUCTION

The applied microwave link must be analysed from compatibility point of view with other systems installed abroad. Taking into account the strong directivity of antennas used in radio relay links it is likely that not all neighbouring countries will be involved in a coordination process. What is more, it may also occur that the link is situated far away from the border and there is no need for coordination at all. One can take some advantages, if such a situation is recognised. Firstly, the link may be put into air immediately not waiting for the answer on a coordination request. Secondly, two parties can avoid superfluous work: the administration sending the coordination request and the administration analysing the request.

But the coordination process for the link can only be omitted, if it is sure, that the link will not produce or get harmful interference from abroad. There are unpleasant consequences of neglecting a coordination process. **A station, which is not coordinated is not protected.** It means that an administration can not protest if its receiver suffers interference coming from abroad or must switch off the transmitter in the case of claims from another administration. Furthermore it also means that the choice of the criteria used for triggering international coordination has no influence on the development of communication systems.

Taking it into account, the following conclusion can be drawn:

The problem of the criteria, which should be used to trigger international coordination, is not an international matter and it must be solved by every administration itself. If a necessary coordination is omitted the administration will experience the consequences of it.

There is one more field where the method for the assessment of the need of an international coordination can be utilised. The same method can be used to reduce the number of foreign links stored in the database. If one wants to avoid assignments, which are not compatible with foreign links, it is a good job to perform compatibility analysis taking into account the registered links. So it is necessary to maintain the database containing microwave links installed abroad. But it is not reasonable to keep in the data base all of them. The number of foreign links must be reduced as much as possible, but anyone, which is important, can not be neglected. Then the spectrum engineer faces the problem: which links should be rejected?

2. THE IDEA OF THE METHOD FOR THE ASSESSMENT OF THE NEED OF AN INTERNATIONAL COORDINATION

It may be supposed that the method, which is based on calculations at points located on the borderline, is the best, because it is secure and it is the least conservative. The method is secure because points on a borderline are expected to have the highest interfering signal level (the distance is the shortest). It is the least conservative because the parameters of the real link can be taken into account (transmitter radiated power, transmitter or receiver antenna radiation pattern, receiver bandwidth, receiver noise figure, and diffraction losses).

Generally, the above statement is true, but in some cases the point inside the foreign country may get the higher interfering signal level than the point on the border. Such a situation is presented on figure 1.

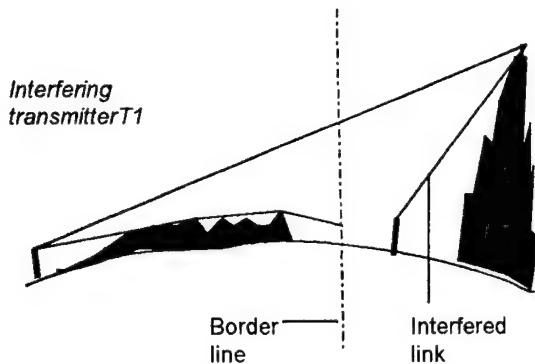


Fig. 1 Point inside the foreign country gets higher interfering signal level than the point on the borderline.

In order to avoid missing a necessary coordination it is proposed to perform additional calculations at "critical points" located on the tops of hills or mountains, where the interfering signal level reaches the local maximum.

3. POINTS FOR CALCULATIONS

The assessment of the need for international coordination is based on the results of calculations of the receiver input power produced by the given transmitter at a potential receiver or produced by a potential transmitter at the given receiver. Potential transmitters or receivers are located at the points where the expected interference level is the highest. These points are located on the borderline or on the tops of hills or mountains inside the foreign country.

3.1. Points on the borderline

There are two methods, which can be used for generation of the points on the borderline. The first method is recommended for administrations with not a long borderline. According to this method points are generated in advance and their data (geographical coordinates and terrain altitude a.s.l.) are stored in a special file. Taking into account a relatively narrow main beam of a microwave antenna points should be generated with the distant of 100 meters. There is a weak point of this method: the calculations will not be performed at the point on the direction of maximum antenna gain. In order to reduce that effect it is proposed to introduce the following correction to the off-axis angle θ :

$$\theta_{cal} = \max \{0, \theta - \theta_{corr}\}, \quad (1)$$

where θ_{cal} is the off-axis angle after correction and θ_{corr} is a correction value, which should be defined (e.g. = 1° or more).

In the second method points on the borderline are generated individually for every transmitter or receiver in the process of calculation. In the first step the point is searched where the main beam direction intersects the borderline. In the next steps the intersection is found for the directions which give the off-axis angles $\theta = 0.2^\circ, 0.4^\circ, 0.7^\circ, 1^\circ, 2^\circ, \dots, 180^\circ$.

3.2. Points on hills or mountains

The steps required to prepare the data file concerning calculation points located on hills or mountains ("critical points") are as follow:

Step 1: Preparation of the file

The file should contain the geographical coordinates, the terrain altitude above sea level and the identifier of the country. The data may be extracted from a suitable map or may be obtained by an exchange with the neighbouring administration. In this step the number of points may be as large as possible.

Step 2: Selection of the significant points

The number of points found in the first step can be considerably reduced selecting only these, which can produce situation presented in Fig. 1. The point is selected if there is any domestic point, which is in the line of sight with the point under selection and is not in the line of sight with the relevant point on the borderline.

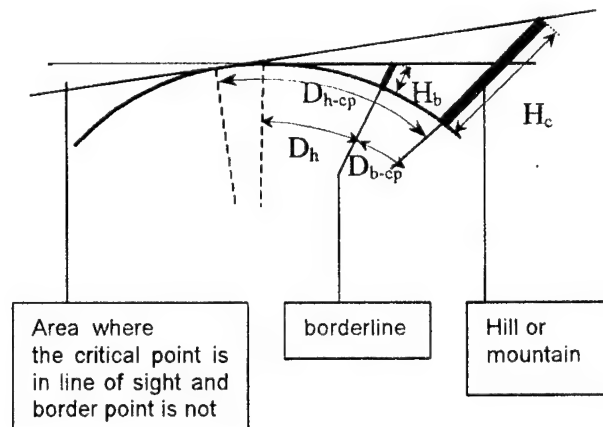


Fig. 2. Example of situation where a critical point is significant.

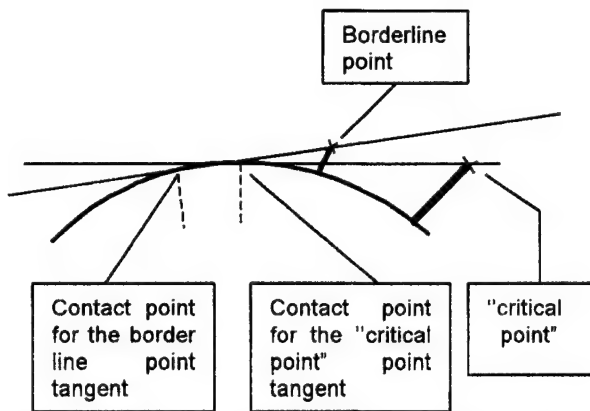


Fig. 3. Example of situation where a critical point is not significant.

Figs. 2 and 3 present situations where a "critical point" generated in step 1 is significant (Fig. 2) and is not (Fig. 3). It can be seen that the "critical point" is significant if the tangent to the smooth earth including the "critical point" is above the tangent including the border line point.

Instead of analysing the position of these two tangents, it is easier to consider mutually position of two contact points related to these lines. If the contact point related to the borderline point tangent is closer to the "critical point" than the contact point related to the "critical point" tangent (Fig. 2), then the "critical point" should be selected and stored in the data base. If not, the "critical point" found in step 1 should be cancelled. In other words the point is selected if the following relation is fulfilled:

$$D_{h-cp} > D_{h-b} + D_{cp-b}, \quad (2)$$

where:

D_{h-cp} = $4.12 \sqrt{H_{cp}}$ is a horizontal distance of the "critical point",

D_{h-b} = $4.12 \sqrt{H_b}$ is a horizontal distance of the point on the borderline,

H_{cp} - the height of the critical point [m a.s.l.],

H_b - the height of the border point [m a.s.l.],

D_{cp-b} - the distance between the "critical point" and the point on the borderline [km].

The above relation should be checked for every point created in step 1 taking into account points on the borderline generated according to the one method described in section 3.1. The height of the critical point and the height of the border point should be determined according section 3.3.

3.3. The height of calculation points

The height of the points where a potential transmitting or receiving antenna is located is

determined as a sum of the terrain altitude above the sea level and antenna mast height. The terrain altitude should be read from the digital terrain database. The antenna mast height is determined as follows:

for the terrain height < 300 m a.s.l. $H_{ant}=600$ m,

for the terrain height ≥ 300 m a.s.l. and < 600 m a.s.l. $H_{ant}+100$ m,

for the terrain height ≥ 600 m a.s.l. $H_{ant}=30$ m.

4. CALCULATIONS

In order to check, if the planned link requires an international coordination, the calculations should be performed to verify if the compatibility criteria are fulfilled. In the first step the calculations refers to the transmitter and it is assessed its compatibility with the potential receivers located in the calculation points (see section 3.). The "worst case" configuration (receiver antenna is pointed exactly to the transmitting antenna, receiver antenna gain is maximum and receiver bandwidth is minimal) is assumed. Because the value of the receiver antenna gain and receiver noise figure are not known they may be taken as a typical for the given range of frequency. If the transmitter is right, the next calculations are performed for the receiver (second step). Assuming that an interfering transmitter can be located at a calculation point and the "worst case" configuration (transmitter antenna is pointed exactly to the receiving antenna, radiated power is 85 dBm) the value of parameter for compatibility assessment is determined. If the transmitter can not produce harmful interference at a receiver located in a calculation point and the receiver can not get harmful interference from a transmitter located in a calculation point there is no need for international coordination. But if a calculation point is found where it is not fulfilled it is better to coordinate the link with the administration to which the point belongs.

If an administration have data of the radio systems installed abroad it is worth to assess expected results of coordination. With that aim the further calculations should be run for the transmitter and the value of parameter for compatibility assessment should be determined for every coordinated receiver located in the country pointed for coordination. If there are not incompatibilities identified the same calculations should be run for the receiver of the link. In the case when the receiver can tolerate arising interference the link may be sent for coordination and it probably will be successful. The negative answer on coordination request may only be got, if a previously coordinated foreign link is missed in the calculations.

In the case when the link is not compatible with a coordinated foreign link the coordination is superfluous because it will not be successful.

5. RESTRICTIONS

Presented method can be used for compatibility criteria relating to the single interfering signal. If administration is obliged to use the criteria relating to the aggregated interfering signals power it is necessary to establish criteria for individual interfering signal. The method can not be also used for compatibility criteria requiring the wanted signal level (e.g. C/I), because for a potential receiver this value is not known.

6. SUMMARISATION

It is not possible to carry out an efficient frequency management without reducing the number of unnecessary coordinations and with the database containing insignificant links. In order to avoid these difficulties the universal and secure method for the assessment of the need of an international coordination is presented. The method is universal because it takes into account various terrain configurations and various compatibility criteria. The method is secure because any necessary coordination or significant link will not be missed. At the same time the method is efficient as much as possible because real link parameters can be taken into account (transmitter power, antenna radiation pattern, diffraction losses, receiver noise figure). The

method can be applied by any administration because the choice of the method used is an internal matter of administrations.

BIOGRAPHICAL NOTES

Wiktor Sęga was graduated from the Technical University of Wrocław (Poland) in 1975, and then he joined the Institute of Telecommunications and Acoustics of this University. In 1979 he obtained a Ph.D. in telecommunications from the Technical University of Wrocław. Since 1979 he has been working in the National Institute of Telecommunications, Wrocław Branch. Dr W. Sęga is involved in preparation of engineering models and software for the computer-aided national spectrum management. He was responsible for elaboration of the digital terrain model for the territory of Poland. Since 1988 to 1989 he worked with Wireless Planning and Coordination Wing of the Ministry of Communications in India, as the UNDP/ITU expert. He is engaged in the ITU-R and CEPT studies. Dr W. Sęga is the Technical Program Coordinator of the International Symposium on EMC.

Wojciech Tyczyński received the M. Sc. degree in physics in 1989 from the Technical University of Wrocław, Poland. Since 1989 he is employed in the National Institute of Telecommunications dealing with compatibility assessment methods. His current research interests are in designing the frequency management system for microwave links. He is also involved in the work of the Temporary Working Group preparing Harmonised Calculation Method used by signatories of Vienna Agreement.

MONITORING OF THE RADIO-FREQUENCY SPECTRUM WITH A DIGITAL ANALYSIS SYSTEM

D. Boudreau*, M. Dufour*, J. Lodge*, D. Paskovich** and F. Patenaude*

*Communications Research Centre, Industry Canada,

PO Box 11490, Station H, 3701 Carling Ave., Ottawa, ON, K2H 8S2 -Canada

** Directorate of Automated Spectrum Monitoring

Industry Canada, 300 Slater Street, Ottawa, ON, K1A 0C8 - Canada

FAX (613) 990-7287, e-mail: paskovich.don@ic.gc.ca

A highly versatile Digital Analysis System (DAS) for spectrum monitoring applications has been developed by the Communications Research Centre of Industry Canada. The system is made from commercially available VXI-based hardware and can be used in both fixed and mobile spectrum monitoring stations. The software control of the equipment, coupled with the use of personal computer for digital signal processing, allows the DAS to be easily reconfigured to address the specific requirements imposed by the modern wideband and narrowband digital systems as well as those of non-digital transmissions. The DAS software measures technical parameters such as power, carrier frequency, S/N ratio, channel and band noise level, modulation type, modulation level, baud rate, signal bandwidth and performs high speed channel occupancy (>20,000 channels/s). The DAS also provides "instantaneous" Line Of Bearing (LOB) for transmitters in a 4.5 MHz band using the Butler matrix technique.

1. The Digital Analysis System

The hardware architecture of the Digital Analysis System (DAS) is briefly described, followed by a general discussion of the signal processing framework.

1.1 Hardware Architecture

The high-speed DAS is based on the hardware architecture shown in Figure 1. This architecture relies on commercially available equipment, using the VXI instrumentation bus. The VXI data bus is an excellent platform for high precision measurements required in the monitoring of high dynamic and frequency range communication signals. The current receiver can be tuned anywhere from 20 MHz to 3 GHz, and provides a RF conversion to the center of the band of a 20 MHz A/D sampling equipment. The conversion image rejection of this receiver is better than 95 dB.

The A/D converter operates at 20 Msamples/s, with a 23-bit amplitude resolution. It includes a digital LO, I/Q data outputs, 24 decimation filters, 64 Mbytes of FIFO memory and high speed local bus support. This equipment allows a wide dynamic range operation, with a free spurious level better than -110 dB. The instantaneous bandwidth, including the receiver conversion chain, is greater than 5.0 MHz (from 2.5 MHz to 8.0 MHz). The 64 Mbyte internal FIFO memory allows the continuous bulk storage of data record for more than one second, even at a sampling rate of 20 MHz. The unit can also operate at different sampling rates, using the external LO input.

The output of the A/D is directed to a personal computer, where digital signal processing (no DSP chips are employed) as well as data analysis and storage are done. The data transfer is done through a VXI instrumentation bus and a VXI controller. The personal computer controls the whole set of equipment, through the VXI controller. The PC also controls one or more drop-down receivers for narrowband processing.

1.2 Signal Processing Framework

Figure 2 illustrates the signal processing architecture of the DAS. The sampled composite signal $s(k)$ undergoes a transformation to enhance the features of interest. Spectral processing is accomplished through a bank of bandpass filters implemented using FFT processing.

In the next stage, the multichannel composite input signal (wideband) that has been transformed in the frequency domain, undergoes a detection stage establishing the channel occupancy. In this wideband setting, it is desirable that the method by which the detection is accomplished uses a constant false alarm rate (CFAR) detection scheme. Adaptive thresholding is also important, and is provided by computing the noise floor level, from a number of subbands of the composite signal.

The information about the channel occupancy, and the results of further analysis on the occupied channels, is stored in a compressed file format. More information is obtained about specific channels by zooming on narrowband portions of the band of interest, or by going to a drop-down receiver.

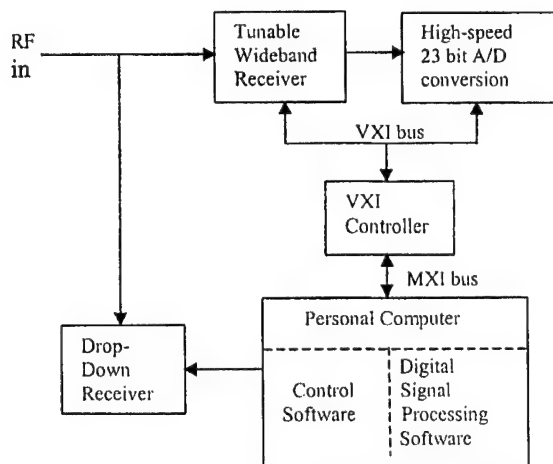


Figure 1: Hardware architecture

2. Specific High-Speed Analysis with the DAS

The current Digital Analysis System capabilities include:

- the control of the VXI equipment with a modular and versatile software architecture, based on object-oriented programming techniques,
- an FFT-based filter bank, transforming the composite signal in the frequency domain,
- noise floor level estimation and CFAR detection of the occupied channels,
- analysis and compression of the occupied channels parameters,
- multichannel direction finding
- modulation recognition
- signal parameter estimation

2.1 Control Software

The DAS is controlled through object-oriented code, which interfaces with the VXI equipment, and allows modularity and versatility. This structure is based on a three-tier implementation. Each piece of equipment, and each function performed by the DAS, is implemented as

a software object, with its own characteristics. The software architecture is shown in Figure 3.

2.2 Filter Bank Processing [1]

A versatile trigger-stop function, for signal acquisition, has been implemented. The sampled signal is presented to the transform stage. The frequency domain signal transform is implemented with a choice of two configurations: a conventional window-based FFT implementation and a more versatile polyphase FFT implementation. The windows or filter impulse responses currently available are Blackman, Hanning, flat-top and rectangular. More windows can easily be added. Based on the output of this filter bank, standard spectrum analyzer functions are available, such as power and frequency marker, trace averaging, etc.

2.3 Noise Level Estimation and CFAR Detection [1]

The constant false alarm rate (CFAR) detection of the active channels, at the output of the frequency domain transform, is performed by using information about the noise floor level. The noise floor level is estimated over a single channel, or over a multichannel frequency band, using second-order statistics computed on the input signal. The CFAR thresholds are adjusted with this information.

2.4 Analysis and Compression of the Occupied Channels Parameters

The compression of the observed data is accomplished by recording the channel power levels, at the output of the filter bank, for periodic time intervals. The power level is quantized and stored with steps of one dB. This provides a picture of the channel occupancy as a function of time. Further analysis capabilities are available, such as the computation of the level crossing rate for a given channel, the cumulative density function of the power levels, and the center frequency of a given channel [2].

2.5 Multichannel Direction Finding

Two parallel receivers are used for multichannel direction finding. The outputs of these two synchronized receivers are processed by two parallel filter banks, and the angle of arrival is computed on the occupied channels only. The result is a vector of angles that can be further processed or archived for statistical purposes. This Butler Matrix technique allows "instantaneous" direction finding on all the occupied channels present in the receiver bandwidth.

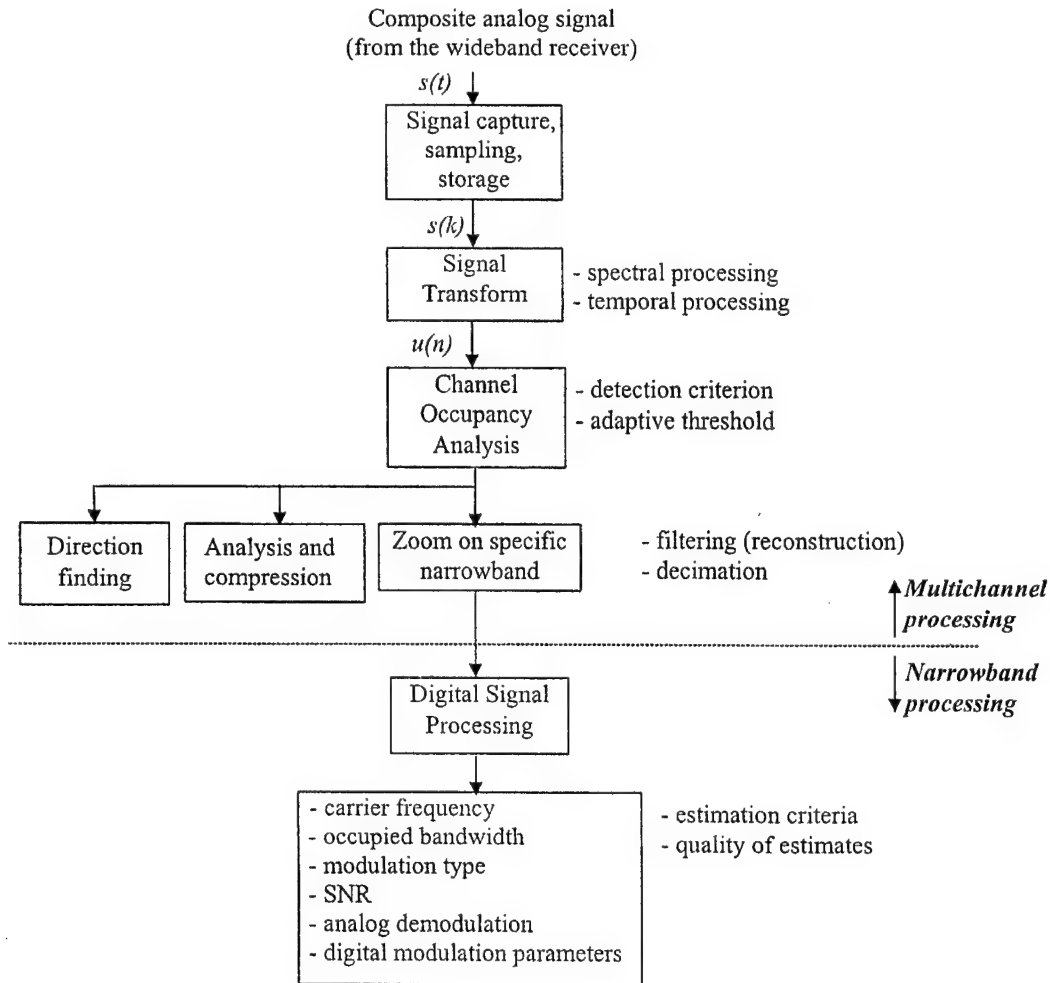


Figure 2: Flow graph of the general framework

2.6 Narrowband Signal Processing

Further analysis is performed on the individual occupied channels, either by dwelling for a short period of time (typically 100 msec) on each occupied channel or by continuously monitoring a single channel. The information that is obtained for every individual channel is the modulation type (within a predetermined set of formats) [3], the carrier frequency, the occupied bandwidth, the narrowband SNR and some modulation parameters, such as the frequency deviation for FM signals, or the number of modulating levels for digital modulated signals.

3. DAS Capabilities

In its current implementation, the DAS is capable of the following performance:

- scanning speed greater than 20,000 channels/s;
 - 1.25 kHz resolution
 - 8.75 kHz channels bandwidth
 - 7 bin points per channels
- sweeping rate greater than 0.5 GHz/s;
 - 7.5 kHz resolution

The occupancy channel speed is currently limited by the data transfer rate between the VXI bus and the PCI bus. As higher data transfer rates are achieved, and as personal computers become more powerful, the receiver settling time will be the ultimate factor determining the DAS scanning speed. This quantity is estimated to be on the order of 60,000 channels/s for the current receiver 5 msec settling time.

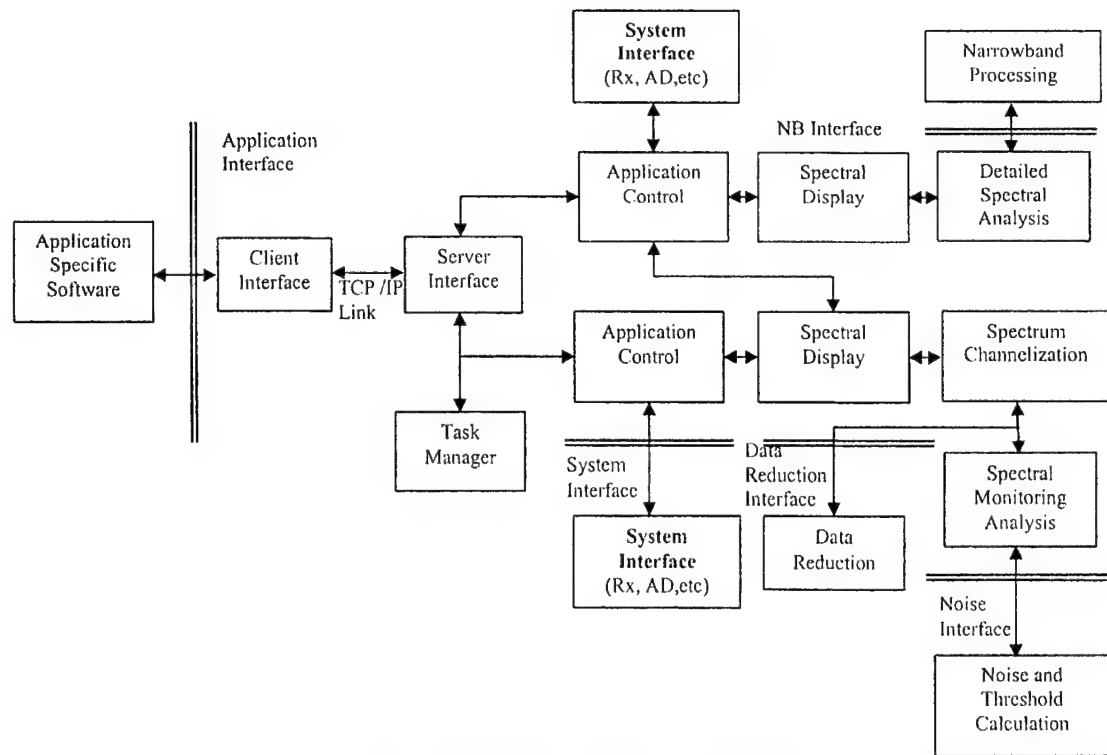


Figure 3: Software architecture and interface

4. DAS Applications and Extensions

The core capabilities of the Digital Analysis System have been included in a few specific applications. In particular, the DAS has been used to build:

- an application for monitoring terrestrial wireless communications, in the spectrum observation centres of the Canadian Government:
 - high speed occupancy measurements of channelized frequency bands, along with the compression and data base storage of the information - currently such measurements are being done in the major Canadian urban centres, to re-allocate spectrum for the introduction of digital services
 - channelization of signals that do not conform to frequency allotment plans - this feature allows the rapid surveying of the radio spectrum to determine if there are any transmissions that do not conform to allocation plans
- an application for satellite carrier monitoring:
 - graphical user interface with the DAS, displaying the status of satellite carrier power and frequency, and setting off alarms in case of misuse
- a specific application for monitoring CDMA signal frequency bands:
 - specialized noise measurement capabilities, allowing the detection of narrowband interferers exceeding the average CDMA signal power - it is also possible to correlate the effect of system occupancy to the "noise level" of the CDMA band
- a generic Spectrum Analyser
- Radio direction finding
 - the DAS has been used in field trials for direction finding of frequency agile (hopping) radios - future plans are to expand the direct finding capability for TDMA and CDMA transmissions
- Internet-controlled applications:
 - remote control of any of the above application; as well as the network transfer of the monitored signals for usage on remote workstations.

5. Conclusions

The Communications Research Centre of Industry Canada has demonstrated the capabilities of a highly efficient Digital Analysis System for spectrum monitoring applications. The use of commercially

available VXI-based hardware offers cheaper and more extensive solutions to the spectrum monitoring problems, than what is currently offered in most conventional monitoring stations. The "open" hardware and object oriented software implementation makes it very flexible, in terms of upgrades and modifications to address specific requirements imposed by the modern wideband and narrowband digital systems and non-digital transmissions.

References

1. F. Patenaude, D. Boudreau and R. Inkol, "CFAR detection based on windowed and polyphase FFT filter banks for channel occupancy measurements," 19th Biennial Symposium on Communications, Queen's University at Kingston, Canada, May 31-June 2, 1998, pp. 339-343.
2. D. Boudreau and F. Patenaude, "Multi-channel carrier frequency estimation using discrete Fourier transform pre-processing," 19th Biennial Symposium on Communications, Kingston, May 31-June 2, 1998, pp. 367-371.
3. C. Dubuc, D. Boudreau, F. Patenaude and R. Inkol, "An automatic modulation recognition algorithm for spectrum monitoring applications," Proceedings of the 1999 IEEE International Communications Conference, Vancouver, June 1999.

BIOGRAPHICAL NOTES

Daniel Boudreau is a research scientist in the Satellite Communications Branch of the Communications Research Centre, Ottawa, Canada. He obtained a PhD in electrical engineering from McGill University, in 1990. He has worked and performed research in the areas of modulation and modem design for mobile satellite communications, adaptive filtering for fading channels and joint source and channel coding. His current interests include speech and video coding for mobile communications, automatic modulation recognition for spectrum monitoring and advanced demodulation and detection techniques for fading channels.

Martial Dufour is a communications Software and RF engineer with 20 years of experience working in the satellite communication branch at CRC, in the area of communication signal processing. Recently he has worked on the design of advanced digital spectrum monitoring systems, aeronautical terminals, software and hardware design for satellite monitoring systems, satellite antenna tracking system and on a new magnetic compass calibration method. Many of his work accomplishments have been successfully licensed for commercial use.

John Lodge received the B.Sc. and Ph.D. degrees in electrical engineering from Queen's University in 1977 and 1981, respectively. From September 1981 to April 1984, he was with Miller Communications Systems Ltd., Kanata, Ontario. He joined the Communications Research Centre in May 1984, where he is currently the Research Manager of Communications Signal Processing.

Don Paskovich has worked since 1978 for the Directorate of Automated Spectrum Management that is responsible for the development and implementation of automated radio monitoring system for the spectrum management activities of the Canadian government.

François Patenaude received his Ph.D. degree in electrical engineering from the University of Ottawa, Canada, in 1996. In 1995, he joined CRC to work on spectrum monitoring and signal processing applications for digital communication over mobile channels. His main research interests comprise statistical subspace signal processing, real-time signal processing, and modulation & coding.

ACCURACY ANALYSIS OF THE HF TRANSMITTER LOCATION PROCEDURE BY THE SINGLE STATION LOCATION (SSL) METHOD

Viktor KOGAN*, Nikolai LOGINOV**,
Alexander PAVLIOUK[^], Vladimir ZAGOSKIN**

*NIIRDAR, 12/11, Buhvostova
str., 107258, Moscow, Russia
Tel.: + 7095 963-50-42
Fax: + 7 095 261-52-68,
E-m.: rezonans@mtu-net.ru

**GOSSVAZNADZOR of the RF, 6,
2nd Spasonalivkovsky per., 117909,
Moscow, Russia
Tel. +7095 238-74-02
Fax +7095 238-51-02
E-m.: gccds100@din.ru

[^] NIIR, 16, Kazakova str.,
103064, Moscow, Russia
Tel. + 7095 261-18-41
Fax: + 7 095 261-52-68,
E-m.: pavliouk@hotmail.com

The problems arising with the application of the Single Station Location (SSL) method for determination of an HF transmitter geographical position are considered. Issues on choosing different ionospheric propagation prediction models for SSL software applications are discussed. The estimations of location errors are given in functions of inaccuracies in ionospheric parameter determination along a propagation path. Despite of a number of not fully solved problems, it is possible to recommend active introduction of the SSL method in newly installed and modernized HF direction-finders (DFs) so the further improvements were reduced only to updating of a DF software.

1. INTRODUCTION

In HF frequency band the geographical position of a transmitter can be determined not only by traditional triangulation method. In this frequency band there is an unique opportunity to determine the position by only one DF and that is inaccessible within other frequency bands. Such determination is carried out by simultaneous measurement of the azimuth and elevation angle of the signal reflected by the ionosphere and received by the antenna array. This method has received the name "Single Station Location" (SSL) one [1]. The SSL concept thus allows performing the location mission when, for geographical, timing, and availability reasons, a complete triangulation DF location system could not be installed. SSL may also be considered as a compliment to an existing location system, by permitting suppression of aberrant bearings.

Principally, the SSL location process is a quite obvious one. After measurement of the elevation angle of the received signal, the trajectory of a beam on the measured frequency is calculated using appropriate

ionospheric propagation model (IPM). The distance by the ground for this beam and relevant azimuth provide required location. However, the practical implementation of this simple concept meets some difficulties associated with the necessity to ensure acceptable accuracy. These difficulties consist in the adequate modeling of the ionosphere properties along the propagation path and in correct interpretation of elevation angle measurement results. Analysis of these factors is the subject of the paper.

2. MODEL AND PARAMETERS OF THE IONOSPHERE

Despite of significant number of available sophisticated IPMs [2], their use for SSL application does not result in considerable success because they estimate only average parameters of the ionosphere. However, current parameters of the ionosphere, which are much more important for SSL application, may deviate from average values up to 15 - 20% even for non-disturbed ionosphere conditions. Thus, increasing of a model complexity does not provide increasing of accuracy above some specified value. Therefore it is more practical to use simplified models, which can be more easily adjusted in accordance with data of current measurements.

The best way of current ionosphere diagnostics along the propagation path is the application of oblique sounding ionosondes, which can provide separation of modes and measurement of their propagation times. However, use of such ionosondes results in pollution of the radio spectrum and requires significant investments for creation and maintenance of the ionosonde network. As means of adjustment, the data of the short-term forecasting of ionospheric propagation conditions can

be used under condition of their availability through relevant national services.

It seems more convenient to use local means of ionosphere diagnostics, belonging to monitoring stations. It concerns ionosondes of vertical sounding, whose negative influence on the radio spectrum pollution is not so great, as for oblique sounding. The results of vertical sounding are applied to the whole path by introduction of corrective coefficients to a mean statistical model.

Cheapest, but the most difficult (from data processing point of view) way of current IPM adjustment is adaptation of measurements results in relation to known transmitter emissions in the direction of measured bearings i.e. use of known test transmitters serving as beacons. The determination of elevation angle of signal radiated by the known beacon under conditions of known distance to it allows, principally, to adjust used IPM based on these measurement data (i.e. by solving an inverse task of the propagation). After such adjustment the model can be used for location of unknown HF transmitters. With the presence of several beacons, there is a task to minimize of a residual error of model adjustment in accordance with a redundant volume of the data. The same problem arises with reception of several modes from one beacon. Let's notice, that the reception of signals from beacons can be also used for correction of an azimuth error due to deviation of a beam azimuth.

The next task requiring appropriate decision is the measurement of elevation angles of a radio wave in a vertical plane and interpretation of measurement results. A mistake in conjunction of the exact elevation angle to one of possible propagation modes can result in essential error in location, especially in the case of the remote stations, propagation from which can occur by several hops. At the present stage of techniques the location with acceptable accuracy is carried out within the limits of one propagation hop, i.e. on distances up to 2000 - 2500 kms [1]. It is clear, that in the case of more accurate elevation angle measurements made and of more mode resolution provided, more precise interpretation of results can be achieved. The most difficult task is the separation of ordinary and extraordinary waves reflected from the same layer. A physical basis of such separation is simultaneous reception and processing of two orthogonal polarizations of the received signal.

These issues should be taken into account under designing of particular DF, following relevant technical specifications, restrictions on cost of DF development and maintenance, and also depending on availability of the short-term forecasts of ionospheric parameters. Thus, achievable technical accuracy of the DF should be correlated with an expected methodical error of location for optimization of the system by the efficiency - cost criterion.

3. ESTIMATION OF THE SSL METOD ACCURACY

Estimations of possible location error values depending on errors in determination of ionosphere parameters are presented below for an orientation. In providing relevant calculations any reasonable IPM can be used. For example, HF propagation model of Recommendation ITU-R P.533-5 [3] or other similar one can be applied. However, for such estimations it is quite sufficient to choose simpler models. Very convenient seems to be the IPM in a form of spherical laminated layer with quasi-parabolic distribution of ionization on height [4]:

$$N(h) = \begin{cases} N_m \cdot \left[1 - \left(\frac{h - h_0}{y_0} \right)^2 \right] & (h_0 - y_0) \leq h \leq (h_0 + y_0) \\ 0 & h < (h_0 - y_0), h > (h_0 + y_0) \end{cases} \quad (1)$$

where:

$N(h)$ - electronic density distribution throughout of a layer height h above the surface of the Earth,

$N_m(h_0)$ - electronic density maximum (EDM) at the height h_0 ,

h_0 - EDM height of the layer,

y_0 - a half-width of the layer.

An advantage of such model is the feature that an integral describing dependence of a hop-length along the ground surface (i.e. required distance to the transmitter R) in function on an elevation angle has the analytical solution in elementary functions in dependence only on three parameters: plasma frequency (PM) at a layer EDM (f_oF), height of the layer EDM above the ground surface (h_0), and a half-thickness of the layer (y_0). The possibility of such analytical solving is provided due to this specific profile of electronic density along the height of the layer, but such kind of the profile almost not differs from a usually accepted parabolic one.

Omitting presentation of further formula derivations, which are rather lengthy and complicated, let us discuss only results of calculations in accordance with general formula (1). For determinacy, the case of the "night" ionosphere with the height of the EDM equals 350 kms and half-width of the layer equals 150 kms is considered.

Dependence of a distance to the transmitter (R) on elevation angle at the ground level (γ) for the case of isotropic ionosphere and for several operating frequencies (f) is presented at Figure 1. The values of operating frequency f at that and subsequent figures are normalized to a PM f_oF at the layer EDM. The point of a minimal distance to the transmitter corresponds to the border of a "dead zone". To the left from this point (at smaller angles) the propagation is provided by "lower"

beams, to the right from this point the propagation is provided by "upper" beams.

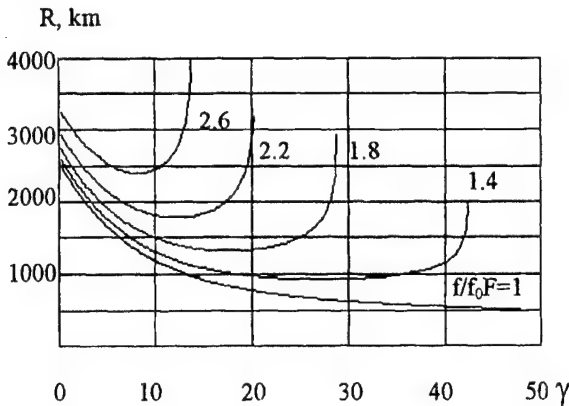


Fig. 1. Dependence of a propagation distance on an elevation angle

As we see, even for the elementary case of single-mode propagation, there are two possible values of elevation angles for one value of distances. This difficulty is partially removed by the fact that for upper beams attenuations at propagation paths considerably exceeds attenuations for lower beams. It is clearly seen from Fig. 2 where dependence of the attenuation on the elevation angle is presented. The attenuation W at Fig. 2 is determined only by divergence of a beam tube of a propagating wave. At Fig. 2 and the next ones point of a minimal distance for each curve is indicated by dot at the axis of abscissae. It is important for SSL method application, that the upper beams (to the right from minimal distance points at Fig. 2) obtain higher attenuation as contrasted to the lower beams (to the left from minimal distance points at Fig. 2). It means, that during observation by a measuring device two groups of elevation angle readings related to lower and upper beams, the readings for lower beams will have larger levels and will be more stable, i.e. they will dominate.

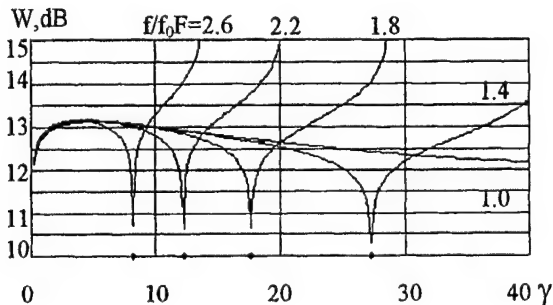


Fig. 2. Dependence of attenuation on elevation angle

Errors in determination of distances to transmitters, which depend on inaccuracy in determination of ionospheric parameters and on errors in elevation angle

measurements, in accordance with the theory of measurements, can be expressed by partial derivatives on relevant parameters. As a parameter under consideration we shall consider estimated distance to a transmitter (R), which is a function of many variables, namely elevation angle (γ), PM (f_0F), height of the layer EDM (h_0) and a half-width of a layer (y_0), i.e.

$$R = R(\gamma, f_0F, h_0, y_0).$$

Thus, absolute values of partial errors in determination of R in dependence on errors of each variable can be expressed as:

$$R'_\gamma = \frac{\partial R}{\partial \gamma} \text{ km/degree}; \quad R'_f = \frac{\partial R}{\partial f_0F} \text{ km/MHz},$$

$$R'_h = \frac{\partial R}{\partial h} \text{ km/km}; \quad R'_y = \frac{\partial R}{\partial y} \text{ km/km}.$$

Relative errors in determination of distances in linear approximation can be determined as:

$$\Delta_\gamma = 100R'_\gamma / R; \quad \Delta_f = 100R'_f / R;$$

$$\Delta_h = 100 \times 10 \times R'_h / R; \quad \Delta_y = 100 \times 10 \times R'_y / R.$$

Based on these formulas relevant errors in determination of distances were calculated for IPM given by formula (1) under different values of a beam elevation angle up to $\gamma = 30^\circ$. The results of calculations are presented at Fig. 3 – 6 below.

Fig. 3 gives errors in determination of distances due to inaccuracy of elevation angle measurements taken as $\partial \gamma = 1^\circ$ for different values of the elevation angle. Under such conditions, for lower beams this relative error of distance measurements does not exceed 8% for lowest values of γ and steadily decreases with increasing of γ up to zero at the minimal distance point. However, under $\partial \gamma = 2^\circ$ this relative error doubles and already obtains significant value.

Fig. 4 gives errors in determination of distances due to inaccuracy of PM estimation at the layer EDM taken as $\partial f_0F = 1 \text{ MHz}$ for different elevation angles. Under such conditions, for lower beams this relative error of distance measurements continuously increases from about 5% at lowest values of γ up to 30% at γ values in the vicinity of the minimal distance point. To provide distance measurements with accuracy not exceeding 10% within this range of γ values, the error in estimation of f_0F should not exceed about 300 kHz.

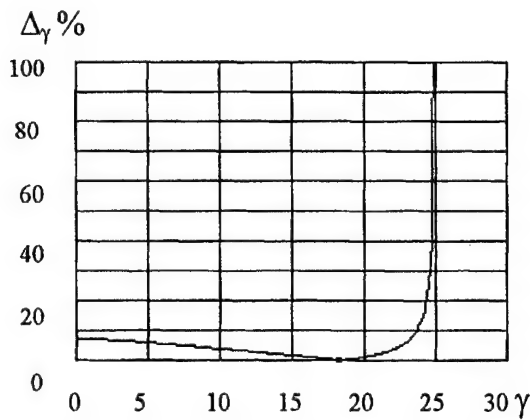


Fig. 3. Relative errors of distance determination in function on error of elevation angle estimation

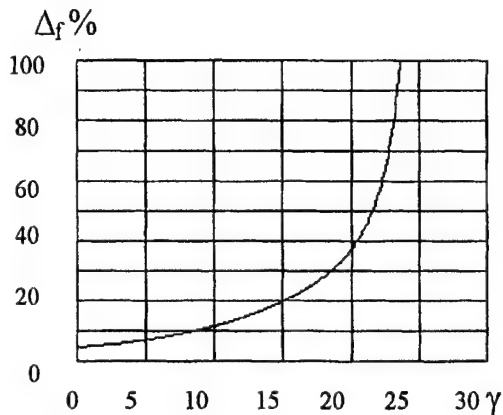


Fig. 4. Relative errors of distance determination in function on error in PM estimation

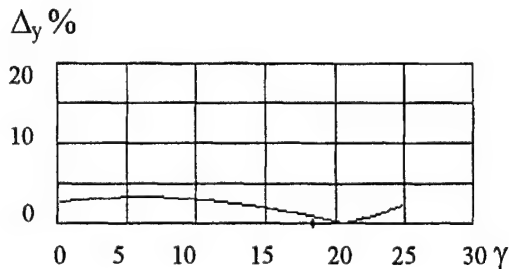


Fig. 5. Relative errors of distance determination in function on error in the layer half-width estimation

Fig. 5 gives errors in determination of distances due to inaccuracy of a layer half-width estimation taken as $\partial h = 10$ km for different elevation angles. Under such conditions, for lower beams this relative error of distance measurements does not exceed 4 - 5% having minimum up to zero at γ values slightly higher than corresponding to the minimal distance point.

Fig. 6 gives errors in determination of distances due to inaccuracy in estimation of a layer EDM height above the ground surface taken as $\partial y = 10$ km for different elevation angles.

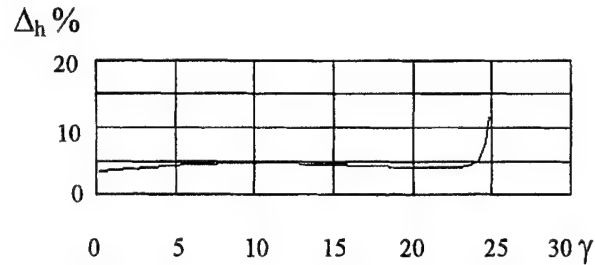


Fig. 6. Relative errors of distance determination in function on error in the layer EDM height estimation

Under such conditions, for lower beams this relative error of distance measurements is a rather stable one and does not exceed 5%.

As we see, the main errors of distance determination are due to errors in measurements of elevation angles (including an error of determination of the mode structure) and in estimation of PM of the layer at its EDM.

The existence of signal fluctuations does not allow obtaining reliable estimations on a single measurement. The mode structure of an observed signal can vary in time due to fading of separate modes. For reduction of errors in determination of a signal mode structure it is necessary to provide accumulation of measurement data. This accumulation should be fulfilled during time periods, which considerably exceeds correlation intervals of fast fluctuations (i.e. on intervals about one minute and more). At the same time there is no sense to accumulate several readings inside the correlation interval. In this connection, it is expedient to provide accumulation in a scanning regime of equipment operation throughout monitored frequency band, returning time to time to the same emissions under considerations.

Despite of significant number of problems peculiar to the SSL method, which have not been solved yet, it is expedient to provide technical possibilities of this method implementation in newly developed DFs and accordingly upgrade those that are in operation. These measures should provide possibility of DFs upgrading only through software improvements.

Increasing of the ionospheric condition interpretation quality is achieved by accumulation of experience on SSL DFs operation and by analysis of the results. Increasing of a DF base and application of recent signal processing technologies can provide enhancing of elevation angle measurement resolution under conditions of large ratios of a signal to interference. Activi-

ties in this direction are continued (see, for example, [5]).

Additional possibilities, which are provided by the SSL method, are already taken into account under modernization of the radio-monitoring network of the Russian Federation [6].

4. CONCLUSIONS

The SSL method provides determination of a transmitter geographical position in HF frequency band by measurements from only one radio monitoring station in a circular sector. It is much cheaper and organizationally easier than location by traditional triangulation method. In a number of cases, when there is no place for installation of the second and third DF with appropriate territory separation of measuring antennas, the SSL method provides the only one practical solution of the problem.

The method demands of high-resolution elevation angle measurement facilities, means for simultaneous receiving of both signal polarizations and means for IPM adjustment based on results of current measurements and relevant software for beam calculations. The main errors of distance determination are caused by inaccuracies in measurement of elevation angles, in identification of the mode composition and in estimation of PM of a layer at its EDM.

The SSL method requires further elaboration, as concerning elevation angle measurement procedure and identification of the mode composition, as well as concerning IPM adjustment based on results of current measurements. These corrections can be made on a basis of propagation information from known transmitters used as beacons or on a basis of data on short-term forecasting of ionospheric propagation conditions provided by relevant national services.

It seems possible to recommend the SSL method implementation in newly developed DFs and accordingly upgrade those that are in the operation. It would be very beneficial to combine operation of HF DFs in SSL and ordinary triangulation regimes for increasing overall efficiency of radio monitoring in this frequency band.

5. REFERENCES

- 5.1. ITU. Spectrum Monitoring Handbook. 1995.
- 5.2. J.M. Goodman. HF Communications Science and Technology. N.Y. VNR. 1992.
- 5.3. ITU-R Recommendations Series P, Geneva, 1995. Recommendation ITU-R P.533-5. HF Propagation Prediction Method.

- 5.4. T.A. Croft, H. Hoogasian. Exact Ray Calculation in a Quasi-Parabolic Ionosphere with no Magnetic Field. Radio Science vol.3, N^o1, January, 1968, pp. 69-74.
- 5.5. Young-Soo Kim, Young-Su Kim. Improved Resolution Capability via Virtual Expansion of Array. Electronics Letters., v35, N^o 19, 1999, pp. 1596-1597.
- 5.6. N.A. Loginov, A.P. Pavliouk. Approach to the automation of the spectrum management system of the Russian Federation (in Russian). Trydy NIIR, 1998, pp.5 – 13.

BIOGRAPHICAL NOTES

Dr. Victor KOGAN – Chief of a laboratory of the Research and Development Institute of Long-Range Radio Communications (NIIDAR), Moscow, Russia. He is an expert in HF propagation and radio communication studies as well as in computer radio communication modeling. About 30 articles and papers published.

Dr. Nikolai LOGINOV – Head of the General State Supervisory Department for Communications of the Russia (GOSSVIAZNADZOR). He is an expert in spectrum management, radio communications and telecommunication economics. Leader of activities on the modernization of the Russian national radio monitoring network. About 50 articles and papers published.

Dr. Alexandre PAVLIOUK – Leading scientist of the Radio Research and Development Institute (NIIR), Moscow, Russia. He is an expert in radio measurements, spectrum management and radio communications. Vice-Chairman of the ITU-R Study Group 1 and a Chairman its Working Party 1B. About 150 articles and papers published.

Vladimir ZAGOSKIN - head of the Radio Monitoring Section of the General State Supervisory Department for Communications of the Russia (GOSSVIAZNADZOR). He is an expert in radio monitoring, spectrum management and radio communications. Executive manager of the modernization of the Russian national radio monitoring network. About 15 articles and papers published.

INTERFEROMETRIC SYSTEM DIRECTION FINDING IMPROVEMENTS ON CIRCULARLY-DISPOSED WIDE-APERTURE DIRECTION FINDING SYSTEM ACCURACY

William A. Luther

Federal Communications Commission, Washington, D.C. 20554

Phone: 202-418-0729; Fax: 202-418-7270; E-mail: wluther@fcc.gov

A modern, interferometric (linear) design direction finder network is shown to be significantly improved over a Wullenweber design (circularly-disposed) direction finder network. The newer technology gives not only faster and more accurate results, but is significantly less expensive to implement. Reliability of the newer, electronic technology is better while maintenance of an interferometric system is much easier. An investigation of the relative accuracy between the two types of systems is conducted and presented. A United States patent has been issued for the new interferometric design. [1.]

1. INTRODUCTION

U.S. government engineers have recently invented a new type of LF/MF/HF interferometer direction finding antenna array and digital signal processing system that allows establishing more accurate transmitter "fixes" throughout the world and subsequent use for appropriate EMC measures. This new interferometric system uses a number of special techniques based both on a unique, minimum-element and minimum-cost array for the desired frequency range, and on simultaneous digital signal processing in a phase-matched receiving system having a separate channel for each antenna element. No equivalent interferometric system is known. A United States patent for the new array and digital processing system has been issued. [1.] The system and network were recently implemented successfully by the U.S. Federal Communications Commission over an eighteen-month period.

The new interferometric direction finder (Type I) replaced on a one-for-one basis, in the identical locations, the Wullenweber (Type W) direction finder. This study examines the results of the new interferometer and compares them directly with results documented and published previously for the Wullenweber [2.].

2. DIRECTION FINDER NETWORK

The new network, comprising fourteen, interconnected, widely-dispersed locations throughout the United States, including in Alaska, Hawaii, and Puerto Rico, was installed at the identical locations where the previously installed, wide-aperture Wullenweber (Type W) direction finder - - which used mechanical, capacitively-coupled goniometers, and which were operating continuously from the early 1960's - - was sited. The new network is completely remote-controlled via telephone lines from one operations center near Washington, D.C. Data from radio frequency signals and digitally processed results have been taken from the new interferometric network to document its performance for this paper, and to allow comparison at the 15th International Wroclaw EMC Conference with results of the best of older (Type W) systems.

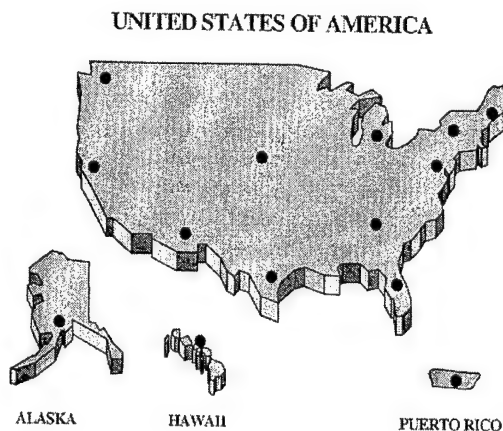


Fig. 1. Direction finding network operated by the Federal Communications Commission of the United States of America

3. ADVANCED INTERFEROMETRY

Advanced interferometry can have a number of advantages over previous technology. With a phase-matched channelized receiver for each antenna element, all antennas in an interferometric array may be monitored simultaneously rather than sampling from one or two at a time. This gives a better, overall understanding of the received signal while allowing direction finding on signals of shorter interval. A completely electronic system such as this new invention has no moving parts (goniometer or commutator), eliminating mechanical complexity, reducing costs, and reducing fabrication and maintenance times, while increasing reliability. The application of digital signal processing removes the burden of manually determining a bearing while reducing both personnel requirements and human errors. A digital, automatic system can be installed in remote locations because today it can send bearing and other information over alternative means of transmission (e.g., where there is access to a telephone, fixed-wireless, or satellite circuit) to a central location. An interferometer can more easily apply a long base line to average out the anomalies normally found in propagation of radio waves, such as multipath or fading. The baseline of an interferometer can be significantly longer, and therefore offer improved performance over a typical baseline of a circularly-disposed, wide-aperture array. Finally, because digital signal processing is used, many modern algorithms (including those yet undevised) can be applied to process data, either at the remote location or at a central processor, providing a broader functionality to the ultimate user. Other functions could include frequency measurement and transmitter characterization ("fingerprinting").

4. INTERFEROMETER DESCRIPTION

The FCC Type I is comprised of eleven active antenna elements, each connected to one channel of an eleven-channel receiver. The antenna elements, vertically polarized with two-meter physical height, are placed in two, suitably-arranged linear arrays, forming a "V," that also can be taken as five similar, equilateral triangles having a common apex. In each linear arm, spacing of the elements from the apex or reference element is 4, 12, 36, 108, and 324 meters, respectively. This spacing provides an extensive baseline for lower frequency applications. The highest frequency of operation of the Type I, determined by the spacing (4 meters) of the elements closest to the apex, is near 40 MHz. This cutoff frequency, determined primarily by the distance between the closest

elements, is also a secondary function of the precision of position in space of the two array arms, and the diameter of the vertical elements. The Type I antenna system has no theoretical lowest frequency of operation, as the 324-meter spacing just becomes progressively smaller compared to the signal wavelength captured, with resulting 6 dB/octave decreasing sensitivity. It is, in fact, the installed RF amplifier characteristics which have the greatest effect on the frequency response of the new system. A description of the interferometric network may be found [3].

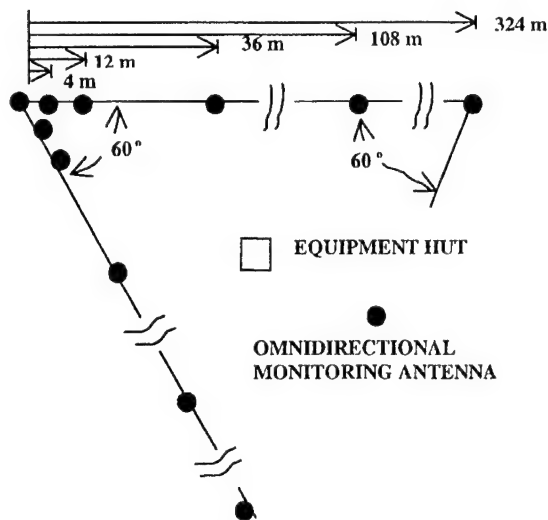


Fig. 2. Plan view of the interferometric direction finder system

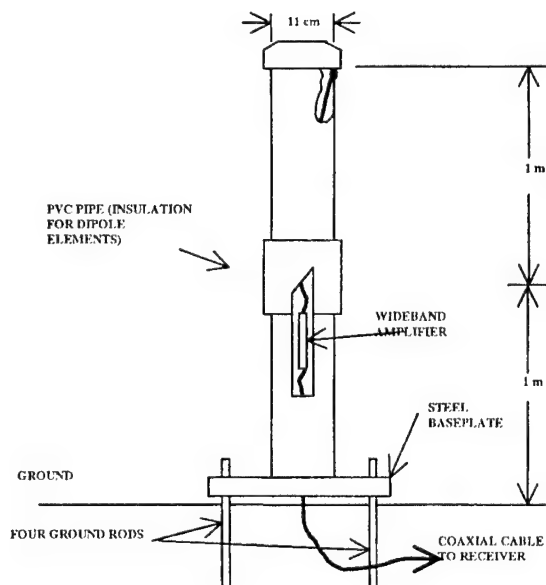


Fig. 3. Interferometer antenna pictorial drawing

5. ERRORS

5.1 Instrument and site errors

Instrument errors can be made small by the design of the DF system. A frequency standard provides accuracy for the RF mixing operations, defines sample increments for the analog to digital conversion process, and allows absolute synchronization of the bearing observations, not only among the various channels of the multi-channel system, but also among multiple DF sites. Calibration processes for the connecting cables, active buffer amplifiers, and preselection filters assure phase match between receiver channels. The use of digital signal processing steps in the intermediate signal processing stages of the receiver guarantees stability in the most troublesome portion of the receiver circuitry [4].

5.2 Lateral deviation errors

These errors are due to random variations in the composition of the ionosphere which ultimately cause the point of reflection of the radio wave to depart from the great circle azimuth between the DF location and the transmitter. A good method of dealing effectively with these errors is to average observations over time. Variations may be leveled by providing, as in this system for example, up to 1024 bearings per second, and remaining on-task for as many minutes as desired.

5.3 Wave polarization and interference errors

These errors arise as a consequence of multipath

propagation, causing the instantaneous polarity of the wavefront to vary, or be distorted, due to the presence of multiple signal sources within the received bandwidth. The DF system can discriminate against polarization changes by responding only to the vertically polarized component of the wavefront. This is accomplished by having the short vertical monopoles accurately erected, and then decoupling the RF cable from any horizontal component of signal which might be induced. Distortion of the wavefront is identified by conducting an analysis of the phases measured across the sampled space. The phases of each adjacent element are referred to the apex element. When the possible phase measurement exceeds 2π radians, the phase measurements are linearly extrapolated, based on the previous element measurement multiplied by a factor of three representing the expansion of the baseline. If the estimated phase can be matched by adding multiple 2π increments, then that value becomes the new absolute phase measurement for that array element. Eventually, the phase of each element in each leg of the array is known. If an undistorted wavefront is being measured, the variance of the data along the array should have a low deviation from the linear extrapolation. Another test may be carried out based on the measured amplitude from the array element. If this amplitude falls below that required to provide adequate phase resolution on a particular channel, the extrapolation process is invalidated and the dataset is rejected. These two data tests can be used to reject many of the bearings which are not valid and which would otherwise clutter the results.

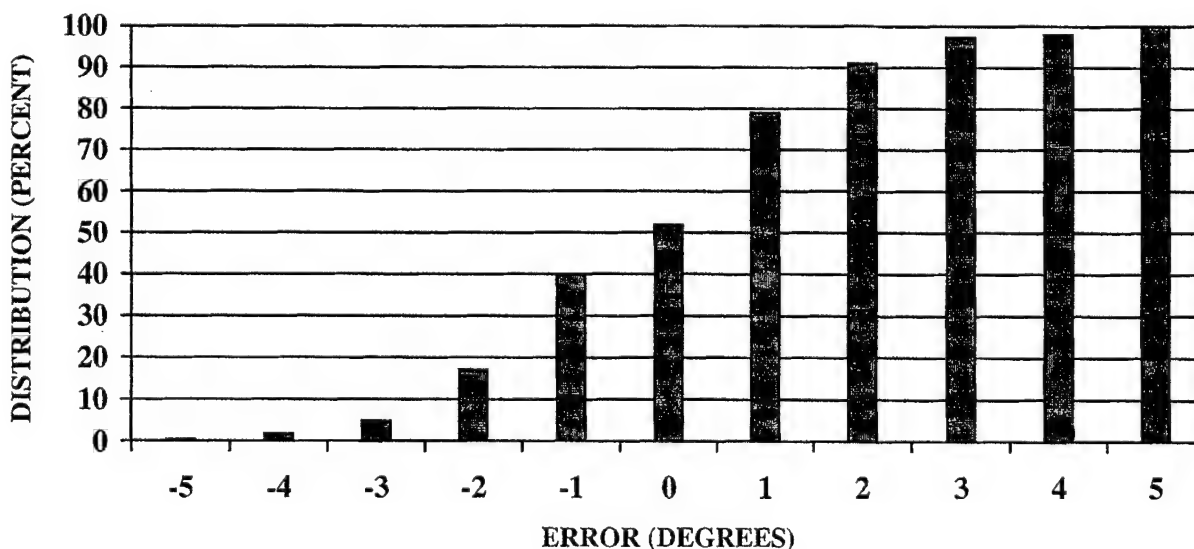


Fig. 4. Interferometer (Type I) bearing error cumulative distribution

6. DIRECTION FINDING DATA

6.1 Interferometer data

Data that characterize the Type I interferometer were taken over a three-month interval. In this interval, an aggregate of 7,980 individual bearings on known sources from all fourteen U.S. direction finding sites was taken. Of the total number of samples, 2,066 possibilities were discarded for cause, including telephone line noise or interruptions, lightning damage, scheduled downtime for maintenance, and signals not heard for any reason during the three-month interval. This indicates a reliability rate of about 74% for the network. When errors were determined on all used bearings (5,914), some 485 were found to be wild, defined as $> \pm 10$ degrees beyond the true bearing. This means that wild bearings under this criterion comprised about 8% of the used bearings, leaving a total of 5,429 samples (68%) representing "valid" bearings on desired signals. These rates compare favorably with previously found probabilities of 32% not heard, and 8% wild, leaving 60% valid bearings [5.]. To present data in a meaningful way which can be compared, and taking bearing error from the interval between $+5$ and -5 degrees, Figure 4 shows in bar graph format, the cumulative distribution of interferometer error over this range.

6.2 Wullenweber data

From documented historic data [2.], bearing distribution statistics from about 1000 valid bearing samples are available. Results of the historic data are presented in summary form below. Approximately 60% of all the bearings used in this analysis fall within 1.5 degrees of the true bearing. Finer statistical analyses [2.] of the Wullenweber data found that bearing error is reduced for bearings of higher classification. This suggests that overall performance of a direction finding system will be improved if bearings are classified accurately and if more importance is given to highly classified bearings in performing calculations. For example [2.]:

BEARING PERFORMANCE BY CLASSIFICATION AND ERRORS OF MEASURED VALUES

BEARING CLASS	NUMBER OF SAMPLES	AVERAGE ERROR (degrees)	STANDARD DEVIATION (degrees)
A	28	0.5	1.6
B	135	0.2	2.1
C	114	0.2	3.4

Bearing classification is explained and documented [6.].

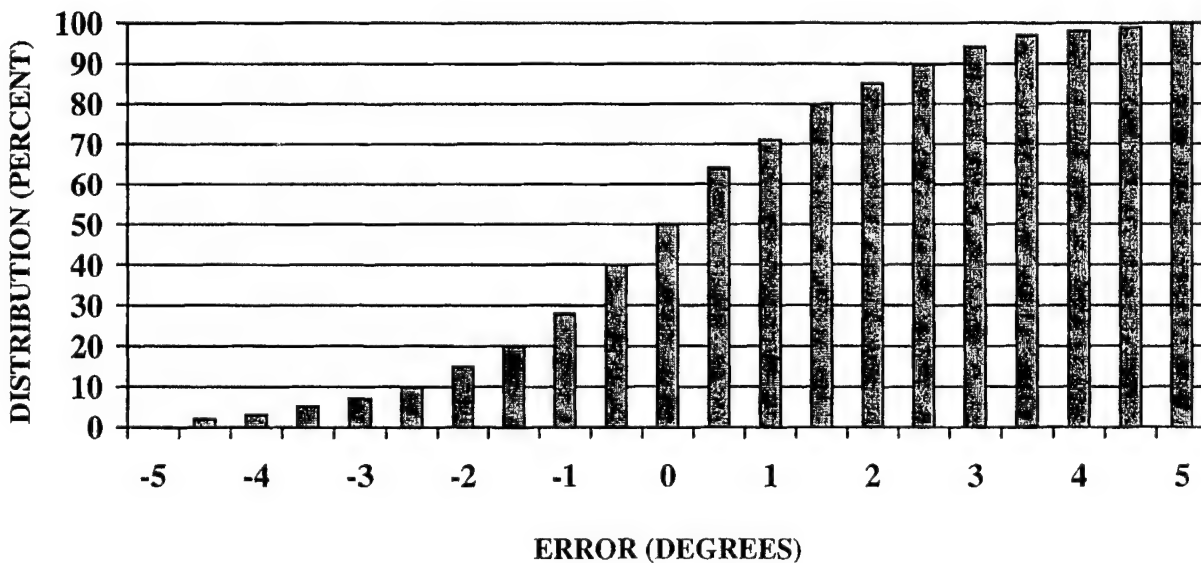


Fig. 5. Wullenweber (Type W) bearing error cumulative distribution

Similarly, if bearing performance is analyzed by signal strength, we find the following [2.]:

BEARING PERFORMANCE BY SIGNAL STRENGTH AND ERRORS OF MEASURED VALUES

SIGNAL STRENGTH	NUMBER OF SAMPLES	AVERAGE ERROR (degrees)	STANDARD DEVIATION (degrees)
S1	2	2.5	4.0
S2	54	0.5	3.4
S3	151	0.1	2.7
S4	63	0.3	1.9
S5	7	-0.3	1.1

Signal strength nomenclature is explained and documented [6.].

Figure 5 shows, again in bar graph format but for the Type W system, the cumulative distribution of error over a range of from +5 to -5 degrees.

6.3 Comparing data

If we directly compare the performance of the Type W direction finding system accuracy to the Type I performance using all available data for both systems, we find:

GROUP STATISTICS

PARAMETER	INTERFEROMETER	WULLENWEBER
STANDARD DEVIATION	2.128 degrees	2.58 degrees
AVERAGE ERROR	0.079 degrees	0.23 degrees

7. CONCLUSIONS

7.1 As direction finding measurements must be made for all qualities of the received signal, it is useful to determine the average operating conditions for direction finding and the performance of the systems under constraints of signal parameters encountered. The typical bearing is taken under less than ideal conditions, which in turn affects the accuracy obtained. Given the realities of operating conditions, it is imperative that direction finder operators accurately determine the parameters of the subject signal so that the quality and description of the bearing and signal parameters may be adequately established.

7.2 Performance of the interferometer direction finder shows substantially improved results over the wide-aperture, Wullenweber design.

7.3 The simpler physical construction of the interferometer intuitively indicates less expensive

installation costs and reduced maintenance requirements.

REFERENCES

1. United States Patent No. 5898402, "A wide Aperture Radio Frequency Data Acquisition System," William L. Kilpatrick, Federal Communications Commission, issued April 27, 1999.
2. CCIR Documents, Volume 1, Report 372-5, International Telecommunication Union, Geneva, 1986.
3. Radiocommunication Study Groups, International Telecommunication Union, Geneva, "Classification of Computer-Generated DF-Bearings," Document 1C/14, 18 July 1997
4. Hosking, R.H., "Digital Receivers: The New Wave for Signal Analysis," RF Design, April 1997.
5. Black, Q.R. and Johnson, R.L., 1995, "Fix Accuracy Improvements in Confirming DF Networks," Symposium on Radiolocation and Direction Finding, Southwest Research Institute, San Antonio, Texas, June 1995.
6. International Telecommunication Union, *Spectrum Monitoring Handbook*, Geneva, Switzerland, 1995, pp 18 and 275.

ACKNOWLEDGEMENT

Acknowledgement is given to Allen K. Yang of the Federal Communications Commission who was responsible for constructing and assembling the diagrams and figures used in this paper.

BIOGRAPHICAL NOTE

William A. Luther is Chief of the Radiocommunication Policy Branch within the International Bureau, and was formerly Chief, Engineering Division within the Field Operations Bureau, both of the Federal Communications Commission, the telecommunications regulatory administration of the United States of America. He holds BSEE and MSEE degrees from Drexel University, Philadelphia, and has been employed at the FCC for forty-one years. He holds 33 awards including the Silver Medal from the FCC, and the Chairman's Special Achievement Award. He has published forty-three scientific and administrative articles, reports, or contributions.

COMPATIBILITY CRITERIA OF MICROWAVE LINKS USED IN INTERNATIONAL COORDINATION

Wiktor Sęga, Wojciech Tyczyński

National Institute of Telecommunications, ul. Swojczycka 38, Wrocław, Poland
wseg@il.wroc.pl, wtyc@il.wroc.pl

Threshold degradation caused by an aggregated interference power is a useful criterion for compatibility assessment from the frequency management point of view, because it allows to ensure the designed availability and performance of a link. In the paper two algorithms for division of allowable receiver threshold degradation between involved administrations are presented. It may be useful for international coordination of microwave links.

1. INTRODUCTION

Nowadays it is not possible for a radio communication system to work in the electromagnetic environment free of interference. So manufactures and system planners must produce their devices and design links which could tolerate certain amount of a power arising from interfering signals. The most harmful is a stationary interference producing the noise, which can be handled in the same way as thermal noise having the same power. As a result of stationary interference the level of a noise power is increased and a fade margin is reduced. In order to ensure the assumed availability and performance of the link a planner should determine the fade margin taking into account the increase of the noise level in the future. This point may occur to be the most difficult. How the maximum interference power can be foreseen?

2. THE ALLOWABLE THRESHOLD DEGRADATION

The satisfactory solution can be found if an administration defines the maximum allowable interference power and ensures that it is not exceeded. In fact this method is applied by some administrations, which will not give the licence if the appeared interference causes degradation of the receiver input power (and fade margin) greater than the defined value. In other words, there is certain amount of dBs in the designed fade

margin, which is assumed to be lost due to the interfering signals. Every new interfering signal increases the total power coming from interference and causes fade margin degradation. If the signal level of the next planned link causes exceeding that value, this link is not put into operation. This approach enables to avoid unexpected situations, when the link suffers unacceptable degradation of availability and performance.

Situation is clear until a link does not get interference from abroad. If it does, this interference must be taken into account. But it is not reasonable to treat foreign links on equal rights with the national, especially if the foreign administration is more advanced in the development of their radio communication systems. In such a case foreign links are in a favour position, because they will occupy a great piece of the allowable fade margin degradation restraining development of national systems. In order to give equal chances to all countries it is proposed to split the value of allowable degradation into two parts; one assigned for national links, second for international.

This approach can be implemented immediately only for the USA, where there is no point where two different borderlines meet together. In Europe interference can come from two or three countries. What to do in such a case? How to manage the allowable fade margin degradation caused by foreign signals?

It is not fair to treat all foreign signals jointly and assign them a common allowable fade margin degradation because one (more advanced) administration may exhaust all interference limit. Therefore the value of allowable degradation assigned for foreign links must be split in to neighbouring countries. But, how to do it and satisfy all of them?

3. DIVISION OF THE ALLOWABLE THRESHOLD DEGRADATION BETWEEN INVOLVED ADMINISTRATIONS

It may be supposed that nobody will raise an objection to the following assumption:

The administration that is likely to have (now and in the future) more interfering transmitters should "take a bigger piece of a cake".

It means that administrations should not participate in the division of the allowable fade margin degradation on equal rights. The administration that may have greater number of transmitters, which could deteriorate the receiver fade margin, should get bigger part of the allowable threshold degradation. But how to assess, which administration may have more interfering transmitters? "May have" denotes that not only existing transmitters should be taken into account, but also those, which may appear in the future.

The answer on the last question may be given if the area, where the interfering transmitters may appear, is defined. There are a lot of methods, which would enable to generate such areas. One of the simplest is the "key whole", where two distances are defined: first (longer) in the main lobe of the antenna, the second (shorter) outside the main lobe (Fig. 1).

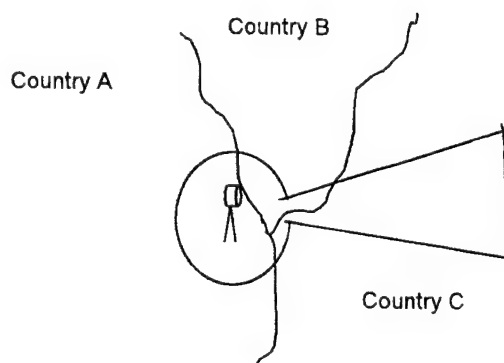


Fig. 1. „Key whole" area on the map

It can be assumed that the surface distribution of transmitters is homogeneous, so the number of interfering transmitters belonging to the Administration is proportional to the surface of the country overlapping the area where the interfering transmitters may appear. The country C from Fig. 1 may have therefore more interfering transmitters than the country B.

Bearing this in mind two algorithms for division of the allowable receiver threshold degradation between involved administrations were elaborated.

Algorithm I.

The idea is as follows:

The value of allowable degradation assigned for foreign links should be divided in to neighbouring administrations in the same ratio that the territory, where the foreign interfering transmitters may appear, is divided between these administrations.

1. Determine the surface of the area where the interfering transmitters may appear (S).	
2. $i = 1$	
3. Take the foreign administration numbered i (A_i)	
4. Does the country of the administration overlap the area where the interfering transmitters may appear?	
Yes	No
4.1 Determine the overlapping surface - $S(A_i)$	Coordination with administration A_i is not required.
4.2 Determine the threshold degradation allowable for transmitters of administration A_i (TD_i) $TD_i = [S(A_i)/\sum S(A_i)] \cdot$ [allowable degradation assigned for foreign links] dB	
5. Have all administrations been analysed?	
Yes	No
5.1 Finish	$i = i + 1$ go to 3

Algorithm II

The idea is as follows:

The administration exploring the given Fig 1. receiver should participate in dividing of the „dB cake" on equal rights with other administrations.

Taking it into account the **Algorithm II** should be modified in the following way:

- „the dB cake" is equal to the whole allowable degradation,
- point 3 should read: Take the administration numbered i (A_i),

- the formula in point 4.2 should read: $TD_i = [S(A_i)/S] \cdot [\text{allowable degradation}] \text{dB}$.

4. SUMMARISATION

Threshold degradation caused by an aggregated interference power is a useful criterion for compatibility assessment from the frequency management point of view, because it allows to ensure the designed availability and performance of a link. The mentioned advantage can be taken if foreign links are treated under the same criterion. If they are the problem of the division of the allowable threshold degradation between involved administrations must be solved. In the paper two solutions are given. Both of them take into account the development of the radio systems by every administration in the future. The algorithms can be incorporated to multilateral agreements.

BIOGRAPHICAL NOTES

Wiktor Sęga was graduated from the Technical University of Wrocław (Poland) in 1975, and then he joined the Institute of Telecommunications and Acoustics of this University. In 1979 he obtained a Ph.D. in telecommunications from the Technical

University of Wrocław. Since 1979 he has been working in the National Institute of Telecommunications, Wrocław Branch. Dr W. Sęga is involved in preparation of engineering models and software for the computer-aided national spectrum management. He was responsible for elaboration of the digital terrain model for the territory of Poland. Since 1988 to 1989 he worked with Wireless Planning and Coordination Wing of the Ministry of Communications in India, as the UNDP/ITU expert. He is engaged in the ITU-R and CEPT studies. Dr W. Sęga is the Technical Program Coordinator of the International Symposium on EMC.

Wojciech Tyczyński received the M. Sc. degree in physics in 1989 from the Technical University of Wrocław, Poland. Since 1989 he is employed in the National Institute of Telecommunications dealing with compatibility assessment methods. His current research interests are in designing the frequency management system for microwave links. He is also involved in the work of the Temporary Working Group preparing Harmonised Calculation Method used by signatories of Vienna Agreement.

SUPPORT OF INTRODUCTION OF DIGITAL BROADCASTING IN EUROPE

Tomáš Český

SES Astra, Luxembourg (until 1999 CEPT/ERO, Denmark)

Societe Europeenne des Satellites, L-6815 Château de Betzdorf, Luxembourg

fax: +352 710 725 9828, e-mail: Tomas_Cesky@ses-astra.com

1 INTRODUCTION

The importance of the introduction of digital broadcasting can hardly be overestimated. The transition from analogue broadcasting to digital will have a major impact on all elements of broadcasting, both technical and non-technical, and will significantly affect hundreds of millions of listeners and viewers. For the first time in the history of broadcasting a standard without backward compatibility will, on a large scale, replace the one in use.

The process of digitalisation takes place in an environment where an unprecedented number of information and communication techniques are being introduced and where new concepts such as multimedia are emerging. This, together with the inherently generic nature of digital technology, is the major factor which will affect the future shape of broadcasting.

From the spectrum management point of view the introduction of terrestrial digital broadcasting presents an extreme challenge which would not be manageable without an appropriate computer support. The role of data exchange and of its software support is discussed in this paper on a case study of two major CEPT activities.

2 BACKGROUND

While digital broadcasting of sound and broadcasting of television have many things in common there are factors which make the process of their introduction quite distinct in some aspects. The major technical features are summarised in the Table 1.

From the spectrum management point of view the main difference between the two is that while the introduction of the DVB-T can be seen as an upgrade of existing form of terrestrial TV broadcasting, the T-DAB introduces an entirely new service into frequency bands which are heavily populated by other services. Consequently: T-DAB is based on the implementation of a CEPT T-DAB Plan (Wiesbaden 95); the introduction of DVB-T is seen as a process of a gradual conversion governed by so-called Chester 97 procedures.

System	T-DAB	DVB-T
ETSI Standard	ETS 300 401	ETS 300 744
Channel width	1.5 MHz	7 or 8 MHz
Modulation	OFDM	OFDM
Channel width compared with analogue	Much bigger	Comparable
Channel raster compared with analogue	N/A	Identical
Target frequency band	VHF/1.5 GHz	UHF/(VHF)
Reception	Mobile	Portable/Fixed

Table 1. Major technical features of T-DAB and DVB-T

2.1 Wiesbaden 1995

After considerable preparations the CEPT T-DAB Planning Meeting took place in summer 1995 at Wiesbaden. Final Acts from this Meeting contain a complete CEPT T-DAB Plan for allotments for Priority 1 and Priority 2 requirements. It also defines all procedures required for maintenance of the Plan including rules for converting allotments into assignments.

The allotment plan for more than 700 allotments was synthesised based on full analysis of compatibility between allotments and between allotments and other services operating on relevant frequencies. This was made possible through an exercise of massive data gathering from CEPT countries, performed by ERO (European Radiocommunications Office of the CEPT), and by advanced computing support of the planning provided by EBU and ERO. The planning process took into account also protection of services other than broadcasting from the T-DAB networks and T-DAB networks from other services. The amount of other services exceeded 90 thousand records.

The CEPT T-DAB Plan is now maintained by the ERO. The maintenance process is based on Circular letters

which are being sent by ERO to notify CEPT administrations about intended modifications such as change in allotment parameters or conversion of an allotment into an assignment. So far more than 50 Circular letters have been sent out and as of today the CEPT T-DAB Plan contains more than 60 co-ordinated or proposed assignments and 800 allotments.

2.2 Chester 1997

The situation in the television broadcasting is different. It is assumed that, in the initial phase, DVB-T will be introduced on the basis of conversion of analogue assignments co-ordinated under the Stockholm 61 Plan to digital and by inserting new assignments in this Plan rather than by the means of massive network re-planning.

In order to facilitate this process the Multilateral Co-ordination CEPT Meeting was held at Chester in summer 1997. This meeting worked out the concept of a *reference situation* which consists of the database of values, such as protected field strength, characterising the situation in so-called test points. Typically 36 test points is associated with one analogue transmitter. The procedure of conversion of an analogue transmitter into digital or introduction of a new digital transmitter is then based on assessing the influence of this change on the *reference situation*.

In order to generate the *reference situation* it was necessary to compile the database of operating co-ordinated transmitters in CEPT countries. Although the Stockholm 61 Plan maintained in ITU gave a good start to this compilation a great majority of CEPT countries opted for supplying new and more complete data to the ERO which is responsible for the CH97 database. The *reference situation* for about 80 thousands television transmitters was then calculated by the EBU and validated by ERO software.

3 DATA PROCESSING ASPECTS

One conclusion from the facts above is that both processes critically depended on an appropriate computer support. It was necessary to gather a considerable amount of data and to achieve quality results of calculations based on this data. Some key issues of this multifaceted task are touched upon in this section.

3.1 Objectives

The overall objective of the computer support was to ensure, throughout the whole exercise, the

- correctness;
- robustness;
- flexibility and
- the openness

in all respects.

The openness and the transparency of the process were instrumental to the success of data gathering and processing. ERO managed the very challenging task of providing CEPT administrations with advanced tools for data compilation, validation and evaluation. The fact that all participants had the most advanced tools for their disposal and could cross-check all interim and final results of data processing done in EBU and ERO can be considered a great stimulant of mutual co-operation and commitment from all participants. Efforts, both in EBU and ERO, proved to be worthwhile.

3.2 Data formats

The data format used for the data gathering was the most straightforward, fixed length ASCII text with one data record on each line. The choice of such format was driven by the necessity of a platform independent solution which would be robust in exchange with numerous national databases. The key requirement was the simplicity and clarity of data format definition and ease of its implementation.

The downside of this choice was a virtual non-existence of commercially available tools for management of data in this format. Since the use of a text editor, such as Notepad, on files with a typical record length of 800 characters is impracticable, it was necessary to develop a set of utilities for data manipulation as a part of the support package.

3.3 Supporting software

The principle desired functions of the system were data collection, validation, rectification as well as presentation of data and presentation of results. A key part of the system functionality was export and import of data facilitating the communication with Compatibility Analysis and Plan Synthesis modules developed and operated by the EBU.

The software addresses a variety of tasks and has multiple functions. Generally it can roughly be divided into several categories as follows:

- Preparation of data
- Manipulation with data
- Validation of data
- Analysis of data
- Display of data and results
- Compatibility calculations
- Reusable software components

Already the initial analysis indicated that the amount of software tools needed to be developed would be of a considerable proportions. The actual extent of the software then was even bigger than expected. However, the experience showed that availability of a good supporting software was crucial to the overall success.

3.4 Publication of results

The openness of the process was maintained by a frequent publication of compiled data and results obtained in calculations. Two lines of relevant CD-ROM publications exist in ERO, DACAN for T-DAB and COCOT for DVB-T. Considerable efforts are being made to supply the data with efficient tool for its analysis.

4 SOFTWARE TECHNIQUES

In order to manage such enormous tasks in given time with available resources (both being much smaller than desired) a number of advanced software techniques was applied such as object oriented programming, component architecture and data encapsulation.

4.1 Object oriented programming

A sound object model of entities described in data files, such as e.g. allotment requirement or TV transmitter, was designed for use throughout the software code. The code itself could than be strictly generic. The overhead of this abstraction paid off very quickly. *Inter alia* it was possible to painlessly reflect all changes in a data specification, some of which happened in an advanced stage of programme development.

The code itself was in C++ which made possible to make the object model portable. This was proved when the entire project migrated in 1996 from 16 to 32 bit platform.

4.2 Component architecture

Most of core software blocks are implemented as COM servers. The decision to adopt this technology was made for a number of reasons. From the point of view of the user the main benefit of this approach is the possibility to use most of the components in his own software. However, it should be noted that some programmes on purpose avoid the use of components. The reason is that basic utilities must run without any "Setup", e.g. directly from the CD-ROM.

4.3 Data encapsulation

The fact that good calculation software should work in an abstraction from format of underlying data is

generally honoured. This abstraction proved to be even more important in projects described here. Data servers encapsulating ASCII files were implemented as COM components. Alternative servers, implementing identical interface, were developed encapsulating a relational database with data converted from these files as well. The possibility of using identical programmes with different data sources proved to be very valuable.

5 CONCLUSION

Frequency management of introduction of terrestrial digital broadcasting within the CEPT is an extremely complex issue which can not be managed without an extensive computer support. In the paper is shown that with use of advanced techniques it is possible to develop and maintain this support within a reasonable short time period and with limited resources. Ways to maintain the transparency and openness of the process and at the same time, achieve the efficiency necessary for its completion are suggested.

The main lesson learned was that application of these techniques should not be compromised. For example the overhead of establishing correct and coherent object model is very quickly paid off by the flexibility gained in the application software.

BIOGRAPHICAL NOTE

Tomáš Český received a PhD from the Czech Technical University, Prague, in microwave antenna theory. During his work at the Telecommunications Research Institute in Prague he was active in microwave propagation studies and later he became responsible for the development of the computer support for frequency spectrum management in Czechoslovakia. In 1991 to 1999 he was at the CEPT European Radiocommunication Office in Copenhagen where his main areas of responsibilities were spectrum engineering and broadcasting issues. Recently he joined SES-Astra as a senior frequency management engineer.

Implementation of Component-based Frequency Spectrum Management Software

Jiří Filčev

CRC Data, spol. s r.o.

U krčské vodárny 26, Prague, CZ 140 00, Czech Republic

E-mail : filcev@crcdata.cz

Continuous requirements for better and better frequency spectrum exploitation are even growing with introduction of digital broadcasting. The necessity of overlapping analogue and digital services increases problem dimension and brings new requirements to computation support for new services planning and co-ordination.

Two years ago a component-based approach for implementing partial services in frequency spectrum management software was presented. Now, after two years of using this technology and extending the number of implemented tasks, we will present our experience in building large-scale systems as digital broadcasting planning system and microwave planning system.

Fundamental criteria for FSM systems quality will be formulated and applied to core groups of components for building large FSM systems

1. Introduction

The following requirements are critical to architecture design and are measure of whole system implementation success

flexibility - system should be easily modified to track algorithm changes and upgrades

adaptability - new data (more precise DTM and morphology data in different formats) should be easily implemented into systems

extensibility - system should expect introducing of new co-ordination procedures, new data exchange formats (ERO, ITU)

reusability - component should be reused between different systems (broadcasting, microwave planning,...) to avoid re-inventing wheel effect

scalability to allow optimum hardware usage and tune system performance for very large scale computational tasks and/or for multi-user operation

robustness - long term rapid development while keeping systems stable and robust, extending system while in continuous usage.

In the next section, components and component groups following these requirements will be presented.

2. Components for FSM systems

From the client side view, component can be considered as black box, implementing certain functionality on some inputs. Such a component can serve for multiple clients - other components or client applications.

From design point of view, component hides the complexity of its functionality implementation. Component is a runtime object, upgrading components can be performed without whole system recompilation in contrast to library oriented systems.

Components are programming language independent, different languages may be used for implementing different functionality (user interface vs. math oriented procedures), component functionality is also accessible from popular scripting languages being a part of operating

system (MS Scripting Engine) or widely spread software (MS Office).

Rich set of components implementing common tasks as DTM data access, radiocommunication object access, standard propagation algorithms and visualization tools are good background for new algorithm development and testing on real sets of data.

Components for FSM systems can be divided into several groups, covering different functionality:

2.1 DTM Components

These components are operating on DTM and morphology data sources (usually databases or binary files) and provides services like GetPoint, GetProfile and GetRectangle.

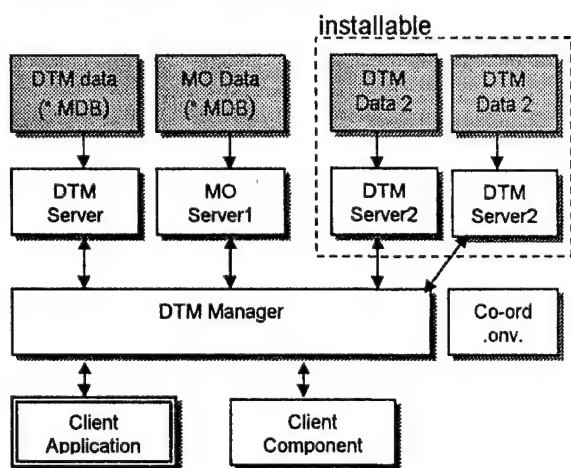


Fig. 1 – DTM Components Architecture

DTM Manager object is the main entry point and allows system extensions by adding of further DTM servers build on different data sources. Such extension can be performed by simple installation of new server into existing system. This way, new DTM data can be introduced into large system without modifying the whole system. Installable components are shown in dashed frame.

2.2 Computational Components

Computational components contain the implementation of algorithms commonly used in all radiocommunication systems. These algorithms use DTM component to query terrain data and work on databases containing some important constants, propagation curve samples etc. Implemented functionality covers profile statistics (effective height, roughness,...), propagation curves, field strength evaluation and propagation attenuations. The functionality of RA Manager is

similar to DTM components, result architecture allows installation of additional computational components like new propagation models into existing system.

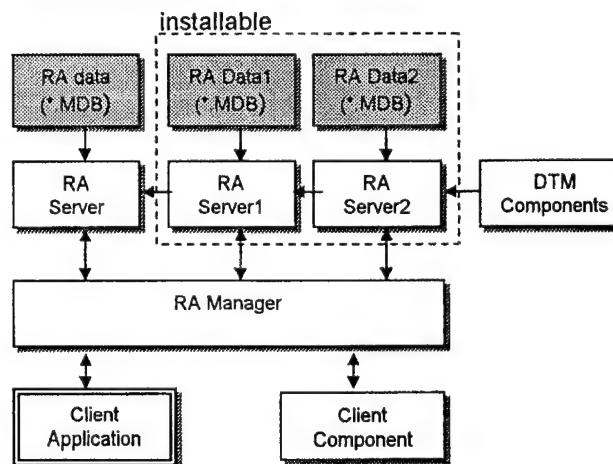


Fig. 2 – RA Components Architecture

2.3 Visualization Components

This group of components is used to display path profiles, radiocommunication objects (transmitters, hops,...) and computation results (testpoints, visibility diagrams, field strength diagrams, raster criteria on raster or vector maps).

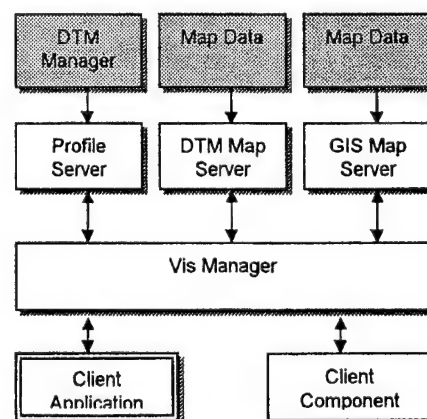


Fig. 3 – Visualisation Components Architecture

Three main components are used for visualization of common situations: Profile for path profile visualization, DTM map without map precise XY projection for preview and more schematic outputs and GIS (Geographical Information System) map, contain GIS engine for displaying requested output on standard map data sources as digitised topographic maps or vector maps. Embedded GIS is capable of using map data in standard formats.

Vis Manager is component for controlling creation of instances and provides support for comparative schemes allowing sending output to appropriate (or new) instance of requested map.

2.4 Data Access Components

These components are more specific to particular radiocommunication service. Data access components encapsulates database operations on certain data source (file database, SQL database engine) and exposes its functionality on radiocommunication data object (transmitter object for broadcasting systems, microwave object for hop representation). Advanced data container techniques were implemented to allow client application to operate on multiple databases and to support collaboration and data exchange between multiple users of system. Block architecture of data access components is shown on following picture.

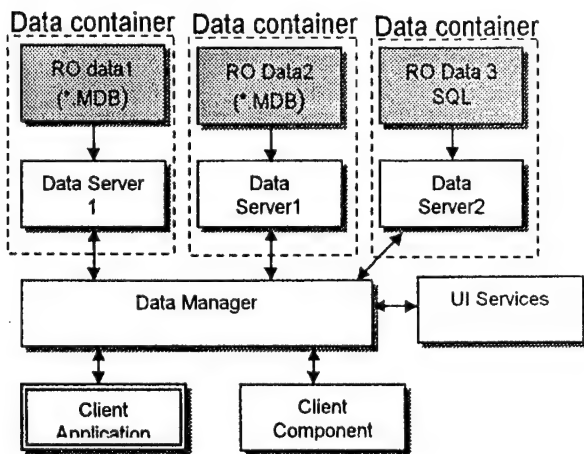


Fig. 4 – Data Components Architecture

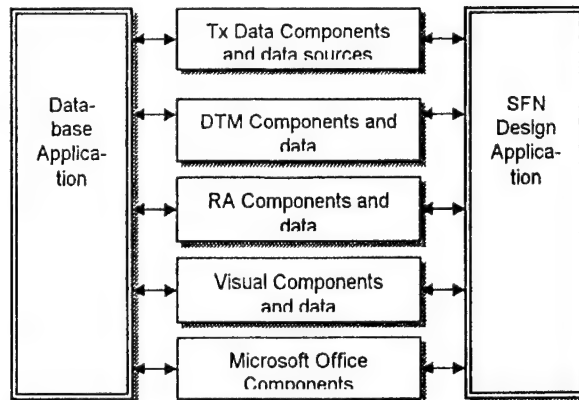
Data container - data server together with data storage - is server component providing data access oriented services on one type of data source. Data manager implements the same functionality but on virtual database consisting of data from all connected data containers. Data access requests are redirected to target container (Load) or compiled from all active data containers (Query). UI Services component implements standard database functionality dialogs for data browsing, editing, querying and selecting for use in client systems.

This architecture is prepared for easy implementation of import/export from/to any new data exchange format simply by creating data server operating on new data storage. Container copy operations in UI services will cover all necessary interfaces for data transfer between external source and other data containers.

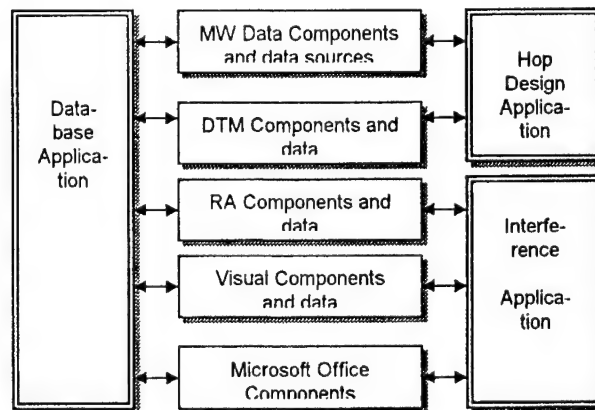
3. Large System Architecture

Component reusability can be demonstrated on principal architecture of two large systems - system for Single Frequency Network Planning designed for coverage and interference calculations for TV, FM, T-DAB and DVB-T systems and microwave system covering hop design, quality computation and interference computations.

3.1 DVB Planning System



3.2 Microwave Planning System



Microsoft Office Components are used in both systems as reporting engine. This way of solving report system is very flexible, report templates are simple Excel templates and can be easily modified by user.

4. Conclusion

The goal of this paper is to demonstrate some results of two year of using component-based approach in building large FSM systems. In addition a poster session is scheduled to present

more detail information together with real system functionality demonstration.

BIOGRAPHICAL NOTE

Jiří Filčev graduated at the Czech Technical University in Prague in 1983, where he also was granted a PhD. degree in 1987 in the field of

speech processing and continued working as assistant professor. His professional work was concentrated to digital signal processing algorithms. In 1993 he co-founded CRC Data company oriented to special software systems development. Currently he is working in radiocommunication software team designing and managing frequency spectrum management systems development.

VIENNA AGREEMENT '99 - HARMONISED CALCULATION METHOD ACTIVITIES

Ján Klima
University of Matthias Bel & PTT Research Institute
Banská Bystrica, Slovak Republic
E-mail: klima@fpv.umb.sk

1. The Vienna Agreement - historical background

In preamble of the first signed Vienna Agreement '93 – VA'93 (Vienna, December 3rd-1993) it is stated: „The representatives of the telecommunications authorities of Belgium, the Federal Republic of Germany, France, Italy, Croatia, Luxembourg, the Netherlands, Austria, Poland, Switzerland, the Slovak Republic, Slovenia, the Czech Republic and Hungary have concluded the present Agreement, under Article 7-of Radio Regulations, on co-ordination of frequencies between 29,7 MHz and 900 MHz for the purposes of preventing mutual harmful interference to the fixed and land mobile services and optimising the use of the frequency spectrum above all on the basis of mutual agreements,,.

The VA93 contains provisions on administrative and technical procedures. It defines different frequency categories (e. g. preferential frequencies, frequencies of geographical network plans) which frequencies have to be co-ordinated, and procedures to be applied for co-ordination (including the data exchange format and timing).

The technical procedures describe the calculation methods determining the interfering field strength and the permissible interference field strength in the different frequency bands. The applied technical tools are described in the 7 Annexes of VA'93.

Fulfilling the technical provisions of the annexes, the signatory countries decided to develop a common computer program based on the Annexes of VA93. This software is called Harmonised Calculation Method (HCM). The program was developed and approved in 1996. For calculations it applies terrain data. The project team (PT-HCM) developed a storage-format for terrain data, which is based on the geographical coordinates in WGS-84 geodetic system.

To get the same results of calculations made by different groups, it is necessary to use the same databases. For this reason a method for mutual exchange of

terrain data was developed. The HCM software is already available in the ITU-R software catalogue.

After successful completion of first phase - developing the HCM for mobile services – it was decided to extend the method to cover the fixed services till 43,5 GHz and the mobile services for the bands around 1 800 MHz. As a second phase, at the end of 1996 (Mainz) and start of the year 1997 (Prague), the project Team of the Vienna Agreement carried on its work under name Technical Working Group Harmonised Calculation Methods (TWG-HCM). For managing a great deal of availed (but also un-availed) work, its organisation was divided into two sub-working groups in accordance with purpose of VA namely to Sub-working group for mobile service (SWG-MS) and Sub-working group for fixed service (SWG-FS).

The detailed tasks for mobile and fixed services were:

- to provide standardised calculation methods,
- to develop unified co-ordination procedures,
- to develop standardised calculation programs,
- to revise documentation of the Vienna Agreement '93 and prepare its new improved version.

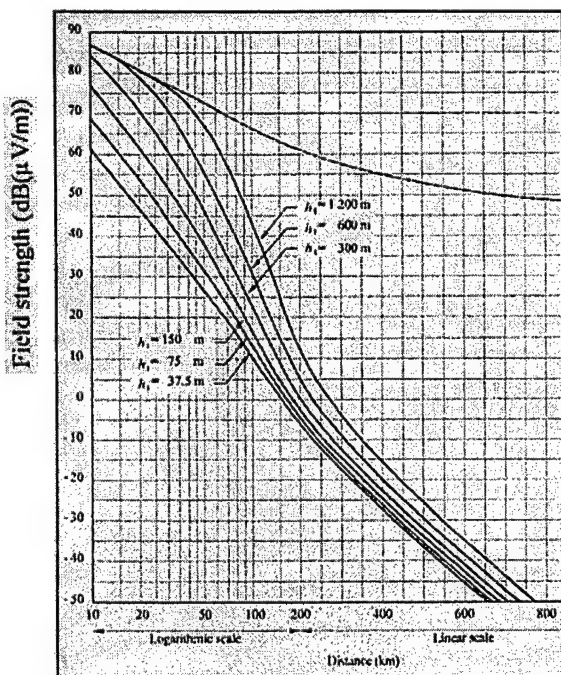
2. Standardised calculation methods

It should be mentioned that there are other organisations working on developing generally valid calculation methods, e. g. ITU-R, CEPT-ERC. The expert's work speciality in frame of TWG-HCM is, that on the basis of knowledge of generally accepted calculation methods, their own experimental works, or works and experiences in certain countries respectively, the experts are searching for common solution of problems, which would be acceptable in all countries, having signed VA. It appeared that the methods of field strength calculation, used in VA'93 were granted to upper limit of frequency interval -to 960 MHz. But the general developmental trend of VA was to expand the frequency interval up to 43,5 GHz, in particular for fixed services. However, the projecting and planning of

fixed services follows different principles and rules comparing with mobile services. First of all, there are power output ratio and calculation of transmission loss instead of field strength calculation and voltage dependent quantities, which are typical for mobile services. Approximately after 3 years work we are able to characterise the results as follows.

2.1 Mobile service - field strength calculation

This part was already quite well solved in VA'93. Basic tool for such activity was set of propagation curves (a functional dependence of field strength on distance from transmitter with effective height of transmitter antenna as parameter) from 30 to 300 and 450 to 1000 MHz - see Fig. 1.



Frequency: 450-1 000 MHz (Bands IV and V); land; 50% of the time;
50% of the locations; $h_2 = 10$ m; $\Delta h = 50$ m

Fig. 1

A-propos - propagation curves. It is a problem for more detailed discussion. There are just sketches of some partial questions:

1. The propagation curves, as they were used in VA, were basically achieved through experiments for purposes and conditions of broadcasting. For these services there was (and still is) typical, that transmitting antennae are installed on the terrain dominants (to obtain the largest area covering by signals). That's why the curves were compiled for effective transmitter antenna high more than 37,5 m and for flat terrain. Moreover, the measurements were made in condition of West Europe.

2. The secondary source of propagation curves set, experimentally achieved, are works by Japanese authors. These curves have been already designed for mobile services, but their basic environment are conditions Japanese cities, with natural conditions for wave propagation totally different from conditions in West Europe.
3. There is a principle question, if there is some correlation between these sets of curves, to make possible to unequivocally define the curves. It has been decided to use the set of curves published in ITU-R, Rec. 370-7 also for mobile service.

However, with developing of new services, above all the systems DCS 1800, a principle problem has been opened: *which set of propagation curves will be used for planning and co-ordination of mobile services in frequency band over 1 GHz?* Sets of propagation curves over 1 GHz are world-wide not enough represented. As author knows, some special experimentally processed propagation curves exist for frequency bands 1600 MHz and 3 GHz (Japanese authors). In context with this one interesting idea occurred: *isn't there some generally valid theorem (functional dependence) derived from known sets of propagation curves in lower frequency bands, which would be able to predict or extrapolate the values of the field strength in higher frequency bands?*

In effort to find such correction factor, author realised extensive analysis of all existing propagation curves. Unfortunately, no unequivocal, even, monotonous, linear dependence has been found, which would enable to predict the field strength in higher frequency bands. The question of appropriate set of curves over 1 GHz is still open for the future.

The positive state is, that (except of small conception details) already processed, improved and by all delegations acceptable algorithm of calculation of the field strength exists, which added (propagation curves) these correction factors to basic tools:

- terrain irregularity Δh ,
- terrain clearance angle,
- correction factor for frequencies in 900 and 1800 MHz bands,
- antenna diagram,
- knife edge diffraction loss.

2.2 Fixed service - calculation of transmission loss

The basic aim of fixed service frequency planning is the choice, or frequency allotment respectively of radio relay link operation, in such a way that:

- this link was interference free, or
- the interference level does not affected a link quality.

As a first step in frequency co-ordination of fixed service links in frame of Vienna Agreement, different possible interference criteria were presented. In order to facilitate comparison between them, a definition of

relevant parameters was decided. At this stage, four possibilities exist:

- minimum C/I,
- maximum threshold degradation (TD); this criterion can be based on two sources (T/I curves or noise of receiver);
- maximum permissible interfering I level;
- minimum [C-(N+I)] under fading conditions.

C (dBm): receiver carrier level at the input of receiver; this value depends on link design and is set by operator of the link. It cannot exceed maximum admissible level (or blocking level).

I (dBm): level of interfering signal at the input of the receiver.

C₀ (dBm): receiver threshold level at the input of the receiver for given Bit Error Rate (BER); this value characterises the sensitivity of the receiver and depends on the technology, the selection of the BER (10⁻³, 10⁻⁴, 10⁻⁶ etc...) being made by the operator.

C_i (dBm): receiver threshold level in an interfering environment at the input of the receiver for given Bit Error Rate (BER).

TD = C_i - C₀ (dB) threshold degradation due to the interferer. This value can be assessed to be identical to the increase of noise at the receiver input; it can also be elaborated more precisely by measurement

M = C - C₀ (dB): fading margin of the link; this value depends on the link design chosen by the operator. This value is the key value to meet the operator's quality and availability objectives, related to a selected BER.

N+I (dBm) aggregated power level of thermal noise with interferer in the receiver bandwidth

The parameters to be protected in the co-ordination process are:

- quality and
- availability objectives of the link.

Those parameters are protected when the fading margin is protected. Thus the fading margin, whatever the value, is the key value for protection in an interfering environment.

As a result of the comparison of possible criteria for the interference calculations there was concluded that the **Threshold Degradation (TD) is the preferred criterion for the Vienna Agreement.**

The elementary TD is the degradation caused by one interferer on a victim receiver.

The technical data necessary for the calculation of different intermediate parameters and finally the interfering signal level I at the input of an interfered receiver are listed in the Annex to Chapter 9 of Vienna Agreement. All those parameters should be a part of the data

being exchanged between the Administrations. Here it is made only a draft of interference level I calculation at the receiver input at the station and the TD calculation:

Interference level (I) at the receiver input of the station can be determined as:

$$I = P_{Tx} - a_{tot} \quad [\text{dBm}]$$

where

a_{tot} [dB] is a total attenuation between transmitter output (point A') and receiver input (point A)

$$a_{tot} = a_{Tx} - G_{Tx} + a_{prop} - G_{Rx} + a_{Rx} + a_{ant} + NFD + ATPC$$

where

a_{prop} [dB] is a propagation attenuation between antennas

a_{ant} [dB] is the attenuation which is a function of both antenna radiation patterns and polarisation discrimination

NFD [dB] is Net Filter Discrimination

ATPC [dB] is the dynamic range of the automatic transmitter power control (when applicable).

Threshold Degradation Calculation

Input:	elementary value I (dB or dBm), interfering power level at the receiver input coming from one identified interfering source.
Necessary data:	FkTB or N (dBW or dBm): noise level in the interfered receiver bandwidth.
Calculation TD (dB):	TD (dB), threshold degradation of the interfered receiver $TD = 10 \log (1 + 10^{(I - N) / 10})$

The question was to find a solution concerning the sharing of the 1 dB aggregated threshold degradation affecting a fixed link receiver and due to multiple foreign links. It was proposed that the individual TD affecting a receiver and due to foreign link must not exceed 0.1 dB. By this way, within the 1 dB maximum aggregated TD criterion it would be possible to cope with different foreign interfering sources.

It appears that:

- 1 dB is a small value that can be too restrictive;
- 10 different interfering sources is probably a too big number, 5 are more realistic.

It was decided to forget the criterion of 1 dB max aggregated TD and to replace it by 0.2 dB maximum individual TD by any foreign source.

Therefore, the criterion of interference between fixed links to be used in the Vienna Agreement co-ordination process becomes:

$$\text{maximum individual TD} < \text{or} = 0.2 \text{ dB}$$

3. Unified co-ordination procedures

Demands on intensive availing of frequencies lead several times to frequency assignments in frame of one service, but also to common availing at frequency bands with different services.

To secure the work of radio-communication devices, it is necessary to predicate possible interferences of the new frequency assignment with those, which already exist, before definitive allotment of the new frequency. This process is called *frequency co-ordination*. Frequency co-ordination for the new frequency assignment runs in several levels:

- *inner-system co-ordination*, in frame of one kind of service,
- *inter-system co-ordination*, the co-ordination between different kinds of services in case of common used frequency bands,
- *in state co-ordination*,
- *international co-ordination*.

The main attention of VA is paid to international co-ordination. This process is essential by those situations, when new frequency assignment is realised in that frequency bands in which electromagnetic waves are propagated on long distances, or is realised near to the country border. Those situations can lead to harmful interference of radio devices not just on the land of neighbouring countries, but also on the land of other countries. That's why the international co-ordination is essential. Rules and procedure for the international co-ordination are described in the Radio Regulations. Any administration, which realizes the new frequency assignment, requests the administration of the country, which could be affected by interference for its statement. It is necessary to include the planning criteria as well as the following data in the request to the co-ordination:

- planned frequencies (transmitting and receiving frequency of the station),
- coverage area of the entire Radiocommunications network,
- class of the station,
- coverage area of the station,
- effective radiated power,
- maximum effective antenna height,
- designation of the emission,
- network development plan,
- antenna patterns for stations belonging to the network.

As it can be seen, for the first fixing of range of co-ordination the *co-ordination area* is used. Its distance from co-ordinated frequency assignment determines this area. *Co-ordination distance* determines the border of interfering – no services are affected by this new frequency and this frequency is not affected by these existing services.

The co-ordination distance is calculated with real technical parameters of investigated frequency assignments and technical parameters of already realised technical assignments. This gives a maximal possible co-ordination area. Co-ordinating distance determines the set of possible frequency assignments (radiocommunication devices), which have to be verified from the point of view of interference.

The co-ordination procedure in both types of services is in VA defined by this way:

- In case of *mobile services* a transmitting frequency shall be co-ordinated if the transmitter produces a field strength, at a border of the country of the administration affected, which at a height of 10 m above ground level exceeds the maximum permissible interference field strength (defined in Annex 1 of VA). A receiving frequency shall be co-ordinated if the receiver requires protection.
- Radio-relay links in the *fixed service* shall be co-ordinated if at least one station is located within the co-ordination zone or if at least one station which can cause harmful interference or required protection even when situated outside the co-ordination zone (described in Annex 11 of VA). In this case the co-ordination procedure is only valid if in both countries involved in the co-ordination process the respective frequency band is allocated to the fixed service and the respective frequency falls under the responsibility of the signatory Administrations.

4. Development of standardised calculation programs

It has to be noted that at present two different states of computer programs HCM exist:

1. For mobile service, which is completed and tested by some Administrations,
2. For fixed service, for which developing a special group of experts has started its work.

The Harmonised Calculation Method for Mobile Service (HCM-MS) is a part of the Vienna Agreement '99. In this document the abbreviation VA'99 is used to Vienna Agreement 1999. Also, the relevant CEPT Recommendations for services (not noted in the VA 99) are included in HCM-MS, as agreed by all Signatories. The HCM-MS subroutine performs calculation from a transmitting station to a receiving station or from a transmitting station to a co-ordination line. HCM-MS subroutine runs with input and output data, which are defined in an interface. Input values (transmitting parameters, receiving parameters or data for line selection and additional information) are mandatory and have to be provided by the surrounding program. This program uses three main subroutines:

- calculation of the field strength,
- calculation of the permissible interference field strength,
- calculation of the maximum field strength on a coordination line.

The current language for programming was chosen to be usable on different platforms (DOS, Windows, Unix, ...). At this time, there are more accurate languages to program. But from the point of view of many Administrations of VA'99 there is a need to have only

one language. There are three possibilities to deal with this problem:

- to have a program in Fortran,
- to have a DLL,
- to have both.

If the program is written in Fortran, it will be necessary to modify the surrounding program for each new version, a DLL will only run under Windows. With both programs all cases be covered. As all Administrations present the using of Windows, SWG-MS decided to exchange the program as a DLL file together with the source code.

The Harmonised Calculation Method for Fixed Service (HCM-FS) is in position of beginning its work. It was decided that its two tasks to be performed should be:

- definition of a module calculating the compatibility between new stations and existing stations,
- definition of a module for evaluating the trigger for co-ordination.

A special problem for both types of services is a morphological database used by the HCM software. Knowing that:

- for the fixed services information is required if the area is: sea, coastal area, or normal land
- and for the mobile service information is required if the area is:
 - land
 - or sea
- and additionally for both services further information is useful about the height of the morphological surface (height of trees or buildings),

There is a proposal to create a morphological database according to the following description:

- A raster database with the same grid and structure as the terrain height database,
- Each entry consists of two bytes, one for the predominant height of the surface (trees, buildings) and one for the class of the morphology.

The class of morphology consists of one byte. Therefore 8 different classes (bits) are possible. For the fixed service only three classes are required, for the mobile service only two classes are required. But it is useful to define all 8 classes as early as possible to avoid later modifications. A set of the 8 possible information bits should be as follows:

- all bits are 0 normal land
- bit 0 is 1 sea, ocean
- bit 1 is 1 small lake, river,
and small portions of water (no sea, no ocean!)
- bit 2 is 1 coastal area
- bit 3 is 1 villages, towns
(buildings)
- bit 4 is 1 trees
- bits 5 to 7 for future use

Note: For the HCM software only the first 4 items have been required till now!

In general, a morphological database is not required for all countries applying the HCM software. If there is no sea or coastal area (e.g. Austria, Slovakia), the use of a morphological database is not mandatory. Therefore the HCM software has to define default values for the absence of that database. The proposal is: The default class of morphology is normal land and the default (additional) height of the morphology is 10 m.

Taking into accounts these definitions, it is up to bilateral agreements to use a morphological database or not.

5. Summary

The article deals with present situation of preparing for signing international agreement – Vienna Agreement '99. As this document contains many technical, legislative, administrative etc. problems, only a sketch of technical tasks is discussed in it. In conclusion some open items have to be mentioned:

For SWG-MS there are e. g.:

- Processing, making algorithms and interpolating of propagation curves for distances from 1 to 10 km, for effective heights of transmitting antenna below 37,5 m (to 1 m, or 0 m respectively) and for receiving antenna heights less then 10 m.
- A need to implement new curves for digital system, as it was stated from increase of permitted interference field strength for TETRA networks based on measurements made for analogue and digital systems.

For SWG-FS there are e. g.:

- *Types of service:* Inter-service co-ordination between different types of services; they are co-ordination of FS against radars, co-ordination of MS against FS and co-ordination of FS against MS.
- *Interference criteria for FS* (short term interference).
- *Passive repeaters* (case of mirrors, ...).
- *Point-to-multipoint* systems.

6. References

Reports of the meetings of the Sub-Working Group Mobile Services and Fixed Services from 1997 to January 2000.

BIOGRAPHICAL NOTES

Mr. Ján Klima finished The Slovak Technical University in Bratislava (Slovak Rep.) in 1971 and received Ph.D. in 1979. From 1991 till now he is a member of TWG HCM of Vienna Agreement. At present he is Assoc. Prof. at the University of Mathias Bel and researcher in the PTT Research Institute in Banská Bystrica (Slovakia), as well. His professional domains are the theory of electromagnetic waves, radio waves propagation and frequency spectrum engineering.

EXCHANGE OF DATA FOR FREQUENCY SPECTRUM MANAGEMENT

Čeněk PAVELKA

TESTCOM

Hvoždanská 3, 148 01 PRAHA 4, Czech Republic

fax: +420 2 7992164, e-mail: Pavelka@TESTCOM.cz

1 INTRODUCTION

The future development of communications is conditioned, to a substantial degree, by quality of frequency spectrum management (FSM). The transition from analogue to digital communications techniques adds another dimension to the importance of FSM, be it national or international. At present FSM depends very much on an intensive use of computer technology, specialised software and advanced data utilisation. The main topic of this presentation is the international exchange of data in the FSM process in European Region.

2 INTERNATIONAL CO-ORDINATION PROCEDURES

In planning radiocommunication services, most cases require, pursuing the provisions of Radio Regulations, international co-ordination. The way and scope of such co-ordination is specific for each service. International co-ordination is used to be performed mainly on a bilateral basis, involving administrations which are concerned. After the co-ordination process had been finalised, its results are reported to the relevant international body responsible for keeping file on utilisation of the frequency spectrum in the given band. (so called notification). As for computer support, all the above steps represent operations upon databases, and eventually, synchronising themselves.

Following are descriptions of co-ordination procedures for individual radiocommunication services.

2.1 Broadcasting Services

Broadcasting in its present stage of development is a service which expands very dynamically. Main reason for that is the transition to digital transmission systems. Today, the experience shows that the success in implementing digital broadcasting is dependent in a limiting manner on international frequency co-ordination. As for digital TV (DVB-T) the transition procedure is, in its

entirety, based on a harmonised chain of co-ordination steps.

2.1.1 Analogue Television and FM Radio

Here the frequency allocation plan together with the rules for international co-ordination were adopted at an ITU regional conference held in Stockholm in 1961. The plan and associated rules for TV broadcasting will be in force until a forthcoming competent conference to be held presumably in 2005 and which should actually close the era of analogue TV. At an ITU regional conference held in Geneva in 1984, the allocation plan for European FM broadcasting was updated and the band used was extended up to 108 MHz. At the beginning, frequency planning was based on applying regular frequency lattices and propagation curves according to CCIR Rec.370. As time passed by, individual administrations began to make use, for their internal purposes, advanced frequency planning procedures to various extents. Interference from broadcasting transmitters was calculated wherein computer techniques, digital terrain maps and various sophisticated models of electromagnetic wave propagation was made use of. However, no amendments were made during the entire period to the co-ordination forms for co-ordination and notification purposes, which serve to international data exchange and submitting technical parameters of transmitters to the ITU. Until nowadays, the forms have survived as paper documents. Fax has become here the peak technical tool for data exchange. This makes, on one hand, the international co-ordination extremely inflexible, on the other hand the IFL in ITU Headquarters merely unusable. A number of administrations ceased to submit to the ITU notifications in form.

The innovation finally comes in these days and is twofold.

The first change is the transition to an electronic form of the data submitted to the ITU for notification. Radiocommunication Bureau is in the process of modernising its information systems,

including moving from the current Frequency Management System (FMS), using a mainframe computer, to a client-serving configuration, using PCs and relational databases under the Terrestrial Radiocommunication System (**TerRaSys**). Unfortunately the ITU has defined the data format only, while it has entirely failed to provide the administrations with even the simplest SW tools for editing and validating of the data, not even mentioning the tools capable of operations over this data and thus assisting international co-ordination. Despite of that, this move undertaken by the ITU has to be praised, and let us hope that as soon as initial difficulties will be overcome, the **TerRaSys** system will become an efficient tool and a source of correct and complete data over which co-ordination calculations can be made.

The other change was triggered in the course of the procedure of implementing digital television which started during the CHESTER97 meeting. One part of CH97 Agreement was the task to define, prior to starting digital broadcasting planning, a reference status of the frequency plan for analogue television with the aim to protect, to the extent necessary, analogue broadcastings. As no use could be made of the ITU database for its incompleteness, a decision was taken to work out a CEPT database. This task has been given to the ERO which then safeguarded not only data capture and distribution but provided the administrations, on a CD ROMs, with a self-contained set of SW tools (COCOT No.1 to 5) for keeping and utilising the data. Thanks to that, analogue television is the only service which has a complete and updated database. However, with the calculation of the reference status the task of ERO will probably finish, and the keeping of the database will no more be continued.

2.1.2 Digital Television

International electronic data exchange on digital television transmitters has been worked out in the course of CH97. However, a couple of unanswered questions remain here, too. Out of them, the most important is where the common European database of digital television will be located, and who will take care for its keeping and maintaining. There are other contributions in this Symposium dealing with planning of digital television and radio, in which are described details of the planning itself. This is why the details are not mentioned here.

2.1.3 Digital Radio

Digital radio, T-DAB, involves the introduction of a new system into frequency bands which are already used by a number of other services. The rules for introducing the system, for frequency planning, for data exchange and for administering the T-DAB database have been agreed at the

Wiesbaden T-DAB meeting in 1995. The ERO safeguards all support including CD ROMs DACAN No. 1 to 7. ERO has also been appointed as the Plan Administrator of the Wiesbaden Plan which contains the database of T-DAB allotments and assignments. The pace of implementation in Europe of T-DAB is less rapid than predicted. However, quite a large number of transmitters have already been put into operation or successfully frequency co-ordinated, especially in Germany. It is necessary for co-ordination procedures to be successful that the updated Plan is at general disposal. The experience shows that in this aspect, there is a considerable amount of spare capacity at the Plan Administrator.

2.2 Mobile and Fixed Services

In Mobile and Fixed Services, international co-ordination is an example of good international co-operation the basis for which has been laid down in Vienna in 1993 and is known as VA93. In 1999 a new agreement VA99 was signed - VA99, by which the co-operation is extended also for Fixed Services. Data formats for co-ordination purposes and for a common DTM have been defined in the framework of VA. Calculation methods for mobiles have also been worked out, and a similar work is in process for fixed service systems. The transition to electronic data exchange and co-ordinations is rather prolonged but some hope exists that it will be brought to an end within two years. VA items are discussed in other Symposium paper.

2.3 One remark on co-ordination procedures itself

When examined today, the co-ordination procedures laid down in the Radio Regulations and in final acts of international conferences (e.g. Stockholm61) are obsolete and lengthy. They have been based on circulation of paper documentation, and time limits for individual co-ordination steps are correspondingly long lasting. The conclusion is that even an easy co-ordination between neighbouring countries of a non-conflict frequency assignment takes six months as a minimum. Solutions of more complex cases are prolonged for several years with humble views to satisfactory outcomes. At present, we are facing the commencement of international frequency co-ordination for implementing DVB-T, and in turn it means that each and every administration will have to co-ordinate many tens of frequencies. I am convinced that this task could hardly be mastered using existing methods and formalistic administrative procedures. The existing approach would result in substantial slow-down in starting DVB-T in Europe. The only realistic outcome, in my opinion, is a close and informal co-operation between neighbouring administrations, especially between their national bodies safeguarding technical assistance in co-ordination tasks. The best approach would be that national

including moving from the current Frequency Management System (FMS), using a mainframe computer, to a client-serving configuration, using PCs and relational databases under the Terrestrial Radiocommunication System (**TerRaSys**). Unfortunately the ITU has defined the data format only, while it has entirely failed to provide the administrations with even the simplest SW tools for editing and validating of the data, not even mentioning the tools capable of operations over this data and thus assisting international co-ordination. Despite of that, this move undertaken by the ITU has to be praised, and let us hope that as soon as initial difficulties will be overcome, the **TerRaSys** system will become an efficient tool and a source of correct and complete data over which co-ordination calculations can be made.

The other change was triggered in the course of the procedure of implementing digital television which started during the CHESTER97 meeting. One part of CH97 Agreement was the task to define, prior to starting digital broadcasting planning, a reference status of the frequency plan for analogue television with the aim to protect, to the extent necessary, analogue broadcastings. As no use could be made of the ITU database for its incompleteness, a decision was taken to work out a CEPT database. This task has been given to the ERO which then safeguarded not only data capture and distribution but provided the administrations, on a CD ROMs, with a self-contained set of SW tools (COCOT No.1 to 5) for keeping and utilising the data. Thanks to that, analogue television is the only service which has a complete and updated database. However, with the calculation of the reference status the task of ERO will probably finish, and the keeping of the database will no more be continued.

2.1.2 Digital Television

International electronic data exchange on digital television transmitters has been worked out in the course of CH97. However, a couple of unanswered questions remain here, too. Out of them, the most important is where the common European database of digital television will be located, and who will take care for its keeping and maintaining. There are other contributions in this Symposium dealing with planning of digital television and radio, in which are described details of the planning itself. This is why the details are not mentioned here.

2.1.3 Digital Radio

Digital radio, T-DAB, involves the introduction of a new system into frequency bands which are already used by a number of other services. The rules for introducing the system, for frequency planning, for data exchange and for administering the T-DAB database have been agreed at the

Wiesbaden T-DAB meeting in 1995. The ERO safeguards all support including CD ROMs DACAN No. 1 to 7. ERO has also been appointed as the Plan Administrator of the Wiesbaden Plan which contains the database of T-DAB allotments and assignments. The pace of implementation in Europe of T-DAB is less rapid than predicted. However, quite a large number of transmitters have already been put into operation or successfully frequency co-ordinated, especially in Germany. It is necessary for co-ordination procedures to be successful that the updated Plan is at general disposal. The experience shows that in this aspect, there is a considerable amount of spare capacity at the Plan Administrator.

2.2 Mobile and Fixed Services

In Mobile and Fixed Services, international co-ordination is an example of good international co-operation the basis for which has been laid down in Vienna in 1993 and is known as VA93. In 1999 a new agreement VA99 was signed - VA99, by which the co-operation is extended also for Fixed Services. Data formats for co-ordination purposes and for a common DTM have been defined in the framework of VA. Calculation methods for mobiles have also been worked out, and a similar work is in process for fixed service systems. The transition to electronic data exchange and co-ordinations is rather prolonged but some hope exists that it will be brought to an end within two years. VA items are discussed in other Symposium paper.

2.3 One remark on co-ordination procedures itself

When examined today, the co-ordination procedures laid down in the Radio Regulations and in final acts of international conferences (e.g. Stockholm61) are obsolete and lengthy. They have been based on circulation of paper documentation, and time limits for individual co-ordination steps are correspondingly long lasting. The conclusion is that even an easy co-ordination between neighbouring countries of a non-conflict frequency assignment takes six months as a minimum. Solutions of more complex cases are prolonged for several years with humble views to satisfactory outcomes. At present, we are facing the commencement of international frequency co-ordination for implementing DVB-T, and in turn it means that each and every administration will have to co-ordinate many tens of frequencies. I am convinced that this task could hardly be mastered using existing methods and formalistic administrative procedures. The existing approach would result in substantial slow-down in starting DVB-T in Europe. The only realistic outcome, in my opinion, is a close and informal co-operation between neighbouring administrations, especially between their national bodies safeguarding technical assistance in co-ordination tasks. The best approach would be that national

EMISSIONS CONTROL TECHNIQUES FOR MSS HANDSET TRANSMITTERS

Christopher N. Kurby

Motorola Inc, 600 N. US Highway 45, Libertyville Illinois, USA; email wck004@email.mot.com

Standards development work during the 1990's for LEO and GEO MSS handsets has been very contentious over the issue of acceptable and realisable conducted transmitter emission limits. Compromised standards eventually were agreed for LEO operation in the 1610 to 1626.5 MHz band and were drafted to protect adjacent MSS services and GNSS composed of GPS and GLONASS systems. Development work continues for the adjacent band above 1626.5 MHz and this is also very contentious. Early transmitters introduced for the Iridium LEO MSS and presented in this paper were straight forward designs and are shown to be compliant with the LEO standards for MSS. This paper also presents more advanced transmitter architectures that reduce complexity, improve efficiency and still provide the necessary conducted emissions control. These techniques can be used for GEO MSS handset transmitters as well as LEO MSS handsets. The paper suggests the performance possible for GEO and LEO MSS handsets and helps set attainable performance useful in subsequent standard development.

1. INTRODUCTION

Mobile satellite terminal emission standards development has been underway under ETSI and ITU forum for many years. Initially they centred on the 1610 to 1626.5 MHz Low Earth Orbit (LEO) uplink band. More development has focused on the Geostationary orbit (GSO or GEO) Mobile Satellite System Band (MSS) of 1626.5 MHz to 1660.5 MHz band. The limits for the LEO system were determined to be compatible with transmitter technology as provided by CDMA [1] proponents and TDMA proponents. The CDMA proponents used very simple transmitter designs employing Class AB High Power Amplifiers as the final radio frequency stage driven heavily into compression. This was established by driving the input of the HPA at the 1 dB compression point of the HPA. Since the PEP to average power ratio (peak to average) is 5.5 dB this represents a very heavy compression of the output signal. The TDMA transmitters were operated in a more linear fashion where the PEP of the modulation was at the input power required for 1 dB compression of the

HPA. Standards were developed for both system types that were compatible for both, the ETSI TBR 041 [2] and corresponding ITU LEO document [3].

The primary concern of these standards is with the out of band emissions into directly adjacent systems, CDMA into TDMA, TDMA into CDMA, and with emissions into adjacent services of GPS, GLONASS, and radio astronomy. Since the in-band emissions are largely an intrasystem matter these limits were not explicitly defined. Rather methods were drafted that provided restrictions on out of band emissions. Thus there is no per channel mask for TDMA systems but there is one for CDMA systems which was offered as a way to show the CDMA systems were less harmful than feared by the TDMA proponents due to cumulative effects of multiple wide bandwidth channels.

The most difficult frequency for TDMA LEO MSS terminals to meet is the 1605 MHz frequency where the level of -70 dBW/MHz EIRP must be met to protect the GLONASS navigation system.

As a way of restricting emissions from multiple carriers in-band the concept of nominated bandwidth (nbw) was introduced in [2]. This required that the nbw be restricted to the licensed band and describes out of band emissions directly adjacent to the operational band. Since this only applies to control emissions at the edge of the band this is not really a per channel mask. However if some liberty is taken with the definition a pseudo per channel mask can be developed and is used in this paper. In the case of the Iridium system the nominated bandwidth is selected to be just under five channel bandwidths wide.

Emission limits have been proposed in the ITU document concerning GSO MSS in [4]. This document contains tables for terminals with EIRP <15 dBW and also >15 dBW. Manufacturers and operators have expressed concern that the limits suggested in the ITU GEO document cannot be met by low power (<15 dBW) handsets and certainly cannot be met by higher power units. Moreover in TBR44 [5] emission limits are given for terminals for GEO MSS which are excessively high compared to the other standards. This paper shows that the proposed limits for <15 dBW terminals are compatible with existing radio technology also shows that higher power terminals can be made compliant which includes aeronautical terminals as well as land mobile.

2. TRANSMITTER TECHNOLOGY

The Iridium system requires a moderately linear transmitter to meet the Iridium system intra band requirements and to meet the ETSI and ITU out of band emission requirements. Linear transmitters require higher battery power than constant envelope systems that can be driven into compression. This motivates the evolution of transmitter technology as we seek higher transmitter efficiency and lower cost while maintaining or improving on transmitter linearity.

This section presents three handset transmitters that were designed for the Iridium system. The overall efficiency will be seen to improve with each generation and the linearity will be maintained. The first subscriber unit shipped, the 9500, used a Doherty amplifier [6]. The complete transmitter line up is shown in Figure 1. This figure gives certain power levels, noted below the elements and signal to noise ratios (SNR's) at 1605 MHz the GLONASS band edge, noted above them. Since the maximum burst power EIRP of an Iridium handset terminal is 11.45 dBW, and the noise limit is -70dBW/MHz the SNR in dBc/Hz can be calculated from

$$\text{SNR} = \text{EIRP} - N + 10 \cdot \log_{10}(1e6) \text{ dBc/Hz} \quad (1)$$

Which after plugging in the values becomes 141.45 dBc/Hz.

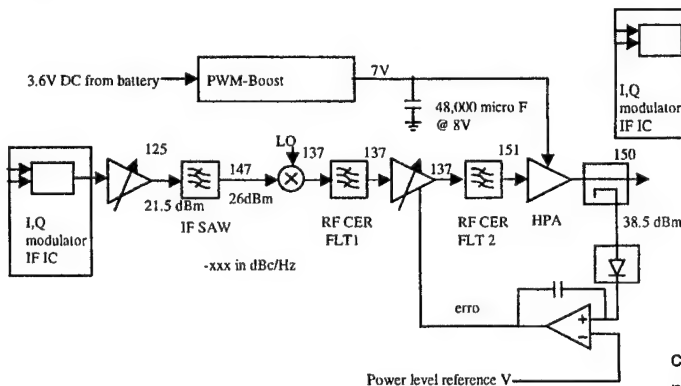


Fig. 1 9500 Transmitter line up with SNR's

In this design ceramic filters 1 and 2 provide sufficient attenuation to provide a 150 dBc/Hz SNR at 1605 MHz.

The next generation transmitter produced similar results but with improved efficiency and smaller size and lower cost. Fig 2. Shows the line-up used in the next generation 9505 model. Here no rf filters are required to make the noise floor of 141.5 dBc/Hz because the up mixer is driven at a higher power and establishes an adequate SNR. However low cost, wide bandwidth rf SAW filters have been substituted for the ceramic filters and provide local oscillator signal rejection primarily.

This transmitter also employs a boost DC to DC converter which is configured to adjust the voltage to the DC output buck converter to correspond to the current output power setting. This results in a significant power savings at reduced transmitter power which occurs most of the time.

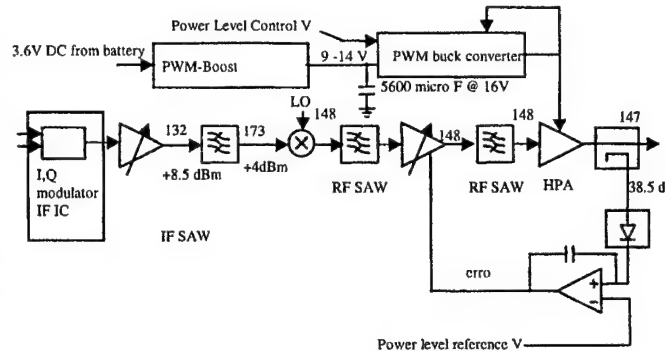


Fig 2. 9505 Transmitter line up with SNR's

The most advanced transmitter technology is provided in the P9373 subscriber unit. This transmitter is similar to the previous 9505 in that it also does not require filter attenuation at 1605 MHz to meet the GLONASS requirement. This transmitter employs an envelope modulation technique [7] technique with a modulated drive signal.

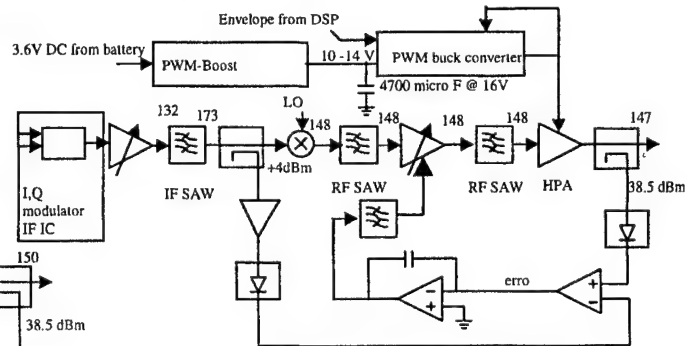


Fig 3. P9373 Transmitter line up with SNR's

The efficiency of the three systems can be indirectly compared by comparing the sine wave driven output power and power added efficiency curves. Fig. 4 gives these for the 9500 and the 9505. The 9500 is restricted to the 7 volt curve due to the constant voltage DC to DC boost converter while the 9505 uses both the 5V and 7V curves. Inspecting the figure we see that for reduced output power if the 5 V curve is used the HPA PAE is increased over the 7 V. As long as the DC to DC buck converter does not reduce the efficiency excessively then the increased PAE will hold up at reduced output power. Since the system normally operates at power cutback the subscriber unit will experience a higher battery life than the fixed 7 volt DC supply system. The efficiency of the buck regulator in the 9505 is in excess of 90% and increased battery life is realised.

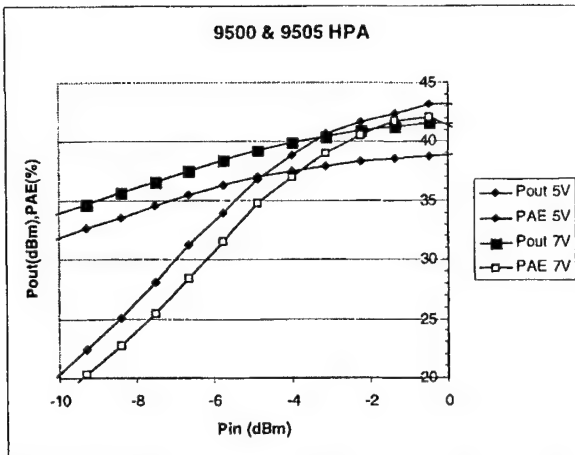


Fig. 4. HPA PAE and Pout curves of the 9500 and 9505 for two voltages

The P9373 of Fig 3. Uses an envelope modulated DC supply to the HPA. This provides an efficiency enhancement over the DC controlled Doherty amplifier. However the linearity is worse in an open loop implementation. Fig 5. Gives the output power, gain and PAE of the output stage used in the P9373.

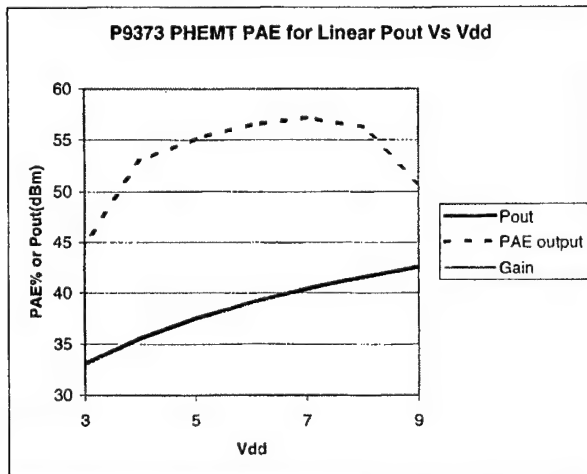


Fig. 5 P9373 HPA open loop Performance curves

The gain is highly non linear especially at low supply voltage. There is about 9 dB of gain distortion from 3 V to 9 V supply voltage. Since the supply is a linear function of the envelope voltage this non constant gain results in AM distortion. The DC supply voltage is described as

$$V_{dd}(t) = K \text{ Envelope} [(I(t) \cos \omega t - q(t) \sin \omega t)] \quad (2)$$

$$V_{dd}(t) = K r(t) \quad (3)$$

Where K is just a DC voltage scaling value and $r(t)$ is the time varying envelope.

In the P9373 a feedback loop is wrapped around the envelope following loop which effectively increases the drive signal as the modulated supply voltage decreases. This results in a highly linear system.

3 EMISSIONS

3.1 Emissions standards scaled

The emission limits set by TBR 041, ITU LEO MSS ITU GEO MSS, TBR 44 and DCS1800 were compared to the actual emission performance of the three respective transmitter technologies. The parameters used for TBR 41 and ITU LEO MSS are a nbw of 208.33 kHz, for the ITU GEO and TBR 44 the nbw is set to the channel separation of 41.67 kHz. The DCS1800 emission levels were applied to the Iridium modulation format transmitters through a simple scaling of the channel separation bandwidths. This was done over the range where the DCS levels scale with power and are then a function of the modulation. The DCS1800 channel separation is 200 kHz while the Iridium system channel separation is 41.66 kHz, this established a roughly 5 to 1 frequency offset scale factor that rounded to exactly 5 and is used for DCS1800 offsets <400 kHz.

The DCS1800 in-band levels are given in terms of off channel power spectral density in 30 kHz to on channel power spectral density in 30 kHz for offsets <=1800 kHz. Since the levels are given in terms of relative psd the same relationship of off channel psd to on channel psd ratio is used for the narrow bandwidth Iridium signal but the psd bw is changed to 3 kHz. The off channel emissions were converted to absolute power using the equation

$$P_{sd_off_3} = P_{sd_on_3} \cdot A \quad (4)$$

Where A is the DCS1800 PSD in 30 kHz spectrum attenuation, and $P_{sd_off_3}$ and $P_{sd_on_3}$ are the power spectrum off and on channel in 3 kHz respectively.

This is converted to absolute power by calculating the on channel spectrum relative to the on channel power. In this analysis the Iridium total on channel power is in a 25 kHz bw. The on channel $P_{sd_on_3}$ is then given by

$$P_{sd_on_3} = P_{tx} + 10 \cdot \log_{10}(3/25) \text{ dB} \quad (5)$$

Where for Iridium the P_{tx} is set to 11.45 dBW.

For offsets greater than 1800 kHz the emissions limits become absolute power limits. The close to carrier spectrum data for the Iridium signals was measured in a 3 kHz bw Vs. the DCS1800 30 kHz limits. The absolute DCS1800 levels were converted to 3 kHz by lowering them 10 dB. The levels for the other standards were also scaled where appropriate.

The out of band emission levels were all converted to dBW/MHz to coincide with the GLONASS and GPS levels of -70 dBW/MHz which also matches how the data was taken on the three transmitters.

3.2 Emission levels in-band

While data exists for all three transmitter types it will only be shown to highlight significant points. Fig. 6 shows how the 9500 transmitter performs relative to the ITU GEO and US Code of federal regulations (CFR) referred to here as FCC. Where it is seen that the limits are roughly equivalent after 200 kHz and are conservative between 200 and 500 kHz offset. There is some narrow band spurious present at 300 kHz due to switching regulator clocks.

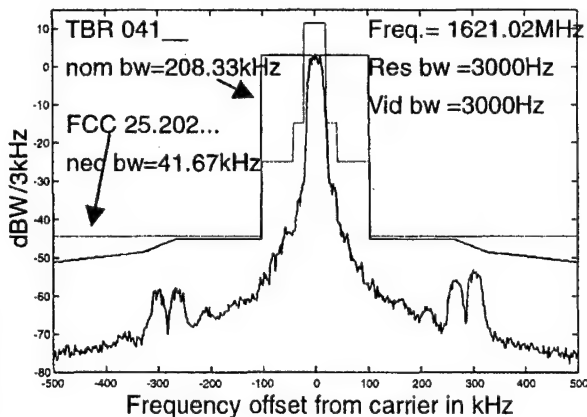


Fig 6. Specimen 9500 Transmitter

Fig. 7 gives spectrum for the P9373 transmitter and compares it to the ITU GEO, TBR44 and the scaled DCS1800 limits for a frequency span of 1 MHz.

This figure highlights the deficiency of the TBR 44 limits compared to actual transmitter performance and to the ITU GEO and DCS1800 limits. TBR44 was drafted to allow GEO data services and is a very old standard that did not recognise the need to protect future satellite systems in the band. Instead it was designed to provide economical transmitters using old transmitter architecture and should be revised.

The DCS1800 scaled limits are seen to be more restrictive than the unit can provide for offsets about 80 kHz. But it is interesting that a transmitter not designed to meet DCS1800 levels nearly does. Since the close in emission levels are due to non linear HPA performance we might expect constant envelope signals to perform better.

The feedback loop wrapped around the envelope modulator for the P9373 in Fig.3 linearizes the system significantly. This is seen when comparing the spectrum of the P9373 in Fig 7 to that of the open loop Doherty transmitter design of the 9500 in Fig 6. This is exemplified between 100 and 200 kHz where the P9373 is seen to be better by about 5 dB. The improvement is measurable for offsets less than 200 kHz and actually results in a lower occupied bandwidth for the P9373. Again narrow band spurious is present but in this case at 400 kHz due to the switching regulators. Once the

frequency offset exceeds the loop bandwidth of about 200 kHz then no more improvement is realised.

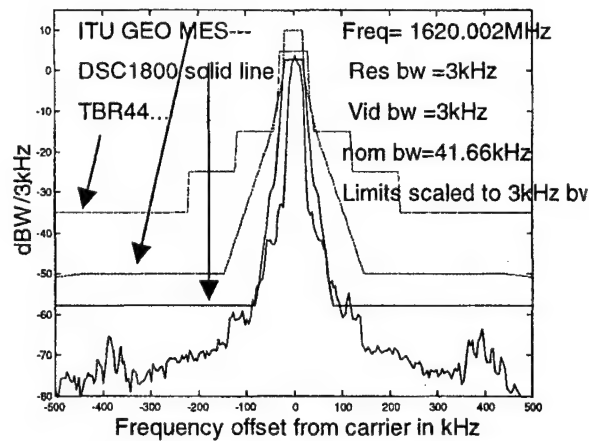


Fig 7. Specimen P9373 Transmitter in-band

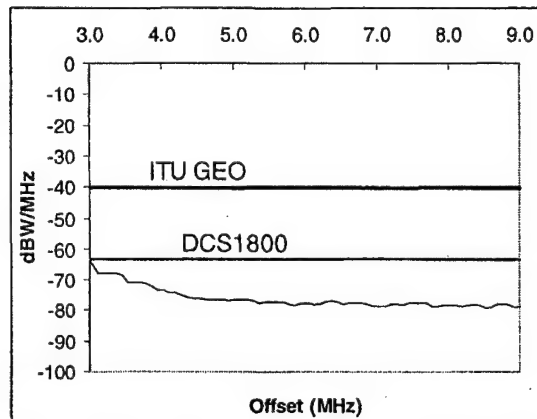


Fig 8. Specimen 9505 Transmitter in-band

Fig. 8 gives a 3 to 10 MHz single sided span of the 9505 but with a 1 MHz bw. The data is only valid for noise and spurious ≥ 3 MHz, but are below the DCS1800 limits and consequently the ITU GEO limits.

3.3 Emission levels out of band

Out of band emission limits for the LEO ITU and ETSI standard are shown in Fig 9 for the 9505 transmitter. The noise spectrum roll off with reduced frequency is flat until the frequency is less than 1600 MHz where the wide bandwidth SAW filter starts to improve the SNR.

ITU GEO, TBR 44 and DCS1800 are compared to specimen transmitters in Fig. 10. But in this case the spectrum is mathematically shifted in the computer from 1620.83 MHz to 1626.75 MHz to see how it would fair in the GEO frequency band. Since the measurements were made with a 1 MHz resolution bandwidth the frequencies in the vicinity of the carrier are invalid as it is more a measurement of the spectrum analyser filter. Comparing Fig 9 to Fig 10 the noise at low frequency offsets for the 9500 improves quickly due to the narrow bandwidth rf ceramic pre-filter. Neither plot reveals any

narrow band spurious because these transmitters employ a limited number of oscillators, use high frequencies (215 MHz) for up mixers and the resolution bandwidth is 1MHz. No spurious is visible at 16.8 MHz offset, the reference oscillator frequency.

The limits set by TBR44 are at 1605 MHz are much higher than either the DCS1800 or ITU GEO limits. The performance of the transmitter is good enough that the spectrum scaled from 11.45 dBW to 29 dBW still meets the out of band emission ITU GEO emission limits for frequencies just below the band edge at 1626.5 MHz.

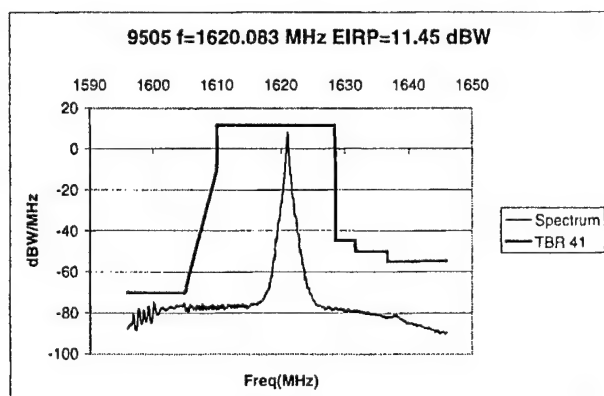


Figure 9 Specimen 9505 Transmitter out of band

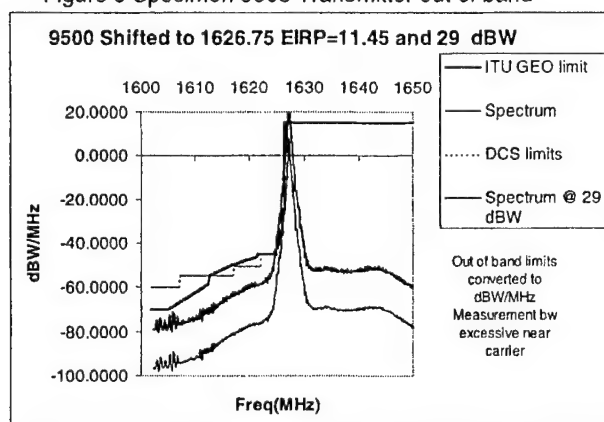


Fig. 10 Specimen 9500 Transmitter GEO out of band

3. Conclusions

This paper showed how the limits set in TBR 44 are excessively high for ordinary handset terminals in the 11.45 dBW EIRP area. The levels are also excessive compared to the ITU GEO limits for EIRP's < 15 dBW. Using low power handset technology higher EIRP terminals can be made to meet the ITU GEO low power limits without extraordinary means just by adding some guardband which is reasonable, since high power terminals can be congregated away from the band edge. Out of band emissions and noise can be controlled by adding narrow band HPA rf pre filters and by driving up mixers at higher power level. Advanced linear transmitter technologies should provide the means to meet stringent out of band emissions while improving overall transmitter efficiency.

Higher power fixed installation terminals including mobiles can employ classical HPA techniques and merely operate below the 1dB compression point of the power out curve to maintain linearity. In this case efficiency is given up but it is also less significant due to the mains power available. They also can employ large pre and post filters if necessary. Spurious is less of a problem due to fewer and higher oscillator frequencies.

4. REFERENCES

1. Alcatel, "Feasible emission mask for CDMA based S-PCN M.E.S.s operating in the 1.6 GHz frequency range" Presented to ETSI/STC/SES5 Tdoc (96)20, January 17, 1996.
2. ETSI, "Satellite Personal Communications Networks (S-PCN); Mobile Earth Stations (MESs), including handheld earth stations, for S-PCN in the 1,6/2,4 GHz bands under the Mobile Satellite Service (MSS); Terminal essential requirements; Terminal essential requirements", ETSI Technical Basis for Regulation, TBR41 February 1998.
3. ITU, "ESSENTIAL TECHNICAL REQUIREMENTS OF MOBILE EARTH STATIONS FOR GLOBAL-NON-GEOSTATIONARY MOBILE-SATELLITE SERVICE SYSTEMS IN THE BANDS 1-3 GHz", ITU-R M.1343.
4. ITU, "ESSENTIAL TECHNICAL REQUIREMENTS OF MOBILE EARTH STATIONS OF GEOSTATIONARY MOBILE-SATELLITE SERVICE SYSTEMS THAT ARE IMPLEMENTING THE GMPCS-MOU ARRANGEMENTS IN PARTS OF THE BAND 1-3 GHz", Rev. 1 to Doc. 8/128-E.
5. ETSI, "Satellite Earth Stations and Systems (SESS), Land Mobile Earth Stations (LMES) operating in the 1.5 and 1.6 GHz bands providing voice and/or data communications", ETSI Technical Basis for Regulation, TBR44 May 1998.
6. F.H. Raab, "Efficiency of Doherty RF-power amplifier systems", IEEE Trans. Broadcasting, vol. BC-33, no. 3, pp. 77-83, September 1987.
7. M. Faulkner and M. Briffa, "Linearized Power Amplifier", US Patent 5,420,536, May 30, 1995.

ACKNOWLEDGEMENTS

Mike Gaynor of Motorola contributed significantly to the content of this paper.

BIOGRAPHICAL NOTE

Chris Kurby received his BSEE from the University of Illinois, in Urbana, he also has a MEE and he has a MEM from Northwestern University, Evanston, Illinois. He works in Personal Communications Sector of Motorola and is a Motorola Science Advisory Board Associate Member. He has 24 US patents and is a member of the IEEE Communications Society.

OUT-OF-BAND EMISSION LIMITS FOR MOBILE SATELLITE EARTH TERMINALS

Reuven Meidan
Motorola Israel

16 Kremenetzki st. Tel Aviv 61250, Israel.
email: reuven.meidan@motorola.com

The satellite-based systems of the past filled only a very partial need for Mobile Satellite Services (MSS). The industry is undergoing an extensive revolution in order to be able to serve the true needs. This includes Non GEO constellations, on-board processing and linear modulation methods. This completely changes the EMC scenario, in a sense that from a relatively low usage and stationary environment it becomes dynamic and denser in emitting sources. This paper addresses the issue of out-of-band emissions. While in the old days, satellite-based earth terminals enjoyed a relaxed requirement, in order to accommodate the new systems a much stricter regime must be adopted, similar to the evolution which the terrestrial-based radio communication industry have gone through.

In this paper the limits required are calculated and shown to be feasible in the light of the development of the technologies that were needed for the modern terrestrial-based systems like GSM.

1. INTRODUCTION

By MSS (Mobile Satellite Service) we refer to non-fixed services, which include mobile operation on land, maritime and aeronautical. These services are about 30 years old now. Originally they were based on GEO (Geostationary Orbit) satellites. The frequency allocation is the, so-called 1.6/1.5 GHz. i.e., a paired nomination based on 2 times 34MHz bands. One at 1,626.5 to 1,660.5 MHz for uplink (earth to space) and the second at 1,525 to 1,559 MHz for downlink (space to earth) communications.

Inmarsat has been the prime operator for these services. It provided since 1979 different MSS systems serving all the 3 mobile components mentioned above. However, in spite of the fact that these services have been offered for 20 years now, the total number of users for all Inmarsat systems is about 140,000, which is low by any standard and clearly far from satisfying any substantial level of demand. In particular, for the aeronautical component the level of services is currently so low that, based on this, Inmarsat requested relief in

protection requirements for out-of-band emission levels into an adjacent (1660 to 1670 MHz) Radio Astronomy band (CEPT PT SE28, Jan. 2000).

Clearly, the demand for satellite-based MSS is large, as they complement the terrestrial-based systems in substantial ways. Indeed, the coverage of terrestrial-based systems is restricted to the populated areas. However, these areas are only a small fraction of the total globe. This implies that only satellite-based systems can provide ubiquitous (in the sense of any time any place) services on a global scale. Furthermore, there is the demand of serving people in the air (aircraft) and in the sea (ships). In these cases satellite-based systems are particularly attractive. Cases of disaster, like earthquakes, floods, etc., where terrestrial-based infrastructure is, either nonexistent or demolished, are another example for the application of satellite-based MSS.

Inmarsat technology, being 20 to 30 years old is based on GEO satellites with relatively small size antennas, which require high power terminals in order to close the link budget. The high terminal power is derived from a high gain terminal antenna. The consequences of this configuration are low capacity due to a low frequency reuse and restricted modes of operation, like the inability to allow true handheld mobile operation and adequate fade margin capabilities associated with mobile operation.

In order to fulfill the real needs for services, the industry has recently been undergoing a far-reaching revolution in applying new technologies. New types of constellations, based on NGE0 (Non GEO) satellites, like LEO (Low Earth Orbit), and MEO (Medium Earth Orbit), have been introduced. The traditional bent-pipe (i.e., satellites operate as radio repeaters) architecture has been complemented by smart satellites, which perform on-board processing and in-the-air satellite-to-satellite routing, based on a network of intersatellite links. NGE0 constellations contribute to MSS revolutionary features like:

1.1 True full global coverage including high latitude areas and the Polar Regions.

This provides ubiquitous (any place any time) coverage on a full global scale, in contrast to GEO, which have coverage limitations due to their equatorial basis.

1.2 Less constrained link budget allowing lower power and nondirective terminal antenna allowing true handheld personal operation. This is due to the substantially lower orbits and high gain satellite antenna.

1.3 High capacity by not limiting satellite orbits to the equator. In contrast GEO have a limited number of available slots along the equator.

1.4 High capacity by better frequency reuse, through satellite multibeam antennas. The lower altitude allows smaller cells on the ground compared to same satellite antenna size in the case of GEO.

1.5 Use of the satellite on-board processing and a network of satellite interlinks to provide trunks to any place without constraining the gateway location like in the bent pipe approach.

1.6 The use of linear multilevel modulation in order to increase spectral efficiency in terms of bits per Hertz.

To accommodate these new NGE0-based systems, so called Big LEOs, a new band, so called the 1.6/2.4 GHz band (1610 to 1626.5 MHz uplink, 1613.8 to 1626.5 and 2483.5 to 2500 MHz downlink) was opened by WARC '92. The systems which were constructed in this band are Iridium® and Globalstar. The former has been in commercial operation for more than a year now and the latter has recently completed the launch of its constellation. Other new bands are being opened for satellite-based MSS systems. e.g., Third Generation (3G) IMT-2000, which includes a satellite component at 1,980 to 2,010 MHz, paired with 2,170 to 2,200 MHz. In this band the ICO system is being constructed.

In addition a new breed of GEO-based systems, so-called Super GEO, has been placed on the design table. These systems are planned with very large size satellite antennas to allow better reuse and reduce link budget limitations thus mitigating their high altitude orbits. Some examples are AceS, THURAYA, EAST.

The ITU space recommendation database for filings of proposed systems reflects this high rate of planning activity of new systems. As of Aug. 1998 more than 200 systems have been advanced published in the L bands (1610 to 1626.5 and 1626.5 to 1660.5 MHz). True, from a construction point of view most of these systems will remain on paper. However, the large number of candidates is clearly indicative of the high need for these services. With these new systems, it appears that the old term MSS had better be changed to S-PCN (Satellite Personal Communications Networks) to better reflect the mission of the new generations of satellite systems for mobile applications.

In order to accommodate these plans for extensive use of MSS old concepts needs to be revisited. This paper deals with the subject of EMC in terms of unwanted emissions, which always accompany radio equipment.

2. THE USER RADIO LINK

In order to increase spectrum efficiency in the form of higher frequency reuse and in order to increase the fade margin for better mobility services, the new generation systems employ higher gain antennas at the satellite. Coupled with the low altitude orbits it will allow operation with terminals with relative low output power. Typically, an average power level of 0dBW will be sufficient for 16dB fade margin for voice services.

In contrast, Inmarsat uses relatively low gain antennas at the satellite, both on the global and local services, thus requiring high EIRP (Effective Isotropic Radiated Power) at the terminal. On a minimum basis, without providing margins for faded mobile EIRP levels of 15 to 25 are typically quoted for voice services.

3. OUT-OF-BAND INTERFERENCE

We consider now the question of intersystem interference due to out-of-band emissions from the terminals.

In terrestrial radio systems one encounters a large dynamic range in terms of received signal levels. This is due to the large variation of ranges and shadowing characteristics of the radio links. For this reason, out-of-band emissions into adjacent bands require a tight control. A good example of the progress made in this field is the GSM standard for out-of-band emission levels.

In contrast, in the satellite arena and in the old days of all GEO systems, dynamic range was limited. Reason was that distance (earth to satellite) was essentially fixed and, as the link budget was constrained, no significant degree of fade margin could be provided. Furthermore, only a small number of systems were in operation. As a result, little was done in terms of controlling the levels of out-of-band emission and the progress made with out-of-band emission did not extend from the terrestrial-based to the satellite-based systems.

However, with the new systems coming on board, the situation with respect to susceptibility to interference of satellite-based systems changes significantly.

3.1. As they operate with higher satellite antenna gains and lower orbits, their uplinks are more sensitive to interference from the transmission of adjacent band terminals..

3.2. As the visibility in the sky to uplink transmission is wide, (Inmarsat high directivity terminal antennas are 60 degrees wide), a victim satellite can be interfered with by a considerable number of terminals.

3.3. Satellite-based systems are power limited. As such, the key factor in these systems operation is the system noise floor, which includes the thermal noise

floor plus other internal noise sources. The desire is to reduce it as much as possible. The harm which interference causes is expressed in terms of the level it raises the system noise floor. This will directly determine the raise of power required from earth terminal in order to mitigate that interference in order to keep the same carrier to interference ratio. As the system is power limited, this degrades the system performance by that amount. For instance, raising the noise floor by 1dB would mean that every terminal would have to be designed with an extra 1dB of radio power in order to combat this interference for keeping the same C/I. Since the power reserve is not there, it would mean a degradation of the quality of service in terms of fade margin to mitigate multipath.

3.4. Statistical analysis of the average based on random distribution of terminals which are sometimes made, are not applicable in this case, as events with high concentrations of terminals in one location (hot spots) are highly probable for satellite systems (e.g., a disaster situation).

3.5. The 2 uplink bands (GEO and NGE0 respectively) are adjacent with 1626.5 being the common edge. This makes the situation particularly problematic.

4. UPLINK INTERFERENCE ANALYSIS

As an example we will use the Iridium system in order to express the connection between the spectral density on the earth of a terminal emission into an Iridium channel and the raise of system noise floor at the satellite receiver. We will take a 1% raise as the point of calculation.

Satellite system noise, N_0 is -201dBW/Hz ($T=500$ K). Earth to satellite bore sight distance 1280km. Satellite antenna gain is 17dB at edge of service. As Iridium channel bandwidth is about 30kHz we will express the results in terms of spectral density measured over 30kHz. While the Iridium footprint contains several types of beams the results among the beam are fairly balanced within about 5dB.

Assuming free space propagation, the above parameters yield an EIRP spectral density on earth measured over 30kHz of about -40dBW.

Interference into a certain victim satellite channel is cumulative effect of all the terminals seen by the antenna beam of said channel. As far as the cumulative effect of interference from all terminals is concerned a distinction should be made between the effects of a narrow band spurious and wide band noise. The wide band noise adds up in a linear way whereas the narrow band discrete spurious components usually occur in random frequencies, so that there is a justification to assume that the cumulative effect from multi-terminals does not add up linearly.

In order to get a requirement for the level of emission From the individual terminal an estimate of the total number of terminals in the footprint of the victim

satellite is needed. The total bandwidth for uplink is 34MHz. Assuming a channel bandwidth of 40kHz, one arrives at a number of 850 channels. Realizing that, by the nature of unwanted emissions, the levels decrease with increasing frequency offset from carrier until a floor, so called the noise floor, is reached, one can assume that, except for the noise floor cumulative effect the interference is dominated by the close in channels, say closest 20 channels occupying 800kHz

5. WHAT SHOULD BE THE LIMITS.

How much should be allowed in terms of intersystem interference? As an example, when the interference from the NGE0 into the GEO band was investigated, Inmarsat required this number to be 0.6% raise of noise floor for total interference from an NGE0 system into a GEO satellite. The argument was based on the many sources of interference from systems sharing the band and from systems occupying other bands, so that the budget allocated to a system from an adjacent band was limited to the above 0.6% (CEPT PG SE28, 1995, 1996).

In terms of noise floor consider GSM (DC1800). The requirement in the standard is -70dBW/30kHz. As can be seen this is adequate. In the close in region from about 100 to 350kHz (see the paper by C. Kurby in this Special Session as to how GSM emission mask should be frequency scaled to a typical satellite channel) GSM limit is -50dBW/30kHz, which is in the right order.

6. CONCLUSIONS

In order to serve the growing need for capabilities, satellite systems are employing new technologies. This requires earth terminals to follow an evolution path to reduce unwanted emissions much like the terrestrial systems have gone through. The good news is that the technology is here, due to the progress made by the terrestrial system designers. In this paper we have derived the necessary limits. In another paper in this Special Session (by C. Kurby) it is shown that these limits are indeed feasible in the sense that they can economically be achieved.

BIOGRAPHICAL NOTES

Reuven Meidan received his B.Sc. and M.Sc., both in Electrical Engineering, from the Technion, Israel Institute of Technology and the Ph.D. in Applied Mathematics from the State University of New York at Stony Brook, LI, NY. Following an academic career, he joined Motorola Israel in 1981, where he currently is Chief Scientist.

Dr. Meidan is an IEEE Fellow and a Motorola Dan Noble Fellow. His main fields of interest are in radio communications, in particular satellite-based systems, both from the technical and standardization aspects.

POLARIZATION CROSS-COUPLING IN LEO AND MEO SATELLITE LINKS

Kazimierz Siwiak

Motorola Labs, Strategic Systems, 1500 Gateway Blvd.

Boynton Beach, FL 33426 USA

Tel: +1 561 739 3443 Fax: +1 561 739 3980 E-mail: k.siwia@motorola.com

Key Words: Satellites, satellite EMC, polarization cross-coupling, spectrum sharing.

1. INTRODUCTION

A strategy of relying on orthogonal polarizations for satellite system isolation, although routinely applied in GEO (geostationary earth orbit) *fixed satellite system* (FSS) to provide isolation between satellites that are spaced in geostationary orbits, is not feasible for *mobile satellite system* (MSS), whether they are LEO (low earth orbit), MEO (medium earth orbit) or GEO, and may also be unsuitable for low elevation angle GEO fixed links. The analysis herein shows that polarization isolation, sometimes contemplated for spectrum sharing among MSS systems to increase the capacity of voice, data and paging, or for sharing with GEO FSS, is flawed because polarization becomes highly randomized in the absence of an unobstructed path between the satellite and mobile earth station, especially at frequencies below 3 GHz. The interference and EMC (electromagnetic compatibility) issues are so severe, as shown herein, that the cross-polarization component becomes a viable diversity branch for path links to the urban environment.

This work proposes geometrically based physical mechanisms for circular polarization cross-coupling which build on an earlier urban terrestrial model [1]. The cross-coupling is related to polarization sensitive diffraction and scattering from building roof tops and corner edges, as well as near-specular reflections from building and street surfaces. Recently reported measurements [2-4] along with the analysis herein show that (1) the power density in the cross-polarized signal can nearly equal that of the co-polarized signal in highly scattered environments, and (2) the polarization randomization inherent in LEO and MEO applications below 3 GHz [2-5] effectively precludes frequency sharing among LEO, MEO and GEO satellite-mobile systems on the basis of polarization discrimination.

2. SATELLITE SYSTEM CHARACTERISTICS

There are fundamental differences in the manner in which satellite-mobile systems are used compared with fixed geometry GEO systems. LEO and MEO

satellite systems like Iridium, Globalstar and ICO provide telecommunications services globally to roaming mobile terminals from satellites that are typically at low elevation angles and that are shadowed or blocked from direct line of sight. GEO FSS terminals, on the other hand, are usually in relatively unobstructed fixed and semi-fixed line of sight paths often employing directive antennas at the mobile. Table 1 lists several current and proposed satellite system characteristics.

Table 1. Global mobile personal satellite system characteristics.

System Characteristics	Iridium LEO	Globalstar LEO	ICO MEO	Next Generation GEOs
Uplink, MHz	1,621.35 - 1,626	1,610 - 1,616.25	1,990 - 2,020	1,525 - 1,559
Downlink, MHz	1,621.35 - 1,626.5	2,483.5 - 2,500	2,065 - 2,100	1,626.5 - 1,660.5
Link margin, dB	16* - 30	11 - 16	8 - 12	8
Altitude, km	780	1,400	10,355	35,800
Access method	TDMA / FDMA	CDMA / FDMA	TDMA / FDMA	TDMA / FDMA

* voice channel

2.1 Propagation Impairments in Fixed Satellite Links

The major factors affecting propagation in fixed geometry systems, GEO FSS, are hydrometeor and gaseous attenuation [6], and rain and ice induced depolarization [7-9]. A recent study [10] in the ACTS (Advanced Communications Technology Satellite) program shows that fixed-link propagation impairments are different at low elevations angles (8 degrees) compared with higher elevation angles (52 degrees).

2.2 Propagation Impairments in Satellite-Mobile Links

The major factors affecting propagation in satellite-mobile links are signal shadowing, blocking, diffraction, scattering and reflection. The result is significant signal attenuation and de-polarization. As

seen in Table 1, the LEOs, MEOs proposed MSS GEOs have significant link margin to help mitigate attenuation in the non-line of sight paths. The same mechanism that produces this attenuation also causes polarization cross-coupling.

3. POLARIZATION CROSS-COUPLING

The polarization cross-coupling for the low elevation angle satellite-mobile link is investigated in this section. The basis for the randomization of polarization in the urban environment is presented. The polarization cross-coupling due to roof top and building corner diffraction is quantified, and polarization cross-coupling model components are suggested. Finally, in-building polarization cross-coupling is quantified for measured signals originating from an airborne transmitter flying paths that simulate the geometry of LEO personal communications satellites and the potential for diversity gain is predicted.

3.1 Polarization Definition

Polarization is defined by a complex vector \mathbf{h}_a in terms of the components h_θ and h_ϕ . The general expression for the polarization vector is

$$\mathbf{h}_a = h_\theta \hat{\theta} + h_\phi \hat{\phi} \quad (1)$$

where θ and ϕ are the usual polar coordinate unit vectors. When h_θ and h_ϕ are in phase, the polarization is linear; when there is a phase difference between h_θ and h_ϕ , the polarization is elliptical. Right-Hand Circular (RHC) polarization is defined $h_\phi = -jh_\theta$ and Left-Hand Circular (LHC) polarization is defined $h_\phi = +jh_\theta$. Thus an antenna matched to RHC, with incident polarization $\mathbf{h}_a = a\hat{\theta} - jb\hat{\phi}$, receives a voltage proportional to $a+b$, while a LHC antenna receives $a-b$.

3.2 Polarization Effects of Diffraction

The fields at the mobile, relative to the free space field from the satellite, behave like cylindrically diffracted waves in the lit and shadow regions added to a direct wave $F_d^{s,h}$ in the lit region

$$F^{s,h} = D^{s,h}(\gamma, \gamma') \frac{e^{-jkd_s}}{\sqrt{d_s}} + F_d^{s,h} \quad (2)$$

where angle γ' and γ are the angles of incidence and diffraction shown in Figure 1, k is the wave number and d_s is the distance from the diffracting edge to the mobile ($d_s=30\text{m}$ in Figure 2). $D^{s,h}(\gamma, \gamma')$ is the rooftop or building corner edge diffraction coefficient using UTD (uniform theory of diffraction) expressions given by Leubbers [11] for perfectly conducting wedges and used in [12] for propagation prediction tools. Superscript h in $F_d^{s,h}$ and $D^{s,h}(\gamma, \gamma')$ is used for the polarization component parallel to the plane of incidence (*hard* boundary condition), and s is used for polarization perpendicular to the plane of incidence (*soft* boundary

condition). Since $D^{s,h}(\gamma, \gamma')$ is polarization dependent, the field at the mobile terminal is also polarization dependent. Polarization randomization due to diffraction alone is investigated by observing the diffracted wave polarization compared to the transmitted polarization.

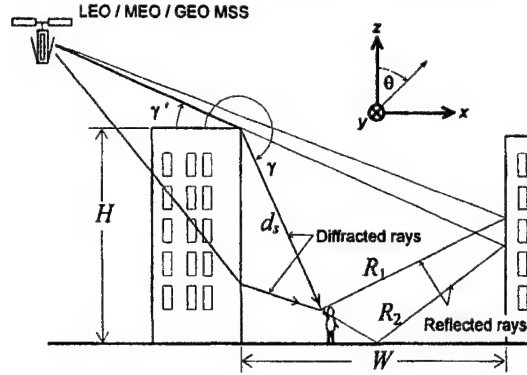


Fig. 1 Geometry for urban diffraction and reflection.

Figure 2 shows the fields including rooftop diffraction for $\gamma'=15$ deg elevation angle to the satellite. The shadow boundary is $\gamma_{\text{shad}}=180+\gamma'=195$ deg.

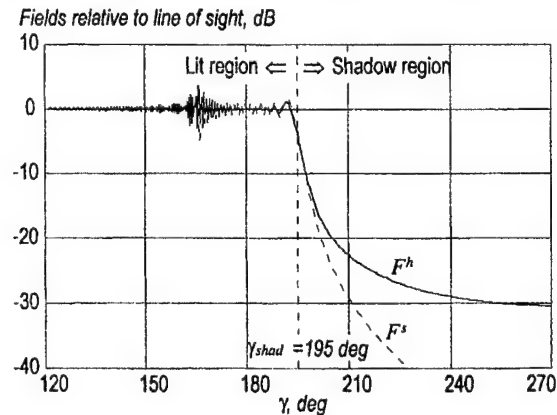


Fig. 2 Fields F^s and F^h for circular polarization incident from $\gamma'=15$ deg elevation on a PEC model of rooftop edge.

3.3 Circularly Polarized Antenna Responses

The mobile terminal antenna is modeled by co-located electric and magnetic dipoles aligned with an axis tilted θ_i from the vertical along the ϕ_i plane. The electric and magnetic dipole outputs are summed or differenced in quadrature to match either RHC or LHC polarization. Thus the co-polarized voltage response in the antenna is

$$V_{\text{copol}} = 20 \log[(F^s + F^h) g(\theta, \phi, \theta_i, \phi_i)] \quad (3)$$

and the cross-polarized response is

$$V_{\text{xpol}} = 20 \log[(F^s - F^h) g(\theta, \phi, \theta_i, \phi_i)] \quad (4)$$

where $g(\theta, \phi, \theta_i, \phi_i)$ is the field pattern of the dipole pair. Such an ideal antenna has perfectly circular polarization response everywhere in space, weighted by the dipole pattern. The cross-polarization coupling is defined as

$$XPOL = V_{xpol} - V_{copol} = 20 \log |(F^e - F^h)/(F^e + F^h)| \quad (5)$$

Note that, unlike V_{copol} and V_{xpol} , $XPOL$ has no pattern dependency for the ideal RHC antenna assumed here.

Figure 3 shows the co-polarization and the cross-polarized responses, as well as the cross-polarization coupling, expressed in decibels, for the roof top diffracted fields shown in Figure 2. The antenna here is tilted $\theta_r = 45$ deg along the $\phi_r = 45$ deg plane.

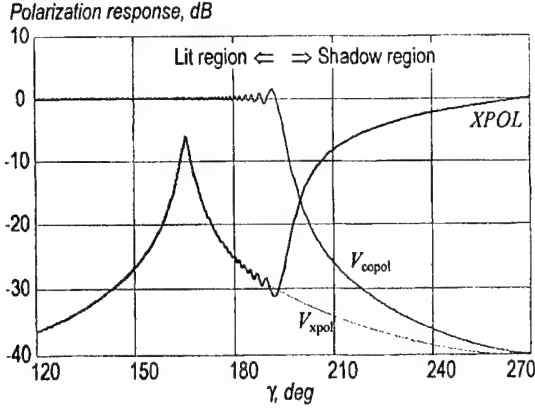


Fig. 3 Cross-polarization coupling ($XPOL$) and responses relative to free space path of RHC and LHC antennas for RHC incident on a roof edge at a 15 deg elevation angle.

In the shadow region the elevation angle to the roof top or "sky line" in degrees is

$$E = \gamma - 180 \quad (6)$$

Akturan and Vogel used photogrammetric techniques [13] to measure the "sky line" and derived probability density functions of sky line elevation angle in suburban and urban areas. Their results show that the skyline elevation angle E is greater than 45 degrees nearly 25% of the time, suggesting that $XPOL$ is between -5 and 0 dB for that time for the rooftop diffracted ray.

3.4 Polarization Randomization due to Reflections

Waves in the urban environment propagate by reflections from buildings and from street surfaces. The cross-polarization coupling for reflected waves is found by applying plane wave reflection coefficients [5], Γ_{par} for the polarization component parallel to the incidence plane, and Γ_{per} for the component perpendicular to the plane of incidence. The coefficients are defined at normal incidence by $\Gamma_{par}(0) = -\Gamma_{per}(0)$. The cross-polarization coupling for a reflection from a building wall (ray R_1 of Figure 1) is

$$XPOL_1 = 20 \log \left| \frac{\Gamma_{par}(90-\theta) - \Gamma_{per}(90-\theta)}{\Gamma_{par}(90-\theta) + \Gamma_{per}(90-\theta)} \right| \quad (7)$$

When an additional ground reflection is considered (ray R_2 in Figure 1) the cross-coupling is

$$XPOL_2 = 20 \log \left| \frac{\Gamma_{par}(90-\theta)\Gamma_{par}(\theta) - \Gamma_{per}(90-\theta)\Gamma_{per}(\theta)}{\Gamma_{par}(90-\theta)\Gamma_{par}(\theta) + \Gamma_{per}(90-\theta)\Gamma_{per}(\theta)} \right| \quad (8)$$

where θ , degrees, is the angle defined in Figure 1.

Figure 4 shows the cross-polarization coupling $XPOL_1$ for a circularly polarized ray R_1 that is reflected once from a vertical building wall, and $XPOL_2$ for a ray R_2 that is additionally reflected from the ground. The two curves begin to separate at an elevation angle near 24 degrees, which is related to Brewster's angle for a dielectric constant of $\epsilon_r = 5$ used here. The cross-polarized signal exceeds the co-polarization by up to tens of decibels, particularly at low elevation angles, and for both low and high elevation angles when an additional street reflection is included. A specularly reflected signal that is otherwise line of sight to the satellite is not significantly attenuated, thus this cross-coupling mechanism may be the dominant impairment to the polarization.

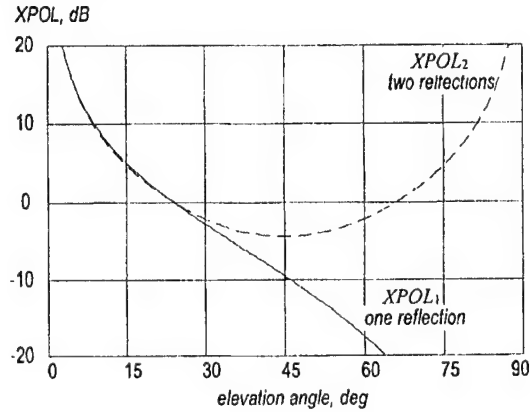


Fig. 4 Polarization cross-coupling after a wall reflection (—), and with the further addition of a ground reflection (---).

4.0 POLARIZATION CROSS-COUPPING MODEL

Signals on urban streets arrive by reflections from buildings, diffraction from roof tops and building edges, and diffraction with subsequent reflection. A model for cross-coupling of circular polarization can be constructed by tracing rays, as shown in Figure 1, for various scenarios, and combining the power in the principal polarization orientations θ and ϕ at the mobile terminal antenna in the manner of the linearly polarized terrestrial model in [1]. Combining signal power is relevant because we are interested in contributions over the multiple rays in a multipath scenario. If the voltage responses are combined as vectors, a full multipath faded response is modeled in the vicinity of the mobile terminal. In this paper all rays are in the x - z plane, and all edges are aligned with x , y or z .

4.1 Model Component for a Rooftop Edge

The power received by RHC and LHC antennas for a single rooftop diffraction are found from the voltage response in (3)-(4). For the co-polarized signal

$$P_{c,D} = |V_{copol}|^2 \quad (9)$$

and for the cross-polarized signal

$$P_{x,D} = |V_{xpol}|^2 \quad (10)$$

4.2 Model Components for Multiple Interactions

Propagation model components of diffracted and/or multiply reflected rays are constructed by ray tracing and multiplying the relevant polarization dependent field modifiers for each geometric interaction, for each of the polarization components. The appropriate diffraction modifier $F^{s,h}$ is applied per polarization at each edge encountered and a reflection coefficient Γ_{per} or Γ_{par} is applied for each reflection. The two polarization components are then combined with the proper antenna pattern weighting as a sum for co-polarization and as a difference for cross-polarization.

Finally, the co- and cross-polarized voltage responses are squared in their magnitude to obtain the power. Power terms can then be summed for each of the co- and cross-polarizations. The power ratio of cross-polarized to co-polarized power is defined as cross-polarization coupling for that set of ray paths under consideration.

5. SIGNAL MEASUREMENTS IN BUILDINGS

Measurements¹ show that circular polarization is nearly completely randomized inside buildings. RHC signals originating from an airborne transmitter were recorded at one millisecond intervals using RHC and LHC receiving antennas. The aircraft traversed paths that simulate the geometry of LEO communications satellites. The signals were received inside a second floor office of a large commercial building.

5.1 Signal Power in RHC and LHC Polarization

Figure 5 shows the RHC and LHC signals measured from the simulated LEO satellite.

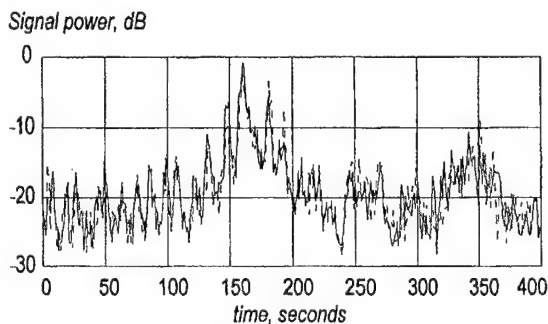


Fig. 5 RHC (—) and LHC (---) signal levels received in a commercial office building and averaged over one second intervals. Source: [3].

The data are averaged over one second intervals to reveal the combined shadowing and free space

propagation loss variations. The power correlation between signals is 0.89, and fast fading was in the range of tens of fades per second.

5.2 Signal Statistics and Diversity Opportunity

The nature of the fast fading is revealed by first “de-meaning” the signals, that is, removing the slow variation shown in Figure 5. The remaining variation is then largely due to multipath. The probability density functions (PDF) of both the RHC and LHC envelopes are shown in Figure 6 along with the difference between them. The two signals differ in average power by 0.7 dB. The PDFs of the two polarizations are nearly identical, indicating a high degree of polarization randomization. The power correlation of the de-meaned signals is 0.10, and the standard deviations of the RHC and LHC signals are 5.13 and 5.07 dB respectively, somewhat below the 5.57 dB of a Rayleigh distributed signal indicating that a dominant signal path exists. The low correlation between the RHC and LHC signals indicates nearly total polarization randomization within the building.

Each of the measured and de-meaned signals were modeled [3] by independent time-space varying multipath components represented by E_{Ray} and a dominant path E_{Dir} having relative power with $K=1.05$. Details of E_{Ray} , E_{Dir} and K are in [14]. The simulated signal PDFs (thin lines) are nearly identical to the measured signal PDFs as seen in Figure 6.

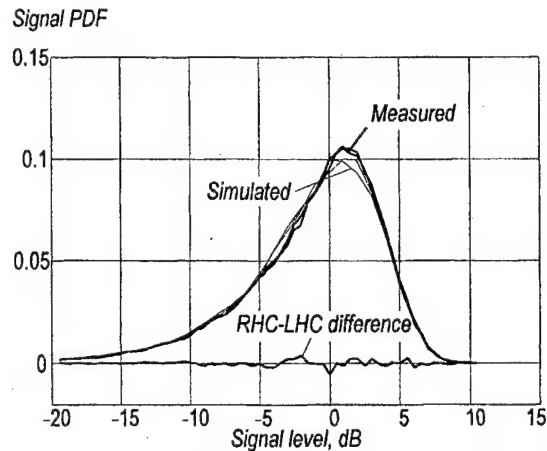


Fig. 6 Measured (bold) and simulated (thin lines) PDFs of the de-meaned RHC and LHC signals and their difference. Source: [3].

Diversity gain is sometimes reported by the “CDF method” [15], defined as the difference between the CDF (cumulative distribution function) of the diversity combined signal and strongest original signal (RHC here) at the 0.1 CDF level. The diversity gain available from the RHC and LHC measurements with PDFs shown in Figure 6 using the “CDF method” is 4.8 dB for selection combining and 6.3 dB for maximal ratio combining.

¹ Data courtesy of Norbert Kleiner, Propagation Engineering Department of Motorola Satellite Communications Group, Phoenix, AZ. Source: [3].

6 SUMMARY AND CONCLUSIONS

The physical basis for the randomization of polarization in the urban environment was presented and polarization cross-coupling due to edge diffraction and to wall and street reflections was quantified. Polarization cross-coupling propagation model components were defined. Building rooftop and corner edges act as polarization "filters" in the diffraction shadow region and impart a cross-polarization component of -5 to 0 dB compared with the co-polarization. Building wall and street reflections result in cross-coupling components that range up to tens of decibels above the co-polarized signal.

Measurements inside buildings indicate that circularly polarized signals are nearly completely randomized hence, the cross-polarization provides a viable diversity branch. The in-building polarization diversity is quantified for signals originating from an airborne transmitter flying paths that simulate the geometry of LEO communications satellites.

The level of the cross-polarization coupling in satellite to low antenna gain mobile terminals in the urban and semi-urban environment effectively precludes the use of orthogonal polarizations as the basis for frequency re-use and spectrum sharing in these systems.

7. REFERENCES

- [1] K. Siwiak, L. A. Ponce de Leon, "Simulation model of urban polarization cross-coupling," *Electron. Lett.*, Vol. 34 No. 22, 29 Oct. 1998, pp. 2168-2169.
- [2] R. Akturan, W. J. Vogel, "Path diversity for LEO satellite-PCS in the urban environment," *IEEE Transactions on Antennas and Propagation*, Vol. 45, No. 7, July 1997, pp. 1107-1116.
- [3] K. Siwiak, "Optimizing body-proximate telecommunications devices in direct and multipath propagation," *Ph.D. Dissertation*, Florida Atlantic University, 1998.
- [4] J. Goldhirsh, W. J. Vogel, *Handbook of Propagation Effects for Vehicular and Personal Mobile Satellite Systems Overview of Experimental and Modeling Results*, Report A2A-98-U-0-021 (APL), EERL-98-12A (EERL), Dec. 1998, Chapter 6.
- [5] K. Siwiak, *Radiowave Propagation and Antennas for Personal Communications, Second Edition*, Artech House: Norwood MA, 1998.
- [6] L. J. Ippolito, "Propagation effects and system performance considerations for satellite communications above 10 GHz," *GLOBECOM '90*, 1990, Vol. 1, pp. 89-91.
- [7] D. J. Bern, J. Janiszewski, A. Paraboni, A. Pawlina, "Rain induced interference between satellite feeder link and direct line-of-sight radio links in K band," *EMC Symposium 1996*, Wroclaw, Poland, June 25-28, 1996, pp. 63-66.
- [8] T. S. Chu, "Rain induced cross-polarization at centimeter and millimeter wavelengths," *Bell Systems Technical Journal*, Vol. 53, No. 8, Oct. 1974, pp. 1557-1579.
- [9] D. V. Rogers, L. J. Ippolito Jr., F. Davarian, "System requirements for Ka-band Earth-satellite propagation data," *Proceedings of the IEEE*, Vol. 85, 6 June 1997, pp. 810-820.
- [10] H. Helmken, R. E. Henning, J. Feil, L. J. Ippolito, C. E. Mayer, "A three-site comparison of fade-duration measurements," *Proceedings of the IEEE* Vol. 85, No. 6, June 1997, pp. 917-925.
- [11] R. Leubbers, "Finite conductivity uniform UTD versus knife edge diffraction prediction of propagation path loss," *IEEE Transactions on Antennas and Propagation*, Vol. 32, No. 1, Jan. 1984, pp. 70-76.
- [12] C. Demetrescu, C. C. Constantinou and M. J. Mehler, "Corner and rooftop diffraction in radiowave propagation prediction tools: a review," *48th International Vehicular Technology Conference*, 18-21 May 1998, pp. 515-519.
- [13] R. Akturan, W. J. Vogel, "Photogrammetric mobile satellite service prediction," *Electron. Lett.*, Vol. 31 No. 3, 2 Feb. 1995, pp. 165-166.
- [14] K. Siwiak, H. Helmken, "Multipath signal model with predetermined statistics," *Electron. Lett.*, Vol. 34 No. 16, 6 Aug. 1998, pp. 1611-1612.
- [15] D. Emmer, E. Humburg, P. Weber, M. Weckerle, "Measurements of base station two-branch polarization diversity reception and a comparison of the diversity gain based on the CDF of signal level and simulations of BER in a GSM system," *48th International Vehicular Technology Conference*, 18-21 May 1998, pp. 5-10.

BIOGRAPHICAL NOTE

Kazimierz (Kai) Siwiak is a Science Advisory Board Associate at Motorola. He is a Registered Professional Engineer and Senior Member of IEEE. He received his B.S.E.E. and M.S.E.E. degrees from the Polytechnic Institute of Brooklyn, Brooklyn, NY, and the Ph.D. from Florida Atlantic University, Boca Raton, FL. Dr. Siwiak holds more than 70 patents, has authored two text book, and has contributed chapters to other books. Prior to joining Motorola, he designed missile antennas and radomes at Raytheon.

SHARING PROPERTIES OF MOBILE SATELLITE SERVICE (MSS) BELOW 1 GHZ AND NATO MILITARY TERRESTRIAL COMMUNICATIONS SYSTEMS

K. S. Kho
NATO HQ C3 Staff / Frequency Management Branch
1110 Brussels
Belgium
Tel. +32.2.707.5504
Fax. +32.2.707.5834 Attn. FMB
E-mail: ks.kho@yucom.be

Low Power Flux Density (PFD) is used in the International Telecommunications Union (ITU) and Conference of European Postal and Telecommunications Administrations (CEPT) as a significant parameter to determine whether a new system could share frequency spectrum with existing systems. The PFD's of systems are made low by spreading the signal leading to a high frequency spectrum bandwidth requirement. This situation is not efficient in case of sharing between civil and military systems since the frequency management of both systems is totally separated. The analysis in this paper is limited only to demonstrate the above phenomena.

Note: In the whole paper "sharing" means "co-channel sharing".

1. INTRODUCTION

CEPT SE 28 carried out studies in supporting sharing of Low Earth Orbit (LEO) Satellite Messaging systems with existing systems.

In addition, CEPT was looking for 2 X 5 MHz Mobile Satellite Service (MSS) band below 1 GHz for civil use. Under the current conditions, use of the spectrum for civil MSS is not allowed due to restrictions imposed under footnotes or other arrangements. CEPT SE 28 carried out the investigation.

The MSS system proposed, is based on Direct Sequence Spread Spectrum (DSSS) with CDMA access mechanism. One of the significant reasons to apply DSSS and CDMA in this regard is to make PFD, especially of the down-link signal, low. With low PFD's, it is hoped that sharing of frequency spectrum with existing systems would be possible.

In the following paragraphs, characteristics of some typical wide- and narrow band military systems will be discussed. It will be demonstrated that the application of DSSS would not always result in sharing behaviour expected.

Finally, the current trend shows that more and more Commercial off The Shelf (COTS) equipment will also be deployed for military use. Therefore, the need for frequency spectrum sharing between military and civil users will occur more frequently. In order to make the frequency spectrum sharing optimal, selection of modulation schemes should be performed carefully. In this regard, trade off between conventional and spread spectrum modulation schemes will be outlined.

2. POWER FLUX DENSITY (PFD)

In the ITU discussions, limit on the PFD's is probably the most important criterion for frequency sharing between systems. Spreading transmitted spectrum under Direct Sequence (DS) or Frequency Hopping (FH) scheme is common to achieve lower PFD's of transmission systems with defined transmission capacities. Low PFD's at the expense of a wider spectrum required should only be useful if sharing with existing systems could be realized. Applying this method, from a frequency management point of view, will result in:

Advantages:

- a. reduced co-ordination distance
- b. reduced required frequency separation

Disadvantage:

- c. more required frequency spectrum/occupied bandwidth.

In a final decision one should consider carefully the advantages and disadvantages of spreading spectrum to lower PFD in lieu of making sharing with existing systems feasible.

Extensive, real time and detailed information of the systems sharing frequency spectrum is required for an efficient frequency management. Therefore, special considerations should be given if two different frequency management authorities manage the systems planned to share a piece of frequency spectrum.

3. SYSTEMS ANALYSED

For illustration purposes, the following systems are considered:

Victim / Military systems:

Tactical Radio Relay (R/R)
Air Ground Air Radio (AGA)

Interferer / MSS Earth terminal:

Mobile Earth Station (MES)

Tactical radio relay represents wide band multi channel ground systems.

Tactical airborne AGA radio represents narrow band single channel airborne systems. The AGA system comprises of ground and airborne terminals.

MES represents a DSSS single channel terminal of mobile satellite service below 1 GHZ systems.

MSS below 1 GHz using Low Earth Orbiting (LEO) satellites is normally aimed for Non Voice and not real time nor interactive communications. The capacity required is normally low. Therefore, the required base band bandwidth should not be more than 25 kHz.

The relevant characteristics of the above mentioned systems are listed in table 1.

4. PROPAGATION MODELS

Two propagation models are used for the calculations. The terrestrial propagation losses were calculated with Okumura-Hatta model for rural area (ITU-R Rec. 529 and Rep. 567-3) and the Ground to Air, Air to Ground and Air-Air propagation losses were calculated using the basic Free Space model.

5. INTERFERENCE CALCULATIONS

Scenario

To illustrate the situations, several scenarios will be described. The situations are concentrated in the cases where military systems could be interfered by MES's deployed in the NATO military 225 – 400 MHz band.

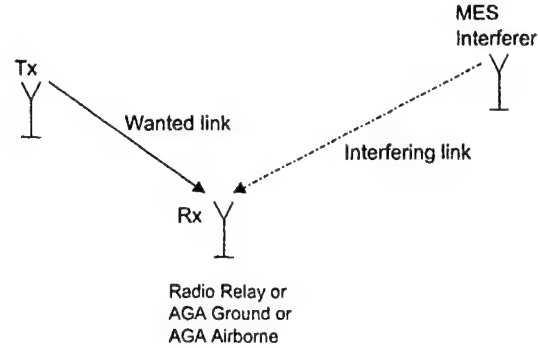


Figure 1: Schematic diagram of the interference scenario

	R/R	AGA Gnd	AGA Airborne	MES
Tx Output Power (Watts)	10	20	10	1
Tx Output Power (dBm)	40	43	40	30
Tx / Rx Antenna Gain (dB)	9	0	0	0
Tx / Rx Antenna Height(m)	22	40	10000	1.5
Opening angle (deg)	60	360	360	360
Occupied Bandwidth (kHz)	1000	25	25	1500
Rx noise factor (dB)	7	10	10	5
Noise (dBm)	-107	-120	-120	-107
Acceptable Degradation due to Sharing with MSS	1 dB (Noise plus Interference level maximally 1 dB higher than Noise level without Interference from MSS)			

Table 1: Characteristics of the discussed systems

On Tune Rejection (OTR)

On Tune Rejection (OTR) is taken into account in the calculations of the interference power.

$$\text{OTR (dB)} = 10 \cdot \log(BW_{\text{Victim}} / BW_{\text{Interferer}}) \\ \text{if } BW_{\text{Victim}} < BW_{\text{Interferer}} \text{ otherwise} \\ = 0 \quad (1)$$

Note: BW = Bandwidth.

Calculations of received power and noise at receiver input

Calculations of the received power is based on the following equation:

$$Pr = Pt + Gt + Gr + \text{OTR} - \text{Pathloss} \quad (2)$$

Where: Pr = Received power (dBm)
Pt = Output power (dBm)
Gt = Transmitter antenna gain (dBi)
Gr = Receiver antenna gain (dBi)
OTR = On Tune Rejection (dB)
Pathloss = Propagation loss (dB)

Noise level at the receiver input is as follows:

$$\text{Noise} = 10 \cdot \log(kT_o) + 10 \cdot \log(B) + \text{NF} \quad (3)$$

Where: P noise = Noise level at the input of the receiver (dB)

K = Boltzmann Constant
 $= 1.38 \cdot 10^{-23}$ (J/K)

B = Bandwidth of the receiver (Hz)

NF = Noise Figure of the receiver (dB)

Scope of calculations

The scope of calculations is limited to the ones required to demonstrate that lowering PDF values at the expense of frequency spectrum is not always appropriate, especially in situations where real-time and detailed frequency management is not practical such as sharing frequency spectrum between civil and military users.

5.1. MES interfering R/R (See: Fig 1)

Noise level at the input of the Rx of R/R is:

$$\begin{aligned} \text{P noise} &= 10 \cdot \log(KT_oB) + 7 \\ &= -174 + 60 + 7 \\ &= -107 \text{ dBm.} \end{aligned}$$

The noise level may increase maximally 1 dB due to interference. Therefore, the maximum interference power falling into the receiver BW (Pint-max) tolerated is:

$$\begin{aligned} \text{Pint-max} + \text{P noise} &= \text{P noise} + 1 \\ \text{Pint-max} + -107 &= -106 \\ \text{Pint-max} &= -112.9 \text{ dBm.} \end{aligned} \quad (4)$$

Pint-max falling into the BW of the victim Rx is:

$$\begin{aligned} \text{Pint-max} &= P_{\text{MES}} + G_{\text{MES}} + G_{\text{R/R}} + \text{OTR} - \text{PathLoss} \\ \text{PathLoss} &= 30 + 0 + 9 + 10 \cdot \log(1000/1500) - -112.9 \\ &= 150.1 \text{ dB.} \end{aligned} \quad (5)$$

Based on Okumura-Hatta model for rural area, pathloss of 150.1 dB corresponds to a distance of 24.6 km.

If the MES signal was not spread, the distance above would be:

Pint-max falling into the BW of the victim Rx is:

$$\begin{aligned} \text{Pint-max} &= P_{\text{MES}} + G_{\text{MES}} + G_{\text{R/R}} + \text{OTR} - \text{PathLoss} \\ \text{PathLoss} &= 30 + 0 + 9 - -112.9 \\ &= 151.9 \text{ dB.} \end{aligned} \quad (6)$$

Based on Okumura-Hatta model for rural area, pathloss of 151.9 dB corresponds to a distance of 26.5 km.

Therefore, in this case, spreading the signal is not decreasing the coordination area.

5.2. MES interfering AGA Ground (GND) (See Fig.1)

Noise level at the input of the Rx of AGA GND is:

$$\begin{aligned} \text{P noise} &= 10 \cdot \log(KT_oB) + 10 \\ &= -174 + 44 + 10 \\ &= -120 \text{ dBm.} \end{aligned}$$

The noise level may increase maximally 1 dB due to interference. Therefore, the maximum tolerated interference power falling into the receiver BW is:

$$\begin{aligned} \text{Pint-max} + \text{P noise} &= \text{P noise} + 1 \\ \text{Pint-max} + -120 &= -119 \\ \text{Pint-max} &= -125.9 \text{ dBm.} \end{aligned} \quad (7)$$

Pint-max falling into the BW of the victim Rx is:

$$\begin{aligned} \text{Pint-max} &= P_{\text{MES}} + G_{\text{MES}} + G_{\text{AGA GND}} + \text{OTR} - \text{PathLoss} \\ \text{PathLoss} &= 30 + 0 + 0 + 10 \cdot \log(25/1500) - -125.9 \\ &= 138.1 \text{ dB.} \end{aligned} \quad (8)$$

Based on Okumura-Hatta model for rural area, pathloss of 138.1 dB corresponds to a distance of 15.3 km.

If the MES signal was not spread, the distance above would be:

Pint-max falling into the BW of the victim Rx is:

$$\begin{aligned} \text{Pint-max} &= P_{\text{MES}} + G_{\text{MES}} + G_{\text{AGA GND}} + \text{OTR} - \text{PathLoss} \\ \text{PathLoss} &= 30 + 0 + 0 + 0 - -125.9 \\ &= 155.9 \text{ dB.} \end{aligned} \quad (9)$$

Based on Okumura-Hatta model for rural area, pathloss of 155.9 dB corresponds to a distance of 36.4 km.

Therefore, in this case, spreading signal is decreasing coordination area and making sharing more practical.

5.3. MES interfering AGA Airborne (AIRB) (See Fig.1)

Noise level at the input of the Rx of AGA AIRB is:

$$\begin{aligned} \text{P noise} &= 10 \cdot \log(KT_oB) + 10 \\ &= -174 + 44 + 10 \\ &= -120 \text{ dBm.} \end{aligned}$$

The noise level may increase maximally 1 dB due to interference. Therefore, the maximum tolerated interference power falling into the receiver BW is:

$$\begin{aligned} \text{Pint-max} + \text{P noise} &= \text{P noise} + 1 \\ \text{Pint-max} + -120 &= -119 \\ \text{Pint-max} &= -125.9 \text{ dBm.} \end{aligned} \quad (10)$$

Pint-max falling into the BW of the victim Rx is:

$$\begin{aligned} \text{Pint-max} &= P_{\text{MES}} + G_{\text{MES}} + G_{\text{AGA AIRB}} + \text{OTR} - \text{PathLoss} \\ \text{PathLoss} &= 30 + 0 + 0 + 10 \cdot \log(25/1500) - -125.9 \end{aligned} \quad (11)$$

=138.1 dB.

At flying altitude of 10000 m, the radio horizon distance of the aircraft is 400 km.

Based on free space model, pathloss at a distance of 400 km is only 123.6 dB which is 14.5 dB less than attenuation required for an acceptable interference.

Therefore, in this case, spreading signal is not decreasing coordination area at all. Any MES within the radio horizon distance of an aircraft would probably interfere reception of an AGA radio in an aircraft despite the wide spectrum used by the MES.

It is clear that in case of airborne receptions, sharing frequency spectrum with base band waveforms is preferred rather than spreading the signal. Eventually, the existing users could offer a single channel to be used exclusively to the other system.

6. CONCLUSIONS

Based on the examples given in this paper, It can be concluded that:

- a. To lower PFD values to allow sharing leads to a need for use of more frequency spectrum.
- b. In ground to ground cases, lowering PFD values by spreading signals leads to smaller co-ordination distances.
- c. Spreading reduces the required co-ordination distance more if the ratio between the bandwidths of the victim and the interferer after spreading is smaller.
- d. However, in airborne cases, spreading interfering signals does not lead to any reduction of co-ordination distances. The co-ordination distance is the radio horizon distance of the aircraft.
- e. If spreading signal does not lead to an advantageous frequency – distance jamming curve, keeping the signal as narrow as possible is more efficient from sharing view point.

7. RECOMMENDATIONS

The following are recommended:

- a. To perform a trade off between spreading and concentrating signals in sharing studies.

- b. In case concentrating signal is more advantageous, to consider the application of multi-level modulation schemes.
- c. To concentrate the signal if different authorities conduct frequency management of systems sharing frequency spectrum.

8. REFERENCES

- a. ITU CCIR
Recommendations and Reports of the CCIR, 1986 Volume V
PROPAGATION IN NON-IONIZED MEDIA
- b. Mischa Schwartz
Information Transmission, Modulation, and Noise Third Edition

BIOGRAPHICAL NOTE

Mr. Kho is graduated in Electrical Engineering at the Surabaya Institute of Technology in 1975 and the Eindhoven University of Technology in 1980. His main projects are as follows:

- a. 1973 - 1979 over water 4 GHz microwave propagation measurements.
- b. 1981 – 1988 Dutch National Defense Research Establishment, TNO Physics and Electronic Laboratory:
 - Development of the Dutch Army Tactical Area Communications System ZODIAC.
 - Development of the Dutch Army Tactical Mobile Communications including Frequency Hopping Combat Net Radio and Single Channel Radio Access (SCRA).
 - Various measurements project in support of development of frequency management systems.
- c. 1988 - 1997 NATO Allied Radio Frequency Agency / CIS Division of IMS
- d. 1998 - NATO HQ C3 Staff, Frequency Management Branch
 - Carrying out NATO EMC Analysis (NEMCA) studies
 - Working in various topics in the frequency management area
 - EMC Analysis of military systems etc.
 - Project Officer for the replacement of the NATO UHF Frequency Assignment System (NUFAS).
 - Supporting various CEPT groups in technical studies regarding sharing between military and civil systems.

EMC 2000

INTERNATIONAL WROCLAW SYMPOSIUM
ON ELECTROMAGNETIC COMPATIBILITY

STANDARDIZATION OF Ka-BAND SATELLITE TERMINALS

Dr. Peter Siebert

Société Européenne des Satellites

L-6815 Chateau de Betzdorf

Grand Duchy of Luxembourg

Fax: +352 710725 482

Peter_Siebert@ses-astra.com

ABSTRACT

Over the last couple of years the global market for direct-to-home (DTH) satellite and cable delivery of broadcast television and radio has seen a considerable growth. This growth is expected to increase even further with the transition to digital multi-channel broadcasting, improving choice and convenience and lowering delivery cost per viewer in the long term. Internet and other interactive services are already driving that growth.

The growing demand for satellite capacity forces satellite operators to explore new frequency bands such as the Ka-band transmit frequencies 27.5 – 31.0 GHz. Interactive multimedia services will use the 29.5 - 30.0 GHz frequency band that has a world-wide exclusive allocation to the Fixed Satellite Service (FSS) on a primary basis by the International Telecommunications Union (ITU).

This frequency band has only been used for experimental purposes to date. Standards specifying the essential requirements under the Radio & Telecommunications Terminal Equipment (R&TTE) Directive are needed to create a mass market in Europe. These standards have to cover safety, ElectroMagnetic Compatibility (EMC) and effective use of spectrum/orbital resources. Once a terminal fulfils these essential requirements it may carry a "CE" mark and can be placed on the European Market without further restrictions.

Recently the European Telecommunications Standards Institute (ETSI) published the standards covering EMC and effective use of spectrum/orbital resources. The ASTRA Broadband Interactive System will be one of the first satellite systems to employ terminals compliant to these standards.

1. SINGLE MARKET AND EUROPEAN DIRECTIVES

One of the most important achievements of the European Union (EU) is the creation of the Single Market consisting of 15 member countries. With 377 million people and a GDP of 7750 Billion USD this market is one of the biggest in the world.

Free movement of goods is a cornerstone of the Single Market. Restrictions to free movement have been diverging national technical standards and regulations. The mechanism to guarantee free movement of products is to prevent trade barriers by mutual recognition and technical harmonization. Mutual recognition means that products legally manufactured or marketed in one country can move freely throughout the community. Technical harmonization is limited to essential requirements that products placed on the Community market must meet to benefit from free movement within the Community. These essential requirements are defined in Directives applicable in all EU countries [1]. The technical specifications of products meeting the essential requirements are laid down in Harmonized Standards. Products manufactured in compliance with Harmonized Standards benefit from presumption of conformity with corresponding essential requirements. However application of harmonized or other standards remains voluntary and the manufacturer may always apply other technical specifications.

Products fulfilling the essential requirements laid down in one or more applicable Directives are subject to free movement. A CE mark on the product indicates that it complies with the essential requirements. The CE marking is proof that the manufacturer is responsible for the conformity of his product to all requirements of

the applicable Community Directives. Hence Member states are not allowed to restrict the placing on the market and putting into service of CE marked products, unless such measures can be justified with proof of non-compliance.

Essential requirements are stated in very broad terms and cover a wide range of products. It is the responsibility of the European Standardization Organizations (SO) to derive technical specification from these requirements for specific products or product classes. These technical specifications are published in Harmonized Standards. The Commission formally requests the European SOs to present Harmonized Standards by issuing a mandate. The technical contents of such standards are under the entire responsibility of the SO. Harmonized Standards provide a presumption of conformity with the essential requirements, if their reference has been published in the Official Journal of the European Communities (OJEC) and if they have been transposed at national level. However it is not necessary that transposition takes place in all Member States.

2. THE R&TTE DIRECTIVE

The applicable Directive for all telecommunication terminals is Directive 99/5/EC on Radio and Telecommunications Terminal Equipment (R&TTE) [2]. It was approved by the European Parliament on March 9 and published in the OJEC on April 7, 1999. It takes effect on April 8, 2000.

The scope of this Directive covers basically all Radio and Terminal equipment. One of the exemptions of particular relevance is broadcast receive equipment.

Essential requirements covered by the Directive are

- the protection of the health and safety of the user and any other person;
- the protection requirement with respect to EMC;
- radio equipment shall be constructed so that it uses effectively the spectrum allocated to terrestrial/space radio communication and orbital resources so as to avoid harmful interference.

The health and safety requirement is quite general and covers all aspects of safety like electrical and mechanical. It extends the scope of the Low Voltage Directive to voltages below 50 V.

The requirements concerning EMC specify that the device must be able to operate in a certain electromagnetic environment. Neither shall its performance be degraded by electromagnetic disturbances coming from this environment, nor shall it add significant amount of disturbance to this environment.

Whereas the first two bullet points apply to all kinds of terminal equipment the last one is limited to radio devices. It shall guarantee that the terminal makes efficient use of the spectrum and/or orbital resources, which are by their nature scarce resources. The term "effective" has not been defined within the Directive leaving the interpretation to the SOs.

The R&TTE Directive will greatly simplify the approval process, reducing testing costs and time to market. For terminal devices, where Harmonized Standards exist the manufacturer may declare conformity to the essential requirements based upon tests to the relevant Harmonized Standard(s), with or without supervision of a notified body, as described in the Annexes to the Directive.

The R&TTE Directive furthermore requires that operators of public networks publish their (air) interface specification to such an extent that manufacturers can design and test equipment accordingly. In addition the network operator has the obligation to give access to all terminals fulfilling the essential requirements.

3. Ka-BAND SATELLITE TERMINALS

The scope of the R&TTE Directive covers all types of satellite earth stations except TeleVision Receive Only (TVRO) terminals. Satellite terminals operate in several frequency bands. Historically satellite services started with C-band terminals covering the 4/6 GHz frequency band. The next frequency band to be employed was Ku-band at 11/12/14 GHz. Limitation of spectrum and orbital resources at C and Ku-band is the reason for deployment of Ka-band frequencies at 20/30 GHz for new services. The ITU has allocated the range 29.5 – 30.0 GHz to Fixed Satellite Service worldwide on a primary basis. It is expected that these Ka-band frequencies will be used for new interactive multimedia services based on a large number of uncoordinated, small and low power earth stations.

Typically the wavelength λ at Ka-band transmit frequencies is about 1 cm. Since the performance of aperture terminals is determined by the ratio D/λ between diameter D and wavelength, Ka-band terminals will perform better than equally sized C or Ku-band equipment.

Ka-band radiation is subject to severe attenuation by water. Heavy rainfalls can reduce the power of a Ka-band signal by up to 10-20 dB. To guarantee a reasonable availability of the telecommunication service, countermeasures like Uplink Power Control (UPC) for transmit terminals or site diversity for receive earth stations may be necessary.

In satellite system with UPC the terminal will employ one or a combination of these countermeasures during fading conditions:

- increase the output power;
- reduce the bandwidth of the transmitted signal;
- increase channel coding while reducing the available data rate for the user.

In general UPC requires powerful amplifiers providing sufficient margin to counteract rainfades. For the time being these amplifiers are one of the main cost drivers of a Ka-band terminal.

There are two different modes for implementing UPC. In the closed loop mode the received power of the transmitted signal is measured by the Network Control Facility (NCF). Based on these measurements UPC commands are sent back to the terminal, which reacts accordingly. The disadvantage of this approach is the long delay introduced by geostationary satellites. Considering typical change rates for rain attenuation at Ka-band frequencies of 1-2 dB/s the system may be too slow to counteract a fade. The second approach is the open-loop concept, where the terminal autonomously performs UPC based on the power of the received signal and no NCF intervention is required. This approach suffers from the fact that receive and transmit frequencies may be affected differently by rain. Especially when reception is in Ku-band the attenuation of the receive signal may not be equivalent to the attenuation of the transmit signal at Ka-band frequencies.

4. STANDARDIZATION OF SATELLITE TERMINALS IN ETSI

The relevant standardization body for all Harmonized Standards falling under the scope of the R&TTE Directive is the European Telecommunications Standards Institute (ETSI), which is responsible for all telecommunication-related standards. The focal point for all satellite-related activities within ETSI is the Technical Committee for Satellite Earth Stations and Systems (TC SES).

In November 1996 TC SES started to work on Harmonized Standards for Ka-band terminals. The Ka-band working group was created and is responsible for the standardization of all kinds of Ka-band satellite terminals. Work items for three different Ka-band terminals were opened, where each work item covers different transmit and/or receive frequency bands. Common to the scope of all three work items is that:

- an NCF is responsible for the monitoring and control of the transmit functions of the terminal;
- the terminals operate through geostationary satellites;
- the transmitted signals are always of digital nature;

- the antenna diameter does not exceed 1.8 m.

The work item for Satellite Interactive Terminals (SIT) covers equipment transmitting in the 29.5-30.0 GHz frequency range and receiving in the 10.7 - 12.75 GHz Ku-band frequency range. Satellite User Terminals (SUT) also transmit at 29.5 - 30.0 GHz and receive in the Ka-band frequencies 17.7 - 20.2 GHz as well as 21.4 - 22.0 GHz. The third work item describes "wideband" SUTs transmitting in the 27.5 - 29.5 GHz frequency range. Reception is in the same frequency bands as defined for SUTs.

5. HARMONIZED STANDARD FOR EFFECTIVE USE OF SPECTRUM/ORBITAL RESOURCES

The Ka-band working group decided that the most urgent demand was for standards for SITs and SUTs. Before starting work on a Harmonized Standard, two voluntary standards should be produced. These voluntary standards are EN 301358 [3] for SUTs and EN 301359 [4] for SITs. After having passed the ETSI approval process these two documents are now publicly available.

After having completed these two ENs the Ka-band working group started to work on the Harmonized Standard by merging the two documents and modifying some of the technical content. The resulting document is prEN 301 459 [5]. The expected date of publication is within the year 2000.

prEN 301459 contains the technical specification, which a SIT or a SUT must be compliant with, to fulfil the essential requirement of effective use of orbital and spectrum resources. This is achieved by defining limits for several types of emissions:

- off-axis spurious radiation;
- on-axis spurious radiation;
- off-axis EIRP emission density within the band;
- transmit polarization discrimination (XPD);
- carrier suppression.

In addition antenna pointing accuracy is specified as well as minimum requirements for Control and Monitoring Functions (CMF). The document also contains detailed test specifications.

5.1. Off-axis spurious radiation

The specification of this parameter covers all kinds of unwanted emission in the frequency range from 10 MHz to 40 GHz with the exception of the operational frequency band (29.5 - 30.0 GHz) itself. All directions are considered except for a cone around the transmit axis with an opening of 7°. The purpose of this specification is to limit interference into other services like e.g. fixed links but also satellite services.

5.2. On-axis spurious emission

This requirement covers all on-axis emission in the operational band 29.5 – 30.0 GHz excluding the transmitted signal itself. Its purpose is to limit interference with other services at the same orbital location operating in the same frequency band.

5.3. Off-axis EIRP density

The purpose of this specification is to limit any radiation to satellite systems at other orbital locations. When specifying the off-axis EIRP density a trade-off has to be made between the power requirement in the desired direction and any transmission in the unwanted direction. Increasing the power density of the transmitted signal automatically increases interference with neighbouring satellite system. Therefore the specification has to take into account the typical orbital separation of satellites as well as the satellite G/T, which is related to the satellite receive spot beam size. Furthermore the specified limits will determine the minimum antenna size and the maximum EIRP spectral density. Whereas the antenna size is an important marketing aspect the latter restricts data rate and availability.

After long and quite controversial discussions the Ka-band working group agreed on a maximum EIRP in any 40 kHz bandwidth not exceeding these limits:

19 - 25 log ϕ dBW	for	$1,8^\circ \leq \phi \leq 7,0^\circ$
-2 dBW	for	$7,0^\circ < \phi \leq 9,2^\circ$
22 - 25 log ϕ dBW	for	$9,2^\circ < \phi \leq 48^\circ$
-10 dBW	for	$\phi > 48^\circ$

Where ϕ is the angle, in degrees, between the main beam axis and the direction considered.

In general this specification can only be fulfilled with a minimum antenna size of at least 65-70 cm and limits the power at the antenna feed to a maximum of -10 dBW/40kHz. It allows a minimum satellite spacing of 2° and a typical satellite receive spot beam opening of about 1° .

For systems using UPC the limits given above apply for clear sky conditions and may be exceeded by the attenuation of the transmit signal relative to clear sky conditions in case of rain fades.

5.4. Cross polar discrimination

This specification is required to protect signals on the orthogonal polarization. Depending on the satellite system architecture the XPD requirements may vary. The XPD specification of 20 dB provides sufficient protection for satellite spotbeam systems without polarization reuse in a spotbeam. More stringent requirements for satellite systems with polarization reuse in a spotbeam will be subject to contractual agreements for the use of the space segment.

5.5. Carrier suppression

This specification limits the radiated power, when the terminal is in the transmission disabled state.

5.6. Antenna pointing accuracy

This requirement shall guarantee that the antenna can be adjusted and fixed with typically 0.1° pointing accuracy. Only for the mechanical capabilities of the antenna are specified. The installation process is not covered!

Furthermore the antenna shall withstand wind speeds of 100 km/h with gusts of 130 km/h without any sign of permanent distortion and no need to repoint.

5.7. Control and monitoring functions

A minimum set of CMFs shall be implemented in the terminals to minimize the probability that they create unwanted transmission:

- Most important is the "no transmission without reception" principle ensuring that the terminal only transmits when it receives the control channel signal of the satellite system it wants to access. This requirement guarantees a proper alignment of the antenna to the desired satellite and minimizes interference into other satellite or terrestrial systems. In addition transmission has to stop as soon as the control channel is lost. This may happen because of misspointing or by human beings standing in front of the antenna.
- The terminal has to monitor all transmission related sub systems and stop transmission immediately when it has detected a μ -processor or transmit sub system (e.g. local oscillator) error.
- In general the terminal may only transmit, when it has received a transmit validation from NCF. The only exception is an initial burst required by some systems after power-on of a terminal for first network access. Because this burst may interfere, its duration and frequency are limited.
- Each terminal must provide a unique identification in the network to allow the NCF to switch off any terminal via the control channel.

6. ESSENTIAL REQUIREMENTS ON SAFETY AND EMC

Beside compliance to the essential requirement of effective use of spectrum/orbital resources Ka-band terminals must also be compliant with the essential requirements on safety including health and EMC. EN 300 673 [6] contains the essential requirements for EMC for all kinds of satellite earth stations operating in the FSS bands of C, Ku and Ka-band frequencies. Concerning safety and health issues no

document specific to satellite earth stations exists. Guidance on these issues can be found in EN 60950 [7] and ENV 50166-2 [8].

7. ASTRA BROADBAND INTERACTIVE SYSTEM

The ASTRA BroadBand Interactive (BBI) system will be one of the first satellite systems to employ SITs in its network. The BBI system provides a Ka-band return path at 29.5-30.0 GHz transmitted from a SIT located at the user premises, thus complementing new and existing ASTRA Ku-band forward path services by forming a 2-way end-to-end network via satellite. The NCC being a part of the Network Control Centre (NCC) assigns all bandwidth and power resources and controls the log-on, authorisation and transmission of the SITs via a forward signalling path in Ku-band frequencies. The forward channel consists out of a standard Ku-band DVB-S/MPEG-2 broadcast signal that uses Multi-Protocol Encapsulation (MPE) [9] to provide services, including IP multicast, to selected users and user groups at up to 38 Mbit/s.

The SITs providing the Ka-band satellite return path from the individual user or group of users will consist of fixed, small antenna (e.g. 75 cm) and an Indoor Unit which can be connected via 10BaseT to a multimedia PC or a Local Area Network.

The return path data received by the NCC is then routed to its final destination either via a Ku-band forward path or terrestrially.

The satellite access protocol is based upon Multi-Frequency Time Division Multiple Access (MF-TDMA) and allows each SIT to dynamically request the satellite capacity required to transmit its traffic. The NCC will allocate the necessary time and frequency slots to the individual SITs and will provide synchronisation information to the network.

The initial end-to-end network is IP-based and provides the industry standard IPsec and its associated key distribution mechanism for security.

8. REFERENCES

- [1] Guide to the implementation of Directives based on New Approach and Global Approach; V1.0, 1998.
- [2] Directive 1999/5/EC on radio equipment and telecommunications terminal equipment and the mutual recognition of their conformity; OJEC, 7.4.1999.

For [1] and [2] see:

<http://forum.europa.eu.int/Public/irc/dg3/tcam/info/data/welcome.html>

[3] EN 301 358: Satellite Earth Stations and Systems (SES); Satellite User Terminals (SUT) using satellites in geostationary orbit operating the 19,7 GHz to 20,2 GHz (space-to-earth) and 29,5 GHz to 30,0 GHz (earth-to-space) frequency bands, V 1.1.1, 1999, ETSI

[4] EN 301 359: Satellite Earth Stations and Systems (SES); Satellite Interactive Terminals (SIT) using satellites in geostationary orbit operating the 11 GHz to 12 GHz (space-to-earth) and 29,5 GHz to 30,0 GHz (earth-to-space) frequency bands, V 1.1.1, 1999, ETSI

[5] prEN 301 459: Satellite Earth Stations and System; Harmonized EN for Satellite Interactive Terminals (SIT) and Satellite User Terminals (SUT) transmitting towards satellites in geostationary orbit in the 29,5 GHz to 30,0 GHz frequency band covering essential requirements under article 3.2 of the R&TTE directive, ETSI

[6] EN 300 673: Electromagnetic compatibility and Radio spectrum Matters (ERM); ElectroMagnetic Compatibility (EMC) standard for Very Small Aperture Terminal (VSAT), Satellite News Gathering (SNG), Satellite Interactive Terminals (SIT) and Satellite User Terminals (SUT) Earth Stations operated in the frequency ranges between 4 GHz and 30 GHz in the Fixed Satellite Service (FSS), V 1.2.1, 1999, ETSI

[7] EN 60950: Safety of information technology equipment; CENELEC

[8] ENV 50166-2: Human exposure to electromagnetic fields; High frequency 10 kHz to 300 GHz; CENELEC

[9] EN 301 192: Digital video broadcasting (DVB); Specification for data broadcasting, V1.2.1, 1999; DVB/ETSI.

BIOGRAPHICAL NOTE

Peter Siebert received his M.Sc. degree in 1984 and his Ph.D. degree in 1989 in physics from the J.W. Goethe University in Frankfurt/Main (Germany), respectively.

Since 1995 he is with SES-ASTRA, a European Satellite operator based in Luxembourg, where he is involved in planning and development of the ASTRA Broadband Interactive system. He also represents his company at ETSI. As ETSI rapporteur he was responsible for drafting EN 301 359 [4] and EN 301 459 [5].

OH SATELLITE, OH SATELLITE!

T.A.Th.Spoelstra

ESF Committee on Radio Astronomy Frequencies
P.O.Box 2, 7990AA Dwingeloo, the Netherlands
email: spoelstra@nfra.nl, URL: <http://www.nfra.nl/craf>

Defective space systems are no longer ghost systems: their number is gradually increasing and must no longer be neglected. This evolution urges the development of adequate regulatory and enforcement instruments to prevent further deterioration of the electromagnetic environment for non-space applications. The paper explains some typical examples of defective space systems and especially their impact on passive radiocommunication services, i.e. radio astronomy, and recommends actions to improve the situation.

To contribute to the improvement of the situation, it is recommended that organizations as the ITU, European Commission, the CEPT and space organizations develop an adequate strategy to manage defective space systems and several recommendations to improve international regulation and development of enforcement tools for administrations are made.

1. INTRODUCTION

With the increasing number of space systems the related EMC issues increase as well. In the design of the space stations the radio frequency protection of and the compatibility with other systems must be taken into account similar as all other radiocommunication systems have to do. Commercial and technological limitations may, however, lead to space systems which do not comply to EMC criteria as they apply to terrestrial systems. This observation leads to distinguish the following categories of space systems:

- a space system in which protection of other radio applications has been or will be implemented;
- a space system which is improved to protect other radio applications;
- a space system in which by design no protection of other radiocommunication services has been built in;
- a space system which causes harmful interference to other radiocommunication services because of malfunctioning of system components.

This paper discusses the issue of noted EM-incompatibility between space systems and passive applications, both space and terrestrial. This is partly due to the allocation status of different space and

terrestrial radiocommunication services sharing the same frequency band or in bands adjacent to each other in the ITU-R Radio Regulations [6]. Another observation which must be made, is that at present adequate EMC guidelines and regulations are lacking for space systems. This environment bears the potential of the development of defective space systems.

It should furthermore be noted that various spectrum policy positions recently developed by organizations such as the European Commission, EC, have been written primarily from the perspective of terrestrial use of radio [5]. At international level a view on a regulatory strategy on defective space systems is lacking. In many cases, these defects are known because they generate harmful interference or produce some other negative impact on other systems. We note that the comments of the ESF Committee in Radio Astronomy Frequencies, CRAF, to the EC spectrum policy document [3] have not found any reflection in the final version of the EC Green Paper on this issue [5].

An adequate strategy on defective space systems and regulatory improvements are of great help to Administrations, especially when it is notified that there are reasons to expect that the extent and impact of this problem on other applications of radio (space based or terrestrial) is rapidly increasing. In various groups, studies are done to develop technical criteria which could be fed in into EMC regulation. However, a strategy on defective space systems has such a complicating aspect that some operators of space applications are reluctant to pay adequate attention to system quality if in their view this is not commercially viable. Furthermore, it is general practice that for space systems operating in the fixed-satellite and mobile-satellite services no mitigation factors are considered and all burden from compatibility issues is put on the terrestrial services.

The paper finally summarizes recommendations for regulatory improvements.

2. SPACE SYSTEMS AND PASSIVE APPLICATIONS

A *passive* service is a receiver-only radiocommunication application. The paramount

example of a passive service is radio astronomy for which the transmitter is a *physical process*. Radio astronomy cannot have any influence on the transmitting source nor on the frequency this source likes to transmit. All other radiocommunication services control both a transmitter and receiver which both can be manipulated by man. The difference between the nature of an active service and a passive service is the major cause of the vulnerability of radio astronomy to interference from active services. For radio astronomy, this vulnerability is enhanced by the fact that the received signals from celestial radio sources are of the order of 10^9 times weaker than common practice in active service applications.

Terrestrial passive services are especially susceptible for interference from aeronautical and space systems because transmissions from such system can easily enter directly into the main lobe of the antenna beam of a receiving installation. Passive space systems receive interference from other space systems through the sidelobes of their antennas and also from ground stations, of course. Active space systems should have been equipped with adequate filtering, spectrum modulation and beam shaping to prevent interference to other services including passive services. It is obvious that defective space systems generate significant EM-incompatibility with passive earth and space stations [1][8]. A space station for passive use of radio is e.g. the Japanese satellite for Very Long Baseline Interferometry, HALCA, which operates as an element of terrestrial VLBI networks. Such a station is susceptible for interference from Earth-to-space transmissions.

The vulnerability for defective space system is enhanced by allocations of frequency bands for space-to-Earth transmissions adjacent to passive services as occurs in many places in the ITU-R Radio Regulations [6].

3. ON THE MEANING OF 'DEFECT' AND 'DEFECTIVE'

We understand that 'a defect apparatus' is 'not satisfying its design objectives or required quality of operation'. In this context 'defective' in the context of radiocommunication systems is defined as 'generating malfunctioning of other radio systems or system components'.

3.1. Internal system defect

A system is considered to be defective when because of defects, it cannot function according to the requirements set by the design objectives.

3.2. External system defect

With respect to other systems, a defective system has degrading impact on the correct functioning of one or more of the other systems. Interpreted in this

way, a defective system generates EM-incompatibility between systems and apparatus.

Following this interpretation, a defective space system is a system that generates EM-incompatibility with other systems and apparatus.

In this document, we address the issue of systems which are EM-incompatible with other systems and apparatus. Obviously this issue is not limited to passive services only, although they are the first to suffer.

4. EXAMPLES

Typical examples of defective systems which cause significant and irrecoverable damage to scientific research using radio frequencies are (see Table 1 for a summary):

- the US military satellite TEX at 328 MHz;
- the Russian system for radionavigation by satellite GLONASS at 1.6 GHz;
- the US based satellite system for mobile communication by satellite Iridium at 1.6 GHz for the user links;
- the fixed-satellite system ASTRA 1-D operated by a Luxembourg based operator at 10.7 GHz.

4.1. The TEX satellite

In 1992, radio astronomers detected in the 322.0 - 328.6 MHz band harmful interference from a space station which was at that time unknown. In the frequency band 322.0-328.6 MHz the Fixed, Mobile and Radio Astronomy services enjoy a primary (shared) allocation. Because of this allocation situation, the operations of a space station in this band were not expected: they do not comply with the ITU-R Radio Regulations.

After several years of investigation it turned out that the interfering source was a US military satellite launched on April 11, 1990: the TEX satellite. The service of this satellite ended in June 1991. However, it was recognized by the company currently responsible for the operations of the satellite that the transmissions of the satellite were not stopped after its exploitation ended: the system kept transmitting a signal at a frequency of 328.25 MHz. The system could not be made silent because intentionally the system has no "off"-switch to prevent fatal unintentional shutdown and it can still receive commands and download telemetry. Also the transmissions into the direction of the earth cannot be suppressed by changing the attitude of the object because the TEX gravity gradient boom was damaged during the process to bring the satellite properly in orbit.

By continuous control from ground stations the system is kept silent [11]. For a final solution of the issue, we have to wait until the space system brakes down.

4.2. The GLONASS system

Interference caused by GLONASS transmissions in the band 1610.6 - 1613.8 MHz degraded radio astronomical observations dramatically in the years between the launch of the first GLONASS satellites. With the full GLONASS constellation the band 1610.6 - 1613.8 MHz would be closed for any radio astronomical research. In 1993 the Inter-Union Commission on the Allocation of Frequencies, IUCAF, representing the international radio astronomy community and the GLONASS administration agreed on a step-by-step plan to clear the band 1610.6-1613.8 MHz of interference by GLONASS. The plan involves the improvement of satellite design, moving the satellite frequencies to an adjacent band, and the filtering of their unwanted emissions. By 2005 this plan will be completed as agreed.

The modernized system will use the same modulation as the current one [1][2][7].

4.3. The Iridium system

The WARC 1992 allocated the band 1610.6-1613.8 MHz to the Radio Astronomy Service on a primary basis. It also allocated the band 1610-1626.5 MHz to the Mobile-Satellite Service, MSS, (Earth-to-space) on a primary basis. MSS (space-to-Earth) got a secondary status in the band 1613.8-1626.5 MHz. Furthermore, in the ITU-R Radio Regulations a footnote was added to the band 1610-1626.5 MHz which states that *harmful interference shall not be caused to stations of the radio astronomy service using the band 1610.6 - 1613.8 MHz by stations of the radiodetermination-satellite and mobile-satellite services.*

The Iridium Satellite System uses the band 1621.35-1626.5 MHz for both Earth-to-space and space-to-Earth transmissions. The Iridium system was designed and built by Motorola Inc, who wrote to IUCAF in 1991 that it was aware of the issue of the protection of radio astronomy in the band 1610.6-1613.8 MHz and that *"Motorola's goal is to share frequencies in a manner that will not interfere with radio astronomy or other MSS/RDSS services."*

In the course of time it became clear that Motorola did not implement measures in the Iridium system to protect any radiocommunication service as can be read from the publications on the design of the system (as can be extracted e.g. from its Main Mission Antenna Concept [10]). Motorola Inc showed that the space-to-Earth transmissions in the band 1621.35-1626.5 MHz will cause harmful interference of up to 30 dB above the levels for detrimental interference for radio astronomy as given in ITU-R Recommendation RA769 presumably except during periods of low communication traffic.

Although the situation for the service links at 1.6 GHz is well-known, the inter-satellite link transmission case causing harmful interference to radio astronomy in the frequency range 22-23 GHz is still under study.

Concrete planning of improvement of the next generation of Iridium satellites is not known to the author of this document and does presumably not exist.

4.4. ASTRA

The frequency band in which the Radio Astronomy Service has a primary allocation, i.e. 10.6 - 10.7 GHz, is adjacent to the band allocated to the Fixed-Satellite Service, i.e. 10.7-11.7 GHz. Out-of-band emissions into the band 10.6 - 10.7 GHz caused by the GDL-6/ASTRA-1D satellite operating at a frequency of 10.71 GHz makes radio astronomical observations in the geographical area served by the ASTRA system impossible. The operator, *Société Européenne des Satellites* in Luxembourg, was informed by CRAF about this harmful interference which is as measurements show 30 dB above the level of detrimental interference a radio astronomy station can tolerate in this frequency band.

The operator confirmed the validity of the complaint of CRAF. Following investigations by the operator, the latter concluded that the uplink transmissions had to be improved. This improvement turned out to alleviate the problem to some extent but far not sufficient to re-open the frequency band 10.6-10.7 GHz for radio astronomy operations by stations in the geographical area served by ASTRA [9]. A defect in the satellite itself may or may not be the cause.

At present no perspective exists that the problem will be solved before the (i.e. geostationary) satellite will be replaced.

5. REGULATIONS

As noted in the introduction, a view on a regulatory strategy on defective space systems is lacking. Also, adequate EMC guidelines and regulations for space systems are not available.

In the examples given above, the acuteness of the impact of the defective systems has been removed by different measures:

- the entity currently responsible for the maintenance of the TEX satellite has taken measures to keep the satellite silent by operational action at ground stations;
- GLONASS is improving its system to improve compliance with the ITU-R Radio Regulations and the protection of the radio astronomy service;
- Motorola Inc and Iridium LLC have made agreements with radio astronomy entities to regulate the pollution generated by the Iridium system [4]. This approach does obviously not comply with the ITU-R Radio Regulations and generates regrettable precedents that may dilute the status of the ITU-R Radio Regulations and ultimately of an international treaty [12]. However, since a clear view on EMC guidelines and regulations for space systems and a strategy on defective space systems is lacking at entities such as the World Trade Organisation and the European Commission, their national equivalents and regulatory authorities significantly dominated by industry such as the US

Federal Communication Commission, FCC, the political pressure on radio astronomers to accept

agreements such as those with Motorola Inc and Iridium LLC was tremendous;

System	Issue	Defect	Perspective	Responsible entity
TEX	Transmission in band not allocated to space service (frequency: 328.25 MHz)	No on/off switch	Operational action to keep suppress transmissions until satellite 'dies'	US Department of Defense
GLONASS	Operations within and adjacent to the band 1610.6-1613.8 MHz.	Inadequate suppression of interfering signal	System is gradually improved to have the interference removed by 2005	GLONASS administration
IRIDIUM	Spurious emission from the band 1616.5-1621.35 MHz into the band 1610.6-1613.8 MHz.	Design	No perspective for improvement	<i>Manufacturer:</i> Motorola Inc <i>Operator:</i> Iridium LLC
ASTRA 1-D	Harmful interference from out-of-band emission into the band 10.6-10.7 GHz to the radio astronomy service.	Space station system defect? Also: wrong allocation: downlink adjacent to passive service	Currently no perspective for improvement	ASTRA/SES

Table 1: Typical examples of defective space systems

- The ASTRA case has not been solved yet in ways similar to the possibilities just mentioned and the discussion to address the adjacent band issues for the Fixed-Satellite Service in the frequency band 10.7-12.75 GHz is subject to further consideration within the CEPT. ASTRA continues to transmit as a broadcasting satellite to household TV systems and the assumed customer interests are considered to have higher priority than action by the operator to comply with international public law, i.e. the ITU-R Radio Regulations [6] and moreover with umbrella treaties such as the UN Outer Space Treaty [13].

These examples show very clearly the consequences of a lacking view, strategy and regulation for defective space systems. It must be said that the ITU-R Radio Regulations contain some articles that address space system operations and their cessation, such as article S22.1 which says that *space systems shall be fitted with devices to ensure immediate cessation of their radio emission by telecommand, whenever such cessation is required under the provisions of these Regulations* but in general the Radio Regulations do not go beyond stating that space systems shall not cause unacceptable interference to other systems and contain therefore tables with power flux density levels that must not be exceeded. Furthermore, the example of the TEX satellite shows that apparently an

article as S22.1 which is very relevant for handling of defective systems can be interpreted in such a way that the manufacturer of a space station does not consider himself bound by this regulation.

In the examples given above, the problems with the TEX satellite and the GLONASS system are managed in compliance with the ITU-R Radio Regulations but obviously the other mentioned systems can continue their operations although they violate these regulations when commercial interest is given priority.

6. RECOMMENDATIONS

In order to improve the handling of defective space systems, the following recommendations could be considered:

- articulation of the UN Liability Convention to issues related with defective space systems into subsequent regulation of the issue [13];
- improvement of the definition of *damage* from the UN Liability Convention;
- international regulation to handle defective space systems. In such regulation key elements should be:
 - a. public interest has higher priority than commercial interest of the private party responsible for the defective system;
 - b. the ITU-R Radio Regulations clauses addressing e.g. necessary cessation of space system operations

(such as article S22.1) need improvement to enhance the responsibility obligations for the space systems and to provide Administrations with adequate enforcement instruments regarding defective space systems;

c. extend the liability towards victims of defective space systems to administration which gave a license to the application of the defective space system on its territory;

- development of adequate satellite monitoring facilities to support administrations in their handling of the issue of defective space systems;

- development of internationally accepted procedures to provide enforcement tools to Administrations in the issue of defective space systems. Issues which need improvement are licensing and legislation to support enforcement to manage defective space systems. Licensing should not be restricted to the country from which territory a space system is launched or the country which hosts the base office of the space system operator [13];

- development of a regime in which the licensing of space system is made subject to the administrative approval of the demonstrated mitigation techniques and measures implemented in the space station to safeguard spectrum purity and prevent harmful interference to other applications using the electromagnetic environment;

- regulations to assist victim services and bodies in the quantification of the claims against defective space systems;

- improvement and adjustment of relevant regional and national legislation wherever necessary.

7. CONCLUSIONS

Defective space systems are no longer ghost systems: real daily practice shows that their number is gradually increasing and must no longer be neglected. This evolution urges the development of adequate regulatory and enforcement instruments to prevent further deterioration of the electromagnetic environment for non-space applications. This issue should find a place high on the agenda of organizations such as the ITU, the EC, the CEPT and national administrations.

8. REFERENCES

- [1] CRAF Handbook for Radio Astronomy, 2nd edition, CRAF secretariat, 1997.
- [2] CRAF Handbook for Radio Astronomy, 2nd edition, CRAF secretariat, 1997, p.107.
- [3] "Public Consultation on EC Green Paper on radio spectrum policy", CRAF Internet page: <http://www.nfra.nl/craf/crafgbcom.htm>, 1999.

- [4] "CRAF Newsletter 1999/2", CRAF Internet page: <http://www.nfra.nl/craf/nwsl9902.htm>, 1999.

- [5] European Commission, "Green Paper on Radio Spectrum Policy", Document COM(1998)596, 1998, Brussels.

- [6] ITU-R Radio Regulations, ITU Publications, Geneva, 1998

- [7] R.J.Cohen, "The GLONASS-Radio Astronomy Joint Experiment", Proceedings of the 12th International Wroclaw Symposium on Electromagnetic Compatibility, Wroclaw, June 28-July 1, editors: J. Janiszewski, W. Moron and W.Sega, 1994, p.530-533

- [8] R. J. Cohen, "Radio pollution: the invisible threat to radio astronomy", *Astronomy & Geophysics*, Vol.40, 1999, p.6.8-6.13.

- [9] K. Ruf, E. Fürst and W. Reich, "At the Limits - Radioastronomical Observations with the Effelsberg 100m Telescope", Proceedings of the 14th International Wroclaw Symposium, June 23-25, 1998, J. Janiszewski, W. Moron and W. Segal, p.625-628.

- [10] J. J. Schuss, J. Upton, B. Myers, T. Sikina, A. Rohwer, P. Makridakas, R. Francois, L. Wardle, W. Kreutel and R. Smith, "The IRIDIUM® Main Mission Antenna Concept", Proceedings of the IEEE International Symposium on Phased Array Systems and Technology, 15-18 October 1996, Boston, MA, pp.411-415.

- [11] T.A.Th.Spoelstra, "The TEX Satellite and Radio Astronomy", Proceedings of the 14th International Wroclaw Symposium on Electromagnetic Compatibility, Wroclaw, June 23-25, editors: J. Janiszewski, W. Moron and W.Sega, 1998, and the CRAF internet page: <http://www.nfra.nl/craf/tex.htm>.

- [12] T.A.Th.Spoelstra, "Regulations and scientific use of radio frequencies", Proceedings of the 15th International Wroclaw Symposium on Electromagnetic Compatibility, Wroclaw, June 27-30, editors: J. Janiszewski, W. Moron and W.Sega, 2000.

- [13] United Nations Treaties and Principle on Outer Space, Vienna, 1994.

BIOGRAPHICAL NOTES

Dr.T.A.Th.Spoelstra is secretary and frequency manager of the Committee on Radio Astronomy Frequencies of the European Science Foundation. His research experience is related with polarization studies of cosmic radio waves, cosmic magnetic fields, radio wave propagation through ionized media, systematic philosophy and philosophy of science. He has served the Netherlands Foundation for Research in Astronomy as Head of Operations of the Westerbork Radio Observatory. He can be reached at: CRAF, NFRA, P.O.Box 2, 7990 AA Dwingeloo, The Netherlands [tel.: +31-521-595100, telefax: +31-521-597332, email: spoelstra@nfra.nl].

RISK OF INTERFERENCE TO AIRCRAFT FROM VSAT, SNG AND SIT TERMINALS

Ryszard J. Zielinski

The Wroclaw University of Technology, Institute of Telecommunication and Acoustics
Wybrzeze St. Wyspianskiego 27, 50-370 Wroclaw, Poland

Phone +48 71 321 49 98, Facsimile +48 71 322 34 73, Email: Dick@zr.ita.pwr.wroc.pl

This paper provides an analysis of the risk of interference resulting from aircraft exposure to the main beam of a satellite terminals of various types.

Presented analysis aimed at determining: the parameters of electromagnetic exposure experienced by an aircraft during landing approach. Three kinds of terminals SNG, VSAT and SIT were analysed. The results were compared with vulnerability limits of existing standards. To complete the analysis some results of fuselage attenuation measurements done by ERA Technology (UK) are described. In the conclusion the potential risk of interference from various satellite terminals is discussed.

1. INTRODUCTION

With the ever increasing use of Very Small Aperture Terminals (VSAT) and Satellite News Gathering Transportable Earth Stations (SNG TES) there is an urgent need to define the potential risk of interference to aircraft passing through the main beams of such stations. This problem was raised in ERC during October 1996 meeting and administrations were encouraged to contact their national Civil Aviation Authority to get information on this subject. Except for Denmark no other Administrations have taken measures as to limit the use of SNG and VSAT terminals in close proximity to airports and glide paths.

This paper provides a detailed analysis of the risk of interference resulting from aircraft exposure to the main beam of a Satellite Earth Station (SES). Since the worst case conditions considered in the study for SNG terminal pertained to the near-field zone of the antenna, use is made of the near-field radiation model [1].

The risk of interference to airborne electronic equipment depends not only on the level of electromagnetic exposure, but also on the attenuation of the fuselage - a parameter which is essential to the systems operating inside the aircraft. Systems involving an external antenna as one of their elements must be analysed separately for the interference transferred via this antenna. Investigations into aircraft fuselage attenuation were carried out in Great Britain [2]. The paper includes a brief description of these studies and of the results obtained in the frequency range which applies to transmissions via VSAT and SNG terminals.

The risk of interference to airborne electronic equipment varies according to the parameters of the interfer-

ence itself and according to the vulnerability of the equipment to relevant type of exposure. It is therefore essential to determine the vulnerability levels at which the functioning of the apparatus is not substantially distorted. In Britain, vulnerability tests have been carried out [3] for some parts of the airborne equipment. It is a well established fact that, having calculated the shapes and levels of electromagnetic pulses (by taking into account fuselage attenuation) and having compared them with the vulnerability levels of the exposed electronic equipment, we can establish the risk of interference to airborne equipment in neuralgic phase of the flight - during landing.

2. PARAMETERS OF TYPICAL VSAT, SNG AND SIT TERMINALS

The analysis of satellite terminals aimed at determining the shapes and levels of electromagnetic exposure experienced by an aircraft during landing approach. VSAT and SNG terminals (Fig. 1 and Fig. 2) with electrical parameters listed in table 1 were analysed in [4, 5].

Table 1. Basic parameters of the typical satellite terminals under analysis

Parameter	VSAT ⁽¹⁾	SNG ⁽²⁾	SIT ⁽³⁾	SIT ⁽⁴⁾
Trans. power P [W]	5	490	0.5	2
Diameter of aperture D [m]	1.8	2.6	0.6	1.2
Frequency f [MHz]	14.125	14.125	29.75	29.75
D/ λ ratio	85	122	60	119
Zone boundary D _{fz} [m]	305	637	71	286

⁽¹⁾ GTE Spacenet Corp. Skystar Plus system

⁽²⁾ Dornier GmbH VMA -2.6/73/25

⁽³⁾ SES Astra SIT for 144 kbps

⁽⁴⁾ SES Astra SIT for 2048 kbps

3. AIRCRAFT EXPOSURE TO THE MAIN BEAM

A satellite terminal produces particular threat to a landing aircraft which makes use of the instrument landing system (ILS). Any interference that might affect the variety of measuring and receiving devices involved

can lead to a catastrophe. For this reason, our analysis concentrates on this part of the flight.

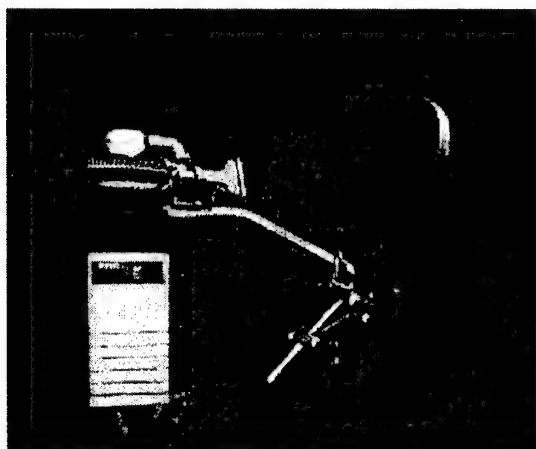


Figure 1. Typical VSAT terminal



Figure 2. Typical SNG terminal

A typical path of approach when the ILS is used was considered [4]. For the needs of analysis we adopted the most common elevation angle of the path of approach in the ILS, which amounts to $\phi=3^\circ$. Irrespective of its type, the aircraft becomes exposed to the beam of the ILS at the distance from 18 to 13 km (10 to 7 nm). At the height $h_G=300$ m (1000 ft) the pilot has to decide whether he is landing or pulling off the machine. Once the decision has been made, the pilot cannot change it. And that is why this altitude is regarded as the most neuralgic point of the landing operation - misinformation coming from the deck part of the ILS may lead to a catastrophe. The height of 300 m has been taken to analyse the potentiality for a terminal induced interference to the ILS. For simplification, analysed is the location of the terminal on the extension of the airstrip.

The member countries of the European Union direct their efforts towards a widespread application of VSAT and SNG systems by liberalising their licence policies. Operators providing such services have been authorised to install VSATs, and SNGs wherever necessary or possible. Advertisements claim that such systems can work at the user's or that they can provide communication from an arbitrary point in Europe (which is of importance in the case of SNG). In the nearest future the new type of satellite terminal SIT with interactive capabilities will be available for everybody. This terminal will receive

DVB-S signal in K_U band from the satellite and use satellite interactive channel in K_a band to send the request for information via satellite to the server. Hence, it cannot be excluded that terminals of that kind will be located at a point where the antenna "illuminates" the path of approach immediately before reaching the critical height at which the pilot has to decide whether to land or to make a re-approach. For this phase of the landing approach, the variations in the amplitude of the electromagnetic field strength (to which the aircraft is exposed) will be determined.

Taking into account the difference in field strength determination between the near zone and the far zone of the antenna radiation, the calculations will involve models for both the zones. If we use the far zone model, initial dissipation of energy in the antenna aperture becomes negligible. But if use is made of the near zone model, the physical dimensions of the antenna aperture must be considered [1].

4. VSAT OF ADMISSIBLE PARAMETER VALUES

From the results of the analysis [6] it can be inferred that VSATs of standard emission parameters produce the smallest threat of interference to the aircrafts. However unlike other terminals, VSATs have a defined admissible level of EIRP, a limited size of antenna aperture and a limited transmission rate. Making use of these parameters, we can construct a model of such a VSAT that produces the highest interference threat, and we can analyse it as if it were a standard VSAT.

Our consideration, which pertain to what is known as the worst case, may soon become an issue of vital importance because of the more and more widespread use of multi-medial systems with much higher demands made on the transmission rate than those made nowadays. These systems may incorporate VSATs with parameter values to the critical ones.

According to the definition proposed by ITU (ETSI), a VSAT should meet the following requirements:

- $EIRP \leq 52$ dBW/40 kHz,
- $D \leq 2,4$ m (ITU) or $D \leq 3,7$ m (ETSI),
- $R_b \leq 2048$ kbps.

On that basis it is possible to determine the maximum EIRP value for the VSAT. The maximum bandwidth covered by the VSAT depends on the modulation used. The spectral effectiveness $\rho = R_b/B$, for selected modulations made use of in satellite radiocommunications is shown in Table 2.

Table 2. Spectrum effectiveness (in theory and in practice) for different types of modulation

Modulation	Spectrum effectiveness ρ [b/s/Hz]	
	Theoretical	Practical
BPSK	0,5	$0,7 \div 0,8$
QPSK	1,0	$1,4 \div 1,6$
MSK	0,67	$0,9 \div 1,1$

Assuming that the VSAT makes use of the least spectrum-effective modulation (BPSK) and transmits at an admissible rate (2048 kbps), we can determine the width of the occupied band, which is 4,096 MHz and 3.0 MHz in theory and practice, respectively. $EIRP_{max,B}$ (in

dB) for the given band is defined by the following relation:

$$EIRP_{\max, B} = EIRP_{\max, 40 \text{ kHz}} + 10 \cdot \log\left(\frac{B_{\text{MHz}}}{40}\right)$$

For the band $B=3 \text{ MHz}$ we have:

$$EIRP_{\max, 3 \text{ MHz}} = 52 + 18,8 = 70,8 \text{ dB.}$$

If the diameter of the antenna aperture D is known, we are able to calculate the power radiated in the main beam, $P_{ef} = EIRP_{\max, B} - G_{VSAT}$. The gain of the antenna is defined by the relation $G_{VSAT} = \eta \left(\frac{\pi \cdot D}{\lambda} \right)^2$,

assuming that the aperture efficiency factor η , is 0,55. Calculations were carried out for three aperture sizes: 1.8 m, 2.4 m, and 3.8 m. A standard aperture has a diameter of 1.8 m, so our previous calculations were performed for this value. Aperture diameter of 2.4 m and 3.8 m are acceptable in terms of ITU and ETSI recommendation, respectively. Table 3 gathers the calculated values of gain G_{VSAT} and of the power radiated in the main beam P_{ef} . If we assume that 90% of the power supplied to the antenna is radiated by the main beam, we will be able to establish the required power at the antenna input.

Table 3. Power radiated by VSAT in the main beam, allowing determination of the admissible EIRP values for various aperture diameters of the antenna (14,125 GHz)

Aperture diameter [m]	Gain [dBi]	Power P_{ef} [dBW]	Power P_{ef} [W]
1,8	45,9	29,8	964
2,4	48,4	27,3	542
3,8	52,4	13,4	216

Table 4. Parameters of VSAT with $EIRP_{\max, 40 \text{ kHz}} = 52 \text{ dBW}$

VSAT	Power P_{ef} [W]	Aperture diameter D [m]	Frequency f [MHz]	D/λ	Zone boundary D_{fz} [m]
#1	964	1,8	14,125	85	305
#2	542	2,4	14,125	113	542
#3	216	3,8	14,125	179	1360

5. RESULTS OF SIMULATION

Making use of the models described in an earlier paper [4], calculations were carried out for terminals characterised by the parameters listed in Table 1 and 4. Two elevation angles ε were adopted, 30° and 10° . These are, respectively, the approximately maximum and the approximately minimum elevation angles for the terminals located throughout Poland and co-operating with geostationary satellites [6, 7]. Figures 3 to 7 show the calculated results obtained with the two elevation angle values for the purpose of comparison. But it is only one of the models that should be taken into account. The choice depends on the distance between the analysed points in the path of approach and the satellite station. If this distance is longer than that to the far zone, the electromagnetic field strength must be established in

terms of the far-zone model. If not, use should be made of the near-zone model. The field strength amplitude for the relevant model is shown by the solid line. There is the distance between the antenna and the points under analysis and distances to the far zone presented in the pictures. The speed with which the aircraft travels during landing approach was assumed to be 77 m/s (about 280 km/h) in every instance.

The first two figures present result of simulation for SIT. Two types of SIT were analysed [8]. The first one for small bit rate 144 kbps and the second one for high bit rate 2048 kbps.

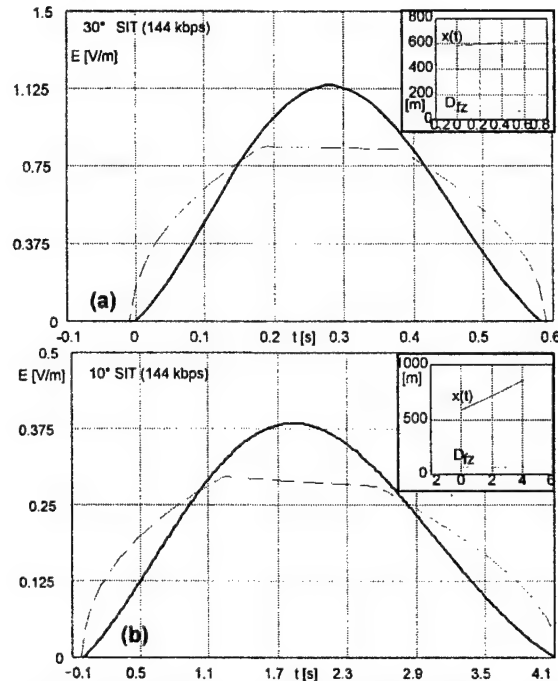


Figure 3. Amplitude of electromagnetic field strength during aircraft travel through the main beam radiated by the antenna of a SIT (144 kbps) for antenna elevation angle a) $\varepsilon=30^\circ$ b) $\varepsilon=10^\circ$ ($x(t)$ - distance to the analysed points, D_{fz} - distance to the far zone)

As far as the SIT (144 kbps) is concerned, the points of interest were located in the far zone at the elevation angle of 30° and 10° . The maximum value of the electric field strength ranged between 1.1 V/m (30°) and 0.4 V/m (10°), whereas the duration of aircraft exposure to the main beam varied from 0.58 s (30°) to 4.1 s (10°). Compared to the vulnerability levels of the electronic equipment (in the K_U band) made use of by the aircraft, these values were of two orders smaller.

The similar situation takes place when SIT with capabilities for transmission rate 2048 kbps is analysed. The points of interest for both elevation angles (30° and 10°) are located in the far zone. The maximum value of the electric field strength ranged between 4.5 V/m (30°) and 1.6 V/m (10°), whereas the duration of aircraft exposure to the main beam varied from 0.29 s (30°) to 2.0 s (10°). The amplitude of interfering signal radiated from SIT (2048 kbps) is four times higher than radiated from SIT (144 kbps) but it is still far below the vulnerability levels of the electronic equipment (in the K_U band) made use of by the aircraft.

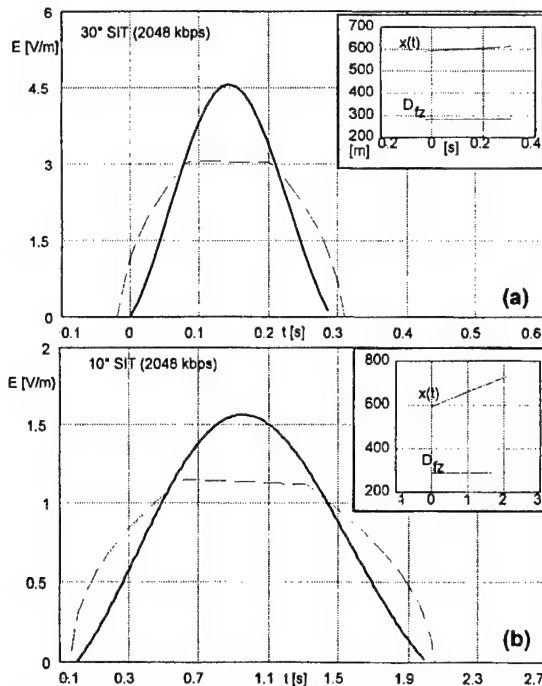


Figure 4. Amplitude of e-m field strength during aircraft travel through the main beam radiated by the antenna of a SIT (2048 kbps) for elevation angle a) $\varepsilon=30^\circ$ b) $\varepsilon=10^\circ$

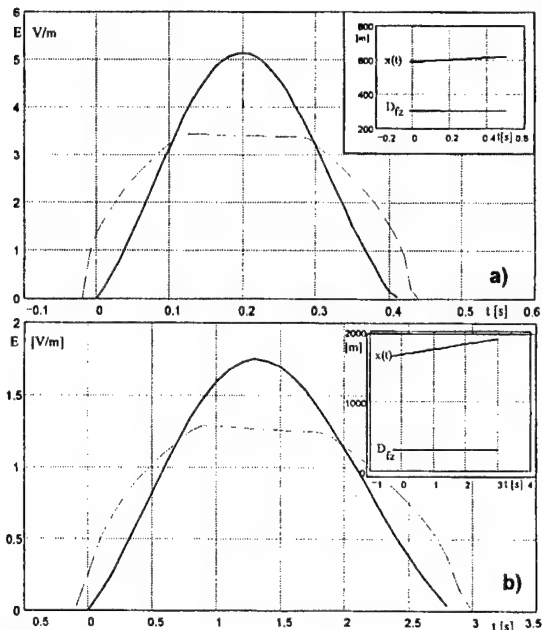


Figure 5. Amplitude of electromagnetic field strength during aircraft travel through the main beam radiated by the antenna of a typical VSAT for antenna elevation angle a) $\varepsilon=30^\circ$ b) $\varepsilon=10^\circ$

When the object under analysis was a conventional VSAT, the points of interest were situated in the far zone. The maximum value of the electric field strength varied from 5.1 V/m (30°) to 1.7 V/m (10°), whereas the duration of aircraft exposure to the main beam ranged from 0.4 s (30°) to 2.8 s (10°). Compared to the vulnerability levels for the electronic equipment of the aircraft [3, 5], these values were small. It should be noted that the agreement of results between the two methods is

quite good. Thus, the near-zone model also applies to the far zone.

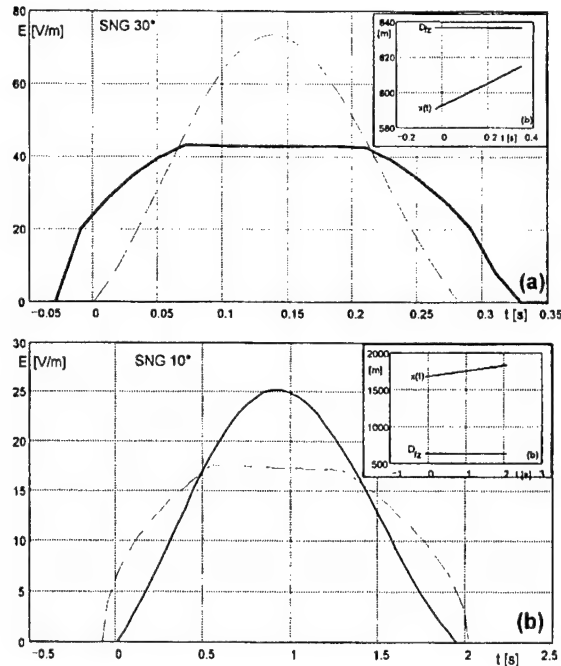


Figure 6. Amplitude of electromagnetic field strength during aircraft travel through the main beam radiated by the antenna of a typical SNG for antenna elevation angle a) $\varepsilon=30^\circ$, b) $\varepsilon=10^\circ$

As far as the SNG terminal is concerned, the points of interest were located in the near zone at the elevation angle of 30° and in the far zone at the elevation angle of 10° . The maximum value of the electric field strength ranged between 42 V/m (30°) and 25 V/m (10°), whereas the duration of aircraft exposure to the main beam varied from 0.35 s (30°) to 1.9 s (10°). Compared to the vulnerability levels of the electronic equipment made use of by the aircraft, these values were of the same order. And this means that the threat of such stations to air traffic is high. This finding has been taken seriously by some European countries, and adequate authorising procedures for transmitting station operators have been implemented [9]. It is worth noting that the results obtained by the two methods are quite consistent - this consistency is better for the far zone, and a little worse for the near zone. And this means that the far-zone model applies to the near zone only to a limited extent.

In the paper there were only presented results of simulation for VSAT#3. As shown by the plots of Fig. 7, the threat produced by VSATs with maximal admissible parameters of the radiated power is comparable to the one produced by the SNG terminals. It should be noted that SNG terminals are designed for temporary uses only, and VSATs may be installed for good.

6. EFFICIENCY OF FUSELAGE SHIELDING

The available literature provides little information about the efficiency of aircraft fuselage shielding in the frequency range of 12.5 to 15.5 GHz and 30 GHz. In April 1993, ERA Technology tested the efficiency of

fuselage shielding [2] under contract with Radiocommunications Agency, UK. The measured results allow corrections and determination of the threat to airborne electronic equipment due to the influence of satellite terminals.

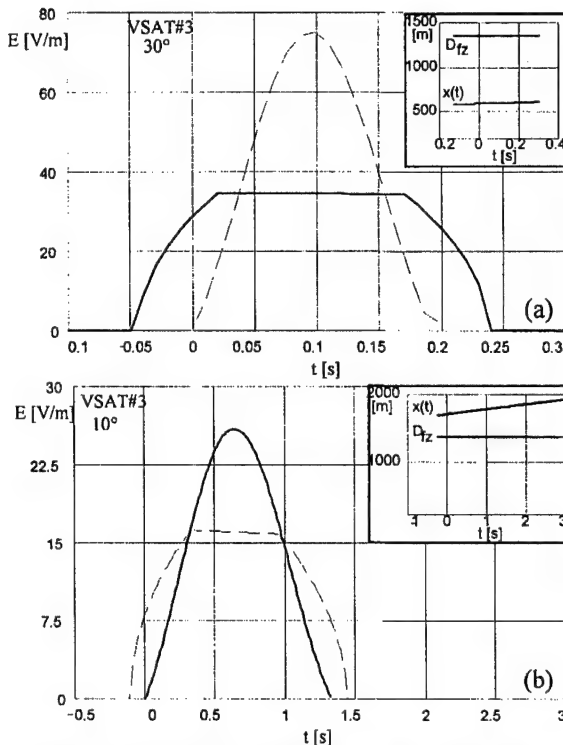


Figure 7. Amplitude of electromagnetic field strength during passage of the aircraft through the main beam of the VSAT#3 antenna for elevation angle of the antenna (a) $\varepsilon=30^\circ$; (b) $\varepsilon=10^\circ$

Measurements were carried out for six aircraft types: Piper PA-31-350 Chieftain, Aerospatiale SA 330E Puma (helicopter), Hawker Siddeley HS 748, BAC One-Eleven, McDonnell Douglas DC-10 and Boeing 747. In most instances, the attenuation characteristics were found to be frequency dependant only to a small extend.

The minimum values of shielding efficiency measured in the cockpit varied from 0 to 16 dB. In the interior of the fuselage shielding efficiency was generally greater, ranging between 12 and 30 dB, except for Aerospatiale SA 330 E Puma, which had a negative efficiency of shielding. This drawback should be attributed to the large fuselage planes made from non-conducting materials and to the internal reflections of the incident wave.

As an example, two measurement results for widely used aeroplanes DC-10 and Boeing 747 are presented in Fig. 8 and Fig. 9.

The results were influenced by the angle of „illumination“ and the height of the illuminating source. The lowest shielding efficiency were those obtained when the cockpit was „illuminated“ through the windows.

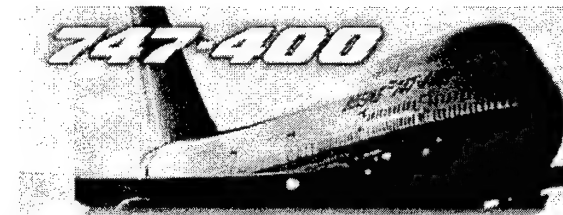
Measurements of electromagnetic fields attenuation by the aircraft fuselage have revealed that the lowest shielding efficiency value for the tested aircrafts was 0 dB. Some of the aircraft, namely those with fuselage made from non-conducting materials, experienced the

effect of a strengthened field induced by reflection and resonance. The measured negative values of signal attenuation approached -6 dB.



Section	Min. attenuation in 12.5 - 15 GHz [dB]
Cockpit	7
Front sec.	20
Middle sec.	26

Figure 8. Minimum attenuation of the Douglas DC-10



Section	Min. attenuation in 12.5 - 15 GHz [dB]
Cockpit	15
Front sec.	31
Middle sec.	31

Figure 9. Minimum attenuation of the Boeing 747 (type 236B)

Nowadays, aircrafts are equipped with instruments which have been investigated for immunity to the field strength of 1 V/m, as postulated by the EUROCAE ED-14B Standard issued in 1984. Recent standards (which take into account the occurrence of high intensity radiated fields) require that the aeronautical equipment should be tested for immunity to field strengths of the order of thousand V/m Table 5). In spite of this requirements, the majority of aircrafts have not been investigated for the compliance with those standards. As the lifetime of the passenger aircraft or a fighter varies from 20 to 30 years, it should be expected that at least after that period such a compliance will be achieved.

The vulnerability levels measured for airborne instruments were found to approach several hundred V/m. However, a small percentage (~5%) showed vulnerability levels below 100 V/m.

There is also issue concerned with characteristics of interfering signal. Taking into account the mode of operation of VSATs and SITs which is bursty in the nature it is possible to select three main phenomena affecting the electronic equipment installed on the board of aeroplane (Fig. 11):

1. the envelope of the pulse,
2. the short pulses caused by bursty transmission,
3. the RF radiation filling the envelope.

These three elements should be simulated during vulnerability tests.

Table 5. Vulnerability levels (standards)

Year	Civil	Military	
		UK	USA
1950	-	-	-
1967	3,7 mV/m, 1 GHz	0,82 V/m, 1 GHz	
1968			1 V/m, 10 GHz
1971			5 V/m, 10 GHz 20 V/m, 40 GHz
1980	0,1 V/m, 1 GHz	5 V/m, 10 GHz cw 20 V/m, 18 GHz mod 100 V/m ext. 200 V/m	
1984	1 V/m, 1,215 GHz		
1986			20 V/m, 40 GHz ext. 200 V/m
1989	200 V/m, 18 GHz		
1992	6,8 kV/m, 18 GHz		

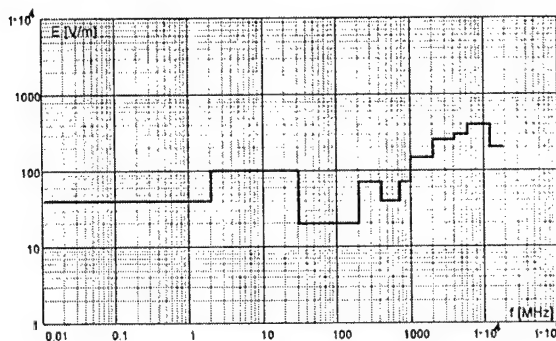


Figure 10. Vulnerability levels (average values) according to EUROCAE JAA (93-01-18)

Summing up what has been said so far, and considering the levels of radiation produced by satellite terminals, it can be inferred that the SNG terminals and VSAT terminals (with maximum EIRP), which have been installed in the vicinity of airports and operate in Fixed Satellite Service, are able to produce interference in the functioning of airborne electronic equipment. That is why a co-ordination of aeronautical services with those provided by the satellite terminals has become urgent. This postulate is in agreement with the one formulated by ERA Technology experts [2] who reported to the UK Radiocommunications Agency that they should make use of the clearance procedure described in RA 172 [9].

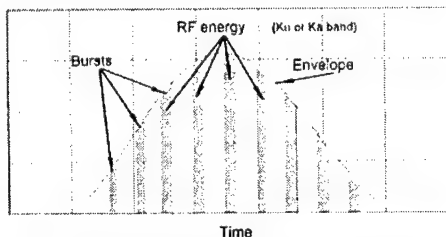


Figure 11. Three elements of the interfering signal affecting the airborne electronic equipment

7. CLEARANCE METHODS

In the majority of European countries, the postulates of non-neglecting the interaction between earth stations and aircraft ILS, or the demands made on the co-ordination of the site and frequency for VSATs and SNGs, are not very strict. In the advertisements for satellite earth stations it is often claimed that they can be installed anywhere.

Presently many efforts are being made to formulate adequate requirements for the protection of airborne instruments and avionics against interference coming from VSAT and SNG systems that have been installed in the vicinity of airports. At the Sesimbra Meeting of January 1997 for the Working Group of Spectrum Engineering, European Radiocommunications Committee (ERC) it was decided that the Danish Administration would collect data pertaining to the available methods by which aircrafts are protected against interference from VSAT and SNG systems. The Administrations of particular European countries were encouraged to enter for co-operation with their national Civil Aviation Authorities in order to have up-to-date information about the analyses and measurements that are underway. The majority of Administrations have poor experience in this sophisticated domain. The problem itself is very difficult to solve - the more so as some of the airports are located in the vicinity of the frontier. And this calls for conclusive decisions made on the forum held by the International Civil Aviation Organisation (ICAO). As a matter of fact, it is only the Danish Administration that has imposed a ban on the operation of satellite terminals in strictly defined areas around the airport of Copenhagen - the distance between the aircraft and the terminal must not be shorter than 500 m, and the adopted admissible electric field strength level for the interfering signal is 50 V/m. Polish Authorities do not allow to operate VSAT and SNG in the area around the airport in which distance to the border of the airport is smaller than 1000 m.

At the ETSI TC SES meeting in Vienna (12-15.04.1999) Eutelsat reported that some European Administrations plan to use their own site clearance procedure for each individual VSAT terminal before permission is granted for transmission. Some countries have unilaterally set technical conditions which should be met, beyond those parameters mentioned in ETSI Technical Basis for Regulations (TBR28) Because Eutelsat is an operator of around 30 000 terminals in Europe, it prefers to follow one common procedure. The work item concerned with elaborating clearance procedure for VSATs was sent to CEPT ERC.

The UK Radiocommunications Agency has established a clearance procedure which must be followed in order to obtain authorisation for the operation of transportable earth stations (TES) and mobile satellite terminals [9]. There is a strict requirement that relevant flight service must be kept informed about any intended operation of a satellite earth station (SES) if it is to be located at a shorter distance than 20 km from the reference point of an airport which makes use of the ILS. Relevant authorities must be forwarded a notice containing at least the following items: the position of the station, the azimuth and elevation angle of the main beam, and the anticipated date and time of transmission. If the operat-

ing conditions of the intended terminal are not acceptable to the airport administration, the operator will be responsible for all the implications that might result.

Every airport making use of ILS is surrounded by what is known as a protected area. Irrespective to the position of the station with respect to the airport, the transmitted beam must not pass through this area unless the administration of the airport or relevant service staff are notified. The notice should include at least the position of the station, the azimuth and elevation angle of the main beam, and the anticipated date and time of transmission.

With such information at hand, the operator or the representative of the airport will be able to analyse the situation and to decide whether or not there is a threat to aircraft (aeronautical services). In this way administration of the airport is given the opportunity to approve or disapprove of the intended terminal operation (after through analysis).

Analysis of the situation is carried out to establish whether or not the main beam passes through the protected area [10]. If so, the operation of the SES will not be approved of. The question arises if authorisation for operation must be equally restrictive for low power satellite terminals as it is for terminals with very high EIRP.

8. SUMMARY

Taking into account the data obtained by simulation, as well as considering the publications on the vulnerability of airborne electronic equipment, the following conclusions can be drawn:

1. Of the various satellite terminals, considerable threat comes from SNG as well as from the VSAT terminals providing satellite services with maximum EIRP. Currently these kinds of VSAT terminals are developed [11].
2. The threat of typical VSAT terminals to air services is noticeably smaller. The maximum field-strength value at a distance of about several hundred meters amounts to several volts per meter.
3. The threat of SIT terminals to the air services seems to be small. But there are not requirements for vulnerability levels in 30 GHz, because standard EUROCAE JAA (93-01-18) specifies limits for certification environment only up to 18 GHz. There is also no information available about fuselage attenuation in this band.
4. Because of the unrestricted transport of VSAT and SNG stations in the member countries of the European Union, there is an urgent need to unify the site clearance procedure.
5. Site clearance procedure may either involve appropriate models of the protected area to analyse each case separately, or make use of special maps which represent the protected areas for particular airports and include all of the available satellites.

9. REFERENCES

- [1] Bem D.J., Janiszewski J.M., Więkowski T.W., Zieliński R.J., „Simple model of reflector antennas for evaluation power flux density in the vicinity of antenna for EMC purposes”. Proceedings of the 13th International Wroclaw Symposium and Exhibition on EMC, Wroclaw, Poland, June 25-28, 1996, pp. 419 - 424.
- [2] Stevens E.G., Watkins P.J., „EMC study phase II - Earth Station/Aircraft Instrument Landing Systems”, Archival Report, ERA Technology, April 1993.
- [3] Colwell B., „Earth Stations/Aircraft Instrument Landing System EMC study”, Final Report, ERA Technology, March 1992.
- [4] Zielinski R.J., „EMC between aircraft onboard electronic equipment and satellite earth stations” Proceedings of the 14th International Wroclaw Symposium and Exhibition on EMC, Wroclaw, Poland, June 23-25, 1998, pp. 320 - 324.
- [5] Zielinski R.J., „Risk of interference to aircraft from VSAT and SNG terminals”, Presented at the Euro Electromagnetics - EUROEM'98, Tel-Aviv, Israel, June 14 - 19, 1998.
- [6] Zielinski R.J., „Electromagnetic compatibility in satellite telecommunication”, (Polish), Wroclaw Technical University Publishers, Wroclaw, 1999, Poland.
- [7] Zielinski R.J., „Satellite Earth Stations with small antenna (VSAT) as a source of interference”, Proceedings of the 12th International Wroclaw Symposium and Exhibition on EMC, Wroclaw, Poland, June 28, July 1, 1994, pp. 235 - 239.
- [8] „Astra Return Channel System - System Description”, Doc.No.:ARCS.240.DC-E001-0.2, Societe Europeenne des Satellites, May 1998.
- [9] „Site Clearance Manual of Code of Practice No. 1, The Clearance Procedure Followed in Order to obtain authorisation for operation of Transportable Earth Stations and Mobile Satellite Terminals”, RA 172, August 1991, Radiocommunications Agency, United Kingdom.
- [10] Bem D.J., Janiszewski J.M., Więkowski T.W., Zieliński R.J., „Coordination of Satellite Earth Station with aeronautical services and airborne equipment”, Proceedings of the 12th International Wroclaw Symposium and Exhibition on EMC, Wroclaw, Poland, June 28, July 1, 1994, pp. 466 - 471.
- [11] Kudelka o., Clausen H.D., Matic V., Collini-Nocker B., Schmidt R., Temel R., Eder T., Birnbacher U., Schrotter P.: „The LISSY Satellite Communications System for Multi-Media Applications”, Presented at the Technical Workshop „Internet Protocols over Satellite”, 12.01.1999, ESTEC, Noordwijk, The Netherlands.
- [12] Zielinski R.J., „EMC analysis of Satellite Earth Stations with small antenna (VSAT)”, Proceedings of the Euro Electromagnetics - EUROEM '94, Bordeaux, France, May 30-31, June 1-2-3, 1994, pp. 702 - 709.

BIOGRAPHICAL NOTE

Ryszard J. Zielinski received the M.S. and Ph.D. degrees in Telecommunications from the Wroclaw University of Technology in 1978 and 1984, respectively. He has been involved in electromagnetic compatibility issues e.g. spectrum management, methods of measurement broadcasting antennas, EMC of ITE, EMC in satellite systems. Currently his main interest is in VSAT networks. He actively participates in the international standardization works of ETSI as an expert and member of TC SES. He is a member of Organizing Committee of The Wroclaw EMC Symposium and Polish Electrical Engineers Association. Mr Zielinski is the author of 1 book and some 60 papers and publications.

RADIO ASTRONOMY IN POLAND

Andrzej J. Kus, Toruń Centre for Astronomy, Nicholas Copernicus University,
87-100 Toruń, Gagarina 11, Poland, tel (+48)-56-6113004, fax: (+48)-56-6113009,
email: ajk@astro.uni.torun.pl, <http://www.astro.uni.torun.pl>

1. INTRODUCTION

From the beginnings of mankind understanding the Universe has become the greatest challenge. Our present knowledge about its nature was gathered laboriously over a very long period in many areas of fundamental research. Though astronomy belongs to the oldest of the sciences, yet the actual scientific attraction in this field is remarkably high. New branches of astronomy emerged in this century. Radio astronomy, which allows us to study the universe in the radio domain, is such an example and certainly can be described as one of the most advanced and successful.

For all of us the Universe is an infinite laboratory to study the extreme conditions and to discover the unknown. Investigations at different wavelengths of electro-magnetic domain reveal rich nature of Cosmos. Gamma-rays and X-rays show the presence of highly energetic activities occurring close to extremely dense objects such as massive black holes or pulsars. The visible range of wavelengths provides us with information on stars and interstellar medium. Radio waves inform us about high energy plasma and magneto-hydrodynamic phenomena.

Research in astronomy puts up the highest demands on modern technology and thus indirectly accelerates commercial applications. Modern radio telescopes and various specialised auxiliary equipment for signal processing and image reconstruction represent technological state of the art.

The global relations and worries about the use of radio wave bands, demands for higher quality commercial electronics, and possible solutions on protection of the environment around radio observatories are very important. The action to preserve part of the radio spectrum for the passive use of radio astronomy is the high priority and has received international recognition and support under the umbrella of OECD, URSI and IAU. Reality of present situation with RFI at each radio observatory requires

from us collective responsibility and the will for co-operation on local, continental and global scales.

2. THE RISE OF RADIO ASTRONOMY

Radio Astronomy [1,2] dates from experiments of Karl Jansky in 1931. Since then we witness enormous progress resulting from technological development of our century. Over the last four decades entirely new observing techniques and sophisticated data analysis methods were developed. The use of these methods provided astronomers with results which changed our understanding of the Universe. Even though radio waves are a million times longer than optical waves, the angular resolution obtained now is three orders of magnitude higher than that of the largest optical telescopes. The sensitivity of our radio telescopes enables the study of the most distant objects in the visible Universe.

Many recent discoveries made in the radio domain have received the highest international recognition. The detection of relic microwave background emission - the remnant of the Big Bang, the discovery of pulsars, observational tests of general relativity, and the development of aperture synthesis techniques are just examples of subjects awarded the Nobel Prize.

Research in astronomy has always been limited by instrumental problems. The struggle for increased sensitivity, higher angular resolution and higher dynamic range remain as the basic goals of observational radio astronomy.

Single dish limitations result from the finite physical size of the aperture. The diffraction limit defines the angular resolution. For the presently used large single radio telescopes it varies between few degrees to about 10 arc sec depending on the frequency used. Sensitivity is defined by the effective collecting area, the noise of receiver and the interference level.

Among others, the limited instantaneous field of view of present telescopes is a particular problem. High

angular resolution results in more pixels per unit area of sky which then takes correspondingly longer to image. Multi-beam systems go some way towards reducing the problem. Paradoxically, we can get more detailed information from smaller and smaller areas when we enlarge the aperture to gain sensitivity. Time resolution is also an important limitation in certain applications, in particular in the study of pulsars.

Frequency resolution and the instantaneously available bandwidth, the recording and data handling methods, are all "back-end" related subjects. Sensitivity to rapid bursts of sporadic emission and ways to distinguish these from man-made interference should also become a common feature of any telescopes.

Despite all these limitations the new high tech telescopes are being designed and constructed. Worth mentioning here are the Green Bank NRAO (USA) 110m antenna, which will soon become operational, 64m antenna built on Sardinia (Italy), 50m antenna built in Spain. Large (1 km²) single aperture telescopes of various form are seriously considered and will be built within 10-15 years, providing astronomers with 100 times better sensitivity over that available now.

A decisive improvement of angular resolution has been achieved by the use of radio interferometry [3]. The technique was developed in parallel at Cambridge and Sidney universities. In the mid sixties the angular resolution of interferometers broke the 1 arc minute limit of the naked eye. This technique allows very accurate position measurements and leads to the optical identifications of many discrete radio sources. It has also proven to be less sensitive to local radio interference.

The major further step was made by the genius idea of aperture synthesis [5]. This new technique was developed at the MRAO Cambridge University by Sir Martin Ryle and his co-workers. Today it remains as the most powerful method of modern radio astronomy. The major world radio telescope operate under this principle. VLA in the USA, MERLIN in the UK, GMRT in India and VLBI (Very Long Baseline Interferometry) - the global array of radio telescopes, all are the aperture synthesis instruments. These instruments have a diffraction equivalent aperture ranging from about 30 km up to continental and global sizes. The resulting angular resolution of radio images reconstructed from the gathered data is better than 0.001 arc sec. The VLBI technique became possible in the late sixties. The radio signal received by an individual telescope of the network is converted to the video band and then independently recorded on magnetic tapes with the phase stability of atomic clocks. The availability of atomic frequency standards was crucial for this technique. VLBI, or any other future array, will also have to rely on high precision frequency standards; the only foreseeable change could eventually occur in the way of data transmission to the central correlator.

High angular resolution of VLBI allows astrometric and geodetic measurements. Point-like objects are measured in the sky with milli-arc-sec precision. At the same time an individual antenna of the network can be located to within few millimetres on intercontinental baselines. The technique is routinely used for study of Earth rotation, tectonic plate motion and the prediction of earth quakes.

In February, 1997 the Japanese Institute of Space and Astronautical Science launched an 8 m antenna into an elliptical orbit around Earth. The project is known as VSOP - VLBI Space Orbiting Programme. Together with the ground based radio telescopes the VSOP antenna expands the capability of the existing array. The maximum baseline, which is defined by the satellite orbit, exceeds 20,000 km. The angular resolution is 2-3 times better than that achieved with the ground network. VSOP is a major step towards the synthesis of a radio telescope bigger than the Earth. Future projects consider larger antennas and the maximum baseline comparable to the Earth - Moon distance. Such projects are realistic and most probably will be successfully completed within the next decade.

Enormous progress has been made in the receivers technologies and digital instrumentation [4]. The Ultra Low Noise preamplifiers cooled to 15 K have only few Kelvins of intrinsic noise. The major contribution to a telescopes system noise temperature comes from the ground, atmosphere and human made radiation. Modern electronics and software help us to study objects with signals well hidden below the system noise. The real limitation to sensitivity [6] in fact comes now from the other users of electromagnetic spectrum. Radio Astronomy - a passive user has to coexist with all other active users. Whereas if bad reception in commercial application occurs, there is always possibility to enlarge the transmitted power. We can not amplify cosmic radio sources. As an example of problem magnitude let me just say that a portable telephone placed on the Moon would be seen by our radio telescopes (at the transmitted frequency band) as the strongest radio source in the sky.

3. RADIO ASTRONOMY IN POLAND

Radio astronomy in Poland was initiated in the mid fifties independently at Cracow's Jagiellonian and Torun's Copernicus universities. At present the Cracow Observatory is equipped with 15 m and 8 m parabolic antennas operating between 200 and 3000 MHz. The major scientific observational interest focuses on studies of the Sun activity. The Torun Centre for Astronomy uses three instruments - the 32m very modern parabolic antenna capable to operate up to 50 GHz, a 15 m paraboloid useable in metre and cm bands and a solar interferometer operating at 127 MHz. The scientific goals here are quite broad. The major activity

concentrates on studies of distant galaxies and quasars, neutron stars as well as molecules in interstellar medium and stellar atmospheres. The methods which we use are: the radio interferometry and sophisticated single dish radiometry.

The dedicated hard work of Torun's team of scientists and engineers over last three decades placed us high among well developed European radio observatories. Our major instrument, the 32m precise parabolic antenna, designed and built in Poland, is one of the best of its class. The new 32m telescope is a fully steerable classical Alt-Az mounted Cassegrain. It's main parabolic reflector is made of 336 panels, each with an accuracy better than 0.35 mm rms. They have been mounted and then adjusted to an accuracy better than 0.2 mm by a classical laser based surveying technique. The final accuracy of the surface is therefore limited by the quality of individual panels. The construction of the dish backing-structure is stiff and based on homological principle. The gravitational deviation from the parabolic shape has been designed to be 0.14 mm rms. The position of the 3.2 m subreflector is continuously adjusted to conform with the homological deformation of the dish. There are four azimuth drives each containing two AC motors and two gear boxes, and two elevation drives each with one gear box but with two AC motors. The complex scheme was chosen to ensure very smooth tracking by having opposed motors working in antibacklash mode. The telescope can point with absolute accuracy of 0.002 deg. Receivers covering the bands 0.75-1.1, 1.4, 1.6, 5 and 6.8 GHz are mounted simultaneously in the vertex cabin. All input amplifiers and waveguides (from above 1.4 GHz band) are cooled down to 20 and 50 K respectively. The best achieved system noise is around 27-30K. The basic auxiliary equipment for the telescope consist of a Hydrogen Maser time and frequency standard, a GPS timing receiver, a VLBI terminal, the pulsar machine, a digital autocorrelating spectrometer and a weather station. The 32m high precision antenna with tavailable auxiliary instruments provides Polish astronomers with the unique tool to study Cosmos. The telescope is part of the European and world-wide network of interferometers - VLBI. This system allows our antenna to be a part of the synthesis radio telescope which has an equivalent aperture size of ~10 thousand kilometres.

This new instrument and the involvement of Polish radio astronomers into international co-operation resulted in the expansion of radio research. VLBI studies of distant galaxies and quasars, the search for new planetary systems around pulsars, the study of interstellar and stellar molecules are the subjects to be mentioned here. The importance of the Torun 32m has been recognised in the astronomical community. The size of the antenna, geographical location and highly professional team of scientists and engineers make the addition of Torun a significant improvements to the

European VLBI Network. Radio astronomy is a very challenging area of modern research for a country like Poland. The European research within EVN is seen in Poland as one of the best examples of scientific, cultural and political co-operation on our continent.

At Toruń radio observatory a systematic monitoring of RFI are being made. This necessary activity takes more and more of our resources and in fact requires now a full appointment of the observatory frequency manager. Using the D=32m antenna, pointed upwards, we measure the level of RFI inside the RA allocated bands. The antenna has considerable gain ($4\pi D^2/\lambda^2$) and the RFI are received by main sidelobes, feed spill over and reflections from secondary mirror support. Thus these are extremely attenuated as compared to ones coming directly into antenna primary beam. Additional less sensitive measurements are done with HP spectrum analysers and simple directional antennas. The graphs are not attached into this paper (too many), these will be shown in the presentation.

Another area of activity for frequency manager is the coordination, with local and central administration, the urban activity and plans. At the moment there is good understanding of our needs and the will to support however, the legal form of the observatory protection zone formally doesn't exist yet.

4. THE FUTURE OF RADIO ASTRONOMY

An ideal radio telescope should have sensitivity of a few mJy, an antenna sensitivity preferably ~1 mK/Jy, and an instantaneous field of view of 2π steradians. It should also have angular resolution selectable between ~1 arc min to ~1 milliarc second depending on the application, time resolution down to microseconds, and frequency resolution selectable between ~1 Hz to ~10 MHz. The last two features are, of course, more dependent on back-end design than on antenna itself; however, the antenna's and receiver's sensitivities are crucial for time and frequency resolutions thus they are mentioned here. Is this an unrealistic dream or can we really design and build such an instrument. I personally think that it will be possible to meet most of these requirements within 20 to 30 years, and some of them much sooner.

At the moment, the most sensible approach is to build special purpose telescopes dedicated to particular tasks: arrays to get high angular resolution and big collecting area elements to get high sensitivity. Very large fully steerable single dishes, built the conventional way, have proved to be very expensive. The weightless environment of space or the far side of the Moon could be better places for the building large apertures, but we know they will not be cheap. Fixed spherical dishes of the Arecibo type are being discussed and they might serve as elements of bigger arrays but it should be noticed that they are not well suited for use at

high frequencies, which we may be forced to use for ground-based radio astronomy sooner than we expect. The rising tide of interference may well deny us the use of the lower (i.e. < 1 GHz) frequencies.

To minimise the interference problem and to further enlarge the angular resolution, space missions with large orbiting antennas combined with ground based telescopes will synthesise a future cosmic radio telescopes. The first successful attempt - VSOP - shows the direction how to use existing, as well as how to create entirely new space technologies in astronomical research.

Despite the push for higher and higher angular resolution - better and sharper images - there is a continuous need for increased sensitivity. One of the big future international projects is known as the Square Kilometre Telescope (SKT) [8]. There are several presently proposed forms of such a large telescope. All assume the effective aperture surface of about 1 square kilometre. The proposals comprise a single aperture with large f/d or else an array of big spherical dishes or a big flat tile integrated antenna & receiver system.

I personally support the idea of a global real-time fibre-optic connected VLBI array with one global correlator centre. This would be an array consisting of up to 1000 single elements, each ~ 32 m in diameter. Used as a phased array, this would provide a collecting area comparable to 1 km² and at the same time would give the maximum angular resolution achievable on our planet. Such an array would also allow great frequency flexibility. Individual countries could contribute effectively since such an enterprise would bring local benefits both scientific and technological. A large number of telescopes similar to Torun's new 32m could be afforded by many countries and therefore this scheme might be a very realistic way of evolving a truly world array of telescopes at a minimal and well shared cost. Questions of concern are related to the cost of the data transmission and to the cost of a mega-baseline correlator at the control centre. The first problem will be solved very soon as multimedia communication systems using fibre optics are being developed with enormous speed. The continuous upgrading of existing correlators could provide the basis for mega-baseline correlator of the future.

One additional feature of radio astronomy research, which adds to the importance of the field is the unique possibility to study complex molecules (see the contribution from Will van Driel). The radio band is the only window in the electromagnetic spectrum where the rotational and vibrational transitions of molecular energy stages can occur. Since the first discovery of the OH radical, molecular radio astronomy has expanded and the interstellar medium has been found to be full of diverse molecular species. Today we study more than 60 species, starting from a simple ones like OH, CO, SO, H₂O and ending with as complex as ethanol, methanol and other C,N,O,H,S combinations. The role

of the interstellar molecular clouds in the formation of stellar and planetary systems is being investigated. Many molecules show maser amplification. Some are so bright, called mega-masers, that could have been found in distant galaxies. The study of molecules in the mm and sub-mm range is becoming a major attraction and activity field for many astronomers. A new project of a multi element mm array is being discussed between the USA, Japan and European countries. The system know now as project ALMA will become operational within next 10-12 years.

Several important points concerning the future of radio astronomy research arise. First, the radio interference problem is a major concern that must be taken into account. The success of the future Large Telescope, no matter how it is designed, depends very much on its location and legal protection. The increasing commercial use of the radio spectrum is pushing astronomers higher and higher in frequency, so we have to design our future instruments to be capable of working at mm and sub-mm wavelength. Being squeezed very exactly into our allocated bands, we cannot in the future improve sensitivity by enlarging bandwidth. Large apertures therefore seem to be the only reliable way to address the problem. Modern receivers have now brought us to practically noiseless preamplifiers, so the main struggle to reduce system noise must concentrate on minimising the ground contribution. Thus the screening of the area around antennas will also have to be considered an important part of future telescopes. To obtain high angular resolution and thus to measure distances, the future instruments would have to be multi-element arrays. The large ground apertures together with the space born antennas, plus radio telescopes located on the Moon and possibly Mars, will serve as our cosmic ear to listen and analyse the most beautiful natural music of the Universe.

5. SPECTRUM MANAGEMENT

In RA we are performing highest sensitivity measurements and these are particularly exposed and vulnerable to man made RFI. The quality of our measurements, and sadly often the survival of some radio astronomical research, are so critically dependent on formal protection and the true respect to the agreed rules. The respecting rules is becoming very difficult and is constraint by rapid expansion of various radio communication systems and their uncontrolled, off the band leakage. Countless low quality home used electronics creates additional serious thread.

Of course radio telescopes are state of the art, but e.g. modulation spectrum recognition techniques are not yet designed nor implemented, and in fact the interference suppression is until now the data removal only. Thus is this the perspective for the next

generation of scientists? What future for RA research can we assure? RA has enormous capability to study Cosmos and should prevail in the coming millennium as the basic source of information about physics, structure and evolution of the Universe.

The situation regarding the level of RFI at both Polish observatories is not acceptable. Their historically conditioned locations happen to be close to the large cities. The rapid expansion of housing area plus flooding of various electrical and electronic appliances make the old times free of RFI gone. The level of man made radio emission has increased dramatically over last two decades. Less and less spectrum is freely available. Formally protected bands allocated for RA by international agreements are contaminated by RFI. At both Polish observatories we had to abandon sensitive measurements below 1 GHz. Situation is changing rapidly to the worse and some areas of important research will have to be completely terminated. In this presentation recent level of RFI as well as undertaken actions will be discussed. Being pushed up from low frequencies means dramatic losses. Most of natural radio emission has nonthermal spectrum (synchrotron mechanism) and the flux density fades away fast with the frequency increase. This is the particular problem for pulsars, and nonthermal galactic sources. The Doppler shift of radiation arriving from distant galaxies and quasars makes the spectra to appear at low frequencies. To study such objects and their evolution we need to have unlimited access to all RA primary allocations.

To protect future research in radio astronomy we need co-ordinated world-wide action [7]. The first and most important issue is to protect the allocated bands. We would like to make other users of electromagnetic waves understand that radio astronomy is a passive use of the band. We never transmit nor generate radio signals. To improve reception of cosmic information we can not go there and increase the transmitted power as the active users would do. The signals which we analyse are so weak that sometimes we integrate for hours in order to get a sufficient S/N ratio. Usually it is 20-30 dB below the noise generated in the receiver and the atmosphere. Any terrestrial interference can ruin our measurements if it falls into our protected bands. Observations of distant quasars, pulsars and molecules can be compromised by commercially used devices such as microwave ovens, cellular telephones faulty TV and radio signals even garage-door openers. Recent experience shows that out of band emission and strong emission in adjacent bands causes severe problems for radio astronomers.

Conditions for coexistence are being discussed on international committees [9]. An agreement has to be reached. Radio quiet zones around observatories, high quality electronics, linearity of power amplifiers and

strict protection of radio astronomy bands are absolutely necessary.

If we do not show sufficient motivation and dedication to this important activity, human kind may lose the unique chance to study the Universe in radio waves in the future.

6. REFERENCES

- 6.1. B.F.Burke, F.Graham-Smith, „An Introduction to Radio Astronomy”, Cambridge University Press, Cambridge UK, 1997.
- 6.2. J.D.Kraus, „Radio Astronomy”, 2nd edition, Cygnus-Quasar Books, 1988.
- 6.3. A.R.Thompson, J.M.Moran, G.W.Swenson, 1986, „Interferometry and Synthesis in Radio Astronomy”, John Wiley & Sons, New York, 1986.
- 6.4. K.Rohlfs, „Tools of Radio Astronomy”, Springer-Verlag, Berlin, 1986.
- 6.5. K.I.Kellermann, „Radio Astronomy in the 21st Century”, Sky & Telescope, February 1997, p.26-33.
- 6.6. J.Roth, „Will the Sun Set on Radio Astronomy”, Sky & Telescope, April 1997, p.41-43.
- 6.7. „CRAF Handbook for Radio Astronomy”, 1997, ESF & NFRA, 7990 Dwingeloo, The Netherlands, <http://www.nfra.nl/craf>.
- 6.8. „Square Kilometre Telescope”, 1998, NFRA, The Netherlands, <http://www.nfra.nl/skai>.
- 6.9. H.Butcher, OECD Working Group on Radio Astronomy, NFRA, The Netherlands, 1988, www.oecd.org/dsti/sti/s_t/ms/act/introra.htm

BIOGRAPHICAL NOTE

Author heads the Department of Radio Astronomy at Toruń Centre for Astronomy. Born in 1944, graduated in astronomy in 1968, Ph.D in 1974, from 1993 university professor. Broad experience in RA techniques and methods. More than 6 years spent at major European and American observatories.

Research activity: VLBI, studies of quasars and radio galaxies, cosmic masers, instrumentation. Last ten years dedicated to building, equipping and commissioning of the largest and most modern astronomical facility in Poland - the 32m radio telescope.

Member of International Astronomical Union, URSI, European Astronomical Society, Associate Member of Royal Astronomical Society.

REGULATIONS AND SCIENTIFIC USE OF RADIO FREQUENCIES

T.A.Th.Spoelstra

ESF Committee on Radio Astronomy Frequencies

P.O.Box 2, 7990AA Dwingeloo, the Netherlands

email: spoelstra@nfra.nl, URL: <http://www.nfra.nl/craf>

Scientific applications of radio frequencies and non-scientific use of the radio spectrum are largely incompatible. The current ITU-R Radio Regulations, EMC directives and standards are inadequate to handle the scientific and the non-scientific services in the physical and technical sense on an equitable basis.

Some recommendations are made for improvement.

1. INTRODUCTION

Radio frequencies are used in many scientific applications and research projects. The paramount example of this is radio astronomy. Other sciences depending on intensive use of radio frequencies are geodesy, meteorology, remote sensing studies and aeronomy. Whether the radio frequency at which the scientific application is operating is a unique requirement that cannot be replaced by another one, depends on physics and on the scientific question. Aeronomy, meteorology and radio astronomy select their radio frequencies on the basis of the physics of the atoms and molecules for their spectral line research and on the physical characteristics of the research objects. The frequency selection for other scientific applications can be based on different arguments.

The framework for radio frequency management is provided by the Radio Regulations of the International Telecommunication Union, ITU [2]. These regulations provide a framework for national administrations to regulate equitable access to the radio frequency spectrum for all entities for which the use of these frequencies is essential: telecommunication industry, safety services, aeronautical services, various scientific and hobby use, etc. This framework also provides a regulatory frame and several criteria to prevent harmful interference. Other criteria are found in regulation dealing with the issue of electromagnetic compatibility, EMC.

Electromagnetic compatibility is managed through standards and EMC directives. The EMC Directive of the European Commission provides such a regulatory framework on electromagnetic compatibility in Europe. Electromagnetic compatibility means "the ability of an electrical and electronic appliance, equipment and installation containing electrical and/or electronic components to function satisfactory in its

electromagnetic environment without introducing intolerable electromagnetic disturbances to anything in that environment" [1]. The main goal of an EMC directive is to ensure that electrical and electronic apparatus do not affect the correct functioning of other apparatus and that each apparatus has an adequate level of immunity to electromagnetic disturbances.

Both frameworks provide a public international legal regulation on interference and compatibility issues and these are articulated in national law. A key question for scientific users of the radio spectrum is to what extent these regulations are sufficient to ensure adequate access to the radio frequency spectrum for scientific research and protection of its operations from radio interference.

2. SCIENCE AND TECHNOLOGY

In scientific experiments and measurement campaigns commercially available equipment is used in several occasions, such as in various geodetic and meteorological programs. For other applications in e.g. remote sensing research and especially in radio astronomy, dedicated instrumentation has to be developed because this equipment and many of its components are commercially not available. In many cases adequate technology does not yet exist, nor even feasibility studies and the design of the instruments so that such investigations will push technology beyond its current limits. This scenario is partly due to the fact that the technical requirements for the scientific and commercially available instruments are very different: e.g. the sensitivity of the receiver may well be several orders of magnitude higher than in industrial applications. Another reason relates to the frequency domain in which the scientific research must be done and for which the state-of-the-art technology does not yet provide the necessary components and/or test instrumentation. This applies especially for passive frequency use. It should be noted that in radio astronomy and some remote sensing applications frequencies up to 2 THz are currently used! In the past 60 years, radio astronomy was noticeably very often leading in technological development and had built the first instruments for the high frequencies at that time.

It is common practice that research instruments and equipment that are developed are designed and built for a specific research program. The characteristics of such a program define the technical requirements. The result of this is that usually each scientific instrument is its own prototype, which is regularly improved to comply with the changing requirements due to scientific programs and technological developments [4]: the scientific instrumentation may be seen as having the characteristics of a laboratory experiment.

In the development of scientific instruments great care is taken to avoid, suppress or remove effects of harmful interference. Also much effort is put into the EMC purity of the instrumentation. The success of this effort depends on the quality characteristics of the commercially available components used and of the components that are developed in-house by the scientific community. Another constraint to this success is the availability of e.g. filtering techniques and test equipment (at present this is especially a concern for frequencies above about 50 GHz).

This scenario implies that at least one common observation during the development of scientific instruments can be made: in a large number of occasions it is noted that current technical standards and EMC directives and regulation are insufficient. This is due to the simple fact that to address compatibility with the characteristics of the specific instrumentation in e.g. radio astronomy, these are not adequate.

During the design and development phase of scientific instruments such as radio telescopes, one is continuously asking the question what action must be taken to build state-of-the-art equipment satisfying the requirements given by the research program. Since nobody can answer the question "How is one supposed to discover what has to be rejected experimentally when building equipment?" scientific usage of radio frequencies is susceptible to the impact of industrial technological development and therefore, their development must take the characteristics and requirements of existing scientific equipment into account.

3. SCIENCE AND THE RADIO ENVIRONMENT

The ITU-R Radio Regulations distinguish 36 different radiocommunication services, of which the earth exploration-satellite service, the radio astronomy service and the space research services are directly serving scientific research programs. Of these science services, the radio astronomy service is the only exclusive passive service. All non-scientific services are active, which means that they use transmitters and receivers for their applications. The requirements of these non-science services are very different and in most cases incompatible with scientific applications. This environment makes scientific usage of radio frequencies vulnerable in many regards:

a. the frequencies of interest for passive scientific applications are given by the laws of physics and cannot be chosen as for active services;

b. the equipment is generally not commercially available and has to be designed and built by the scientists themselves (generally for use in frequency domains in which neither standards nor EMC guidelines exist yet);

c. for scientific research projects, access to all radio frequencies is desirable but such a demand is regulatory and practicably extremely difficult to manage;

d. the regulations consider square boundaries between different frequency bands but perfectly square filters to prevent or suppress unwanted emissions do not exist which poses difficult compatibility and coordination questions in relation with applications in adjacent frequency bands.

Another fact is that for commercial reasons some operators and manufacturers do not sufficiently comply with the Radio Regulations or EMC directives, especially when it concerns space-based systems in the Mobile-Satellite Service and Fixed-Satellite Service. This may lead to defective systems which happen to occur more and more often [5]. Since receiving instruments used by scientific users of radio frequencies are usually the most sensitive which exist, these sciences are the most vulnerable for defective systems and the first to suffer.

It is extremely difficult or even impossible for scientific programs using radio frequencies to conclude whether the measurement data are contaminated by interference and to which extent. One reason for this is the fact that much interference mimics signal characteristics which cannot be distinguished from those in which the scientist is interested: an example concerns spectral line measurements which are fundamental for many research programs. Another reason is that in order to distinguish, calibrate and remove interference, it must be accurately known which part of the antenna pattern received the harmful signal: it is generally not possible to determine this and therefore the unwanted signal cannot be calibrated and removed properly.

The effect of this situation is that it is extremely difficult and often impossible for scientists to quantify accurately the impact of unwanted emissions. To complete a research program with adequate quality, the scientist must therefore trust that the measurement data are not corrupted and therefore considered to be correct. Daily practice shows that this assumption cannot be maintained [3][7][8]. Considering this fact, scientists wish that Administrations play a more assertive role to enforce necessary protection measures that manufacturers and operators must take.

4. SCIENCE AND REGULATIONS

The vulnerability of scientific usage of radio frequencies is in some cases built in into regulations. An example of this is Article S4.6 of the ITU-R Radio Regulations which reads:

"For the purpose of resolving cases of harmful interference, the radio astronomy service shall be treated as a radiocommunication service. However,

protection from services in other bands shall be afforded the radio astronomy service only to the extent that such services are afforded protection from each other."

Article S4.6 may be read as that radio astronomy on the one hand and other radiocommunication services on the other hand are treated on an equitable basis in the regulatory or legal sense. This observation holds, however, for the science services in general as follows from other articles in the ITU-R Radio Regulations (e.g. S4.7). However, article S4.6 does not consider the fundamental difference in characteristics between active and passive services. Because of this lacking distinction, the protection of passive services is unavoidably structurally an extremely difficult issue. This is especially the case since the ITU-R Radio Regulations do not contain a definition for *harmful interference to a passive service* nor a definition for the *level of harmful interference to a passive service*. The absence of such definitions hampers quantification of the protection requirements for radio astronomy.

Although it is the mission of the ITU, i.e. of its Radiocommunication Sector, to ensure the rational, equitable, efficient and economical use of the radio-frequency spectrum by all radiocommunication services, the specific case of passive services is thus not handled on an equitable basis in the physical and technical sense. It is common practice in the design of applications in active services that the power of emitted signals is raised to the point that the level of natural, additive noise onto the received signal is made negligible. In such a context where active spectrum users may raise their transmit powers beyond that, spectrum management reduces to ensuring each user some required signal-to-interference ratio, i.e. handling relative signal power levels. Passive services are based on measurements of natural radiation, sometimes of very low levels. They need protection in *absolute* terms.

This situation is basically not different for each of the science services, although the radio astronomy case is the most striking one.

5. SCIENCE AND STANDARDS

An EMC directive applies to apparatus liable to cause electromagnetic disturbances or whose normal operations may be affected by such disturbances [1]. The last fraction of this sentence could imply that the considered EMC directive explicitly applies to scientific instrumentation for passive use of radio frequencies, especially radio astronomy receivers with the well-known very high sensitivity requirements. However, this aspect is usually beyond the scope of EMC considerations, which apply to apparatus generating electromagnetic radiation exceeding specified limits, i.e. to electromagnetically active equipment. Although a radio astronomy receiver as such is also an electromagnetically active equipment, the emission it generates is usually below any level relevant for EMC considerations: if that were not the case, it could not work at all. Components and sub-

systems of such an instrument, such as computers integrated in the receiver system, must of course comply with the available regulations. But that is too obvious: the most vulnerable for inadequate components are the scientists themselves!

Current technical standards form a fundament in EMC regulation. Such standards are usually result of industrial development and commercial interests in an often unclear mixture. Many standards have been developed without adequate consideration of passive scientific use of radio frequencies and also the regulations providing adequate criteria for standard development are often not sufficient as well. Experience in technical study groups developing such criteria shows how difficult it is to reach agreement on numbers which enter public regulation, especially when they have to satisfy the requirements of passive services. Often commercial interest dominates the reluctance to accept what is technically feasible.

Although the standards may well be very adequate for industrial and commercial applications, the aspect of electromagnetic compatibility with passive scientific equipment should receive better attention. This is not always easy to realize in practice, even when the scientific community is participating in the work of standard development. The reason for this is the large imbalance between the requirements of commercial apparatus and scientific equipment.

When a case of incompatibility occurs and a regulatory authority may not be able to apply the regulatory framework in a straightforward way, he may urge private users of the radio spectrum to reach an agreement on their use of radio frequencies. Such agreements may more and more address a "regulation" of interference tolerance or spectrum pollution. These agreements may be incorporated in e.g. licensing conditions to one or both of the parties to the agreement. However, administrations should consider such a regulatory "escape" as undesirable since when it becomes publicly accepted that agreements to regulate pollution that a victim has to accept, are becoming common practice for whatever purpose, this development dilutes public regulation and the legal status of an international treaty such as the ITU-R Radio Regulations. Administrations should prevent such agreements instead of suggesting or even asking them to solve an issue.

Also, the pollution victim should not accept an agreement. If he does, he contributes to a precedent that private agreements can be made to regulate this pollution separate from available legislation to protect the victim but to make the life easier for the polluter. Organizations such as the World Trade Organization, WTO, and the European Commission, EC, must not sympathize with such pollution agreements either. However, it is becoming more common practice that with the (usually hardly justified) argument that one must not hamper new developments, curative measures are taken after the problem has been created. This scenario gives implicit priority to presumed new developments at the expenses of existing applications

which by consequence are automatically placed in a victim position.

Also organizations such as the WTO and EC must use their political weight to put pressure on the "polluter" to create an interference-free radio environment which also for the polluter will pay off in the future.

6. RECOMMENDATIONS AND CONCLUSIONS

To improve the regulatory context for scientific research using radio frequencies and to fill the existing regulatory gaps, we recommend that

- [a] scientists participate more actively in the process of standard development and technical studies developing elements for this process so that in its results the scientific requirements are taken into account in a better way;
- [b] administrations play a more assertive role to enforce necessary mitigation and protection measures that manufacturers and operators must take to maintain spectrum purity and to ensure adequate access to the radio frequency spectrum to other users of the radio spectrum, i.e. for scientific applications;
- [c] adequate monitoring facilities should be made available for regulatory authorities for their spectrum management and related enforcement work;
- [d] adequate and explicit definitions dealing with the specific characteristics and requirements of both *active* and *passive* services be included in the ITU-R Radio Regulations;
- [e] in the ITU-R Radio Regulations a definition for *harmful interference to a passive service* and for the *level of harmful interference to a passive service* be included;
- [f] scientists should evaluate and where necessary develop and improve the criteria quantifying the protection requirements for specific research;
- [g] scientists should study improvement of those particular regulatory articles and clauses which do not adequately take the requirements of the scientific applications of radio frequencies into account. Such a study could be performed in e.g. ITU-R Study Group 7.

These recommendations are considered necessary to

enable an escape from the scenario provided unintentionally by the current regulations and directives that in the radio frequency spectrum the specific requirements of scientific research doom science to be placed in a victim position by its nature.

7. REFERENCES

- [1] European Commission, "Guidelines on the application of Council Directive 89/336/EEC of 3 May 1989 on the approximation of the laws of the Member States relating to electromagnetic compatibility", 1989, p.12.
- [2] ITU-R Radio Regulations, edition 1998, International Telecommunication Union, Geneva.
- [3] A.J.Kus, "Radio practice in Poland", elsewhere in these proceedings
- [4] K. Ruf, "Technical and Engineering Challenges for the Future of Radio Astronomy", Radio Science Bulletin No.291, 1999, pp.13-18.
- [5] T.A.Th. Spoelstra, "Oh Satellite, Oh Satellite!", elsewhere in these proceedings.
- [6] T.A.Th. Spoelstra, "Public and Private – Regulations and Agreements".
- [7] W. van Driel, "The need for radio astronomical line observations: from hydrogen to formaldehyde", elsewhere in these proceedings
- [8] A. Winnberg, "Scientific Use of Radio – Challenges from Space", elsewhere in these proceedings

BIOGRAPHICAL NOTES

Dr. T.A.Th. Spoelstra is secretary and frequency manager of the Committee on Radio Astronomy Frequencies of the European Science Foundation. His research experience is related with polarization studies of cosmic radio waves, cosmic magnetic fields, radio wave propagation through ionized media, systematic philosophy and philosophy of science. He has served the Netherlands Foundation for Research in Astronomy as Head of Operations of the Westerbork Radio Observatory. He can be reached at: CRAF, NFRA, P.O.Box 2, 7990 AA Dwingeloo, The Netherlands [tel.: +31-521-595100, telefax: +31-521-597332, email: spoelstra@nfra.nl].

THE NEED FOR RADIO ASTRONOMICAL LINE OBSERVATIONS: FROM HYDROGEN TO ALCOHOL

W. van Driel

Unité Scientifique Nançay, Observatoire de Paris, Section de Meudon
5 place Jules Janssen, F-92195 Meudon, France

E-mail: Wim.vanDriel@obspm.fr, fax: +33-248518318

Abstract

Radio astronomical spectral line observations give us irreplaceable windows to study complex physical processes crucial for our understanding of the origin, present state and future of the Universe. In order to continue these observations the spectral windows allocated for them need to be kept very clean, i.e. free from harmful interference - an increasingly difficult task seen the continued crowding of the spectrum as well as the increasing sensitivity of radio telescopes. Here, the scientific importance of astronomical observations made in spectral lines will be discussed. Most of these are made in the so-called 21-cm line of neutral hydrogen, HI, which show the presence of the elusive Dark Matter, and allow measurements of the expansion of the Universe and local digressions from it. The lines of the OH radical in the 18 cm range are observed in such diverse objects as comets, evolved stars and distant megamaser galaxies. The CO molecular lines at millimetric wavelengths are found in dense interstellar clouds throughout the Universe. New-generation giant radio telescopes are being planned, capable of detecting redshifted radio lines in very distant objects far outside the bands allocated for observations in their rest frequencies.

1. RADIO ASTRONOMY - WHY AND WHAT

The Universe is, per definition, the largest laboratory one can imagine for testing and developing our understanding of physics. Astrophysicists may not be able to perform the kind of hands-on experiments in this huge laboratory that most of their colleague physicists can do in theirs, but they can observe (from a safe distance) an extremely broad range of physical conditions and processes that cannot be reproduced at all on Earth, now or in the foreseeable future.

To observe the Universe, astronomers have access to a wide range of wavelength domains, all providing complementary information on the state of the multitude of objects found in the Universe. Of these domains, only two are readily accessible from the ground: optical/near-

infrared (roughly 0.3-10 μm) and radio waves (about 150 μm - 50 m, or about 10 MHz to 2 THz).

Whereas optical observations study the electromagnetic waves from relatively hot objects such as stars (for example, the surface temperature of the Sun is about 5,600 K), celestial radio waves mainly originate from cooler objects, such as the gas between stars (generally at temperatures of a few tens of K), or from electrons in ordered motion in magnetic fields. Radio astronomical studies cover many of the same kind of objects as optical studies, but in addition they have revealed new classes of objects and quite unexpected forms of activity.

Celestial radio sources can emit electromagnetic radiation all over the electromagnetic spectrum, but often their emission at frequencies outside the radio domain is so weak that they can be studied by radio telescopes only.

Radio observations are crucial for our continued exploration and understanding of the origin, early phases, present state and ultimate future of the Universe. In order to continue these observations the spectral windows allocated to the Radio Astronomy Service need to be kept very clean, i.e., free from harmful interference - an increasingly difficult task seen the mounting (commercial) pressure on and crowding of the spectrum as well as the increasing sensitivity of radio telescopes, needed to detect the extremely faint celestial sources, both those in operation and the huge telescopes being planned.

2. RADIO LINES

The spectrum of celestial radio waves reaching the Earth has a very broad continuum, covering the entire range of radio frequencies that can penetrate the Earth's atmosphere (from decametric to sub-millimetric waves) as well as a large range of atomic and molecular spectral lines, each of which is confined to a quite narrow frequency range for any given object.

The radio continuum arises from two principal mechanisms: thermal emission, produced in an ionized gas of free electrons and ions, and nonthermal (or synchrotron) emission generated by relativistic particles

moving in magnetic fields - as observed in radio galaxies, quasars and supernova remnants.

Thousands of radio spectral lines have been detected in over 100 different molecules in interstellar space. Many of these are organic molecules, often of great complexity, leading to intriguing questions about the way in which they developed and on the origin of life in the Universe.

To understand physical and chemical conditions in interstellar clouds, or in specific regions within a cloud, it is necessary to intercompare observations made in a large number of lines: of different transitions from the same atoms and molecules (including their isotopes) and between transitions of different atoms and molecules.

Here, the scientific importance of radio astronomical observations made in spectral lines will be addressed. EMC and regulatory issues, interference from ground-based and satellite systems will be addressed in more detail elsewhere in these Proceedings [1] [2] [3].

3. RADIO LINE OBSERVATIONS

The Radio Astronomy Service is unique among the Radio Communication Services, in the sense that it is the only "passive" science Service, i.e., it is solely concerned with the detection of naturally occurring radio waves and not involved in any man-made transmissions. All non-scientific Services are active, on the other hand, meaning that they use both transmitters and receivers for their purposes, and that their requirements are often incompatible with scientific applications, which creates an electromagnetic environment that makes scientific radio frequency observations vulnerable in many respects [2].

To analyze the spectral characteristics of radio lines from celestial sources (ranging from comets to clusters of galaxies) observations are usually made within many frequency channels (several thousands is common, up to several million channels) within the receiver bandwidth - which can range from a few kHz for stellar line observations to several tens of MHz for studies of galaxies and clusters of galaxies.

Each radio telescope usually is its own prototype, as such dedicated research instruments are designed and developed for specific research programs, and need many components which are not commercially available. With time, each telescope is being constantly improved in order to comply with scientific and technological development [4].

Practically all radio line observations require a high sensitivity, as celestial sources generally are very weak, as well as a high dynamical range, as weak spectral features need to be studied in or around strong radio sources (previously mainly of celestial origin, but nowadays frequently of man-made origin).

Radio telescopes therefore tend to be big: the largest presently operational single-dish radio telescope observing below 10 GHz (Arecibo, on the island of Puerto Rico) has a diameter of 300 meters.

The Very Large Array (VLA) radio interferometer in New Mexico consists of 27 parabolic antennas of 25 meter diameter each, movable along a Y-shaped system of rail tracks extending to about 30 km from the center. The largest single-dish telescope operating at millimeter wavelengths, at Nobeyama in Japan, has a diameter of 45 m and the largest mm-wave interferometer, of IRAM in France, has 7 15 m parabolic dishes. Much larger instruments are being planned for observations throughout the radio domain, though, see Sect. 5 for a brief summary.

Single-dish telescopes provide detailed spectra of celestial objects within their beam, while radio interferometers provide detailed 3-dimensional image cubes of celestial line sources, using the Doppler effect to map the distribution and kinematics of atoms and molecules.

Modern large radio telescopes routinely provide spectral line data with a sensitivity of order of a millijansky (1 mJy corresponds to $10^{-29} \text{ W m}^{-2} \text{ Hz}^{-1}$) within integration times varying from minutes to hours, depending on the instrument's size and nature (single-dish or interferometer), though they can also achieve sensitivity levels of a few microJanskys. To achieve these state-of-the-art high quality results often long integration times are needed, and an EMC environment that does not generate harmful interference.

Unfortunately, the tremendous sensitivity of large radio telescopes makes them able to pick up harmful interference through their sidelobes in virtually any direction, often from outside the allocated and protected radio astronomy bands in which the celestial sources are actually being observed. So on top of the extremely weak radio lines from the astronomical source they are pointed at, they superpose omnidirectionally collected out-of-band RFI signals.

In practice, it is extremely difficult, or even impossible, to conclude if, and to what extent, astronomical measurements are contaminated by interference (RFI). One reason is that RFI often mimics the signal the scientist is interested in, and another is that in order to distinguish, calibrate and ultimately remove interference, it must be accurately known which part of the antenna pattern received the harmful signal, which is generally not possible.

4. SCIENTIFIC INTERESTS

Here, the scientific interests of astronomical radio line observations are briefly discussed, in order of increasing frequency of the allocated bands.

322-328.6 MHz: Deuterium (D)

Besides its use for continuum observations of radio galaxies, it contains a spectral line of deuterium at a rest frequency of 327.4 MHz. The relative abundance of deuterium and hydrogen is related to problems of the origin of the Universe and the primordial synthesis of elements in the Big Bang.

1330-1400/1400-1427 MHz: neutral hydrogen (H I)

Most radio astronomical line observations are made in the so-called 21-cm line (at 1420.4 MHz rest frequency) of neutral hydrogen, H I. Hydrogen is by far the most abundant (90%) element in the Universe, it has been virtually omnipresent in both space and time and most atoms are in the ground state, the state in which the line occurs.

Since its discovery in 1951, it serves as the most critical tracer of the structure and dynamics of the Milky Way galaxy, as indicator of redshift (distance) dynamics and mass of other galaxies, to measure the Hubble expansion flow of the Universe (and local digressions from it) and as probe of the early phases of the Universe.

Of external galaxies the observed, doppler-shifted H I line frequency measures its velocity along the line of sight, the redshift, which determines its distance from us in the expanding Universe. The H I redshifts of about 10,000 galaxies have already been measured. Local digressions of galaxies from the global expansion flow indicate the presence of local mass concentrations (groups and (super)clusters of hundreds up to ten thousands of galaxies) and allow an estimate of their total gravitational masses, of which usually only a small fraction can be traced through observations in the electromagnetic spectrum (like of stars in visible light and of H I gas in the 21 cm line).

In the local Universe, mapping galaxy redshifts has revealed the presence of a huge mass concentration, dubbed the Great Attractor, at a distance of about 200,000 lightyears. At optical wavelengths, this structure lies completely hidden behind the dense dust and gas clouds in the plane of the Milky Way and only radio line observations could reveal it and probe its properties.

The main mass component in the Universe, sensed through line measurements of galaxy kinematics, remains as yet unidentified and has been dubbed Dark Matter. This elusive material appears to be present practically everywhere and may be able to "close" the Universe, i.e., its gravitational pull may slow down the expansion of the Universe, started in the Big Bang explosion, and ultimately stop it.

The total mass of individual galaxies can be estimated from the width of the H I line, as measured with single dish telescopes, which measures the rotation velocity of the gas in the galactic disks. Using radio interferometer observations, sophisticated mass distribution models can be made using surface photometry, obtained from optical or infrared CCD imaging, and the H I rotation curve (i.e., the rotation velocity of the gas as function of its distance to the center of the galaxy) - these models have shown that the H I rotation velocities are strikingly constant in a given galaxy, even far outside the visible stellar galactic disks, where H I gas can still be detected, implying the need for large fractions of Dark Matter inside and around galaxies, surrounding the radiating stellar and gaseous disk in a dark halo.

As the Universe is expanding, the H I line emission of other galaxies is observed as redshifted towards lower frequencies, and as the sensitivity of radio telescopes improves increasingly distant galaxies can in principle be detected in H I at ever lower frequencies - even around 327 MHz giant clouds are being observed, sampling a "look-back" time of over 10 billion years ago, preceding the epoch of galaxy formation.

Clearly, many scientific reasons drive astronomers to observe at frequencies below 1400 MHz, where the tremendous distances of the objects observed make their H I lines extremely weak, and much fainter than most man-made transmissions. Hence the critical importance of the regulation of frequency usage and its restriction to well-defined narrow bands as well as the limitation of spurious emission within the radio astronomy bands in order to allow the continued use of this unique probe of the history and evolution of the Universe.

1610.6-1613.8/1660-1670/1718.8-1722.2 MHz: OH

Another well-observed series of lines are those of the OH radical which has 4 so-called primary and satellite lines in the 1.6 GHz range. OH is a widespread and abundant molecule, observed throughout the Galaxy and in other galaxies. Under special conditions these lines can be greatly enhanced by stimulated emission, creating powerful maser sources. They are found in a quite diverse range of objects, such as:

Comets, great balls of dirty water ice which evaporates when heated in the vicinity of the Sun, surrounding them by a cloud of OH gas. Radio observations can determine the rate of outgassing of a comet as a function of time, as well as very accurate radial velocities and the influence of the pressure by solar wind particles.

Massive stars, considerably heavier than the Sun, when nearing the final phases of their life, become unstable. Their light output becomes variable on periods of months to years as they undergo a regular contraction and expansion stage, and they start shedding the outermost layers of their atmosphere, forming circumstellar gas shells around themselves, which are expanding with several tens of kilometers per second. Radio line observations permit a study of these expanding shells, providing accurate radial velocities (important for mapping the Milky Way, as these amplified maser sources can be traced to its very edges) and giving inside into basic questions of stellar structure and evolution. The structure and kinematics of the shell can be mapped using radio interferometers with baselines of up to several hundred kilometers, such as MERLIN in the UK and the VLBA in the U.S.A., or through VLBI (Very Large Baseline Interferometry) networks spanning the dimensions of the Earth itself.

The most powerful maser sources known occur in the centers of so-called OH megamaser galaxies, with outputs sometimes exceeding 10^{29} W. They are located in the dust-shrouded nuclei of infrared luminous galaxies, which are often violently interacting or merging galaxy

at less than 3 times the line's rest frequency and thus far outside the frequency band allocated for its observation.

Molecules have series of lines, and lines of higher transitions, occurring at higher frequencies, can sometimes be observed within a band allocated to the rest frequency of a lower transition. Linking observations of quite different lines in different redshift ranges made within a single band is very difficult, however, as they are formed under quite different physical conditions.

Frequency protection at mm wavelengths

As is clear from the previous section, the entire mm-wave spectrum is full of lines, each potentially providing information inaccessible through other means. Many lines remain unidentified. The International Astronomical Union has compiled a list [6] of the 72 "astrophysically most important spectral lines", with rest frequencies covering the 327 MHz to 809 GHz range, in an attempt to assign relative scientific priorities, but it can only serve as a guide as we cannot foresee future discoveries or needs. In principle, astronomers need access to the entire mm-window, and the presently allocated bands, determined in the early 70's when only a few strong lines had been detected, are hugely inadequate.

As the commercial exploitation of the spectrum moves towards ever increasing frequencies, serious thought needs to be given to ensure the survival of mm- and submm-wave astronomy. It seems clear that radio astronomy can share the spectrum with several fixed services, for example through coordination or radio-quiet zones. This will be impossible, however, in the case of the satellite services. There, for example, "guard" bands could be set up around radio astronomy allocations which could be allocated to some of the fixed services more compatible with the strict requirements of the Radio Astronomy Service.

5. FUTURE GIANT RADIO TELESCOPES

The radio astronomical community plans to build new-generation radio telescopes with very large collecting surfaces which will drastically improve the sensitivity of observations over a very wide frequency range (about 20 MHz to 800 GHz):

- ALMA, a millimeter wavelength interferometer, consisting of 60-odd parabolic dishes of about 15 meter diameter each (the largest existing millimeter interferometer at IRAM consists of 6 15 m dishes), -
- LOFAR, an interferometer for use at decametric wavelengths with a collective surface of about a square kilometer (the largest existing decametric array, at Kharkov, has a surface of about 20,000 square meters) and
- the Square Kilometer Array, SKA, an interferometer for use in the metric to centimetric range, also with a collective surface of a square kilometer (the largest operational interferometer, VLA, has 27 25 m dishes) [7].

These will revolutionize radio astronomical research in about all scientific fields. In extragalactic research, for

example, SKA will allow the detailed imaging of ordinary spiral galaxies in the 21 cm H_I line out to a redshift of about 2 (where most of the objects in the Hubble Telescope Deep Field lie) and H_I detections of normal spiral galaxies out to redshifts z of about 5; OH megamaser starburst galaxies can readily be detected out to $z=8$. This view of the distant Universe, complemented by those of other planned very large ground-based and space observatories, like the two other planned radio interferometers ALMA and LOFAR, will revolutionize our knowledge of these seminal early epochs as well as of closerby objects.

These are long-term multinational, if not basically world-wide, projects with budgets of up to about half a billion current US dollars each. The LOFAR array could be completed by the year 2005, while for ALMA and SKA operation dates of 2008 and 2012 are being planned.

Clearly, the arrival of such giant instruments potentially capable of tracing line emission of at least hundreds of atoms and molecules redshifted throughout the radio spectrum out to the edges of the Universe, requires that careful thought has to be given to spectral management aspects, the establishment of (international) radio protection zones around the instruments and the design of interference-robust instruments in order to allow these giant radio telescopes to attain their scientific goals.

Recommendations from an astronomical point of view on the improvement of the regulatory context for scientific research using radio frequencies are given elsewhere in the present Proceedings [2].

6. REFERENCES

- [1] A. Winnberg, "Scientific use of radio - challenges from Space", in the present Proceedings
- [2] T.A.Th. Spoelstra, "Regulations and scientific use of radio frequencies", in the present Proceedings
- [3] T.A.Th. Spoelstra, "Oh Satellite, oh satellite", in the present Proceedings
- [4] K. Ruf, "Technical and engineering challenges for the future of radio astronomy", Radio Sciences Bulletin No. 291, pp. 13-18
- [5] ITU-R Radio Regulations, ITU Publications, Geneva, 1998
- [6] CRAF handbook for radio astronomy - 2nd edition, ESF-CRAF, Dwingeloo, 1997, pp. 81-82
- [7] Web page <http://www.nfra.nl/skai/>

BIOGRAPHICAL NOTE

Dr. W. van Driel is astronomer at the Paris Observatory, specialized in extragalactic research, and Director of its Nançay Radio Observatory. He is member of the Committee on Radio Astronomy Frequencies (CRAF) of the European Science Foundation and of the Commission on Frequency Allocations for Radio Astronomy and Space Sciences (IUCAF) of the IUT.

pairs being shaped into a single entity. The presence of the OH line is an indicator for this rare kind of activity, and because of the maser enhancement these powerful sources can be observed out to very large distances. The redshift of these distant objects takes them well outside the protected bands and the most distant are actually observed in the 21 cm band.

Though the Radio Astronomy Service has primary allocations in this domain, where no other radio spectrum user should disturb its observations, according to the ITU-R Radio Regulations [5], two satellite systems, designed badly and without taking the rights of radio astronomy into account have threatened our observations in recent years: the Russian global navigation system GLONASS and the commercial mobile satellite communication system Iridium [3], and radio astronomy has found itself in the peculiar situation of being forced to negotiate a limited access to its own allocated, protected bands and to accept their pollution by another spectrum user who had taken no steps to prevent this pollution, despite warnings by the radio community. Such an obviously unwanted situation could lead to dangerous precedents for all radio services [2].

3100-3400 MHz: CH

In this band, three lines of the CH molecule have been detected at rest frequencies of 3263, 3335 and 3349 MHz. The study of interstellar CH is considered to be extremely important in understanding the chemistry of interstellar material. Its presence suggests the existence of the molecule CH₄ (methane), considered as one of the basic molecules for the initial stages of the formation of life in the Universe. These frequencies have, unfortunately, only been allocated to radio astronomy by a footnote in the Radio Regulations.

4950-4990 MHz: formaldehyde (H₂CO)

Besides its wide use for radio continuum studies, one of the most important uses of this band is the study of formaldehyde (H₂CO) in interstellar clouds, which has a rest frequency of 4829.7 MHz. The importance of the line lies in the fact that it can be detected in absorption against continuum sources, even against the 3K cosmic background radiation. Isotopic abundance studies have also been made using its carbon and oxygen isotopes, providing insight in the state and distribution of these elements, produced earlier in the interiors of massive stars and flung into the interstellar medium during supernovae explosions.

Around 20 GHz: molecular lines

In particular the band between 18 and 30 GHz is densely packed with spectral lines, but only 37 out of the 173 lines listed in 1986 lie inside protected bands. So it is feared that many lines will become unobservable, seen the increased usage of this spectral region, especially for

satellite downlinks like those for HDTV broadcasts. Astronomers would like to be able to observe occasionally in certain bands, in agreement with the relevant ITU-R recommendation to administrations.

Beyond 30 GHz: (sub)millimeter wavelengths

In space, matter can exist in molecular form if it is far enough away from the ultraviolet radiation from hot stars, which can split molecules into their atomic components. Spectral line radiation from a given kind of molecule occurs as a series of lines, which are different for each molecule, and whose relative intensities depend on the physical conditions in which the molecule is situated, such as temperature and density.

Spectroscopy is one of the main tools of millimeter-wave radio astronomy, as it is frequently necessary to observe several lines, or transitions, of a given molecule to determine local physical conditions, or to unambiguously identify the emitting molecule, whose individual lines may be masked by lines from other molecules and whose observed line frequencies are shifted because of the source's radial motion in space.

At present, thousands of spectral lines have been identified in the millimetric and submillimetric spectral domain, representing well over a hundred different molecules found in a diverse array of objects. These objects, which in general cannot be studied in other frequency domains, include proto-planetary disks around young stars, low-temperature, dense and dusty cocoons surrounding protostars and young galaxies at high redshift in the early Universe. Some of the identified molecules are quite complex organic species consisting of up to a dozen atoms. Quantities can be astronomical indeed: the nucleus of the Milky Way contains enough C₂H₅OH to fill 10²⁸ bottles of 80 proof alcohol. Astronomical observations are already being made up to frequencies of about 2 THz. An example of well-observed lines is:

105-116/217-231 GHz: carbon monoxide (CO)

These are the most frequently observed millimeter bands, equal in importance to the 21 cm H_I line band at 1400-1427 MHz, as they contain lines of carbon monoxide (CO) and its isotopes.

These lines provide powerful tools for the study of cosmic isotope ratios, as CO is a relative stable molecule compared to others found in interstellar space and as it appears to be relatively abundant and widespread in the disk of spiral galaxies, like the Milky Way, where they can be used to trace the spiral arms.

It seems to play an important role in the chemistry of the interstellar medium and its high abundance may be due to an efficient formation mechanism.

Where these lines have been detected in other galaxies, their observed redshifted frequencies will be (radically) different from the rest frequencies. CO lines have been detected in very distant galaxies undergoing intense bursts of star formation at redshifts of over 3, i.e.,

SCIENTIFIC USE OF RADIO – CHALLENGES FROM SPACE

Anders Winnberg
Onsala Space Observatory
SE – 439 92 Onsala, Sweden
fax: +46 31 772 5590; e-mail: anders@oso.chalmers.se

Astronomy, several geophysical sciences including meteorology, and various remote sensing sciences use radio receivers to register extremely weak natural radio radiation from a multitude of objects and media. The sensitivity requirements of all these sciences, and in particular radio astronomy, make them very vulnerable to interference from man-made radio signals. Even out-of-band emission from active radio services in nearby frequency bands could be harmful to a passive scientific radio service. As long as the interfering radio transmitters are ground-based, geographic coordination could solve the problem, in principle. In recent years, however, many satellite-borne radio services have been defined, using low polar orbits. Such satellites cover the entire surface of the Earth in a short time and therefore no place is geographically protected from interference. Due to the increasing congestion in the radio spectrum, several satellite services have been allocated in frequency bands adjacent to or close to bands allocated to the radio astronomy service. There still is a danger that many future satellite services will be allocated in bands close to radio astronomy bands. Examples of such cases are given.

1. INTRODUCTION

There are several scientific radio services, but only some of them are registered as Radio Communication Services within the International Telecommunication Union (ITU). Many scientific radio services are 'passive', i.e. they only receive natural radio radiation and do not transmit any artificial radio signals. Examples of such services are radio astronomy and aeronomy. Other scientific radio services are 'active', i.e. they receive reflected or backscattered echoes from transmitted signals like a radar system. Examples of such services are remote sensing using Synthetic Aperture Radar (SAR) and Ionospheric Incoherent Scatter Radars, like the EISCAT installations.

I will limit myself to passive scientific radio services in this paper, however, because they are the most vulnerable services to man-made radio signals. First I will give a brief description of scientific radio services (Section 2) followed by a description of satellite radio services (Section 3). Then I will give examples of interference from satellites (Section 4) and of future chal-

lenges (Section 5) followed by brief conclusions (Section 6).

For a recent account of the threat to radio astronomy, the reader is referred to [1].

2. SCIENTIFIC RADIO SERVICES

2.1 Radio astronomy

Radio astronomy was registered as a Radiocommunication Service with the ITU in 1959. Some of the frequency bands reserved for the Radio Astronomy Service (RAS) originate from the World Administrative Radio Conference that same year (WARC59).

Radio astronomy is a division of the science of astronomy, and it studies the universe with the help of natural radio radiation. Due to its extreme sensitivity radio astronomy is very vulnerable to interference. Many countries in the world, including third-world countries, have invested large sums of money in radio astronomy and they have the obligation to enable the efficient operation of these expensive facilities.

Traditionally radio astronomy observatories have been built far from populated regions, sometimes in valleys, to avoid man-made radio signals. This solution to the interference problem, however, is not sufficient any longer since several satellite-borne radiocommunication services have been introduced. There is no place on our planet that is protected from interference from down-looking transmitters carried onboard non-geostationary (NGSO) polar-orbit satellites.

One place that is often mentioned in the context of interference to radio astronomy is the backside of the moon. There would be several advantages with a radio observatory on that site, such as the great distance and shielding from the terrestrial interference sources and the low gravity. As a matter of fact a commission within the International Astronomical Union (IAU) is working on this idea. However, the cost for the construction and running of such a station would exceed the total cost for all existing ground-based radio observatories. The question is whether such a project would become financially feasible before the space beyond the moon would be filled with interfering space vehicles!

Of course the reason for the vulnerability of radio astronomy is its great sensitivity necessitated by the

extreme weakness of natural radio radiation from extra-terrestrial sources. This is reflected in the special unit for spectral flux density that was introduced in radio astronomy in its early days: 1 Jansky = 1 Jy = 10^{-26} W m⁻² Hz⁻¹, i.e. -260 dB(W m⁻² Hz⁻¹). Many modern radio astronomy instruments are capable of detecting noise signals with an intensity of the order of a few μ Jy.

Radio astronomy was the first new division of astronomy that, after the Second World War, introduced electronic techniques to astronomy on a large scale. This revolutionized the science and today there is no part of observational astronomy – not even the classical optical astronomy – that is not heavily dependent on electronics. The constant quest for better sensitivity and resolution by the astronomers has led to a rapid rate of electronic inventions and development of know-how within the astronomical science. This in turn has had a cross-fertilization effect between astronomy and industry.

2.2 Geodesy

The science of geodesy measures the shape of the earth. Geodetic data taken at many time epochs are used by geophysical sciences like geodynamics which deals with motions of the earth crust and changes in the axis of rotation. In the seventies geodesy got a very powerful tool from radio astronomy: Very Large Baseline Interferometry (VLBI). This is perhaps the most sophisticated technique in radio astronomy, enabling enormous angular resolutions. It involves radio telescopes separated by very large distances across continents and even on different continents. These radio telescopes observe the same cosmic radio source simultaneously, but since the distances between them are so large, the signals cannot be brought together online with preserved phase. Therefore they are recorded on magnetic video tape at each station together with accurate time codes and when the observing session is over, these tapes are transported to a special correlator where the signals are correlated pairwise. The correlated signals are further reduced in a general purpose computer and the end product is a map of the radio source with very high magnification. The record angular resolution achieved to date is 50 micro arcsecond, about 10^{-8} °, or the angle that a golf ball on the moon would occupy as seen from the earth!

The astronomical use of the VLBI technique is based on the assumption that the geographical positions of the participating radio telescopes are well known. In the course of time a long list of point-like, distant radio sources with accurate celestial positions has been compiled. By observing these sources over and over again one could determine the geographical positions of the radio telescopes with increasing accuracy. This is how geodesy is using the VLBI technique.

Geodetic VLBI uses two frequency bands, at about 2.2 GHz and 8.5 GHz. These two bands are observed simultaneously in order to correct for ionospheric effects. The VLBI technique is rather robust against interference since the interfering signal must be phase coherent

to at least two participating radio telescopes to cause a signal in the correlated output, a situation which could occur only for relatively close telescopes or for a transmitter on a distant satellite or space probe. A strong interfering signal, however, could drive one of the VLBI receivers into saturation.

Space geodesy is not a separate radio service. It uses bands allocated to Space Research and Earth Exploration-Satellite services and sometime it goes outside these bands on its own risk. A potential threat to space geodesy has emerged in the United States where the band 2.31 - 2.36 GHz has been allocated to the Broadcasting-Satellite Service for digital audio broadcasting from geostationary satellites. Two operators are scheduled to start operations this year.

2.3 Aeronomy

The science of aeronomy is dealing with the physics and chemistry of planetary atmospheres, including the atmosphere of our own planet. Within the last twenty years microwave technique has been introduced in aeronomy, again as a 'gift' from radio astronomy, as a very powerful tool to probe the terrestrial 'middle atmosphere', i.e. the stratosphere and the mesosphere (altitudes 10 to 100 km). Several gases (ClO, CO, H₂O and O₃) can be detected and studied through rotational spectral lines in the millimetre and sub-millimetre wave range. The dominating line broadening mechanism is pressure broadening and therefore, by analyzing the shape of the line profile, one can deduce the abundance of the species as a function of pressure, i.e. altitude.

'Radio aeronomy' measurements are carried out both from the ground and from satellites. The atmospheres of Venus, Jupiter and Saturn can be studied also using large radio telescopes or interferometers. This is considered as radio astronomy, though.

'Radio aeronomy', like 'space geodesy', is not a separate radio service either. Several of its requirements, however, hopefully will be taken care of during the next World Radiocommunication Conference (WRC2000). Active radio operators in the millimetre wave bands are still rare but several services are planned for the future (see Section 5).

2.4 Remote sensing

A great variety of techniques is collected into the conception of 'remote sensing'. These techniques are used in both basic research and in applied research and they can be both passive and active.

One research area which uses remote sensing is meteorology. Another example of remote sensing is the monitoring of the earth surface from satellites to estimate resources, e.g. forest, or to study the seas.

There are three Radiocommunication Services which are associated with remote sensing. Meteorological-Satellite Service (MetS), Meteorological Aids Service (MetA) and Earth Exploration-Satellite Service (EESS). MetA is mainly instruments onboard balloons.

3. SATELLITE RADIO SERVICES

The following commercial and utility satellite radio services have been defined and registered within ITU: Amateur-Satellite Service (AmSS), Broadcasting Satellite Service (BSS), Fixed-Satellite Service (FSS), Inter-Satellite Service (ISS), Mobile-Satellite Service (MSS), Radiodetermination-Satellite Service (RDSS), Radio-location-Satellite Service (RLSS), Radionavigation-Satellite Service (RNSS) and Space Operation Service (SpO).

MSS and RNSS are subdivided into Aeronautical, Land and Maritime sections.

I will not deal with the AmSS and SpO services because they are not causing any problem for scientific radio services to my knowledge.

3.1 Broadcasting Satellite Service

This service, established already in 1971, is predominantly used for television broadcasting but Digital Audio Broadcasting (DAB) is coming soon. The satellites usually are geostationary. The allocated bands are 1452 – 1492 MHz, 11.7 – 12.5 GHz, 21.4 – 22.0 GHz, 40.5 – 42.5 GHz and 84 – 86 GHz. The band 11.7 – 12.5 GHz is a problem, because one operator is causing heavy pollution in the RAS band 10.6 – 10.7 GHz (see section 4). The band 40.5 – 42.5 GHz is a potential problem because it is adjacent to the RAS band 42.5 – 43.5 GHz containing spectral lines of silicon monoxide. However, so far no operator has taken up this band in Europe and the European administrations will try to delete the BSS from this band at the WRC2000. The band in the 3-mm wavelength range (84 – 86 GHz) has not been used so far either. It probably will be moved to 74 – 76 GHz at WRC2000.

3.2 Fixed-Satellite Service

This is one of the oldest satellite services and it is used for communication between fixed earth stations via satellite both as audio and video. A large number of frequency bands have been allocated to FSS but the need for more band is still strong. The American administration is trying to get the band 40.5 – 42.5 GHz allocated to FSS (Teledesic) but most European administrations are against this, mainly because they want to protect terrestrial systems in the Fixed Service (FS) and the Broadcasting Service (BS). Again the RAS band 42.5 – 43.5 GHz is at stakes. Already FSS is allocated inside the RAS band but only for uplinks which are easier to coordinate, especially for fixed earth stations.

3.3 Inter-Satellite Service

Many satellite systems need to have communication between the satellites. This could cause problems for satellite-borne scientific radio services using bands close to ISS bands. There is an ISS band around 23

GHz which lies between two RAS bands for spectral-line observations (water vapour and ammonia). This could cause problems in the future.

3.4 Mobile-Satellite Service

This service is providing communication between mobile terminals via a fleet of satellites. The terminals can be onboard vessels or transported in cars or lorries. The latest development, and probably something for the future, is the MSS application with handheld terminals, similar to mobile telephones. There are several bands allocated to MSS at frequencies below 1 GHz. In addition there are bands within the 1.4 – 1.7 GHz range which are close to important RAS bands (hydrogen and hydroxyl). One operator (see section 4) chose to run both the uplinks and the downlinks in a band close to the RAS band 1610.6 – 1613.8 GHz. This has caused strong interference to radio astronomy in this band used for observations of OH.

3.5 Radionavigation-Satellite Service

So far there are two operators in this service: GLONASS and GPS. GLONASS is a Russian system set up during the 1980ies to enable accurate navigation for vessels and airplanes based on delay measurements of signals from several satellites which are above the horizon at any time and at any geographical site. GPS is a similar American system established by the US Air Force but with several code levels, some of which can be used by civilian equipment.

Both systems operate in the 1.6 GHz range. When the GLONASS satellites were launched some of them were transmitting right inside the RAS band 1610.6 – 1613.8 GHz (see section 4). There are no known interferences from the GPS satellites any longer after an initial disaster with the first satellites, launched at the end of the eighties.

Both the European Space Agency (ESA) and the National Space Development Agency of Japan (NASDA) are planning their own navigation systems based on satellites. The European system will be called Galileo and one of the bands that have been proposed is close to the RAS band 4990 – 5000 MHz.

4. EXAMPLES OF SATELLITE INTERFERENCE

4.1 TEX

In 1992 radio astronomers in India and in the Netherlands detected a radio signal at a frequency of 328.25 MHz which is in a band which is shared by Fixed, Mobile, and Radio Astronomy services. The characteristics of the signal led to the conclusion that it originated from a satellite. The Dutch frequency administration filed a complaint with ITU who brought the issue to the attention of the American, Chinese, and Russian administrations. After a long and persistent investigation by the US administration and by the spectrum manager of the

1998 that the culprit was an American military satellite by the name of TEX which was out of function.

TEX was launched in April 1990 and taken out of service in June 1991. The satellite attitude control did not function properly and there is no 'off button' for security reasons. And of course the frequency is illegal. The situation is now that Boeing Company – the corporation responsible for the satellite – is constantly monitoring TEX and when necessary sending 'keep quiet signals' to it.

We can learn two things from this: a) administrations should be extra alert on the frequency selection and coordination process for space stations; b) every satellite transmitter should have an 'off button'.

4.2 Astra D

This is a geostationary satellite for TV broadcasting for Germany and neighbouring countries. The operator is Société Européenne des Satellites in Luxembourg and it has a license for broadcasting in a band above the radio astronomy band 10.6 – 10.7 GHz. Due to a malfunction of the transmitter, however, Astra D causes severe interference in the radio astronomy band. Therefore, no observations are possible in this band in Europe. Again, this case teaches us that a much stricter mechanism has to be found for the licensing of satellite services.

4.3 GLONASS

In 1984 it was discovered that many of the GLONASS satellites transmitted in or close to the radio astronomy band at 1610.6 – 1613.8 MHz. This band is mainly used for studies of a spectral line from the hydroxyl radical (OH) at 1612.321 MHz. The radio astronomy service was upgraded to primary status in 1992 and shortly afterwards negotiations started between the Interunion Commission on the Allocation of Frequencies to radio astronomy and space research (IUCAF) and the GLONASS administration [2]. This led to a step-by-step plan to clear the radio astronomy band from interference from GLONASS. This agreement served as a model for similar agreements between the frequency administration of the Russian Federation and those of other countries having radio observatories using the band. According to these agreements the transmitters of all the GLONASS satellites should be outside the protected band and filters be installed before the end of 2005. This is to be accomplished by replacement of satellites as the old ones cease to operate. So far the timetable seems to be followed.

4.4 Iridium

The WARC 1992 allocated the band 1610.0 – 1626.5 MHz to the uplinks of the MSS on a primary basis and the same band to the MSS downlinks on a secondary basis. However, the following footnote was added to the Radio Regulations: *"Harmful interference shall not be caused to stations of the radio astronomy service*

using the band 1610.6 – 1613.8 MHz by stations of the... mobile-satellite services".

Several of the MSS operators are using the band 1610.0 – 1626.5 MHz for their uplinks. One operator, the Motorola-lead international consortium Iridium LLC, however, chose to use the same band for their downlinks as well. Iridium got an American license in the band 1621.35 – 1626.5 MHz and soon started negotiations with other administrations for licenses in this band.

In the course of time it became clear that Motorola did not implement measures in the Iridium system to protect any other radio service, including the radio astronomy service, in their own band or in adjacent bands. The main source of interference in adjacent bands is the wide-spread intermodulation products caused by simultaneous transmission at several frequencies using the same transmitter. For radio astronomy Motorola Inc. did suggest some operational solutions, but these would affect radio astronomy *only* and have no impact on the operation of the Iridium system.

In 1994 the US National Radio Astronomy Observatory agreed to restrict observations of the OH line to 4 hours during the night when the Iridium traffic is low. A similar agreement was signed with the National Astronomy and Ionospheric Center at Arecibo in Puerto Rico stating that during about 8 hours per day the Iridium interference would be below the ITU recommended level for harmful interference [-238 dB (W/m²/Hz)].

In Europe Iridium has met strong resistance from radio astronomers. The 1612-MHz band is used much more in Europe than elsewhere in the world and European radio astronomy is well organized under the European Science Foundation (ESF) Committee on Radio Astronomy Frequencies (CRAF). CRAF brought its concern to the attention of the 'Conférence des Administrations Européennes des Postes et des Télécommunications' (CEPT) who ordered CRAF and Iridium to negotiate about compromise conditions valid during a limited period. After very difficult negotiations an agreement was reached which is valid for the time 1 May 1999 to 1 January 2006.

According to this agreement, four major radio observatories in western Europe are protected from interference during 7 hours per day and during 2 weekends per month around the clock. Other European observatories can get the same amount of protection after notification of need (collectively). After the 1 January 2006 the Iridium system shall not cause any harmful interference to radio astronomy.

This agreement is the most favorable one of all agreements signed between Iridium LLC and radio astronomy organizations. Still it should be pointed out that the Iridium case is a an example of an inferior method of solving an interference problem. The victim should not have to share a frequency band with the pollution from the perpetrator!

5. CHALLENGES IN THE FUTURE

5.1 Cloud profiling radar

A Cloud Profiling Radar is one of the instruments investigated within the ESA for its Earth Observations Preparatory Program (EOPP). It will record the water droplet size as a function of altitude through the clouds. This is of great importance for predictions of and warnings against hail storms and similar meteorological phenomena but also for longterm modelling of global warming.

This satellite-borne radar will operate in the band 94.0 – 94.1 GHz which is in the astronomically important 3-mm 'atmospheric window'. In this band and in the higher-frequency mm-wave bands, radio astronomers study many spectral lines from various molecules in interstellar space.

CRAF informed ESA about the potential problem of interference to the very sensitive radio astronomy mixer receivers used in this frequency range. The mixer element, Superconductor-Insulator-Superconductor (SIS), is inherently very broadband and open for interference from signals far away in frequency from the frequency of the spectral line under study. In the case of a mainlobe-to-mainlobe line-up between the mm-wave telescope and the radar telescope an SIS mixer could even be destroyed.

ESA contracted the Italian branch of the Swiss company Oerlikon-Contraves to investigate the problem and to suggest solutions. The best solution turned out to be the installation of band-stop filters in front of the mm-wave mixers of radio telescopes covering the 100-MHz band of the radar signal. Prototypes of filters of various design were manufactured and tested and the most promising design was a ring-loaded circular waveguide filter. It is extremely difficult to make these filters due to the very small mechanical tolerances. But in any case the first step has been taken in the development of high-Q, low-loss filters for mm-wave applications.

5.2 Sky stations

This is another planned system but it will not be based on satellites. Instead it will consist of geostationary platforms located in the stratosphere at an altitude between 20 and 30 km. Therefore the system also is called High Altitude Platform System (HAPS). Each platform will be a giant helium-filled 'blimp' with solar panel arrays for its entire energy need, including the energy for its engines that will keep it close to its nominal geographical position. The stations will be hovering over populated areas and there will be at least 250 of them. The platforms will be the backbone in a global Internet system with variable broadband data rates at a nominal

rate of 1.5 Mbps to portable terminals and up to 155 Mbps to fixed terminals.

Sky Stations will use the band 47.2 – 47.5 GHz for its downlinks and the band 47.9 – 48.2 GHz for its uplinks. The potentially threatened radio astronomy bands are 42.5 – 43.5 and 48.94 – 49.04 GHz.

5.3 Teledesic

This is a subsidiary of Microsoft Inc. and its purpose is to provide broad-band communication service via 288 satellites in non-geostationary orbits and a large number of fixed earth stations. The system therefore is part of the FSS. Teledesic has requested two uplink bands at 17.8 – 18.6 GHz and 18.8 – 19.3 GHz and two downlink bands at 27.6 – 28.4 GHz and 28.6 – 29.1 GHz. The radio astronomy bands that could become affected by the downlink signals, if insufficient precautions are taken, are 23.6 – 24.0 GHz and 31.3 – 31.8 GHz.

6. CONCLUSIONS

Passive scientific radio services are very vulnerable to radio interference due to their extreme sensitivity. Satellite-borne sources of interference are especially harmful since there is no place on Earth where a scientific radio station could 'hide away' from such interference. For radio astronomy and for aeronomy such sources of interference are harmful also because they are situated in the sky where radio telescopes are pointed during measurements.

International regulation, licensing procedures and equipment approval for satellite systems have to be improved in order to avoid mistakes and malfunctions.

7. REFERENCES

- 7.1 J. Cohen "Radio pollution: the invisible threat to radio astronomy", *Astronomy & Geophysics*, Vol. 40, 1999, pp. 6.8 - 6.13.
- 7.2 B. Robinson, "Frequency allocation: The first forty years", *Annual Reviews of Astronomy & Astrophysics*, Vol. 37, 1999, pp. 65 - 96.

BIOGRAPHICAL NOTE

The author is Professor at Onsala Space Observatory, Chalmers University of Technology, Göteborg, Sweden. He got a PhD at Chalmers in 1970 and worked at the Max-Planck-Institut für Radioastronomie in Bonn, Germany, in the 1970ies. His scientific interests lie in the areas of late-type stars, galactic structure, comets, and the earth atmosphere (aeronomy). He is a member of the ESF Committee for Radio Astronomy Frequencies (CRAF).

NATO APPROACH TO HARMONIZATION OF CIVIL AND MILITARY EMC STANDARDS

Invited sessions NATO/1 to NATO/4 organized by:

CAPT. R. AZZARONE, *General Directorate TELEDIFE, Rome, Italy*

DR M. KUKULKA, *Polish Navy HQ, Gdynia, Poland*

CDR. R. ARCHER, *Nato HQ, Brussels, Belgium*

(sponsored by NATO Special WG10 "EM Environment Effects")

EMC 2000

INTERNATIONAL WROCLAW SYMPOSIUM
ON ELECTROMAGNETIC COMPATIBILITY

PROVISION OF EMC IN BULGARIAN NAVY AND HARMONIZATION OF NAVAL AND CIVIL E3 STANDARDS

Captain eng. Dimitar Dimitrov
Navy Staff, Bulgaria

INTRODUCTION

The problem of electro-magnetic compatibility (EMC) of radio-electronic equipment on board of ships, submarines and aircraft has gained nowadays a great importance.

When a ship is out at sea almost all radio-electronic equipment (REE) functions at one and the same time and that forms a complicated electromagnetic situation. We have a great number of REE, auxiliary installations and generators working in a comparatively small area.

The impact of this electro-magnetic situation on REE comes through the low-frequency electromagnetic field on the ship, the transient process in the networks, the high frequency electromagnetic field as well as through the electromagnetic effects in the atmosphere. Placing a great number of radio engineering installations in a comparatively small area is characterized by the increase of active interference and the arising of the problem of their electro-magnetic compatibility.

I. PROVISION OF EMC ON BOARD THE SHIPS OF BULGARIAN NAVY

We assume that the creating of a complex electro-magnetical condition on a board of ship can bring the following hazards:

- destruction of electronic hardware
- communication breakdown
- threat of human life (crew of the ships).

The electronic hardware can be physically damaged in case of high-powered interference fields. Communications breakdown happens most frequently when the parameter of signal-to-noise ratio is affected. The

peak level depends on the kind of modulation and coding.

The biggest typical military electro-magnetic threats on ships are considered to be the 1000 Watt HF-transmitters and the radars. The Bulgarian Navy has required specific installation measures on their latest ships to attenuate outer deck EM-fields generated by these sources. In inner deck areas the field strength was reduced to below 1 V/m in the frequency band from 2 to 30 MHz. Also field strengths caused by radar were reduced to below 1 V/m in below deck areas.

We assume that this process is particularly applicable now when on board the naval ships of Partners there will be installed new additional appliances of communication that are compatible with NATO's installations.

Obviously that will make the radio electronic environment of the ships more difficult and new decisions will have to be found, one of which is the deconstruction of a part of the old equipment with the aerial systems.

To solve these problems of providing EMC, the following four tasks should be fulfilled in sequence:

1. Investigation of the electromagnetic environment in which radio-electronic equipment functions.
2. Estimation of the electro-magnetic compatibility.
3. Development of new methods and devices providing EMC on the ships.
4. Harmonization of naval and civil E3 standards.

To discuss all the problems concerning the provision of EMC is practically impossible, therefore I will concentrate on the harmonization of naval and civil E3 standards.

II. HARMONIZATION OF NAVAL AND CIVIL E3 STANDARDS

The National Board of the health service and safety is a central organ that works upon the matters of the working time and environment in Bulgaria.

In the Ministry of Defense the following organs are created to be responsible for providing EMC and harmonization of the standards.

There is an organized agency within the Ministry of Defense called "Military insurance expedition and codification" and a department for "Military Standardization".

Their task is to insure all kinds of Standards both civil and military.

The central laboratory for measurement instruments is authorized to be responsible for the control connected with the establishment of the requirements of the working environment. It establishes inspection procedures and their mechanisms.

The laboratory performs measurements not only of the civil working environment, but also on the military units and equipment. In the course of that activity the laboratory makes proposals for the working up of new methods of control and measurement, their technical forming, etc.

There is a Central Military Inspection constructed within the Ministry of Defense. Its task is to perform radio activity investigations of the electromagnetic environment and the emissions from the military equipment.

The basic Bulgarian specification document by which measurements are made aboard Bulgarian Navy ships is the Bulgarian National standard BNS - 14 525 - 90 and BNS-17137-91.

The determination of the intensity of the electric compound (E) and magnetic constitutive (H) of the equipment is done in compliance with the Bulgarian State Standard-14525-90. Electromagnetic fields frequency acceptable values requirements for the control of the frequency range from 60 KHz to 300 MHz.

The determination of the density of the energetic current is done in compliance with the requirement of the Bulgarian State Standard 17137-91 for the frequency range 300 MHz to 300 GHz.

	FREQUENCY RANGE	LIMIT VALUE
1	30 - 300 KHz	25 V / m
2	0.3 - 3 MHz	15 V / m
3	3 - 30 MHz	10 V / m
4	30 - 300 MHz	3 V / m
5	0.06 - 1.5 MHz	5 V / m
6	30 - 50 MHz	0.3 A / m
7	0.3 - 300 MHz contin.	0.1mkW / cm2
8	0.3 - 300 MHz up to 8 h	10 mkW / cm2
9	0.3 - 300 MHz up to 2 h	< 100 mkW / cm2
10	0.3 - 300 MHz up to 20min	< 1mkW / cm2

Tab. No 1 Admissible limits of the strength and density of the energy flux of EMC in populated areas.

The admissible limits are pointed out in table No 1. In the frequency range between 30 KHz and 300 MHz the electric component in V/m and the magnetic field in A/m are measured, while above 300 MHz the energy flux density is measured in W / m-2 or mkrW / sm-2 .

For populated areas the rate is more restrictive and must not exceed admissible limits of 10 mkW/cm2.

We do not have any military standards for EMC. For basis we use that are shown above following two civil standards.

When we ordered from the equipment makers creating a new military equipment, in the beginning we specified military requirements, which are more complex than the civil standards.

The basic regulating document is "Design and incorporating of a goods with military designation" in which are requirements for the equipment makers, stage of control and methods for testing the new equipment.

To achieve these goals it is necessary the performing of the following formalized tasks:

-The comparison of the fundamental civil and military E3 standards.

-The comparison of the common military limits and the determination of the degree to which they can be common.

Comparison the military and civil environment.

The military environment distinguishes itself from a commercial one by radar, communication antennas, EMP, and in inner deck places by a high density of equipment in a commercial environment equipment is placed in an open field while the hull off a frigate provides a screening for the inner deck equipment against the rest of the world. This screening by the hull causes several areas with a different environment depending on the quality of the screening.

Field forces under 1V/m are not deemed to be dangerous. Our opinion is that the cargo equipment can be placed in the below deck and Internal space, which has not direct connection except through cables to the external area. In this case, however, we must look at the density of the equipment.

Most frequently forced by possible cost reduction, we buy civil equipment. Placed in the military electro-magnetic situation, even in the inner deck this equipment can cause damage. Consequently it is necessary to remake and improve this equipment using military standards, and so after this operation the price become higher.

These low field strengths in specific areas made the application of commercial standards feasible. Therefore, a profound study analysis and application of civil standards are necessary in the complex military condition.

In the last years commercial standards have been used often on board the Bulgarian ships.

Up to now they haven't caused a big problem. The problem of the Bulgarian Navy is the lack of experience with commercial standards in the military environment.

Our main task at this stage is to adopt all NATO standardized documents applying to EMC and their improvement and application in the Bulgarian navy.

CONCLUSION

A review of the problem shows that up to now there isn't a common criterion established in the world to estimate the impact of electro-magnetic field on the human organism and to define the admissible limits of the field characteristics. This leads to substantial differences between specification documents of different countries.

Numerous publications on this problem show that at present there are common standards, not only civil but military too, that refer to electro-magnetic radiation and to the norms for protection of human life. Our main task is therefore the creation of common normative document and harmonization of civil and military standards.

REFERENCES:

1. Design and incorporating of a goods with military designation - MoD 1990
2. Bulgarian State Standard-14525-1990.
3. Bulgarian State Standard-17137-1991.
4. Electromagnetic Compatibility – Symposium EMC -1994 and 1996
5. Pajii. AI – “ Radioelektronnaia borba “ –Moskva 1990.

RISK ANALYSIS BY THE USE OF COMMERCIAL EQUIPMENT IN A MILITARY ENVIRONMENT

Henk A. Klok
Royal Netherlands Navy
Postbox 1260
2340 BG Oegstgeest
The Netherlands
phone: 00 31 71 305 2173
fax: 00 31 71 305 2606

e-mail: ha.klok@mindef.nl or adv@meobo.navy.disp.mindef.nl

The use of Commercial off the Shelf equipment is widely accepted, even in a military electromagnetic environment. Since this equipment has to meet the European EMC-directive 89/336/EC, it is expected that in those cases where equipment needs to comply to the basic EMC-requirements a considerable amount of money will be saved.

In this paper, the differences between the military EMI-standard MIL-STD 461D/462D together with the civil EMI-requirements are compared with respect to measurement methods, frequency range and limits. Also the applicability of the test methods will be taken into account.

In the second place, the electromagnetic environment existing on board of Navy ships has been determined to evaluate the risk of using the COTS equipment in this environment. Within these established EM-environments the necessary EMC-requirements applied to the equipment are defined. A few of the assumptions made in the theoretical approach of the comparison are verified by using measurement data taken from commercial equipment.

It is noted that in case the necessary requirements could not be met with civil EMC standards, it is examined whether additional installation rules, or other additional constraints, would lead to the feasibility of using commercial equipment with a acceptable risk of EMI.

1. INTRODUCTION

In the Royal Netherlands Navy a project is running to investigate and analyse the risk of installing commercial equipment in a military electromagnetic environment. Because of the fact that in general equipment fulfilling military EMC standards are expensive and that commercial equipment has to fulfil the EMC directive, it can be acceptable to install this equipment on board. However, it has to be taken into

account that the environment of a naval ship is very different from an industrial and residential environment. To investigate the difference and to prepare recommendations, the study will focus on a comparison of standards and environments.

The first step is to collect commercial standards, relating to electric and electronic equipment with respect to EMC requirements. Secondly a comparison was made with the MIL-STD-461D/462D focusing on the frequency band of interest, the measurement methods, the limits, etc.

To analyse the risk by installing commercial equipment, the electromagnetic environment is determined and with respect to this conclusions can be made.

The main conclusion is that for operational and tactical equipment it is not allowed to use commercial equipment. The frequency range of a ships EM-environment does not correspond to the measuring frequency range for radiated emissions and immunity methods of the civil standards. It can be recommended to the civil organisations at least to extend the frequency range. More investigations will perform to the installations rules on board if stricter rules can partly solve this problem.

Another very important point will be to start discussions on the harmonisation of measurement methods. When the methods are harmonised for the civil as well as the military organisations, the limits can be different depending on the applicability, electromagnetic environment, etc. of the equipment.

2. COMPARISON OF DIFFERENT STANDARDS

With respect to the commercial standards, different of them are included in the study:

- EN 50081
- EN 50082
- IEC 60533
- IEC 945

The IEC 60533 is an interesting standard, applicable for electromagnetic compatibility of electrical and electronic installations in merchant ships. This makes a comparison with the military standards more in line of the naval ship's environment. The IEC 945 is an interference standard for navigation equipment installed in a ship's environment.

The other European EN standards are both generic standards for equipment not dealing with a product standard and installed in an industrial environment. EN 50081 is an emission standard, EN 80082 an immunity standard.

Comparing the commercial standards with the MIL-STD-461D/462D, it can easily be concluded that most of the tests differ too much for a theoretical correct comparison. However since there is a need for a well founded standpoint regarding the application of commercial standards, so one must make use of the experience, good practice and even experiments.

In general, the commercial standards differ from the military standards in two ways:

1. Incomplete frequency range;
2. Tests differently executed (where frequencies are involved).

Below, the different methods and limits will be compared and discussed.

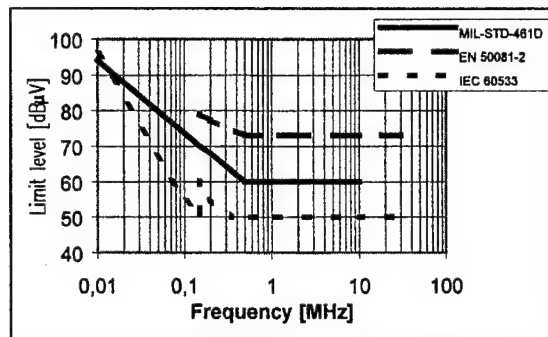
2.1. Conducted Emission

Focusing on the MIL-STD, it can be concluded that compared with the last versions (461C) of the MIL-STD, the D and E version use a Line Impedance Stabilisation Network (LISN) instead of a feedthrough capacitor.

This makes the comparison with the commercial standards more easily, because the civil standards also use a LISN. Before comparing the limit lines, some differences are to be noted:

- There is a difference between the characteristics (components, frequency range versus impedance response, etc.) between the LISN's.
- The MIL-STD measures in the frequency range from 30 Hz to 10 kHz the current. In the frequency range from 10 kHz to 10 MHz, the voltage will be measured.
- The commercial standards measure only the voltage between 150 kHz to 30 MHz.

With these differences in mind, the limit lines over the common frequency range can be compared. This comparison shows that the IEC 60533 is more stringent than the other standards. See graph 1 for the different limit lines. With respect to the IEC limit line it should be noted that this limit is for equipment installed in the bridge and deck zone. For equipment installed in the general power distribution zone the limit is about 20 dB less severe.



Graph 1: Comparison of conducted emission limits

2.2. Radiated Emission

In the harmonised commercial standards, only the electric field will be measured. There is a method under consideration for the magnetic field emission. This test method is compatible with the MIL-STD-461/462.

In radiated emission tests for the electric field, the measuring distance and the environment are not similar. The commercial standards require an open site environment, while the military standard requires a shielded room. The effect of the cage is responsible for a deviation to open site measurements results of maximum 6 dB.

However, the commercial standards are more open for the applicability for a screened room instead of the open area. Measurements in an open area are difficult to perform, due to the high ambient. To avoid reflections, a compact range (fully anechoic chamber) can be used.

This test environment makes a comparison easier, but special attention should be paid to for performing radiated measurements in screened rooms. The results are very depending on the amount of absorbing material in the room. Investigations and tests showed a difference of over 15 dB in different cages. When the cage is fully equipped with absorbing material with the proper specifications, the difference will increase to not more than 3 dB.

With respect to the measuring distance, in the commercial standards the distance in most cases is 30 metres, or sometimes, depending on the standard, 10 metres. In some cases a measuring distance of 3 metres is allowable.

In the IEC 60533 however, the measuring distance is 3 metres in all cases. Comparing with the MIL-STD measuring distance of 1 metres, the distance is a problem because of the fact that the antenna is placed in the near field.

In the commercial standards it should be noted that the limit can be corrected linearly as a function of the distance from 30 metres up to 3 metres (far field correction). For a measuring distance to 1 metres, the transfer function is frequency dependent due to near- and far field corrections.

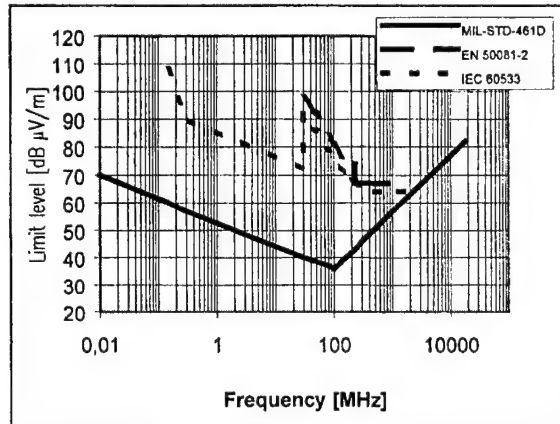
In the study this correction factor is calculated by assuming the fact that the field of the equipment under

test is characterised as a field generated by a halve wave dipole.

It is also important to note that the frequency range of measuring of most of the commercial standards is from 30 MHz to 1 GHz. Only in the IEC 60533, the starting frequency is 150 kHz. This will be a very important change.

Comparing the different limits over the common frequency range, taken into account the differences in measuring distances, it shows that the MIL-STD is more stringent than the commercial standards. For the comparison of the limits, see graph 2.

It should also be noted that the frequency range of the MIL-STD is from 10 kHz up to 18 GHz.



Graph 2: Comparison of radiated emission limits

2.3. Conducted susceptibility

The methods of military and commercial standards are not really comparable because of the method of injection and differences in injection signals.

An experiment was to relate the methods by the data resulted from the product investigation. An equipment under test shall tested conform both methods. During both tests the stress factor is raised until the equipment under test fails. Comparing the stress factors should give information about the relation between the commercial and military standards.

2.4. Radiated Susceptibility

The radiated susceptibility test with respect to the electric field, refers to a field measured at the location of the equipment under test. This causes no significant difference with the MIL-STD test.

An important difference will be the covered frequency range of both standards. In the MIL-STD the test has to be performed over a very wide frequency range from 10 kHz up to 40 GHz. In the commercial standards this will be from 30 MHz to 1 GHz (80 MHz to 2 GHz in the IEC 60533).

It can be seen that the frequency range from 2 MHz to 30 MHz is not covered in the commercial standards.

Focusing on the limits of the different standards, it can be noted that equipment fulfilling the MIL-STD has

to withstand 200 V/m over the complete frequency range for outerdeck purposes. For other purposes different values are applicable depending on the environment (below deck of a metal hull, non-metallic ship, etc.) and can be increased to 10 V/m. This is the same value as the commercial standard for industrial environment.

In the MIL-STD application, the test signal is unmodulated in the frequency range below 1 GHz.

Due to the modulation of 80 % with a 1 kHz signal the commercial test may be considered more severe than the MIL-STD for below deck equipment.

In this study special attention is paid to the frequency range below 30 MHz and above 1 GHz.

See table 1 for an overview of the comparison.

	MIL-STD-461D	EN 50082-2	IEC 60533
Freq. Range	10 kHz - 40 GHz	80 MHz - 1 GHz	80 MHz - 2 GHz
Measuring Method	monitor the field during the test at location of EUT	define a certain area of homogenous field within 6 dB on the place where the EUT will be located	
Limit	up to 200 V/m	10 V/m	up to 10 V/m
Modulation	< 1 GHz: CW > 1 GHz: pulse 1 kHz	Amplitude modulation (AM) with 1 kHz and modulation depth 80 %	

Table 1: Radiated Immunity comparison

3. DEFINITION OF THE ELECTROMAGNETIC ENVIRONMENT

The military environment differentiates itself from a commercial by radar transmissions, communications in a wide frequency range, electromagnetic pulse (EMP), and in innerdeck situations by a highly density of equipment. In a commercial environment equipment is placed in an open field while the hull of a frigate provides a screening for the innerdeck equipment against the outside world.

This screening by the hull will create several areas with a different EM-environment, depending of the quality of the screening.

The electromagnetic environment on board of the Royal Netherlands Navy ships (due to the outside threat), is highly dependent of the policy of the RNLN to built their own ships. The policy during the design of a ship is that the fieldstrength inside the ship has to be as low as possible. To create an environment as "nice" as possible, installation rules are to be used. These rules are laid down in a Defence document KN 12330. This document is developed by the RNLN, based on theoretical measures and investigations to very practical guidelines.

Some of these are for example:

- Use of screened cable all over the ship.
- Outerdeck cables as few as possible and as short as possible.

- Use of special cable glands to connect the cable screening over 360 degrees to the hull of the ship, the cabinets or equipment.
- Cable separation of the different cable categories.
- Design electronic compartments with special installation rules.

These measures result in an EM-environment due to outside threats as radar, communications and EMP, which can be described as follows in the next table 2.

Source	Frequency	EM-environment		
		Outerdeck	Innerdeck	
		whole ship	Above maindeck	Below maindeck
MF/HF comm.	0,5 - 30 MHz	200 V/m	1 V/m	1 V/m
VHF/UHF comm.	30 - 400 MHz	20 V/m	< 0,1 V/m	< 0,1 V/m
Search radar	1 - 10 GHz	2500 V/m	20 V/m	3 V/m
Track radar	5 - 35 GHz	2500 V/m	-	-
EMP	< 1 GHz	50 kV/m	500 V/m	50 V/m

Table 2: Electromagnetic environment of a metal ship

A fieldstrength below 1 V/m is considered as no threat. Regarding the above table, it seems that commercial equipment can be placed in below- and innerdeck areas, which have no direct link (by cable) to outerdeck areas. However, in these situations it should still be considered if the density of equipment in which the equipment has to work without EMI-problems.

As already noted, the typical military EM-environment is caused by emissions from noisy innerdeck equipment as static inverters at one hand and radar- and communication transmitters outside on the other hand.

In most below deck areas the effect of the outside transmitters is negligible due to the installation rules. The concentration of equipment inside the ships hull is therefore considered a much greater danger.

4. RISK EVALUATION

Over the last five years commercial standards have been used incidentally on board RNLN ships. Up to now they have not given a big problem, but is has to be taken into account that this was only valid for ships which are not acting as a real warship (frigate), such as a LPD or Oil Replenisher.

For frigates, the MIL-STD is still in the specification of all the equipment to be installed on board. In special cases, it is allowed to deliver equipment which fulfil the commercial standard, but some additional tests has to be performed to make sure that no problems will raise when installing these.

During a part of the study, manufacturers were invited to have a CE-marked product tested conform the commercial standard as well as conform the military standard. About over hundred manufacturers were invited of which twenty five responded. Most of them are active in the control- and monitoring- and in the static inverter industry. All manufacturers have contacts with the RNLN and should have been aware of EMC-requirements on board of the Navy ships.

As a result is can be noted that in some cases, in the frequency range below 30 MHz radiated problems (due to both emission as immunity) were found.

This underlined the importance of having radiated limits for emissions as well as susceptibility tests in the HF-range from 1 MHz to 30 MHz.

So, the product investigations showed that most of the emitted energy is below 30 MHz and this is not covered in the commercial standards except the IEC 60533.

That is one part of the hardening, the other part is of course the susceptibility to electric fields, which is not implemented in the commercial standards.

A risk is taken when relying fully on the CE-marking of a product. The product investigation showed that not all equipment complies to the required standards. This is assumed to be a short term effect. To minimise the risk it is advisable to add EMC-tests to the factory acceptance tests.

5. CONCLUSIONS AND RECOMMENDATIONS

From a technical point of view, it can be concluded that the commercial standards do not cover the military environment as the MIL-STD will do. The IEC-60533 is the most comparable standard which can be used, but with respect to the radiated immunity, also the IEC does not cover the military environment over the whole frequency range, so still problems can be expect.

As a commercial conclusion, it can be noted that the use of commercial EMC-standards as a way to save money, influences the safety margin by an unknown factor. This causes an undefined environment and just saves a considerable amount of money for large quantity of goods, bought from the shelf. Unfortunately there is no way to know if these savings are in balance with possible costs to solve EMI-incidents for ships beyond the period of guarantee.

Saving costs and having a defined environment can be established by specifying engineering requirements and having the tests done by the Navy itself.

Regarding the applicability of commercial standards the following can be stated at this moment:

- Due to the threat of radar-, HF-communications and electromagnetic pulse, commercial limits are insufficient in outerdeck areas. This means indirectly that systems complying to commercial limits, should not be located in outerdeck areas or have a direct (cable)link with the outerdeck area.

- In above deck areas innerdeck, like the mast, commercial equipment should at least be able to withstand radar signals. A test or extra specifications should safeguard this.
- In most innerdeck areas, commercial seems to be complying, however since there is an undefined safety margin, it makes sense to avoid high densities of equipment or take extra installation measures.
- Since there is no commercial test available that relates to the threat of EMP, great care should be exercised with commercial equipment on ships that are designed to withstand an EMP of 50 kV/m.
- Equipment installed in innerdeck areas and not involved with the operational and tactical activities of the ship, can be accepted as commercial equipment as far as susceptible is concerned. All equipment with has to operate under all circumstances of the ships operations and which is not allowed to fail, has to meet the MIL-STD.

For current projects as well as for future projects it is very important to specify the EMI/EMC-requirements in an early phase. It is recommended to specify only the MIL-STD-461D/462D or MIL-STD 461E.

When a manufacturer offers commercial equipment, additional tests have to be performed to check if the desired standards are sufficient, taken into account the place of installing and the electromagnetic environment over there.

Very important at this additional test is the frequency range of interest. Special care should be taken of the frequency range of 1 MHz to 30 MHz.

To minimise the risk it is therefore advisable to add these EMC-tests to the factory acceptance tests.

6. HARMONISATION OF METHODS

A last point, and in the opinion of the defence organisation a very important point, is the discussion on the harmonisation of at least measuring methods.

The study has shown that the difference in test methods of commercial and military standards are that big, that

comparing is rather impossible. It will be a big step in the good direction if at least the measuring methods of the military and the commercial standards are the same. It is well known that some defence organisations started a discussion on this item, but it looks that it will be a very long way to go.

The methods can be the same over the total frequency range of threat for the commercial world as well as the military world.

With respect to the limitation, different limits can be proposed for the different environments.

It is expected that equipment installed in an industrial environment in a ground facility without transmitters in the neighbourhood, has to fulfil other limits and to meet other EM-requirements, than equipment installed in a navy environment with a lot of radar- and communication transmitters on board the same platform.

As a starting point for further discussion, find below a proposal for the measurement methods to be performed as a minimum. The methods cover the whole frequency range of the total EM-environment for all applicability's.

- Conducted Emissions: 30 Hz to 10 kHz
- Conducted Emissions: 10 kHz to 30 MHz
- Conducted Immunity: 30 Hz to 10 kHz
- Conducted Immunity: 10 kHz to 30 MHz
- Radiated Emissions: 30 Hz to 10 kHz
- Radiated Emissions: 10 kHz to 10 GHz
- Radiated Immunity: 30 Hz to 10 kHz
- Radiated Immunity: 10 kHz to 10 GHz

Further discussions can be focused on the method itself, for example what LISN shall be used, measuring voltage or current, magnetic field and electric field, frequency range, measuring distances, etc.

Before starting discussions on the limits, the methods has to be agreed by all bodies, civil as well as military.

7. REFERENCES

- [1] Different EMC standards as MIL-STD-461/462, IEC 60533, EN 50081 and EN 50082.
- [2] TNO-FEL-96-A028 (Use of commercial standards on board RNLN-ships) by A.B. Woltering and H.A. Klok.

HARMONISATION OF EMC STANDARDS FOR THE NAVAL ENVIRONMENT A UNITED KINGDOM APPROACH.

Alan Lavell-Smith

DERA Portsmouth West, Portsmouth Hill Road, Fareham, Hampshire, PO17 6AD, United Kingdom.
Telephone: +44 (0) 23-92337357. Fax: +44 (0) 23-92336505 Email: APLSMITH@dera.gov.uk

This paper provides an overview of some of the work conducted by the United Kingdom (UK) concerning harmonisation of Civil and Military Electromagnetic Compatibility (EMC) Standards for the naval environment. This paper considers the main standards that are applicable to both the civil and military environments. It addresses some of the main difficulties in comparing these standards and identifies areas where commonality can be found. This is of particular relevance due to the increasing use of "Commercial Off The Shelf" (COTS) equipment in modern military systems. This paper also provides an overview of the United Kingdom's new approach to the selection of suitable standards for defence procurement.

1. INTRODUCTION

Since the introduction of the EMC Directive (89/336/EEC), considerable effort has concentrated on the harmonisation of civilian EMC standards from different European nations. This has resulted in the Euro Norm (EN) and European Telecommunications Standards Institute (ETSI) series of EMC standards published in the Official Journal of the European Community, which have become a set of internationally recognised standards used for free trade purposes inside the Europe Union (EU).

To date comparatively little effort has been given to the problems associated with harmonising civil and military standards. It has always been understood that the military Electromagnetic (EM) environment is more severe than the commercial environment. Accordingly, equipment procured for use in the military environment needed to meet an acceptable recognised standard, typically the national military EMC standard.

1.1 Problems and use of COTS

However, over the last eight years there has been a significant decline in many national defence budgets and a need to rethink how equipment is procured. One of the easiest solutions is to procure "Commercial Off The Shelf" (COTS) equipment.

Consequently, COTS equipment has allowed the armed services to obtain modern state-of-the-art technology, faster and cheaper than before. However, the problem with most COTS equipment is that it has been built to commercial standards and assessments are required to ensure that the equipment will work in the harsher military environment. This is particularly true for

the EM environment, where there are strict controls on the amount of EM emissions. And equipment is required to have a high level of immunity over a wide frequency range. Therefore, a good understanding of the EM environment into which the COTS equipment is to be placed is essential.

1.2 Naval EM environment

The naval electromagnetic environment experienced by equipment mounted on a naval platform is extremely harsh. Equipment must operate efficiently in close proximity to many high power emitters, for example radios, radars and degaussing systems, generating very high field strengths over a wide frequency range. Consideration must also be given to the EM environment generated by escorting platforms, including other naval warships, auxiliaries, helicopters and aircraft.

In the UK, the naval EM environment is categorised into two specific areas for equipment EMC testing, known as Above Decks and Below Decks which are defined as follows:

- 'Above deck' limits apply to equipments fitted or used outside the metallic structure of surface ships. This includes equipments fitted in non-metallic ship structures or within a metallic Bridge or Hangar (with the exception of equipment located in screened compartments on non-metallic vessels). It shall also apply to equipment fitted between the pressure hull and outer case of submarines [1].
- 'Below deck' limits apply to equipments fitted in submarines or within the metallic structure of surface ships (but not within the Bridge or Hangar space) [1].

The Above Deck environment is the harsher EM Environment. Above Decks' equipment must have a high level of immunity and produce very low levels of unintentional emissions. The Below Decks environment has a much more controlled EM environment due to the screening nature of the metallic hull and its superstructure. In some respects, the Below Decks environment is more like the industrial/commercial environments but with more restrictions over EM emissions and immunity. Broad definitions of these environments can be found in a variety of documents produced by both the UK Ministry of Defence and NATO (North Atlantic Treaty Organisation), for example UK Interim Defence Standard (Def Stan) 08-46 and NATO Standardization Agreement (STANAG) 4435.

2. BENEFITS OF USING STANDARDS

In any new equipment, material or service procurement the intelligent use of standards offers significant benefits and helps to make the acquisition process more effective. Some of the most important benefits of using standards are that they

- Set performance requirements that promote innovation.
- Define unambiguous technical and performance requirements, which can be used in contracts and specifications.
- Provide recognised benchmarks against which products, processes and services can be measured.
- Promote improvements in the quality of products, processes and services,
- Promote improvement in the health, safety, and the environment.

In addition to the above general benefits, standardisation in the UK MOD also promotes operational effectiveness through improved interoperability and supportability of defence equipment.

These benefits can only be achieved through the selection of the most appropriate standards [2]. Guidance on the correct choice of standards is important, as is the understanding of the implications of choosing one standard over another. This becomes very important when considering the procurement of COTS equipment for use in a military environment. Thus, there is a need to look more closely at the harmonisation of civil and military standards and the likely impact of choosing one over the other. In order to achieve this, it is important to understand each of the relevant standards and the differences between them.

3. CURRENT UK MILITARY EMC STANDARDS

The UK naval military EMC standard work of reference has been developed over a large number of years and has seen many changes. The changes were introduced to address problems found with the original standards. Such changes have included identification of limits levels set too low, changes in the EM environment as more equipment has been added to ships and practical experience with naval equipment installations. Over the last forty years, Directorate General Ships (DG Ships) 250B, Naval EMC B Specification B768, and Naval Weapon Specification (NWS) 3, have been the main naval EMC specifications. However, these standards have now replaced by the current military standard Def Stan 59-41 (Parts 1 to 7) [1].

Def Stan 59-41 is an UK Tri-Service Defence Standard; it contains the limits and measurement methodologies for performing military equipment/system EMC testing and verification. This standard was originally started in 1971 and has been in use and under revision ever since. It has seen the incorporation of many aspects over the years including the main parts of the previous naval standards above. Currently, the main documentation of the standard is at issue six. It defines limits for both the Above and Below Decks environments and contains numerous tests to cover all aspects of Naval equipment EMC and performance.

4. RELEVANT EUROPEAN EMC STANDARDS

Currently there is no single EMC Euro Norm that covers all the requirements for equipment to be installed both Above and Below Decks, as in Def Stan 59-41. The Marine Equipment Directive (96/98/EC), defines a range of electrical and electronic equipment that is to be installed in a maritime platform, e.g. boat, dinghy or warship. This Directive has its own specific EMC section, which overrides the EMC Directive and mandates its own EMC standards for all covered equipment. The EMC Directive and its applicable standards cover equipment not covered by the Marine Directive. An important aspect is the need to effectively consider the "Above" and "Below" decks environments. Therefore, any consideration of equipment needs to be split into that covered by the Marine Directive EMC standards and covered by other EMC standards.

4.1 Marine EMC standards

The following is a short list of the most applicable EN and British Standards that might be chosen to allow EMC testing of equipment that is to be used in a maritime environment.

- **BS EN 60945:1997** - *Marine Navigational Equipment - general equipment. Methods of testing and required test results*
- **BS 1597:1985** - *Specification for limits and methods of measurement of electromagnetic interference generated by marine equipment and installations.*
- **BS 5260:1975** - *Code of practice for radio interference suppression on marine installations.*
- **BS 7027:1990** - *Limits and methods of measurement of immunity of marine electrical and electronic equipment to conducted and radiated electromagnetic interference.*

It should be noted that currently only one maritime EMC standard, EN 60945, is published as part of the harmonised standards list, and several British Standards had to be used to complement the list. These standards do not cover the entire tests that may be required to complete installation in a naval platform, but cover the major requirements. Several of these standards specifically define limits for "Above" and "Below" decks equipment.

Note: Effectively BS EN 60945 replaces the older British Standards and any future equipment will only be tested to this standard, unless the manufacturers decide otherwise. Whilst BS EN 60945 contains many of the requirements from the British Standards there are areas where it does not effectively replace them, for example changes in limit levels and frequency ranges.

4.2 Other EMC standards.

The EMC Directive will cover any other equipment that may be installed in a naval platform, if not already covered by the Marine Equipment or other specialist Directive. This means that the European Harmonised EMC standards must be used for all other electronic and electrical equipment. A short list of applicable standards that might be considered is produced below.

- *BS EN 50065-1:1992*
- *prEN 50065-2:1992*
- *BS EN 50081-1:1992*
- *BS EN 50081-2:1994*
- *BS EN 50082-1:1998*
- *BS EN 50082-2:1995*
- *BS EN 50130-4:1996*
- *BS EN 55015:1997*
- *BS EN 55020:1997*
- *BS EN 55022:1995*
- *BS EN 60721-1:1996*

This list is not exhaustive, but some of the main standards that are applicable have been identified. As indicated above nearly all the harmonised product specific EMC standards can apply.

5. COMPARING CIVIL AND MILITARY STANDARDS

In the UK a number of studies have been conducted to compare the Def Stan 59-41 [1] with the European commercial standards. These studies were conducted to consider the potential for harmonisation between these standards and, more importantly, to assist the project acquisition staff to choose the most appropriate standards. All these studies have been reliant upon a good understanding of the naval EM environments and of the relevant standards themselves.

Most of the studies have been comparisons between the Def Stan [1] and one or two specific commercial standards. However, the largest study has considered all the commercial standards identified above [3].

During these studies areas of commonality have been established, but were outweighed by the number of comparison problems encountered. Areas of commonality were found, they tended to be over limited parts of the frequency range required by the Def Stan [1]. The marine immunity standards showed the closest commonality, with several areas of overlap in frequency ranges and limit levels, but the overall range did not satisfy the military environment requirements. Other immunity standards also showed some commonality but were more limited than the marine standards. There was limited commonality between the commercial emissions standards and those requirements in the Def Stan [1].

6. COMPARISON PROBLEMS

Problems found during the studies varied in their significance and are explained below.

6.1 Frequency Ranges

One of the most prominent factors in trying to compare the standards is the difference in the frequency ranges. Whilst there were large portions of the measurement ranges where both were in agreement, there were also distinct areas where the civil standards did not cover frequencies required in the Def Stan.

Many of the ENs did not have any coverage above 1000 MHz, and those that did only covered the odd frequency, whilst the military requires coverage up to 18 GHz. There were also significant gaps in the coverage requirements at the lower end of the frequency range.

6.2 Measurement Detector Types

Detector types are another major area of difference. The Def Stan uses a PEAK detector to perform its measurements. This allows the effect of both continuous and pulsed interference to be fully assessed. However, the Euro Norms use either a QUASI-PEAK or AVERAGE measurement detector, depending upon the test undertaken.

The Quasi-Peak is an integration detector and has a known charge and discharge time, which affects its measurement capability. This means that short pulse-width interference with low repetition rates, are not detected as easily as is possible with a peak detector. As the repetition rate goes up so does the quasi-peak detectors measurements. The Average detector is even less sensitive to short interference pulses. Both Quasi-Peak and Average detectors are very dependent upon measurement dwell time to produce accurate results.

It must be remembered that the military EMC scenario is concerned with interference from all sources, including false switching effects, transients, etc. The civil EMC scenario has been concerned about the affect to audio broadcast systems where occasional fast transient signals do not have a significant effect. Both Quasi-Peak and Average detectors are ideally suited to measuring interference in audio broadcast systems as they are not sensitive to these occasional transients.

6.3 Distances For Measuring Emissions

When considering radiated emissions from equipment, there is a notable difference between the Def Stan and the ENs. The Def Stan conducts all measurements at 1m, whilst the ENs can allow measurements to be taken at 3 metres, 10m and 30m. This makes any comparison very difficult due to field effects and is very dependent upon the antennas used for testing.

6.4 Probe Types and Antenna Types

Both standard types identify many different tests and the methods of conducting them. A large number of the tests, whilst trying to identify similar effects use very different test apparatus to measure the required effect. This results in different probes and antennas being used to measure the interference and leads to different results, due to the impact of the measurement system on the result.

6.5 Different Measurement Units

With the differences in measurement methodologies there is also a variation in the units used to set levels and to make measurements. Although, it is generally possible to compare these, in the more extreme cases it can be very difficult. One such example is magnetic emissions, where the Def Stan uses dBpT, whilst the commercial standards use dBµA, dBµV/m and dBµV.

6.6 Different Acceptance Levels

Another major difference is between the limits chosen for acceptance of equipment. The Def Stan identifies two limits depending upon whether the equipment is Above Decks or Below Decks. The majority of commercial standards also identify different levels, but these are dependent upon the equipment use and Class.

These levels are difficult to compare easily; for example, commercial standards sometimes recommend a higher immunity level but over a limited frequency range.

7. OTHER HARMONISATION ISSUES

In addition to limit level and measurement methodology problems, the comparison studies have also identified a number of other issues. These issues do need to be considered as part of the overall harmonisation effort. The two main issues are discussed below.

7.1 Presentation of Results

At the moment there is no standard format for presenting test results, making it difficult to compare results of the same standard from different test houses. When trying to compare across different standards the task is even more complicated.

7.2 "Need To Test" ?

The second issue is one of concern for the non-diligent procurer. The issue is to do with the European Legislation and the wording of the EMC Directive. Directive Article 10.1, "The standards compliance route", states that equipment is presumed to comply when the manufacturer has applied the appropriate standards. However, "apply" can be interpreted with enormous flexibility and raises an important question: Is it possible to "apply" a test standard to a product without actually testing it? [4].

Although the Directive requires every item to be compliant, it is impossible to do so economically and the best manufacturers only test limited samples. Thus, they are "applying" the results of their tests to products, which have not been tested. Therefore, "apply a standard" does not necessarily mean "test to a standard" and effectively any manufacturer makes a legal statement that the product would pass, were it to be tested to the standards "applied". This cannot be guaranteed and comes down to achieving sufficient confidence in the EMC performance of the commercial products. The difference between having a technical rationale for such confidence and just hoping for the best comes under the terms of "due diligence". Like many other business decisions there will always be a commercial cost versus risk decision to consider, when deciding what quantity and quality of EMC testing is necessary. Once it is recognised that testing, per se, is not mandatory, there are a number of options, each having different levels of risk and cost [4].

8. CURRENT PROCUREMENT METHODOLOGY

The following is a brief summary of the procurement methodology that has been in use recently. Whilst there is a significant drive to use COTS technology wherever possible, it is recognised that there is still a need to ensure that performance is not compromised. There have been a number of minor EMC instances from COTS equipment procured to commercial standards.

Consequently, there is still a need to look at having COTS equipment tested to Def Stan 59-41, if there is any doubt about suitability of the procured equipment. The following guidance has been provided to the defence procurer when considering standards:

- *"The Project Manager shall instruct the Design Authority to take into account the EMC characteristics of all proprietary equipment being procured by MOD, to ensure that it complies with the terms of the relevant National Standard. Where EMC requirements for equipment differ from those of the National Standard, then Defence Standard 59-41 shall be invoked and the appropriate test methods and limits identified in order to ensure acceptable equipment performance in its intended environment"* [1].

9. NEW APPROACH TO USE OF STANDARDS IN PROCUREMENT

The above situation has been under review for some time. Over the last couple of years there have been several major changes to the structure and methodology of defence procurement in the UK Ministry of Defence (MOD). The main change has been the introduction of "Smart Procurement", which dramatically alters the defence procurement process. As a result of this and the review process, the UK Defence Standards (DStan) has implemented a set of changes to guide the selection of standards. These changes have a direct impact on the possibility of harmonisation between civil and military standards, as they identify a hierarchy of choice of standards for use in contracts. The following is a short overview of the recently introduced DStan changes [2].

It is UK government policy to encourage the use of standards that are applicable to world markets and to use internationally recognised standards wherever possible. This is to reduce barriers to trade. Also the UK is obliged under the EU directive for the Co-ordinating of Procedures for the Award of Public Supply Contracts to give preference to national standards which implement European Standards.

UK MOD policy is in support of these requirements and **civil standards are to be used wherever appropriate in preference to international military standards such as NATO STANAGs and UK Defence Standards**. The order of preference for the selection of standards for defence acquisition is shown in Table 1. This order of preference is to be applied, where practicable, in all defence contracts and sub contracts.

The effect of these changes is to promote the use of civil standards, particularly Euro Norms, over military standards, where possible. Therefore, military standards will need to be carefully considered as to why they are being implemented and further harmonisation work may be required to support the decision making process. DStan have issued this new approach through a variety of publications and over the Internet, via their web-site: <http://www.dtsan.mod.uk> [2, 5].

Hierarchy	Type of Document
1	Regional (British Standards implementing European standards) European Committee for Standardization (CEN) European Committee for Electrotechnical Standardization (CENELEC) European Telecommunications Standards Institute (ETSI)
2	International (British Standards implementing international standards) International Organization for Standardization (ISO) International Electrotechnical Commission (IEC) International Telecommunication Union (ITU)
3	National (Other British Standards) - British Standards Institution (BSI)
4	International Military Standards (NATO / ABCA) NATO Standardization Agreements (STANAGs) Allied Publications (AP) ABCA Quadripartite Standardization Agreements (QSTAGs)
5	UK MOD Defence Standards (Def Stans)
6	UK MOD Departmental Standards and Specifications e.g. Naval Engineering Standards (NES)
7	Other nation's military standards e.g. DoD Mil Specs and Standards
8	Recognised Industry/ Partnership/Consortium Standards e.g. PANAIA, AIRBUS, etc, Trade Association standards (e.g. American Society for Testing and Materials (ASTM)),

Table (1) – The order preference for the selection of standards for MOD procurement.

10. CONCLUSIONS

This paper has identified the importance of standards and why special consideration needs to be given to the Naval EM environment and hence to EMC. It has identified the main UK military EMC standard, Def Stan 59-41 and some of the commercial EMC standards that may be used as alternatives. In particular it has differentiated between those commercial EMC standards specifically developed for a marine EM environment, typically EN 60945, and those associated with the commercial and industrial environments.

An overview of the comparison work conducted by the UK has been declared and areas of commonality identified. The major problems associated with trying to compare the civil and military standards have been discussed in detail, and shows that further harmonisation work is still required. Finally, the UK new approach, to define a standards hierarchy, has been presented. This and the current harmonisation effort in the UK area of Naval EMC standards concludes that:

- It is difficult to compare between the tests and limit levels of the UK Def Stan and those of the identified civil EMC standards.
- Areas of commonality do exist but are limited at present.
- There is still a need to conduct further harmonisation work to help the defence procurer to make the right choice of standards depending upon an appreciation of the environment that the equipment is to be used in.
- There is now a definitive hierarchy for choosing standards for contracts.

11. REFERENCES

1. DStan, "Electromagnetic Compatibility", Defence Standard 59-41, Parts 1 to 7, Issue 6, UK MOD Directorate of Standardization, 29 September 1995.
2. A. Stirling, "Selection of Standards for use in defence Acquisition", Standards in Defence News, Serial 174, January 2000.
3. R.M.Turner, A.P.Smith, P.J.Goddard. "Unpublished DERA/MOD Report". 30 June 1998.
4. N.Harvey, K.Armstrong, "How much to test, is a question of cost", Approval Magazine, March/April 1998.
5. DStan, "Standards for Defence, UK MOD Standardization Policy", Defence Standard 00-00, Parts 1, Issue 3, UK MOD Directorate of Standardization, 04 July 1999.
6. UK department of Trade and Industry/Federation of the Electronics Industry, "EMC and LVD Yearbook 1998", Nutwood UK Ltd.

ACKNOWLEDGEMENT

The author gratefully acknowledges Messieurs Calum Sim and Henry Burrows of UK Defence Standards for their contributions and review of this paper. The author would also like to acknowledge the help of Messieurs Geoff Nixon, Luke Turnbull and Mike Hawken in reviewing this paper

BIOGRAPHICAL NOTE

ALAN LAVELL-SMITH is head of engineering for the Electromagnetic Engineering Group at DERA Portsdown West. He specialises in Naval EM Engineering, EMC and Topside design of maritime platforms. He obtained his Bachelor of Engineering Degree in Electrical and Electronic Engineering at Polytechnic SouthWest in 1991. He is a member of the Institute of Electrical and Electronic Engineers, Inc in the EMC and Antennas and Propagation Societies. He has also recently joined as a member of the Institution of Electrical Engineers.

© British Crown copyright 2000. Published with the permission of the Defence Evaluation and Research Agency on behalf of the Controller of HMSO.

EMC 2000

INTERNATIONAL WROCLAW SYMPOSIUM ON ELECTROMAGNETIC COMPATIBILITY

Harmonization of E3 Standards

By F. Michael Stewart
U.S. Space and Naval Warfare Systems Command
San Diego, California
United States of America
Tele: (619) 524 7230 Email: stewartm@spawar.navy.mil

1. INTRODUCTION.

As more the military uses equipment built to commercial standards, the need becomes greater to compare military and civilian E³ requirements. The development of guidance to both the civilian and military E³ communities for the utilization and application of available civilian standards is important. The process of comparing military standards to civilian standards in order to harmonize requirements is underway.

2. SCOPE.

The efforts towards E³ standard harmonization are centered on the DOD/Industry E³ Standards Committee (DIESC). The DIESC is made up of representatives from DoD and Industry. The DIESC was established in 1994. The goal of the DIESC is to foster cooperation between DoD and Industry for harmonization of military and commercial electromagnetic compatibility standards. The primary effort of this committee has been directed at comparing the military's MIL-STD-461D and MIL-STD-462D to major national and international commercial E³ requirements. These commercial standards were developed by the Federal Communication Commission (FCC), the Radio Technical Commission for Aeronautics (RTCA) DO-160D, the American National Standards Institute (ANSI), the International Electrotechnical Commission (IEC), the International Special Committee on Radio Interference (CISPR) and the Institute of Electrical and Electronics Engineers (IEEE) standards. Since the start of this effort in 1994, MIL-STD-461D and MIL-STD-462D have been incorporated in a the new MIL-STD-461E, dated 20 August 1999.

3. THE GUIDE.

A guide has been drafted documenting the results on the comparisons between the military's MIL-STD-461D and MIL-STD-462D and the commercial standards along with some ideas as how to use the information. The specific commercial standards that the military standards were compared with are:

- (a). FCC, Part 15, RF Devices.
- (b). FCC, Part 18, Industrial, Scientific and Medical Equipment.
- (c). DO-160D, Environmental Conditions and Test Procedures for Airborne Equipment.
- (d). ANSI C63.4, Radio noise emissions from low-voltage electrical and electronic equipment in the range of 10 kHz to 1 GHz - methods of measurement
- (e). IEC 61000-3-2, Limits - Section 2, Limits for harmonic currents emissions (equipment input current \leq 16A per phase).
- (f). IEC 61000-3-8, Limits - Section 8, Signaling on low voltage electrical installations - emission levels frequency bands and electromagnetic disturbance levels.
- (g). IEC 61000-4-3, Testing and Measurement Techniques - Section 3, Radiated, radio frequency, EM field immunity test.
- (h). IEC 61000-4-4, Testing and Measurement Techniques - Section 4, Electrical Fast Transient/burst immunity test.
- (i). IEC 61000-4-6, Testing and Measurement Techniques - Section 6, Immunity to conducted disturbances induced by radio-frequency fields.
- (j). IEC 61000-4-8, Testing and Measurement Techniques - Section 8, Power frequency magnetic field immunity test Basic EMC Publication.

(k). IEC 61000-4-9, Testing and Measurement Techniques - Section 9, Pulse magnetic field immunity test Basic EMC Publication.

(l). IEC 61000-4-10, Testing and Measurement Techniques - Section 10, Damped oscillatory magnetic field immunity test Basic EMC Publication.

(m). IEC 61000-4-13, (in preparation) Testing and Measurement Techniques - Section 13, Tests for immunity to voltage fluctuations, unbalance, variation in power frequency

(n). IEC 61000-4-16, (in preparation) Testing and Measurement Techniques - Section 16, Conducted disturbances in the frequency range DC to 150 kHz immunity.

(o). IEC 61000-4-20, (in preparation) Testing and Measurement Techniques - Section 20, Immunity and Emission Testing in TEM Cells.

(p). IEC 61000-4-25, (in preparation) Testing and Measurement Techniques - Section 25, HEMP Equipment and systems.

(q). IEC 61533, EMC of electrical and electronic installations in ships and of mobile and fixed offshore units.

(r). CISPR 11, Limits and methods of measurement of electromagnetic disturbance characteristics of industrial, scientific and medical radio-frequency equipment.

(s). CISPR-13, Limits and methods of measurement of radio interference characteristics of sound and television broadcast receivers and associated equipment.

(t). CISPR 14, Requirements for household appliances, electric tools and similar apparatus.

(u). CISPR 15, Limits and methods of measurement of radio interference characteristics of fluorescent lamps and luminaries.

(v). CISPR 16, Specification for radio disturbance and immunity measuring apparatus and methods.

(w). CISPR 22, Limits and methods of measurement of radio interference characteristics of information technology equipment.

(x). IEEE Std. 187, Open field method of measurement of spurious radiation from FM and TV broadcast receivers.

(y). IEEE Std. 1140, (in preparation) Standard Procedures for the Measurement of Electric and Magnetic Fields from Video Display Terminals (VDTs).

A large portion of the guide is devoted to providing guidance on determining the risk of using a particular commercial standard for a specific military application. The guide emphasizes that the overall evaluation process is complicated by a large number of factors that must be considered. Included in the guide are equipment factors that need to be considered in evaluating the risk of using commercial equipment for military applications. Some of these factors are:

a. System performance requirements.

b. Impact on mission and safety.

c. Operational electromagnetic environment.

d. Platform installation characteristics.

e. Equipment EMI characteristics.

This complicated evaluation process will most likely require personnel who have specialized knowledge in EMI requirements and testing and who have the skills necessary to apply the guide to the circumstances of specific procurements. To aid in the initial evaluation process the guide provides a flow chart for the procurement of EMC for systems and equipment and a risk evaluation matrix.

The guide also provides a list of relevant military and commercial standards and an annotated classification of these standards. The guide is intended to assist personnel in evaluating equipment qualified to commercial Electromagnetic Interference / Electromagnetic Compatibility (EMI/EMC) standards for use in military application. This guide is expected to be released as an engineering study latter this year.

4. DIFFERENCES BETWEEN COMMERCIAL AND MILITARY STANDARDS.

While performing the comparisons, two distinctive differences between the military and commercial standards became apparent.

The first deals with a system's requirements, which are driven by its intended environment. As an example, there is a high concentration of electronic emitters and receivers on military platforms, especially ships. For this reason, the military's "radiation emission limits" are much more severe than the corresponding civilian limits. Mainly, the military places more stringent spectral immunity requirements on devices exposed to nearby international emitters over a wider frequency range than the commercial standards.

The second deals with the fact that both the military and the commercial developers have documented successful test methods and philosophies. Some which are significantly different, but achieve the same result, the environment notwithstanding. As an example, in the area of "grounding of the test sample": Equipment mounted on military vessels is usually mounted on grounded conductive material or on ground planes for testing. Most commercial equipment, being lightweight and portable, is usually tested while mounted on an ungrounded tabletop.

5. HARMONIZATION PROGRESS

Since the start of the DIESC and the development of the guide, there has been one step towards the harmonization between MIL-STD-461E and the international standard (IEC 61000-4-8). MIL-STD-461E has been revised to include an additional test method for conducting magnetic field susceptibility testing

(RS101). The method uses Helmholtz coils to produce a magnetic field. The equipment under test is immersed in the field during testing. This is a change from the normal proximity test method of RS101, and is basically the same testing contained in ICE 61000-4-8. The requirements of MIL-STD-461E (RS101) testing and IEC 61000-4-8 remain very different in frequency and amplitude. Test RS101 of MIL-STD-461E will cover the frequency range of 30 Hz to 100 kHz. IEC 61000-4-8 only addresses the frequency of the AC power distribution networks.

6. FUTURE OF HARMONIZATION.

Communities have developed our E³ standards to satisfy their differing missions, e.g., military vs civilian communities. For the most part, a given E3 standard was developed by a community to satisfy a problem, or to ensure alignment with international rules and regulations. Therefore it is a difficult task to reach complete agreement on the exact wording or test procedure without much more research and coordination among the interested committees.

It is expected that harmonization will be a long and arduous process, but well worth the effort!

BIOGRAPHICAL NOTE

Mr. Stewart has worked in the E3 area since 1987. He earned his Electrical Engineer graduate (BSEE) from the University of Arkansas; and his Masters degree in Engineering Management from George Washington University.

His present job includes Electromagnetic Environmental Effects (E3); Shipboard Topside Design & Integration; and Research and Development of EMC Software products for the US Navy.



EMC 2000

INTERNATIONAL WROCLAW SYMPOSIUM
ON ELECTROMAGNETIC COMPATIBILITY

NUMERICAL PREDICTION OF SHIP ANTENNA PERFORMANCE IN THE RADAR BAND

Mauro Bandinelli, Antonio Benedetti, Stefano Chiti, Riccardo Cioni

IDS Ingegneria Dei Sistemi S.p.A. - Via Livornese 1019 56010 PISA Italy

Tel. +39 050 312411 - fax +39 050 3124201 - e-mail: idspisa@ids-spa.it - URL: www.ids-spa.it

This paper presents the results of a preliminary validation assessment of a new Electromagnetic Framework environment called EMIPT (ElectroMagnetic Interference Prediction Tool), developed to answer the requirements of accurate numerical modelling for the prediction of the performance of radar antenna installed in a real ship environment.

The EMIPT is close to the final delivery to the UK Navy after a multiple step validation programme carried out by comparisons between simulations and measurements performed by DERA (Defence Evaluation and Research Agency) as expert support to the MoD (UK Ministry of Defence).

1. INTRODUCTION

The needs of accurate electromagnetic (e.m.) modelling to approach real ship design projects have been addressed into a numerical tool suited to both support ship projects at system level and to provide rules and guidelines to be used in the EMC behaviour of ships with respect to the applicable EMC standards. The EMIPT includes a wide set of features capable of manage the complex scenario to be deal with, involving the management of 3D CAD representations of the ship with its combat system, the database of the equipment and of the e.m. design data, the set of e.m. techniques needed to simulate the interaction between antennas and structures. In the version considered for this work, the system has been configured to be applied to frequencies above 0,5 GHz, thus it is mainly applicable to radar band problems.

The prediction tool is aimed at supporting the naval Engineer with the following main features:

- ✦ Electromagnetic Design of modern Naval Units, taking account of:
- ✦ realistic Antenna and 3D structure environment modelling, and operating on the:
- ✦ 500 MHz to 40 GHz band (in the release here considered), capable of predicting:
- ✦ Antenna radiation pattern and related 3D coverage

- ✦ Electromagnetic Radiation Hazard aboard the ship
- ✦ Inter Antenna Coupling and related EMI on fix/rotating antennas in:
- ✦ Radar, EW, Satcom applications

Furthermore, the EMIPT has been conceived to provide the following additional features:

- ✦ The CAD is always available for geometry import and manipulations on the ship
- ✦ There is a continuous link between the CAD elements and the database
- ✦ There is a continuous link between the simulation procedures and the database
- ✦ A common Equipment/Material database is available and can be queried at every stage of the operations
- ✦ The system has an high portability due to development environments (C++, Java)

The fig. 1. shows a typical view of the graphical user interface where the 3D CAD scenario has been taken as the central environment of the system, supporting the input of project data, the management of antennas aboard ships, the display of result on the 3D ship CAD representation.

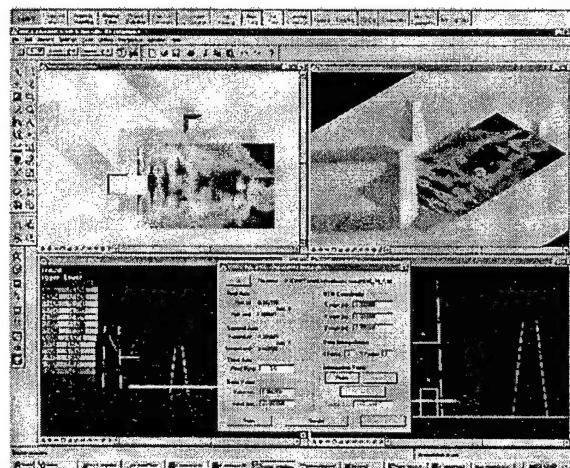


Fig. 1 – EMIPT main front end

2. BRIEF OUTLINE OF THE EMIPT

2.1 The Modelling of Antennas

A model for aperture and array antennas (typically used in radar band application) was developed, based on the following main requirements :

- the model must be as general as possible, capable to cope the main part of the antennas typically used in the band of frequencies of interest
- the model must be effective in the frame of the analysis of the e.m. interaction among antennas and ship superstructures; in particular it must be suitable to be used with scattering modelling methods such as GTD (Geometrical Theory of Diffraction) and, in this frame, it must be effective from the point of view of the required CPU time
- the model must be accurate from the point of view of the antenna radiation pattern and near field behaviour; it is not foreseen to be used in the frame of antenna design, so the characterisation of antenna input impedance is a not interesting topic.

The model selected is based on the Aperture Integration Method [1], and it has been implemented in the IDS proprietary code AAM (Aperture Antenna Modeller).

The code is able to model both well defined antennas such as conical corrugated or smoothed horns and more general aperture antennas. On the basis of the user input data AAM synthesises a set of equivalent electric $J(P)$ and magnetic $J_m(P)$ sources located on a finite set of points on a plan shaped surface (usually the reference aperture of the antenna) :

$$\begin{aligned}\vec{J}(P) &= \hat{n} \wedge \vec{H}_a(P), \\ \vec{J}_m(P) &= -\hat{n} \wedge \vec{E}_a(P)\end{aligned}$$

Such a set of equivalent currents can be used both for e.m. field evaluation (near and far) and for inter-antenna coupling evaluation, by referring to well known techniques such as the Reaction Integral Equation.

Only magnetic equivalent currents (located on a perfectly conducting plane) are needed to represent the main lobe and the nearest secondary lobes of the antenna, but also the electric ones (in this case both the equivalent currents are working in free space) are needed to well simulate the antenna radiative behaviour at endfire angles and besides, also on backward directions.

The wave impedance $Z_w(P) = \left| \vec{E}_a(P) \right| / \left| \vec{H}_a(P) \right|$ can be defined by the user. It has been demonstrated that this capability is particularly useful to model the backward radiation of horn type antennas in a heuristic but very effective manner.

In Para. 3.1 an example of the performance of such model is reported by comparing a simulated radiation

pattern with a measured one, on the overall $[0^\circ-360^\circ]$ circular scan plane.

2.2 The Modelling of Structures

Starting from the geometrical model of the environment under test, the pertinent electromagnetic model has been defined by means of the Microstation CAD tool, embedded within EMI-PT.

In order to perform this step, a special purpose electromagnetic meshing application developed at IDS, and embedded within the CAD tool, has been used. Since the GTD_EM solver tool (a IDS proprietary code based on the Uniform Theory of Diffraction) is used, the electromagnetic model must be defined by a set of canonical shapes, whose closed form scattering formulation is known (known as canonical problems).

By means of the electromagnetic mesher, the user can define the CAD model by a proper set of the following canonical shapes:

- Multisided Flat Plates
- Cones and cone frustums
- Cylinders
- Disks

2.3 The EM Computation

Results have been computed by means of the GTD_EM code embedded within the EMI-PT.

By means of this code, it is possible to separately select a large set of propagation mechanisms and verify the main scattering contributions to the received field.

Moreover, since ray tracing and field computation are computed into two separate steps, it is also possible to visualise all the ray paths and the relevant field contribution, thus performing a sort of diagnostic check to the problem under investigation and ensuring the understanding of all the involved propagation phenomena.

Moreover, the code is also able to account for non perfectly conductive materials and simulate the behaviour of RAMs.

3. VALIDATION RESULTS

The development of the EMIPT has been carried out under a contract from the UK MoD and has been conceived on the basis of a pre-existing tool called "Ship EDF" that has been widely validated during many years of application to complex e.m. projects of ship, mainly on behalf of the Italian Navy. In particular the two tools includes the same electromagnetic solver engines that have been subjected to a wide validation programme on behalf of the UK MoD.

The following paragraphs present some examples of validation taken from this activity, that has been focused on the application to the radar band scenario, giving a lot of useful information on the problem of accuracy when

dealing with very short wavelength in a real environment and on the physical behaviour of some parameters that must be carefully considered in performing analysis and measurement.

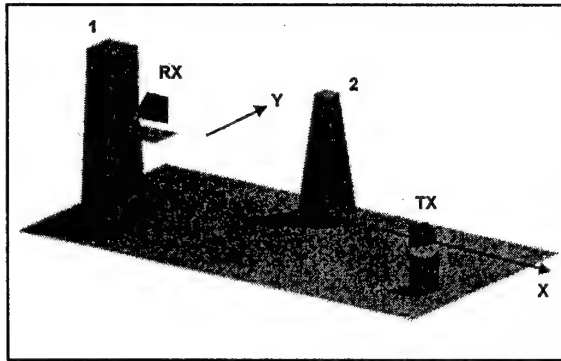


Fig. 2 – Initial Validation scenario (VP1)

The validation procedure has been scheduled according to a three step process, with increasing complexity of the scenario. The first, identified as Validation Pack 1 (VP1) refers to the structure shown in Fig.2, that represents the simpler scenario. The second step called VP2 refers to a real scale model of a ship superstructure shown in Fig. 3, and involves horns as well as navigation radar antennas. The final third step involves a real ship platform with horns and navigation radar antennas and all the structural complexity associated with it.

In the next chapters a few examples of validations are given to provide an overview of the obtainable accuracy and of the applicability of the numerical prediction tools.

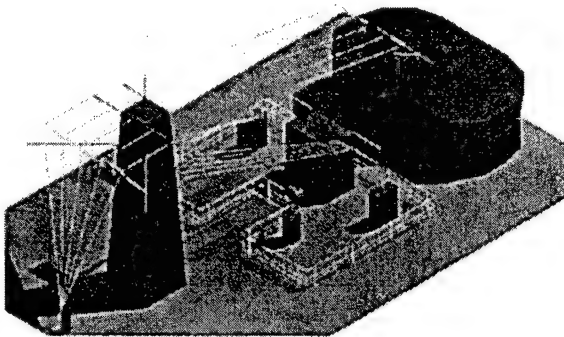


Fig. 3 – Second step validation scenario (VP2)

3.1 Validation of the Antenna Model

The numerical antenna model has been built up by using the IDS Aperture Antenna Modeller (AAM). The model is validated by checking its far field radiation pattern in free space against the measured one. Fig. 4 shows an example of validation related with the radiation pattern of a Horn operating at 3 GHz, on the full azimuth scan. By using the same technique all the mostly used antenna in

the radar band are modelled, from reflector to aperture and array, and horns.

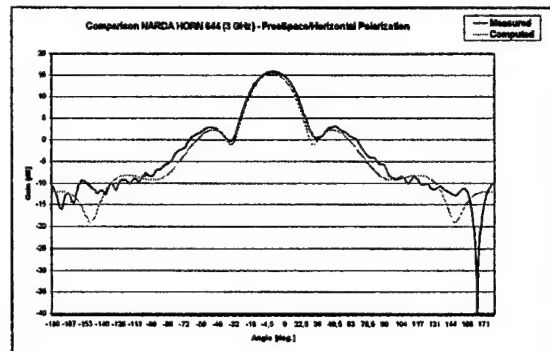


Fig. 4 – Antenna Numerical Model validation

3.2 Far Field Validation

The far field validation of antenna interacting with the structures has been performed in VP1 according to a set of many different orientation of horn antennas operating from 3 to 18 GHz. Fig. 5 shows the geometry considered for the validation result presented in Fig. 6.

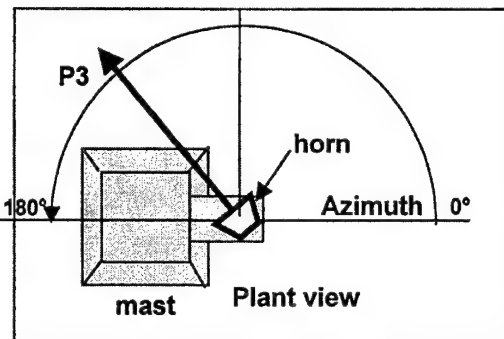


Fig. 5 – Antenna pointing for the test of Fig. 6

The transmitting antenna is pointed to the wedge of the supporting mast and the pattern is splitted into two beams, one coming from the reflection on the mast wall and the other degraded by the masking from the mast. Furthermore the example show the behaviour along near and far side-lobes regions.

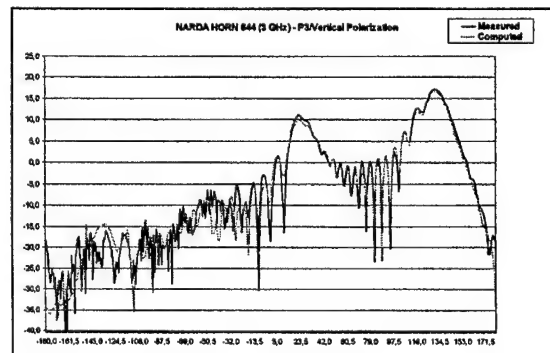


Fig. 6 – Comparison on far field for the configuration shown in Fig.5

3.3 Near Field Validation

The near field validation was carried out according to the scenario of Fig.7, where the details of the measurements grid are highlighted; the field strength were measured in the cross points of the grid lines and, for each point, three measurements have been done, at the nominal point, and at two more points moved by $\lambda/3$ and $2\lambda/3$ along the X direction.

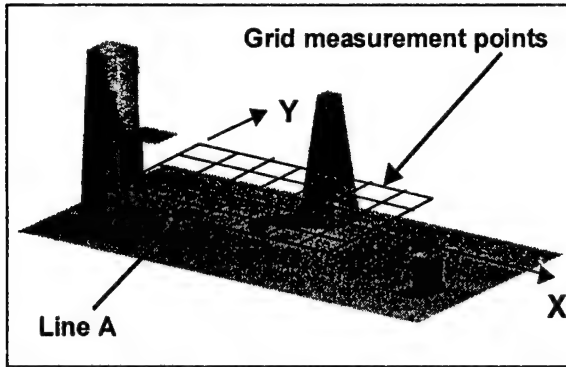


Fig. 7 – VP1 near field validation scenario

An example of validation result is presented in Fig.8 concerned with a scan along the line A. The result show the details of the behaviour of the computed field strength with respect to the measured one; as expected, the finer sampling rate of the simulations highlights the interesting features of the true physical behaviour of the field. The multipath effects due to the superposition of many scattering contributions give the information of the range of the field values for the different sampling points. This kind of result suggested also some interesting review of the criteria for performing more effective near field measurements aboard real ships that are under discussion.

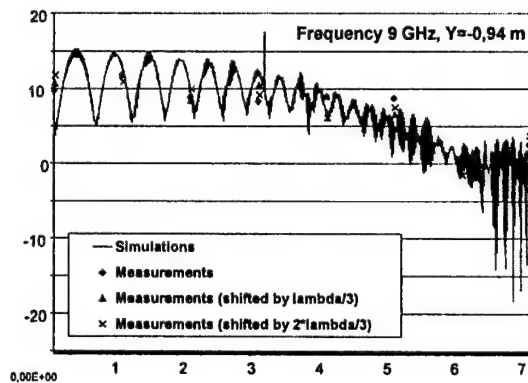


Fig. 8 - Validation Pack 1 Near Field example

Following the same approach, a further example related to the VP2 scenario is presented according to the configuration of Fig.9.

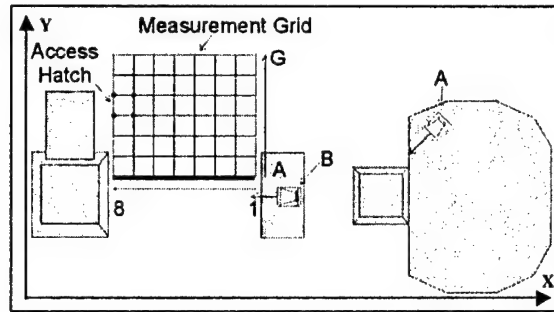


Fig.9 – VP2 near field validation scenario

An example of validation result is shown in Fig. 10. The result highlights propagation effects similar to those observed for the VP1 case, confirming that the near field behaviour in typical ship environments have basic common features that must be carefully considered when dealing with near field analysis both by prediction and measurements.

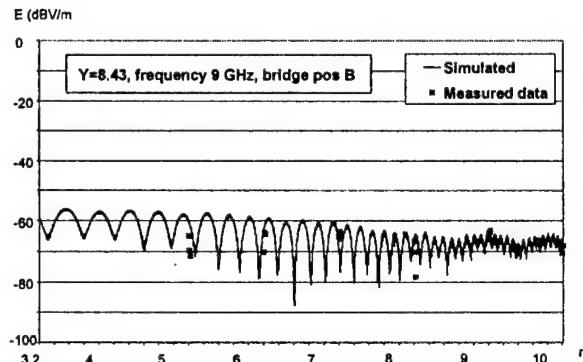


Fig.10.- Validation Pack 2 Near Field example

The whole set of the considered cases gave much information on the confidence achievable using the prediction for such complex real scenarios.

3.4 Coupling Validation

The geometry for the VP1 coupling validation is shown in Fig. 2; in the example here presented both the transmitting and the receiving horn are pointed toward the mast No.2, so the coupling occurs via direct ray along the line of sight between the two antennas, weighted by the sidelobe of the horns, and via reflected waves on the mast 2, weighted by the main beam of the horns.

The result of the validation is shown in Fig. 11, where the coupling behaviour on the 8 to 12 GHz band is presented.

The effect of multipath due to different path contributions is highlighted on such frequency scan analysis.

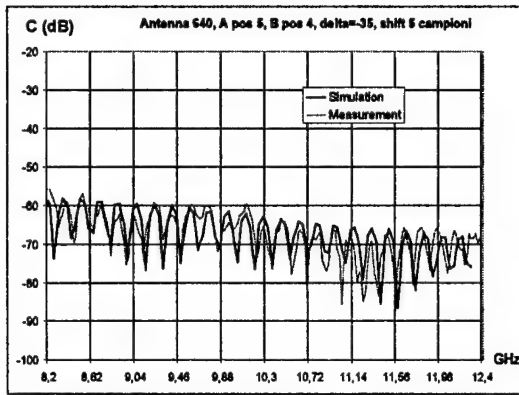


Fig. 11 - VP1 coupling validation example

In Fig. 12 the layout of an example concerned with the validation pack 2 is shown.

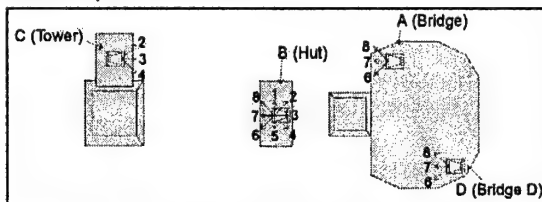


Fig. 12 - VP2 coupling scenario example

According to such configuration, the Fig. 13 shows the result of the frequency swept coupling validation. The VP2 scenario shows several effects arising from the scattering of the structures; however there are some fast oscillations in the measured curves that could be produced by additional noise sources not included in the prediction.

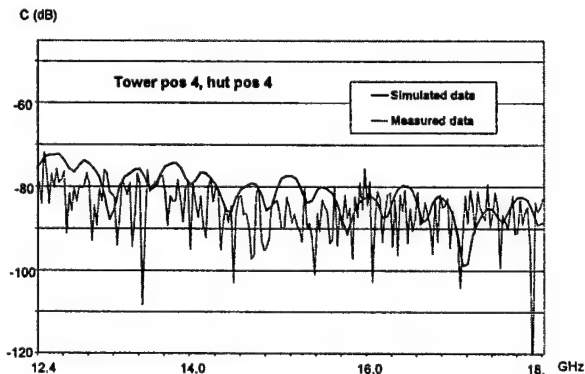


Fig. 13 - VP2 coupling validation example

4. CONCLUSIONS

This paper presents a limited selection of the whole set of results obtained during a large validation programme of the EMIPT code, in order to give an overview of the performance of the numerical prediction approach to the design of modern ship platforms.

The work highlighted not only the validation aspects of the tool, but gave many important information on the problems that the e.m. engineer can experience when dealing with antenna and EMC problems, on real ship environment, in the radar bands.

It is worth noting that in many practical situations it is very difficult to characterise properly the behaviour of some specific e.m. parameters, such as the near field on areas close to the structures. In this scenario the work pointed out the usefulness of integrating with additional information the possible measurement campaigns, that seems to be potentially limited in providing the amount of data needed to sample the parameter with the proper step.

From this last point of view, the numerical prediction showed the capability of providing a very efficient means to improve the characterisation of the e.m. environment especially for checking its behaviour with respect to the applicable norms threshold, as happens in the case of radiation hazard assessment.

Furthermore, in the frame of this assessment process, the application of the prediction showed the capability to provide powerful diagnostics tools, in terms of ray tracing and induced currents analysis based on graphical display on the 3D CAD ship model. This capability was usefully employed to investigate many e.m. phenomena features that helped in a better understanding of the real e.m. scenario and, in some way, gave useful inputs for optimising the measurement procedures and related standards.

5. ACKNOWLEDGMENTS

The authors wish to advice Mr. Geoff Nixon from the UK MoD for his helpful review and suggestions during the activity, and Mr. Ivan Boswell and his team from DERA Funtington who performed all the scenario setup and the measurements campaign used for this work.

PREDICTION OF E.M. FIELD LEVELS INSIDE CLOSED STRUCTURES BY A STATISTICAL APPROACH

Riccardo Cioni, Francesco Teti

IDS Ingegneria dei Sistemi S.p.A. – Via Livornese 1019, 56010 Pisa, Italy

Tel. +39 050 312411 – fax +39 050 3124201 – e-mail: ids_pisa@ids-spa.it – URL: <http://www.ids-spa.it>

The present paper deals with the possibility of predicting the electromagnetic field levels into a closed volume by means of a statistical formulation.

The source of radiation can be both internal (e.g. an equipment with parasitic radiation) or external (e.g. an electromagnetic field due to equipment or antennas placed externally to the volume itself).

The interface between the internal volume and the external one is constituted by a set of apertures. The mean dimensions of the apertures must be in the order of the wavelength or greater.

The formulation is based on the oversized cavity method: the main principle is that, if the volume dimensions are greater than a few wavelengths, a lot of resonant modes are excited and the electromagnetic field level is characterised by a mean value that is rather independent from the volume structure.

On a spacecraft, the available volume is reduced by practical reasons, whereas the number of payloads is very high. The EMI problem of predicting the field inside the spacecraft body is thus an important and actual problem.

To apply the formulation to a spacecraft, a set of extensions to the formulation itself have been performed, in order to take into account:

- *Multiple volumes separated by conductive interfaces each one with a set of holes that allow propagation effects between neighbouring volumes.*
- *The presence of lumped absorbers, aimed at reducing the field levels inside the volume.*

Due to its computational efficiency, this approach is very useful for preliminary and large scale investigations.

1. THEORETICAL FORMULATION

The oversize cavity approach is based on the concept of the reverberating chambers, used for EMI assessment of consumer and industrial products.

Under this concept, when a volume of irregular shape, delimited by conductive walls, is excited by a source of e.m. radiation whose wavelength is much smaller than

the dimensions of the volume itself, the internal field can be represented by the sum of a lot of characteristic modes: the resulting field averages around a settled value, independently from the position into the volume itself.

Basing on this concept and resorting to the principle of energy conservation, the simple cases of an external source and of an internal source can be considered in order to point out the main characteristics of this theory. The reader can find in [1,2] the full analytical approach and all the details of the theory.

For both the following examples it is supposed that the walls defining the volume are conductive materials without losses and the volume is characterised by an apertures set whose total area is A_t .

If the source is internal and is radiating a power P_i , in absence of losses all the energy will flow through the apertures and the r.m.s. field value will be given by:

$$P = \frac{E^2}{\eta} A_t, \text{ hence } E = \sqrt{\eta \frac{P}{A_t}} \quad (1)$$

Assuming a steady condition, if E is the field value at the interface, it will also be the field internal to the volume itself.

If an external source it is exciting one of apertures of the volume, with an area equal to A_e , and the field due to the external source on the interface is equal to E_e , then the field level within the considered volume will be:

$$\frac{E_e^2}{\eta} A_e = \frac{E^2}{\eta} A_t, \text{ hence } E = E_e \sqrt{\frac{A_e}{A_t}} \quad (2)$$

However, the following considerations apply must be taken into account:

1. In the energy flux it has been supposed that an asymptotic approximation of field constant across the aperture is applicable (hence the aperture much greater than the wavelength): this hypothesis must be verified.
2. At low frequencies, some cables passing through holes can modify the way energy propagates between the external and the internal sides of the volume.
3. The settled field level can be assumed valid at a distance sufficiently far from the feeding source (either

an internal source or an aperture in case of external excitations)

4. In the case of internal source, if the apertures are reduced to a minimum area and no losses are assumed, the computed value can diverge from the real one: however, this is a situation in which also the use of exact methods is very critical.

About the considerations (1) and (2), it has been verified that:

- if the aperture has no passing cables and characteristic dimensions are in the order of half a wavelength or greater, then the energy flux rapidly converge to the asymptotic value: a dumping coefficient, to be applied to the aperture area, can however be considered in order to account of small apertures: note that for resonant apertures this coefficient can be greater than 1. In case of doubts, each aperture can be separately analysed by means of exact methods and its equivalent area can be readily obtained.
- If some cables pass through the apertures, the problem is somewhat more complex, since also the grounding details must be considered and the use of an exact method is required; however, if the net area of the aperture is greater than λ^2 the asymptotic approximation applies, but the net area must be considered.

Finally, some extensions are required in order to manage interfaces with neighbouring volumes (hence propagation across different regions) and the presence of absorbers aimed at reducing the internal field level.

2. COMPUTER CODE

Based on the previous theoretical formulation a software tool has been developed; it is able to evaluate the expected e.m. field levels in a cavity caused by device's radiated e.m. emission or by incident external e.m. field for frequencies greater than 1 GHz. The tool was developed to perform analyses of EMC/EMI risk assessment on satellite but its use is very general and it can find applications where the objective is to evaluate e.m. field levels in cavity with dimensions greater than many wavelengths. The 'Oversize' tool is able to:

- consider the presence of e.m. absorbers in the cavity;
- consider cavities composed by multiple communicating volumes;
- define radiated emission measure for each installed equipment and use it for the definition of internal sources;
- perform analyses based on a predefined environment (geometry, equipment configuration) and 'what if' type;
- define all the input data and compute options by a user friendly interface;
- produce reports resuming results and compute options selection.

The following picture shows the main menu window of the tool 'Oversize'.

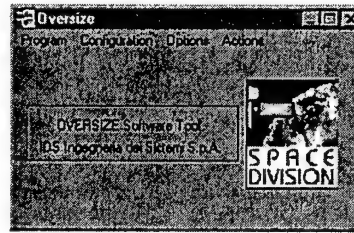


Fig. 1 – Main window

The tool permits to define and manipulate the geometry of the model modifying apertures area, panel area and conductivity, absorber efficiency etc.. Fig.2 shows the graphic user interface which permits the user to change the previous geometrical and electrical parameters.

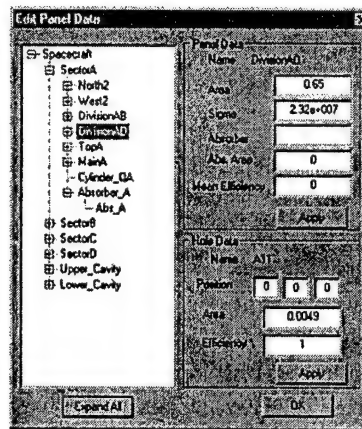


Fig. 2 – Geometry data definition window

The user can also change the equipment characteristics in terms of emissions, operative frequency and position inside the cavity. Fig.3 shows the window with the option that the user can change. All the previous parameter changes are fundamental to conduce 'what if' type analyses.

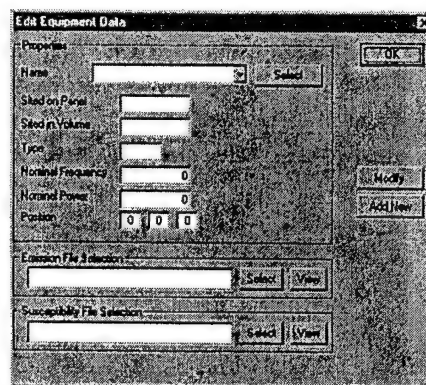


Fig. 3 – Equipment data definition window

3. VALIDATION RESULTS

The software tool, briefly described in the previous chapter, has been validated by Finite Difference Time Domain (FDTD) analyses of the expected e.m. levels into a spacecraft sector excited by an external field source at 1.55 GHz located on the top of the cavity. The geometrical model represents a spacecraft volume with apertures for solar array booms and for waveguides. The following two pictures show an external and an internal view of the cavity; the modelling was almost complete as it considers the presence of apertures and devices occupation space.

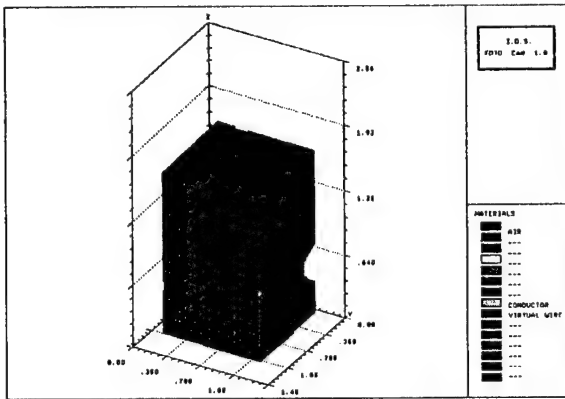


Fig. 4 – External view

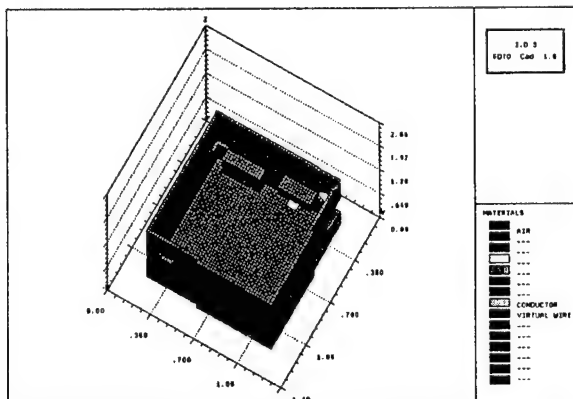


Fig. 5 – Internal view

The first main result of the simulations is that the field level in the cavity is constant on average. The following picture shows the e.m. field level along the Z axis from the top to the floor of the sector. As it can be noticed at $Z=80u$ the field takes its higher value which accounts for the aperture excited by the external field source but rapidly, just about 0.2 m from the top of the cavity, it tends to a steady value.

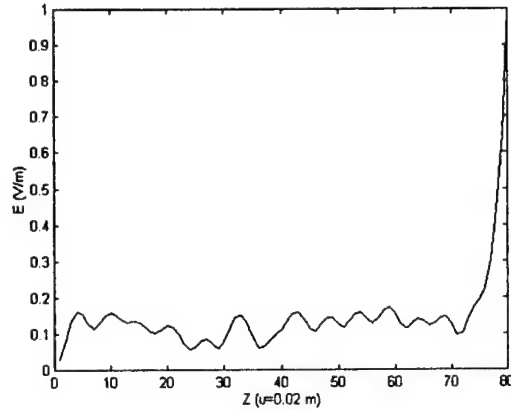


Fig. 6 – Field level along Z axis

It is necessary to point out that the high level at $Z=80u$ is caused by the presence of an hole which feeds the cavity with the e.m. energy used for this test.

The constant distribution inside the cavity is also confirmed by the following statistic parameters evaluated on the field values obtained from the simulations.

Mean value	0.113 V/m
Standard deviation	0.0407 V/m
Effective Value	0.120 V/m

Tab. 1 – FDTD field levels statistics

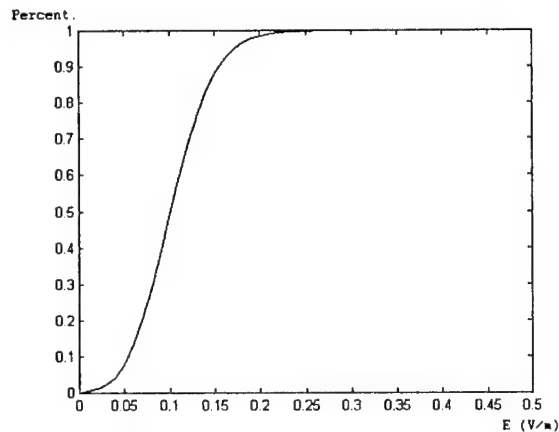


Fig. 7 – FDTD percentiles curve

All the previous results confirm that the basic hypothesis of the oversize cavity formulation about the uniformity of the field level inside a cavity at high frequency is correct. The most important result which validates the software tool 'Oversize' is that the effective value obtained it is

very near to the result obtained by the FDTD simulation, in fact it results to be 0.122 V/m.

4. CONCLUSIONS

A statistical approach, known as oversize cavity, has been tested in order to analyse the e.m. fields inside a closed volume. Validation has been performed by means of FDTD and a good agreement between the two methods has been demonstrated. Since this statistical approach is based on asymptotic assumptions, it is expected to be more and more valid as the ratio between the volume dimensions and the wavelength increases, so it can replace the use of exact methods especially when they are no more applicable due to memory and CPU time requirements.

Even if it has been applied to the assessment of EMI compatibility for spacecraft, it could also be applied to other kind of problems, such as for e.m. field levels

inside instrumentation racks and in general whenever the field level into large cavities must be predicted.

5. REFERENCES

- [1] R. Gutierrez, J. Thuery - "Etude du couplage entre les antennes et les équipements d'un satellite"- Proc. Of the 11th ESTEC Antenna Workshop on antenna Measurement. Gothenburg, Sweden 20-22 June 1988.
- [2] J. Thuery, R. Gutierrez, J. Ramis - "A model for spurious RF coupling on board communication satellites" - Proc. of the International Conference on Electromagnetic in Aerospace Applications - September 12-15, 1989 - Polytechnic of Turin - ITALY.

EMC 2000

INTERNATIONAL WROCLAW SYMPOSIUM
ON ELECTROMAGNETIC COMPATIBILITY

MODELLING OF MICROWAVE ELECTROMAGNETIC INTERFERENCE IN A COMPLEX COUPLING ENVIRONMENT

Sebastian A Di Laura

EM Engineering Group, Concepts and Integration, Room C109, DERA Portsdown West, Portsdown Hill Road, Fareham, Hants PO17 6AD, UK. Fax (+44) (0) 23-9233-7338, Email: sadilaura@dera.gov.uk

ABSTRACT

Electromagnetic Interference (EMI) on the topside of modern naval platforms is becoming an increasing problem because of the high density of competing antenna systems. The prediction of EMI is complex, time consuming and expensive. The advent of high specification computers now makes computer simulation predictions a cost-effective means of identifying EMI whilst the platform is still in its design stages. DERA has acknowledged the EMI problem and is developing an EMI prediction code called the Mutual Interference Simulation Tool (MIST). This paper will explain how MIST works, and demonstrate its advantages and capabilities.

1. INTRODUCTION

Electromagnetic Interference (EMI) on the topside of modern naval platforms is becoming an increasing problem because of the high density of competing antenna systems (Figure 1).

Intra-ship EMI is caused by the propagation of electromagnetic energy from a radiating source (transmitter) to a "victim" (receiver) on the same platform. The propagation path may be direct between the source and victim, or indirect where energy reaches the victim after first reflecting/diffracting from the superstructure.

The problem of EMI on naval platforms is extremely complex and growing. Not only are more systems being introduced to the average topside, but their sensitivity to noise is also increasing. EMI reduces the signal to noise ratio of systems, and is particularly serious for surveillance and tracking radars. Figure 2, shows the range of systems that might typically be fitted to a modern naval platform and the regions of the frequency spectrum that they occupy.

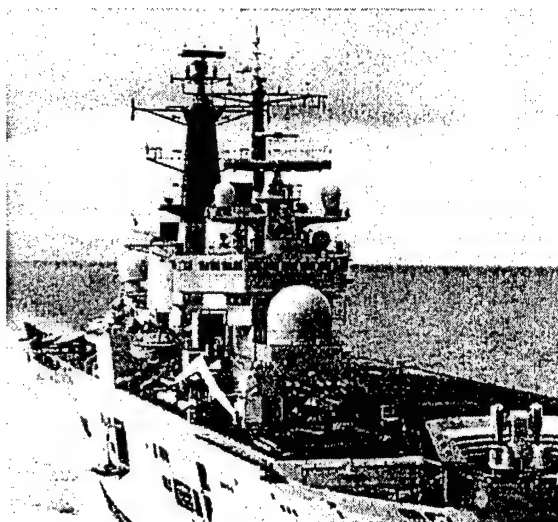


Figure 1. An example of a topside electromagnetic environment

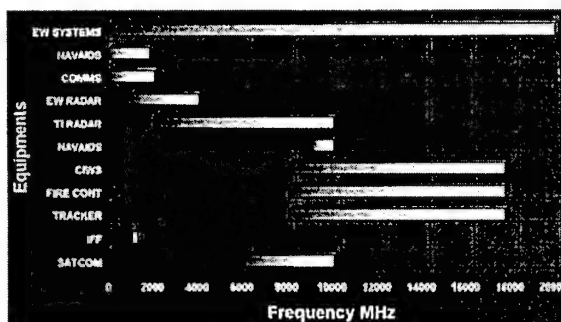


Figure 2. Sensor/Frequency Chart

EMI problems are usually identified once the platform is in service. Combating the EMI involves expensive retrospective modifications. This may require large structural alterations to the topside (e.g. antenna relocation, Radar Absorbing Material (RAM) application, structural reshaping) in order to achieve a tolerable level of EMI. The sensible approach is to predict the causes and magnitude of the EMI using computer-modelling tools while the platform is in its conceptual or design stage, avoiding costly modifications later on.

In order to address this DERA is developing the Mutual Interference Simulation Tool (MIST) to predict EMI on naval platforms. This tool models frequencies ranging from High Frequency (HF) to the microwave bands. This paper deals only with MIST's microwave modelling capability.

2. BENEFITS OF EM MODELLING

There are three methods of assessing EMI on naval platforms. The first involves measurements taken on sea trials. Here all the environmental information is available but this type of trial is difficult to control, is very time consuming and expensive. The second method involves laboratory trials. These are highly controllable and give an insight into the basic EMI mechanisms. However, unlike the sea trials, most of the environmental parameters cannot be represented. They too are time consuming and expensive. The third method uses computer simulation or EMI prediction tools. These are generally highly controllable, fast, inexpensive to use, and highly flexible. They are best utilised during the conceptual/design phase of a platform. Computer modelling though is only as accurate as the parameters fed into the software, in this case the antenna parameters and the CAD representation of the platform. The benefits of computer simulation can be summarised as follows:

- The effects of EMI on "victim" receiver antennas can be quantitatively and qualitatively assessed.
- EMI problems can be identified earlier on in the project life cycle while the platform is in the concept/design stage. This leads to lower downstream costs and a better final system performance.
- Once problems are identified solutions to reduce EMI can be modelled. These include the application of RAM, repositioning of antennas and/or reshaping parts of the superstructure to reflect Electromagnetic Radiation (EMR) into low risk directions.
- EMI predictions using EM modelling tools like MIST saves time and money.
- All modelling can be tailored to the customer's needs.

3. HOW EMI IS MODELLED

Modelling a naval platform is a complex procedure and should normally be performed by an experienced operator. From the CAD model design of the platform through the final analysis of the results the necessary steps to carry out a complete assessment are described below.

The shipbuilder/customer supplies the necessary antenna parameters, CAD model data of the platform and the type of EMI assessment that is required. The surface CAD model representation of the platform is converted into a solid representation by subdividing it into small flat patches. This process is referred to as "meshing" (Figure 3). We note here that to maintain a high fidelity representation of the model, the mesh density applied should vary with the surface contour, especially when curved surfaces are found (Figure 4). In general the mesh density is dependent on several factors. The size of the platform, whether the observation point is in the far field criterion of the source and the accurate representation of micro-geometry are some to mention. Generally, mesh sizes range from tens to hundreds of thousands of elements, increasing as the complexity of the model increases. A meshed model is shown below.

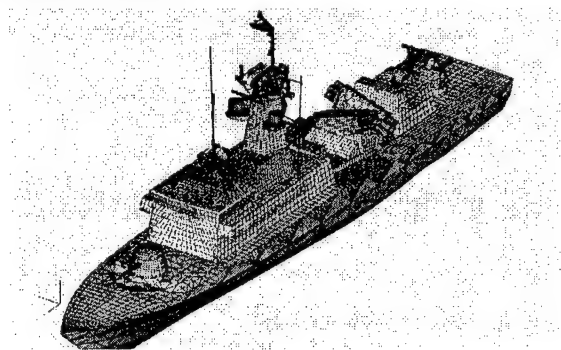


Figure 3. A meshed model

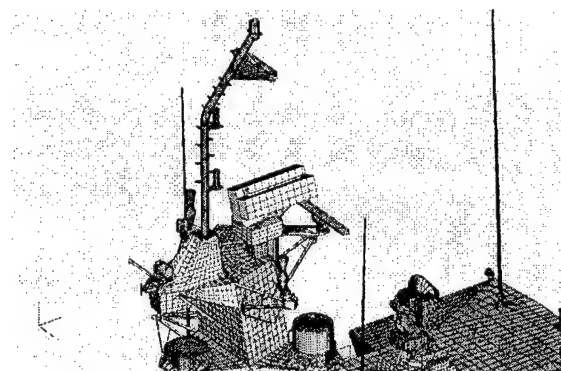


Figure 4. Close-up view of topside

Antennas are imported and "joined" to the structure from the MIST Antenna database. This database contains all the physical and electrical parameters of most common Electromagnetic (EM) sensors. At this stage the CAD model is ready and the geometrical data are extracted. An edge detection routine is executed and diffracting edges are automatically identified.

In order to model complex interactions such as double and triple reflection/diffraction, the line of sight (LOS) between scatterers in the structure must be determined. This is achieved via a sophisticated ray-tracing algorithm. Edge and LOS identification take about 90% of the total runtime, but do not require any human intervention and are therefore cheap and easy to accomplish.

The Electromagnetic interactions are modelled by using three high frequency approximation techniques. These are Physical Optics (PO), the Physical Theory of Diffraction (PTD) and Geometrical Optics (GO), which are implemented into the MIST EM solver. For multiple reflections the combination GO/PO is used. The EM data output by MIST can be visualised in several different ways as described below. This output can also be analysed using "Commercial of the Shelf (COTS) software.

4. MIST CAPABILITIES/VISUALISATION

MIST outputs can be analysed/visualised in a variety of formats. The EM solvers are set to calculate the total scattered electromagnetic field for a particular source/victim pair. With this information quantities such as Propagation Loss can be extracted. The visualisation of high return scatterers on the superstructure is shown as "hotspots" (Figure 5), and complex energy (ray) paths (Figure 6) are displayed as lines as shown in the figures below. A combination of the two displays is also possible.

MIST can be used to model a source/victim pair and in general it can determine electromagnetic field densities at any observation point specified by the user.

The output here can determine what treatments are most appropriate to reduce EMI, e.g. special coatings, alternative materials, reshaping or relocation.

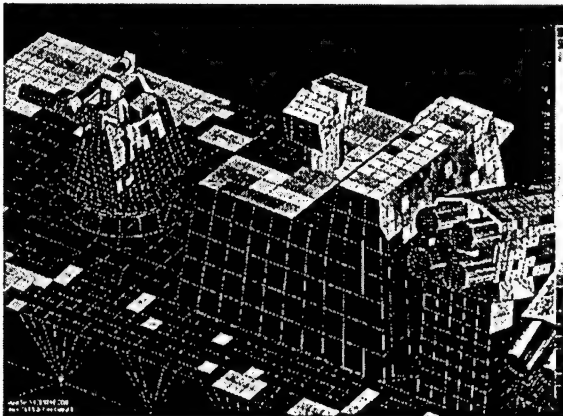


Figure 5. Hotspots display

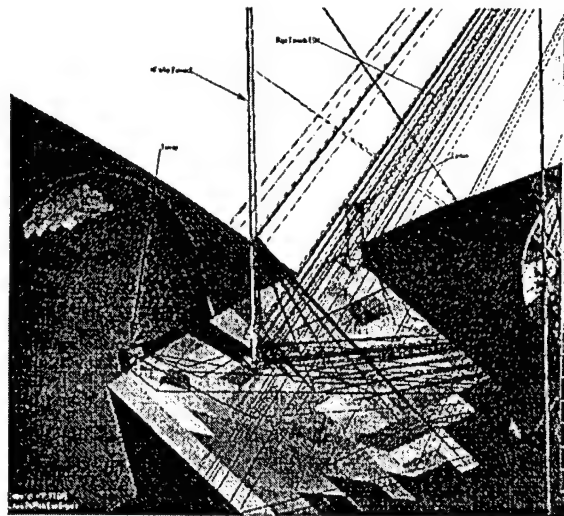


Figure 6. Display of complex ray paths

Another visualisation format is the polar plot display of the change of EMI with antenna orientation, as shown below in Figure 7.

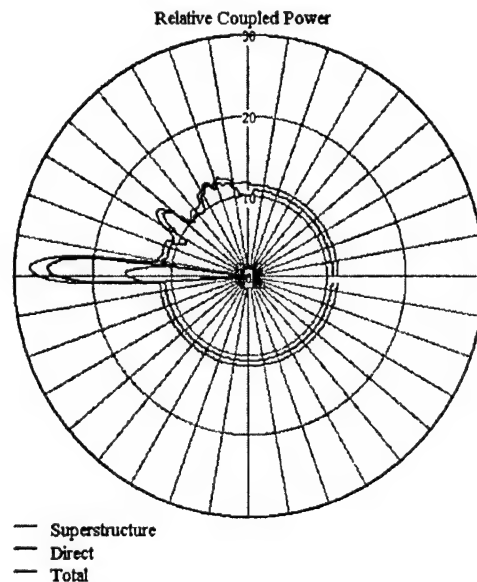


Figure 7. Polar Plot

A very useful tool that might be used during the concept/design or retrofit stages of a platform is the blockage display. Areas of the superstructure blocking the visibility of a sensor or directional weapon can be readily identified, as shown in Figure 8.

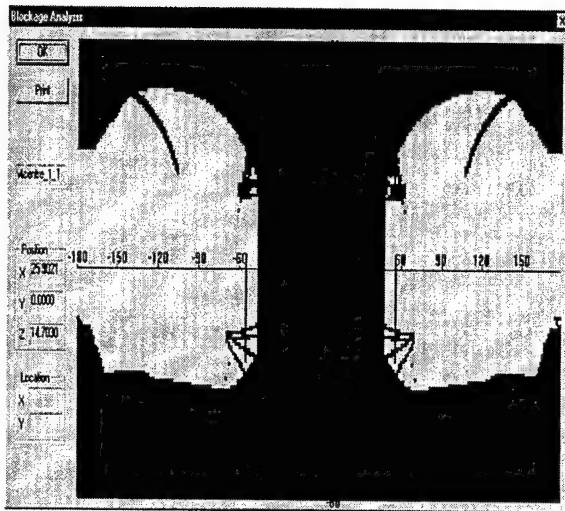


Figure 8. Blockage Analysis Display

MIST can run on a standard PC without the need for expensive workstations. Access to the EM solvers, CAD software and output data is achieved via a simple standard windows graphical user interface (GUI). The GUI allow the user to readily create / modify the actual platform being modelled, transfer data files and post-process results from the EM solver. The COTS CAD package used to create the model geometry and view post-processing is very intuitive and versatile, and is able to import a variety of standard file formats including stereolithography files.

With the aim on minimising human intervention and thus increasing the cost-effectiveness of the process, MIST also features automatic identification of edges and multiple reflections.

MIST capabilities can be summarised as follows:

- Prediction of sources of EMI on complex platforms.
- Clear visualisation of EMR propagation in the form of "hotspots", ray paths, polar plots and field densities.
- User friendly interface to EM solver, CAD software and data output via simple standard windows GUI.
- MIST is compatible with standard COTS CAD packages.
- Realistic antenna representation and comprehensive database.

- Automatic diffracting edge and multiple interactions detection.
- Ability to use a variety of input file formats.

5. CONCLUSIONS

The problem of EMI on topside of naval platforms is complex and needs to be addressed. Sea and laboratory trials, although possible, are no longer an option when these are compared to the more cost-effective computer simulation approach.

DERA is developing the MIST modelling tool which is designed to predict the sources and magnitude of EMI on naval platforms, ideally when they are in their concept/design stage. A comprehensive antenna database provides the necessary information to assess EMI qualitatively and quantitatively.

Future capabilities will include the modelling of composite materials, which at present are beginning to populate the topsides of naval platforms.

ACKNOWLEDGEMENT

The author gratefully acknowledges Mr Steve Turner of DERA for their contribution and review of this paper. The author would also like to acknowledge the help of Mr Alan Lavell-Smith in reviewing this paper.

BIOGRAPHICAL NOTE

SEBASTIAN DI LAURA is the main software developer for the MIST microwave module programme. He specialises in electromagnetic high frequency techniques and ray tracing. He graduated with a Bachelor of Science Degree in Physics and Mathematics at the University of Portsmouth in 1995. He also obtained a Master of Science degree in Microwave Communications at Portsmouth University in 1998.

© British Crown copyright 2000. Published with the permission of the Defence Evaluation and Research Agency on behalf of the controller of HMSO.

VALIDATION OF A TIME-DOMAIN MOM SIMULATOR FOR EMC STANDARD GUIDELINES

G. Manara, A. Monorchio

Dipartimento di Ingegneria della Informazione, Università di Pisa

Via Diotisalvi 2, I-56126 Pisa (Italy)

Tel. +39-050-568511, Fax. +39-050-568522, E-mail manara(mono)@iet.unipi.it

Numerical results obtained by applying a stable marching-on-in-time solution scheme of the Electric Field Integral Equation (EFIE) are compared with experimental data relevant to the case of scattering from continuous metallic bodies and metallic shelters with apertures. The experiments have been performed in an Electromagnetic Pulse (EMP) hardware simulator, reproducing plane wave illumination conditions. The above comparisons are used to discuss the limits of applicability, with specific reference to numerical stability, of the corresponding simulator, which is based on a Method of Moments (MoM) solution of the EFIE in time domain. The observations drawn may be useful to define general EMC standard guidelines for validating application oriented software packages.

1. INTRODUCTION

Numerical techniques for the prediction of electromagnetic fields scattered by complex objects, directly operating in time domain (TD), have recently received considerable attention. The availability of computer codes based on such techniques is of remarkable importance, for instance, in the field of electromagnetic compatibility, where the interest is often extended to wide frequency bands.

Among the algorithms proposed in the literature for TD analysis of electromagnetic scattering, we mention the TD formulation of the well-known method of moments (MoM), which proves computationally efficient [1]. However this algorithm suffers from a definite tendency to instability, that is, the calculated induced current and field distributions typically exhibit spurious fluctuations of growing amplitude and eventually diverge. These unintended instabilities are introduced at the system discretization stage, i.e., in the conversion of the Electric Field Integral Equation (EFIE) to a discrete space-time model. Similar problems arise in the application of the magnetic and combined field integral equations. In particular, the

achievement of a stable numerical procedure strongly depends on how the original problem is discretized, both in space (size and shape of the triangular patches) and time (time step and shape of basis functions) [2].

This paper deals with the validation of a numerically stable simulation procedure, based on a formulation of the Electric Field Integral Equation in Time Domain (EFIE-TD). In particular, simulation data are compared with results obtained from experiments performed on a set of canonical metallic bodies. The experiments have been carried out in an open-site Electromagnetic Pulse (EMP) hardware simulator. The induced current densities on the exterior surface of metallic bodies have been measured by broad-band sensors which are coupled to the magnetic field components tangential to the above surfaces. The measured current densities have therefore been processed in order to eliminate the effects introduced by the measuring instruments chain and those of air humidity that strongly affects the results. In particular, a procedure is shown which allows us to reconstruct the actual amplitude of the electric field impinging on the scattering object. In this way, the statistical approach is avoided and no averaging of the measurements is needed to compare the predicted and measured results. A set of conducting canonical bodies has been tested, either open or closed. The limits of applicability of the EFIE are discussed for the case of open bodies. Finally, we point out that, due to the large time constants characterizing the measurement setup, comparisons between experimental and numerical data can be performed only if the employed method is stable also at late times; in our case this long term stability has been obtained by the analysis developed in [2].

Finally, we note that, once validated, the TD electromagnetic simulator presented in this paper may constitute a valid alternative to measurement procedures in the analysis of electromagnetic field distribution in complex environments. It allows us not only to formulate predictions, but also to verify and interpret experimental data.

2. A STABLE MoM-TD FORMULATION

A TD version of the EFIE suitable for solving the scattering problem of interest is described in this section and solved through a MoM approach. Let S be the exterior surface of a perfectly conducting body, which can be either closed or open, illuminated by an arbitrarily polarized plane wave; \vec{E}^i denotes the incident electric field and \vec{J} the surface current density induced on S .

Since the body is a perfect electric conductor, the tangential component of the total electric field on S must vanish. This leads to an integro-differential vector equation in the unknown induced current density \vec{J} . The forcing term of this equation is given by the tangential component of the incident electric field \vec{E}_{tang}^i :

$$\frac{\partial}{\partial t} \left[\frac{\mu}{4\pi} \int_S \frac{\vec{J}(\vec{r}', t - R/c)}{R} dS \right] - \nabla \left[\frac{1}{4\pi\epsilon} \int_S \frac{1}{R} \int_{-\infty}^{t-R/c} \nabla \cdot \vec{J}(\vec{r}', \tau) d\tau dS \right] = \vec{E}_{\text{tang}}^i \quad (1)$$

In (1), $R = |\vec{r} - \vec{r}'|$ denotes the distance between an arbitrarily located observation point \vec{r} and a source point \vec{r}' on S ; $t - R/c$ is the retarded time and μ, ϵ are the permeability and permittivity of the medium surrounding the scatterer, respectively. In order to obtain a numerical solution of equation (1), a suitable expansion of the unknown current $\vec{J}(\vec{r}, t)$ is employed. In particular, the spatial variation of surface currents induced on the body can be accurately approximated by discretizing its surface into N_T triangular patches over which a set of basis functions can be defined. As far as the temporal variation is concerned, a time discretization scheme can be assumed, provided that the time step ΔT is properly chosen. Hence, the surface current distribution can be numerically approximated as

$$\vec{J}(\vec{r}, t) = \sum_{j=-\infty}^{+\infty} \sum_{n=0}^{N_e} I_{n,j} T_j(t) \vec{f}_n(\vec{r}), \quad (2)$$

where N_e is the number of edges of the triangles which model the scatterer, excluding the boundary edges if S is open. Each unknown coefficient $I_{n,j}$ represents the value of the component of the surface current normal to the n -th edge at the instant $j\Delta T$.

The basis functions $\vec{f}_n(\vec{r})$ that have been utilized are known as "roof-top" functions [3]; they are defined over each triangle pair that discretizes the body surface (triangular patch modeling). Basis functions

$T_j(t)$ with a triangular shape have been commonly used to discretize the temporal evolution [1]. However, in order to guarantee the algorithm stability according to the criteria defined in the next section, different interpolating functions have been employed here. Specifically, pulses ensuring quadratic approximation over temporal sub-domains have been used. In particular, the second order polynomial used to describe time evolution over each sub-domain is an arc of the parabola passing through the samples at: $t = (j-1)\Delta T$, $t = j\Delta T$, and $t = (j+1)\Delta T$. The result is a continuous piece-wise quadratic function, with a piece-wise linear derivative, which is discontinuous at the integer multiples of ΔT , except when the function to be interpolated is exactly linear or quadratic.

From (1) and (2), adopting a testing procedure as that used in the frequency domain approach [3], the following set of equations is obtained at the instant $t_j = j\Delta T$:

$$\begin{aligned} & \frac{l_n}{2} (\bar{\rho}_n^{c+} + \bar{\rho}_n^{c-}) \cdot \frac{\partial \bar{A}(\vec{r}_n^*, t_j)}{\partial t} + \\ & + l_n [\phi(\vec{r}_n^{c+}, t_j) - \phi(\vec{r}_n^{c-}, t_j)] = \\ & = \frac{l_n}{2} (\bar{\rho}_n^{c+} + \bar{\rho}_n^{c-}) \cdot \vec{E}_{\text{tang}}^i(\vec{r}_n^*, t_j), \quad n = 1, 2, \dots, N_e. \end{aligned} \quad (3)$$

In the derivation of (3), testing functions coincide with basis functions (Galerkin's method). Moreover, the vector potential \bar{A} is evaluated at the center \vec{r}_n^* of each edge, while the scalar potential ϕ is calculated at the centroid $\vec{r}_n^{c\pm}$ of each triangle Γ_n^{\pm} . Finally, $\bar{\rho}_n^{c\pm}$ denotes the same centroid with respect to the free vertices of the pertinent triangles, while l_n is the length of the edge.

For obtaining a numerical implementation of (3), we substitute explicit free-space expressions in TD for the vector and the scalar potential and approximate the surface current distribution as in (2). In particular, the use of the quadratic interpolating functions enables us to evaluate in a closed form the derivatives with respect to time in (3). Finally, a linear system of equations is obtained which relates the unknown coefficients $I_{n,j}$ to the incident electric field. It can be expressed in matrix form as follows:

$$\underline{I}(j+1) = \sum_{k=0}^j \underline{M}^{-1} \cdot \underline{F}_{j-k} \cdot \underline{I}(k) + \underline{M}^{-1} \cdot \underline{B} \cdot \underline{E}_{\text{tang}}^i(j), \quad (4)$$

where $\underline{I}(j)$ is a column vector with N_e elements representing the unknown coefficients at the instant t_j , $\underline{E}_{\text{tang}}^i(j)$ is the vector containing the values of the

incident electric field at each edge at the same instant. The matrices $\underline{\underline{M}}$, $\underline{\underline{F}}_{j-k}$ and $\underline{\underline{B}}$ assume values depending upon both geometrical and temporal parameters; however, they do not explicitly depend on time. The first term at the right-hand side of (4) reveals the recursive nature of the system, since the coefficients at a fixed instant of time depend on the values assumed by the same coefficients at previous instants.

Extensive numerical tests carried out for various geometries and discretization schemes suggested heuristic expressions for a lower and an upper limit, ΔT_{\min} and ΔT_{\max} , of the time step ΔT for which system stability is ensured. In particular, the above limits were found to depend on both size and shape of the triangular elements used for space discretization. Both ΔT_{\min} and ΔT_{\max} vary with the size of the patches as well with their quality factor [4] according to a simple proportionality law. Furthermore, ΔT_{\max} was also seen to be affected by the relative positions of the patches. In conclusion, the stability interval strongly depends on the geometrical discretization of the body. In particular, the more uniform and regular is the patch modeling of the scatterer, the wider is likely to be the set of values of ΔT leading to a stable behavior of the algorithm. Depending on the scatterer and on the particular mesh employed, this interval may sometimes be void so that stability cannot be ensured. This frequently occurs when the body has wedges or tips. However, even if a stability interval does not exist, it is convenient to choose ΔT close to the values ΔT_{\min} and ΔT_{\max} , in order to delay instability phenomena as much as possible. Further details can be found in [2].

3. EXPERIMENTAL SET-UP

The experiments have been conducted in an Electromagnetic Pulse (EMP) open-site hardware simulator, 95 m long and 28 m wide, and whose height is 19 m. The basis of the simulator is a metallic plane while all the supporting structure are made of wood and kevlar for keeping the electromagnetic interference as low as possible. The effective test volume is a box with a basis of 10m×10m and a height of 6 m.

A Marx type generator provides the excitation of the electromagnetic field; the output voltage ranges from 400kV to 1.3MV and the pulse shape can be modeled as a double exponential with a rise time, computed between 10% and 90% of the maximum value, lower than 5 nsec.

The acquisition system is a MELOPEE type with sensors of reduced dimensions so that the field under measurement is perturbed very lowly. Additionally, the sensors have a very high dynamic (they are able to measure electric field from several mV/m to 1 MV/m)

and wide band working frequencies (from several kHz to more than 1 GHz).

Specifically, the probes that have been used are the ones with code H1601 and E1602. The former is a probe that is coupled to the tangential component of the magnetic field present on a surface, so that a direct measure of the surface current density is obtained. It is a derivative type and it is connected to an integrator-transmitter (T1060) through a shielded coaxial cable 0.2 m long. The transmission between the device under test and the control room is made with fiber optic cables.

The probe H1601 allows the detection of signals from DC up to 1.3 GHz. The system H1601-T1060 is able to measure surface current densities from $\pm 2.65 \text{ A/m}$ to $\pm 2.65 \text{ kA/m}$ with a noise level of 33 mA_{rms}/m.

The electric field probe E1602 is suitable for free space measurements. It has small dimensions and is of derivative kind, so that an integrator T1060 must be used in conjunction. The frequency band ranges from 150 KHz to 1.5 GHz, and the sensitivities of the system is from $\pm 1 \text{ kV/m}$ to $\pm 1 \text{ MV/m}$. The noise level is 4V_{rms}/m.

It is important to observe that the overall frequency band of the measuring chain allows very reliable measurements being assured a minimal interval between 200 KHz and 1.2 GHz. This band is sufficient to contain the 99% of the energy produced by a Nuclear Electromagnetic Pulse (NEMP).

In order to compare the results produced by the measurements and the calculation performed with the MoM-TD, some canonical configurations have been used, as for instance cubes, cylinders either closed or open with some apertures. These scattering objects have been placed at the center of the EMP simulator, where the incident EM field has a plane wave behavior. However, due to the extreme variability from pulse to pulse, the incident field should be evaluated at each measurement. A direct measure of the incident plane wave is not possible when the scattering body is placed in the test region, due to the simultaneous presence of the scattering and the incident fields. To overcome this problem a statistical analysis should be performed, *i.e.*, several measurements should be made with and without the scattering object, the final average of the results providing the measured incident and scattered field to be compared with theory. This way is cumbersome and, in some cases, not reliable. An alternative procedure is proposed here, which is based on the definition of a suitable system transfer function. In particular, a probe has been placed at the input section of the transmission line constituting the core of the open-site hardware simulator, far from the location of the scattering objects. A further probe has been located at the center of the test volume, in the absence of any scattering object. The Fourier transform of the ratio between the measurement of the second probe to the first one has been assumed to be the system transfer function. At each measurement, in the presence of the scattering object, we retain the first

probe recording the field at input stage of the hardware simulator. This signal, multiplied by the transfer function, is assumed to represent the incident field for that particular measurement. In this way, we avoid a statistical treatment of the signals. Moreover, we found that the transfer function can be considered stationary with respect to the typical evolution time of the illuminating pulse, resulting stable for some hours or even for a whole day, but strongly depending on the relative humidity of the environment.

4. NUMERICAL RESULTS

Samples of numerical results are presented in this section to show the agreement between predicted and measured results. In particular, two classes of object are considered, *i.e.*, closed metallic bodies and metallic shelters with apertures.

Let us first present the results related to closed metallic bodies. Specifically, a metallic cube 1 m on a side has been built and tested. The presence of the metallic plane in the EMP simulator has been accounted for in the simulations by doubling the dimensions of the objects with respect to the ground plane according to the image theorem. The measured and calculated current densities vs. time for the cube are shown in Fig. 1, when it is illuminated by a vertically polarized plane wave. The probe location is shown in the same figure (point A). As apparent from the results presented, the agreement between measured and computed results is very good, confirming the accuracy of both the measurements and simulations.

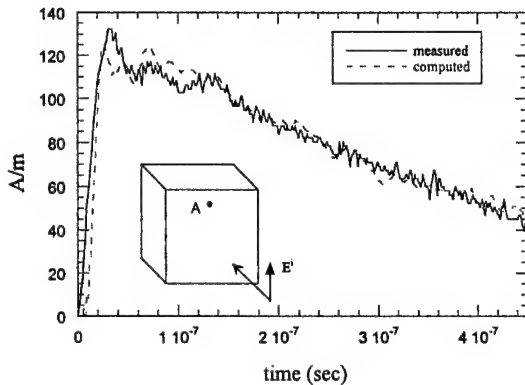


Fig. 1 – Induced current density on a PEC cube at the location A. Continuous line: measurements; dashed line: MoM-TD simulation.

The limits of applicability of the simulation scheme illustrated above have been tested by considering the presence of apertures in the scattering objects. In this case, among the various parameters which might be of interest, we quote the transmitted field inside the objects. However, it is well known that accurate results for this class of problems can be accomplished only if the magnetic equivalent currents at the aperture are

considered. This has been confirmed in our experiments performed on a cube with an aperture in one of its metallic walls. In particular, we observed that quite a good agreement exists between simulations and measurements for what concerns the near field and the external induced currents, when the aperture is not small. Nevertheless, the transmitted field inside the objects is not properly evaluated by the EFIE in time domain. This fact has been summarized in the next Fig. 2, where the radar cross section normalized with respect to the surface S of the cube, has been calculated and compared with results obtained with a MoM formulation in frequency domain, which accounts for the equivalent magnetic currents on the aperture [5]. In particular, by considering apertures of different dimensions, it is shown that the EFIE formulation provides very similar results to those obtained by the frequency domain MoM formulation with magnetic currents, when the ratio A/a approaches unity.

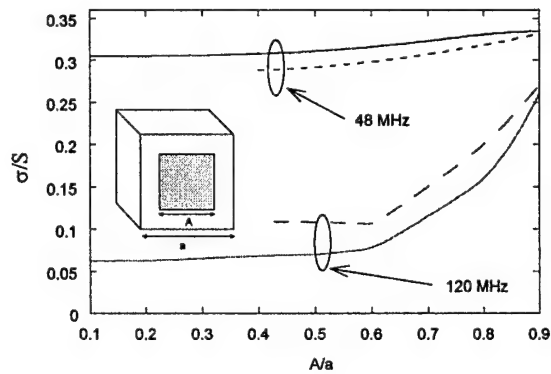


Fig. 2 – Radar cross section normalized to the side surface as a function of the aperture dimensions. Continuous line: after [5]; dashed line: MoM-TD simulation.

5. CONCLUSIONS

In this paper we addressed the problem of transient scattering from conducting objects. A set of measurements has been performed in an open-site EMP hardware simulator and compared with a corresponding set of numerical data obtained through the application of a stable formulation of the MoM in time domain. A specific measurement procedure has been adopted which allows us to avoid a statistical approach and reconstruct the actual amplitude of the electric field impinging on the scattering object. The agreement between simulated and measured data confirms the accuracy and effectiveness of both the simulation scheme and the measurement procedure. In particular, general EMC standard guidelines can be derived for the definition of stable and accurate simulation procedures in time domain. In particular, we observe that once the proposed MoM-TD simulator

has been validated with respect to a set of significant application issues, it may represent a valid alternative to measurements for verifying the compliance of specific requirements on the electromagnetic field distribution in complex environments.

6. REFERENCES

- 6.1. S. M. Rao and D. R. Wilton, "Transient scattering by conducting surfaces of arbitrary shape," *IEEE Trans. Antennas Propagat.*, vol. 39, no. 1, pp. 56-61, January 1991.
- 6.2. G. Manara, A. Monorchio and R. Reggiannini, "A Space-Time Discretization Criterion for a Stable Time-Marching Solution of the Electric Field Integral Equation," *IEEE Trans. on Antennas and Propagation*, Special Issue on Advanced Numerical Techniques in Electromagnetics, vol. 45, no. 3, pp. 527-532, March 1997.
- 6.3. S. M. Rao, D. R. Wilton, and A. W. Glisson, "Electromagnetic scattering by surfaces of arbitrary shape," *IEEE Trans. Antennas and Propagation*, Vol. 30, No. 5, pp. 409-419, May 1982.
- 6.4. D. A. Lindholm, "Automatic triangular mesh generation on surfaces of polyhedra," *IEEE Trans. Magnetics*, Vol. 19, No. 6, pp. 2539-2542, Nov. 1983.
- 6.5. T. Wang, J.R. Mautz, "Electromagnetic Scattering From And Transmission Through Arbitrary Apertures In Conducting Bodies," *IEEE Transactions on Antennas and Propagation*, vol. 38, no. 11, pp. 1805-1814, Nov. 1990.

ACKNOWLEDGMENTS

The EMP simulator is a facility of C.I.S.A.M. (Centro Interforze di Studi ed Applicazioni Militari) of the Italian Ministry of Defense, San Piero a Grado, Pisa. The authors wish to express their gratefulness to the personnel of C.I.S.A.M. for providing the measurements.

BIOGRAPHICAL NOTES

Giuliano Manara was born in Florence, Italy, on October 30, 1954. He received the Laurea (Doctor) degree in electronics engineering (*summa cum laude*) from the University of Florence, Italy, in 1979.

He was first with the Department of Electronics Engineering of the University of Florence, Italy, as a Postdoctoral Research Fellow. Then, in 1987, he joined the Department of Information Engineering of the University of Pisa, where he currently works as a Full Professor of Electromagnetic Fields. Since 1980, he has been collaborating with the Department of Electrical Engineering of the Ohio State University, Columbus, Ohio, where, in the summer and fall of 1987, he was involved in research at the ElectroScience Laboratory. His current research interests include remote sensing, electromagnetic compatibility, frequency selective surfaces (FSS), and, mainly, asymptotic and numerical techniques for the analysis of electromagnetic scattering and radiation, both in frequency and time domain.

Dr. Manara is a Senior Member of the Institute of Electrical and Electronics Engineers (IEEE).

Agostino Monorchio was born in Reggio Calabria, Italy, on March 16, 1966. He received the Laurea degree in electronics engineering and the Ph.D. degree in "methods and technologies for environmental monitoring" in 1991 and 1994, both from the University of Pisa, Italy.

During 1995, he joined the Radioastronomic Group at the Arcetri Astrophysical Observatory, Florence, Italy, as a Postdoctoral Research Fellow, working in the area of microwave systems. He is currently an Assistant Professor at the School of Engineering of the University of Pisa. During 1997 he was involved in research at the Electromagnetic Communication Laboratory of the Pennsylvania State University, State College, Pennsylvania, where he is presently an adjunct member. His research interests include numerical and asymptotic methods for applied electromagnetics, both in frequency and time domains. He has also been involved in research concerning frequency selective surfaces (FSS) and the analysis and definition of electromagnetic models of the scattering from the sea surface for remote sensing applications.

Dr. Monorchio is a Member of the Institute of Electrical and Electronics Engineers (IEEE).

APPLICATION OF CIVILIAN AND MILITARY STANDARDS TO CARRY OUT TRANSIENT ELECTROMAGNETIC FIELD MEASUREMENTS AT CISAM EMP FACILITIES

Major M. Agostinelli, Italian Army

Centro Interforze Studi per le Applicazioni Militari

56010 S. Piero a Grado, Pisa- Italy

Phone: +39. 050.964350-Fax: +39 .050.964332-E mail: massimo.agostinelli@cisam.it

ABSTRACT

The ever increasing sophistication, miniaturisation and the more recent introduction and dependence on " digital electronics ", using low power semiconductor devices and commercial off the shelf (COTS) components, raise the problem of weapon system reliability against impulsive electromagnetic stresses, generated either naturally or artificially for offensive purposes. Currently, the transients regarded as having the highest damage capability are from nuclear and lightning electromagnetic pulses (EMP).

The threats mentioned above are the same for civilian equipment and systems and the concept of protection is common. Nevertheless, there are many international, national, civilian and military standards to protect equipment or systems.

A survey of the application of civilian and military standards for transient electromagnetic field protection tests, measurements and studies, using the EMP test facilities at CISAM (Centro Interforze Studi Applicazioni Militari), is the subject of the present article along with the necessity for a unified approach to the EMP protection.

1. INTRODUCTION

CISAM is a military centre that, among other tasks, conduct studies, analyses and verifications directed towards the protection of military electronic systems against both nuclear and lightning threats; this is also true for ESD (ElectroStatic Discharge) problems.

CISAM is also involved in a NATO effort to establish a unified protection against all electromagnetic environmental effects (E3), in order to avoid:

- the lack of a central NATO focus to co-ordinate a joint E3 initiative along with E3 protection terminology, standards and test methods;
- the indiscriminate proliferation of standards;
- conflicting and redundant standards and specifications [1].

For the reasons mentioned above and in the aim of investigation in the electromagnetic field, the tests and measurements performed at CISAM EMP facilities are related not only with the check for the fulfilment of the systems EMP hardening requirement, but they are also useful to investigate the behaviour of the systems tested, in terms of susceptibility, and for studies and applications of the results in military, civilian and industrial topics.

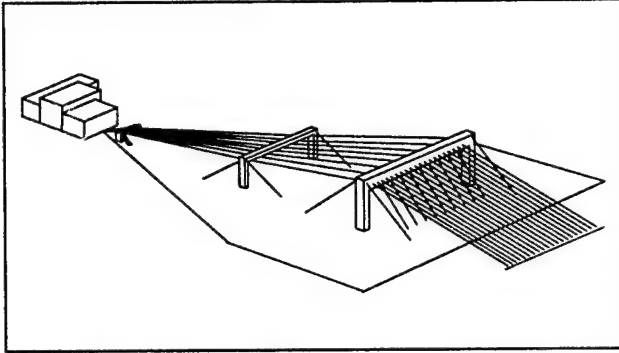
2. EMP TEST FACILITIES

The EMP test facilities available at CISAM allow development, qualification and acceptable test in accordance with some civilian and military standards. The facilities are the result of a co-operation between MOD (Military Of Defence) personnel and national and international industries.

The type and the main features of the test facilities are listed below.

EMP SIMULATOR

Name: INSIEME



Overall dimensions Working Volume dimensions

Length: 96 m	Lenght: 15 m
Width: 28 m	Width: 14 m
Height: 19 m	Height: 06 m

Description and type of the facility

A transmission line simulator (vertically polarized guided wave with conical longitudinal cross section). A high voltage pulse generator (Marx generator) is connected at one hand, a terminating resistor at the other hand.

Both the generator and the termination are matched to the impedance of the transmission line structure to avoid reflections (the impedance of the line, generator and load is 100Ω).

Technical performance data

Pulse waveshape:	double exponential
Pulse polarity:	positive or negative
Repetition capability:	1 pulse per minute
Electric field peak Value (E_p):	from 50 to 100KV/m
Rise time (10%-90% of E_p , τ_r):	≤ 5 ns
FWHM:	200 ns $\pm 10\%$
Overall duration (10% of E_p , τ_d):	600 ns $\pm 10\%$
Field polarization:	vertical

Instrumentation

Control and computing system

Personal computer Pentium
Software Femto_V3 by Thomson-CSF
Color printer
Scanner

Detection and transmission system

Melopee 1000 by Thomson-CSF:

- ⇒ free field and ground plane electric and magnetic sensors
- ⇒ current probes
- ⇒ optical data links

Acquisition system

Six digitizing oscilloscopes for simultaneous acquisition of them:

- ⇒ 2 are used for measurement channels at the Sample Rate of 1 Gs/s
- ⇒ 4 are used for measurement channels at the Sample Rate of 2 Gs/s

Measurements

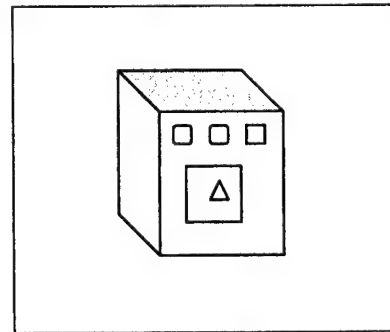
NEMP test according to the following standards:

- ⇒ AEP-4 ed. 1986
- ⇒ FINABEL 2.C.10. Chapter V, Section 53
- ⇒ MIL-STD 461C-461D

Due to the phenomenology stemming from it, the EMP range affords very limited test time.

Normally, a NEMP test doesn't go beyond one working day. However, setting up, calibration of range and instruments pertaining to the test unit, the drawing up of test and report procedures may take from 10 to 15 working days.

NEMP-LEMP INJECTION CURRENT SYSTEM



Description

The system is designed and manufactured to generate biexponential pulsed signals for lightning and/or nuclear EMP simulation in single stroke test.

It is featuring a cabinet including several plug-in drawers, each drawer corresponding to a definite type of wave.

The output level is continuously adjustable from 0 to U_{max} or to I_{max} . The output accepts any type of load: from open circuit to short circuit.

Technical performance data

Load impedances: 0 to ∞ Ohm
 Minimum lifetime: 500.000 pulses
 Triggering: Manual
 Power supply: 220V \pm 10%, 50/60Hz

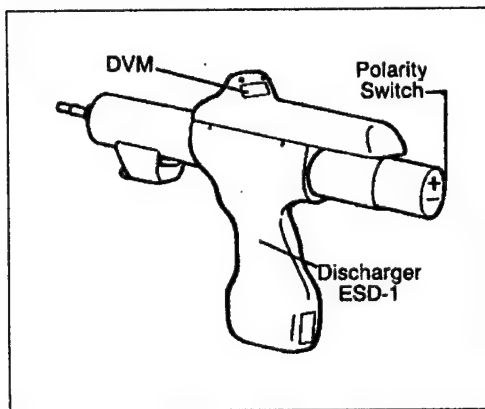
Measurements

NEMP-LEMP INJECTION CURRENT TEST
 according to the following standards:

\Rightarrow FINABEL 2.C.10, Chapter V, Section 53
 \Rightarrow EFA-EMC " Specification for equipment "
 SPE-J-000-E-1000 ed. 1991, test LEMP
 -EFA 1 and LEMP-EFA 2.

These current injection tests have variable duration:
 from 2 to 5 working days.

ESD TEST SYSTEM



The system is housed in two basic, interconnected units: the ESD-1 Discharger (or gun), which may be either hand-held or tripod mounted, and its associated Power-Supply Control Unit PSC-1.

The ESD-1 Discharger is made up of the basic handle, polarity switch, high voltage set knob and digital display. The unit PSC-1 includes selectors for repetition rate, charging rate and burst/normal modes. Interchangeable Discharge Networks, Current Injection Adapters and Tips, all plug directly into the Discharger's barrel.

Technical performance data

Voltage range: 1 to 25 KV with ball tip
 Polarity: selectable (+ or -)
 Operating mode: Single shot and Repetitive
 Repetition rates: 1 shot per 0.05, 1, 3 10 s

Measurement

ESD test according to the following standards:

\Rightarrow MIL-STD 883 C

\Rightarrow STANAG 4239

\Rightarrow IEC 801-2 (CENELEC EN 61000-4-2)

These ESD tests have variable duration: from 2 to 4 working days.

3. A SURVEY OF THE MEASUREMENTS PERFORMED

In order to test the NEMP hardening of military systems and the effectiveness of the protection devices for equipment and systems, several objects have been tested, using the NEMP simulator INSIEME, according to the standards mentioned above.

Electro explosive devices (EED), Back up Power Systems, Command, Control, Communications and Information systems (C3I) are only a set of the objects tested and the activity developed can be considered as a matter of routine.

The employment of the Simulator for studies deserves a special mention; in the framework of a joint research program with CISAM, CESI

(Centro Elettrotecnico Sperimentale Italiano) and ENEL (Ente Nazionale Energia Elettrica), based on the use of military facilities for further understanding of typical civilian-industrial topics like the generation and propagation of induced overvoltages on power lines due to lightning, a feasibility study has been developed to verify the capability of the NEMP Simulator to illuminate an entire wing span of a MV power transmission line.

The possibility to install an effective MV power transmission line in the NEMP Simulator has been successfully assessed [2].

Although the frequency spectrum of the NEMP (up to 100 MHz) is quite different from the Lightning one (up to 1 MHz in the literature), nevertheless, the higher spectrum content of the NEMP has allowed to study the coupling and the propagation phenomena of the induced overvoltages using a scale model of a power transmission line.

The NEMP-LEMP lightning injection system has been used to test the NEMP-LEMP protection of the systems by the current direct injection method.

The NEMP tests have been performed for C3I systems. The LEMP EFA -1 (slow pulse) and LEMP EFA-2 (fast pulse) tests [3,4] have been performed on an hydraulic pressure switch, installed on board the EFA 2000 (Euro Fighter Aircraft), to verify that lightning induced signals on power and signal lines will not cause degradation of performance or malfunction, for the object under test, in accordance with the specified requirements.

The shielding effectiveness of advanced composite materials (ACM) panels, made of fiber composites and used in the aircraft industry, have been investigated by means of the NEMP-LEMP injection system and the detection, transmission and data acquisition system of the NEMP simulator. The first system has been used to generate the stimulus, applied to the only face (made of fiber composites) of a metallic (aluminium) cube (dimensions 1m x 1m x 1m), in accordance with the LEMP standards mentioned above, whereas the second one, due to its high sensitivity, accuracy and miniaturisation of the sensors employed, has allowed to detect the strength of the electromagnetic field inside the cube.

The ESD effects on a device or on a system can be predicted and investigated through the use of both numerical simulation and experimental measurements. The efficiency of equipotential and grounding systems with respect to an electrostatic discharge has been investigated from an experimental point of view by carrying out measurements for the conducted interferences in metallic objects connected to ground and stroked by ESD; then, experimental measurements have been used to validate a numerical procedure made with the use of Finite-Difference in Time Domain (FDTD) algorithms.

Due to the relevance of topic, related to the health of the personnel performing ESD tests with high level discharge voltages (15, 20, 25 kV), measurements have been carried out to detect the level of the electromagnetic field, that arises from this type of test, by means the ESD test system and the detection, transmission and data acquisition system of the NEMP simulator. The results will be the topics of a next article.

4. CONCLUSIONS

Several tests, performed by means of the EMP test facilities and in accordance with a set of civilian and military standards, have been shown in this article, as

well as the efforts to unify the results, obtained for military and civilian applications, for a good comprehension of the phenomena and the best solutions of the related topics.

Due to the relevance of the subjects and the experience in the field, a further investigation will be performed in the aim of a unified protection against electromagnetic environmental effects.

5. REFERENCES

1. NATO Policy for Unified Protection against Electromagnetic Environmental Effects (E3) Enclosure to D/ND&ES/11/35, 28 January 2000.
2. C. Imposimato, M. Agostinelli, A. Longhi, L. Pandini, L. Inzoli, "A feasibility analysis to carry out measurements on effective power transmission lines illuminated by e.m. transients fields produced inside the CISAM EMP facility" (English), Proceedings of the Symposium on Electromagnetic Compatibility, San Miniato (Florence), Italy 23-25 October 1996,
3. Electromagnetic Compatibility Specifications for equipment-SPE-J-000-E- 1000, Issue 1, February 1991.
4. M. Agostinelli " Lightning Test Standards for military and civilian Applications. " Conference on Electromagnetic Compatibility, Florence 10 November 1995.

BIOGRAPHICAL NOTES

Major Massimo Agostinelli received his degree in Electronic Engineering from the University of Ancona, Italy. In 1988 he began work at Centro Tecnico Militare delle Trasmissioni in Rome, as Head of the Radio Section, and there he gained experience in the field of Electronic Counter-Counter Measures (ECCM) for radio systems and was involved in the test of the C3I CATRIN System.

From 1993 he is in charge of the EMP Section at CISAM and he is also the national delegate of the AC/225 NAAG (NATO Army Armament Group)-Land Group 7 (LG7)-Nuclear Protection Sub-Group (NPSG).

ALTERNATIVE METHODS FOR RADIATED EMISSION MEASUREMENTS

Daniel J. Bem, Zbigniew M. Jóskiewicz, Tadeusz W. Więckowski

Wrocław University of Technology
Institute of Telecommunication and Acoustics
Wybrzeże Wyspiańskiego 27, 50-370 Wrocław, POLAND
Phone: +48 71 3214998, Fax: +48 71 3223473

The paper herein presents alternative methods for radiated emission measurements for various devices. Several of the various measurement methods have been reviewed paying special attention to the measurement setups using loop antennas. A method for expanding the measurement functionality of the test setup for higher frequencies has also been shown.

1. INTRODUCTION

The effectiveness and reliability of telecommunication systems is nowadays a decisive factor for the functioning and development of the national economy. This to a large extent depends on the immunity to electromagnetic fields (both continuous and impulse-type) as well as the level of interference present within the telecommunication or IT systems environment. The problems related to establishing the level of interference radiated by the devices, systems and installations is important not only for electromagnetic compatibility, but also because of the frequent need to maintain a certain secrecy of the transmitted or processed information. There are devices available today that allow for such data to be retrieved based on spurious radiated electromagnetic fields. This is the main reason why highly developed countries pay so much attention to emission research. The emission requirements are nowadays considered as basic parameters, like the mechanical and environmental requirements for various devices - especially in the field of telecommunications and IT.

The measurement of the radiated interference boils down to defining the strength of the electromagnetic field in the direction of maximum radiation. Most of the standards recommend the Open Area Test Site (OATS) measurements or the use of a semi-anechoic chamber. The availability of OATS is somewhat limited considering the environmental conditions and the level of naturally occurring electromagnetic interference. This inconvenience can be alleviated using measurements in the semi-anechoic chamber. However,

the costs of building such a chamber of adequate size are very high. Taking this into account, within the last ten years there has been an evident heightened interest in alternative radiated emission measurement methods.

The alternative methods rely on measuring the parameters of the interference generating sources instead of measuring the strength of actual radiated electromagnetic field. Of course, the measurement of these parameters is not simple. For certain types of objects, especially small ones in comparison to the wavelength of the radiated field, this is however currently not a problem. There are several known alternative methods for measurements of radiated electromagnetic fields: a method using three frame antennas [10][12], a method using the TEM cell [2], and a method using the GTEM cell [4]. First we will pay special attention to the method using three frame antennas.

Based on the works of Ma, Koepke, Hansen and Wilson it is clearly evident that the source of interference (the device under test - DUT) can be simulated by equivalent dipoles: an electric one with the moment (\vec{p}), a magnetic one with the moment (\vec{m}) and a quadrupole with the moment (\vec{q}).

If the dimensions of the DUT are less than the minimum wavelength of the radiated electromagnetic field, then in order to properly determine the value of the vector potential characterising the radiating object, it is necessary to consider the moments of the equivalent dipoles: the electric and magnetic ones [2][4]. Thus:

$$\vec{A}(\vec{r}) \approx \frac{\mu_0}{4\pi} \cdot \frac{e^{-jk_0 r}}{r} [\vec{p} - jk_0 \vec{r} \times \vec{m}] = \frac{\mu_0}{4\pi} [\vec{A}_p(\vec{r}) - jk_0 \vec{A}_m(\vec{r})] \quad (1)$$

The total vector potential at the observation point caused by the radiation from the tested object consists of the superposition of the vector potential from the equivalent electric dipole

$$\vec{A}_p(\vec{r}) = \frac{e^{-jk_0 r}}{r} \vec{p} \quad (2)$$

and the equivalent magnetic dipole

$$\bar{A}_m(\bar{r}) = \frac{e^{-jk_0 r}}{r} \bar{I}_r \times \bar{m} \quad (3)$$

Knowing the moments of the equivalent electric and magnetic dipoles, it is possible to calculate the field radiated by the DUT equivalent to open area test site conditions. This case is relative to when the device under test is placed above a conductive surface, thus the radiated field is not just the superposition of the equivalent electric and magnetic dipoles, but also of their mirror reflections [4]. The electric field strength is described by following relation:

$$\bar{E}(\bar{r}) = -j \frac{k_0 \zeta_0}{4\pi} \left[\frac{e^{-jk_0 r_1}}{r_1} \bar{F}_p(\bar{r}_1, \bar{p}) + \frac{e^{-jk_0 r_2}}{r_2} \bar{F}_p(\bar{r}_2, \bar{p}') + \right. \\ \left. jk_0 \left[\frac{e^{-jk_0 r_1}}{r_1} \bar{F}_m(\bar{r}_1, \bar{m}) + \frac{e^{-jk_0 r_2}}{r_2} \bar{F}_m(\bar{r}_2, \bar{m}') \right] \right] \quad (4)$$

where:

$$\bar{F}_p(\bar{r}, \bar{p}) = \left[\bar{I}_x \left[p_x \left(\frac{x^2 z^2}{\rho^2 r^2} + \frac{y^2}{\rho^2} \right) - p_y \frac{xy}{r^2} - p_z \frac{xz}{r^2} \right] + \right. \\ \left. + \bar{I}_y \left[-p_x \frac{xy}{r^2} + p_y \left(\frac{y^2 z^2}{\rho^2 r^2} + \frac{x^2}{\rho^2} \right) - p_z \frac{yz}{r^2} \right] + \right. \\ \left. + \bar{I}_z \left[-p_x \frac{xz}{r^2} - p_y \frac{yz}{\rho^2} + p_z \left(\frac{\rho^2}{r^2} \right) \right] \right] \quad (5)$$

$$\bar{F}_m(\bar{r}, \bar{m}) = \left[\bar{I}_x \left[m_y \frac{z}{r} - m_z \frac{y}{r} \right] + \right. \\ \left. + \bar{I}_y \left[-m_x \frac{z}{r} + m_z \frac{x}{r} \right] + \right. \\ \left. + \bar{I}_z \left[m_x \frac{y}{r} - m_y \frac{x}{r} \right] \right] \quad (6)$$

in which r_1 is the distance of the observation point to the device under test

$$r_1 = \sqrt{r^2 + (z-h)^2} \quad (7)$$

and where r_2 is the distance of the observation point to the mirror reflection of the DUT

$$r_2 = \sqrt{r^2 + (z+h)^2} \quad (8)$$

We would like to remind that the mirror reflection of the equivalent electric dipole with the moment (\bar{p}) having the components (p_x, p_y, p_z) is a dipole with a moment (\bar{p}') having the components ($-p_x, -p_y, p_z$). On the other hand the mirror reflection of the equivalent magnetic dipole with the moment (\bar{m}) with the components (m_x, m_y, m_z) is a dipole with a moment (\bar{m}') with the components ($m_x, m_y, -m_z$).

2. MEASUREMENTS METHODS

2.1. THE TEM CELL METHOD

The first alternative electromagnetic field radiation measurement method has been elaborated for the Craford type TEM cell (fig. 1). The main part of this setup is the TEM cell - being a rectangular section of a

transmission line with matching transformers at both ends for matching the wave impedance of the line to the load impedance. The internal conductor - septum - is a wide metal plate allowing for a homogenous electric field to be achieved within the working volume, that is where the device under test is placed.

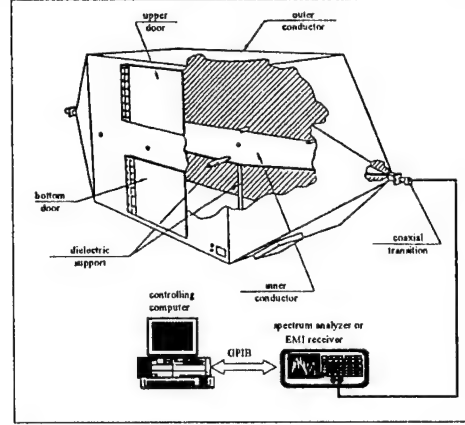


Fig. 1. Radiated emission test set-up using a TEM cell

As one can see, this cell forms is a broadband converter with a linear amplitude/phase characteristic, converting electromagnetic fields into radio-frequency voltages or vice-versa. The key advantage of this cell is the total isolation of the tested object from external electromagnetic fields. It has to be considered however, that placing any tested object inside the TEM cell changes the parameters of the cell as well as of the tested device itself. Wilson and Change have theoretically resolved this problem [1] for a rectangular coaxial line. There have also been many experimental tests for various types of antenna inside a TEM cell. In the publication [2] of Sreenivasiah, Chang, Koepke and Ma, they presented a method of replacing an electrically small object inside the cell with a system of three orthogonal magnetic dipole moments and three orthogonal electric dipole moments. The parameters of these dipoles (amplitudes and phases) are calculated based on the power measurements at both ports of the cell, for six positions of the DUT within the working volume of the TEM cell (fig. 2).

During the measurements the DUT is placed inside the TEM cell, with its centre being at the point of the centre of the working volume of the cell and having its (x') axis parallel to the (x) axis of the cell, the (y') axis in line with the (y) axis of the cell and the (z') axis in line with the (z) axis of the cell. The first two positions of the tested object are achieved by rotating it around an axis parallel to the (z) axis of the cell and going through the centre of the DUT at angles of $\pi/4$ and $3\pi/4$. For both of these positions a measurement is made of the voltage sums and differences occurring at the matched loads. By analogy the measurements for the next orthogonal positions of the tested object are made. It is very important to keep the centre of the tested object in one fixed point throughout the tests.

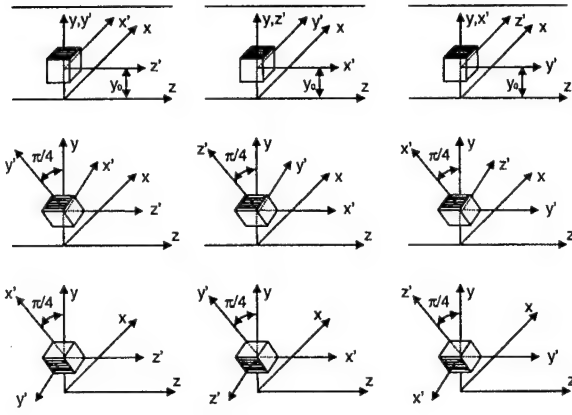


Fig. 2. DUT's positions in the working volume of a TEM cell

Based on the measured values of the sums and differences at the input and output of the cell we can determine the amplitude and phase of the electric dipole moments:

$$p_x^2 = (P_{s1} + P_{s2} - P_{s3} - P_{s4} + P_{s5} + P_{s6}) / (2s^2), \quad (9)$$

$$p_y^2 = (P_{s1} + P_{s2} + P_{s3} + P_{s4} - P_{s5} - P_{s6}) / (2s^2), \quad (10)$$

$$p_z^2 = (-P_{s1} - P_{s2} + P_{s3} + P_{s4} + P_{s5} + P_{s6}) / (2s^2), \quad (11)$$

$$\cos(\phi_{px} - \phi_{py}) = (P_{s1} - P_{s2}) / (2s^2 p_x p_y), \quad (12)$$

$$\cos(\phi_{py} - \phi_{pz}) = (P_{s3} - P_{s4}) / (2s^2 p_y p_z), \quad (13)$$

$$\cos(\phi_{pz} - \phi_{px}) = (P_{s5} - P_{s6}) / (2s^2 p_z p_x), \quad (14)$$

as well as the magnetic ones:

$$m_x^2 = (P_{d1} + P_{d2} - P_{d3} - P_{d4} + P_{d5} + P_{d6}) / (2k^2 s^2), \quad (15)$$

$$m_y^2 = (P_{d1} + P_{d2} + P_{d3} + P_{d4} - P_{d5} - P_{d6}) / (2k^2 s^2), \quad (16)$$

$$m_z^2 = (-P_{d1} - P_{d2} + P_{d3} - P_{d4} + P_{d5} + P_{d6}) / (2k^2 s^2), \quad (17)$$

$$\cos(\phi_{mx} - \phi_{my}) = (P_{d1} - P_{d2}) / (2s^2 m_x m_y), \quad (18)$$

$$\cos(\phi_{my} - \phi_{mz}) = (P_{d3} - P_{d4}) / (2s^2 m_y m_z), \quad (19)$$

$$\cos(\phi_{mz} - \phi_{mx}) = (P_{d5} - P_{d6}) / (2s^2 m_z m_x). \quad (20)$$

The P_{si} and P_{di} (where $i = 1..6$) presented in the shown relations are the appropriate sums and differences of the measured power of signals for the six positions of the tested object within the working measurement volume of the cell. On the other hand (s) is the value of the electric field strength at the point of the DUT, equivalent to a cell input signal of 1 W. The value of normalising field strength can be elaborated through measurements or through a numerical simulation taking into account the following condition:

$$\iint_S \vec{E}_{Tn} \times \vec{H}_{Tm} \cdot \vec{T}_z dS = \delta_{nm}, \quad (21)$$

where: S is the cross-section of the cell, and where δ_{nm} is the Kronecker delta:

$$\delta_{nm} = \begin{cases} 0 [W], & \text{when } m \neq n, \\ 1 [W], & \text{when } m = n. \end{cases} \quad (22)$$

In order to verify the elaborated theory, an electrically

small frame antenna has been placed in the TEM cell. The magnetic dipole moment has been calculated theoretically and based on the measurements conducted in the TEM cell. The accuracy of the obtained results was 3%. A detailed analysis of the measurement errors has been presented by Ma [3].

There is a technical inconvenience to applying the TEM cell because of limitations for higher measurement frequencies. This limitation arises to the limited cross-width of the cell. A TEM cell for 1 GHz has a very small measurement area (<7.5 cm), thus only very small devices can be tested. It has been proposed that in order to increase the cells operating frequency above the borderline values it should be partially filled with an absorbent material. This cannot be done, as one of the presumptions made for the purpose of calculations would become invalid: i.e. the chamber surface integral will not be zero. It will also be impossible to work out a relation tying the cell input signal power with the source parameters of the device under test – the electric and magnetic dipole moments.

2.2. THE GTEM CELL METHOD

Considering the above-mentioned limitations of the TEM cell, a GTEM cell (fig. 3) is used for emission measurements of electrically small devices. The GTEM cell allows the use of alternative measurement methods for a much wider frequency range than the TEM cell. It is also an entirely shielded structure conducting a TEM wave between two conductors, thus it does not radiate an external field and it is not influenced by external interference. The input module is an exchangeable module, thus not only an EMI receiver, spectrum analyser or a signal generator can be connected to it, but a high voltage pulse generator as well. Considering this, the GTEM cell can be used for both emission tests as well as for the susceptibility of the devices to continuous and pulse electromagnetic fields. The broadband frequency measurements are possible due to a special construction of the cell's load. For low frequencies, the cell's load consists of distributed resistance loads, whilst for higher frequencies there are special graphite absorbers placed at the back wall of the cell, which absorb the electromagnetic energy.

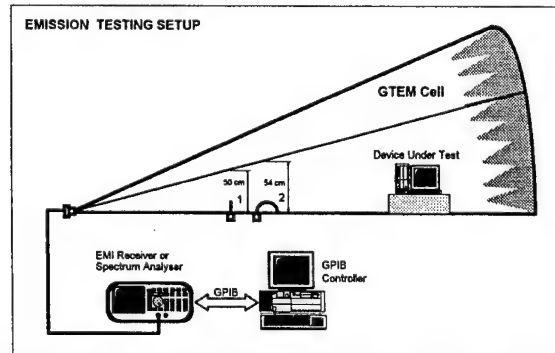


Fig. 3. Example of the emission testing set-up equipped with a GTEM cell

Similar to the TEM cell, an alternative method of elaborating the emissions of electronic and electrical devices has been prepared for the GTEM cell, based on the determined parameters of the radiation source. The substitute model determined through measurements consists of three orthogonal electric dipoles, three orthogonal magnetic dipoles and a quadrupole. Because of the construction of the GTEM cell, an additional simplification presumption has to be made as opposed to the TEM cell. The difference is that the GTEM cell has one input only, thus it is not possible to determine the phase difference between the dipoles. It has been presumed thus that the phase of all dipole moments is zero.

The proposed method [4][5] allows for the equivalent electric and magnetic dipole moments to be determined for the DUT based on power measurements at the input of the GTEM cell for twelve different positions of the device under test in the cell's working volume. The placement of the DUT within the working volume has been chosen appropriately, such that each component of the dipole moment is strongly coupled to the vertical component of the electric field and the horizontal component of the magnetic field in the GTEM cell. The above is achieved for three orthogonal placements of the tested object within the cell's working volume (placements: xx' , xy' , xz' - fig. 4). For each of these placements the tested object has to be additionally rotated around its vertical axis by an angle of $\pi/4$, $\pi/2$ and $3\pi/4$.

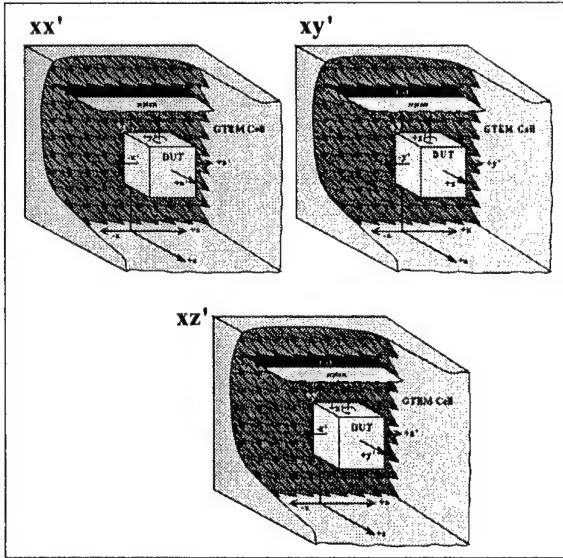


Fig. 4. Basic DUT positions in the working volume of a GTEM cell

Based on the voltage measurements at the input of the GTEM cell the magnetic dipole moment components can be determined [4]:

$$m_x^2 = \frac{M_{3xx'} M_{3yy'}}{k_0^2 M_{3xx'}}, \quad (23)$$

$$m_y^2 = \frac{M_{3yy'} M_{3xz'}}{k_0^2 M_{3xx'}}, \quad (24)$$

$$m_z^2 = \frac{M_{3xz'} M_{3yy'}}{k_0^2 M_{3xx'}}, \quad (25)$$

as well as the electric dipole moment:

$$p_x = M_{1xx'} - k_0^2 m_x^2 = M_{2xx'} - k_0^2 m_y^2, \quad (26)$$

$$p_y = M_{1xx'} - k_0^2 m_x^2 = M_{2xx'} - k_0^2 m_z^2, \quad (27)$$

$$p_z = M_{1yy'} - k_0^2 m_y^2 = M_{2yy'} - k_0^2 m_z^2. \quad (28)$$

The M variables are proportional to the modules of normalising power measured at the input of the GTEM cell for the predetermined positions of the device under test. For the xx' placement (the x' axis of the device under test is parallel to the x axis of the GTEM cell) we have the following [4]:

$$M_{1xx'} = |\tilde{P}(0)|_{xx'}, \quad (29)$$

$$M_{2xx'} = |\tilde{P}(\pi/2)|_{xx'}, \quad (30)$$

$$M_{3xx'} = \frac{1}{2} \left[|\tilde{P}(\pi/4)|_{xx'} - |\tilde{P}(3\pi/4)|_{xx'} \right]. \quad (31)$$

Additional methods have also been elaborated, in order to allow the determination of the equivalent dipole moments based on measurements from nine [6] and seven [7] positions of the device under test in the working volume of the GTEM cell.

In many practical applications, the knowledge of the full radiation characteristics is not necessary. For precompliance emission tests the most crucial information is the total power radiated by the device under test, based on which it is possible to calculate the maximum component of strengths (horizontal and vertical) of the electric field for any point surrounding the DUT. For this case, we assume a half-wave dipole radiating the same power as an equivalent model of the device under test. The following relation describes the total power radiated by the DUT:

$$P_c = 10k_0^2 [M_{1xx'} + M_{1yy'} + M_{1zz'}]. \quad (32)$$

The electric field strength calculations can be conducted for both models in free space as well as ones above a conductive plane. In order to determine the total power radiated by the device under test, it is necessary to measure the voltage at the GTEM cell input for just three basic positions of the DUT within the cell (fig. 4). The relations necessary to perform these calculations can be found for example in [8].

If the electric field strengths calculated using this method in reference to an open area test site (OATS) are below the allowable levels, it can be stated that the device complies with the relevant standards. However, if the calculated values are above the values stated in the standards, then the measurements shall be repeated for all twelve positions of the DUT within the working volume. Only after this it will be possible to state if the DUT conforms to the requirements.

The literature presents numerous examples verifying the

presented methods, proving a high consistence of the obtained results to the measurements at the OATS. The authors of this paper have also conducted such a verification using a spherical radiation source KSQ manufactured by MEB Schaffner Berlin as the device under test, having the dimensions of 11cm x 11 cm x 11 cm. Calculated values of electric field strength for 3 and 12 positions in a GTEM and measured in an OATS has been presented in figure 5.

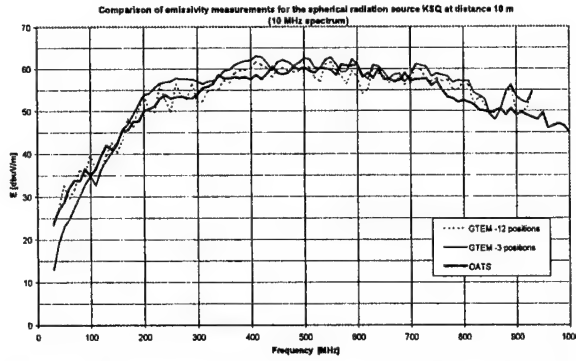


Fig. 5. Comparison of the measured electric field strength (for a spherical radiation source KSQ) obtained using a GTEM-aided setup and in an OATS

2.3. THE THREE LOOP ANTENNAS METHOD

A setup with an array of three double-loaded loop antennas arranged orthogonally to each other (fig. 6) also allows the equivalent electric and magnetic dipole moments to be determined based on the current flows of the antenna loads. The first concept for such a system has been presented in [9], which has been further evolved by Kanda [10][11] and the authors of this paper [12].

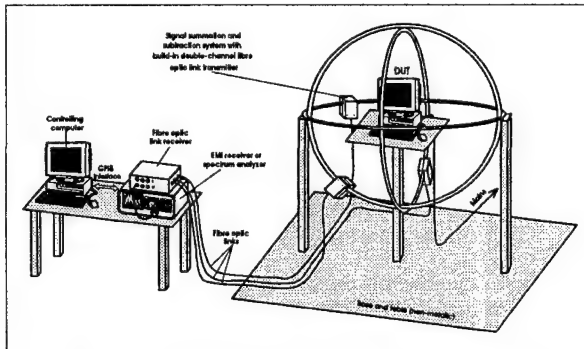


Fig. 6. Example of a set-up using an array of three double-loaded loop antennas arranged orthogonally to each other to enable alternative measurement of the radiated electromagnetic field

A theoretical analysis has shown, that for an electrically small device placed in the centre of this setup, the sum of the currents ($I_s = I(0) + I(\pi)$), flowing through the loads of each antenna, depends only on the magnetic dipole moment normal component (perpendicular) to the

surface of this antenna. On the other hand, the current difference ($I_d = I(0) - I(\pi)$), flowing through the loads of each of the antennas, depends on the electric dipole moment component tangent to the antenna surface and perpendicular to the line between its loads.

Knowing the sums and differences of the currents flowing through the loads of each of the antennas it is possible to determine the values of the equivalent dipole moments. For an antenna placed in the XY plane, the appropriate relations published by Kanda in [10] are as follows:

$$m_z = \frac{I_s [1 + 2Y_0 Z_L]}{4\pi b g_m Y_0} = I_s \cdot F_m, \quad (33)$$

$$p_y = \frac{I_d [1 + 2Y_1 Z_L]}{4\pi b g_e Y_1} = I_d \cdot F_e. \quad (34)$$

where: Y_0 and Y_1 is the respective admittance for the magnetic and electric fields, Z_L is the resistance value of the load, and g_e and g_m are the electric field components tangent to the surface of the loop antenna:

$$g_m = \frac{k^2 \cdot \zeta_0}{4\pi} \cdot \left[1 - \frac{j}{k \cdot b} \right] \cdot \frac{e^{-jkb}}{b}, \quad (35)$$

$$g_e = -\frac{j \cdot k \cdot \zeta_0}{4\pi} \cdot \left[1 - \frac{j}{k \cdot b} - \frac{1}{(k \cdot b)^2} \right] \cdot \frac{e^{-jkb}}{b}. \quad (36)$$

The presumption made for these relations, limiting the number of $a(n)$ coefficients depending on the admittance of the antennas, limits the applicability of this method to a frequency range of just a few tenths MHz. The above mentioned limitation causes discrepancies between the theoretical calculations and actual measurement results. This has been confirmed by test results presented by Kanda in 1999 during the EMC Symposium [13].

The article [12] has also shown that when determining the transition function tying the sums and differences of current to the appropriate dipole moments, the number of $a(n)$ coefficients shall not be limited in the relations describing the admittance Y_0 and Y_1 . The minimal number of these coefficients depends on the radius of the loop antenna and the frequency range:

$$n > k \cdot b. \quad (37)$$

Taking into account the above facts, the relations look as follows [12]:

$$m_z = \frac{j \cdot \pi \cdot \zeta \cdot a(0) \cdot I_s \cdot (1 + 2 \cdot Y_0 \cdot Z_L)}{4 \cdot \pi \cdot b \cdot g_m} = I_s \cdot F_m, \quad (38)$$

$$p_y = \frac{j \cdot \pi \cdot \zeta \cdot a(1) \cdot I_d \cdot (1 + 2 \cdot Y_1 \cdot Z_L)}{4 \cdot \pi \cdot b \cdot g_e} = I_d \cdot F_e, \quad (39)$$

where:

$$Y_0 = \frac{1}{j\pi\zeta} \left[\frac{1}{a(0)} + 2 \cdot \sum_{n=1}^{\infty} \frac{1}{a(2n)} \right], \quad (40)$$

$$Y_1 = \frac{2}{j\pi\zeta} \left[\sum_{n=1}^{\infty} \frac{1}{a(2n-1)} \right]. \quad (41)$$

In order to prove that these relations are true for higher frequencies, the transfer functions F_e and F_m have been

calculated numerically (using the moment method - the NEC program) for a few double loaded loop antenna models. The results of the above calculations have been compared to the values calculated based on the relations (38) and (39). A transfer function has also been established for the Y_0 and Y_1 admittance, determined only based on the $a(0)$ and $a(1)$ coefficients (the Kanda assumption). A sample comparison of the results for 1 m and 2 m radius loop (the conductor radius $a=0.0075$ m. and load impedance $Z_L=100\Omega$) antennas have been presented in figures from 7 to 10.

Using a test setup with three double-loaded loop antennas allows for the elimination of the basic inconveniences present during the measurements in a TEM or GTEM cell. The propagation conditions are similar to the free space. As for the influence of the loop antennas onto the device under test and the device onto the parameters of the antennas, these can be omitted if the antennas are of sufficient diameter.

The key advantage of this method is that the equivalent dipole moments can be determined without having to change the placement of the DUT. This is especially important for devices powered from mains. Each change of placement of the device causes also the change in the placement of the power supply cables, thus changing the parameters of the field source. It is not possible to obtain an accurate value for the electric and magnetic dipole moment components. This test setup does not provide a significant isolation from external electromagnetic interference as with the using TEM cell or the GTEM cell. Placing the loop antenna setup in a fully anechoic chamber can alleviate this inconvenience.

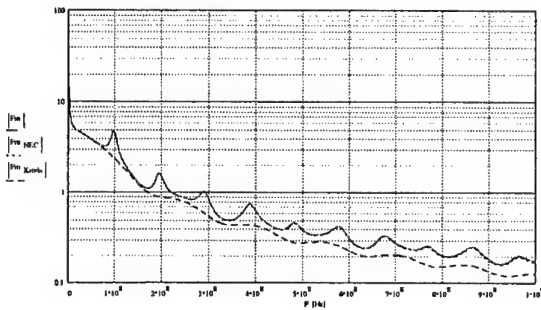


Fig. 7. Comparison of the calculated modules of function F_m in the frequency domain ($b=1$ m.)

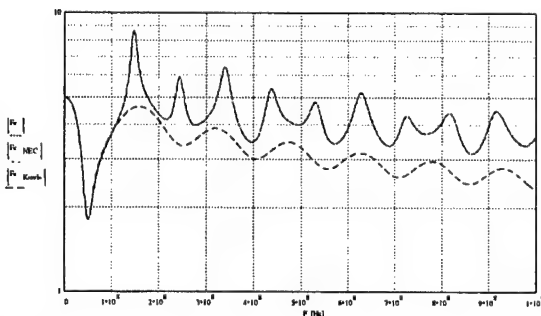


Fig. 8. Comparison of the calculated modules of function F_e in the frequency domain ($b=1$ m.)

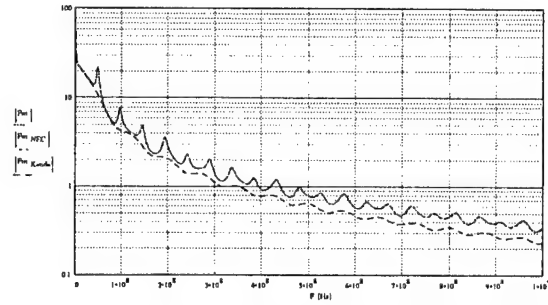


Fig. 9. Comparison of the calculated modules of function F_m in the frequency domain ($b=2$ m.)

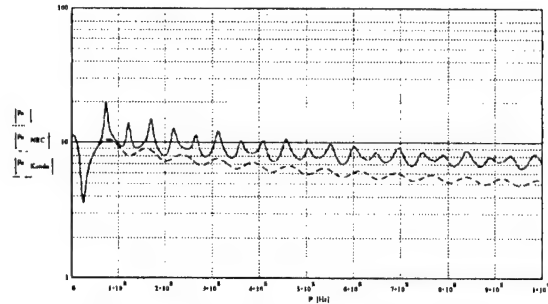


Fig. 10. Comparison of the calculated modules of function F_e in the frequency domain ($b=2$ m.)

3. SUMMARY

Within the last years various alternative emission test methods for electric and electronics devices are becoming more popular. One of the unquestionable advantages is the ability to determine the emission of the device under test in any environment based on the elaborated equivalent radiation model (without the need of additional measurements). The other advantages are the relative low costs of building and using such setups as compared to an open area test site, as well as a shortened test cycle.

The TEM and GTEM cell setups as well as the three orthogonal double-loaded loop antenna setup can be used for precoppliance evaluation of device emissions. However, one has to note that even though these alternative emission measurement methods have many advantages, they cannot be used for measurements of all device emissions as opposed to an open area test site. The basic limitation relates to the geometrical size of the tested device. The TEM and GTEM cells cannot be used for testing devices, which must remain stationary during use. Considering the above, EMC laboratories should be also equipped with standard measurement setups as described by the relevant standards.

The Institute of Telecommunication and Acoustics of the Wrocław University of Technology has been conducting research related to device emission measurement methods including alternative methods for many years. Most of these works has been financed from the national Science Research Committee (Pol. "Komitet Badań Naukowych").

4. REFERENCES

- [1] P.F. Wilson, D.C. Chang, "Probe Excitation of a Rectangular Coaxial Transmission Line", 1981 IEEE International Symposium on EMC, Boulder, Colorado, August 1981, pp. 495-498.
- [2] H. Koepke, M. T. Ma, "A New Method for Determining the Emission Characteristics of Unknown Interference Source", Proc. of the 5th Symposium and Exhibition on EMC, Zurich, March 1983, pp.35-40.
- [3] M.T. Ma, "Error Analysis of Radiation Characteristics of an Unknown Interference Source Based on Power Measurements", Proc. of the International Symposium on EMC, Tokyo 1984, pp. 39-44.
- [4] P. Wilson, D. Hansen, D. Hoitink, "Emission Measurements in a GTEM Cell: Simulating Free Space and Ground Screen Radiation of a Test Device", Research Report, Baden, June 1988.
- [5] P. Wilson, D. Hansen, D. Koenigstein, "Simulating Open Area Test Site Emission Measurements Based on Data Obtained in a Novel Broadband TEM Cell", International IEEE Symposium on EMC, Denver, 1989, pp. 171-177.
- [6] S. Berger, "A Variable Position, Gravity Down G-TEM Configuration", Proc. of the International Symposium on EMC, Zurich, March 1995.
- [7] L. Carbonini, "A New Procedure for Evaluating Radiated Emissions from Wideband TEM Cell Measurements", Proc. of the International Conference on Electromagnetic in Advanced Application, Turin, Italy, Sept. 1995, pp. 133-136.
- [8] A. Nothofer, A.C. Marvin, T. Konefal, "Radiated Emission measurements in GTEM Cells Compared with Those of an OATS", Proc. of the 12th International Symposium on EMC, Zurich, 1997, pp. 317-320.
- [9] T. W. Wieckowski, "Loop antennas in electromagnetic field metrology", Scientific Papers of the Institute of Telecommunication and Acoustics of the Technical University of Wrocław, No. 34, Wrocław 1992.
- [10] M. Kanda, D. A. Hill, "New Emission Measurement Method for an Electrically Small Source: a Three Loop Method and TEM Cell Method", Proc. of the 11th Symposium on EMC, Wrocław, June 1992, pp. 310-312.
- [11] M. Kanda, D. A. Hill, "A Three Loop Method for Determining of an Electrically Small Source", IEEE Transactions on EMC, Vol. 34, No. 1, August 1994, pp. 1-3.

- [12] T.W. Wieckowski, Z.M. Jóskiewicz, "Loop antennas in the EMC metrology", Proc. of the 14th Symposium on EMC, Wrocław, June 1998, pp. 242-246.
- [13] M. Kanda: *An Optically Linked Three-Loop Antenna System for Determining the Near Field Characteristics from an Electrically Small Source*, Supplement of Proc. of the 13th International Symposium on EMC, Zurich, 1999, pp. 155-160.

5. BIOGRAPHICAL NOTES

Daniel J. Bem received the Ingenieur degree in radiocommunication from Wrocław University of Technology (Poland) in 1953, The M.Sc., Ph.D. and D.Sc. degrees in 1957, 1956 and 1975, respectively. From 1966 to 1967 he was associated with the Electrical Engineering Department at the University of Birmingham as a Graduate Research Associate. Since 1953 he had been employed at the Wrocław University of Technology where at present he is Professor of Telecommunications and holds the Chair of Radiocommunications.

His research has concerned on satellite communications, radiocommunications and electromagnetic compatibility. He has 10 books, 7 monographs, 5 textbooks, 198 papers presented on international and national conferences. Since 1986 he has been the Chairman of the Wrocław International Symposia on EMC.

Zbigniew M. Joskiewicz received his MSc degree in telecommunications in 1994 from the Wrocław University of Technology (Poland). Since 1994 he has been working as an Assistant Professor at the Institute of Telecommunication and Acoustics of the Wrocław University of Technology. His field of work is electromagnetic compatibility and radiocommunication systems. He is an author of some 8 papers presented on international and national conferences.

Tadeusz W. Wieckowski is with the Institute of Telecommunication and Acoustics of the Wrocław University of Technology (Poland), where he works as a Professor in the field of communications systems and electromagnetic compatibility. He received his MSc and Ph.D. degrees in telecommunication in 1976 and 1980, respectively. He is a member of the Association of Polish Electrical Engineers and the Organising Committee of the Wrocław Symposia. Mr. Wieckowski is an author of some 120 papers presented on international and national conferences.

APPLICATIONS OF NATO STANDARDS FOR EVALUATING BULKHEAD SHIELDING IN THE OPERATIONAL ROOMS ON BOARD OF SHIPS

Giancarlo Misuri

Vinicio Procacci

Institute for Telecommunications and Electronics "Giancarlo Vallauri" (Mariteleradar)

Viale Italia, 72 – 57100 Livorno Italy

Fax 0586 238205 (e-mail: telerada@tin.it)

ABSTRACT

This paper presents the methodology of performing the shielding effectiveness measurements of operational rooms on board of Italian Navy ships, according to STANAG 4557 "EM Shielding: Methods of standard attenuation measurements for naval enclosures". After a description of the measurement system and methods, the results of some measurements carried out in the radio room of an Italian military ship are shown. The applicability of the adopted methodology is limited to the frequency band 10 KHz – 1 GHz for electric field attenuation measurement, and 10 KHz – 30 MHz for magnetic field attenuation measurement. At the end, the applicability of the aforesaid methodology in the civil context is briefly analysed.

1. INTRODUCTION

The measurement of shipboard operational rooms shielding effectiveness is an important test for the Italian Navy in order to verify the level of security of the transmissions and to ensure the correct functioning of the equipments that shall operate in the operational rooms.

2. MEASUREMENT SYSTEM

On board it is necessary to measure the behaviour of shielded enclosure including doors, penetrations, equipments, ducting, etc. In the real condition attenuation measurements shall be given by the difference between field strengths induced in receiving antenna (and produced by transmitting antenna) during calibration measurements and during shipboard measurements. The instrument of the measurement system shall be tested and calibrated before executing the measure.

The measurement system employed to perform the measurements is schematically illustrated in Fig. 1. STANAG 4557 determines the following measurement system instrumentation. Signal source may be either a signal generator or a power oscillator with CW (or modulated output) and with enough power to endow the whole system with an adequate measurement range.

The detector may be any receiver or field strength meter with sufficient sensitivity such that its dynamic range is greater than the maximum attenuation required to be measured.

Antennas to be employed over the different frequency bands are:

- for magnetic field attenuation measurement: "loop antenna for frequency range from 10 KHz to 30 MHz;
- for electric field attenuation measurement:
 - Frequency range from 10 kHz to 30 MHz: electric field source provided with rod receiving antennas;
 - Frequency range from 30 MHz to 200 MHz : Biconical antenna
 - Frequency range 200 MHz to 1 GHz : Tuned dipole antenna.

In particular, for the measurements performed in the radio room of a military ship, the following instrumentation has been used:

- A signal generator Rohde & Schwarz SMGL, operating in the frequency range 10 KHz – 1 GHz;
- A spectrum analyzer HP8593A, operating in the frequency range 3 KHz – 22 GHz;
- an active EATON pair TX and RX 96020 for magnetic field attenuation measurement and the following antennas for electric field attenuation measurement:
 - a TX EATON antenna N° 3303 and RX EATON N° 3301B (10 kHz to 30 MHz);
 - a tuned dipole antenna EATON DM-105A-T1 (30 MHz to 200 MHz);
 - EATON DM-105A-T2 antenna up to 400 MHz and EATON DM-105A-T3 beyond 400 MHz (200 MHz to 1 GHz).

3. METHODS OF MEASUREMENTS

The following measurements methodology has been extracted from STANAG 4557.

During measurements, in order to reduce the possibility of electromagnetic influence between human body and antennas, only the test personnel is allowed to access the location and the operational enclosure cannot be used.

The room under test must be clear of all extension cables and non permanent equipments. Cables normally connected inside the space should be terminated to permanently mounted equipment. This will prevent parasitic reradiations within the shielded room. No electrical or electronic equipment should be running in the enclosure while the measurement is taken place. According to STANAG 4557, the attenuation assessment consists of the following phases.

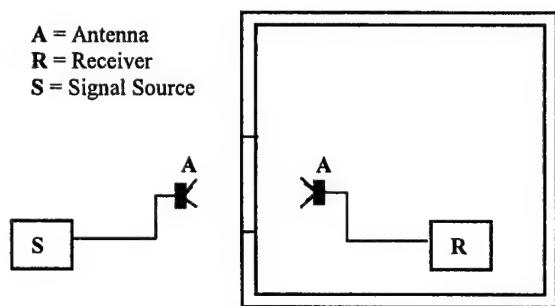


Fig. 1: Measurement system scheme

3.1 Arrangement of instrumentation

Instrumentation has been arranged as shown in fig. 1. The receiver has been laid inside the enclosure and the transmitting antenna outside.

3.2 On board measurements positions

The measurements positions has been selected on the basis of an inspection of the enclosure under test. Selection criteria take into account each point of the enclosure that can increase the risk of undesired electromagnetic radiated emissions.

Measurement should be made close to:

- Apertures (e.g. doors, ventilation ducts, mesh gratings, etc.);
- Penetration cables and conducting pipes as these can pick up signals on one side of the screen and re-radiated on the other;
- Seams and other weak features of the shielding and bonding.

3.3 On board dynamic range measurement

In order to ascertain the capability of the system of revealing the attenuation value that is intended to be gauged, it is necessary to perform a check in advance on the intended operational attenuation measurement range. The test of attenuation measurement range shall consist of the following steps:

- The instrumentation shall be placed inside the enclosure, (maintained in maximum shielding conditions); RX and TX antennas shall be positioned with mutual distances as indicated in Fig. 2.
- Accordingly with the dimensions of the on board rooms, there should be no metallic items placed between antennas or in their proximity.
- Two readings of the amplitude levels (provided by the detector and expressed in $\text{dB}_{\mu\text{V}}$) shall be taken in the following conditions:

- a) maximum output power level of the signal generator (this could also include an amplifier). Let V_1 ($\text{dB}_{\mu\text{V}}$) be the level read from the detector. If the high power transmit level saturate either the receiving antenna (if active antenna) or the receiver it is possible to reduce the power level of the signal generator and take in account this reduction for calculate V_1 ;
 - b) signal source switched off and detector still operating in the previous conditions. Let V_2 ($\text{dB}_{\mu\text{V}}$) be the read amplitude level (it consists of the instrumental noise plus environmental noise).
- Measurement system range is calculated as follows:
- $$\text{Range (dB)} = V_1 (\text{dB}_{\mu\text{V}}) - V_2 (\text{dB}_{\mu\text{V}}).$$

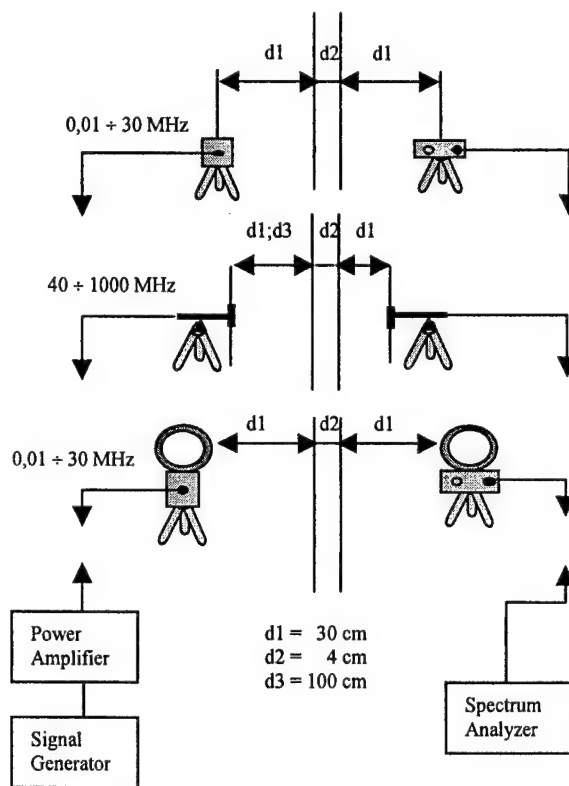


Fig. 2: Dynamic range measurement: mutual distances of Rx and Tx antennas

The range validation must concern horizontal and vertical orientation of antennas.

In order to make the attenuation measurement possible, range must be larger than expected attenuation value over the intended frequency range, otherwise the measurement signal level will need to be increased turning up the amplification.

The available instrumentation should provide a dynamic range of $80+100$ dB, but it will be considered that this resulting range will be the maximum attenuation measurable level; if the attenuation measurement is limited by the background noise (V_2), the real

attenuation is over the measured attenuation and over the dynamic range.

3.4 Shipboard measurement

Special attention must be paid when recording the parameters set during the attenuation measurements (receiver band, signal source output level, type of employed modulation, length of tuned dipoles and so on). Antennas should be aligned over two planes, horizontal and vertical, perpendicular to the plane of the shielding on the opposite sides of it.

The positions of instruments and antennas in the various frequency bands are the same as during dynamic range measurement. The distances between the antennas are mandatory but they can be modified, because of lack of available space, and such modifications must be reported in the trial report.

3.5 Calibration measurement

Calibration measurements are to be performed after shipboard measurements, in a shielded anechoic enclosure (fig. 4) or in an open-site, without metallic items placed between the antennas or in their proximity. Antennas must be carefully placed in the same conditions (fig. 3) as during the shipboard measurements.

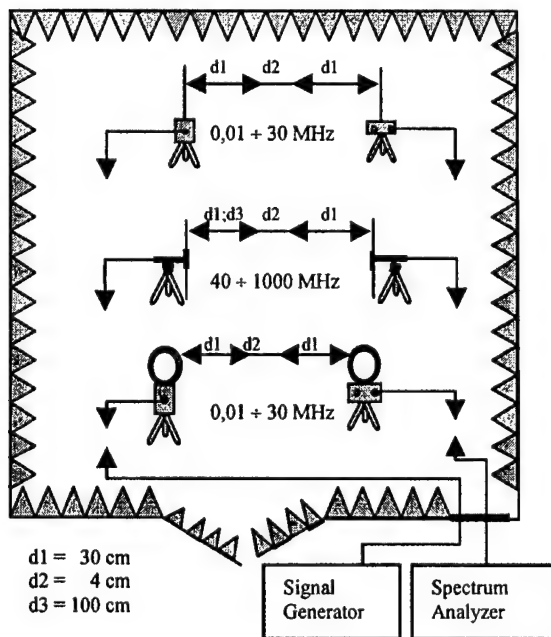


Fig.3:Antennas position during calibration measurement

The same cables as were used on the ship should also be used for this calibration measurements. Also the operational modes of the measurement chain must be thoroughly reproduced on the basis of the indications reported in the tables (receiver band, signal source level, type of modulation employed, length of tuned dipoles and so on).

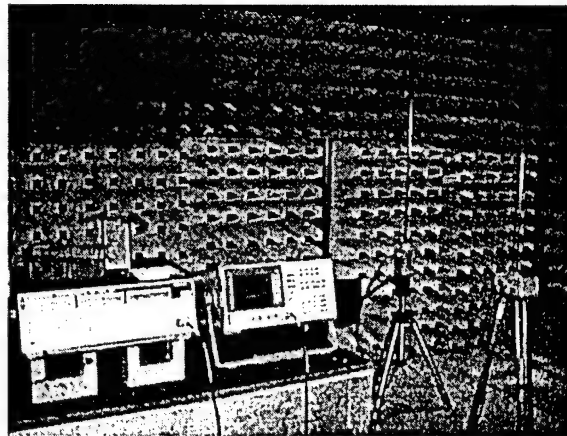


Fig. 4: Calibration measurement in the shielded anechoic chamber

If the high power transmit level saturate either the receiving antenna (if active antenna) or the receiver it is possible to reduce the power level of calibration and take in account this reduction for calculate V_o . If we reduced the power level of K dB we will considered that V_o will be the value measured plus the 2K factor.

3.6 Attenuation calculation

The following formula expresses the value of attenuation:

$$\text{Attenuation (dB)} = V_o(\text{dB}\mu\text{V}) - V(\text{dB}\mu\text{V}),$$

where V_o and V are the values of the voltage read on the receiver as a function of frequency respectively during the calibration during the trial.

Since two measures are performed, with antennas placed on horizontal and vertical planes, two different values will be achieved. As a value of attenuation, the least must be chosen.

4. RESULTS

The shielding effectiveness measurements of an Italian Navy ship radio room have been performed in two test points (door and bulkhead) for the following three conditions:

- Radio room clear of all extension cables and non permanent equipments;
- Radio room including equipments (operational condition);
- Radio room including equipments (after corrective actions).

In fig. 5 and fig. 6 the results are reported for magnetic and electric field attenuation measurements (the door as test point) in the frequency range 10 KHz - 30 MHz, in both conditions a) and b). As easily deductible by the diagram analysis, fig. 6 shows a maximum 44 dB degradation of attenuation at the frequency of 600 KHz.

In fig. 7 and fig. 8 the results are reported for magnetic and electric field attenuation measurements (the bulkhead as test point) in the frequency range 10 KHz - 1 GHz in both conditions a) and b). The diagram

obtained in fig. 8 shows a maximum 59 dB degradation of attenuation at the frequency of 1 GHz.

While in the case of the magnetic field the attenuation degradation is more limited, in the case of the electric field some corrective actions were necessary to bring the attenuation values to an acceptable level of shielding effectiveness.

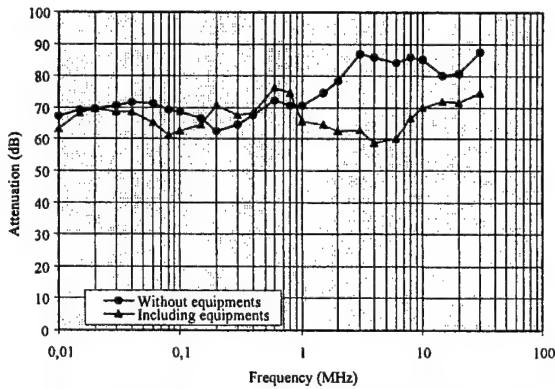


Fig. 5: Shielding effectiveness of magnetic field.
Test point: door

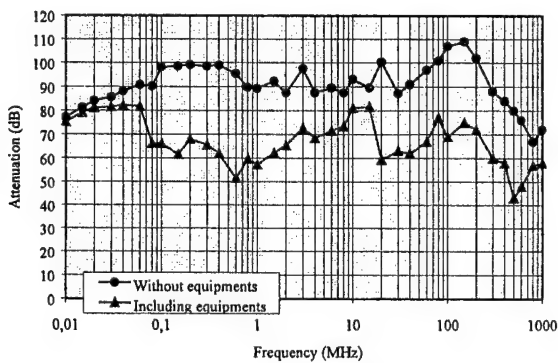


Fig. 6: Shielding effectiveness of electric field.
Test point: door

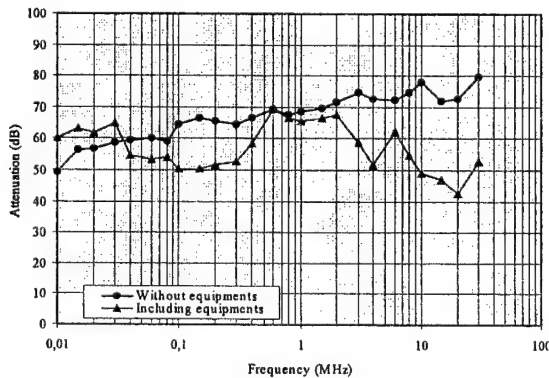


Fig. 7: Shielding effectiveness of magnetic field
Test point: Bulkhead

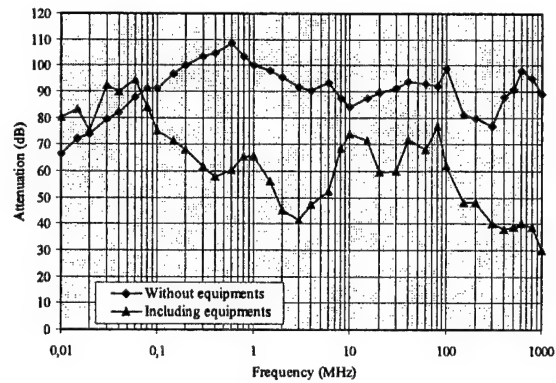


Fig. 8: Shielding effectiveness of electric field.
Test point: Bulkhead

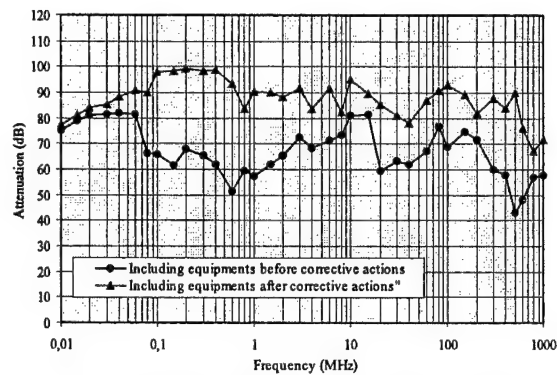


Fig. 9: Shielding effectiveness of electric field
Test point: door

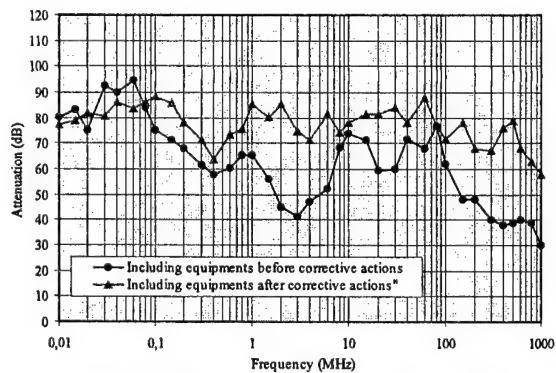


Fig. 10: Shielding effectiveness of electric field.
Test point: bulkhead

Following actions were performed:

- accurate cleaning of door "fingers";
- substitution of damaged door "fingers";
- restoration of acceptable RF characteristics of an aperture for penetrating cables.

After these corrective actions the electric field attenuation values increased, as shown in fig. 9 and fig. 10. In fig. 11 is illustrated the tuned dipole antenna used during the shipboard measurements.

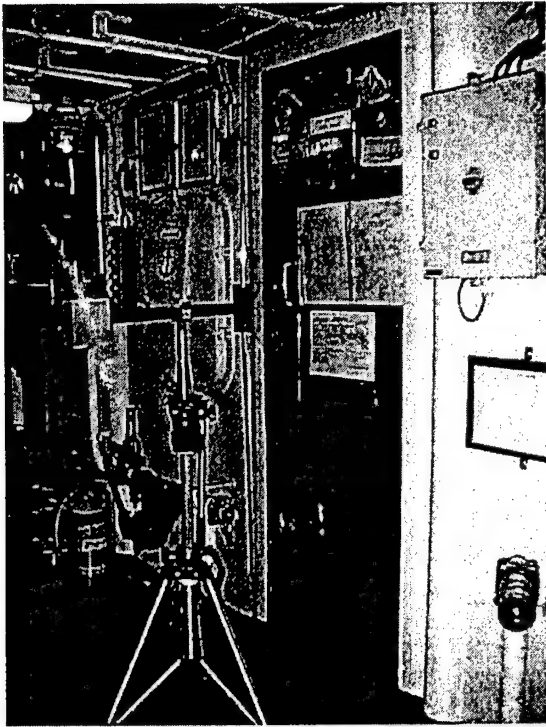


Fig. 11: Tuned dipole antenna used during shipboard measurement

5. CONCLUSIONS

The Italian Navy began several years ago to adopt the aforesaid methodology, described in STANAG 4557, of measuring shipboard operational rooms shielding effectiveness. The application of this EMC standard in many cases has permitted the identification of shielding and bonding problems, due to bulkheads imperfect integrity, bad RF characteristics of apertures for penetrating cables, etc.

Also in civil context we can find analogous requirements of shielding effectiveness verification for places like for example:

- radio rooms of merchant/passenger ships;
- radio rooms of public order control forces;
- companies and government agencies data processing centers;
- research and experimentation laboratories;
- intensive care hospital departments;
- in general, rooms that need shielding for RADHAZ requirements.

In conclusion we think that this methodology can be usefully and successfully applicable to the aforesaid cases and so we wish the extension of STANAG 4557 to the civil context.

TESTING THE EMP EFFECT ON AN ORDNANCE SYSTEM

Fatih USTUNER, Isa ARAZ, Mehmet YAZICI, Senol PAZAR

TUBITAK National Research Institute of Electronics and Cryptology
Gebze, 41470, Kocaeli - TURKEY
Phone: +90-262-6481202
Fax: +90-262-6481100
ustuner@mam.gov.tr

Published experimental work on the effect of electromagnetic pulse over the electro-explosive devices (EED) is scarce in the literature. The effect may be perceived in two different modes on the bridgewire type EEDs. One is the pin-to-pin mode and the other is the pin-to-case mode. In this work, the authors attempt to measure the pin-to-pin effect using the energy concept. An ordnance system comprising of passive elements was subjected to an electromagnetic pulse. A method is devised to measure the energy induced to the hot bridgewire type electro-explosive device.

Briefly, the method is as follows: the components of the equipment under test was placed inside a GTEM cell. One end of the EED wire was brought to the outside of the GTEM cell. The induced current on the wire was picked up by an RF current probe in the differential mode. The output of the current probe was sampled by a digitizing oscilloscope. The sampled time domain waveform was transformed to the frequency domain by applying FFT. Afterwards, the correction factors of the current probe was introduced. By using the frequency domain current components then obtained, the energy dissipated on the bridgewire resistance was calculated. The test results will be given in the paper. The validity of the applied method is to be discussed.

1. INTRODUCTION

Ordnance systems may be susceptible to electromagnetic environmental effects if proper EMC measures are not taken. The electroexplosive device (EED) which is a device used to start an explosive train using an electrical energy constitutes the most vulnerable part of an ordnance system. Inadvertent initiation of such devices could result personnel hazards and/or mission failures. Almost all ordnance systems use hot bridge wire type EEDs. The primary characteristic of these types of EEDs is that they

are passive and therefore they exhibit linear behaviour. The direct current joule heating (I^2R) is the normal initiation mode for these types of EEDs. Since the EEDs are actuated electrically and these devices may receive an RF conduction current through a pair of transmission line, the electromagnetic energy in the environment may constitute a potential threat.

The electromagnetic environmental effects that can affect an ordnance system may be one of the followings:

- Electromagnetic radiation from intentional transmitters.
- Electromagnetic pulse after a nuclear detonation.
- Lightning
- Electrostatic discharge

These effects may use the following two ways to cause inadvertent ignition:

- Pin-to-pin mode
- Pin-to-case mode

1.1. Structure of Electroexplosive Device

To understand these two ways, one must first consider the structure of an EED. A typical EED with complete firing mechanism can be simply depicted as in Fig. 1. An EED usually consists of a small bridgewire surrounded by an explosive compound (primary and secondary charges). The bridgewire and explosive compound are enclosed in a metal case and the bridge wire is electrically isolated from the case.

The electrical energy is provided from a current source through a pair of conducting wires which is connected to the EED terminals. The normal initiation process is the heating of the bridge wire by supplying it with a differential mode current. After the bridge wire reaches a critical temperature, the primary charge detonates which

in turn causes the explosion of the secondary charge. This is the normal initiation or ignition mode and it is called as "pin-to-pin" mode. The other way, which may be classified as the abnormal way, is the dielectric breakdown of the explosive due to the pin-to-case voltage difference. The breakdown exhibits itself with an arc formation between a pin and the case. This arc can cause an ignition to the primary or/and the secondary charge. This way is called as pin-to-case and is the primary way whereby the electrostatic discharge can affect an EED.

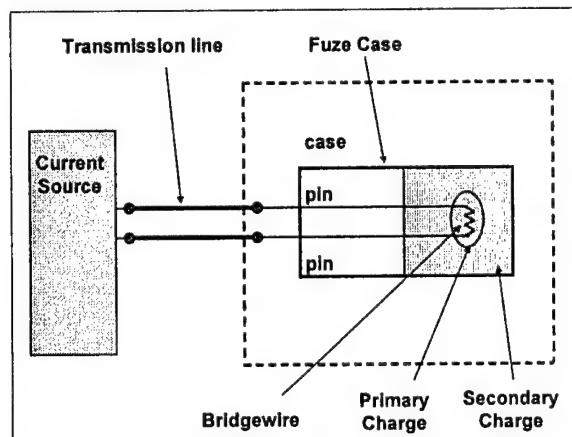


Fig. 1. An Electroexplosive Device

1.2. Bridge wire Heating

As seen in the previous section, the primary factor of the ignition process in the normal (pin-to-pin) mode is the heat quantity on the bridge wire. Depending upon the time constant, the energy needed to fire varies. Pulsed high currents need lower energy to start the ignition as compared to the continuous low currents. The ignition characteristics of the squib MK1 MOD 0 can be given as an example. According to the specification MIL-PRF-14977C[1], the squib can be fired within a 5 ms after applying 1.5 A at 21°C. On the other hand, the same squib shall not fire when energized with 0.2 A for 5 s. If the energy quantity needed for each case is calculated, one can find that the energy in the first case is around 11.25 mJ while in the second case is around 200 mJ. This controversial phenomenon can be explained as follows:

- In the first case, the bridge wire reaches a thermal balance in which the supplied energy couldn't increase further the heat.
- In the second case, the bridgewire finds no time to cool down and the ignition starts with the initial application of the current.

There are experimental results for this phenomenon [2]. From this point of view, one can propose two types of criterion for the bridge wire ignition:

- Current/power criteria for continuous stimulus
- Energy criteria for pulsed stimulus

Either criteria can be selected as the minimum no fire stimulus (MNFS) criteria depending upon the type of the electromagnetic environmental effect. In this work, only the pin-to-pin mode is considered and it is investigated whether an EMP effect can accumulate a sufficient energy deposition over the bridge wire which in turn lead to an ignition of the primary charge. The measurement parameter will be the current flowing through the bridge wire in the differential mode. Since the present work is interested in the EMP effect, the energy criteria was chosen for determining the firing threshold.

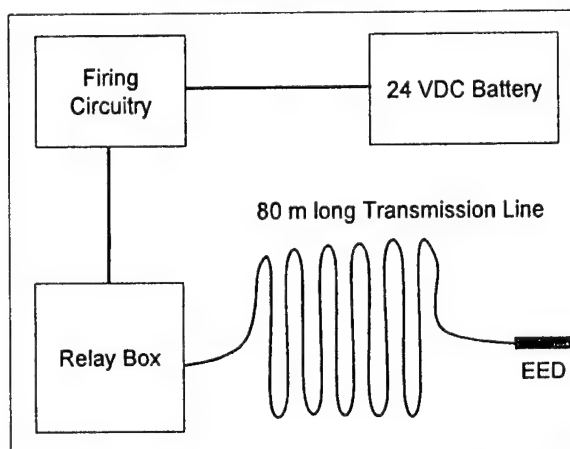


Fig. 2. Electrical Sub-system

2. TESTING

2.1. Description of the system under test

In this description, only the electrical sub-system of the overall ordnance system will be considered since only this part is subjected to the test. The electrical sub-system is depicted in Fig. 2. As seen, it simply consists of a battery supplying the energy, the firing device containing the necessary control circuitry, a relay box supplying the firing current, an 80 meter long unshielded pair transmission line which connects the EED and the squib of type MK1 MOD 0. As can be easily foreseen, it is the transmission line that will act as an unintentional antenna facilitating the coupling and transmission of the RF energy to the EED. Therefore the primary element of the test setup will be the lying down of this transmission line.

2.2. Test Limit

The minimum no fire stimulus energy is taken as 10 mJ energy in the light of the characteristics of the squib MK1 MOD 0 and the published experimental work. The test limit was set to 16.5 dB below the MNFS as the military standard MIL-

STD-464 recommends[3]. This corresponds to 224 μJ as the test limit.

2.3. Test Method

2.3.1. Test Setup

The test room used in the test is a GTEM cell having a 1.5 m septum height. The transmission line between the relay box and the fuze was placed inside a non-conducting box in a zig-zag form. The fuze end of the transmission line was brought to the outside of the GTEM cell through a metal pipe having a 0.9 meter length. The actual fuze was replaced by a carbon composition type resistor having the same DC resistance value. The RF current probe was placed on the transmission line near the simulating resistor in such a way that it pick ups the differential mode current. It was connected to the oscilloscope through a 40 dB attenuator. The EMP generator was connected to the feed point the GTEM.

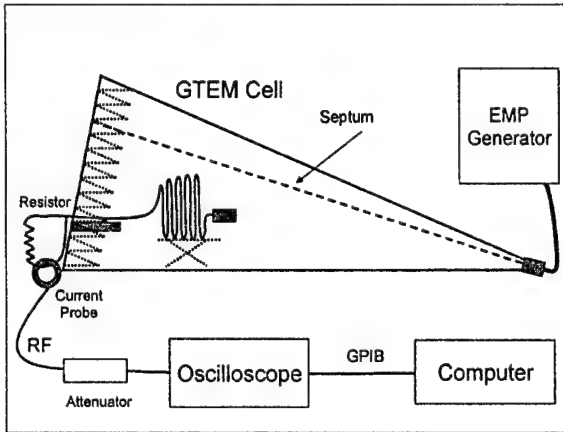


Fig. 3. Test Setup

2.3.2. Test Procedure

The electromagnetic pulse is generated by an EMP generator capable of delivering a double exponential pulse whose time domain waveform is given in Fig. 4.

The output of the current probe was sampled by a digitizing oscilloscope and captured by a computer via GPIB bus. The sampled time domain waveform was transformed to the frequency domain by applying FFT. Afterwards, the correction factors of the current probe was introduced. Using the resulting spectra of the fuze current and benefiting from the Parseval's theorem, one can find the energy dissipated on the bridge wire resistance using the following equation:

$$E = \left(\sum_{n=1}^{N/2} I_n^2 \cdot R \right) \cdot \Delta t \quad (1)$$

Where I_n is the fuze current, R is the fuze resistance, Δt is the sampling interval time and N is the number of sampling points (In this work $N=1024$ and $\Delta t = 5 \text{ ns}$). Δt is used as a scaling measure.

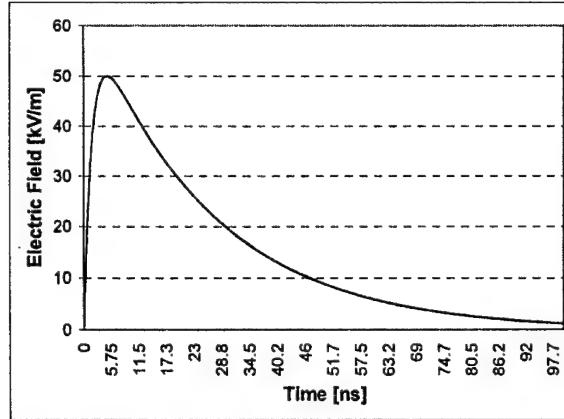


Fig. 4. Electromagnetic Pulse

3. MEASUREMENT RESULTS

The measurement results are given for three cases depending upon the position of the box containing the transmission line. These are as follows (see Fig. 6 for the coordinate axis of GTEM):

- Position 1: the transmission line zigzags are parallel to the x-axis
- Position 2: the transmission line zigzags are parallel to the z-axis
- Position 3: the transmission line zigzags are parallel to the y-axis

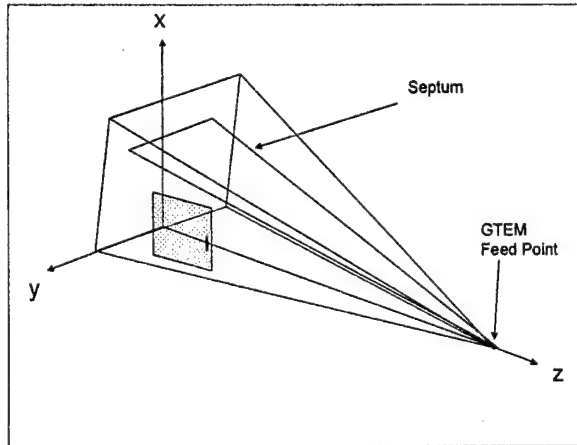


Fig. 5. GTEM Cell Coordinates

The time domain waveform captured by the digitizing oscilloscope for the position 1 is depicted in order to illustrate the damped sinusoidal type of change in the time (Fig. 6). The frequency of the damped sinusoid is 10 MHz.

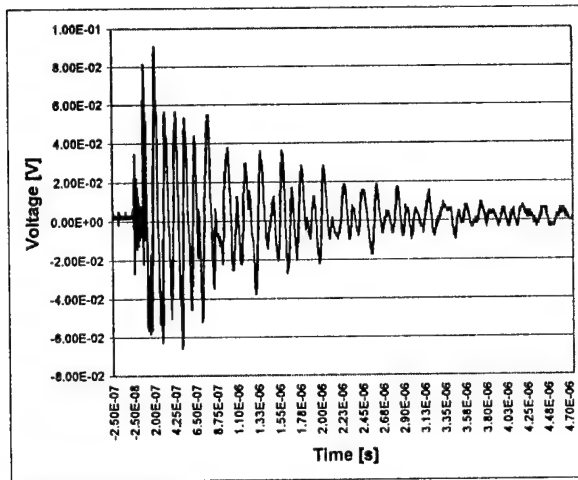


Fig. 6. Time Domain Waveform

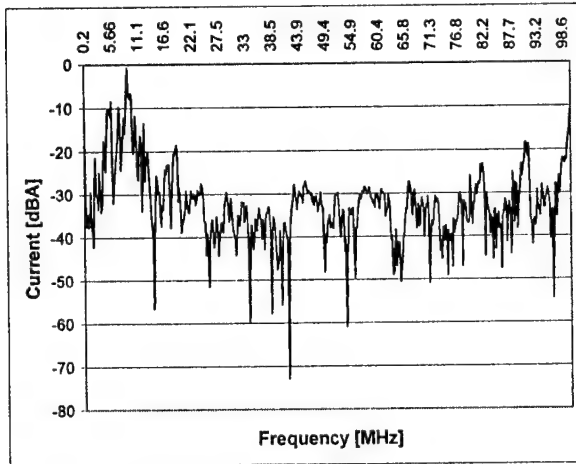


Fig. 7. Current Spectra (Position 1)

The frequency domain current components for position 1,2,3 is seen in figure 7, 8, 9 respectively. As expected, the peak of current spectra is around 10 MHz. Using Equation 1, the total energy induced to the fuze was calculated. The results are given in Table 1 with the limit level. The highest calculated energy is obtained in position 1 in which the transmission line is parallel with the electric field inside GTEM cell. On the other hand, all the calculated energies are below the limit with safety margin.

Table 1. Test Results

Position	Limit (μJ)	Result (μJ)
1	224	28
2	224	22.6
3	224	21.2

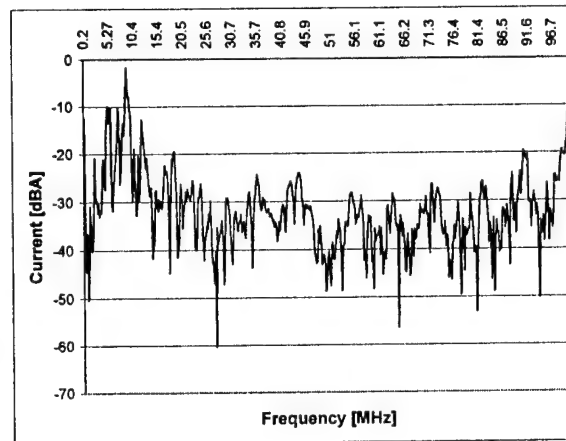


Fig. 8. Current Spectra (Position 2)

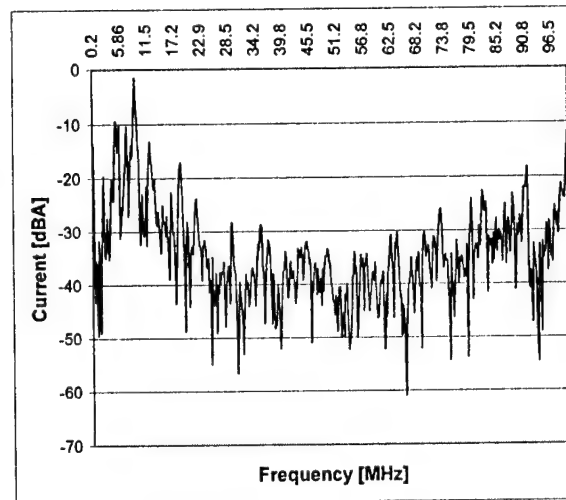


Fig. 9. Current Spectra (Position 3)

4. VALIDITY OF THE RESULTS

Although the test logic is tried to be well defined, the test instrumentation has many drawbacks. Some of them are as follows:

- The use of a carbon resistor to simulate a fuze. The carbon resistor RF characteristics couldn't be the same with the fuze.
- The transmission line end was brought out of the test cell thereby disturbing the test setup integrity.

5. CONCLUSION

The EMP effect on an ordnance system was assessed experimentally. According to the results, the ordnance system is not susceptible to EMP. However, there are several drawbacks of the current test setup and the experimental work must

be redone by using more sophisticated sensors and test equipment.

6. REFERENCES

- 6.1. MIL-PRF-14977C, "Performance Specification Squib, Mark 1 Mod 0 for 2.75 inch rocket", US Department of Defense, 1997
- 6.2. Jenkins, Olohan, "Some UK techniques for assessing RF susceptibility of electro-explosive devices in aircraft systems", IEEE EMC Symposium Digest, pp. 361 – 367, 1976.
- 6.3. MIL-STD-464, "Electromagnetic Environmental Effects, Requirements for Systems", US Department of Defense, 1997

BIOGRAPHICAL NOTES



Fatih Ustuner: Born in 1967 in Istanbul. He took his BS and MS degrees in electrical engineering from Middle East Technical University. Currently he is working as an EMC researcher at TUBITAK National Institute of Electronics and Cryptology.



Isa Araz: Born in 1969 in Ankara. He took BS degree in physics from Middle East Technical University and MS degree in electrical engineering from Sakarya University. Currently he is working as an EMC researcher at TUBITAK National Institute of Electronics and Cryptology. He is a PhD student at Sakarya University.



Mehmet Yazici: Born in 1972 in Rize. He took BS degree in electrical engineering from Yildiz Technical University and MS from Gebze Institute of Technology. Currently he is working as an EMC researcher at TUBITAK National Institute of Electronics and Cryptology.



Senol Pazar: He was born in 1970 in Zonguldak. He took his BS in electrical engineering from Middle East Technical University and MS degree from Dumlupinar University. Currently he is working as a DSP researcher at TUBITAK National Institute of Electronics and Cryptology. He is a PhD student at Middle East Technical University.

IMPLEMENTATION OF STANDARDISED EMC CRITERIA DURING THE WARSHIP DESIGN PROCESS IN POLAND

K. Dymarkowski, J. Uczciwek, R. P. Zając
R&D Marine Technology Centre (CTM), 81-109 Gdynia, Dickmana 62, Poland
Tel.: (+48 58) 6665381, Fax: (+ 48 58) 665 6487 E-mail: rz@ctm.gdynia.pl

The paper presents the way of formulating requirements, which should be complied with by systems, i.e. navigation system, with respect to electromagnetic compatibility. The principle of acceptance process and minimum requirements, which should be complied with by normative documents is presented. Technical Criteria of Product (TCP), which is a temporary document, defining technical requirements and testing procedures fulfilling the requirements, is presented. Inclusion of the Polish Military Standards and the Polish Industry Standards with respect to electromagnetic compatibility is also described. The requirements, as well as recommended tests methods related to ships' navigation system are presented.

1. INTRODUCTION

The use of COTS equipment in military procurement is likely to become increasingly common. However, the use of COTS equipment in the generally more severe military environment raises the need for protection against each of Electromagnetic Environmental Effects (E3).

All electric and electronic apparatus carried into EU market have to meet the EMC Directive-89/336/EEC, amended by 92/31/EEC and 93/68/EEC.

It is necessary to take into consideration the differences between civil and military environments, limits and test methods using the COTS equipment in the military applications. That is one of the reasons why comparison of civil and military standards on E3 is necessary.

Another reason of necessity to use civil standards in E3 area regarding to military equipment and materials is presented in the paper.

Polish MOD has introduced the obligation of certification of military equipment and materials in order to ensure their proper reliability level. The base of certification process is reference document based on the referenced standards. The best situation is when referred product or product family standards are available.

In Poland, but not only, the comprehensive system of military standards in the area of E3 threats has not yet been established.

There are very many military and civilian, national and international E3 protection standards. However, some particular EM phenomenon has not been covered by military standards. Then additional EMC assessment referred to civilian standards may be required.

One of the more important elements of ship designing process is devices and systems for ships equipping definition and checking. It is connected with defining of utility, safety and reliability parameters of equipment in the area of Electromagnetic Environmental Effects. One of the basic instruments in that process are standards. So again, the best situation is when product standards are available.

As will be shown in the next part of the paper in majority of cases it is not possible to find E3 referenced product standards for military equipment and materials.

2. POLISH MILITARY STANDARDS IN E3 AREA

During last 40 years, there have been published a number of E3 protection standards in the world. There are basic, generic, product and product family standards obligatory in civil and military applications. In that area in Poland up to early 90's system of national standards which was composition of own study and implementation of international standards was accepted.

Referring to military equipment and materials there were in force Polish Military Standards (PMS) [1]. They were the result of implementation of international (in force in bloc of eastern countries) standards, CT B CEB 065-81 + CT B CEB 072-81. These standards include general resolutions, environmental immunity requirements, guides of tests methods definition etc. No specific limits and method of tests in E3 area except effects of NEMP are included in them.

Within Polish integration with western structures (EWG, NATO) there have been undertaken intensive actions to harmonisation of Polish standards with the standards being in force in these structures. It concerns military standards in E3 area, too.

In reference to naval equipment and materials, actually there are in force four Military Standards (MS). Two of them are basic, self-elaborated standards [2,3] and another two generic standards [4,5] which are implementation of MIL-STD-461D and MIL-STD-462D.

Table 1 – List of required tests standards DS (NO), PMS (WPN) and NS (PN) of electromagnetic compatibility ship's systems

No	Required tests	DS (NO) and/or PMS (WPN) limits/test methods	NS (PN) limits/ test methods	International standards limits/test methods
1	Electromagnetic disturbance radiated emission	NO-06-A200 NO-06-A500	PN-EN 55022 CISPR-16-1	MIL-STD-461D MIL-STD-462D
2	Electromagnetic disturbance conducted emission	NO-06-A200 NO-06-A500	PN-EN 55022 CISPR-16-1	MIL-STD-461D MIL-STD-462D
3	Electrostatic discharge immunity	Non	PN-IEC 801 – 2	IEC 801 – 2
4	Burst immunity	Non	PN-IEC 801- 4	IEC 801- 4
5	Surge immunity	Non	PN-EN 61000-4-5	EN 61000-4-5
6	50 Hz magnetic field immunity	Non	PN EN 61000-4 -8	EN 61000-4-8
7	Pulse magnetic field immunity	Non	PN EN 61000-4-9	EN 61000-4-9
8	Damped oscillatory magnetic field immunity	Non	PN-EN 61000-4-10	EN 61000-4-10
9	Oscillatory waves immunity	NO-06-A200 NO-06-A500	PN-EN 61000-4-12	EN 61000-4-12 MIL-STD-461D MIL-STD-462D
10	Voltage variations, dips and short interruptions	Non	PN EN 61000-4-11	EN 61000-4-11
11	Radiated, (10 kHz to 40 GHz), electromagnetic field immunity	NO-06-A200 NO-06-A500	PN-IEC 1000-4-3 PN-EN 55020	MIL-STD-461D MIL-STD-462D
12	Conducted, (10 kHz to 400 MHz), electromagnetic field immunity	NO-06-A200 NO-06-A500	PN-EN 61000-4-6 PN-EN 55020	MIL-STD-461D MIL-STD-462D
13	NEMP immunity	WPN-84/N-01003 NO-06-A200 NO-06-A500	Non	MIL-STD-461D MIL-STD-462D

To take into account all possible E3 threats in ship's environment in process of requirements formulation and ship's equipment authorisation, it is necessary to apply limits and test methods from different military and civil standards.

The specific EM effects, limits and tests from available military and civil standards, which should be taken into account for naval equipment, are arranged in table 1.

3. BASIC DOCUMENT FOR MILITARY EQUIPMENT CERTIFICATION

Specialists meet the basic difficulty in establishing process of military equipment and materials acceptance. It is lack of referenced product standards. They have to interpret many different basic and generic standards and to extract suitable requirements and testing methods.

It is very long and complex process to establish suitable product standard. So, in the Polish Armed Forces there has been established quick procedure to prepare temporary normative document, Technical Criteria of Product (TCP) defining technical requirements and testing procedures. Three sides agree on that document. They are supplier of equipment,

purchaser and Competent Body responsible on certification process. National Defence Standards Directorate accepts the document. The TCP has the form of product standard and should include following information:

- all required utility, safety and reliability of equipment and materials,
- methods of tests and tests sequences,
- principles of assessment of equipment compliance with requirements.

The following hierarchy of respective normative documents is adopted in the process of TCP in EM effects preparation:

- national military/defence standards,
- international ratified military standards,
- other international military standards,
- national civilian standards,
- international civilian standards.

Additionally, there other documents like handbooks, AEP's, ANEP's etc. are taken into account. Scope of EM effects, limits, testing methods and respective standards included into TCP for as specific ship's device as radio-navigation receiver, which have been taken into account is arranged in the tables 2 and 3.

Table 2 – Electromagnetic disturbance emission requirements

No.	Description of test	Standardised limit of disturbance	Standardised test method
1	2	3	4
1	Electromagnetic disturbance radiated emission:		
	a) magnetic field emissions in the frequency range of 30 Hz to 100 kHz	Requirement KRE-01 NO-06-A200	NO-06-A500
	b) electric field emissions in the frequency range of 10 kHz to 18 GHz	Requirement KRE-02 NO-06-A200	
2	Electromagnetic disturbance conducted emission:		
	a) conducted emission power leads in the frequency range of 10 kHz to 10 MHz	Requirement KCE-02 NO-06-A200	NO-06-A500
	b) conducted disturbance antenna terminal in the frequency range of 10 kHz to 40 GHz	Requirement KCE-03 NO-06-A200	

Table 3 – Electromagnetic immunity requirements

No.	Description of test	Standardised limit of disturbance	Standardised test method
1	2	3	4
1	Electrostatic discharge immunity:		
	a) direct	6 kV ± 10% PN– IEC 801- 2	PN– IEC 801- 2
	b) indirect	8 kV ± 10% PN– IEC 801- 2	
2	EFT/Burst immunity	4 kV ± 10% PN– IEC 801- 4	PN– IEC 801- 4
3	Surge immunity	2 kV ± 10% PN-EN 61000-4-5	PN-EN 61000-4-5
4	50 Hz Magnetic field immunity	50 A/m ± 10% PN - EN 61000-4-8	PN-EN 61000-4-8
5	Pulse magnetic field immunity	1 500 A/m ± 10% PN - EN 61000-4-9	PN-EN 61000-4-9
6	Radiated, (10 kHz to 40 GHz), electromagnetic field immunity	10 V/m ± 10% NO-06-A200	NO-06-A500
7	Conducted, (10 kHz to 400 MHz), electromagnetic field immunity	Requirement KCS-06 NO-06-A200	NO-06-A500
8	Voltage variations, dips and short interruptions:		
	a) voltage variations	± 20% U _N *) PN EN 61000-4-11	PN EN 61000-4-11
	b) short interruptions (dips)	(100% + 0%) U _N *) PN EN 61000-4-11	
U _N – nominal EUT voltage *) accuracy ± 5%			

4. TCP IN SHIP DESIGN AND CONSTRUCTION PROCESS

Modern ships are very complex systems consisting of combat sub-systems, platform, platform sub-systems and additional equipment. During the ship design process, among other things, detailed requirements for equipment and its installation conditions are formulated. During all stages of ship designing and constructing that process is developed.

During different phases of equipment, systems and ship trials requirements are verified and may change. Some of the initial requirements may be subject to very strong EM environment, out of standardised limits. It is the reason, why chosen requirements included in related to normative document should be changed during process of prototype ship designing and constructing. It is easier to change some requirements in the document like TCP than in standard.

The impact of tests and trails on TCP requirements formulation process in different ship designing and constructing phases is shown on the figure 1.

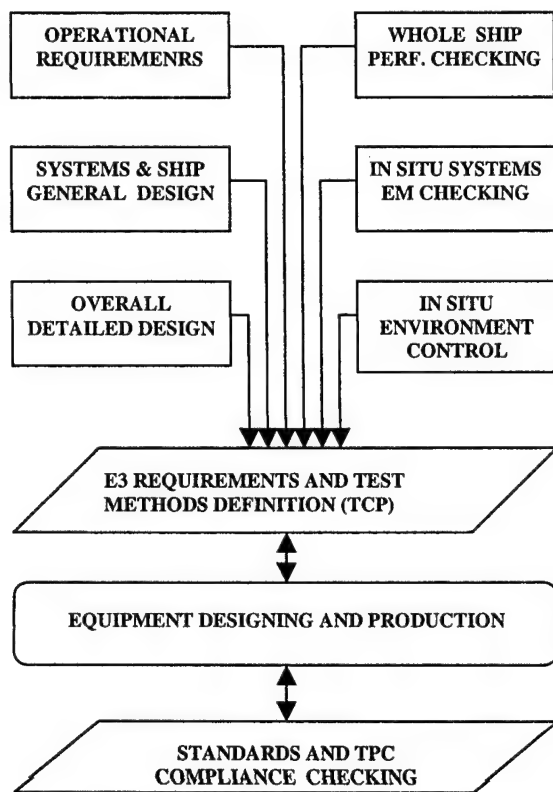


Fig. 1. The block diagram of ship designing and construction steps impact on E3 requirements defining process

The initiative to develop the harmonised NATO approach to E3 protection is very valuable in the light of the problems presented in the paper. Comprehensive system of harmonised standards, guides and other normative documents will be very useful for all specialists are committed on ships designing and construction process.

5. REFERENCES

- 5.1. Polish Military Standards, WPN-84/N-01001-01007, Military apparatus, devices and equipment-Generic technical requirements, methods of tests and trails.
- 5.2. Defence Standard, NO-19-A500, Electromagnetic compatibility of ships' devices-Methods of tests and criteria of evaluation.
- 5.3. Defence Standard, NO-20-A500-6, Technical requirements and methods of tests of ships' devices-Electromagnetic compatibility -General
- 5.4. Defence Standard, NO-06-A200, Electromagnetic compatibility- Characteristics requirements for equipment.
- 5.5. Defence Standard, NO-06-A500, Electromagnetic compatibility of ships' devices-Procedures of tests of electromagnetic interference characteristics.

BIOGRAPHICAL NOTES

Krzysztof DYMARKOWSKI received his M.Sc. degree in 1976 and D. Sc. degree in 1992 from the Technical University of Gdańsk both in electroengineering. His technical activity concentrates on developing and designing protection systems in wide scope of electromagnetic effects. He is the Chief Engineer of Naval Systems Department at the R&D Marine Technology Centre in Gdynia

Jerzy UCZCIWEK was graduated from the Technical Military University in Warsaw in 1975. He received the D. Sc. degree in 1996 in the Naval Academy in Gdynia. His research interests are in measurement and analysis of electromagnetic phenomena especially in naval environment. He is the Chief Engineer at the R&D Marine Technology Centre in Gdynia

Ryszard ZAJĄC received his M. Sc. degree in 1970 and D. Sc. in 1978 in the Technical Military University of Warsaw. Now he is the head of Naval Systems Department at the R&D Marine Technology Centre in Gdynia. His present scientific interests are all technical problems of EMC.

EMC 2000

INTERNATIONAL WROCLAW SYMPOSIUM ON ELECTROMAGNETIC COMPATIBILITY

Cost- and time-effective EMC testing of equipment used in safety critical environments

Dipl.-Ing. Rudolf Harms, Daimler-Chrysler Aerospace AG, Space Infrastructure Division
Hünefeldstraße 1-5, D-28199 Bremen, Germany
Phone: +49-421-5394706, FAX: +49-421-5395763, e-mail: rudolf.harms@ri.dasa.de

Dipl.-Ing. Ludger Revermann, Wehrtechnische Dienststelle 71, Dezernat 620
Berliner Straße 115, D-24340 Eckernförde, Germany
Phone: +49-4308-186331, FAX: +49-4308-186310, e-mail: LRevermann@wtd71.de

A new set of time- and cost-effective EMC test-methods is presented.

Based on a number of different existing EMC-standards and the use of common test-equipment the procedures are designed to be used for tests of safety-critical (not only military) components.

The main advantages will be:

- *reduced preparation time due to the use of only one test setup for all measurements,*
- *same physical values (i.e. currents) will be used for emission- and susceptibility-tests - safety margins can simply be determined,*
- *methods are designed to make the tests applicable on equipment level as well as on system and installation (mil.: platform) level.*

1. Introduction

More and more EMC requirements are put on the market, increasing the costs of electrical and electronic equipment – but not reducing the number of EMI-problems. Too many organizations produce "specialized" EMC-standards, which do neither fulfill the needs of the rest of the world nor take system aspects into account.

In the near future there might exist about 1500 EMI product standards, each providing a specialized set of tests tailored to the needs of a certain E.U.T., but, of course, slightly different of the generic standards.

On the other hand NATO's ministries of defense (also, but not only, Germany) force the procurement and use of equipment, developed and specified for the civil market. Will it be possible to verify the Electromagnetic Compatibility (including safety margins) of a complex system, consisting of

equipment tested in accordance with different standards and (incomparable) limits ?

To get rid of this problem the existing German military EMC-standards (VG 95370 series) are completely revised at this moment with the main goals:

- reducing the costs of EMC-tests due to the use of common test equipment,
- reducing the time for EMC-tests by using only one test setup,
- defining test methods that can be used as well on equipment as on system level,
- in combination with appropriate limits the tests qualify the E.U.T. for the system – by reducing the EMC-risk to nearly zero.

Using the tests of radiated emission and susceptibility as examples the structure and main aspects of the new standard will be described.

2. THE MATCHED PAIR PRINCIPLE

The uncertainties of EMC-measurements normally are relative large. Some reasons (among others) are standing waves and resonance effects. During EMC-tests of equipment these effects can be reduced by:

- the use of absorbing materials on the walls of the shielded test room,
- performing the tests on an OATS (open area test site),
- the use of round cable suppression cores of ferrite material.

If the instruments however are integrated into a real system, all these previously suppressed ef-

fects will be back again, maybe at other frequencies.

The VG draft assumes that resonance effects are unavoidable; these however should remain identical during all tests. Thus the norm only uses one test setup – with exactly defined position and alignment of sensors (antennas, current probes) and injectors. The measured and/or tested physical unit has to be the same during emission and immunity tests. Furthermore during tests in the frequency domain the parameters have to be determined using the same measurement equipment (i.e. test receivers) and detector functions (bandwidth, peak measurement) for both kinds of tests.

The impedances of the circuitry of the E.U.T and resonance effects are unknown and will remain so. Leaving these effects unchanged during all tests (as described before) makes it possible to evaluate the EMI-safety margin of an E.U.T. without performing calculations due to different impedances and/or physical units.

3. TEST ANTENNAS AND ANTENNA-POSITION

For all tests the antenna distance should be 1 meter. There is no electrical reason to do so, but in real life the systems space is limited, so the short antenna distance seems to be the only way to perform equipment tests comparable with system tests. Knowing that wave front curvature is the result of this short antenna distance, the goal is to make tests possible and reproducible – instead of getting most precise field intensity results. Furthermore it has to be taken into account, that in most cases EMI-antennas are calibrated for this distance.

All antennas, magnetic loops excepted, should be linearly polarized. Broadband antennas should be used.

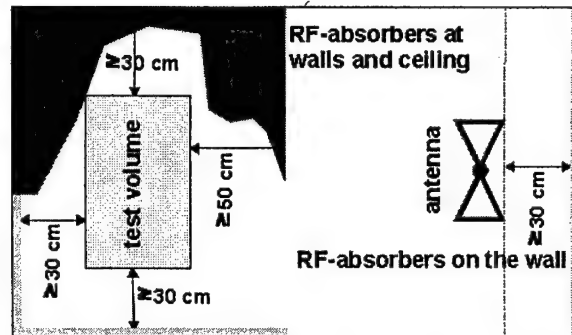
The same type of antennas shall be used for emission and immunity tests for better compensation of proximity effects.

At lower frequencies (licenses are granted starting at 9 kHz – so this has to be the lowest test frequency) a magnetic antenna should be used (up to 30 MHz). One reason is that in this frequency range the case of the E.U.T. is nearly transparent for magnetic fields, another one is the better testing of components (i.e. power supplies) with high currents and low voltages.

From 30 MHz to 200 MHz the biconical antenna is used. Unfortunately no good alternative has been found.

Above 200 MHz horn antennas with a specified antenna gain are used. They are preferred because of their better suppression capabilities of environmental effects. They integrate the radiation

lobes of the E.U.T. and have a good directivity. The use of absorbing material at the walls of the test site can be limited to some regions and is therefore less expensive.



The proposed procedures have been tested in the frequency range up to 100 GHz. It has to be noted that the calculation of the generated field strength, using the transmitting antenna factor, gives the same results as the former calibration with an isotropic field sensor.

All antennas above 30 MHz have a linear polarization. The alignment of the antenna (in relation to the ground plane) should be $\pm 45^\circ$ - tests using horizontal polarization will (because the ground plane's short circuiting effects) no longer be performed.

The distance antenna – E.U.T. of 1 meter and the height of the antenna of 1.2 meters above ground leads, if the antenna's gain is not less than 6 dB, to the effect, that no ground reflected signals of the E.U.T. are received – absorbing material on the floor of the test site is not essential.

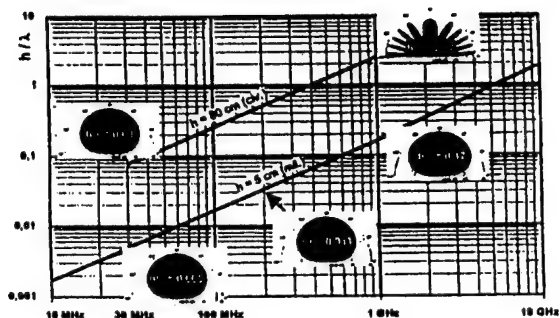
4. SETUP OF THE E.U.T.

For equipment testing a conductive reference ground plane is required by two reasons:

- The ground plane reduces the lobing of the radiation emitted by the E.U.T.
- The resonance effects of the shielded enclosure are masked by the ground plane effects.

It might be necessary to define the dimensions more exactly (i.e. 0.8 m x 2.5 m) instead of the presently used term "greater than 2.25 m²".

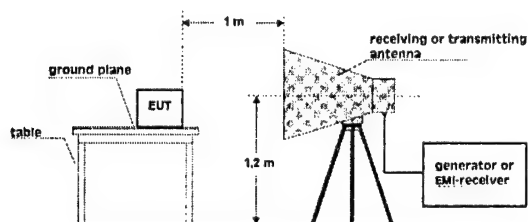
The following picture shows the lobing effects of an E.U.T. as an radiator in the civilian test setup (80 cm above the reflecting floor on a non-conductive test bench) and the military test set up (calculated per [1]). It is evident that the lobing is linearly decreased by the E.U.T.'s proximity to the ground plane. The use of a reference ground plane will make the height scan of the receiving antenna obsolete.



In civilian standards a turntable is used for radiated emission testing. However, E.U.T. emitting signals in their vertical axis are not covered by this method.

Military standards require all sides of an E.U.T. to be probed with an antenna to define the side with the maximum emissions which has to face the antenna.

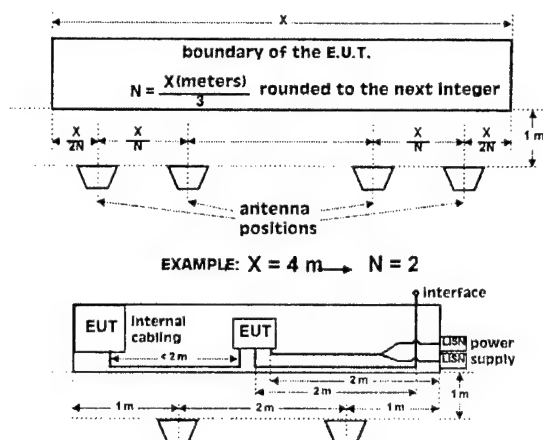
Presently the distance between the cabling of the E.U.T. and the ground plane is 5 cm. It's possible that in the near future this distance has to be reduced because of the necessity of increasing the upper frequency limit of radiated emission tests - operating frequencies for radars for automotive and flight applications are now in the range between 70 and 93 GHz.



The definition of standard lengths for the cabling of the E.U.T. will be kept unchanged. Under some circumstances lower lengths might be allowed - greater lengths will not be tested, that means that these might be shielded.

As LISN the 50 μ H (according to C.I.S.P.R.) network will be used.

Depending on the dimensions of the E.U.T. the position(s) of the test antenna(s) are calculated - this helps to reproduce the results.



5. MEASUREMENT PARAMETERS

Swept measurements in the frequency domain are necessary as the spectral lines of digital signals might be missed by spot frequency measurements as allowed by civil standards. A minimum frequency resolution of 1% would be sufficient, but an increase to 0.1% could be necessary, where high Q-factors occur. During the immunity tests the signal should not be switched off during frequency changing. Still under discussion is to sweep from the highest to the lowest frequency - the influence on the E.U.T. then would occur first with the base frequency - not with one of its harmonics.

As the victims in future systems are unknown during the tests, a worst case detector has to be chosen: the peak detector. For system planning corrections could be applied, depending on the demodulation methods used by possible victims in the system. Additionally the peak detector allows shortest sweep times during testing.

During immunity tests the minimum dwell time per frequency should be 1 second, depending on the E.U.T.; in some cases this time has to be increased.

Also for common reference only one type of modulation should be used for frequency domain testing. The 1 kHz, 100% pulse amplitude modulation seems to be a good choice. The modulation shape looks like a digital signal and its frequency is audible.

6. DOCUMENTATION OF THE RESULTS

At least the more important EMC-laboratories generate the test results in digital form and store them i.e. on diskettes, tape recorders etc.

To make the results more useful for system analyses a suggestion should be made for a standardized data storage in ASCII format.

In the future this data, stored on a standard medium (CD-ROM preferred) has to be part of the (written) test report. If later the data will be needed for further analysis and/or system planning this might reduce the risk of errors.

7. SUMMARY

Parts of the new VG-draft for military equipment have been explained. In the same manner, procedures and test setup for conducted tests (emission and immunity) will be simplified.

It has been shown that not only the resources (money, time and equipment), needed to perform complete and valuable EMC-tests, can be reduced-new test procedures and/or parameters further-more decrease the risk of EM Incompatibilities.

8. LITERATURE

[1] ANSI C63.5/1988, American National Standard for Calibration of Antennas used for Radiated Emission Measurement in EMI Control, IEEE, N.Y.

[2] R. Harms, Let's make the Compatibility Requirements Compatible, 1999 IEEE EMC Symposium

[3] R. Harms, Harmonization and Simplification of future EMC-standards (german), EMV 2000, Dueseldorf,

BIOGRAPHICAL NOTE

Ludger Revermann is with the Bundeswehr Technical Center for Ships and Naval Weapons in Eckernfoerde, Germany, part of the procurement organization of the German MoD. In the department Navigation, Communication, EMC he is responsible for EMI/EMC-matters of Naval Systems and Equipment.

EMC ASSESSMENT USING THE TRANSMISSION LINE MATRIX METHOD (TLM)

J J Kazik

EM Engineering Group, Concepts and Integration, Room C109, DERA Portsdown West Portsdown Hill Road,
Fareham, PO17 6AD, UK. Fax: (+44) (0)23 92337338, Email: JJKAZIK@dera.gov.uk

ABSTRACT

This paper describes the Transmission Line Matrix Method, (TLM) and its potential application to the assessment of EMC via the prediction of electromagnetic fields and currents surrounding structures constructed from either metal or composite materials or both.

1. INTRODUCTION

1.1. Conventionally, numerical modelling has been the domain of powerful workstations and outside the scope of a stand-alone PC. Cheaper memory and faster processors, however, have enabled computational electromagnetic techniques to be ported to the PC environment. This has enabled the direct numerical electromagnetic assessment of novel materials and technologies, particularly for stealth purposes, to be performed on desktop computers.

1.2. One such numerical method is the Transmission Line Matrix Method, (TLM). TLM has the potential for being used to assess EMC and EMI problems by predicting the electromagnetic environment surrounding structures constructed from either metal, composite materials or both.

1.3. This paper introduces the TLM technique and illustrates areas of applicability by describing general modelling and validation of the prediction of electromagnetic fields and currents, demonstrating the applicability to the assessment of EMC/EMI. The paper demonstrates that TLM has the potential for becoming a highly efficient and accurate technique for the assessment of EMC and EMI.

1.4. The technique demonstrates how EMI and EMC problems can be minimised by the prediction and identification of areas of high electromagnetic fields and surface current densities at the concept stage of a typical platform.

2. THE TRANSMISSION LINE MATRIX METHOD

2.1. TLM is a time domain technique based on the analogy between the propagation of electromagnetic waves in a medium and signals propagating along a transmission line [1]. This is illustrated in figure 1 and equations 1 and 2, representing the correspondence between a one dimensional transmission line with inductance L, capacitance C and admittance G, and an electromagnetic wave in a medium with permeability μ , permittivity ϵ , and conductivity σ :

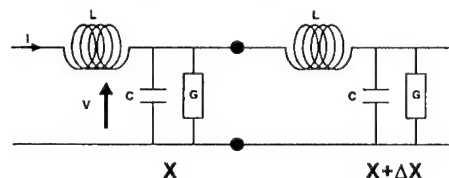


Fig. 1: 1-D Transmission Line

$$\frac{\partial^2 i}{\partial x^2} = \frac{LC}{(\Delta x)^2} \frac{\partial^2 i}{\partial t^2} + \frac{L}{(\Delta x)^2 G} \frac{\partial i}{\partial t} \quad (1)$$

$$\frac{\partial^2 H}{\partial x^2} = \mu \epsilon \frac{\partial^2 H}{\partial t^2} + \mu \sigma \frac{\partial H}{\partial t} \quad (2)$$

2.2. From the above the following equivalencies can be drawn:

Transmission Line		EM Field
i	\Leftrightarrow	H
$\frac{L}{\Delta x}$	\Leftrightarrow	μ
$\frac{C}{\Delta x}$	\Leftrightarrow	ϵ
$\frac{1}{G \Delta x}$	\Leftrightarrow	σ

Fig. 2: 1-D Transmission Line and Electromagnetic Field Equivalencies

2.3. TLM essentially models the propagation of voltage impulses along a network of transmission lines. These impulses are then scattered at each junction of the transmission lines.

2.4. The structure to be modelled is represented as a cartesian mesh of transmission lines, joined where they cross. Each TLM cell is therefore one of these junctions, termed a node. Different materials are therefore modelled according to their electromagnetic properties via appropriate choices of the values of the transmission line inductance, capacitance, and admittance.

2.5. Thin complex materials can be modelled as resistive ladder networks attached between nodes, enabling thin material modelling without direct representation by a TLM cell, saving on memory and run time. TLM can also model features such as lossy dielectrics, finite conductivity and thin wires.

2.6. This process is depicted in Figure 3, illustrating a 3-D TLM node and a junction of transmission lines with a thin material.

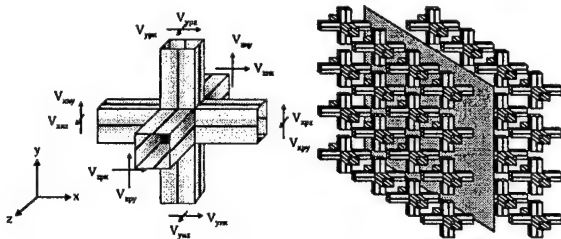


Fig. 3: 3D TLM Node and Modelling with TLM

2.7. As long as the spacing between adjacent nodes is less than $1/10$ of the wavelength being studied, the waves will propagate along the mesh with very little wave propagation velocity error. Accordingly, TLM has a low wave dispersion error [2].

2.8. TLM cells may also vary in size enabling a tight fit to a geometry. In this way, problems with modelling areas of detail are largely eliminated (though TLM still uses a staircase approximation to the geometry).

2.9. Model excitation is via the introduction of a pulse of a specified bandwidth introduced at one or more of the nodes. At successive time steps, these impulses travel along the transmission lines, scattering at the junctions and connecting across to neighbouring nodes within the time step.

2.10. Frequency domain data can be extracted from the time domain TLM simulation either via a Fourier transform or via a sinusoidal excitation (monochromatic wave). This enables a complete characterisation of the electromagnetic environment surrounding a complex object to be performed.

3. MATERIAL MODELLING WITH TLM.

3.1. Transmission Loss.

3.1.1. Figure 4 depicts a TLM model for assessing the transmission loss through two material layers (glass reinforced plastic and nickel/copper coated polyester).

3.1.2. Figure 5 depicts the comparison of the TLM predicted transmission loss with the analytic solution.

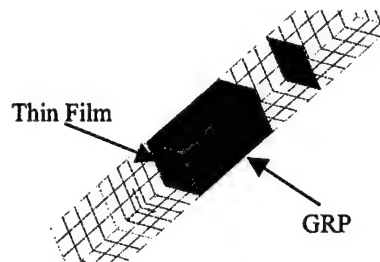


Fig. 4: TLM representation of two layer material

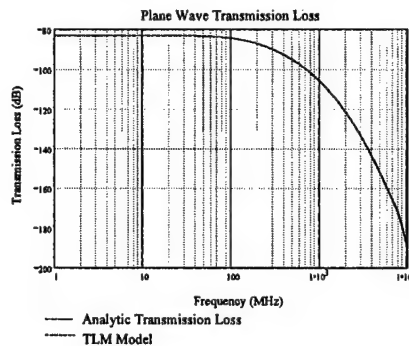


Fig. 5: Comparison between TLM and Analytical Two Layer Material Transmission Loss

3.1.3. This material model was validated at HF via a comparison of the measured and predicted screening performance of a panel of the copper/nickel coated polyester mesh in a split-screened room. Figure 6 represents the TLM model and figure 7 is the comparison of the predictions with the experimental data in the range 1–20 MHz.

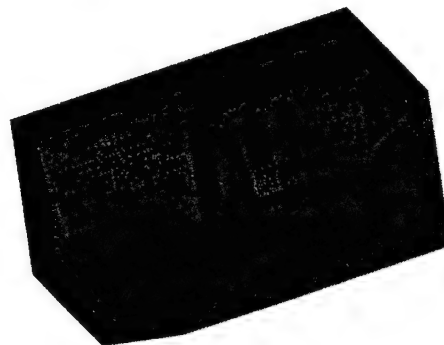


Fig. 6: TLM model of the split screened room with a material panel

3.1.4. From figure 7 it can be seen that there is exceptionally good agreement with the experimental data.

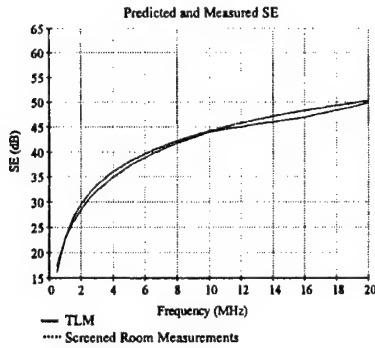


Fig 7: Comparison with experimental data of the TLM model of the screened room with a flecron panel

3.2. Antenna Ground Plane.

3.2.1. TLM models have been created, replicating the geometry of a flame sprayed zinc antenna ground plane (AGP) supported by a composite glass reinforced plastic substrate, placed onto top of a steel enclosure [3]. Predictions of the isolation between the inside and the outside were compared to measurements at various frequencies. Figure 8 depicts the TLM model of the AGP.

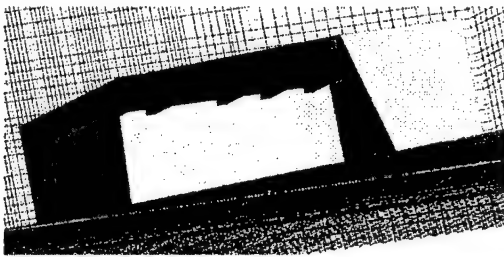


Fig. 8: TLM model of AGP

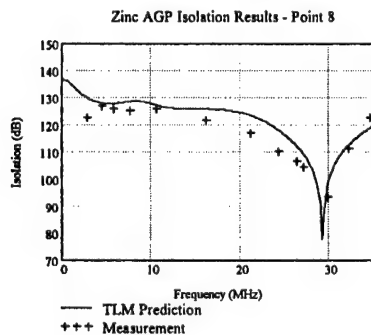


Fig. 9: Comparison between isolation measurements and TLM predictions.

3.2.2. Screening performance results are presented in figure 9 for one test position. The correlation between the two data sets is excellent.

4. SOURCE MODELS IN TLM

4.1. 10 Metre Whip Monopole

4.1.1. Cross-code validation between NEC 4 and TLM has also been performed for a model of a 10-metre monopole whip at HF [4].

4.1.2. Two equivalent models of a 10-metre monopole whip were created for NEC 4 and TLM, with a radius for both models set at 10 mm. For both models, the currents along the whip and the elevation radiation patterns were determined together with the input impedance and VSWR of the whip. Both NEC and TLM models are depicted in figure 10.

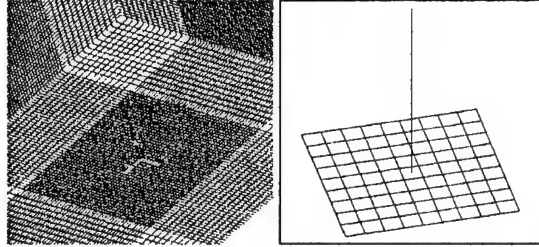


Fig. 10: TLM and NEC models of a 10 metre whip monopole on a ground plane

4.1.3. Note that depiction of the extent of the ground plane in figure 10 is misleading. The ground plane extends to infinity and is perfectly conducting. In the TLM model, the vertical walls are the extent of the workspace representing the terminating boundaries for the model.

4.1.4. Figure 11 represents the absolute current distributions along the whip for both sets of predictions.

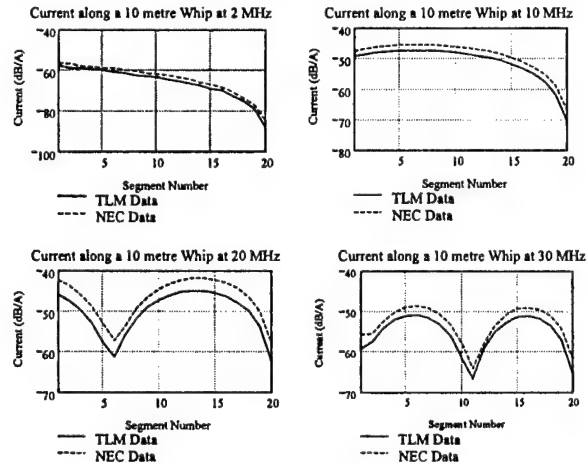


Fig. 11: TLM and NEC currents along monopole.

4.1.5. Both NEC and TLM are in good agreement, correlating to within 3-4 dB, with the TLM predicted current being lower than the corresponding NEC values.

4.1.6. Figure 12 represents the elevation radiation patterns for the 10-metre whip monopole. Note that these are the absolute TLM and NEC values.

4.1.7. The NEC and TLM radiation patterns are in very good agreement, correlating to within 3-4 dB across all frequencies modelled.

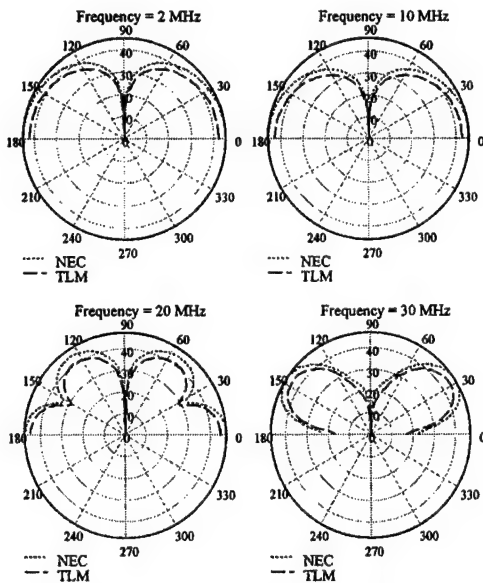


Fig. 12: TLM and NEC elevation radiation patterns for 10 metre monopole.

4.1.8. The predicted voltage standing wave ratio (VSWR) and impedance were also compared for both techniques. These are depicted in figure 13.

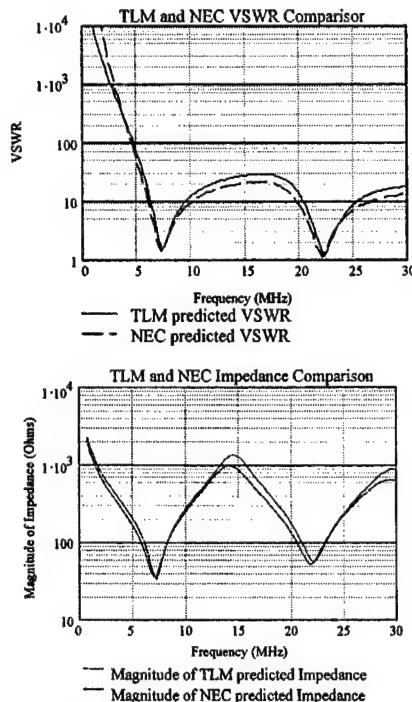


Fig. 13: NEC and TLM VSWR and magnitude of impedance for the 10 metre whip monopole.

4.1.9. Calculation of impedance and VSWR for both simulations show that there is excellent correlation between the two numerical techniques. The magnitude of the impedance determined via both techniques differs by only ~ 1 to 2 dB across the HF band. Similarly, the VSWR varies by ± 1 to 2 dB across the band.

4.1.10. The real and imaginary components of the impedance are also in excellent agreement with standard published texts [6], [7].

4.1.11. The results of this work indicate that TLM modelling can provide results as good as those of NEC.

5. WHOLE SHIP MODELLING.

5.1. A large ship has also been modelled using TLM and NEC in order to assess installed monopole antenna performance [5]. Figures 14, 15 and 16 depict the TLM model and results of a comparison with NEC for the same antenna.

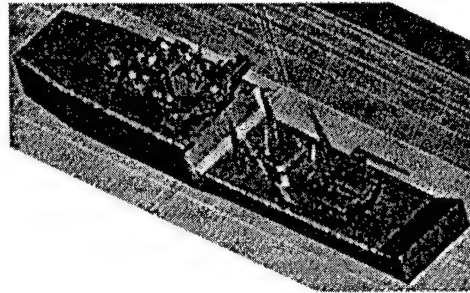


Fig. 14: TLM model of a Ship

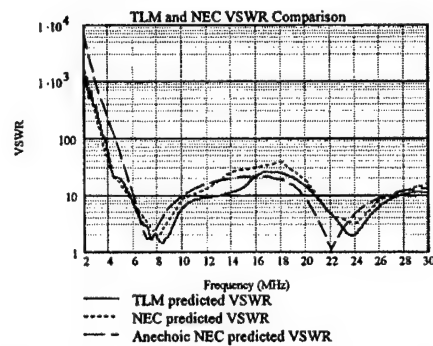


Fig. 15: NEC and TLM VSWR for a ship monopole

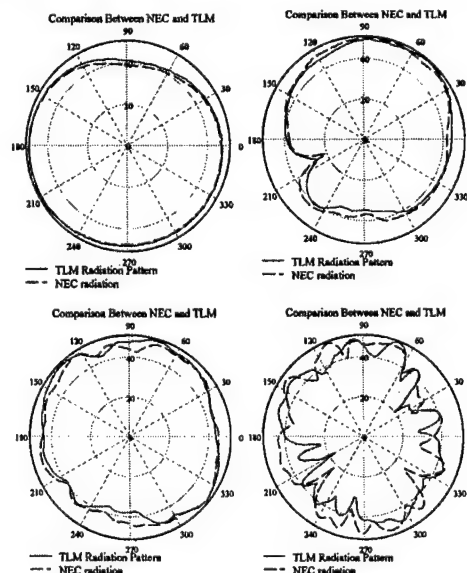


Fig. 16: NEC and TLM Patterns at 2, 10, 20 & 30 MHz

5.2. From figure 16, it can be seen that other than at 30 MHz, the patterns agree to within ~5 dB. However, the discrepancy results from exceeding the frequency limit of the NEC model owing to computer limitations.

5.3. The results from this ship modelling indicate that TLM is capable of providing results comparable to those produced via NEC.

6. SUMMARY AND WAY FORWARD

6.1. TLM is proving to be capable of providing results at least as good, if not better than NEC. Combined with the capability to assess different materials, TLM has the potential to supersede NEC as a tool for the numerical assessment of the electromagnetic environment from radiators and surrounding complex structures.

6.2. It should be noted that comparisons have been focused toward the HF range, where many materials can be modelled as a homogeneous layer. At present, the modelling of inhomogeneous materials can only be performed for very small sections, where the inhomogeneity of the material is modelled directly.

6.3. Though techniques are being developed to address this shortcoming, they are still at the developmental stage [8]. Further work is therefore required in order to develop TLM techniques capable of dealing with these complex materials.

6.4. However, the TLM technique can be run on a commercially available desktop PC, with a reasonable amount of RAM (all TLM models were run on a Pentium II 300 MHz machine with 256 Mbytes, whereas the NEC ship model was run on a SG 2000).

6.5. When run time and the type of workstation required are considered for very complex models such as the ship, TLM can be seen to be more efficient. A Comparison of the SPEC95fp and SPECfp_rate95 (© 1996 Standard Performance Evaluation Corporation) benchmarks for each processor illustrates the difference in efficiency of both techniques.

6.6. The PII 300 has a SPEC95fp and SPECfp_rate95 of 8.49 and 75.1 respectively (© 1998 Intel Corporation). The Origin 2000 has values of 24.5 and 190 respectively (© 1998 SGI). By scaling run times according to these results, the NEC ship model would have taken 30-40 times as long as the TLM model when run on comparable machines for the same output.

6.7. TLM may therefore provide a viable alternative to traditional methods such as NEC for electromagnetic modelling of complex structures, particular those comprised of complex dielectric materials outside the realm of numerical modelling with NEC.

7. REFERENCES

- 7.1. C Christopoulos, 1995 "The Transmission Line Modelling Method", (English) IEEE/OUP IEEE ISBN 0-7803-1017-9, OUP ISBN 0-19-856533-X.
- 7.2. Simons N R S, et al, "Comparison of the TLM and FD-TD Methods for a Problem Containing a Sharp Metallic Edge" (English), IEEE Trans. MTT, Vol. 47 No. 10, 1999.
- 7.3. Kazik, J J, "Prediction of Shielding Performance via the Transmission Line Matrix Method (TLM)" (English) Colloquium on Shielding and Grounding Digest, IEE, London, Jan 2000.
- 7.4. Kazik, J J, (Awaiting Publication) "Cross Code Validation Between NEC 4 and TLM for a 10-metre Whip Monopole", (English), Eighth International Conference on HF Systems and Techniques, University of Guildford UK 10-13 July 2000.
- 7.5. Kazik, J J, "Cross Code Comparison Between NEC 4 AND Transmission Line Matrix (TLM) Methods for Whole Ship Modelling", (English), Digest of the 3rd International Workshop on TLM, IEEE/MMT Society/University of Nice-Sophia Antipolis, France, Oct 1999.
- 7.6. Schelkunoff, S A, "Advanced Antenna Theory", (English), John Wiley & Sons, Inc., page 82, 1952.
- 7.7. Harrington, R F "Time Harmonic Electromagnetic Fields", (English), McGraw-Hill Book Company Inc., page 352, 1961.
- 7.8. Christopoulos C, et al, "Materials Modelling in TLM and EMC Applications", (English), Digest of the 3rd International Workshop on TLM, IEEE/MMT Society/University of Nice-Sophia Antipolis, France, Oct 1999.

BIOGRAPHY

John J Kazik is Head of Theory and Modelling for the EM Engineering Group at DERA Portsmouth West. His main interests are in the development of numerical computational electromagnetic tools, such as TLM and PO/PTD. He obtained his Bachelor's Degree in Physics from Imperial College, London in 1982 and his Masters Degree in Applied Mathematics from Kings College London in 1985. He is an Associate of the Royal College of Science, a Member of the Institute of Electrical and Electronic Engineers, Member of the Institute of Physics and a Chartered Physicist. He is also currently studying for his Doctorate with Nottingham University in TLM.

British Crown Copyright 2000 DERA. Published with the Permission of the Defence Evaluation and Research Agency on behalf of Controller HMSO.

EMC 2000

INTERNATIONAL WROCLAW SYMPOSIUM
ON ELECTROMAGNETIC COMPATIBILITY

ELECTROMAGNETIC ENVIRONMENTAL EFFECTS (E3) AWARENESS IN THE U.S. NAVY

Mr. F.M. Stewart

Space and Naval Warfare Systems Command, attn: Code 051-1E

4301 Pacific Highway, San Diego, California, USA 92110-3127

Voice Tel: USA (619) 524 7230; Fax Tel: USA (619) 524 7224; email: stewartm@spawar.navy.mil

1. INTRODUCTION

The U.S. Navy established an E3 Awareness Program to implement instructions, procedures, and guidelines for system operators so they readily identify EMI problems, institute corrective action, and restore electronic systems to a combat ready status.

2. SCOPE

An initiative has been started within the NATO Naval Armaments Group, Special Working Group Ten (NNAG SWG/10) on Naval Electro-Magnetic Environment Effects to examine E3 Awareness in NATO member nations with the goal of minimizing the effects of EMI.

3. TOPICS

The following are descriptions of E3 related areas. The descriptions are of seminars or technical materials that have been used in classes and briefings.

Understanding & Applying MIL-STD-461D

A practical interpretation of the standard including design, testing and control requirements. Discusses the emission and susceptibility requirements of each part in detail, test instrumentation and facilities needs and the EMI control requirements, including contract data requirements, EMI Test Plan, EMI Test Report and EMI Control Plan.

Design and Test to Meet E3 Requirements

This is design requirements for project engineers. The sources of EMC requirements, their justification, and their interpretation. Specific design techniques are presented with rationale and objectives.

Application and Use of MIL-STD-237 (Overview) Training Course

This provides E3 guidance for Program Managers responsible for acquisitions and explains the new DoD acquisition process now reflected in Revision B to MIL-HDBK-237. Special emphasis is given to the acquisition of non-developmental items (NDI)

and commercial items (CI) for use in unique military operational environments. Expands on the material provided in the PM E3 Awareness course. (1/2) day.

MIL-STD-462D Testing

This seminar is a hands-on testing course specifically tailored for DoD personnel who perform testing performed in accordance with MIL-STD-462D. Includes design, testing and control requirements and discusses emission and susceptibility requirements, test instrumentation and essential facilities. Features hands-on test workshops in R&B's extensive laboratory. (3 days).

MIL-STD-461/462 Testing

This seminar is specially tailored for DoD personnel who witness, supervise or review for compliance, testing in accordance with MIL-STD-461/462. It provides an overview of the Navy's E3 program and the necessity for compliance. Additionally, the purpose, performance criteria, and acceptable alternatives for each test. Typical contractor shortcuts and avoidance techniques are summarized.

EMI Controls for Shore Installations

This describes the causes of EMI problems found at ground installations and how they may be corrected and /or precluded. Guidelines for purchasing equipment and modifying existing equipment to improve its EMI immunity are provided. Facilities design and modification is covered. The testing procedures for ground installations, including site surveys, ESD evaluations and related documentation is covered. Non-military EMI controls, such as FCC requirements and IEEE evaluation criteria are included. This information is intended for personnel responsible for facility design, equipment acquisition, equipment installation and equipment operations for ground installations.

Electromagnetic Radiation Hazards Awareness

The purpose of this seminar is to provide information on the potential hazards to humans from electromagnetic radiation, sometimes called microwave radiation. This knowledge should enable the participant to intelligently deal with any RADHAZ problems that he encounters. The material covered includes background information, requirements, definitions, permissible exposure limits, electromagnetic fields, calculation of electromagnetic fields, measurements, protective measures, reporting of overexposure and RADHAZ related organizations.

Electromagnetic Pulse (EMP)

An introduction to understanding the EMP phenomenon, the causes and effects of EMP, EMP hardening and effective testing programs. Addresses effects in cables and antennas, EMP standards, lightning, and personnel safety. The requirements for CS116 and RS105 in MIL-STD-461D including equipment requirements, conducted susceptibility and radiated susceptibility testing methods are reviewed and discussed.

Grounding, Bonding & Shielding

A broad-based treatment of the elements of design and materials selection to provide EMI protection and suppression. Covers grounding considerations, categories and safety. Types and methods of bonding and examples are given. Shielding techniques, including near/far field considerations, gaskets, apertures, and cabling, as well as a brief review of printed circuit board considerations, are discussed.

Transient Testing

Introduces laboratory personnel to the phenomena of Electromagnetic Pulse (EMP), Lightning and Electrostatic Discharge (ESD), and discusses safety precautions and test methods. Particular attention is paid to EMI/EMC testing in accordance with MIL-STD-461D, RTCA DO-160, MIL-STD-1757 and related specifications and standards.

Electromagnetic Compatibility (EMC) by Design

An in-depth technical treatment of the design criteria of a wide spectrum of EMI considerations. Includes EMC management, cable coupling, grounding, bonding and shielding, filters, receivers and transmitters, transient suppression, and other topics.

Guidelines for the Use of Commercial Technologies for Military E3 Applications

The major emphasis of this is the evaluation and selection, from an E3 perspective, of already developed equipment capable of fulfilling Navy operational requirements with little or no modification. These nondevelopmental items (NDI) allow the Navy to take advantage of technological advances resulting from the competitive pressures of the commercial marketplace as well as developments in other DoD or Government agencies. However, the implications on electromagnetic compatibility of the overall weapon system must be carefully considered. Understanding EC and Other Commercial Requirements & Test Methods

Comprehensive overview of European Community (EC) requirements and the EMC Directive. Explains test standards and procedures, preparation of a TCF, application of CE mark and other requirements. Includes laboratory demonstrations of emissions and immunity testing. Removes all mystery and confusion.

Introduction to EMI

A basic treatment of the "whys and hows" of EMI/EMC for non-EMC personnel, those new to the EMC field and/or those desiring a review of the essential principles. Includes terms and definitions, sources and effects of EMI, some design and testing considerations, concepts of retrofits and the financial impact of cost-effective planning.

Guidelines for the Use of MIL-STD-464, Interface Standard for System Electromagnetic Environmental Effects Requirements

This seminar explains the evolution of MIL-STD-464 and the new system level E3 requirements it mandates. The seminar details the baseline requirements of the new specification and covers the E3 interface and performance requirements, and verification requirements for airborne, sea, space and ground systems, including ordnance. The effects of the increasing use of commercial items and NDI in military operational environments is also discussed.

4. SUMMARY

Awareness of these topics in the engineering, technical and programmatic communities will lead to reducing incidents of EMI.

BIOGRAPHICAL NOTE

Mr. Stewart has worked in the E3 area since 1987. He earned his Electrical Engineer graduate (BSEE) from the University of Arkansas; and his Masters degree in Engineering Management from George Washington University. His present job includes Electromagnetic Environmental Effects (E3); Shipboard Topside Design & Integration; and Research and Development of EMC Software for the US Navy.



III WORKSHOPS

EMC 2000

INTERNATIONAL WROCLAW SYMPOSIUM ON ELECTROMAGNETIC COMPATIBILITY WORKSHOP

Automotive EMC Directive and the use of radio products in vehicles

Detlev Aust
Chairman of ETSI ERM TG4,
Nokia GmbH, Meesmannstraße 103, D-44807 Bochum, Germany,
e-mail: detlev.aust@nokia.com

1. ABSTRACT

Radio and telecommunication testing issues have always been a part of ETSI work, especially in the field of EMC. For radio and telecommunication equipment generally the requirements of the R&TTE Directive 1999/5/EC [1] have to be fulfilled before introducing new radio products into the European market. Additionally there are product specific Council Directives, which have to be applied, when a product falls under their particular scope. For radio and telecommunication equipment and their ancillary equipment intended for installation into vehicles the requirements of the automotive directive 95/54/EC [2] need to be considered. This paper describes the activities of ETSI ERM Task Group 4 to minimise practical problems in the application of Council Directive 95/54/EC on radio communication equipment.

2. INTRODUCTION

The number of wireless data systems, radio communication equipment and telematic traffic systems designed for the installation into vehicles have increased heavily in the last years. Basically there are terrestrial mobile systems (e.g. GSM, TETRA, D-AMPS), two-way satellite communication systems (e.g. Globalstar, INMARSAT), broadcast receivers (e.g. GPS, FM radio) providing the driver of a vehicle with a variety of useful services (e.g. traffic information, emergency services, entertainment). This development will even go on with several new technologies (e.g. UMTS, WAP, Bluetooth) making available additional value added services to the customer in the near future.

In the area of EMC for the systems above, two product specific Directives have to be taken into account: the R&TTE Directive and the automotive EMC directive. (Fig. 1.). Both vertical Directives are designed to ensure electromagnetic compatibility,

but due to the different history and evolution of the two Directives there are great differences in type approval process and measurement methods.

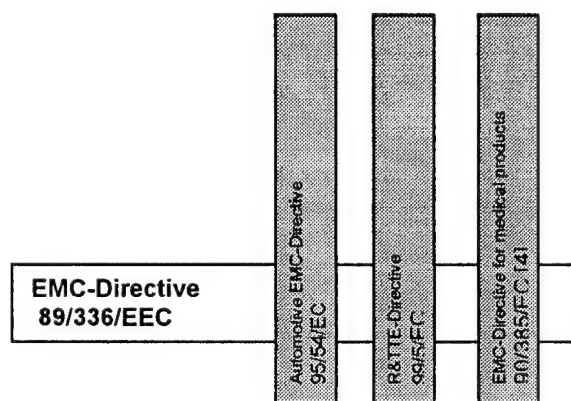


Fig.1: Selection of Council Directives covering EMC

3. COMPARISON OF AUTOMOTIVE EMC AND R&TTE DIRECTIVE

The general horizontal EMC Directive 89/336/EEC [3] (Fig. 1) states that where a vertical Directive for a specific product exists, then this should take precedence. Based on the Directive 72/245/EEC [5] dealing with the interference of ignition systems the Directive 95/54/EC was created to modify the existing directive to become a product-specific Directive. The aim was to define a minimum set of EMC requirements needed for the certification of a vehicle or independent technical unit intended for fitment into vehicles.

Contrary to 'new approach' Directives like R&TTE which focus on the objectives and the necessary type approval procedures, the automotive EMC Directive was designed as an 'old approach'

Directive including all technical specifications like test methods and limits (e.g. Fig. 2 and Fig. 3).

'New approach' Directives (e.g. 89/336/EEC, 1999/5/EC) use harmonised Standards (e.g. EN 55022 [6]) to define the testing methods and limits with the advantage of more flexibility to adapt the objectives to different product types and technical evolutions.

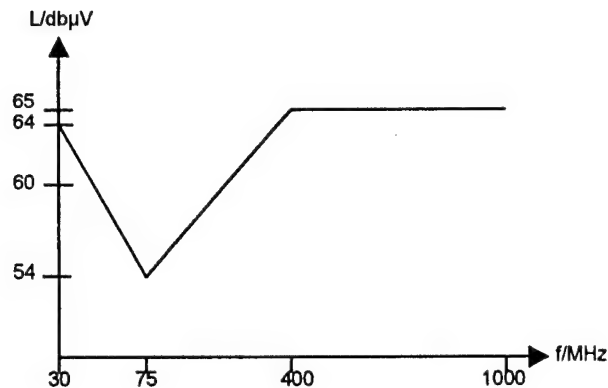


Fig. 2: Emission requirements in 95/54/EC:
Limit Broadband

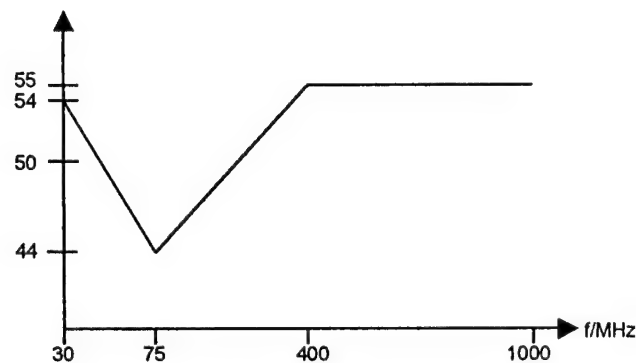


Fig. 3: Emission requirements in 95/54/EC:
Limit Narrowband

The Directive 95/54/EC applies to all vehicles and their components, which come under the scope of the framework directive 70/156/EEC [7] (amended by 92/53/EEC [8]). These covers vehicles, which have a maximum speed exceeding 25 km/h, 4 or more wheels and are intended for use on public roads. Vehicle trailers are included in the framework, but agricultural tractors, mobile machinery and vehicles, which run on rails, are excluded.

For the certification of a vehicle or an electric/electronic subassembly (ESA) it is

mandatory to include a competent authority. The directive allows the certification of a vehicle either by testing the complete vehicle or by testing all relevant independent components. Vehicles certified to Directive 95/54/EC will require an 'e'-marking incorporating a reference number, which identifies the Member State that has granted the type-approval, the amendment number of the directive and the unique reference number of the type approval certificate.

The R&TTE Directive gives the possibility of four different type approval routes based in principle on a technical documentation and the presumption of conformity to harmonised standards. The manufacturer can choose the procedure. E.g. by implementing and maintaining a full quality management system certified by a notified body the manufacturer is allowed to issue declaration of conformity for a product if harmonised standards are applied. This leads to the consequence that manufacturer has the complete responsibility of introducing new products into the market with the advantage of better flexibility and more accurate timing. A radio-transmitting product, which is in conformity with the R&TTE directive, must bear a 'CE'-mark.

4. PROBLEM FIELDS

Due to the fact that the Directive 95/54/EC was designed in principal for the type approval of vehicles, several different product specific characteristics of radio transmitters are not explicitly defined in this Directive. This leads to different interpretations of the requirements either by vehicle and radio equipment manufacturers, competent authorities and technical services (test laboratories). Especially in case of aftermarket products this may result in potential difficulties to enter the EU market. Additional there are overlaps in the Directives resulting in different, duplicated test methods for same protection objectives.

One specific clause (Annex I, article 4.3.2.3) of the Directive 95/54/EC requires the vehicle manufacturer to define the maximum power which may be used by a transmitter installed in the vehicle, if requested by a competent authority. Due to the fact that digital mobile communication networks are designed to interoperate with transmitters using defined power levels, any modification of the levels will harm the functionality of such a system.

The use of mobile communications devices in vehicles is becoming more and more a part of our daily live, e.g. the use of mobile phones in the

backseats of taxis is a common known everyday event. Some not unambiguous clauses set out in the Directive 95/54/EC can lead to interpretations, which are in contradiction with the requirements of the users of mobile communication equipment, such as businessmen, policemen, fire brigade, emergency and security services.

5. SOLUTIONS

ETSI ERM established a joint working group with ACEA (European Automobile Manufacturers Association) in 1998 to agree on common interpretation and application of the automotive EMC Directive concerning radio products. The issue has been driven and co-ordinated by a Task Group founded inside the committee for this special purpose (TG4 'automotive directive').

Different activities were initiated through the working groups like the development of 'EMC guidelines for installation of aftermarket radio frequency transmitting equipment in road vehicles' by ISO (International Standardisation Organisation; responsible working group ISO TC 22/SC3/WG3).

One major target was to ensure that EMC tests should be performed just once to meet the objectives of both Directives. Several discussions with the European Commission resulted in the decision of DG (Direction Générale) Enterprise / Vehicle department to set up a study on the application of Directive 95/54/EC, especially considering aftermarket products.

The study was launched in April 2000 and is supported by ETSI, ACEA, CLEPA (car suppliers' association) and EACEM (consumer electronics manufacturers association).

5. CONCLUSION

The study of the European commission on the Directive 95/54/EC will try to identify the problems of all concerned industries and competent Services in application of the latter Directive. Based on the results, which are expected for autumn 2000 a decision will be taken by the EU Commission, if changes, amendments or an additional interpretation is necessary for clarification. The working group ETSI ERM TG4 will accompany the activities.

6. REFERENCES

[1] European Commission, Directive 1999/5/EC of the European Parliament and of the Council of 9 March 1999 on radio equipment and

telecommunications terminal equipment and the mutual recognition of their conformity

[2] European Commission, Commission Directive 95/54/EC of 31 October 1995 adapting to technical progress Council Directive 72/245/EEC on the approximation of the laws of the Member States relating to the suppression of radio interference produced by spark-ignition engines fitted to motor vehicles and amending Directive 70/156/EEC on the approximation of the laws of the Member States relating to the type-approval of motor vehicles and their trailers

[3] European Commission, Council Directive 89/336/EEC of 3 May 1989 on the approximation of the laws of the Member States relating to electromagnetic compatibility

[4] European Commission, Council Directive 90/385/EEC of 20 June 1990 on the approximation of the laws of the Member States relating to active implantable medical devices

[5] European Commission, Council Directive 72/245/EEC of 20 June 1972 on the approximation of the laws of the Member States relating to the suppression of radio interference produced by spark-ignition engines fitted to motor vehicles

[6] CENELEC, Standard EN 55022: Information technology equipment - Radio disturbance characteristics - Limits and methods of measurement

[7] European Commission, Council Directive 70/156/EEC of 6 February 1970 on the approximation of the laws of the Member States relating to the type-approval of motor vehicles and their trailers

[8] European Commission, Council Directive No 92/53/EEC of 18 June 1992 amending Directive 70/156/EEC on the approximation of the laws of the Member States relating to the type-approval of motor vehicles and their trailers

BIOGRAPHICAL NOTE

Detlev Aust received the M.S. degree from the University of Dortmund, Germany in the field of electrical engineering. From 1990 he worked on the test development for automotive IC's in semiconductor industry. In 1994 he joined the network operator e-plus responsible for the quality management of mobile phones. Since 1999 he is with Nokia, Germany as Standardisation Engineering Manager. Inside ETSI he is the chairman of ETSI ERM Task Group 4.

EMC 2000

INTERNATIONAL WROCLAW SYMPOSIUM ON ELECTROMAGNETIC COMPATIBILITY WORKSHOP

MARITIME EMC AND THE INTERNATIONAL COMMUNITY

Eirik O. Blikrud
Norwegian Post and Telecommunications Authority
P.O.Box 447, 0104 Oslo
Norway

Tel: + 47 22 82 48 75
Fax: + 47 22 82 48 90

eirik.blikrud@npt.no

The maritime community is inherently truly global and therefore dependent on international agreements and regulations. ETSI is playing an important role in this work by preparing EMC standards for maritime equipment in accordance with relevant European Directives as well as international requirements and recommendations and in co-operation with other international standardisation organisations.

1. INTRODUCTION

The maritime world is by nature truly international and the maritime community embraces most countries with a sea shore and even some land locked countries.

The global nature of the maritime world has necessitated international agreements and the maritime community consists of a number of international organisations. As for telecommunications, this is indicated as up to recently, more than 90 % of ITU's Radio Regulations [1] concerned maritime frequency matters, technical parameters and operational procedures for maritime communications, and the International Maritime Organization (IMO), which today is the United Nations' special agency on maritime safety matters, has roots back to the very beginning of last century.

The environment on board a ship is a closed world with a large number of electrical and electronic equipment and has experienced EMI and EMC

problems long before these topics were as clearly identified as they are today.

2. MARITIME EMC

2.1 GENERAL

The nature of maritime EMC is not in principle different from other EMC environments, but the EMC sensitive elements are packed closely together and some of the element parameters are large: A ship may well have generators producing 2 MW, consumer elements may often consume 400 kW, HF transmitters have generally 2 kW output power and radar transmitters may have pulse powers of several hundred kW.

The sensitivity of a radio receiver may be around 1 μ V and a radar installation may have sensitivity of - 100 dBm.

In addition to the fact that the dynamic power range of such installations may be more than 190 dB, malfunctioning of the system may seriously jeopardise the safety of shipping as well as the safety of life at sea.

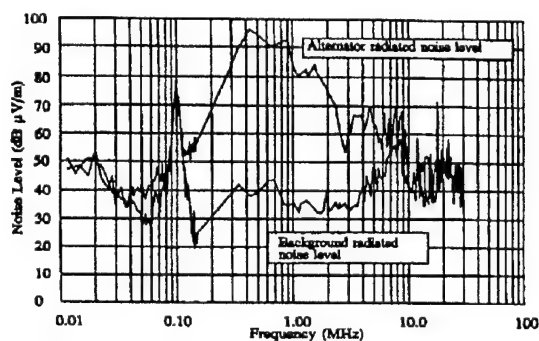
2.2 IMO REQUIREMENTS ON EMC

Already for many years, IMO has required that all reasonable and practicable steps should be taken to ensure electromagnetic compatibility between any equipment concerned and other mandatory

radio communication and navigational equipment carried on board. Lately, IMO has recognised the need to prepare standards on EMC for all electrical and electronic ship's equipment to ensure the operational reliability of such equipment and is inviting Governments to ensure that all ship's electrical and electronic equipment are tested to relevant EMC standards, cf. IMO Resolution A.813(19) [2].

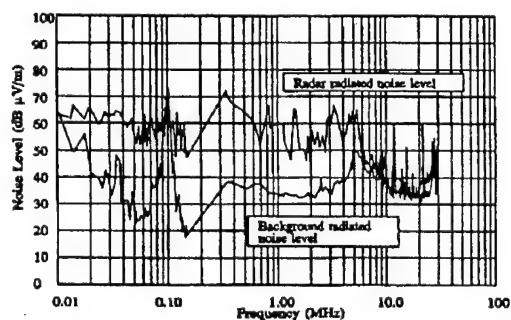
2.3 LEVEL OF EMI ON BOARD SHIPS

To indicate the levels of interference that may be found on board ships, Figure 1 shows the radiated noise pattern from an alternator and Figure 2 shows the radiated noise from a 9 GHz radar installation.



Typical alternator radiated noise pattern.

Fig. 1



Typical radiated noise level from a radar installation.

Fig. 2

3. ETSI's WORK WITH MARITIME EMC

ETSI's work with maritime EMC is taking place in the technical committee for electromagnetic compatibility and radio spectrum matters (TC ERM) and in its sub-groups WG EMC and RP-01

as well as in a special task group on maritime EMC (TG5).

Up to now, requirements for each category of maritime radio equipment have been included in two separate standards, one with radio related requirements and one with EMC requirements. This has led to a large number of standards where the different EMC standards only had minor differences. TG5 was set up in order to identify and systemise the maritime EMC requirements and propose actions to reduce the number of standards.

TG5 has prepared a draft ETSI Guide concerning EMC requirements in maritime standards. The Guide is intended to have two purposes:

- serve as a single, general source containing all maritime EMC requirements that may be relevant when preparing maritime EMC standards
- give guidance how to prepare standards for maritime radio equipment that combine EMC and radio technical requirements in one standard (integrated standard)

The Guide describes how integrated standards combining EMC and radio technical requirements may be structured. Further, the Guide describes the sequence of tests and tables all relevant EMC requirements.

Although an integrated standard amalgamates both the radio technical and EMC requirements, all EMC requirements are still easily identifiable as both the EMC and the radio parameters are put in different, dedicated clauses.

Technical requirements related to the antenna port of a radio equipment are found in the radio technical part of an integrated standard and the EMC part contains technical requirements related to the other ports of an equipment (classical EMC parameters).

The Guide contains also a library of proposed text modules for different EMC measurements where it is the intention that relevant text modules may be used directly in an integrated standard.

4. CO-OPERATION WITH IEC/CENELEC

ETSI is co-operating with IEC/CENELEC through a co-operation agreement of 1995. The purpose of this agreement is to ensure maximum coherence between ETSI and IEC standards, to avoid

duplication of standardisation activities between ETSI, IEC and CENELEC and to promote further co-operation in the standardisation processes.

As for maritime equipment, ETSI is responsible for preparing standards for radio communications equipment while CENELEC (IEC) shall prepare standards for maritime navigational equipment. The standards should include both radio technical and EMC requirements.

When ETSI prepares EMC standards for maritime equipment, due considerations are given to the CENELEC/IEC standard 60945 [3] which is a basic product family standard for maritime radio equipment with general requirements for both communication and navigation equipment

5. ETSI's MARITIME EMC STANDARDS

5.1 MARINE EQUIPMENT DIRECTIVE

The EU Directive on marine equipment (96/98/EC [4] as amended) is applicable for ships subject to the IMO SOLAS Convention (generally ships above 300 tons in international trade). This Directive states clearly that such equipment shall be subject only to that Directive and it excludes all other directives, like the EMC Directive [5].

Based on the ETSI Guide concerning maritime EMC requirements, single integrated standards for maritime equipment subject to the Marine Directive may be prepared.

5.2 R&TTE DIRECTIVE

Maritime radio equipment which falls outside the Marine Directive, are subject to the R&TTE Directive [6]. For such equipment, a standard should distinguish between the different categories of requirements, however, all requirements may still be contained in one standard if the EMC requirements are clearly identifiable.

6. MARITIME EMC REQUIREMENTS

The relevant EMC requirements for maritime communication equipment are listed in the ETSI Guide and includes the following technical parameters:

- 6.1 EMC radiated emissions for ancillary equipment which are measured in the frequency range 30 MHz to 1 GHz

- 6.2 Conducted emissions on the power ports that are measured in the frequency range 10 kHz to 30 MHz
- 6.3 RF electromagnetic immunity tests that are carried out in the frequency range 80 MHz to 1 GHz. The test level is 10 V/m
- 6.4 Immunity against electrostatic discharge that are measured with 6 kV contact discharge and 8 kV air discharge
- 6.5 Immunity against fast transients on the power lines that are measured a number of 15 ms bursts with 2 kV test level
- 6.6 Immunity against conducted disturbances that are measured with radio frequencies applied on the power ports. In some frequency bands, the test signal level is 10 V rms
- 6.7 Immunity against short term power supply variations that are tested with variations in the supply voltage of ± 20 V
- 6.8 Immunity against power supply failure that is tested with a power supply break of 60 s
- 6.9 With a 0,5 kV line-to-line and a 1 kV line-to-ground voltage added on the power supply, the immunity against surges are tested

7. CONCLUSIONS

Standards for maritime EMC are of essential importance for international shipping and for safety of life at sea. The EMC requirements in the standards prepared by ETSI have been selected to ensure an adequate level of compatibility for apparatus intended to be used in maritime environments.

8. REFERENCES

- 8.1 International Telecommunication Union: Radio Regulations, Geneva 1998
- 8.2 International Maritime Organization Resolution A.813(19): General requirements for electromagnetic compatibility (EMC) for all electrical and electronic ship's equipment, London, 1995

- 8.3 EN 60945: "Maritime navigation and radio communication equipment and systems. General requirements - Methods of measurement and required results".
- 8.4 Council Directive 96/98/EC on marine equipment, Brussels, 1996
- 8.5 Council Directive 89/336/EEC on the approximation of the laws of the Member States relating to electromagnetic compatibility
- 8.6 Directive 1999/5/EC of the European Parliament and of Council of 9 March 1999 on radio equipment and telecommunications terminals and the mutual recognition of their conformity

BIOGRAPHICAL NOTE

Eirik O. Blikrud is an electrotechnical engineer from the Norwegian Technical University. He is now working for the Norwegian Post and Telecommunications Authority with international standardisation for maritime communications and navigation equipment.

He has been chairman of ETSI STC RES-01 and ETSI ERM TG5, and is presently chairman of the technical working group in the IMO COMSAR Sub-Committee.

EMC 2000

INTERNATIONAL WROCLAW SYMPOSIUM ON ELECTROMAGNETIC COMPATIBILITY WORKSHOP

THE INTERFACE BETWEEN ETSI AND THE SPECTRUM MANAGERS IN THE EUROPEAN RADIOCOMMUNICATIONS COMMITTEE (ERC) OF THE EUROPEAN CONFERENCE OF POSTAL AND TELECOMMUNICATIONS ADMINISTRATIONS (CEPT)

by Georges de Brito
France Telecom R&D
38 - 40, rue du Général Leclerc
92 794 Issy les Moulineaux Cedex 9
France

Tel : 00 33 1 45 29 45 93
Fax : 00 33 1 45 29 69 62

georges.debrito@francetelecom.fr

Bacchus was born from the leg (more precisely the thigh) of Jupiter ... as also happened with ETSI... ever since, CEPT and ETSI have been enjoying parallel lives.

This paper, relating to a series of presentations for a dedicated session, provides a simplistic picture of both ETSI and CEPT/ERC, in order to focus specifically on the relations between these two organisations, in their joint effort to support the definition and use of radio equipment.

1. INTRODUCTION

ETSI is one of the Standards Organisations recognised by the European Commission.

Among its "Technical Bodies", a number are dealing with radio products. Obviously, such products require spectral resources for their normal operation. Their design may be depending on the resources made available ... by CEPT; conversely, the spectrum allocations may depend on market needs, which to a certain extent may be best known by some of the typical ETSI members such as operators, manufacturers and users (which are not "CEPT members").

As a result a very close co-operation is required between ETSI and CEPT in order to enhance efficiency in the use of the radio spectrum. One of the Working Groups of TC-ERM, WG ERM - RM, is responsible (from the ETSI side) for the interface between these two organisations.

After a brief presentation of the two organisations, this paper will focus on the role of ETSI WG ERM - RM in the relations between the two organisations and the methods used; the full terms of reference and working procedures of the WG are provided in an annex.

2. THE PARTNERS

Their names have already been identified, but further details are necessary in order to allow for a clear understanding of the mechanisms and of the relations between them (and also of the problems these relations, in turn, may generate).

2.1. ETSI

ETSI was born at the end of the eighties (it is just over 10 years now) when a number of standardisation work items were brought over from CEPT (e.g. GSM).

Its structure has hopefully been made clear in other papers ... In short, it is an association under French law (the so called "1901 Law") having a very wide membership and where a significant number of Technical Bodies (TBs), Technical Committees (TCs) and ETSI Projects (EPs), prepare, among others, a variety of types of standards (ENs, ESs, etc) for the benefit of the Telecommunications Community.

TBs often have Working Groups to support their activities. Among them, WG RM (Radio Matters) which is often quoted in this paper. WG RM reports to TC-

ERM (the TC dealing with Electro Magnetic Compatibility and Radio Spectrum Matters).

Further information concerning ETSI may be found in the ETSI web site : <http://www.etsi.org>.

2.2. ERC

CEPT, the European Conference of Postal and Telecommunications Administrations has some 43 Members; Poland is one of them. Its legal basis is also close to those of an association.

The European Radiocommunications Committee (ERC) is clearly the more relevant committee of CEPT for the area of radiocommunications, while other committees handle topics such as telecommunications in general; satellite communications are also covered by CEPT.

ERC has three permanent Working Groups (FM, SE and RR as shown in the diagram below), and a number of other groups and Task Groups (TGs).

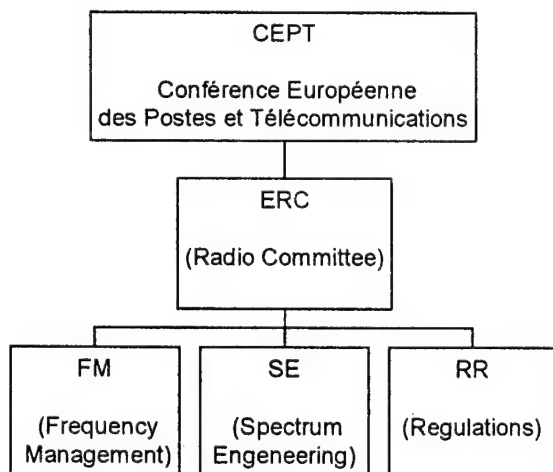
Among the usual outputs of the work and decisions reached by ERC are Recommendations, Reports and Decisions.

"CEPT Decisions" are binding for the Administrations that have indicated their intention to follow them.

WG ERM - RM has a closer co-operation with these 3 permanent groups as well as with TG1 (which focus on UMTS) and CPG (which focus on the WRC Conference).

CPG and TG1 are more task oriented, while FM, SE and RR are "horizontal" groups.

CEPT and ERC



FM is the Working Group responsible, among others, for the decisions concerning frequencies. These are to be harmonised across Europe, but at the moment, this is not, unfortunately, always the case...

Its decisions are often based on technical analysis performed by SE: the Spectrum Engineering WG.

As it is indicated by its name, RR deals with Regulations ... and is at the moment quite busy with the effects of the implementation in Europe of the R&TTE Directive (within the European Community, it is mandatory for all Members States to implement all the Directives).

The work of ERC is supported by a permanent organisation, the European Radiocommunications Office (ERO). ERO is providing support to ERC (e.g. defining and maintaining a number of databases and servers) but also has its own activities, including studies and surveys.

Further information on ERC and ERO can be found in the ERO web site: <http://www.ero.dk>.

3. THE ROLE OF WG ERM - RM

The need for a close co-operation had been identified since day one; it has been materialised by the signature of a Memorandum of Understanding (MoU) between the two organisations.

Furthermore, most (if not all) of the Administrations members of CEPT are also ETSI members, so a number of participants in ERC meetings are also participating in ETSI meetings; but the responsibilities are different, even when the topics discussed are related.

ETSI having both a vertical (EPs) and horizontal structure (TCs), one of the task of RM is to convert these vertical and possibly conflicting flows of information and views into, hopefully, some more homogeneous material usable by the various ERC bodies (typically horizontal). The difference of structure between ETSI and ERC (there are not many horizontal TBs within ETSI) make this interface particularly important and difficult to handle.

In these relations, ETSI is often the body asking for frequencies (for new products and services, handled by one of the various TBs) and ERC is the body trying to find resources (frequency bands) which have to fit in an already overcrowded spectrum...

In return, ERC may request technical constraints for equipment using such or such frequency band, e.g. for co-existence and/or compatibility purposes.

In order for such iteration process to converge quickly, fast routes are required!

4. METHODS AND PEOPLE

In order to facilitate this process, the following methods are generally used:

- the requests originated in ETSI are often supported by a brief description of the proposal and of the

corresponding needs in terms of spectrum, the System Reference Document (the SRDoc), which is easier to handle and has a broader scope than the corresponding Draft Standard ;

- these request are usually sent using "Liaison Statements" (LSs) ;
- the liaison statements are supported by the RM Liaison Officers (LOs have been nominated so far for liaison with FM, SE, RR, CPG and TG1); LOs attend regularly the corresponding meetings ;
- the Liaison Officers (LOs) are expected to present (only) harmonised ETSI views ;
- the Liaison Officers can be assisted, as needed, by experts from the appropriate TB(s).

The Chairman of WG RM is also a regular participant in the ERC committee meetings.

A number of SRDocs have been made available so far, based on a model SRDoc drafted by RM and published by ETSI as an ETSI Report (TR 101 788).

Typically, the TB in charge of the topic drafts SRDocs. WG RM subsequently offers them for approval. At that time, the views of the TB in charge are confronted with the views of the representatives of other TBs, which may also have (diverging) interests for the same spectrum. From the confrontation will hopefully rise an ETSI harmonised view...

More technical debates may also occur in WG RM when technical requirements relating to a certain type of equipment or technology are in conflict with the needs or interest of others. In such case, co-operation with WG SE of ERC can also be very fruitful. WG SE and its Project Teams (PTs) have carried out a number of compatibility studies, in particular for systems operating in adjacent bands (e.g. in SE 7).

The end result of such technical work is normally two fold:

- publication by CEPT of Decisions and/or Recommendations as appropriate ;
- publication by ETSI of the Standard(s) for the corresponding products.

Last but not least, it has to be noted that there are also regular meetings between ERC and ETSI.

Such meetings focus normally on general questions, while WG RM addresses normally the technical issues.

5. CONCLUSIONS

This paper has briefly presented the flow of information across the interface between ERC and ETSI and its implications.

However, it has to be made clear that both organisations are quite fast moving universes and that the

legislation in the European Community may also change quite fast.

As a result, it has to be noted that the interface has to be adapted and adjusted every day to the evolution of the various roles and needs...

This paper tried to briefly present to-day's situation...

ANNEXES

A.1 TERMS OF REFERENCE

In order to provide the full visibility of this interface, the terms of reference of

"WORKING GROUP RADIO MATTERS (RM)
OF THE ETSI TECHNICAL COMMITTEE
EMC AND RADIO SPECTRUM MATTERS (ERM)"

have been provided here after.

RESPONSIBILITY

- On behalf of TC ERM, WG RM is responsible for spectrum parameters in ETSI deliverables in order to ensure the efficient use of the radio spectrum and inter-system compatibility.
- WG RM administers the CEPT ERC / ETSI MoU on behalf of ETSI.
- WG RM co-ordinates the ETSI positions on the efficient use of the radio spectrum and on spectrum allocations.
- WG RM acts on behalf of TC ERM as the formal ETSI-interface to other organisations (e.g. CEPT, EU, ITU-R, etc.) relating radio spectrum matters.

AREAS OF ACTIVITY

- WG RM will establish a close liaison and an interactive process of consultation with CEPT ERC and its Working Groups FM, SE, RR and the CPG by the nomination of Liaison Officers representing ETSI views in meetings of these committees.
- WG RM will, from the beginning and for the duration of the standardisation process, establish a close liaison with the ETSI NBDG and the ETSI technical bodies that produce standards for radio equipment and systems by requesting the nomination of Experts Rapporteurs to provide liaison with the RM Working Group.
- WG RM will, as required, convene temporary Task Groups for specific work items, e. g. to review and endorse ETSI deliverables prior to Public Enquiry.
- In co-operation with ERC WGs and other specialised bodies, WG RM will prepare, as necessary, Technical Reports on radio spectrum efficiency and inter-system compatibility.
- In co-operation with external specialised bodies (e.g. ERC), WG RM will act as ETSI co-ordination centre of technical expertise in the field of radio spectrum matters.

- WG RM will report to TC ERM on its activities.

To achieve the above, the following Working Procedures will be used.

A.2 Working Procedures of WG RM

To improve the efficiency of the execution of the CEPT ERC/ETSI MoU, the following working procedures apply:

- To ensure a good co-ordination in line with the CEPT ERC/ETSI MoU, WG RM will nominate Liaison Officers to attend the ERC and ERC Working Groups meetings. The WG RM Chairman shall represent ETSI views in the ERC and the WG RM vice-Chairmen in the ERC Working Groups.
- WG RM will require the appointment of expert(s) from the originating ETSI Technical Bodies producing radio standards. These will act as expert rapporteurs for the specific work programme, e.g. radio standards, and will attend the relevant ETSI WG RM and ERC Working Group's project teams.
- The aforementioned expert rapporteurs from the ETSI bodies should participate in any task group that WG RM may establish for the purpose of reviewing and endorsing radio parameters contained in radio standards which those ETSI bodies may be developing.
- In order to co-ordinate the spectrum demand and ensure inter-system compatibility, WG RM:
 - will require from the originating ETSI Technical bodies and as soon as a new Work Item using radio technology is proposed, a 'System Reference Document' giving the working assumptions as required by the CEPT ERC/ETSI MoU (see section 3.2);
 - will then circulate the 'System Reference Document' among all ETSI bodies involved for potential comments.

The 'System Reference Document' for which a framework template will be defined by WG RM, will include as a minimum:

- A System Description, e.g. the type of service, the traffic evaluation etc;
- Information on key spectrum parameters e.g. RF power, bandwidth, access method, proposed frequency bands and channel arrangement etc.

In case of conflict, WG RM will manage the co-ordination to achieve a consensus. If no consensus can be achieved, the issue is deferred to TC-ERM for final decision.

If no problem is detected, WG RM will then supply the approved 'System Reference Document' and other relevant information to CEPT ERC. This documentation will start the subsequent co-ordination activities between ETSI WG RM and ERC according to sections 3.5 and 3.6 of the CEPT ERC/ETSI MoU.

- To facilitate an efficient bi-directional co-ordination between ETSI and ERC, ETSI will encourage the ERC to nominate responsible persons on the specific issues identified by WG RM.
- Progress on the co-ordination activities with ERC will be reported to WG RM by the ETSI Liaison Officers.
- A work plan, which identifies and tracks the progress on specific radio issues will be handled by WG RM.

The outcome of the above-mentioned joint CEPT/ETSI co-ordinated studies and activities will result in co-ordinated ETSI deliverables and CEPT ERC Recommendations and Decisions.

BIOGRAPHICAL NOTE

Georges de Brito is presently the Chairman of WG ERM - RM of ETSI, after having participated in the GSM adventure, in particular in the definition of the GSM architecture, as Vice-Chairman of COST 207 and 231, and Vice-Chairman of SCEG and SCEG - DTX (Groups responsible, among others, for the definition of the speech codec for GSM).

He is presently working in the research centre of France Telecom R&D situated in Issy les Moulineaux, France (a suburban part of Paris).

After completing the "Ecole Polytechnique", in Paris, he specialised in Telecommunications in the ENST (Ecole Nationale Supérieure des Telecommunications), followed by a "DEA" in Optimal Control, both also in Paris.



He also holds a number of flying certificates, which have enabled him to fly as a hobby over 4 Continents (including flights between Paris and both North and South America, China, Poland, Arctic Ice Cap, etc.).

EMC 2000

INTERNATIONAL WROCLAW SYMPOSIUM ON ELECTROMAGNETIC COMPATIBILITY WORKSHOP

OVERVIEW OF ETSI ACTIVITIES

Michael Sharpe
ETSI
650 Route des Lucioles
F-06921 Sophia Antipolis CEDEX
FRANCE

Tél: +33 4 92 94 43 02

Fax: +33 4 92 38 49 02

e-mail: mike.sharpe@etsi.fr

The telecommunications market is innovative and dynamic. It has seen far-reaching changes in the last decade in terms of technical evolution, convergence of markets and developments at the political level.

This paper provides a summary of how ETSI, the European body which sets technical standards in this sector, has optimised its working methods to serve the needs of this fast-moving market.

1. INTRODUCTION

1.1. The Telecommunications Market

The last decade has seen far-reaching changes in the telecommunications market place. A combination of technical innovation and changes to the international regulatory environment have brought telecommunications products and services within the reach of more customers than seen before.

This decade has seen explosive growth in the use of the Internet and the use of mobile communications. Users demand rapid access to up-to-date information and communications facilities from their offices and their homes, and expect similar facilities when on the move.

The telecommunications sector used to be dominated by national telecommunications operators who had a monopoly within their national territories. Most European countries are now open to competition for traditional communications services, and we see an increasing number of operators offering mobile telephony Internet services.

On a technology level, the use of software in networks and in terminals is increasing. Technical inno-

vations can therefore be rapidly deployed, allowing the end user to benefit from advancing technology quickly.

Industries that have traditionally been separate are finding that they use similar technology and provide similar services. Incumbent telecommunications operators find themselves in competition with cable television broadcasters and electrical power operators to provide high-bandwidth data telecommunications services over their existing networks. Broadcast television receivers give access to interactive multimedia services. Even traditional white goods are being developed which include telecommunications devices in order to be integrated into a home environment.

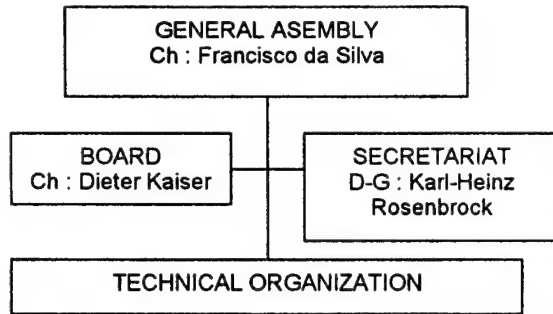
Such a dynamic marketplace requires a standards body, which is capable of reacting rapidly to market, needs and is flexible in its approach. This paper describes the activities of ETSI, which is the European body, which sets the standards for this sector and how it is optimised its organisation to provide the best service in the most efficient way.

2. ETSI ORGANISATION

ETSI is an association of members. Membership is open to any organisation, which has an interest in the telecommunications sector. Most ETSI members are national administrations, telecommunications network operators or manufacturers. However, research institutes, test houses and trade associations also join ETSI and take full part in its activities.

Being a member of ETSI allows an organisation to take part in the development of international standards directly, without having to pass via a national standardisation organisation. ETSI full membership is open to

organisations incorporated in a CEPT member state; other organisations may become associate members, with the same rights as full members except for certain aspects specific to European activity.



All ETSI members have the right to attend the *General Assembly*, the highest decision making body of ETSI, which normally meets twice per year (Spring and Autumn). ETSI *Board* members are elected by the General Assembly and have powers specifically delegated from the General Assembly.

The technical output of ETSI is developed by the *Technical Organisation*, a group of Technical Committees, ETSI Projects and ETSI Partnership Projects that are responsible for specific areas. Each technical body operates largely independently, and is responsible for the approval of its own output. ETSI members (full and associate) may send representatives on a voluntary basis to any technical body and directly input to the technical work.

To complement the voluntary work of the Technical Bodies, ETSI also has funds to employ technical experts on a temporary basis in *Specialist Task Forces* to carry out work of an urgent nature. Specialist Task Forces are funded either from members' contributions or from the European Commission. They are managed by the ETSI Secretariat and their technical output is approved by one or more technical bodies.

The work of ETSI is supported by a permanent secretariat of about 100 staff based in the Technology Park of Sophia Antipolis in southern France.

The fact that players in the telecommunications market can influence ETSI directly at both the management level and the technical level allows ETSI to maintain an clear understanding of market requirements and to react quickly to developments.

3. TECHNICAL OUTPUT

The objective of the Institute is to produce and perform the maintenance of the technical standards and other deliverables, which are required by its members.

As a recognised European standards organisation, an important task is to produce and perform the maintenance of the technical standards, which are necessary to achieve a large unified European market for telecommunications, and related areas.

The technical output of ETSI is in the form of documents of the following types:

- European Standards (telecommunications series) (EN)

ENs are produced by the relevant technical bodies and submitted to public approval procedures for adoption as European Standards. The approval procedures may include a phase for public comment. ENs is adopted by a vote of national representatives. National Standards Organisations in CEPT countries are committed to transpose ENs into national standards.

The public approval procedures for an EN give a technical document a formal status as a European Standard, but are time-consuming for the telecommunications sector, which requires rapid technical standardisation. For this reason, ETSI has introduced deliverables which are developed by the same technical experts who develop European Standards, but which have shorter formal procedures.

- ETSI Standards (ES) and ETSI Guides (EG)

These deliverables are developed by the same ETSI Technical Bodies as develop ENs, and so contain the same level of technical expertise. Once completed by the ETSI Technical Body they are submitted to a 60-day vote by correspondence of ETSI members.

- Technical Specifications (TS) and Technical Reports (TR)

The same technical bodies that develop the other ETSI deliverables, and therefore represent the agreed technical view of the relevant experts in the field also produce these deliverables. Once agreed by the technical body they are published by ETSI.

Technical Specifications and Technical Reports are the quickest way of bringing the agreed position of European technical expertise into the public domain. They are sometimes used to publish technical documentation while the formal public approval procedures to produce European Standards are underway.

This ability to agree a specification and bring it to the public domain quickly, either as an ES or as a TS, has been introduced by ETSI in order to be able to react quickly to market developments.

4. SOME ETSI TECHNICAL BODIES

4.1. 3GPP, SMG and UMTS

3GPP is an ETSI Partnership Project, set up as a partnership between CWTS (China), ETSI, T1 (USA), TTA (Japan), TTA (Korea) and TTC (Japan). The project was set up to co-operate for the production of Technical Specifications for a 3rd Generation Mobile System based on the evolved GSM core networks and the radio access technologies that the Organizational Partners support (i.e. UTRA both FDD and TDD modes).

SMG is the ETSI Technical Body responsible for the maintenance of the GSM standards. UMTS is the project to further develop 3GPP on a European basis.

ETSI created the Mobile Competence Centre (MCC) in March 1999 to provide support to 3GPP as well as to ETSI's Technical Committee SMG and ETSI Project UMTS.

Specifications produced by 3GPP will be published as regional specifications by the partner standards bodies. ETSI will publish 3GPP deliverables as TSs or TRs as appropriate. Where needed for specific regional requirements (for example, Harmonised Standards under European Directives), ETSI will publish ENs based on the 3GPP specifications.

4.2. BRAN

EP BRAN is responsible for the development of Broadband radio access networks. HIPERLAN Type 1 is a wireless LAN that is ISO 8802 compatible. It is intended to allow high performance wireless networks to be created, without existing wired infrastructure. In addition it can be used as an extension of a wired LAN.

HIPERLAN/2 is a short-range variant intended for complementary access mechanism for UMTS systems as well as for private use as a wireless LAN type system. It will offer high speed access (25 Mbit/s typical data rate) to a variety of networks including the UMTS core networks, ATM networks and IP based networks.

HIPERACCESS is a long range variant intended for point-to-multipoint, high speed access (25 Mbit/s typical data rate) by residential and small business users to a wide variety of networks including the UMTS core networks, ATM networks and IP based networks.

HIPERLINK is a variant, which provides short-range very high-speed interconnection of HIPERLANs and HIPERACCESS, e.g. up to 155 Mbit/s over distances up to 150 m. Spectrum for HIPERLINK, is available in the 17 GHz range.

4.3. Broadcast

BROADCAST is a joint CENELEC/EBU/ETSI Technical Committee which co-ordinates the drafting of

standards in the field of broadcasting and related fields. The committee assesses the work performed within external bodies, for example, the Digital Video Broadcasting (DVB) project and the WorldDAB forum) for standardisation. The Technical Committee is responsible for broadcast systems (emission-reception combination) for television, radio, data and other services via satellite, cable and terrestrial transmitters. CENELEC is responsible for the standardization of radio and television receivers (TC 203, 206, 209).

4.4. DECT

The DECT Project has overall responsibility within ETSI for the development and maintenance of standards for Digital Enhanced Cordless Telecommunications (DECT).

DECT is becoming a worldwide standard for short-range cordless mobility, and can be adapted for many other cordless applications (Wireless Local Loop, Cordless PBX, etc.). Interest in the DECT standard is global, as it can easily be adapted for use in other frequency allocations than the European allocation.

DECT/GSM Interworking and Dual-Mode standards have been developed, and DECT technology is relevant to the future Universal Mobile Telecommunications System (UMTS) currently being developed by ETSI.

4.5. ERM

ETSI ERM is a "horizontal" technical committee that is responsible for the standardization of electromagnetic compatibility (EMC) and radio spectrum matters on behalf of all other technical bodies of ETSI. Its work can be considered in three main areas:

"Horizontal" issues: The Electromagnetic Compatibility (EMC) working group is responsible for all ETSI Harmonised Standards related to the EMC Directive (89/336/EEC) and article 3.1b of the R&TTE Directive (1999/5/EC).

ETSI has an agreement with CENELEC in which EMC for fixed telecommunication terminal equipment is standardised by CENELEC; EMC for network equipment and radio equipment is standardised by ETSI. This group is also responsible for liaison on behalf of ETSI with CENELEC on EMC issues.

ETSI is also represented on the steering committee of CISPR. The EMC working group is responsible for co-ordinating ETSI inputs to CISPR.

The Radio Matters (RM) working group is responsible for co-operation with the European Radiocommunications Committee (ERC) to secure appropriate spectrum allocations in the CEPT countries for standardised systems, in order to ensure co-existence between different communications systems standardised by ETSI.

"Radio Project" activities: ERM has long-term working groups providing expertise in the following areas:

- Land-mobile radio (RP02 and RP08)
- Maritime radio (RP01)
- Aeronautical radio (RP05)
- Radio site engineering (RP11)

"Task group" activities: ERM has a number of task groups which are set up on a short-term basis to deal with particular issues, and which disband on the resolution of the task. Current task groups are looking at:

- Issues for radio equipment installed in motor vehicles (TG4),
- EMC requirements for marine radio (TG5) and aeronautical radio (TG15),
- ETSI input to the ERO Detailed Spectrum Review (TG7),
- Interference potential of CB radio (TG8),
- requirements for Radio LAN (TG11) and Cordless Telephone (TG13) equipment,
- requirements for the declaration of interfaces under the R&TTE Directive (TG14).

4.6 Powerline Telecommunications (PLT)

The PLT project develops the necessary standards and specifications to cover the provision of voice and data services over the mains power transmission and distribution network and/or in-building electricity wiring.

The standards are being developed in sufficient detail to allow interoperability between equipment from different manufacturers and co-existence of multiple powerline systems within the same environment.

EMC requirements for Powerline Telecommunications are being developed in a joint group with CENELEC. The ETSI Radio Matters group is also studying possible frequency allocations for powerline systems to avoid interference in the HF band.

4.7 SES

ETSI SES is responsible for all types of satellite communication services (including mobile and broadcasting) and for all types of earth station equipment (especially the radio frequency interfaces and network and/or user interfaces).

The technical activities fall into the following areas:

- Fixed Satellite Service (FSS) and Broadcast Satellite Service (BSS): VSAT, TVRO, SNG

- Mobile Satellite Service (MSS) Land, Maritime and Aircraft Earth Stations
- Little Low Earth Orbit Satellite (LEOS) terminals and Space Standardization (ECSS)
- Satellite Personal Communications Networks (S-PCN) and GEO satellites - Mobile Radio (GMR) interfaces
- Satellite Interactive Terminal (SIT) in Ku/Ka and Ka/Ka bands, using GEO or non-GEO satellites
- Satellite Broadband Multimedia and Satellite component of UMTS

4.8 TETRA

With the support of the European Commission and the ETSI members, the Terrestrial Trunked Radio (TETRA) standard has been developed over a number of years by the co-operation of manufacturers, users, operators and other experts, with emphasis on ensuring that the standard will support the needs of emergency services throughout Europe and beyond.

The standard builds upon the lessons and techniques of previous analogue trunked radio systems and the successful development of GSM during the 1980's.

The TETRA trunking facility provides a pooling of all radio channels, which are then allocated on demand to individual users, in both voice and data modes. By the provision of national networks, countrywide roaming can be supported (the user being in constant seamless communications with his colleagues). TETRA supports point-to-point and point-to-multipoint communications both by the use of the TETRA infrastructure and by the use of Direct Mode without infrastructure.

4.9 Transmission and Multiplexing (TM)

The aim of ETSI TM is to standardize the functionality and performance of transport networks and their elements. Transport networks include everything necessary to provide digital paths between end users and switching nodes. This includes:

- optical fibre cables and components
- line systems and multiplexers
- cross connection equipment
- end to end performance aspects, including network protection
- fixed radio systems
- digital subscriber line systems for metallic cables

This group, through its working group TM4, is also responsible for the standards for radio links used in transport networks, including point-to-point and point-to-multipoint distribution systems.

5. ETSI AND EUROPEAN REGULATION

Some ETSI standards are used for regulatory purposes within the European Union. The European Union has a number of Directives, which give ETSI standards a specific legal effect.

The Directive 98/13/EC on Telecommunication Terminal Equipment and Satellite Earth Station equipment is being replaced by Directive 1999/5/EC on Radio equipment and Telecommunication Terminal Equipment ("the R&TTE Directive").

ETSI has a mandate from the European Commission to produce Harmonised Standards to address the essential requirements of this Directive, which covers all radio equipment and all telecommunications terminal equipment, with certain specific exceptions. EU member states are required to presume that equipment which complies with these Harmonised Standards (which are all ENs) complies with the Directive. Equipment which complies with ETSI Harmonised Standards therefore enjoys free circulation and can be freely marketed anywhere within the European Community.

ETSI has a work programme consisting of 91 Harmonised Standards being developed under this Directive. The development of these Harmonised Standards is being co-ordinated by a Specialist Task Force (STF 149).

Many of the Harmonised Standards that were developed under 98/13/EC are being modified to meet the requirements of the new Directive. Some of the 98/13/EC Harmonised Standards are being maintained in order to retain their technical value. In many cases they are also used as the basis for regulation in non-EU countries.

ETSI has also developed Harmonised Standards under the EMC Directive (89/336/EC as amended), and is in the process of developing a consolidated set of EMC requirements for all radio equipment (EN 301 489).

ETSI standards are also quoted in other European Directives, for example the Marine Equipment Directive (96/98/EC) which sets requirements for equipment used for safety of life at sea.

6. ETSI AND GLOBAL STANDARDISATION

ETSI supports the work of the International Telecommunications Union and many ETSI standards are contributed to the ITU and form part of ITU Recommendations.

ETSI co-operates actively with other regional standardisation bodies, see section 4.1 on 3GPP. ETSI takes an active role in the Global Standards Collaboration (GSC) and the associated Radio Standardisation (RAST) groups.

ETSI has formal working relations with ISO, IEC and CISPR on matters of common interest.

7. CONCLUSION

ETSI is a regional standardisation body with a global membership. Its working methods are different from traditional international standardisation bodies, and have been tailored to be able to react quickly to the telecommunications sector.

ETSI members benefit from being able to take part in international standardisation activities directly. ETSI gathers an expertise from a broad range of telecommunications market players, including national administrations, network operators and manufacturers, and can publish the results of technical consensus building quickly. ETSI is also recognised as a competent European Standards body, which develops Harmonised Standards allowing access to the single market within the European Community.

BIOGRAPHICAL NOTE

Michael Sharpe received a BSc degree from the University of Essex, UK in 1986, followed by a degree of Doctor of Philosophy in 1990.

He joined the British Broadcasting Corporation, working in an engineering project management department responsible for television capital projects. He worked as an EMC engineer for Ford Motor Company before moving to the Radiocommunications Agency (UK) to work on the implementation of the EMC Directive into UK law. He joined ETSI as a Technical Editor in 1995, and is now the ETSI Technical Officer responsible for EMC and radio spectrum matters, and is responsible for regulatory affairs.

EMC 2000

INTERNATIONAL WROCLAW SYMPOSIUM ON ELECTROMAGNETIC COMPATIBILITY WORKSHOP

European Legislation Initiatives: the R&TTE Directive and SLIM Initiative

Speaker: Oliver J. Wheaton, *Radiocommunications Agency, DTI, London, UK*,
Chairman of ETSI Technical Committee TC-ERM "EMC & Radio Spectrum Matters"

The Radio and Telecommunications Terminal Equipment Directive (R&TTE)

Background

The R&TTE Directive 99/5/EC or to give it its correct title " Directive 99/5/EC of the European Parliament and of the Council relating radio equipment and telecommunications terminal equipment and the mutual recognition of their conformity", was published in the Official Journal of the European Communities (OJEC) on 7 April 1999.

The Directive is now in force and applicable to all radio and telecommunications terminal equipment and products, which are now required to comply fully with its provisions i.e. from 8 April 2000 when it entered into force. Some transitional provisions for one year after that date are provided to cover products placed on the market via the Directives that it superseded, i.e. the TTE Directive with its Satellite amendment.

The R&TTE Directive is a 'new approach' Directive, (c.f. the EMC Directive, 89/336/EEC), which means that the product is required to comply with the **essential requirements** identified in the Directive. It embodies the protection/essential requirements identified in the Low Voltage Directive (LVD) and the EMC Directive as indicated below.

It should be noted that for radio products the R&TTE Directive relates to placing goods on the market; their **use** is still subject to the National provision of a **radio** licence regime. This could mean an **individual** licence or a **class** licence that provides for exemption from having a **radio** licence.

The R&TTE Directive, **Article 5.1** provides for a **presumption of conformity** with the **essential requirements** of the Directive, if the product is compliant with a harmonised standard, the reference for which has been published in the OJEC under the Directive.

Harmonised standards are being prepared by ETSI

under a **mandate** from the European Commission, they will provide the prime route to the market for radio equipment (with a few exceptions) in both **harmonised** and **non-harmonised frequency bands**, and equally for telecommunications terminal equipment which can also be radio equipment.

The R&TTE Directive

As noted above the R&TTE Directive covers all radio equipment (with a few exceptions) in both harmonised and non-harmonised frequency bands, it replaces the codified Telecommunications Terminal Equipment Directive 98/13/EC.

The Directive provides a **number of routes** for a manufacturer's product to access the market, the preferred route is via the **harmonised standard**. Market access is based on the manufacturer's declaration of conformity with the essential requirements of the R&TTE Directive, a pre-requisite before the manufacturer places goods on the market and affixes the **CE mark**.

In the event that a harmonised standard is not available for radio products e.g. in the case of innovative technology, a **Notified Body** can be used to specify a **test suite** and in this case the manufacturer is required to prepare a technical construction file as per the EMC Directive.

The R&TTE Directive covers the protection/essential requirements identified in:

- 1) Low Voltage Directive (LVD) 73/23/EEC under **Article 3.1(a) – Health and Safety**,
- 2) EMC Directive 89/336/EEC under **Article 3.1(b) – EMC**

plus

- 3) Those essential requirements needed for spectrum management under **Article 3.2 – effective use of the spectrum and avoidance of harmful interference**.

plus

- 4) Any additional essential requirements under Article 3.3 parts (a) to (e) which cover
 - a) interworking via networks with other apparatus
 - b) harm to or misuse of network resources
 - c) personal privacy
 - d) avoidance of fraud
 - e) access to emergency services
 - f) disability features

The European Commission following a consultation of the Member States via a committee known as the Telecommunication Conformity Assessment and Market Surveillance Committee (TCAM), composed of representatives of the Member States, will identify any additional essential requirements and notify the Member States.

Role and Activities in ETSI

ETSI as indicated above, has received a standardisation mandate from the Commission and also funding to support a Specialist Task Force (hired help). ETSI's activities are co-ordinated by the R&TTE Steering Committee and are preparing harmonised standards across the full range of its portfolio for both radio and telecommunications terminal equipment.

An ETSI Guide, to the preparation of harmonised standards EG 201 399 has been prepared and published, it provides a basis for a technical body to determine if an attribute or parameter is essential under the terms of the R&TTE Directive. The Guide contains a decision tree that can be used to assist in this determination i.e. is it to be considered essential or not?

The inclusion of market forces in this determination has been opposed by some administrations. The principle of proportionality (to regulate by allowing market forces) enshrined in the R&TTE Directive and expanded in the ETSI Guide is not well understood

In addition a draft harmonised pro forma has been prepared to assist the technical bodies in generating the necessary standards within the short time-scales available. The pro forma has been published as an ETSI Special Report SR 001 470

To provide for the potential diversity of the standards that can relate to a specific product, a modular

approach has been adopted (for the standards generation) and manufacturers will need to select the appropriate standard(s) or module(s) that relate to the applicable Articles of the R&TTE Directive. This modular concept is explained in the pro forma document as part of the Introduction.

Summary

The R&TTE Directive is a de-regulatory measure that replaces the concept of a priori type approval with a manufacturer's declaration of conformity with the essential requirements of the Directive.

In doing so it also places on the recognised European Standards bodies, i.e. CEN, CENELEC and ETSI, but primarily ETSI the responsibility for preparing harmonised standards to meet the market's needs.

For maximum effect these standards needed to be in place, and listed in the OJEC, by 8 April 2000. In the event this has not been achieved but considerable progress has been made and it is expected that the majority of the harmonised standards will be in place before the end of 2000.

The SLIM Initiative in Europe (EMC)

Background

Legislation in this sector the EMC Directive 89/336/EEC and the R&TTE Directive 99/5/EC are designed to remove trade barriers within the European Economic Area (EEA).

The SLIM initiative relates to the Simplification of Legislation for the Internal Market, the EMC Directive has been reviewed by the SLIM panel and their initial report identified a number of areas where they believe that beneficial changes could be made to further improve the legislation.

Their proposals can be summarised as:

- a) incorporation into the EMC Directive of a number of definitions taken from the European Commission's published Guidance document;
- b) consideration as to whether environment classes should be explicitly defined;
- c) anticipation of the protection requirements;
- d) the treatment of fixed installations;
- e) the deletion of Article 10(5) of the EMC Directive following the introduction of the R&TTE Directive 99/5/EC (now dropped due to the exclusions in the R&TTE Directive).

- f) the possible exclusion of identified equipment;
- g) a strategic review of the notified standards.

These are **proposals** that have no specific status at this stage, but work is continuing in a small task group looking at the options available for updating the legislation.

Activities in ETSI

Representatives from ETSI's **EMC** community are participating in the on-going discussion, **item g)** above has particular significance for the **ETSI radio** community.

Initially **ETSI** prepared some **30 radio EMC** standards; which relate to specific radio products, this was deemed essential, as they included a cross-reference to **spurious emissions**, originally seen as an **EMC** parameter, which formed part of the radio product standard.

The changes to the European legislation with the introduction of the **R&TTE Directive 99/5/EC** has now made it possible to remove these cross-references, (see above). **ETSI** decided to re-write its radio **EMC** standards portfolio, work which is now nearing completion, to simplify them in two respects:

- a) that the radio **EMC** standards will in future only refer to classical **EMC** phenomena and **ETSI** will now classify as 'spectrum management' parameters all radio phenomena associated with the antenna and the antenna port including case radiation.
- b) that the new radio **EMC** standard will be a multi-part standard which brings together all of the common aspects such as test methods in a part 1 (common technical requirements) and then allocates individual parts for product specific aspects.

Summary

Work is now well advanced in that all of the constituent parts (22) for the new multi-part radio **EMC** standard **EN 301 489** have been written, and it is expected that they will be approved by **ETSI TC-ERM** when it meets May 2000.

The radio **EMC** standards have thus been simplified and when published by **ETSI** will be listed in the **OJEC** under both the **EMC** and **R&TTE Directives**.

Biographical Note

Oliver J. Wheaton B.Tech, MSc., C.Eng, MIEE, joined the Radiocommunications Agency - DTI in 1987 as Deputy Director responsible for Mobile Services. He is presently responsible for the Agency's standardisation policy and reviewing the Agency's international commitments/activities.

He chairs the UK ETSI Members Conference and is the head of the UK delegation at the ETSI General Assembly.

He chairs the ETSI Technical Committee - EMC and Radio Spectrum Matters (TC-ERM) which is the group within ETSI that deals with the horizontal issues associated with electromagnetic and radio spectrum compatibility and a number of radio /wireless project activities, which includes aeronautical, maritime and land mobile applications.

He also chairs the ETSI group R&TTE Steering Committee responsible for the co-ordination of the standardisation activities within ETSI in support of the R&TTE Directive. He is a member of the UK delegation to TCAM, the Commission's Members States committee responsible for the R&TTE Directive.

Prior to joining DTI Olly Wheaton was with the UK Ministry of Defence (Procurement Executive) (MoD (PE)) in a number of roles. He joined the MoD (PE) following 13 years with the Marconi Company - which he joined in 1960 as a student apprentice.

Olly Wheaton was educated at Loughborough University of Technology, from which he holds Bachelor and Master degrees, he is also a chartered engineer and a member of the Institution of Electrical Engineers.

EMC 2000

INTERNATIONAL WROCLAW SYMPOSIUM ON ELECTROMAGNETIC COMPATIBILITY WORKSHOP

THE SPECTRUM ENGINEERING ADVANCED MONTE CARLO ANALYSIS TOOL (SEAMCAT)¹

Abdelkrim Benamar, Prakash Moorut, Dragan Boscovic
Motorola Labs - Centre de Recherche de Motorola - Paris(*)
Espace Technologique - SaintAubin
91193 Gif-sur-Yvette Cedex
FRANCE

Tell: +33 (0)1 69 34 25 15 Fax: +33 (0)1 69 35 25 01
E-mail: benamar, moorut, boscovic@crm.mot.com

(*) on behalf of CEPT SE21 members

The deregulation of the telecommunications industry, the massive development in mobile and personal communications and the emergence of a diversity of radio applications and services are some of the key elements which have contributed towards the growth of the telecommunications market in recent years. Sustaining future growth is strongly dependent upon the efficiency with which the radio spectrum is used.

This paper describes a software tool based upon the statistical Monte Carlo technique, the Spectrum Engineering Advanced Monte Carlo Analysis Tool (SEAMCAT) [1], which provides a spectrally efficient solution to spectrum engineering problems.

1. INTRODUCTION

The development of mobile and personal communications is one of the key elements contributing towards the growth of the telecommunication market in recent years. The initial limiting factors for higher take up of mobile communications equipment were linked to lack of reliable and efficient communication schemes and their high cost. Future growth is strongly dependent upon improving the efficiency with which radio frequency spectrum is used.

Throughout the last decade, there has been a major emphasis on source and channel coding, digital modulation, multiple access schemes and channel equalisation. Each of these technologies helps in some way to improve the rate at which information can be transmitted in a given bandwidth. However, in addition to these methods which are aimed primarily at improving the performance of a single system, the compatibility between different systems must be studied. When several systems, possibly employing different technologies are operating in the same or neighbouring geographic areas and are using frequency bands

relatively close to one another, then proper spectrum engineering techniques need to be exercised in order to minimise likelihood of inter-system interference. Indeed, activity of one system may degrade the availability of the other. End users of the affected system will intuitively blame their own equipment whereas in practice the problem is being generated by transmissions unknown to the user. Traditionally spectrum engineers have avoided these consequences by introducing guard bands (or frequency separations) between different radio systems. This has been relatively effective but associated with it has been decreased spectrum efficiency. The traditional analytical methods used to determine the size of guard bands make use of worst case assumptions (e.g. the Minimum Coupling Loss method) and may lead to frequency separations considerably greater than necessary.

This paper describes a software tool based upon the statistical Monte Carlo technique, the Spectrum Engineering Advanced Monte Carlo Analysis Tool (SEAMCAT) [1], which provides a spectrally efficient solution to many spectrum engineering problems. The Monte Carlo methodology has been adopted by the CEPT and is under study within ITU-R Task Group 1/5. The Monte Carlo technique functions by considering many independent instants in time (or in space). For each instant, or simulation trial, a scenario is built up using a number of different random variables, i.e. where the interferers are with respect to the victim, how strong the wanted signal strength is, which channels the victim and interferer are using etc. If a sufficient number of simulation trials are considered then the probability of a certain event occurring can be calculated with a high level of accuracy.

In this way, the tool is able to quantify levels of interference between radio systems and is able to help determine appropriate frequency planning rules or specify limits for transmitter / receiver performance.

¹ SEAMCAT is the name chosen by the MoU group of European administrations and industry members for their development of a software tool based on the CEPT/ERC "Monte Carlo Radio Compatibility Tool" algorithm. Further information on the project is available from <http://www.ero.dk>

2. SEAMCAT METHODOLOGY

The statistical methodology briefly described here is known as the Monte Carlo technique [2]. Statistical simulation methods may be contrasted to conventional analytical methods, which are typically applied to ordinary or partial differential equations that describe some underlying physical or mathematical system. In many applications of the Monte Carlo technique, the physical process is simulated directly, and there is no need to even write down the differential equations that describe the behaviour of the system.

The only requirement is that the physical or mathematical system be described by probability density functions (pdf's). Once the pdf's of the relevant parameters are known, the Monte Carlo simulation can proceed by random sampling of them. Many simulations trials are performed and the desired result is taken as an average over the number of observations. In many practical applications, one can predict the statistical error in this average result, and hence an estimate of the number of Monte Carlo trials that are needed to achieve a given error.

The SEAMCAT tool models a victim receiver operating amongst a population of interferers. These interferers may belong to the same system as the victim, a different system or a mixture of both. The interferers are randomly distributed around the victim in a manner decided by the user. It is common practice to use a uniform random distribution. The density of interferers is set in line with the environment being modelled, i.e. an urban environment has a higher density than a rural environment. Only a proportion of the interferers is active at any one time. This proportion is known as the utilisation and will depend upon the day of the week as well as the time of day. Fig. 1 illustrates how the interferers and victim may appear for one simulation trial. Also illustrated is the transmitter providing the victim's wanted signal.

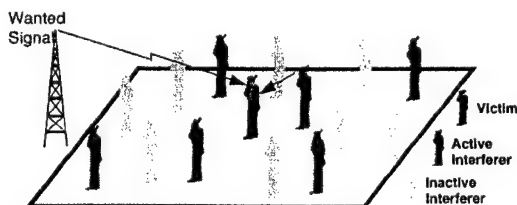


Figure 1 - A typical victim and interferer scenario for a Monte Carlo simulation trial

The effect of each interferer upon the victim is summed. Several interference mechanisms are included such as unwanted emissions, receiver blocking, intermodulation products, co-channel and adjacent channel interference phenomena are also considered in the methodology. The level of unwanted emissions falling within the victim's receiver bandwidth is determined using the interferer's transmit mask,

interferer / victim frequency separation, antenna gains and propagation loss. The receiver blocking power, i.e. the power captured from the on-channel transmissions of the interferer due to selectivity imperfections of the victim's receiver, is determined using the interferer's transmit power, victim receiver blocking performance, interferer / victim frequency separation, antenna gains and propagation loss.

The criterion for interference to occur is for the victim receiver to have a carrier to interference ratio (C/I) less than the minimum allowable value (often known as the protection ratio). In order to calculate the victim's C/I it is necessary to establish the victim's wanted signal strength as well as the interfering signal strength. The position of the victim's wanted signal transmitter is identified and a link budget calculation completed. Having knowledge of both the interfering signal strength and the wanted signal strength allows the victim's C/I ratio to be computed. Figure 2 illustrates the various signal levels.

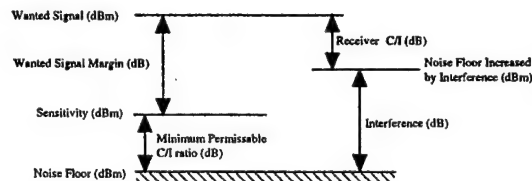


Figure 2 - The signal levels used to determine whether or not interference is occurring

The left-hand side of the diagram represents the situation when there is no interference and the victim is receiving the desired signal with some margin. In this case the victim's C/I ratio is given by the sum of the wanted signal margin and the minimum permissible C/I. The right hand side of the diagram illustrates what happens when interference is introduced. The interference adds to the noise floor and the victim's C/I ratio is reduced. The new C/I ratio is defined by the number of dBs difference between the wanted signal strength and the increased noise floor. This ratio must be greater than the minimum permissible C/I if interference is to be avoided. The Monte Carlo simulation tool checks for this condition and records whether or not interference is occurring.

The simulation considers many instants in time by using the probability distribution functions modelling each of the parameters describing the victim and interferer systems. The simulation is complete once sufficient instants in time, or simulation trials have been completed to provide an accurate probability of interference result.

3. APPLICABILITY OF THE SEAMCAT TOOL TO SPECTRUM ENGINEERING PROBLEMS

The SEAMCAT tool as applied to radio system compatibility is able to provide solutions to a number of problems commonly encountered in the field of spectrum engineering. These include the ability to -

- identify candidate frequency bands for radio systems;
- determine the appropriate size of frequency separations (or guard bands);
- derive transmitter emission masks needed to protect adjacent services;
- specify receiver susceptibility to preserve system performance in a given radio environment;
- identify band sharing issues between different services and technologies;
- help provide smooth band refarming strategies

The Monte Carlo technique provides a solution, which is spectrally efficient and helps to ensure that levels of interference are acceptable. The technique can address any radio interference scenario regardless of the interfering and victim systems. For example, a population of cellular mobile telephones interfering with a wireless local loop base receiver or a constellation of low earth orbit satellites interfering with a terrestrial mobile receiver. There is no restriction upon the victim or interfering systems. The only requirement is that there is knowledge of the parameters, which can be used to model them. This includes the receiver and transmitter specifications, the propagation model associated with the medium of communication and a measure of the quality of service required.

4. CONCLUSION

In this contribution, we have described a software tool, SEAMCAT, based upon the statistical Monte Carlo technique which is capable of analysing complex radio system compatibility issues. Such a tool is valuable for providing solutions to spectrum engineering problems in a spectrally efficient manner.

Further information on the project is available from <http://www.ero.dk>.

5. REFERENCES

- [1] "Monte Carlo Radio Compatibility Tool", Document CEPT/ERC/SE(97)30.
- [2] R. Y. Rubinstein, "Simulation and the Monte Carlo method", Wiley Series in Probability and Mathematical Statistics, 1981.

Abdelkrim Benamar received the Engineering Degree in Telecommunications from the National Institute of Telecommunications (Evry, France) and the Ph.D. degree in electronics and signal processing from Orsay University (France) in 1993 and 1996 respectively.

In 1993, he joined Alcatel Mobile Phones and has been engaged in a collaborative program with France Telecom CNET aiming to develop acoustic echo canceller and noise reduction schemes for hands-free GSM telephony in cars. Since October 1996, he has been with Motorola Labs, Centre de Recherche de Motorola - Paris, where he is currently leading the Spectrum Engineering Research Team.

His current research interests are in statistical methodologies to analyse complex radio compatibility issues involving terrestrial and satellite systems, and the spectrum allocation and sharing techniques for optimal spectrum utilisation.

Prakash Moorut received the Engineering Degree in Telecommunications from Ecole Supérieure d'Electricité, Paris, in 1997. Since 1997, he has been working with Motorola Labs, Paris, in the Spectrum Engineering Research Team. He conducts system simulation activities involving radio systems such as GSM, IS-95, ReFLEX, TETRA, FM PMR, WiLL, PCS1900, UMTS, MSS. He develops methodologies to tackle spectrum engineering issues and performs radio system coexistence analysis involving both terrestrial and satellite systems. He also actively contributes to the development of the Monte Carlo radio system compatibility methodology within CEPT.

Dragan Bosovic received the Dip. Ing. in 1983 and the MSc degree in 1988 from University of Belgrade Faculty of Electrical Engineering and the PhD from University of Bath School of Electrical Engineering in 1991.

From 1982 to 1988, he worked as a R & D Engineer at the Institute of Applied Physics, Belgrade and was engaged in research into and development of ultra-broadband microwave components. From 1988 to 1991 he worked as a Research Officer and Consultant at University of Bath and Wessex Electronics Ltd., Bristol Consulting, respectively. He was engaged in numerical modelling of electro-magnetic phenomena and its application.

Since 1991, he has been a Member of Technical Staff and Deputy Research Director of Motorola, Basingstoke and Paris. At Basingstoke, he was responsible for planning, tracking and control of advanced research programmes related to system design of the digital mobile radio systems, private trunked networks and public cellular networks. At Paris, his research interests are in the characterisation of radio environment and radio system design for optimum coexistence with other radio systems. He also actively participates in the activities of various working groups, project teams and committees in ETSI, CEPT and ITU forums.

IV

**OPEN MEETING OF URSI COMMISSION E
"EM NOISE AND INTERFERENCE"**

EMC 2000

INTERNATIONAL WROCLAW SYMPOSIUM ON ELECTROMAGNETIC COMPATIBILITY

URSI COMMISSION E OPEN MEETING

COMMISSION E OPEN MEETING

Robert L. Gardner, Chairman
Commission E, Noise and Interference Control
International Union of Radio Science
6152 Manchester Park Circle
Alexandria, VA 22310-4957
703-924-9370 GardnerR@aol.com

The technical interests of the International Union of Radio Science (URSI) are considered within ten Scientific Commissions. Commission E is charged with the topics under interference and noise control. This is very broad and encourages researches in the following terms of reference:

- (a) Terrestrial and planetary noise of natural origin; man-made noise;
- (b) The composite noise environment;
- (c) The effects of noise on system performance;
- (d) The lasting effects of natural and intentional emissions on equipment performance;
- (e) The scientific basis of noise and interference control;
- (f) Spectrum management/utilization and wireless telecommunications;
- (g) Geo-electric and -magnetic fields and seismic associated electromagnetic fields.

Note : Many of the subjects mentioned are treated under the common title of Electromagnetic Compatibility.

In turn, the work of Commission E is primarily accomplished through its working groups. Each working group organizes sessions and encourages research in their areas of interest. Those working groups and their various Chairs are:

E.1. Spectrum Utilization Management and Wireless Telecommunications
Co-Chairs: G. Hurt (U.S.A.), R. Struzak (Switzerland);

E.2. Intentional Electromagnetic Interference
Co-Chairs: M. Wik (Sweden) and W. Radasky (USA)

E.3. High Power Electromagnetics
Co-Chairs: C.E. Baum (U.S.A.) and R.L. Gardner (U.S.A.);

E.4. Terrestrial and Planetary Lightning Generation of Electromagnetic Noise
Co-Chairs: Z. Kawasaki (Japan) and V. Cooray (Sweden)

E.5. Interaction with, and Protection of, Complex Electronic Systems
Co-Chairs : J. Nitsch (Germany), P. Degauque (France), M. Ianoz (Switzerland), J-P. Parmentier (France);

E.6. Effects of Transients on Equipment
Co-Chairs: J. ter Haseborg (Germany), V. Scuka (Sweden), and B. Demoulin (France);

E.7. Extra-Terrestrial and Terrestrial Meteorologic-Electric Environment
Chair: H. Kikuchi (Japan);

E.8. Geo-electromagnetic Disturbances and Their Effects on Technological Systems
Co-Chairs: M. Hayakawa (Japan) and R. Pirjola (Finland)

E.9. Interference and Noise at Frequencies above 30 MHz
Chair : J. Gavan (Israel)

This open meeting is meant to bring this group together to discuss progress, plans and problems. Meetings are typically held at the beginning of the important international URSI sponsored EMC conferences. Working group chairmen usually present various issues associated with their technical areas followed by a short discussion of a technical area of interest.

EMC 2000

INTERNATIONAL WROCLAW SYMPOSIUM
ON ELECTROMAGNETIC COMPATIBILITY

URSI COMMISSION E OPEN MEETING

URSI WG E1: Spectrum Management/ Utilisation and Wireless Telecommunications

Ryszard Struzak, Co-Chair WG E1

Route du Boiron 45, CH-1260 Nyon, Switzerland

ryszard.struzak@ties.itu.int

This overview brings together information relevant to activities of the working group E1 that has been made available to the author. It covers the period since the URSI General Assembly, Toronto, Ontario, Canada, August 13-21, 1999.

The 1999 Assembly

The increasing gap between developed and developing countries and the spectrum congestion are the main problems that confront the scientists. That is the key message of the sixteenth URSI General Assembly, as I understood it. The spectrum congestion threatens the future of wireless telecommunications and other uses of radio waves. The development gap threatens global stability, not to mention humanitarian and moral issues; it is, however, beyond the scope of this overview.

WG Sessions

The scientific sessions of the working group E1 held during the Assembly and entitled "Spectrum Management and Utilisation" included ten presentations, five in the oral session and five in the poster one. The aim was to gather those interested in solving problems of RF spectrum congestion and mutual interference among communication systems to discuss the progress made and new problems that appeared since the previous Assembly.

The oral session began with contribution by J. Shapira, URSI Vice-President. Its purpose was to emphasize the significance of the spectrum congestion issues and the need for active URSI attitude. His contribution "Spec-

tral Congestion and URSI" noted growing influence of commercial entities and endangered spectrum usage by short-term politics. Although spectrum allocation and coordination are the responsibility of ITU, the scope and the threat of the problem call for intensive contributions from radio scientists in most areas of URSI activity. URSI should maintain dialog with all players and be more active in finding appropriate long-term solutions acceptable to all parties involved in the uses made of the radio frequency spectrum. K Hughes of the ITU reviewed results of the most recent international sharing studies in the framework of ITU R SG3. His contribution was entitled "Sharing Consideration Issues in ITU-R propagation Studies".

G Hurt of NTIA (USA) addressed the issues related to the increasing uses of low-power radio devices. Low-power radio covers a wide range of devices, including short-range communication, remote control, cordless telephones, and radiolocation. These devices must share the spectrum with other licensed radio services on an unprotected, non-interference basis. In certain instances, transmit power up to 1W has been authorized, but generally spectral power density is restricted to minus 70dBW/MHz. In his contribution "Unlicensed Radio Devices", he presented results of recent research in the USA and ITU R, including measurements, and methodology for evaluating the aggregate interference effects of dense deployment of unlicensed radio devices based on Monte Carlo simulation techniques. V Rawat presented spectrum management practices developed in Canada. S Hess, discussed the European approach to spectrum management, with emphasis on detailed spectrum investigation project running in European Radio-

communications Office, and on the European table of frequency allocations expected beyond the year 2008.

In the poster session of the working group, D Cohen discussed work undertaken in the USA on "Interference Avoidance Methods for Wireless Communications in Unlicensed Spectrum". It covered the ISM bands (902-928MHz, 2400-2483.8MHz, and 5725-5850MHz), PCS band 1910-1920MHz, and U-NII band around 5 GHz. E Medeiros and L Bermudez in their contribution "Study of the Non-Flat Broadcast Band In Multichannel Multipoint Distribution Service MMDS" presented results of research made in Brazil on the implementation of MMDS multi-channel transmission systems. B Nurmatov and A Pavliouk, in their input "Experience in Development of a Method for Calculating Spectrum Use Fees", presented an approach to the solution of spectrum scarcity problem. The approach consists in setting fees to be collected for the uses made of the radio frequency spectrum - the issue under discussion in several countries and in the ITU. D Guerrero, H Zaharia, S Primak, and D Makrakis discussed "Performance Analysis of Turbo Codes Communication Channel with Fading". J Pawelec, D Wieczorek, A Janulewicz and A Przybysz contributed with poster "IS Interference Rejection Using Adaptive Lattice Filters"

The abstracts of the contributions presented at the assembly are available in printed form [2].

Other Sessions

In addition to working group E1 sessions, the scientific programme of the assembly included a number of items relevant to spectrum management/ utilisation and wireless telecommunications. Working Group E9 addressed issues of interference in communication; details are given in a separate report by J Gavan.

However, the inter-commission coordination was non-ideal and, as a consequence, it was not always easy to take part in discussions of the same or close topic that were distributed randomly among different sessions. For instance, a discussion on a crucial issue of spectrum access fees was held in session of our WG E and also at session C3 "Radio Spectrum Utilisation and their Technologies" (contribution "Economic Value of Radio Frequencies" by T Jitsuzumi and T Ishida). That session included also other papers that might be of interest to WG E1 members, such as, for instance, contributions by S Komaki, K Tsukamoto and M Okada ("Radio Ecology: Social and Economic Strategies and Technologies"), J Scott ("Adjacent Channel Power Distortion Measurement"), and Y. Cheng, and Y. Fei ("Study on Generation and Radiation of Ultra-Wideband Radio Spectrum"). Discussions of topics of common interest to two or more commissions would be more fruitful at common meetings.

Session EA "Electromagnetic Compatibility and EM Pollution", organized by P Degauque and M D'Amore,

included a number of contribution of interest to E1 WG members. Among others, M Selivanov discussed problems of frequency sharing between IS-95 CDMA based wireless local loop and other systems in the 800MHz band. J Dai presented a model of anti-interference performance evaluation for the electrical information system.

Session JCEG "Interference Protection Measures" included, among others, paper by S Ellingson on the frequency-, time-, and multi-domain approaches in suppression of radio interference in radio astronomy. Adaptive interference mitigation strategies were discussed by J Bell, R Ekers, P Hall, R Smegal, W Wilson, A Hopkins and B Thomas. A similar topic was addressed by R Bradley and R Fisher. A cross-correlation interference excision technique was discussed by L Kewley and B Sault and R Ekers.

Many interesting contributions were included in the programme of other commissions. Commission C "Signals and Systems" can serve as an example. Session C3 "Radio Spectrum Utilization and Their Technologies", session C4 "Space-Time Blind Signal Processing for Communications, Intelligent Antenna and Adaptive Equalization" and session C6 "Software Radio for Future Communications", for instance, contained a number of contributions relevant to the use of spectrum resources.

General & Tutorial Lectures

Few general and tutorial lectures deserve mentioning here as being potentially of special interest to the E1 WG membership. J Bach Andersen in his general lecture addressed the future generations of mobile communications from the scientific point of view. Commission C-Tutorial by G Delisle, K Hettak, and J Lucas dealt with intelligent antennas for future wireless communications.

The culmination of discussions on spectrum management/ utilisation and wireless telecommunications was expected at the special lecture closing the Assembly. The lecture was offered by P Delogne and W Baan on behalf of special Inter-Commission Working Group on Spectrum Congestion. The authors reviewed the status-of-the-art of spectrum utilization, with emphasis on specific case of science services. They discussed the role of source coding, channel coding, signal processing, and explained concepts of spectrum efficiency, Shannon's limit, as well as implementation constraints. Finally, they suggest on how can URSI help solving the spectrum congestion problem. Among other things, they suggest stronger collaboration with ITU-R and with industry.

Unfortunately, due to time-planning errors, the lecture could not be delivered as planned and no discussion was possible. However, as the full text of the lecture has been made available [1], the discussion was continued

by correspondence. The first voice in discussion was published in the December issue of *The Radio Science Bulletin* [5]. That contribution proposed a quantitative approach to spectrum congestion issues and a modification to Shannon's formula on radio channel capacity. The proposed modification accounts for spectrum congestion effects - an element absent in the Shannon's formula and all derivative works. Discussions of spectrum congestion issues were continued at the international School on Data and Multimedia Communications Using Terrestrial and Satellite Radio Links, directed by S. Radicella and myself [4].

EMC 2000 Wroclaw

In addition to the open meeting of URSI Commission E, the Wroclaw Symposium EMC 2000 contains a number of contributions relevant to WG E1 activities, including plenary lectures, workshops, and sessions. They are not discussed here as they are presented elsewhere in this volume.

References

1. Delogne P, Baan W: Spectrum Congestion; in *Modern Radio Science 1999*, ed. by M Stuchly, Oxford University Press 1999, p. 309-327
2. Proceedings (Abstracts) of the XXVIth General Assembly of URSI, Toronto, Ontario, Canada, August 13-21, 1999,
3. Proceedings of the XVth International Wroclaw Symposium on Electromagnetic Compatibility, Wroclaw, Poland, June 27-30, 2000 (This volume)
4. Lecture Notes, The School on Data and Multimedia Communications Using Terrestrial and Satellite Radio Links, The Abdus Salam International Centre for Theoretical Physics, Trieste, Italy, 7-25 February 2000
5. Struzak R: Spectrum Congestion - a Voice in Discussion; *The Radio Science Bulletin URSI No 291*, December 1999, p. 4-5

EMC 2000

INTERNATIONAL WROCLAW SYMPOSIUM
ON ELECTROMAGNETIC COMPATIBILITY

URSI COMMISSION E OPEN MEETING

THE STANDARDISATION OF HIGH POWER ELECTROMAGNETIC TRANSIENT PHENOMENA IN THE IEC Report of Working Group E2

William A. Radasky
Metatech Corporation
358 S. Fairview Ave. Suite E
GOLETA CA 93117, USA
E-mail: wradasky@aol.com

Manuel W. Wik
Defence Materiel Administration
Electronic Systems Directorate
S-115 88 Stockholm, Sweden
E-mail: mawik@fmv.se

This paper introduces the standardisation work underway in Subcommittee 77C in the International Electrotechnical Commission (IEC). This committee is developing protection standards dealing with the disturbances due to high altitude electromagnetic pulse (HEMP) and due to intentionally produced high power EM transients.

1. INTRODUCTION

The objective of the International Electrotechnical Commission (IEC) is to produce civilian standards for electrical and electronic equipment and systems. In particular, the electromagnetic compatibility (EMC) aspects are of interest worldwide for the electronics and power industries in order to harmonise methods of protection and to develop protection devices. All information used and developed is openly available. The intention of IEC SC77C, which deals with high power EM phenomena, is to reference and apply existing IEC EMC standards wherever possible, so that there is no duplication of effort. Those working in the SC77C subcommittee and on particular projects are representatives of their countries and not of organisations (civilian or military).

Subcommittee 77C currently has sixteen participating member nations: Austria, China, Czech Republic, Finland, France, Germany, Italy, Japan, Mexico, Romania, Russia, Spain, Sweden, Switzerland, United Kingdom and USA. In addition there are fourteen observing member nations: Belgium, Canada, Croatia, Denmark, Ireland, Israel, Netherlands, Norway, Poland, Portugal, Slovakia, Thailand, Turkey and Ukraine. The Chairman is Dr. W. A. Radasky (USA) and the Secretariat is undertaken by Sweden (Messrs M. W. Wik, T. Wedin).

The preparation of SC77C standards is consistent with the development of EMC standards within other parts of TC77 (EMC) and is thus structured according to "IEC Publication 61000" which is divided into seven major parts. Only Parts 1, 2, 4, 5 and 6 are utilised by SC77C at present. The current development of standards and reports includes fifteen active projects, which are summarised below.

2. PROGRESS OF WORK AND HIGHLIGHTS

2.1. 61000-1-X

Part 1 "General" is planned to include terminology, definitions and other general aspects. "The effects of high-altitude EMP (HEMP) on civil equipment and systems" (61000-1-3, W. A. Radasky, USA) will provide information concerning the effects of high-altitude EMP (HEMP) on electrical and electronic equipment and systems. This information is based on effects observed during high altitude nuclear testing and from tests performed in HEMP simulators in several countries. The project is intended to be published as a Technical Report and is presently circulating as a 1CD.

2.2. 61000-2-X

Part 2 "Environment" gives a description of the high power electromagnetic environment and is divided into radiated and conducted parts. "Description of HEMP environment - Radiated disturbance" (61000-2-9, G. Champiot, France) is published as an IEC International Standard. It contains a number of definitions and the radiated parameters for early-time, intermediate-time and late-time HEMP waveforms. This includes electric and magnetic field time waveforms, HEMP

frequency amplitude and energy, weighting of the early, intermediate and late-time HEMP, and also deals with reflections and transmission of the HEMP at the earth's surface.

"Description of HEMP environment - Conducted disturbance" (61000-2-10, W. A. Radasky, USA) is based on the radiated waveforms in standard 61000-2-9 and is published as an IEC International Standard. It describes the conducted environment applicable for categories of conductors for different positions and illumination cases statistically taken into account. The specified environments are based on extensive theoretical calculations and experimental measurements.

Part 2 also includes "Classification of HEMP environment" (61000-2-11, W. A. Radasky, USA) and groups HEMP environments present at various locations outside and inside of civilian systems. The project is published as an IEC International Standard. One reason for classification is to provide guidance for equipment manufacturers to help them decide on the proper immunity test levels appropriate for their equipment. Another reason is to provide systems designers with guidance regarding construction methods and protective measures needed to achieve defined EM classes.

2.3. 61000-4-X

Part 4 "Testing and Measurement Techniques" presently includes five projects. "Test methods for protective devices for HEMP and other radiated disturbances" (61000-4-23, F. Tesche, USA) is approved for circulation as a FDIS. The document contains definitions, shielding effectiveness measurement methods of shielding materials, gaskets and shielded enclosures, and transfer impedance measurement methods for coaxial cables.

"Test methods for protective devices for HEMP conducted disturbance" (61000-4-24, W. K. Buechler, Switzerland) is published as an International Standard. It describes methods to measure the residual voltage on protective devices under HEMP conditions, i. e. for the case of very fast changes of voltage and current as a function of time. This standard complements the standard 61000-5-5 "Specification of protective devices for conducted disturbance".

"HEMP immunity test methods for

equipment and systems" (61000-4-25, P. R. Barnes, USA) is distributed as a fourth Committee Draft. The draft presently includes a list of immunity tests, environmental conditions, guidance for the selection of immunity tests, selection of severity levels, test levels, selection of test methods, test equipment, test set-up, test procedure and evaluation of test results. Efforts are being made to employ as many existing EMC test techniques as possible and to avoid more costly special HEMP tests.

"HEMP simulator compendium" (61000-4-32, J. C. Giles, USA) has been approved as a new work item. The specific aim of this project is to provide information on the various types of existing large HEMP simulators and their uses, performance parameters, limitations, and availability. This will allow all potential simulator users to evaluate the adequacy of available simulators for testing large systems.

"Measurement Methods for High-Power Transients", (61000-4-33, A. Kaelin, Switzerland), has recently been approved as a new project. The intention of this work is to identify appropriate sensor calibrations and measurement methods to be used for the measurement of high-power transient electromagnetic disturbances.

2.4. 61000-5-X

Part 5 "Installation and Mitigation Guidelines" presently includes five projects. "HEMP protection concepts" (61000-5-3, M. Ianoz, Switzerland) is published as a Technical Report. The concepts presented are based on general principles such as zoning, grounding, component selection, and circuit and equipment design.

"Specification of protective devices for HEMP radiated disturbance" (61000-5-4, J. Delaballe, France), is published as a Technical Report. This document identifies the parameters required to accurately specify protection to HEMP radiated fields.

"Specification of protective devices for HEMP conducted disturbance" (61000-5-5, W. K. Buechler, Switzerland), is published as an IEC International Standard. This standard identifies the parameters required to accurately specify protection for HEMP conducted environments.

A work originally started by SC77B, "Mitigation of external EM influences" (61000-5-6, J. Philip Castillo, USA) has been

transferred to SC77C. The project is distributed as 1CD. The intention is that the document will contain specific information on installation practises. As indicated by the title, this publication will cover HEMP and other external EM disturbances such as lightning.

"Degrees of protection against electromagnetic disturbances provided by enclosures (EM code)" (61000-5-7, C. Jones, USA) will describe protection properties offered by different types of enclosures with respect to electromagnetic fields. In addition, standardised test methods are identified along with a codification system that is consistent with the IP code already established by the IEC. This project is approved for circulation as an FDIS.

2.5. 61000-6-X

Part 6 "Generic Standard for HEMP Immunity for Indoor Equipment", (61000-6-6, P. R. Barnes, USA) has recently been approved as a new project. The plan for this work is to identify a generic set of environments and test levels to be applied to electronic equipment to survive the effects of HEMP.

3. CONCLUSIONS

IEC Subcommittee 77C is in the process of developing a family of HEMP and high power EM transient standards and publications that will help manufacturers and facility owners to protect their equipment from the effects of these disturbances. The entire program of work has been summarised in this paper.

frequency amplitude and energy, weighting of the early, intermediate and late-time HEMP, and also deals with reflections and transmission of the HEMP at the earth's surface.

"Description of HEMP environment - Conducted disturbance" (61000-2-10, W. A. Radasky, USA) is based on the radiated waveforms in standard 61000-2-9 and is published as an IEC International Standard. It describes the conducted environment applicable for categories of conductors for different positions and illumination cases statistically taken into account. The specified environments are based on extensive theoretical calculations and experimental measurements.

Part 2 also includes "Classification of HEMP environment" (61000-2-11, W. A. Radasky, USA) and groups HEMP environments present at various locations outside and inside of civilian systems. The project is published as an IEC International Standard. One reason for classification is to provide guidance for equipment manufacturers to help them decide on the proper immunity test levels appropriate for their equipment. Another reason is to provide systems designers with guidance regarding construction methods and protective measures needed to achieve defined EM classes.

2.3. 61000-4-X

Part 4 "Testing and Measurement Techniques" presently includes five projects. "Test methods for protective devices for HEMP and other radiated disturbances" (61000-4-23, F. Tesche, USA) is approved for circulation as a FDIS. The document contains definitions, shielding effectiveness measurement methods of shielding materials, gaskets and shielded enclosures, and transfer impedance measurement methods for coaxial cables.

"Test methods for protective devices for HEMP conducted disturbance" (61000-4-24, W. K. Buechler, Switzerland) is published as an International Standard. It describes methods to measure the residual voltage on protective devices under HEMP conditions, i. e. for the case of very fast changes of voltage and current as a function of time. This standard complements the standard 61000-5-5 "Specification of protective devices for conducted disturbance".

"HEMP immunity test methods for

equipment and systems" (61000-4-25, P. R. Barnes, USA) is distributed as a fourth Committee Draft. The draft presently includes a list of immunity tests, environmental conditions, guidance for the selection of immunity tests, selection of severity levels, test levels, selection of test methods, test equipment, test set-up, test procedure and evaluation of test results. Efforts are being made to employ as many existing EMC test techniques as possible and to avoid more costly special HEMP tests.

"HEMP simulator compendium" (61000-4-32, J. C. Giles, USA) has been approved as a new work item. The specific aim of this project is to provide information on the various types of existing large HEMP simulators and their uses, performance parameters, limitations, and availability. This will allow all potential simulator users to evaluate the adequacy of available simulators for testing large systems.

"Measurement Methods for High-Power Transients", (61000-4-33, A. Kaelin, Switzerland), has recently been approved as a new project. The intention of this work is to identify appropriate sensor calibrations and measurement methods to be used for the measurement of high-power transient electromagnetic disturbances.

2.4. 61000-5-X

Part 5 "Installation and Mitigation Guidelines" presently includes five projects. "HEMP protection concepts" (61000-5-3, M. Ianoz, Switzerland) is published as a Technical Report. The concepts presented are based on general principles such as zoning, grounding, component selection, and circuit and equipment design.

"Specification of protective devices for HEMP radiated disturbance" (61000-5-4, J. Delaballe, France), is published as a Technical Report. This document identifies the parameters required to accurately specify protection to HEMP radiated fields.

"Specification of protective devices for HEMP conducted disturbance" (61000-5-5, W. K. Buechler, Switzerland), is published as an IEC International Standard. This standard identifies the parameters required to accurately specify protection for HEMP conducted environments.

A work originally started by SC77B, "Mitigation of external EM influences" (61000-5-6, J. Philip Castillo, USA) has been

EMC 2000

INTERNATIONAL WROCLAW SYMPOSIUM
ON ELECTROMAGNETIC COMPATIBILITY

URSI COMMISSION E OPEN MEETING

INTENTIONAL ELECTROMAGNETIC INTERFERENCE (EMI) -- WHAT IS THE THREAT AND WHAT CAN WE DO ABOUT IT?

Report of Working Group E2

Manuel W. Wik
Defence Materiel Administ.
Electronic Systems Direct.
SE-115 88 Stockholm
mawik@fmv.se

William A. Radasky
Metatech Corporation
358 S. Fairview Ave., Suite E
Goleta, CA 93117, USA
Wradasky@aol.com

Robert L. Gardner
6152 Manchester Park Circle
Alexandria, VA 22310, USA
GardnerR@aol.com

Intentional Electromagnetic Interference (EMI) is a new threat to electronic systems. Society's dependence on computer systems has increased rapidly over the past decade, and the susceptibility of these electronic systems to EM interference is increasing every year. At the same time hackers, criminals and terrorists are able to build EMI sources that can readily produce high level transient radiated and conducted disturbances. This paper reviews the overall threat and recommends actions to deal with the problem.

1. INTRODUCTION

There is likely to be an increase in the number of incidents involving intentional EMI in the future. It is important that engineers be aware of the threat that it poses and that those who design critical applications where malicious damage would have serious consequences should start to consider this in their designs and the layout of their systems. Engineers need to be aware of the problem, assess the risks posed to their equipment and applications and then take appropriate counter measures.

Intentional EMI can be attractive, because it can be undertaken covertly, anonymously and at some distance away from physical barriers, such as fences and walls. It can cover a great number of targets and leave minor traces or none at all. Those involved can range from careless people to pranksters, vandals, criminals and terrorists, whether state-sponsored or otherwise.

Electronic components and circuits, such as microprocessors, are working at increasingly higher frequencies and lower voltages and thus are increasingly more susceptible to electromagnetic

interference (EMI). At the same time, there have been rapid advances in radio frequency (RF) sources and antennae, and there is an increasing variety of equipment capable of generating very short RF pulses that can disrupt sophisticated electronics.

Pulse radiation devices may consist of two main types. They may be high power microwave (HPM) devices producing high power in a narrow frequency band, which could cause "front door" damage, or ultra-wide-band (UWB) devices, which produce a narrow time-domain pulse, and are more likely to cause "back door" disruption or damage. As the power density of the EM field decreases with the square of the distance from the source, the proximity of an EM generator to the targeted equipment is clearly a major factor in the damage likely to be caused.

Other types of EM sources are radiating continuous narrowband or wideband jammers, and EM injectors that are coupled (galvanic or inductive) directly to cables entering a facility.

2. RECOGNITION OF THE PROBLEM

Intentional EMI has been recognised as an area that needs to be considered by representatives of the International Union on Radio Science (URSI) and the International Electrotechnical Commission (IEC). The URSI General Assembly in August 1999 in Toronto issued a resolution recommending the scientific community in general and the EMC community in particular to take into account the threats of intentional EMI and to undertake a number of actions.

Earlier in the same year the IEC Technical Committee on EMC recommended that its subcommittee SC 77C deal with high power transient phenomena under a wider scope of work. The new scope is: "Standardisation in the field of electromagnetic compatibility to protect civilian equipment, systems and installations from threats by man-made high power phenomena including the electromagnetic fields produced by nuclear detonations at high altitude."

Hearings in the US Congress on 17 June 1997 and 25 February and 20 May 1998 on Radio Frequency Weapons and their proliferation indicate the seriousness of EMI as a present and future threat.

Commercial aircraft regulations which require that all radios, mobile phones, computers, CD players, etc. be turned off before take-off and landing, are well known to the public and indicate the seriousness of EMI in general. Similarly, hospitals restrict the use of mobile phones, which can affect patient monitoring and other medical equipment.

The possibility of EMI involvement in the crash of TWA Flight 800 has been discussed in published articles. (The Boeing 747 exploded at a height of about 13,000 feet near Long Island, New York in July 1996. There has been much speculation about the cause of the explosion, which has still not been definitely established.)

A Swedish study has revealed that high-power microwave (HPM) sources can stop cars at a distance of 900 meters and cause serious damage at a distance of 30 meters. Although dangerous in the wrong hands, this type of application could be of interest to law-enforcement agencies if it would allow stolen or fugitive vehicles to be brought safely to a halt from high speeds.

High-power EM emitters could be installed in vans along highways in order to stop car traffic and to cause malfunctioning of traffic signals. Similarly, if the vans were parked outside the perimeter of a large airport, they could disrupt the proper functioning of systems for take-off and landing. If such vans were left outside computer centres, they could cause malfunctioning of computer systems and would result in very high costs in lost business, mistrust and a bad reputation among customers. Of course, if the computer centre controlled critical industrial systems, the results could be even more serious in terms of injury and loss of life.

3. WHAT CAN BE DONE ABOUT IT?

The electromagnetic compatibility (EMC) community must be prepared to deal with new threats as they emerge. This article is intended to make people aware of the following:

- the existence of intentional EMI and associated phenomena;
- the fact that Intentional EMI can be undertaken covertly and anonymously and that physical boundaries such as fences and walls can be penetrated by electromagnetic fields;
- the potentially serious nature of the effects of intentional EMI on the infrastructure and important functions in society, such as transportation, communication, security and medicine;
- the major potential impact of such major disruptions of these important functions, in terms of loss of life, health, money, information, trust, time, and possibly other areas;
- the need for additional research into intentional EMI in order to understand the large variation of susceptibility levels and system weaknesses and to establish appropriate levels for dealing with such threats;
- the need for the development and recognition of techniques for appropriate protection against intentional EMI and of methods that can be used to protect the public from the damage to the infrastructure that could occur as a result of such intentional EMI;
- the need to develop special EM monitors to determine when an attack is underway;
- the necessity for high-quality testing and assessment of system performance when exposed to these special electromagnetic environments;
- the need for the EMC community to provide usable data to support the formulation of standards of protection.

4. CONCLUSIONS

Intentional EMI is a new threat to electronic systems. Fortunately this threat has been recognised by several international organisations, the IEC and URSI, and new work is underway to deal with the threat.

EMC 2000

INTERNATIONAL WROCLAW SYMPOSIUM
ON ELECTROMAGNETIC COMPATIBILITY

URSI COMMISSION E OPEN MEETING

TESTING STRATEGIES FOR SUSCEPTIBILITY TESTING IN HIGH POWER ELECTROMAGNETICS

Robert L. Gardner, Consultant and David C. Stoudt
Joint Program Office for Special Technology Countermeasures (JPO/STC)
Mail Stop Code B20
NAVSURFWARCENDIV
17320 Dahlgren Road
Dahlgren, VA 22448-5100
540-653-2715, GardnerRL@nswc.navy.mil
540-653-8050, StoudtDC@nswc.navy.mil

Carl E. Baum
Air Force Research Laboratory DEHE
3550 Aberdeen Ave SE
Kirtland AFB
Albuquerque, NM 87117-5776
505-846-5092

The Commission E Open Meeting papers consist of a combination of a status report for the working group of interest and a short paper in the area of interest of the working group. Recent work in high power electromagnetics (HPE) has been reported in the Reviews of Radio Science 1996-1999, at the US National Radio Science Meeting and most recently at the EuroEM Conference in Edinburgh. Activities are varied and range from models of the electrical properties of the center of a lightning return stroke to transient antenna design to the design of gas switches.

HPE fields impact equipment in a variety of ways and can include the usual interference, disruption and damage. One of the challenges of determining the lethality of HPE waveforms is the extreme variability of the effects. Complete conclusions about the systems require thorough test techniques. HPE tests are very expensive so that choosing an efficient test strategy is important. This paper outlines some of those test strategies based on "Design of Experiment" techniques.

1. HPE COMMITTEE ACTIVITIES

High Power Electromagnetics (HPE) has been an important part of Commission E's research interests since the formation of Commission E. HPE is the study of electromagnetic field generation, coupling, and system interaction for those cases where nonlinear phenomena in air become an important part of the interaction process. This work includes high power microwaves, electromagnetic pulse, lightning source

region interactions and related phenomena. There is close interaction between this working group and the working groups on Interaction with, and Protection of, Complex Electronic Systems and Effects of Transients on Equipment as well as the newly formed working group on Intentional Electromagnetic Interference.

Recent activities of the HPE Working Group have included preparation of two articles for the Reviews of Radio Science [1,2], support of an HPE session for the North American Radio Science Meeting, and preparations for the upcoming EuroEM meeting scheduled for 28 May 2000 in Edinburgh. The two RRS papers were a review of research on the impulse radiating antenna (IRA) and a review of some of the analytic techniques of high power electromagnetics (HPE).

The IRA is a new and exciting antenna design that is well suited for radiating fast pulses in a narrow beam. Its high gain at early times (high frequencies) comes from the optical like behavior of its dish and at later times from a unique loading design in its feed arms. There are variations of the design that allow additional flexibility through use of the symmetry features of the antenna.

HPE modeling, by definition, requires the application of Maxwell's equations with various models of plasma physics. The geometries are often so complex that it is necessary to simplify the treatment considerably and still describe the important physical

effects. This RRS chapter includes some of these simplifications like an analytic equation of state for air and a transmission line model of the lightning return stroke.

The HPE session at the US National Radio Science Meeting that was held in January 2000 in Boulder, CO included a variety of topics. There were two different designs of transient antennas presented. Several different varieties of IRA were considered in the session. Fast closing switches are used to drive IRAs and other broadband antennas. Three papers discussed the characteristics of these switches. Finally, there were papers on lightning, laser induced microwave emission and HPM susceptibility.

The EuroEM conference promises to be the highlight of the biennium for the HPE community. There are sessions being organized in most of the components of HPE. Topics include high power microwave sources and effects, electromagnetic pulse, lightning, and other topics in HPE research. The technical basis for HPE including coupling, generation, and vulnerability are all part of the program.

This promises to be an exciting year in HPE research. There is increased understanding of the phenomena of interest gained through better analytic and computer models as well as significant effects research.

2. ISSUES IN SUSCEPTIBILITY TESTING

RF weapons are complex assemblies of RF oscillators, pulse forming networks and antennas. These weapons interact with targets along complex paths that are difficult to predict. Complex coupling geometries and varying tactical scenarios lead to varying susceptibility levels that complicate the weapon assessment process. This situation requires a combination of empirical and analytical techniques for RF system analysis. Even with complete treatment of all of these issues, the variability of HPE effects ranges over 10 or more orders of magnitude in power density [3].

Drawing conclusions from the RF susceptibility data requires careful planning and attention to the requirements of statistical significance. [4,5]. The chief difficulties in RF susceptibility data analysis are the large number of parameters and the sensitivity of the data to small variations in test conditions. Susceptibility or immunity levels can vary a great deal with changes in any of the parameters. Developing trends in the data therefore requires sample sizes of usually 20 or more examples of the target. On the other hand, large numbers of the test objects are usually not available or are very expensive.

3. OBJECTIVES OF VULNERABILITY TESTING

The first step in assessing the response of a system to RF attack is to clearly state the objectives of the experiments and/or analysis [6]. For protection, we want to know the potential weaknesses or failures of a system when exposed to a variety of potential threats. The type of threat can be limited by a clear definition of the potential adversary [7]. We will want to know if there are any particularly soft conditions or sweet spots in the defended system we need to consider.

Once the system and threat are described we will need to know what effects are important to the system. Upset of a computer may be catastrophic to one system and an irritation to another.

Our final task is to determine and state clearly the most important parameters in the scenario and to state the potential system effects as functions of system configuration and source parameters. There are potentially 10s to hundreds of parameters available in the total source-target interaction. The large number of parameters makes the determination of susceptibility or vulnerability a difficult task whether done experimentally or analytically.

4. PARAMETER DEFINITION

So, what we want to do is to map out the failures in a large parameter space and specifically identify particular system weaknesses. This process is a challenge with the large number of parameters available to the source designers and required to describe the protected system.

Still there are a number of parameters that must be considered coming to a conclusion about a system. For the source, some parameters are:

- a. Field strength at the target.
- b. Waveform of each pulse
 - 1) Rise time
 - 2) Area or energy
 - 3) Center frequency
 - 4) Bandwidth
- c. Total number of pulses
- d. Pulse rate.
- e. Field level as a function of distance
- f. Reflected fields
- g. Access to the target by the weaponer

An electromagnetic description of the target system is more difficult and usually requires a topological decomposition of the system. Our process is aided by the likelihood that our defined task is to protect some particular facility or system. Even for a single system, there are many remaining parameters. There may be

doors that can be opened or closed. The system may have connections that can be in place or not or the system may even be portable so its location must be described.

Locations of individual wires in a system may make a difference in susceptibility and our physical understanding of the interaction is not sufficient to determine the threshold for wire movement that changes the result of a susceptibility experiment. Some particular modulations or waveforms may be particularly effective against some targets. For example LoVetri, et al [8] found that certain modulations on carriers tuned to a computer case caused failures at field strengths as low as 30 V/m. As noted, it is this kind of vulnerability that causes the largest problem for systems that requires protection from RF attack.

5. AN EXPERIMENT STRATEGY

Most experiments in HPE susceptibility are anecdotal experiments. That is, one test object is placed in front of a source and the target system either fails or it doesn't. Experiments of this type yield little information that can be used to predict the outcomes of other experimental or operational situations. Next, there are some limited parameter variations. Test objects and test execution are expensive so there are few repetitions. The results are not statistically significant at any useful confidence level. If there is an effort to make statistically significant experiments, the experimenters will usually only consider one parameter. That parameter might be distance from the source or it might be test object serial number. For many of the situations of interest to this community, 30-50 tests are required to complete a study of one parameter. The number of tests here is typically known as the number of degrees of freedom when calculating descriptive statistics. There are rarely sufficient resources to investigate one parameter in this manner, much less the number required for a coherent physical review of the interaction with the target. This method is known as the one-variable-at-a-time approach. We need a better strategy to treat all of the parameters efficiently.

With all of these parameters we must find out which ones are most important by some means other than intuition. Fortunately, there are statistical tools available to make that determination [9]. First, we need to have a numerical scheme to describe the effects. One might use a sliding scale of interference, disturbance, disruption, and damage, for example. The next step is to take each of the parameters and plan experiments for high and low values of each of them. Experiments like this are called factorial designs and the number of experiments goes up as 2^n . That can be a lot of experiments, but significantly less than the one-variable-at-a-time technique. When the experiments are

done, we have values describing system effect as a function of the many parameters. In other words, we have a multidimensional conceptual plot of effects level. The response to variation in the parameters must be smooth and relatively monotonic for this technique to work. Resonant response cannot be treated effectively with this method. Simultaneous solution and determination of the sensitivity of the effects level to each parameter can be found by analysis of variance techniques. A standard analysis of variance (ANOVA) relates the changes in variance to the particular parameter. The method also will determine similar relations for combinations of variables or cross terms. Information on the sensitivity of effects to combinations of variable is not available through "one-variable-at-a-time" techniques.

Examining data in this way is a well-understood process in reliability engineering and related disciplines, but is rarely used in engineering experiments. The technique is known as Design of Experiment concepts. In this method only a few (2-3) values of each of the parameters is considered in the experiment planning. This method of experiment planning greatly reduces the total number of tests necessary for statistical significance. For this technique the number of degrees of freedom is related to the number of experiments not to the number of experiments per parameter as it is in the one-variable-at-a-time technique.

This technique is best applied in stages. In the first pass, we can eliminate many of the parameters that don't change the effects level very much. With a few remaining parameters we can treat the variations more carefully, particularly if the variation with the parameter is not linear. Three or more experiments per parameter allow the possibility of a maximum within the parameter space examined. Complex response functions require many data points to resolve the parameter sensitivity.

This strategy allows us to efficiently design susceptibility tests. It also allows us to quantitatively examine a number of important parameters that are needed to describe a particular engagement scenario. Further work is required to understand the uncertainties that are introduced by specific sampling methods.

6. REFERENCES

- 6.1. R. L. Gardner, "Methods of High Power Electromagnetics, *Review of Radio Science 1996-1999*, Oxford, New York, 1999, pp. 387-402.
- 6.2. C. E. Baum, E. G. Farr, and D. V. Giri, "Review of Impulse-Radiating Antennas", *Review of Radio Science 1996-1999*, Oxford, New York, 1999, pp. 403-439.

6.3. R. L. Gardner and C. W. Jones, "System Lethality: Perspective on High Power Microwaves", *System Design and Assessment Notes*, Note 34, EMP Note Series, AFRL/DEPE, Air Force Research Laboratory, Kirtland AFB, NM, 1995.

6.4. I. Kohlberg and R. L. Gardner, "Interpreting Electronic System Response to Unwanted Electromagnetic Signals Using Non-Parametric Statistics", *Proceedings of the International Symposium on Electromagnetic Compatibility*, Magdeburg, p 37, Oct 99.

6.5. R. Holland and R. H. St. John, *Statistical Electromagnetics*, Taylor & Francis, New York, 1999.

6.6. C. E. Baum, "From the Electromagnetic Pulse to High-Power Electromagnetics," *Proc. IEEE.*, 1992, pg. 789-817, Sec. VI.

6.7. R. L. Gardner, M. W. Wik, and D. C. Stoudt, "Intentional Electromagnetic Interference", *Review of Radio Science 1996-1999*, Oxford University Press, New York, 1999, Ch. 13, p. 349.

6.8. J. LoVetri, A. T. M. Wilbers, A. P. M. Zwamborn, "Microwave Interaction With A Personal Computer: Experiment and Modeling", *Proceedings of the 13th International Zurich Symposium and Technical Exhibition on Electromagnetic Compatibility*, 1999, p. 39G6.

6.9. W. J. Diamond, *Practical Experiment Design*, Wiley, New York, 1989.

Dr. Robert L. Gardner received his PhD from the University of Colorado in 1980. He has been active in High Power Electromagnetics since that time and is now Co-Chairman of the International Working Group on High-Power Electromagnetics (HPE). He is Chairman of Commission E of the International Union of Radio Science. Dr. Gardner has worked in the EMP, lightning, and high power microwave communities in a variety of positions with the US Navy and the US Air

Force advising them on various aspects of the effects and interaction of HPE. He has published widely in these areas and. Dr. Gardner is currently a Consultant supporting the JPO-STC located in Dahlgren, VA.

Dr. David C. Stoudt's current research efforts include the effects of high-power microwaves on electronic equipment, the development of high-power photoconductive switches, and the development and evaluation of other high-power electromagnetic sources. He is currently the US Senior National Representative to the NATO SCI-019 Panel on "Tactical Implications of High Power Microwaves," and the Counter-RF Program Manager for the JPO-STC. In 1999 he was awarded the Navy's Meritorious Civilian Service Award. He is widely published with thirty-five refereed journal and conference papers, two book chapters, and has been awarded five patents.

Dr. Carl E. Baum received the BS, MS, and PhD degrees from the California Institute of Technology in 1962, 1963, and 1969. Since his completion of military service in 1971 he has served as Senior Scientist at the Air Force Research Laboratory. His research is highly acclaimed. Among his many awards are the Air Force Research and Development Award, The AFSC Harold Brown Award, the Richard C. Stoddard award of the IEEE EMC Society, and the 1987 IEEE Harry Diamond Award. He is a Fellow of the IEEE and has been named a Phillips Laboratory Fellow. Dr. Baum has published numerous papers, reports and book chapters and has published four books. The titles are: *Transient Lens Synthesis: Differential Geometry in Electromagnetic Theory*, *Electromagnetic Symmetry*, *Ultra-Wideband, Short-Pulse Electromagnetics 3*, and *Detection and Identification of Usually Obscured Targets*. He is a member of Commissions A, B, and E of the US National Committee of the International Union of Radio Science and Co-Chair of the International Working Group on High Power Electromagnetics.

EMC 2000

INTERNATIONAL WROCLAW SYMPOSIUM
ON ELECTROMAGNETIC COMPATIBILITY

URSI COMMISSION E OPEN MEETING

IMPACT OF THE 1997-98 EL NIÑO EVENT ON LIGHTNING ACTIVITY OVER INDONESIA

Effrina Y. Hamid, Zen-Ichiro Kawasaki, and Redy Mardiana

Department of Electrical Engineering, Osaka University

Yamadaoka 2-1, Suita, Osaka 565-0871, JAPAN

Fax: +81-6-6879-7724

Email: zen@pwr.eng.osaka-u.ac.jp

Abstract: *The 1997-98 El Niño is one of the strongest El Niño Southern Oscillation (ENSO) events of this century. The major impact of the sea surface temperature (SST) change during this El Niño event was the shift in the convection activity from the western to the central and eastern Pacific affecting the response of rain-producing cumulonimbus. As a result, convective rainfalls were suppressed near the western Pacific regions and maritime continents including Indonesia. On the other hand, the lightning activity during El Niño period increased in contrast (on the average of 57%). As observed by the Tropical Rainfall Measuring Mission (TRMM) Lightning Imaging Sensor (LIS) and Precipitation Radar (PR), the convective storms during El Niño were more intense. This was supported by the facts that the El Niño's storms had greater vertical developments and thicker zones containing ice phase precipitation.*

1. INTRODUCTION

The 1997-98 El Niño event is the strongest on record, comparable in magnitude to 1982-1983 episode [Chandra et al., 1998; McPhaden and Yu, 1999]. The El Niño began to develop in March 1997 and has strengthened rapidly since then. The western Pacific warm pool migrated eastward with the collapse of the trade winds [Chandra et al., 1998; McPhaden and Yu, 1999; Lau and Wu, 1999]. After a gradual decline in the intensity of these thermal anomalies in early 1998, the El Niño event abruptly ended during May-June 1998 and then the SST reverted to a normal condition (some investigators confirmed that a La Niña event appeared after El Niño event). The major impact of the El Niño was less convection in the Western Pacific and maritime continent including Indonesia, or approximately from Papua New Guinea to the eastern and central Indian Ocean and central East Asia. As a result, there has been a significant decrease in rainfall and convection activity over the western Pacific and maritime continent [Chandra et al., 1998; Lau and Wu, 1999; Shen and Kimoto, 1999]. These changes during El Niño affected atmospheric circulation. Since tropical storms and deep convection are directly linked to the transport of momentum, heat, and moisture in the atmosphere, several changes on atmospheric circulation during El Niño could possibly influence storm frequency and intensity [Williams, 1992b]. One aspect of storms is lightning activity.

Several investigators have documented relating lightning-producing storms. Lightning activity is related to the stage of convective cloud development [Williams et al., 1989], the intensity of updrafts [Lhermitte and Williams, 1983; Williams et al., 1992a], cloud structure [Rust and Doviak, 1982], convective available potential energy (CAPE) [Williams et al., 1992a; Williams and Renno, 1993] and even surface air temperature [Williams et al., 1992a; Williams, 1992b; Williams, 1994; Price, 1993]. Williams et al. [1992a] reported that the vertical development of convection is positively correlated with updraft intensity that transport supercooled drops and ice particles into the mixed phase regions (between 0°C and 40°C), so that it can be shown that the vertical development is also strongly related to lightning activity. Observations over the oceans have found that oceanic storms, compared to continental storms, showed very weak updraft, and consequently they have vertical reflectivity profiles exhibiting modest at low levels, and decreasing rapidly with height above the freezing level [Jorgensen and LeMone, 1989; Szoke et al., 1986].

The purpose of this study is to investigate the implications of the change in convective precipitation due to 1997-98 El Niño event on the lightning activity in a certain tropical region and their possible correlation with some parameters for storms. The tropical region, which was selected, is Indonesia (6°N - 11°S and 95°E - 141°E).

2. DATA SETS

For this work, we used data set scanned by the Tropical Rainfall Measuring Mission (TRMM) satellite. The TRMM is a joint effort between the National Aeronautics and Space Administration (NASA) of U.S. and the National Space Development Agency (NASDA) of Japan to study tropical and subtropical rain systems. The TRMM satellite carries five sensors and the characteristics of each sensor have been described by Kummerow et al. [1998]. The TRMM satellite crosses over Indonesia at least two times and a maximum of six times a day during ascending and descending passes. Therefore the collected data are not full time observations over Indonesia but are collected just during the TRMM overpasses Indonesia. The data sets used are from two of the sensors, as follows:

i) Lightning data from the TRMM Lightning Imaging Sensor (LIS): provided by the Global Hydrology Resource Center (GHRC), the Information Technology

component of the Global Hydrology and Climate Center in Huntsville, Alabama (URL: <http://ghrc.msfc.nasa.gov/>). Since LIS detects optical emissions during lightning discharges, the data sets used correspond to intra-cloud and cloud-to-ground flashes.

ii) Precipitation data from TRMM precipitation radar (PR): supplied by the TRMM Science Data and Information System (TSDIS) and distributed to the public by the Distributed Active Archive Center (DAAC) (URL: <http://daac.gsfc.nasa.gov/>) at NASA Goddard Space Flight Center. The TRMM PR data used are: (a) 3A-25 Planetary Grid 1 which has 0.5° grid intervals ranged from 6°N to 11°S and 95°E to 141°E . These include the mean convective rainfall (convRainMean2), the mean convective storm height (stormHeightMean), the mean depth of ice phase precipitation (sdepthMean2), and the mean bright band height (bbheightMean), (b) 3A-25 Planetary Grid 2 which has 5° grid intervals ranged from 5°N to 10°S and 95°E to 140°E , and the data are histogram for convective rainfall (convrainH).

3. RESULTS

Figure 1 shows the monthly variation and diurnal variation of lightning flashes over Indonesia from December 1997 to May 1999. No lightning data are provided before December 1997 because the TRMM satellite was launched in November 1997. Indonesia has relatively high lightning activity from November to April (corresponding to the rainy season) and a low lightning activity from May to October (corresponding to the dry season) [Hamid et al., 1999]. The rainy season also relates to the Asian winter monsoon, which coincides, in part, with the Australian summer monsoon. A key point in this figure is the contrast in number of flashes between December 1997 to May 1998 and December 1998 to May 1999 with the highest incident times in the early to the late afternoon (about 13 to 19 local time). It is noted that December 1997 to May or June 1998 correspond to El Niño period, which intercepts with rainy season period. On the average the number of flashes increases about 57% during El Niño

lightning flashes occurred during those months (a 92% increase during March 1998). We use the term number of lightning flashes rather than the lightning flash rate to represent the lightning activity in the discussion.

The spatial distribution of lightning flashes during March 1998 and 1999 is shown in Fig. 2. The figure clearly shows that in March 1998 the lightning activity was generally more intense, but not everywhere. However, the number of pixels of convective rainfalls in March 1998 as shown in Fig. 3 was apparently lower than that in March 1999. The number of pixels of convective rainfalls can be an indicator of convective storm activity.

Figure 4 shows that the convective rainfalls were more widespread across the ocean in March 1999 than those in March 1998. The larger number of convective rainfalls in March 1999 occurred both on the land/coast and ocean (see Fig. 3). From Fig. 2, it is obvious that lightning flashes were concentrated on land and the coast and were very rare lightning on the ocean, even though in March 1999 the convective rainfalls were widespread across the ocean. This behavior has been observed in previous studies. Jorgensen and LeMone [1989] made observations of oceanic storms and stated that oceanic storms show very weak updraft, even though the convective clouds develop to great depths in the oceanic atmosphere. Due to weak updrafts, oceanic storms rarely have high reflectivity regions extending above the freezing level (0°C), meaning there will be few large ice phase particles therein [Szoke et al., 1986]. However, typical freezing level locations for oceanic and continental storms are similar [Jorgensen and LeMone, 1989] (see later Fig. 7).

From the spatial distribution of convective storm heights as shown in Fig. 5 it is shown that in March 1999 the storms were more widely distributed across the land and ocean (like the distribution of convective rainfalls) and can develop to quite high altitude (7000-9000 m) in the atmosphere. The storm height in this study is the height of a storm from the ground level to the minimum detectable reflectivity value ($\sim 16 - 18$ dBz). The interesting part in Fig. 5 is that the storms were more concentrated on land and coast and had higher vertical developments during March 1998 than

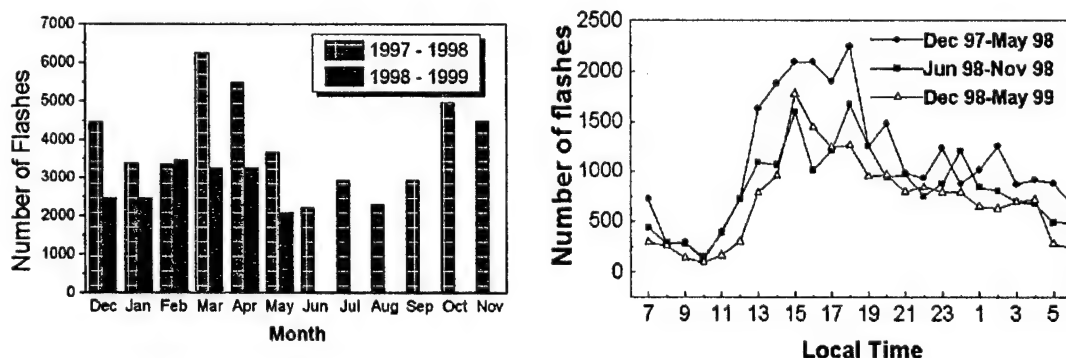


Fig. 1. Monthly variation (left) and diurnal variation (right) of lightning activity over Indonesia (6°N - 11°S and 95°E - 141°E). December 1997 to May or June 1998 correspond to the El Niño period and the other months correspond to the normal period.

period. As a case study we focus on the comparison of lightning activity between March 1998 and March 1999, since some of the greatest difference in the number of

the storms during March 1999. The spatial locations of the storms that have high vertical reflectivity were the same with those of intense lightning activity as seen in

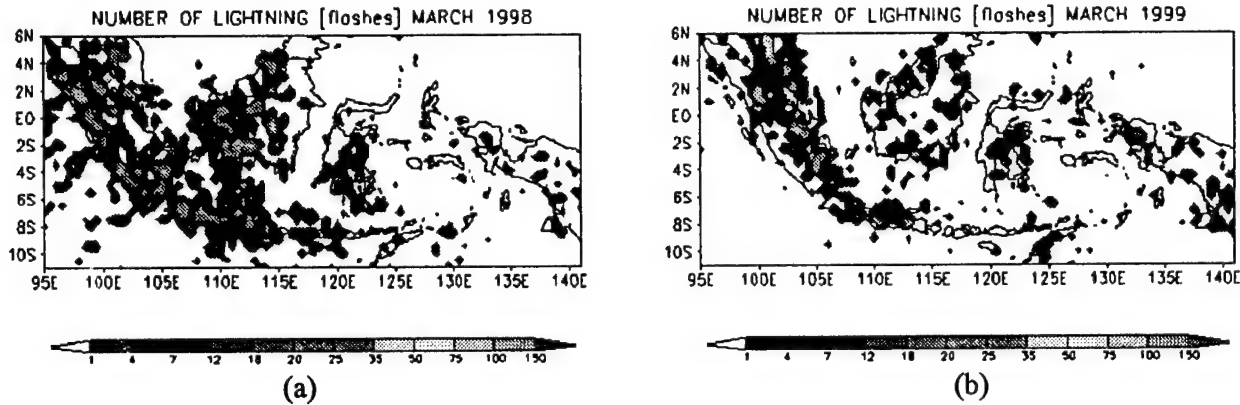


Fig. 2. Spatial distribution of lightning activity, (a) March 1998, and (b) March 1999. The number of flashes is sampled every $0.5^\circ \times 0.5^\circ$.

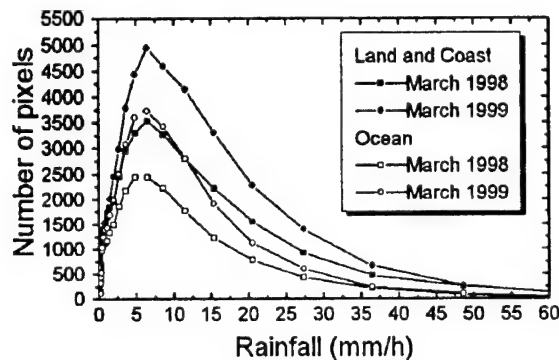


Fig. 3. Number of pixels of convective rainfalls over Indonesia at an altitude of 2 km during March 1998 and March 1999. One pixel corresponds to an instantaneous field of view (IFOV) during TRMM PR scanning (similar to $\sim 4.3 \times 4.3 \text{ km}^2$ at ground level). Selected grids for the land and coast are ($0^\circ\text{--}5^\circ\text{N}$ and $95^\circ\text{E}\text{--}105^\circ\text{E}$), ($0^\circ\text{--}5^\circ\text{N}$ and $110^\circ\text{E}\text{--}120^\circ\text{E}$), ($0^\circ\text{--}5^\circ\text{S}$ and $100^\circ\text{E}\text{--}105^\circ\text{E}$), ($0^\circ\text{--}5^\circ\text{S}$ and $110^\circ\text{E}\text{--}125^\circ\text{E}$), ($0^\circ\text{--}5^\circ\text{S}$ and $130^\circ\text{E}\text{--}140^\circ\text{E}$), ($5^\circ\text{S}\text{--}10^\circ\text{S}$ and $105^\circ\text{E}\text{--}125^\circ\text{E}$), and ($5^\circ\text{S}\text{--}10^\circ\text{S}$ and $135^\circ\text{E}\text{--}140^\circ\text{E}$). The rest grids are for the ocean.

Fig. 2. Since the lightning activity took place primarily on land and coast, the search for the explanation of the large difference in number of flashes between March 1998 and March 1999 is, therefore, focused on the storms that occurred on the land and the coast.

Figure 5, as discussed earlier, shows that during March 1998 the land and coast have higher vertical developments than those during March 1999. Since higher vertical developments is positively correlated with stronger updraft, it can be shown that higher vertical developments also relates to higher lightning activity [Williams et al., 1992a]. Larger updraft velocities within the electrified clouds must be sufficiently intense to carry larger particles in the solid phase by riming and with a larger accumulation of ice-phase condensate in the mixed phase region. A larger accumulation of ice-phase causes a more vigorous separation of positive and negative charge by ice particles collision [Williams, 1994]; this charge separation then would result in more rapid breakdown and hence more frequent lightning [Solomon and Baker, 1998; Takahashi et al., 1999]. As shown in Fig. 2, large lightning activity occurred wherever high vertical

developments were present (compare with Figure 5). Additional evidence that the storms in March 1998 contained larger amount of precipitation particles above the freezing level, which are responsible for electrical discharges, is indicated by the snow depth as seen in Fig. 6. The snow depth is the thickness of the cloud containing snow, graupel, and other precipitation particles above the freezing level. However, the locations of the freezing level above the ground, represented by the bright band heights in Fig. 7, were not significantly different between March 1998 and March 1999. They were in a range of 4000 - 4750 m on the land and coast. This means that the height of storms is not or less affected by the height of freezing levels, but it is due to the thickness of ice phase precipitation zones.

4. SUMMARY AND DISCUSSIONS

The increase in number of lightning flashes during El Niño over Indonesia has been studied by taking a comparison of lightning activity between March 1998, corresponding to El Niño period, and March 1999,

corresponding to normal period. The main differences are summarized as follows:

- i) On ocean: During El Niño period (normal period) the number of convective storms decreases (increases), meanwhile the number of lightning flashes remains low.
- ii) On land and coast: During El Niño period (normal period) the number of convective storms decreases (increases), on the contrary, the number of lightning flashes increases (decreases). These indicate that convective storms are more intense during El Niño period so that they can produce more lightning discharges. The higher intensity of convective storms is supported by the facts that the storms have higher vertical developments and thicker ice phase precipitation zones.

phase. The point deserving greater emphasis, particularly for the tropics, is that the production of rainfall in the tropics requires only very modest lifting (because only the liquid phase is necessary for abundant rainfall) but the production of active lightning requires deep lifting (because a vigorous ice phase is essential). No wonder the lightning-rainfall relationship is non-unique [Earle Williams, personal communication, 2000]. This means that one must be cognizant of meteorological regime in generalizing about lightning-rainfall relationship [Petersen and Rutledge, 1998; Williams et al., 1992a].

Turning now to the effect of surface air temperature. Since lightning frequencies in the tropics are very sensitive to small increase in surface air temperature

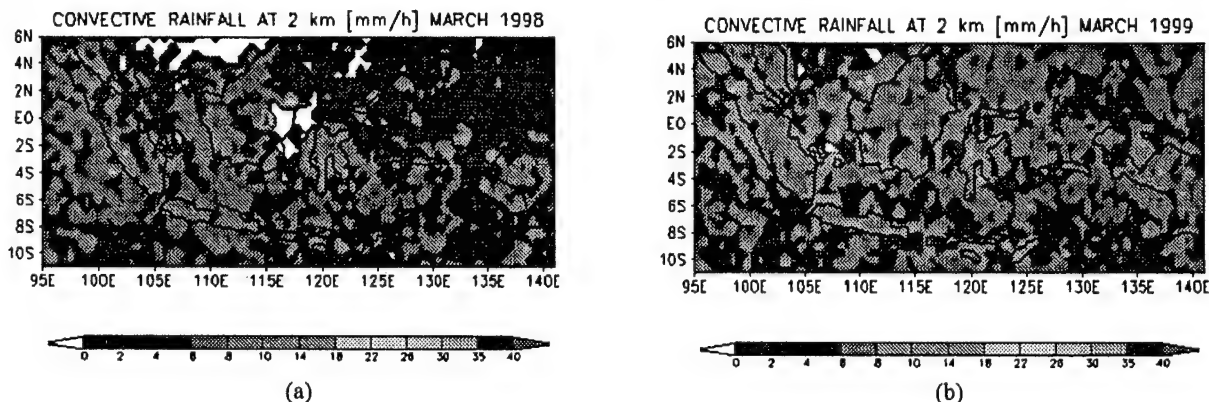


Fig. 4. Spatial distribution of the mean convective rainfalls at an altitude of 2 km, (a) March 1998, and (b) March 1999. The convective rainfalls were uniformly distributed across land/coast and ocean during March 1999, but more concentrated on land and coast during March 1998.

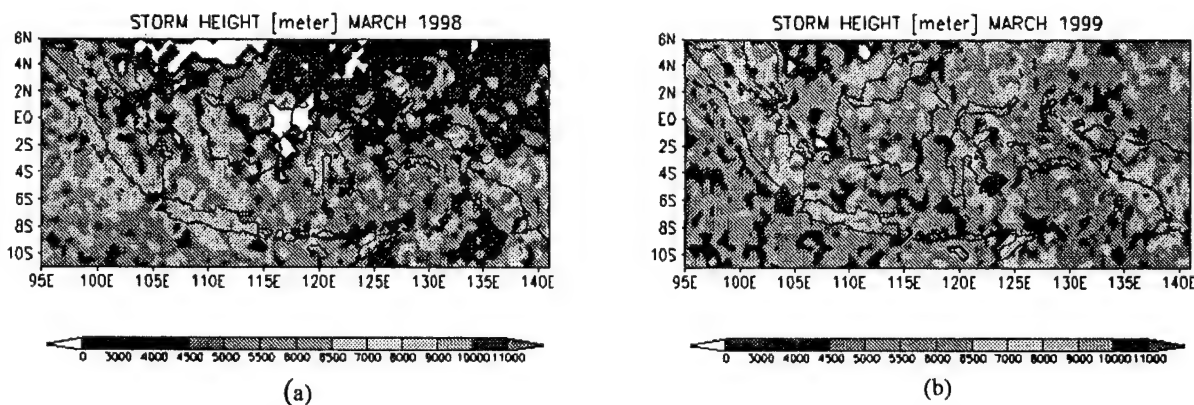


Fig. 5. Spatial distribution of the mean convective storm heights, (a) March 1998, and (b) March 1999. The storm height corresponds to the vertical development of convection.

Previous studies of El Niño over land areas in other parts of the world have emphasized that El Niño is the warm phase (higher surface air temperature than during normal period) and the dry phase [Amarasekera et al., 1997; Kent et al., 1995]. Numerous other studies have pointed out to a proportionality between rainfall and lightning, leading to the inference that the wet phase (abundant rainfall) is the active lightning phase. This latter result runs counter to the result in this study and also to the study of Williams [1992b] that concluded that the warm phase was also the active lightning

[Williams, 1992b] and the surface air temperature over the majority of tropical lands increases during El Niño years [Hansen and Lebedeff, 1987], then the warm phase of El Niño may cause larger lightning activity, because the increase in surface air temperature affects to the larger CAPE, which is associated to the deeper clouds and larger updrafts in episodic deep convection [Williams and Renno, 1993]. Additionally, satellite observations (SAGE - Stratospheric Aerosol and Gas Experiment) of upper tropospheric cirrus by Kent et al. [1995] have found more cirrus during the warm phase

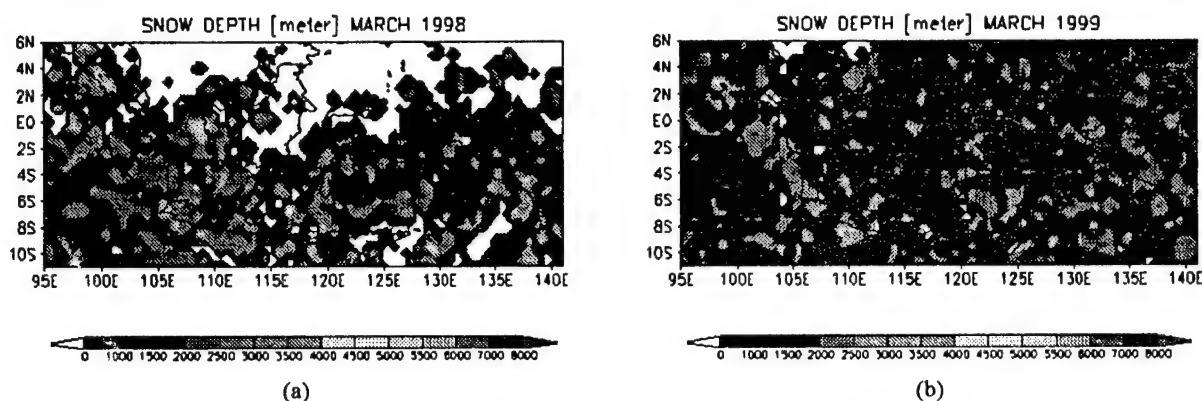


Fig. 6. Spatial distribution of the mean depth of ice phase precipitation, (a) March 1998, and (b) March 1999.

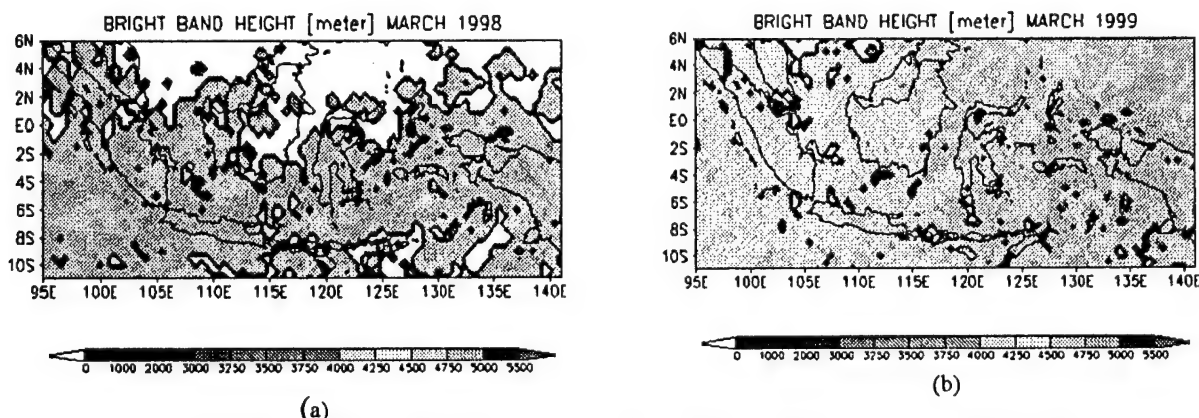


Fig. 7. Spatial distribution of the mean bright band height, (a) March 1998, and (b) March 1999. Bright band is a melting region, which is lying at or just below 0°C isotherm. The height of bright band levels is not different for land/coast and ocean for both months.

El Niño at many places throughout the tropics, including Indonesia. These observations are consistent with larger vertical development (where the cirrus detrains) in this study. Furthermore, Rutledge et al. [1992] and William et al. [1992a] reported during the Down Under Doppler and Electricity Experiment (DUNDEE) in Darwin that within the Australian monsoon two primary modes of convection exist over land areas, one characteristic of tropical oceanic convection (during the active monsoon) and another of continental convection (during the break monsoon). Continental convection can produce lightning rate larger than oceanic storms, and this is because oceanic convection often display no electrification and show rapid decrease in vertical radar reflectivity above the freezing level even when precipitation is heavy. Continental and oceanic convection that exhibit very different radar reflectivity about freezing levels can often grow to considerable depth (15–20 km). If the differences between continental and oceanic convection during DUNDEE are representative of differences elsewhere in the tropical lands, then the convection during El Niño period in Indonesia is more "continental like" because the vertical reflectivity development of the storms is larger and the rainfall yield per lightning flash (e.g. March 1998) decrease.

Other mechanisms of producing larger lightning activity that should also be considered are land-sea

breeze circulations over the numerous islands contained in Indonesian maritime continent. Since the SST is suppressed [Chandra et al., 1998; McPhaden and Yu, 1999; Lau and Wu, 1999] and the surface air temperature over tropical lands increases during El Niño years [Hansen and Lebedeff, 1987], then there will be more significant land vs. ocean differences in heating profiles within the maritime continent. Due to these temperature contrasts, it can be expected that over islands where sea breeze and topographic effects can be important, deeper convection may occur during El Niño than during normal period. The deeper convection may have greater vertical developments, which are responsible for producing larger lightning flashes.

Acknowledgments. We acknowledge with gratitude the contribution of GHRC for providing worldwide lightning data and to the TSDIS for supplying precipitation data via DAAC. Discussions with Earle Williams were most helpful.

5. REFERENCES

1. Amarasekara, K. N., R. F. Lee, E. R. Williams, and E. A. B. Eltahir, ENSO and the natural variability in

- the flow of tropical rivers, *J. Hydrology*, 200, 24-39, 1997.
2. Chandra, S., J. R. Ziemke, W. Min, and W. G. Read, Effects of 1997-1998 El Niño on tropospheric ozone and water vapor, *Geophys. Res. Lett.*, 25, 3867-3870, 1998.
 3. Hamid, E. Y., Z.-I. Kawasaki, R. Mardiana, and K. Matsuura, TRMM/LIS observations of lightning activity over Indonesia and comparison with ground-based measurement around Java Island, *J. Atmos. Elect.*, 19, 153-164, 1999.
 4. Hansen, J., and S. Lebedeff, Global trends of measured surface air temperature, *J. Geophys. Res.*, 92, 13345-13372, 1987.
 5. Jorgensen, D. P., and M. A. LeMone, Vertical velocity characteristics of oceanic convection, *J. Atmos. Sci.*, 46, 621-640, 1989.
 6. Kent, G. S., E. R. Williams, P. H. Wang, M. P. McCormick, and K. M. Skeens, Surface temperature related variations in tropical cirrus cloud as measured by SAGE II, *J. Climate*, 8, 2577-2594, 1995.
 7. Kummerow, C., W. Barnes, J. Shiue, and J. Simpson, The Tropical Rainfall Measuring Mission (TRMM) sensor package, *J. Atmos. and Ocean Tech.*, 15, 809-817, 1988.
 8. Lau, K. M., and H. T. Wu, Assessment of the impacts of the 1997-98 El Niño on the Asian-Australia monsoon, *Geophys. Res. Lett.*, 26, 1747-1750, 1999.
 9. Lhermitte, R., and E. R. Williams, Cloud electrification, *Rev. Geophys.*, 21, 984-992, 1983.
 10. McPhaden, M. J., and X. Yu, Equatorial waves and the 1997-98 El Niño, *Geophys. Res. Lett.*, 26, 2961-2964, 1999.
 11. Petersen, W. A., and S. A. Rutledge, On the relationship between cloud-to-ground lightning and convective rainfall, *J. Geophys. Res.*, 103, 14,025-14,040, 1998.
 12. Price, C., Global surface temperatures and the atmospheric electrical circuit, *Geophys. Res. Lett.*, 20, 1363-1366, 1993.
 13. Rust, W. D., and R. J. Doviak, Radar research on thunderstorms and lightning, *Nature*, 297, 461-468, 1982.
 14. Rutledge, S. A., E. R. Williams, and T. D. Keenan, The down under doppler and electricity experiment (DUNDEE): Overview and preliminary results, *Bull. Am. Meteorol. Soc.*, 73, 3-16, 1992.
 15. Shen, X., and M. Kimoto, Influence of El Niño on the 1997 Indian summer monsoon, *J. Meteor. Soc. Japan*, 77, 1023-1037, 1999.
 16. Solomon, R., and M. Baker, Lightning flash rate and type in convective storms, *J. Geophys. Res.*, 103, 14041-14057, 1998.
 17. Szoke, E. J., E. J. Zipser, and D. P. Jorgensen, A radar study of convective cells in mesoscale systems in GATE. Part I: Vertical profiles statistics and comparison with hurricanes, *J. Atmos. Sci.*, 43, 182-197, 1986.
 18. Takahashi, T., T. Tajiri, and Y. Sonoi, Charges on graupel and snow crystals and the electrical structure of winter thunderstorms, *J. Atmos. Sci.*, 56, 1561-1578, 1999.
 19. Williams, E. R., M. E. Weber, and R. E. Orville, The relationship between lightning type and convective state of thunderclouds, *J. Geophys. Res.*, 94, 13,213-13,220, 1989.
 20. Williams, E. R., S. A. Rutledge, S. G. Geotis, N. Renno, E. Rasmussen, and T. Rickenbach, A radar and electrical study of tropical "Hot Tower", *J. Atmos. Sci.*, 49, 1386-1395, 1992a.
 21. Williams, E. R., The Schumann Resonance: a global tropical thermometer, *Science*, 256, 1184-1187, 1992b.
 22. Williams, E. R., and N. Renno, An analysis of the conditional instability of the tropical atmosphere, *Mon. Wea. Rev.*, 121, 31-26, 1993.
 23. Williams, E. R., Global circuit response to seasonal variations in global surface air temperature, *Mon. Wea. Rev.*, 122, 1917-1929, 1994.

BIOGRAPHIES

Effrina Yanti Hamid. She was born in Medan, Indonesia. She received B.Eng. and M.Eng. degrees from Bandung Institute of Technology in 1995 and 1998, respectively. Now, she is a Ph.D. student in Department of Electrical Engineering, Osaka University, Japan.

Zen-ichiro Kawasaki. He received his B.S., M.S. and Dr. Eng. degrees in communication engineering from Osaka University in 1973, 1975 and 1978, respectively. In 1989, he joined the Department of Electrical Engineering, Osaka University and he is currently an professor. His researches mainly concern the observation of lightning discharges and the diagnosis techniques for power apparatus. Dr. Kawasaki is also a member of IEEE, IEE Japan, AGU and SAE of Japan.

Redy Mardiana. He was born in Bandung, Indonesia. He received B.Eng. and M.Eng. degrees from Bandung Institute of Technology in 1992 and 1997, respectively. Now, he is a Ph.D. student in Department of Electrical Engineering, Osaka University, Japan.

EMC Problems Connected to the Use of the Low Voltage Power Network for Information Transmission

Michel Ianoz

Swiss Federal Institute of Technology, Power Systems Laboratory, CH-1015 Lausanne, Switzerland
michel.ianoz@epfl.ch

The Commission E Open Meetings papers are a choice between a status report for the Working Group activity or a short presentation of a subject in the area of the respective WG, which seems more relevant for the period between two such Open Meetings.

The problem discussed in this short review paper is far from being solved. On the contrary one could say that it has just been put forward and that it will represent a research item for the next few years. It is however typical for the new trend in which power and information technology are closely related.

A session dedicated to this item is organized by the Wroclaw EMC 2000 symposium.

I. INTRODUCTION

Distribution power lines have been used for long time to transmit specific information pertaining to the network operation or to various services which electric utilities are offering to their customers. The range of frequencies used for this service was from a few hundred of Hz up to 150 kHz, where the public radio frequency band begins.

In the last 2 – 3 years, feasibility studies have been performed in various countries to check the possibility of using the low voltage distribution network to provide data transmission and eventually also telephonic links to individual customers at frequencies up to 30 MHz [1]. This application is particularly interesting for power utilities which can enter in this way the telecommunication market.

However, this transmission mode in the frequency band extending from 1 to 30 MHz will present various and quite complex EMC problems. The main problem will probably be the emission of electromagnetic noise which can interfere with public radio. Some immunity aspects should probably also be considered.

II. GENERAL VIEW OF THE METHOD

A modem connected to the Ethernet network is installed at the customer (fig. 1). One or several PCs can be connected to the Ethernet network. The modem is connected through a coupling unit to the LV distribution

network. The signals coming from the PC through the Ethernet network and the coupling unit are transmitted through the LV network to a MV/LV substation where is a so-called base station. The signal is deviated to this base station before entering the MV/LV transformer.

The connection between the base stations which are collecting the information at the level of a town district and the long distance links between different towns can be achieved in different ways :

- optical fiber links dedicated to this connection;
- radio links already existing and used by the utility for its own services.
-

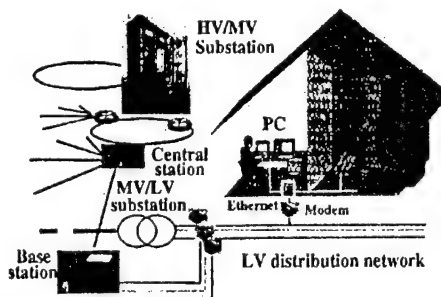


Fig. 1 – Principle arrangement for the use of the LV power network for information transmission.

III. EMC EMISSION PROBLEMS

The power distribution network at the level of a town district is used to transmit information by sending it from a so-called backbone station through cables running along the streets which then enter individual houses, administrative buildings or industries (fig. 2).

EMC emission problem due to the use of the LV power network for information transmission are at three different levels :

- indoor level;
- street level;
- general environment level.

III.1 Indoor level

When signals at frequencies up to 30 MHz are transmitted through the low voltage distribution network, indoor disturbances can occur due to the possible interference of the electromagnetic field radiated by the network with various installations : radio receivers, video equipment, CD players and others.

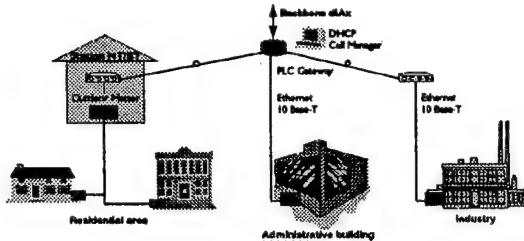


Fig. 2 – Use of the LV distribution power network in a district of the town for information transmission

The difficulties to determine the level of such disturbances are connected to :

- the complicated and very big variety of the possible arrangements of the LV network in a house;
- the small dimensions of the rooms which does not permit to perform measurements at distances from the disturbance source larger than about 1 m. The consequence is that these measurements will be performed in a strongly non-uniform field.

This means that for modeling the LV circuit in an individual house or public building (administrative or industry) in order to calculate radiation, codes like NEC can be used, but for this task one needs computers with large memory; and a large number of calculations to include a big variety of configurations and obtain a statistical result.

For the experimental part, due to the high non-uniformity of the field in the small rooms of the houses, a field mapping over the room surface will be needed. Like for the calculations, due to the big variety of configurations, in order to have reliable results, a large number of measurements will be needed.

The first published results in this direction [2], show that the CISPR 22 limit for conducted emission is not respected for a PLT (power line technology) modem connected on the LV network (fig. 3). Even if this result should be taken with precaution because it shows the peak value, while the limit is fixed for the quasi-peak, it gives an indication that EMC problems might arise when this power line technology (PLT) or power line communication (PLC) are used inside a house.

III.2 Out door level

It can be assumed that at some moments of the day, due to the simultaneous input coming from a large number of individual connections, the total traffic

flowing in the outdoor cables along a street can be quite high.

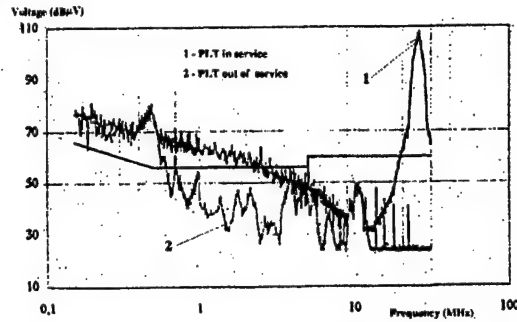


Fig. 3 – Conducted emission of a PLT modem

This can mean that these cables can radiate a significant field in the environment and eventually in the vertical direction, where there is no barrier for the field, this disturbance can reach flying objects and interfere with their electronics. For the moment, this is a non-verified assumption, but it represents a potential danger which must be checked.

III.3 General environment level

In a very populated town, the addition of signals in many outdoor cables, can even represent a kind of very large antenna which will eventually send such noise signals into the ionosphere. Of course this is also for the moment a speculation which possible occurrence must be checked by modeling or experiments.

IV. EMC IMMUNITY PROBLEMS

The immunity problems will probably be less important than the emission ones, but if the integrity of the transmitted signal is less in danger, the attenuation and the problem of the large impedance variation of power network the as a function of the loads connected to it can be an obstacle to this so attractive application.

V. STANDARDIZATION ASPECTS

Concerning standardization there is practically a complete lack of existing documents. Radiated emission standards are probably not applicable, due to the difficulty to perform field measurements at 3 m distance from the power circuits in small rooms. CISPR 22 which considers conducted disturbances is probably the only standard which can be used without modifications.

REFERENCES

- [1] K. Dostert, "Möglichkeiten und Grenzen neuer, alternativer TK-Festnetz Zugänge im Spannungsfeld bestehender Dienste und Randbedingungen", Funkschau-Intensiv Seminar "PLC und EMV", 1 Juli, 1999, München.
- [2] O. Daguillon et al., "Etude sur le brouillage éventuel des radiocommunications par le rayonnement des systèmes de transmission haut débit", 10^{ème} Colloque Int. Sur la CEM, Clermont-Ferrand, 15-17 mars, 2000, pp. 183-188.

EMC 2000

INTERNATIONAL WROCLAW SYMPOSIUM
ON ELECTROMAGNETIC COMPATIBILITY

URSI COMMISSION E OPEN MEETING

ACTIVITY OF URSI COMMISSION E WORKING GROUP: E-7 ON EXTRATERRESTRIAL AND TERRESTRIAL METEOROLOGICO-ELECTRIC ENVIRONMENT WITH NOISE AND CHAOS

INCLUDING THE RESULTS:

GRAVITO-ELECTRODYNAMICS OF DUST AND ITS APPLICATIONS TO PRE-EARTHQUAKE EFFECTS AND TORNADOES

Hiroshi Kikuchi

Institute for Environmental Electromagnetics
3-8-18, Komagome, Toshima-ku, Tokyo 170, Japan
Fax: +81-3-3917-9418; E-mail: hkikuchi@mars.dti.ne.jp

This article is an updated version of review of the progress made by URSI Working Group E-7 (Chairman: H. Kikuchi; Co-Chairman: S.S. Moiseev) on Extraterrestrial and Terrestrial Meteorologico-Electric Environment with Noise and Chaos, and complements the last report published in the Proceedings of EMC Zurich Symposium in 1999.

1. INTRODUCTION

The content is based on the activity of URSI Working Group E-7 on Extraterrestrial and Terrestrial Meteorologico-Electric Environment with Noise and Chaos, including papers presented at the XXV URSI General Assembly in Toronto and significant results obtained from a series of URSI Workshops and Symposia held in Tokyo, more recently in Niigata, Japan in 1997 and in Urbana-Champaign, U.S.A. in 1999, some of which are contained in a book, *Dusty and Dirty Plasmas, Noise, and Chaos in Space and in the Laboratory* published by Plenum [1], in *Proceedings of International Symposium on Unconventional Plasmas with Noise and Chaos* [2], and in *Proceedings of International Workshop on Radio Method for Studying Turbulence* [3].

Although some of the content overlap an article „Activity of URSI Commission E Working Group: E-7 on Extraterrestrial and Terrestrial Meteorologico-Electric Environment with Noise and Chaos”, reported in 1999 [4], the present review aims at a most updated version.

2. DUSTY AND DIRTY PLASMAS IN SPACE AND IN THE LABORATORY

2.1 Cosmic dusty plasmas

The recent in-situ detection of very small grains by the Ulysses mission suggests that Jupiter's magnetosphere is not merely a sink but also a source of fine inter-

planetary dust in a particular size range. This is the unexpected finding of quasi-periodic streams of submicron grains ($1.6 \times 10^{-16} \text{ g} < m_d < 1.1 \times 10^{-14} \text{ g}$, m_d : dust mass) travelling at high speeds ($20 \text{ km/s} < v < 56 \text{ km/s}$) during its distant Jovian encounter. From the encounter geometry, it can be concluded that these grains come from, their initial source being the observed volcanoes of the Jovian satellite, Io [5, 6]. Along this line, a scenario has been given on how Io's dust could enter Jupiter's magnetosphere, based on joint effects of the electric force produced by thundercloud charges in Io's atmosphere and Jupiter's gravitational force [7].

2.2 Laboratory dusty plasmas

It has been shown that Coulomb crystallization of a dusty plasma occurs in rf-glow discharges, forming a 'plasma crystal'. Charged dust particles (monodisperse, spherical latex spheres) embedded in a neutralizing plasma interact due to their charge and form 2-dimensional lattice structures. The dynamical behaviour of the lattice points at phase transitions from solid to liquid and gas has been investigated [8, 9, 10].

Most recently, there has been appeared a study of effects of a probe placed within a plasma above a plasma crystal [11]. A biased probe in an argon plasma near to the sheath-edge has been found to alter significantly the structure and properties of a plasma crystal, inducing particle circulation around a stable crystal island. The formation of the island and the circulation are attributed to a nonuniform electric field in the crystal region caused by the presence of the biased probe.

In contrast to laboratory experiments as mentioned above, few theoretical model exist up-to now for plasma crystal except numerical simulations. An attempt has been made, based upon a model of wake potential [12, 13]. It has been shown that charged dust grains in a sheath region with plasma ion flow can attract each

other in the wake potential cone of an upstream dust particulate. Because of the periodic nature of the potential, periodic structures of the dust grains can be formed in a base plane of the cone.

As typical examples of strongly coupled classical plasmas, plasmas of highly charged dust particles and ion plasmas in traps have been reviewed from the theoretical aspect with particular reference to the layered structures of these plasmas at low temperatures. It has been structured to a good accuracy when the effect of correlation between charges is taken into account properly [14].

As one of studies of unconventional plasmas, the subject of waves in weakly ionized gases is continuing. Using a basic system of magnetoacoustic hydromagnetics, it has been shown that low frequency solitary waves may exist in a cold weakly ionized gas pervaded by a magnetic field. One of basic features is that the neutrals and charged particles move together, provided the collision frequency (essentially of the neutral particles with charged ones) is sufficiently large [15].

2.3 Gravito-electrodynamics of dust in an electric cusp and in an electric mirror

In the presence of electromagnetic and gravitational fields, a dust particle, charged or uncharged, is usually considered a point charge and/or material point, making the so-called 'test particle' approach feasible and the motion of the dust particle in space is governed by the Lorentz and gravitational forces. Accordingly, no electric but a gravitational force is exerted on a neutral or uncharged dust particle. The test particle is, however, not always valid for a sizeable dust in an electric field due to nonuniform charges induced or polarised on the dust grain even if the grain is electrically neutral and uncharged. This is particularly true when a dust grain is placed in a special electric configuration such as forming an electric cusp or an electrically neutral point, causing a novel but ubiquitous phenomenon of electric reconnection. The significance of this effect has been introduced for an electric cusp formed by a quadrupole and a sequence of periodical cusps that constitute an 'electric mirror', leading to the discovery of particle acceleration in a cusp region and of particle trapping in an electric mirror analogous to the magnetic mirror. High-energy dust particles which escaped from electric mirrors could be populated over a very wide range of altitudes beyond mirror points in the planetary atmosphere with the aid of additional electric fields. Some of them could penetrate into the ionosphere and even magnetosphere. These findings have led to an explanation of dust layer and ring formation in the planetary atmosphere, ionosphere, and magnetosphere such as Jupiter's *gossamer ring*, diffuse dust layers in the terrestrial atmosphere, and in particular, a variety of *pre-earthquake effects* [7, 16-19].

Gravito-electrodynamics of dust has been extended to three-dimensional motion of dust not in the ecliptic plane of an electric quadrupole. Then, a particle exhibits a helical motion and an important role of the quadrupole in helicity or vortex generation in particle- or electrohydrodynamics has been stressed with its direct rele-

vance to *tornadoes* [20, 21].

3. METEOROLOGICO-ELECTRIC ENVIRONMENT WITH NOISE AND CHAOS

3.1 EHD and EMHD transport and electric reconnection

There are a variety of dusty or dirty plasma and meteorologico-electric environments, containing charged or polarized dust grains or aerosols in the terrestrial, planetary, and cometary atmospheres and in interstellar dark space. In such environments, electric phenomena are taking place predominantly rather than magnetic phenomena, involving or accompanying electrification, electric charging or discharge, ionization or recombination, particle disruption, or agglomeration, and space charge and/or electric field transport. Space charges are carried on an underlying stream, convection or diffusion in a variety of forms charged streams and/or vortices in external and internal electric fields. Examples are thunderstorms, cold and jet fronts, hurricanes, typhoons, cyclones, tornadoes, sandstorms, whirlwinds and corn circles in the terrestrial environment, planetary lightnings, aurorae, rings, nebular lightnings, cometary tails, and dark interstellar clouds in the extraterrestrial environment. Accordingly, conventional hydrodynamics (HD) or magnetohydrodynamics (MHD) breaks down, and even conventional plasma physics is not relevant, since their environments now contain dust grains or aerosols, and are considered neither conducting nor collisionless plasmas as often assumed for conventional plasmas. They may be partially ionized, collisional gases, dusty or dirty plasmas, dielectric or semiconducting fluids where electrohydrodynamic (EHD) or more generally electromagnetohydrodynamic (EMHD) transport processes are taking place significantly rather than HD or MHD processes.

A new equation of electric field transport, including space charge, ponderomotive, and gravitational forces, has been obtained, being supplemented by the equations of fluid vorticity, magnetic field, and energy transport extended also to the EHD and EMHD regimes. The 'electric Reynolds number' newly introduced, analogous to the Reynolds and magnetic Reynolds numbers, plays an important role in the EHD and EMHD regimes as a criterion of relative importance of convection, diffusion, dissipation, propagation, and radiation [22-24].

The study of ion-aerosol balance and Poisson's equation in a non-equilibrium system composed of positive and negative light ions and aerosol particles in an external electric field shows that the system may lose stability, if ion-aerosol attachment coefficients increase with the electric field growth. The model can explain meso-scale electric field structure formation in the surface atmospheric layer. In this connection, the analysis sensitive measurements at Borok (58°N, 38°E) indicates existence of spatio-temporal structures of electric field and space charge with local spatial scales in the surface atmospheric layer. Based on these studies, influence of dust (aerosol) particles on terrestrial electromagnetic environment is discussed [25, 26].

A new model of global electric field and current with magnetospheric and atmospheric electric sources has been put forward, taking into account the effect of both the complex inner structure of the ground and inhomogeneity of the atmospheric conductivity. Calculated ground-ionosphere voltage depends on the thunderstorm activity distribution and appears to be about a few hundreds kilovolts, and atmospheric current density at the planetary surface is approximately 10^{-12} A/m². They are close to measured values at middle latitudes. [27].

On the basis of new EHD with the equation of electric field transport, it has been shown that any perturbation exerted on an electric cusp can lead to electric field line merging-reconnection. Such a perturbation can usually be done by dust or object that plays crucial and significant roles in electric reconnection and subsequent electric discharge or lightning, thus for many geophysical, astrophysical, and meteorological phenomena such as thunderstorms, rocket and tower triggered lightning, ball lightning, nebular lightning, tornadic thunderstorms, and Chondrules formation in meteorites [28, 29].

New observational evidence supporting such a cusp model has been obtained from natural lightning observations during winter thunderstorms in a coastal region of the Sea of Japan [30].

If the concentration N of ice crystallites exceeds M/ν^2 (M : critical value of the product $n\nu$, $n = \nu N$: number of molecules per unit volume of the cloud, ν : number of water molecules in an aggregate) spontaneous polarization catastrophe (PC) occurs, and this leads to the atmospheric masers feeding plasma solitons that provides a ball lightning formation [31].

3.2 Self-organization, chaos, turbulence, and vortices

Relationship between self-organization and chaos depends strongly on a dissipation, and reducing of dissipative transfer are caused by the reduction of frictions related to viscosity, magnetic viscosity, and thermal conductivity. It has been shown that the effective viscosity coefficient in helical turbulence is smaller than in usual turbulence due to the existence of long-lived vortices tending to coalesce. The conditions under which the viscosity becomes negative has been discussed with a variety of atmospheric and oceanic applications. In summary, characteristic properties of usual and magnetic viscosity has been studied in the framework of HD, MHD, and EMHD media [32–35].

The study of large-scale coherent HD vortex generation has been extended to electrified charged dusty vortices to be termed as 'EHD vortices', incorporating helical turbulence in electric and magnetic fields into that in fluid velocity, which are all due to the anisotropy created by an external electric field on the background. A new equation of EHD vortices has been introduced on the basis of a set of EHD or EMHD equations together with the equation of state and a full set of Maxwell's equations. In fact, EHD vortices can be more explosive with larger instabilities than HD vortices. In addition, it is inferred that an external electric field could provide the origin of additional self-organization to a coalescence of fluid vortex and electric

field lines as a manifestation of a new frozen-in field concept for electric fields when the fluid and electric Reynolds numbers are sufficiently high. Consequently, a coalescence of fluid vortex breakdown or merging point and electric reconnection point, X-type or O-type, could be expected in a local cusp region where a local decrease in both the fluid and electric Reynolds numbers occur due to any perturbations. In fact, an artificial mapping of electric field lines onto fluid vortex lines with breakdown and merging points typically sketched for tornadoes, based on an updated model, could produce a reasonable consistent charge distribution on thunderclouds that is thought most likely to occur from observations of tornadic thunderstorms available so far. The fact that charged EHD tornadoes with thunderstorms are more severe than uncharged tornadoes could be explained on the basis of HD and EHD vortices, noticing that the growth rate of EHD vortices can be greater than that of HD vortices [36, 37].

Common character of the behavior of atmospheric and laboratory MHD turbulence results from the fact that energy spectra of these turbulence cases are similar. They are characterized by the presence of $-5/3$ and $-7/3$ exponent values, and an inverse cascade from smaller to larger scales within the inertial interval. In both cases, simplest mechanism of such turbulence behavior and such spectra formation is the violation of mirror symmetry in the initial (undisturbed) turbulence and the appearance of nonzero helicity. The comparison of theoretical results with the known, as well as with new experimental data obtained in the laboratory has been made [38].

Experimental data indicate a number of different turbulent regimes whose spectral properties are shown to depend on two parameters: $\gamma = f_0 \tau_0^2 / r_0$ and $\Gamma = \gamma^{4/3} Re$, where f_0 is the force setting the fluid in motion, r_0 , τ_0 its spatial and temporal correlation scales, and Re is the Reynolds number. It is shown further that there is a possibility of excitation of intense vortices not only of a large scale, but also of relatively small scales, which is known to occur in natural conditions. The microstructure of a turbulent flow is formed from several universal dependences whose appearance and arrangement depend on γ and Γ . In particular, Kolmogorov's mode appears for $\gamma \ll 1$ and $\Gamma \ll 1$. Comparison with experiments for large-scale turbulence (MHD flows and wind spectra observed in the atmosphere) reveals good agreement [39, 40].

There are a number of physical mechanisms to produce various electromagnetic indicators by tropical cyclones perturbations at high altitudes. Tropical cyclone electromagnetic indicators include the following: transient electric fields in the upper atmosphere and lower ionosphere; ionospheric irregularities; charge separation electric fields; low-frequency electromagnetic emissions; precipitating energetic particles; bremsstrahlung X-rays; and gas ionization enhancement. These electromagnetic indicators could be used for tropical cyclone monitoring [41, 42].

Topological diagrams for turbulent vorticity in shearing plasma layers have been developed as strings of identical helix units smoothly jointed at their junctions. Helix strings tying loops, knots, links, and braids on

tetragonal and cubic lattices are obtained. A scaling cycle of vortex stretching, twisting, breaking, and reconnection at high Reynolds number forming vortex lattices at arbitrary mesh refinement are also presented. Its exponential particle acceleration brings ion circulation energy within a range of high-energy events associated with lightning and ball lightning. This vortex plasma has a state equation with negative pressure for self-confinement. It is argued that its energy surface in phase space favours self-organization [43].

Log-normal statistics for (ball) lightning, VLF radio noise and rainfall indicates power-law relations of atmospheric parameters with fractal dimensions as exponent. Universal shear flow parameters emerge from stretching transition layer vorticity along scaling and differentiable fractal curves from circle arcs or helix units that are also useful for modeling observed properties of vortex structures in atmospheric turbulence [44, 45].

4. APPLICATIONS OF DUST GRAVITO-ELECTRODYNAMICS AND EHD TO PRE-EARTHQUAKE ATMOSPHERIC, IONOSPHERIC, AND MAGNETOSPHERIC EFFECTS

Relevance of the electric cusp and reconnection model to pre-earthquake effects has been pointed out for an attempt to interpret ionospheric effects and to unite the processes in the earth crust, atmospheric electricity, and ionosphere. They are variations of phase of VLF signals and of HF signal intensity on passes over the epicenter of preparing earthquake, appearance or increase of E_s layers and additional layers, spread phenomena on bottom side ionograms within a whole range of altitudes, sometimes large-scale variations of electron density in F-layer occupying the area over the future epicenter with a diameter more than 1000 km, strong plasma density depletion within the upper atmosphere over the region of the preparing earthquake, and emanation of aerosol particles by the crust with a large content of metals which takes place before and some time after the earthquake and which could be explained as follows. Due to a high pressure within the crust, two effects may take place: piezoelectric field generation and fluidity of hard materials. Fluidity leads to appearance of microparticles which can move under the piezoelectric force action. Charged microparticles and metallic ions are accelerated by the piezo-electric field due to the electric reconnection process and are injected into the atmosphere. This flow of aerosols leads to the increase of atmospheric conductivity and other effects connected with penetration of metallic ions and aerosols into the ionosphere [46–48].

5. REFERENCES

- [1] H. Kikuchi (Ed.), *Dusty and Dirty Plasmas, Noise, and Chaos in Space and in the Laboratory*, New York: Plenum, 1994.
- [2] *Proceedings of International Symposium on Unconventional Plasmas with Noise and Chaos*, 31 August - 1 September, 1997, Niigata, Japan.
- [3] *Proceedings of International Workshop on Radio Method for Studying Turbulence*, 9-12, August, 1999, Urbana-Champaign, U.S.A..
- [4] H. Kikuchi, „Activity of URSI Commission E Working Group: E-7 on Extraterrestrial and Terrestrial Meteorological-Electric Environment with Noise and Chaos”, *Proceedings of 1997 EMC Zurich Symposium*, Zurich, Switzerland.
- [5] M. Horanyi, G. Morfill, and E. Grün, „Mechanism for the acceleration and ejection of dust grains from Jupiter's magnetosphere”, *Nature*, 363, 144-146, 1993.
- [6] D.A. Mendis, M. Rosenberg, and V.W. Chow, „Cosmic dusty plasmas”, in [1], 1994, p.15.
- [7] H. Kikuchi, „Gravito-electrodynamics of dust in electric cusps and electric mirrors and its applications to planetary dust layers and rings”, in *XXVIIth URSI GA-99 (Abstracts)*, E3.2, 1999, p.277.
- [8] J.H. Chu and I. Lin, *Phys. Rev. Lett.*, 72, 4009, 1994.
- [9] H. Thomas and G. Morfill, *Phys. Rev. Lett.*, 73, 652, 1994.
- [10] Y. Hayashi, „Observation of Coulomb crystals in dusty plasmas”, in [2], p.20.
- [11] D.A. Law, W.H. Steel, B. Annaratone, and J.E. Allen, „Probe-induced particle circulation in a plasma crystal”, in *Proc. 23rd International Conference on Phenomena in Ionised Gases*, Vol.1, 1997, pp.192-193.
- [12] S.V. Vladimirov and O. Ishihara, „On plasma crystal formation”, *Phys. Plasmas*, 3, 444-446, 1996.
- [13] O. Ishihara and S.V. Vladimirov, „Wake potential of a dust grain in a plasma with ion flow”, *Phys. Plasmas*, 4, 69-74, 1997.
- [14] H. Totsuji, „Strongly coupled nonneutral plasmas: simulation and theory on dusty plasmas and plasmas in traps”, in [2], p.18.
- [15] D.K. Callebaut and N.L. Tsintsadze, „Low-frequency solitary waves in cold weakly ionised gases in a magnetic field”, in [2], p.12.
- [16] H. Kikuchi, „Gravito-electrodynamics of dust in an electric cusp”, in *XXII EGS NP4.2 (Abstracts)*, 1997.
- [17] H. Kikuchi, „Uncharged particle acceleration and gas discharges by electric reconnection”, in [2], p.3.
- [18] H. Kikuchi, „Gravito-electrodynamics of dust in electric cusps and electric mirrors with electric reconnection and its applications to diffuse dust layers in the troposphere and pre-earthquake atmospheric and ionospheric effects”, in *Proc. EMC Wrocław 2000 Symp.* this issue, 2000.
- [19] H. Kikuchi, „Gravito-electrodynamics of dust in periodical electric cusps and mirrors with electric reconnection and its applications to planetary dust layers and rings”, in *Proc. PIERS*, 2000.
- [20] H. Kikuchi, „electrodynamics of dust with a helical motion in an electric quadrupole and its application to tornadic thunderstorms”, in *Proc. EGS*, 2000.
- [21] H. Kikuchi, „The role of an electric quadrupole in helicity and vortex generation and the role of horizontal thundercloud electrification in tornado generation”, in *Proc. EGS*, 2000.
- [22] H. Kikuchi, „Meteorological-electric phenomena

- and electrohydrodynamics (EHD)/electromagnetohydrodynamics (EMHD)", in *Environmental and Space Electro-magnetics*, H. Kikuchi (Ed.), Springer-Verlag, Tokyo, 1991, pp.561-575.
- [23] H.Kikuchi, "EHD and EMHD transport processes in dusty and dirty plasmas", in [1], 1994, pp.139-148.
- [24] H.Kikuchi, "EHD/EMHD transport processes and electric reconnection in dusty and dirty plasmas", in P. Fauchais, P., J. van der Mullen, and J. Heberlein (eds.), *Heat and Mass Transfer under Plasma Conditions, Annals of the New York Academy of Sciences*, Vol.89, pp.246-258.
- [25] E.A. Mareev, "Influence of dust particles on terrestrial electromagnetic environment", in *XXVth URSI GA-99 (Abstracts)*, E3.5, 1999, p.279.
- [26] S.V. Anisimov, S.S. Bakastov, and E.A. Mareev, "Spatio-temporal structures of electric field and space charge in the surface atmospheric layer", *J. Geophys. Res.*, 99, 10603-10610, 1994.
- [27] S.S. Davydenko, "A model of global electric field and current with magnetospheric and atmospheric electric sources", in *XXVth URSI GA-99 (Abstracts)*, E3.3, 1999, p.278.
- [28] H. Kikuchi, "Electric reconnection and chaos in dusty and dirty plasmas", in [1], 1994, pp.535-544.
- [29] H. Kikuchi, "Roles of dust or object perturbing an electric cusp in electric reconnection and consequent electric discharge or lightning", *Physics and Chemistry of the Earth*, 21, 549-557, 1996.
- [30] H. Sakurano, Y. Kito, S. Isozumi, and T. Saida, *Trans.IEE Japan (in Japanese)*, 11-B, 38-42, 1991.
- [31] P.H. Handel, "Nonlinear dynamics of the polarization catastrophe in clouds and of the atmospheric masers feeding plasma solitons", in [2], p.1.
- [32] S.S. Moiseev, "Flow with reduced and negative transport coefficients in fluctuating geophysical, MHD and EMHD media", in *XXVth URSI CA-96 (Abstracts)*, E1.2.4, 1996, p.210.
- [33] S.S. Moiseev and O.Onishchenko, "Helicoidal media: properties of chaos and structures, *Physica B*, 228, 83-90, 1996.
- [34] S.S. Moiseev, A.V. Belyan, V.G. Pungin, and O.G. Chkhetiani, "Amplification of fluctuations and current dynamo due to helical and chiral effects in geophysical and plasma-like media", in *XXII EGS NP4.2 (Abstracts)*, 1997.
- [35] S.S. Moiseev, "Feedbacks and multicative noise in helical and chiral media", in [2], p.16.
- [36] H. Kikuchi, "EHD vortices in the atmosphere with helical turbulence in electric and space-charge fields", in *Nonlinear Dynamics of Structures*, R.Z. Sagdeev et al. (Eds.), Singapore: World Scientific, 1991, pp.261-272.
- [37] H. Kikuchi, "Electrohydrodynamic (EHD) vortices in helical turbulence", *Physica Scripta*, T63, 91-98, 1996.
- [38] H. Branover, A. Eidelman, E. Golbraikh, and S.S. Moiseev, "Magnetohydrodynamic simulation of atmospheric helical turbulence", in *XXXth URSI GA-96 (Abstracts)*, E1.2.7, 1996, p.211.
- [39] S.S. Moiseev, S.N. Gordienko, V.G. Pungin, "Dynamo and turbulence types in planetary media", in *XXVth URSI GA-99 (Abstracts)*, E3.10, 1999, p.281.
- [40] S.N. Gordienko and S.S. Moiseev, "Spectra of hydrodynamical turbulence and their applications", in [3], 1999.
- [41] N.S. Erokhin and S.S. Moiseev, "On the tropical cyclones electromagnetic indicators", in *XXVth URSI GA-96 (Abstracts)*, E1.2.2, 1996, p.209.
- [42] N.S. Erokhin, L.A. Mikhailovskaya, and N.N. Zolnikova, "Disturbances of electromagnetic environment produced by powerful atmospheric vortices", in *XXVth URSI GA-99 (Abstracts)*, E3.6, 1999, p.279.
- [43] G.C. Dijkhuis, Helix string model for turbulent vorticity and cavitation in shearing arc plasma", in P. Fauchais, P., J. van der Mullen, and J. Heberlein (eds.), *Heat and Mass Transfer under Plasma Conditions, Annals of the New York Academy of Sciences*, Vol.89, pp.259-272.
- [44] G.C. Dijkhuis, "Verhulst dynamics and fractal stretching of transition layer vorticity", in [1], 1994, pp.163-176.
- [45] G.C. Dijkhuis, "Dimensional eigenvalues for scaling structures in atmospheric turbulence", in *XXVth URSI GA-96 (Abstracts)*, E1.2.5, 1996, p.210.
- [46] S.A. Pulinets, A.D. Legen'ka, and V.A. Alekseev, "Pre-earthquake ionospheric effects and their possible mechanisms", in [1], 1994, pp.545-557.
- [47] S.A. Pulinets, A.D. Legen'ka, V.A. Alekseev, and V.V. Afonin, "Variations within the ionosphere observed before the strong earthquakes and their possible causes", in *XXVth URSI GA-96 (Abstracts)*, HEG.6, 1996, p.669.
- [48] S.A. Pulinets, K.A. Boyarchuk, V.V. Hegai, and D.R. Shklyar, "Ground-atmosphere-ionosphere magnetosphere coupling conception including seismic activity", in *XXVth URSI GA-99 (Abstracts)*, GH1.10, 1999, p.747.

EMC 2000

INTERNATIONAL WROCLAW SYMPOSIUM
ON ELECTROMAGNETIC COMPATIBILITY

URSI COMMISSION E OPEN MEETING

GEOELECTROMAGNETIC DISTURBANCES AND THEIR EFFECTS ON TECHNOLOGICAL SYSTEMS

M. Hayakawa¹⁾ and R. Pirjola²⁾

1) Department of Electronic Engineering, The University of Electro-Communications, 1-5-1 Chofugaoka, Chofu Tokyo 182-8585, Japan // fax: +81 (0)424 43 5783 // e-mail: hayakawa@whistler.ee.uec.ac.jp

2) Finnish Meteorological Institute, Geophysical Research Division, P. O. Box 503, FIN-00101 Helsinki, Finland // fax: +358-9-19294603 // e-mail: risto.pirjola@fmi.fi

Main topics of our URSI Commission E Working Group, "Geoelectromagnetic disturbances and their effects on technological systems," will be reviewed here. First of all, we present the latest results on the seismo-ULF emissions, and then we report on the ELF wave phenomena associated with atmospheric optical emissions. Finally, we will report on the geomagnetic induced current on the transmission lines. The analyses of ULF magnetic fields associated with a large earthquake, have been performed and it is shown by means of the polarization and fractal analyses that there occur precursory ULF emissions. Recent studies on optical emissions (Red sprites, blue jets etc.) and ELF emissions have been presented. At the earth's surface "space weather" manifests itself as geomagnetic storms and geomagnetically induced currents (GIC) in electric power transmission grids, pipelines etc. Several studies aiming at space weather and GIC forecasting are being performed by sophisticated modelling techniques.

1. INTRODUCTION

Geoelectromagnetic disturbances take place in a wide frequency range from DC to higher frequency. In the ULF range (frequency below 10Hz), the most important geoelectromagnetic disturbances are geomagnetic disturbances and geomagnetic pulsations as the consequence of solar-wind effect onto the magnetosphere and ionosphere, and also wave-particle interaction in the magnetosphere. In the frequency range higher than ULF, there is so-called the ELF and VLF range, where the lightning discharge is the main noise source. Our recent greatest concerns are ELF wave associated with the cloud-ionosphere discharges and also Schumann resonances to be used for the monitoring of global warming.

Space weather refers to conditions in the Sun and in the solar wind, magnetosphere and ionosphere that can influence the performance of space-borne and ground-based technological systems and can even endanger human life or health. Systems affected by space weather include satellites and communication and navigation systems. At the earth's surface, space weather effects are known as GIC since they refer to geomagnetically induced currents flowing in conductor networks, like electric power transmission grids, pipelines, phone

cables and railway systems.

This paper deals with the general review of the studies associated with our Working Group entitled, "Geoelectromagnetic disturbances and their effects on technological systems."

2. GEOELECTROMAGNETIC DISTURBANCES

2.1. Seismogenic ULF emissions

One of the important signatures of the geoelectromagnetic disturbances is the detection of seismogenic ULF emissions, which are recently known to be very useful for the short-term earthquake prediction [1]. There have been published two important papers on the ULF signatures of earthquakes (Spitak and Loma Prieta earthquakes) [2], and it is highly required that we accumulate more convincing data for seismogenic ULF emissions. Later, Hayakawa et al. [3] have obtained an additional convincing signature of ULF emissions for a large Guam earthquake on 8 August, 1993, and they have been based on the newly developed analysis of method (polarization analysis). Furthermore, the simultaneous use of fractal analysis has yielded further confirmation on the presence of seismo-ULF emissions before the Guam earthquake [4]. A new event for the earthquake in Biak, Indonesia on February 17, 1996, has been analyzed extensively by using our proposed polarization and fractal analyses, together with the use of a remote reference station [5]. As the result, it is found that there exists the appearance of seismo-ULF emissions about 1.5-1.0 month before the quake, with the intensity of the order of 0.2-0.3nT.

A network for the observation of seismo-ULF emissions has been established in the Tokyo area of Japan (Izu, Chiba, Kakioka, Chichibu and Matsushiro). Especially, in the areas of Izu and Chiba, we have installed 3-4 sites spaced by 5-10km in order to form a differential array in order to increase the S/N ratio for seismo-ULF emissions. Since there have not been many strong earthquakes, we have not yet obtained any results.

2.2. Acoustic Emissions

Attempts to find acoustic emission (AE) associated with earthquakes (EQs) have been undertaken for some

years. An anomaly in AE behavior in the range 800-1200 Hz was recorded about 16 hours before the Spitak earthquake, at the distance 80 km from the epicenter. However, their conclusions were not completely convincing due to extremely weak signals, of which amplitude spectrum sharply declines with the frequency. Here we report the facts of possibly extreme importance that clear AE intensification associated with EQs was recorded in the tunnel at the depth of about 100 meters at Matsushiro Seismological Observatory of Japan Meteorological Agency. We used special receivers with magneto-elastic detectors of which sensitivity increases as cube of frequency. The AE intensification has been verified at four frequency bands, namely 30, 160, 500 and 1000 Hz for several EQs in the surrounding area; EQs with $M \sim 3-5$, distance $\sim 20-150$ km. It was also found that the increase in AE activity started at about 12 hours before EQs and decreased after the EQs in a similar manner [6].

The correlation between AE and ULF emissions have also been investigated at Matsushiro, and it is found that there was observed an increase in ULF emissions a few days before the quake. As the result, we can say that microfracturing would be responsible for the generation of ULF emissions as suggested by Molchanov and Hayakawa (1995) [7].

3. ELF WAVES

The effects considered are those which are involved in the generation and propagation of terrestrial radio noise. Such radio noise consists of 'sferics' or 'atmospherics' produced by, or associated with, lightning discharges. Attention is confined to the ELF (Extremely Low Frequency - 3 Hz to 3 kHz) band and particularly to the lower-ELF ('Schumann resonance') band - 5 Hz to 60 Hz. This reflects the upsurge in research publications in this area over the past decade and the recent comparisons of the occurrence of transient optical emissions in the mesosphere and lower ionosphere called sprites (or red sprites), elves and blue jets with the characteristics of the causative lightning source as deduced from observations of ELF sferics propagated to great, even global, distances. The following is mainly based on the review by Jones [1999] [8].

3.1. Schumann resonances

The Schumann resonances are simply the electromagnetic resonances of the global earth-ionosphere (quasi) spherical-shell cavity. For lossless (perfectly reflecting) boundaries W. O. Schumann showed that the resonance frequencies are given by an equation of the form $f_n = c\sqrt{n(n+1)}/(2\pi a)$ (a : Earth's radius; c : light velocity). This predicts a fundamental mode frequency ($n=1$) of $f_1 = 10.6$ Hz and overtones at 18.4, 26.0, 33.5 and 41.1 Hz. Recent reviews of both experimental data and theory have been given by Sentman [1995] [9] and Nikolaenko [1997] [10].

The resonances are excited by global lightning

activity and are evident in experimental atmospheric noise spectra in the band 5 Hz to 60 Hz. The noise spectra have maximums near 7.8, 14.2, 19.6, 25.9 and 32 Hz corresponding to the modes $n = 1$ to $n = 5$ in Schumann's formula. The measured frequencies are lower than predicted by the formula because of ionospheric losses and are thus diagnostic of these losses. The amplitude and frequency of the Schumann modes is determined by the temporal and spatial distribution of global lightning - this being most intense in the tropics. We have studied the temporal variations of the level of global lightning activity from the long-term Schumann resonance monitoring at Tottori, and have found annual and semi-annual components in the variations of global thunderstorm activity between 1967 and 1970. Further sophisticated propagation modelling with taking into account the inhomogeneities (like the inclusion of day/night asymmetry etc.) would be highly required to interpret the actually observed diurnal pattern of resonance frequencies.

3.2. ELF transients

Within the past 5 years or so, it has been recognized that many of the lightning sources responsible for generating transient ELF electromagnetic signatures ('events') in the Schumann resonance band and at higher ELF frequencies (where the signal is referred as a 'slow tail' sferic), are the same sources which frequently, but not necessarily, produce the luminous phenomena in the upper atmosphere above some of the thunderclouds. It is now established that the essential connection between the electromagnetic and optical effects is positive cloud-to-ground (+CG) lightning discharges with high peak currents and large charge transfers. Mesoscale convective systems (MCSs) appear to play an important role in both the optical and sferic cases. However, sprites are observed over smaller convective systems and only a minority of ELF sferics are associated with the spectacular upper atmosphere occurrences. Some sprites and elves have an association with ELF events.

3.3. Positive CG lightning, sferics, sprites and MCSs

A positive cloud-ground (+CG) lightning stroke is defined as a stroke that lowers positive electrical charge to the ground. In the electromagnetic theory used for sferic analysis, the convention is to take the positive direction as upwards. This convention, adopted here, is opposite to that used in studies of atmospheric electricity where the positive direction is downwards - the direction of the 'fair weather' field. A positive stroke lowers positive charge to the ground by a 'conventional' current I flowing in a channel of length dl and has a current moment $I dl$ (I : Amp metre) which is negative in the theory, i.e. directed downwards. This negative current moment generates a vertical electric field pulse that is positive (upwards). Confusingly, this positive field pulse generates a negative voltage pulse on the receiving antenna.

It is generally accepted that the vast majority (over 90%) of sferics observed in the upper ELF band (where

they are called 'slow tails') and in the VLF band have a negative initial polarity - at least in mid-latitudes. These are generated by 'normal thunderclouds in which the charge distribution is 'positive over negative'. The normal -CG stroke taps the main negative charge centre at the base of the cloud. Positive CG strokes have to be initiated from the upper region of the cloud. This can be displaced laterally from the base region by wind shear, facilitating a +CG discharge. This is the conventional mechanism for +CG stroke generation and is invoked in many of the theories of the atmospheric optical phenomena. A lightning flash usually comprises several strokes (about 4) blazing essentially the same channel below the cloud charge center(s). The number of strokes per flash is the multiplicity of the flash and is typically four. In the tropics the situation may be different.

Laterally extensive mesoscale convective systems (MCSs) have been described in which the normal 'positive over negative' charge distribution is inverted. The positive charge reservoir is near the base and the 0°C isotherm, at some 4-6 km height. The total amount of positive charge available in such a system may be thousands of coulombs.

Positive CG lightning appears as an essential ingredient for generating sprites. The data support the hypothesis that sprites are uniquely associated with +CG flashes which have a large peak current. However, most +CG flashes (including some with a large peak current) do not produce sprites.

Much of the recent experimental work on sprites and sferics has used data from the US National Lightning Detection Network (NLDN). This locates sferic sources using a bandwidth of 5 kHz to 500 kHz and reports time-marked locations ('fixes') of individual sources and their peak amplitudes. The peak current in the discharge may be estimated from these data. However, it should be noted that the peak current occurs a few microseconds after leader touch-down when the return stroke channel is less than 1 km long. The peak current is not simply related to the total charge removed by the whole discharge that is an important parameter in ELF sferic characteristics.

3.4. Experimental results on ELF transients

(a) Source locations

Huang et al. [1999] [11] has produced monthly maps showing several thousand sources locations for each month. These locations are in accord with what is known of global thunderstorm activity with the storm centres mainly located in low latitudes and moving southwards in the northern hemisphere summer-winter transition.

An important feature of Huang's work is that the source locations found were compared with those for sferics located by the National Lightning Detection Network (NLDN). There was a systematic periodic bearing error (which was allowed for). It was noted that the ELF location method, using their propagation constant model, overestimated the range by about

100km.

(b) Source Polarity

In Huang et al.'s larger data set of 400 events, 66% were of positive polarity. They note that the flashes which produce ELF events are overwhelmingly of positive polarity and are associated with NLDN-deduced peak cloud-to-ground currents of 20-70 kA.

(c) Charge Moment Amplitude (A) and Time Constant (τ)

Burke and Jones [1996] [12] data set is a selection of large amplitude events propagated over global paths. The system bandwidth was 5-50 Hz. They present statistical distributions of the two parameters A and τ with mean values of $A = 5.1 \times 10^7$ Am for positive strokes and $A = 3.2 \times 10^7$ Am for negative strokes. For τ the mean values were 32 ms and 26 ms for positive and negative strokes respectively. These give values of the charge moment change $\Delta M_Q = A\tau$ (which excludes the ground image) of 1630 C km and 830 C km for positive and negative strokes respectively. In this work it was not known if the event sources were associated with sprites or elves. It should be noted that the A and τ values obtained in this recent study are typical of those obtained over some three decades at King's College and refer to the largest sources which occur globally at a rate of about 1 per minute. Only about 1 in 10,000 strokes produce the ELF event signatures which correspond to the above parameter values.

(d) ELF Transients associated with sprites and elves

Boccippio et al. [1995] [13] report the results of a comprehensive study in which NLDN and ELF sferic electromagnetic data were obtained in conjunction with simultaneous low-light monochrome LLTV imaging of sprites with 17 ms resolution at Yucca Ridge, N. Colorado. The ELF receiving system bandwidth was 3-120 Hz and was located in Rhode Island, 2300 km from the LLTV station. 56% of the +CG flashes produced sprites and these flashes fell within the upper 3-15% of the NLDN positive peak current distribution (Currents of 100 - 200 kA). About 80% of the sprites were coincident with +CG strokes and ELF transients.

In Huang et al. [1999] [11], simultaneous NLDN, ELF and LLTV data were obtained and elves as well as sprites were observed. The ELF recording system was the same as that used for the study of the preceding paragraph. The ELF data showed that the 40 sprites observed produced a 'red' ELF spectrum with an average value of τ of 5.4 ms and ΔM_Q in the range 200-1500 C km. In contrast the 15 elves recorded produced a 'winter' spectrum in the lower-ELF band with an average τ of 3.6 ms and smaller values of ΔM_Q . The τ values here, derived from ELF sferics produced by one MCS, are much less than those reported above and would not be atypical of a normal (-CG) stroke.

4. GEOMAGNETIC INDUCED CURRENTS

4.1. General description of GIC

In power systems, transformers may be saturated due to GIC possibly leading to different kinds of

problems. As extreme consequences, a complete black-out of the whole network and a permanent damage of transformers may result. A very famous GIC event occurred in Québec, Canada, during a large magnetic storm in March 1989. The province suffered from an electric black-out lasting for several hours. In the same storm a transformer was damaged by GIC and had to be replaced by a new one in the USA. In pipelines, GIC enhance corrosion and interfere with corrosion control and protection equipment. The first GIC observations were made in early telegraph systems already about 150 years ago [14]. GIC phenomena are more probable in high-latitude auroral regions than at lower latitudes.

GIC research, as well as other space weather studies, is particularly important in the present years because of the sunspot maximum with a higher probability of solar activity and magnetic storms at the earth's surface. However, remarkable space weather and GIC events are possible at any time during the eleven-year solar cycle.

GICs are driven in a network by the electric field accompanying a geomagnetic variation at the earth's surface. Both the electric and the magnetic fields are primarily caused by a magnetospheric-ionospheric current distribution and secondarily affected by currents induced in the earth. Thus, the calculation of the fields requires a space and geophysical model and leads to complicated formulas, which are exact but unpractical for applications [15]. An important aim of today's space weather and GIC research is the development of forecasting and warning methods, and then all computations should be fast. The complex image method (CIM) provides an appropriate technique since it permits accurate and fast calculations of the electric and magnetic fields.

After knowing the electric field, the determination of GIC is straightforward using a matrix formalism for a discretely-earthed power grid [16], and the distributed-source transmission line (DSTL) theory for a continuously-earthed buried pipeline [17].

4.2. Calculation of the electric field

The horizontal electric field occurring at the earth's surface during a geomagnetic storm is the key quantity for GIC in a technological network at the earth's surface. A calculation of the field requires a model of the currents in the magnetosphere and ionosphere and of the earth's conductivity distribution. Formulas expressing the electric and magnetic fields at the surface of a layered earth produced by a general three-dimensional magnetospheric-ionospheric current system are derived in [15]. Although possible, the computations are laborious and time-consuming in practice, and therefore they are not applicable to GIC forecasting or warning purposes, which would be based on satellite observations of charged particles emitted by the Sun. This difficulty can be avoided by using CIM for determining the electric and magnetic fields at the earth's surface [18].

CIM was developed in connection with radio engineering research about thirty years ago [19]. It was

introduced in earth electromagnetic induction studies in the 1970's [20]. Not until recently, CIM has started to become a standard tool in GIC studies.

CIM is based on a quantity dependent on the frequency and on the earth's conductivity structure and called the complex skin depth. In CIM, the earth is formally replaced by a perfect conductor at this depth. Then it is possible to (mathematically) express the secondary contribution to the surface fields in a closed form as the field produced by the mirror image of the primary source. This further means that the expressions of the surface fields become convenient for fast numerical computations. CIM has been shown to be very accurate, and it easily allows for investigations of any complicated ionospheric current distributions with vertical (geomagnetic-field-aligned) currents coupling the ionosphere to the magnetosphere. For all these reasons, CIM is now becoming a practical technique in association with investigations of space weather effects on the ground.

4.3. GIC in power systems

In comparison with the 50 or 60 Hz frequency used in electric power transmission, geomagnetic variations are very slow having frequencies typically in the mHz range. Therefore transformers experience GIC as dc currents. In normal operation circumstances of transformers, the relation between the ac exciting current needed to provide the magnetic flux for the voltage transformation and the voltage is linear [21]. However, the presence of GIC implies that the operation is no more linear resulting in saturation of the transformer during one half of the ac cycle and in a large and distorted exciting current. The electricity will contain both even and odd harmonics, which can cause relaying problems.

The increased exciting current also results in reactive power losses in the transformer leading to voltage drops and even to a collapse of the whole system. The saturation also affects the transformer itself, and overheating may occur with possible permanent damage

The most famous GIC problem occurred in the Hydro-Québec power system during a large magnetic storm on March 13, 1989, at 2.45 a.m. local time [22]. The cascading phenomena resulted in the loss of 21500 MW of energy, and the time between the onset of the magnetic storm and the collapse of the network was only about one and a half minutes. After nine hours 17 % of the load were still out of service. The March 1989 storm gave rise to an intensive GIC investigation in the Hydro-Québec system and corrective measures against GIC have been taken later.

In the same March 1989 storm, a transformer was seriously damaged in New Jersey, USA, causing a cost of several million US dollars together with replacement energy costs of about 400 kUSD per day.

4.4. GIC in pipelines

GIC-related problems in pipelines arise from voltages between the pipe and the surrounding soil. The electrochemical conditions at the pipe-soil interface are

changed by voltage fluctuations leading to the possibility of corrosion of the pipe steel. In addition, the voltages interfere with corrosion control surveys, in which the potential between the pipe and the soil is monitored.

To prevent corrosion, the pipeline should be in a small negative (~ 1 V) potential with respect to the ground. Such a voltage is maintained by a cathodic protection system. During a geomagnetic storm pipe-to-soil voltages of several volts have been observed, thus clearly exceeding the protection voltage.

Locations near inhomogeneities of a pipeline, like ends, bends and branches, are prone to large pipe-to-soil voltages. Therefore long electrically continuous pipeline sections are preferable, so that the number of section ends is minimized. On the other hand, the voltages at the ends of a long section are larger than those corresponding to a shorter one. Thus, the design of a pipeline system such that corrosion problems will be avoided is an optimizing task in which suitable compromises should be found.

5. CONCLUSIONS

Seismogenic ULF emissions have been analyzed by means of different kinds of data base. An additional convincing evidence was obtained for a large earthquake at Biak, Indonesia on February 17, 1996 on the basis of the sophisticated analysis methods (polarization and fractal analyses), and also a network of ULF observation in Japan was described.

The existence of slow tail sferics has been known for over 6 decades. The majority of these are well accounted for by accepted 'normal' lightning-stroke characteristics. The lower ELF band transient events have been the subject of study for 3 decades, with greatly increased activity in the past 10 years. There continues to be speculation as to the nature of the source currents which produce these signals which are so large that, for a time interval of the order of 100 ms, the electromagnetic signature dwarfs that of the whole global lightning distribution, even when the source is 10,000 or more kilometers distant.

The 1990s have seen the recognition of the various high-altitude luminous phenomena known as sprites, elves and blue jets. It appears that these are produced exclusively by +CG lightning and especially (but not exclusively) above mesoscale convective storm systems. Recent work shows that both in-sprite currents and continuing currents in the +CG discharge can produce ΔM_Q values of the order measured experimentally. It should be recalled, however, that a significant proportion of ELF events (and most slow tails) are generated by -CG discharges. The negative events involve somewhat lower values of ΔM_Q than positive events, but in the -CG case no sprites are generated.

Space weather conditions are determined by the activity of the Sun, which statistically follows the eleven-year sunspot cycle. A maximum of the cycle is taking place in 2000 making space weather issues particularly important now. Another fact emphasizing

the significance of space weather is the increasing dependence of people on reliable technological systems.

At the earth's surface, electric power transmission systems may experience problems due to space weather. These are produced by saturation of transformers caused by geomagnetically induced currents (GIC). Oil and gas pipelines can suffer from problems associated with corrosion due to voltages created by space weather. GIC can also affect phone cables and railway equipment. Observations of the Sun and of charged particles emitted by the Sun provide possibilities of forecasting space weather and of giving early warnings of large events. To predict GIC in a system, it is necessary to be able to estimate the electric field occurring at the earth's surface. This requires an accurate, but fast, calculation method. It has been realized recently that the complex image method (CIM) obviously involves a good opportunity in this respect.

6. REFERENCES

- 6.1. Hayakawa, M., Editor, "Atmospheric and Ionospheric Electromagnetic Phenomena Associated with Earthquakes," TERRAPUB, 997p., Tokyo, 1999.
- 6.2. Molchanov, O. A., et al., "Results of ULF magnetic field measurements near the epicenters of the Spitak ($M_s=6.9$) and Loma Prieta ($M_s=7.1$) earthquakes: Comparative analysis," *Geophys. Res. Lett.*, 19, 1495-1498, 1992.
- 6.3. Hayakawa, M., R. Kawate, O. A. Molchanov and K. Yumoto, "Results of ultra-low-frequency magnetic field measurement, during the Guam earthquake of 8 August 1993," *Geophys. Res. Lett.*, 23, 241-244, 1996.
- 6.4. Hayakawa, M., T. Ito and N. Smirnova, "Fractal analysis of geomagnetic ULF data associated with the Guam earthquake on August 8, 1993," *Geophys. Res. Lett.*, 26, 2797-2800, 1999.
- 6.5. Hayakawa, M., T. Ito, K. Hattori and K. Yumoto, "ULF electromagnetic precursors for an earthquake at Biak, Indonesia on February 17, 1996," *Geophys. Res. Lett.*, in press, 2000.
- 6.6. Gorbarikov, A., et al., "Acoustic emission response to earthquakes," *Geophys. Res. Lett.*, submitted, 2000.
- 6.7. Molchanov, O. A. and M. Hayakawa, "Generation of ULF electromagnetic emissions by microfracturing," *Geophys. Res. Lett.*, 22, 3091-3094, 1995.
- 6.8. Jones, D. L., "ELF sferics and lightning effect on the middle and upper atmosphere," *Modern Radio Sci.*, Oxford Univ. Press, 171-180, 1999.
- 6.9. Sentman, D. D., "Schumann resonances," Ed. by H. Volland, CRC Press, 267-310, 1995.
- 6.10. Nickolaenko, A. P., "Modern aspects of Schumann resonance studies," *J. Atmos. Solar-terr. Phys.*, 59, 505-516, 1997.
- 6.11. Huang, E., E. Williams, R. Boldi, S. Heckman, W. Lyons, M. Taylor, T. Nelson and C. Wong, "Criteria for Sprites and Elves Based on Schumann Resonance Observations," *J. Geophys. Res.*, 104, 16943-16964, 1999.
- 6.12. Burke, C. P. and D. L. Jones, "On the polarity and

continuing currents in unusually large lightning flashes deduced from ELF events," *J. Atmos. Terr. Phys.*, 58, 531-540, 1996.

6.13. Boccippio, D. J., E. R. Williams, S. J. Heckman, W. A. Lyons, I. T. Baker and R. Boldi, "Sprites, ELF Transients, and Positive Ground Strokes," *Science*, 269, 1088-1091, 1995.

6.14. Boteler, D. H., Pirjola, R. J. and Nevanlinna, H., "The effects of geomagnetic disturbances on electrical systems at the earth's surface," *Adv. Space Res.*, 22, 17-27, 1998.

6.15. Häkkinen, L., and Pirjola, R., "Calculation of electric and magnetic fields due to an electrojet current system above a layered Earth," *Geophysica*, 22, 31-44, 1986.

6.16. Lehtinen, M. and Pirjola, R., "Currents produced in earthed conductor networks by geomagnetically-induced electric fields," *Annales Geophysicae*, 3, 479-484, 1985.

6.17. Pulkkinen, A., Pirjola, R., Boteler, D., Viljanen, A. and Yegorov, I., "Modelling of space weather effects on

pipelines," Submitted to *J. Appl. Geophysics*, 2000.

6.18. Pirjola, R. and Viljanen, A., "Complex image method for calculating electric and magnetic fields produced by an auroral electrojet of finite length," *Annales Geophysicae*, 16, 1434-1444, 1998.

6.19. Wait, J. R. and Spies, K. P., "On the representation of the quasi-static fields of a line current source above the ground," *Canadian J. Phys.*, 27, 2731-2733, 1969.

6.20. Thomson, D. J. and Weaver, J. T., "The Complex Image Approximation for Induction in a Multilayered Earth," *J. Geophys. Res.*, 80, 123-129, 1975.

6.21. Kappenman, J. G. and Albertson, V. D., "Bracing for the geomagnetic storms," *IEEE Spectrum*, March, 27-33, 1990.

6.22. Chech, P., Chano, S., Huynh, H. and Dutil, A., "1992 The Hydro-Québec system blackout of 13 March system response to geomagnetic disturbance," *EPRI Report*, TR-100450, Proceedings of Geomagnetically Induced Currents Conference, Millbrae, California, USA, November 8-10, 19.1-19.21, 1989.

EMC 2000

INTERNATIONAL WROCLAW SYMPOSIUM
ON ELECTROMAGNETIC COMPATIBILITY

URSI COMMISSION E OPEN MEETING

Report of the Working Group E URSI/Commission E 9 Interference and Noise at Frequencies above 30MHz

Activities for the period September 1998 to April 2000

including a joint E/F Session at the URSI General Assembly of Toronto

"RADIO NOISE AND INTERFERENCE ABOVE 30MHZ"

Holon Academic Institute of Technology

52 Golomb Street, POB 305, Holon 58102, Israel

Professor Jacob Gavan – Head of Communication Engineering Dept.

Tel: 972-3-502-6686; Fax: 972-3-502-6685; <http://www.cteh.ac.il> – email gavan@barlev.cteh.ac.il

A joint Session E/F on Interference in Communication was held in Toronto, Canada at the XXVI General Assembly of the URSI in September 1999.

The organizers and leading conveners of the session were:

- Prof. Jacob Gavan, Head of Communication Engineering Department at the Holon Academic Institute of Technology, Israel,

and

- Dr. Bertram Arbesser-Rastburg Head of Wave Interaction and Propagation Section at the European Space Agency ESTEC Noordwijk the Netherlands. Fax No 31 71 5654999. After well planned preparations, cooperation and the efficient support of Prof. Masashi Hayakawa, Commission E Vice Chairman, we organized an interesting program for the session.

The summary of the E/F session targets is:

There has been exponential growth of Radio Mobile Systems equipment and users and considerable progress in the design and realization of Radio equipments, especially receivers. The effects of intra and inter Mutual interference have become more important than the internal, man made and atmospheric noise, especially for frequency bands above 30MHz.

Therefore the E/F session will concentrate on deterministic and empirical investigations on terrestrial and space propagation effects and analysis of Linear and Non Linear Interference affecting radio systems, especially at frequency bands of cellular, Personal and Satellite systems. This session will also include development of mitigation methods to enhance radio systems performance in consideration of even hostile wireless media propagation conditions."

The following abstracts for the session are:

CONTRIBUTION ORAL PAPERS

Original Abstract	PRESENTING AUTHOR And Country	ABSTRACT TITLE	FULL ADDRESS
EF.01	BLAUNSTEIN N.SH Israel	Co-channel interference prediction for Different microcell urban environments	Dept. of Electrical and Computer Engineering, Ben-Gurion - University of the Negev, P.O.Box 653, Beer Sheva 84105, ISRAEL - Fax : 972 7 6472 949,
EF.02	DINWIDDY, SIMON E. The Netherlands	A short history of space and how to get through free of interference	ESA (European Space Agency) ESTEC, P.O. Box 299 - 2200 AG - Noordwijk, The Netherlands
EF.03	SMITH, ERNEST K. USA	Interference due to Sporadic E over Japan	University of Colorado, Boulder Colorado, 80309-0425 - USA-
EF.04	LOYKA, S.L. Switzerland and Ukraine	Numerical Simulation of Nonlinear Inter- ference in Radio Systems	Swiss Federal Institute of Technology - LEMA-EPFL- Ecublens, CH-1015 Lausanne, Switzerland - Fax : +41.21.6932673
EF.05	GAVAN JACOB ISRAEL	Nowadays Cosited Radio Systems Inter- ference Effects: Analysis, Computation and Mitigation Techniques	Holon Institute of Technology, Arts and Sciences, Head of Communication Engineering Department - 52 Golomb St. POB 305, Holon 58102, Israel -
EF.06	AL-NUAIMI, M.O. UK	Site Shielding - An Effective Interference Control Tool -	School of Electronics, University of Glamorgan - Pontypridd, CF37 IDL, United Kingdom - Tel : +44 (0) 1443 482524, Fax : +44 (0) 1443 482541,

Original Abstract	PRESENTING AUTHOR And Country	ABSTRACT TITLE	FULL ADDRESS
EF.07	PEREZ REINALDO USA	A Major Threat to Satellites Radio Systems in Low Earth Orbit	Jet Propulsion Laboratory California Institute of Technology - Pasadena, California - Fax 3039714306

The Authors presented their abstracts on Interference in Communication and all the participants found them most interesting. Unfortunately, we were unable to grant a scholarship to Dr. Loyka SC - Hence he don't attend the conference. So we decided to prolong the time of presentation of our remaining

six presentations. The full abstracts can be found in the URSI Toronto XXVe General Assembly Book of Abstracts 1999 pp 718-721.

The following abstracts were chosen for poster presentations.

CONTRIBUTION (POSTER) PAPERS

E/F - Interference in Communication (1)

Original Abstract	PRESENTING AUTHOR and Country	ABSTRACT TITLE	FULL ADDRESS
P1	HRYTSKIV, Z.D. UKRAINE	Impulse Noise Influence on Image Transmission in Telecommunication System - EA	State University "Lvivska Polytechnika" 12 S. Bandery St., Lviv, 290646, Ukraine Tel : 0322 398519 - Fax:0322 744300,
EF.P2	DAI, JIN F. CHINA	The Model of Anti-Interfere Performance Evaluation for the Electric Information System (EIS) EA	Nanjing Research Institute of Electrical Engineering P.O.B. 1406- 52 - 210014 Nanjing China - Tel :025-4433457 - Fax:025-4433457,
EF.P3	LIU, YUAN-AN CHINA	Electromagnetic Hazard and Correlated EMI from Local Radiating Sources and the Related EMC Problems - EA -	Liu Yuan An Pob 171, Telecommunication Engineering School Beijing University of Posts and Telecommunications Beijing 100088, P.R. CHINA - Tel : (10)6228-1027, Fax : (10) 6228- 1774,
EF.P4	PRIMAK, SERGUEI CANADA	A statistical Approach to Modelling Electromagnetic Field Coupling E7	The University of Western Ontario London, Ontario, N6A 5B9, Canada Tel : 1-519-679-2111 ext.8355 - Fax : 1-519-661-34-88,
EF.P5	GUERRERO, DURAND CANADA	Performance Analysis of Turbo Codes Communication Channel with Fading E4	Advanced Communications Engi- neering Center - Dept. of Electrical and Computer Engineering - The University of Western Ontario, London, Ontario, N6a 5B9, Canada primak@gauss.enga.uwo.ca
EF.P6	PAWALEC, J.J. POLAND	Interference Rejection Using Adaptive Lattice Filters - E4	Radom University of Technology Frcta 14/2, 00-227 Warszawa, Poland, tel/fax 48-226358913,

These abstracts can also be found in the (abstract book)URSI XXVI Toronto General Assembly abstract book.

After the conference I gave several seminars and lectures in the USA (Qualcomm- San Diego, ITU Palo-Alto and Monterey at the International Symposium on Infrared and Millimeter waves where I entitled presented two papers entitled "Multi-mode LADAR/RADAR and Transponder Systems for tracking remote cooperative targets" and "Hypothesis of Natural RADAR DETECTION AND Navigation Guiding Hornets Flight",) and also in Israel. The last two conference papers deal with pioneers frequency ranges were mutual interference are still negligible and the main limitations to the RADAR and communications links are cluttering, scattering and absorption losses. Extension of these two conference papers where

accepted at the International Journal of Infrared and Millimeter Waves. The Hornet paper was published in the February 2000 edition and the LADAR/RADAR a few months later. A second paper was published on the fascinating hypothesis that hornets own a sophisticated detection and tracking system similar to the bats, but more sophisticated and accurate.

S. Ishay, J. Gavan

"Hypothesis Stipulating that a Natural RADAR
Navigation of Systems Guides Hornet Flight"
Journal of Electromagnetic Waves and
Applications

Vol.13, October 1999 (pp.1611-1625)
Cambridge, U.S.A.

J. Gavan, J.S. Ishay

"Hypothesis of Natural Radar Detection and Navigation Guiding Hornets Flight"
February 2000

I calculated that the operation of the Radar submillimeter system is limited to a distance of 70 meters due only to the high dispersion and atmospheric attenuation. Recently, together with a PHD student of Prof. J.S. Ishay, we discovered that the hornets antennas also have electrical energy and sub-millimetric wavelength antenna arrays. Thus the hornets own three receiving transmitting radiation sources which enable a Direction Finder Communication system up to a range of a few kms. (Paper in preparation for PIERS 2000). In the near future we intend proving these hypothesis by innovative detectors in the sub-millimeter waves (THz frequency ranges).

On the 15th February 2000, the Israeli National Committee for URSI organized the 4th Annual Symposium at the Campus of Tel-Aviv University of. In the morning the following lectures were presented:

Professor John Mc Coy, Catholic University, Washington, DC: *Accommodating Complexity in Propagation and Scattering* (45 minutes)
and:

Dr. Joseph Shapira, Vice President, URSI Int'l; President, Celler Ltd: *Radio Optimization of Cellular Networks* (45 minutes) and Dr. Noah Brosh on Radio Astronomy in Israel : Yes or No? (15 minutes).

In the afternoon, (6 sessions were opened in parallel: Commission A organized and chaired by Dr. Jacob Halevi on Electromagnetic Metrology; Commission B on Fields and Waves organized and chaired by Prof. R. Kastner and Dr. A. Boag; Commission C organized and chaired by Prof. S. Shamai and S. Litsin. Commission D on Electronics and Photonics organized and chaired by Prof. Y. Nemirowsky; Commission J on Radio Astronomy organized and chaired by Dr. N. Brosh and Commission E organized and chaired by Prof. J. Gavan. The lectures presented in our Commission E session on "Electromagnetics Noise and Interference" were as follows:

Electromagnetic Noise and Interference : Commission E

- Prof. Nathan Blaunstein, Ben Gurion University:
"Parameters affecting interference in a cellular radio urban propagation environment."
- Prof. Jacob Gavan, Holon Academic Institute of Technology:
"Analysis and mitigation methods for collocated radio systems interference and radiation effects."
- Dr. Moshe Rousseau, RAFAEL:
"Do electromagnetic system failure result from conducted or from radiated emissions? This is the Question."
- Dr. Alexander Axelrod, EMC consultant:
"New mechanisms of conducted emission in electrical power lines."
- Dr. Vladimir Liandres, Ben-Gurion University:
"Algorithm of frequency assignment in cellular communication to reduce interference."
- Dr. Haim Matsner, Holon Academic Institute of Technology:
"Analysis and computation of EMI leakage interference from waveguide connections."

There were only about 15 to 20 participants, due to the competition between parallel sessions. However the lectures were followed by very animated and useful discussions. The time allocated to each speaker was more than 30 minutes due to the absence of Dr. Moshe Rousseau who was ill. Four of the five presented lectures dealt with the interference above

30MHz which is the subject of Work Group E9. The first lecture was on cellular system frequency bands which one of the most expanding fields in telecommunications. One lecture deals with collocation radio systems interference with emphasis high power HF, UHF and UHF radio systems, which in some cases can also occur for cellular systems. The subject of this lecture was an improved extended version of the paper I gave at the URSI General Assembly in September 1999 in Toronto (mentioned earlier before and whose summary is presented here). One lecture dealt with the interference in Microwaves systems only. Dr. A. Axelrod presented his lecture on quite a different subject but strongly related to EMC. "Conducted emission in electronic power lines. some of the questions raised were about the radiation of power lines, especially due to the new trend to use them for Internet transmission even for long distances. Thus, high frequency bands are required on the power lines which causes radiation to occur.

Analysis and Mitigation Methods for collocated
Radio Systems Interference and Radiation effects:

Summary

Nowadays interference and radiation effects from radio systems especially for collocated transmitters (Tx) and receiver (Rx) have become very common and complex and have to be treated more seriously.

This is due to the tremendous growth in the number of wireless users and equipment and the necessity for coexistence of Tx and Rx on the same site, where mutual interference effects are significantly more harmful than natural, transceiver internal and industrial noise.

In radio systems, the output power of the Tx has to be high enough to provide sufficient desired signals even at long distances remote Rx. This also applies to cases of multipaths plus shadowing in realistic worst case propagation conditions, where non favorable Rayleigh and Log Normal statistical distributions are the rule, especially for ground mobile communication. However, the Tx desired signal for suitable Rx become interference for all other users of the radio spectrum. Therefore, optimization of the Tx output power is useful especially for collocated equipments. Nowadays, improvements are achieved partially in radio systems by using the following Digital Signal Processing (DSP) techniques: Automatic power control, dynamic channel frequency assignment, especially for reducing adjacent channel interference and smart antennas adaptive arrays. This will provide a reduction in interference by optimized space filtering and maximal signal to interference ratio to the desired mobile Rx or headset in case of cellular paging and Personal Communication Systems (PCS).

The collocated Tx interference are usually non linear affecting victim Rx, especially by blocking, broadband desensitization or spot frequency intermodulation (IM). Collocated Tx and Rx parameters simulation computation tools are required to estimate the Rx interference power levels under realistic worst case conditions, taking into account the positions and distances between the respective antennas including near field propagation scenarios. Most useful mitigation techniques will be presented to reduce harmful interference from the adaptive frequency selective filters, attenuators partial spatial shielding to the mentioned DSP solutions and efficient amplifier linearization methods up to complex electronic interference cancellation sub-systems. In the case of several cosited radio equipments operating simultaneously, a second (Computation)

simulation interaction is required using the Monte-Carlo statistical method.

Analysis and methods of protection will also be presented against threats of radiation hazards to site operators and hand-phone users in function of Tx effective radiation power and separation distances. This is important owing to the excess field and power levels which are present in the case of severe desensitization and blocking of victim Rx. The users or operators standing in close proximity to the near field zone by can also become victims, due to the exposure to the radiation level exceeding even the thermal limit regulations.

Main References

- [1] J. Gavan, "Nowadays Cosited Radio Systems Interference Effects: Analysis, Computation and Mitigation Techniques" Invited Lecture XXVI Toronto URSI (General Assembly) Abstracts EFS P720, August 1999
- [2] M.O. Al Nuaimi, "Site Shielding - An effective Interference Control Tool" Abstracts EFS P720, August 1999.
- [3] J. Gavan, F. Handler, Analysis, Computation and Mitigation of the Interference to a Remote Receiver from Two Collocated Vehicular Transceivers, IEEE Transactions on VT, vol. 45, no. 2, pp. 431-442, August 1996.

Additional Commission E Israeli National Activities

Under the leadership of Elya B. Joffe we are preparing the IEEE EMC Society 2003 International Symposium which will be held in Israel.

At the 27 of January 2000 we organized with the national IEEE EMC section a symposium on Grounding, Shielding and Radiation at the Holon Academic Institute of Technology. This symposium included the visit and operation of a new anachoid chamber part of an extended Antenna Laboratory for BSc level students of the Communication Engineering Department and for the staff research. This chamber will be extended and serve us also for EMC measurements in the forth coming EMC laboratory which will be designed next year. In spite of a stormy weather and heavy rains about 80 participants were present at the symposium and more than one hundred at the chamber visit.

Coming Scientific Activities

I am preparing with a few colleagues, included Prof. N. Blaustein, research tasks and papers on interference in urban and indoor situations, Blue tooth and Radio Frequency Identification systems for short ranges and long distance scenarios, radiation effects from headsets and other collocated Tx and the novel hypothesis of a sophisticated Hornets RADAR and Communication tracking and Direction Finding (DF) systems. I am presenting two papers on "Hypothesis of Natural Radar Tracking and Communication Direction Finding Systems Affecting Hornets Flight" at the Israeli IEEE Conference in Tel-Aviv, April 2000 and at the Progress in Electromagnetizing Research Symposium (PIERS) at Cambridge US, July 2000. This summer I intent also to participate to the Annual Virginia Tech Symposium on wireless Personal Communication and to the IEEE Int. Conference on communication in New Orleans this June. I shall also present seminars at the Toronto and Mexico Universities on interference problems.

During a sabbatical year which will begin in October 2000 I intent to collaborate with Dr. Arbesser-Rastburg and other well known scientists to prepare sessions for the URSI general Assembly in 2002. It is also included a participation as Convener to the session on EMC in communication in the 2001 Asia Pacific Radio Science conference at Tokyo, where I hope to initiate also useful contributions for the coming URSI General Assembly.

LIST OF EXHIBITORS

AM Technologies Sp. z o.o.

Ochota Office Park, Al. Jerozolimskie 181, PL-02-222 Warszawa, Poland

Phone: +48 22 608 45 55, Fax: +48 22 608 45 54,

e-mail: info@am-tech.pl

ASTAT Sp. z o.o.

Dabrowskiego 461, PL-60-451 Poznan, Poland

Phone: +48 61 848 88 71, Fax: +48 61 848 82 76,

e-mail: info@astat.com.pl

ELSINCO POLSKA Sp. z o.o.

Gdanska 50, PL-01-691 Warsaw, Poland

Phone: +48 22 832 40 42, Fax: +48 22 832 22 38,

e-mail: elsinco.warsaw@it.com.pl

NATIONAL INSTITUTE OF TELECOMMUNICATIONS

Wroclaw Branch

Swojczycka 38, PL-51-501 Wroclaw, Poland

Phone: +48 71 348 30 51, Fax: 48 71 372 88 78,

e-mail: hlug@il.wroc.pl

ROHDE UND SCHWARZ OESTERREICH

Sonnleithnergasse 20, A-1100 Vienna, Austria

ODDZIAŁ W WARSZAWIE

Stawki 2, floor 28, PL-00-193 Warsaw, Poland

Phone: +48 22 860 6490 to 6498, Fax: +48 22 860 6499,

e-mail: rohdepl@rsoe.com

SCHROFF GMBH

Feldrennach, Langenalberstr. 96-100, D-75334 Straubenhardt, Germany

Phone: +49 7082 794-0, Fax: +49 7082 794-2 00,

e-mail: info@schroff.de

TECHTRONIC

Grabiszynska 85, PL-53-503 Wroclaw, Poland

Phone: +48 71 342 5856, Fax: +48 71 342 0264,

e-mail: tom@techtronic.com.pl

TEKTRONIX POLSKA Sp. z o.o.

Pulawska 15, PL-02-515 Warsaw, Poland

Phone: +48 22 521 53 40, Fax: +48 22 521 53 41,

e-mail: measurement.poland@tektronix.com

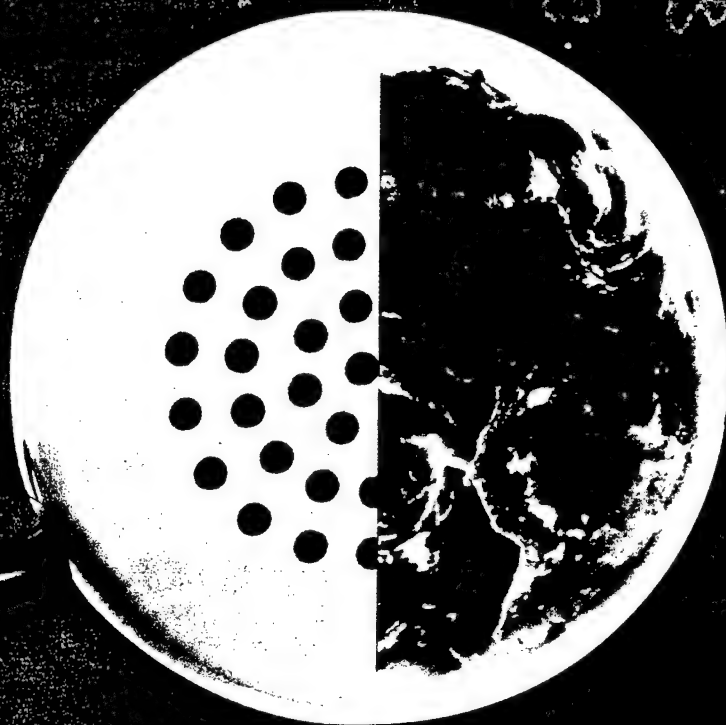
UNITRONEX POLAND Sp. z o.o.

Grzybowska 87, PL-00-844 Warsaw, Poland

Phone: +48 22 631 26 43, Fax: +48 22 632 75 59,

e-mail: uwo@unitronex.com

WE CARE FOR EACH CONNECTION, SO MILLIONS OF THEM ARE POSSIBLE



Telekomunikacja Polska S.A. enables you to make any call you want.

Reliability, experience, advanced technology and expertise
are the cornerstones of our growing success.

And as we enter the 21st century, its demands are not a mystery to us.

We have a digital network with fully integrated services.

A satellite communications system. Secure electronic mail.

A data transmission network. An Internet link with the entire world.

We have all that assures a constant, fast, and reliable flow of information.





anex[®]

ANDRZEJ POSTAWKA
Przedsiębiorstwo
Wielobranżowe
ul. Jerzmanowska 99
54-430 Wrocław

Anex Multibranch Company manufactures, as one of its main fields of activity since 1989, broadcast **antennas**, **antenna systems**, and antenna equipment for **radio and television** networks. The Company has its own **development and design** division, its own measuring **equipment**, and means of transport, including the big **terrain trucks**. We have set into operation over **150 antenna systems** of various size.

e-mail: anex@k.pl
tel. (071) 349 30 80
(071) 349 31 32
(071) 349 32 16
(090) 664 154
(071) 349 31 77



Plus

GSM

business

business to business

business to business

business to business

business to business

business to business

business to business

business to business

business to business

business to business

business to business

business to business

business to business

business to business

business to business

business to business

business to business

business to business

business to business

business to business

business to business

business to business

business to business

business to business



Plus GSM is the unquestionable leader in the supply of mobile telephone services to the corporate market. More than 66% of 500 largest Polish businesses have already chosen Plus GSM.

Why do these leading companies choose Plus GSM?

- we guarantee the highest quality of service
- we offer solutions adjusted to individual requirements
- we are constantly introducing new state of the art technologies

Our success is built on the trust of our clients. We would like to thank all our corporate clients and wish them many successful business conversations.

Internet: www.plusgsm.pl

Call free: 0 800 683 683

W@P

Z Idea po Internecie.

W@P IDEA - WHAT IS IT?

W@P Idea is a new service offered by the Idea network. It opens a whole new world of web opportunities for mobile phone users. You can browse information resources and use various services offered on the Internet through your WAP (Wireless Application Protocol) compatible phone.

USING W@P IDEA

To access WAP services on the Idea network, you must have:

- a) the Standard Data Transmission Service set up on your account (available with no additional connection charge and no monthly fee to all Idea users, i.e. Idea Optima and Meritum service plans plus POP pre-paid service users),

- b) a WAP-enabled phone with appropriate settings programmed.

The Standard Data Transmission Service is available to all Idea network users from March 1, 2000.

All customers who signed a contract with PTK Centertel earlier and chose the Idea 50 or Idea 150 service plans can activate the Standard Data Transmission Service by sending an "AKT DATA" text message (SMS) to the 555 number", or by ordering the service directly through the Customer Service Centre (dial *22 from your handset).

the SMSC Idea Messaging Centre number (+48 501 200 777) must be set on your phone





**PREMISE
NETWORKS**

A Division of Molex

Authorized
**PROMETRIC
TESTING CENTER**

Microsoft Certified

**Technical
Education**
Center

Microsoft Certified
Solution Provider

TECHTRONIC

RANGE OF TECHTRONIC SERVICES:

- comprehensive delivering of computers and computer equipment warranty and after-warranty computers and computer equipment service
- installation of computer networks
- designs and installations of telecommunication networks
- designs and installations of dedicated supply systems for computer networks
- designs and installations of sprinkler systems
- designs and installations of emergency supply systems
- designs and installations of following telecommunication engineering systems:
 - * structured cabling systems
 - * fire alarm signaling
 - * communication and security systems
 - * presence control
 - * providing sound
 - * TV + TVSAT
 - * industrial TV
- system integration
- computer training and courses

www.techtronic.com.pl
e-mail: system@techtronic.com.pl

NATIONAL INSTITUTE OF TELECOMMUNICATIONS

WROCLAW BRANCH • ul. Swojczycka 38, 50-501 Wrocław
tel. (+4871) 348-30-51 • fax (+4871) 3728878



EMC MEASUREMENT DIVISION

M.Pietranik@il.wroc.pl

EMC measurements
according to IEC-61000-4-
-2/3/4/5/6/11,
EN-55011/13/14/20/22,
ISO-7637 standards

Expert opinions,
measurements in situ, advice
on compliance with EMC
Directive (89/336/EEC)

Advice on, and organisation
of measurement set-ups, test
equipment completion,

Design and delivery of
specialised measuring
equipment,

Development of software for
automatic EMC
measurements

Verification of parameters of
EMC test equipment used for
emission measurements;
special laboratory certified b
the Polish Central House of
Measures (GUM)

SPECTRUM MANAGEMENT DIVISION

W.Sega@il.wroc.pl

Many years' experience in
radio network planning and
development of frequency
management support
systems for government and
private sector

Turn-key systems containing
all you need to solve your
frequency management
problems

Creation of planning tools,
propagation models, and
digital terrain models

Seminars in network
planning, network
optimization, spectrum
engineering, and spectrum
management

Evaluation of trends in
spectrum management

Strategic spectrum planning
(evaluation of spectrum
requirements and availability,
and spectrum allocation
plans)

Studies on strategy for
introducing the new
radiocommuniacion services

ANTENNA AND FIELD DIVISION

M.Kaluski@il.wroc.pl

Spectrum monitoring systems
in frequency range 0,1 MHz
to 3 GHz. Design, turn-key
delivery, installation, service

EM fields measurements in
the frequency range 0,1 MHz
to 5 GHz

Hazardous EM fields
measurements in the
frequency range 0,1 MHz
to 6 GHz

Computer modeling for the
EM fields evaluation

Antenna and antenna
systems design, and
parameters measurements

Antenna measurements for
certification and technical
approval

Adaptive antennas design
and consulting, high
frequency digital signal
processing using DSP

Visit our web site <http://www.il.wroc.pl>